

Refining and enhancing the modelling of vehicle-track interaction

Von der Fakultät für Maschinenbau
der Gottfried Wilhelm Leibniz Universität Hannover
zur Erlangung des akademischen Grades
Doktor-Ingenieur
genehmigte

Dissertation

von
Dipl.-Ing. Ingo Kaiser
geb. am 14. August 1972 in Hannover

2018

1. Referent: Prof. Dr.-Ing. Gerhard Poll
 2. Referent: Prof. Dr.-Ing. Prof. E.h. Dr.h.c.mult. Werner Schiehlen
 3. Referent: Prof. Dipl.-Ing. Dr. Ing. E.h. Gerhard Voß
- Tag der Promotion: 9.6.2017

Abstract

The interaction of a railway vehicle and the track is of significant importance for the operational safety and the economic efficiency of the entire system “railway”. Generally, the wheel-rail contact possesses a high stiffness so that very high dynamic contact forces and strong interactions between vehicle and track can occur. For the operational safety, it has to be guaranteed that the forces do not cause damage of vehicle and track. Furthermore, wear occurs in the wheel-rail contact. The rate of the wear progress and the distribution of the wear on the running surfaces of wheels and rails have a significant impact on the maintenance effort and thereby on the economic efficiency of the entire system “railway”.

Real-life experiments concerning railway vehicles require a high effort and thereby are costly. Moreover, they can be quite risky especially during the test phase of a new vehicle or for new operational conditions. Therefore, the computational simulation has become an important tool for the investigation of the dynamic behaviour of a railway vehicle.

Generally, every simulation model is a simplification of the real system to be investigated. For the simulation of the dynamic behaviour of a railway vehicle the modelling as a multi-body system is applied very often. For this purpose, commercially available programs exist. For the modelling of a railway vehicle as a multi-body system, components like the wheelsets, bogie frames, car body and track are described by rigid bodies. These bodies are connected to each other by force elements representing the suspension and the wheel-rail contacts.

Since the wheel-rail contact is very stiff, strong dynamic forces can occur in the contact; these forces are acting on the wheelset and the rail. Because of these strong forces it seems to be obvious to model the wheelset and the rail as flexible bodies. This modelling, however, is not used as the standard method. Furthermore, it is known from earlier investigations that for certain profiles the wheel-rail contact is very sensitive to relative motions between wheel rim and rail head. Since such relative motions can also be caused by deformations, modelling these components as flexible bodies and investigating the impact of these flexibilities on the behaviour of the system seems to be desirable.

As already mentioned, the wheel-rail contact is the essential element for the wear of wheels and rails. Many simulations for the investigation of the wear either use quite rough types of modelling or the dynamic behaviour of the vehicle is determined first using a simulation model for the dynamics and the wear is determined afterwards using a detailed contact model. Both methods have several drawbacks so that the development of a simulation model, which is capable to calculate the dynamic behaviour of the vehicle-track system and the wear occurring in the contact simultaneously, is desirable. The base for such a model is the integration of a detailed model for the wheel-rail contact into the entire system.

The elements “wheelset”, “rail” and “wheel-rail contact” are the three essential components for the vehicle-track interaction. In the present work, the modelling of these three components is enhanced

and refined in the following way:

1. The wheelset is modelled as a flexible body. Here, the essential issues are to fully take into account the rotation of the wheelset due to the overturning and the related gyroscopic effects as well as to describe the forces resulting from the wheel-rail contact; due to the overturning, these forces act as a circulating load.
2. In the enhanced track model, the rail is modelled as flexible bodies, which are supported by discrete sleepers. In order to describe the motion of the rail head in a more accurate way, the model of the rail also takes deformations of the cross section into account; such deformations are not described by the usually used beam models.
3. The modelling of the wheel-rail contact is based on a consideration of wheel and rail as elastic halfspaces. Using the contact model, which is developed here, also non-elliptic contact areas can be determined; such contact areas can occur for several profile combinations of wheel and rail, but cannot be described by the widely used Hertzian theory. For the contact model, an iterative solution of the discretized contact equations is used. A particular challenge is the development of a fast solving algorithm for the contact equations.

Based on the refined and enhanced models for the subsystems “wheelset”, “rail” and “wheel-rail contact” a vehicle-track model is developed. This model describes a passenger coach having two bogies, each one equipped with two wheelsets; this coach is running on a straight track. Using this model, the functional efficiency of the newly developed models for the subsystems as well as the impact of the flexibilities of wheelsets and rails on the running behaviour of the coach are investigated. This is done for two running states, i.e. the centred running and the permanent hunting. Furthermore, the impact of the flexibilities of wheelsets and rails is compared with those of different contact geometries and different friction coefficients in the wheel-rail contact.

Keywords: railway vehicle, flexible wheelset, flexible rail, flexible track, wheel-rail contact, rolling contact, non-elliptic contact, elastic multibody system, finite element model, cyclic system, vehicle-track interaction, hunting.

Zusammenfassung

Die Wechselwirkung von Schienenfahrzeug und Gleis ist von erheblicher Bedeutung für die Sicherheit und die Wirtschaftlichkeit des Gesamtsystems „Eisenbahn“. Generell besitzt der Rad-Schiene-Kontakt eine hohe Steifigkeit, so dass hier sehr hohe dynamische Kontaktkräfte und starke Wechselwirkungen von Fahrzeug und Fahrweg auftreten können. Für die Sicherheit des Betriebs muss gewährleistet sein, dass die Kräfte nicht zu Beschädigungen von Fahrzeug und Fahrweg führen. Weiterhin tritt im Rad-Schiene-Kontakt Verschleiß auf. Die Geschwindigkeit des Verschleißfortschritts und die Verteilung des Verschleißes auf den Laufflächen von Rädern und Schienen haben einen erheblichen Einfluss auf den Wartungsaufwand und damit auf die Wirtschaftlichkeit des Gesamtsystems „Eisenbahn“.

Reale Versuche mit Schienenfahrzeugen sind sehr aufwendig und damit teuer. Zudem können sie insbesondere während der Erprobungsphase eines neuen Fahrzeugs oder neuer Betriebsbedingungen mit erheblichen Risiken verbunden sein. Aus diesem Grund ist die computergestützte Simulation ein wichtiges Werkzeug zur Untersuchung des dynamischen Verhaltens von Schienenfahrzeugen geworden.

Prinzipiell stellt jedes Simulationsmodell eine Vereinfachung des untersuchten realen Systems dar. Für die Simulation des dynamischen Verhaltens von Schienenfahrzeugen wird sehr häufig die Modellierung als Mehrkörpersystem verwendet. Für diese Aufgabe existieren kommerziell erhältliche Simulationsprogramme. Bei der Modellierung eines Schienenfahrzeugs als Mehrkörpersystem werden Komponenten wie Radsätze, Fahrwerkrahmen, Wagenkasten und Gleis durch starre Körper beschrieben. Diese Körper sind durch Krafterelemente, die die Federung und die Rad-Schiene-Kontakte repräsentieren, miteinander verbunden.

Da der Rad-Schiene-Kontakt sehr steif ist, können starke dynamische Kräfte im Kontakt auftreten, die auf den Radsatz und die Schiene einwirken. Aufgrund dieser starken Kräfte erscheint es naheliegend, sowohl den Radsatz als auch die Schiene als flexible Körper zu modellieren. Diese Modellierung wird jedoch bis heute nicht standardmäßig verwendet. Weiterhin ist aus früheren Untersuchungen bekannt, dass der Rad-Schiene-Kontakt für einige Profile sehr empfindlich auf Relativbewegungen des Radkranzes und des Schienenkopfes reagiert. Da derartige Relativbewegungen auch durch Deformationsbewegungen von Radsatz und Schiene verursacht werden, erscheinen eine Modellierung dieser Komponenten als flexible Körper und eine Untersuchung des Einflusses dieser Flexibilitäten auf das Systemverhalten ebenfalls wünschenswert.

Wie schon erwähnt, stellt der Rad-Schiene-Kontakt das entscheidende Element für den Verschleiß von Rad und Schiene dar. Viele Simulationen zur Untersuchung des Verschleißes verwenden entweder relativ grobe Modellierungen, oder es werden zunächst das dynamische Verhalten des Fahrzeugs mit einem Simulationsmodell für die Dynamik und anschließend der Verschleiß mit einem detaillierteren Kontaktmodell bestimmt. Beide Vorgehensweisen weisen Nachteile auf, so dass die Entwicklung eines Simulationsmodells wünschenswert ist, mit dem sowohl das dynamische Verhalten des Fahrzeug-Fahrweg-Systems als auch der im Kontakt auftretende Verschleiß simultan

berechnet werden können. Die Basis für ein solches Modell besteht in der Integration eines detaillierten Modells für den Rad-Schiene-Kontakt in das Gesamtmodell.

Die Elemente „Radsatz“, „Schiene“ und „Rad-Schiene-Kontakt“ sind die drei wesentlichen Komponenten für die Fahrzeug-Fahrweg-Wechselwirkung. In der vorliegenden Arbeit werden die Modellierungen dieser drei Komponenten in folgender Weise erweitert und verfeinert:

1. Der Radsatz wird als flexibler Körper modelliert. Die wesentliche Problemstellung besteht hierbei sowohl in der vollen Berücksichtigung der Rotation des Radsatzes infolge des Abrollens und der damit verbundenen Kreiseffekte als auch in der Beschreibung der aus dem Rad-Schiene-Kontakt resultierenden Kräfte, die aufgrund des Abrollens für den Radsatz eine umlaufende Belastung darstellen.
2. In dem erweiterten Gleismodell werden die Schienen als flexible Körper modelliert, die von diskreten Schwellen gestützt werden. Um die Bewegung des Schienenkopfes genauer zu beschreiben, berücksichtigt das Modell der Schiene auch Deformationen des Querschnitts, die von den üblicherweise verwendeten Balkenmodellen nicht abgebildet werden.
3. Die Modellierung des Rad-Schiene-Kontakts beruht auf der Beschreibung von Rad und Schiene als elastische Halbräume. Mit dem hier entwickelten Kontaktmodell lassen sich auch nicht-elliptische Kontaktflächen bestimmen, die für mehrere Profilkombinationen von Rad und Schiene auftreten können, jedoch von der häufig verwendeten Hertz'schen Theorie nicht erfasst werden. Das Kontaktmodell verwendet eine iterative Lösung der diskretisierten Gleichungen für den Kontakt. Eine besondere Herausforderung besteht in der Entwicklung eines schnellen Lösungsalgorithmus für die Kontaktgleichungen.

Auf der Basis der verfeinerten und erweiterten Modelle für die Subsysteme „Radsatz“, „Schiene“ und „Rad-Schiene-Kontakt“ wird ein Fahrzeug-Fahrweg-Modell entwickelt. Dieses Modell beschreibt einen vierachsigen Reisezugwagen mit zwei Drehgestellen, der auf einem geraden Gleis läuft. Mit diesem Modell werden sowohl die Funktionstüchtigkeit der neu entwickelten Modellierungen der Subsysteme als auch der Einfluss der Flexibilität von Radsätzen und Schienen auf das Laufverhalten des Wagens untersucht. Dies geschieht anhand zweier Fahrscenarien, nämlich dem zentrischen Geradeauslauf und dem Wellenlauf, auch Schlingern genannt. Weiterhin wird der Einfluss der Flexibilitäten von Radsätzen und Schienen mit den Einflüssen unterschiedlicher Kontaktgeometrien und unterschiedlicher Reibbeiwerte im Rad-Schiene-Kontakt verglichen.

Schlagnvorte: Schienenfahrzeug, flexibler Radsatz, flexible Schiene, flexibles Gleis, Rad-Schiene-Kontakt, Rollkontakt, nicht-elliptischer Kontakt, elastisches Mehrkörpersystem, Finite-Elemente-Modell, zyklisches System, Fahrzeug-Fahrweg-Wechselwirkung, Schlingerlauf.

Contents

1	Introduction	11
1.1	Specific characteristics of the railway	13
1.2	Requirements to a railway vehicle	16
1.3	Motivation, aim and goal of this work	18
1.4	Structure of the work	22
2	Modelling of railways: State of the art	24
2.1	Modelling methods	26
2.1.1	Multibody models	26
2.1.2	Finite element systems	28
2.1.3	Flexible multibody systems	30
2.2	Vehicle models	31
2.2.1	Characteristic behaviour of the wheelset	31
2.2.2	Low frequency range	39
2.2.3	High frequency range	42
2.2.4	Medium-frequency range	43
2.3	Track models	45
2.3.1	Substitution track models	48
2.3.2	Aspects of structural track models	50
2.3.3	Examples for structural track models	56
2.4	Wheel-rail contact models	57
2.4.1	Elliptic contact	58
2.4.2	Normal contact	60
2.4.3	Tangential contact	62
3	Cyclic systems	64
3.1	Fourier series	66
3.1.1	Continuous Fourier series	66
3.1.2	Discrete Fourier series	68
3.1.3	Fourier series for real functions	73

3.2	Transformation of the linear cyclic system	76
3.3	Modal decomposition of a cyclic system	86
3.3.1	Modal decomposition of an ordinary linear system	88
3.3.2	Eigenvectors of a linear cyclic system	92
3.3.3	Damped cyclic systems	104
3.4	Conclusion	110
4	Structural dynamics of the wheelset and the rail	116
4.1	Finite element modelling	118
4.2	Prismatic solid	120
4.3	Solid of revolution	129
4.4	Bilinear interpolation	140
4.5	Formulation of the semi-analytic elements	145
4.5.1	Bilinear prism element	145
4.5.2	Bilinear annular element	147
4.5.3	Numerical integration	149
5	Description of the rotating flexible wheelset	151
5.1	Kinematics of the wheelset	151
5.1.1	Rigid body motions	152
5.1.2	Relative motions	153
5.1.3	Summary	155
5.2	Generalization of a cyclic structure: The n -tuple of particles	156
5.3	Description in the sliding frame	160
5.4	Transformation of the linear cyclic system	163
5.5	Modal synthesis	166
5.6	Structural dynamics model of the wheelset	170
5.7	Inertia terms for a cyclic structure: General principle	174
5.8	Inertia terms for a cyclic structure: Structure of the terms	184
5.8.1	Rigid body terms	187
5.8.2	Terms of first order	189
5.8.3	Terms of second order	191
5.9	External forces	193
5.9.1	Wheel-rail contact forces	194
5.9.2	Bearing forces	198
6	Modelling of the track	199
6.1	Structure of the track model	199

6.2	Modelling of the rail	201
6.3	Modelling of the sleeper	204
6.3.1	Kinematics of the sleeper	205
6.3.2	Inertia terms for the sleeper	207
6.3.3	Modelling of the underground	209
6.3.4	Rail seat	211
6.4	The track as a cyclic structure	213
6.4.1	Rails	214
6.4.2	Sleepers	215
6.4.3	Modelling of the pads	216
6.4.4	Equations of motion	217
6.5	Influence of the length of the track model	218
7	Modelling of the wheel-rail contact	223
7.1	Kinematics	225
7.1.1	Rotation of the surface	227
7.1.2	Angular velocity of the surface	232
7.1.3	Application to the rail	238
7.1.4	Application to the wheel	244
7.2	Geometry and kinematics of the contact	249
7.2.1	Determination of the wheel envelope	251
7.2.2	Determination of the interpenetration	253
7.3	Contact mechanics	257
7.4	Discretization of the contact problem	258
7.5	Normal contact	269
7.5.1	Solving algorithm	270
7.6	Tangential contact	277
7.6.1	Solving algorithm	279
8	Simulation results	284
8.1	Centred running	286
8.2	Hunting behaviour	293
8.2.1	Influence of the flexibilities on the hunting	294
8.2.2	Influence of the friction	303
8.2.3	Influence of the conicity	310
8.3	Conclusion	318
9	Conclusion and outlook	320

A	Mathematical basics	328
A.1	Summation	328
A.2	Complex numbers	329
A.3	Exponential function for complex exponents	330
A.4	Polynomial interpolation	331
A.5	Matrices and vectors	333
A.5.1	Vector product	333
A.5.2	Scalar triple product	334
A.5.3	Vector triple product	335
A.6	Evaluation of geometric series	336
B	Description of a continuum in cylindrical coordinates	338
B.1	Derivatives	338
B.2	Strains	341
B.3	Virtual work	347
B.4	Navier's equation	352
C	Derivation of the kinematics and the inertial terms for a flexible body	357
C.1	Kinematics: Floating frame of reference formulation	357
C.2	Description of the relative kinematics	359
C.3	Inertia terms	360
C.3.1	Translational motions	362
C.3.2	Rotational motions	363
C.3.3	Relative motions	366
D	Rotation matrices	368
D.1	Elementary rotation matrices	368
D.2	Composed rotation matrices	371
D.3	Formulation by column vectors	372
D.4	Angular velocity	374
E	Compliance coefficients	378
E.1	Local coordinates	381
E.2	Integration over the polar coordinates	385
E.2.1	Integration for constant ξ	388
E.2.2	Integration for constant η	390
E.2.3	Evaluation of the integrals	392

Chapter 1

Introduction

The introduction of the railways meant a tremendous increase of mobility. Until the 19th century, the only ways to travel on ground were walking or for the few, who could afford, riding on a horse or using a carriage hauled by horses. The railway however provided an affordable travelling even to further destinations to a high percentage of people. The railway also enabled new, up to then unknown possibilities concerning the transport of cargo. It can be seen as an indicator for this strong improvement of performance that the railway networks in Europe and North America grew and expanded very fast. Another indicator for the high transport performance of the railway is the fact that it became very soon an integral part of strategic military planning¹, which relied on the railways' high transport capacity and high transport speed compared to the other ways of transport.

In the 20th century the railways were confronted with new competitors. In Europe and North America the automobile, which had been a very luxurious and exquisite article in the first decades after its invention in 1886, evolved after World War 2 into an affordable product: Privately owned cars became a common standard even for the middle class. Trucks, mostly originally designed for military purposes, were becoming widely used for cargo transport. Also, the building of motorways allowed for an increase of driving speed. Concerning passenger travel, also air traffic became a stronger competitor even for travelling within a continent. In America the long-distance passenger trains nearly vanished as a consequence of this competition. In Middle and Western Europe the state-owned railway companies took the challenge by improving their offer, which meant a higher standard of comfort as well as higher travelling speeds to shorten the travelling time; one example for these improved offers were the Trans Europ Express (TEE) trains, which were introduced in 1957, see e.g. Mertens [44]. One aspect to improve the competitiveness of the railway was replacing the steam locomotives which hauled most of the trains before World War 2 by vehicles equipped with diesel motors or electrical propulsion. These propulsion systems, especially the electric propulsion, enable higher power and performance combined with better energetic efficiency and less maintenance effort of the vehicles. Another aspect was the development of new running gears which provided save operation and good ride comfort even at higher running speeds. An overview of the development of running gears and their design features is e.g. given by Baur in his bilingual book [5] about bogies. In his thesis [36], Kratochville also gives an overview on this development with special focus on the yaw damper, which is an essential component for many running gears designed for high speeds.

In 1969 the German Federal Ministry for Transport gave order to carry out a study officially called

¹It can be seen as an indicator for the high importance of the railways for military strategy that taking photographs of railways was prohibited for a long time in many countries, especially in Europe.

“Studie über ein Hochleistungsschnellverkehrssystem” (study on a high-performance rapid transport system), short “HSB-Studie” (HSB study). This study [18] was completed in 1971 and covered several aspects concerning railway operation at higher speed. It should be kept in mind that at this time the regular maximum speed for trains in Germany was 160 km/h with very few exceptions. One of these exceptions were the demonstration runs during the International Traffic Exhibition in 1965 in Munich; these trains, which consisted of regular passenger coaches hauled by the electric locomotives of the series E03, were publically accessible and ran regularly with a top speed of 200 km/h between Munich and Augsburg. One appendix of the HSB study dealt with running dynamics, which was investigated using mechanical models of the vehicles. The study concluded that concerning the guidance of the vehicles within in the track the limiting speed is located at about 270 km/h. The study also mentioned the world speed record set in France in 1955, when a test train consisting of the electric locomotive BB-9004 and three passenger coaches reached a maximum speed of 331 km/h on the line south of Bordeaux, but stated that “after this, damages were detected.”²

An overview on the actual development of high-speed railways is given by Hughes [19]; some milestones regarding the development of high speed traffic shall be cited here:

- 1955: World speed record 331 km/h set by the French locomotive BB-9004 hauling three coaches
- 1964: Begin of regular operation of the Japanese Shinkansen train between Tokyo and Osaka at 210 km/h
- 1965: First publically accessible runs at 200 km/h in Europe by special trains hauled by the German locomotives of the type E03 during the International Traffic Exhibition in Munich
- 1967: First regular service at 200 km/h in Europe by the French train “Le Capitole” hauled by specially modified locomotives of the type BB-9200, see [44]
- 1981: World speed record 380 km/h set by the French high-speed train TGV 16 (“Train á Grande Vitesse” = high-speed train); begin of regular operation of the TGV-SE (“Sud-Est” = South-East) at 270 km/h
- 1988: World speed record 406 km/h set by the German high-speed train ICE-V (“Intercity Experimental”, later “Intercity Express”, “Vorserie” = prototype)
- 1989: Begin of regular operation of the French high-speed train TGV-A (“Atlantique” = atlantic) at 300 km/h
- 1990: World speed record 515 km/h set by the French high-speed train TGV-A 325
- 2007: World speed record 574 km/h set by the French high-speed trainset TGV-V150 (“Vitesse 150” = speed 150 [m/s], i.e. 540 km/h)

²Original quote from [18], section A7/1, page 38: “Die größte bisher kurzzeitig gefahrene Geschwindigkeit gibt die SNCF mit 331 km/h an, wonach allerdings Schäden auftraten, wobei aber zu bedenken ist, daß es sich um konventionellen Oberbau (nicht einmal durchgehend geschweißt) handelte.” Free translation: “The highest speed achieved until now for a short time is reported by SNCF [“Soci t  Nationale des Chemins de fer Franais” = French national railways] with 331 km/h, but after this, damages were detected; it has, however, to be considered that it was a conventional track, ([the rails were] not even continuously welded).”

It should be noted that the world speed records were set in experimental runs which were not accessible for public. Also, the TGV trainsets used for these record runs were specially modified or even specially composed as it was the case for the trainset TGV-V150. – The chronology shows a remarkable increase of the speeds, especially the development between 1981 and 2007. Starting with the world record run of 380 km/h in 1981 it proves in an impressive and convincing way that the speed limit of 270 km/h assumed in the HSB study was incorrect; the question which maximum speed can be achieved by a railway vehicle isn't completely answered till today. It should be pointed out that before the high-speed runs the behaviour of the vehicles was carefully studied on the base of mathematical-mechanical models, see e.g. [61] and [10]. These investigations helped to reduce the risks of exploring unknown speed ranges during the practical test runs. This may illustrate the advance of the simulation models as well as of the design of the running gears.

Altogether, this short overview shows the importance of mechanical modelling of railway vehicles and the simulation of their dynamic behaviour, which have become an important part of the development of the railway. The dynamic behaviour of railway vehicles is influenced by several factors; to get a better understanding of these factors, of the problems they cause and of the requirements the specific characteristics of the railway will be considered in the following and it will be discussed how these characteristics are influencing the entire behaviour of the complete railway system.

1.1 Specific characteristics of the railway

Like many transport systems, railways consists of both infrastructure and vehicles. In the following, some specific characteristics of railways in contrast to other transport systems will be considered. Generally, the motions of a vehicle and the forces related to them can be categorized with respect to the vehicle's own orientation:

- vertical motions and forces: Support
- lateral motions and forces: Guidance
- longitudinal motions: Propulsion and braking

The railway is a *track-guided ground vehicle*, i.e.:

- For support and guidance a *ground vehicle* interacts with solid ground in contrast to ships and aircrafts, which interact with water and air, respectively.
- The trajectory of a *track-guided vehicle* is given by the trajectory of the track, i.e. the vehicle operator can only determine the speed, but not the course of the vehicle in contrast to road vehicle where the course can be changed by steering. This means that a railway vehicle needs an automatic guidance mechanism, which corrects deviations from the ideal trajectory.

For all railways, forces responsible for support and for guidance are transmitted by a solid contact between a wheel and a rail which are usually made of steel. This wheel-rail contact transmits forces by two principles: Forces which act normal to the contact surface are transmitted by positive interlocking, while forces acting tangential to the contact surface are transmitted by friction. With very few exceptions, propulsion and braking forces are also transmitted by the wheel-rail contact. Exceptions, in which braking forces are transmitted independently of the wheel-rail contact, are

vehicles equipped with electromagnetic track brakes or linear eddy current brakes. The best known exceptions concerning the transmission of propulsion forces are rack railways or cog railways, which use a toothed rack rail and a cog wheel to transmit longitudinal forces. It should be pointed out that due to the transmission of forces by friction in the rolling contact, slip and hence wear in the contact occurs; this cannot be avoided.

From these principles

1. transmission of supporting, guiding, propulsion, and braking forces by a solid contact of a steel wheels and steel rails
2. automatic guidance by the running gear and the infrastructure

which are specific for the railway a number of specific characteristics of the entire system “railway” arise.

Since the support and guiding forces of the railway vehicle are transmitted by a solid contact, the railway vehicle has to be in contact with the infrastructure at any time; a loss of this contact usually means a derailment, which generally implies severe damage to the infrastructure and the vehicle and sometimes also includes casualties and therefore has to be avoided by all means. Due to this, the railway requires a continuous infrastructure, which is costly with respect to building and to maintenance. In contrast to this, aircrafts and watercrafts usually just need a punctual infrastructure like airports and harbours, respectively.

Since the wheels and the rails of a railway are usually made of steel, the wheel-rail contact is very stiff. This means that unevennesses of the running surfaces in the magnitude of less than 1 mm can already cause high dynamic forces in the wheel-rail contact, which should be avoided. Such an accuracy can only be achieved by a specifically built infrastructure. It is evident that this required accuracy makes the building and the maintenance of the infrastructure costly. For road vehicles, these requirements to the infrastructure are in contrast to this less strong: Road vehicles are usually equipped with rubber tyres, which can cushion unevennesses of the infrastructure in the magnitude of few millimeters.³

A specific characteristic of a railway is that a comparatively fine tuning of the vehicle and the infrastructure is required. Of course, all kinds of vehicles are subjected to certain geometrical limits given by their infrastructure, which limit their main dimensions like length, width and height; this also applies for aircrafts and watercrafts especially regarding airports and harbours, respectively. Regarding ground vehicles in general, the geometry of the infrastructure, which the vehicles have to follow, gives certain restrictions to the vehicles and their operation: The space around a road or a track, which is generally kept clear, limits the admissible width and height of the vehicle; the radius of a curve limits the admissible length of the vehicle in order to ensure that it doesn't exceed the aforementioned space. It is also obvious that the radius of a curve together with the cant, i.e. the inclination with respect to the longitudinal axis, limits the admissible speed at which the vehicle can pass the curve. But regarding the cross section of the running surface, it can be said that an ideal road has a plain surface, which may have a cross slope; ruts, i.e. longitudinal depressions of the road surface, are an unwanted result of wear and thereby considered as a deviation from

³For road vehicles, the line for a built infrastructure, which is required for operation, is difficult to draw. At slow speeds, most cars can also run on unmade or nearly unmade ways like country roads or rural roads. Some road vehicles like dump trucks, which are used e.g. on construction sites, or agricultural vehicles are specially designed for off-road operation on unmade ground. However, such vehicles can be considered as special cases; the majority of road vehicles, which are used for passenger traffic or cargo transport, are designed to be operated on tarmac roads, i.e. they require a built infrastructure.

the ideal plain. The width of the road puts an upper, but no lower limit on the track axle, i.e. the transverse distance between the wheels. To put it bluntly: Each road, on which a truck can run, can also be used with a car and even with a bicycle from the technical point of view. In contrast to this, the track gauge, i.e. the transverse distance between the two rails of a track, prescribes a certain range with an upper and a lower limit for the wheel gauge, i.e. the transverse distance between the two wheels, for a railway vehicle which shall run on this track. Furthermore, the shape of the rail profile has an impact on a basic function of a railway vehicle: Since a railway vehicle has no steering devices by which the driver could influence the vehicle's course, it needs an automatic guidance mechanism. This guiding mechanism is strongly influenced by the shape of the profiles of both wheel and rail; this will be discussed in detail in section 2.2.1. The wheel profile of a vehicle is usually adapted to the rail profile of the network on which the vehicle shall run in order to achieve the resulting geometry which is required for a good running behaviour. Therefore, it can't be said that there is an ideal cross sectional geometry of a railway track in general, whilst for a road a plain surface can be considered to be the ideal running surface.

It can be concluded that for a railway the vehicles are very tightly bound to a continuous built infrastructure having relatively narrow tolerances. This fact makes the railway comparatively vulnerable even to small local faults. Of course, at many transport systems the infrastructure and the vehicles are subjected to interaction forces leading to a deterioration of both subsystems over time. In the case of the railway, such deterioration is caused by the wear of wheels and rails and by damage of the subgrade due to the loads, temperature changes and vegetation. Therefore, costly maintenance of the vehicles as well as of the infrastructure is required. The more, in the case of the railway, the maintenance of the infrastructure usually means a stronger disturbance of the regular operation. For the general maintenance of a motorway, for instance, the traffic may be reduced from several lanes to one lane in one direction, but this still allows a reduced operation. In contrast to this, a railway track has to be closed completely for general maintenance. Furthermore, a railway vehicle needs a turnout to change from one track to another, while road vehicles can change the lane of a road at every location of the road from the technical point of view. Since turnouts are comparatively complex and expensive constructions, they are installed only at very few points. As a consequence, the maintenance of even a very short section of the track can require the temporary closure of a far longer section depending on the distance between two turnouts, which may strongly reduce the capacity of the railway line. All this underlines the need for long maintenance intervals especially for the track; however, this can only be achieved by a proper adaptation of vehicle and track.

As already mentioned, because of the stiffness of the wheel-rail contact using steel, even geometric disturbances having a magnitude of about 1 mm can lead to high dynamic forces in the contact. Such dynamic forces are undesirable for several reasons. High dynamic forces cause strong loads on the components, which may lead to fatigue or even catastrophic failure. Furthermore, dynamic forces having higher frequencies can excite structural vibrations of the wheels and the rails. Such structural vibrations can cause noise which is annoying for the passengers as well as for the residents living near a railway line.

Thus it is highly desirable to design railway vehicles and tracks in such a way that the damage caused by the vehicle-track interaction is low. However, as explained before, this requires a good adaptation between vehicles and tracks. This adaptation is not limited to the geometry of the track and the running gears but also applies for their dynamic behaviour. In real life, there are a lot of factors like the geometrical shape of the components which have an influence on their structural dynamics and parameters like masses, stiffnesses and dampings. Although field measurements are valuable, it is sometimes difficult to trace back an effect to few specific parameters on the base

of field measurements only and to separate characteristic effects from random influences. Here, a computer-based simulation provides a more systematic investigation, because single parameters can be changed in a defined way to study their influence on the behaviour of the entire system. However, this requires a sufficient accuracy of the modelling of the system. These aspects will be discussed in later sections of this work.

1.2 Requirements to a railway vehicle

The essential task of a railway vehicle is to fulfil a given mission profile, i.e. the transport of passengers or cargo on one or several defined networks, in an economically efficient way and by keeping the requirements with respect to safety and environmental compliance. The following consideration is limited to aspects, which are related to the dynamics of the running gear. Other mechanical problems like e.g. energy consumption, braking or aerodynamics and non-mechanical problems like constructional design (general architecture, gauging, maintenance friendliness etc.), vehicle equipment (energy supply, air conditioning, passenger information etc.) or certain environmental issues (recycling of materials, environmental compliance of operational materials etc.) will not be discussed in this work.

The requirements for the running gears which arise from the general requirements for the vehicle can be described by the following main topics although there may be some interference between the single topics:

1. *Running stability*: Since a railway vehicle is a track guided vehicle, it has to be guaranteed that the vehicle follows the trajectory which is given by the track within a certain range of tolerance. Exceeding this range of tolerance leads to the derailment of the vehicle which usually causes considerable damage to the vehicle and the track. The vehicle is guided by forces acting in the wheel-rail contact. If these forces exceed certain limits severe damage to the track may ensue which again can lead to a derailment of the vehicle. Therefore, the running stability is a safety aspect.
2. *Vibration insulation*: Mechanical vibrations are uncomfortable to the human body and can also cause damage and failure of vehicle components. Mechanical vibrations of the running gear are mainly excited by track imperfections; therefore they cannot be completely avoided. Nevertheless, their propagation and transmission to other parts of the vehicle, especially to the passengers and to the cargo, should be minimised. Regarding the effect of mechanical vibrations on the human body, the frequency plays an important role. The issue of comfort is related to the low-frequency range below 80 Hz, especially below 20 Hz. From the mechanical point of view, the human body is a vibration system, which has certain eigenfrequencies. Exciting the human body with these frequencies may result e.g. in nausea. This problem is of concern for the passengers and the operation personnel of the vehicle. High-frequent vibrations are related to noise, which is not only relevant for the passengers, but also for persons in the neighbourhood of the railway line. Therefore, vibration insulation has also an environmental aspect.
3. *Durability*: For a safe operation it must be guaranteed that the materials of which the vehicle and the track consist can take the loads occurring during operation without failing. Therefore, also the durability is relevant for safety. To fulfil this requirement, the components must be properly designed and dimensioned on the one hand. On the other hand, dynamic effects, which lead to high peaks of the loads, should be minimized.

4. *Wear behaviour*: In the contact between wheel and rail forces are transmitted and tangential relative motions occur. The contact area is very small; therefore, high local stresses occur. Furthermore, the tangential forces are transmitted by friction and are inevitably linked to slip; together, they cause wear of the running surfaces which cannot be completely avoided. Therefore, wheels and rails have to be maintained, i.e. they are reprofiled or replaced as soon as a certain limit regarding the deviation from the ideal shape is reached. As discussed in section 1.1, especially the maintenance of the railway track often causes strong restrictions of operation. Therefore it is evident that the intervals of maintenance have a strong impact on the economical efficiency of the entire railway system including the vehicle and the track. A non-uniform wear, i.e. an inhomogeneous distribution of the wear on the running surfaces, is especially disadvantageous: As mentioned before in section 1.1, the profiles of the wheel and the rail have a strong impact on the vehicle's running behaviour. If the wear is non-uniform in lateral direction, the shapes of the profiles are changed. This can cause changes of the running behaviour, mostly deterioration. The non-uniform distribution of wear in the circumferential direction of the wheel and in the longitudinal direction of the rail is known as corrugation. Corrugated running surfaces, either of the wheel, of the rail or of both, lead to high dynamic forces. Such forces can cause high stresses in the components of the vehicle and the track with negative impact on the durability, as mentioned in topic 3. Furthermore, high frequent dynamic forces can excite structural vibrations of the wheel and the rails and thereby cause noise.

Moreover, it has to be ensured that the running gear fulfils these requirements, especially those, which are relevant for the operational safety, under varying conditions. Some of these conditions are random within a certain range, while others are defined. Probably the best known example for a randomly varying operational condition is the friction in the wheel-rail contact. As mentioned in section 1.1, the friction is one principle for the transmission of the forces acting in the wheel-rail contact; it is obvious that the wheel-rail forces have a strong impact on the dynamic behaviour of the vehicle. The friction depends on the current state of the contact surfaces; it can be affected by environmental conditions like temperature or moisture. Regarding the railway, this is especially important since the track is located outdoors and thereby subjected to changing environmental conditions. An example for varying, but defined conditions is the operation of one and the same vehicle on two or more different railway networks. As described in section 1.1, it is a special characteristic of railways that they need a comparatively fine adaptation between the vehicle and the infrastructure compared to other transport systems like cars, ships and planes. Even if two railway networks use the same track gauge, the tracks can still differ in other geometric properties like e.g. the profile shape of the rail head or the inclination of the rails which can influence the contact geometry, i.e. the position of the contact on the running surfaces of wheel and rail. This again has an impact on the forces acting in the wheel-rail contact and thereby on the vibrations of the entire vehicle and on its running stability. This problem is one aspect of interoperability, i.e. the capacity of a railway vehicle to be operated on different networks which is especially important in the context of cross-border traffic in Europe: Due to historical reasons, many states of Europe or private companies developed their own networks which were initially insulated from each other; only later, connections between the networks were established. Thereby, the aforementioned parameters of the track geometry can vary from country to country or even within one country; in some cases, this may lead to undesired mechanical behaviour of a vehicle, when it is operated on a network for which it was not designed originally.

To make sure that the actual design of the running gear fulfils these requirements, the behaviour of the vehicle is simulated before the actual manufacturing of the vehicle or before operating it

under new, hitherto not encountered conditions: By using suitable mathematical-mechanical models which are realised on the base of computer software the motions of the vehicle's components and the loads acting on them are calculated. Thereby, dangerous states like derailment or overloading and subsequent damage and failure of a component can be recognized in time. But also within the safe range, i.e. below the safety limits, the vehicle or the vehicle-track system can be optimised to match criteria like low noise emission or good wear behaviour to minimise the maintenance effort. The mechanical properties and characteristics of the components, of which the vehicle-track system consists, as well as the operating conditions given by the trajectory of the track, the track geometry, friction etc. are described by parameters, i.e. numerical values, which can be comparatively easily modified. Thereby, the behaviour of different variants of the vehicle in different operational scenarios can be studied and investigated to find the version which meets the requirements best.

1.3 Motivation, aim and goal of this work

In order to specify the aim and the goal of this work, several various aspects regarding the modelling and the requirements to a railway, which are relevant for the modelling, will be considered and discussed first. Although some of the topics seem to be basically unrelated and although there may also be some interference and overlapping between other ones, they all are relevant for the motivation of this work; thus, they are all treated in this section.

The topics listed and discussed in section 1.2 show that the running gear, which is even a subsystem of the entire vehicle and of the entire system "railway", has to fulfil several different requirements. It has also been said already that the computer-based simulation of the mechanical behaviour enables an assessment and an optimization of a railway system and its subsystems and components at comparatively low efforts and costs and low risk. However, there is no "universal model" for a railway system. The choice of the modelling regarding the scope and the detailing depends on several factors. In this context, "scope" means, which components are taken into account, i.e. a single component like a wheelset, a subsystem like a bogie or an entire railway vehicle both consisting of several components or even a complete train including several vehicles; "detailing" means, how accurate the components included in the model are modelled, e.g. whether a component is considered as a rigid body or its structural dynamics is taken into account.

Generally, the modelling should follow the principle "as simple as possible, as complex as necessary", i.e. all components and all effects, which are relevant, shall be taken into account and everything, which is not relevant, should be neglected. However, distinguishing between what is relevant and what is not may sometimes be difficult so that this question can only be answered based on a comparison of the results obtained with different models; for instance, if the results obtained from a very detailed and from a simpler model hardly differ from each other, this strengthens the reliability of the simpler model. Of course, the choice of a suitable model requires a certain experience. This experience again depends on the technical system itself and on the issues and aspects to be investigated. If the system itself and its operating conditions are similar to existing examples and if it is investigated with respect to known aspects, then there is a high amount of experience. Conversely, if a system differs from its precursors e.g. by its structure, if it is operated under different conditions or if it is investigated with respect to a new, hitherto unknown aspect, then there is less experience so that a new assessment of the modelling itself may be necessary.

Regarding railway vehicles and their running gears, there are certain designs like bogies equipped with wheelsets, which have basically the same structure, although different types differ from each

other in specific design details. They also differ in the values of their mechanical parameters like the stiffness and damping of the suspensions, but the feasible range of these parameters is limited because of certain requirements⁴. Therefore and since these constructions have been used for a long time, there is a high amount of experience, so that their dynamic behaviour is basically known. Moreover, for a long time railway vehicles have to be assessed with respect to certain issues like running stability, safety against derailment or ride comfort. The survey paper by Bruni, Vinolas, Berg, Polach and Stichel [8] from 2011 gives a list of common analysis types; the frequency range, which is of interest in this context, is located between 0 Hz and 20 Hz. The paper states also that the modelling of railway vehicles as multibody systems has become a major design instrument in railway engineering. Already 15 years earlier in 1996, Vohla [77] stated in his thesis that simulating the running of a railway vehicle on a straight track and its quasi-static running in a curve can be considered as state of the art, while the simulation of the dynamic running in a curve is considered as nearly state of the art. Moreover, Vohla classified the running on a straight track and in a curve as “classical running dynamics” and low frequent dynamics, i.e. located in the frequency range below 20 Hz. Thereby, the multibody modelling of railway vehicles can be regarded as an established standard modelling method.

As already mentioned, the question of the necessary complexity may be rethought if a system is operated under different conditions or if it is investigated regarding new aspects. Probably the best known example for a change of the operational conditions is the increase of the running speed, as shown by the milestones listed in section 1. However, the size of the wheels used for high-speed trains is practically the same as for passenger coaches and freight cars used since the introduction of the railway; due to the height of the floor above the rail head, the wheel diameter for such railway vehicles is usually limited to about 1 m⁵; for locomotives, a larger diameter of about 1.2 m is usual, but also this value is rarely exceeded. As a result, the angular speed of the wheels has increased in nearly the same way as the running speed. Thereby, the influence of gyroscopic effects resulting from the overturning motion of the wheelset increases so that a suitable mechanical model for a high-speed railway vehicle should take this effect into account.

An example for a case, in which investigations with respect to a hitherto unknown problem became necessary, is given by Popp, Knothe and Pöpper in [54]: When high-speed trains were introduced in Germany at the beginning of the 1990s, problems like ballast deterioration and corrugation of both wheels and rails, which also lead to an increase of noise emission, occurred in an up-to-then unknown and unexpected degree. Against the background of the characteristics of the railway system and its requirements as described before, it is evident that this required an increased maintenance effort and worsened the cost-efficiency of the entire system. The phenomena of corrugation and ballast deterioration are located in the medium frequency range between 40 Hz and 400 Hz according to [54]. The work by Heiß [17] showed that the lowest structural eigenfrequencies for a trailer wheelset of a passenger coach occur at 76.0 Hz (first antimetric torsional eigenmode), 76.7 Hz (first symmetric bending eigenmode) and 148.4 Hz (first antimetric bending eigenmode), i.e. several eigenfrequencies associated with structural vibrations are lying in this frequency range. It is obvious that modelling the wheelset as a rigid body, as it is used in the “classical” running

⁴For instance, in order to achieve a good ride comfort the suspension of a railway vehicle for passenger traffic is designed in such a way that the eigenfrequencies associated to eigenmodes including large motions of the carbody lie below 2 Hz. The criteria for comfort are based on the mechanical properties of the human body. Since these properties haven't changed drastically in the past and since it is very unlikely that they will drastically change in the next decades, carbody eigenmodes below 2 Hz can be considered as a specific characteristics of a railway vehicle for passenger traffic.

⁵The TGV-V150 trainset, which set the current world speed record of 574.8 km/h, was equipped with larger wheels than the serial version of the train; they had a diameter of 1.092 m so that the limit of 1 m was only slightly exceeded.

dynamics, is not sufficient to describe the effects occurring in the medium frequency range.

In the context of the specific characteristics of the railway system described in section 1.1 it has been explained how tightly bound a railway vehicle is to its infrastructure. Furthermore, under the topic 4 listed in section 1.2 the problem of wear has been discussed; furthermore, the impact of the wear on the economy of the railway was considered. In this context it should be noted that the economic pressure on the railways has increased; in Europe it may be seen as an indicator for this that the formerly public railway companies⁶ have been converted into private enterprise companies taking part in economic competition. Therefore, the issue of wear is becoming more and more important for the railway so that an optimization of the wear behaviour in order to reduce maintenance costs is desirable. It has already been mentioned that there are different types of wear. As described in the previous paragraph, the investigation of corrugation at high-speed railways requires a modelling, which takes into account the structural dynamics of the wheelset. According to the survey paper by Bruni, Vinolas, Berg, Polach and Stichel [8], considering the frequency range between 0 Hz and 20 Hz is sufficient for wear issues; although not explicitly stated, the authors apparently refer to profile wear in this context. But although the modelling of the wheelsets as rigid bodies seems to be appropriate for this frequency range, the extension to describe the wheelsets and also the track as flexible structures may also be useful with respect to wear. Generally, wear only occurs where two bodies are actually in contact; therefore, an investigation of the wear behaviour requires a comparatively precise determination of the actual position of the contact area. For several combinations of wheel and rail profiles it is known that the contact geometry can be very sensitive to the relative kinematics, i.e. even a small change of the position of the wheel rim relative to the rail head can lead to a drastic change of the position of the contact area. It seems to be possible that structural deformations of the wheelset and the rail can also cause such changes of the relative kinematics, especially against the background to the high loads, to which these components are subjected. At least, an investigation of the impact, which structural deformations of wheelsets and rails have on the wheel-rail contact, seems to be sensible.

It is evident that the complexity of a computer-based mathematical-mechanical model is limited by the performance of the available computer hardware. In some cases it can therefore be necessary either to reduce the scope or the detailing of the model or both or to split the calculation into separate steps, in which models with different detailing and different scope are used. For instance, since considerable motions of the carbody mainly occur in the frequency range below 2 Hz, the scope of a model for an investigation of the behaviour in the medium frequency range between 40 Hz and 400 Hz may be reduced to one bogie. However, this strategy may contain a risk: One objective of the simulation is the optimization of the components and their design. Usually, a component is optimized with respect to one or several optimization criteria. If the model, which is used for the optimization, is focused on one or only few components, the optimization might be disadvantageous to the behaviour of the entire system. This is especially true for railways, since here a very strong interdependence between the vehicle and the track exists. Of course, a “universal model” of a railway system covering *all* aspects of analysis is not recommendable, but a modelling, which is suitable for different types of analysis, should make sense, even if not every single detail is absolutely necessary for each analysis. Also for the sake of consistency such a modelling covering not all, but several aspects seems reasonable. – An example for a calculation split into several steps is the investigation of wear: In the first step a multibody system of the vehicle-track system including a simpler model for the wheel-rail contact could be used to

⁶Even the names of some railway companies indicate their past as public companies, e.g. FS (Italy) = “Ferrovie dello Stato” = “railways of the state”, SJ (Sweden) = “Statens Järnvägar” = “railways of the state” or PKP (Poland) = “Polskie Koleje Państwowe” = “Polish state railways”.

determine the relative motions between the wheel rim and the rail head in the contact. For the multibody simulation only the resulting wheel-rail force is required so that local deviations of the stress distribution in the contact can be tolerated. In the second step, these relative motions could be applied to a detailed contact model to determine the wear occurring in the contact. As already mentioned, wear can only occur where the two bodies are actually in contact; thus a contact model for the investigation of wear should precisely determine the position and the shape of the contact area and the distribution of the stresses and relative tangential motions in this area. Since two different contact models can have slightly different characteristics, some adaptation of the data gained from the multibody simulation may be required, before it can be applied to the wear model. Therefore, a consistent modelling, where the wear or at least the stress distribution is calculated simultaneously to the motions of the vehicle-track system, should be preferable.

In the last decades the performance of computers has significantly increased so that considerable computational power is also affordable even for non-professional users and consumers. This enables also more complex calculations within an acceptable time. Although it is not a direct comparison, an example may illustrate this: In his thesis [77] Vohla estimated the required CPU time for simulating the dynamic behaviour of a single wheelset, whereby the two rolling contacts are described by the detailed program CONTACT; this program is based on an iterative solution of the discretized contact problem. Based on the technology of a RISC processor from 1990, the simulation of five seconds real time would require 100 years of CPU time. In the present work, calculation results will be presented, which were obtained with a model describing an entire passenger coach and using an iterative solution for all eight wheel-rail contacts. Depending on the configuration of the model, the simulation of one second real time took between two and sixteen hours using a PC for private consumers without parallelization of the code. Therefore, it may also be an interesting aspect to explore the possibilities of current computer performance regarding the scope and the detailing of models, which can be handled.

Based on these considerations the aim and the goal of the present work are formulated. The goal is to develop an enhanced and refined modelling of a railway vehicle running on a track. The wheel-rail contact is the connection between the railway vehicle and the infrastructure; here, the forces are transmitted and the wear occurs. The closest components to the contact are the wheelset and the rail. Therefore, in the new vehicle-track model the components “wheelset”, “rail” and “wheel-rail contact”, which are the key components for the vehicle-track interaction, are described by refined models. The wheelsets and the rails are modelled as flexible bodies. Thereby, the frequency range, for which the refined model is valid, is extended; furthermore, taking into account structural deformations of the wheelset and the rail provides a more precise description of the relative kinematics of wheel and rail in the contact. The model of the flexible wheelset also takes gyroscopic effects resulting from the overturning into account so that it is suitable for high running speeds as discussed before. To provide a basis for wear investigations, a very precise model for the wheel-rail contact, which enables the direct calculation of the contact stresses, is developed. By investigating two scenarios, i.e. the centred running and the permanent or “unstable” hunting⁷ both on an ideal track without imperfections, the influences of the structural flexibilities of both wheelsets and rails on the behaviour of the entire system and on the wheel-rail contact are investigated. For these investigations, different model versions are used, in which the wheelsets and the rails are either modelled as flexible or as rigid bodies; the comparison of the results obtained from the different model variants show the impact of the flexibilities. Furthermore,

⁷From the mathematical point of view, the expression “unstable hunting” is incorrect, since the amplitudes of the attractor for the permanent hunting are limited and not infinite. However, since the expression “unstable hunting” is widely used, it is also used here.

the calculations are carried out using different wheel-rail geometries and different values for the friction coefficient of the wheel-rail contact. Thereby, the impacts on the running behaviour of the structural flexibilities of wheelsets and rails on the one hand and of the varied parameters on the other hand can be compared. Moreover, this also helps to answer the question, whether structural flexibilities always have the same impact or whether this impact varies depending on other conditions.

1.4 Structure of the work

Chapter 2 contains an overview of the state of the art regarding the mechanical modelling of railway systems. Section 2.1 gives a brief general overview on different methods of mechanical modelling. Section 2.2 presents selected works regarding the modelling of a railway vehicle and discusses them with respect to their aim and the used modelling method. In section 2.3 different methods to model a railway track are presented and selected works covering the track modelling are presented. Section 2.4 deals with models for the wheel-rail contact.

The concept of cyclic structures is very useful for the modelling of the wheelsets as well as of the track. Therefore, in the chapter 3, this concept and some important properties of cyclic systems will be shown and discussed.

The modelling of the wheelsets and the rails as flexible bodies requires a structural dynamics model; the basis of the models used for these two bodies will be presented in the chapter 4. Like for many technical structures, the finite element method (FEM) is a suitable modelling method. Both the wheelset and the rail possess a particular geometry, which enables a description based on the concept of cyclic systems; this concept provides a drastic reduction of the computational effort without loss of accuracy.

The following three chapters 5, 6 and 7 deal with the refined models for the three key components “wheelset”, “track” and “wheel-rail contact” for the vehicle-track interaction.

In chapter 5 a mechanical description of the wheelset as a rotating flexible body is developed. This formulation combines the description of a flexible body with the concept of cyclic systems described in the section 3. Some basic characteristics of the resulting equations of motion are presented and discussed. Section 5.6 describes the finite element model of a wheelset based on the modelling developed in the chapter 4; from this model, the shape functions used to describe the structural deformations are obtained.

Chapter 6 presents a track model, which is developed based on the concept of cyclic systems. A special focus lies on the modelling of the rail, since this component is closely connected to the wheel-rail contact.

Chapter 7 deals with several aspects regarding the modelling of the wheel-rail contact. A method to connect the wheel-rail contact model to the flexible bodies representing the wheelset and the rail is developed in section 7.1. In section 7.2 the analysis of the contact geometry is presented. The section 7.3 treats the modelling of the contact mechanics, i.e. the basic formulation, the discretization and the solving algorithm for the discretized problem.

In the chapter 8 two scenarios are investigated using the refined modelling. In the section 8.1 the centred running on an undisturbed straight track is considered, while the section 8.2 deals with the permanent hunting motion. In this chapter different model versions are used, in which the structural flexibilities of the wheelsets and of the rails are either taken into account or neglected. By comparing the results obtained from the different model variants the influence of the structural

flexibilities can be analyzed. Furthermore, the calculations are carried out using different track geometries and different values of the friction coefficient.

Chapter 9 contains final conclusions and an outlook.

Chapter 2

Modelling of railways: State of the art

The modelling of a railway, i.e. the vehicle and the track, as a mechanical system includes several topics. Roughly spoken, the entire railway system can be split into three main subsystems, which are interacting with each other:

1. the vehicle
2. the wheel-rail contact
3. the track

A schematic overview on the structure of the railway system and its subsystems is given in Fig.2.0.1. The subsystems “vehicle” and “track” are connected by n wheel-rail contact elements.

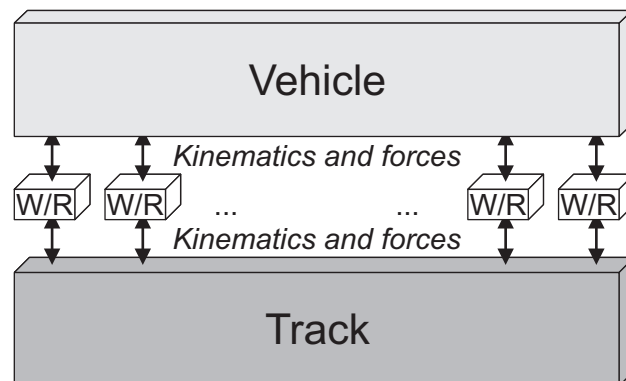


Figure 2.0.1: General structure of a railway system (W/R: wheel-rail contact)

Between the vehicle and the track on the one hand and the wheel-rail contacts on the other hand forces and kinematical quantities like displacements and velocities are exchanged.

There are several methods to model the subsystems “vehicle”, “wheel-rail contact” and “track”, which differ with respect to detailing, effort and validity. Although it might sound rather trivial, the choice of the entire model depends on the phenomenon, which shall be modelled. This question can be split into several aspects. The limits between the following topics are sometimes a bit blurred and there are also some interdependencies. However, some important aspects determining the choice of the model are:

- Scope of the model: Which components shall be modelled, e.g. an entire vehicle, a single running gear etc.?

- Focus of the model: What is of main interest, e.g. the vehicle or the track?
- Frequency range: Which frequencies can be expected to occur?

As it will turn out, the frequency range is an important aspect, not only for the modelling of the subsystems themselves, but also for the amount of the model. For instance, since at a common passenger coach eigenfrequencies including motions of the entire carbody are located below 10 Hz, the influence of the carbody motions can be neglected e.g. in an investigation concerning curve squealing, which is located in the range of several kHz.

A very general criterion is the distinction between planar and spatial vehicle-track models. In Fig.2.0.2 and Fig.2.0.3 a planar and a spatial vehicle-track model are displayed in principle. The

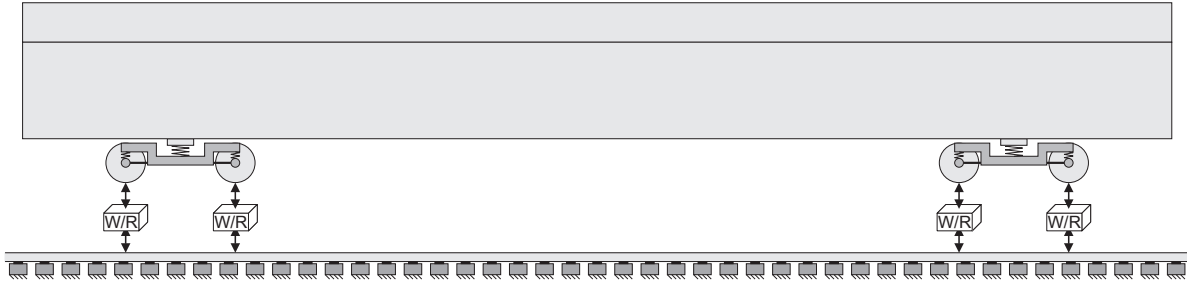


Figure 2.0.2: Planar vehicle-track model

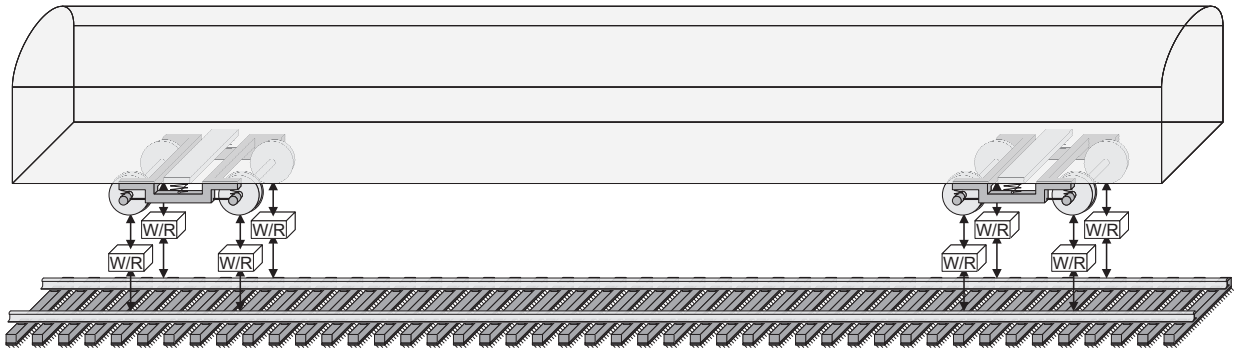


Figure 2.0.3: Spatial vehicle-track model

basic assumption for a planar model is that the complete vehicle-track system is strictly symmetric of with respect to the middle cross plain, i.e. the plain spanned by the longitudinal and the vertical axis. Therefore, only translational motions in vertical and longitudinal directions and pitch motions, i.e. rotational motions around the lateral axis, are possible. Due to this planar models are mainly used for investigations of the vertical dynamics. If also lateral, yaw and roll motions are taken into account, the symmetry with respect to the middle cross plain is lost. Thereby, for the modelling of lateral dynamics a spatial model is required.

Splitting the entire system “railway” into several subsystems suggests a modular structure of the model. If interfaces between the subsystems are defined, then the subsystems can be described by different models with different degrees of detailing and different modelling depth. This works in both ways: On the one hand, a detailed model can be simplified by replacing the models for the subsystems step-by-step by simpler models. The comparison of the results obtained with the different model variants helps to ensure the reliability of the modelling. On the other hand, a mechanical design, which has been obtained by a simple model, can be validated using a detailed model to make sure that no unwanted effects have been overlooked.

In the following sections an overview on different methods of mechanical modelling and on different models for the aforementioned subsystems “vehicle”, “track”, and “wheel-rail contact” will

be given.

2.1 Modelling methods

A very comprehensive overview on different modelling methods for technical systems and their applicability is given by Schiehlen and Eberhard in [64] and [63]; in [55] and [56], Popp and Schiehlen present a similar overview. Based on [64], [63], [55] and [56], the different modelling methods and their characteristics listed in Table 2.1.1. The main aspects of these modelling meth-

Mechanical model	Geometric shape	Stiffness distribution	Number of degrees of freedom
Multi-body system	complicated	inhomogeneous	finite (small)
Finite element system	complicated	homogeneous	finite (large)
Continuous system	simple	homogeneous	infinite

Table 2.1.1: Models of mechanical systems according to Schiehlen and Eberhard [64], [63] and Popp and Schiehlen [55], [56]

ods, especially with respect to the modelling of railways, will be presented in the following considerations.

2.1.1 Multibody models

The method of multibody modelling is nowadays a widely used method to simulate the mechanical behaviour of technical systems such as vehicles or robots. There are several books dealing with the fundamentals of multibody modelling such as e.g. the books by Roberson and Schwertassek [59], by Shabana [68] or by Schiehlen and Eberhard [64], [63]. Several simulation software systems, which are based on the multibody modelling, are commercially available. Many of these programs offer a graphical user interface, which makes the generation of the model comparatively easy. The equations of motion are generated automatically and solved numerically. The post-processing of many MBS models includes animation tools, which give an instructive impression of the system's motions, but also diagrams for certain physical quantities, e.g. displacements, forces etc., can be created. Altogether this underlines that this method is well established. In the following considerations the method of multibody modelling will be very briefly described; also some mathematical aspects are presented, since this will be an important topic for some modelling aspects.

A “classical” multibody system (MBS) consists of several rigid bodies, which have an inertia with respect to translational and rotational motions. The motions of the bodies are described by joints, which allow translations and rotations depending on the type of the joint. Thereby, the degrees of freedom (DOFs) of the system are defined. Between the bodies, force elements are acting, which are connected to the bodies at special points, the so-called markers. The force of the element depends on the relative motions, i.e. relative position and relative velocity, of the points, between which the element acts. The best-known force elements are springs and dampers, but also the rolling contact between wheel and rail can be modelled as a force element.

Schiehlen and Eberhard [64], [63] give the following equations of motion for a multibody system:

$$\mathbf{M}(\mathbf{y}, t) \ddot{\mathbf{y}}(t) + \mathbf{k}(\dot{\mathbf{y}}, \mathbf{y}, t) = \mathbf{q}(\dot{\mathbf{y}}, \mathbf{y}, t) \Rightarrow \mathbf{M}(\mathbf{y}, t) \ddot{\mathbf{y}}(t) + \mathbf{f}(\dot{\mathbf{y}}, \mathbf{y}, t) = \mathbf{0} \quad (2.1.1)$$

Here, the vector $\mathbf{y} = \mathbf{y}(t)$ contains the degrees of freedom of the multibody system. The matrix $\mathbf{M}(\mathbf{y}, t)$ is the mass matrix. The vectors $\mathbf{k}(\dot{\mathbf{y}}, \mathbf{y}, t)$ and $\mathbf{q}(\dot{\mathbf{y}}, \mathbf{y}, t)$ represent the Coriolis forces and the generalized external forces, respectively. From the mathematical point of view the equation of motion according to (2.1.1) is a system of nonlinear ordinary differential equations (ODE). Usually, the initial state described by the position $\mathbf{y}(t = t_0) = \mathbf{y}_0$ and the velocity $\dot{\mathbf{y}}(t = t_0) = \dot{\mathbf{y}}_0$ is given; then, the wanted solution of the equation of motion (2.1.1) is the time history of the system's motions described by $\mathbf{y}(t)$ and $\dot{\mathbf{y}}(t)$ for $t_0 \leq t \leq T_{end}$. Thus the mathematical problem to be solved is an initial value problem. The solution of this problem is usually obtained from a numerical integration; to this end the equation of motion can be reformulated using the state vector $\mathbf{z}(t)$ in order to obtain an system of ordinary differential equations of first order:

$$\mathbf{z}(t) = \begin{bmatrix} \mathbf{y}(t) \\ \dot{\mathbf{y}}(t) \end{bmatrix}, \underbrace{\begin{bmatrix} \dot{\mathbf{y}}(t) \\ \dot{\mathbf{y}}(t) \end{bmatrix}}_{\dot{\mathbf{z}}(t)} = \underbrace{\begin{bmatrix} \dot{\mathbf{y}}(t) \\ -\mathbf{M}(\mathbf{y}(t), t)^{-1} \mathbf{f}(\dot{\mathbf{y}}(t), \mathbf{y}(t), t) \end{bmatrix}}_{\mathbf{F}(\dot{\mathbf{y}}(t), \mathbf{y}(t), t) = \mathbf{F}(\mathbf{z}(t), t)} \Rightarrow \dot{\mathbf{z}}(t) = \mathbf{F}(\mathbf{z}(t), t), \mathbf{z}(t = t_0) = \mathbf{z}_0 \quad (2.1.2)$$

The determination of the wanted solution $\mathbf{z}(t)$ is called integration of the differential equation. Usually, the solution can only be determined numerically. There are a lot of numerical algorithms to solve this problem; an overview is given e.g. by Roos and Schwetlick in [60]. In this book [60], on which the following considerations are based, a scalar initial value problem of the following kind

$$u'(x) = f(x, u(x)), u(x_0) = u_0 \quad (2.1.3)$$

is discussed; according to [60] the results can, however, also be applied on a system of differential equations using vectors. The numerical solution for the interval $[x_0, b]$ provides the wanted solution $\mathbf{u}(x)$ at $N + 1 \in \mathbb{N}$ discrete points x_k :

$$x_k = x_0 + kh, h = \frac{b - x_0}{N}, k = 0, \dots, N \Rightarrow u_k = u(x_k) \quad (2.1.4)$$

The parameter N denotes the number of time steps; the parameter h is the stepsize. The methods for numerical integration can be classified with respect to several aspects. One of these classifications distinguishes between **explicit** and **implicit** methods. According to [60] a multistep integration method to solve the scalar initial value problem (2.1.3) has the following structure:

$$\frac{1}{h} (\alpha_k u_{i+k} + \alpha_{k-1} u_{i+k-1} + \dots + \alpha_0 u_i) = \beta_k f_{i+k} + \beta_{k-1} f_{i+k-1} + \dots + \beta_0 f_i, f_k = f(x_k, u_k) \quad (2.1.5)$$

The values u_j and $f_j = f(x_j, u_j)$ for $j = i, \dots, i+k-1$ are known and thereby available; the value u_{i+k} is the new value to be determined. For an **explicit** method it is valid $\beta_k = 0$; therefore the equation (2.1.5) can be resolved with respect to the new value u_{i+k} so that it can be determined from known values without any iteration:

$$u_{i+k} = \frac{1}{\alpha_k} [h (\beta_{k-1} f_{i+k-1} + \dots + \beta_0 f_i) - (\alpha_{k-1} u_{i+k-1} + \dots + \alpha_0 u_i)] \quad (2.1.6)$$

For $\beta_k \neq 0$ the method is **implicit**; in this case the equation contains the new value u_{i+k} and the function $f_{i+k} = f(u_{i+k}, x_{i+k})$:

$$\begin{aligned} u_{i+k} - \frac{\beta_k}{h \alpha_k} f_{i+k} &= u_{i+k} - \frac{\beta_k}{h \alpha_k} f(u_{i+k}, x_{i+k}) \\ &= \frac{1}{\alpha_k} [h (\beta_{k-1} f_{i+k-1} + \dots + \beta_0 f_i) - (\alpha_{k-1} u_{i+k-1} + \dots + \alpha_0 u_i)] \end{aligned} \quad (2.1.7)$$

Since the function $f(x, u)$ is usually nonlinear, the wanted solution u_{i+k} can only be obtained from solving a nonlinear equation. Usually, this requires an iteration, i.e. the function $f(x_{i+k}, u_{i+k})$ has to be evaluated several times. It is evident that thereby the computational effort for each time step is higher for an implicit integration method than for an explicit one. By transferring the implicit integration method on the initial value problem for the multibody model it is obtained:

$$\begin{aligned} t_k &= t_0 + kh, \quad h = \frac{T_{end} - t_0}{N}, \quad \mathbf{z}_k = \mathbf{z}(t_k), \quad \mathbf{F}_k = (\mathbf{z}_k, t_k) \\ \Rightarrow \mathbf{z}_{i+k} - \frac{\beta_k}{h\alpha_k} \mathbf{F}_{i+k} &= \mathbf{z}_{i+k} - \frac{\beta_k}{h\alpha_k} \mathbf{F}(\mathbf{z}_{i+k}, t_{i+k}) \\ &= \frac{1}{\alpha_k} [h(\beta_{k-1} \mathbf{F}_{i+k-1} + \dots + \beta_0 \mathbf{F}_i) - (\alpha_{k-1} \mathbf{z}_{i+k-1} + \dots + \alpha_0 \mathbf{z}_i)] \quad (2.1.8) \end{aligned}$$

In many cases the equations of motion for a multibody system require an implicit integration method. Therefore, the function $\mathbf{F}_{i+k} = \mathbf{F}(\mathbf{z}_{i+k}, t_{i+k})$ usually has to be evaluated several times for each part \mathbf{z}_{i+k} of the wanted solution. From this it follows that the function $\mathbf{F}(\mathbf{z}, t)$, which represents the mechanical modelling, should be numerically efficient to provide a low computational effort. As (2.1.2) shows the function $\mathbf{F}(\mathbf{z}, t)$ contains the function $\mathbf{f}(\dot{\mathbf{y}}, \mathbf{y}, t)$, which describes the generalized forces acting on the bodies. In some cases these forces cannot be determined by a simple explicit equation, but by an algorithm consisting of several steps. This is the case e.g. for several models describing the wheel-rail contact. Thus the aspect of numerical efficiency will be discussed later in the context of different models for the wheel-rail contact.

2.1.2 Finite element systems

The finite element method (FE method or FEM) is basically a discretization method for boundary value problems, see e.g. the book by Roos and Schwetlick [60]. It is used to determine an approximative solution of a differential equation for a certain region for given conditions at the boundaries of the region. The wanted solution is the function $\mathbf{f}(\mathbf{x})$ describing the distribution of the physical quantity \mathbf{f} across the region, in which the location is denoted by \mathbf{x} . This region can have a different number of dimensions, i.e. it can be a one-dimensional, two-dimensional or three-dimensional region, so that the coordinate \mathbf{x} can be a scalar variable or a two-dimensional or three-dimensional vector. The physical quantity \mathbf{f} , too, can be scalar or a vector. Generally, the FE method can be applied to several physical problems having different physical quantities, e.g. displacements due to deformation, the temperature or the intensity of electric and magnetic fields.

A short description of the basic idea for the FE method shall be given. The following consideration, which is quite rough, follows the book about finite elements by Schwarz [67], although the nomenclature is modified. The region, for which the solution $\mathbf{f}(\mathbf{x})$ shall be determined, is divided into several smaller regions E_k , which have a simple geometry; these regions describe the finite elements. Within one element, the distribution of \mathbf{f} is expressed by local shape functions $\mathbf{n}_i^{(k)}(\mathbf{x})$. The shape functions are scaled by the values $\mathbf{f}_i = \mathbf{f}(\mathbf{x}_i)$ at certain points P_i defined by \mathbf{x}_i ; these points are called “nodes”. The shape functions are defined in such a way that the function $\mathbf{n}_i^{(k)}$ has the value 1 at the point P_i and vanishes at all other points. This leads to:

$$\mathbf{f}(\mathbf{x}) = \sum_{i=1}^{N_k} \mathbf{n}_i^{(k)}(\mathbf{x}) \mathbf{f}_i, \quad \mathbf{n}_i^{(k)}(\mathbf{x}_j) = \begin{cases} 1 & \text{for } j = i \\ 0 & \text{for } j \neq i \end{cases}, \quad \mathbf{f}_i = \mathbf{f}(\mathbf{x}_i) \quad (2.1.9)$$

The number N_k denotes the number of the nodes of the element E_k . Here, the discretization becomes visible: The distribution $\mathbf{f}(\mathbf{x})$ within the element is expressed by the values \mathbf{f}_i at the nodes P_i ,

i.e. it depends on a finite number of variables. Within the element E_k , the shape functions $\mathbf{n}_i^{(k)}(\mathbf{x})$ are usually defined by simple functions like polynomials; outside the element, the shape functions vanish. The union of the elements E_k is the complete region, for which the wanted solution $\mathbf{f}(\mathbf{x})$ shall be determined. Based on the single elements, the complete solution is approximated in the following way:

$$\mathbf{f}(\mathbf{x}) = \sum_{i=1}^{N_N} \mathbf{N}_i(\mathbf{x}) \mathbf{f}_i, \quad \mathbf{N}_i(\mathbf{x}_j) = \begin{cases} 1 & \text{for } j = i \\ 0 & \text{for } j \neq i \end{cases}, \quad \mathbf{f}_i = \mathbf{f}(\mathbf{x}_i) \quad (2.1.10)$$

Here, the functions $\mathbf{N}_i(\mathbf{x})$ are the global shape functions; they are determined by all local shape function $\mathbf{n}_i^{(k)}$, which don't vanish at the point P_i .

By applying this method on a deformable mechanical structure a finite element system (FE system) is obtained. According to Schiehlen and Eberhard [64], [63] such an FE system consists of deformable elements possessing a mass and thereby an inertia; at the nodes discrete forces and torques are applied to the system. As a result,

The finite elements can be classified in various ways regarding mathematical mechanical aspects. Some of these aspects are:

1. Dimension and shape of the element:
 - (a) One-dimensional elements
 - (b) Two-dimensional elements: triangular shape or trapezoidal shape
 - (c) Three-dimensional elements: tetrahedron shape or hexahedron shape
2. Type of the shape function: Linear functions, quadratic functions, cubic functions
3. Type of the deformation:
 - (a) One-dimensional elements: bending, torsion, axial deformation
 - (b) Two-dimensional elements: plane element, plate element, shell element
 - (c) Three-dimensional elements: volume element

The aspects are not completely independent from each other. For instance, a beam element, which describes bending motions, usually requires cubic shape functions; linear shape functions are not sufficient.

The single finite elements have a simple geometry. However, from these elements also geometrically complex structures can be composed if a sufficient number of elements is used. But due to the comparatively simple spline functions also for simpler geometries a certain number of elements may be necessary to achieve the required accuracy of the solution. From the mathematical and numerical point of view, the FE system is usually described by a large system of coupled equations, i.e. a system of high order; the number of the equations depends on the number of the nodes and the type of the shape functions. Therefore, the system of equations can usually only be solved by a computer.

Since the FE method can be applied even to geometrically complex structures, it has become a widely used method in engineering; several commercial software systems based on this method are available. Usually these software systems include a graphical interface for the generation of the model and for the visualization of the results.

The application of the FE method to deformation mechanics covers several problems in mechanical engineering. Here, only two problems shall be briefly described. For the strength analysis the FE method is used to determine the stresses acting in the structure for given loads. The comparison of these stresses to the specific strength of the used material shows, whether the structure withstands the loads or whether a failure is to be expected. In the structural eigenfrequency analysis, the values of the eigenfrequencies and the mode shapes, to which the eigenfrequencies are associated, are determined. This analysis is important insofar as an excitation of a structure with its eigenfrequencies can cause large deformations, which again can lead to high stresses in the structure and even to its subsequent failure.

2.1.3 Flexible multibody systems

As described in section 2.1.1, a “classical” multibody system consists of rigid bodies connected by joints, i.e. the bodies can’t perform any deformations. In some cases, the modelling of a component as a rigid body can be insufficient. This can be the case if the forces acting on the body are so high that the deformations of the body can’t be neglected. Another possible case is that the forces acting on the body excite structural vibrations of the body; this occurs if the frequency of the forces approaches a structural eigenfrequency of the body.

There are several possibilities to deal with this problem. One possibility is to resolve the component into several rigid bodies, which are connected by flexible elements. An example in the context of railway vehicle dynamics is the work by Morys [46]; in this work, a wheelset is described by eight rigid bodies, which are connected by elastic elements. The advantage of this method is that it can be performed within the multibody formalism, i.e. no extension of the multibody formalism is necessary. The main effort of this modelling method is required for choosing a suitable partition of the entire body into single rigid bodies and determining and “tuning” the parameters for masses and stiffnesses in such a way that the combination of rigid bodies and elastic elements reproduces the structural dynamics for the relevant eigenmodes. As a main disadvantage, Morys himself mentions that several types of eigenmodes cannot be described using this method.

Another possibility is the extension to elastic multibody systems or flexible multibody systems, where deformations of certain bodies are admissible. There are several approaches; according to Schiehlen and Eberhard [64], [63] the floating frame of reference formulation (FFRF) can be applied if the deformations are small. In this formulation the motion of the flexible body is described by superposing the large nonlinear motion of the floating frame of reference and the small linearized deformations with respect to this frame. For the description of the structural dynamics an FE model of the body, as described in section 2.1.2, can be used. However, as mentioned in section 2.1.2, an FE model is usually described by a system of high order. Therefore, the original FE model is often reduced for this application. For instance, the deformation field of the flexible body can be described by a modal synthesis; here, shape functions, which are obtained from the FE model, are scaled by modal coordinates, which constitute the degrees of freedom for the deformations. As an example, the eigenmodes of the flexible body can be used as shape functions. For the shape functions, coefficients based on integrals have to be calculated.

2.2 Vehicle models

As described in section 1.2, a vehicle has to match several requirements and criteria, which are related to different phenomena. These phenomena are located in different frequency ranges and therefore require different types of models, which are suitable for their description. In this section, problems located in different frequency ranges and models for their description will be presented and discussed.

The physical behaviour of the wheelset on a straight track is closely related to the running stability of the vehicle and essential for the function, for the construction and for the mechanical design of the vehicle. Therefore, this behaviour will be discussed first, also with respect to different modelling depths and to the phenomena, which can be described by these models.

2.2.1 Characteristic behaviour of the wheelset

Railway vehicles are track-guided vehicles, i.e. they don't possess any steering devices, by which the driver can influence the course of the vehicle. The vehicle's course is determined by the track and the vehicle needs an automatic steering mechanism to follow the track and to compensate deviations. The essential element for the track guidance of a vehicle is the wheelset. In addition to the supporting function and to the propulsion and the braking the wheelset is also responsible for the guidance. The two characteristic features of a conventional wheelset are:

1. The wheels are coupled by a rigid axle. Thereby, both wheels have the same rotational speed.
2. The wheels have a non-cylindrical shape¹. Thereby, the current rolling radius of each wheel depends on the effective position of the wheelset relative to the track.

Up to today, several alternative concepts for the track guidance have been developed, e.g. constructions based on independently rotating wheels, which use mechatronic control in newer time. However, the vast majority of railway vehicles all over the world still uses conventional wheelsets.

A detailed description of the modelling of a railway vehicle's running behaviour is given by Knothe and Stichel in [35] and by Wickens in [80]. In these books, also the historical development of the modelling is described. Therefore, the following discussion is limited to the essential methods, concepts and features of different types of modelling. Furthermore, the performance of the different modelling types will be discussed, i.e. which modelling concepts are necessary for the description of several phenomena. An overview on the different modelling methods is given in Tab.2.2.2. This also underlines the motivation of this work and its classification.

The following considerations shall give a more detailed description of the modelling methods.

¹In a few cases, cylindrical wheels are used. An example is the underground railway in Berlin. However, wheelsets having cylindrical wheels don't show the hunting behaviour.

Modelling	Described phenomena
Kinematical rolling	<ul style="list-style-type: none"> • Periodical lateral and yaw motions (hunting motion) • Qualitative impact of running speed, conicity, rolling radius and track gauge
Linear dynamical equations of motion	<ul style="list-style-type: none"> • Existence of the critical speed (increasing and decreasing of the hunting motion) • Interaction with other components, e.g. bogie frame, track etc.
Nonlinear contact modelling	<ul style="list-style-type: none"> • Limit cycle behaviour, i.e. existence of limit cycles with defined amplitudes • Flange contact
Flexible wheelset	<ul style="list-style-type: none"> • Deformation of the wheelset under static and dynamical loads • Impact of the deformation on the contact and thereby on the running behaviour

Table 2.2.2: Modelling methods for the wheelset's running behaviour

Kinematical rolling: Klingel's equation

The first and probably best known modelling of the wheelset's running behaviour was published by Klingel in 1883 [32]. The basic assumptions for this modelling are:

1. The wheels have the shape of a truncated cone. The rails have a rectangular cross section.
2. The wheelset and the track are rigid.
3. Kinematical rolling is assumed, i.e. no relative velocities between wheel and rail occur in the contact point.

An overview on the model is given in Fig.2.2.4.

Here, $2a_0$, r_0 and δ_0 denote the track gauge, the nominal rolling radius and half the cone angle. Based on this, Klingel's equation can be derived:

$$y''(x) + \frac{\tan \delta_0}{a_0 r_0} y(x) = 0 \quad (2.2.11)$$

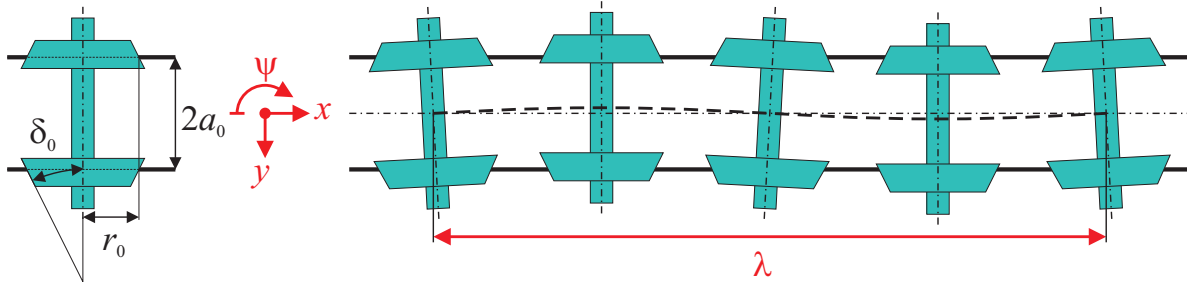


Figure 2.2.4: Hunting according to Klingel

The equation is solved by a periodic function. Thereby, the wavelength λ of the hunting motion is obtained²:

$$y(x) = \hat{y} \sin\left(\frac{2\pi}{\lambda}x + \phi\right) \Rightarrow \lambda = 2\pi \sqrt{\frac{a_0 r_0}{\tan \delta_0}} \quad (2.2.12)$$

Apparently, the hunting motion has a constant wavelength. It should be pointed out that this equation is obtained from purely kinematical considerations, i.e. concerning forces acting on the wheelset it is assumed that the forces are sufficient to generate this motion.

For a long time, Klingel's equation was used for the mechanical design of railway vehicles. It provided an estimation of the hunting frequency in a given range of the running speed. However, to describe the running behaviour of the wheelset at higher speed, Klingel's equation is not suitable. The limits of its validity can be demonstrated in a comparatively simple way: Let v_0 be a constant running speed so that there is a proportional relation $x = v_0 t$ between the covered distance x and the time t . After inserting this relation into the solution (2.2.12) of Klingel's equation the lateral acceleration of the wheelset is obtained by the second derivative with respect to time:

$$x = v_0 t \Rightarrow y(t) = \hat{y} \sin\left(\frac{2\pi}{\lambda}v_0 t + \phi\right) \Rightarrow \ddot{y}(t) = \underbrace{-\hat{y} \left(\frac{2\pi}{\lambda}\right)^2}_{\hat{y}} v_0^2 \sin\left(\frac{2\pi}{\lambda}v_0 t + \phi\right) \quad (2.2.13)$$

The amplitude \hat{y} of the lateral acceleration grows with the square of the running speed v_0^2 . Since an acceleration is caused by forces acting on a body, also the guiding forces accelerating the wheelset in lateral direction have to grow proportionally to v_0^2 to provide this motion. However, the guidance of the wheelset is mostly performed by frictional forces and – in a small amount – by normal forces acting in the contact. Both forces are limited by the weight of the wheelset in the case of a free wheelset or by the weight of the vehicle, if the wheelset is assumed to be mounted to a vehicle. Thereby, the guiding forces cannot be arbitrarily high and hence Klingel's equation cannot describe the running behaviour at high running speeds.

As already mentioned, the motion described by Klingel's equation is obtained from purely kinematical considerations. The only requirement is that the forces acting in the contact are high enough to enable the described motion; in other words: Forces can be determined as reaction forces for a given motion, but the equation is not derived from a formulation based on forces. Therefore, Klingel's equation cannot describe interactions between the wheelset and other components of the vehicle like the bogie frame: If a wheelset described by Klingel's equation is coupled to a vehicle by suspension elements like springs and dampers, then the motion of the wheelset acts

²According to [76] and [16], the expression “hunting” denotes a coupled lateral and yaw motion (or “nosing” as the rotation around the vertical axis is called in [76]) of the wheelset, i.e. it is a pure kinematical expression, which makes no statement on the stability of the motion, i.e. whether it increases or decreases.

as a given kinematical excitation for the vehicle and the other components have no influence on the wheelset's running behaviour. This also limits the applicability of Klingel's equation.

Nevertheless, Klingel's equation gives an estimation, which parameters have an influence on the running behaviour: A higher value for the half cone angle δ_0 leads to a shorter wavelength λ and thereby to a higher frequency f of the motion due to the relation $f = v_0/\lambda$. This relation also shows that the frequency of the hunting motion increases with the running speed v_0 , although in real life this increase is not linear, since the wavelength is not constant. Thereby, higher lateral contact forces between wheel and rail are to be expected for higher running speeds.

Linear equations of motions for the wheelset

To model the effects, which occur at higher running speeds and result from interactions with other components of the vehicle, the equations of motion for the wheelset are derived based on the laws by Newton and Euler. This requires also a description of the forces acting in the wheel-rail contact, especially the lateral and longitudinal forces, which are important for the lateral and the yaw motions, respectively. In his book [26] Kalker gives very detailed descriptions of different theories regarding the rolling contact. Generally, the tangential forces transmitted by friction depend on the creepages in the contact. The creepage is defined as the ratio of the relative velocity in the contact to the running speed v_0 . In reverse, this means that for the equations of motions relative motions in the contact are admissible in contrast to the kinematical rolling, where it was assumed that the relative velocities in the contact vanish. One theory described in [26] is Kalker's linear theory; a shorter description of this theory can be found in e.g. [3] or [55]. For small creepages v_i the relation between the tangential forces and the creepages is given by the following relations:

$$F_1 = - \underbrace{abGC_{11}}_{f_{11}} \underbrace{\frac{v_{1,rel}}{v_0}}_{v_1} \quad (2.2.14)$$

$$F_2 = - \underbrace{abGC_{22}}_{f_{22}} \underbrace{\frac{v_{2,rel}}{v_0}}_{v_2} - \underbrace{(ab)^{3/2}GC_{23}}_{f_{23}} \underbrace{\frac{\omega_{3,rel}}{v_0}}_{v_3} \quad (2.2.15)$$

$$M_3 = \underbrace{(ab)^{3/2}GC_{23}}_{f_{23}} \underbrace{\frac{v_{2,rel}}{v_0}}_{v_2} - \underbrace{(ab)^2GC_{33}}_{f_{33}} \underbrace{\frac{\omega_{3,rel}}{v_0}}_{v_3} \quad (2.2.16)$$

Here, F_1 , F_2 and M_3 denote the longitudinal tangential force, the lateral tangential force and the spin torque acting around the axis normal to the contact. Furthermore, $v_{1,rel}$, $v_{2,rel}$ and $\omega_{3,rel}$ represent the relative translational velocities in longitudinal and lateral direction and the relative angular velocity around the normal axis of the contact. As already mentioned, the creepages v_i are defined as the ratio of the relative velocity to the running speed v_0 . According to the Hertzian contact theory, on which Kalker's linear theory is based, the contact area of two elastic bodies is an ellipse having the semiaxes a and b . The material properties of wheel and rail are represented by the shear modulus G . The coefficients C_{ij} are the so-called Kalker coefficients, which depend on the ratio a/b of the semiaxes of the contact ellipse and on Poisson's ratio ν for the materials of wheel and rail. A more detailed discussion of Kalker's linear theory will be given in section 2.4.1. For a better overview, the products of the semiaxes a and b , the shear modulus G and the Kalker coefficients C_{ij} are represented by the coefficients f_{ij} for the following considerations.

Based on this theory, the linear dynamical equations of motions for the free wheelset can be derived, as given e.g. by Popp and Schiehlen in [55]:

$$\begin{aligned} \begin{bmatrix} m_w & 0 \\ 0 & J_{A,w} \end{bmatrix} \begin{bmatrix} \ddot{y}(t) \\ \ddot{\psi}(t) \end{bmatrix} + \left(\frac{2}{v_0} \begin{bmatrix} f_{22} & f_{23} \\ -f_{23} & a_0^2 f_{11} + f_{33} \end{bmatrix} + J_{P,w} \frac{\delta_0 v_0}{a_0 r_0} \begin{bmatrix} 0 & -1 \\ 1 & 0 \end{bmatrix} \right) \begin{bmatrix} \dot{y}(t) \\ \dot{\psi}(t) \end{bmatrix} \\ + \begin{bmatrix} m_w g \frac{\delta_0}{a_0} & -2f_{22} \\ 2f_{11} \frac{\delta_0 a_0}{r_0} & 2f_{23} \end{bmatrix} \begin{bmatrix} y(t) \\ \psi(t) \end{bmatrix} = \begin{bmatrix} 0 \\ 0 \end{bmatrix} \end{aligned} \quad (2.2.17)$$

Here, m_w , $J_{A,w}$ and $J_{P,w}$ denote the mass, the equatorial and the polar moment of inertia of the wheelset, respectively. The coefficient g is the acceleration due to the earth's gravitation. Furthermore, the conicity $\delta_0 \ll 1$ is assumed to be very small so that the approximations $\sin \delta_0 \approx \delta_0$, $\cos \delta_0 \approx 1$ and $\tan \delta_0 \approx \delta_0$ are admissible.

The structure of the equations of motion already shows several characteristics of the wheelset's dynamical running behaviour: The damping effect of the contact forces diminishes with increasing running speed v_0 . Furthermore, the matrix of the forces depending on the displacements is non-symmetric, which indicates circulatoric forces, i.e. non-conservative forces. The combination of both influences leads to the effect that the wheelset's lateral and yaw motions are asymptotically stable below a certain running speed, which is called *critical speed* $v_{0,crit}$. For $v_0 < v_{0,crit}$, the lateral and the yaw motions decay, so that the wheelset centres itself within the track. Above the critical speed, the wheelset shows unstable behaviour, i.e. an initial disturbance of the lateral and the yaw motion increases. The stability of the motion can be determined by inserting the usual solution for a linear differential equation based on the exponential function. Thereby, the system of linear equations can be reduced to an algebraic problem:

$$\mathbf{M}\ddot{\mathbf{y}}(t) + \mathbf{P}\dot{\mathbf{y}}(t) + \mathbf{Q}\mathbf{y}(t) = \mathbf{0}, \mathbf{y}(t) = \hat{\mathbf{y}}_i e^{\lambda_i t} \Rightarrow \left[\mathbf{M}\lambda_i^2 + \mathbf{P}\lambda_i + \mathbf{Q} \right] \hat{\mathbf{y}}_i = \mathbf{0} \quad (2.2.18)$$

The non-trivial solution is obtained by solving the eigenvalue problem:

$$\hat{\mathbf{y}}_i \neq \mathbf{0} \Rightarrow \det \left[\mathbf{M}\lambda_i^2 + \mathbf{P}\lambda_i + \mathbf{Q} \right] = 0 \quad (2.2.19)$$

At the critical speed, the maximum real part of all eigenvalues vanishes:

$$v_0 = v_{0,crit} \Rightarrow \max_i \Re \lambda_i = 0 \quad (2.2.20)$$

As already mentioned, the equations of motions are derived based on forces and torques acting on the wheelset. Thereby, the model of the wheelset can be extended to the model of a bogie or of a complete vehicle, where the interactions, i.e. the mutual influence of the bodies' motions on each other, are taken into account. Such models are presented in the thesis by Ihme [20] and in the book by Garg and Dukkipatti [14]. Based on such a model, the influences of mechanical parameters like the suspensions' stiffnesses and dampings on the running behaviour can be investigated. As a further extension of this modelling, track disturbances exciting oscillations of the vehicle can be taken into account. This also was presented by Ihme [20].

Nonlinear influences and effects

As shown in the previous section, the linear equations of motion show several considerable advantages compared Klingel's equation based on the purely kinematical consideration. However, as their name already says, the linear equations of motion don't take nonlinear effects into account. However, nonlinear effects can have a strong influence on the running behaviour of the vehicle. In his thesis [76] van Bommel lists two important nonlinear influences regarding the wheelset:

1. The geometry of the wheel-rail contact is nonlinear, i.e. the relation between the lateral displacement y and the difference of the rolling radii Δr of the right and the left wheel is nonlinear. Here the wheel flanges, which limit the lateral displacement of the wheelset, play an important role. In Fig.2.2.5 the difference of the rolling radii vs. the lateral displacement for the wear-optimized wheel profile S1002 combined with the rail profile UIC60 is shown; this profile combination is widely used in railway operation. In this figure, the strong increase of the rolling radii difference for high lateral displacements, which results from the flange contact, can clearly be seen. Fig.2.2.5 also shows that a nonlinear relation between the rolling radii and the lateral displacement can already occur for lateral displacements below the flange contact.
2. The traction characteristics, i.e. the relation between the creepages and the tangential forces, is nonlinear. The tangential forces are caused by friction and can thereby not exceed a limit $T_{max} = \mu N$ given by the current normal force N and the friction coefficient μ . For high creepages, the nonlinear characteristics has a considerable influence.

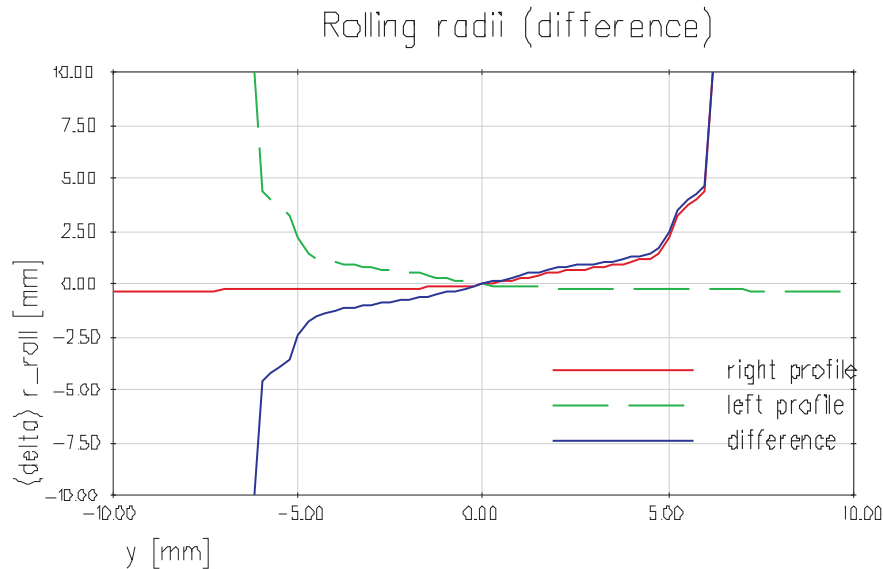


Figure 2.2.5: Function of the rolling radii difference depending on the lateral displacement. Wheel profile: S1002, rail profile: UIC 60, cant 1/40

As it has been shown in (2.2.18) and (2.2.19), the analysis and the mathematical treatment of a linear system is comparatively easy; the eigenvalues λ_i obtained from the analysis give a good characterization of the system's behaviour. In contrast to this, the analysis of a nonlinear system is far more difficult. A nonlinear system can be characterised by its attractors. An attractor is a state or a certain sequence of states, towards which the dynamical behaviour of the system evolves. There are several types of attractors: *Fixed points*, *limit cycles*, *limit tori* and *strange attractors*, see e.g. the book by Magnus, Popp, and Sextro [41] on oscillations.

In the case of the railway vehicle, the desired attractor is a fixed point attractor, which describes the centred position of the wheelset within the track. A fixed point attractor is characterised by a constant, time-invariant state \mathbf{y}_{fp} of the system. The stability of such an attractor can be investigated by linearisation based on a Taylor expansion. A nonlinear function $f(x)$ can be approximated in the range around the reference point x_0 by the following linear function $f_{lin}(x)$ using the first

derivative $f'(x_0)$ of the original function at the reference point as the gradient:

$$f_{lin}(x) = f(x_0) + f'(x_0)(x - x_0), \quad f'(x) = \frac{df(x)}{dx} \quad (2.2.21)$$

Linearising the function of the rolling radii difference around the wheelset's centred position, i.e. for $y_0 = 0$ and $\psi_0 = 0$, gives a linearised conicity $\tan \delta_0$. From the linearisation of the traction characteristics for very small creepages, the coefficients f_{11} , f_{22} , f_{23} and f_{33} are obtained, which have already been introduced in the equations (2.2.14), (2.2.15) and (2.2.16). These coefficients and the linearised conicity $\tan \delta_0 \approx \delta_0$ can be inserted in to the equations of motion (2.2.17). By varying the running speed v_0 the value can be found, at which an eigenvalue having a non-negative real part occurs, see (2.2.20). This value will be called *linear critical speed* $v_{crit,lin}$. Below this running speed, the centred position is stable, i.e. after a disturbance the wheelset tries to reach this attractor again. Above this critical speed, the amplitudes of the wheelset's motion grows and exceeds all limits, according to the solution of given by the exponential function with a positive real part $\Re \lambda_i$, as described in (2.2.18).

In real life, the lateral motion of the wheelset is limited by its flanges. Therefore, a limit cycle attractor can occur for a wheelset. A limit cycle is a periodic oscillation of the system with a defined amplitude. Although the lateral motion of the wheelset doesn't exceed all limits, the limit cycle oscillation can be dangerous: For the flange contact, very high forces can occur, which can cause considerable damage of the track.

In total, the dynamical behaviour of the wheelset under consideration of the nonlinear contact geometry and the nonlinear traction characteristics can be described by the diagram shown in Fig.2.2.6. Here, the attractors are displayed as the relation between the maximum lateral displacement \hat{y} and the running speed v_0 .

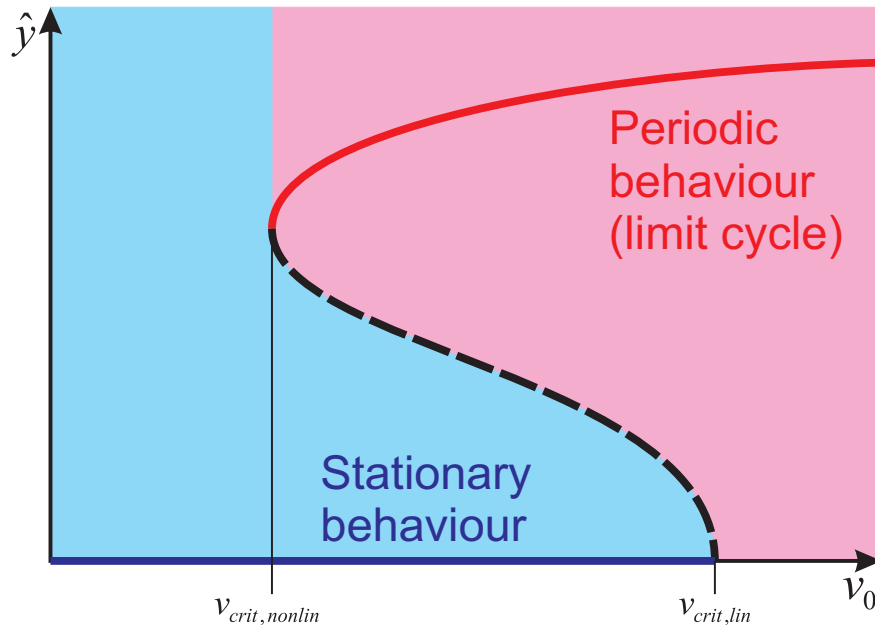


Figure 2.2.6: Generic scheme of the wheelset's attractors

The attractors only exist for certain ranges of the running speed: The centred position only is a stable attractor for $v_0 < v_{crit,lin}$ and the limit cycle only exists for $v_0 > v_{crit,nonlin}$. Each attractor possesses a certain basin of attraction: If the initial condition of the system lies within the basin of attraction of a certain attractor, then the motions of the system will approach this attractor, if now other external disturbances are applied. If the running speed lies below both critical speeds,

i.e. $v_0 < v_{crit,lin} \wedge v_0 < v_{crit,nonlin}$, then only one attractor, namely the centred position, exists so that the wheelset will centre itself within the track for every initial condition. If the running speed is higher than both critical speeds, i.e. $v_0 > v_{crit,lin} \wedge v_0 > v_{crit,nonlin}$, then a limit cycle oscillation will occur for each initial condition. In many cases, the nonlinear critical speed is lower than the linear critical speed, i.e. $v_{0,crit,nonlin} < v_{0,crit,lin}$: The lowest speed, at which a permanent hunting can occur, is lower than the speed, at which the centred position becomes unstable. In the range of $v_{crit,nonlin} < v_0 < v_{crit,lin}$ both attractor coexist. It depends on the initial conditions of the system, which attractor the system tries to reach. Since on the one hand the limit cycle motion can cause damages to the track and can therefore be dangerous and since on the other hand the nonlinear critical speed $v_{crit,nonlin}$, at which the limit cycle motion starts, is lower than the linear critical speed $v_{crit,lin}$, the knowledge of $v_{crit,nonlin}$ is important for the mechanical design of the vehicle. However, the determination of this nonlinear critical speed requires suitable methods for analysing the nonlinear dynamics of the vehicle. Such methods will be presented and discussed in the following considerations.

It should be pointed out explicitly that Fig.2.2.6 gives only a qualitative description of the wheelset's dynamical behaviour. A complete vehicle possesses several wheelsets, which can also be arranged in bogies. The wheelsets, the bogie frames and the carbody are coupled by elements, which can also have nonlinear characteristics. Examples are rubber springs, bumpstops for limiting motions or dry friction elements as used for the yaw damping in the bogies of the types MD 522 or SGP 300. The latter problem of a moment caused by dry friction, which can also occur in the pivot connecting the car body and the bogie, has also been investigated by van Bommel in his work [76]. Due to the coupling elements acting between the wheelsets and the bogie frame and between the bogie frames and the car body very complex dynamical interactions can occur. Thereby, the permanent hunting motion may not appear as a limit cycle, i.e. a strictly periodic motion, but as a limit torus, i.e. a quasi-periodic motion. Such a quasi-periodic motion consists of several harmonic functions, whereas the quotient of at least two frequencies is not rational.

The nonlinear effects occurring at a railway vehicle have a strong impact on the running behaviour and thereby are relevant for the mechanical design of the vehicle. Hence, there are several ways to treat these nonlinear effects:

1. Since the analysis of linear systems is comparatively easy to handle and gives a quick and descriptive insight into the systems behaviour, one possibility is to approximate the nonlinear system by a linear one. The "strict linearisation" in the sense of approximating the nonlinear function $f(x)$ by the first terms of a Taylor expansion according to (2.2.21) is only valid for small motions around the centred position. Therefore, for larger displacements the quasi-linearisation can be applied; this method is also known as the Krylov-Bogoliubov method, see e.g. [41]³. Here, x is assumed to be a harmonic function with the amplitude \hat{x} . Thereby, the linearisation of the function $f(x)$ is performed by:

$$k = \frac{1}{\pi \hat{x}} \int_0^{2\pi} f(\hat{x} \cos \phi) \cos \phi d\phi \Rightarrow f(x) \approx kx \quad (2.2.22)$$

Here, the coefficient k depends on the amplitude \hat{x} , which has to be chosen. Applying this method to the difference of the rolling radii depending on the lateral displacement of the wheelset leads to the well-known equivalent conicity. The advantage of this method is that it works very fast and is thereby well suited for parameter studies, e.g. for parameters of the primary or secondary suspension as shown by Diepen in [11]. Its disadvantage is that it uses a very rough approximation of the actual motion.

³In [41] the German transliteration "Bogoljubov" is used.

2. The numerical integration is the most universal method to analyse the behaviour of a nonlinear system. If the vehicle is modelled as a multibody system as described in section 2.1.1, its dynamics can be formulated as an initial value problem, i.e. a system of differential equations described in the state space and a given initial value:

$$\dot{\mathbf{z}}(t) = \mathbf{F}(\mathbf{z}(t), t), \mathbf{z}(t = t_0) = \mathbf{z}_0 \quad (2.2.23)$$

The application of this method only requires that the solution exists. Therefore, its advantage is its universal applicability. The disadvantage is that in some cases a very high computational effort is necessary: To find an attractor, e.g. a limit cycle or a limit torus, an integration over a very long simulation interval may be required to make sure that all transient motions have died out. Furthermore, the differential equations describing the motion of a railway vehicle can be very stiff; there are several books like e.g. [60] dealing with the problem of stiff differential equations. The numerical integration of such stiff differential equations requires an implicit integration method, which usually leads to a higher computational effort than an explicit method, as discussed in section 2.1.1.

3. The main problem to determine the attractor of a nonlinear system is that transient motions have to die out completely. In some cases this can require a long time and thereby a high computational effort. Since the attractor of permanent hunting is often a limit cycle, it is obvious to exploit the strict periodicity of the limit cycle $\mathbf{z}(t) = \mathbf{z}(t + T)$, i.e. after one period of the duration T the same state described by the state vector $\mathbf{z}(t)$ occurs. Moelle [45] used a Galerkin method, whereas the state vector is described by a Fourier series. Thereby, a numerical integration of the system's equations is avoided in this method. Kaas-Petersen [22] applied the method of path-following on the hunting of a railway vehicle. This approach has been successfully applied by Schupp [66] to more complex systems. Also its applicability was extended by Schupp from systems of ordinary differential equations (ODE) to systems of differential-algebraic equations (DAE). The limit cycle is obtained by a direct calculation: A residual function $\mathbf{R} = \mathbf{z}(\mathbf{z}_0, T) - \mathbf{z}_0$, which depends on the initial state \mathbf{z}_0 and the duration T of the period, is minimised. The state $\mathbf{z}(\mathbf{z}_0, T)$ is obtained by solving the initial value problem (2.2.23). The advantage of such methods is that they calculate the limit cycle attractor directly and thereby avoid long numerical integrations, which may be necessary for a pure numerical integration. The disadvantage is that the applicability of such methods is limited to limit cycle attractors, since these methods exploit the periodicity of such an attractor.

2.2.2 Low frequency range

In the low frequency range mostly problems of running dynamics are located. In a recent paper by Bruni, Vinolas, Berg, Polach, and Stichel [8] a list of analysis types is given; this list includes issues like carbody sway in curves, safety against derailment, track shift forces, stability, ride comfort, wear and gauging. It is explicitly stated that for some issues like carbody sway, gauging, wear and ride comfort the frequency range between 0 Hz and 20 Hz is of main interest.

Generally, a railway vehicle possesses at least one carbody, which contains the payload or the passengers or in the case of a locomotive the propulsion plant, and several wheelsets. If the vehicle uses bogies running gears, the vehicle also possesses bogie frames. The carbody, the wheelsets, and the bogie frames are connected by flexible elements forming the primary suspension acting between the wheelset and the bogie frame and the secondary suspension acting between the bogie frame and the carbody. With respect to Tab. 2.1.1 the railway vehicle has a complex geometry.

Furthermore, the flexible elements of the primary and secondary suspensions are usually distinctly softer than the comparatively stiff wheelsets, bogie frames, and carbody. Therefore it is obvious to model a railway vehicle as a multibody system.

In this frequency range, the entire vehicle is considered and modelled as a multi-body system. Usually, the main components like the carbody, the bogie frame and the wheelset are modelled as rigid bodies. The bodies are connected by force elements representing the springs and dampers of the primary and the secondary suspension. In some cases this modelling is enhanced, e.g. by modelling motor units or wheelset bearings as separate bodies or by splitting the carbody, the bogie frame or the wheelset into several separate bodies to approximate the structural dynamics. The survey by Bruni, Vinolas, Berg, Polach, and Stichel [8] gives an overview on modelling of the suspension components and track in multibody models of railway vehicles, since the modelling of these components is highly important for the accuracy of the model.

In his thesis van Bommel [76] investigates the hunting motion of a two-axled vehicle; it is explicitly mentioned that this can also represent a bogie. The system consists of three bodies representing the two wheelsets and the carbody, which are connected by linear springs and dampers; thus the mechanical model is a multibody system even if van Bommel didn't use this expression⁴. This work is one of the earliest, in which the influence of the nonlinearities resulting from the wheel-rail contact geometry and from the friction characteristics, as discussed in section 2.2.1, are taken into account.

The HSB study [18] is a study about several problems related to railway operations at higher speed; it had been ordered by the German Federal Ministry of Transport. In Appendix 7 of the HSB study several different mechanical models are presented to investigate the running behaviour at higher speeds. For the vertical dynamics a quite simple model is used; here, the vehicle model consists of just two rigid bodies describing the wheelset and a part of the carbody. The model is excited by sinusoidal rail irregularities. Furthermore, a more complex vehicle-track model is presented. The vehicle model describes an entire passenger coach equipped with two two-axle bogies. The model consists of seven rigid bodies, which represent the carbody, the two bogie frames, and the four wheelsets. The wheel-rail contact geometry is nonlinear so that the influence of the flange is taken into account. With this model the stability of the running behaviour is investigated. In the simulated scenario the vehicle is excited by a lateral wind gust; thereby hunting of the vehicle is initiated. The diagrams show a hunting frequency of approx. 2.75 Hz at a running speed of 270 km/h, which is clearly located in the low frequency range.

Sauvage [61] gives an overview on the influence of several parameters on the running behaviour at high speeds. The critical speed is determined depending on the equivalent conicity, the longitudinal and lateral stiffnesses of the primary suspension etc.

Diepen [11] investigated the running behaviour of a passenger coach used for intercity traffic. The bogie frames and the wheelsets are modelled as rigid bodies. The carbody is represented by two rigid bodies, which are connected by a spherical joint and rotational springs. Thereby, the lowest bending and torsional eigenmodes of the carbody are approximated. This is an example for the approximation of a flexible structure by connected rigid bodies within the multi-body formalism. Based on this model, Diepen analyzes the influence of several parameters like stiffnesses of the primary and the secondary suspension on the riding comfort.

Kratochwille [36] investigated the influence of switchable yaw dampers on the running behaviour

⁴According to Schiehlen and Eberhard [64], [63] the interest in multibody systems didn't increase until after 1965, when a need for this arose from space technology; since then also computer-based formalisms are developed. The thesis by van Bommel [76] appeared in 1964, i.e. before this time.

of a passenger coach. On the one hand, stiff yaw dampers have a stabilizing effect on the running behaviour and thereby enable higher running speeds. On the other hand, on curved lines stiff yaw dampers are disadvantageous, since the moment against relative yaw motions, which is caused by the dampers, leads to higher lateral forces and thereby to increased wear. The multi-body model describes a trailer coach of the German ICE train equipped with prototype bogies. The model includes seven rigid bodies representing the carbody, the two bogie frames and the four wheelsets. Using this model, the running through different curves with varying radius for different characteristics of the yaw damper is simulated. A special focus lies on the resulting lateral force ΣY between the wheelset and the track, since this is relevant for the operational safety and the homologation of the vehicle.

In the works of Zhai, Wang and Cai [83] and by Xiao, Jin, Wen, Zhu and Zhang [82] a passenger coach is modelled by a multi-body system, which includes seven rigid bodies to describe the carbody, the two bogie frames and the four wheelsets. Zhai, Wang and Cai [83] investigate two scenarios of passing a curve, i.e. a tight curve at low running speeds and a curve having a large radius at high speeds. The evaluation focuses on the vertical and lateral wheel-rail forces. Xiao, Jin, Wen, Zhu and Zhang [82] analyse the scenario of passing a track buckle having different shapes with respect to the risk of derailment. It can be concluded that in both cases the low-frequent running dynamics is considered.

The work of Polach and Kaiser [53] is focused on the nonlinear analysis of the running stability with special respect to the applicability of the path-following method. The model represents a double-deck passenger coach. The model is developed in a commercially available multi-body simulation software environment. The carbody consists of two bodies, which are connected by a revolute joint and a rotational spring to approximate torsional deformations. In a similar way, the bogie frames are modelled by two bodies so that twisting deformations of the frames are taken into account. The running behaviour is investigated for different wheel-rail profile combinations and different characteristics of the yaw dampers.

Multi-body models consisting of rigid bodies are also used to determine loads, which are acting on certain components. The works of Flach [13] and Stichel [70] are focused on the durability of the bogie frame. In both works, a passenger coach of the ICE train of the first generation is modelled as a multi-body system using rigid bodies. By simulating different scenarios using the multi-body model the forces acting on the bogie frame are determined. They are put as loads on a finite element model of the frame to analyze stresses and fatigue. Thus, the finite element analysis is used as a postprocessing, i.e. structural deformations of the bogie frame are not taken into account in the simulation of the dynamics.

Wear problems concerning the profiles of wheel and rail are also phenomena, which are located in the low-frequency range. Due to the sliding friction, which occurs the wheel-rail contact, wear occurs. With ongoing wear the shapes of the profiles are changing. The changed geometry of the profiles leads to changes of the running behaviour. Therefore, the evolution of the wear is usually simulated by an interplay between the running dynamics and the wear behaviour. The modelling of the wear requires a more realistic determination of the actual location of the wheel-rail contact and of the stresses occurring in the contact.

Kim [30] investigated the running of a passenger coach on the Gotthard line in Switzerland, which is characterized by many curves. The model of the passenger coach is a multi-body model, where rigid bodies represent the carbody and the bogie frames. The wheelset is composed of several rigid bodies connected by rotational springs: The axle is split into two bodies for an approximation of torsional motions. The bending deformation of the wheelset is approximated by modelling the

wheels as separate rigid bodies, which are connected to the axle by spherical joints. This modelling can be seen as an example for a lumped-mass modelling of a flexible structure. Compared to the modelling of the wheelset as one rigid body, a more realistic determination of the actual contact geometry is provided.

Weidemann [79] investigates the running dynamics and the wear behaviour for monobloc wheels and resilient wheels. At resilient wheels, the wheel disc including the hub on the one hand and the wheel rim on the other hand are separate parts; between the wheel discs and the wheel rim a rubber layer is placed. The model by Weidemann is a multi-body model consisting of rigid bodies. It describes a passenger coach with two bogies and four wheelsets. Therefore, the wheelset having resilient wheels consists of the “basic wheelset”, which includes the axle, the two brake discs and the two wheel discs, and of two wheel rims. The wheel rims can perform translations around the symmetry axis of the wheelset and all three relative rotations. The rubber elements are modelled by force elements.

Schelle [62] investigated the wear occurring at the wheels of freight locomotives, which run on a curvy line in the Harz mountains in Germany. The locomotive is modelled as a multi-body system consisting of rigid bodies, which represent the carbody, the bogie frames, the wheelsets, but also the traction motor units, the wheelset bearings and the traction rods. Realistic operation scenarios of the locomotive are simulated using a detailed representation of the topology of the track. The wear is calculated by evaluating the stresses in the wheel-rail contact. Based on the wear, changes of the profiles of wheel and rail are calculated. The evolution of the profiles is a result of the interplay between the dynamical behaviour, which causes wear in the contact and thereby slowly changes the shapes of the profiles, and the evolution of the profiles, which have an impact on the running behaviour.

In the work by Kaiser and Popp [23] also the limit cycle behaviour of a passenger coach is investigated; here, the wheelsets are modelled as flexible bodies. The results show a destabilizing effect of the wheelsets’ structural flexibility, i.e. the permanent hunting starts at lower running speeds and the lateral amplitudes of the wheelsets increase. In [24] this investigation was continued using a refined finite element model for the wheelset and a detailed model of the track; in the track model, the rails are modelled as flexible bodies and the periodic support by discrete sleepers is taken into account. The results confirmed the destabilizing effect of the structural flexibilities of the wheelsets and also showed a destabilizing effect of the track flexibility.

2.2.3 High frequency range

Phenomena located in the high frequency range are usually related to structural vibrations of components. Due to structural vibrations and motions of the surface sound can be radiated, which is heard as noise. In the context of vehicle dynamics, investigations of the high frequency behaviour are mainly focused on the wheelsets. High-frequent structural vibrations of the wheelsets are mainly caused by two different excitation mechanisms resulting in two different types of noise. The rolling noise is caused by irregularities of the running surfaces of wheels and rails, e.g. due to corrugation. These irregularities cause dynamic fluctuations of the normal forces in the contact leading to structural vibrations of the wheelsets. The other mechanism is the squealing noise, which can occur during the passing of a curve. In this case the structural vibrations are excited by tangential forces acting in the wheel-rail contact; the squealing noise is usually related to high lateral creepages in the contact. Therefore, it mainly occurs for high angles of attack between the wheel and the rail, e.g. in tight curves.

It is obvious that the description of phenomena, which are strongly related to structural vibrations of the wheelset, requires a comparatively detailed modelling of the wheelsets. Here, the finite element method is mainly used, since it has nearly no restrictions with respect to the geometry of the structure. There are several commercially available software systems based on the finite element method.

In his work [17] Heiß develops a finite element model of a trailing wheelset to analyze the acoustic behaviour. This model consists of brick elements, i.e. three-dimensional elements with the shape of a hexahedron. By exploiting symmetry properties of the structure, the model is reduced to one eighth of the original structure; the eigenmodes having different symmetry properties are obtained by applying suitable boundary conditions to the reduced model. Heiß gives an overview of the eigenmodes and classifies them with respect to their symmetry properties and other characteristics like e.g. node lines. Since this provides a basic understanding of the structural dynamics not only of a wheelset, but generally of a rotational symmetric structure, a comprehensive discussion of the results can be found in the book by Gasch, Knothe, and Liebich [15].

The problem of curve squealing has been investigated in many works so that only a small selection of such works is given here. Works dealing with this phenomenon have been given published by Schneider [65], Fingberg [12], Périard [50], and Ben Othman [6]. In all these works, the wheelset has been modelled by finite elements.

Fingberg [12] used a self-developed finite element model for the wheelset. By exploiting the symmetry of the wheelset with respect to the middle cross plain the wheelset is reduced to one half; the eigenmodes with different symmetry properties are obtained by applying different boundary conditions to the node in the middle cross plain. The wheel is modelled by annular shell elements exploiting the rotational symmetry of the wheel.

Périard [50] used a commercially available software package to model a wheelset; the whole model consists of three-dimensional brick elements.

Ben Othman [6] developed a finite element model of a wheelset using commercially available software tools. In his model the wheels consisting of the wheel disc, the wheel rim, and a rubber layer between the disc and the rim is modelled by volume elements, i.e. three-dimensional elements, while beam elements are used for the axle.

In models for the investigation of the curve squealing the dynamical behaviour of the other components like the carbody and the bogie frame are less important. In his work [6] Ben Othman states that for the squealing noise the influence of other components besides the wheel can be neglected without loss of accuracy. In the works by Schneider [65] and Fingberg [12] only one wheelset is considered. A quasi-static curve running is assumed, so that the position of the wheelset within the track is constant with respect to the lateral displacement and to the yaw angle. In contrast to this Périard [50] considers the curve squealing of a tram as a transient process; thus a multibody model of the tram is used to determine the position of the wheelset within the track.

2.2.4 Medium-frequency range

The medium-frequency range can be characterised by a combination of several characteristics of the low-frequency range as well as of the high-frequency range. On the one hand, the frequency is low enough that interactions between the different bodies, e.g. between the wheelset and the bogie frame, have to be taken into account. On the other hand, the frequency is high enough that effects of structural dynamics have an influence. For instance, the lowest structural eigenfrequencies of a trailer wheelset used for passenger coaches are located at approx. 80 Hz, where the

first antisymmetric torsional eigenmode and the first symmetric bending eigenmode occur. Therefore, Popp, Knothe and Pöpper [54] defined the range between approx. 40 Hz and 400 Hz as the medium-frequency range. Due to the combination of the interaction of several bodies on the one hand and the consideration of structural dynamics on the other hand, models for the medium frequency range possess a rather high number of degrees of freedom.

An important phenomenon, which is located in the medium frequency range, is the corrugation. This denotes an irregular distribution of wear over the circumference of the wheel or over the length of the rail. In the case of the wheel, periodic deviations of the running surface from the ideal rotational symmetric shape are also known as “polygonalization”. Since the wheel and the rail consist of steel, they are very stiff. Therefore, high dynamic normal forces occur during running even for small deviations of the running surfaces from the “ideal”, i.e. a rotational symmetric shape in the case of the wheel and a prismatic shape in the case of the rail. Such high dynamic forces cause high loads for the wheel and the rail, which increase the material damage and can lead to fatigue and thereby to failure. Furthermore, dynamic forces excite structural vibrations of the wheel and the rail, which can cause noise.

The “grumbling noise” of the German ICE trains of the first generation is a phenomenon located in the medium frequency range. This noise was related to an irregular wear of the wheels with respect to the circumference. This type of wear is known as polygonalization in the case of the wheels or as corrugation. The term “corrugation” also denotes an irregular distribution of wear over the length of the rails.

Morys [46] developed a model for the investigation of the polygonalization of the ICE wheels. The model includes a bogie with two wheelsets, a carbody and a flexible track. The carbody is connected to the bogie by the one pivot. At its other pivot a longitudinal motion along the track is applied. Each wheelset consists of 8 rigid bodies representing the two wheels and the four brake discs including the corresponding parts of the axle and the journals. The rigid bodies are connected by spherical joints and rotational springs. By comparing the eigenfrequencies of the wheelset model with those obtained from a finite element model and by measurements, the springs are tuned. While the lowest eigenmodes are represented very well, differences occur for eigenmodes, which include deformations of the wheel disc. The advantage of the wheelset model is that it is developed completely within a commercially available multibody system simulation environment, i.e. no extension of the multibody system formalism is required. Since the wheels are modelled as rigid bodies, their coupling with the wheel-rail contact module is quite easy. As a disadvantage, Morys himself mentions that not all eigenmodes obtained from the finite element model can be reproduced by the multibody model of the wheelset. – The model of the track will be discussed in the section about track modelling.

Also in order to investigate the “grumbling noise” of the ICE train, Szolc modelled the wheelset as a discrete-continuous structure in [72] and [73]. The wheelset’s axle is considered as a shaft, which can describe bending deformations according to the Bernoulli-Euler beam theory and torsional deformations. The deformation is described by a modal synthesis using the eigenmodes of the beam and the rod. The wheels and the brake discs are modelled as rigid rings, which are coupled to the axle by massless isotropic membranes. Since the wheel rim is considered as a rigid body, the problem of coupling the flexible wheelset with the wheel-rail contact is solved in a very easy way. In [72] the model contains only one wheelset, which is connected by linear springs and dampers to an infinite mass moving along the track. Later in [73] Szolc extended the modelling to a bogie with two wheelsets, both modelled as discrete-continuous systems. Here, the bogie frame is modelled as a rigid body, to which the wheelsets are connected by linear springs and dampers. The bogie frame is connected by linear springs and dampers, which represent the secondary suspension, to

the carbody, which is guided along the track.

The thesis by Küsel [38] also deals with the polygonalization of the wheels. In this work Küsel uses a wheelset model, which can also be described as a discrete-continuous model. The wheelset model describes a trailing wheelset equipped with four brake discs. The model consists of eight rigid bodies; two bodies represent the wheel hubs including the journals; two further bodies represent the wheel rims. Each brake disc is also represented by a rigid body. In total the wheelset model possesses 15 degrees of freedom: Each wheel hub can perform independent longitudinal and vertical displacements and three independent rotations; the lateral displacement is equal for both wheel hubs. Furthermore, each wheel rim can perform two inclinations relative to the wheel hubs. The axle is modelled as a continuum, which can perform bending motions and torsional motions; their distribution is described by a cubic polynomial for the bending motions and a linear polynomial for the torsional motions. The current shape of the axle is determined by the relative motions of the wheel hubs. Each wheel hub is connected to one wheel rim by a plate representing the wheel web; a cubic polynomial describes the distribution of the deformation along the radial coordinate. Also here, the current deformation of the wheel web depends on the relative motions between the wheel hub and the wheel rim. The complete model consists of one wheelset connected by linear springs and dampers to the bogie frame, which is guided along the track.

In [23], Kaiser and Popp present the model of a vehicle in which the wheelsets are modelled as flexible bodies; here, a comparatively simple finite element model is used for the wheelsets. By applying a formulation based on the Arbitrary Lagrangian Eulerian (ALE) approach, the equations of motion can be formulated as a system of linear differential equations with constant coefficients whereby gyroscopic effects are fully taken into account. This enables the calculation of a frequency response function for an excitation force acting at the wheel-rail contact. The results show several resonance peaks in the medium-frequency range which cannot be obtained by using a rigid body model.

The variety of modeling methods described above shows that there is yet no “standard modelling” for the modelling in the medium frequency range, in contrast to the low frequency range, where the multibody modelling can be considered as the standard method. A possible reason might be that problems occurring in the medium frequency range like the “grumbling noise” of the ICE train have recently emerged and are therefore comparatively new, as described by Popp, Knothe, and Pöpper in [54].

2.3 Track models

The track links the vehicle to the environment. It transmits the forces at the wheel-rail contact, which are responsible for support, guidance, driving and braking, to the subgrade or the substructure like e.g. a bridge.

One of the basest problems concerning the modelling of a railway system is that the length of the track is far higher than the length of the vehicles: For instance, a common passenger coach as used in Europe has a length over buffers of 25.4 m or 26.4 m, depending on the standard. In contrast to this, a track covers a length of several kilometers. It is evident that those zones of the track are of highest interest, where the vehicles are currently located and where thereby the load are applied on the track; this is valid for practically all investigations, be the vehicle or the track in the focus of the investigation.

Nevertheless, the high length of the track in combination with the structural damping has an im-

portant impact on its dynamical behaviour: The structural vibrations of a flexible structure can be interpreted as waves travelling through the structure; these waves are reflected and the boundaries of the structure. As a result, for certain wavelengths the interference of the waves travelling through the structure forms a standing wave; the associated frequencies are the eigenfrequencies of the structure. However, for a railway track things become more complicated: On the one hand the track has a high length; on the other hand the track possesses a considerable damping resulting from the subgrade and from the fastening between the rail and the sleeper so that the waves become weaker while they are travelling through the track. As a result the wave reflection at the ends of the track plays hardly a role regarding the dynamic behaviour of the track.

Furthermore, a vehicle covers a very long distance when running at high speeds: For a running speed of $v_0 = 270$ km/h, which lies in the range of regular operation speed for several of high speed railway systems, the vehicle covers a distance of $\Delta s = v_0 \Delta t = 75$ m within a time interval of $\Delta t = 1$ s. Thus, the simulation of a time interval of 10 s would require a track model having a length of at least 750 m. Assuming a sleeper spacing of $\Delta s_S = 0.6$ m this results in 1250 sleeper bays. It is evident that such a large model is difficult to handle even for today's computer systems.

An overview on the modelling of railway tracks is given by Knothe in [33]. In [34] Knothe and Grassie give an overview on track models for higher frequency ranges; this article the lower bound for higher frequencies is assumed at 20 Hz. In the following, some aspects concerning the methods of track modelling will be discussed. Based on these considerations, the track models are categorized, although the limits between the different categories are sometimes a bit blurred.

Track models can be divided into **inertially fixed models** and **moved models**. The basic principles of these two modelling types are illustrated in Fig.2.3.7.

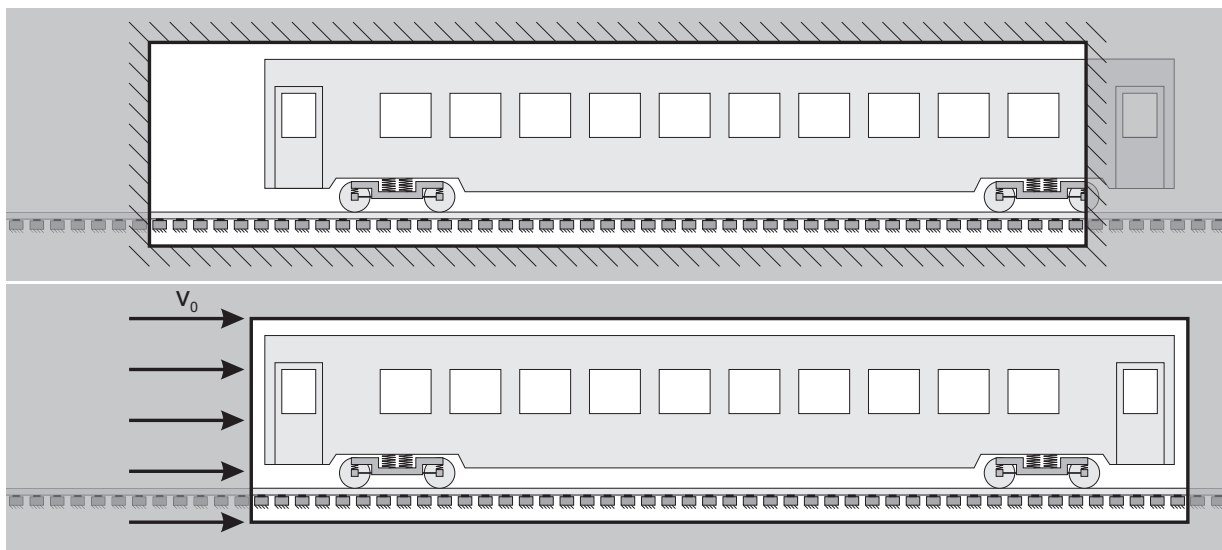


Figure 2.3.7: Above: Inertially fixed track model; below: Moving track model

In an **inertially fixed track model**, the section of the track, which is considered, is constant, i.e. the same track section is considered all the time, while the vehicle is passing through the considered section. In contrast to this, in a **moving track model** the track section, where the vehicle is currently located, is considered, i.e. the actual section of the track, which is considered, is changing over time.

Generally, it can be said that inertially fixed track models are used for investigations focused on the track and on the subgrade, while moving track models are used for investigations focused on the

vehicle. For instance, the impact of a load history by a passing train on the track and its components like pads and sleepers and on the subgrade can be analyzed using an inertially fixed track model.

As illustrated in the figures Fig.2.0.1, Fig.2.0.2, and Fig.2.0.3 the subsystems “vehicle” and “track” are not connected directly, but indirectly by the wheel-rail contact elements. Usually, the wheel-rail contact is modelled by a force element. The inputs of such a force element are the relative kinematics of the coupling points, between which the force element acts. Its outputs are the forces and torques, which are determined based on the relative kinematics and on the specific force law of the element. These forces and torques are applied on the aforementioned points. In the case of the wheel-rail contact the kinematical inputs are usually determined for the lowest point of the wheel and for the point on the rail head, where the wheel is currently located.

Regarding the kinematics and the forces, which are exchanged by the subsystems “vehicle” and “track” on the one hand and the subsystem “wheel-rail contact” on the other hand, only the receptance behaviour of the subsystems “vehicle” and “track” is relevant, i.e.: The relation between a dynamical force acting on the coupling point and the kinematics of the point as a reaction to the excitation is important, but not the actual mechanical structure of the subsystem. Thus there are two basic modelling strategies for moving track models, if the investigation focuses on the vehicle: **Structural models** and **substitution models**. Also between these two categories, the limits are sometimes a bit blurred; nevertheless some basic characteristics can be formulated.

Structural models consist of elements, which represent actual components of the track like rails, sleepers, pads etc. Therefore, the parameters of the elements are physical quantities like e.g. the mass of a sleeper or the bending stiffness of a rail. Thereby, the influence of such parameters on the dynamical behaviour can be investigated. However, in some cases like e.g. for the stiffness and the damping of a pad are difficult to be determined. The modelling effort is relatively high: The rail is usually modelled as a continuum, e.g. as a beam. This contributes to the relatively high order of the mathematical description. Since the rail is modelled as a continuum, it is usually not a problem to apply several wheel-rail contact forces on the rail and thereby to take the interaction of wheelsets via the track into account. Also, physical effects like wave propagation within the track can be taken into account.

Substitution models reproduce the dynamical behaviour of the track, i.e. the motion of the rail head under the influence of wheel-rail forces, without taking care of its actual structure. A substitution model can be formulated in a “purely mathematical” way or consist of “mechanical standard elements” like masses, springs and dampers. In the second case, the substitution track model can be easily integrated into an MBS formalism. The parameters of substitution models have no physical meaning. They are tuned in such a way that the model shows the same receptance behaviour as the actual track. Thereby, measured track receptances can be reproduced. Usually, the receptance is measured by inertially fixed devices. Thereby, the substitution model usually doesn’t take into account effects of wave propagation within the track, which is a justified approach as long as the running speed is far lower than the speed of wave propagation. It is also evident that, since the substitution model only reproduces the receptance of the rail head, “internal” physical quantities of the track like e.g. the forces acting between the rail and the sleepers are not available. The complexity of a substitution model, i.e. its structure of the model and its number of degrees of freedom depends on the desired accuracy of the model. To model the dynamical behaviour of the track required for low-frequent running dynamics a model with less than 10 degrees of freedom may be sufficient. Usually, each wheelset is supported by one separate substitution track model. In order to model interactions between the wheelsets via the track coupling elements between the single track models are required, which make the entire model more complex. As already mentioned, a substitution model only represents the receptance behaviour of the track; therefore structural track

models are usually moving track models. Since a structural track model is not suitable to determine “internal” physical quantities of the track, a fixed track model, which usually focuses on the track and its internal processes, based on the substitution approach doesn’t appear to be sensible.

In the following sections, some substitution and structural models for the track will be considered.

2.3.1 Substitution track models

As already mentioned, substitution track models reproduce the receptance behaviour of the rail head to excitation by wheel-rail forces. This can be done in different ways.

A substitution model with a purely mathematical description was developed by Fingberg [12]. In this model, the receptance behaviour of the track is described by several decoupled modal equations:

$$m_{C_i} \ddot{u}_{C_i}(t) + d_{C_i} \dot{u}_{C_i}(t) + c_{C_i} q_{C_i}(t) = F_C(t), u_C = \sum_{i=1}^{n_C} u_{C_i}(t) \quad (2.3.24)$$

The receptance behaviour of the track is described for several spatial directions (longitudinal, lateral, vertical), which are here indicated by C .

Another possibility is to assemble the substitution track model of masses, springs and dampers, i.e. of standard elements of multi-body system modelling. Thereby, such models can be easily described within the multi-body formalism, which is also used for the modelling of vehicles. The overview given by Bruni, Vinolas, Berg, Polach, and Stichel [8] also deals with the of track modelling using the multibody method and presents several track models consisting of the masses, springs and dampers.

Substitution track models, which are based on the multi-body modelling, have different modelling depths. Comparatively simple models were used by Kim [30] and by Netter [48].

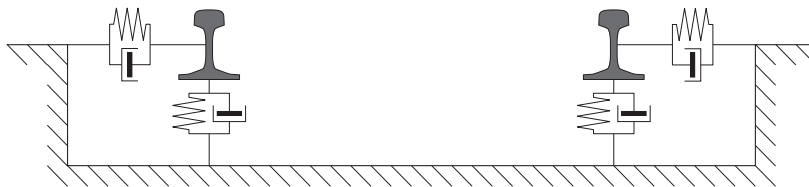


Figure 2.3.8: Substitution track model according to [18] and [30].

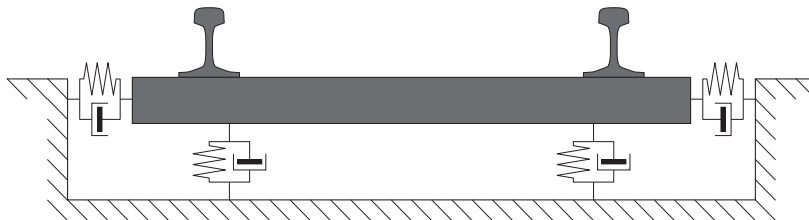


Figure 2.3.9: Substitution track model according to [48] and [8].

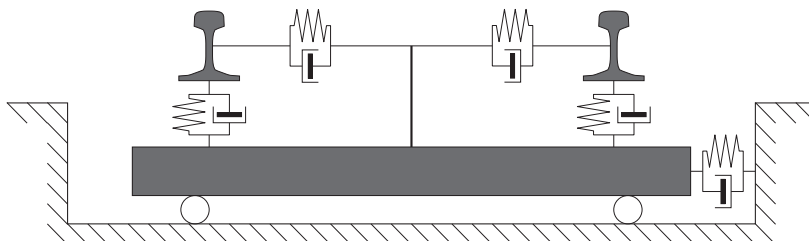


Figure 2.3.10: Substitution track model according to [21].

A more complex model was presented in the Manchester benchmark by Iwnicki [21]. This model was e.g. used by Mahr [42] and by Schelle [62]. In both works, existing multi-body simulation programs were used, so that the integration of the track model into the complete vehicle-track system model was quite easy.

In the work of Berg and Char [9] several substitution models with different complexity are presented. The parameters of the models are tuned to reproduce receptances, which were obtained

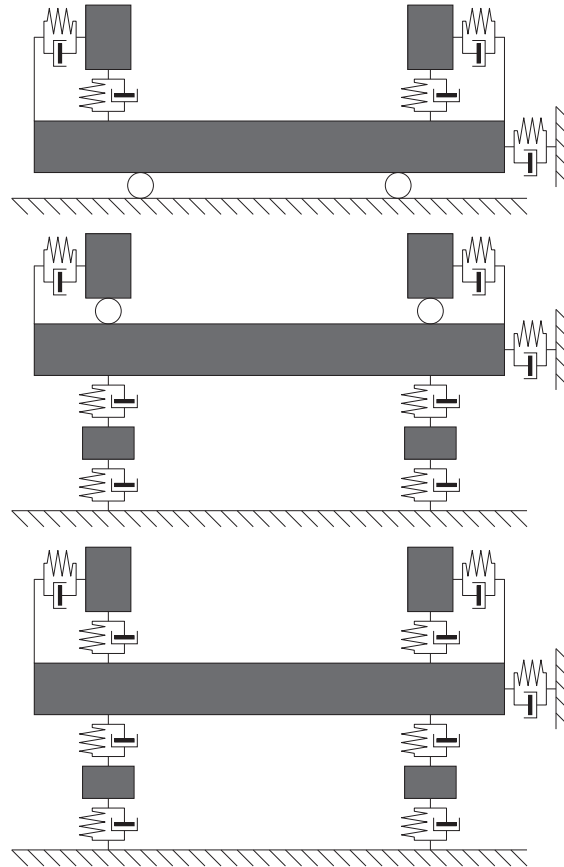


Figure 2.3.11: Substitution track models according to Char and Berg [9].

from field measurements.

In the works by Kurzeck [37] and by Szolc [72], [73] phenomena located in the medium frequency range are investigated. The track models used in these works can be categorized as substitution models, since they don't describe the rail by a flexible continuum. However, these models have a higher degree of detailing. The work by Kurzeck [37] is focused on roaring noise occurring at urban light railways; its frequency is located near 80 Hz. The track model developed by Kurzeck contains a flexible component assembled from finite beam elements to include the effect of structural vibrations of the sleeper in the vertical-lateral plain. – The works of Szolc [72], [73] deal with the vehicle-track interaction in the range between 30 Hz and 500 Hz. The model presented by Szolc in [72] describes a single wheelset, which is supported by track model system composed of masses, springs and dampers. The parameters of these elements are, however, not constant, but vary depending on the longitudinal coordinate of the track. Thereby, it is taken into account that the dynamical behaviour of the track is different for excitations above one sleeper on the one hand and between two sleepers on the other hand. In [73] Szolc extended the model from a single wheelset to a bogie having two wheelsets. In the extended model each wheelset is supported by one aforementioned track model system. To take the interaction between the wheelsets via the

track into account both track model systems are coupled by springs so that an interaction between the two wheelsets via the track is possible. – The track models by Kurzeck [37] and by Szolc [72], [73] can be seen as examples that substitution models can also be used for problems located above the frequency range of pure running dynamics.

Wu [81] developed a substitution model for the track, which is valid for the medium and high frequency range; here, the medium frequency range is located between 50 Hz and 500 Hz. The substitution model consists of linear springs and dampers and of masses performing translations. The parameters of these elements are tuned by comparing the frequency response function of the substitution model with the one of a detailed structural track model. For different cases of excitation, e.g. vertical or lateral excitation or symmetric or antimetric excitation with respect to the plane spanned by the longitudinal and vertical axis, different substitution models are developed. Furthermore, the influence of the discrete support of the rail by sleepers is taken into account by using parameters depending on the longitudinal coordinate of the track.

2.3.2 Aspects of structural track models

Structural models are based on the actual structure of the track. Usually, the rail is modelled as a continuum, which can at least perform bending motions, but also other motions like torsion. This modelling enables to take the effects of wave propagation within the track into account. At high speeds, effects of wave propagation become more important, since the running speed of the vehicle comes closer to the propagation velocity of the waves. This was e.g. substantiated by Triantafyllidis and Prange: In [74] and [75] Triantafyllidis and Prange analyzed measurements taken during the world record run of the German ICE prototype train, which reached a top speed of 406 km/h on May 1st, 1988. The evaluation showed a considerable influence of the Doppler effect.

The class of structural track models covers a wide range of different model types. Thus in this section some important aspects regarding structural track models will be discussed. In the next section, some existing track models will be discussed with respect to their modelling regarding these aspects and to their purpose. Some of these aspects are:

- Modelling of the rail
- Modelling of the support, number of layers
- Inertially fixed track model or moving track model
- Linear track model or nonlinear track model
- Length and boundary conditions of the track model
- Domain of the model: Time domain or frequency domain

These aspects will be discussed in the following; it will turn out that some of these aspects are not independent from each other. Generally, the first three aspects focus mainly on the mechanical modelling, while the last three aspects are more relevant for the mathematical treatment of the model.

Basically the railway track consists of two rails and a support, by which they are connected to the subgrade. Since the rails and the support are the main elements of the rail, it is obvious to consider first their characteristics and their modelling, i.e. their mechanical representation in a track model.

Modelling of the rail: As already said, in a structural track model the rail is modelled as a flexible, deformable structure, i.e. as a continuum. Two important characteristics of the rails are:

- The dimension of the rail regarding its length is far higher than regarding its cross section. The widely used rail profile 60E1 has a width of 150 mm and a height of 172 mm, while a track is several kilometers long and the rails are nowadays usually welded.
- Usually the rail has a prismatic shape, i.e. its cross section is constant over its length; exceptions mainly occur for turnouts and crossings.

From this it follows that the rail has a simple geometry. With respect to the different modelling method listed in Tab. 2.1.1 this means that the rail can be modelled as a continuous system; of course, it can also be modelled as a finite element system. In the first approach, there are generally two aspects regarding the modelling of the rail:

1. Longitudinal distribution of the deformations
2. Degrees of freedom of the deformations

Regarding the longitudinal distribution of the deformations, there are two basic strategies:

1. *Modelling as a continuous system:* The distribution of the rail's deformations is described by continuous functions, i.e. the functions are defined for the whole length of the modelled rail. In many cases, the exponential function and the sine and the cosine function derived from it are used.
2. *Modelling as a finite element system:* The distribution of the rail's deformations is described by local functions, which are only defined piecewise for finite intervals.

The categorization of the degrees of freedom of deformation and the related models is more complex:

1. Rail models assuming undeformed cross sections (one-dimensional continua)
 - (a) Vertical bending
 - i. Bernoulli-Euler beam
 - ii. Timoshenko beam
 - (b) Vertical and lateral bending plus torsion
 - i. Bernoulli-Euler beam
 - ii. Timoshenko beam
2. Rail models taking into account cross sectional deformations
 - (a) Two-dimensional models
 - (b) Three-dimensional models

The aspects, by which the different categories are distinguished, will be discussed in the following considerations.

One-dimensional models assume that the continuum is composed of sections having the infinitesimal length dx . A further assumption is that each section is rigid, i.e. the shape of the cross section remains unchanged and deformations are described by motions of the sections relative to each other. Each infinitesimal section of such a rail model can have at most six degrees of freedom, i.e. three translational and three rotational degrees of freedom, since this is the maximum number of degrees of freedom for a rigid body.

At railway systems the vertical forces resulting mainly from the weight of the vehicles are generally larger than lateral forces, since the lateral forces are limited by the vertical forces, the friction coefficient μ in the contact and the inclination of the running surfaces. Therefore, most track models take at least the vertical motions of the rail into account; these vertical motions are related to bending deformations of the rail. In cases, in which the vertical dynamics of the vehicle-track system is of interest as e.g. the influence of corrugated rails or wheel flats, a model considering only the vertical bending is sufficient. With respect to the distinction between plain and spatial models, as discussed in section 2 a plain model usually describes the vertical bending.

The vertical bending of the rail can be extended to bending in vertical and lateral direction. If lateral motions of the rail head are described, usually also torsional motions of the rail are taken into account. The wheel-rail forces are acting on the rail head, while the rail is connected to the sleeper by a pad at its foot. Thereby, regarding the lateral direction the rail is loaded by eccentric forces; thus, the consideration of torsion in addition to lateral bending motions is obvious. The torsion causes not only a lateral displacement of the rail head, but also a roll motion of the rail head, i.e. a rotation around the longitudinal axis of the rail. In this context it should be pointed out that the wheel-rail contact geometry, i.e. the location of the actual contact area between wheel and rail, can be very sensitive to changes of the relative position of the rail head and the wheel rim. Bezin, Iwnicki, and Cavalletti [7] underline the impact of the rail head's roll motion on the contact geometry.

If the rail is modelled as a one-dimensional continuum, then its bending motions in vertical and, if taken into account, in lateral direction are described based on a beam theory. Probably the simplest model for the rail is the Bernoulli-Euler beam. In this theory it is assumed that the cross section is always perpendicular to the bending line; thus no shear deformations are taken into account. Each infinitesimal section possesses one degree of freedom per translational displacement, i.e. one degree of freedom, if bending only in vertical direction is possible, and two degrees of freedom, if vertical and lateral bending is taken into account. The deformation with respect to one direction is described by the displacement $w(x, t)$ depending on the longitudinal coordinate x and the time t . The rotation angle $\gamma(x, t)$ of the infinitesimal section is approximately determined by the inclination, i.e. $\gamma(x, t) \approx w'(x, t) = \frac{\partial}{\partial x} w(x, t)$; thus it is dependent on $w(x, t)$ in a kinematical way and thereby it is not a degree of freedom. Furthermore, the rotational inertia of the cross section is neglected in the Bernoulli-Euler beam theory. Thus this theory is mainly suited for long slender beams and large wavelengths of the bending deformation.

The Timoshenko beam theory is a more detailed theory to describe bending motions. This theory takes the rotational inertia of the cross sections and the shear deformation, which are both neglected in the Bernoulli-Euler beam theory, into account. Therefore, the translational displacement $w(x, t)$ and the rotational displacement $\gamma(x, t)$ of an infinitesimal section are separate degrees of freedom. The Timoshenko beam theory is suitable for shorter beams and bending deformations of shorter wavelengths, where the wavelength of the rail's deformation comes closer to the dimensions of

the cross section. Such shorter wavelengths are usually related to higher frequencies so that a rail model based on the Timoshenko beam theory is valid for a greater frequency range than a model based on the Bernoulli-Euler beam theory. A recent work, in which the influence of the beam modelling on the dynamic behaviour of the track model is investigated, is the thesis by Kaps [28]. The advantage of the Timoshenko beam theory is its applicability to more cases and its wider range of validity. Its disadvantage is that it requires a higher mathematical effort; as already described, an infinitesimal section has two degrees of freedom per direction of bending, i.e. two degrees of freedom for vertical bending and four degrees of freedom for vertical and lateral bending.

As already mentioned, one-dimensional models are based on the assumption that the cross section remains undeformed and maintains its original shape. However, this assumption may be problematic in some cases. As already mentioned in the context of lateral motions, the rail is subjected to eccentric lateral loads. Furthermore, the rail has a comparatively thin web. Thereby, deformations of the cross section may be expected. Deformations of the cross section can include lateral and roll motions of the rail head; since the wheel-rail contact geometry can be very sensitive even to the relative kinematics of the rail head and the wheel rim, such deformations of the cross section may also have an impact on the wheel-rail interaction. Regarding the behaviour at frequencies of several kHz, deformations of the cross section also occur for vertical loading.

There are several possibilities to formulate rail models, which take cross-sectional deformations into account. The rail can be assembled from one-dimensional elements like beams and two-dimensional elements like plates and shells. It can also be modelled by three-dimensional finite elements, i.e. by volume elements.

Modelling of the support: At a real track the rails are supported by sleepers or slabs; between the rails on the one hand and the sleepers or slabs on the other hand flexible pads are installed. It should be pointed out that in real life the rail is not continuously supported, but periodically by discrete fastening elements. In [33] Knothe gives a hierarchy of track models with respect to two aspects:

- Number of the layers
 1. *One-layer model:* The rails and the sleepers are represented by one layer having an inertia.
 2. *Two-layer model:* The rails and the sleepers are represented by two separate layers, both having a mass; thereby, relative motions between the rails and the sleepers are possible.
 3. *Two-layer model with elastic sleepers:* The upper and the lower layer represent the rails and the sleepers, respectively; in addition deformations of the sleepers are taken into account.
 4. *Three-layer model:* In addition to the rails and the sleepers the ballast is represented by a separate third layer having a mass.
- Modelling of the support; this modelling aspect can be split into two subaspects so that there are four possible combinations:
 1. (a) *Continuous support:* The sleepers and, if modelled as a separate layer, the ballast are modelled as continuous layers having a mass. Between the layers having a mass continuous viscoelastic layers are located.

- (b) *Discrete support*: The sleepers and, if modelled as a separate layer, the ballast are modelled by discrete bodies. The rail is not continuously, but non-uniformly supported.
- 2. (a) *Foundation models*: The lowest layer is connected to a rigid ground by a viscoelastic foundation.
- (b) *Halfspace models*: The lowest layer is supported by a halfspace representing the underground.

As already mentioned, rails are connected by sleepers or slabs by discrete fastening elements. A usual value for the longitudinal spacing between two fastening elements is $\Delta s = 0.6$ m. The modelling approach of a *continuous support* replaces the discrete fastening elements by a continuous visco-elastic layer, which has constant parameters with respect to the longitudinal direction. The advantage of this approach is that the equations describing the model can be treated in an easier way regarding their mathematical solution. However, this modelling is only admissible if the wavelength of the rail's deformations are far higher than the spacing of the fastenings. Probably the best known effect, which cannot be reproduced by a continuous support, is the so-called pinned-pinned mode of the rails; for this motion, the vibration nodes of the rails occur at the location of the fastenings so that the vibration of the rails is only weakly damped. The modelling of a *discrete support* considers the fastening elements as single discrete elements. Thereby, effects resulting from the non-uniform support like the pinned-pinned mode can be modelled so that a track model using a discrete support is usually valid for higher frequency ranges. The disadvantage is the higher mathematical effort for the solution of the model. Due to the discrete support the dynamic properties of the track model vary along the longitudinal coordinate; for instance, if a force acts on the rail in the middle of a sleeper bay, it causes a larger deformation than it would do, if it acts directly above one sleeper.

Furthermore, the supporting elements can be modelled with different detailing. Regarding the discrete sleeper the representation by a rigid body is the simplest model. More refined models of the sleepers and of the slabs take their deformational motions into account, e.g. by modelling the sleeper as a beam or by modelling the slab as a plate. There are also different aspects regarding the modelling of the fastening system, which connects the rail and the sleeper. In many cases the fastening is modelled as a force element; here, different characteristics for the relation between the deformation and the force can be applied. Furthermore, the pad, which acts between the rail foot and the rail seat of the sleeper, can either be modelled as a compact force element, i.e. a single discrete force element acting between two points, or by distributed force elements or a layer taking into account its actual geometric dimensions.

Linear and nonlinear track models: Usually, the motions for the several elements of a structural track model are comparatively small; therefore, a linearization with respect to the kinematics is possible in many cases, e.g. approximating the sine function $\sin \varphi \approx \varphi$ for very small angles φ . Nevertheless, also in track models nonlinear effects can occur. Such a nonlinear phenomenon is a sleeper void, i.e. in the unloaded state the sleeper is not supported by the subgrade, but only hangs under the rail. A nonlinearity occurs if the deformation of the track is high enough so that the gap between the sleeper and the support vanishes and forces start to act between these two components. The calculation of the track model in the frequency domain and the modal decomposition of a track model are methods, which can only be applied on linear models; a nonlinear track model cannot be treated with these methods.

Domain of the model: Generally, it can be distinguished between **frequency domain models** and **time domain models**. In the frequency domain, usually the receptance function, i.e. the

response of the model to a harmonic excitation, is determined. Thereby, also infinitely long track models can be handled. However, the dynamics can only be determined for a harmonic excitation, i.e. for a periodic excitation; transient processes cannot be described. Furthermore, as already mentioned before, the model has to be linear to treat it in the frequency domain. In contrast to this, time domain models can describe transient processes; they can also contain nonlinear elements. However, a model has to be finite to be treated in the time domain.

Model length and boundary conditions: As already mentioned a real track has a much larger longitudinal dimension than a railway vehicle. Thereby, the effect of reflection for deformation waves, which are excited by the wheel-rail contact forces acting on the track and are propagating through the track structure, is extremely weak. This lack of wave reflection has a strong impact on the track's dynamic behaviour; therefore, a structural track model should reproduce it with a sufficient accuracy. One possibility is to model the track as an infinite structure. However, the dynamic behaviour of an infinite structure can only be treated in the frequency domain; for a harmonic excitation the frequency response function can be calculated. In order to model transient dynamics the calculation has to be done in the time domain; this requires a finite model. To limit the computational effort a finite structural track model is much shorter than a real track. In this context the question arises how long the model has to be and which boundary conditions have to be applied at its ends. Simply spoken it can be said that the track model has to be long enough so that the influence of the boundary conditions at its ends on the dynamic behaviour at the current location of the wheel-rail contact is negligible. To say it more precisely, the track model has to be long enough to make sure that the waves, which are propagating through the track, are so weak, when they reach the end, that their reflection at the ends has practically no influence.

It is obvious that in order to minimize the aforementioned influence of wave reflection at the rails' ends, the ends of the track have to be located as far as possible from the zone, where the wheel-rail forces are acting on the rail. For a finite track model this zone is typically located in the middle of the track model. In the case of an **inertially fixed** finite **track model** the locations of the ends remain constant. However, for a **moving** finite **track model** it has to be ensured that the vehicle never reaches the end of the track; one reason is to avoid that the vehicle falls off the track, another reason is that the effect of the wave reflection at the end of the track model becomes stronger, when the vehicle approaches this end. There are several possibilities to solve this problem:

- The track model is assembled before the vehicle and dismounted behind the vehicle, i.e. if an element of the track is far enough behind the vehicle, it is separated from the track at the rear end and connected to the track at the front end.
- The deformations of the rail are described by shape functions, which are moving together with the vehicle. If the support is modelled by discrete elements, then the supporting elements, i.e. the sleepers and the fastening elements connecting the rails and the sleepers, are moving along the rails with the running speed v_0 in the opposite direction of the vehicle's running.
- The boundary conditions at the ends of the track model are set equal. Thereby the track model forms a ring so that the vehicle never reaches the end of the track model. It should be pointed out that this does not necessary mean that the track is curved; the topology of the structural track model on the one hand and the topology of the trajectory of the track are separated from each other.

2.3.3 Examples for structural track models

In the following, some structural track models based on these modelling principles will be discussed.

The vehicle-track models used by Zhai, Wang and Cai [83] and by Xiao, Jin, Wen, Zhu, and Zhang [82] are similar in several aspects: The track models can be categorized as discrete-continuous models: They consist of two rails modelled by beams, which can perform bending motions in vertical and lateral direction and also torsional motions. In [83], the Euler-Bernoulli beam theory is used, while in [82] the Timoshenko beam theory is applied. The rails are described by a modal synthesis using trigonometric functions.

to be continued...

For the investigation of wheel polygonalization, Morys [46] developed track model, which consists of a chain of 30 track modules. Each module includes two Euler-Bernoulli beams representing the rails and a rigid body representing the sleeper. The beams can perform vertical and lateral bending deformations. Springs and dampers connect the sleeper to the rails and to the fixed ground. At the rear end of the last module and at the front end of the first module, boundary conditions for a rigid support are applied. The number of the track modules, which determine the length of the track model, is chosen in such a way that the reaction forces at the end of the flexible track model become sufficiently low. While the bogie moves along the track, the currently last track module is disconnected from the currently second-last one, shifted forward and connected to the front end of the currently first track module. Thereby, the track is disassembled behind the bogie and assembled before the bogie so that the bogie is always located in the middle of the flexible track.

For cyclic track models the boundary conditions at the ends of the rails are set equal. Thereby, the track forms a “ring with neglected curvature”. As a consequence, the vehicle never reaches an end of the track and therefore cannot “fall off the track”. This modelling class covers a wide range of models with different modelling depth. A comparatively simple cyclic track model is used by Mazzola, Bruni, Martínez-Casas and Baeza in [43]. For the track symmetric motions are assumed so that only one half of the track has to be modelled. The rail can perform bending motions in the vertical and lateral direction as well as torsional motions; the bending is described based on the Timoshenko beam theory. The rail is supported by discrete sleepers; they are modelled as rigid bodies and can perform only vertical translations. Each sleeper is connected to the rail and to the fixed environment by springs and dampers representing the pads and the underground.

The model developed by Ripke [58] considers the track as a cyclic structure. The boundary conditions at both ends of the track model are set equal. Thereby, the track forms a “ring with neglected curvature”. As a consequence, the vehicle never reaches an end of the track and therefore cannot “fall off the track”.

A recent track model has been presented by Baeza and Ouyang [4]. This model is a cyclic track model, i.e. a finite model, where the boundary conditions at its ends are set equal. The rail can perform bending motions in vertical and lateral direction and torsional motions. The bending of the rail is described by the Timoshenko beam theory. The longitudinal distribution of the deformations is described by sine and cosine functions so that the cyclic boundary condition is automatically fulfilled. The sleepers are modelled by finite beam elements using the Timoshenko beam theory. They are connected by a viscoelastic foundation to a rigid ground; thus the model can be classified as a two-layer model with elastic sleepers. Baeza and Ouyang give an interesting interpretation of their model: On the track, which is considered to be infinite, an infinite number of identical vehicles is rolling; the distance between two vehicles is the length L . Therefore the cyclic

model represents one characteristic sample of the infinite train-track system, which has the length L . Furthermore, Baeza and Ouyang mention explicitly that the model can consider nonlinearities. to be continued...

2.4 Wheel-rail contact models

In real life the wheel-rail contact is a small region, in which forces are transmitted between the wheel and the rail. The forces are transmitted by two principles, form closure, i.e. normal stresses, and force closure, i.e. tangential stresses caused by friction.

In multibody models the wheel-rail contact is usually modelled as a force element. This force element acts between two coupling points or markers, one belonging to the rail, the other one belonging to the wheel. The inputs of the force element are the kinematics of the two points; its outputs are the resulting forces, which are applied on the bodies. Thus it can be said that the kinematics and forces are interchanged at the coupling points. Regarding the modelling of the wheel-rail contact within a multibody model several aspects should be considered:

1. As described in section 2.1.1 the equations of motion for a multibody system are a system of ordinary differential equations (ODE) or of differential-algebraic equations (DAE). The mathematical problem is an initial value problem, i.e. the wanted solution $\mathbf{z}(t)$ is obtained by integrating the equations of motion starting from a given initial value $\mathbf{z}_0 = \mathbf{z}(t = t_0)$. In many cases an implicit integration is necessary; such an implicit integration requires an iterative solution of a system of nonlinear equations for each time step and thereby usually several evaluations of the equation of motion $\dot{\mathbf{z}}(t) = \mathbf{F}(\mathbf{z}(t), t)$. The procedure to calculate the resulting forces for a kinematical input has to be carried out for each evaluation. In this context it becomes clear that a wheel-rail contact model used for a multibody simulation needs a high computational efficiency.
2. As mentioned before, kinematics and forces are interchanged between the bodies on the one hand and the force element on the other hand at the coupling points. The discrete forces applied on the bodies are the resulting wheel-rail forces resulting from integrating the stress field over the contact area A_C :

$$\mathbf{f}_{WR,res} = \int_{A_C} \begin{bmatrix} \tau_1(x,y) \\ \tau_2(x,y) \\ p(x,y) \end{bmatrix} dA \quad (2.4.25)$$

Since for the dynamics of the multibody system only the resulting force $\mathbf{f}_{WR,res}$ is required, local deviations of the stress distributions $\tau_1(x,y)$, $\tau_2(x,y)$, and $p(x,y)$ from the exact solution can be tolerated.

Owing to these aspects, i.e. on the one hand the need for a fast calculation and on the other hand a greater tolerance with respect to the actual stress distribution, wheel-rail contact models used in multibody modelling are often based on simplified solutions for the wheel-rail contact.

In the context of multibody dynamics the Hertzian theory and Kalker's linear theory are often used. Thus these theories will be presented and discussed shortly in the following section, also with respect to the aforementioned aspects. The discussion of their limitations for the application on the wheel-rail contact will help to understand the aim of other models.

Since the wheel-rail contact area is very small compared to the dimensions of the wheel and the rail, the modelling of the contact area requires a finer resolution for the description of the elasticity. Therefore, the “local elasticity” describing the deformations in the contact is often separated from the “global elasticity” describing deformations of the entire structure, e.g. bending. Models describing the contact between a wheel and a rail, which are both modelled as flexible bodies, are comparatively rare. An example is the work by Pletz, Daves and Ossberger [52], who simulated the passing of a railway wheel through the crossing nose of a switch in a finite element environment. Here, the local and the global elasticity are not treated separately, but due to the high computational effort the model is limited to one wheel and a section of 3 m of the switch.

Usually, the treatment of the wheel-rail contact is split into several steps; this is e.g. described by Vohla [77]:

1. Contact geometry problem
2. Normal contact problem
3. Tangential contact problem

In the following sections, an overview on models for the normal and the tangential contact problem will be given.

2.4.1 Elliptic contact

A well known theory for the contact of two elastic bodies was developed by Hertz. An overview of this theory is given e.g. by Ayasse and Chollet in [3]; the following considerations are based on this source. A more detailed description is given e.g. by Kalker in [26]. The Hertzian theory gives a solution of the equation of Boussinesq and Cerrutti for the normal contact. The theory assumes that in the contact region, the undeformed surfaces of the two bodies are described by elliptic paraboloids of the following form:

$$z_1(x,y) = -A_1x^2 - B_1y^2, \quad z_2(x,y) = A_2x^2 + B_2y^2 \quad (2.4.26)$$

The parameters A_i and B_i are determined from the curvature radii $r_{x,i}$ and $r_{y,i}$ of the bodies in the contact:

$$A_i = \frac{1}{2r_{x,i}}, \quad B_i = \frac{1}{2r_{y,i}} \quad (2.4.27)$$

If the surface of the body is convex, the radius is positive. The formulation of the surfaces assumes that the curvatures of the surfaces are constant within the contact region.

The approach of the bodies caused by the deformation in the contact is expressed by δ_0 . Thereby an interpenetration $\delta(x,y)$ of the undeformed surfaces occurs, which can be formulated as:

$$\delta(x,y) = z_2(x,y) + \delta_0 - z_1(x,y) = \delta_0 - (A_1 + A_2)x^2 - (B_1 + B_2)y^2 = \delta_0 - Ax^2 - By^2 \quad (2.4.28)$$

In the following considerations the resulting curvature parameters A and B are assumed to be positive, i.e. $A > 0$ and $B > 0$. – The boundary of the interpenetration area is obtained by setting $\delta(x,y) = 0$. It turns out that the interpenetration area is an ellipse having the semi-axes a_g and b_g :

$$0 = \delta_0 - Ax^2 - By^2 \Rightarrow 1 = \frac{Ax^2}{\delta_0} + \frac{By^2}{\delta_0} = \left(\frac{x}{a_g}\right)^2 + \left(\frac{y}{b_g}\right)^2 \Rightarrow a_g = \sqrt{\frac{\delta_0}{A}}, \quad b_g = \sqrt{\frac{\delta_0}{B}} \quad (2.4.29)$$

The actual contact area is smaller than the interpenetration area, but has also the shape of an ellipse. The semi-axes are determined by:

$$a = m \left[\frac{3}{2} N \frac{1-\nu^2}{E} \frac{1}{A+B} \right]^{1/3}, \quad b = n \left[\frac{3}{2} N \frac{1-\nu^2}{E} \frac{1}{A+B} \right]^{1/3} \quad (2.4.30)$$

Here, E and ν denote Young's modulus and Poisson's ratio of the material, respectively; N is the normal force pressing the two bodies against each other. The dimensionless coefficients m and n are the Hertzian coefficients, which will be explained later on. The relation between the approach δ_0 and the normal force N is given by:

$$\delta_0 = r \left[\left(\frac{3}{2} N \frac{1-\nu^2}{E} \right)^2 (A+B) \right]^{1/3} \quad (2.4.31)$$

Also r is a dimensionless Hertzian coefficient. The distribution of the pressure $p(x,y)$ is given by a half ellipsoid:

$$p(x,y) = p_{max} \sqrt{1 - \left(\frac{x}{a}\right)^2 - \left(\frac{y}{b}\right)^2}, \quad p_{max} = \frac{3}{2} \frac{N}{\pi a b} \quad (2.4.32)$$

The coefficients m , n , and r are obtained from evaluating elliptic integrals, see e.g. Kalker [26]:

$$\begin{aligned} \frac{a}{b} &= \sqrt{1-k^2} \\ \Rightarrow D &= \int_0^{\pi/2} \frac{\sin^2 \psi}{(1-k^2 \sin^2 \psi)^{1/2}} d\psi, \quad C = \int_0^{\pi/2} \frac{\sin^2 \psi \cos^2 \psi}{(1-k^2 \sin^2 \psi)^{3/2}} d\psi, \quad E = \int_0^{\pi/2} (1-k^2 \sin^2 \psi)^{1/2} d\psi \end{aligned} \quad (2.4.33)$$

These integrals can be evaluated only numerically; this requires a considerable computational effort. Usually, the coefficients m , n , and r are precalculated and stored in tables depending on the auxiliary parameter $\cos \theta$, which is defined by:

$$\cos \theta = \frac{|A-B|}{A+B} \quad (2.4.34)$$

Assuming that A and B are positive the expression can be reformulated to:

$$\cos \theta = \frac{|A-B|}{A+B} = \frac{|1-(B/A)|}{1+(B/A)} \quad (2.4.35)$$

As already mentioned, the Hertzian coefficients m , n , and r are usually given in tables depending on the parameter $\cos \theta$. Since the parameter $\cos \theta$ is related to the ratio B/A , also the coefficients m , n , and r finally depend on A/B .

Based on the equations (2.4.30) and (2.4.31) a direct relation between the semiaxes a and b and the approach δ_0 can be formulated. For the square of the semiaxis a it is valid:

$$a^2 = m^2 \left(\frac{3}{2} N \frac{1-\nu^2}{E} \right)^{2/3} \left(\frac{1}{A+B} \right)^{2/3} \Rightarrow \left(\frac{3}{2} N \frac{1-\nu^2}{E} \right)^{2/3} = \frac{a^2}{m^2} (A+B)^{2/3} \quad (2.4.36)$$

By inserting this into (2.4.31) the normal force N and the material parameters E and ν are eliminated:

$$\delta_0 = r \left(\frac{3}{2} N \frac{1-\nu^2}{E} \right)^{2/3} (A+B)^{1/3} = r \frac{a^2}{m^2} \underbrace{(A+B)^{2/3} (A+B)^{1/3}}_{(A+B)} \Rightarrow a = m \sqrt{\frac{\delta_0}{r(A+B)}} \quad (2.4.37)$$

In an analogous way the semiaxis b can be expressed by:

$$b = n \sqrt{\frac{\delta_0}{r(A+B)}} \quad (2.4.38)$$

These relations show that the semiaxes a and b of the contact ellipse can be determined purely based on the geometry of the contact. As described above the curvature parameters A and B are given by the geometrical shape of the two bodies in contact; the Hertzian parameters m , n , and r depend on the ratio A/B and thereby also on the geometry.

For the tangential contact, the linear theory by Kalker is widely used. This theory gives a relation between the creepages in the contact patch and the transmitted tangential forces. The creepages are defined as the ratio between the relative velocity and the running speed v_0 . The relative motions in the contact are described by the longitudinal relative velocity $v_{1,rel}$, the lateral relative velocity $v_{2,rel}$ and the relative angular velocity $\omega_{3,rel}$ around the normal axis of the contact area. In Kalker's linear theory it is assumed that the creepages are very small. In this case the relation between the relative velocities and the longitudinal force F_1 , the lateral force F_2 and the spin moment M_3 , which are transmitted in the contact, is given by:

$$F_1 = -abGC_{11} \frac{v_{1,rel}}{v_0} \quad (2.4.39)$$

$$F_2 = -abGC_{22} \frac{v_{2,rel}}{v_0} - (ab)^{3/2} GC_{23} \frac{\omega_{3,rel}}{v_0} \quad (2.4.40)$$

$$M_3 = (ab)^{3/2} GC_{23} \frac{v_{2,rel}}{v_0} - (ab)^2 GC_{33} \frac{\omega_{3,rel}}{v_0} \quad (2.4.41)$$

Here, a and b denote the semiaxes of the contact ellipse, as determined according to (2.4.30). The shear modulus of the material is denoted by G . The coefficients C_{ij} are the so-called Kalker coefficients. They depend on the minimum ratio of the semiaxes $g = \min(a/b, b/a)$ and on Poisson's ratio ν . Therefore, the coefficients can be precalculated and stored in tables, as done by Kalker.

The big advantage of the Hertzian theory and Kalker's linear theory is their very low computational effort: The coefficients m , n , r , and C_{ij} required by the calculation depend on just one or two parameters. Thereby, values of the coefficients can be precalculated for discrete values of the parameters; the values required for the actual calculation can then be determined by interpolation between the precalculated values.

2.4.2 Normal contact

The application of the Hertzian theory on wheel-rail contacts can be problematic in several cases. As described above, a basic assumption of the Hertzian theory is that the curvatures of the surfaces are constant within the contact region. However, this assumption isn't always valid for wheel-rail contacts, because many rail profiles are composed of circular arcs having different radii. Thereby, discontinuities of the curvature occur, which lead to non-elliptic contact areas. It should be pointed out that this problem isn't just a theoretical consideration. Kleiner [31] conducted experiments, in which a pressure sensitive film was placed between a railway wheel and a rail. At such films the colour changes, when a specific pressure is exceeded. Therefore, the boundary between the regions of different colours can be interpreted as an isobar. The experimental results obtained by Kleiner clearly showed that non-elliptic contact areas occur in wheel-rail contacts for several relative positions.

The Hertzian theory assumes that the interpenetration area and the contact area are ellipses. Since ellipses are uniquely defined by their two semi-axes, they form a family of curves, which are characterised by two parameters. As the short discussion of the Hertzian theory and Kalker's linear theory in section 2.4.1 shows, only the ratio of the semi-axes, i.e. only one parameter, is actually needed for the determination coefficients required for the calculation of the forces. In contrast to this, the non-elliptic contact areas, which can occur in wheel-rail contacts, cannot be described by a family of curves depending on so few parameters. There are several ways to treat the problem of non-elliptic contact areas. An overview is given by Piotrowski and Chollet in [51]. Generally, there are three possibilities to treat the non-elliptic contact:

1. Replacing the non-elliptic contact area by an equivalent ellipse
2. Estimation of the non-elliptic contact area based on the geometrically determined interpenetration area
3. Determination of the non-elliptic contact area by solving the equations based on the contact mechanics

One possibility is to replace the non-elliptic contact area by an equivalent ellipse. An example is the method presented by Vollebregt, Weidemann and Kienberger in [78]: The semi-axes of the ellipse are set equal to the maximum dimensions of the interpenetration area in longitudinal and lateral direction.

A further possibility is the estimation of the contact area. In the Hertzian theory, the interpenetration area as well as the contact area are ellipses, i.e. geometrically similar shapes. According to (2.4.29) the semi-axes of the interpenetration ellipse are given by:

$$a_g = \sqrt{\frac{\delta_0}{A}}, \quad b_g = \sqrt{\frac{\delta_0}{B}} \quad (2.4.42)$$

Furthermore the semi-axes a and b of the contact ellipse can be determined purely based on the contact geometry, as shown in section 2.4.1. According to (2.4.37) and (2.4.38) it is valid:

$$a = m\sqrt{\frac{\delta_0}{r(A+B)}}, \quad b = n\sqrt{\frac{\delta_0}{r(A+B)}} \quad (2.4.43)$$

The actual contact ellipse having the semi-axes a and b is always smaller than the interpenetration ellipse having the semi-axes a_g and b_g . Thus the contact ellipse can be obtained from the interpenetration ellipse by reducing the approach δ_0 and correcting the ratio of the resulting semi-axes, since the ratio a_g/b_g is not identical to the ration a/b .

Furthermore, at least the radius of the wheel in circumferential direction is constant. Based on this, some properties of the Hertzian contact can be applied on the non-elliptic contact to estimate the contact area and the pressure distribution. An approximation for the contact area can be obtained by reducing the interpenetration between the surfaces of wheel and rail, thereby reducing the interpenetration area and considering the reduced interpenetration area as the contact area. Since the ratio of the semi-axes is not the same for the interpenetration ellipse and the contact ellipse, a shape correction can be applied, as presented by Ayasse and Chollet in [2]. Models, which are based on an estimation of the contact area, were developed by Kik and Piotrowski [29], Linder [40], Quost, Sebes, Eddhahak, Ayasse, Chollet, Gautier and Thouverez [57]. The model by Linder was enhanced by Weidemann [79] to calculate the wear occurring in the wheel-rail contact.

The third possibility is to determine the stress distribution in the contact by solving the mechanical equations, which describe the contact. The main difficulty in this context is that the solution has to be determined iteratively. Probably the best known program for this task is the software CONTACT originally developed by Kalker; basics for this program can be found in Kalker's fundamental book [26].

2.4.3 Tangential contact

The tangential contact model describes the forces transmitted by friction. Due to the characteristics of the dry friction, the transmittable tangential tension is limited by the normal pressure and the friction coefficient. As a result, the relation between the creepage in the contact and the tangential forces shows a saturation characteristics, i.e. the tangential force cannot exceed a certain value. The appropriate modelling of this characteristics can be seen as a main problem regarding the modelling of the tangential contact. A survey on different tangential contact models is given e.g. by Kalker in [27].

The model by Shen, Hedrick and Elkins [69] uses a heuristic approach to describe the transition between the nearly linear behaviour for very small creepages and the saturation. In the first step the longitudinal and lateral tangential forces F'_1 and F'_2 are calculated using Kalker's linear theory.

$$F'_1 = -abGC_{11} \frac{v_{1,rel}}{v_0}, F'_2 = -abGC_{22} \frac{v_{2,rel}}{v_0} - (ab)^{3/2} GC_{23} \frac{\omega_{3,rel}}{v_0} \quad (2.4.44)$$

The spin moment is neglected. Since the resulting tangential force F'_R determined by

$$F'_R = \sqrt{F_1'^2 + F_2'^2} \quad (2.4.45)$$

may exceed the maximum transmittable tangential force μN , a parameter τ is introduced

$$\tau = \frac{F'_R}{3\mu N} \Rightarrow \frac{F_R}{\mu N} = \begin{cases} 1 - (1 - \tau)^3 & \text{for } 0 \leq \tau < 1 \\ 1 & \text{for } \tau \geq 1 \end{cases} \quad (2.4.46)$$

For $\tau \geq 1$ the saturation is reached. After determining F_R according to (2.4.46) the actual tangential forces F_1 and F_2 are obtained by scaling the forces F'_1 and F'_2 :

$$F_1 = \frac{F_R}{F'_R} F'_1, F_2 = \frac{F_R}{F'_R} F'_2 \quad (2.4.47)$$

The FASTSIM algorithm developed by Kalker [25] avoids the iterative calculation of the tangential stresses. To illustrate the simplification, the relation between the tangential deformations and the tangential stresses should be considered once again: If the two bodies in contact are described by half-spaces, which show linear material behaviour and have the same material parameters G and ν , then the relation between the tangential deformations u_1 and u_2 on the one hand and the tangential stresses τ_1 and τ_2 on the other hand are given by the following equations of Boussinesq and Cerrutti:

$$u_1(X, Y) = \frac{1}{\pi G} \int_{A_c} H_{11}(X-x, Y-y) \tau_1(x, y) dA + \frac{1}{\pi G} \int_{A_c} H_{12}(X-x, Y-y) \tau_2(x, y) dA \quad (2.4.48)$$

$$u_2(X, Y) = \frac{1}{\pi G} \int_{A_c} H_{12}(X-x, Y-y) \tau_1(x, y) dA + \frac{1}{\pi G} \int_{A_c} H_{22}(X-x, Y-y) \tau_2(x, y) dA \quad (2.4.49)$$

Since the influence functions H_{11} and H_{22} are always positive, i.e. $H_{11}(X-x, Y-y) > 0$ and $H_{22}(X-x, Y-y) > 0$, the determination of the tangential displacements $u_1(X, Y)$ and $u_2(X, Y)$ required the evaluation the entire stress field given by $\tau_1(x, y)$ and $\tau_2(x, y)$. For the FASTSIM algorithm this relation is replaced by the much more simpler relation

$$\tau_1(X, Y) = L_1 u_1(X, Y), \quad \tau_2(X, Y) = L_2 u_2(X, Y) \quad (2.4.50)$$

i.e. the deformations $u_1(X, Y)$ and $u_2(X, Y)$ only depend on the stresses $\tau_1(X, Y)$ and $\tau_2(X, Y)$, respectively, at the particular point defined by X and Y , but not on the entire stress distribution $\tau_1(x, y)$ and $\tau_2(x, y)$. Kalker gave a very illustrating interpretation of this simplification, see [26]: “In this theory the elastic wheel and rail are modelled by a set of springs [...]. Each set consists of a number of small three-spring systems so that each point of the surface of wheel and rail can elastically displace in any direction independently of its neighbours.” – The coefficients L_1 and L_2 depend on the Kalker coefficients C_{11} , C_{22} and C_{23} . In the practical application, the contact ellipse is separated in longitudinal stripes so that a particle, which travels through the contact area, moves along a stripe. The stripes are again separated into rectangles. Starting at the leading edge, the tangential stresses are evaluated successively by going along the stripe. At each step it is checked, whether calculated stresses $\tilde{\tau}_1(x, y)$ and $\tilde{\tau}_2(x, y)$ exceed the local transmittable stress $\tau_{max}(x, y)$, which is determined by the local pressure $p(x, y)$ and the friction coefficient μ . If the maximum transmittable stress is exceeded, then the stresses $\tilde{\tau}_1(x, y)$ and $\tilde{\tau}_2(x, y)$ are scaled down.

$$\sqrt{\tilde{\tau}_1(x, y)^2 + \tilde{\tau}_2(x, y)^2} \leq \tau_{max}(x, y) = \mu p(x, y) \Rightarrow \tau_i(x, y) = \tilde{\tau}_i(x, y) \quad (2.4.51)$$

$$\sqrt{\tilde{\tau}_1(x, y)^2 + \tilde{\tau}_2(x, y)^2} > \tau_{max}(x, y) = \mu p(x, y) \Rightarrow \tau_i(x, y) = \frac{\tau_{max}(x, y)}{\sqrt{\tilde{\tau}_1(x, y)^2 + \tilde{\tau}_2(x, y)^2}} \tilde{\tau}_i(x, y) \quad (2.4.52)$$

In the FASTSIM algorithm the contact area is divided into longitudinal stripes, which are considered separately. Therefore, it is possible to combine the FASTSIM algorithm with normal contact models based on a description of the contact area by stripes, see e.g. the works by Linder [40], by Weidemann [79] or by Quost, Sebes, Eddhahak, Ayasse, Chollet, Gautier and Thouverez [57].

Chapter 3

Cyclic systems

A cyclic system consists of n identical segments, which are arranged in a circular way; the number n of the segments is a natural number and it is greater than 2, i.e. $n \in \mathbb{N}$, $n > 2$. Here, the zeroth and the n -th segment are identical. In technical systems components, which can be considered as cyclic systems, are not rare. Such components are usually rotational symmetric like e.g. turbines or wheels. Axisymmetric structures, too, can be considered as cyclic structures; here, the number of segments n can be chosen arbitrarily.

The description of structures as cyclic systems enables a distinct reduction of the computational effort without loss of accuracy. Therefore, this concept has been used for various applications like in the work by Panning [49] about the vibration of turbines. Although a railway track is not a circular structure, it nevertheless consists of identical segments and is thereby a periodic structure, so that it can also be approximated as a cyclic structure as done by Ripke [58]. In this work, the concept of the cyclic system is an important base for the description of the wheelset and the track. Therefore, the characteristics of a linear cyclic system shall be considered in this section.

Following the nomenclature given in [64], [63] and [55], the equation of motion for an ordinary linear mechanical system is given by:

$$\mathbf{M}\ddot{\mathbf{y}}(t) + \mathbf{P}\dot{\mathbf{y}}(t) + \mathbf{Q}\mathbf{y}(t) = \mathbf{h}(t), \mathbf{M} = \mathbf{M}^T, \mathbf{x} \neq \mathbf{0} \Rightarrow \mathbf{x}^T \mathbf{M} \mathbf{x} > 0 \quad (3.0.1)$$

For the matrices, it is valid:

$$\mathbf{M} = \mathbf{M}^T, \mathbf{x} \neq \mathbf{0} \Rightarrow \mathbf{x}^T \mathbf{M} \mathbf{x} > 0, \mathbf{P} = \mathbf{D} + \mathbf{G}, \mathbf{D} = \mathbf{D}^T, \mathbf{G} = -\mathbf{G}^T, \mathbf{Q} = \mathbf{K} + \mathbf{N}, \mathbf{K} = \mathbf{K}^T, \mathbf{N} = -\mathbf{N}^T \quad (3.0.2)$$

The equation of motion for a linear cyclic system have the same structure as the one for an ordinary linear mechanical system:

$$\mathbf{M}_C \ddot{\mathbf{y}}_C(t) + \mathbf{P}_C \dot{\mathbf{y}}_C(t) + \mathbf{Q}_C \mathbf{y}_C(t) = \mathbf{h}_C(t) \quad (3.0.3)$$

Here and in the following, the index C is used to denote the vectors and matrices for a cyclic system. The vector $\mathbf{y}_C(t)$, which describes the current displacements, has the following structure:

$$\mathbf{y}_C(t) = \begin{bmatrix} \mathbf{y}^{(0)}(t) \\ \mathbf{y}^{(1)}(t) \\ \vdots \\ \mathbf{y}^{(n-1)}(t) \end{bmatrix} \quad (3.0.4)$$

The subvector $\mathbf{y}^{(j)}(t)$ describes the displacements for the j -th segment; it is of order N_S . Since the cyclic structure consists of n identical segments, the vector $\mathbf{y}_C(t)$ is of order $n \cdot N_S$. The properties of the matrices \mathbf{M}_C , \mathbf{P}_C and \mathbf{Q}_C are exemplified for the matrix \mathbf{Q}_C ; this matrix has the following structure:

$$\mathbf{Q}_C = \begin{bmatrix} \mathbf{Q}^{(0)} & \mathbf{Q}^{(1)} & \mathbf{0} & \dots & \mathbf{0} & \mathbf{Q}^{(-1)} \\ \mathbf{Q}^{(-1)} & \mathbf{Q}^{(0)} & \mathbf{Q}^{(1)} & \dots & \mathbf{0} & \mathbf{0} \\ \mathbf{0} & \mathbf{Q}^{(-1)} & \mathbf{Q}^{(0)} & \ddots & \mathbf{0} & \mathbf{0} \\ \vdots & \vdots & \ddots & \ddots & \ddots & \vdots \\ \mathbf{0} & \mathbf{0} & \mathbf{0} & \ddots & \mathbf{Q}^{(0)} & \mathbf{Q}^{(1)} \\ \mathbf{Q}^{(1)} & \mathbf{0} & \mathbf{0} & \dots & \mathbf{Q}^{(-1)} & \mathbf{Q}^{(0)} \end{bmatrix} \quad (3.0.5)$$

For the matrices \mathbf{M}_C and \mathbf{P}_C the submatrices $\mathbf{Q}^{(l)}$ have to be replaced by the related submatrices $\mathbf{M}^{(l)}$ and $\mathbf{P}^{(l)}$, respectively. The submatrices $\mathbf{Q}^{(l)}$, $\mathbf{P}^{(l)}$ and $\mathbf{M}^{(l)}$ are of order $N_S \times N_S$; thereby, the matrices \mathbf{Q}_C , \mathbf{P}_C and \mathbf{M}_C are of order $(n \cdot N_S) \times (n \cdot N_S)$.

In a cyclic system the n segments are arranged in a circular way, so that the zeroth and the n -th element are identical. Because of this, it is rather obvious to describe the cyclic system by a Fourier series, since this description is very useful for periodic functions. Therefore, the main characteristics of Fourier series shall be considered in the following section 3.1. In the section 3.2, the discrete Fourier series is used to describe the motions for the individual segments, which form the cyclic structure; based on this, a transformation, which enables a very efficient formulation of the linear cyclic system, will be developed. The modal decomposition is an established method of analyzing linear systems and reducing the computational effort for their evaluation; in the section 3.3, this method will be described and subsequently applied to the linear cyclic system. The most important results will finally be concluded and discussed in the section 3.4; in this section, also practical aspects of the computation will be addressed.

As already mentioned, a cyclic system consists of $n > 2$ circularly arranged identical segments. Here, n is a natural number, i.e. $n \in \mathbb{N}$. Furthermore, the following relation, which will be used several times in this work, is valid:

$$n > 2 \Rightarrow 0 < \frac{1}{n} < \frac{1}{2} \Rightarrow -\frac{1}{2} < -\frac{1}{n} < 0 \quad (3.0.6)$$

In the present work the matrices \mathbf{M}_C , \mathbf{P}_C and \mathbf{Q}_C are assumed to be real matrices; therefore, their submatrices $\mathbf{M}^{(l)}$, $\mathbf{P}^{(l)}$ and $\mathbf{Q}^{(l)}$ are real matrices, too. Nevertheless, in the following considerations complex numbers will be used in the context of Fourier series since they provide a very compact formulation. Therefore, some relations, which are applied several times, shall briefly be summarized here; these relations are derived in the appendix A.2. A complex number $z \in \mathbb{C}$ can be expressed in the following way.

$$z = a + ib = \Re z + i\Im z, \quad \Re z = a, \quad \Im z = b, \quad a, b \in \mathbb{R} \quad (3.0.7)$$

Here, $\Re z$ and $\Im z$ denote the real part and the imaginary part, respectively, of z . The complex conjugate \bar{z} of a complex number z is obtained by changing the sign of the imaginary part.

$$\bar{z} = \Re z - i\Im z \quad (3.0.8)$$

As it is shown in the appendix A.2, the conjugation on the one hand and the addition, the subtraction and the multiplication of complex numbers on the other hand can be carried out independently; therefore, it is valid:

$$z_1, z_2, z_3, z_4 \in \mathbb{C} : \overline{z_1 z_2 + z_3 z_4} = \bar{z}_1 \bar{z}_2 + \bar{z}_3 \bar{z}_4, \quad \overline{z_1 z_2 - z_3 z_4} = \bar{z}_1 \bar{z}_2 - \bar{z}_3 \bar{z}_4 \quad (3.0.9)$$

The addition and multiplication of matrices is defined by appropriate additions and multiplications of their coefficients. Based on (3.0.9) it is therefore valid for the linear combination of two matrices \mathbf{A} and \mathbf{B} , which uses the scalar factors c and d :

$$c, d \in \mathbb{C}, \mathbf{A}, \mathbf{B} \in \mathbb{C}^{N \times P} : \overline{c\mathbf{A} + d\mathbf{B}} = \bar{c}\bar{\mathbf{A}} + \bar{d}\bar{\mathbf{B}} \quad (3.0.10)$$

Also based on (3.0.9), it is valid for the multiplication and addition of the matrices \mathbf{A} , \mathbf{B} , \mathbf{X} and \mathbf{Y} :

$$\mathbf{A}, \mathbf{B} \in \mathbb{C}^{N \times P}, \mathbf{X}, \mathbf{Y} \in \mathbb{C}^{P \times Q} : \overline{\mathbf{A}\mathbf{X} + \mathbf{B}\mathbf{Y}} = \bar{\mathbf{A}}\bar{\mathbf{X}} + \bar{\mathbf{B}}\bar{\mathbf{Y}} \quad (3.0.11)$$

3.1 Fourier series

A Fourier series describes a function $f(x)$ by a linear combination of trigonometric functions. For the following considerations, the properties of the exponential function and its relation to the trigonometric functions play an essential role. The mathematical basics are presented and discussed in the appendix A.3; here, only the results shall be given. According to Euler's formula it is valid for an exponential function with an imaginary exponent:

$$\phi \in \mathbb{R} : e^{i\phi} = \cos \phi + i \sin \phi \Rightarrow \Re e^{i\phi} = \cos \phi, \Im e^{i\phi} = \sin \phi \quad (3.1.12)$$

Here and in the following, the argument ϕ is generally assumed to be a real number, i.e. $\phi \in \mathbb{R}$. For the complex conjugate of $e^{i\phi}$ it is valid:

$$e^{-i\phi} = \overline{e^{i\phi}} = \cos \phi - i \sin \phi \quad (3.1.13)$$

By solving the sum and the difference of the relations (3.1.12) and (3.1.13) the cosine function and the sine function can be expressed in the following way:

$$\cos \phi = \frac{e^{i\phi} + e^{-i\phi}}{2}, \sin \phi = \frac{e^{i\phi} - e^{-i\phi}}{2i} = i \frac{e^{-i\phi} - e^{i\phi}}{2} \quad (3.1.14)$$

For the exponential function it is valid:

$$m \in \mathbb{Z} \Leftrightarrow e^{2\pi m i} = \underbrace{\cos(2\pi m)}_1 + i \underbrace{\sin(2\pi m)}_0 = 1 \quad (3.1.15)$$

Based on this, it can be derived:

$$m \in \mathbb{Z} : 1 = e^{2\pi i m} \Rightarrow e^{im\phi} = e^{im\phi} e^{2\pi i m} = e^{im\phi + 2\pi i m} = e^{im(\phi + 2\pi)} \quad (3.1.16)$$

$$\Rightarrow \cos(m(\phi + 2\pi)) = \Re e^{im(\phi + 2\pi)} = \Re e^{im\phi} = \cos(m\phi) \quad (3.1.17)$$

$$\Rightarrow \sin(m(\phi + 2\pi)) = \Im e^{im(\phi + 2\pi)} = \Im e^{im\phi} = \sin(m\phi) \quad (3.1.18)$$

3.1.1 Continuous Fourier series

A Fourier series describes a function $f(\phi)$ by a linear combination of trigonometric functions having different periodicities k :

$$f(\phi) = A_0 + \sum_{K=1}^{\infty} [A_K \cos(K\phi) + B_K \sin(K\phi)], \phi \in \mathbb{R}, f(\phi), A_K, B_K \in \mathbb{C}, K \in \mathbb{Z} \quad (3.1.19)$$

As shown in (3.1.17) and (3.1.18) the functions $\cos(K\phi)$ and $\sin(K\phi)$ are periodic with period 2π :

$$k \in \mathbb{Z} : \cos(K(\phi + 2\pi)) = \cos(K\phi), \quad \sin(K(\phi + 2\pi)) = \sin(K\phi) \quad (3.1.20)$$

Thereby, also their linear combination describing the function $f(\phi)$ is periodic with period 2π , i.e. $f(\phi + 2\pi) = f(\phi)$.

By applying the relations according to (3.1.14) the expression contained in the bracket of (3.1.19) can be reformulated in the following way:

$$\begin{aligned} K \neq 0 : A_K \cos(K\phi) + B_K \sin(K\phi) &= A_K \frac{e^{iK\phi} + e^{-iK\phi}}{2} + B_K \frac{e^{iK\phi} - e^{-iK\phi}}{2i} \\ &= \underbrace{\left(\frac{A_K}{2} + \frac{B_K}{2i} \right)}_{C_K} e^{iK\phi} + \underbrace{\left(\frac{A_K}{2} - \frac{B_K}{2i} \right)}_{C_{-K}} e^{-iK\phi} \end{aligned} \quad (3.1.21)$$

Thereby, the new Fourier coefficients C_K and C_{-K} are defined. The relations between C_K , C_{-K} , A_K and B_K are obtained to:

$$C_K = \frac{A_K}{2} + \frac{B_K}{2i}, \quad C_{-K} = \frac{A_K}{2} - \frac{B_K}{2i} \Rightarrow C_K + C_{-K} = A_K, \quad C_K - C_{-K} = \frac{B_K}{i} \Rightarrow B_K = i(C_K - C_{-K}) \quad (3.1.22)$$

The coefficients C_K and C_{-K} can be simplified in the following way:

$$1 = -i^2 \Rightarrow i^{-1} = -i \Rightarrow C_K = \frac{A_K}{2} + \frac{B_K}{2i} = \frac{A_K}{2} - i \frac{B_K}{2}, \quad C_{-K} = \frac{A_K}{2} - \frac{B_K}{2i} = \frac{A_K}{2} + i \frac{B_K}{2} \quad (3.1.23)$$

In total, it is valid for the relations between C_K and C_{-K} on the one hand and A_K and B_K on the other hand:

$$C_K = \frac{A_K - iB_K}{2}, \quad C_{-K} = \frac{A_K + iB_K}{2}, \quad A_K = C_K + C_{-K}, \quad B_K = i(C_K - C_{-K}) \quad (3.1.24)$$

By defining

$$C_0 = A_0 \quad (3.1.25)$$

and applying the following transformation of a sum, which is derived in the appendix A.1:

$$\sum_{K=-\hat{K}}^{\hat{K}} X_K = X_0 + \sum_{K=1}^{\hat{K}} (X_K + X_{-K}) \quad (3.1.26)$$

the Fourier series can be formulated in a very compact way:

$$\begin{aligned} f(\phi) &= A_0 + \sum_{K=1}^{\infty} (A_K \cos(K\phi) + B_K \sin(K\phi)) \\ &= \underbrace{C_0 e^{i \cdot 0 \cdot \phi}}_1 + \sum_{K=1}^{\infty} (C_K e^{iK\phi} + C_{-K} e^{-iK\phi}) = \sum_{K=-\infty}^{\infty} C_K e^{iK\phi} \end{aligned} \quad (3.1.27)$$

It can be shown that the coefficients C_K are uniquely defined for a given function $f(\phi)$. In this context, the orthogonality of the exponential functions is an essential property. In order to consider this, the integral of the product of two functions $e^{iK\phi}$ and $e^{iL\phi}$ over one period $0 \leq x \leq 2\pi$ has to be considered:

$$\int_0^{2\pi} e^{iK\phi} e^{iL\phi} d\phi = \int_0^{2\pi} e^{i(K+L)\phi} d\phi \quad (3.1.28)$$

For the evaluation of the integral two cases have to be distinguished. For $K + L = 0$ it is valid:

$$K + L = 0 \Rightarrow e^{i(K+L)\phi} = e^{i \cdot 0 \cdot \phi} = e^0 = 1 \Rightarrow \int_0^{2\pi} e^{i(K+L)\phi} d\phi = \int_0^{2\pi} d\phi = 2\pi \quad (3.1.29)$$

For $K + L \neq 0$ it is obtained:

$$\int_0^{2\pi} e^{i(K+L)\phi} d\phi = \left. \frac{e^{i(K+L)\phi}}{i(K+L)} \right|_0^{2\pi} = \frac{e^{2\pi i(K+L)} - e^{i(K+L) \cdot 0}}{i(K+L)} = \frac{e^{2\pi i(K+L)} - e^0}{i(K+L)} = \frac{e^{2\pi i(K+L)} - 1}{i(K+L)} \quad (3.1.30)$$

Since K and L are integers, their sum $K + L$ is an integer, too. By applying the relation (3.1.15), the integral (3.1.30) can be evaluated:

$$K, L \in \mathbb{Z} \Rightarrow K + L \in \mathbb{Z} \Rightarrow e^{2\pi i(K+L)} = 1 \Rightarrow \int_0^{2\pi} e^{i(K+L)\phi} d\phi = \frac{e^{2\pi i(K+L)} - 1}{i(K+L)} = \frac{1 - 1}{i(K+L)} = 0 \quad (3.1.31)$$

In total, it is valid:

$$\int_0^{2\pi} e^{i(K+L)\phi} d\phi = \begin{cases} 2\pi & \text{for } K + L = 0 \Leftrightarrow K = -L \\ 0 & \text{for } K + L \neq 0 \Leftrightarrow K \neq -L \end{cases} \quad (3.1.32)$$

Multiplying the equation (3.1.27) by $e^{iL\phi}$, $L \in \mathbb{Z}$, rearranging it and applying the relation (3.1.32) leads to:

$$\int_0^{2\pi} f(\phi) e^{iL\phi} d\phi = \int_0^{2\pi} \left(\sum_{K=-\infty}^{\infty} C_K e^{iK\phi} e^{iL\phi} \right) d\phi = \sum_{K=-\infty}^{\infty} C_K \int_0^{2\pi} e^{i(K+L)\phi} d\phi = 2\pi C_{-L} \quad (3.1.33)$$

Solving this relation to C_{-L} and using the substitution $K = -L$ leads to:

$$\int_0^{2\pi} f(\phi) e^{iL\phi} d\phi = 2\pi C_{-L} \Rightarrow C_{-L} = \frac{1}{2\pi} \int_0^{2\pi} f(\phi) e^{iL\phi} d\phi \Rightarrow C_K = \frac{1}{2\pi} \int_0^{2\pi} f(\phi) e^{-iK\phi} d\phi \quad (3.1.34)$$

This result indicates that the Fourier coefficient C_K is uniquely defined for a given function $f(\phi)$ and a given periodicity $K \in \mathbb{Z}$.

3.1.2 Discrete Fourier series

A discrete Fourier series is obtained if the function $f(\phi)$ is evaluated only for $n \in \mathbb{N}$ discrete values ϕ_j , $j \in \{\mathbb{N}_0 \mid 0 \leq j \leq n-1\}$. Although there is in principle no restriction with respect to the selection of the values for ϕ_j , it is nevertheless reasonable to choose n equidistant values within the interval $\phi_0 \leq \phi_j < \phi_0 + 2\pi$, whereas the length of the interval results from the periodicity of the function $f(\phi)$ with period 2π :

$$\phi_j = \phi_0 + \frac{2\pi}{n} j, \quad n \in \mathbb{N}, \quad j \in \{\mathbb{N}_0 \mid 0 \leq j \leq n-1\}, \quad \phi_0 \in \mathbb{R} \quad (3.1.35)$$

Inserting the discrete values ϕ_j into the the Fourier series given by (3.1.27) leads to:

$$f(\phi_j) = \sum_{K=-\infty}^{\infty} C_K e^{iK\phi_j} = \sum_{K=-\infty}^{\infty} C_K e^{iK(\phi_0 + \frac{2\pi}{n}j)} = \sum_{K=-\infty}^{\infty} C_K e^{iK\phi_0} e^{iK\frac{2\pi}{n}j} = \sum_{K=-\infty}^{\infty} C_K e^{iK\phi_0} \left(e^{\frac{2\pi}{n}i}\right)^{Kj} \quad (3.1.36)$$

For the sake of brevity and of a better overview the root of unity ζ will be used in the following. The root of unity is defined by:

$$\zeta = e^{\frac{2\pi}{n}i} \quad (3.1.37)$$

Based on the relation (3.1.15), the following relation, which will be used several times in this work, can be derived:

$$p \in \mathbb{Z} \Leftrightarrow 1 = e^{2\pi pi} = e^{\frac{2\pi}{n}pni} = \left(e^{\frac{2\pi}{n}i}\right)^{pn} = \zeta^{pn} \quad (3.1.38)$$

Using the definition of the root of unity ζ according to (3.1.37) the discrete Fourier series can be formulated in the following way:

$$e^{iK\frac{2\pi}{n}j} = \left(e^{\frac{2\pi}{n}i}\right)^{Kj} = \zeta^{Kj} \Rightarrow f_j = f(\phi_j) = \sum_{K=-\infty}^{\infty} C_K e^{iK\phi_0} e^{iK\frac{2\pi}{n}j} = \sum_{K=-\infty}^{\infty} C_K e^{iK\phi_0} \zeta^{Kj} \quad (3.1.39)$$

By applying (3.1.38) it can be derived:

$$M, j \in \mathbb{Z} \Rightarrow M \cdot j \in \mathbb{Z} \Rightarrow \zeta^{Mjn} = \zeta^{Mnj} = 1 \Rightarrow \zeta^{Kj} = \zeta^{Kj} \zeta^{Mnj} = \zeta^{(K+Mn)j} \quad (3.1.40)$$

Apparently, the value $\zeta^{(K+Mn)j}$, $M \in \mathbb{Z}$, does not depend on M . Therefore, it is reasonable to express the periodicity K in the following way by using a basic periodicity k and an integer m .

$$K = k + mn, K, k, m \in \mathbb{Z} \Rightarrow \zeta^{Kj} = \zeta^{(k+mn)j} = \zeta^{kj} \underbrace{\zeta^{mnj}}_1 \quad (3.1.41)$$

In order to assign a unique value for the basic periodicity k to each periodicity K , an interval for k has to be defined:

$$k_{\min} \leq k \leq k_{\max}, k_{\min}, k_{\max} \in \mathbb{Z} \quad (3.1.42)$$

The bounds k_{\min} and k_{\max} have to be defined in such a way that for $m \neq 0$ a periodicity $K = k + mn$ lies outside the interval. This is achieved by the following relation between the bounds k_{\min} and k_{\max} :

$$k_{\min} + n = k_{\max} + 1 \Leftrightarrow k_{\min} = k_{\max} + 1 - n \Leftrightarrow k_{\min} + n - 1 = k_{\max} \quad (3.1.43)$$

As long as this condition is fulfilled, the bounds k_{\min} and k_{\max} can be chosen arbitrarily. This will be considered later.

By using the formulation $K = k + mn$ the discrete Fourier series according to (3.1.39) is reformulated in the following way:

$$\begin{aligned} f_j &= \sum_{K=-\infty}^{\infty} C_K e^{iK\phi_0} \zeta^{Kj} = \sum_{k=k_{\min}}^{k_{\max}} \sum_{m=-\infty}^{\infty} C_{k+mn} e^{i(k+mn)\phi_0} \underbrace{\zeta^{(k+mn)j}}_{\zeta^{kj}} \\ &= \sum_{k=k_{\min}}^{k_{\max}} \underbrace{\left[\sum_{m=-\infty}^{\infty} C_{k+mn} e^{i(k+mn)\phi_0} \right]}_{c_k} \zeta^{kj} = \sum_{k=k_{\min}}^{k_{\max}} c_k \zeta^{kj} \end{aligned} \quad (3.1.44)$$

While the continuous Fourier series can be a sum of an infinite number of terms, the discrete Fourier series only consists of a limited number n of terms. Therefore, the relation between the values f_j and the coefficients c_k can be formulated as a system of linear equations:

$$\underbrace{\begin{bmatrix} f_0 \\ \vdots \\ f_j \\ \vdots \\ f_{n-1} \end{bmatrix}}_{\mathbf{f}} = \underbrace{\begin{bmatrix} \zeta^{k_{\min} \cdot 0} & \dots & \zeta^{k \cdot 0} & \dots & \zeta^{k_{\max} \cdot 0} \\ \vdots & & \vdots & & \vdots \\ \zeta^{k_{\min} \cdot j} & \dots & \zeta^{k \cdot j} & \dots & \zeta^{k_{\max} \cdot j} \\ \vdots & & \vdots & & \vdots \\ \zeta^{k_{\min} \cdot (n-1)} & \dots & \zeta^{k \cdot (n-1)} & \dots & \zeta^{k_{\max} \cdot (n-1)} \end{bmatrix}}_{\mathbf{T}} \underbrace{\begin{bmatrix} c_{k_{\min}} \\ \vdots \\ c_k \\ \vdots \\ c_{k_{\max}} \end{bmatrix}}_{\mathbf{c}} \quad (3.1.45)$$

As it has been done for the continuous Fourier series in the previous section 3.1.1, the orthogonality of the functions used for the Fourier series shall also be considered here. Since the function ζ^{kj} is only evaluated for a finite number of points defined by j , it is obvious to arrange the powers ζ^{kj} for the periodicity k in a vector \mathbf{t}_k ; thereby, the transformation matrix \mathbf{T} can be described by arranging the vectors \mathbf{t}_k for $k_{\min} \leq k \leq k_{\max}$ as column vectors.

$$\mathbf{t}_k = \begin{bmatrix} \zeta^{k \cdot 0} \\ \vdots \\ \zeta^{k \cdot j} \\ \vdots \\ \zeta^{k \cdot (n-1)} \end{bmatrix} \Rightarrow \mathbf{T} = [\mathbf{t}_{k_{\min}} \quad \dots \quad \mathbf{t}_k \quad \dots \quad \mathbf{t}_{k_{\max}}] \quad (3.1.46)$$

In order to consider the orthogonality, the scalar product of two vectors \mathbf{t}_k and \mathbf{t}_l has to be evaluated:

$$\mathbf{t}_k^H \mathbf{t}_l = \overline{\mathbf{t}_k}^T \mathbf{t}_l \quad (3.1.47)$$

Since the vector \mathbf{t}_k is complex, the Hermitian transposition $\mathbf{z}^H = \overline{\mathbf{z}}^T$ is used instead of the “normal” transposition \mathbf{z}^T according to Strang [71]. One reason given by Strang is the following: The module of a real vector \mathbf{x} is obtained in the following way:

$$\mathbf{x}^T = [x_1 \quad x_2 \quad \dots \quad x_n] \Rightarrow |\mathbf{x}| = \sqrt{\mathbf{x}^T \mathbf{x}} = \sqrt{x_1^2 + x_2^2 + \dots + x_n^2} \quad (3.1.48)$$

The application of this rule to a complex vector \mathbf{z} , however, may lead to an apparently wrong result, as it can be seen from the following example:

$$\mathbf{z} = \begin{bmatrix} 1 \\ i \end{bmatrix} \Rightarrow \mathbf{z}^T = [1 \quad i] \Rightarrow \sqrt{\mathbf{z}^T \mathbf{z}} = \sqrt{1^2 + i^2} = \sqrt{1 - 1} = 0 \quad (3.1.49)$$

According to this, the module $|\mathbf{z}|$ of the vector \mathbf{z} would be zero. Based on the rule for the absolute value $|z|$ of a complex number z , which is derived in the appendix A.2:

$$|z| = \sqrt{z \overline{z}} = \sqrt{(\Re z)^2 + (\Im z)^2} \quad (3.1.50)$$

the scalar product $\mathbf{z}^H \mathbf{z}$ using the Hermitian transposition leads to the following correct result:

$$\mathbf{z} = \begin{bmatrix} 1 \\ i \end{bmatrix} \Rightarrow \mathbf{z}^H = [1 \quad -i] \Rightarrow |\mathbf{z}| = \sqrt{\mathbf{z}^H \mathbf{z}} = \sqrt{1^2 - i^2} = \sqrt{1 + 1} = \sqrt{2} \quad (3.1.51)$$

For the Hermitian transpose \mathbf{t}_k^H the complex conjugate $\overline{\zeta^{kj}}$ is required. Based on the relation (3.1.13) it is valid:

$$\overline{e^{i\phi}} = e^{-i\phi} \Rightarrow \overline{\zeta^{kj}} = \overline{e^{\frac{2\pi}{n}ikj}} = e^{-\frac{2\pi}{n}ikj} = \zeta^{-kj} \quad (3.1.52)$$

Thereby, the scalar product of the two vectors \mathbf{t}_k and \mathbf{t}_l can be formulated:

$$\mathbf{t}_k^H \mathbf{t}_l = \begin{bmatrix} \zeta^{-k \cdot 0} & \dots & \zeta^{-k \cdot j} & \dots & \zeta^{-k \cdot (n-1)} \end{bmatrix} \begin{bmatrix} \zeta^{l \cdot 0} \\ \vdots \\ \zeta^{l \cdot j} \\ \vdots \\ \zeta^{l \cdot (n-1)} \end{bmatrix} = \sum_{j=0}^{n-1} \zeta^{-k \cdot j} \zeta^{l \cdot j} = \sum_{j=0}^{n-1} \zeta^{(-k+l) \cdot j} \quad (3.1.53)$$

It will turn out later that the evaluation of a sum of this kind is fundamental in the context of cyclic systems; therefore, this problem shall be considered in a more generalized way by using the power ζ^{pj} , $p \in \mathbb{Z}$, from which the expression (3.1.53) can be derived as a special case $p = -k + l$. For the evaluation, the following rule for a geometric series, which is derived in the appendix A.6 is used:

$$\sum_{j=0}^{n-1} q^j = \begin{cases} \frac{1-q^n}{1-q} & \text{for } q \neq 1 \wedge q \neq 0 \\ n & \text{for } q = 1 \end{cases} \quad (3.1.54)$$

By reformulating the power ζ^{pj} and setting $\zeta^p = q$ it is obtained based on (3.1.54):

$$\sum_{j=0}^{n-1} \zeta^{pj} = \sum_{j=0}^{n-1} (\zeta^p)^j = \begin{cases} \frac{1-(\zeta^p)^n}{1-\zeta^p} & \text{for } \zeta^p \neq 1 \wedge \zeta^p \neq 0 \\ n & \text{for } \zeta^p = 1 \end{cases} \quad (3.1.55)$$

Based on the relation (3.1.38) the numerator can be evaluated immediately; since p is an integer, it is valid:

$$p \in \mathbb{Z} : \zeta^{pn} = 1 \Rightarrow 1 - (\zeta^p)^n = 1 - \zeta^{pn} = 1 - 1 = 0 \quad (3.1.56)$$

Transforming the power ζ^p leads to:

$$\zeta^p = \left(e^{\frac{2\pi}{n}i} \right)^p = e^{2\pi i \frac{p}{n}} \quad (3.1.57)$$

Here, it becomes evident that the case $\zeta^p = 0$ cannot occur so that the requirement $\zeta^p \neq 0$ can be omitted in the following. According to (3.1.15), it is valid:

$$m \in \mathbb{Z} \Leftrightarrow e^{2\pi i m} = 1 \quad (3.1.58)$$

Applying this relation to the power ζ^p leads to:

$$\frac{p}{n} \in \mathbb{Z} \Leftrightarrow \zeta^p = e^{2\pi i \frac{p}{n}} = 1 \quad (3.1.59)$$

As discussed in the appendix A.3, where the relation (3.1.58) is derived, the deduction can be made in both directions. In the present case this means that the case $q = \zeta^p = 1$ occurs if and only if the quotient $\frac{p}{n}$ is an integer. Thereby, the evaluation of the sum over j leads to the following result:

$$\sum_{j=0}^{n-1} \zeta^{pj} = \sum_{j=0}^{n-1} e^{2\pi i \frac{p}{n}j} = \begin{cases} 0 & \text{for } \frac{p}{n} \notin \mathbb{Z} \\ n & \text{for } \frac{p}{n} \in \mathbb{Z} \end{cases} \quad (3.1.60)$$

The result indicates that the sum is either equal to n or vanishes, i.e. for a given n there are only two possible results; this corresponds to the orthogonality relation for the functions e^{iKx} , which has been considered for the continuous Fourier series in the previous section 3.1.1. However, in contrast to the continuous Fourier series, where the periodicity K is unlimited, the periodicity k used in the discrete Fourier series is limited by the bounds k_{\min} and k_{\max} . Therefore, the pairs $\langle k, l \rangle$, for which the scalar product $\mathbf{t}_k^H \mathbf{t}_l$ does not vanish, have to fulfil three conditions; the first two are determined by the range of the periodicity and the third one results from the condition according to (3.1.60):

$$k_{\min} \leq k \leq k_{\max} \wedge k_{\min} \leq l \leq k_{\max} \wedge \frac{-k+l}{n} \in \mathbb{Z} \Rightarrow \mathbf{t}_k^H \mathbf{t}_l = n \neq 0 \quad (3.1.61)$$

Since the third condition contains the expression $-k+l$, its range has to be determined first. To this end, the range of k is reformulated:

$$k_{\min} \leq k \leq k_{\max} \Leftrightarrow -k_{\min} \geq -k \geq -k_{\max} \quad (3.1.62)$$

Combining this with the range of l leads to

$$-k_{\max} \leq -k \leq -k_{\min} \wedge k_{\min} \leq l \leq k_{\max} \Rightarrow -k_{\max} + k_{\min} \leq -k + l \leq -k_{\min} + k_{\max} \quad (3.1.63)$$

The relation between k_{\min} and k_{\max} according to (3.1.43) is transformed in the following way:

$$k_{\min} + n = k_{\max} + 1 \Rightarrow n - 1 = k_{\max} - k_{\min} \quad (3.1.64)$$

Since n is a natural number, it is positive so that dividing an inequation by n does not change the relations. Therefore, inserting the relation (3.1.64) into (3.1.63) and dividing the result by n leads to:

$$-k_{\max} + k_{\min} = -n + 1 \leq -k + l \leq -k_{\min} + k_{\max} = n - 1 \Rightarrow -1 + \frac{1}{n} \leq \frac{-k+l}{n} \leq 1 - \frac{1}{n} \quad (3.1.65)$$

Also from $n \in \mathbb{N}$ it can be derived:

$$n \in \mathbb{N} \Rightarrow n \geq 1 \Rightarrow 0 < \frac{1}{n} \leq 1 \Rightarrow -1 < -1 + \frac{1}{n} \leq 0 \Rightarrow 1 > 1 - \frac{1}{n} \geq 0 \quad (3.1.66)$$

Thereby, the range of the quotient $\frac{-k+l}{n}$ is finally determined:

$$-1 < -1 + \frac{1}{n} \leq \frac{-k+l}{n} \leq 1 - \frac{1}{n} < 1 \Rightarrow -1 < \frac{-k+l}{n} < 1 \quad (3.1.67)$$

Based on this, the condition (3.1.61) can be formulated in the following way:

$$-1 < \frac{-k+l}{n} < 1 \wedge \frac{-k+l}{n} \in \mathbb{Z} \Rightarrow \mathbf{t}_k^H \mathbf{t}_l = n \neq 0 \quad (3.1.68)$$

Apparently, in the range $-1 < M < 1$, $M = 0$ is the only integer $M \in \mathbb{Z}$. Thereby, it is valid:

$$-1 < \frac{-k+l}{n} < 1 \wedge \frac{-k+l}{n} \in \mathbb{Z} \Rightarrow \frac{-k+l}{n} = 0 \Rightarrow k = l \Rightarrow \mathbf{t}_k^H \mathbf{t}_k = n \neq 0 \quad (3.1.69)$$

Conversely, this means based on (3.1.60) that for $k \neq l$ the scalar product $\mathbf{t}_k^H \mathbf{t}_l$ vanishes. In total it is valid:

$$k_{\min} \leq k \leq k_{\max} \wedge k_{\min} \leq l \leq k_{\max} : \mathbf{t}_k^H \mathbf{t}_l = \sum_{j=0}^{n-1} \zeta^{(-k+l)j} = \begin{cases} 0 & \text{for } k \neq l \\ n & \text{for } k = l \end{cases} \quad (3.1.70)$$

This shows that the column vectors \mathbf{t}_k and \mathbf{t}_l , $k \neq l$, are orthogonal. Based on (3.1.70), it is obtained for the matrix product $\mathbf{T}^H \mathbf{T}$:

$$\mathbf{T}^H \mathbf{T} = \begin{bmatrix} \mathbf{t}_{k_{\min}}^H \\ \vdots \\ \mathbf{t}_k^H \\ \vdots \\ \mathbf{t}_{k_{\max}}^H \end{bmatrix} \begin{bmatrix} \mathbf{t}_{k_{\min}} & \cdots & \mathbf{t}_l & \cdots & \mathbf{t}_{k_{\max}} \end{bmatrix} = \begin{bmatrix} n & 0 & \cdots & 0 & 0 \\ 0 & n & \ddots & 0 & 0 \\ \vdots & \ddots & \ddots & \ddots & \vdots \\ 0 & 0 & \ddots & n & 0 \\ 0 & 0 & \cdots & 0 & n \end{bmatrix} = n \mathbf{I} \Rightarrow \frac{1}{n} \mathbf{T}^H = \mathbf{T}^{-1} \quad (3.1.71)$$

Thereby, the inverse matrix \mathbf{T}^{-1} is determined; it is valid:

$$\mathbf{f} = \mathbf{T} \mathbf{c} \Rightarrow \mathbf{c} = \mathbf{T}^{-1} \mathbf{f} = \frac{1}{n} \mathbf{T}^H \mathbf{f} \quad (3.1.72)$$

The existence of \mathbf{T}^{-1} proves that for n given values f_j vector contained in the vector \mathbf{f} the coefficients c_k of the discrete Fourier series, which form the vector \mathbf{c} , are uniquely defined. By inserting the matrix \mathbf{T} according to (3.1.45) into (3.1.72) and by applying the relation $\overline{\zeta^{kj}} = \zeta^{-kj}$ derived in (3.1.52) it is obtained:

$$\underbrace{\begin{bmatrix} c_{k_{\min}} \\ \vdots \\ c_k \\ \vdots \\ c_{k_{\max}} \end{bmatrix}}_{\mathbf{c}} = \frac{1}{n} \underbrace{\begin{bmatrix} \zeta^{-k_{\min} \cdot 0} & \cdots & \zeta^{-k_{\min} \cdot j} & \cdots & \zeta^{-k_{\min} \cdot (n-1)} \\ \vdots & & \vdots & & \vdots \\ \zeta^{-k \cdot 0} & \cdots & \zeta^{-k \cdot j} & \cdots & \zeta^{-k \cdot (n-1)} \\ \vdots & & \vdots & & \vdots \\ \zeta^{-k_{\max} \cdot 0} & \cdots & \zeta^{-k_{\max} \cdot j} & \cdots & \zeta^{-k_{\max} \cdot (n-1)} \end{bmatrix}}_{\mathbf{T}^H = \overline{\mathbf{T}}^T} \underbrace{\begin{bmatrix} f_0 \\ \vdots \\ f_j \\ \vdots \\ f_{n-1} \end{bmatrix}}_{\mathbf{f}} \Rightarrow c_k = \frac{1}{n} \left(\sum_{j=0}^{n-1} f_j \zeta^{-kj} \right) \quad (3.1.73)$$

Thereby, the determination of the coefficients c_k for the given values f_j is obtained.

3.1.3 Fourier series for real functions

In the previous sections 3.1.1 the description of a function $f(\phi)$ by a continuous Fourier series has been developed; from this the description of the values $f_j = f(\phi_j)$ for discrete equidistant arguments ϕ_j by a discrete Fourier series has been derived in 3.1.2. Here, the arguments ϕ and ϕ_j were assumed to be real numbers, while the function $f(\phi)$ was assumed to be complex. Since set of the real numbers \mathbb{R} is a subset of the set of the complex numbers \mathbb{C} , the methods described in the sections 3.1.1 and 3.1.2 can also be applied to a real function $f(\phi) \in \mathbb{R}$. This case shall be considered in the following.

In the section 3.1.1 the following two formulations of a continuous Fourier series have been shown:

$$f(\phi) = A_0 + \sum_{K=1}^{\infty} [A_K \cos(K\phi) + B_K \sin(K\phi)] = \sum_{K=-\infty}^{\infty} C_K e^{iK\phi}, \quad \phi \in \mathbb{R}, \quad K \in \mathbb{Z} \quad (3.1.74)$$

For a given function $f(\phi)$ the coefficients C_K are obtained according to the following relation:

$$C_K = \frac{1}{2\pi} \int_0^{2\pi} f(\phi) e^{-iK\phi} d\phi \quad (3.1.75)$$

The variable ϕ and the fraction $\frac{1}{2\pi}$ are real numbers so that they are not affected by the conjugation. By applying the relation (3.1.13) it is obtained for the complex conjugate $\overline{C_K}$:

$$\overline{C_K} = \overline{\frac{1}{2\pi} \int_0^{2\pi} f(\phi) e^{-iK\phi} d\phi} = \frac{1}{2\pi} \int_0^{2\pi} \overline{f(\phi) e^{-iK\phi}} d\phi = \frac{1}{2\pi} \int_0^{2\pi} \overline{f(\phi)} e^{iK\phi} d\phi \quad (3.1.76)$$

If the values of $f(\phi)$ are real, too, then it is valid:

$$f(\phi) \in \mathbb{R} \Rightarrow f(\phi) = \overline{f(\phi)} \Rightarrow \overline{C_K} = \frac{1}{2\pi} \int_0^{2\pi} \overline{f(\phi)} e^{iK\phi} d\phi = \frac{1}{2\pi} \int_0^{2\pi} f(\phi) e^{-i(-K)\phi} d\phi = C_{-K} \quad (3.1.77)$$

The result indicates that for a real function $f(\phi) \in \mathbb{R}$ it is valid for the coefficients $C_{-K} = \overline{C_K}$. From this, it follows for $K = 0$:

$$f(\phi) \in \mathbb{R} \Rightarrow C_0 = \overline{C_0} \Rightarrow 0 = C_0 - \overline{C_0} = 2i\Im C_0 \Rightarrow \Im C_0 = 0 \Rightarrow C_0 \in \mathbb{R} \quad (3.1.78)$$

The same considerations can be applied to the coefficients c_k of the discrete Fourier series. As derived in the previous section 3.1.2, it is valid:

$$f_j = \sum_{k=k_{\min}}^{k_{\max}} c_k \zeta^{kj}, \quad c_k = \frac{1}{n} \left(\sum_{j=0}^{n-1} f_j \zeta^{-kj} \right) \quad (3.1.79)$$

By taking $n \in \mathbb{N}$ into account and applying the relation $\overline{\zeta^{kj}} = \zeta^{-kj}$ according to (3.1.52) it is obtained for the complex conjugate $\overline{c_k}$:

$$\overline{c_k} = \overline{\frac{1}{n} \left(\sum_{j=0}^{n-1} f_j \zeta^{-kj} \right)} = \frac{1}{n} \left(\sum_{j=0}^{n-1} \overline{f_j} \overline{\zeta^{-kj}} \right) = \frac{1}{n} \left(\sum_{j=0}^{n-1} \overline{f_j} \zeta^{kj} \right) \quad (3.1.80)$$

If the values f_j are real numbers, it can be derived:

$$f_j \in \mathbb{R} \Rightarrow f_j = \overline{f_j} \Rightarrow \overline{c_k} = \frac{1}{n} \left(\sum_{j=0}^{n-1} \overline{f_j} \zeta^{kj} \right) = \frac{1}{n} \left(\sum_{j=0}^{n-1} f_j \zeta^{-(-k)j} \right) = c_{-k} \quad (3.1.81)$$

Also here, for a real function $f_j \in \mathbb{R}$ the relation $\overline{c_k} = c_{-k}$ is valid. From this it follows for $k = 0$:

$$f_j \in \mathbb{R} \Rightarrow \overline{c_0} = c_0 \Rightarrow 0 = c_0 - \overline{c_0} = 2i\Im c_0 \Rightarrow \Im c_0 = 0 \Rightarrow c_0 \in \mathbb{R} \quad (3.1.82)$$

As described in the previous section 3.1.2, for the derivation of a discrete Fourier series from a continuous Fourier series it is necessary to a basic periodicity k to each periodicity K used in the continuous Fourier series. To this end, the range of the basic periodicity k has to limited:

$$k_{\min} \leq k \leq k_{\max}, \quad k_{\max} = k_{\min} + n - 1 \Leftrightarrow k_{\max} - k_{\min} = n - 1 \quad (3.1.83)$$

For the evaluation of the product $\mathbf{T}^H \mathbf{T}$ and for the determination of the inverse matrix \mathbf{T}^{-1} only the difference $k_{\max} - k_{\min} = n - 1$ has been used so that one bound k_{\min} or k_{\max} can be chosen arbitrarily, while other bound is determined by $k_{\max} = k_{\min} + n - 1$ or $k_{\min} = k_{\max} - n + 1$, respectively. Of course, there are some obvious choices for reasonable values. One possibility is the following interval:

$$k_{\min} = 0 \leq k \leq k_{\max} = n - 1 \quad (3.1.84)$$

Here, the values for k are non-negative and as small as possible. Another possibility is to choose the bounds in a similar way as for the continuous Fourier series according to (3.1.74), i.e. defining an interval, which is centred around zero. Thereby, the relation (3.1.81) can be applied for $f_j \in \mathbb{R}$; this enables a simpler and more instructive interpretation of the result. If the interval is centred around zero, then the upper and the lower bounds have the same absolute values and differ only by their signs, i.e. $-k_{\min} = k_{\max}$. Combining this condition with the relation (3.1.83) leads to:

$$-k_{\min} = k_{\max} \wedge k_{\max} - k_{\min} = n - 1 \Rightarrow 2k_{\max} = n - 1 \Rightarrow k_{\max} = -k_{\min} = \frac{n-1}{2} = \frac{n}{2} - \frac{1}{2} \quad (3.1.85)$$

The bounds k_{\min} and k_{\max} have to be integers. Based on (3.1.85) this can only be achieved if n is an odd number; therefore, the condition for the lower and upper bound has to be modified, e.g. in the following way:

$$-k_{\min} = k_{\max} - 1 \wedge k_{\max} - k_{\min} = n - 1 \Rightarrow 2k_{\max} = n \Rightarrow k_{\max} = \frac{n}{2} \Rightarrow k_{\min} = -\frac{n}{2} + 1 \quad (3.1.86)$$

In total, the bounds for the discrete Fourier series can be formulated in the following way:

$$\text{Odd number } n : n \in \mathbb{N} \wedge \frac{n}{2} \notin \mathbb{N} : k_{\min} = -\frac{n-1}{2}, k_{\max} = \frac{n-1}{2} \Rightarrow k_{\min} = -k_{\max} \quad (3.1.87)$$

$$\text{Even number } n : n \in \mathbb{N} \wedge \frac{n}{2} \in \mathbb{N} : k_{\min} = -\frac{n}{2} + 1, k_{\max} = \frac{n}{2} \Rightarrow k_{\min} = -k_{\max} + 1 \quad (3.1.88)$$

From the comparison of the bounds k_{\min} and k_{\max} for the two different cases it can be concluded:

$$k_{\min} \geq -\frac{n-1}{2}, k_{\max} \leq \frac{n}{2} \Rightarrow -\frac{n}{2} + \frac{1}{2} \leq k_{\min} \leq k \leq k_{\max} \leq \frac{n}{2} \Rightarrow -\frac{n}{2} + \frac{1}{2} \leq k \leq \frac{n}{2} \quad (3.1.89)$$

Thereby, a generalized formulation for the range of k , which covers all numbers n , is obtained.

In the section 3.1.1 the following relation has been derived:

$$C_K e^{iK\phi} + C_{-K} e^{-iK\phi} = \underbrace{(C_K + C_{-K})}_{A_K} \underbrace{\cos(K\phi)}_{\Re e^{iK\phi}} + i \underbrace{(C_K - C_{-K})}_{B_K} \underbrace{\sin\phi}_{\Im e^{iK\phi}} \quad (3.1.90)$$

The power ζ^{kj} is obtained from $e^{iK\phi}$ for $K = k$ and $\phi = \frac{2\pi}{n}j$; based on (3.1.90), it can be formulated:

$$e^{ik\frac{2\pi}{n}j} = \left(e^{\frac{2\pi}{n}i}\right)^{kj} = \zeta^{kj} \Rightarrow c_k \zeta^{kj} + c_{-k} \zeta^{-kj} = \underbrace{(c_k + c_{-k})}_{a_k} \underbrace{\cos\left(\frac{2\pi}{n}kj\right)}_{\Re \zeta^{kj}} + i \underbrace{(c_k - c_{-k})}_{b_k} \underbrace{\sin\left(\frac{2\pi}{n}kj\right)}_{\Im \zeta^{kj}} \quad (3.1.91)$$

Thereby, the coefficients a_k and b_k are defined. It can be shown that for real values f_j the coefficients a_k and b_k are real numbers, too:

$$\begin{aligned} f_j \in \mathbb{R} \Rightarrow c_{-k} = \overline{c_k} \Rightarrow a_k = c_k + c_{-k} = c_k + \overline{c_k} = 2\Re c_k \in \mathbb{R} \Rightarrow a_k \in \mathbb{R} \\ \Rightarrow b_k = i(c_k - c_{-k}) = i(c_k - \overline{c_k}) = 2\Im c_k \in \mathbb{R} \Rightarrow b_k \in \mathbb{R} \end{aligned} \quad (3.1.92)$$

By applying the transformation

$$\sum_{K=-\hat{K}}^{\hat{K}} X_K = X_0 + \sum_{K=1}^{\hat{K}} (X_K + X_{-K}) \quad (3.1.93)$$

and by setting $a_0 = c_0$ the discrete Fourier series for an odd number n can be formulated in the following way:

$$f_j = \sum_{k=-\frac{n-1}{2}}^{\frac{n-1}{2}} c_k \zeta^{kj} = c_0 + \sum_{k=1}^{\frac{n-1}{2}} (c_k \zeta^{kj} + c_{-k} \zeta^{-kj}) = a_0 + \sum_{k=1}^{\frac{n-1}{2}} \left[a_k \cos\left(\frac{2\pi}{n}kj\right) + b_k \sin\left(\frac{2\pi}{n}kj\right) \right] \quad (3.1.94)$$

For an even number n the periodicity $k = \frac{n}{2}$ has to be treated separately; here, it is valid:

$$j \in \mathbb{Z} : \zeta^{\frac{n}{2}j} = e^{i\frac{2\pi}{n}\frac{n}{2}j} = e^{i\pi j} = (e^{i\pi})^j = (\cos\pi + i\sin\pi)^j = (-1)^j \in \{-1, 1\} \quad (3.1.95)$$

Therefore, it is obtained for $c_{\frac{n}{2}}$:

$$\zeta^{-\frac{n}{2}j} = \frac{1}{\zeta^{\frac{n}{2}j}} = \frac{1}{(-1)^j} = \left(\frac{1}{-1}\right)^j = (-1)^j \Rightarrow c_{\frac{n}{2}} = \frac{1}{n} \left(\sum_{j=0}^{n-1} f_j \zeta^{-\frac{n}{2}j} \right) = \frac{1}{n} \left(\sum_{j=0}^{n-1} f_j (-1)^j \right) \quad (3.1.96)$$

It can be shown that if the values f_j are real then the coefficient $c_{\frac{n}{2}}$, too, is a real number:

$$f_j \in \mathbb{R} \wedge (-1)^j \in \{-1, 1\} \subset \mathbb{R} \Rightarrow f_j \zeta^{-\frac{n}{2}j} \in \mathbb{R} \Rightarrow c_{\frac{n}{2}} \in \mathbb{R} \quad (3.1.97)$$

By splitting the sum, applying the transformation (3.1.93) and setting $c_0 = a_0$ and $c_{\frac{n}{2}} = a_{\frac{n}{2}}$ the discrete Fourier series for an even number n can be formulated in the following way:

$$\begin{aligned} f_j &= \sum_{k=-\frac{n}{2}+1}^{\frac{n}{2}} c_k \zeta^{kj} = \sum_{k=-\frac{n}{2}+1}^{\frac{n}{2}-1} c_k \zeta^{kj} + c_{\frac{n}{2}} \zeta^{\frac{n}{2}j} = c_0 + \sum_{k=1}^{\frac{n}{2}-1} (c_k \zeta^{kj} + c_{-k} \zeta^{-kj}) + c_{\frac{n}{2}} (-1)^j \\ &= a_0 + \sum_{k=1}^{\frac{n}{2}-1} \left[a_k \cos\left(\frac{2\pi}{n}kj\right) + b_k \sin\left(\frac{2\pi}{n}kj\right) \right] + a_{\frac{n}{2}} (-1)^j \end{aligned} \quad (3.1.98)$$

3.2 Transformation of the linear cyclic system

In the section 3.1, continuous and discrete Fourier series have been considered. According to (3.1.44), the n discrete values f_j of the function $f(x)$ are expressed in the following way:

$$\begin{aligned} \phi_j &= \phi_0 + \frac{2\pi}{n}j, \quad n \in \mathbb{N}, \quad j \in \{\mathbb{N}_0 \mid 0 \leq j \leq n-1\}, \quad \phi_0 \in \mathbb{R} \\ f(\phi_j) &= f_j = \sum_{k=k_{\min}}^{k_{\max}} c_k \zeta^{kj}, \quad \zeta = e^{\frac{2\pi}{n}i}, \quad k \in \mathbb{Z}, \quad k_{\max} = k_{\min} + n - 1 \end{aligned} \quad (3.2.99)$$

The formulation for scalar values f_j can be extended easily for vectors and matrices. Based on this, the vector $\mathbf{y}^{(j)}$ describing the displacements of the j -th segment is formulated in the following way:

$$\mathbf{y}^{(j)}(t) = \sum_{k=k_{\min}}^{k_{\max}} \mathbf{y}_k(t) \zeta^{kj}, \quad \zeta = e^{\frac{2\pi}{n}i}, \quad k \in \mathbb{Z}, \quad k_{\max} = k_{\min} + n - 1 \quad (3.2.100)$$

The relation between the vector \mathbf{y}_C containing the subvectors $\mathbf{y}^{(j)}$ for the segments on the one hand and the vector \mathbf{y}_F containing the Fourier vectors \mathbf{y}_k on the other hand can be expressed by the

following matrix equation:

$$\underbrace{\begin{bmatrix} \mathbf{y}^{(0)}(t) \\ \vdots \\ \mathbf{y}^{(j)}(t) \\ \vdots \\ \mathbf{y}^{(n-1)}(t) \end{bmatrix}}_{\mathbf{y}_C(t)} = \underbrace{\begin{bmatrix} \mathbf{I}\zeta^{k_{\min}\cdot 0} & \dots & \mathbf{I}\zeta^{k\cdot 0} & \dots & \mathbf{I}\zeta^{k_{\max}\cdot 0} \\ \vdots & & \vdots & & \vdots \\ \mathbf{I}\zeta^{k_{\min}\cdot j} & \dots & \mathbf{I}\zeta^{k\cdot j} & \dots & \mathbf{I}\zeta^{k_{\max}\cdot j} \\ \vdots & & \vdots & & \vdots \\ \mathbf{I}\zeta^{k_{\min}\cdot(n-1)} & \dots & \mathbf{I}\zeta^{k\cdot(n-1)} & \dots & \mathbf{I}\zeta^{k_{\max}\cdot(n-1)} \end{bmatrix}}_{\mathbf{T}_{CF}} \underbrace{\begin{bmatrix} \mathbf{y}_{k_{\min}}(t) \\ \vdots \\ \mathbf{y}_k(t) \\ \vdots \\ \mathbf{y}_{k_{\max}}(t) \end{bmatrix}}_{\mathbf{y}_F(t)} \quad (3.2.101)$$

For the sake of clarity, it is indicated here that the vectors $\mathbf{y}^{(j)}(t)$ and $\mathbf{y}_k(t)$ forming the vectors $\mathbf{y}_C(t)$ and $\mathbf{y}_F(t)$, respectively, depend on the time t , while the powers $\zeta^{k\cdot j}$ and the transformation matrix \mathbf{T}_{CF} are constant. The transformation matrix \mathbf{T}_{CF} can be described by the submatrices \mathbf{T}_k representing the hypercolumns:

$$\mathbf{T}_k = \begin{bmatrix} \mathbf{I}\zeta^{k\cdot 0} \\ \vdots \\ \mathbf{I}\zeta^{k\cdot j} \\ \vdots \\ \mathbf{I}\zeta^{k\cdot(n-1)} \end{bmatrix} \Rightarrow \mathbf{T} = [\mathbf{T}_{k_{\min}} \cdots \mathbf{T}_k \cdots \mathbf{T}_{k_{\max}}] \quad (3.2.102)$$

In order to clarify the structure of the transformation matrix \mathbf{T}_{CF} , also exponents containing zero as a factor are written in full. – Since the matrix \mathbf{T}_{CF} is constant, it obtained for the vectors of the velocity and of the acceleration:

$$\mathbf{y}_C(t) = \mathbf{T}_{CF} \mathbf{y}_F(t) \Rightarrow \dot{\mathbf{y}}_C(t) = \mathbf{T}_{CF} \dot{\mathbf{y}}_F(t) \Rightarrow \ddot{\mathbf{y}}_C(t) = \mathbf{T}_{CF} \ddot{\mathbf{y}}_F(t) \quad (3.2.103)$$

For the derivatives of the subvectors $\mathbf{y}^{(j)}(t)$ it is valid:

$$\mathbf{y}^{(j)}(t) = \sum_{k=k_{\min}}^{k_{\max}} \mathbf{y}_k(t) \zeta^{kj} \Rightarrow \dot{\mathbf{y}}^{(j)}(t) = \sum_{k=k_{\min}}^{k_{\max}} \dot{\mathbf{y}}_k(t) \zeta^{kj} \Rightarrow \ddot{\mathbf{y}}^{(j)}(t) = \sum_{k=k_{\min}}^{k_{\max}} \ddot{\mathbf{y}}_k(t) \zeta^{kj} \quad (3.2.104)$$

The vector of the virtual velocity $\delta'\dot{\mathbf{y}}_C$ is derived from the vector $\dot{\mathbf{y}}_C(t)$:

$$\dot{\mathbf{y}}_C(t) = \mathbf{T}_{CF} \dot{\mathbf{y}}_F(t) \Rightarrow \delta'\dot{\mathbf{y}}_C = \mathbf{T}_{CF} \delta'\dot{\mathbf{y}}_F \quad (3.2.105)$$

Thereby, it is valid for its subvectors $\delta'\dot{\mathbf{y}}^{(j)}$

$$\dot{\mathbf{y}}^{(j)}(t) = \sum_{k=k_{\min}}^{k_{\max}} \dot{\mathbf{y}}_k(t) \zeta^{kj} \Rightarrow \delta'\dot{\mathbf{y}}^{(j)} = \sum_{k=k_{\min}}^{k_{\max}} \delta'\dot{\mathbf{y}}_k \zeta^{kj} \quad (3.2.106)$$

For the following considerations it is assumed that the vector of the virtual velocity $\delta'\dot{\mathbf{y}}_C$ is a real vector, i.e. its imaginary part vanishes so that it is equal to its complex conjugate vector.

$$\Im \delta'\dot{\mathbf{y}}_C = \mathbf{0} \Rightarrow \delta'\dot{\mathbf{y}}_C = \overline{\delta'\dot{\mathbf{y}}_C} = \overline{\mathbf{T}_{CF} \delta'\dot{\mathbf{y}}_F} = \overline{\mathbf{T}_{CF}} \overline{\delta'\dot{\mathbf{y}}_F} \quad (3.2.107)$$

The transposition of the vector $\delta'\dot{\mathbf{y}}_C$ leads to

$$\delta'\dot{\mathbf{y}}_C^T = \left(\overline{\mathbf{T}_{CF}} \overline{\delta'\dot{\mathbf{y}}_F} \right)^T = \overline{\delta'\dot{\mathbf{y}}_F}^T \overline{\mathbf{T}_{CF}}^T = \delta'\dot{\mathbf{y}}_F^H \mathbf{T}_{CF}^H \quad (3.2.108)$$

The relations (3.2.103) and (3.2.108) are now inserted into the equation of motion for the linear cyclic system. For the sake of brevity and of a better overview, the dependency of the vectors $\mathbf{y}_C(t)$, $\dot{\mathbf{y}}_C(t)$ and $\ddot{\mathbf{y}}_C(t)$ on the time t will not be indicated explicitly in the following. By inserting the relations it is obtained:

$$\begin{aligned} \delta \dot{\mathbf{y}}_C^T (\mathbf{M}_C \ddot{\mathbf{y}}_C + \mathbf{P}_C \dot{\mathbf{y}}_C + \mathbf{Q}_C \mathbf{y}_C) &= \delta \dot{\mathbf{y}}_F^H \mathbf{T}_{CF}^H (\mathbf{M}_C \mathbf{T}_{CF} \ddot{\mathbf{y}}_F + \mathbf{P}_C \mathbf{T}_{CF} \dot{\mathbf{y}}_F + \mathbf{Q}_C \mathbf{T}_{CF} \mathbf{y}_F) \\ &= \delta \dot{\mathbf{y}}_F^H (\mathbf{T}_{CF}^H \mathbf{M}_C \mathbf{T}_{CF} \ddot{\mathbf{y}}_F + \mathbf{T}_{CF}^H \mathbf{P}_C \mathbf{T}_{CF} \dot{\mathbf{y}}_F + \mathbf{T}_{CF}^H \mathbf{Q}_C \mathbf{T}_{CF} \mathbf{y}_F) \end{aligned} \quad (3.2.109)$$

In the following considerations the matrix products $\mathbf{T}_{CF}^H \mathbf{M}_C \mathbf{T}_{CF}$, $\mathbf{T}_{CF}^H \mathbf{P}_C \mathbf{T}_{CF}$ and $\mathbf{T}_{CF}^H \mathbf{Q}_C \mathbf{T}_{CF}$ will be evaluated. To this end, the product $\mathbf{T}_{CF}^H \mathbf{C}_C \mathbf{T}_{CF}$ will be considered; here, \mathbf{C}_C is a generalized matrix, which has the following structure:

$$\mathbf{C}_C = \begin{bmatrix} \mathbf{C}_{1|1} & \mathbf{C}_{1|2} & \mathbf{C}_{1|3} & \cdots & \mathbf{C}_{1|n} \\ \mathbf{C}_{2|1} & \mathbf{C}_{2|2} & \mathbf{C}_{2|3} & \cdots & \mathbf{C}_{2|n} \\ \mathbf{C}_{3|1} & \mathbf{C}_{3|2} & \mathbf{C}_{3|3} & \cdots & \mathbf{C}_{3|n} \\ \vdots & \vdots & \vdots & \ddots & \vdots \\ \mathbf{C}_{n|1} & \mathbf{C}_{n|2} & \mathbf{C}_{n|3} & \cdots & \mathbf{C}_{n|n} \end{bmatrix} = \begin{bmatrix} \mathbf{C}^{(0)} & \mathbf{C}^{(1)} & \mathbf{C}^{(2)} & \cdots & \mathbf{C}^{(n-1)} \\ \mathbf{C}^{(n-1)} & \mathbf{C}^{(0)} & \mathbf{C}^{(1)} & \cdots & \mathbf{C}^{(n-2)} \\ \mathbf{C}^{(n-2)} & \mathbf{C}^{(n-1)} & \mathbf{C}^{(0)} & \cdots & \mathbf{C}^{(n-3)} \\ \vdots & \vdots & \vdots & \ddots & \vdots \\ \mathbf{C}^{(1)} & \mathbf{C}^{(2)} & \mathbf{C}^{(3)} & \cdots & \mathbf{C}^{(0)} \end{bmatrix} \quad (3.2.110)$$

Here, it is valid for the submatrices $\mathbf{C}_{I|J}$:

$$\mathbf{C}_{I|J} = \begin{cases} \mathbf{C}^{(J-I)} & \text{for } J \geq I \\ \mathbf{C}^{(J-I+n)} & \text{for } J < I \end{cases} \quad (3.2.111)$$

As it will be shown later, the wanted products $\mathbf{T}_{CF}^H \mathbf{M}_C \mathbf{T}_{CF}$, $\mathbf{T}_{CF}^H \mathbf{P}_C \mathbf{T}_{CF}$ and $\mathbf{T}_{CF}^H \mathbf{Q}_C \mathbf{T}_{CF}$ can be derived from the product $\mathbf{T}_{CF}^H \mathbf{C}_C \mathbf{T}_{CF}$ by replacing the submatrices $\mathbf{C}^{(K)}$ with the corresponding submatrices $\mathbf{M}^{(K)}$, $\mathbf{P}^{(K)}$ and $\mathbf{Q}^{(K)}$, respectively.

For the following considerations the description of the transformation matrix \mathbf{T}_{CF} by hypercolumns \mathbf{T}_k according to (3.2.102) is used. Based on this, it is obtained for the product $\mathbf{C}_C \mathbf{T}_{CF}$:

$$\mathbf{C}_C \mathbf{T}_{CF} = \mathbf{C}_C [\mathbf{T}_{k_{\min}} \cdots \mathbf{T}_l \cdots \mathbf{T}_{k_{\max}}] = [\mathbf{C}_C \mathbf{T}_{k_{\min}} \cdots \mathbf{C}_C \mathbf{T}_l \cdots \mathbf{C}_C \mathbf{T}_{k_{\max}}] \quad (3.2.112)$$

The successive multiplication by \mathbf{T}_{CF}^H leads to:

$$\begin{aligned} \mathbf{T}_{CF}^H \mathbf{C}_C \mathbf{T}_{CF} &= \begin{bmatrix} \mathbf{T}_{k_{\min}}^H \\ \vdots \\ \mathbf{T}_k^H \\ \vdots \\ \mathbf{T}_{k_{\max}}^H \end{bmatrix} [\mathbf{C}_C \mathbf{T}_{k_{\min}} \cdots \mathbf{C}_C \mathbf{T}_l \cdots \mathbf{C}_C \mathbf{T}_{k_{\max}}] \\ &= \begin{bmatrix} \mathbf{T}_{k_{\min}}^H \mathbf{C}_C \mathbf{T}_{k_{\min}} & \cdots & \mathbf{T}_{k_{\min}}^H \mathbf{C}_C \mathbf{T}_l & \cdots & \mathbf{T}_{k_{\min}}^H \mathbf{C}_C \mathbf{T}_{k_{\max}} \\ \vdots & & \vdots & & \vdots \\ \mathbf{T}_k^H \mathbf{C}_C \mathbf{T}_{k_{\min}} & \cdots & \mathbf{T}_k^H \mathbf{C}_C \mathbf{T}_l & \cdots & \mathbf{T}_k^H \mathbf{C}_C \mathbf{T}_{k_{\max}} \\ \vdots & & \vdots & & \vdots \\ \mathbf{T}_{k_{\max}}^H \mathbf{C}_C \mathbf{T}_{k_{\min}} & \cdots & \mathbf{T}_{k_{\max}}^H \mathbf{C}_C \mathbf{T}_l & \cdots & \mathbf{T}_{k_{\max}}^H \mathbf{C}_C \mathbf{T}_{k_{\max}} \end{bmatrix} \end{aligned} \quad (3.2.113)$$

For the evaluation of the products $\mathbf{T}_k^H \mathbf{C}_C \mathbf{T}_l$, of which the matrix $\mathbf{T}_{CF}^H \mathbf{C}_C \mathbf{T}_{CF}$ is composed, it is useful to adapt the indices. By using the substitution $J = j + 1 \Leftrightarrow j = J - 1$ the column matrix \mathbf{T}_l

of the transformation matrix \mathbf{T}_{CF} is formulated in the following way:

$$j = J - 1, 0 \leq j \leq n - 1 \Rightarrow \mathbf{T}_l = \begin{bmatrix} \mathbf{I} \zeta^{l \cdot 0} \\ \vdots \\ \mathbf{I} \zeta^{l \cdot j} \\ \vdots \\ \mathbf{I} \zeta^{l \cdot (n-1)} \end{bmatrix} = \begin{bmatrix} \mathbf{I} \zeta^{l \cdot 0} \\ \vdots \\ \mathbf{I} \zeta^{l \cdot (J-1)} \\ \vdots \\ \mathbf{I} \zeta^{l \cdot (n-1)} \end{bmatrix}, 1 \leq J \leq n \quad (3.2.114)$$

The multiplication of the matrix \mathbf{C}_C with the column matrix \mathbf{T}_l from the right hand side leads to:

$$\mathbf{C}_C \mathbf{T}_l = \begin{bmatrix} \mathbf{C}_{1|1} & \cdots & \mathbf{C}_{1|J} & \cdots & \mathbf{C}_{1|n} \\ \vdots & & \vdots & & \vdots \\ \mathbf{C}_{I|1} & \cdots & \mathbf{C}_{I|J} & \cdots & \mathbf{C}_{I|n} \\ \vdots & & \vdots & & \vdots \\ \mathbf{C}_{n|1} & \cdots & \mathbf{C}_{n|J} & \cdots & \mathbf{C}_{n|n} \end{bmatrix} \begin{bmatrix} \mathbf{I} \zeta^{l \cdot 0} \\ \vdots \\ \mathbf{I} \zeta^{l \cdot (J-1)} \\ \vdots \\ \mathbf{I} \zeta^{l \cdot (n-1)} \end{bmatrix} = \sum_{J=1}^n \begin{bmatrix} \mathbf{C}_{1|J} \zeta^{l \cdot (J-1)} \\ \vdots \\ \mathbf{C}_{I|J} \zeta^{l \cdot (J-1)} \\ \vdots \\ \mathbf{C}_{n|J} \zeta^{l \cdot (J-1)} \end{bmatrix} \quad (3.2.115)$$

In order to take advantage from the structure of the matrix \mathbf{C}_C , the submatrices $\mathbf{C}_{I|J}$ are replaced according to (3.2.111). While for $I = 1$ the condition $J \geq I$ is always fulfilled so that the sum can be treated in whole, the sums for $2 \leq I \leq n$ have to be split up in order to cover both conditions $J \geq I$ and $J < I$.

$$I = 1 : \sum_{J=1}^n \mathbf{C}_{I|J} \zeta^{l \cdot (J-1)} = \sum_{J=1}^n \mathbf{C}^{(J-I)} \zeta^{l \cdot (J-1)} \quad (3.2.116)$$

$$\begin{aligned} 2 \leq I \leq n : \sum_{J=1}^n \mathbf{C}_{I|J} \zeta^{l \cdot (J-1)} &= \sum_{J=1}^{I-1} \mathbf{C}_{I|J} \zeta^{l \cdot (J-1)} + \sum_{J=I}^n \mathbf{C}_{I|J} \zeta^{l \cdot (J-1)} \\ &= \sum_{J=1}^{I-1} \mathbf{C}^{(J-I+n)} \zeta^{l \cdot (J-1)} + \sum_{J=I}^n \mathbf{C}^{(J-I)} \zeta^{l \cdot (J-1)} \end{aligned} \quad (3.2.117)$$

For the following transformations, the index shift for a sum, which is derived in the appendix A.1, will be applied several times. It is valid:

$$l = k + c \Rightarrow \sum_{k=k_{\min}}^{k_{\max}} X_k = \sum_{l=k_{\min}+c}^{k_{\max}+c} X_{l-c}, k, l, c \in \mathbb{Z} \quad (3.2.118)$$

Based on this, the sum (3.2.116) and the second partial sum of (3.2.117) are transformed in the following way:

$$J = i + I \Rightarrow i = J - I \Rightarrow \sum_{J=I}^n \mathbf{C}^{(J-I)} \zeta^{l \cdot (J-1)} = \sum_{i=0}^{n-I} \mathbf{C}^{(i)} \zeta^{l \cdot (i+I-1)} = \sum_{i=0}^{n-I} \mathbf{C}^{(i)} \zeta^{l \cdot i} \zeta^{l \cdot (I-1)} \quad (3.2.119)$$

For the first partial sum of (3.2.117) the following index shift is applied:

$$\begin{aligned} J = i + I - n \Rightarrow i = J - I + n \\ \Rightarrow \sum_{J=1}^{I-1} \mathbf{C}^{(J-I+n)} \zeta^{l \cdot (J-1)} &= \sum_{i=n-I+1}^{n-1} \mathbf{C}^{(i)} \zeta^{l \cdot (i+I-n-1)} = \sum_{i=n-I+1}^{n-1} \mathbf{C}^{(i)} \zeta^{l \cdot i} \zeta^{l \cdot (I-1)} \zeta^{-l \cdot n} \end{aligned} \quad (3.2.120)$$

As derived in (3.1.38) it is valid:

$$p \in \mathbb{Z}, n \in \mathbb{N} : \zeta^{pn} = 1 \quad (3.2.121)$$

Since l is an integer, this relation can be used in order to simplify the sum (3.2.120). Finally, the two transformed partial sums (3.2.119) and (3.2.120) can be merged; thereby, it is obtained:

$$\begin{aligned} \sum_{J=1}^n \mathbf{C}_{I|J} \zeta^{l \cdot (J-1)} &= \sum_{J=I}^n \mathbf{C}^{(J-I)} \zeta^{l \cdot (J-1)} + \sum_{J=1}^{I-1} \mathbf{C}^{(J-I+n)} \zeta^{l \cdot (J-1)} \\ &= \sum_{i=0}^{n-I} \mathbf{C}^{(i)} \zeta^{l \cdot i} \zeta^{l \cdot (I-1)} + \sum_{i=n-I+1}^{n-1} \mathbf{C}^{(i)} \zeta^{l \cdot i} \zeta^{l \cdot (I-1)} \underbrace{\zeta^{-l \cdot n}}_1 = \sum_{i=0}^{n-1} \mathbf{C}^{(i)} \zeta^{l \cdot i} \zeta^{l \cdot (I-1)} \end{aligned} \quad (3.2.122)$$

It can be seen that for setting $I = 1$ the expressions (3.2.119) and (3.2.122) yield the same result so that the formulation (3.2.122) is valid for all values of I , i.e. for $1 \leq I \leq n$.

After merging the sums, the index I has disappeared from the bounds and is contained only in the power $\zeta^{l \cdot (I-1)}$, which is independent from the summation index i . Therefore, this power can be factored out so that it is obtained:

$$\sum_{J=1}^n \mathbf{C}_{I|J} \zeta^{l \cdot (J-1)} = \sum_{i=0}^{n-1} \mathbf{C}^{(i)} \zeta^{l \cdot i} \zeta^{l \cdot (I-1)} = \underbrace{\left[\sum_{i=0}^{n-1} \mathbf{C}^{(i)} \zeta^{l \cdot i} \right]}_{\mathbf{C}_l} \zeta^{l \cdot (I-1)} = \mathbf{C}_l \zeta^{l \cdot (I-1)} \quad (3.2.123)$$

Based on this, the product $\mathbf{C}_C \mathbf{T}_l$ can be formulated in the following way:

$$\mathbf{C}_C \mathbf{T}_l = \sum_{J=1}^n \begin{bmatrix} \mathbf{C}_{1|J} \zeta^{l \cdot (J-1)} \\ \vdots \\ \mathbf{C}_{I|J} \zeta^{l \cdot (J-1)} \\ \vdots \\ \mathbf{C}_{n|J} \zeta^{l \cdot (J-1)} \end{bmatrix} = \begin{bmatrix} \mathbf{C}_l \zeta^{l \cdot 0} \\ \vdots \\ \mathbf{C}_l \zeta^{l \cdot (I-1)} \\ \vdots \\ \mathbf{C}_l \zeta^{l \cdot (n-1)} \end{bmatrix} \quad (3.2.124)$$

By applying the relation $\overline{\zeta^{k \cdot j}} = \zeta^{-k \cdot j}$ according to (3.1.52) it is obtained for the complex conjugate $\overline{\mathbf{T}}_k$ of the column matrix \mathbf{T}_k :

$$\mathbf{T}_k = \begin{bmatrix} \mathbf{I} \zeta^{k \cdot 0} \\ \vdots \\ \mathbf{I} \zeta^{k \cdot j} \\ \vdots \\ \mathbf{I} \zeta^{k \cdot (n-1)} \end{bmatrix} \Rightarrow \overline{\mathbf{T}}_k = \begin{bmatrix} \mathbf{I} \zeta^{-k \cdot 0} \\ \vdots \\ \mathbf{I} \zeta^{-k \cdot j} \\ \vdots \\ \mathbf{I} \zeta^{-k \cdot (n-1)} \end{bmatrix} \quad (3.2.125)$$

In order to adapt the indices used in the submatrices, the substitution $j = I - 1 \Leftrightarrow I = j + 1$ is applied to the product $\mathbf{C}_C \mathbf{T}_l$; this leads to:

$$I = j + 1, 1 \leq J \leq n \Rightarrow \mathbf{C}_C \mathbf{T}_l = \begin{bmatrix} \mathbf{C}_l \zeta^{l \cdot 0} \\ \vdots \\ \mathbf{C}_l \zeta^{l \cdot (I-1)} \\ \vdots \\ \mathbf{C}_l \zeta^{l \cdot (n-1)} \end{bmatrix} = \begin{bmatrix} \mathbf{C}_l \zeta^{l \cdot 0} \\ \vdots \\ \mathbf{C}_l \zeta^{l \cdot j} \\ \vdots \\ \mathbf{C}_l \zeta^{l \cdot (n-1)} \end{bmatrix}, 0 \leq j \leq n - 1 \quad (3.2.126)$$

Using this, the matrix product $\mathbf{T}_k^H \mathbf{C}_C \mathbf{T}_l$ can be determined:

$$\begin{aligned} \mathbf{T}_k^H \mathbf{C}_C \mathbf{T}_l &= \overline{\mathbf{T}_k}^T \mathbf{C}_C \mathbf{T}_l = [\mathbf{I} \zeta^{-k \cdot 0} \dots \mathbf{I} \zeta^{-k \cdot j} \dots \mathbf{I} \zeta^{-k \cdot (n-1)}] \begin{bmatrix} \mathbf{C}_l \zeta^{l \cdot 0} \\ \vdots \\ \mathbf{C}_l \zeta^{l \cdot j} \\ \vdots \\ \mathbf{C}_l \zeta^{l \cdot (n-1)} \end{bmatrix} \\ &= \sum_{j=0}^{n-1} \zeta^{-k \cdot j} \mathbf{C}_l \zeta^{l \cdot j} = \mathbf{C}_l \sum_{j=0}^{n-1} \zeta^{(-k+l) \cdot j} \end{aligned} \quad (3.2.127)$$

In the section 3.1.2 the following orthogonality relation (3.1.70) has been derived:

$$k_{\min} \leq k \leq k_{\max} \wedge k_{\min} \leq l \leq k_{\max} : \sum_{j=0}^{n-1} \zeta^{(-k+l) \cdot j} = \begin{cases} 0 & \text{for } k \neq l \\ n & \text{for } k = l \end{cases} \quad (3.2.128)$$

Based on this, it is obtained for the matrix product $\mathbf{T}_k^H \mathbf{C}_C \mathbf{T}_l$:

$$\mathbf{T}_k^H \mathbf{C}_C \mathbf{T}_l = \mathbf{C}_l \sum_{j=0}^{n-1} \zeta^{(-k+l) \cdot j} = \begin{cases} n \mathbf{C}_k & \text{for } k = l \\ \mathbf{0} & \text{for } k \neq l \end{cases} \quad (3.2.129)$$

From this, it follows for the transformed matrix $\mathbf{T}_{CF}^H \mathbf{C}_C \mathbf{T}_{CF}$:

$$\begin{aligned} \mathbf{T}_{CF}^H \mathbf{C}_C \mathbf{T}_{CF} &= \begin{bmatrix} \mathbf{T}_{k_{\min}}^H \mathbf{C}_C \mathbf{T}_{k_{\min}} & \dots & \mathbf{T}_{k_{\min}}^H \mathbf{C}_C \mathbf{T}_k & \dots & \mathbf{T}_{k_{\min}}^H \mathbf{C}_C \mathbf{T}_l & \dots & \mathbf{T}_{k_{\min}}^H \mathbf{C}_C \mathbf{T}_{k_{\max}} \\ \vdots & \ddots & \vdots & & \vdots & & \vdots \\ \mathbf{T}_k^H \mathbf{C}_C \mathbf{T}_{k_{\min}} & \dots & \mathbf{T}_k^H \mathbf{C}_C \mathbf{T}_k & \dots & \mathbf{T}_k^H \mathbf{C}_C \mathbf{T}_l & \dots & \mathbf{T}_k^H \mathbf{C}_C \mathbf{T}_{k_{\max}} \\ \vdots & & \vdots & \ddots & \vdots & & \vdots \\ \mathbf{T}_l^H \mathbf{C}_C \mathbf{T}_{k_{\min}} & \dots & \mathbf{T}_l^H \mathbf{C}_C \mathbf{T}_k & \dots & \mathbf{T}_l^H \mathbf{C}_C \mathbf{T}_l & \dots & \mathbf{T}_l^H \mathbf{C}_C \mathbf{T}_{k_{\max}} \\ \vdots & & \vdots & & \vdots & \ddots & \vdots \\ \mathbf{T}_{k_{\max}}^H \mathbf{C}_C \mathbf{T}_{k_{\min}} & \dots & \mathbf{T}_{k_{\max}}^H \mathbf{C}_C \mathbf{T}_k & \dots & \mathbf{T}_{k_{\max}}^H \mathbf{C}_C \mathbf{T}_l & \dots & \mathbf{T}_{k_{\max}}^H \mathbf{C}_C \mathbf{T}_{k_{\max}} \end{bmatrix} \\ &= n \begin{bmatrix} \mathbf{C}_{k_{\min}} & \dots & \mathbf{0} & \dots & \mathbf{0} & \dots & \mathbf{0} \\ \vdots & \ddots & \vdots & & \vdots & & \vdots \\ \mathbf{0} & \dots & \mathbf{C}_k & \dots & \mathbf{0} & \dots & \mathbf{0} \\ \vdots & & \vdots & \ddots & \vdots & & \vdots \\ \mathbf{0} & \dots & \mathbf{0} & \dots & \mathbf{C}_l & \dots & \mathbf{0} \\ \vdots & & \vdots & & \vdots & \ddots & \vdots \\ \mathbf{0} & \dots & \mathbf{0} & \dots & \mathbf{0} & \dots & \mathbf{C}_{k_{\max}} \end{bmatrix} \end{aligned} \quad (3.2.130)$$

This result indicates that the transformed matrix $\mathbf{T}_{CF}^H \mathbf{C}_C \mathbf{T}_{CF}$ is a block-diagonal matrix. It should be pointed out that for the matrix \mathbf{C}_C no further properties are assumed than the structure described in (3.2.110), i.e. if \mathbf{C}_C has this structure the block-diagonal structure of the product $\mathbf{T}_{CF}^H \mathbf{C}_C \mathbf{T}_{CF}$ is obtained regardless of whether the matrix \mathbf{C}_C is real or complex or whether it is symmetric, skew-symmetric or has no symmetry property at all.

By comparing the generalized matrix \mathbf{C}_C and the matrix \mathbf{Q}_C

$$\mathbf{C}_C = \begin{bmatrix} \mathbf{C}^{(0)} & \mathbf{C}^{(1)} & \mathbf{C}^{(2)} & \dots & \mathbf{C}^{(n-1)} \\ \mathbf{C}^{(n-1)} & \mathbf{C}^{(0)} & \mathbf{C}^{(1)} & \dots & \mathbf{C}^{(n-2)} \\ \mathbf{C}^{(n-2)} & \mathbf{C}^{(n-1)} & \mathbf{C}^{(0)} & \dots & \mathbf{C}^{(n-3)} \\ \vdots & \vdots & \vdots & \ddots & \vdots \\ \mathbf{C}^{(1)} & \mathbf{C}^{(2)} & \mathbf{C}^{(3)} & \dots & \mathbf{C}^{(0)} \end{bmatrix}, \mathbf{Q}_C = \begin{bmatrix} \mathbf{Q}^{(0)} & \mathbf{Q}^{(1)} & \mathbf{0} & \dots & \mathbf{Q}^{(-1)} \\ \mathbf{Q}^{(-1)} & \mathbf{Q}^{(0)} & \mathbf{Q}^{(1)} & \dots & \mathbf{0} \\ \mathbf{0} & \mathbf{Q}^{(-1)} & \mathbf{Q}^{(0)} & \dots & \mathbf{0} \\ \vdots & \vdots & \vdots & \ddots & \vdots \\ \mathbf{Q}^{(1)} & \mathbf{0} & \mathbf{0} & \dots & \mathbf{Q}^{(0)} \end{bmatrix} \quad (3.2.131)$$

it can be seen that the matrix product $\mathbf{T}_{CF}^H \mathbf{Q}_C \mathbf{T}_{CF}$ can be derived from the product $\mathbf{T}_{CF}^H \mathbf{C}_C \mathbf{T}_{CF}$ by substituting the submatrices $\mathbf{C}^{(I)}$ in the following way:

$$\mathbf{C}^{(I)} = \begin{cases} \mathbf{Q}^{(0)} & \text{for } I = 0 \\ \mathbf{Q}^{(1)} & \text{for } I = 1 \\ \mathbf{0} & \text{for } 2 \leq I \leq n-2 \\ \mathbf{Q}^{(-1)} & \text{for } I = n-1 \end{cases} \quad (3.2.132)$$

By inserting this into (3.2.129) and applying the relation $\zeta^{kn} = 1$ derived from (3.2.121) the matrix \mathbf{Q}_k is obtained:

$$\begin{aligned} \mathbf{Q}_k &= \sum_{i=0}^{n-1} \mathbf{Q}^{(i)} \zeta^{k \cdot i} = \mathbf{Q}^{(0)} \zeta^{k \cdot 0} + \mathbf{Q}^{(1)} \zeta^{k \cdot 1} + \underbrace{\sum_{i=2}^{n-2} \mathbf{Q}^{(i)} \zeta^{k \cdot i}}_{\mathbf{0}} + \mathbf{Q}^{(n-1)} \zeta^{k \cdot (n-1)} \\ &= \mathbf{Q}^{(0)} + \mathbf{Q}^{(1)} \zeta^k + \mathbf{Q}^{(-1)} \zeta^{-k} \underbrace{\zeta^{k \cdot n}}_1 = \mathbf{Q}^{(-1)} \zeta^{-k} + \mathbf{Q}^{(0)} + \mathbf{Q}^{(1)} \zeta^k \end{aligned} \quad (3.2.133)$$

Based on this, the product $\mathbf{T}_{CF}^H \mathbf{Q}_C \mathbf{T}_{CF}$ is formulated in the following way:

$$\mathbf{T}_{CF}^H \mathbf{Q}_C \mathbf{T}_{CF} = n \begin{bmatrix} \mathbf{Q}_{k_{\min}} & \dots & \mathbf{0} & \dots & \mathbf{0} & \dots & \mathbf{0} \\ \vdots & \ddots & \vdots & & \vdots & & \vdots \\ \mathbf{0} & \dots & \mathbf{Q}_k & \dots & \mathbf{0} & \dots & \mathbf{0} \\ \vdots & & \vdots & \ddots & \vdots & & \vdots \\ \mathbf{0} & \dots & \mathbf{0} & \dots & \mathbf{Q}_l & \dots & \mathbf{0} \\ \vdots & & \vdots & & \vdots & \ddots & \vdots \\ \mathbf{0} & \dots & \mathbf{0} & \dots & \mathbf{0} & \dots & \mathbf{Q}_{k_{\max}} \end{bmatrix} \quad (3.2.134)$$

As already mentioned, the matrices \mathbf{Q}_C , \mathbf{P}_C and \mathbf{M}_C have an analogous structure. Therefore, it is valid for the products $\mathbf{T}_{CF}^H \mathbf{P}_C \mathbf{T}_{CF}$ and $\mathbf{T}_{CF}^H \mathbf{M}_C \mathbf{T}_{CF}$:

$$\mathbf{P}_C = \begin{bmatrix} \mathbf{P}^{(0)} & \mathbf{P}^{(1)} & \mathbf{0} & \dots & \mathbf{P}^{(-1)} \\ \mathbf{P}^{(-1)} & \mathbf{P}^{(0)} & \mathbf{P}^{(1)} & \dots & \mathbf{0} \\ \mathbf{0} & \mathbf{P}^{(-1)} & \mathbf{P}^{(0)} & \dots & \mathbf{0} \\ \vdots & \vdots & \vdots & \ddots & \vdots \\ \mathbf{P}^{(1)} & \mathbf{0} & \mathbf{0} & \dots & \mathbf{P}^{(0)} \end{bmatrix} \Rightarrow \mathbf{T}_{CF}^H \mathbf{P}_C \mathbf{T}_{CF} = n \begin{bmatrix} \mathbf{P}_{k_{\min}} & \dots & \mathbf{0} & \dots & \mathbf{0} & \dots & \mathbf{0} \\ \vdots & \ddots & \vdots & & \vdots & & \vdots \\ \mathbf{0} & \dots & \mathbf{P}_k & \dots & \mathbf{0} & \dots & \mathbf{0} \\ \vdots & & \vdots & \ddots & \vdots & & \vdots \\ \mathbf{0} & \dots & \mathbf{0} & \dots & \mathbf{P}_l & \dots & \mathbf{0} \\ \vdots & & \vdots & & \vdots & \ddots & \vdots \\ \mathbf{0} & \dots & \mathbf{0} & \dots & \mathbf{0} & \dots & \mathbf{P}_{k_{\max}} \end{bmatrix} \quad (3.2.135)$$

$$\mathbf{M}_C = \begin{bmatrix} \mathbf{M}^{(0)} & \mathbf{M}^{(1)} & \mathbf{0} & \dots & \mathbf{M}^{(-1)} \\ \mathbf{M}^{(-1)} & \mathbf{M}^{(0)} & \mathbf{M}^{(1)} & \dots & \mathbf{0} \\ \mathbf{0} & \mathbf{M}^{(-1)} & \mathbf{M}^{(0)} & \dots & \mathbf{0} \\ \vdots & \vdots & \vdots & \ddots & \vdots \\ \mathbf{M}^{(1)} & \mathbf{0} & \mathbf{0} & \dots & \mathbf{M}^{(0)} \end{bmatrix} \Rightarrow \mathbf{T}_{CF}^H \mathbf{M}_C \mathbf{T}_{CF} = n \begin{bmatrix} \mathbf{M}_{k_{\min}} & \dots & \mathbf{0} & \dots & \mathbf{0} & \dots & \mathbf{0} \\ \vdots & \ddots & \vdots & & \vdots & & \vdots \\ \mathbf{0} & \dots & \mathbf{M}_k & \dots & \mathbf{0} & \dots & \mathbf{0} \\ \vdots & & \vdots & \ddots & \vdots & & \vdots \\ \mathbf{0} & \dots & \mathbf{0} & \dots & \mathbf{M}_l & \dots & \mathbf{0} \\ \vdots & & \vdots & & \vdots & \ddots & \vdots \\ \mathbf{0} & \dots & \mathbf{0} & \dots & \mathbf{0} & \dots & \mathbf{M}_{k_{\max}} \end{bmatrix} \quad (3.2.136)$$

The relations between the matrices $\mathbf{P}^{(l)}$ and $\mathbf{M}^{(l)}$ on the one hand and the matrices \mathbf{P}_k and \mathbf{M}_k on the other hand are given by

$$\mathbf{P}_k = \mathbf{P}^{(-1)} \zeta^{-k} + \mathbf{P}^{(0)} + \mathbf{P}^{(1)} \zeta^k \quad (3.2.137)$$

$$\mathbf{M}_k = \mathbf{M}^{(-1)} \zeta^{-k} + \mathbf{M}^{(0)} + \mathbf{M}^{(1)} \zeta^k \quad (3.2.138)$$

For the product of the transformed matrix $\mathbf{T}_{CF}^H \mathbf{Q}_C \mathbf{T}_{CF}$ and the vector \mathbf{y}_F it is obtained:

$$\mathbf{T}_{CF}^H \mathbf{Q}_C \mathbf{T}_{CF} \mathbf{y}_F = n \begin{bmatrix} \mathbf{Q}_{k_{\min}} & \dots & \mathbf{0} & \dots & \mathbf{0} & \dots & \mathbf{0} \\ \vdots & \ddots & \vdots & & \vdots & & \vdots \\ \mathbf{0} & \dots & \mathbf{Q}_k & \dots & \mathbf{0} & \dots & \mathbf{0} \\ \vdots & & \vdots & \ddots & \vdots & & \vdots \\ \mathbf{0} & \dots & \mathbf{0} & \dots & \mathbf{Q}_l & \dots & \mathbf{0} \\ \vdots & & \vdots & & \vdots & \ddots & \vdots \\ \mathbf{0} & \dots & \mathbf{0} & \dots & \mathbf{0} & \dots & \mathbf{Q}_{k_{\max}} \end{bmatrix} \begin{bmatrix} \mathbf{y}_{k_{\min}} \\ \vdots \\ \mathbf{y}_k \\ \vdots \\ \mathbf{y}_l \\ \vdots \\ \mathbf{y}_{k_{\max}} \end{bmatrix} = n \begin{bmatrix} \mathbf{Q}_{k_{\min}} \mathbf{y}_{k_{\min}} \\ \vdots \\ \mathbf{Q}_k \mathbf{y}_k \\ \vdots \\ \mathbf{Q}_l \mathbf{y}_l \\ \vdots \\ \mathbf{Q}_{k_{\max}} \mathbf{y}_{k_{\max}} \end{bmatrix} \quad (3.2.139)$$

Due to the block-diagonal structure of the transformed matrices, each subvector of the vector $\mathbf{T}_{CF}^H \mathbf{P}_C \mathbf{T}_{CF} \dot{\mathbf{y}}_F$ contains one and only one vector \mathbf{y}_k . Conversely, this means that there are no coupling terms and thereby no interactions of different periodicities $k \neq l$. In an analogous way, it is obtained for the products $\mathbf{T}_{CF}^H \mathbf{M}_C \mathbf{T}_{CF} \dot{\mathbf{y}}_F$ and $\mathbf{T}_{CF}^H \mathbf{M}_C \mathbf{T}_{CF} \ddot{\mathbf{y}}_F$:

$$\mathbf{T}_{CF}^H \mathbf{P}_C \mathbf{T}_{CF} \dot{\mathbf{y}}_F = n \begin{bmatrix} \mathbf{P}_{k_{\min}} \dot{\mathbf{y}}_{k_{\min}} \\ \vdots \\ \mathbf{P}_k \dot{\mathbf{y}}_k \\ \vdots \\ \mathbf{P}_l \dot{\mathbf{y}}_l \\ \vdots \\ \mathbf{P}_{k_{\max}} \dot{\mathbf{y}}_{k_{\max}} \end{bmatrix}, \quad \mathbf{T}_{CF}^H \mathbf{M}_C \mathbf{T}_{CF} \ddot{\mathbf{y}}_F = n \begin{bmatrix} \mathbf{M}_{k_{\min}} \ddot{\mathbf{y}}_{k_{\min}} \\ \vdots \\ \mathbf{M}_k \ddot{\mathbf{y}}_k \\ \vdots \\ \mathbf{M}_l \ddot{\mathbf{y}}_l \\ \vdots \\ \mathbf{M}_{k_{\max}} \ddot{\mathbf{y}}_{k_{\max}} \end{bmatrix} \quad (3.2.140)$$

In total it is valid for the left-hand side of the equation of motion:

$$\begin{aligned}
& \delta' \dot{\mathbf{y}}_C^T (\mathbf{M}_C \ddot{\mathbf{y}}_C + \mathbf{P}_C \dot{\mathbf{y}}_C + \mathbf{Q}_C \mathbf{y}_C) \\
&= \delta' \dot{\mathbf{y}}_F^H (\mathbf{T}_{CF}^H \mathbf{M}_C \mathbf{T}_{CF} \ddot{\mathbf{y}}_F + \mathbf{T}_{CF}^H \mathbf{P}_C \mathbf{T}_{CF} \dot{\mathbf{y}}_F + \mathbf{T}_{CF}^H \mathbf{Q}_C \mathbf{T}_{CF} \mathbf{y}_F) \\
&= \left[\delta' \dot{\mathbf{y}}_{k_{\min}}^H \cdots \delta' \dot{\mathbf{y}}_k^H \cdots \delta' \dot{\mathbf{y}}_l^H \cdots \delta' \dot{\mathbf{y}}_{k_{\max}}^H \right] n \begin{bmatrix} \mathbf{M}_{k_{\min}} \ddot{\mathbf{y}}_{k_{\min}} + \mathbf{P}_{k_{\min}} \dot{\mathbf{y}}_{k_{\min}} + \mathbf{Q}_{k_{\min}} \mathbf{y}_{k_{\min}} \\ \vdots \\ \mathbf{M}_k \ddot{\mathbf{y}}_k + \mathbf{P}_k \dot{\mathbf{y}}_k + \mathbf{Q}_k \mathbf{y}_k \\ \vdots \\ \mathbf{M}_l \ddot{\mathbf{y}}_l + \mathbf{P}_l \dot{\mathbf{y}}_l + \mathbf{Q}_l \mathbf{y}_l \\ \vdots \\ \mathbf{M}_{k_{\max}} \ddot{\mathbf{y}}_{k_{\max}} + \mathbf{P}_{k_{\max}} \dot{\mathbf{y}}_{k_{\max}} + \mathbf{Q}_{k_{\max}} \mathbf{y}_{k_{\max}} \end{bmatrix} \\
&= n \sum_{k=k_{\min}}^{k_{\max}} \delta' \dot{\mathbf{y}}_k^H (\mathbf{M}_k \ddot{\mathbf{y}}_k + \mathbf{P}_k \dot{\mathbf{y}}_k + \mathbf{Q}_k \mathbf{y}_k) \tag{3.2.141}
\end{aligned}$$

The result shows that the formulation of the motions of a cyclic system by discrete Fourier series enables a very simple formulation.

The block-diagonal structure of the matrix products $\mathbf{T}_{CF}^H \mathbf{Q}_C \mathbf{T}_{CF}$, $\mathbf{T}_{CF}^H \mathbf{P}_C \mathbf{T}_{CF}$ and $\mathbf{T}_{CF}^H \mathbf{M}_C \mathbf{T}_{CF}$ has been derived from the consideration of the product $\mathbf{T}_{CF}^H \mathbf{C}_C \mathbf{T}_{CF}$. The evaluation of this product takes advantage of the structure of the generalized matrix \mathbf{C}_C according to (3.2.110), but no further properties have been assumed; in particular this means that the matrix \mathbf{C}_C can be complex and that it doesn't have to have any symmetry properties. However, as mentioned at the beginning of this chapter, the matrices \mathbf{Q}_C , \mathbf{P}_C and \mathbf{M}_C are assumed to be real matrices. Furthermore, for an ordinary linear mechanical system the matrix \mathbf{M} is always symmetric, while the matrices \mathbf{P} and \mathbf{Q} can be split up into a symmetric and a skew-symmetric part; since a linear cyclic system is a special case of an ordinary linear mechanical system, this is also valid for the matrices \mathbf{M}_C , \mathbf{M}_k and \mathbf{M}_l . The properties of the matrices \mathbf{M}_k , \mathbf{P}_k and \mathbf{Q}_k , which are derived from these additional properties, will be considered in the following.

Again, the matrix \mathbf{Q}_C shall serve as an example. According to (3.2.133) the matrix \mathbf{Q}_k is obtained from the submatrices $\mathbf{Q}^{(l)}$ of \mathbf{Q}_C in the following way:

$$\mathbf{Q}_k = \mathbf{Q}^{(-1)} \zeta^{-k} + \mathbf{Q}^{(0)} + \mathbf{Q}^{(1)} \zeta^k \tag{3.2.142}$$

If the matrix \mathbf{Q}_C is a real matrix, i.e. $\mathbf{Q}_C = \overline{\mathbf{Q}_C}$, then its submatrices $\mathbf{Q}^{(l)}$ are real matrices, too, i.e. $\mathbf{Q}^{(l)} = \overline{\mathbf{Q}^{(l)}}$. In this case, the following relation between the matrices \mathbf{Q}_k and \mathbf{Q}_{-k} can be derived based on the relation (3.1.52):

$$\begin{aligned}
\zeta^{-k} = \overline{\zeta^k}, \quad \mathbf{Q}^{(l)} = \overline{\mathbf{Q}^{(l)}} \Rightarrow \overline{\mathbf{Q}_k} &= \overline{\mathbf{Q}^{(-1)} \zeta^{-k} + \mathbf{Q}^{(0)} + \mathbf{Q}^{(1)} \zeta^k} = \overline{\mathbf{Q}^{(-1)}} \overline{\zeta^{-k}} + \overline{\mathbf{Q}^{(0)}} + \overline{\mathbf{Q}^{(1)}} \overline{\zeta^k} \\
&= \mathbf{Q}^{(-1)} \zeta^{-(-k)} + \mathbf{Q}^{(0)} + \mathbf{Q}^{(1)} \zeta^{-k} = \mathbf{Q}_{-k} \tag{3.2.143}
\end{aligned}$$

In an analogous way it is valid for the real matrices $\mathbf{P}_C = \overline{\mathbf{P}_C}$ and $\mathbf{M}_C = \overline{\mathbf{M}_C}$:

$$\mathbf{Q}_C = \overline{\mathbf{Q}_C} \Rightarrow \mathbf{Q}^{(l)} = \overline{\mathbf{Q}^{(l)}} \Rightarrow \mathbf{Q}_{-k} = \overline{\mathbf{Q}_k} \tag{3.2.144}$$

$$\mathbf{P}_C = \overline{\mathbf{P}_C} \Rightarrow \mathbf{P}^{(l)} = \overline{\mathbf{P}^{(l)}} \Rightarrow \mathbf{P}_{-k} = \overline{\mathbf{P}_k} \tag{3.2.145}$$

$$\mathbf{M}_C = \overline{\mathbf{M}_C} \Rightarrow \mathbf{M}^{(l)} = \overline{\mathbf{M}^{(l)}} \Rightarrow \mathbf{M}_{-k} = \overline{\mathbf{M}_k} \tag{3.2.146}$$

Next, the symmetry properties shall be considered. Based to the formulation of an ordinary linear mechanical system according to (3.0.1) and (3.0.2), it is obtained for the matrices of the linear

cyclic system:

$$\mathbf{M}_C = \mathbf{M}_C^T \quad (3.2.147)$$

$$\mathbf{P}_C = \mathbf{D}_C + \mathbf{G}_C, \quad \mathbf{D}_C = \mathbf{D}_C^T, \quad \mathbf{G}_C = -\mathbf{G}_C^T \quad (3.2.148)$$

$$\mathbf{Q}_C = \mathbf{K}_C + \mathbf{N}_C, \quad \mathbf{K}_C = \mathbf{K}_C^T, \quad \mathbf{N}_C = -\mathbf{N}_C^T \quad (3.2.149)$$

In order to shorten the derivation of the symmetry properties, a generalized matrix \mathbf{B}_C shall be considered:

$$\mathbf{B}_C = \sigma \mathbf{B}_C^T \Rightarrow \begin{bmatrix} \mathbf{B}^{(0)} & \mathbf{B}^{(1)} & \mathbf{0} & \dots & \mathbf{B}^{(-1)} \\ \mathbf{B}^{(-1)} & \mathbf{B}^{(0)} & \mathbf{B}^{(1)} & \dots & \mathbf{0} \\ \mathbf{0} & \mathbf{B}^{(-1)} & \mathbf{B}^{(0)} & \dots & \mathbf{0} \\ \vdots & \vdots & \vdots & \ddots & \vdots \\ \mathbf{B}^{(1)} & \mathbf{0} & \mathbf{0} & \dots & \mathbf{B}^{(0)} \end{bmatrix} = \sigma \begin{bmatrix} \mathbf{B}^{(0)T} & \mathbf{B}^{(-1)T} & \mathbf{0} & \dots & \mathbf{B}^{(1)T} \\ \mathbf{B}^{(1)T} & \mathbf{B}^{(0)T} & \mathbf{B}^{(-1)T} & \dots & \mathbf{0} \\ \mathbf{0} & \mathbf{B}^{(1)T} & \mathbf{B}^{(0)T} & \dots & \mathbf{0} \\ \vdots & \vdots & \vdots & \ddots & \vdots \\ \mathbf{B}^{(-1)T} & \mathbf{0} & \mathbf{0} & \dots & \mathbf{B}^{(0)T} \end{bmatrix} \quad (3.2.150)$$

Here, σ is a scalar factor indicating the sign. For $\sigma = 1$, the matrix \mathbf{B}_C is symmetric; for $\sigma = -1$ it is skew-symmetric. From the comparison of the corresponding submatrices it is obtained:

$$\mathbf{B}_C = \sigma \mathbf{B}_C^T \Rightarrow \mathbf{B}^{(0)} = \sigma \mathbf{B}^{(0)T}, \quad \mathbf{B}^{(1)} = \sigma \mathbf{B}^{(-1)T}, \quad \mathbf{B}^{(-1)} = \sigma \mathbf{B}^{(1)T} \quad (3.2.151)$$

The matrix \mathbf{B}_k is defined in a way analogous to the definition of \mathbf{Q}_k according to (3.2.142):

$$\mathbf{B}_k = \mathbf{B}^{(-1)} \zeta^{-k} + \mathbf{B}^{(0)} + \mathbf{B}^{(1)} \zeta^k \quad (3.2.152)$$

For further considerations, it is assumed that the matrix \mathbf{B}_C is a real matrix, i.e. $\mathbf{B}_C = \overline{\mathbf{B}_C}$. For this, it follows based on (3.3.252):

$$\mathbf{B}_C = \overline{\mathbf{B}_C} \Rightarrow \mathbf{B}^{(l)} = \overline{\mathbf{B}^{(l)}} \Rightarrow \mathbf{B}_k = \underbrace{\mathbf{B}^{(0)} + \Re \zeta^k (\mathbf{B}^{(1)} + \mathbf{B}^{(-1)})}_{\Re \mathbf{B}_k} + i \underbrace{\Im \zeta^k (\mathbf{B}^{(1)} - \mathbf{B}^{(-1)})}_{\Im \mathbf{B}_k} \quad (3.2.153)$$

By transposing the matrix \mathbf{B}_k and applying the relations according to (3.2.151) it is obtained:

$$\begin{aligned} \mathbf{B}_k^T &= \mathbf{B}^{(0)T} + \Re \zeta^k (\mathbf{B}^{(1)T} + \mathbf{B}^{(-1)T}) + i \Im \zeta^k (\mathbf{B}^{(1)T} - \mathbf{B}^{(-1)T}) \\ &= \sigma \mathbf{B}^{(0)} + \Re \zeta^k (\sigma \mathbf{B}^{(-1)} + \sigma \mathbf{B}^{(1)}) + i \Im \zeta^k (\sigma \mathbf{B}^{(-1)} - \sigma \mathbf{B}^{(1)}) \\ &= \sigma \left(\underbrace{\mathbf{B}^{(0)} + \Re \zeta^k (\mathbf{B}^{(1)} + \mathbf{B}^{(-1)})}_{\Re \mathbf{B}_k} \right) - i \sigma \underbrace{\Im \zeta^k (\mathbf{B}^{(1)} - \mathbf{B}^{(-1)})}_{\Im \mathbf{B}_k} \\ &= \sigma (\Re \mathbf{B}_k - i \Im \mathbf{B}_k) = \sigma \overline{\mathbf{B}_k} \end{aligned} \quad (3.2.154)$$

The transposition of the results leads to:

$$\mathbf{B}_k^T = \sigma \overline{\mathbf{B}_k} \Rightarrow \mathbf{B}_k = \sigma \mathbf{B}_k^T = \sigma \overline{\mathbf{B}_k^T} = \sigma \mathbf{B}_k^H \quad (3.2.155)$$

Based on this relation, the symmetry properties of the matrices \mathbf{M}_k , \mathbf{D}_k , \mathbf{G}_k , \mathbf{K}_k and \mathbf{N}_k can be derived. The mass matrix \mathbf{M}_C , the damping matrix \mathbf{D}_C and the stiffness matrix \mathbf{K}_k symmetric

matrices; if they are also real matrices the symmetry properties of the matrices \mathbf{M}_k , \mathbf{D}_k and \mathbf{K}_k can be derived from (3.2.155) by setting $\sigma = 1$. This leads to:

$$\mathbf{M}_C = \mathbf{M}_C^T = \overline{\mathbf{M}_C} \Rightarrow \mathbf{M}_k = \mathbf{M}^{(-1)}\zeta^{-k} + \mathbf{M}^{(0)} + \mathbf{M}^{(1)}\zeta^k = \mathbf{M}_k^H \quad (3.2.156)$$

$$\mathbf{D}_C = \mathbf{D}_C^T = \overline{\mathbf{D}_C} \Rightarrow \mathbf{D}_k = \mathbf{D}^{(-1)}\zeta^{-k} + \mathbf{D}^{(0)} + \mathbf{D}^{(1)}\zeta^k = \mathbf{D}_k^H \quad (3.2.157)$$

$$\mathbf{K}_C = \mathbf{K}_C^T = \overline{\mathbf{K}_C} \Rightarrow \mathbf{K}_k = \mathbf{K}^{(-1)}\zeta^{-k} + \mathbf{K}^{(0)} + \mathbf{K}^{(1)}\zeta^k = \mathbf{K}_k^H \quad (3.2.158)$$

The matrices \mathbf{M}_k , \mathbf{D}_k and \mathbf{K}_k are Hermitian matrices, i.e. their real parts are symmetric, while their imaginary parts are skew-symmetric. – The gyroscopic matrix \mathbf{G}_C and the circulatoric matrix \mathbf{N}_C are skew-symmetric matrices. If they are also real, the symmetry properties of the matrices \mathbf{G}_k and \mathbf{N}_k are obtained from (3.2.155) by setting $\sigma = -1$. This results in:

$$\mathbf{G}_C = -\mathbf{G}_C^T = \overline{\mathbf{G}_C} \Rightarrow \mathbf{G}_k = \mathbf{G}^{(-1)}\zeta^{-k} + \mathbf{G}^{(0)} + \mathbf{G}^{(1)}\zeta^k = -\mathbf{G}_k^H \quad (3.2.159)$$

$$\mathbf{N}_C = -\mathbf{N}_C^T = \overline{\mathbf{N}_C} \Rightarrow \mathbf{N}_k = \mathbf{N}^{(-1)}\zeta^{-k} + \mathbf{N}^{(0)} + \mathbf{N}^{(1)}\zeta^k = -\mathbf{N}_k^H \quad (3.2.160)$$

The matrices \mathbf{G}_k and \mathbf{N}_k are skew-Hermitian, i.e. their real parts are skew-symmetric, while their imaginary parts are symmetric.

3.3 Modal decomposition of a cyclic system

Depending on the system's size and complexity, the matrices \mathbf{M} , \mathbf{P} and \mathbf{Q} for a linear mechanical system can be rather large; as a result, the calculation effort to solve the system's equations of motion can be high. Therefore, it is desirable to transform the equations of motion into a form, which is easier to handle from the computational point of view. Here, the modal description of the system is a highly useful method, which is described in several books, e.g. [15]. In several cases, this transformation also enables a reduction of number of the degrees of freedom with a relatively small loss of accuracy.

In the following considerations, the principle of the modal decomposition and of the modal transformation will be developed and applied to the cyclic system. The relations will be developed for several types of systems, whereas in the following sequence each system can be considered as a special case of the previous system.

1. The most generalized type of linear dynamic system is described by the state space representation given by the following equation:

$$\dot{\mathbf{z}}(t) = \mathbf{A}\mathbf{z}(t) + \mathbf{b}(t) \quad (3.3.161)$$

Here, $\mathbf{z}(t)$ is the state vector, \mathbf{A} is the system matrix, and $\mathbf{b}(t)$ is the input vector. In the state space representation, the system is described by a system of ordinary linear first order differential equations.

2. An ordinary linear mechanical system is described by the following equation of motion:

$$\mathbf{M}\ddot{\mathbf{y}}(t) + \mathbf{P}\dot{\mathbf{y}}(t) + \mathbf{Q}\mathbf{y}(t) = \mathbf{h}(t), \quad \mathbf{M} = \mathbf{M}^T \quad (3.3.162)$$

The equation of motion is a system of ordinary linear second order differential equations. The corresponding state space equation is obtained to:

$$\underbrace{\begin{bmatrix} \mathbf{0} & \mathbf{I} \\ -\mathbf{M}^{-1}\mathbf{Q} & -\mathbf{M}^{-1}\mathbf{P} \end{bmatrix}}_{\mathbf{A}} \underbrace{\begin{bmatrix} \mathbf{y}(t) \\ \dot{\mathbf{y}}(t) \end{bmatrix}}_{\mathbf{z}(t)} + \underbrace{\begin{bmatrix} \mathbf{0} \\ \mathbf{M}^{-1}\mathbf{h}(t) \end{bmatrix}}_{\mathbf{b}(t)} \quad (3.3.163)$$

This equation is a special case of (3.3.161) in so far as in this case the system matrix \mathbf{A} has a particular structure, i.e. it is composed by submatrices, which again are based on the matrices \mathbf{M} , \mathbf{P} and \mathbf{Q} , while in (3.3.161) no particular structure \mathbf{A} is required.

3. The equation of motion for a linear cyclic system is given by:

$$\mathbf{M}_C \ddot{\mathbf{y}}_C(t) + \mathbf{P}_C \dot{\mathbf{y}}_C(t) + \mathbf{Q}_C \mathbf{y}_C(t) = \mathbf{h}_C(t), \quad \mathbf{M}_C = \mathbf{M}_C^T \quad (3.3.164)$$

While the equation of motion has the same structure as for the ordinary linear mechanical system, the matrices \mathbf{M}_C , \mathbf{P}_C and \mathbf{Q}_C and the vectors $\ddot{\mathbf{y}}_C(t)$, $\dot{\mathbf{y}}_C(t)$, $\mathbf{y}_C(t)$ and $\mathbf{h}_C(t)$ and have a special structure; therefore, the linear cyclic system is a special case of the ordinary linear mechanical system. These structures of the matrices and the vectors are exemplified for the matrices \mathbf{Q}_C and $\mathbf{y}_C(t)$:

$$\mathbf{Q}_C = \begin{bmatrix} \mathbf{Q}^{(0)} & \mathbf{Q}^{(1)} & \mathbf{0} & \dots & \mathbf{0} & \mathbf{Q}^{(-1)} \\ \mathbf{Q}^{(-1)} & \mathbf{Q}^{(0)} & \mathbf{Q}^{(1)} & \dots & \mathbf{0} & \mathbf{0} \\ \mathbf{0} & \mathbf{Q}^{(-1)} & \mathbf{Q}^{(0)} & \ddots & \mathbf{0} & \mathbf{0} \\ \vdots & \vdots & \ddots & \ddots & \ddots & \vdots \\ \mathbf{0} & \mathbf{0} & \mathbf{0} & \ddots & \mathbf{Q}^{(0)} & \mathbf{Q}^{(1)} \\ \mathbf{Q}^{(1)} & \mathbf{0} & \mathbf{0} & \dots & \mathbf{Q}^{(-1)} & \mathbf{Q}^{(0)} \end{bmatrix}, \quad \mathbf{y}_C(t) = \begin{bmatrix} \mathbf{y}^{(0)}(t) \\ \mathbf{y}^{(1)}(t) \\ \vdots \\ \mathbf{y}^{(j)}(t) \\ \vdots \\ \mathbf{y}^{(n-1)}(t) \end{bmatrix} \quad (3.3.165)$$

4. For a damped linear cyclic system the equation of motion is given by:

$$\mathbf{M}_C \ddot{\mathbf{y}}_C(t) + \mathbf{D}_C \dot{\mathbf{y}}_C(t) + \mathbf{K}_C \mathbf{y}_C(t) = \mathbf{h}_C(t), \quad \mathbf{M}_C = \mathbf{M}_C^T, \quad \mathbf{D}_C = \mathbf{D}_C^T, \quad \mathbf{K}_C = \mathbf{K}_C^T \quad (3.3.166)$$

Here, the damping matrix \mathbf{D}_C and the stiffness matrix \mathbf{K}_C have structure analogous to the one shown for \mathbf{Q}_C in (3.3.165). In addition to this, the matrices \mathbf{D}_C and \mathbf{K}_C are symmetric matrices; thereby, the damped linear cyclic system is a special case of the linear cyclic system described by (3.3.164), where no symmetry properties for the matrices \mathbf{P}_C and \mathbf{Q}_C are required. – Generally, a damped linear system is a special case of an ordinary linear mechanical system described by (3.3.162), for which it is set $\mathbf{P} = \mathbf{D} = \mathbf{D}^T$ and $\mathbf{Q} = \mathbf{K} = \mathbf{K}^T$. The designation “damped system” for such a system is taken from [15].

Since each of the systems listed above can be considered as a special case of the previous system, all relations developed for one system can also be applied on the following one, i.e. for instance, all relations, which are valid for the ordinary linear mechanical system, are also valid for a linear cyclic system and thereby also for a damped linear cyclic system. By taking advantage from the additional properties, which are valid for the special cases, further relations for the considered special case will be derived.

In the section 3.3.1, the principle of the modal decomposition and of the modal transformation will be considered for the systems described by (3.3.161) and (3.3.162). These considerations are based on the book by Gasch, Knothe, and Liebich [15] on structural dynamics, although some modifications are made, especially with respect to some mathematical formulations according to the book by Strang [71] on linear algebra. Also, the nomenclature of the matrices used in [15] is adapted to the one used in [64], [63] and [55]. – In the section 3.3.2, the methods developed in the section 3.3.1 will be applied to a linear cyclic system described by (3.3.164) and the specific results will be discussed. The special case of a damped cyclic system described by (3.3.166) will be considered in the section 3.3.3.

3.3.1 Modal decomposition of an ordinary linear system

Since the state space representation given by (3.3.161) is the most generalized formulation for a linear dynamic system, the transformation of this equation shall be considered first. This transformation is based on the diagonalization of the matrix \mathbf{A} using its eigenvectors. An eigenvector \mathbf{w}_I of a matrix \mathbf{A} is defined in the following way:

$$\mathbf{A} \mathbf{w}_I = \lambda_I \mathbf{w}_I \Leftrightarrow (\mathbf{A} - \lambda_I \mathbf{I}) \mathbf{w}_I = \mathbf{0}, \mathbf{w}_I \neq \mathbf{0} \quad (3.3.167)$$

Here, λ_I is the eigenvalue, to which the eigenvector \mathbf{w}_I is associated. For the non-trivial solution $\mathbf{w}_I \neq \mathbf{0}$ it is valid:

$$(\mathbf{A} - \lambda_I \mathbf{I}) \underbrace{\mathbf{w}_I}_{\neq \mathbf{0}} = \mathbf{0} \Rightarrow \det(\mathbf{A} - \lambda_I \mathbf{I}) = 0 \quad (3.3.168)$$

The problem (3.3.167) is a right eigenvector problem, because the matrix \mathbf{A} is multiplied by the vector \mathbf{w}_I from the right side. A left eigenvector problem is obtained by multiplying the matrix \mathbf{A} with the vector \mathbf{v}_I from the left hand side; if $\mathbf{v}_I \neq \mathbf{0}$ is a left eigenvector associated with the eigenvalue λ_I , it has to fulfil the following condition:

$$\mathbf{v}_I^H \mathbf{A} = \lambda_I \mathbf{v}_I^H \Leftrightarrow \mathbf{v}_I^H (\mathbf{A} - \lambda_I \mathbf{I}) = \mathbf{0}, \mathbf{v}_I \neq \mathbf{0} \quad (3.3.169)$$

As discussed in the section 3.1.2 the Hermitian transpose \mathbf{v}_I^H is used instead of the “simple” transpose \mathbf{v}_I^T , as recommended by Strang [71]. In this context it should be mentioned that e.g. in the algorithms contained in the well-known software library LAPACK [1] the Hermitian transpose is used for the left eigenvectors. – It should be noted that for the indexing of the eigenvalues and eigenvectors uppercase letters like I and J will be used in order to avoid confusion with the segment index j or the periodicities k , which are written as lowercase letters as introduced in the previous section 3.2.

Multiplying the equations (3.3.167) and (3.3.169) by \mathbf{v}_J^H and \mathbf{w}_I , respectively, and subtracting the results leads to:

$$\mathbf{A} \mathbf{w}_I = \lambda_I \mathbf{w}_I \Rightarrow \mathbf{v}_J^H \mathbf{A} \mathbf{w}_I = \lambda_I \mathbf{v}_J^H \mathbf{w}_I \quad (3.3.170)$$

$$\mathbf{v}_J^H \mathbf{A} = \lambda_J \mathbf{v}_J^H \Rightarrow \mathbf{v}_J^H \mathbf{A} \mathbf{w}_I = \lambda_J \mathbf{v}_J^H \mathbf{w}_I \quad (3.3.171)$$

$$\Rightarrow 0 = (\lambda_I - \lambda_J) \mathbf{v}_J^H \mathbf{w}_I \quad (3.3.172)$$

A product vanishes if at least one of its factors vanishes. Based on this the orthogonality of two eigenvectors \mathbf{v}_J and \mathbf{w}_I belonging to two different eigenvalues $\lambda_I \neq \lambda_J$ can be derived:

$$\lambda_I \neq \lambda_J \Rightarrow \lambda_I - \lambda_J \neq 0 \Rightarrow \mathbf{v}_J^H \mathbf{w}_I = 0 \quad (3.3.173)$$

Of course, the matrix \mathbf{A} can also have multiple eigenvectors so that the eigenvectors \mathbf{v}_j and \mathbf{w}_I are orthogonal, although the eigenvalues, to which they are associated, are equal, i.e. $\lambda_i = \lambda_j$ for $i \neq j$. This case will be considered later, when it becomes relevant. For the following consideration it is assumed that all eigenvectors of the matrix \mathbf{A} are orthogonal and that the eigenvectors are normalized in the following way:

$$\mathbf{v}_I^H \mathbf{w}_J = \begin{cases} 1 & \text{for } I = J \\ 0 & \text{for } I \neq J \end{cases} \quad (3.3.174)$$

Based on this orthogonality relation the state space equation according to (3.3.163):

$$\dot{\mathbf{z}}(t) = \mathbf{A} \mathbf{z}(t) + \mathbf{b}(t) \quad (3.3.175)$$

can now be transformed. To this end, the state vector $\mathbf{z}(t)$ is formulated as a linear combination of the right eigenvectors \mathbf{w}_J ; here, the time-dependent scalar factors $q_J(t)$ are the modal coordinates. According to Strang [71], a matrix of the order $N \times N$ has N eigenvalues and thereby N eigenvectors. By using all N eigenvectors of the matrix \mathbf{A} it is obtained for $\mathbf{z}(t)$ and its derivative $\dot{\mathbf{z}}(t)$:

$$\mathbf{z}(t) = \sum_{J=1}^N \mathbf{w}_J q_J(t) \Rightarrow \dot{\mathbf{z}}(t) = \sum_{J=1}^N \mathbf{w}_J \dot{q}_J(t) \quad (3.3.176)$$

Inserting this formulation into the state space representation (3.3.175) and applying the condition for the right eigenvector according to (3.3.167) leads to:

$$\underbrace{\sum_{J=1}^N \mathbf{w}_J \dot{q}_J(t)}_{\dot{\mathbf{z}}(t)} = \mathbf{A} \underbrace{\sum_{J=1}^N \mathbf{w}_J q_J(t)}_{\mathbf{z}(t)} + \mathbf{b}(t) = \sum_{J=1}^N \mathbf{A} \mathbf{w}_J q_J(t) + \mathbf{b}(t) = \sum_{J=1}^N \lambda_J \mathbf{w}_J q_J(t) + \mathbf{b}(t) \quad (3.3.177)$$

Multiplying the equation by \mathbf{v}_I^H leads to:

$$\mathbf{v}_I^H \sum_{J=1}^N \mathbf{w}_J \dot{q}_J(t) = \mathbf{v}_I^H \left(\sum_{J=1}^N \lambda_J \mathbf{w}_J q_J(t) + \mathbf{b}(t) \right) \Rightarrow \sum_{J=1}^N \mathbf{v}_I^H \mathbf{w}_J \dot{q}_J(t) = \sum_{J=1}^N \lambda_J \mathbf{v}_I^H \mathbf{w}_J q_J(t) + \mathbf{v}_I^H \mathbf{b}(t) \quad (3.3.178)$$

According to the orthogonality relation (3.3.174), the products $\mathbf{v}_I^H \mathbf{w}_J$ vanish for $I \neq J$. Therefore, also the summands for $I \neq J$ vanish so that only the summand for $I = J$ remains. Since the vectors are normalized so that it is valid $\mathbf{v}_I^H \mathbf{w}_I = 1$, it is finally obtained:

$$\sum_{J=1}^N \mathbf{v}_I^H \mathbf{w}_J \dot{q}_J(t) = \sum_{J=1}^N \lambda_J \mathbf{v}_I^H \mathbf{w}_J q_J(t) + \mathbf{v}_I^H \mathbf{b}(t) \Rightarrow \dot{q}_I(t) = \lambda_I q_I(t) + \mathbf{v}_I^H \mathbf{b}(t) \quad (3.3.179)$$

Since the matrix \mathbf{A} has N eigenvectors, N decoupled differential equations are obtained. It is evident that the solution process of the N decoupled equations requires a far lower computational effort than the one of the original state space representation according to (3.3.163). Of course, the determination of the eigenvalues and eigenvectors of \mathbf{A} requires a certain effort; however, this has to be carried out only once.

The conditions described above, i.e.

$$\det(\mathbf{A} - \lambda_I \mathbf{I}) = 0, \mathbf{A} \mathbf{w}_I = \lambda_I \mathbf{w}_I, \mathbf{w}_I \neq \mathbf{0}, \mathbf{v}_I^H \mathbf{A} = \lambda_I \mathbf{v}_I^H, \mathbf{v}_I \neq \mathbf{0} \quad (3.3.180)$$

are the standard formulation for the problem of determining eigenvalues λ_I and their associated eigenvectors \mathbf{w}_I and \mathbf{v}_I . The majority of computational algorithms like e.g. those contained in the well-known software library LAPACK [1] are adapted to this formulation. Practically, this means that the square matrix \mathbf{A} of the order $N \times N$ has to be provided and the algorithm returns the eigenvalues λ_I and the associated eigenvectors.

An ordinary linear mechanical system is a special case of a linear dynamic system. Therefore, as discussed in the section 3.3, for an ordinary linear mechanical system the system matrix \mathbf{A} has a particular structure, as shown in (3.3.163). In the followig considerations, the conditions according to (3.3.180) will be reformulated by taking advantage from the structure of \mathbf{A} describing an ordinary linear mechanical system. In this case the matrix \mathbf{A} is composed of submatrices, which again are derived from the matrices \mathbf{M} , \mathbf{P} and \mathbf{Q} used in the equations of motion. Therefore, also

the vectors \mathbf{w}_I and \mathbf{v}_I will be formulated using subvectors. By using this formulation it is obtained for the right eigenvector problem:

$$\mathbf{w}_I = \begin{bmatrix} \mathbf{y}_{I|1} \\ \mathbf{y}_{I|2} \end{bmatrix} \Rightarrow \lambda_I \begin{bmatrix} \mathbf{y}_{I|1} \\ \mathbf{y}_{I|2} \end{bmatrix} = \underbrace{\begin{bmatrix} \mathbf{0} & \mathbf{I} \\ -\mathbf{M}^{-1}\mathbf{Q} & -\mathbf{M}^{-1}\mathbf{P} \end{bmatrix}}_{\mathbf{A}} \begin{bmatrix} \mathbf{y}_{I|1} \\ \mathbf{y}_{I|2} \end{bmatrix} = \begin{bmatrix} \mathbf{y}_{I|2} \\ -\mathbf{M}^{-1}\mathbf{Q}\mathbf{y}_{I|1} - \mathbf{M}^{-1}\mathbf{P}\mathbf{y}_{I|2} \end{bmatrix} \quad (3.3.181)$$

$$\Rightarrow \lambda_I \mathbf{y}_{I|1} = \mathbf{y}_{I|2} \quad (3.3.182)$$

$$\lambda_I \mathbf{y}_{I|2} = -\mathbf{M}^{-1}\mathbf{Q}\mathbf{y}_{I|1} - \mathbf{M}^{-1}\mathbf{P}\mathbf{y}_{I|2} \Rightarrow \mathbf{0} = \lambda_I \mathbf{y}_{I|2} + \mathbf{M}^{-1}\mathbf{P}\mathbf{y}_{I|2} + \mathbf{M}^{-1}\mathbf{Q}\mathbf{y}_{I|1} \quad (3.3.183)$$

Multiplying the relation (3.3.183) by \mathbf{M} , eliminating the vector $\mathbf{y}_{I|2}$ according to (3.3.182) and setting $\mathbf{y}_{I|1} \equiv \mathbf{y}_I$ leads to:

$$\mathbf{0} = \mathbf{M}\lambda_I \underbrace{\lambda_I \mathbf{y}_{I|1}}_{\mathbf{y}_{I|2}} + \underbrace{\mathbf{M}\mathbf{M}^{-1}\mathbf{P}}_{\mathbf{I}} \lambda_I \mathbf{y}_{I|1} + \underbrace{\mathbf{M}\mathbf{M}^{-1}\mathbf{Q}}_{\mathbf{I}} \mathbf{y}_{I|1} = (\lambda_I^2 \mathbf{M} + \lambda_I \mathbf{P} + \mathbf{Q}) \mathbf{y}_I \quad (3.3.184)$$

For the non-trivial solution the following condition has to be fulfilled:

$$\mathbf{0} = (\lambda_I^2 \mathbf{M} + \lambda_I \mathbf{P} + \mathbf{Q}) \mathbf{y}_I \wedge \mathbf{y}_I \neq \mathbf{0} \Rightarrow \det(\lambda_I^2 \mathbf{M} + \lambda_I \mathbf{P} + \mathbf{Q}) = 0 \quad (3.3.185)$$

Due to the condition $\mathbf{y}_{I|1} = \mathbf{y}_I \neq \mathbf{0}$ it is ensured that at least one subvector of \mathbf{w}_I is different from the zero vector $\mathbf{0}$ so that also \mathbf{w}_I is different from $\mathbf{0}$. This is also valid for the case $\lambda_I = 0$, for which the vector $\mathbf{y}_{I|2} = \lambda_I \mathbf{y}_{I|1}$ is equal to $\mathbf{0}$.

The evaluation of the left eigenvector problem leads to:

$$\mathbf{v}_I = \begin{bmatrix} \mathbf{x}_{I|1} \\ \mathbf{x}_{I|2} \end{bmatrix} \Rightarrow \lambda_I \begin{bmatrix} \mathbf{x}_{I|1}^H & \mathbf{x}_{I|2}^H \end{bmatrix} = \begin{bmatrix} \mathbf{x}_{I|1}^H & \mathbf{x}_{I|2}^H \end{bmatrix} \begin{bmatrix} \mathbf{0} & \mathbf{I} \\ -\mathbf{M}^{-1}\mathbf{Q} & -\mathbf{M}^{-1}\mathbf{P} \end{bmatrix} \\ = \begin{bmatrix} -\mathbf{x}_{I|2}^H \mathbf{M}^{-1}\mathbf{Q} & \mathbf{x}_{I|1}^H - \mathbf{x}_{I|2}^H \mathbf{M}^{-1}\mathbf{P} \end{bmatrix} \quad (3.3.186)$$

$$\Rightarrow \lambda_I \mathbf{x}_{I|1}^H = -\mathbf{x}_{I|2}^H \mathbf{M}^{-1}\mathbf{Q} \Rightarrow \mathbf{0} = \lambda_I \mathbf{x}_{I|1}^H + \mathbf{x}_{I|2}^H \mathbf{M}^{-1}\mathbf{Q} \quad (3.3.187)$$

$$\lambda_I \mathbf{x}_{I|2}^H = \mathbf{x}_{I|1}^H - \mathbf{x}_{I|2}^H \mathbf{M}^{-1}\mathbf{P} \Rightarrow \mathbf{x}_{I|1}^H = \lambda_I \mathbf{x}_{I|2}^H + \mathbf{x}_{I|2}^H \mathbf{M}^{-1}\mathbf{P} \quad (3.3.188)$$

The vector $\mathbf{x}_{I|1}$ can be eliminated by inserting the relation (3.3.188) into (3.3.187). This leads to:

$$\mathbf{0} = \lambda_I \underbrace{(\lambda_I \mathbf{x}_{I|2}^H + \mathbf{x}_{I|2}^H \mathbf{M}^{-1}\mathbf{P})}_{\mathbf{x}_{I|1}^H} + \mathbf{x}_{I|2}^H \mathbf{M}^{-1}\mathbf{Q} = \lambda_I^2 \mathbf{x}_{I|2}^H + \lambda_I \mathbf{x}_{I|2}^H \mathbf{M}^{-1}\mathbf{P} + \mathbf{x}_{I|2}^H \mathbf{M}^{-1}\mathbf{Q} \quad (3.3.189)$$

By substituting $\mathbf{x}_{I|2}^H$ in an appropriate way the inverse \mathbf{M}^{-1} is eliminated.

$$\mathbf{x}_{I|2}^H = \mathbf{x}_I^H \mathbf{M} \Rightarrow \mathbf{0} = \lambda_I^2 \mathbf{x}_I^H \mathbf{M} + \lambda_I \mathbf{x}_I^H \underbrace{\mathbf{M}\mathbf{M}^{-1}\mathbf{P}}_{\mathbf{I}} + \mathbf{x}_I^H \underbrace{\mathbf{M}\mathbf{M}^{-1}\mathbf{Q}}_{\mathbf{I}} = \mathbf{x}_I^H (\lambda_I^2 \mathbf{M} + \lambda_I \mathbf{P} + \mathbf{Q}) \quad (3.3.190)$$

Here, the non-trivial solution has to fulfil the following condition:

$$\mathbf{0} = \mathbf{x}_I^H (\lambda_I^2 \mathbf{M} + \lambda_I \mathbf{P} + \mathbf{Q}) \wedge \mathbf{x}_I \neq \mathbf{0} \Rightarrow \det(\lambda_I^2 \mathbf{M} + \lambda_I \mathbf{P} + \mathbf{Q}) = 0 \quad (3.3.191)$$

It should be noted that for the ordinary linear mechanical system the formulations (3.3.185) and (3.3.191) are equivalent to the formulations according to (3.3.180). For the numerical treatment,

the formulations (3.3.185) and (3.3.191) are not very suitable; however, as it will turn out later, they can be useful in some special cases like e.g. double eigenvalues.

In the equations (3.3.170), (3.3.171), (3.3.172) and (3.3.173) it has been shown that eigenvectors \mathbf{v}_J^H and \mathbf{w}_I , which are associated to different eigenvalues $\lambda_J \neq \lambda_I$, are orthogonal. However, in some cases, double or multiple eigenvalues can occur. In order to evaluate the orthogonality in this case, the scalar product $\mathbf{v}_J^H \mathbf{w}_I$ of a left eigenvector and a right eigenvector shall be expressed based on the matrices \mathbf{M} , \mathbf{P} and \mathbf{Q} of the original equation. Using the subvectors $\mathbf{y}_{I|1}$, $\mathbf{y}_{I|2}$, $\mathbf{x}_{J|1}$ and $\mathbf{x}_{J|2}$ it is valid:

$$\mathbf{v}_J^H \mathbf{w}_I = [\mathbf{x}_{J|1}^H \quad \mathbf{x}_{J|2}^H] \begin{bmatrix} \mathbf{y}_{I|1} \\ \mathbf{y}_{I|2} \end{bmatrix} = \mathbf{x}_{J|1}^H \mathbf{y}_{I|1} + \mathbf{x}_{J|2}^H \mathbf{y}_{I|2} \quad (3.3.192)$$

The vector $\mathbf{y}_{I|2}$ can be eliminated immediately by applying the relation (3.3.182); furthermore, it is set $\mathbf{y}_I \equiv \mathbf{y}_{I|1}$; thereby, it is obtained:

$$\lambda_I \mathbf{y}_{I|1} = \mathbf{y}_{I|2} \Rightarrow \mathbf{v}_J^H \mathbf{w}_I = \mathbf{x}_{J|1}^H \mathbf{y}_{I|1} + \mathbf{x}_{J|2}^H \mathbf{y}_{I|2} = \mathbf{x}_{J|1}^H \mathbf{y}_{I|1} + \mathbf{x}_{J|2}^H \lambda_I \mathbf{y}_{I|1} = \mathbf{x}_{J|1}^H \mathbf{y}_I + \lambda_I \mathbf{x}_{J|2}^H \mathbf{y}_I \quad (3.3.193)$$

The vector $\mathbf{x}_{J|1}^H$ can be eliminated in two ways. The first possibility is to resolve the relation (3.3.188) to $\mathbf{x}_{J|1}^H$ and to substitute the index I by J :

$$\mathbf{0} = \lambda_I \mathbf{x}_{J|2}^H + \mathbf{x}_{J|2}^H \mathbf{M}^{-1} \mathbf{P} - \mathbf{x}_{J|1}^H \Rightarrow \mathbf{x}_{J|1}^H = \lambda_J \mathbf{x}_{J|2}^H + \mathbf{x}_{J|2}^H \mathbf{M}^{-1} \mathbf{P} \quad (3.3.194)$$

Inserting this into (3.3.193) leads to:

$$\begin{aligned} \mathbf{v}_J^H \mathbf{w}_I &= \mathbf{x}_{J|1}^H \mathbf{y}_I + \lambda_I \mathbf{x}_{J|2}^H \mathbf{y}_I = (\lambda_J \mathbf{x}_{J|2}^H + \mathbf{x}_{J|2}^H \mathbf{M}^{-1} \mathbf{P}) \mathbf{y}_I + \lambda_I \mathbf{x}_{J|2}^H \mathbf{y}_I \\ &= (\lambda_I + \lambda_J) \mathbf{x}_{J|2}^H \mathbf{y}_I + \mathbf{x}_{J|2}^H \mathbf{M}^{-1} \mathbf{P} \mathbf{y}_I \end{aligned} \quad (3.3.195)$$

The second possibility uses the relation (3.3.188); substituting the index I by J leads to:

$$\lambda_I \mathbf{x}_{J|1}^H = -\mathbf{x}_{J|2}^H \mathbf{M}^{-1} \mathbf{Q} \Rightarrow \lambda_J \mathbf{x}_{J|1}^H = -\mathbf{x}_{J|2}^H \mathbf{M}^{-1} \mathbf{Q} \quad (3.3.196)$$

After multiplying the scalar product (3.3.193) by λ_J , the expression $\lambda_J \mathbf{y}_{J|1}$ can be substituted. Thereby, it is obtained:

$$\lambda_J \mathbf{v}_J^H \mathbf{w}_I = \lambda_J \mathbf{x}_{J|1}^H \mathbf{y}_I + \lambda_J \lambda_I \mathbf{x}_{J|2}^H \mathbf{y}_I = -\mathbf{x}_{J|2}^H \mathbf{M}^{-1} \mathbf{Q} \mathbf{y}_I + \lambda_I \lambda_J \mathbf{x}_{J|2}^H \mathbf{y}_I \quad (3.3.197)$$

By applying the substitution $\mathbf{x}_{J|2}^H = \mathbf{x}_J^H \mathbf{M}$ the two results (3.3.195) and (3.3.197) are reformulated in the following way:

$$\mathbf{v}_J^H \mathbf{w}_I = (\lambda_I + \lambda_J) \mathbf{x}_{J|2}^H \mathbf{y}_I + \mathbf{x}_{J|2}^H \mathbf{M}^{-1} \mathbf{P} \mathbf{y}_I = (\lambda_I + \lambda_J) \mathbf{x}_J^H \mathbf{M} \mathbf{y}_I + \mathbf{x}_J^H \underbrace{\mathbf{M} \mathbf{M}^{-1}}_{\mathbf{I}} \mathbf{P} \mathbf{y}_I \quad (3.3.198)$$

$$\lambda_J \mathbf{v}_J^H \mathbf{w}_I = -\mathbf{x}_{J|2}^H \mathbf{M}^{-1} \mathbf{Q} \mathbf{y}_I + \lambda_I \lambda_J \mathbf{x}_{J|2}^H \mathbf{y}_I = -\mathbf{x}_J^H \underbrace{\mathbf{M} \mathbf{M}^{-1}}_{\mathbf{I}} \mathbf{Q} \mathbf{y}_I + \lambda_I \lambda_J \mathbf{x}_J^H \mathbf{M} \mathbf{y}_I \quad (3.3.199)$$

Thereby, the product $\mathbf{v}_J^H \mathbf{w}_I$ can be expressed in the two ways using the matrices \mathbf{M} , \mathbf{P} and \mathbf{Q} :

$$\mathbf{v}_J^H \mathbf{w}_I = (\lambda_I + \lambda_J) \mathbf{x}_J^H \mathbf{M} \mathbf{y}_I + \mathbf{x}_J^H \mathbf{P} \mathbf{y}_I \quad (3.3.200)$$

$$\lambda_J \mathbf{v}_J^H \mathbf{w}_I = -\mathbf{x}_J^H \mathbf{Q} \mathbf{y}_I + \lambda_I \lambda_J \mathbf{x}_J^H \mathbf{M} \mathbf{y}_I \quad (3.3.201)$$

3.3.2 Eigenvectors of a linear cyclic system

As mentioned before, a cyclic linear system is a special case of an ordinary mechanical linear system. Therefore, the relations developed in the previous section 3.3.1 can be applied also to the cyclic linear system. The equation of motion and the state space representation are obtained by simply replacing the generalized matrices \mathbf{M} , \mathbf{P} and \mathbf{Q} and the vectors $\mathbf{y}(t)$ and $\mathbf{h}(t)$ by the matrices \mathbf{M}_C , \mathbf{P}_C and \mathbf{Q}_C and by the vectors $\mathbf{h}_C(t)$ and $\mathbf{h}_C(t)$, respectively. Thereby, it is obtained:

$$\mathbf{M}_C \ddot{\mathbf{y}}_C(t) + \mathbf{P}_C \dot{\mathbf{y}}_C(t) + \mathbf{Q}_C \mathbf{y}_C(t) = \mathbf{h}_C(t) \quad (3.3.202)$$

$$\Leftrightarrow \underbrace{\begin{bmatrix} \dot{\mathbf{y}}_C(t) \\ \mathbf{y}_C(t) \end{bmatrix}}_{\mathbf{z}_C(t)} = \underbrace{\begin{bmatrix} \mathbf{0} & \mathbf{I} \\ -\mathbf{M}_C^{-1} \mathbf{Q}_C & -\mathbf{M}_C^{-1} \mathbf{P}_C \end{bmatrix}}_{\mathbf{A}_C} \underbrace{\begin{bmatrix} \mathbf{y}_C(t) \\ \dot{\mathbf{y}}_C(t) \end{bmatrix}}_{\mathbf{z}_C(t)} + \underbrace{\begin{bmatrix} \mathbf{0} \\ \mathbf{M}_C^{-1} \mathbf{h}_C(t) \end{bmatrix}}_{\mathbf{b}_C(t)} \quad (3.3.203)$$

Based on relations for an ordinary linear mechanical system the eigenvectors \mathbf{w}_{CI} and \mathbf{v}_{CI} for a linear cyclic system will be considered in the following. The relations for the eigenvectors of a cyclic system are formulated by replacing the matrices \mathbf{M} , \mathbf{P} and \mathbf{Q} in the relations developed in the section 3.3.1 by the matrices \mathbf{M}_C , \mathbf{P}_C and \mathbf{Q}_C , respectively. Thereby, it is obtained for the right eigenvector problem of the cyclic system:

$$\lambda_I \underbrace{\begin{bmatrix} \mathbf{y}_{CI1} \\ \mathbf{y}_{CI2} \end{bmatrix}}_{\mathbf{w}_{CI}} = \underbrace{\begin{bmatrix} \mathbf{0} & \mathbf{I} \\ -\mathbf{M}_C^{-1} \mathbf{Q}_C & -\mathbf{M}_C^{-1} \mathbf{P}_C \end{bmatrix}}_{\mathbf{A}_C} \underbrace{\begin{bmatrix} \mathbf{y}_{CI1} \\ \mathbf{y}_{CI2} \end{bmatrix}}_{\mathbf{w}_{CI}} \quad (3.3.204)$$

$$\Rightarrow \mathbf{0} = \left(\lambda_I^2 \mathbf{M}_C + \lambda_I \mathbf{P}_C + \mathbf{Q}_C \right) \mathbf{y}_{CI}, \mathbf{y}_{CI} = \mathbf{y}_{CI1} \neq \mathbf{0} \quad (3.3.205)$$

For the left eigenvector problem of the cyclic system it is valid:

$$\lambda_I \underbrace{\begin{bmatrix} \mathbf{x}_{CI1}^H & \mathbf{x}_{CI2}^H \end{bmatrix}}_{\mathbf{v}_{CI}^H} = \underbrace{\begin{bmatrix} \mathbf{x}_{CI1}^H & \mathbf{x}_{CI2}^H \end{bmatrix}}_{\mathbf{v}_{CI}^H} \underbrace{\begin{bmatrix} \mathbf{0} & \mathbf{I} \\ -\mathbf{M}_C^{-1} \mathbf{Q}_C & -\mathbf{M}_C^{-1} \mathbf{P}_C \end{bmatrix}}_{\mathbf{A}_C} \quad (3.3.206)$$

$$\Rightarrow \mathbf{0} = \mathbf{x}_{CI}^H \left(\lambda_I^2 \mathbf{M}_C + \lambda_I \mathbf{P}_C + \mathbf{Q}_C \right), \mathbf{x}_{CI}^H \mathbf{M}_C = \mathbf{x}_{CI2}^H, \mathbf{x}_{CI} \neq \mathbf{0} \quad (3.3.207)$$

In the following considerations, the specific properties of the eigenvectors of a linear cyclic system will be derived by applying the transformation developed in the section 3.2; this transformations takes advantage from the structure of the matrices \mathbf{M}_C , \mathbf{P}_C and \mathbf{Q}_C according to (3.0.5). Here, the formulations (3.3.205) and (3.3.207) will be used since they are more suitable than the formulations (3.3.204) and (3.3.206).

For a linear cyclic system the eigenvectors \mathbf{y}_{CI} and \mathbf{x}_{CI} can be formulated in the following way:

$$\underbrace{\begin{bmatrix} \mathbf{y}_I^{(0)} \\ \vdots \\ \mathbf{y}_I^{(j)} \\ \vdots \\ \mathbf{y}_I^{(n-1)} \end{bmatrix}}_{\mathbf{y}_{CI}} = \underbrace{\begin{bmatrix} \mathbf{I} \zeta^{k_{\min} \cdot 0} & \dots & \mathbf{I} \zeta^{k \cdot 0} & \dots & \mathbf{I} \zeta^{k_{\max} \cdot 0} \\ \vdots & & \vdots & & \vdots \\ \mathbf{I} \zeta^{k_{\min} \cdot j} & \dots & \mathbf{I} \zeta^{k \cdot j} & \dots & \mathbf{I} \zeta^{k_{\max} \cdot j} \\ \vdots & & \vdots & & \vdots \\ \mathbf{I} \zeta^{k_{\min} \cdot (n-1)} & \dots & \mathbf{I} \zeta^{k \cdot (n-1)} & \dots & \mathbf{I} \zeta^{k_{\max} \cdot (n-1)} \end{bmatrix}}_{\mathbf{T}_{CF}} \underbrace{\begin{bmatrix} \mathbf{y}_{I,k_{\min}} \\ \vdots \\ \mathbf{y}_{I,k} \\ \vdots \\ \mathbf{y}_{I,k_{\max}} \end{bmatrix}}_{\mathbf{y}_{FI}} \Rightarrow \mathbf{y}_I^{(j)} = \sum_{k=k_{\min}}^{k_{\max}} \mathbf{y}_{I,k} \zeta^{k \cdot j} \quad (3.3.208)$$

$$\underbrace{\begin{bmatrix} \mathbf{x}_I^{(0)} \\ \vdots \\ \mathbf{x}_I^{(j)} \\ \vdots \\ \mathbf{x}_I^{(n-1)} \end{bmatrix}}_{\mathbf{x}_{CI}} = \underbrace{\begin{bmatrix} \mathbf{I}\zeta^{k_{\min}\cdot 0} & \dots & \mathbf{I}\zeta^{k\cdot 0} & \dots & \mathbf{I}\zeta^{k_{\max}\cdot 0} \\ \vdots & & \vdots & & \vdots \\ \mathbf{I}\zeta^{k_{\min}\cdot j} & \dots & \mathbf{I}\zeta^{k\cdot j} & \dots & \mathbf{I}\zeta^{k_{\max}\cdot j} \\ \vdots & & \vdots & & \vdots \\ \mathbf{I}\zeta^{k_{\min}\cdot(n-1)} & \dots & \mathbf{I}\zeta^{k\cdot(n-1)} & \dots & \mathbf{I}\zeta^{k_{\max}\cdot(n-1)} \end{bmatrix}}_{\mathbf{T}_{CF}} \underbrace{\begin{bmatrix} \mathbf{x}_{I,k_{\min}} \\ \vdots \\ \mathbf{x}_{I,k} \\ \vdots \\ \mathbf{x}_{I,k_{\max}} \end{bmatrix}}_{\mathbf{x}_{FI}} \Rightarrow \mathbf{x}_I^{(j)} = \sum_{k=k_{\min}}^{k_{\max}} \mathbf{x}_{I,k} \zeta^{k\cdot j} \quad (3.3.209)$$

By multiplying the condition (3.3.205) by \mathbf{T}_{CF}^H and inserting the formulation of the eigenvector according to (3.3.208) it is obtained:

$$\begin{aligned} \mathbf{0} &= \mathbf{T}_{CF}^H \left(\lambda_I^2 \mathbf{M}_C + \lambda_I \mathbf{P}_C + \mathbf{Q}_C \right) \underbrace{\mathbf{T}_{CF} \mathbf{y}_{FI}}_{\mathbf{y}_{CI}} \\ &\Rightarrow \mathbf{0} = \left(\lambda_I^2 \mathbf{T}_{CF}^H \mathbf{M}_C \mathbf{T}_{CF} + \lambda_I \mathbf{T}_{CF}^H \mathbf{P}_C \mathbf{T}_{CF} + \mathbf{T}_{CF}^H \mathbf{Q}_C \mathbf{T}_{CF} \right) \mathbf{y}_{FI} \end{aligned} \quad (3.3.210)$$

In the section 3.2 it has been determined that the product $\mathbf{T}_{CF}^H \mathbf{Q}_C \mathbf{T}_{CF}$ is a block-diagonal matrix. Thereby, it is valid:

$$\mathbf{T}_{CF}^H \mathbf{Q}_C \mathbf{T}_{CF} \mathbf{y}_{FI} = n \begin{bmatrix} \mathbf{Q}_{k_{\min}} & \dots & \mathbf{0} & \dots & \mathbf{0} & \dots & \mathbf{0} \\ \vdots & \ddots & \vdots & & \vdots & & \vdots \\ \mathbf{0} & \dots & \mathbf{Q}_k & \dots & \mathbf{0} & \dots & \mathbf{0} \\ \vdots & & \vdots & \ddots & \vdots & & \vdots \\ \mathbf{0} & \dots & \mathbf{0} & \dots & \mathbf{Q}_J & \dots & \mathbf{0} \\ \vdots & & \vdots & & \vdots & \ddots & \vdots \\ \mathbf{0} & \dots & \mathbf{0} & \dots & \mathbf{0} & \dots & \mathbf{Q}_{k_{\max}} \end{bmatrix} \begin{bmatrix} \mathbf{y}_{I,k_{\min}} \\ \vdots \\ \mathbf{y}_{I,k} \\ \vdots \\ \mathbf{y}_{I,l} \\ \vdots \\ \mathbf{y}_{I,k_{\max}} \end{bmatrix} = n \begin{bmatrix} \mathbf{Q}_{k_{\min}} \mathbf{y}_{I,k_{\min}} \\ \vdots \\ \mathbf{Q}_k \mathbf{y}_{I,k} \\ \vdots \\ \mathbf{Q}_J \mathbf{y}_{I,l} \\ \vdots \\ \mathbf{Q}_{k_{\max}} \mathbf{y}_{I,k_{\max}} \end{bmatrix} \quad (3.3.211)$$

The matrices \mathbf{P}_C and \mathbf{M}_C have a structure analogous to \mathbf{Q}_C . Thereby, it is valid:

$$\begin{bmatrix} \mathbf{0} \\ \vdots \\ \mathbf{0} \\ \vdots \\ \mathbf{0} \\ \vdots \\ \mathbf{0} \end{bmatrix} = \lambda_I^2 n \underbrace{\begin{bmatrix} \mathbf{M}_{k_{\min}} \mathbf{y}_{I,k_{\min}} \\ \vdots \\ \mathbf{M}_k \mathbf{y}_{I,k} \\ \vdots \\ \mathbf{M}_J \mathbf{y}_{I,l} \\ \vdots \\ \mathbf{M}_{k_{\max}} \mathbf{y}_{I,k_{\max}} \end{bmatrix}}_{\mathbf{T}_{CF}^H \mathbf{M}_C \mathbf{T}_{CF} \mathbf{y}_{FI}} + \lambda_I n \underbrace{\begin{bmatrix} \mathbf{P}_{k_{\min}} \mathbf{y}_{I,k_{\min}} \\ \vdots \\ \mathbf{P}_k \mathbf{y}_{I,k} \\ \vdots \\ \mathbf{P}_J \mathbf{y}_{I,l} \\ \vdots \\ \mathbf{P}_{k_{\max}} \mathbf{y}_{I,k_{\max}} \end{bmatrix}}_{\mathbf{T}_{CF}^H \mathbf{P}_C \mathbf{T}_{CF} \mathbf{y}_{FI}} + n \underbrace{\begin{bmatrix} \mathbf{Q}_{k_{\min}} \mathbf{y}_{I,k_{\min}} \\ \vdots \\ \mathbf{Q}_k \mathbf{y}_{I,k} \\ \vdots \\ \mathbf{Q}_J \mathbf{y}_{I,l} \\ \vdots \\ \mathbf{Q}_{k_{\max}} \mathbf{y}_{I,k_{\max}} \end{bmatrix}}_{\mathbf{T}_{CF}^H \mathbf{Q}_C \mathbf{T}_{CF} \mathbf{y}_{FI}} \quad (3.3.212)$$

The evaluation of the subvectors leads to:

$$\begin{aligned} k \in \{k \in \mathbb{Z} \mid k_{\min} \leq k \leq k_{\max}\} : \mathbf{0} &= \lambda_I^2 n \mathbf{M}_k \mathbf{y}_{I,k} + \lambda_I n \mathbf{P}_k \mathbf{y}_{I,k} + n \mathbf{Q}_k \mathbf{y}_{I,k} \\ &\Rightarrow \mathbf{0} = \left(\lambda_I^2 \mathbf{M}_k + \lambda_I \mathbf{P}_k + \mathbf{Q}_k \right) \mathbf{y}_{I,k} \end{aligned} \quad (3.3.213)$$

It should be noted that the factor $n > 2$, which results from the transformation, is eliminated since it appears in all three terms. – In an analogous way the left eigenvector problem is multiplied by

\mathbf{T}_{CF} and the formulation of the left eigenvector according to (3.3.209) is applied. This leads to:

$$\begin{aligned} \mathbf{0} &= \underbrace{\mathbf{x}_{FI}^H \mathbf{T}_{CF}^H}_{\mathbf{x}_{CI}^H} \left(\lambda_I^2 \mathbf{M}_C + \lambda_I \mathbf{P}_C + \mathbf{Q}_C \right) \mathbf{T}_{CF} \\ &\Rightarrow \mathbf{0} = \mathbf{x}_{FI}^H \left(\lambda_I^2 \mathbf{T}_{CF}^H \mathbf{M}_C \mathbf{T}_{CF} + \lambda_I \mathbf{T}_{CF}^H \mathbf{P}_C \mathbf{T}_{CF} + \mathbf{T}_{CF}^H \mathbf{Q}_C \mathbf{T}_{CF} \right) \end{aligned} \quad (3.3.214)$$

Due to the block-diagonal structure of the product $\mathbf{T}_{CF}^H \mathbf{Q}_C \mathbf{T}_{CF}$ it is obtained:

$$\begin{aligned} \mathbf{x}_{FI}^H \mathbf{T}_{CF}^H \mathbf{Q}_C \mathbf{T}_{CF} &= \left[\mathbf{x}_{I,k_{\min}}^H \cdots \mathbf{x}_{I,k}^H \cdots \mathbf{x}_{I,l}^H \cdots \mathbf{x}_{I,k_{\max}}^H \right] n \begin{bmatrix} \mathbf{Q}_{k_{\min}} & \cdots & \mathbf{0} & \cdots & \mathbf{0} & \cdots & \mathbf{0} \\ \vdots & \ddots & \vdots & & \vdots & & \vdots \\ \mathbf{0} & \cdots & \mathbf{Q}_k & \cdots & \mathbf{0} & \cdots & \mathbf{0} \\ \vdots & & \vdots & \ddots & \vdots & & \vdots \\ \mathbf{0} & \cdots & \mathbf{0} & \cdots & \mathbf{Q}_J & \cdots & \mathbf{0} \\ \vdots & & \vdots & & \vdots & \ddots & \vdots \\ \mathbf{0} & \cdots & \mathbf{0} & \cdots & \mathbf{0} & \cdots & \mathbf{Q}_{k_{\max}} \end{bmatrix} \\ &= n \left[\mathbf{x}_{I,k_{\min}}^H \mathbf{Q}_{k_{\min}} \cdots \mathbf{x}_{I,k}^H \mathbf{Q}_k \cdots \mathbf{x}_{I,l}^H \mathbf{Q}_J \cdots \mathbf{x}_{I,k_{\max}}^H \mathbf{Q}_{k_{\max}} \right] \end{aligned} \quad (3.3.215)$$

Also here, the analogous structure of the matrices \mathbf{Q}_C , \mathbf{P}_C and \mathbf{M}_C is applied; from this it follows:

$$\begin{aligned} &\left[\mathbf{0} \cdots \mathbf{0} \cdots \mathbf{0} \cdots \mathbf{0} \right] \\ &= \lambda_I^2 n \underbrace{\left[\mathbf{x}_{I,k_{\min}}^H \mathbf{M}_{k_{\min}} \cdots \mathbf{x}_{I,k}^H \mathbf{M}_k \cdots \mathbf{x}_{I,l}^H \mathbf{M}_J \cdots \mathbf{x}_{I,k_{\max}}^H \mathbf{M}_{k_{\max}} \right]}_{\mathbf{x}_{FI}^H \mathbf{T}_{CF}^H \mathbf{M}_C \mathbf{T}_{CF}} \\ &+ \lambda_I n \underbrace{\left[\mathbf{x}_{I,k_{\min}}^H \mathbf{P}_{k_{\min}} \cdots \mathbf{x}_{I,k}^H \mathbf{P}_k \cdots \mathbf{x}_{I,l}^H \mathbf{P}_J \cdots \mathbf{x}_{I,k_{\max}}^H \mathbf{P}_{k_{\max}} \right]}_{\mathbf{x}_{FI}^H \mathbf{T}_{CF}^H \mathbf{P}_C \mathbf{T}_{CF}} \\ &+ n \underbrace{\left[\mathbf{x}_{I,k_{\min}}^H \mathbf{Q}_{k_{\min}} \cdots \mathbf{x}_{I,k}^H \mathbf{Q}_k \cdots \mathbf{x}_{I,l}^H \mathbf{Q}_J \cdots \mathbf{x}_{I,k_{\max}}^H \mathbf{Q}_{k_{\max}} \right]}_{\mathbf{x}_{FI}^H \mathbf{T}_{CF}^H \mathbf{Q}_C \mathbf{T}_{CF}} \end{aligned} \quad (3.3.216)$$

By evaluating the subvectors it is obtained:

$$\begin{aligned} k \in \{k \in \mathbb{Z} \mid k_{\min} \leq k \leq k_{\max}\} : \mathbf{0} &= \lambda_I^2 n \mathbf{x}_{I,k}^H \mathbf{M}_k + \lambda_I n \mathbf{x}_{I,k}^H \mathbf{P}_k + n \mathbf{x}_{I,k}^H \mathbf{Q}_k \\ &\Rightarrow \mathbf{0} = \mathbf{x}_{I,k}^H \left(\lambda_I^2 \mathbf{M}_k + \lambda_I \mathbf{P}_k + \mathbf{Q}_k \right) \end{aligned} \quad (3.3.217)$$

According to (3.3.208) and (3.3.209) the vectors \mathbf{y}_{FI} and \mathbf{x}_{FI} are composed of subvectors $\mathbf{y}_{I,k}$ and $\mathbf{x}_{I,k}$, respectively. For the wanted non-trivial solutions $\mathbf{y}_{FI} \neq \mathbf{0}$ and $\mathbf{x}_{FI} \neq \mathbf{0}$ it is sufficient if at least one subvector is different from the zero vector $\mathbf{0}$. Therefore, it is set for the subvectors $\mathbf{y}_{I,k}$ and $\mathbf{x}_{I,k}$, which form the vectors \mathbf{y}_{FI} and \mathbf{x}_{FI} :

$$\mathbf{y}_{I,k} = \begin{cases} \mathbf{Y}_I \neq \mathbf{0} & \text{for } k = k_I \\ \mathbf{0} & \text{for } k \neq k_I \end{cases} \Rightarrow \mathbf{y}_{FI} \neq \mathbf{0} \quad (3.3.218)$$

$$\mathbf{x}_{I,k} = \begin{cases} \mathbf{X}_I \neq \mathbf{0} & \text{for } k = k_I \\ \mathbf{0} & \text{for } k \neq k_I \end{cases} \Rightarrow \mathbf{x}_{FI} \neq \mathbf{0} \quad (3.3.219)$$

Here, k_I is the periodicity for the eigenvectors \mathbf{y}_{CI} and \mathbf{x}_{CI} of the cyclic system. For the periodicities $k \neq k_I$ the chosen vectors $\mathbf{y}_{I,k} = \mathbf{0}$ and $\mathbf{x}_{I,k} = \mathbf{0}$ are the trivial solutions, which generally fulfil the

conditions (3.3.213) and (3.3.217):

$$k \neq k_I : \mathbf{y}_{I,k} = \mathbf{0} \Rightarrow \left(\lambda_I^2 \mathbf{M}_k + \lambda_I \mathbf{P}_k + \mathbf{Q}_k \right) \mathbf{y}_{I,k} = \mathbf{0} \quad (3.3.220)$$

$$\mathbf{x}_{I,k} = \mathbf{0} \Rightarrow \mathbf{x}_{I,k}^H \left(\lambda_I^2 \mathbf{M}_k + \lambda_I \mathbf{P}_k + \mathbf{Q}_k \right) = \mathbf{0} \quad (3.3.221)$$

The eigenvalue λ_I and the vectors \mathbf{Y}_I and \mathbf{X}_I are determined by solving the decoupled eigenvector problems for the periodicity k_I ; this problem is described by the following equations:

$$\det \left(\lambda_I^2 \mathbf{M}_{k_I} + \lambda_I \mathbf{P}_{k_I} + \mathbf{Q}_{k_I} \right) = 0 \quad (3.3.222)$$

$$\left(\lambda_I^2 \mathbf{M}_{k_I} + \lambda_I \mathbf{P}_{k_I} + \mathbf{Q}_{k_I} \right) \mathbf{Y}_I = \mathbf{0}, \mathbf{Y}_I \neq \mathbf{0} \quad (3.3.223)$$

$$\mathbf{X}_I^H \left(\lambda_I^2 \mathbf{M}_{k_I} + \lambda_I \mathbf{P}_{k_I} + \mathbf{Q}_{k_I} \right) = \mathbf{0}, \mathbf{X}_I \neq \mathbf{0} \quad (3.3.224)$$

By solving these equations the non-trivial solutions \mathbf{Y}_I and \mathbf{X}_I , which fulfil the conditions (3.3.213) and (3.3.217) for $k = k_I$, are determined. For the vectors $\mathbf{y}_I^{(j)}$ and $\mathbf{x}_I^{(j)}$, which form the eigenvectors \mathbf{y}_{CI} and \mathbf{x}_{CI} , respectively, it is obtained:

$$\mathbf{y}_{I,k} = \begin{cases} \mathbf{Y}_I \neq \mathbf{0} & \text{for } k = k_I \\ \mathbf{0} & \text{for } k \neq k_I \end{cases} \Rightarrow \mathbf{y}_I^{(j)} = \sum_{k=k_{\min}}^{k_{\max}} \mathbf{y}_{I,k} \zeta^{kj} = \mathbf{Y}_I \zeta^{k_I j} \neq \mathbf{0} \Rightarrow \mathbf{y}_{CI} \neq \mathbf{0} \quad (3.3.225)$$

$$\mathbf{x}_{I,k} = \begin{cases} \mathbf{X}_I \neq \mathbf{0} & \text{for } k = k_I \\ \mathbf{0} & \text{for } k \neq k_I \end{cases} \Rightarrow \mathbf{x}_I^{(j)} = \sum_{k=k_{\min}}^{k_{\max}} \mathbf{x}_{I,k} \zeta^{kj} = \mathbf{X}_I \zeta^{k_I j} \neq \mathbf{0} \Rightarrow \mathbf{x}_{CI} \neq \mathbf{0} \quad (3.3.226)$$

As a result, the eigenvectors \mathbf{y}_{CI} and \mathbf{x}_{CI} for the entire cyclic system are found; together with the eigenvalue λ_I , to which the vectors are associated, they fulfil the following conditions:

$$\left(\lambda_I^2 \mathbf{M}_C + \lambda_I \mathbf{P}_C + \mathbf{Q}_C \right) \mathbf{y}_{CI} = \mathbf{0}, \mathbf{y}_{CI} \neq \mathbf{0} \quad (3.3.227)$$

$$\mathbf{x}_{CI}^H \left(\lambda_I^2 \mathbf{M}_C + \lambda_I \mathbf{P}_C + \mathbf{Q}_C \right) = \mathbf{0}, \mathbf{x}_{CI} \neq \mathbf{0} \quad (3.3.228)$$

As it can be seen from (3.3.225) and (3.3.226) each eigenvector has only one periodicity k_I due to the decoupling of the motions for different periodicities. Of course, it is possible that double eigenvalues occur, i.e. for $I \neq J$ two eigenvalues $\lambda_I = \lambda_J$ are equal; in this case, a linear combination of the two right eigenvectors \mathbf{y}_{CI} and \mathbf{y}_{CJ} , too, is a right eigenvector:

$$\left(\lambda_I^2 \mathbf{M}_C + \lambda_I \mathbf{P}_C + \mathbf{Q}_C \right) \mathbf{y}_{CI} = \mathbf{0}, \left(\lambda_J^2 \mathbf{M}_C + \lambda_J \mathbf{P}_C + \mathbf{Q}_C \right) \mathbf{y}_{CJ} = \mathbf{0} \quad (3.3.229)$$

$$\lambda_I = \lambda_J \Rightarrow \left(\lambda_I^2 \mathbf{M}_C + \lambda_I \mathbf{P}_C + \mathbf{Q}_C \right) (a_I \mathbf{y}_{CI} + a_J \mathbf{y}_{CJ}) = \mathbf{0}, a_I, a_J \in \mathbb{C} \quad (3.3.230)$$

$$\Rightarrow a_I \mathbf{y}_I^{(j)} + a_J \mathbf{y}_J^{(j)} = a_I \mathbf{Y}_I \zeta^{k_I j} + a_J \mathbf{Y}_J \zeta^{k_J j} \quad (3.3.231)$$

In an analogous way, this is valid for the left eigenvectors, i.e. the linear combination $b_I \mathbf{x}_{CI} + b_J \mathbf{x}_{CJ}$, $b_I, b_J \in \mathbb{C}$ of the left eigenvectors \mathbf{x}_{CI} and \mathbf{x}_{CJ} , too, is a left eigenvector. If the eigenvectors have different periodicities $k_I \neq k_J$, the resulting linear combination has more than one periodicity. In the present case, where no further properties of the matrices \mathbf{M}_C , \mathbf{P}_C and \mathbf{Q}_C are assumed, the occurrence of such double eigenvalues is a coincidence, which cannot be assumed in general.

In the previous section 3.3.1 the eigenvector problem has been formulated in two ways, one based on the original equation of motion, the other one using the state space representation. These

relations are relevant for the formulating the eigenvector problem in the standardized form, so that existing numerical algorithms e.g. as contained in the well-known software library LAPACK [1] can be applied; this aspect will be considered later. Furthermore, these relations are important in the context of the orthogonality of eigenvectors, particularly in the context to the already mentioned problem of double eigenvalues. For a right eigenvector \mathbf{w}_I associated to the eigenvalue λ_I and a left eigenvector \mathbf{v}_J associated to the eigenvalue λ_J it is valid:

$$\lambda_I \underbrace{\begin{bmatrix} \mathbf{y}_{I1} \\ \mathbf{y}_{I2} \end{bmatrix}}_{\mathbf{w}_I} = \underbrace{\begin{bmatrix} \mathbf{0} & \mathbf{I} \\ -\mathbf{M}^{-1}\mathbf{Q} & -\mathbf{M}^{-1}\mathbf{P} \end{bmatrix}}_{\mathbf{A}} \underbrace{\begin{bmatrix} \mathbf{y}_{I1} \\ \mathbf{y}_{I2} \end{bmatrix}}_{\mathbf{w}_I}, \quad \mathbf{y}_I = \mathbf{y}_{I1} \quad (3.3.232)$$

$$\lambda_J \underbrace{\begin{bmatrix} \mathbf{x}_{J1}^H & \mathbf{x}_{J2}^H \end{bmatrix}}_{\mathbf{v}_J^H} = \underbrace{\begin{bmatrix} \mathbf{x}_{J1}^H & \mathbf{x}_{J2}^H \end{bmatrix}}_{\mathbf{v}_J^H} \underbrace{\begin{bmatrix} \mathbf{0} & \mathbf{I} \\ -\mathbf{M}^{-1}\mathbf{Q} & -\mathbf{M}^{-1}\mathbf{P} \end{bmatrix}}_{\mathbf{A}}, \quad \mathbf{x}_J^H = \mathbf{x}_{J2}^H \mathbf{M} \quad (3.3.233)$$

$$\Rightarrow \mathbf{v}_J^H \mathbf{w}_I = (\lambda_I + \lambda_J) \mathbf{x}_J^H \mathbf{M} \mathbf{y}_I + \mathbf{x}_J^H \mathbf{P} \mathbf{y}_I \quad (3.3.234)$$

$$\Rightarrow \lambda_J \mathbf{v}_J^H \mathbf{w}_I = -\mathbf{x}_J^H \mathbf{Q} \mathbf{y}_I + \lambda_I \lambda_J \mathbf{x}_J^H \mathbf{M} \mathbf{y}_I \quad (3.3.235)$$

By applying this to the eigenvector problem of the cyclic system described by (3.3.204), (3.3.205), (3.3.206) and (3.3.207) it is obtained:

$$\begin{aligned} \mathbf{v}_{CJ}^H \mathbf{w}_{CI} &= (\lambda_I + \lambda_J) \mathbf{x}_{CJ}^H \mathbf{M}_C \mathbf{y}_{CI} + \mathbf{x}_{CJ}^H \mathbf{P}_C \mathbf{y}_{CI} \\ &= (\lambda_I + \lambda_J) \mathbf{x}_{FJ}^H \mathbf{T}_{CF}^H \mathbf{M}_C \mathbf{T}_{CF} \mathbf{y}_{FI} + \mathbf{x}_{FJ}^H \mathbf{T}_{CF}^H \mathbf{P}_C \mathbf{T}_{CF} \mathbf{y}_{FI} \end{aligned} \quad (3.3.236)$$

$$\begin{aligned} \lambda_J \mathbf{v}_{CJ}^H \mathbf{w}_{CI} &= -\mathbf{x}_{CJ}^H \mathbf{Q}_C \mathbf{y}_{CI} + \lambda_I \lambda_J \mathbf{x}_{CJ}^H \mathbf{M}_C \mathbf{y}_{CI} \\ &= -\mathbf{x}_{FJ}^H \mathbf{T}_{CF}^H \mathbf{Q}_C \mathbf{T}_{CF} \mathbf{y}_{FI} + \lambda_I \lambda_J \mathbf{x}_{FJ}^H \mathbf{T}_{CF}^H \mathbf{M}_C \mathbf{T}_{CF} \mathbf{y}_{FI} \end{aligned} \quad (3.3.237)$$

The product $\mathbf{x}_{FJ}^H \mathbf{T}_{CF}^H \mathbf{Q}_C \mathbf{T}_{CF} \mathbf{y}_{FI}$ is evaluated based on (3.3.211); by multiplying this expression by \mathbf{x}_{FJ}^H it is obtained:

$$\underbrace{\begin{bmatrix} \mathbf{x}_{J,k_{\min}}^H & \cdots & \mathbf{x}_{J,k}^H & \cdots & \mathbf{x}_{J,l}^H & \cdots & \mathbf{x}_{J,k_{\max}}^H \end{bmatrix}}_{\mathbf{x}_{FJ}^H} n \underbrace{\begin{bmatrix} \mathbf{Q}_{k_{\min}} \mathbf{y}_{I,k_{\min}} \\ \vdots \\ \mathbf{Q}_k \mathbf{y}_{I,k} \\ \vdots \\ \mathbf{Q}_l \mathbf{y}_{I,l} \\ \vdots \\ \mathbf{Q}_{k_{\max}} \mathbf{y}_{I,k_{\max}} \end{bmatrix}}_{\mathbf{T}_{CF}^H \mathbf{Q}_C \mathbf{T}_{CF} \mathbf{y}_{FI}} = n \sum_{k=k_{\min}}^{k_{\max}} \mathbf{x}_{J,k}^H \mathbf{Q}_k \mathbf{y}_{I,k} \quad (3.3.238)$$

For the vectors $\mathbf{y}_{I,k}$ it is valid:

$$\mathbf{y}_{I,k} = \begin{cases} \mathbf{Y}_I \neq \mathbf{0} & \text{for } k = k_I \\ \mathbf{0} & \text{for } k \neq k_I \end{cases} \quad (3.3.239)$$

Since only one vector $\mathbf{y}_{I,k}$ is different from the zero vector, all summands of the sum contained in (3.3.238) except the one for $k = k_I$ vanish immediately so that it is obtained:

$$\mathbf{x}_{CJ}^H \mathbf{Q}_C \mathbf{y}_{CI} = \mathbf{x}_{FJ}^H \mathbf{T}_{CF}^H \mathbf{Q}_C \mathbf{T}_{CF} \mathbf{y}_{FI} = n \sum_{k=k_{\min}}^{k_{\max}} \mathbf{x}_{J,k}^H \mathbf{Q}_k \mathbf{y}_{I,k} = n \mathbf{x}_{J,k_I}^H \mathbf{Q}_{k_I} \mathbf{Y}_I \quad (3.3.240)$$

Based on (3.3.226) it is valid for the vectors $\mathbf{x}_{J,k}$:

$$\mathbf{x}_{J,k} = \begin{cases} \mathbf{X}_J \neq \mathbf{0} & \text{for } k = k_J \\ \mathbf{0} & \text{for } k \neq k_J \end{cases} \quad (3.3.241)$$

Applying this to the expression (3.3.240) leads to:

$$\mathbf{x}_{CJ}^H \mathbf{Q}_C \mathbf{y}_{CI} = n \mathbf{x}_{J,k_I}^H \mathbf{Q}_{k_I} \mathbf{Y}_I = \begin{cases} n \mathbf{X}_J^H \mathbf{Q}_{k_I} \mathbf{Y}_I & \text{for } k_I = k_J \\ \mathbf{0} & \text{for } k_I \neq k_J \end{cases} \quad (3.3.242)$$

Due to the analogous structure of the matrices \mathbf{Q}_C , \mathbf{P}_C and \mathbf{M}_C it is valid:

$$\mathbf{x}_{CJ}^H \mathbf{P}_C \mathbf{y}_{CI} = n \mathbf{x}_{J,k_I}^H \mathbf{P}_{k_I} \mathbf{Y}_I = \begin{cases} n \mathbf{X}_J^H \mathbf{P}_{k_I} \mathbf{Y}_I & \text{for } k_I = k_J \\ \mathbf{0} & \text{for } k_I \neq k_J \end{cases} \quad (3.3.243)$$

$$\mathbf{x}_{CJ}^H \mathbf{M}_C \mathbf{y}_{CI} = n \mathbf{x}_{J,k_I}^H \mathbf{M}_{k_I} \mathbf{Y}_I = \begin{cases} n \mathbf{X}_J^H \mathbf{M}_{k_I} \mathbf{Y}_I & \text{for } k_I = k_J \\ \mathbf{0} & \text{for } k_I \neq k_J \end{cases} \quad (3.3.244)$$

For different periodicities $k_I \neq k_J$ the eigenvectors \mathbf{x}_{CJ} and \mathbf{y}_{CI} are orthogonal with respect to all three matrices \mathbf{M}_C , \mathbf{P}_C and \mathbf{Q}_C . By inserting these results into the relations (3.3.236) and (3.3.236) that for different periodicities $k_I \neq k_J$ also the eigenvectors \mathbf{w}_{CI} and \mathbf{v}_{CJ} , which are obtained for the system matrix \mathbf{A}_C , are orthogonal:

$$k_I \neq k_J \Rightarrow \mathbf{v}_{CJ}^H \mathbf{w}_{CI} = (\lambda_I + \lambda_J) \underbrace{\mathbf{x}_{CJ}^H \mathbf{M}_C \mathbf{y}_{CI}}_0 + \underbrace{\mathbf{x}_{CJ}^H \mathbf{P}_C \mathbf{y}_{CI}}_0 = 0 \quad (3.3.245)$$

$$k_I \neq k_J \Rightarrow \lambda_J \mathbf{v}_{CJ}^H \mathbf{w}_{CI} = - \underbrace{\mathbf{x}_{CJ}^H \mathbf{Q}_C \mathbf{y}_{CI}}_0 + \lambda_I \lambda_J \underbrace{\mathbf{x}_{CJ}^H \mathbf{M}_C \mathbf{y}_{CI}}_0 = 0 \quad (3.3.246)$$

Since for different periodicities $k_I \neq k_J$ the products $\mathbf{x}_{CJ}^H \mathbf{M}_C \mathbf{y}_{CI}$, $\mathbf{x}_{CJ}^H \mathbf{P}_C \mathbf{y}_{CI}$ and $\mathbf{x}_{CJ}^H \mathbf{Q}_C \mathbf{y}_{CI}$ vanish, the orthogonality of the vectors does not depend on the eigenvalues λ_I and λ_J . As it can be seen from (3.3.211) and (3.3.238) the orthogonality results from the block-diagonal structure of the product $\mathbf{T}_{CF}^H \mathbf{Q}_C \mathbf{T}_{CF}$; as discussed in the section 3.2, this block-diagonal structure, in turn, is a consequence of the structure of the original matrix \mathbf{Q}_C indicated in (3.0.5). In an analogous way this is valid for the products $\mathbf{T}_{CF}^H \mathbf{P}_C \mathbf{T}_{CF}$ and $\mathbf{T}_{CF}^H \mathbf{M}_C \mathbf{T}_{CF}$.

Up to here, only the structure of the matrices \mathbf{M}_C , \mathbf{P}_C and \mathbf{Q}_C according to (3.0.5) has been used. For the following considerations, it is assumed in addition that the matrices \mathbf{M}_C , \mathbf{P}_C and \mathbf{Q}_C and thereby also their submatrices $\mathbf{M}^{(I)}$, $\mathbf{P}^{(I)}$ and $\mathbf{Q}^{(I)}$ are real matrices. The matrices \mathbf{M}_k , \mathbf{P}_k and \mathbf{Q}_k are defined in the following way:

$$\begin{aligned} \mathbf{M}_k &= \mathbf{M}^{(-1)} \zeta^{-k} + \mathbf{M}^{(0)} + \mathbf{M}^{(1)} \zeta^k, \quad \mathbf{P}_k = \mathbf{P}^{(-1)} \zeta^{-k} + \mathbf{P}^{(0)} + \mathbf{P}^{(1)} \zeta^k, \\ \mathbf{Q}_k &= \mathbf{Q}^{(-1)} \zeta^{-k} + \mathbf{Q}^{(0)} + \mathbf{Q}^{(1)} \zeta^k \end{aligned} \quad (3.3.247)$$

As derived in the previous section 3.2 it is valid for the matrices \mathbf{M}_k , \mathbf{P}_k and \mathbf{Q}_k :

$$\mathbf{Q}_C = \overline{\mathbf{Q}_C} \Rightarrow \mathbf{Q}^{(I)} = \overline{\mathbf{Q}^{(I)}} \Rightarrow \mathbf{Q}_{-k} = \overline{\mathbf{Q}_k} \quad (3.3.248)$$

$$\mathbf{P}_C = \overline{\mathbf{P}_C} \Rightarrow \mathbf{P}^{(I)} = \overline{\mathbf{P}^{(I)}} \Rightarrow \mathbf{P}_{-k} = \overline{\mathbf{P}_k} \quad (3.3.249)$$

$$\mathbf{M}_C = \overline{\mathbf{M}_C} \Rightarrow \mathbf{M}^{(I)} = \overline{\mathbf{M}^{(I)}} \Rightarrow \mathbf{M}_{-k} = \overline{\mathbf{M}_k} \quad (3.3.250)$$

For the following considerations it is assumed that the range of the periodicity k is centred or nearly centred around zero, as discussed in the section 3.1.3. As derived in (3.1.89), it is valid:

$$-\frac{n}{2} < k_{\min} \leq k \leq k_{\max} \leq \frac{n}{2} \Rightarrow -\frac{n}{2} < k \leq \frac{n}{2} \quad (3.3.251)$$

Since the range for k is nearly centred around zero, for nearly each periodicity k a corresponding negative value $-k$, too, is contained in the interval so that the relations (3.3.248), (3.3.249) and (3.3.250) can be used.

Since the submatrices $\mathbf{M}^{(l)}$, $\mathbf{P}^{(l)}$ and $\mathbf{Q}^{(l)}$ are real, the matrices \mathbf{M}_k , \mathbf{P}_k and \mathbf{Q}_k can easily be split up into their real and imaginary parts. As an example, the matrix \mathbf{Q}_k shall be considered; it is valid:

$$\begin{aligned} \zeta^{-k} = \overline{\zeta^k}, \mathbf{Q}^{(l)} = \overline{\mathbf{Q}^{(l)}} &\Rightarrow \mathbf{Q}_k = \mathbf{Q}^{(-1)} \underbrace{\left(\Re \zeta^k - i \Im \zeta^k \right)}_{\zeta^{-k}} + \mathbf{Q}^{(0)} + \mathbf{Q}^{(1)} \underbrace{\left(\Re \zeta^k + i \Im \zeta^k \right)}_{\zeta^k} \\ &= \underbrace{\mathbf{Q}^{(0)} + \Re \zeta^k \left(\mathbf{Q}^{(1)} + \mathbf{Q}^{(-1)} \right)}_{\Re \mathbf{Q}_k} + i \underbrace{\Im \zeta^k \left(\mathbf{Q}^{(1)} - \mathbf{Q}^{(-1)} \right)}_{\Im \mathbf{Q}_k} \end{aligned} \quad (3.3.252)$$

It shall first be checked, for which periodicities k the matrix \mathbf{Q}_k is real; to this end, the power ζ^k has to be considered:

$$\zeta^k = e^{\frac{2\pi}{n}ik} = \cos\left(\frac{2\pi}{n}k\right) + i \sin\left(\frac{2\pi}{n}k\right) \Rightarrow \Re \zeta^k = \cos\left(\frac{2\pi}{n}k\right), \Im \zeta^k = \sin\left(\frac{2\pi}{n}k\right) \quad (3.3.253)$$

For the sine function it is valid:

$$m \in \mathbb{Z} \Leftrightarrow \sin(m\pi) = 0 \quad (3.3.254)$$

By applying this to the imaginary part $\Im \zeta^k$ according to (3.3.253) it is obtained:

$$\Im \zeta^k = \sin\left(\frac{2\pi}{n}k\right) = 0 \Leftrightarrow \frac{2k}{n} \in \mathbb{Z} \quad (3.3.255)$$

By dividing the relation (3.3.251) by $\frac{n}{2}$, the range for the quotient $\frac{2k}{n}$ is obtained so that the values for $\frac{2k}{n} \in \mathbb{Z}$ can be determined:

$$-\frac{n}{2} < k \leq \frac{n}{2} \Rightarrow -1 < \frac{2k}{n} \leq 1, -1 < \frac{2k}{n} \leq 1 \wedge \frac{2k}{n} \in \mathbb{Z} \Rightarrow \frac{2k}{n} \in \{0, 1\} \quad (3.3.256)$$

The periodicities k , for which the power ζ^k is a real number, are obtained to:

$$\frac{2k}{n} = 0 \Rightarrow k = 0 \Rightarrow \zeta^k = \zeta^0 = 1 \quad (3.3.257)$$

$$\frac{2k}{n} = 1 \Rightarrow k = \frac{n}{2} \Rightarrow \zeta^k = \zeta^{\frac{n}{2}} = e^{\frac{2\pi}{n}i\frac{n}{2}} = e^{\pi i} = \cos(\pi) + i \sin(\pi) = -1 \quad (3.3.258)$$

Based on the definition of the matrices \mathbf{Q}_k , \mathbf{P}_k and \mathbf{M}_k according to (3.3.247), the matrices \mathbf{Q}_0 , \mathbf{P}_0 and \mathbf{M}_0 are given by:

$$\zeta^k = \zeta^0 = 1 \Rightarrow \mathbf{Q}_0 = \mathbf{Q}^{(-1)} + \mathbf{Q}^{(0)} + \mathbf{Q}^{(1)}, \mathbf{P}_0 = \mathbf{P}^{(-1)} + \mathbf{P}^{(0)} + \mathbf{P}^{(1)}, \mathbf{M}_0 = \mathbf{M}^{(-1)} + \mathbf{M}^{(0)} + \mathbf{M}^{(1)} \quad (3.3.259)$$

The eigenvectors of the cyclic system, which have the periodicity $k_I = 0$, are obtained to:

$$k_I = 0 \Rightarrow \zeta^{k_I j} = \zeta^0 = 1 \Rightarrow \mathbf{y}_I^{(j)} = \mathbf{Y}_I, \mathbf{x}_I^{(j)} = \mathbf{X}_I \quad (3.3.260)$$

While the periodicity $k = 0$ occurs for all values n , the second periodicity $k = \frac{n}{2}$, for which the matrices \mathbf{Q}_k , \mathbf{P}_k and \mathbf{M}_k are real matrices, only occurs for an even number n , i.e. $\frac{n}{2} \in \mathbb{N}$, because the periodicity k is an integer. Then, the matrices $\mathbf{Q}_{\frac{n}{2}}$, $\mathbf{P}_{\frac{n}{2}}$ and $\mathbf{M}_{\frac{n}{2}}$ are obtained to:

$$\zeta^k = \zeta^{\frac{n}{2}} = -1 \Rightarrow \mathbf{Q}_0 = \mathbf{Q}^{(0)} - \mathbf{Q}^{(1)} - \mathbf{Q}^{(-1)}, \mathbf{P}_0 = \mathbf{P}^{(0)} - \mathbf{P}^{(1)} - \mathbf{P}^{(-1)}, \mathbf{M}_0 = \mathbf{M}^{(0)} - \mathbf{M}^{(1)} - \mathbf{M}^{(-1)} \quad (3.3.261)$$

For the eigenvectors having the periodicity $k_I = \frac{n}{2}$ it is valid:

$$k_I = \frac{n}{2} \Rightarrow \zeta^{k_I j} = \left(\zeta^{k_I}\right)^j = (-1)^j \Rightarrow \mathbf{y}_I^{(j)} = (-1)^j \mathbf{Y}_I, \mathbf{x}_I^{(j)} = (-1)^j \mathbf{X}_I \quad (3.3.262)$$

For all other periodicities, i.e. for $k \neq 0 \wedge k \neq \frac{n}{2}$, the imaginary parts of the power ζ^k and thereby also of the power $\zeta^{-k} = \overline{\zeta^k}$ do not vanish, so that the matrices \mathbf{Q}_k , \mathbf{P}_k and \mathbf{M}_k can be complex. However, by taking advantage from the relations $\mathbf{Q}_{-k} = \overline{\mathbf{Q}_k}$, $\mathbf{P}_{-k} = \overline{\mathbf{P}_k}$ and $\mathbf{M}_{-k} = \overline{\mathbf{M}_k}$ according to (3.3.248), (3.3.249) and (3.3.250) the eigenvector problem can be formulated using real matrices. The basis is the condition (3.3.213), which must be fulfilled for each eigenvalue λ_I and for each periodicity k . For the two periodicities k and $-k$ it is valid:

$$\mathbf{0} = \left(\lambda_I^2 \mathbf{M}_k + \lambda_I \mathbf{P}_k + \mathbf{Q}_k\right) \mathbf{y}_{I,k} \quad (3.3.263)$$

$$\mathbf{0} = \left(\lambda_I^2 \mathbf{M}_{-k} + \lambda_I \mathbf{P}_{-k} + \mathbf{Q}_{-k}\right) \mathbf{y}_{I,-k} \quad (3.3.264)$$

By splitting the matrices \mathbf{M}_k , \mathbf{P}_k and \mathbf{Q}_k into their real and imaginary parts the content of the bracket in (3.3.263) is reformulated in the following way:

$$\begin{aligned} \lambda_I^2 \mathbf{M}_k + \lambda_I \mathbf{P}_k + \mathbf{Q}_k &= \lambda_I^2 (\Re \mathbf{M}_k + i \Im \mathbf{M}_k) + \lambda_I (\Re \mathbf{P}_k + i \Im \mathbf{P}_k) + (\Re \mathbf{Q}_k + i \Im \mathbf{Q}_k) \\ &= \lambda_I^2 \Re \mathbf{M}_k + \lambda_I \Re \mathbf{P}_k + \Re \mathbf{Q}_k + i \left(\lambda_I^2 \Im \mathbf{M}_k + \lambda_I \Im \mathbf{P}_k + \Im \mathbf{Q}_k\right) \end{aligned} \quad (3.3.265)$$

It should be noted that although the terms are grouped with respect to the factor i the two groups $\lambda_I^2 \Re \mathbf{M}_k + \lambda_I \Re \mathbf{P}_k + \Re \mathbf{Q}_k$ and $\lambda_I^2 \Im \mathbf{M}_k + \lambda_I \Im \mathbf{P}_k + \Im \mathbf{Q}_k$ are not necessarily equal to the real part and the imaginary part of $\lambda_I^2 \mathbf{M}_k + \lambda_I \mathbf{P}_k + \mathbf{Q}_k$, since the eigenvalue λ_I can be a complex number. – By applying the relations (3.3.248), (3.3.249) and (3.3.250) the expression contained in (3.3.264) is treated in an analogous way:

$$\begin{aligned} \lambda_I^2 \mathbf{M}_{-k} + \lambda_I \mathbf{P}_{-k} + \mathbf{Q}_{-k} &= \lambda_I^2 \overline{\mathbf{M}_k} + \lambda_I \overline{\mathbf{P}_k} + \overline{\mathbf{Q}_k} \\ &= \lambda_I^2 (\Re \mathbf{M}_k - i \Im \mathbf{M}_k) + \lambda_I (\Re \mathbf{P}_k - i \Im \mathbf{P}_k) + (\Re \mathbf{Q}_k - i \Im \mathbf{Q}_k) \\ &= \lambda_I^2 \Re \mathbf{M}_k + \lambda_I \Re \mathbf{P}_k + \Re \mathbf{Q}_k - i \left(\lambda_I^2 \Im \mathbf{M}_k + \lambda_I \Im \mathbf{P}_k + \Im \mathbf{Q}_k\right) \end{aligned} \quad (3.3.266)$$

Adding the two equations (3.3.263) and (3.3.264) and applying the relations (3.3.265) and (3.3.266) leads to:

$$\begin{aligned} \mathbf{0} &= \left(\lambda_I^2 \mathbf{M}_k + \lambda_I \mathbf{P}_k + \mathbf{Q}_k\right) \mathbf{y}_{I,k} + \left(\lambda_I^2 \mathbf{M}_{-k} + \lambda_I \mathbf{P}_{-k} + \mathbf{Q}_{-k}\right) \mathbf{y}_{I,-k} \\ &= \left[\lambda_I^2 \Re \mathbf{M}_k + \lambda_I \Re \mathbf{P}_k + \Re \mathbf{Q}_k + i \left(\lambda_I^2 \Im \mathbf{M}_k + \lambda_I \Im \mathbf{P}_k + \Im \mathbf{Q}_k\right)\right] \mathbf{y}_{I,k} \\ &\quad + \left[\lambda_I^2 \Re \mathbf{M}_k + \lambda_I \Re \mathbf{P}_k + \Re \mathbf{Q}_k - i \left(\lambda_I^2 \Im \mathbf{M}_k + \lambda_I \Im \mathbf{P}_k + \Im \mathbf{Q}_k\right)\right] \mathbf{y}_{I,-k} \\ &= \left(\lambda_I^2 \Re \mathbf{M}_k + \lambda_I \Re \mathbf{P}_k + \Re \mathbf{Q}_k\right) (\mathbf{y}_{I,k} + \mathbf{y}_{I,-k}) + \left(\lambda_I^2 \Im \mathbf{M}_k + \lambda_I \Im \mathbf{P}_k + \Im \mathbf{Q}_k\right) (i \mathbf{y}_{I,k} - i \mathbf{y}_{I,-k}) \end{aligned} \quad (3.3.267)$$

By multiplying both equations (3.3.263) and (3.3.264) by i , subtracting them and again applying

the transformations (3.3.265) and (3.3.266) it is obtained:

$$\begin{aligned}
\mathbf{0} &= i \left(\lambda_I^2 \mathbf{M}_k + \lambda_I \mathbf{P}_k + \mathbf{Q}_k \right) \mathbf{y}_{I,k} - i \left(\lambda_I^2 \mathbf{M}_{-k} + \lambda_I \mathbf{P}_{-k} + \mathbf{Q}_{-k} \right) \mathbf{y}_{I,-k} \\
&= i \left[\lambda_I^2 \Re \mathbf{M}_k + \lambda_I \Re \mathbf{P}_k + \Re \mathbf{Q}_k + i \left(\lambda_I^2 \Im \mathbf{M}_k + \lambda_I \Im \mathbf{P}_k + \Im \mathbf{Q}_k \right) \right] \mathbf{y}_{I,k} \\
&\quad - i \left[\lambda_I^2 \Re \mathbf{M}_k + \lambda_I \Re \mathbf{P}_k + \Re \mathbf{Q}_k - i \left(\lambda_I^2 \Im \mathbf{M}_k + \lambda_I \Im \mathbf{P}_k + \Im \mathbf{Q}_k \right) \right] \mathbf{y}_{I,-k} \\
&= \left(\lambda_I^2 \Re \mathbf{M}_k + \lambda_I \Re \mathbf{P}_k + \Re \mathbf{Q}_k \right) i \left(\mathbf{y}_{I,k} - \mathbf{y}_{I,-k} \right) + i^2 \left(\lambda_I^2 \Im \mathbf{M}_k + \lambda_I \Im \mathbf{P}_k + \Im \mathbf{Q}_k \right) \left(\mathbf{y}_{I,k} + \mathbf{y}_{I,-k} \right) \\
&= \left(\lambda_I^2 \Re \mathbf{M}_k + \lambda_I \Re \mathbf{P}_k + \Re \mathbf{Q}_k \right) \left(i \mathbf{y}_{I,k} - i \mathbf{y}_{I,-k} \right) - \left(\lambda_I^2 \Im \mathbf{M}_k + \lambda_I \Im \mathbf{P}_k + \Im \mathbf{Q}_k \right) \left(\mathbf{y}_{I,k} + \mathbf{y}_{I,-k} \right)
\end{aligned} \tag{3.3.268}$$

There are several possibilities to formulate the two equations as a right eigenvector problem using real matrices. In following formulation, the equation (3.3.267) is expressed by the first hyperrow, while the equation (3.3.268) is expressed by the second hyperrow:

$$\begin{bmatrix} \mathbf{0} \\ \mathbf{0} \end{bmatrix} = \left(\lambda_I^2 \begin{bmatrix} \Re \mathbf{M}_k & \Im \mathbf{M}_k \\ -\Im \mathbf{M}_k & \Re \mathbf{M}_k \end{bmatrix} + \lambda_I \begin{bmatrix} \Re \mathbf{P}_k & \Im \mathbf{P}_k \\ -\Im \mathbf{P}_k & \Re \mathbf{P}_k \end{bmatrix} + \begin{bmatrix} \Re \mathbf{Q}_k & \Im \mathbf{Q}_k \\ -\Im \mathbf{Q}_k & \Re \mathbf{Q}_k \end{bmatrix} \right) \begin{bmatrix} \mathbf{y}_{I,k} + \mathbf{y}_{I,-k} \\ i \mathbf{y}_{I,k} - i \mathbf{y}_{I,-k} \end{bmatrix} \tag{3.3.269}$$

In an alternative formulation, the first hyperrow represents the equation (3.3.268), while the evaluation of the second hyperrow yields the equation (3.3.268) multiplied by -1 :

$$\begin{bmatrix} \mathbf{0} \\ \mathbf{0} \end{bmatrix} = \left(\lambda_I^2 \begin{bmatrix} \Re \mathbf{M}_k & \Im \mathbf{M}_k \\ -\Im \mathbf{M}_k & \Re \mathbf{M}_k \end{bmatrix} + \lambda_I \begin{bmatrix} \Re \mathbf{P}_k & \Im \mathbf{P}_k \\ -\Im \mathbf{P}_k & \Re \mathbf{P}_k \end{bmatrix} + \begin{bmatrix} \Re \mathbf{Q}_k & \Im \mathbf{Q}_k \\ -\Im \mathbf{Q}_k & \Re \mathbf{Q}_k \end{bmatrix} \right) \begin{bmatrix} i \mathbf{y}_{I,k} - i \mathbf{y}_{I,-k} \\ -\mathbf{y}_{I,k} - \mathbf{y}_{I,-k} \end{bmatrix} \tag{3.3.270}$$

It should be pointed out that both formulations (3.3.269) and (3.3.270) are based on the equations (3.3.267) and (3.3.268), which again are obtained from combining the eigenvector conditions (3.3.263) and (3.3.264) for the periodicities k and $-k$.

Both formulations (3.3.269) and (3.3.270) use the same matrices, but a different formulation for the eigenvector. According to (3.3.218), the subvectors $\mathbf{y}_{I,k}$ of the eigenvector \mathbf{y}_F have been chosen as zero vectors except the vector $\mathbf{y}_{I,k_I} = \mathbf{Y}_I \neq \mathbf{0}$.

$$\mathbf{y}_{I,k} = \begin{cases} \mathbf{Y}_I \neq \mathbf{0} & \text{for } k = k_I \\ \mathbf{0} & \text{for } k \neq k_I \end{cases} \tag{3.3.271}$$

Therefore, it is valid for $k_I \neq 0$:

$$k_I \neq 0 \Rightarrow k_I \neq -k_I \Rightarrow \mathbf{y}_{I,k_I} = \mathbf{Y}_I \wedge \mathbf{y}_{I,-k_I} = \mathbf{0} \tag{3.3.272}$$

Based on this, the conditions (3.3.263) and (3.3.264) for $k = k_I$ are formulated and subsequently expressed by the two formulations (3.3.269) and (3.3.270). As a result, it is obtained:

$$\mathbf{0} = \left(\lambda_I^2 \mathbf{M}_{k_I} + \lambda_I \mathbf{P}_{k_I} + \mathbf{Q}_{k_I} \right) \mathbf{y}_{I,k_I}, \mathbf{y}_{I,k_I} = \mathbf{Y}_I \neq \mathbf{0} \tag{3.3.273}$$

$$\mathbf{0} = \left(\lambda_I^2 \mathbf{M}_{-k_I} + \lambda_I \mathbf{P}_{-k_I} + \mathbf{Q}_{-k_I} \right) \mathbf{y}_{I,-k_I}, \mathbf{y}_{I,-k_I} = \mathbf{0} \tag{3.3.274}$$

$$\Rightarrow \mathbf{0} = \left(\lambda_I^2 \begin{bmatrix} \Re \mathbf{M}_{k_I} & \Im \mathbf{M}_{k_I} \\ -\Im \mathbf{M}_{k_I} & \Re \mathbf{M}_{k_I} \end{bmatrix} + \lambda_I \begin{bmatrix} \Re \mathbf{P}_{k_I} & \Im \mathbf{P}_{k_I} \\ -\Im \mathbf{P}_{k_I} & \Re \mathbf{P}_{k_I} \end{bmatrix} + \begin{bmatrix} \Re \mathbf{Q}_{k_I} & \Im \mathbf{Q}_{k_I} \\ -\Im \mathbf{Q}_{k_I} & \Re \mathbf{Q}_{k_I} \end{bmatrix} \right) \underbrace{\begin{bmatrix} \mathbf{Y}_I \\ i \mathbf{Y}_I \end{bmatrix}}_{\mathbf{Y}_{I1}^*} \tag{3.3.275}$$

$$\mathbf{0} = \left(\lambda_I^2 \begin{bmatrix} \Re \mathbf{M}_{k_I} & \Im \mathbf{M}_{k_I} \\ -\Im \mathbf{M}_{k_I} & \Re \mathbf{M}_{k_I} \end{bmatrix} + \lambda_I \begin{bmatrix} \Re \mathbf{P}_{k_I} & \Im \mathbf{P}_{k_I} \\ -\Im \mathbf{P}_{k_I} & \Re \mathbf{P}_{k_I} \end{bmatrix} + \begin{bmatrix} \Re \mathbf{Q}_{k_I} & \Im \mathbf{Q}_{k_I} \\ -\Im \mathbf{Q}_{k_I} & \Re \mathbf{Q}_{k_I} \end{bmatrix} \right) \underbrace{\begin{bmatrix} i \mathbf{Y}_I \\ i^2 \mathbf{Y}_I \end{bmatrix}}_{\mathbf{Y}_{I2}^*} \tag{3.3.276}$$

It is evident that the two vectors \mathbf{Y}_{I1}^* and \mathbf{Y}_{I2}^* differ only by the factor i . Generally, if the vector $\mathbf{w}_I \neq \mathbf{0}$ is an eigenvector for a matrix \mathbf{A} , than the vector $c\mathbf{w}_I$, $c \in \mathbb{C}$, too, is an eigenvector so that a scalar factor is not relevant. Therefore, both equations (3.3.275) and (3.3.276) are equivalent. For this reason, the formulation (3.3.269) will be used for further considerations.

As mentioned before, the two formulations (3.3.269) and (3.3.270), which are valid for the periodicity k , are derived from the conditions (3.3.263) and (3.3.264), which are valid for the periodicities k and $-k$, respectively. Therefore, by solving the following equation, which is derived from (3.3.269) for $k = |k_I|$, both vectors $\mathbf{y}_{I,|k_I|}$ and $\mathbf{y}_{I,-|k_I|}$ are obtained:

$$\mathbf{0} = \left(\lambda_I^2 \begin{bmatrix} \Re \mathbf{M}_{|k_I|} & \Im \mathbf{M}_{|k_I|} \\ -\Im \mathbf{M}_{|k_I|} & \Re \mathbf{M}_{|k_I|} \end{bmatrix} + \lambda_I \begin{bmatrix} \Re \mathbf{P}_{|k_I|} & \Im \mathbf{P}_{|k_I|} \\ -\Im \mathbf{P}_{|k_I|} & \Re \mathbf{P}_{|k_I|} \end{bmatrix} + \begin{bmatrix} \Re \mathbf{Q}_{|k_I|} & \Im \mathbf{Q}_{|k_I|} \\ -\Im \mathbf{Q}_{|k_I|} & \Re \mathbf{Q}_{|k_I|} \end{bmatrix} \right) \begin{bmatrix} \mathbf{y}_{I,|k_I|} + \mathbf{y}_{I,-|k_I|} \\ i\mathbf{y}_{I,|k_I|} - i\mathbf{y}_{I,-|k_I|} \end{bmatrix} \quad (3.3.277)$$

For the vectors $\mathbf{y}_I^{(j)}$, which form the right eigenvectors \mathbf{w}_{CI} , it is valid:

$$\mathbf{y}_{I,k} = \begin{cases} \mathbf{y}_{I,k_I} = \mathbf{Y}_I \neq \mathbf{0} & \text{for } k = k_I \\ \mathbf{0} & \text{for } k \neq k_I \end{cases} \Rightarrow \mathbf{y}_I^{(j)} = \sum_{k=k_{\min}}^{k_{\max}} \mathbf{y}_{I,k} \zeta^{kj} = \mathbf{Y}_I \zeta^{k_I j} \quad (3.3.278)$$

From this, the following formulation, which covers both cases $k_I > 0$ and $k_I < 0$ is derived. By using the absolute value $|k_I|$ it is valid:

$$k_I > 0 : \mathbf{y}_{I,|k_I|} = \mathbf{y}_{I,k_I} = \mathbf{Y}_I \neq \mathbf{0} \wedge \mathbf{y}_{I,-|k_I|} = \mathbf{y}_{I,-k_I} = \mathbf{0} \quad (3.3.279)$$

$$k_I < 0 : \mathbf{y}_{I,|k_I|} = \mathbf{y}_{I,-k_I} = \mathbf{0} \quad \wedge \mathbf{y}_{I,-|k_I|} = \mathbf{y}_{I,k_I} = \mathbf{Y}_I \neq \mathbf{0} \quad (3.3.280)$$

By using the relation $\zeta^{-kj} = \overline{\zeta^{kj}}$ it is obtained:

$$\begin{aligned} \mathbf{y}_I^{(j)} &= \mathbf{y}_{I,|k_I|} \zeta^{|k_I|j} + \mathbf{y}_{I,-|k_I|} \zeta^{-|k_I|j} = \mathbf{y}_{I,|k_I|} \zeta^{|k_I|j} + \mathbf{y}_{I,-|k_I|} \overline{\zeta^{|k_I|j}} \\ &= \mathbf{y}_{I,|k_I|} \left(\Re \zeta^{|k_I|j} + i \Im \zeta^{|k_I|j} \right) + \mathbf{y}_{I,-|k_I|} \left(\Re \zeta^{|k_I|j} - i \Im \zeta^{|k_I|j} \right) \\ &= (\mathbf{y}_{I,|k_I|} + \mathbf{y}_{I,-|k_I|}) \Re \zeta^{|k_I|j} + (i\mathbf{y}_{I,|k_I|} - i\mathbf{y}_{I,-|k_I|}) \Im \zeta^{|k_I|j} \end{aligned} \quad (3.3.281)$$

For the sake of brevity and for a better overview the vectors $\Sigma \mathbf{Y}_I$ and $\Delta \mathbf{Y}_I$ shall be introduced:

$$\Sigma \mathbf{Y}_I = \mathbf{y}_{I,|k_I|} + \mathbf{y}_{I,-|k_I|} \quad \Delta \mathbf{Y}_I = i\mathbf{y}_{I,|k_I|} - i\mathbf{y}_{I,-|k_I|} \quad (3.3.282)$$

$$\Leftrightarrow \mathbf{y}_{I,|k_I|} = \frac{1}{2} (\Sigma \mathbf{Y}_I - i \Delta \mathbf{Y}_I) \quad \mathbf{y}_{I,-|k_I|} = \frac{1}{2} (\Sigma \mathbf{Y}_I + i \Delta \mathbf{Y}_I) \quad (3.3.283)$$

In total, the determination of the subvectors $\mathbf{y}_I^{(j)}$ can be formulated in the following way:

$$\mathbf{0} = \left(\lambda_I^2 \begin{bmatrix} \Re \mathbf{M}_{|k_I|} & \Im \mathbf{M}_{|k_I|} \\ -\Im \mathbf{M}_{|k_I|} & \Re \mathbf{M}_{|k_I|} \end{bmatrix} + \lambda_I \begin{bmatrix} \Re \mathbf{P}_{|k_I|} & \Im \mathbf{P}_{|k_I|} \\ -\Im \mathbf{P}_{|k_I|} & \Re \mathbf{P}_{|k_I|} \end{bmatrix} + \begin{bmatrix} \Re \mathbf{Q}_{|k_I|} & \Im \mathbf{Q}_{|k_I|} \\ -\Im \mathbf{Q}_{|k_I|} & \Re \mathbf{Q}_{|k_I|} \end{bmatrix} \right) \begin{bmatrix} \Sigma \mathbf{Y}_I \\ \Delta \mathbf{Y}_I \end{bmatrix}, \begin{bmatrix} \Sigma \mathbf{Y}_I \\ \Delta \mathbf{Y}_I \end{bmatrix} \neq \mathbf{0} \quad (3.3.284)$$

$$\mathbf{y}_I^{(j)} = \underbrace{\Sigma \mathbf{Y}_I \cos\left(\frac{2\pi}{n}|k_I|j\right)}_{\Re \zeta^{|k_I|j}} + \underbrace{\Delta \mathbf{Y}_I \sin\left(\frac{2\pi}{n}|k_I|j\right)}_{\Im \zeta^{|k_I|j}} = \begin{bmatrix} \Re \zeta^{|k_I|j} & \Im \zeta^{|k_I|j} \end{bmatrix} \begin{bmatrix} \Sigma \mathbf{Y}_I \\ \Delta \mathbf{Y}_I \end{bmatrix} \quad (3.3.285)$$

The solution of the equation (3.3.284) yields the vectors $\Sigma \mathbf{Y}_I$ and $\Delta \mathbf{Y}_I$, from which the vectors $\mathbf{y}_I^{(j)}$ are determined according to (3.3.285). For many practical applications, this formulation should be sufficient. If however, the ‘‘original’’ eigenvectors according to (3.3.225) are required, i.e. the

formulation using one periodicity $k_I \in \mathbb{Z}$, which can be negative, then this formulation can be reconstructed by combining the relations (3.3.281) and (3.3.283):

$$\mathbf{y}_I^{(j)} = \mathbf{y}_{I,|k_I|} \zeta^{|k_I|j} + \mathbf{y}_{I,-|k_I|} \zeta^{-|k_I|j} = \frac{1}{2} (\Sigma \mathbf{Y}_I - i \Delta \mathbf{Y}_I) \zeta^{|k_I|j} + \frac{1}{2} (\Sigma \mathbf{Y}_I + i \Delta \mathbf{Y}_I) \zeta^{-|k_I|j} \quad (3.3.286)$$

If λ_I is a single eigenvector, either the vector $\mathbf{y}_{I,|k_I|}$ or the vector $\mathbf{y}_{I,-|k_I|}$ vanishes.

The left eigenvector problem is reformulated in an analogous way. From the condition (3.3.217) it follows for k and $-k$:

$$\mathbf{0} = \mathbf{x}_{I,k}^H \left(\lambda_I^2 \mathbf{M}_k + \lambda_I \mathbf{P}_k + \mathbf{Q}_k \right) \quad (3.3.287)$$

$$\mathbf{0} = \mathbf{x}_{I,-k}^H \left(\lambda_I^2 \mathbf{M}_{-k} + \lambda_I \mathbf{P}_{-k} + \mathbf{Q}_{-k} \right) \quad (3.3.288)$$

Adding these two equations and applying the transformations (3.3.265) and (3.3.266) leads to:

$$\begin{aligned} \mathbf{0} &= \mathbf{x}_{I,k}^H \left(\lambda_I^2 \mathbf{M}_k + \lambda_I \mathbf{P}_k + \mathbf{Q}_k \right) + \mathbf{x}_{I,-k}^H \left(\lambda_I^2 \mathbf{M}_{-k} + \lambda_I \mathbf{P}_{-k} + \mathbf{Q}_{-k} \right) \\ &= \mathbf{x}_{I,k}^H \left[\lambda_I^2 \Re \mathbf{M}_k + \lambda_I \Re \mathbf{P}_k + \Re \mathbf{Q}_k + i \left(\lambda_I^2 \Im \mathbf{M}_k + \lambda_I \Im \mathbf{P}_k + \Im \mathbf{Q}_k \right) \right] \\ &\quad + \mathbf{x}_{I,-k}^H \left[\lambda_I^2 \Re \mathbf{M}_k + \lambda_I \Re \mathbf{P}_k + \Re \mathbf{Q}_k - i \left(\lambda_I^2 \Im \mathbf{M}_k + \lambda_I \Im \mathbf{P}_k + \Im \mathbf{Q}_k \right) \right] \\ &= (\mathbf{x}_{I,-k}^H + \mathbf{x}_{I,k}^H) \left(\lambda_I^2 \Re \mathbf{M}_k + \lambda_I \Re \mathbf{P}_k + \Re \mathbf{Q}_k \right) \\ &\quad - (i \mathbf{x}_{I,-k}^H - i \mathbf{x}_{I,k}^H) \left(\lambda_I^2 \Im \mathbf{M}_k + \lambda_I \Im \mathbf{P}_k + \Im \mathbf{Q}_k \right) \end{aligned} \quad (3.3.289)$$

By multiplying the equations (3.3.287) and (3.3.288) by i , subtracting them and again applying the transformations (3.3.265) and (3.3.266) it is obtained:

$$\begin{aligned} \mathbf{0} &= -i \mathbf{x}_{I,k}^H \left(\lambda_I^2 \mathbf{M}_k + \lambda_I \mathbf{P}_k + \mathbf{Q}_k \right) + i \mathbf{x}_{I,-k}^H \left(\lambda_I^2 \mathbf{M}_{-k} + \lambda_I \mathbf{P}_{-k} + \mathbf{Q}_{-k} \right) \\ &= -i \mathbf{x}_{I,k}^H \left[\lambda_I^2 \Re \mathbf{M}_k + \lambda_I \Re \mathbf{P}_k + \Re \mathbf{Q}_k + i \left(\lambda_I^2 \Im \mathbf{M}_k + \lambda_I \Im \mathbf{P}_k + \Im \mathbf{Q}_k \right) \right] \\ &\quad + i \mathbf{x}_{I,-k}^H \left[\lambda_I^2 \Re \mathbf{M}_k + \lambda_I \Re \mathbf{P}_k + \Re \mathbf{Q}_k - i \left(\lambda_I^2 \Im \mathbf{M}_k + \lambda_I \Im \mathbf{P}_k + \Im \mathbf{Q}_k \right) \right] \\ &= (i \mathbf{x}_{I,-k}^H - i \mathbf{x}_{I,k}^H) \left(\lambda_I^2 \Re \mathbf{M}_k + \lambda_I \Re \mathbf{P}_k + \Re \mathbf{Q}_k \right) \\ &\quad + \underbrace{(-i^2)}_1 (\mathbf{x}_{I,-k}^H + \mathbf{x}_{I,k}^H) \left(\lambda_I^2 \Im \mathbf{M}_k + \lambda_I \Im \mathbf{P}_k + \Im \mathbf{Q}_k \right) \end{aligned} \quad (3.3.290)$$

Also here, the two resulting equations (3.3.289) and (3.3.290) can be arranged in two ways. Here, the matrices are arranged in the same way as in the formulations (3.3.269) and (3.3.270):

$$\begin{aligned} [\mathbf{0} \quad \mathbf{0}] &= [\mathbf{x}_{I,-k}^H + \mathbf{x}_{I,k}^H \quad i \mathbf{x}_{I,-k}^H - i \mathbf{x}_{I,k}^H] \left(\lambda_I^2 \begin{bmatrix} \Re \mathbf{M}_k & \Im \mathbf{M}_k \\ -\Im \mathbf{M}_k & \Re \mathbf{M}_k \end{bmatrix} \right. \\ &\quad \left. + \lambda_I \begin{bmatrix} \Re \mathbf{P}_k & \Im \mathbf{P}_k \\ -\Im \mathbf{P}_k & \Re \mathbf{P}_k \end{bmatrix} + \begin{bmatrix} \Re \mathbf{Q}_k & \Im \mathbf{Q}_k \\ -\Im \mathbf{Q}_k & \Re \mathbf{Q}_k \end{bmatrix} \right) \end{aligned} \quad (3.3.291)$$

$$\begin{aligned} [\mathbf{0} \quad \mathbf{0}] &= [i \mathbf{x}_{I,-k}^H - i \mathbf{x}_{I,k}^H \quad -\mathbf{x}_{I,-k}^H - \mathbf{x}_{I,k}^H] \left(\lambda_I^2 \begin{bmatrix} \Re \mathbf{M}_k & \Im \mathbf{M}_k \\ -\Im \mathbf{M}_k & \Re \mathbf{M}_k \end{bmatrix} \right. \\ &\quad \left. + \lambda_I \begin{bmatrix} \Re \mathbf{P}_k & \Im \mathbf{P}_k \\ -\Im \mathbf{P}_k & \Re \mathbf{P}_k \end{bmatrix} + \begin{bmatrix} \Re \mathbf{Q}_k & \Im \mathbf{Q}_k \\ -\Im \mathbf{Q}_k & \Re \mathbf{Q}_k \end{bmatrix} \right) \end{aligned} \quad (3.3.292)$$

The vectors $\mathbf{x}_{I,k}$ are chosen in the same way as the vectors $\mathbf{y}_{I,k}$:

$$\mathbf{x}_{I,k} = \begin{cases} \mathbf{X}_I \neq \mathbf{0} & \text{for } k = k_I \\ \mathbf{0} & \text{for } k \neq k_I \end{cases} \quad (3.3.293)$$

Thereby, for $k_I \neq 0$ it is valid $k_I \neq -k_I$; from this it follows $\mathbf{x}_{I,k_I} = \mathbf{X}_I \neq \mathbf{0}$ and $\mathbf{x}_{I,-k_I} = \mathbf{0}$. Setting $k = k_I$, inserting the vectors \mathbf{x}_{I,k_I} and $\mathbf{x}_{I,-k_I}$ and applying the relation $i^2 = -1$ leads to:

$$\mathbf{0} = \mathbf{x}_{I,k}^H \left(\lambda_I^2 \mathbf{M}_{k_I} + \lambda_I \mathbf{P}_{k_I} + \mathbf{Q}_{k_I} \right), \quad \mathbf{x}_{I,k_I} = \mathbf{X}_I \neq \mathbf{0} \quad (3.3.294)$$

$$\mathbf{0} = \mathbf{x}_{I,-k}^H \left(\lambda_I^2 \mathbf{M}_{-k_I} + \lambda_I \mathbf{P}_{-k_I} + \mathbf{Q}_{-k_I} \right), \quad \mathbf{x}_{I,-k_I} = \mathbf{0} \quad (3.3.295)$$

$$\Rightarrow \mathbf{0} = \begin{bmatrix} \mathbf{X}_I^H & -i\mathbf{X}_I^H \end{bmatrix} \left(\lambda_I^2 \begin{bmatrix} \Re \mathbf{M}_{k_I} & \Im \mathbf{M}_{k_I} \\ -\Im \mathbf{M}_{k_I} & \Re \mathbf{M}_{k_I} \end{bmatrix} + \lambda_I \begin{bmatrix} \Re \mathbf{P}_{k_I} & \Im \mathbf{P}_{k_I} \\ -\Im \mathbf{P}_{k_I} & \Re \mathbf{P}_{k_I} \end{bmatrix} + \begin{bmatrix} \Re \mathbf{Q}_{k_I} & \Im \mathbf{Q}_{k_I} \\ -\Im \mathbf{Q}_{k_I} & \Re \mathbf{Q}_{k_I} \end{bmatrix} \right) \quad (3.3.296)$$

$$\mathbf{0} = \begin{bmatrix} -i\mathbf{X}_I^H & i^2\mathbf{X}_I^H \end{bmatrix} \left(\lambda_I^2 \begin{bmatrix} \Re \mathbf{M}_{k_I} & \Im \mathbf{M}_{k_I} \\ -\Im \mathbf{M}_{k_I} & \Re \mathbf{M}_{k_I} \end{bmatrix} + \lambda_I \begin{bmatrix} \Re \mathbf{P}_{k_I} & \Im \mathbf{P}_{k_I} \\ -\Im \mathbf{P}_{k_I} & \Re \mathbf{P}_{k_I} \end{bmatrix} + \begin{bmatrix} \Re \mathbf{Q}_{k_I} & \Im \mathbf{Q}_{k_I} \\ -\Im \mathbf{Q}_{k_I} & \Re \mathbf{Q}_{k_I} \end{bmatrix} \right) \quad (3.3.297)$$

It is evident that the equation (3.3.296) can be transformed into the equation (3.3.297) by multiplying it by $-i$; therefore, both equations (3.3.296) and (3.3.297) are equivalent.

By setting $k = |k_I|$ it is obtained:

$$\mathbf{0} = \begin{bmatrix} \mathbf{x}_{I,-|k_I|}^H + \mathbf{x}_{I,|k_I|}^H & i\mathbf{x}_{I,-|k_I|}^H - i\mathbf{x}_{I,|k_I|}^H \end{bmatrix} \left(\lambda_I^2 \begin{bmatrix} \Re \mathbf{M}_{|k_I|} & \Im \mathbf{M}_{|k_I|} \\ -\Im \mathbf{M}_{|k_I|} & \Re \mathbf{M}_{|k_I|} \end{bmatrix} + \lambda_I \begin{bmatrix} \Re \mathbf{P}_{|k_I|} & \Im \mathbf{P}_{|k_I|} \\ -\Im \mathbf{P}_{|k_I|} & \Re \mathbf{P}_{|k_I|} \end{bmatrix} + \begin{bmatrix} \Re \mathbf{Q}_{|k_I|} & \Im \mathbf{Q}_{|k_I|} \\ -\Im \mathbf{Q}_{|k_I|} & \Re \mathbf{Q}_{|k_I|} \end{bmatrix} \right) \quad (3.3.298)$$

The left eigenvectors have the same structure as the right eigenvectors; therefore, the following reformulation, which has been derived for the subvectors $\mathbf{y}_I^{(j)}$, is also applied here:

$$\mathbf{x}_I^{(j)} = \mathbf{x}_{I,|k_I|} \zeta^{|k_I|j} + \mathbf{x}_{I,-|k_I|} \zeta^{-|k_I|j} = \underbrace{(\mathbf{x}_{I,|k_I|} + \mathbf{x}_{I,-|k_I|})}_{\Sigma \mathbf{X}_I} \Re \zeta^{|k_I|j} + \underbrace{(i\mathbf{x}_{I,|k_I|} - i\mathbf{x}_{I,-|k_I|})}_{\Delta \mathbf{X}_I} \Im \zeta^{|k_I|j} \quad (3.3.299)$$

The Hermitian transposition consists of a transposition and a conjugation; while this poses no problem for the vector $\Sigma \mathbf{X}_I$, it has to be noted that the scalar factors i have to be conjugated. Thereby, it is obtained for the Hermitian transposes $\Sigma \mathbf{X}_I$ and $\Delta \mathbf{X}_I$:

$$\Sigma \mathbf{X}_I = \mathbf{x}_{I,|k_I|} + \mathbf{x}_{I,-|k_I|} \Rightarrow \Sigma \mathbf{X}_I^H = \mathbf{x}_{I,|k_I|}^H + \mathbf{x}_{I,-|k_I|}^H \quad (3.3.300)$$

$$\Delta \mathbf{X}_I = i\mathbf{x}_{I,|k_I|} - i\mathbf{x}_{I,-|k_I|} \Rightarrow \Delta \mathbf{X}_I^H = \bar{i} \mathbf{x}_{I,|k_I|}^H - \bar{i} \mathbf{x}_{I,-|k_I|}^H = -i\mathbf{x}_{I,|k_I|}^H + i\mathbf{x}_{I,-|k_I|}^H \quad (3.3.301)$$

Thereby, the left eigenvector problem is finally formulated in the following way:

$$\mathbf{0} = \underbrace{\begin{bmatrix} \Sigma \mathbf{X}_I^H & \Delta \mathbf{X}_I^H \end{bmatrix}}_{\neq \mathbf{0}} \left(\lambda_I^2 \begin{bmatrix} \Re \mathbf{M}_{|k_I|} & \Im \mathbf{M}_{|k_I|} \\ -\Im \mathbf{M}_{|k_I|} & \Re \mathbf{M}_{|k_I|} \end{bmatrix} + \lambda_I \begin{bmatrix} \Re \mathbf{P}_{|k_I|} & \Im \mathbf{P}_{|k_I|} \\ -\Im \mathbf{P}_{|k_I|} & \Re \mathbf{P}_{|k_I|} \end{bmatrix} + \begin{bmatrix} \Re \mathbf{Q}_{|k_I|} & \Im \mathbf{Q}_{|k_I|} \\ -\Im \mathbf{Q}_{|k_I|} & \Re \mathbf{Q}_{|k_I|} \end{bmatrix} \right) \quad (3.3.302)$$

The subvectors $\mathbf{x}_I^{(j)}$ are obtained in an analogous way as the subvectors $\mathbf{y}_I^{(j)}$:

$$\mathbf{x}_I^{(j)} = \underbrace{\Sigma \mathbf{X}_I \cos\left(\frac{2\pi}{n}|k_I|j\right)}_{\Re \zeta^{|k_I|j}} + \underbrace{\Delta \mathbf{X}_I \sin\left(\frac{2\pi}{n}|k_I|j\right)}_{\Im \zeta^{|k_I|j}} = \begin{bmatrix} \mathbf{I} \Re \zeta^{|k_I|j} & \mathbf{I} \Im \zeta^{|k_I|j} \end{bmatrix} \begin{bmatrix} \Sigma \mathbf{X}_I \\ \Delta \mathbf{X}_I \end{bmatrix} \quad (3.3.303)$$

Furthermore, also the “original” formulation using only one periodicity can be determined from the following relation:

$$\mathbf{x}_I^{(j)} = \mathbf{x}_{I,|k_I|} \zeta^{|k_I|j} + \mathbf{x}_{I,-|k_I|} \zeta^{-|k_I|j} = \frac{1}{2} (\Sigma \mathbf{X}_I - i \Delta \mathbf{X}_I) \zeta^{|k_I|j} + \frac{1}{2} (\Sigma \mathbf{X}_I + i \Delta \mathbf{X}_I) \zeta^{-|k_I|j} \quad (3.3.304)$$

3.3.3 Damped cyclic systems

As already mentioned in Section 3.3.1, damped linear systems, i.e. systems, in which no gyroscopic forces and no circulatoric forces occur, are an important special case of an ordinary linear mechanical system. The equation of motion is derived from (3.0.1) by setting $\mathbf{G} = \mathbf{0} \Leftrightarrow \mathbf{P} = \mathbf{D}$ and $\mathbf{N} = \mathbf{0} \Leftrightarrow \mathbf{Q} = \mathbf{K}$; this leads to:

$$\mathbf{M} \ddot{\mathbf{y}}(t) + \mathbf{D} \dot{\mathbf{y}}(t) + \mathbf{K} \mathbf{y}(t) = \mathbf{h}(t), \quad \mathbf{M} = \mathbf{M}^T, \quad \mathbf{D} = \mathbf{D}^T, \quad \mathbf{K} = \mathbf{K}^T \quad (3.3.305)$$

Therefore, for a damped cyclic system, the equation of motion is given by:

$$\mathbf{M}_C \ddot{\mathbf{y}}_C(t) + \mathbf{D}_C \dot{\mathbf{y}}_C(t) + \mathbf{K}_C \mathbf{y}_C(t) = \mathbf{h}_C(t), \quad \mathbf{M}_C = \mathbf{M}_C^T, \quad \mathbf{D}_C = \mathbf{D}_C^T, \quad \mathbf{K}_C = \mathbf{K}_C^T \quad (3.3.306)$$

Since a damped linear system is a special case of an ordinary linear system, so that all relations, which have been developed in the previous section 3.3.2, can be applied also here. Practically, this means that these relations are still valid after replacing the non-symmetric matrices \mathbf{Q}_C and \mathbf{P}_C by the symmetric matrices \mathbf{K}_C and \mathbf{D}_C . In particular, the products $\mathbf{T}_{CF}^H \mathbf{D}_C \mathbf{T}_{CF}$ and $\mathbf{T}_{CF}^H \mathbf{K}_C \mathbf{T}_{CF}$ have the same block-diagonal structure as the products $\mathbf{T}_{CF}^H \mathbf{P}_C \mathbf{T}_{CF}$ and $\mathbf{T}_{CF}^H \mathbf{Q}_C \mathbf{T}_{CF}$. Therefore, an eigenvector \mathbf{y}_{CI} for damped linear cyclic system is determined in the same way as for a linear cyclic system, for which the matrices \mathbf{P}_C and \mathbf{Q}_C don't have any symmetry properties. The vectors $\mathbf{y}_I^{(j)}$ and $\mathbf{x}_I^{(j)}$, which form the eigenvectors \mathbf{y}_{CI} and \mathbf{x}_{CI} , are chosen to:

$$\mathbf{y}_{I,k} = \begin{cases} \mathbf{Y}_I \neq \mathbf{0} & \text{for } k = k_I \\ \mathbf{0} & \text{for } k \neq k_I \end{cases} \Rightarrow \mathbf{y}_I^{(j)} = \mathbf{Y}_I \zeta^{k_I j} \quad (3.3.307)$$

$$\mathbf{x}_{I,k} = \begin{cases} \mathbf{X}_I \neq \mathbf{0} & \text{for } k = k_I \\ \mathbf{0} & \text{for } k \neq k_I \end{cases} \Rightarrow \mathbf{x}_I^{(j)} = \mathbf{X}_I \zeta^{k_I j} \quad (3.3.308)$$

The vectors \mathbf{Y}_I and \mathbf{X}_I have to fulfill the following conditions:

$$\mathbf{0} = \left(\lambda_I^2 \mathbf{M}_{k_I} + \lambda_I \mathbf{D}_{k_I} + \mathbf{K}_{k_I} \right) \mathbf{Y}_I, \quad \mathbf{Y}_I \neq \mathbf{0} \quad (3.3.309)$$

$$\mathbf{0} = \mathbf{X}_I^H \left(\lambda_I^2 \mathbf{M}_{k_I} + \lambda_I \mathbf{D}_{k_I} + \mathbf{K}_{k_I} \right), \quad \mathbf{X}_I \neq \mathbf{0} \quad (3.3.310)$$

As introduced in the section 3.2, the matrix \mathbf{M}_k is defined by:

$$\mathbf{M}_k = \mathbf{M}^{(-1)} \zeta^{-k} + \mathbf{M}^{(0)} + \mathbf{M}^{(1)} \zeta^k \quad (3.3.311)$$

If \mathbf{M}_C is a real matrix, then the following relation between \mathbf{M}_k and \mathbf{M}_{-k} is valid:

$$\mathbf{M}_C = \overline{\mathbf{M}_C} \Rightarrow \mathbf{M}^{(l)} = \overline{\mathbf{M}^{(l)}} \Rightarrow \mathbf{M}_{-k} = \overline{\mathbf{M}_k} \quad (3.3.312)$$

It should be noted that this relation is a consequence of the structure of \mathbf{M}_C , which is analogous to the structure of \mathbf{Q}_C shown in (3.0.5), i.e. it is independent from the symmetry. Furthermore, it has been shown in the section 3.2 that if \mathbf{M}_C is a real symmetric matrix then the \mathbf{M}_k is a Hermitian matrix:

$$\mathbf{M}_C = \mathbf{M}_C^T = \overline{\mathbf{M}_C} \Rightarrow \mathbf{M}_k = \mathbf{M}_k^H = \overline{\mathbf{M}_k}^T \quad (3.3.313)$$

In contrast to the relation (3.3.312), this one is derived from the symmetry of \mathbf{M}_C . By combining the two relations (3.3.312) and (3.3.313) it is obtained:

$$\mathbf{M}_C = \mathbf{M}_C^T = \overline{\mathbf{M}_C} \Rightarrow \mathbf{M}_k = \overline{\mathbf{M}_k}^T = \mathbf{M}_{-k}^T \Rightarrow \mathbf{M}_k^T = \mathbf{M}_{-k} \quad (3.3.314)$$

The matrices \mathbf{D}_C and \mathbf{K}_C have the same relevant properties as the matrix \mathbf{M}_C , i.e. they have the structure according to (3.0.5), they are real matrices and they are symmetric. Therefore it is valid:

$$\mathbf{M}_C = \overline{\mathbf{M}_C} = \mathbf{M}_C^T \Rightarrow \mathbf{M}_k = \mathbf{M}_{-k}^T \Rightarrow \mathbf{M}_k^T = \mathbf{M}_{-k} \quad (3.3.315)$$

$$\mathbf{D}_C = \overline{\mathbf{D}_C} = \mathbf{D}_C^T \Rightarrow \mathbf{D}_k = \mathbf{D}_{-k}^T \Rightarrow \mathbf{D}_k^T = \mathbf{D}_{-k} \quad (3.3.316)$$

$$\mathbf{K}_C = \overline{\mathbf{K}_C} = \mathbf{K}_C^T \Rightarrow \mathbf{K}_k = \mathbf{K}_{-k}^T \Rightarrow \mathbf{K}_k^T = \mathbf{K}_{-k} \quad (3.3.317)$$

For the following consideration it is useful to express the Hermitian transpose \mathbf{X}_I^H by transposition and conjugation. Thereby, the left eigenvector problem according to (3.3.310) is reformulated in the following way:

$$\mathbf{X}_I^H = \overline{\mathbf{X}_I}^T \Rightarrow \mathbf{0} = \overline{\mathbf{X}_I}^T \left(\lambda_I^2 \mathbf{M}_{k_I} + \lambda_I \mathbf{D}_{k_I} + \mathbf{K}_{k_I} \right) \quad (3.3.318)$$

By transposing the right eigenvector problem according to (3.3.309) and the left eigenvector problem (3.3.318) and applying the relations (3.3.317), (3.3.316) and (3.3.315) it is obtained:

$$\mathbf{0} = \mathbf{Y}_I^T \left(\lambda_I^2 \mathbf{M}_{k_I}^T + \lambda_I \mathbf{D}_{k_I}^T + \mathbf{K}_{k_I}^T \right) = \mathbf{Y}_I^T \left(\lambda_I^2 \mathbf{M}_{-k_I} + \lambda_I \mathbf{D}_{-k_I} + \mathbf{K}_{-k_I} \right) \quad (3.3.319)$$

$$\mathbf{0} = \left(\lambda_I^2 \mathbf{M}_{k_I}^T + \lambda_I \mathbf{D}_{k_I}^T + \mathbf{K}_{k_I}^T \right) \overline{\mathbf{X}_I} = \left(\lambda_I^2 \mathbf{M}_{-k_I} + \lambda_I \mathbf{D}_{-k_I} + \mathbf{K}_{-k_I} \right) \overline{\mathbf{X}_I} \quad (3.3.320)$$

According to (3.3.318) the vector \mathbf{X}_I is different from the zero vector so that its complex conjugate $\overline{\mathbf{X}_I}$, too, is different from the zero vector. Apparently, the vector $\overline{\mathbf{X}_I}$ is a right eigenvector associated with the eigenvalue λ_I for the periodicity $k = -k_I$.

For the sake of clarity, two indices $I \neq J$ shall be used in the following considerations in order to distinguish the two eigenvectors. The structure and the conditions for the eigenvectors \mathbf{y}_{CI} and \mathbf{x}_{CI} , which are associated to the eigenvalue λ_I , are already described by the equations (3.3.307), (3.3.308), (3.3.309) and (3.3.318). The eigenvectors \mathbf{y}_{CJ} and \mathbf{x}_{CJ} , which are associated with the eigenvalue λ_J are defined in an analogous way:

$$\mathbf{y}_{J,k} = \begin{cases} \mathbf{Y}_J \neq \mathbf{0} & \text{for } k = k_J \\ \mathbf{0} & \text{for } k \neq k_J \end{cases} \Rightarrow \mathbf{y}_J^{(j)} = \mathbf{Y}_J \zeta^{k_J j} \quad (3.3.321)$$

$$\mathbf{x}_{J,k} = \begin{cases} \mathbf{X}_J \neq \mathbf{0} & \text{for } k = k_J \\ \mathbf{0} & \text{for } k \neq k_J \end{cases} \Rightarrow \mathbf{x}_J^{(j)} = \mathbf{X}_J \zeta^{k_J j} \quad (3.3.322)$$

For the vectors \mathbf{Y}_J and \mathbf{X}_J it is valid:

$$\mathbf{0} = \left(\lambda_J^2 \mathbf{M}_{k_J} + \lambda_J \mathbf{D}_{k_J} + \mathbf{K}_{k_J} \right) \mathbf{Y}_J, \mathbf{Y}_J \neq \mathbf{0} \quad (3.3.323)$$

$$\mathbf{0} = \mathbf{X}_J^H \left(\lambda_J^2 \mathbf{M}_{k_J} + \lambda_J \mathbf{D}_{k_J} + \mathbf{K}_{k_J} \right), \mathbf{X}_J \neq \mathbf{0} \quad (3.3.324)$$

For the double eigenvalue it is valid $\lambda_J = \lambda_I = \lambda_J^*$, while the relation between the two periodicities is given by $k_J = -k_I$. Thereby, the transposed left eigenvector problem for $k = k_I$, as derived in (3.3.320), can also be interpreted as the right eigenvector problem for $k = k_J$:

$$\mathbf{0} = \left(\lambda_I^2 \mathbf{M}_{-k_I} + \lambda_I \mathbf{D}_{-k_I} + \mathbf{K}_{-k_I} \right) \overline{\mathbf{X}}_I = \left(\lambda_J^{*2} \mathbf{M}_{k_J} + \lambda_J^* \mathbf{D}_{k_J} + \mathbf{K}_{k_J} \right) \mathbf{Y}_J \Rightarrow \mathbf{Y}_J = \overline{\mathbf{X}}_I \quad (3.3.325)$$

In an analogous way, the relation between the transposed right eigenvector problem for $k = k_I$ described by (3.3.319) and the left eigenvector problem for $k = k_J$ is obtained:

$$\mathbf{0} = \mathbf{Y}_I^T \left(\lambda_I^2 \mathbf{M}_{-k_I} + \lambda_I \mathbf{D}_{-k_I} + \mathbf{K}_{-k_I} \right) = \overline{\mathbf{X}}_J^T \left(\lambda_J^{*2} \mathbf{M}_{k_J} + \lambda_J^* \mathbf{D}_{k_J} + \mathbf{K}_{k_J} \right) \Rightarrow \overline{\mathbf{X}}_J = \mathbf{Y}_I \Rightarrow \mathbf{X}_J = \overline{\mathbf{Y}}_I \quad (3.3.326)$$

In the section 3.3.2 the products $\mathbf{x}_{cI}^H \mathbf{M}_C \mathbf{y}_{cJ}$, $\mathbf{x}_{cI}^H \mathbf{P}_C \mathbf{y}_{cJ}$ and $\mathbf{x}_{cI}^H \mathbf{Q}_C \mathbf{y}_{cJ}$, which are relevant for the orthogonality of two eigenvectors, have been considered. If the vectors $\mathbf{y}_{I,k}$ and $\mathbf{x}_{J,k}$ are chosen in the following way:

$$\mathbf{y}_{I,k} = \begin{cases} \mathbf{Y}_I \neq \mathbf{0} & \text{for } k = k_I \\ \mathbf{0} & \text{for } k \neq k_I \end{cases}, \quad \mathbf{x}_{J,k} = \begin{cases} \mathbf{X}_J \neq \mathbf{0} & \text{for } k = k_J \\ \mathbf{0} & \text{for } k \neq k_J \end{cases} \quad (3.3.327)$$

then the evaluation of the products $\mathbf{x}_{cI}^H \mathbf{M}_C \mathbf{y}_{cJ}$, $\mathbf{x}_{cI}^H \mathbf{P}_C \mathbf{y}_{cJ}$ and $\mathbf{x}_{cI}^H \mathbf{Q}_C \mathbf{y}_{cJ}$ leads to:

$$\mathbf{x}_{cJ}^H \mathbf{M}_C \mathbf{y}_{cI} = \begin{cases} n \mathbf{X}_J^H \mathbf{M}_{k_I} \mathbf{Y}_I & \text{for } k_I = k_J \\ \mathbf{0} & \text{for } k_I \neq k_J \end{cases} \quad (3.3.328)$$

$$\mathbf{x}_{cJ}^H \mathbf{P}_C \mathbf{y}_{cI} = \begin{cases} n \mathbf{X}_J^H \mathbf{P}_{k_I} \mathbf{Y}_I & \text{for } k_I = k_J \\ \mathbf{0} & \text{for } k_I \neq k_J \end{cases} \quad (3.3.329)$$

$$\mathbf{x}_{cJ}^H \mathbf{Q}_C \mathbf{y}_{cI} = \begin{cases} n \mathbf{X}_J^H \mathbf{Q}_{k_I} \mathbf{Y}_I & \text{for } k_I = k_J \\ \mathbf{0} & \text{for } k_I \neq k_J \end{cases} \quad (3.3.330)$$

These relations are solely based on the structure of the matrices \mathbf{M}_C , \mathbf{P}_C and \mathbf{Q}_C , i.e. no further properties like e.g. symmetry properties were assumed for the matrices. Therefore, these relations are also valid for the special case $\mathbf{P}_C = \mathbf{D}_C = \mathbf{D}_C^T$ and $\mathbf{Q}_C = \mathbf{K}_C = \mathbf{K}_C^T$:

$$\mathbf{x}_{cJ}^H \mathbf{D}_C \mathbf{y}_{cI} = \begin{cases} n \mathbf{X}_J^H \mathbf{D}_{k_I} \mathbf{Y}_I & \text{for } k_I = k_J \\ \mathbf{0} & \text{for } k_I \neq k_J \end{cases}, \quad \mathbf{x}_{cJ}^H \mathbf{K}_C \mathbf{y}_{cI} = \begin{cases} n \mathbf{X}_J^H \mathbf{K}_{k_I} \mathbf{Y}_I & \text{for } k_I = k_J \\ \mathbf{0} & \text{for } k_I \neq k_J \end{cases} \quad (3.3.331)$$

According to (3.3.307) and (3.3.308), the eigenvectors \mathbf{y}_{cI} and \mathbf{x}_{cI} have the periodicity k_I , while the eigenvectors \mathbf{y}_{cJ} and \mathbf{x}_{cJ} have the periodicity k_J according to (3.3.321) and (3.3.322). The periodicities k_I and k_J only differ by the sign, i.e. $k_I = -k_J$, so that for $k_I \neq 0$ the periodicities k_I and k_J are in fact different, i.e. $k_I \neq k_J$. From (3.3.328), (3.3.328) and (3.3.328) it follows that eigenvectors, which have different periodicities, are orthogonal. Thereby, it is shown that for $k_J = -k_I \neq 0$ the vectors \mathbf{y}_{cI} and \mathbf{x}_{cI} on the one hand and \mathbf{y}_{cJ} and \mathbf{x}_{cJ} on the other hand are orthogonal. From this it follows that the eigenvalue $\lambda_J^* = \lambda_I = \lambda_J$ is in fact a double eigenvalue.

If the right eigenvectors \mathbf{y}_{cI} and \mathbf{y}_{cJ} are associated to a double eigenvalue $\lambda_I = \lambda_J = \lambda_J^*$, then their linear combination, too, is a right eigenvector, as it is shown in the following:

$$\mathbf{0} = \left(\lambda_I^2 \mathbf{M}_C + \lambda_I \mathbf{D}_C + \mathbf{K}_C \right) \mathbf{y}_{cI} \Rightarrow \mathbf{0} = \left(\lambda_I^{*2} \mathbf{M}_C + \lambda_I^* \mathbf{D}_C + \mathbf{K}_C \right) a_I \mathbf{y}_{cI}, \quad a_I \in \mathbb{C} \quad (3.3.332)$$

$$\mathbf{0} = \left(\lambda_J^2 \mathbf{M}_C + \lambda_J \mathbf{D}_C + \mathbf{K}_C \right) \mathbf{y}_{cJ} \Rightarrow \mathbf{0} = \left(\lambda_I^{*2} \mathbf{M}_C + \lambda_I^* \mathbf{D}_C + \mathbf{K}_C \right) a_J \mathbf{y}_{cJ}, \quad a_J \in \mathbb{C} \quad (3.3.333)$$

$$\mathbf{0} = \left(\lambda_I^{*2} \mathbf{M}_C + \lambda_I^* \mathbf{D}_C + \mathbf{K}_C \right) (a_I \mathbf{y}_{cI} + a_J \mathbf{y}_{cJ}) \quad (3.3.334)$$

In an analogous way it is valid for the left eigenvectors \mathbf{x}_{CI} and \mathbf{x}_{CJ} , which are associated with the double eigenvalue $\lambda_I = \lambda_J = \lambda_I^*$:

$$\mathbf{0} = \mathbf{x}_{CI}^H \left(\lambda_I^2 \mathbf{M}_C + \lambda_I \mathbf{D}_C + \mathbf{K}_C \right) \Rightarrow \mathbf{0} = \bar{b}_I \mathbf{x}_{CI}^H \left(\lambda_I^{*2} \mathbf{M}_C + \lambda_I^* \mathbf{D}_C + \mathbf{K}_C \right), b_I \in \mathbb{C} \quad (3.3.335)$$

$$\mathbf{0} = \mathbf{x}_{CJ}^H \left(\lambda_J^2 \mathbf{M}_C + \lambda_J \mathbf{D}_C + \mathbf{K}_C \right) \Rightarrow \mathbf{0} = \bar{b}_J \mathbf{x}_{CJ}^H \left(\lambda_J^{*2} \mathbf{M}_C + \lambda_J^* \mathbf{D}_C + \mathbf{K}_C \right), b_J \in \mathbb{C} \quad (3.3.336)$$

$$\mathbf{0} = (\bar{b}_I \mathbf{x}_{CI}^H + \bar{b}_J \mathbf{x}_{CJ}^H) \left(\lambda_I^{*2} \mathbf{M}_C + \lambda_I^* \mathbf{D}_C + \mathbf{K}_C \right) \quad (3.3.337)$$

The complex conjugates \bar{b}_I and \bar{b}_J are used because of the Hermitian transposition, which consists of a transposition and a conjugation, which also affects the scalar factors.

Both linear combinations $a_I \mathbf{y}_{CI} + a_J \mathbf{y}_{CJ}$ and $b_I \mathbf{x}_{CI} + b_J \mathbf{x}_{CJ}$ can be formulated in the following way using sums and differences:

$$a_I \mathbf{y}_{CI} + a_J \mathbf{y}_{CJ} = \frac{a_I + a_J}{2} (\mathbf{y}_{CI} + \mathbf{y}_{CJ}) + \frac{a_I - a_J}{2} (\mathbf{y}_{CI} - \mathbf{y}_{CJ}) \quad (3.3.338)$$

$$b_I \mathbf{x}_{CI} + b_J \mathbf{x}_{CJ} = \frac{b_I + b_J}{2} (\mathbf{x}_{CI} + \mathbf{x}_{CJ}) + \frac{b_I - b_J}{2} (\mathbf{x}_{CI} - \mathbf{x}_{CJ}) \quad (3.3.339)$$

It can be shown that the sums and the differences of the vectors are orthogonal for all three matrices. As an example, the matrix \mathbf{M}_C shall be considered; it is valid:

$$\begin{aligned} (\mathbf{x}_{CI} + \mathbf{x}_{CJ})^H \mathbf{M}_C (\mathbf{y}_{CI} - \mathbf{y}_{CJ}) &= (\mathbf{x}_{CI}^H + \mathbf{x}_{CJ}^H) \mathbf{M}_C (\mathbf{y}_{CI} - \mathbf{y}_{CJ}) \\ &= \mathbf{x}_{CI}^H \mathbf{M}_C \mathbf{y}_{CI} - \underbrace{\mathbf{x}_{CI}^H \mathbf{M}_C \mathbf{y}_{CJ}}_0 + \underbrace{\mathbf{x}_{CJ}^H \mathbf{M}_C \mathbf{y}_{CI}}_0 - \mathbf{x}_{CJ}^H \mathbf{M}_C \mathbf{y}_{CJ} \end{aligned} \quad (3.3.340)$$

$$\begin{aligned} (\mathbf{x}_{CI} - \mathbf{x}_{CJ})^H \mathbf{M}_C (\mathbf{y}_{CI} + \mathbf{y}_{CJ}) &= (\mathbf{x}_{CI}^H - \mathbf{x}_{CJ}^H) \mathbf{M}_C (\mathbf{y}_{CI} + \mathbf{y}_{CJ}) \\ &= \mathbf{x}_{CI}^H \mathbf{M}_C \mathbf{y}_{CI} + \underbrace{\mathbf{x}_{CI}^H \mathbf{M}_C \mathbf{y}_{CJ}}_0 - \underbrace{\mathbf{x}_{CJ}^H \mathbf{M}_C \mathbf{y}_{CI}}_0 - \mathbf{x}_{CJ}^H \mathbf{M}_C \mathbf{y}_{CJ} \end{aligned} \quad (3.3.341)$$

The evaluation is based on the relation (3.3.328). According to this, the second and the third term vanish immediately because of the different periodicities $k_I \neq k_J$. For the evaluation of the remaining terms, the relations $\mathbf{Y}_J = \bar{\mathbf{X}}_I$ and $\bar{\mathbf{X}}_J = \mathbf{Y}_I$, which are obtained from (3.3.325) and (3.3.326), respectively, are applied. This leads to:

$$\mathbf{Y}_J = \bar{\mathbf{X}}_I \Rightarrow \mathbf{x}_{CI}^H \mathbf{M}_C \mathbf{y}_{CI} = n \mathbf{X}_I^H \mathbf{M}_{k_I} \mathbf{Y}_I = n \bar{\mathbf{X}}_I^T \mathbf{M}_{k_I} \mathbf{Y}_I = n \mathbf{Y}_J^T \mathbf{M}_{k_I} \mathbf{Y}_I \quad (3.3.342)$$

$$\mathbf{Y}_J = \bar{\mathbf{X}}_I \Rightarrow \mathbf{x}_{CJ}^H \mathbf{M}_C \mathbf{y}_{CJ} = n \mathbf{X}_J^H \mathbf{M}_{k_J} \mathbf{Y}_J = n \bar{\mathbf{X}}_J^T \mathbf{M}_{k_J} \mathbf{Y}_J = n \mathbf{Y}_I^T \mathbf{M}_{k_J} \mathbf{Y}_J \quad (3.3.343)$$

The product $\mathbf{Y}_I^T \mathbf{M}_{k_J} \mathbf{Y}_J$ is a scalar so that it is not affected by a transposition:

$$\mathbf{x}_{CJ}^H \mathbf{M}_C \mathbf{y}_{CJ} = n \mathbf{Y}_I^T \mathbf{M}_{k_J} \mathbf{Y}_J = n (\mathbf{Y}_I^T \mathbf{M}_{k_J} \mathbf{Y}_J)^T = n \mathbf{Y}_J^T \mathbf{M}_{k_J}^T \mathbf{Y}_I \quad (3.3.344)$$

For the matrix $\mathbf{M}_{k_J}^T$ it is valid based on (3.3.315) and on $k_J = -k_I$:

$$\mathbf{M}_k^T = \mathbf{M}_{-k}, k_J = -k_I \Rightarrow \mathbf{M}_{k_J}^T = \mathbf{M}_{-k_J} = \mathbf{M}_{k_I} \quad (3.3.345)$$

Thereby, it is valid:

$$\mathbf{x}_{CJ}^H \mathbf{M}_C \mathbf{y}_{CJ} = n \mathbf{Y}_J^T \mathbf{M}_{k_J}^T \mathbf{Y}_I = n \mathbf{Y}_J^T \mathbf{M}_{k_I} \mathbf{Y}_I = \mathbf{x}_{CI}^H \mathbf{M}_C \mathbf{y}_{CI} \quad (3.3.346)$$

From this it follows:

$$(\mathbf{x}_{CI} + \mathbf{x}_{CJ})^H \mathbf{M}_C (\mathbf{y}_{CI} - \mathbf{y}_{CJ}) = \mathbf{x}_{CI}^H \mathbf{M}_C \mathbf{y}_{CI} - \mathbf{x}_{CJ}^H \mathbf{M}_C \mathbf{y}_{CJ} = 0 \quad (3.3.347)$$

$$(\mathbf{x}_{CI} - \mathbf{x}_{CJ})^H \mathbf{M}_C (\mathbf{y}_{CI} + \mathbf{y}_{CJ}) = \mathbf{x}_{CI}^H \mathbf{M}_C \mathbf{y}_{CI} - \mathbf{x}_{CJ}^H \mathbf{M}_C \mathbf{y}_{CJ} = 0 \quad (3.3.348)$$

Since the matrices \mathbf{K}_C and \mathbf{D}_C have the same structure and the same symmetry property as the matrix \mathbf{M}_C , it is valid:

$$(\mathbf{x}_{CI} + \mathbf{x}_{CJ})^H \mathbf{M}_C (\mathbf{y}_{CI} - \mathbf{y}_{CJ}) = 0, (\mathbf{x}_{CI} - \mathbf{x}_{CJ})^H \mathbf{M}_C (\mathbf{y}_{CI} + \mathbf{y}_{CJ}) = 0 \quad (3.3.349)$$

$$(\mathbf{x}_{CI} + \mathbf{x}_{CJ})^H \mathbf{D}_C (\mathbf{y}_{CI} - \mathbf{y}_{CJ}) = 0, (\mathbf{x}_{CI} - \mathbf{x}_{CJ})^H \mathbf{D}_C (\mathbf{y}_{CI} + \mathbf{y}_{CJ}) = 0 \quad (3.3.350)$$

$$(\mathbf{x}_{CI} + \mathbf{x}_{CJ})^H \mathbf{K}_C (\mathbf{y}_{CI} - \mathbf{y}_{CJ}) = 0, (\mathbf{x}_{CI} - \mathbf{x}_{CJ})^H \mathbf{K}_C (\mathbf{y}_{CI} + \mathbf{y}_{CJ}) = 0 \quad (3.3.351)$$

Also here, the two eigenvector problems for $k = k_I$ and $k = k_J = -k_I$ shall be transformed into an eigenvector problem using real matrices. In section 3.3.2, the following reformulation, which is based on the relations $\mathbf{M}_{-k} = \overline{\mathbf{M}_k}$, $\mathbf{P}_{-k} = \overline{\mathbf{P}_k}$ and $\mathbf{Q}_{-k} = \overline{\mathbf{Q}_k}$ has been derived:

$$\mathbf{0} = \left(\lambda_I^2 \mathbf{M}_k + \lambda_I \mathbf{P}_k + \mathbf{Q}_k \right) \mathbf{y}_{I,k} \quad (3.3.352)$$

$$\mathbf{0} = \left(\lambda_I^2 \mathbf{M}_{-k} + \lambda_I \mathbf{P}_{-k} + \mathbf{Q}_{-k} \right) \mathbf{y}_{I,-k} \quad (3.3.353)$$

$$\Rightarrow \mathbf{0} = \left(\lambda_I^2 \begin{bmatrix} \Re \mathbf{M}_k & \Im \mathbf{M}_k \\ -\Im \mathbf{M}_k & \Re \mathbf{M}_k \end{bmatrix} + \lambda_I \begin{bmatrix} \Re \mathbf{P}_k & \Im \mathbf{P}_k \\ -\Im \mathbf{P}_k & \Re \mathbf{P}_k \end{bmatrix} + \begin{bmatrix} \Re \mathbf{Q}_k & \Im \mathbf{Q}_k \\ -\Im \mathbf{Q}_k & \Re \mathbf{Q}_k \end{bmatrix} \right) \begin{bmatrix} \mathbf{y}_{I,k} + \mathbf{y}_{I,-k} \\ i\mathbf{y}_{I,k} - i\mathbf{y}_{I,-k} \end{bmatrix} \quad (3.3.354)$$

$$\mathbf{0} = \left(\lambda_I^2 \begin{bmatrix} \Re \mathbf{M}_k & \Im \mathbf{M}_k \\ -\Im \mathbf{M}_k & \Re \mathbf{M}_k \end{bmatrix} + \lambda_I \begin{bmatrix} \Re \mathbf{P}_k & \Im \mathbf{P}_k \\ -\Im \mathbf{P}_k & \Re \mathbf{P}_k \end{bmatrix} + \begin{bmatrix} \Re \mathbf{Q}_k & \Im \mathbf{Q}_k \\ -\Im \mathbf{Q}_k & \Re \mathbf{Q}_k \end{bmatrix} \right) \begin{bmatrix} i\mathbf{y}_{I,k} - i\mathbf{y}_{I,-k} \\ -\mathbf{y}_{I,k} - \mathbf{y}_{I,-k} \end{bmatrix} \quad (3.3.355)$$

If $\lambda_I = \lambda_J = \lambda_I^*$ is a double eigenvalue, for which it is valid $k_I = -k_J \neq 0$, then it is obtained:

$$\mathbf{0} = \left(\lambda_I^2 \mathbf{M}_{k_I} + \lambda_I \mathbf{D}_{k_I} + \mathbf{K}_{k_I} \right) \mathbf{Y}_I = \left(\lambda_I^{*2} \mathbf{M}_{k_I} + \lambda_I^* \mathbf{D}_{k_I} + \mathbf{K}_{k_I} \right) \mathbf{Y}_I, \mathbf{Y}_I \neq \mathbf{0} \quad (3.3.356)$$

$$\mathbf{0} = \left(\lambda_J^2 \mathbf{M}_{k_J} + \lambda_J \mathbf{D}_{k_J} + \mathbf{K}_{k_J} \right) \mathbf{Y}_J = \left(\lambda_I^{*2} \mathbf{M}_{-k_I} + \lambda_I^* \mathbf{D}_{-k_I} + \mathbf{K}_{-k_I} \right) \mathbf{Y}_J, \mathbf{Y}_J \neq \mathbf{0} \quad (3.3.357)$$

$$\Rightarrow \mathbf{0} = \left(\lambda_I^2 \begin{bmatrix} \Re \mathbf{M}_{k_I} & \Im \mathbf{M}_{k_I} \\ -\Im \mathbf{M}_{k_I} & \Re \mathbf{M}_{k_I} \end{bmatrix} + \lambda_I \begin{bmatrix} \Re \mathbf{D}_{k_I} & \Im \mathbf{D}_{k_I} \\ -\Im \mathbf{D}_{k_I} & \Re \mathbf{D}_{k_I} \end{bmatrix} + \begin{bmatrix} \Re \mathbf{K}_{k_I} & \Im \mathbf{K}_{k_I} \\ -\Im \mathbf{K}_{k_I} & \Re \mathbf{K}_{k_I} \end{bmatrix} \right) \underbrace{\begin{bmatrix} \mathbf{Y}_I + \mathbf{Y}_J \\ i\mathbf{Y}_I - i\mathbf{Y}_J \end{bmatrix}}_{\mathbf{Y}_{I1}^*} \quad (3.3.358)$$

$$\mathbf{0} = \left(\lambda_I^2 \begin{bmatrix} \Re \mathbf{M}_{k_I} & \Im \mathbf{M}_{k_I} \\ -\Im \mathbf{M}_{k_I} & \Re \mathbf{M}_{k_I} \end{bmatrix} + \lambda_I \begin{bmatrix} \Re \mathbf{D}_{k_I} & \Im \mathbf{D}_{k_I} \\ -\Im \mathbf{D}_{k_I} & \Re \mathbf{D}_{k_I} \end{bmatrix} + \begin{bmatrix} \Re \mathbf{K}_{k_I} & \Im \mathbf{K}_{k_I} \\ -\Im \mathbf{K}_{k_I} & \Re \mathbf{K}_{k_I} \end{bmatrix} \right) \underbrace{\begin{bmatrix} i\mathbf{Y}_I - i\mathbf{Y}_J \\ -\mathbf{Y}_I - \mathbf{Y}_J \end{bmatrix}}_{\mathbf{Y}_{I2}^*} \quad (3.3.359)$$

In the previous section 3.3.2 it has been shown that for a single eigenvalue the two formulations (3.3.354) and (3.3.355) can be transformed into each other by multiplying the vector by a scalar factor and are thereby equivalent. The comparison of the two formulations (3.3.358) and (3.3.359), however, shows that the sum $\mathbf{Y}_I + \mathbf{Y}_J$ is contained in the upper subvector of \mathbf{Y}_{I1}^* and in the lower subvector of \mathbf{Y}_{I2}^* , while the difference $\mathbf{Y}_I - \mathbf{Y}_J$ is contained in the other subvector. Since both vectors \mathbf{Y}_I and \mathbf{Y}_J are different from the zero vector, the two vectors \mathbf{Y}_{I1}^* and \mathbf{Y}_{I2}^* cannot be transformed into each other by a multiplication by a scalar factor and are thereby linearly independent.

As shown in the previous section 3.3.2, the formulations (3.3.354) and (3.3.355) are obtained by adding and subtracting the conditions (3.3.352) and (3.3.353). Therefore, it is obvious to evaluate the vectors \mathbf{Y}_{I1}^* and \mathbf{Y}_{I2}^* based on the consideration of the sum and the difference of the vectors \mathbf{y}_{CI} and \mathbf{y}_{CJ} , which is a special case of a linear combination. Since the periodicities k_I and k_J of the eigenvectors associated with the double eigenvalue $\lambda_I^* = \lambda_I = \lambda_J$ only differ by the sign, i.e. $k_J = -k_I$, it is assumed for the following consideration that k_I is positive, while k_J is negative. Based on the relation

$$k_J = -k_I \Rightarrow \zeta^{k_J j} = \zeta^{-k_I j} = \overline{\zeta^{k_I j}} \quad (3.3.360)$$

it is obtained for the sum $\mathbf{y}_I^{(j)} + \mathbf{y}_J^{(j)}$:

$$\begin{aligned} \mathbf{y}_I^{(j)} + \mathbf{y}_J^{(j)} &= \mathbf{Y}_I \zeta^{k_I j} + \mathbf{Y}_J \zeta^{k_J j} = \mathbf{Y}_I \left(\Re \zeta^{k_I j} + i \Im \zeta^{k_I j} \right) + \mathbf{Y}_J \left(\Re \zeta^{k_I j} - i \Im \zeta^{k_I j} \right) \\ &= \underbrace{(\mathbf{Y}_I + \mathbf{Y}_J)}_{\Sigma \mathbf{Y}_I^*} \Re \zeta^{k_I j} + i \underbrace{(\mathbf{Y}_I - \mathbf{Y}_J)}_{\Delta \mathbf{Y}_I^*} \Im \zeta^{k_I j} \end{aligned} \quad (3.3.361)$$

For the difference $\mathbf{y}_I^{(j)} - \mathbf{y}_J^{(j)}$ it is valid:

$$\begin{aligned} \mathbf{y}_I^{(j)} - \mathbf{y}_J^{(j)} &= \mathbf{Y}_I \zeta^{k_I j} - \mathbf{Y}_J \zeta^{k_J j} = \mathbf{Y}_I \left(\Re \zeta^{k_I j} + i \Im \zeta^{k_I j} \right) - \mathbf{Y}_J \left(\Re \zeta^{k_I j} - i \Im \zeta^{k_I j} \right) \\ &= (\mathbf{Y}_I - \mathbf{Y}_J) \Re \zeta^{k_I j} + i (\mathbf{Y}_I + \mathbf{Y}_J) \Im \zeta^{k_I j} \end{aligned} \quad (3.3.362)$$

The multiplication by i leads to:

$$i \left(\mathbf{y}_I^{(j)} - \mathbf{y}_J^{(j)} \right) = i (\mathbf{Y}_I - \mathbf{Y}_J) \Re \zeta^{k_I j} + i^2 (\mathbf{Y}_I + \mathbf{Y}_J) \Im \zeta^{k_I j} = \underbrace{i (\mathbf{Y}_I - \mathbf{Y}_J)}_{\Delta \mathbf{Y}_I^*} \Re \zeta^{k_I j} - \underbrace{(\mathbf{Y}_I + \mathbf{Y}_J)}_{\Sigma \mathbf{Y}_I^*} \Im \zeta^{k_I j} \quad (3.3.363)$$

Based on this, the eigenvectors of the damped linear cyclic system can be formulated using the equations (3.3.358) and (3.3.359):

$$\mathbf{0} = \left(\lambda_I^2 \begin{bmatrix} \Re \mathbf{M}_{k_I} & \Im \mathbf{M}_{k_I} \\ -\Im \mathbf{M}_{k_I} & \Re \mathbf{M}_{k_I} \end{bmatrix} + \lambda_I \begin{bmatrix} \Re \mathbf{D}_{k_I} & \Im \mathbf{D}_{k_I} \\ -\Im \mathbf{D}_{k_I} & \Re \mathbf{D}_{k_I} \end{bmatrix} + \begin{bmatrix} \Re \mathbf{K}_{k_I} & \Im \mathbf{K}_{k_I} \\ -\Im \mathbf{K}_{k_I} & \Re \mathbf{K}_{k_I} \end{bmatrix} \right) \begin{bmatrix} \Sigma \mathbf{Y}_I^* \\ \Delta \mathbf{Y}_I^* \end{bmatrix}, \begin{bmatrix} \Sigma \mathbf{Y}_I^* \\ \Delta \mathbf{Y}_I^* \end{bmatrix} \neq \mathbf{0} \quad (3.3.364)$$

$$\mathbf{y}_{I1}^{(j)} = \mathbf{y}_I^{(j)} + \mathbf{y}_J^{(j)} = \Sigma \mathbf{Y}_I^* \Re \zeta^{k_I j} + \Delta \mathbf{Y}_I^* \Im \zeta^{k_I j} = \begin{bmatrix} \Re \zeta^{k_I j} & \Im \zeta^{k_I j} \end{bmatrix} \begin{bmatrix} \Sigma \mathbf{Y}_I^* \\ \Delta \mathbf{Y}_I^* \end{bmatrix} \quad (3.3.365)$$

$$\mathbf{0} = \left(\lambda_I^2 \begin{bmatrix} \Re \mathbf{M}_{k_I} & \Im \mathbf{M}_{k_I} \\ -\Im \mathbf{M}_{k_I} & \Re \mathbf{M}_{k_I} \end{bmatrix} + \lambda_I \begin{bmatrix} \Re \mathbf{D}_{k_I} & \Im \mathbf{D}_{k_I} \\ -\Im \mathbf{D}_{k_I} & \Re \mathbf{D}_{k_I} \end{bmatrix} + \begin{bmatrix} \Re \mathbf{K}_{k_I} & \Im \mathbf{K}_{k_I} \\ -\Im \mathbf{K}_{k_I} & \Re \mathbf{K}_{k_I} \end{bmatrix} \right) \begin{bmatrix} \Delta \mathbf{Y}_I^* \\ -\Sigma \mathbf{Y}_I^* \end{bmatrix}, \begin{bmatrix} \Delta \mathbf{Y}_I^* \\ -\Sigma \mathbf{Y}_I^* \end{bmatrix} \neq \mathbf{0} \quad (3.3.366)$$

$$\mathbf{y}_{I2}^{(j)} = i \left(\mathbf{y}_I^{(j)} - \mathbf{y}_J^{(j)} \right) = \Delta \mathbf{Y}_I^* \Re \zeta^{k_I j} - \Sigma \mathbf{Y}_I^* \Im \zeta^{k_I j} = \begin{bmatrix} \Re \zeta^{k_I j} & \Im \zeta^{k_I j} \end{bmatrix} \begin{bmatrix} \Delta \mathbf{Y}_I^* \\ -\Sigma \mathbf{Y}_I^* \end{bmatrix} \quad (3.3.367)$$

Also here, the “original” eigenvectors \mathbf{Y}_I and \mathbf{Y}_J can be determined from the vectors $\Sigma \mathbf{Y}_I^*$ and $\Delta \mathbf{Y}_I^*$.

$$\Sigma \mathbf{Y}_I^* = \mathbf{Y}_I + \mathbf{Y}_J \wedge \Delta \mathbf{Y}_I^* = i (\mathbf{Y}_I - \mathbf{Y}_J) \Leftrightarrow \mathbf{Y}_I = \frac{1}{2} (\Sigma \mathbf{Y}_I^* - i \Delta \mathbf{Y}_I^*) \wedge \mathbf{Y}_J = \frac{1}{2} (\Sigma \mathbf{Y}_I^* + i \Delta \mathbf{Y}_I^*) \quad (3.3.368)$$

The left eigenvectors are treated in an analogous way as the right eigenvectors. For the sum and the difference of $\mathbf{x}_I^{(j)}$ and $\mathbf{x}_J^{(j)}$ it is valid:

$$\mathbf{x}_I^{(j)} + \mathbf{x}_J^{(j)} = \mathbf{X}_I \zeta^{k_I j} + \mathbf{X}_J \zeta^{k_J j} = (\mathbf{X}_I + \mathbf{X}_J) \Re \zeta^{k_I j} + i (\mathbf{X}_I - \mathbf{X}_J) \Im \zeta^{k_I j} \quad (3.3.369)$$

$$i \left(\mathbf{x}_I^{(j)} - \mathbf{x}_J^{(j)} \right) = i \left(\mathbf{X}_I \zeta^{k_I j} + \mathbf{X}_J \zeta^{k_J j} \right) = i (\mathbf{X}_I - \mathbf{X}_J) \Re \zeta^{k_I j} - (\mathbf{X}_I + \mathbf{X}_J) \Im \zeta^{k_I j} \quad (3.3.370)$$

For the damped linear cyclic system, the vectors \mathbf{X}_I and \mathbf{X}_J don't have to be determined separately, but are already known from the comparison for the transposed right eigenvector problems (3.3.319) and (3.3.320). Inserting these relations and applying the relation $\bar{\bar{i}} = -i$ leads to:

$$\mathbf{Y}_J = \overline{\mathbf{X}_I} \Leftrightarrow \mathbf{X}_I = \overline{\mathbf{Y}_J}, \mathbf{X}_J = \overline{\mathbf{Y}_I} \quad (3.3.371)$$

$$\Rightarrow \mathbf{X}_I + \mathbf{X}_J = \overline{\mathbf{Y}_J} + \overline{\mathbf{Y}_I} = \overline{\mathbf{Y}_J + \mathbf{Y}_I} = \overline{\Sigma \mathbf{Y}_I^*} \quad (3.3.372)$$

$$i(\mathbf{X}_I - \mathbf{X}_J) = -\bar{i}(\overline{\mathbf{Y}_J} - \overline{\mathbf{Y}_I}) = \bar{i}(\overline{\mathbf{Y}_I} - \overline{\mathbf{Y}_J}) = \overline{i(\mathbf{Y}_I - \mathbf{Y}_J)} = \overline{\Delta \mathbf{Y}_I^*} \quad (3.3.373)$$

Based on this, the left eigenvectors are obtained to:

$$\mathbf{x}_I^{(j)} + \mathbf{x}_J^{(j)} = (\mathbf{X}_I + \mathbf{X}_J) \Re \zeta^{k_I j} + i(\mathbf{X}_I - \mathbf{X}_J) \Im \zeta^{k_I j} = \overline{\Sigma \mathbf{Y}_I^*} \Re \zeta^{k_I j} + \overline{\Delta \mathbf{Y}_I^*} \Im \zeta^{k_I j} \quad (3.3.374)$$

$$i(\mathbf{x}_I^{(j)} - \mathbf{x}_J^{(j)}) = i(\mathbf{X}_I - \mathbf{X}_J) \Re \zeta^{k_I j} - (\mathbf{X}_I + \mathbf{X}_J) \Im \zeta^{k_I j} = \overline{\Delta \mathbf{Y}_I^*} \Re \zeta^{k_I j} - \overline{\Sigma \mathbf{Y}_I^*} \Im \zeta^{k_I j} \quad (3.3.375)$$

The comparison of this result with the formulation of the right eigenvectors $\mathbf{y}_{I1}^{(j)}$ and $\mathbf{y}_{I2}^{(j)}$ leads to:

$$\mathbf{y}_{I1}^{(j)} = \mathbf{y}_I^{(j)} + \mathbf{y}_J^{(j)} = \Sigma \mathbf{Y}_I^* \Re \zeta^{k_I j} + \Delta \mathbf{Y}_I^* \Im \zeta^{k_I j} \quad (3.3.376)$$

$$\Rightarrow \overline{\mathbf{y}_{I1}^{(j)}} = \overline{\Sigma \mathbf{Y}_I^* \Re \zeta^{k_I j} + \Delta \mathbf{Y}_I^* \Im \zeta^{k_I j}} = \overline{\Sigma \mathbf{Y}_I^*} \Re \zeta^{k_I j} + \overline{\Delta \mathbf{Y}_I^*} \Im \zeta^{k_I j} = \mathbf{x}_I^{(j)} + \mathbf{x}_J^{(j)} \quad (3.3.377)$$

$$\mathbf{y}_{I2}^{(j)} = i(\mathbf{y}_I^{(j)} - \mathbf{y}_J^{(j)}) = \Delta \mathbf{Y}_I^* \Re \zeta^{k_I j} - \Sigma \mathbf{Y}_I^* \Im \zeta^{k_I j} \quad (3.3.378)$$

$$\Rightarrow \overline{\mathbf{y}_{I2}^{(j)}} = \overline{\Delta \mathbf{Y}_I^* \Re \zeta^{k_I j} - \Sigma \mathbf{Y}_I^* \Im \zeta^{k_I j}} = \overline{\Delta \mathbf{Y}_I^*} \Re \zeta^{k_I j} - \overline{\Sigma \mathbf{Y}_I^*} \Im \zeta^{k_I j} = i(\mathbf{x}_I^{(j)} - \mathbf{x}_J^{(j)}) \quad (3.3.379)$$

As shown before, the sums $\mathbf{y}_{CI} + \mathbf{y}_{CJ}$ and $\mathbf{x}_{CI} + \mathbf{x}_{CJ}$ are orthogonal to the differences $\mathbf{y}_{CI} - \mathbf{y}_{CJ}$ and $\mathbf{x}_{CI} - \mathbf{x}_{CJ}$. The orthogonality is not affected by any scalar factor. Therefore, it is reasonable to define the left eigenvectors $\mathbf{x}_{I1}^{(j)}$ and $\mathbf{x}_{I2}^{(j)}$ in the following way:

$$\mathbf{y}_{I1}^{(j)} = \mathbf{y}_I^{(j)} + \mathbf{y}_J^{(j)} \Rightarrow \overline{\mathbf{y}_{I1}^{(j)}} = \mathbf{x}_I^{(j)} + \mathbf{x}_J^{(j)} = \mathbf{x}_{I1}^{(j)} \quad (3.3.380)$$

$$\mathbf{y}_{I2}^{(j)} = i(\mathbf{y}_I^{(j)} - \mathbf{y}_J^{(j)}) \Rightarrow \overline{\mathbf{y}_{I2}^{(j)}} = i(\mathbf{x}_I^{(j)} - \mathbf{x}_J^{(j)}) = \mathbf{x}_{I2}^{(j)} \quad (3.3.381)$$

3.4 Conclusion

In this chapter, the equations of motion for a linear cyclic system given by

$$\mathbf{M}_C \ddot{\mathbf{y}}_C(t) + \mathbf{P}_C \dot{\mathbf{y}}_C(t) + \mathbf{Q}_C \mathbf{y}_C(t) = \mathbf{h}_C(t) \quad (3.4.382)$$

have been considered; in this section, the results of the consideration shall be concluded briefly.

The vectors $\mathbf{y}^{(j)}$, which describe the displacements for the j -th segment, can be described by a discrete Fourier series using the root of unity ζ :

$$\mathbf{y}^{(j)}(t) = \sum_{k=k_{\min}}^{k_{\max}} \mathbf{y}_k(t) \zeta^{kj}, \quad \zeta = e^{\frac{2\pi}{n}i}, \quad k \in \mathbb{Z}, \quad k_{\max} = k_{\min} + n - 1 \quad (3.4.383)$$

$$\Rightarrow \underbrace{\begin{bmatrix} \mathbf{y}^{(0)}(t) \\ \vdots \\ \mathbf{y}^{(j)}(t) \\ \vdots \\ \mathbf{y}^{(n-1)}(t) \end{bmatrix}}_{\mathbf{y}_C(t)} = \underbrace{\begin{bmatrix} \mathbf{I} \zeta^{k_{\min} \cdot 0} & \dots & \mathbf{I} \zeta^{k \cdot 0} & \dots & \mathbf{I} \zeta^{k_{\max} \cdot 0} \\ \vdots & & \vdots & & \vdots \\ \mathbf{I} \zeta^{k_{\min} \cdot j} & \dots & \mathbf{I} \zeta^{k \cdot j} & \dots & \mathbf{I} \zeta^{k_{\max} \cdot j} \\ \vdots & & \vdots & & \vdots \\ \mathbf{I} \zeta^{k_{\min} \cdot (n-1)} & \dots & \mathbf{I} \zeta^{k \cdot (n-1)} & \dots & \mathbf{I} \zeta^{k_{\max} \cdot (n-1)} \end{bmatrix}}_{\mathbf{T}_{CF}} \underbrace{\begin{bmatrix} \mathbf{y}_{k_{\min}}(t) \\ \vdots \\ \mathbf{y}_k(t) \\ \vdots \\ \mathbf{y}_{k_{\max}}(t) \end{bmatrix}}_{\mathbf{y}_F(t)} \quad (3.4.384)$$

Although the bounds k_{\min} and k_{\max} , which limit the range of the periodicity k , can be chosen arbitrarily as long as the condition $k_{\max} = k_{\min} + n - 1$ is fulfilled, it is nevertheless reasonable to use a range for k , which is exactly or nearly centred around zero. Therefore, it is valid for k :

$$-\frac{n}{2} < k \leq \frac{n}{2} \quad (3.4.385)$$

By assuming that the vector $\delta\dot{\mathbf{y}}_C$, which describes the virtual velocities, is a real vector, the left hand side of the equations of motion can be transformed in the following way:

$$\begin{aligned} \delta\dot{\mathbf{y}}_C^T (\mathbf{M}_C \ddot{\mathbf{y}}_C + \mathbf{P}_C \dot{\mathbf{y}}_C + \mathbf{Q}_C \mathbf{y}_C) &= \delta\dot{\mathbf{y}}_F^H (\mathbf{T}_{CF}^H \mathbf{M}_C \mathbf{T}_{CF} \ddot{\mathbf{y}}_F + \mathbf{T}_{CF}^H \mathbf{P}_C \mathbf{T}_{CF} \dot{\mathbf{y}}_F + \mathbf{T}_{CF}^H \mathbf{Q}_C \mathbf{T}_{CF} \mathbf{y}_F) \\ &= n \sum_{k=k_{\min}}^{k_{\max}} \delta\dot{\mathbf{y}}_k^H (\mathbf{M}_k \ddot{\mathbf{y}}_k + \mathbf{P}_k \dot{\mathbf{y}}_k + \mathbf{Q}_k \mathbf{y}_k) \end{aligned} \quad (3.4.386)$$

Due to the transformation, the terms of the left-hand side of the equation of motion are decoupled for different periodicities k , i.e. there is no interaction between motions having different periodicities. The matrices \mathbf{Q}_k , \mathbf{P}_k and \mathbf{M}_k are determined in the following way:

$$\mathbf{Q}_C = \begin{bmatrix} \mathbf{Q}^{(0)} & \mathbf{Q}^{(1)} & \mathbf{0} & \dots & \mathbf{0} & \mathbf{Q}^{(-1)} \\ \mathbf{Q}^{(-1)} & \mathbf{Q}^{(0)} & \mathbf{Q}^{(1)} & \dots & \mathbf{0} & \mathbf{0} \\ \mathbf{0} & \mathbf{Q}^{(-1)} & \mathbf{Q}^{(0)} & \ddots & \mathbf{0} & \mathbf{0} \\ \vdots & \vdots & \ddots & \ddots & \ddots & \vdots \\ \mathbf{0} & \mathbf{0} & \mathbf{0} & \ddots & \mathbf{Q}^{(0)} & \mathbf{Q}^{(1)} \\ \mathbf{Q}^{(1)} & \mathbf{0} & \mathbf{0} & \dots & \mathbf{Q}^{(-1)} & \mathbf{Q}^{(0)} \end{bmatrix} \Rightarrow \mathbf{Q}_k = \mathbf{Q}^{(-1)} \zeta^{-k} + \mathbf{Q}^{(0)} + \mathbf{Q}^{(1)} \zeta^k \quad (3.4.387)$$

$$\mathbf{P}_C = \begin{bmatrix} \mathbf{P}^{(0)} & \mathbf{P}^{(1)} & \mathbf{0} & \dots & \mathbf{0} & \mathbf{P}^{(-1)} \\ \mathbf{P}^{(-1)} & \mathbf{P}^{(0)} & \mathbf{P}^{(1)} & \dots & \mathbf{0} & \mathbf{0} \\ \mathbf{0} & \mathbf{P}^{(-1)} & \mathbf{P}^{(0)} & \ddots & \mathbf{0} & \mathbf{0} \\ \vdots & \vdots & \ddots & \ddots & \ddots & \vdots \\ \mathbf{0} & \mathbf{0} & \mathbf{0} & \ddots & \mathbf{P}^{(0)} & \mathbf{P}^{(1)} \\ \mathbf{P}^{(1)} & \mathbf{0} & \mathbf{0} & \dots & \mathbf{P}^{(-1)} & \mathbf{P}^{(0)} \end{bmatrix} \Rightarrow \mathbf{P}_k = \mathbf{P}^{(-1)} \zeta^{-k} + \mathbf{P}^{(0)} + \mathbf{P}^{(1)} \zeta^k \quad (3.4.388)$$

$$\mathbf{M}_C = \begin{bmatrix} \mathbf{M}^{(0)} & \mathbf{M}^{(1)} & \mathbf{0} & \dots & \mathbf{0} & \mathbf{M}^{(-1)} \\ \mathbf{M}^{(-1)} & \mathbf{M}^{(0)} & \mathbf{M}^{(1)} & \dots & \mathbf{0} & \mathbf{0} \\ \mathbf{0} & \mathbf{M}^{(-1)} & \mathbf{M}^{(0)} & \ddots & \mathbf{0} & \mathbf{0} \\ \vdots & \vdots & \ddots & \ddots & \ddots & \vdots \\ \mathbf{0} & \mathbf{0} & \mathbf{0} & \ddots & \mathbf{M}^{(0)} & \mathbf{M}^{(1)} \\ \mathbf{M}^{(1)} & \mathbf{0} & \mathbf{0} & \dots & \mathbf{M}^{(-1)} & \mathbf{M}^{(0)} \end{bmatrix} \Rightarrow \mathbf{M}_k = \mathbf{M}^{(-1)} \zeta^{-k} + \mathbf{M}^{(0)} + \mathbf{M}^{(1)} \zeta^k \quad (3.4.389)$$

The right eigenvector \mathbf{y}_{CI} and the left eigenvector \mathbf{x}_{CI} of a linear cyclic system fulfil the following conditions:

$$\mathbf{0} = (\lambda_I^2 \mathbf{M}_C + \lambda_I \mathbf{P}_C + \mathbf{Q}_C) \mathbf{y}_{CI}, \quad \mathbf{y}_{CI} \neq \mathbf{0} \quad (3.4.390)$$

$$\mathbf{0} = \mathbf{x}_{CI}^H (\lambda_I^2 \mathbf{M}_C + \lambda_I \mathbf{P}_C + \mathbf{Q}_C), \quad \mathbf{x}_{CI} \neq \mathbf{0} \quad (3.4.391)$$

Each eigenvector \mathbf{y}_{CI} and \mathbf{x}_{CI} can be formulated in the following way using the periodicity k_I :

$$\mathbf{y}_{CI} = \begin{bmatrix} \mathbf{y}_I^{(0)} \\ \vdots \\ \mathbf{y}_I^{(j)} \\ \vdots \\ \mathbf{y}_I^{(n-1)} \end{bmatrix} = \begin{bmatrix} \mathbf{Y}_I \\ \vdots \\ \mathbf{Y}_I \zeta^{k_I j} \\ \vdots \\ \mathbf{Y}_I \zeta^{k_I(n-1)} \end{bmatrix}, \quad \mathbf{x}_{CI} = \begin{bmatrix} \mathbf{x}_I^{(0)} \\ \vdots \\ \mathbf{x}_I^{(j)} \\ \vdots \\ \mathbf{x}_I^{(n-1)} \end{bmatrix} = \begin{bmatrix} \mathbf{X}_I \\ \vdots \\ \mathbf{X}_I \zeta^{k_I j} \\ \vdots \\ \mathbf{X}_I \zeta^{k_I(n-1)} \end{bmatrix} \quad (3.4.392)$$

If two eigenvectors \mathbf{x}_{CI} and \mathbf{y}_{CI} have different periodicities $k_I \neq k_J$, they are orthogonal regardless of their eigenvalues λ_I and λ_J , to which they are associated, because of the decoupling shown in (3.4.386). The eigenvalue λ_I and the vectors \mathbf{Y}_I and \mathbf{X}_I fulfil the following conditions:

$$\det(\lambda_I^2 \mathbf{M}_{k_I} + \lambda_I \mathbf{P}_{k_I} + \mathbf{Q}_{k_I}) = 0 \quad (3.4.393)$$

$$(\lambda_I^2 \mathbf{M}_{k_I} + \lambda_I \mathbf{P}_{k_I} + \mathbf{Q}_{k_I}) \mathbf{Y}_I = \mathbf{0}, \quad \mathbf{Y}_I \neq \mathbf{0} \quad (3.4.394)$$

$$\mathbf{X}_I^H (\lambda_I^2 \mathbf{M}_{k_I} + \lambda_I \mathbf{P}_{k_I} + \mathbf{Q}_{k_I}) = \mathbf{0}, \quad \mathbf{X}_I \neq \mathbf{0} \quad (3.4.395)$$

The matrices \mathbf{M}_C , \mathbf{P}_C and \mathbf{Q}_C are usually real matrices; thereby, also their submatrices $\mathbf{M}^{(J)}$, $\mathbf{P}^{(J)}$ and $\mathbf{Q}^{(J)}$, too, are real. According to (3.4.387), (3.4.388) and (3.4.389), the matrices \mathbf{M}_k , \mathbf{P}_k and \mathbf{Q}_k are linear combination of the submatrices $\mathbf{M}^{(J)}$, $\mathbf{P}^{(J)}$ and $\mathbf{Q}^{(J)}$ using the powers ζ^k and $\zeta^{-k} = \overline{\zeta^k}$ as scalar factors. Based on this, three different cases can be distinguished. For $k = 0$ the matrices \mathbf{M}_k , \mathbf{P}_k and \mathbf{Q}_k are real matrices:

$$k = 0 : \mathbf{M}_0 = \mathbf{M}^{(0)} + \mathbf{M}^{(-1)} + \mathbf{M}^{(1)}, \quad \mathbf{P}_0 = \mathbf{P}^{(0)} + \mathbf{P}^{(-1)} + \mathbf{P}^{(1)}, \quad \mathbf{Q}_0 = \mathbf{Q}^{(0)} + \mathbf{Q}^{(-1)} + \mathbf{Q}^{(1)} \quad (3.4.396)$$

In this case, all segment vectors $\mathbf{y}_I^{(j)}$ and $\mathbf{x}_I^{(j)}$ are equal, respectively; it is valid:

$$k_I = 0 \Rightarrow \zeta^{k_I j} = 1 \Rightarrow \mathbf{y}_I^{(j)} = \mathbf{Y}_I, \quad \mathbf{x}_I^{(j)} = \mathbf{X}_I \quad (3.4.397)$$

The second case $k = \frac{n}{2}$ only occurs for even numbers n ; here, it is valid for the matrices \mathbf{M}_k , \mathbf{P}_k and \mathbf{Q}_k :

$$k = \frac{n}{2} : \mathbf{M}_{\frac{n}{2}} = \mathbf{M}^{(0)} - \mathbf{M}^{(-1)} - \mathbf{M}^{(1)}, \quad \mathbf{P}_{\frac{n}{2}} = \mathbf{P}^{(0)} - \mathbf{P}^{(-1)} - \mathbf{P}^{(1)}, \quad \mathbf{Q}_{\frac{n}{2}} = \mathbf{Q}^{(0)} - \mathbf{Q}^{(-1)} - \mathbf{Q}^{(1)} \quad (3.4.398)$$

Here, the vectors $\mathbf{y}_I^{(j)}$ and $\mathbf{x}_I^{(j)}$ differ only by sign, which alternates; therefore, it is valid:

$$k_I = \frac{n}{2} \Rightarrow \zeta^{k_I j} = (-1)^j \Rightarrow \mathbf{y}_I^{(j)} = (-1)^j \mathbf{Y}_I, \quad \mathbf{x}_I^{(j)} = (-1)^j \mathbf{X}_I \quad (3.4.399)$$

For all other periodicities, i.e. $k \neq 0 \wedge k \neq \frac{n}{2}$, the matrices \mathbf{M}_k , \mathbf{P}_k and \mathbf{Q}_k can be complex; splitting these matrices into their real parts and imaginary parts leads to:

$$\Re \mathbf{M}_k = \mathbf{M}^{(0)} + \Re \zeta^k (\mathbf{M}^{(1)} + \mathbf{M}^{(-1)}), \quad \Im \mathbf{M}_k = \Im \zeta^k (\mathbf{M}^{(1)} - \mathbf{M}^{(-1)}) \quad (3.4.400)$$

$$\Re \mathbf{P}_k = \mathbf{P}^{(0)} + \Re \zeta^k (\mathbf{P}^{(1)} + \mathbf{P}^{(-1)}), \quad \Im \mathbf{P}_k = \Im \zeta^k (\mathbf{P}^{(1)} - \mathbf{P}^{(-1)}) \quad (3.4.401)$$

$$\Re \mathbf{Q}_k = \mathbf{Q}^{(0)} + \Re \zeta^k (\mathbf{Q}^{(1)} + \mathbf{Q}^{(-1)}), \quad \Im \mathbf{Q}_k = \Im \zeta^k (\mathbf{Q}^{(1)} - \mathbf{Q}^{(-1)}) \quad (3.4.402)$$

Here, it is valid for the matrices:

$$\mathbf{M}_{-k} = \overline{\mathbf{M}_k}, \mathbf{P}_{-k} = \overline{\mathbf{P}_k}, \mathbf{Q}_{-k} = \overline{\mathbf{Q}_k} \quad (3.4.403)$$

In this case it is useful to combine the conditions for the corresponding periodicities k and $-k$. The advantage of this formulation is that it uses real matrices and covers both periodicities k and $-k$

$$\begin{aligned} \mathbf{0} &= (\lambda_I^2 \mathbf{M}_k + \lambda_I \mathbf{P}_k + \mathbf{Q}_k) \mathbf{y}_{I,k} \wedge \mathbf{0} = (\lambda_I^2 \mathbf{M}_{-k} + \lambda_I \mathbf{P}_{-k} + \mathbf{Q}_{-k}) \mathbf{y}_{I,-k} \\ &\Rightarrow \mathbf{0} = \left(\lambda_I^2 \begin{bmatrix} \Re \mathbf{M}_k & \Im \mathbf{M}_k \\ -\Im \mathbf{M}_k & \Re \mathbf{M}_k \end{bmatrix} + \lambda_I \begin{bmatrix} \Re \mathbf{P}_k & \Im \mathbf{P}_k \\ -\Im \mathbf{P}_k & \Re \mathbf{P}_k \end{bmatrix} + \begin{bmatrix} \Re \mathbf{Q}_k & \Im \mathbf{Q}_k \\ -\Im \mathbf{Q}_k & \Re \mathbf{Q}_k \end{bmatrix} \right) \begin{bmatrix} \mathbf{y}_{I,k} + \mathbf{y}_{I,-k} \\ i \mathbf{y}_{I,k} - i \mathbf{y}_{I,-k} \end{bmatrix} \end{aligned} \quad (3.4.404)$$

The subvectors $\mathbf{y}_I^{(j)}$ having the periodicity k_I are now determined in the following way:

$$\mathbf{0} = \left(\lambda_I^2 \begin{bmatrix} \Re \mathbf{M}_{|k_I|} & \Im \mathbf{M}_{|k_I|} \\ -\Im \mathbf{M}_{|k_I|} & \Re \mathbf{M}_{|k_I|} \end{bmatrix} + \lambda_I \begin{bmatrix} \Re \mathbf{P}_{|k_I|} & \Im \mathbf{P}_{|k_I|} \\ -\Im \mathbf{P}_{|k_I|} & \Re \mathbf{P}_{|k_I|} \end{bmatrix} + \begin{bmatrix} \Re \mathbf{Q}_{|k_I|} & \Im \mathbf{Q}_{|k_I|} \\ -\Im \mathbf{Q}_{|k_I|} & \Re \mathbf{Q}_{|k_I|} \end{bmatrix} \right) \begin{bmatrix} \Sigma \mathbf{Y}_I \\ \Delta \mathbf{Y}_I \end{bmatrix} \quad (3.4.405)$$

$$\mathbf{y}_I^{(j)} = [\mathbf{I} \Re \zeta^{|k_I|j} \quad \mathbf{I} \Im \zeta^{|k_I|j}] \begin{bmatrix} \Sigma \mathbf{Y}_I \\ \Delta \mathbf{Y}_I \end{bmatrix} = \Sigma \mathbf{Y}_I \cos\left(\frac{2\pi}{n} |k_I|j\right) + \Delta \mathbf{Y}_I \sin\left(\frac{2\pi}{n} |k_I|j\right) \quad (3.4.406)$$

A damped linear cyclic system is a special case of a linear cyclic system. Its equation of motion is given by:

$$\mathbf{M}_C \ddot{\mathbf{y}}_C(t) + \mathbf{D}_C \dot{\mathbf{y}}_C(t) + \mathbf{K}_C \mathbf{y}_C(t) = \mathbf{h}_C(t), \mathbf{M}_C = \mathbf{M}_C^T, \mathbf{D}_C = \mathbf{D}_C^T, \mathbf{K}_C = \mathbf{K}_C^T \quad (3.4.407)$$

Here, the matrices \mathbf{D}_C and \mathbf{K}_C have the same structure as indicated for the matrices \mathbf{P}_C and \mathbf{Q}_C in (3.4.388) and (3.4.387), respectively; in addition, all matrices are symmetric, so that it is valid for their submatrices:

$$\mathbf{M}^{(0)} = \mathbf{M}^{(0)T}, \mathbf{M}^{(-1)} = \mathbf{M}^{(1)T}, \mathbf{D}^{(0)} = \mathbf{D}^{(0)T}, \mathbf{D}^{(-1)} = \mathbf{D}^{(1)T}, \mathbf{K}^{(0)} = \mathbf{K}^{(0)T}, \mathbf{K}^{(-1)} = \mathbf{K}^{(1)T} \quad (3.4.408)$$

In this case, all matrices \mathbf{M}_k , \mathbf{D}_k and \mathbf{K}_k are Hermitian matrices, i.e. their real parts are symmetric, while their imaginary parts are skew-symmetric:

$$\mathbf{M}_k = \mathbf{M}^{(-1)} \zeta^{-k} + \mathbf{M}^{(0)} + \mathbf{M}^{(1)} \zeta^k = \mathbf{M}_k^H \Rightarrow \Re \mathbf{M}_k = \Re \mathbf{M}_k^T, \Im \mathbf{M}_k = -\Im \mathbf{M}_k^T \quad (3.4.409)$$

$$\mathbf{D}_k = \mathbf{D}^{(-1)} \zeta^{-k} + \mathbf{D}^{(0)} + \mathbf{D}^{(1)} \zeta^k = \mathbf{D}_k^H \Rightarrow \Re \mathbf{D}_k = \Re \mathbf{D}_k^T, \Im \mathbf{D}_k = -\Im \mathbf{D}_k^T \quad (3.4.410)$$

$$\mathbf{K}_k = \mathbf{K}^{(-1)} \zeta^{-k} + \mathbf{K}^{(0)} + \mathbf{K}^{(1)} \zeta^k = \mathbf{K}_k^H \Rightarrow \Re \mathbf{K}_k = \Re \mathbf{K}_k^T, \Im \mathbf{K}_k = -\Im \mathbf{K}_k^T \quad (3.4.411)$$

Based on this, all eigenvalues of a damped linear system for the periodicity $k_I \neq 0 \wedge k_I \neq \frac{n}{2}$ are double eigenvalues. For a double eigenvalue $\lambda_I = \lambda_J = \lambda_I^*$ it is valid:

$$\mathbf{0} = \left(\lambda_I^{*2} \begin{bmatrix} \Re \mathbf{M}_{|k_I|} & \Im \mathbf{M}_{|k_I|} \\ -\Im \mathbf{M}_{|k_I|} & \Re \mathbf{M}_{|k_I|} \end{bmatrix} + \lambda_I^* \begin{bmatrix} \Re \mathbf{D}_{|k_I|} & \Im \mathbf{D}_{|k_I|} \\ -\Im \mathbf{D}_{|k_I|} & \Re \mathbf{D}_{|k_I|} \end{bmatrix} + \begin{bmatrix} \Re \mathbf{K}_{|k_I|} & \Im \mathbf{K}_{|k_I|} \\ -\Im \mathbf{K}_{|k_I|} & \Re \mathbf{K}_{|k_I|} \end{bmatrix} \right) \begin{bmatrix} \Sigma \mathbf{Y}_I^* \\ \Delta \mathbf{Y}_I^* \end{bmatrix} \quad (3.4.412)$$

$$\Rightarrow \mathbf{y}_{I1}^{(j)} = [\mathbf{I} \Re \zeta^{|k_I|j} \quad \mathbf{I} \Im \zeta^{|k_I|j}] \begin{bmatrix} \Sigma \mathbf{Y}_I^* \\ \Delta \mathbf{Y}_I^* \end{bmatrix} = \Sigma \mathbf{Y}_I^* \cos\left(\frac{2\pi}{n} |k_I|j\right) + \Delta \mathbf{Y}_I^* \sin\left(\frac{2\pi}{n} |k_I|j\right) \quad (3.4.413)$$

$$\mathbf{0} = \left(\lambda_I^{*2} \begin{bmatrix} \Re \mathbf{M}_{|k_I|} & \Im \mathbf{M}_{|k_I|} \\ -\Im \mathbf{M}_{|k_I|} & \Re \mathbf{M}_{|k_I|} \end{bmatrix} + \lambda_I^* \begin{bmatrix} \Re \mathbf{D}_{|k_I|} & \Im \mathbf{D}_{|k_I|} \\ -\Im \mathbf{D}_{|k_I|} & \Re \mathbf{D}_{|k_I|} \end{bmatrix} + \begin{bmatrix} \Re \mathbf{K}_{|k_I|} & \Im \mathbf{K}_{|k_I|} \\ -\Im \mathbf{K}_{|k_I|} & \Re \mathbf{K}_{|k_I|} \end{bmatrix} \right) \begin{bmatrix} \Delta \mathbf{Y}_I^* \\ -\Sigma \mathbf{Y}_I^* \end{bmatrix} \quad (3.4.414)$$

$$\Rightarrow \mathbf{y}_{I2}^{(j)} = [\mathbf{I} \Re \zeta^{|k_I|j} \quad \mathbf{I} \Im \zeta^{|k_I|j}] \begin{bmatrix} \Delta \mathbf{Y}_I^* \\ -\Sigma \mathbf{Y}_I^* \end{bmatrix} = \Delta \mathbf{Y}_I^* \cos\left(\frac{2\pi}{n} |k_I|j\right) - \Sigma \mathbf{Y}_I^* \sin\left(\frac{2\pi}{n} |k_I|j\right) \quad (3.4.415)$$

The double eigenvectors represent the isotropy of the cyclic structure. Since the structure consists of n identical segments, which are arranged circularly, it has no preferred spatial orientation with respect to this circle. Therefore, for each motion, which is not rotational symmetric ($k_I = 0$) or described by alternating signs ($k_I = \frac{n}{2}$), two parameters are required in order to determine the amplitude and the spatial orientation of the resulting motion.

For the practical determination of the eigenvalues and eigenvectors, the conditions (3.4.393), (3.4.394) and (3.4.395) have to be transformed into the following formulation, which is used by many solving algorithms like e.g. those contained in the widely used library LAPACK [1]:

$$\det(\mathbf{A} - \lambda_I \mathbf{I}) = 0, \mathbf{A} \mathbf{w}_I = \lambda_I \mathbf{w}_I, \mathbf{v}_I^H \mathbf{A} = \lambda_I \mathbf{v}_I^H \quad (3.4.416)$$

In the present case, this formulation is obtained by using the state space representation of an ordinary linear mechanical system. Here, the matrix \mathbf{A} has the following structure:

$$\mathbf{M} \ddot{\mathbf{y}}(t) + \mathbf{P} \dot{\mathbf{y}}(t) + \mathbf{Q} \mathbf{y}(t) = \mathbf{h}(t) \Rightarrow \mathbf{A} = \begin{bmatrix} \mathbf{0} & \mathbf{I} \\ -\mathbf{M}^{-1} \mathbf{Q} & -\mathbf{M}^{-1} \mathbf{P} \end{bmatrix} \quad (3.4.417)$$

According to (3.4.387), (3.4.388) and (3.4.389) the matrices \mathbf{Q}_k , \mathbf{P}_k and \mathbf{M}_k are linear combinations of the submatrices $\mathbf{Q}^{(j)}$, $\mathbf{P}^{(j)}$ and $\mathbf{M}^{(j)}$, which are of order $N_S \times N_S$. Therefore, also the matrices \mathbf{Q}_k , \mathbf{P}_k and \mathbf{M}_k are of order $N_S \times N_S$. As discussed before, for the periodicities $k = 0$ and $k = \frac{n}{2}$ the matrices \mathbf{M}_k , \mathbf{P}_k and \mathbf{Q}_k are always real matrices. In this case, the matrix \mathbf{A}_k can be derived directly from the conditions (3.4.394) and (3.4.395). It is valid:

$$k = 0 \vee k = \frac{n}{2} : \mathbf{A}_k = \begin{bmatrix} \mathbf{0} & \mathbf{I} \\ -\mathbf{M}_k^{-1} \mathbf{Q}_k & -\mathbf{M}_k^{-1} \mathbf{P}_k \end{bmatrix}, \mathbf{A}_k \in \mathbb{R}^{2 \cdot N_S \times 2 \cdot N_S} \quad (3.4.418)$$

Here, the vectors $\mathbf{y}_I^{(j)}$ are determined in the following way:

$$(\mathbf{A}_k - \lambda_I \mathbf{I}) \mathbf{w}_I = \mathbf{0} \Rightarrow \mathbf{w}_I = \begin{bmatrix} \mathbf{Y}_I \\ \lambda_I \mathbf{Y}_I \end{bmatrix} \Rightarrow \mathbf{y}_I^{(j)} = \begin{cases} \mathbf{Y}_I & \text{for } k_I = 0 \\ \mathbf{Y}_I (-1)^j & \text{for } k_I = \frac{n}{2} \end{cases} \quad (3.4.419)$$

For all other periodicities $k \neq 0 \wedge k \neq \frac{n}{2}$, the matrices \mathbf{M}_k , \mathbf{P}_k and \mathbf{Q}_k can be complex. In this case, the real and imaginary parts of the matrices are rearranged in order to formulate the eigenvector problem using real matrices. As mentioned before, this formulation covers the corresponding periodicities k and $-k$, which differ only by the sign; therefore, this calculation has to be carried out only for positive periodicities $k > 0$.

$$\begin{aligned} 0 < k < \frac{n}{2} : \mathbf{M}_k^* &= \begin{bmatrix} \Re \mathbf{M}_k & \Im \mathbf{M}_k \\ -\Im \mathbf{M}_k & \Re \mathbf{M}_k \end{bmatrix}, \mathbf{P}_k^* = \begin{bmatrix} \Re \mathbf{P}_k & \Im \mathbf{P}_k \\ -\Im \mathbf{P}_k & \Re \mathbf{P}_k \end{bmatrix}, \\ \mathbf{Q}_k^* &= \begin{bmatrix} \Re \mathbf{Q}_k & \Im \mathbf{Q}_k \\ -\Im \mathbf{Q}_k & \Re \mathbf{Q}_k \end{bmatrix}, \mathbf{M}_k^*, \mathbf{P}_k^*, \mathbf{Q}_k^* \in \mathbb{R}^{2 \cdot N_S \times 2 \cdot N_S} \\ \Rightarrow \mathbf{A}_k^* &= \begin{bmatrix} \mathbf{0} & \mathbf{I} \\ -\mathbf{M}_k^{*-1} \mathbf{Q}_k^* & -\mathbf{M}_k^{*-1} \mathbf{P}_k^* \end{bmatrix}, \mathbf{A}_k^* \in \mathbb{R}^{4 \cdot N_S \times 4 \cdot N_S} \end{aligned} \quad (3.4.420)$$

In this case, the vectors $\mathbf{y}_I^{(j)}$ are obtained in the following way:

$$\begin{aligned} (\mathbf{A}_k - \lambda_I \mathbf{I}) \mathbf{w}_I &= \mathbf{0} \\ \Rightarrow \mathbf{y}_I^{(j)} &= [\mathbf{I} \Re \zeta^{kj} \quad \mathbf{I} \Im \zeta^{kj} \quad \mathbf{0} \quad \mathbf{0}] \begin{bmatrix} \Sigma \mathbf{Y}_I \\ \Delta \mathbf{Y}_I \\ \lambda_I \Sigma \mathbf{Y}_I \\ \lambda_I \Delta \mathbf{Y}_I \end{bmatrix} = \Sigma \mathbf{Y}_I \cos\left(\frac{2\pi}{n} k j\right) + \Delta \mathbf{Y}_I \sin\left(\frac{2\pi}{n} k j\right) \end{aligned} \quad (3.4.421)$$

At first glance the formulation using the matrices \mathbf{M}_k^* , \mathbf{P}_k^* and \mathbf{Q}_k^* of order $2 \cdot N_S \times 2 \cdot N_S$ instead of the matrices \mathbf{M}_k , \mathbf{P}_k and \mathbf{Q}_k of order $N_S \times N_S$ seems to require an increased computational effort. However, while the matrices \mathbf{M}_k^* , \mathbf{P}_k^* and \mathbf{Q}_k^* are real, the matrices \mathbf{M}_k , \mathbf{P}_k and \mathbf{Q}_k can be complex. Regarding the computing, a complex number is stored and processed as two floating point numbers; furthermore, the multiplication of two complex numbers requires four multiplications and two additions. Therefore, the formulation using the matrices \mathbf{M}_k^* , \mathbf{P}_k^* , $\mathbf{Q}_k^* \in \mathbb{R}^{2 \cdot N_S \times 2 \cdot N_S}$ matrices instead of the matrices $\mathbf{M}_k, \mathbf{P}_k, \mathbf{Q}_k \in \mathbb{C}^{N_S \times N_S}$ does not mean an increased computational effort.

The original matrices \mathbf{M}_C , \mathbf{P}_C and \mathbf{Q}_C are of order $n \cdot N_S \times n \cdot N_S$. Therefore, it is valid for the untransformed linear cyclic system:

$$\mathbf{A}_C = \begin{bmatrix} \mathbf{0} & \mathbf{I} \\ -\mathbf{M}_C^{-1} \mathbf{Q}_C & -\mathbf{M}_C^{-1} \mathbf{P}_C \end{bmatrix}, \mathbf{A}_C \in \mathbb{R}^{2 \cdot n \cdot N_S \times 2 \cdot n \cdot N_S} \quad (3.4.422)$$

The required computational effort for the analysis of a linear cyclic system of order $n \cdot N_S \times n \cdot N_S$ shall now be compared:

- For an odd number n it has to be solved:
 - 1 eigenvector problem of the order $2 \cdot N_S$ for $k = 0$
 - $\frac{n-1}{2}$ eigenvector problems of the order $4 \cdot N_S$ for $0 < k < \frac{n}{2}$
- For an even number n it has to be solved:
 - 2 eigenvector problems of the order $2 \cdot N_S$ for $k = 0$ and $k = \frac{n}{2}$
 - $\frac{n}{2} - 1$ eigenvector problems of the order $4 \cdot N_S$ for $0 < k < \frac{n}{2}$
- Without applying the transformation it has to be solved:
 - 1 eigenvector problem of the order $2 \cdot n \cdot N_S$

There are different algorithms for the numerical solution of an eigenvector problem. The computational effort depends on the order of the problem and for some algorithms on the density or the sparsity of the matrix, i.e. how many elements are different from zero. However, for nearly all solving algorithms, the computational effort grows disproportional with the order, see e.g. [60], i.e. if the order is doubled from N to $2 \cdot N$, then the computational effort for solving a problem of order $2 \cdot N$ is more than twice the one required for solving a problem of order N . Thereby, a splitting of one eigenvalue problem into several separate problems of lower order practically always means a reduced computational effort. Furthermore, the transformation of the cyclic system is an analytic method, i.e. the problem is transformed without loss of accuracy. Therefore, the description of a cyclic system by the method presented in this chapter is useful for the analysis of such a system.

Chapter 4

Structural dynamics of the wheelset and the rail

In the vehicle-track model, which is developed in this work, the structural flexibility of the wheelsets and the rails is essential. In order to describe the deformations of a flexible structure, a modal synthesis is used, i.e. shape functions, which are scaled by modal coordinates, are superposed. It is advantageous to use the eigenmodes of the structure as shape functions. This requires a model for the structural dynamics in order to determine the eigenmodes.

The finite element (FE) method is a widely used method for the analysis of the structural dynamics, which provides a great flexibility regarding the geometry of the structure. As already discussed in the section 2.1.2, the modelling of a structure by finite elements results in very large systems of equations; it is evident that with growing size of the system also the effort for the solution increases. It should also be kept in mind that the FE method is an approximative method, i.e. it usually doesn't determine the exact solution, but only an approximation. For both reasons, it is advantageous to exploit known properties of the wanted solution in order to reduce the size of the system; such known properties are in particular symmetries of the structure, which is analyzed.

With the exception of turnouts and crossings, a rail has a prismatic structure. The essential characteristic of a prismatic structure is that its cross section is constant along the axis of the extrusion. A wheelset having disc wheels can be considered as a solid of revolution, i.e. it has a rotational symmetry with respect to any angle.

A prism is generated by extruding an area, the so-called cross-sectional area. A solid of revolution is generated by rotating an area around the axis of symmetry. In the case of the rail and of the wheelset, the generating areas have a relatively complicated shape so that the distribution of the displacements over these areas cannot be determined analytically, but only in an approximative way, e.g. by finite elements. However, the distribution along the axis of extrusion in the case of the prism and over the circumference can be described by analytical functions. Therefore, it is advantageous to use a semi-analytic method for the modelling of the structural dynamics of the rail and the wheelset.

In this chapter, the semi-analytic solution for a prism and for a solid of revolution and finite elements, which are based on these solutions, will be presented. Although the wheelset and the rail belong to different subsystems, i.e. the wheelset belongs to the vehicle and the rail belongs to the track, both structures have several properties in common so that it is obvious to treat them in one chapter.

The rail and the wheelset will be modelled as three-dimensional solids. Therefore, the basis for

the structural dynamics is the equation of motion for an isotropic linear elastic medium, as given e.g. by Landau and Lifshitz in [39]; this is also known as Navier's equation. By modifying the nomenclature¹ and applying the relation

$$E = 2G(1 + \nu) \quad (4.0.1)$$

between Young's modulus E , the shear modulus G and Poisson's ratio ν the equation can be written in the following way:

$$\rho \ddot{\mathbf{w}} = \frac{E}{2(1+\nu)} \Delta \mathbf{w} + \frac{E}{2(1+\nu)(1-2\nu)} \mathbf{grad} \operatorname{div} \mathbf{w} = G \left[\Delta \mathbf{w} + \frac{1}{1-2\nu} \mathbf{grad} \operatorname{div} \mathbf{w} \right] \quad (4.0.2)$$

Here, ρ denotes the density of the material. The displacement vector \mathbf{w} has the following structure:

$$\mathbf{w} = \begin{bmatrix} U(x, y, z, t) \\ V(x, y, z, t) \\ W(x, y, z, t) \end{bmatrix} \quad (4.0.3)$$

Based on this, the equations of motions for the different coordinates can be formulated; for the sake of brevity, the dependency of the displacements U , V and W on the spatial coordinates x , y and z and on the time t is not indicated explicitly.

$$\frac{\partial^2 U}{\partial x^2} + \frac{\partial^2 U}{\partial y^2} + \frac{\partial^2 U}{\partial z^2} + \frac{1}{1-2\nu} \frac{\partial}{\partial x} \left(\frac{\partial U}{\partial x} + \frac{\partial V}{\partial y} + \frac{\partial W}{\partial z} \right) - \frac{\rho}{G} \frac{\partial^2 U}{\partial t^2} = 0 \quad (4.0.4)$$

$$\frac{\partial^2 V}{\partial x^2} + \frac{\partial^2 V}{\partial y^2} + \frac{\partial^2 V}{\partial z^2} + \frac{1}{1-2\nu} \frac{\partial}{\partial y} \left(\frac{\partial U}{\partial x} + \frac{\partial V}{\partial y} + \frac{\partial W}{\partial z} \right) - \frac{\rho}{G} \frac{\partial^2 V}{\partial t^2} = 0 \quad (4.0.5)$$

$$\frac{\partial^2 W}{\partial x^2} + \frac{\partial^2 W}{\partial y^2} + \frac{\partial^2 W}{\partial z^2} + \frac{1}{1-2\nu} \frac{\partial}{\partial z} \left(\frac{\partial U}{\partial x} + \frac{\partial V}{\partial y} + \frac{\partial W}{\partial z} \right) - \frac{\rho}{G} \frac{\partial^2 W}{\partial t^2} = 0 \quad (4.0.6)$$

...

The infinitesimal volume dV can be considered as a triple scalar product. The triple scalar product of the three vectors \vec{a} , \vec{b} and \vec{c} is the volume of the parallelepiped given by the three vectors:

$$V = (\vec{a} \times \vec{b}) \cdot \vec{c} \quad (4.0.7)$$

$$dV = \left(\frac{\partial \mathbf{x}}{\partial x} dx \times \frac{\partial \mathbf{x}}{\partial y} dy \right) \cdot \frac{\partial \mathbf{x}}{\partial z} dz = \left(\begin{bmatrix} 1 \\ 0 \\ 0 \end{bmatrix} \times \begin{bmatrix} 0 \\ 1 \\ 0 \end{bmatrix} \right) \cdot \begin{bmatrix} 0 \\ 0 \\ 1 \end{bmatrix} dx dy dz \quad (4.0.8)$$

$$\begin{aligned} dV &= \left(\frac{\partial \mathbf{x}}{\partial \phi} d\phi \times \frac{\partial \mathbf{x}}{\partial y} dy \right) \cdot \frac{\partial \mathbf{x}}{\partial r} dr = \left(\begin{bmatrix} r \cos \phi \\ 0 \\ -r \sin \phi \end{bmatrix} \times \begin{bmatrix} 0 \\ 1 \\ 0 \end{bmatrix} \right) \cdot \begin{bmatrix} \sin \phi \\ 0 \\ \cos \phi \end{bmatrix} d\phi dy dr \\ &= \begin{bmatrix} r \sin \phi \\ 0 \\ r \cos \phi \end{bmatrix} \cdot \begin{bmatrix} \sin \phi \\ 0 \\ \cos \phi \end{bmatrix} d\phi dy dr = r (\sin^2 \phi + \cos^2 \phi) d\phi dy dr = r d\phi dy dr \end{aligned} \quad (4.0.9)$$

¹In [39], the symbol \mathbf{u} is used for the displacement. In this work, the symbol \mathbf{u} is used for displacements in the directions of cylindrical coordinates, while displacements in the directions of cartesian coordinates are denoted by \mathbf{w} .

4.1 Finite element modelling

The finite element (FE) method is a widely used and well established method for the solution of field problems including problems of elasticity. There are several books describing the method, e.g. the book by Zienkiewicz and Taylor [84]. Therefore, only a brief overview on the FE method will be given, which is based on [84]. Nevertheless, these fundamentals are required for the development of the finite elements for a prismatic solid and for a solid of revolution.

The goal of the analysis is to determine the displacement $\mathbf{w}(\mathbf{x})$ at an arbitrary point denoted by \mathbf{x} . First, an element e is considered. This element has certain points, which are called “nodes”; these nodes will be denoted by the index k . This distribution is approximated by superposing shape functions $\mathbf{N}_k(\mathbf{x})$, which are scaled by the displacements \mathbf{w}_k^e at the nodes.

$$\mathbf{w}(\mathbf{x}) \approx \tilde{\mathbf{w}}(\mathbf{x}) = \sum_k \mathbf{N}_k(\mathbf{x}) \mathbf{w}_k^e = \mathbf{N}(\mathbf{x}) \mathbf{w}^e \quad (4.1.10)$$

The shape functions have to fulfil the following condition:

$$\mathbf{N}_k(\mathbf{x}_l) = \begin{cases} \mathbf{I} & \text{for } l = k \\ \mathbf{0} & \text{for } l \neq k \end{cases} \Rightarrow \tilde{\mathbf{w}}(\mathbf{x}_k) = \mathbf{w}_k^e \quad (4.1.11)$$

From the displacement $\tilde{\mathbf{u}}$ the strains $\tilde{\boldsymbol{\varepsilon}}$ are derived by applying a suitable operator \mathbf{S} , which gives the required derivatives:

$$\boldsymbol{\varepsilon}(\mathbf{x}) \approx \tilde{\boldsymbol{\varepsilon}}(\mathbf{x}) = \mathbf{S} \tilde{\mathbf{w}}(\mathbf{x}) = \underbrace{\mathbf{S} \mathbf{N}(\mathbf{x})}_{\mathbf{B}(\mathbf{x})} \mathbf{w}^e = \mathbf{B}(\mathbf{x}) \mathbf{w}^e \quad (4.1.12)$$

The element is loaded by nodal forces \mathbf{q}_k^e , which are acting at the nodes; the nodal forces for all nodes form the vector \mathbf{q}^e . Furthermore, the element is subjected to distributed body forces $\mathbf{b}(\mathbf{x})$. Setting the virtual work of the external nodal forces \mathbf{q}_k^e equal to the total virtual work of the internal forces, which is obtained from the integral over the volume V^e of the element, leads to:

$$\begin{aligned} \delta \mathbf{w}^{eT} \mathbf{q}^e &= \int_{V^e} \left(\delta \tilde{\boldsymbol{\varepsilon}}(\mathbf{x})^T \boldsymbol{\sigma}(\mathbf{x}) - \delta \tilde{\mathbf{w}}(\mathbf{x})^T \mathbf{b}(\mathbf{x}) \right) dV \\ &= \delta \mathbf{w}^{eT} \int_{V^e} \left(\mathbf{B}(\mathbf{x})^T \boldsymbol{\sigma}(\mathbf{x}) - \mathbf{N}(\mathbf{x})^T \mathbf{b}(\mathbf{x}) \right) dV \end{aligned} \quad (4.1.13)$$

In this work, the modelling of the wheelset and the rail as flexible structures is focused on the analysis of the structural dynamics including the determination of structural eigenmodes. In this context, initial strains and initial residual stresses are neglected; furthermore, a linear elastic behaviour of the material is assumed. Thereby, the relation between the stress $\boldsymbol{\sigma}(\mathbf{x})$ and the strain $\boldsymbol{\varepsilon}(\mathbf{x})$ is formulated in the following way:

$$\boldsymbol{\sigma}(\mathbf{x}) = \mathbf{D} \boldsymbol{\varepsilon}(\mathbf{x}) \approx \mathbf{D} \tilde{\boldsymbol{\varepsilon}}(\mathbf{x}) = \mathbf{D} \mathbf{B}(\mathbf{x}) \mathbf{w}^e \quad (4.1.14)$$

Here, the matrix \mathbf{D} is the elasticity matrix, which contains the material parameters like Young's modulus E , the shear modulus G and Poisson's ratio ν . It is assumed that within one element these parameters and thereby also the elasticity matrix \mathbf{D} are constant.

In the context of the structural dynamics, the inertia has to be taken into account; this can be done by the body forces $\mathbf{b}(\mathbf{x})$. Moreover, it is assumed that there are no further body forces. Thereby, it is valid:

$$\mathbf{b}(\mathbf{x}) = -\rho \ddot{\mathbf{w}}(\mathbf{x}) \approx -\rho \ddot{\tilde{\mathbf{w}}}(\mathbf{x}) = -\rho \mathbf{N}(\mathbf{x}) \ddot{\mathbf{w}}^e \quad (4.1.15)$$

Inserting the relations (4.1.14) and (4.1.15) into (4.1.13) and factoring out the nodal displacement vector \mathbf{w}^e and its derivative leads to:

$$\begin{aligned}
\delta \mathbf{w}^{eT} \mathbf{q}^e &= \int_{V^e} \left(\delta \tilde{\boldsymbol{\varepsilon}}(\mathbf{x})^T \boldsymbol{\sigma}(\mathbf{x}) + \delta \tilde{\mathbf{w}}(\mathbf{x})^T \rho \ddot{\mathbf{w}}(\mathbf{x}) \right) dV \\
&= \int_{V^e} \left(\delta \tilde{\boldsymbol{\varepsilon}}(\mathbf{x})^T \mathbf{D} \tilde{\boldsymbol{\varepsilon}}(\mathbf{x}) + \delta \tilde{\mathbf{w}}(\mathbf{x})^T \rho \ddot{\mathbf{w}}(\mathbf{x}) \right) dV \\
&= \int_{V^e} \left(\delta \mathbf{w}^{eT} \mathbf{B}(\mathbf{x})^T \mathbf{D} \mathbf{B}(\mathbf{x}) \mathbf{w}^e + \delta \mathbf{w}^{eT} \mathbf{N}(\mathbf{x})^T \rho \mathbf{N}(\mathbf{x}) \ddot{\mathbf{w}}^e \right) dV \\
&= \delta \mathbf{w}^{eT} \left(\int_{V^e} \mathbf{B}(\mathbf{x})^T \mathbf{D} \mathbf{B}(\mathbf{x}) dV \mathbf{w}^e + \int_{V^e} \mathbf{N}(\mathbf{x})^T \rho \mathbf{N}(\mathbf{x}) dV \ddot{\mathbf{w}}^e \right) \\
&= \delta \mathbf{w}^{eT} (\mathbf{K}^e \mathbf{w}^e + \mathbf{M}^e \ddot{\mathbf{w}}^e)
\end{aligned} \tag{4.1.16}$$

Here, \mathbf{K}^e and \mathbf{M}^e are the stiffness matrix and the mass matrix of the element, respectively:

$$\mathbf{K}^e = \int_{V^e} \mathbf{B}(\mathbf{x})^T \mathbf{D} \mathbf{B}(\mathbf{x}) dV, \quad \mathbf{M}^e = \int_{V^e} \mathbf{N}(\mathbf{x})^T \rho \mathbf{N}(\mathbf{x}) dV \tag{4.1.17}$$

The stiffness matrix and the mass matrix can also be split into submatrices, which refer to the single nodes. It is valid:

$$\tilde{\mathbf{w}}(\mathbf{x}) = \mathbf{N}(\mathbf{x}) \mathbf{w}^e = \sum_k \mathbf{N}_k(\mathbf{x}) \mathbf{w}_k^e \tag{4.1.18}$$

$$\Rightarrow \tilde{\boldsymbol{\varepsilon}}(\mathbf{x}) = \mathbf{S} \tilde{\mathbf{w}}(\mathbf{x}) = \mathbf{S} \left(\sum_k \mathbf{N}_k(\mathbf{x}) \mathbf{w}_k^e \right) = \sum_k \underbrace{\mathbf{S} \mathbf{N}_k(\mathbf{x})}_{\mathbf{B}_k(\mathbf{x})} \mathbf{w}_k^e = \sum_k \mathbf{B}_k(\mathbf{x}) \mathbf{w}_k^e \tag{4.1.19}$$

From these formulations, the expressions for the virtual displacement and for the virtual strain are derived; regarding the products contained in the integrand, it is necessary to use a different summation index:

$$\tilde{\mathbf{w}}(\mathbf{x}) = \sum_k \mathbf{N}_k(\mathbf{x}) \mathbf{w}_k^e \Rightarrow \delta \tilde{\mathbf{w}}(\mathbf{x}) = \sum_i \mathbf{N}_i(\mathbf{x}) \delta \mathbf{w}_i^e \tag{4.1.20}$$

$$\tilde{\boldsymbol{\varepsilon}}(\mathbf{x}) = \sum_k \mathbf{B}_k(\mathbf{x}) \mathbf{w}_k^e \Rightarrow \delta \tilde{\boldsymbol{\varepsilon}}(\mathbf{x}) = \sum_i \mathbf{B}_i(\mathbf{x}) \delta \mathbf{w}_i^e \tag{4.1.21}$$

By inserting these expressions into (4.1.16) it is obtained:

$$\begin{aligned}
&\int_{V^e} \left(\delta \tilde{\boldsymbol{\varepsilon}}(\mathbf{x})^T \mathbf{D} \tilde{\boldsymbol{\varepsilon}}(\mathbf{x}) + \delta \tilde{\mathbf{w}}(\mathbf{x})^T \rho \ddot{\mathbf{w}}(\mathbf{x}) \right) dV \\
&= \int_{V^e} \left(\left[\sum_i \mathbf{B}_i(\mathbf{x}) \delta \mathbf{w}_i^e \right]^T \mathbf{D} \left[\sum_k \mathbf{B}_k(\mathbf{x}) \mathbf{w}_k^e \right] + \left[\sum_i \mathbf{N}_i(\mathbf{x}) \delta \mathbf{w}_i^e \right]^T \rho \left[\sum_k \mathbf{N}_k(\mathbf{x}) \ddot{\mathbf{w}}_k^e \right] \right) dV \\
&= \sum_i \sum_k \int_{V^e} \left(\delta \mathbf{w}_i^{eT} \mathbf{B}_i(\mathbf{x})^T \mathbf{D} \mathbf{B}_k(\mathbf{x}) \mathbf{w}_k^e + \delta \mathbf{w}_i^{eT} \mathbf{N}_i(\mathbf{x})^T \rho \mathbf{N}_k(\mathbf{x}) \ddot{\mathbf{w}}_k^e \right) dV \\
&= \sum_i \sum_k \delta \mathbf{w}_i^{eT} \left(\int_{V^e} \mathbf{B}_i(\mathbf{x})^T \mathbf{D} \mathbf{B}_k(\mathbf{x}) dV \mathbf{w}_k^e + \int_{V^e} \mathbf{N}_i(\mathbf{x})^T \rho \mathbf{N}_k(\mathbf{x}) dV \ddot{\mathbf{w}}_k^e \right) \\
&= \sum_i \sum_k \delta \mathbf{w}_i^{eT} \left(\mathbf{K}_{i|k}^e \mathbf{w}_k^e + \mathbf{M}_{i|k}^e \ddot{\mathbf{w}}_k^e \right)
\end{aligned} \tag{4.1.22}$$

Here, the matrices $\mathbf{K}_{i|k}^e$ and $\mathbf{M}_{i|k}^e$ are defined in the following way:

$$\mathbf{K}_{i|k}^e = \int_{V^e} \mathbf{B}_i(\mathbf{x})^T \mathbf{D} \mathbf{B}_k(\mathbf{x}) dV, \quad \mathbf{M}_{i|k}^e = \int_{V^e} \mathbf{N}_i(\mathbf{x})^T \rho \mathbf{N}_k(\mathbf{x}) dV \quad (4.1.23)$$

The indices i and k refer to the nodes of the element so that the matrices $\mathbf{K}_{i|k}^e$ and $\mathbf{M}_{i|k}^e$ describe the interaction between the i -th and the k -th node of the element. By using a matrix notation, the result of (4.1.22) can be formulated in the following way:

$$\begin{aligned} & \int_{V^e} \left(\delta \tilde{\mathbf{e}}(\mathbf{x})^T \mathbf{D} \tilde{\mathbf{e}}(\mathbf{x}) + \delta \tilde{\mathbf{w}}(\mathbf{x})^T \rho \ddot{\tilde{\mathbf{w}}}(\mathbf{x}) \right) dV \\ &= \sum_i \sum_k \delta \mathbf{w}_i^e{}^T \left(\mathbf{K}_{i|k}^e \mathbf{w}_k^e + \mathbf{M}_{i|k}^e \ddot{\mathbf{w}}_k^e \right) \\ &= \begin{bmatrix} \delta \mathbf{w}_1^e{}^T \\ \vdots \\ \delta \mathbf{w}_i^e{}^T \\ \vdots \end{bmatrix}^T \left(\begin{bmatrix} \mathbf{K}_{1|1}^e & \cdots & \mathbf{K}_{1|k}^e & \cdots \\ \vdots & & \vdots & \\ \mathbf{K}_{i|1}^e & \cdots & \mathbf{K}_{i|k}^e & \cdots \\ \vdots & & \vdots & \end{bmatrix} \begin{bmatrix} \mathbf{w}_1^e \\ \vdots \\ \mathbf{w}_k^e \\ \vdots \end{bmatrix} + \begin{bmatrix} \mathbf{M}_{1|1}^e & \cdots & \mathbf{M}_{1|k}^e & \cdots \\ \vdots & & \vdots & \\ \mathbf{M}_{i|1}^e & \cdots & \mathbf{M}_{i|k}^e & \cdots \\ \vdots & & \vdots & \end{bmatrix} \begin{bmatrix} \ddot{\mathbf{w}}_1^e \\ \vdots \\ \ddot{\mathbf{w}}_k^e \\ \vdots \end{bmatrix} \right) \end{aligned} \quad (4.1.24)$$

The complete element stiffness matrix \mathbf{K}^e and the complete element mass matrix \mathbf{M}^e are composed of the submatrices $\mathbf{K}_{i|k}^e$ and $\mathbf{M}_{i|k}^e$.

4.2 Prismatic solid

In this section, the basis for a finite element for prismatic structure will be developed. The prismatic structure is characterized by its length ℓ and its cross-sectional area A_C . The structure is considered in the cartesian coordinates x , y and z . The coordinate x is pointing in the direction of the 1-axis, which is the axis of the extrusion. Therefore, the coordinates y and z are the cross-sectional coordinates. An overview is given in Fig.4.2.1.

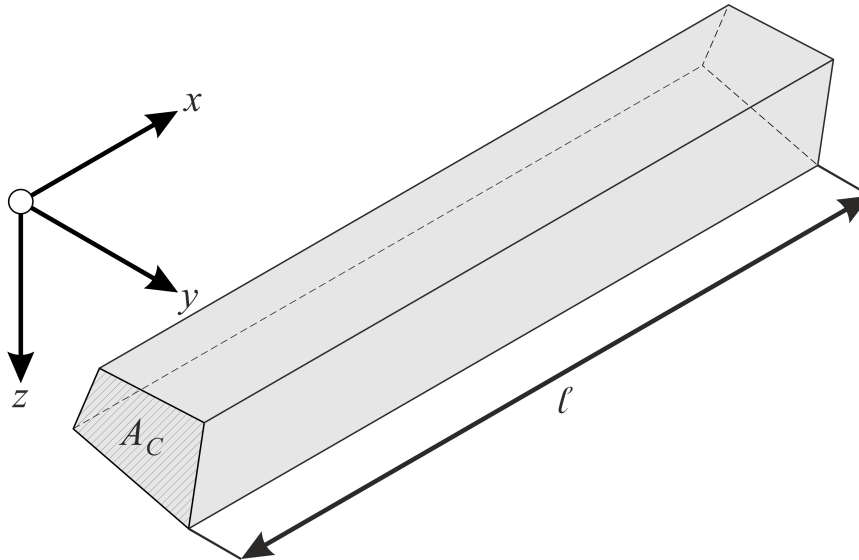


Figure 4.2.1: Finite prism element with quadrilateral cross section

As it can be seen from Fig.4.2.1, the element is a three-dimensional volume element. Therefore, the displacement \mathbf{w} is expressed by the following vector:

$$\mathbf{w} = \begin{bmatrix} U(x, y, z, t) \\ V(x, y, z, t) \\ W(x, y, z, t) \end{bmatrix} \quad (4.2.25)$$

Furthermore, it is assumed that the boundary conditions at both ends of the prismatic structure are equal; therefore, it is valid:

$$\mathbf{w}(x = 0, y, z, t) = \mathbf{w}(x = \ell, y, z, t) \quad (4.2.26)$$

It should be pointed out that in this section the shape of the cross section and the shape functions, which describe the distribution of the displacement, are not specified so that the derivation given in this section is valid for any arbitrary cross section and for any arbitrary shape functions.

Since the element is a three-dimensional volume element, the basis for the following consideration are Navier's equations, as introduced in (4.0.2), (4.0.4), (4.0.5) and (4.0.6).

$$\frac{\partial^2 U}{\partial x^2} + \frac{\partial^2 U}{\partial y^2} + \frac{\partial^2 U}{\partial z^2} + \frac{1}{1-2\nu} \frac{\partial}{\partial x} \left(\frac{\partial U}{\partial x} + \frac{\partial V}{\partial y} + \frac{\partial W}{\partial z} \right) - \frac{\rho}{G} \frac{\partial^2 U}{\partial t^2} = 0 \quad (4.2.27)$$

$$\frac{\partial^2 V}{\partial x^2} + \frac{\partial^2 V}{\partial y^2} + \frac{\partial^2 V}{\partial z^2} + \frac{1}{1-2\nu} \frac{\partial}{\partial y} \left(\frac{\partial U}{\partial x} + \frac{\partial V}{\partial y} + \frac{\partial W}{\partial z} \right) - \frac{\rho}{G} \frac{\partial^2 V}{\partial t^2} = 0 \quad (4.2.28)$$

$$\frac{\partial^2 W}{\partial x^2} + \frac{\partial^2 W}{\partial y^2} + \frac{\partial^2 W}{\partial z^2} + \frac{1}{1-2\nu} \frac{\partial}{\partial z} \left(\frac{\partial U}{\partial x} + \frac{\partial V}{\partial y} + \frac{\partial W}{\partial z} \right) - \frac{\rho}{G} \frac{\partial^2 W}{\partial t^2} = 0 \quad (4.2.29)$$

Here, G , ν and ρ denote the shear modulus, Poisson's ratio and the density of the material, respectively.

Similar to a notepad, a prismatic structure can be regarded as a stack of identical sheets, which are infinitesimally thin. The coordinates of each sheet are the cross-sectional coordinates y and z . If all sheets are identical, then the material parameters can depend on the cross-sectional coordinates, but are independent from the longitudinal coordinate x :

$$G = G(y, z), \quad \nu = \nu(y, z), \quad \rho = \rho(y, z) \quad (4.2.30)$$

Therefore, the following semi-analytical solution, which separates the longitudinal coordinate x from the cross-sectional coordinates y and z can be applied:

$$\mathbf{w} = \mathbf{w}_k(x, y, z, t) = \underbrace{\begin{bmatrix} U_k(y, z) \\ V_k(y, z) \\ W_k(y, z) \end{bmatrix}}_{\hat{\mathbf{w}}_k(y, z)} e^{ik\kappa x} e^{i\omega_k t} = \underbrace{\hat{\mathbf{w}}_k(y, z)}_{\mathbf{w}_k(x, y, z)} e^{ik\kappa x} e^{i\omega_k t}, \quad \kappa = \frac{2\pi}{\ell}, \quad k \in \mathbb{Z} \quad (4.2.31)$$

Inserting this semi-analytic solution into Navier's equations and factoring out the functions $e^{ik\kappa x}$

and $e^{i\omega_k t}$ leads to:

$$0 = \left[-k^2 \kappa^2 U_k + \frac{\partial^2 U_k}{\partial y^2} + \frac{\partial^2 U_k}{\partial z^2} + \frac{ik\kappa}{1-2\nu} \left(ik\kappa U_k + \frac{\partial V_k}{\partial y} + \frac{\partial W_k}{\partial z} \right) + \frac{\rho}{G} U_k \omega_k^2 \right] e^{ik\kappa x} e^{i\omega_k t} \quad (4.2.32)$$

$$0 = \left[-k^2 \kappa^2 V_k + \frac{\partial^2 V_k}{\partial y^2} + \frac{\partial^2 V_k}{\partial z^2} + \frac{1}{1-2\nu} \frac{\partial}{\partial y} \left(ik\kappa U_k + \frac{\partial V_k}{\partial y} + \frac{\partial W_k}{\partial z} \right) + \frac{\rho}{G} V_k \omega_k^2 \right] e^{ik\kappa x} e^{i\omega_k t} \quad (4.2.33)$$

$$0 = \left[-k^2 \kappa^2 W_k + \frac{\partial^2 W_k}{\partial y^2} + \frac{\partial^2 W_k}{\partial z^2} + \frac{1}{1-2\nu} \frac{\partial}{\partial z} \left(ik\kappa U_k + \frac{\partial V_k}{\partial y} + \frac{\partial W_k}{\partial z} \right) + \frac{\rho}{G} W_k \omega_k^2 \right] e^{ik\kappa x} e^{i\omega_k t} \quad (4.2.34)$$

According to (4.2.38) the functions $U_k = U_k(y, z)$, $V_k = V_k(y, z)$, and $W_k = W_k(y, z)$ depend only on the coordinates y and z of the cross section. Therefore, the original three-dimensional field problem is reduced to a two-dimensional one:

$$0 = -k^2 \kappa^2 U_k + \frac{\partial^2 U_k}{\partial y^2} + \frac{\partial^2 U_k}{\partial z^2} + \frac{ik\kappa}{1-2\nu} \left(ik\kappa U_k + \frac{\partial V_k}{\partial y} + \frac{\partial W_k}{\partial z} \right) + \frac{\rho}{G} U_k \omega_k^2 \quad (4.2.35)$$

$$0 = -k^2 \kappa^2 V_k + \frac{\partial^2 V_k}{\partial y^2} + \frac{\partial^2 V_k}{\partial z^2} + \frac{1}{1-2\nu} \frac{\partial}{\partial y} \left(ik\kappa U_k + \frac{\partial V_k}{\partial y} + \frac{\partial W_k}{\partial z} \right) + \frac{\rho}{G} V_k \omega_k^2 \quad (4.2.36)$$

$$0 = -k^2 \kappa^2 W_k + \frac{\partial^2 W_k}{\partial y^2} + \frac{\partial^2 W_k}{\partial z^2} + \frac{1}{1-2\nu} \frac{\partial}{\partial z} \left(ik\kappa U_k + \frac{\partial V_k}{\partial y} + \frac{\partial W_k}{\partial z} \right) + \frac{\rho}{G} W_k \omega_k^2 \quad (4.2.37)$$

It can be seen that the angular velocity ω_k appears only as the square ω_k^2 ; thereby, the sign of ω_k has no influence on the reduced equation. Thus, the following expression leads to the same reduced equations and is thereby a solution, too:

$$\mathbf{w} = \mathbf{w}_k(x, y, z, t) = \underbrace{\begin{bmatrix} U_k(y, z) \\ V_k(y, z) \\ W_k(y, z) \end{bmatrix}}_{\hat{\mathbf{w}}_k(y, z)} e^{ik\kappa x} e^{-i\omega_k t} \quad (4.2.38)$$

In an analogous way the following expression

$$\mathbf{w} = \mathbf{w}_{-k}(x, y, z, t) = \underbrace{\begin{bmatrix} U_{-k}(y, z) \\ V_{-k}(y, z) \\ W_{-k}(y, z) \end{bmatrix}}_{\hat{\mathbf{w}}_{-k}(y, z)} e^{-ik\kappa x} e^{i\omega_{-k} t} \quad (4.2.39)$$

leads to:

$$0 = -k^2 \kappa^2 U_{-k} + \frac{\partial^2 U_{-k}}{\partial y^2} + \frac{\partial^2 U_{-k}}{\partial z^2} + \frac{-ik\kappa}{1-2\nu} \left(-ik\kappa U_{-k} + \frac{\partial V_{-k}}{\partial y} + \frac{\partial W_{-k}}{\partial z} \right) + \frac{\rho}{G} U_{-k} \omega_{-k}^2 \quad (4.2.40)$$

$$0 = -k^2 \kappa^2 V_{-k} + \frac{\partial^2 V_{-k}}{\partial y^2} + \frac{\partial^2 V_{-k}}{\partial z^2} + \frac{1}{1-2\nu} \frac{\partial}{\partial y} \left(-ik\kappa U_{-k} + \frac{\partial V_{-k}}{\partial y} + \frac{\partial W_{-k}}{\partial z} \right) + \frac{\rho}{G} V_{-k} \omega_{-k}^2 \quad (4.2.41)$$

$$0 = -k^2 \kappa^2 W_{-k} + \frac{\partial^2 W_{-k}}{\partial y^2} + \frac{\partial^2 W_{-k}}{\partial z^2} + \frac{1}{1-2\nu} \frac{\partial}{\partial z} \left(-ik\kappa U_{-k} + \frac{\partial V_{-k}}{\partial y} + \frac{\partial W_{-k}}{\partial z} \right) + \frac{\rho}{G} W_{-k} \omega_{-k}^2 \quad (4.2.42)$$

The comparison shows that the equations (4.2.41) and (4.2.42) for $-k$ can easily be converted into the equations (6.2.11) and (6.2.12), respectively, by the following substitutions:

$$U_{-k} = -U_k, V_{-k} = V_k, W_{-k} = W_k, \omega_{-k} = \omega_k \quad (4.2.43)$$

By applying these substitutions to the equation (4.2.41) and by subsequently multiplying it by -1 , it is converted into the equation (6.2.10). Based on this semi-analytic solution, a finite element for the prismatic structure is now developed. It is assumed that the material parameters G , ν and ρ are constant within one element.

As already mentioned, the prismatic structure can be considered as a stack of identical sheets. A certain sheet is indicated by the longitudinal coordinate x . Using the basic idea of the finite element discretization, the distribution of the displacement \mathbf{w} over the cross section A_C , which is the area of the sheet, is expressed by shape functions $\mathbf{N}_i(y, z)$, which are scaled by the nodal displacements $\mathbf{w}_i^e(x, t)$ at the i -th node of n_N nodes of the element. Since the shape functions describe the distribution over the cross section, they only depend on the cross-sectional coordinates y and z .

$$\mathbf{w}(x, y, z, t) = \sum_{i=1}^{n_N} \mathbf{N}_i(y, z) \mathbf{w}_i^e(x, t) \quad (4.2.44)$$

For the shape functions $\mathbf{N}_i(y, z)$ and for the nodal displacements $\mathbf{w}_i^e(x, t)$ it is valid:

$$\mathbf{N}_i(y_j, z_j) = \begin{cases} \mathbf{I} & \text{for } j = i \\ \mathbf{0} & \text{for } j \neq i \end{cases}, \mathbf{w}_i^e(x, t) = \mathbf{w}_i(x, y_i, z_i, t) \quad (4.2.45)$$

According to (4.2.38), a semi-analytic solution of Navier's equation is given by:

$$\mathbf{w}_k(x, y, z, t) = \hat{\mathbf{w}}_k(y, z) e^{ik\kappa x} e^{i\omega_k t} \quad (4.2.46)$$

Since Navier's equation is a linear differential equation, also the linear combination of several solutions is a solution. Therefore, a general solution is given by:

$$\mathbf{w}(x, y, z, t) = \sum_K \sum_I \hat{\mathbf{w}}_{K,I}(y, z) e^{i\omega_{K,I} t} e^{iK \frac{2\pi}{\ell} x} \quad (4.2.47)$$

In each solution, the longitudinal coordinate x only appears as the argument of the function $e^{iK \frac{2\pi}{\ell} x}$. Based on this, the nodal displacement $\mathbf{w}_i^e(x, t)$ can be formulated as a Fourier series of the following form:

$$\mathbf{w}(x, y_i, z_i, t) = \mathbf{w}_i^e(x, t) = \sum_K \mathbf{w}_{i,K}^e(t) e^{iK \frac{2\pi}{\ell} x} \quad (4.2.48)$$

Finally, the distribution of the displacements within the finite element is formulated in the following way:

$$\mathbf{w}(x, y, z, t) = \sum_{i=1}^{n_N} \mathbf{N}_i(y, z) \mathbf{w}_i^e(x, t) = \sum_{i=1}^{n_N} \hat{\mathbf{N}}_i(y, z) \left[\sum_K \mathbf{w}_{i,K}^e(t) e^{iK \frac{2\pi}{\ell} x} \right] = \sum_K \sum_{i=1}^{n_N} \hat{\mathbf{N}}_i(y, z) \mathbf{w}_{i,K}^e(t) e^{iK \frac{2\pi}{\ell} x} \quad (4.2.49)$$

The vectors $\mathbf{w}_{i,K}^e(t)$ and the shape functions $\mathbf{N}_i(y, z)$ can be arranged in a vector and a matrix in the following way:

$$\begin{aligned} \mathbf{w}_K^e(t) &= \begin{bmatrix} \mathbf{w}_{1,K}^e(t) \\ \mathbf{w}_{2,K}^e(t) \\ \vdots \\ \mathbf{w}_{n_N,K}^e(t) \end{bmatrix}, \hat{\mathbf{N}}(y, z) = [\hat{\mathbf{N}}_1(y, z) \quad \hat{\mathbf{N}}_2(y, z) \quad \dots \quad \hat{\mathbf{N}}_{n_N}(y, z)] \\ &\Rightarrow \sum_{i=1}^{n_N} \hat{\mathbf{N}}_i(y, z) \mathbf{w}_{i,K}^e(t) = \hat{\mathbf{N}}(y, z) \mathbf{w}_K^e(t) \end{aligned} \quad (4.2.50)$$

Thereby, the displacement can be written as:

$$\mathbf{w}(x, y, z, t) = \sum_K \sum_{i=1}^{n_N} \hat{\mathbf{N}}_i(y, z) \mathbf{w}_{i,K}^e(t) e^{iK \frac{2\pi}{\ell} x} = \sum_K \hat{\mathbf{N}}(y, z) \mathbf{w}_K^e(t) e^{iK \frac{2\pi}{\ell} x} \quad (4.2.51)$$

Based on Zienkiewicz and Taylor² [84], for a three-dimensional continuum, the stress vector $\boldsymbol{\sigma}$, the elasticity matrix \mathbf{D} and the strain vector $\boldsymbol{\varepsilon}$ are given by:

$$\underbrace{\begin{bmatrix} \sigma_x \\ \sigma_y \\ \sigma_z \\ \tau_{xy} \\ \tau_{yz} \\ \tau_{zx} \end{bmatrix}}_{\boldsymbol{\sigma}} = \frac{G}{1-2\nu} \underbrace{\begin{bmatrix} 2(1-\nu) & 2\nu & 2\nu & 0 & 0 & 0 \\ 2\nu & 2(1-\nu) & 2\nu & 0 & 0 & 0 \\ 2\nu & 2\nu & 2(1-\nu) & 0 & 0 & 0 \\ 0 & 0 & 0 & 1-2\nu & 0 & 0 \\ 0 & 0 & 0 & 0 & 1-2\nu & 0 \\ 0 & 0 & 0 & 0 & 0 & 1-2\nu \end{bmatrix}}_{\mathbf{D}} \underbrace{\begin{bmatrix} \frac{\partial U}{\partial x} \\ \frac{\partial V}{\partial y} \\ \frac{\partial W}{\partial z} \\ \frac{\partial U}{\partial y} + \frac{\partial V}{\partial x} \\ \frac{\partial V}{\partial z} + \frac{\partial W}{\partial y} \\ \frac{\partial W}{\partial x} + \frac{\partial U}{\partial z} \end{bmatrix}}_{\boldsymbol{\varepsilon}} \quad (4.2.52)$$

The strain vector can be formulated in the following way:

$$\begin{aligned} \boldsymbol{\varepsilon} &= \begin{bmatrix} \frac{\partial U}{\partial x} \\ \frac{\partial V}{\partial y} \\ \frac{\partial W}{\partial z} \\ \frac{\partial U}{\partial y} + \frac{\partial V}{\partial x} \\ \frac{\partial V}{\partial z} + \frac{\partial W}{\partial y} \\ \frac{\partial W}{\partial x} + \frac{\partial U}{\partial z} \end{bmatrix} = \underbrace{\begin{bmatrix} 1 & 0 & 0 \\ 0 & 0 & 0 \\ 0 & 0 & 0 \\ 0 & 1 & 0 \\ 0 & 0 & 0 \\ 0 & 0 & 1 \end{bmatrix}}_{\mathbf{T}_x} \underbrace{\begin{bmatrix} \frac{\partial U}{\partial x} \\ \frac{\partial V}{\partial x} \\ \frac{\partial W}{\partial x} \end{bmatrix}}_{\frac{\partial \mathbf{w}}{\partial x}} + \underbrace{\begin{bmatrix} 0 & 0 & 0 \\ 0 & 1 & 0 \\ 0 & 0 & 0 \\ 1 & 0 & 0 \\ 0 & 0 & 1 \\ 0 & 0 & 0 \end{bmatrix}}_{\mathbf{T}_y} \underbrace{\begin{bmatrix} \frac{\partial U}{\partial y} \\ \frac{\partial V}{\partial y} \\ \frac{\partial W}{\partial y} \end{bmatrix}}_{\frac{\partial \mathbf{w}}{\partial y}} + \underbrace{\begin{bmatrix} 0 & 0 & 0 \\ 0 & 0 & 0 \\ 0 & 0 & 1 \\ 0 & 0 & 0 \\ 0 & 1 & 0 \\ 1 & 0 & 0 \end{bmatrix}}_{\mathbf{T}_z} \underbrace{\begin{bmatrix} \frac{\partial U}{\partial z} \\ \frac{\partial V}{\partial z} \\ \frac{\partial W}{\partial z} \end{bmatrix}}_{\frac{\partial \mathbf{w}}{\partial z}} \\ &= \mathbf{T}_x \frac{\partial \mathbf{w}}{\partial x} + \mathbf{T}_y \frac{\partial \mathbf{w}}{\partial y} + \mathbf{T}_z \frac{\partial \mathbf{w}}{\partial z} \end{aligned} \quad (4.2.53)$$

For the derivatives of the displacement $\mathbf{w}(x, y, z, t)$ it is valid:

$$\frac{\partial \mathbf{w}}{\partial x} = \begin{bmatrix} \frac{\partial U}{\partial x} \\ \frac{\partial V}{\partial x} \\ \frac{\partial W}{\partial x} \end{bmatrix} = \frac{\partial}{\partial x} \left(\sum_K \hat{\mathbf{N}}(y, z) \mathbf{w}_K^e(t) e^{iK \frac{2\pi}{\ell} x} \right) = \sum_K \hat{\mathbf{N}}(y, z) \mathbf{w}_K^e(t) iK \frac{2\pi}{\ell} e^{iK \frac{2\pi}{\ell} x} \quad (4.2.54)$$

$$\frac{\partial \mathbf{w}}{\partial y} = \begin{bmatrix} \frac{\partial U}{\partial y} \\ \frac{\partial V}{\partial y} \\ \frac{\partial W}{\partial y} \end{bmatrix} = \frac{\partial}{\partial y} \left(\sum_K \hat{\mathbf{N}}(y, z) \mathbf{w}_K^e(t) e^{iK \frac{2\pi}{\ell} x} \right) = \sum_K \frac{\partial}{\partial y} \hat{\mathbf{N}}(y, z) \mathbf{w}_K^e(t) e^{iK \frac{2\pi}{\ell} x} \quad (4.2.55)$$

$$\frac{\partial \mathbf{w}}{\partial z} = \begin{bmatrix} \frac{\partial U}{\partial z} \\ \frac{\partial V}{\partial z} \\ \frac{\partial W}{\partial z} \end{bmatrix} = \frac{\partial}{\partial z} \left(\sum_K \hat{\mathbf{N}}(y, z) \mathbf{w}_K^e(t) e^{iK \frac{2\pi}{\ell} x} \right) = \sum_K \frac{\partial}{\partial z} \hat{\mathbf{N}}(y, z) \mathbf{w}_K^e(t) e^{iK \frac{2\pi}{\ell} x} \quad (4.2.56)$$

Inserting these expressions into (4.2.57) and factoring out the function $e^{iK \frac{2\pi}{\ell} x}$ and the vectors $\mathbf{w}_K^e(t)$

²In [84], Young's modulus E is used to formulate the matrix \mathbf{D} . By applying the relation $E = 2G(1 + \nu)$, where G is the shear modulus, enables a more compact notation.

of the nodal displacements leads to the following formulation of the strain vector:

$$\begin{aligned}
\varepsilon(\mathbf{x}) &= \mathbf{T}_x \left[\sum_K \hat{\mathbf{N}}(y,z) \mathbf{w}_K^e(t) iK \frac{2\pi}{\ell} e^{iK \frac{2\pi}{\ell} x} \right] + \mathbf{T}_y \left[\sum_K \frac{\partial}{\partial y} \hat{\mathbf{N}}(y,z) \mathbf{w}_K^e(t) e^{iK \frac{2\pi}{\ell} x} \right] \\
&\quad + \mathbf{T}_z \left[\sum_K \frac{\partial}{\partial z} \hat{\mathbf{N}}(y,z) \mathbf{w}_K^e(t) e^{iK \frac{2\pi}{\ell} x} \right] \\
&= \sum_K \underbrace{\left[\mathbf{T}_x \hat{\mathbf{N}}(y,z) iK \frac{2\pi}{\ell} + \mathbf{T}_y \frac{\partial}{\partial y} \hat{\mathbf{N}}(y,z) + \mathbf{T}_z \frac{\partial}{\partial z} \hat{\mathbf{N}}(y,z) \right]}_{\hat{\mathbf{B}}_K(y,z)} \mathbf{w}_K^e(t) e^{iK \frac{2\pi}{\ell} x} \\
&= \sum_K \hat{\mathbf{B}}_K(y,z) \mathbf{w}_K^e(t) e^{iK \frac{2\pi}{\ell} x} \tag{4.2.57}
\end{aligned}$$

It can be seen that the matrix $\hat{\mathbf{B}}_K(y,z)$ contains the periodicity K as a factor; this results from the derivatives with respect to x . Therefore, the matrices $\hat{\mathbf{B}}_K(y,z)$ have to be denoted using the index K in contrast to the matrices $\hat{\mathbf{N}}(y,z)$, which are equal for all periodicities K so that a distinction with respect to K is not necessary. – Resolving the matrix $\hat{\mathbf{N}}$ and the vector \mathbf{w}_K^e into the shape functions and displacements for the single nodes leads to the following formulation of the strain vector:

$$\begin{aligned}
\hat{\mathbf{N}}(y,z) \mathbf{w}_K^e(t) &= \sum_{i=1}^{n_N} \hat{\mathbf{N}}_i(y,z) \mathbf{w}_{i,K}^e(t) \\
\Rightarrow \frac{\partial}{\partial y} \hat{\mathbf{N}}(y,z) \mathbf{w}_K^e(t) &= \sum_{i=1}^{n_N} \frac{\partial}{\partial y} \hat{\mathbf{N}}_i(y,z) \mathbf{w}_{i,K}^e(t), \quad \frac{\partial}{\partial z} \hat{\mathbf{N}}(y,z) \mathbf{w}_K^e(t) = \sum_{i=1}^{n_N} \frac{\partial}{\partial z} \hat{\mathbf{N}}_i(y,z) \mathbf{w}_{i,K}^e(t) \tag{4.2.58} \\
\varepsilon(\mathbf{x}) &= \mathbf{T}_x \left[\sum_K \left(\sum_{i=1}^{n_N} \hat{\mathbf{N}}_i(y,z) \mathbf{w}_{i,K}^e(t) \right) iK \frac{2\pi}{\ell} e^{iK \frac{2\pi}{\ell} x} \right] + \mathbf{T}_y \left[\sum_K \left(\sum_{i=1}^{n_N} \frac{\partial}{\partial y} \hat{\mathbf{N}}_i(y,z) \mathbf{w}_{i,K}^e(t) \right) e^{iK \frac{2\pi}{\ell} x} \right] \\
&\quad + \mathbf{T}_z \left[\sum_K \left(\sum_{i=1}^{n_N} \frac{\partial}{\partial z} \hat{\mathbf{N}}_i(y,z) \mathbf{w}_{i,K}^e(t) \right) e^{iK \frac{2\pi}{\ell} x} \right] \\
&= \sum_K \sum_{i=1}^{n_N} \underbrace{\left[\mathbf{T}_x \hat{\mathbf{N}}_i(y,z) iK \frac{2\pi}{\ell} + \mathbf{T}_y \frac{\partial}{\partial y} \hat{\mathbf{N}}_i(y,z) + \mathbf{T}_z \frac{\partial}{\partial z} \hat{\mathbf{N}}_i(y,z) \right]}_{\mathbf{B}_{i,K}(y,z)} \mathbf{w}_{i,K}^e(t) e^{iK \frac{2\pi}{\ell} x} \\
&= \sum_K \sum_{i=1}^{n_N} \hat{\mathbf{B}}_{i,K}(y,z) \mathbf{w}_{i,K}^e(t) e^{iK \frac{2\pi}{\ell} x} \tag{4.2.59}
\end{aligned}$$

Comparing the expressions (4.2.57) and (4.2.59) leads to:

$$\hat{\mathbf{B}}_K(y,z) \mathbf{w}_K^e(t) = \sum_{i=1}^{n_N} \hat{\mathbf{B}}_{i,K}(y,z) \mathbf{w}_{i,K}^e(t) \tag{4.2.60}$$

The resolved formulation according to (4.2.59) will be used later.

The displacement $\mathbf{w}(x,y,z)$ and the strain $\varepsilon(x,y,z)$ have been formulated in the following way:

$$\mathbf{w}(x,y,z,t) = \sum_K \hat{\mathbf{N}}(y,z) e^{iK \frac{2\pi}{\ell} x} \mathbf{w}_K^e \tag{4.2.61}$$

$$\varepsilon(x,y,z,t) = \sum_K \hat{\mathbf{B}}_K(y,z) e^{iK \frac{2\pi}{\ell} x} \mathbf{w}_K^e \tag{4.2.62}$$

Here and in the following, the dependence of the discretized displacements \mathbf{w}_K^e on the time t will not be indicated explicitly for the sake of brevity. From these formulations, the expressions for the variation of the displacement and of the strain are derived. By replacing the periodicity K by $L \in \mathbb{Z}$, which is necessary for the following formulation, it is valid:

$$\delta \mathbf{w}(x, y, z) = \sum_L \hat{\mathbf{N}}(y, z) e^{iL \frac{2\pi}{\ell} x} \delta \mathbf{w}_L^e \Rightarrow \delta \mathbf{w}(x, y, z)^T = \sum_L \delta \mathbf{w}_L^e{}^T \hat{\mathbf{N}}(y, z)^T e^{iL \frac{2\pi}{\ell} x} \quad (4.2.63)$$

$$\delta \boldsymbol{\varepsilon}(x, y, z) = \sum_L \hat{\mathbf{B}}_L(y, z) e^{iL \frac{2\pi}{\ell} x} \delta \mathbf{w}_L^e \Rightarrow \delta \boldsymbol{\varepsilon}(x, y, z)^T = \sum_L \delta \mathbf{w}_L^e{}^T \hat{\mathbf{B}}_L(y, z)^T e^{iL \frac{2\pi}{\ell} x} \quad (4.2.64)$$

Inserting these expressions into the right-hand side of (4.1.13) leads to:

$$\begin{aligned} & \int_{V^e} \left(\delta \tilde{\boldsymbol{\varepsilon}}(\mathbf{x})^T \mathbf{D} \tilde{\boldsymbol{\varepsilon}}(\mathbf{x}) + \delta \tilde{\mathbf{w}}(\mathbf{x})^T \rho \ddot{\tilde{\mathbf{w}}}(\mathbf{x}) \right) dV \\ &= \int_{V^e} \left[\sum_L \delta \mathbf{w}_L^e{}^T \hat{\mathbf{B}}_L(y, z)^T e^{iL \frac{2\pi}{\ell} x} \right] \mathbf{D} \left[\sum_K \hat{\mathbf{B}}_K(y, z) e^{iK \frac{2\pi}{\ell} x} \mathbf{w}_K^e \right] dV \\ & \quad + \int_{V^e} \left[\sum_L \delta \mathbf{w}_L^e{}^T \hat{\mathbf{N}}(y, z)^T e^{iL \frac{2\pi}{\ell} x} \right] \rho \left[\sum_K \hat{\mathbf{N}}(y, z) e^{iK \frac{2\pi}{\ell} x} \ddot{\mathbf{w}}_K^e \right] dV \\ &= \sum_L \sum_K \delta \mathbf{w}_L^e{}^T \left[\int_{V^e} \hat{\mathbf{B}}_L(y, z)^T \mathbf{D} \hat{\mathbf{B}}_K(y, z) e^{i(L+K) \frac{2\pi}{\ell} x} dV \mathbf{w}_K^e \right. \\ & \quad \left. + \int_{V^e} \hat{\mathbf{N}}(y, z)^T \rho \hat{\mathbf{N}}(y, z) e^{i(L+K) \frac{2\pi}{\ell} x} dV \ddot{\mathbf{w}}_K^e \right] \quad (4.2.65) \end{aligned}$$

The infinitesimal volume dV can be expressed based on the triple scalar product, which is also known as the mixed product. The triple scalar product of the three vectors \vec{a} , \vec{b} and \vec{c} can be formulated several different ways; its result is the volume V_P of the parallelepiped, for which the three vectors define the edges. It is valid:

$$V_P = \vec{a} \cdot (\vec{b} \times \vec{c}) = \begin{bmatrix} a_1 \\ a_2 \\ a_3 \end{bmatrix} \cdot \left(\begin{bmatrix} b_1 \\ b_2 \\ b_3 \end{bmatrix} \times \begin{bmatrix} c_1 \\ c_2 \\ c_3 \end{bmatrix} \right) = \det \begin{bmatrix} a_1 & b_1 & c_1 \\ a_2 & b_2 & c_2 \\ a_3 & b_3 & c_3 \end{bmatrix} \quad (4.2.66)$$

In the present case the vectors defining the edges of the infinitesimal volume are obtained from the partial derivatives of the reference position vector \mathbf{x} with respect to the coordinates. Thus, it can be formulated for the infinitesimal volume dV :

$$\mathbf{x} = [x \quad y \quad z]^T \quad (4.2.67)$$

$$dV = \frac{\partial \mathbf{x}}{\partial x} dx \cdot \left(\frac{\partial \mathbf{x}}{\partial y} dy \times \frac{\partial \mathbf{x}}{\partial z} dz \right) = \begin{bmatrix} 1 \\ 0 \\ 0 \end{bmatrix} \cdot \left(\begin{bmatrix} 0 \\ 1 \\ 0 \end{bmatrix} \times \begin{bmatrix} 0 \\ 0 \\ 1 \end{bmatrix} \right) dx dy dz = \underbrace{\begin{bmatrix} 1 \\ 0 \\ 0 \end{bmatrix} \cdot \begin{bmatrix} 1 \\ 0 \\ 0 \end{bmatrix}}_1 dx dy dz \quad (4.2.68)$$

The essential characteristic of a prismatic structure is that the shape of the cross section is independent from the coordinate pointing in the direction of the extrusion. For the integration over the volume V^e of the prismatic element, the integrations have to be carried out over the length ℓ and over the cross-sectional area A_C . It can be seen that the integrands consist of factor, which contain

either the longitudinal coordinate x or the cross sectional coordinates y and z , so that the two integrations are completely separated from each other. Thereby, the integrals can be reformulated in the following way:

$$\begin{aligned} \int_{V^e} \hat{\mathbf{B}}_L(y, z)^T \mathbf{D} \hat{\mathbf{B}}_K(y, z) e^{i(L+K)\frac{2\pi}{\ell}x} dV &= \int_{A_C} \int_0^\ell \hat{\mathbf{B}}_L(y, z)^T \mathbf{D} \hat{\mathbf{B}}_K(y, z) e^{i(L+K)\frac{2\pi}{\ell}x} dx dy dz \\ &= \int_{A_C} \hat{\mathbf{B}}_L(y, z)^T \mathbf{D} \hat{\mathbf{B}}_K(y, z) dy dz \int_0^\ell e^{i(L+K)\frac{2\pi}{\ell}x} dx \quad (4.2.69) \end{aligned}$$

$$\begin{aligned} \int_{V^e} \hat{\mathbf{N}}(y, z)^T \rho \hat{\mathbf{N}}(y, z) e^{i(L+K)\frac{2\pi}{\ell}x} dV &= \int_{A_C} \int_0^\ell \hat{\mathbf{N}}(y, z)^T \rho \hat{\mathbf{N}}(y, z) e^{i(L+K)\frac{2\pi}{\ell}x} dx dy dz \\ &= \int_{A_C} \hat{\mathbf{N}}(y, z)^T \rho \hat{\mathbf{N}}(y, z) dy dz \int_0^\ell e^{i(L+K)\frac{2\pi}{\ell}x} dx \quad (4.2.70) \end{aligned}$$

In order to evaluate the integral over the longitudinal coordinate x , the two cases $L+K=0$ and $L+K \neq 0$ have to be distinguished. It is valid:

$$L+K=0 : \int_0^\ell e^{i(L+K)\frac{2\pi}{\ell}x} dx = \int_0^\ell e^0 dx = \int_0^\ell dx = \ell \quad (4.2.71)$$

$$\begin{aligned} L+K \neq 0 : \int_0^\ell e^{i(L+K)\frac{2\pi}{\ell}x} dx &= \frac{1}{L+K} \frac{\ell}{2\pi} e^{i(L+K)\frac{2\pi}{\ell}x} \Big|_0^\ell = \frac{1}{L+K} \frac{\ell}{2\pi} \left[e^{2\pi i(L+K)} - e^0 \right] \\ &= \frac{1}{L+K} \frac{\ell}{2\pi} \left[1^{(L+K)} - 1 \right] = 0 \quad (4.2.72) \end{aligned}$$

Thereby, only the integrals for $L+K=0 \Leftrightarrow K=-L$ remain, while all other integrals vanish. This leads to:

$$\begin{aligned} &\int_{V^e} \left(\delta \tilde{\mathbf{e}}(\mathbf{x})^T \mathbf{D} \tilde{\mathbf{e}}(\mathbf{x}) + \delta \tilde{\mathbf{w}}(\mathbf{x})^T \rho \tilde{\mathbf{w}}(\mathbf{x}) \right) dV \\ &= \sum_L \sum_K \delta \mathbf{w}_L^e{}^T \left[\int_{V^e} \hat{\mathbf{B}}_L(y, z)^T \mathbf{D} \hat{\mathbf{B}}_K(y, z) e^{i(L+K)\frac{2\pi}{\ell}x} dV \mathbf{w}_K^e \right. \\ &\quad \left. + \int_{V^e} \hat{\mathbf{N}}(y, z)^T \rho \hat{\mathbf{N}}(y, z) e^{i(L+K)\frac{2\pi}{\ell}x} dV \tilde{\mathbf{w}}_K^e \right] \\ &= \sum_L \delta \mathbf{w}_L^e{}^T \left[\int_{A_C} \hat{\mathbf{B}}_L(y, z)^T \mathbf{D} \hat{\mathbf{B}}_{-L}(y, z) dy dz \ell \mathbf{w}_{-L}^e + \int_{A_C} \hat{\mathbf{N}}(y, z)^T \rho \hat{\mathbf{N}}(y, z) dy dz \ell \tilde{\mathbf{w}}_{-L}^e \right] \quad (4.2.73) \end{aligned}$$

It can be seen that beneath the virtual displacement $\delta \mathbf{w}_L$ each summand only contains the displacement \mathbf{w}_{-L} and its second derivative $\tilde{\mathbf{w}}_{-L}$; this means that with respect to the elasticity and to the inertia the motions for different periodicities L are decoupled from each other. – The substitution $L=-K$ for the periodicity gives:

$$\begin{aligned} &\delta \mathbf{w}^e{}^T \left(\int_{V^e} \mathbf{B}(\mathbf{x})^T \mathbf{D} \mathbf{B}(\mathbf{x}) dV \mathbf{w}^e + \int_{V^e} \mathbf{N}(\mathbf{x})^T \rho \mathbf{N}(\mathbf{x}) dV \tilde{\mathbf{w}}^e \right) \\ &= \sum_L \delta \mathbf{w}_L^e{}^T \left[\int_{A_C} \hat{\mathbf{B}}_L(y, z)^T \mathbf{D} \hat{\mathbf{B}}_{-L}(y, z) dy dz \ell \mathbf{w}_{-L}^e + \int_{A_C} \hat{\mathbf{N}}(y, z)^T \rho \hat{\mathbf{N}}(y, z) dy dz \ell \tilde{\mathbf{w}}_{-L}^e \right] \\ &= \sum_K \delta \mathbf{w}_{-K}^e{}^T \left[\int_{A_C} \hat{\mathbf{B}}_{-K}(y, z)^T \mathbf{D} \hat{\mathbf{B}}_K(y, z) dy dz \ell \mathbf{w}_K^e + \int_{A_C} \hat{\mathbf{N}}(y, z)^T \rho \hat{\mathbf{N}}(y, z) dy dz \ell \tilde{\mathbf{w}}_K^e \right] \\ &= \sum_K \delta \mathbf{w}_{-K}^e{}^T \left[\mathbf{K}_K^e \ell \mathbf{w}_K^e + \mathbf{M}^e \ell \tilde{\mathbf{w}}_K^e \right] \quad (4.2.74) \end{aligned}$$

Here, the matrices \mathbf{K}_K^e and \mathbf{M}^e are the element stiffness matrices and the element mass matrices, respectively. It can be seen that the mass matrix \mathbf{M}^e of the element is independent from the periodicity K ; therefore, the index K is not required for the mass matrix:

$$\mathbf{M}^e = \int_{A_C} \hat{\mathbf{N}}(y,z)^T \rho \hat{\mathbf{N}}(y,z) dy dz \quad (4.2.75)$$

By using the formulation of the strain matrix according to (4.2.57), the integrand of the stiffness matrix can be resolved in the following way:

$$\begin{aligned} \mathbf{K}_K^e &= \int_{A_C} \hat{\mathbf{B}}_{-K}(y,z)^T \mathbf{D} \hat{\mathbf{B}}_K(y,z) dy dz \\ &= \int_{A_C} \left[-\mathbf{T}_x \hat{\mathbf{N}} iK \frac{2\pi}{\ell} + \mathbf{T}_y \frac{\partial \hat{\mathbf{N}}}{\partial y} + \mathbf{T}_z \frac{\partial \hat{\mathbf{N}}}{\partial z} \right]^T \mathbf{D} \left[\mathbf{T}_x \hat{\mathbf{N}} iK \frac{2\pi}{\ell} + \mathbf{T}_y \frac{\partial \hat{\mathbf{N}}}{\partial y} + \mathbf{T}_z \frac{\partial \hat{\mathbf{N}}}{\partial z} \right] dy dz \\ &= \underbrace{-i^2}_{1} K^2 \left(\frac{2\pi}{\ell} \right)^2 \int_{A_C} \hat{\mathbf{N}}^T \mathbf{T}_x^T \mathbf{D} \mathbf{T}_x \hat{\mathbf{N}} dy dz \\ &\quad + iK \frac{2\pi}{\ell} \int_{A_C} \left[-\hat{\mathbf{N}}^T \mathbf{T}_x^T \mathbf{D} \left(\mathbf{T}_y \frac{\partial \hat{\mathbf{N}}}{\partial y} + \mathbf{T}_z \frac{\partial \hat{\mathbf{N}}}{\partial z} \right) + \left(\frac{\partial \hat{\mathbf{N}}^T}{\partial y} \mathbf{T}_y^T + \frac{\partial \hat{\mathbf{N}}^T}{\partial z} \mathbf{T}_z^T \right) \mathbf{D} \mathbf{T}_x \hat{\mathbf{N}} \right] dy dz \\ &\quad + \int_{A_C} \left(\frac{\partial \hat{\mathbf{N}}^T}{\partial y} \mathbf{T}_y^T + \frac{\partial \hat{\mathbf{N}}^T}{\partial z} \mathbf{T}_z^T \right) \mathbf{D} \left(\mathbf{T}_y \frac{\partial \hat{\mathbf{N}}}{\partial y} + \mathbf{T}_z \frac{\partial \hat{\mathbf{N}}}{\partial z} \right) dy dz \end{aligned} \quad (4.2.76)$$

The result shows that the complete element stiffness matrix is composed from three types of integrals: the first type contains a product of the shape functions $\hat{\mathbf{N}}$, the second one contains a product of the shape functions and one of their derivatives and the third one contains the product of two derivatives.

In section 4.1, a formulation of the element matrices using submatrices, which refer to single nodes, has been developed. This formulation shall also be applied to the equations describing the prism element. According to (4.2.50) and (4.2.59) it is valid:

$$\hat{\mathbf{N}}(y,z) \mathbf{w}_K^e(t) = \sum_{i=1}^{n_N} \hat{\mathbf{N}}_i(y,z) \mathbf{w}_{i,K}^e(t) \quad (4.2.77)$$

$$\hat{\mathbf{B}}_K(y,z) \mathbf{w}_K^e(t) = \sum_{i=1}^{n_N} \underbrace{\left[\mathbf{T}_x \hat{\mathbf{N}}_i(y,z) iK \frac{2\pi}{\ell} + \mathbf{T}_y \frac{\partial \hat{\mathbf{N}}_i(y,z)}{\partial y} + \mathbf{T}_z \frac{\partial \hat{\mathbf{N}}_i(y,z)}{\partial z} \right]}_{\mathbf{B}_{i,K}(y,z)} \mathbf{w}_{i,K}^e(t) \quad (4.2.78)$$

Using these expressions, the terms for the stiffness matrix \mathbf{K}_K^e and for the mass matrix \mathbf{M}^e accord-

ing to (4.2.74) are reformulated. It is valid:

$$\begin{aligned}
\delta \mathbf{w}_{-K}^e \mathbf{T} \mathbf{K}_K^e \mathbf{w}_K^e &= \delta \mathbf{w}_{-K}^e \mathbf{T} \int_{A_C} \hat{\mathbf{B}}_{-K}(y, z) \mathbf{T} \mathbf{D} \hat{\mathbf{B}}_K(y, z) dy dz \mathbf{w}_K^e \\
&= \int_{A_C} \delta \mathbf{w}_{-K}^e \mathbf{T} \hat{\mathbf{B}}_{-K}(y, z) \mathbf{T} \mathbf{D} \hat{\mathbf{B}}_K(y, z) \mathbf{w}_K^e dy dz \\
&= \int_{A_C} \left[\sum_{i=1}^{n_N} \delta \mathbf{w}_{i,K}^e \mathbf{T} \hat{\mathbf{B}}_{i,-K}(y, z) \mathbf{T} \right] \mathbf{D} \left[\sum_{k=1}^{n_N} \hat{\mathbf{B}}_{k,K}(y, z) \mathbf{w}_{k,K}^e \right] dy dz \\
&= \sum_{i=1}^{n_N} \sum_{k=1}^{n_N} \delta \mathbf{w}_{i,K}^e \mathbf{T} \int_{A_C} \hat{\mathbf{B}}_{i,-K}(y, z) \mathbf{T} \mathbf{D} \hat{\mathbf{B}}_{k,K}(y, z) dy dz \mathbf{w}_{k,K}^e \\
&= \sum_{i=1}^{n_N} \sum_{k=1}^{n_N} \delta \mathbf{w}_{i,K}^e \mathbf{T} \mathbf{K}_{i|k,K}^e \mathbf{w}_{k,K}^e
\end{aligned} \tag{4.2.79}$$

$$\begin{aligned}
\delta \mathbf{w}_{-K}^e \mathbf{T} \mathbf{M}^e \ddot{\mathbf{w}}_K^e &= \delta \mathbf{w}_{-K}^e \mathbf{T} \int_{A_C} \hat{\mathbf{N}}_{-K}(y, z) \mathbf{T} \rho \hat{\mathbf{N}}_K(y, z) dy dz \ddot{\mathbf{w}}_K^e \\
&= \int_{A_C} \delta \mathbf{w}_{-K}^e \mathbf{T} \hat{\mathbf{N}}(y, z) \mathbf{T} \rho \hat{\mathbf{N}}(y, z) \ddot{\mathbf{w}}_K^e dy dz \\
&= \int_{A_C} \left[\sum_{i=1}^{n_N} \delta \mathbf{w}_{i,K}^e \mathbf{T} \hat{\mathbf{N}}_i(y, z) \mathbf{T} \right] \rho \left[\sum_{k=1}^{n_N} \hat{\mathbf{N}}_k(y, z) \ddot{\mathbf{w}}_{k,K}^e \right] dy dz \\
&= \sum_{i=1}^{n_N} \sum_{k=1}^{n_N} \delta \mathbf{w}_{i,K}^e \mathbf{T} \int_{A_C} \hat{\mathbf{N}}_i(y, z) \mathbf{T} \rho \hat{\mathbf{N}}_k(y, z) dy dz \ddot{\mathbf{w}}_{k,K}^e \\
&= \sum_{i=1}^{n_N} \sum_{k=1}^{n_N} \delta \mathbf{w}_{i,K}^e \mathbf{T} \mathbf{M}_{i|k}^e \ddot{\mathbf{w}}_{k,K}^e
\end{aligned} \tag{4.2.80}$$

By applying the definition for the strain matrix $\hat{\mathbf{B}}_{i,K}(y, z)$ according to (4.2.78), the stiffness matrix $\mathbf{K}_{i|k,K}^e$ is resolved in the following way:

$$\begin{aligned}
\mathbf{K}_{i|k,K}^e &= \int_{A_C} \hat{\mathbf{B}}_{i,-K}(y, z) \mathbf{T} \mathbf{D} \hat{\mathbf{B}}_{k,K}(y, z) dy dz \\
&= \int_{A_C} \left[-\mathbf{T}_x \hat{\mathbf{N}}_i iK \frac{2\pi}{\ell} + \mathbf{T}_y \frac{\partial \hat{\mathbf{N}}_i}{\partial y} + \mathbf{T}_z \frac{\partial \hat{\mathbf{N}}_i}{\partial z} \right] \mathbf{T} \mathbf{D} \left[\mathbf{T}_x \hat{\mathbf{N}}_k iK \frac{2\pi}{\ell} + \mathbf{T}_y \frac{\partial \hat{\mathbf{N}}_k}{\partial y} + \mathbf{T}_z \frac{\partial \hat{\mathbf{N}}_k}{\partial z} \right] dy dz \\
&= K^2 \left(\frac{2\pi}{\ell} \right)^2 \int_{A_C} \hat{\mathbf{N}}_i \mathbf{T}_x \mathbf{T} \mathbf{D} \mathbf{T}_x \hat{\mathbf{N}}_k dy dz - iK \frac{2\pi}{\ell} \int_{A_C} \hat{\mathbf{N}}_i \mathbf{T}_x \mathbf{T} \mathbf{D} \left(\mathbf{T}_y \frac{\partial \hat{\mathbf{N}}_k}{\partial y} + \mathbf{T}_z \frac{\partial \hat{\mathbf{N}}_k}{\partial z} \right) dy dz \\
&\quad + iK \frac{2\pi}{\ell} \int_{A_C} \left(\frac{\partial \hat{\mathbf{N}}_i}{\partial y} \mathbf{T}_y \mathbf{T} + \frac{\partial \hat{\mathbf{N}}_i}{\partial z} \mathbf{T}_z \mathbf{T} \right) \mathbf{D} \mathbf{T}_x \hat{\mathbf{N}}_k dy dz \\
&\quad + \int_{A_C} \left(\frac{\partial \hat{\mathbf{N}}_i}{\partial y} \mathbf{T}_y \mathbf{T} + \frac{\partial \hat{\mathbf{N}}_i}{\partial z} \mathbf{T}_z \mathbf{T} \right) \mathbf{D} \left(\mathbf{T}_y \frac{\partial \hat{\mathbf{N}}_k}{\partial y} + \mathbf{T}_z \frac{\partial \hat{\mathbf{N}}_k}{\partial z} \right) dy dz
\end{aligned} \tag{4.2.81}$$

4.3 Solid of revolution

As it can be seen from Fig. 4.3.2, the solid of revolution or annular element is generated by the rotation of the area A_C around the 2-axis. The area A_C is the cross-sectional area; it lies in the 2-3-plane. The 2-axis is chosen as the axis of the axisymmetry, because the finite element, which

will be developed, is intended to be used for the modelling of the wheelset; in the MBS description of railway vehicles, the 2-axis is usually the lateral axis.

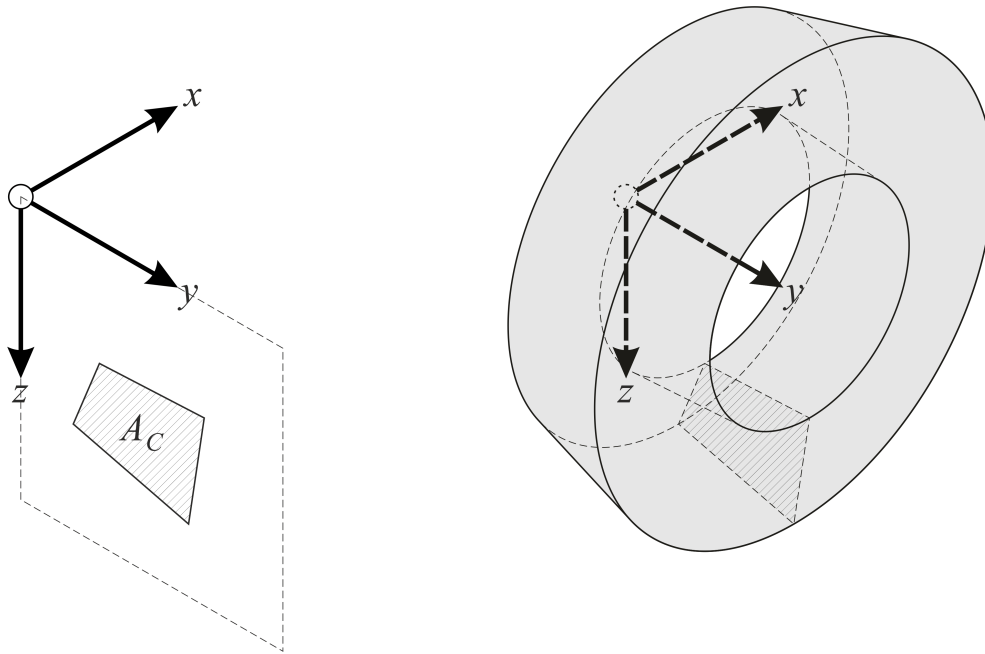


Figure 4.3.2: Finite annular element with quadrilateral cross section A_C

For a solid of revolution, it is advantageous to use cylindrical coordinates. Here, the coordinate y pointing in the direction of the 2-axis is used as the axial coordinate, while the cartesian coordinates x and z are replaced by the polar coordinates r and ϕ . Thereby, the reference position \mathbf{x} is given in the following way:

$$\underbrace{\begin{bmatrix} x \\ y \\ z \end{bmatrix}}_{\mathbf{x}} = \underbrace{\begin{bmatrix} \cos \phi & 0 & \sin \phi \\ 0 & 1 & 0 \\ \sin \phi & 0 & \cos \phi \end{bmatrix}}_{\mathbf{S}_2(\phi)} \underbrace{\begin{bmatrix} 0 \\ y \\ r \end{bmatrix}}_{\mathbf{c}} = \begin{bmatrix} r \sin \phi \\ y \\ r \cos \phi \end{bmatrix} \Rightarrow x = r \sin \phi, z = r \cos \phi \quad (4.3.82)$$

The relation between the derivatives of a function f with respect to the cartesian coordinates x , y and z on the one hand and those with respect to the cylindrical coordinates r , ϕ and y can be formulated in the following way:

$$\begin{bmatrix} \frac{1}{r} \frac{\partial f}{\partial \phi} \\ \frac{\partial f}{\partial y} \\ \frac{\partial f}{\partial r} \end{bmatrix} = \underbrace{\begin{bmatrix} \cos \phi & 0 & -\sin \phi \\ 0 & 1 & 0 \\ \sin \phi & 0 & \cos \phi \end{bmatrix}}_{\mathbf{S}_2(-\phi)} \begin{bmatrix} \frac{\partial f}{\partial x} \\ \frac{\partial f}{\partial y} \\ \frac{\partial f}{\partial z} \end{bmatrix} \Rightarrow \begin{bmatrix} \frac{\partial f}{\partial x} \\ \frac{\partial f}{\partial y} \\ \frac{\partial f}{\partial z} \end{bmatrix} = \underbrace{\begin{bmatrix} \cos \phi & 0 & \sin \phi \\ 0 & 1 & 0 \\ -\sin \phi & 0 & \cos \phi \end{bmatrix}}_{\mathbf{S}_2(\phi) = \mathbf{S}_2(-\phi)^{-1}} \begin{bmatrix} \frac{1}{r} \frac{\partial f}{\partial \phi} \\ \frac{\partial f}{\partial y} \\ \frac{\partial f}{\partial r} \end{bmatrix} \quad (4.3.83)$$

Using the directions of cylindrical coordinates r , ϕ and y , the displacements are described by the radial displacement R , the tangential displacement T and the axial displacement V . For the chosen orientation of the cylindrical coordinates, the relation between these displacements on the one hand and the displacements U , V and W in the directions of cartesian coordinates can be formulated in

the following way:

$$\underbrace{\begin{bmatrix} U \\ V \\ W \end{bmatrix}}_{\mathbf{w}} = \underbrace{\begin{bmatrix} \cos \phi & 0 & \sin \phi \\ 0 & 1 & 0 \\ -\sin \phi & 0 & \cos \phi \end{bmatrix}}_{\mathbf{S}_2(\phi)} \underbrace{\begin{bmatrix} T \\ V \\ R \end{bmatrix}}_{\mathbf{u}} \Rightarrow \mathbf{w} = \mathbf{S}_2(\phi) \mathbf{u} \quad (4.3.84)$$

Generally, the derivation of the formulations for the cylindrical coordinates is not very complicated, but quite laborious. Therefore, only the final formulas are presented here. The complete derivation from the formulation using cartesian coordinates can be found in appendix B.

Also here, Navier's equations for a linear elastic material are the basis for the structural dynamics:

$$\frac{\partial^2 U}{\partial x^2} + \frac{\partial^2 U}{\partial y^2} + \frac{\partial^2 U}{\partial z^2} + \frac{1}{1-2\nu} \frac{\partial}{\partial x} \left(\frac{\partial U}{\partial x} + \frac{\partial V}{\partial y} + \frac{\partial W}{\partial z} \right) - \frac{\rho}{G} \frac{\partial^2 U}{\partial t^2} = 0 \quad (4.3.85)$$

$$\frac{\partial^2 V}{\partial x^2} + \frac{\partial^2 V}{\partial y^2} + \frac{\partial^2 V}{\partial z^2} + \frac{1}{1-2\nu} \frac{\partial}{\partial y} \left(\frac{\partial U}{\partial x} + \frac{\partial V}{\partial y} + \frac{\partial W}{\partial z} \right) - \frac{\rho}{G} \frac{\partial^2 V}{\partial t^2} = 0 \quad (4.3.86)$$

$$\frac{\partial^2 W}{\partial x^2} + \frac{\partial^2 W}{\partial y^2} + \frac{\partial^2 W}{\partial z^2} + \frac{1}{1-2\nu} \frac{\partial}{\partial z} \left(\frac{\partial U}{\partial x} + \frac{\partial V}{\partial y} + \frac{\partial W}{\partial z} \right) - \frac{\rho}{G} \frac{\partial^2 W}{\partial t^2} = 0 \quad (4.3.87)$$

Based on these equations, the formulation for the cylindrical coordinates r , ϕ and y and for the displacements R , T and V is developed in detail in appendix B.4. As the result, is it obtained:

$$0 = \frac{1}{r^2} \frac{\partial^2 T}{\partial \phi^2} + \frac{\partial^2 T}{\partial y^2} + \frac{\partial^2 T}{\partial r^2} - \frac{1}{r} \frac{\partial T}{\partial r} - \frac{1}{r^2} T + \frac{2}{r^2} \frac{\partial R}{\partial \phi} + \frac{1}{1-2\nu} \frac{1}{r} \frac{\partial}{\partial \phi} \left(\frac{1}{r} \frac{\partial T}{\partial \phi} + \frac{R}{r} + \frac{\partial R}{\partial r} + \frac{\partial V}{\partial y} \right) - \frac{\partial^2 T}{\partial t^2} \quad (4.3.88)$$

$$0 = \frac{1}{r^2} \frac{\partial^2 V}{\partial \phi^2} + \frac{\partial^2 V}{\partial y^2} + \frac{\partial^2 V}{\partial r^2} - \frac{1}{r} \frac{\partial V}{\partial r} + \frac{1}{1-2\nu} \frac{\partial}{\partial y} \left(\frac{1}{r} \frac{\partial T}{\partial \phi} + \frac{R}{r} + \frac{\partial R}{\partial r} + \frac{\partial V}{\partial y} \right) - \frac{\rho}{G} \frac{\partial^2 V}{\partial t^2} \quad (4.3.89)$$

$$0 = \frac{1}{r^2} \frac{\partial^2 R}{\partial \phi^2} + \frac{\partial^2 R}{\partial y^2} + \frac{\partial^2 R}{\partial r^2} - \frac{1}{r} \frac{\partial R}{\partial r} - \frac{1}{r^2} R - \frac{2}{r^2} \frac{\partial T}{\partial \phi} + \frac{1}{1-2\nu} \frac{\partial}{\partial r} \left(\frac{1}{r} \frac{\partial T}{\partial \phi} + \frac{R}{r} + \frac{\partial R}{\partial r} + \frac{\partial V}{\partial y} \right) - \frac{\rho}{G} \frac{\partial^2 R}{\partial t^2} \quad (4.3.90)$$

Similar to the solution for the prism, which has been discussed in section 4.2, a semi-analytic solution can also be given for the an axisymmetric structure. Regarding the axial symmetry, it is assumed that the material parameters G , ν and ρ are constant over the circumference, i.e. these parameters depend on the radial coordinate r and the axial coordinate y , but not on the azimuth ϕ :

$$G = G(r, y), \quad \nu = \nu(r, y), \quad \rho = \rho(r, y) \quad (4.3.91)$$

The body of revolution can be considered to be consisting of rings having an infinitesimal cross section; these rings are defined by the radius r and the axial coordinate y . Therefore, it is obvious to separate the cross sectional coordinates r and y from the azimuth ϕ . From the relations

$$x = r \sin \phi, \quad z = r \cos \phi \quad (4.3.92)$$

it is evident that the cylindrical coordinates $\langle r, \phi, y \rangle$ and $\langle r, \phi + 2\pi m, y \rangle$, $m \in \mathbb{Z}$ denote the same point. Therefore, it is obvious to use a the exponential function having an imaginary exponent

for the function depending on the azimuth ϕ . Therefore, the following expression is used as the semi-analytic solution for the body of revolution:

$$\mathbf{u} = \mathbf{u}_k(r, \phi, y, t) = \underbrace{\begin{bmatrix} T_k(r, y) \\ V_k(r, y) \\ R_k(r, y) \end{bmatrix}}_{\hat{\mathbf{u}}_k(y, z)} e^{ik\phi} e^{i\omega_k t} = \underbrace{\hat{\mathbf{u}}_k(r, y)}_{\mathbf{u}_k(r, \phi, y)} e^{ik\phi} e^{i\omega_k t}, k \in \mathbb{Z} \quad (4.3.93)$$

By inserting this into the equations (4.3.88), (4.3.89) and (4.3.90) and factoring out the functions $e^{ik\phi}$ and $e^{i\omega_k t}$ gives:

$$0 = \left(-\frac{1}{r^2} k^2 T_k + \frac{\partial^2 T_k}{\partial y^2} + \frac{\partial^2 T_k}{\partial r^2} - \frac{1}{r} \frac{\partial T_k}{\partial r} - \frac{1}{r^2} T_k + \frac{2}{r^2} ik R_k \right. \\ \left. + \frac{1}{1-2\nu} \frac{ik}{r} \left(\frac{1}{r} ik T_k + \frac{R_k}{r} + \frac{\partial R_k}{\partial r} + \frac{\partial V_k}{\partial y} \right) + \omega_k^2 T_k \right) e^{ik\phi} e^{i\omega_k t} \quad (4.3.94)$$

$$0 = \left(-\frac{1}{r^2} k^2 V_k + \frac{\partial^2 V}{\partial y^2} + \frac{\partial^2 V}{\partial r^2} - \frac{1}{r} \frac{\partial V}{\partial r} \right. \\ \left. + \frac{1}{1-2\nu} \frac{\partial}{\partial y} \left(\frac{1}{r} ik T_k + \frac{R_k}{r} + \frac{\partial R_k}{\partial r} + \frac{\partial V_k}{\partial y} \right) + \omega_k^2 V_k \right) e^{ik\phi} e^{i\omega_k t} \quad (4.3.95)$$

$$0 = \left(-\frac{1}{r^2} k^2 R_k + \frac{\partial^2 R_k}{\partial y^2} + \frac{\partial^2 R_k}{\partial r^2} - \frac{1}{r} \frac{\partial R_k}{\partial r} - \frac{1}{r^2} R_k - \frac{2}{r^2} ik T_k \right. \\ \left. + \frac{1}{1-2\nu} \frac{\partial}{\partial r} \left(\frac{1}{r} ik T_k + \frac{R_k}{r} + \frac{\partial R_k}{\partial r} + \frac{\partial V_k}{\partial y} \right) + \omega_k^2 T_k \right) e^{ik\phi} e^{i\omega_k t} \quad (4.3.96)$$

Since the functions $T_k = T_k(r, y)$, $V_k = V_k(r, y)$ and $R_k = R_k(r, y)$ only depend on the coordinates r and y , the original three-dimensional problem is reduced to a two-dimensional field problem, similar as for the prismatic body discussed in section 4.2. This field problem is given by:

$$0 = -\frac{k^2 + 1}{r^2} T_k + \frac{\partial^2 T_k}{\partial y^2} + \frac{\partial^2 T_k}{\partial r^2} - \frac{1}{r} \frac{\partial T_k}{\partial r} + \frac{2ik}{r^2} R_k \\ + \frac{1}{1-2\nu} \frac{ik}{r} \left(\frac{ik}{r} T_k + \frac{R_k}{r} + \frac{\partial R_k}{\partial r} + \frac{\partial V_k}{\partial y} \right) + \omega_k^2 T_k \quad (4.3.97)$$

$$0 = -\frac{k^2}{r^2} V_k + \frac{\partial^2 V}{\partial y^2} + \frac{\partial^2 V}{\partial r^2} - \frac{1}{r} \frac{\partial V}{\partial r} + \frac{1}{1-2\nu} \frac{\partial}{\partial y} \left(\frac{ik}{r} T_k + \frac{R_k}{r} + \frac{\partial R_k}{\partial r} + \frac{\partial V_k}{\partial y} \right) + \omega_k^2 V_k \quad (4.3.98)$$

$$0 = -\frac{k^2 + 1}{r^2} R_k + \frac{\partial^2 R_k}{\partial y^2} + \frac{\partial^2 R_k}{\partial r^2} - \frac{1}{r} \frac{\partial R_k}{\partial r} - \frac{2ik}{r^2} T_k \\ + \frac{1}{1-2\nu} \frac{\partial}{\partial r} \left(\frac{ik}{r} T_k + \frac{R_k}{r} + \frac{\partial R_k}{\partial r} + \frac{\partial V_k}{\partial y} \right) + \omega_k^2 R_k \quad (4.3.99)$$

In an analogous way, the following expression:

$$\mathbf{u} = \mathbf{u}_{-k}(r, \phi, y, t) = \underbrace{\begin{bmatrix} T_{-k}(r, y) \\ V_{-k}(r, y) \\ R_{-k}(r, y) \end{bmatrix}}_{\hat{\mathbf{u}}_{-k}(y, z)} e^{-ik\phi} e^{i\omega_{-k} t} = \underbrace{\hat{\mathbf{u}}_{-k}(r, y)}_{\mathbf{u}_{-k}(r, \phi, y)} e^{-ik\phi} e^{i\omega_{-k} t}, k \in \mathbb{Z} \quad (4.3.100)$$

leads to the following equations for the two-dimensional problem:

$$0 = -\frac{k^2+1}{r^2}T_{-k} + \frac{\partial^2 T_{-k}}{\partial y^2} + \frac{\partial^2 T_{-k}}{\partial r^2} - \frac{1}{r} \frac{\partial T_{-k}}{\partial r} - \frac{2ik}{r^2}R_{-k} - \frac{1}{1-2\nu} \frac{ik}{r} \left(-\frac{ik}{r}T_{-k} + \frac{R_{-k}}{r} + \frac{\partial R_{-k}}{\partial r} + \frac{\partial V_{-k}}{\partial y} \right) + \omega_{-k}^2 T_{-k} \quad (4.3.101)$$

$$0 = -\frac{k^2}{r^2}V_{-k} + \frac{\partial^2 V}{\partial y^2} + \frac{\partial^2 V}{\partial r^2} - \frac{1}{r} \frac{\partial V}{\partial r} + \frac{1}{1-2\nu} \frac{\partial}{\partial y} \left(-\frac{ik}{r}T_{-k} + \frac{R_{-k}}{r} + \frac{\partial R_{-k}}{\partial r} + \frac{\partial V_{-k}}{\partial y} \right) + \omega_{-k}^2 V_{-k} \quad (4.3.102)$$

$$0 = -\frac{k^2+1}{r^2}R_{-k} + \frac{\partial^2 R_{-k}}{\partial y^2} + \frac{\partial^2 R_{-k}}{\partial r^2} - \frac{1}{r} \frac{\partial R_{-k}}{\partial r} + \frac{2ik}{r^2}T_{-k} + \frac{1}{1-2\nu} \frac{\partial}{\partial r} \left(-\frac{ik}{r}T_{-k} + \frac{R_{-k}}{r} + \frac{\partial R_{-k}}{\partial r} + \frac{\partial V_{-k}}{\partial y} \right) + \omega_{-k}^2 R_{-k} \quad (4.3.103)$$

From the comparison of the equations (4.3.98) and (4.3.102) and of the equations (4.3.99) and (4.3.103), it can be seen that the equations (4.3.102) and (4.3.103) for $-k$ can be converted into the equations (4.3.98) and (4.3.99) for k , respectively, by applying the following substitutions:

$$T_{-k} = -T_k, \quad V_{-k} = V_k, \quad R_{-k} = R_k, \quad \omega_{-k} = \omega_k \quad (4.3.104)$$

The equation (4.3.101) is converted into the equation (4.3.97) by applying these substitutions and subsequently multiplying the equation by -1 .

Based on this semi-analytic solution, the finite element for the body of revolution is developed in a similar way, as it has been used in for the prismatic element in section 4.2. In order to determine an approximation for the functions $T_k(r, y)$, $V_k(r, y)$ and $R_k(r, y)$, which are the solution of the two-dimensional field problem described by the equations (4.3.97), (4.3.97) and (4.3.99), the following discretization is used:

$$\begin{bmatrix} T_k(r, y, t) \\ V_k(r, y, t) \\ R_k(r, y, t) \end{bmatrix} = \sum_{i=1}^{n_N} \mathbf{N}_i(r, y) \mathbf{u}_{i,K}^e(t) = \hat{\mathbf{N}}(r, y) \mathbf{u}_K^e(t), \quad \hat{\mathbf{N}}_i(r_j, y_j) = \begin{cases} 1 & \text{for } j = i \\ 0 & \text{for } j \neq i \end{cases} \quad (4.3.105)$$

$$\mathbf{u}_K^e(t) = \begin{bmatrix} \mathbf{u}_{1,K}^e(t) \\ \mathbf{u}_{2,K}^e(t) \\ \vdots \\ \mathbf{u}_{n_N,K}^e(t) \end{bmatrix}, \quad \hat{\mathbf{N}}(r, y) = [\hat{\mathbf{N}}_1(r, y) \quad \hat{\mathbf{N}}_2(r, y) \quad \dots \quad \hat{\mathbf{N}}_{n_N}(r, y)] \quad (4.3.106)$$

Based on this, the displacement $\mathbf{u}(r, \phi, y, t)$ in the direction of cylindrical coordinates is formulated in the following way:

$$\mathbf{u}(r, \phi, y, t) = \sum_K \sum_{i=1}^{n_N} \mathbf{N}_i(r, y) \mathbf{u}_{i,K}^e(t) e^{iK\phi} = \sum_K \hat{\mathbf{N}}(r, y) \mathbf{u}_K^e(t) e^{iK\phi} \quad (4.3.107)$$

As discussed in section 4.1, the basis for the formulation of the finite element modelling for the structural dynamics is the following expression:

$$\begin{aligned} \delta \mathbf{w}^{eT} \mathbf{q}^e &= \int_{V^e} \left(\delta \tilde{\mathbf{E}}(\mathbf{x})^T \boldsymbol{\sigma}(\mathbf{x}) + \delta \tilde{\mathbf{w}}(\mathbf{x})^T \rho \ddot{\mathbf{w}}(\mathbf{x}) \right) dV \\ &= \delta \mathbf{w}^{eT} \left(\int_{V^e} \mathbf{B}(\mathbf{x})^T \mathbf{D} \mathbf{B}(\mathbf{x}) dV \mathbf{w}^e + \int_{V^e} \mathbf{N}(\mathbf{x})^T \rho \mathbf{N}(\mathbf{x}) dV \ddot{\mathbf{w}}^e \right) \\ &= \delta \mathbf{w}^{eT} (\mathbf{K}^e \mathbf{w}^e + \mathbf{M}^e \ddot{\mathbf{w}}^e) \end{aligned} \quad (4.3.108)$$

In the present case, the integrand has to be formulated for cylindrical coordinates. For the term representing the inertia, this is quite simple. It is valid:

$$\begin{aligned} \mathbf{w} &= \mathbf{S}_2(\phi) \mathbf{u} \Rightarrow \delta \mathbf{w} = \mathbf{S}_2(\phi) \delta \mathbf{u}, \quad \ddot{\mathbf{w}} = \mathbf{S}_2(\phi) \ddot{\mathbf{u}} \\ &\Rightarrow \delta \mathbf{w}^T \rho \ddot{\mathbf{w}} = \delta \mathbf{u}^T \mathbf{S}_2(\phi)^T \rho \mathbf{S}_2(\phi) \ddot{\mathbf{u}} = \delta \mathbf{u}^T \underbrace{\mathbf{S}_2(-\phi) \mathbf{S}_2(\phi)}_{\mathbf{I}} \rho \ddot{\mathbf{u}} = \delta \mathbf{u}^T \rho \ddot{\mathbf{u}} \quad (4.3.109) \end{aligned}$$

The derivation of the term for the virtual work of the deformation is quite laborious. The full derivation can be found in the sections B.2 and B.3 of the appendix B. Here, only the result shall be given. It is valid:

$$\delta \boldsymbol{\varepsilon}^T \boldsymbol{\sigma} = \underbrace{\begin{bmatrix} \frac{1}{r} \frac{\partial \delta T}{\partial \phi} + \frac{\delta R}{r} \\ \frac{\partial \delta V}{\partial y} \\ \frac{\partial \delta R}{\partial r} \\ \frac{1}{r} \frac{\partial \delta V}{\partial \phi} + \frac{\partial \delta T}{\partial y} \\ \frac{\partial \delta V}{\partial r} + \frac{\partial \delta R}{\partial y} \\ \frac{1}{r} \frac{\partial \delta R}{\partial \phi} - \frac{\delta T}{r} + \frac{\partial \delta T}{\partial r} \end{bmatrix}^T}_{\boldsymbol{\varepsilon}_{cyl}^T} \underbrace{\begin{bmatrix} 2G \left[\frac{1}{r} \frac{\partial T}{\partial \phi} + \frac{R}{r} + \frac{\nu}{1-2\nu} \left(\frac{1}{r} \frac{\partial T}{\partial \phi} + \frac{R}{r} + \frac{\partial V}{\partial y} + \frac{\partial R}{\partial r} \right) \right] \\ 2G \left[\frac{\partial V}{\partial y} + \frac{\nu}{1-2\nu} \left(\frac{1}{r} \frac{\partial T}{\partial \phi} + \frac{R}{r} + \frac{\partial V}{\partial y} + \frac{\partial R}{\partial r} \right) \right] \\ 2G \left[\frac{\partial R}{\partial r} + \frac{\nu}{1-2\nu} \left(\frac{1}{r} \frac{\partial T}{\partial \phi} + \frac{R}{r} + \frac{\partial V}{\partial y} + \frac{\partial R}{\partial r} \right) \right] \\ G \left[\frac{1}{r} \frac{\partial V}{\partial \phi} + \frac{\partial T}{\partial y} \right] \\ G \left[\frac{\partial V}{\partial r} + \frac{\partial R}{\partial y} \right] \\ G \left[\frac{1}{r} \frac{\partial R}{\partial \phi} - \frac{T}{r} + \frac{\partial T}{\partial r} \right] \end{bmatrix}}_{\boldsymbol{\sigma}_{cyl}} = \delta \boldsymbol{\varepsilon}_{cyl}^T \boldsymbol{\sigma}_{cyl} \quad (4.3.110)$$

The relation between the stresses contained in the vector $\boldsymbol{\sigma}_{cyl}$ and the strains contained in the vector $\boldsymbol{\varepsilon}_{cyl}$ is given by:

$$\underbrace{\begin{bmatrix} \boldsymbol{\sigma}_t \\ \boldsymbol{\sigma}_y \\ \boldsymbol{\sigma}_r \\ \boldsymbol{\tau}_{ty} \\ \boldsymbol{\tau}_{yr} \\ \boldsymbol{\tau}_{rt} \end{bmatrix}}_{\boldsymbol{\sigma}_{cyl}} = \frac{G}{1-2\nu} \underbrace{\begin{bmatrix} 2(1-\nu) & 2\nu & 2\nu & 0 & 0 & 0 \\ 2\nu & 2(1-\nu) & 2\nu & 0 & 0 & 0 \\ 2\nu & 2\nu & 2(1-\nu) & 0 & 0 & 0 \\ 0 & 0 & 0 & 1-2\nu & 0 & 0 \\ 0 & 0 & 0 & 0 & 1-2\nu & 0 \\ 0 & 0 & 0 & 0 & 0 & 1-2\nu \end{bmatrix}}_{\mathbf{D}} \underbrace{\begin{bmatrix} \frac{1}{r} \frac{\partial T}{\partial \phi} + \frac{R}{r} \\ \frac{\partial V}{\partial y} \\ \frac{\partial R}{\partial r} \\ \frac{1}{r} \frac{\partial V}{\partial \phi} + \frac{\partial T}{\partial y} \\ \frac{\partial V}{\partial r} + \frac{\partial R}{\partial y} \\ \frac{1}{r} \frac{\partial R}{\partial \phi} - \frac{T}{r} + \frac{\partial T}{\partial r} \end{bmatrix}}_{\boldsymbol{\varepsilon}_{cyl}} \quad (4.3.111)$$

Therefore, it can be formulated:

$$\delta \boldsymbol{\varepsilon}^T \boldsymbol{\sigma} = \delta \boldsymbol{\varepsilon}_{cyl}^T \boldsymbol{\sigma}_{cyl} = \delta \boldsymbol{\varepsilon}^T \mathbf{D} \boldsymbol{\varepsilon}_{cyl} \quad (4.3.112)$$

The strain vector $\boldsymbol{\varepsilon}_{cyl}$ can be formulated in the following way:

$$\begin{aligned}
\boldsymbol{\varepsilon}_{cyl} &= \begin{bmatrix} \frac{1}{r} \frac{\partial T}{\partial \phi} + \frac{R}{r} \\ \frac{\partial V}{\partial y} \\ \frac{\partial R}{\partial r} \\ \frac{1}{r} \frac{\partial V}{\partial \phi} + \frac{\partial T}{\partial y} \\ \frac{\partial V}{\partial r} + \frac{\partial R}{\partial y} \\ \frac{1}{r} \frac{\partial R}{\partial \phi} - \frac{T}{r} + \frac{\partial T}{\partial r} \end{bmatrix} \\
&= \frac{1}{r} \underbrace{\begin{bmatrix} 0 & 0 & 1 \\ 0 & 0 & 0 \\ 0 & 0 & 0 \\ 0 & 0 & 0 \\ 0 & 0 & 0 \\ -1 & 0 & 0 \end{bmatrix}}_{\mathbf{T}_0} \underbrace{\begin{bmatrix} T \\ V \\ R \end{bmatrix}}_{\mathbf{u}} + \frac{1}{r} \underbrace{\begin{bmatrix} 1 & 0 & 0 \\ 0 & 0 & 0 \\ 0 & 0 & 0 \\ 0 & 1 & 0 \\ 0 & 0 & 0 \\ 0 & 0 & 1 \end{bmatrix}}_{\mathbf{T}_\phi} \underbrace{\begin{bmatrix} \frac{\partial T}{\partial \phi} \\ \frac{\partial V}{\partial \phi} \\ \frac{\partial R}{\partial \phi} \end{bmatrix}}_{\frac{\partial \mathbf{u}}{\partial \phi}} + \underbrace{\begin{bmatrix} 0 & 0 & 0 \\ 0 & 0 & 0 \\ 0 & 0 & 1 \\ 0 & 0 & 0 \\ 0 & 1 & 0 \\ 1 & 0 & 0 \end{bmatrix}}_{\mathbf{T}_r} \underbrace{\begin{bmatrix} \frac{\partial T}{\partial r} \\ \frac{\partial V}{\partial r} \\ \frac{\partial R}{\partial r} \end{bmatrix}}_{\frac{\partial \mathbf{u}}{\partial r}} + \underbrace{\begin{bmatrix} 0 & 0 & 0 \\ 0 & 1 & 0 \\ 0 & 0 & 0 \\ 1 & 0 & 0 \\ 0 & 0 & 1 \\ 0 & 0 & 0 \end{bmatrix}}_{\mathbf{T}_y} \underbrace{\begin{bmatrix} \frac{\partial T}{\partial y} \\ \frac{\partial V}{\partial y} \\ \frac{\partial R}{\partial y} \end{bmatrix}}_{\frac{\partial \mathbf{u}}{\partial y}} \\
&= \frac{1}{r} \mathbf{T}_0 \mathbf{u} + \frac{1}{r} \mathbf{T}_\phi \frac{\partial \mathbf{u}}{\partial \phi} + \mathbf{T}_r \frac{\partial \mathbf{u}}{\partial r} + \mathbf{T}_y \frac{\partial \mathbf{u}}{\partial y} \tag{4.3.113}
\end{aligned}$$

For the displacement \mathbf{u} and its derivatives it is valid:

$$\mathbf{u} = \begin{bmatrix} T \\ V \\ R \end{bmatrix} = \sum_K \hat{\mathbf{N}}(r, y) \mathbf{u}_K^e(t) e^{iK\phi} \tag{4.3.114}$$

$$\frac{\partial \mathbf{u}}{\partial \phi} = \begin{bmatrix} \frac{\partial T}{\partial \phi} \\ \frac{\partial V}{\partial \phi} \\ \frac{\partial R}{\partial \phi} \end{bmatrix} = \frac{\partial}{\partial \phi} \left(\sum_K \hat{\mathbf{N}}(r, y) \mathbf{u}_K^e(t) e^{iK\phi} \right) = \sum_K \hat{\mathbf{N}}(r, y) \mathbf{u}_K^e(t) iK e^{iK\phi} \tag{4.3.115}$$

$$\frac{\partial \mathbf{u}}{\partial r} = \begin{bmatrix} \frac{\partial T}{\partial r} \\ \frac{\partial V}{\partial r} \\ \frac{\partial R}{\partial r} \end{bmatrix} = \frac{\partial}{\partial r} \left(\sum_K \hat{\mathbf{N}}(r, y) \mathbf{u}_K^e(t) e^{iK\phi} \right) = \sum_K \frac{\partial}{\partial r} \hat{\mathbf{N}}(r, y) \mathbf{u}_K^e(t) e^{iK\phi} \tag{4.3.116}$$

$$\frac{\partial \mathbf{u}}{\partial y} = \begin{bmatrix} \frac{\partial T}{\partial y} \\ \frac{\partial V}{\partial y} \\ \frac{\partial R}{\partial y} \end{bmatrix} = \frac{\partial}{\partial y} \left(\sum_K \hat{\mathbf{N}}(r, y) \mathbf{u}_K^e(t) e^{iK\phi} \right) = \sum_K \frac{\partial}{\partial y} \hat{\mathbf{N}}(r, y) \mathbf{u}_K^e(t) e^{iK\phi} \tag{4.3.117}$$

It can be seen that all vectors contain the function $e^{iK\phi}$. Thereby, it can be formulated:

$$\begin{aligned}
\boldsymbol{\varepsilon}_{cyl} &= \frac{1}{r} \mathbf{T}_0 \mathbf{u} + \frac{1}{r} \mathbf{T}_\phi \frac{\partial \mathbf{u}}{\partial \phi} + \mathbf{T}_r \frac{\partial \mathbf{u}}{\partial r} + \mathbf{T}_y \frac{\partial \mathbf{u}}{\partial y} \\
&= \frac{1}{r} \mathbf{T}_0 \left(\sum_K \hat{\mathbf{N}}(r, y) \mathbf{u}_K^e(t) iK e^{iK\phi} \right) + \frac{1}{r} \mathbf{T}_\phi \left(\sum_K \hat{\mathbf{N}}(r, y) \mathbf{u}_K^e(t) iK e^{iK\phi} \right) \\
&\quad + \mathbf{T}_r \left(\sum_K \frac{\partial}{\partial r} \hat{\mathbf{N}}(r, y) \mathbf{u}_K^e(t) e^{iK\phi} \right) + \mathbf{T}_y \left(\sum_K \frac{\partial}{\partial y} \hat{\mathbf{N}}(r, y) \mathbf{u}_K^e(t) e^{iK\phi} \right) \\
&= \sum_K \underbrace{\left(\frac{1}{r} [\mathbf{T}_0 + \mathbf{T}_\phi iK] \hat{\mathbf{N}}(r, y) + \mathbf{T}_r \frac{\partial}{\partial r} \hat{\mathbf{N}}(r, y) + \mathbf{T}_y \frac{\partial}{\partial y} \hat{\mathbf{N}}(r, y) \right)}_{\hat{\mathbf{B}}_K(r, y)} \mathbf{u}_K^e(t) e^{iK\phi} \\
&= \sum_K \hat{\mathbf{B}}_K(r, y) \mathbf{u}_K^e(t) e^{iK\phi} \tag{4.3.118}
\end{aligned}$$

In an analogous way to the prismatic solid, also here the strain matrix $\hat{\mathbf{B}}_K(r, y)$ contains the periodicity K , which results from the derivative with respect to the angle ϕ . Therefore, the index K is required for the matrices $\hat{\mathbf{B}}_K(r, y)$ in contrast to the matrices $\hat{\mathbf{N}}(r, y)$, which are equal for all periodicities.

Also here, the strain vector $\boldsymbol{\varepsilon}_{cyl}$ is resolved with respect to the single nodes:

$$\begin{aligned}
\hat{\mathbf{N}}(r, y) \mathbf{u}_K^e(t) &= \sum_{i=1}^{n_N} \hat{\mathbf{N}}_i(r, y) \mathbf{u}_{i,K}^e(t) \\
\Rightarrow \frac{\partial}{\partial y} \hat{\mathbf{N}}(r, y) \mathbf{u}_K^e(t) &= \sum_{i=1}^{n_N} \frac{\partial}{\partial y} \hat{\mathbf{N}}_i(r, y) \mathbf{u}_{i,K}^e(t), \quad \frac{\partial}{\partial z} \hat{\mathbf{N}}(r, y) \mathbf{u}_K^e(t) = \sum_{i=1}^{n_N} \frac{\partial}{\partial r} \hat{\mathbf{N}}_i(r, y) \mathbf{u}_{i,K}^e(t) \tag{4.3.119}
\end{aligned}$$

$$\begin{aligned}
\boldsymbol{\varepsilon}_{cyl} &= \frac{1}{r} \mathbf{T}_0 \left[\sum_K \left(\sum_{i=1}^{n_N} \hat{\mathbf{N}}_i(r, y) \mathbf{u}_{i,K}^e(t) \right) e^{iK\phi} \right] + \frac{1}{r} \mathbf{T}_\phi \left[\sum_K \left(\sum_{i=1}^{n_N} \hat{\mathbf{N}}_i(r, y) \mathbf{u}_{i,K}^e(t) \right) iK e^{iK\phi} \right] \\
&\quad + \mathbf{T}_y \left[\sum_K \left(\sum_{i=1}^{n_N} \frac{\partial}{\partial y} \hat{\mathbf{N}}_i(r, y) \mathbf{u}_{i,K}^e(t) \right) e^{iK\phi} \right] + \mathbf{T}_r \left[\sum_K \left(\sum_{i=1}^{n_N} \frac{\partial}{\partial r} \hat{\mathbf{N}}_i(r, y) \mathbf{u}_{i,K}^e(t) \right) e^{iK\phi} \right] \\
&= \sum_K \sum_{i=1}^{n_N} \underbrace{\left[\frac{1}{r} [\mathbf{T}_0 + iK \mathbf{T}_\phi] \hat{\mathbf{N}}_i(r, y) + \mathbf{T}_y \frac{\partial}{\partial y} \hat{\mathbf{N}}_i(r, y) + \mathbf{T}_r \frac{\partial}{\partial r} \hat{\mathbf{N}}_i(r, y) \right]}_{\mathbf{B}_{i,K}(r, y)} \mathbf{u}_{i,K}^e(t) e^{iK\phi} \\
&= \sum_K \sum_{i=1}^{n_N} \hat{\mathbf{B}}_{i,K}(r, y) \mathbf{u}_{i,K}^e(t) e^{iK\phi} \tag{4.3.120}
\end{aligned}$$

From the comparison with (4.3.118) it follows:

$$\hat{\mathbf{B}}_K(r, y) \mathbf{u}_K^e(t) = \sum_{i=1}^{n_N} \hat{\mathbf{B}}_{i,K}(r, y) \mathbf{u}_{i,K}^e(t) \tag{4.3.121}$$

The displacements \mathbf{u} and the strains $\boldsymbol{\varepsilon}_{cyl}$ are formulated in the following way:

$$\mathbf{u}(r, \phi, y, t) = \sum_K \hat{\mathbf{N}}(r, y) \mathbf{u}_K^e e^{iK\phi} \tag{4.3.122}$$

$$\boldsymbol{\varepsilon}_{cyl}(r, \phi, y, t) = \sum_K \hat{\mathbf{B}}_K(r, y) \mathbf{u}_K^e e^{iK\phi} \tag{4.3.123}$$

Here and in the following considerations, the dependence of the displacement vectors \mathbf{u}_K^e on the time t is not indicated explicitly for the sake of brevity. From these expressions, the virtual displacement and the virtual strain are derived; again, the periodicity K is substituted by L :

$$\delta \mathbf{u}(r, \phi, y) = \sum_L \hat{\mathbf{N}}(r, y) \delta \mathbf{u}_L^e e^{iL\phi} \Rightarrow \delta \mathbf{u}(r, \phi, y)^T = \sum_L \delta \mathbf{u}_L^e{}^T \hat{\mathbf{N}}(r, y)^T e^{iL\phi} \quad (4.3.124)$$

$$\delta \varepsilon_{cyl}(r, \phi, y) = \sum_L \hat{\mathbf{B}}_L(r, y) \delta \mathbf{u}_L^e e^{iL\phi} \Rightarrow \delta \varepsilon_{cyl}(r, \phi, y)^T = \sum_L \delta \mathbf{u}_L^e{}^T \hat{\mathbf{B}}_L(r, y)^T e^{iL\phi} \quad (4.3.125)$$

By subsequently inserting the expressions for the cylindrical coordinates according to (4.3.109) and (4.3.112) and the discretisation of the displacements and strains, it is obtained:

$$\begin{aligned} \int_{V^e} \left(\delta \varepsilon^T \boldsymbol{\sigma} + \delta \mathbf{w}^T \rho \ddot{\mathbf{w}} \right) dV &= \int_{V^e} \left(\delta \varepsilon_{cyl}^T \mathbf{D} \varepsilon_{cyl} + \delta \mathbf{u}^T \rho \ddot{\mathbf{u}} \right) dV \\ &= \int_{V^e} \left(\left[\sum_L \delta \mathbf{u}_L^e{}^T \hat{\mathbf{B}}_L(r, y)^T e^{iL\phi} \right] \mathbf{D} \left[\sum_K \hat{\mathbf{B}}_K(r, y) \mathbf{u}_K^e e^{iK\phi} \right] \right. \\ &\quad \left. + \left[\sum_L \delta \mathbf{u}_L^e{}^T \hat{\mathbf{N}}(r, y)^T e^{iL\phi} \right] \rho \left[\sum_K \hat{\mathbf{N}}(r, y) \ddot{\mathbf{u}}_K^e e^{iK\phi} \right] \right) dV \\ &= \sum_L \sum_K \delta \mathbf{u}_L^e{}^T \left(\int_{V^e} \hat{\mathbf{B}}_L(r, y)^T \mathbf{D} \hat{\mathbf{B}}_K(r, y) e^{i(L+K)\phi} dV \mathbf{u}_K^e \right. \\ &\quad \left. + \int_{V^e} \hat{\mathbf{N}}(r, y)^T \rho \hat{\mathbf{N}}(r, y) e^{i(L+K)\phi} dV \ddot{\mathbf{u}}_K^e \right) \quad (4.3.126) \end{aligned}$$

The infinitesimal volume dV , which is required for the integration, is determined in an analogous way as it has been done in section 4.2 for the cartesian coordinates: it is obtained by the triple scalar product of the partial derivatives of the reference position vector with respect to the coordinates:

$$\begin{aligned} \mathbf{x} &= [x \ y \ z]^T = [r \sin \phi \ y \ r \cos \phi]^T \quad (4.3.127) \\ dV &= \frac{\partial \mathbf{x}}{\partial \phi} d\phi \cdot \left(\frac{\partial \mathbf{x}}{\partial y} dy \times \frac{\partial \mathbf{x}}{\partial r} dr \right) = \begin{bmatrix} r \cos \phi \\ 0 \\ -r \sin \phi \end{bmatrix} \cdot \left(\begin{bmatrix} 0 \\ 1 \\ 0 \end{bmatrix} \times \begin{bmatrix} \sin \phi \\ 0 \\ \cos \phi \end{bmatrix} \right) d\phi \ dy \ dr \\ &= \begin{bmatrix} r \cos \phi \\ 0 \\ -r \sin \phi \end{bmatrix} \cdot \begin{bmatrix} \cos \phi \\ 0 \\ -\sin \phi \end{bmatrix} d\phi \ dy \ dr = (r \cos^2 \phi + r \sin^2 \phi) d\phi \ dy \ dr = r \ d\phi \ dy \ dr \quad (4.3.128) \end{aligned}$$

For a body of revolution, the integration has to be carried out over the full circumference, i.e. from 0 to 2π with respect to the angle ϕ and over the cross-sectional area A_C with respect to the axial coordinate y and the radial coordinate r . The essential property of the body of revolution is that the cross section is independent from the angle of rotation. Therefore, the integrals for the stiffness matrix and for the mass matrix can be formulated as a product of one integral over the

cross-sectional area A_C and another one over the circumference:

$$\begin{aligned} \int_{V^e} \hat{\mathbf{B}}_L(r,y)^T \mathbf{D} \hat{\mathbf{B}}_K(r,y) e^{i(L+K)\phi} dV &= \int_{A_C} \int_0^{2\pi} \hat{\mathbf{B}}_L(r,y)^T \mathbf{D} \hat{\mathbf{B}}_K(r,y) e^{i(L+K)\phi} r d\phi dr dy \\ &= \int_{A_C} \hat{\mathbf{B}}_L(r,y)^T \mathbf{D} \hat{\mathbf{B}}_K(r,y) r dr dy \int_0^{2\pi} e^{i(L+K)\phi} d\phi \quad (4.3.129) \end{aligned}$$

$$\begin{aligned} \int_{V^e} \hat{\mathbf{N}}(r,y)^T \rho \hat{\mathbf{N}}(r,y) e^{i(L+K)\phi} dV &= \int_{A_C} \int_0^{2\pi} \hat{\mathbf{N}}(r,y)^T \rho \hat{\mathbf{N}}(r,y) e^{i(L+K)\phi} r d\phi dr dy \\ &= \int_{A_C} \hat{\mathbf{N}}(r,y)^T \rho \hat{\mathbf{N}}(r,y) r dr dy \int_0^{2\pi} e^{i(L+K)\phi} d\phi \quad (4.3.130) \end{aligned}$$

In order to evaluate the integral over the circumference, two cases $L+K=0$ and $L+K \neq 0$ have to be considered. It is valid:

$$L+K=0 : \int_0^{2\pi} e^{i(L+K)\phi} d\phi = \int_0^{2\pi} e^0 d\phi = \int_0^{2\pi} d\phi = 2\pi \quad (4.3.131)$$

$$\begin{aligned} L+K \neq 0 : \int_0^{2\pi} e^{i(L+K)\phi} d\phi &= \frac{1}{L+K} \frac{\ell}{2\pi} e^{i(L+K)\phi} \Big|_0^{2\pi} = \frac{1}{L+K} [e^{2\pi i(L+K)} - e^0] \\ &= \frac{1}{L+K} [1^{(L+K)} - 1] = 0 \quad (4.3.132) \end{aligned}$$

For $L+K \neq 0$ the integral over the circumference vanishes; since this integral is contained as a factor in (4.3.129) and (4.3.130), the complete left-hand sides of (4.3.129) and (4.3.130) vanish in this case. Only the integrals for $L+K=0 \Leftrightarrow K=-L$ don't vanish. Thereby, the following result is obtained:

$$\begin{aligned} \int_{V^e} (\delta \boldsymbol{\varepsilon}^T \boldsymbol{\sigma} + \delta \mathbf{w}^T \rho \ddot{\mathbf{w}}) dV &= \sum_L \sum_K \delta \mathbf{u}_L^e{}^T \left[\int_{V^e} \hat{\mathbf{B}}_L(r,y)^T \mathbf{D} \hat{\mathbf{B}}_{-L}(r,y) e^{i(L+K)\phi} dV \mathbf{u}_K^e(t) \right. \\ &\quad \left. + \int_{V^e} \hat{\mathbf{N}}(r,y)^T \rho \hat{\mathbf{N}}(r,y) e^{i(L+K)\phi} dV \ddot{\mathbf{u}}_K^e(t) \right] \\ &= \sum_L \delta \mathbf{u}_L^e{}^T \left[2\pi \int_{A_C} \hat{\mathbf{B}}_L(r,y)^T \mathbf{D} \hat{\mathbf{B}}_{-L}(r,y) r dr dy \mathbf{u}_{-L}^e(t) \right. \\ &\quad \left. + 2\pi \int_{A_C} \hat{\mathbf{N}}(r,y)^T \rho \hat{\mathbf{N}}(r,y) r dr dy \ddot{\mathbf{u}}_{-L}^e(t) \right] \quad (4.3.133) \end{aligned}$$

The result shows that each summand contains the virtual displacement $\delta \mathbf{u}_L^e$ and the displacement \mathbf{u}_{-L}^e and its second derivative $\ddot{\mathbf{u}}_{-L}^e$. This indicates that motions with different periodicities are decoupled from each other with respect to the elasticity and to the inertia. – By using the substitution $K=-L$ for the indices it is finally obtained:

$$\begin{aligned} \int_{V^e} (\delta \boldsymbol{\varepsilon}^T \boldsymbol{\sigma} + \delta \mathbf{w}^T \rho \ddot{\mathbf{w}}) dV &= \sum_L \delta \mathbf{u}_L^e{}^T \left[2\pi \int_{A_C} \hat{\mathbf{B}}_L(r,y)^T \mathbf{D} \hat{\mathbf{B}}_{-L}(r,y) r dr dy \mathbf{u}_{-L}^e(t) \right. \\ &\quad \left. + 2\pi \int_{A_C} \hat{\mathbf{N}}(r,y)^T \rho \hat{\mathbf{N}}(r,y) r dr dy \ddot{\mathbf{u}}_{-L}^e(t) \right] \\ &= \sum_K \delta \mathbf{u}_{-K}^e{}^T \left[2\pi \int_{A_C} \hat{\mathbf{B}}_{-K}(r,y)^T \mathbf{D} \hat{\mathbf{B}}_K(r,y) r dr dy \mathbf{u}_K^e(t) \right. \\ &\quad \left. + 2\pi \int_{A_C} \hat{\mathbf{N}}(r,y)^T \rho \hat{\mathbf{N}}(r,y) r dr dy \ddot{\mathbf{u}}_K^e(t) \right] \\ &= \sum_K \delta \mathbf{u}_{-K}^e{}^T [2\pi \mathbf{K}_K^e \mathbf{u}_K^e(t) + 2\pi \mathbf{M}^e \ddot{\mathbf{u}}_K^e(t)] \quad (4.3.134) \end{aligned}$$

Like for the prismatic element, the mass matrix for the axisymmetric element is independent from the periodicity K .

Also here, the integrand of the stiffness matrix is resolved using the formulation of the strain vector according to (4.3.118). It is valid:

$$\begin{aligned}
\mathbf{K}_K^e &= \int_{Ac} \hat{\mathbf{B}}_{-K}(r,y)^T \mathbf{D} \hat{\mathbf{B}}_K(r,y) r dr dy \\
&= \int_{Ac} \left[\frac{1}{r} (\mathbf{T}_0 - \mathbf{T}_\phi iK) \hat{\mathbf{N}} + \mathbf{T}_r \frac{\partial \hat{\mathbf{N}}}{\partial r} + \mathbf{T}_y \frac{\partial \hat{\mathbf{N}}}{\partial y} \right]^T \mathbf{D} \left[\frac{1}{r} (\mathbf{T}_0 + \mathbf{T}_\phi iK) \hat{\mathbf{N}} + \mathbf{T}_r \frac{\partial \hat{\mathbf{N}}}{\partial r} + \mathbf{T}_y \frac{\partial \hat{\mathbf{N}}}{\partial y} \right] r dr dy \\
&= \int_{Ac} \frac{1}{r} \hat{\mathbf{N}}^T [\mathbf{T}_0^T - iK \mathbf{T}_\phi^T] \mathbf{D} [\mathbf{T}_0 + iK \mathbf{T}_\phi] \hat{\mathbf{N}} dr dy \\
&\quad + \int_{Ac} \hat{\mathbf{N}}^T [\mathbf{T}_0^T - iK \mathbf{T}_\phi^T] \mathbf{D} \left[\mathbf{T}_r \frac{\partial \hat{\mathbf{N}}}{\partial r} + \mathbf{T}_y \frac{\partial \hat{\mathbf{N}}}{\partial y} \right] dr dy \\
&\quad + \int_{Ac} \left[\frac{\partial \hat{\mathbf{N}}^T}{\partial r} \mathbf{T}_r^T + \frac{\partial \hat{\mathbf{N}}^T}{\partial y} \mathbf{T}_y^T \right] \mathbf{D} [\mathbf{T}_0 + iK \mathbf{T}_\phi] \hat{\mathbf{N}} dr dy \\
&\quad + \int_{Ac} \left[\frac{\partial \hat{\mathbf{N}}^T}{\partial r} \mathbf{T}_r^T + \frac{\partial \hat{\mathbf{N}}^T}{\partial y} \mathbf{T}_y^T \right] \mathbf{D} \left[\mathbf{T}_r \frac{\partial \hat{\mathbf{N}}}{\partial r} + \mathbf{T}_y \frac{\partial \hat{\mathbf{N}}}{\partial y} \right] r dr dy \tag{4.3.135}
\end{aligned}$$

In a similar way to the stiffness matrix of the prismatic element, the stiffness matrix of the annular element is composed of three types of integrals, i.e. integrals over a product of the shape functions, over a product of the shape function and its derivatives and over a product of two derivatives of the shape functions.

Based on the following relations

$$\hat{\mathbf{N}}(r,y) \mathbf{u}_K^e(t) = \sum_{i=1}^{nN} \hat{\mathbf{N}}_i(r,y) \mathbf{u}_{i,K}^e(t) \tag{4.3.136}$$

$$\hat{\mathbf{B}}_K(r,y) \mathbf{u}_K^e(t) = \sum_{i=1}^{nN} \underbrace{\left[\frac{1}{r} [\mathbf{T}_0 + iK \mathbf{T}_\phi] \hat{\mathbf{N}}_i(r,y) + \mathbf{T}_y \frac{\partial \hat{\mathbf{N}}_i(r,y)}{\partial y} + \mathbf{T}_r \frac{\partial \hat{\mathbf{N}}_i(r,y)}{\partial r} \right]}_{\mathbf{B}_{i,K}(r,y)} \mathbf{u}_{i,K}^e(t) \tag{4.3.137}$$

the stiffness matrix and the mass matrix can be resolved into submatrices, which refer to single

nodes. Inserting these relations into the expressions according to (4.3.134) leads to:

$$\begin{aligned}
\delta \mathbf{u}_{-K}^e \mathbf{T} \mathbf{K}_K^e \mathbf{u}_K^e(t) &= \delta \mathbf{u}_{-K}^e \mathbf{T} \int_{A_C} \hat{\mathbf{B}}_{-K}(r, y)^T \mathbf{D} \hat{\mathbf{B}}_K(r, y) r dr dy \mathbf{u}_K^e(t) \\
&= \int_{A_C} \delta \mathbf{u}_{-K}^e \mathbf{T} \hat{\mathbf{B}}_{-K}(r, y)^T \mathbf{D} \hat{\mathbf{B}}_K(r, y) \mathbf{u}_K^e(t) r dr dy \\
&= \int_{A_C} \left[\sum_{i=1}^{n_N} \delta \mathbf{u}_{i,K}^e \mathbf{T} \mathbf{B}_{i,-K}(r, y)^T \right] \mathbf{D} \left[\sum_{k=1}^{n_N} \mathbf{B}_{k,K}(r, y) \mathbf{u}_{k,K}^e(t) \right] r dr dy \\
&= \sum_{i=1}^{n_N} \sum_{k=1}^{n_N} \delta \mathbf{u}_{i,K}^e \mathbf{T} \int_{A_C} \mathbf{B}_{i,-K}(r, y)^T \mathbf{D} \mathbf{B}_{k,K}(r, y) r dr dy \mathbf{u}_{k,K}^e(t) \\
&= \sum_{i=1}^{n_N} \sum_{k=1}^{n_N} \delta \mathbf{u}_{i,K}^e \mathbf{T} \mathbf{K}_{i|k,K}^e \mathbf{u}_{k,K}^e(t) \tag{4.3.138}
\end{aligned}$$

$$\begin{aligned}
\delta \mathbf{u}_{-K}^e \mathbf{T} \mathbf{M}^e \ddot{\mathbf{u}}_K^e(t) &= \delta \mathbf{u}_{-K}^e \mathbf{T} \int_{A_C} \hat{\mathbf{N}}(r, y)^T \rho \hat{\mathbf{N}}(r, y) r dr dy \ddot{\mathbf{u}}_K^e(t) \\
&= \int_{A_C} \delta \mathbf{u}_{-K}^e \mathbf{T} \hat{\mathbf{N}}(r, y)^T \rho \hat{\mathbf{N}}(r, y) \ddot{\mathbf{u}}_K^e(t) r dr dy \\
&= \int_{A_C} \left[\sum_{i=1}^{n_N} \delta \mathbf{u}_{i,K}^e \mathbf{T} \mathbf{N}_i(r, y)^T \right] \rho \left[\sum_{k=1}^{n_N} \mathbf{N}_k(r, y) \ddot{\mathbf{u}}_{k,K}^e(t) \right] r dr dy \\
&= \sum_{i=1}^{n_N} \sum_{k=1}^{n_N} \delta \mathbf{u}_{i,K}^e \mathbf{T} \int_{A_C} \mathbf{N}_i(r, y)^T \rho \mathbf{N}_k(r, y) r dr dy \ddot{\mathbf{u}}_{k,K}^e(t) \\
&= \sum_{i=1}^{n_N} \sum_{k=1}^{n_N} \delta \mathbf{u}_{i,K}^e \mathbf{T} \mathbf{M}_{i|k}^e \ddot{\mathbf{u}}_{k,K}^e(t) \tag{4.3.139}
\end{aligned}$$

Using the definition of the strain matrix $\hat{\mathbf{B}}_{i,K}(r, y)$ according to (4.3.137) the stiffness matrix $\mathbf{K}_{i|k,K}^e$ is resolved in the following way:

$$\begin{aligned}
\mathbf{K}_{i|k,K}^e &= \int_{A_C} \hat{\mathbf{B}}_{i,-K}(r, y)^T \mathbf{D} \hat{\mathbf{B}}_{k,K}(r, y) r dr dy \\
&= \int_{A_C} \left[\frac{\mathbf{T}_0 - \mathbf{T}_\phi iK}{r} \hat{\mathbf{N}}_i + \mathbf{T}_r \frac{\partial \hat{\mathbf{N}}_i}{\partial r} + \mathbf{T}_y \frac{\partial \hat{\mathbf{N}}_i}{\partial y} \right]^T \mathbf{D} \left[\frac{\mathbf{T}_0 + \mathbf{T}_\phi iK}{r} \hat{\mathbf{N}}_k + \mathbf{T}_r \frac{\partial \hat{\mathbf{N}}_k}{\partial r} + \mathbf{T}_y \frac{\partial \hat{\mathbf{N}}_k}{\partial y} \right] r dr dy \\
&= \int_{A_C} \frac{1}{r} \hat{\mathbf{N}}_i^T [\mathbf{T}_0^T - iK \mathbf{T}_\phi^T] \mathbf{D} [\mathbf{T}_0 + iK \mathbf{T}_\phi] \hat{\mathbf{N}}_k dr dy \\
&\quad + \int_{A_C} \hat{\mathbf{N}}_i^T [\mathbf{T}_0^T - iK \mathbf{T}_\phi^T] \mathbf{D} \left[\mathbf{T}_r \frac{\partial \hat{\mathbf{N}}_k}{\partial r} + \mathbf{T}_y \frac{\partial \hat{\mathbf{N}}_k}{\partial y} \right] dr dy \\
&\quad + \int_{A_C} \left[\frac{\partial \hat{\mathbf{N}}_i}{\partial r} \mathbf{T}_r^T + \frac{\partial \hat{\mathbf{N}}_i}{\partial y} \mathbf{T}_y^T \right] \mathbf{D} [\mathbf{T}_0 + iK \mathbf{T}_\phi] \hat{\mathbf{N}}_k dr dy \\
&\quad + \int_{A_C} \left[\frac{\partial \hat{\mathbf{N}}_i}{\partial r} \mathbf{T}_r^T + \frac{\partial \hat{\mathbf{N}}_i}{\partial y} \mathbf{T}_y^T \right] \mathbf{D} \left[\mathbf{T}_r \frac{\partial \hat{\mathbf{N}}_k}{\partial r} + \mathbf{T}_y \frac{\partial \hat{\mathbf{N}}_k}{\partial y} \right] r dr dy \tag{4.3.140}
\end{aligned}$$

4.4 Bilinear interpolation

In the sections 4.2 and 4.3 the general basis for a prismatic and for an annular finite element, respectively, has been developed. In this derivation, the shape functions $\mathbf{N}_i(y, z)$ and $\mathbf{N}_i(y, r)$, which

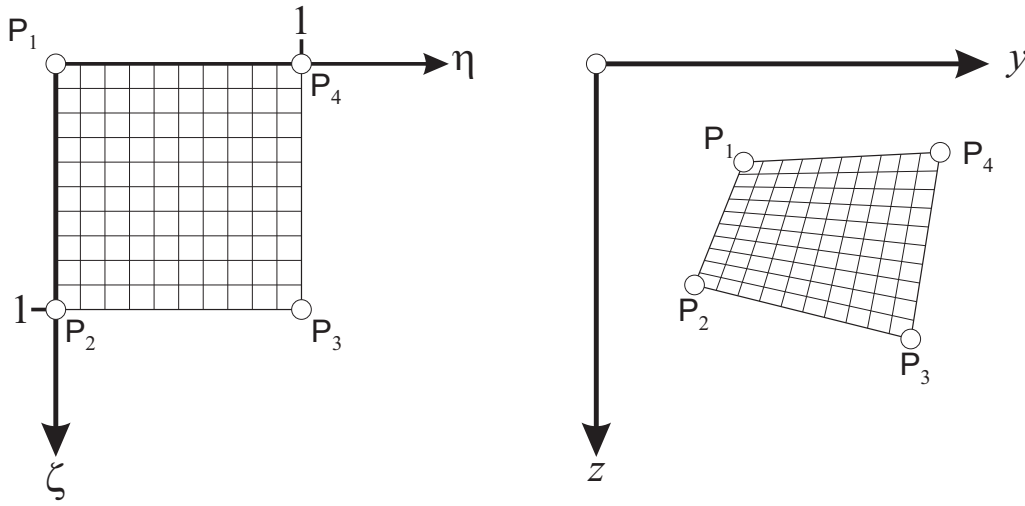


Figure 4.4.3: Left: unit square of the local coordinates η and ζ ; right: actual cross section A_C

describe the distribution of the displacement over the cross section of the prism and the annular solid, respectively, and the nodal displacements \mathbf{w}_K^e and \mathbf{u}_K^e haven't been specified except for the basic conditions, which are generally required for the finite element formulation:

$$\mathbf{N}_i(y_j, z_j) = \begin{cases} \mathbf{I} & \text{for } j = i \\ \mathbf{0} & \text{for } j \neq i \end{cases}, \quad \mathbf{w}_i^e(x, t) = \mathbf{w}_i(x, y_i, z_i, t) \quad (4.4.141)$$

$$\mathbf{N}_i(y_j, r_j) = \begin{cases} \mathbf{I} & \text{for } j = i \\ \mathbf{0} & \text{for } j \neq i \end{cases}, \quad \mathbf{u}_i^e(x, t) = \mathbf{u}_i(x, y_i, z_i, t) \quad (4.4.142)$$

In this section, a formulation will be developed, which uses a quadrilateral area for the cross section and a bilinear interpolation. The four nodes P_1 , P_2 , P_3 and P_4 are located at the corners of the quadrilateral area. In the following, an area located in the plane using the coordinates y and z will be considered. This is the description used of the cross-sectional area of the prismatic element. Nevertheless, the considerations are also valid for the cross-sectional area of the annular element; the cartesian coordinate z has simply to be replaced by the radial coordinate r .

For the description of the area, the local coordinates η and ζ are used. The range of these coordinates is given by:

$$\eta \in \{\mathbb{R} | 0 \leq \eta \leq 1\}, \quad \zeta \in \{\mathbb{R} | 0 \leq \zeta \leq 1\} \quad (4.4.143)$$

so that the complete domain defined by the coordinates is the unit square. This unit square is mapped to the actual shape of the cross sectional area A_C , as shown in Fig. 4.4.3. The mapping is done by the scalar shape functions $N_i(\eta, \zeta)$, which fulfil the following condition:

$$N_i(\eta_j, \zeta_j) = \begin{cases} 1 & \text{for } j = i \\ 0 & \text{for } j \neq i \end{cases} \quad (4.4.144)$$

For a bilinear interpolation and for the mapping displayed in Fig. 4.4.3, the shape functions are given by the following expressions:

$$N_1(\eta, \zeta) = (1 - \eta)(1 - \zeta), \quad N_2(\eta, \zeta) = (1 - \eta)\zeta, \quad N_3(\eta, \zeta) = \eta\zeta, \quad N_4(\eta, \zeta) = \eta(1 - \zeta) \quad (4.4.145)$$

The functions $N_i(\eta, \zeta)$ are displayed in Fig. 4.4.4. Using these functions, the two-dimensional

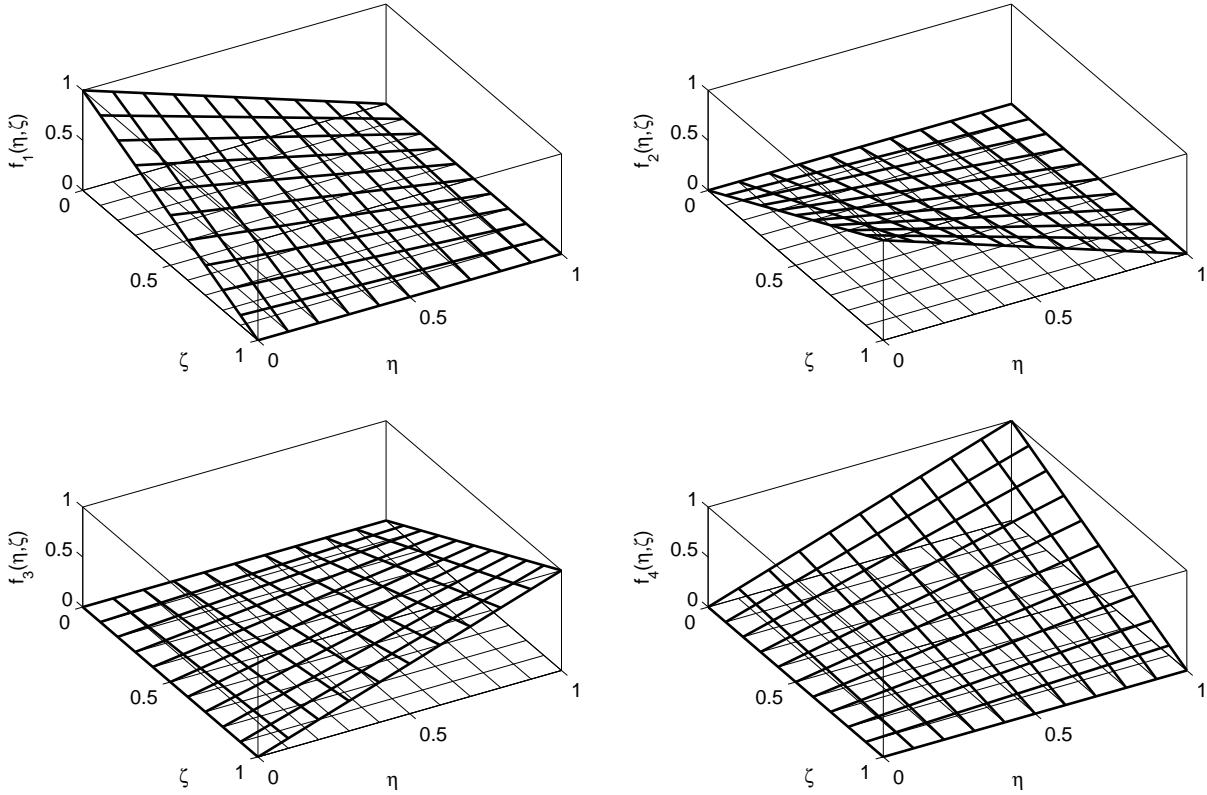


Figure 4.4.4: Interpolation functions for a bilinear quadrilateral finite element

vector \mathbf{y} is described in the following way:

$$\mathbf{y} = \begin{bmatrix} y \\ z \end{bmatrix} = \underbrace{\begin{bmatrix} y_1 \\ z_1 \end{bmatrix}}_{\mathbf{y}_1} N_1(\eta, \zeta) + \underbrace{\begin{bmatrix} y_2 \\ z_2 \end{bmatrix}}_{\mathbf{y}_2} N_2(\eta, \zeta) + \underbrace{\begin{bmatrix} y_3 \\ z_3 \end{bmatrix}}_{\mathbf{y}_3} N_3(\eta, \zeta) + \underbrace{\begin{bmatrix} y_4 \\ z_4 \end{bmatrix}}_{\mathbf{y}_4} N_4(\eta, \zeta) = \sum_{i=1}^4 \mathbf{y}_i N_i(\eta, \zeta) \quad (4.4.146)$$

Here, the vectors \mathbf{y}_i contain the coordinates y_i and z_i of the nodes P_i . Since the shape functions according to (4.4.145) fulfil the condition (4.4.144), it is valid: They fulfil the condition:

$$\mathbf{y}(\eta, \zeta) = \sum_{i=1}^4 \mathbf{y}_i N_i(\eta, \zeta), \quad N_i(\eta_j, \zeta_j) = \begin{cases} 1 & \text{for } j = i \\ 0 & \text{for } j \neq i \end{cases} \Rightarrow \mathbf{y}(\eta_i, \zeta_i) = \mathbf{y}_i \quad (4.4.147)$$

In an analogous way, the following mapping is used for the annular element:

$$\mathbf{y} = \begin{bmatrix} y \\ r \end{bmatrix} = \underbrace{\begin{bmatrix} y_1 \\ r_1 \end{bmatrix}}_{\mathbf{y}_1} N_1(\eta, \zeta) + \underbrace{\begin{bmatrix} y_2 \\ r_2 \end{bmatrix}}_{\mathbf{y}_2} N_2(\eta, \zeta) + \underbrace{\begin{bmatrix} y_3 \\ r_3 \end{bmatrix}}_{\mathbf{y}_3} N_3(\eta, \zeta) + \underbrace{\begin{bmatrix} y_4 \\ r_4 \end{bmatrix}}_{\mathbf{y}_4} N_4(\eta, \zeta) = \sum_{i=1}^4 \mathbf{y}_i N_i(\eta, \zeta) \quad (4.4.148)$$

In order to determine the stiffness matrix and the mass matrix of the element, an integration over the area has to be carried out. In section 4.2 the infinitesimal volume dV has been formulated using the triple scalar product:

$$dV = \frac{\partial \mathbf{x}}{\partial x} dx \cdot \left(\frac{\partial \mathbf{x}}{\partial y} dy \times \frac{\partial \mathbf{x}}{\partial z} dz \right) \quad (4.4.149)$$

Based on this, the infinitesimal area dA can be formulated by replacing the differential with respect to x by the unity vector \mathbf{e}_1 pointing in the direction of the 1-axis. Furthermore, the differentials with

respect to the coordinates y and z have to be replaced by those with respect to the local coordinates η and ζ . This leads to:

$$\begin{aligned} dA &= \mathbf{e}_1 \cdot \left(\frac{\partial \mathbf{x}}{\partial \eta} d\eta \times \frac{\partial \mathbf{x}}{\partial \zeta} d\zeta \right) = \begin{bmatrix} 1 \\ 0 \\ 0 \end{bmatrix} \cdot \left(\begin{bmatrix} 0 \\ \frac{\partial y}{\partial \eta} \\ \frac{\partial z}{\partial \eta} \end{bmatrix} d\eta \times \begin{bmatrix} 0 \\ \frac{\partial y}{\partial \zeta} \\ \frac{\partial z}{\partial \zeta} \end{bmatrix} d\zeta \right) \\ &= \begin{bmatrix} 1 \\ 0 \\ 0 \end{bmatrix} \cdot \begin{bmatrix} \frac{\partial y}{\partial \eta} \frac{\partial z}{\partial \zeta} - \frac{\partial z}{\partial \eta} \frac{\partial y}{\partial \zeta} \\ 0 \\ 0 \end{bmatrix} d\eta d\zeta = \underbrace{\left(\frac{\partial y}{\partial \eta} \frac{\partial z}{\partial \zeta} - \frac{\partial z}{\partial \eta} \frac{\partial y}{\partial \zeta} \right)}_J d\eta d\zeta = J d\eta d\zeta \quad (4.4.150) \end{aligned}$$

The scalar J is the determinant of the Jacobian \mathbf{J} :

$$\mathbf{J} = \begin{bmatrix} \frac{\partial y}{\partial \eta} & \frac{\partial y}{\partial \zeta} \\ \frac{\partial z}{\partial \eta} & \frac{\partial z}{\partial \zeta} \end{bmatrix} \Rightarrow \det \mathbf{J} = \det \begin{bmatrix} \frac{\partial y}{\partial \eta} & \frac{\partial y}{\partial \zeta} \\ \frac{\partial z}{\partial \eta} & \frac{\partial z}{\partial \zeta} \end{bmatrix} = \frac{\partial y}{\partial \eta} \frac{\partial z}{\partial \zeta} - \frac{\partial y}{\partial \zeta} \frac{\partial z}{\partial \eta} = J \quad (4.4.151)$$

For the used shape functions, the partial derivatives are obtained to:

$$\begin{aligned} N_1 &= (1 - \eta)(1 - \zeta), \quad N_2 = (1 - \eta)\zeta, \quad N_3 = \eta\zeta, \quad N_4 = \eta(1 - \zeta) \\ \Rightarrow \frac{\partial N_1}{\partial \eta} &= -(1 - \zeta), \quad \frac{\partial N_2}{\partial \eta} = -\zeta, \quad \frac{\partial N_3}{\partial \eta} = \zeta, \quad \frac{\partial N_4}{\partial \eta} = 1 - \zeta \quad (4.4.152) \end{aligned}$$

$$\Rightarrow \frac{\partial N_1}{\partial \zeta} = -(1 - \eta), \quad \frac{\partial N_2}{\partial \zeta} = 1 - \eta, \quad \frac{\partial N_3}{\partial \zeta} = \eta, \quad \frac{\partial N_4}{\partial \zeta} = -\eta \quad (4.4.153)$$

Thereby, it is valid for the elements of the Jacobian:

$$\begin{aligned} \begin{bmatrix} \frac{\partial y}{\partial \eta} \\ \frac{\partial z}{\partial \eta} \end{bmatrix} &= \frac{\partial \mathbf{y}}{\partial \eta} = \frac{\partial}{\partial \eta} \left(\sum_{i=1}^4 \mathbf{y}_i N_i(\eta, \zeta) \right) = -\mathbf{y}_1(1 - \zeta) - \mathbf{y}_2\zeta + \mathbf{y}_3\zeta + \mathbf{y}_4(1 - \zeta) \\ &= \begin{bmatrix} y_4 - y_1 \\ z_4 - z_1 \end{bmatrix} (1 - \zeta) + \begin{bmatrix} y_3 - y_2 \\ z_3 - z_2 \end{bmatrix} \zeta \quad (4.4.154) \end{aligned}$$

$$\begin{aligned} \begin{bmatrix} \frac{\partial y}{\partial \zeta} \\ \frac{\partial z}{\partial \zeta} \end{bmatrix} &= \frac{\partial \mathbf{y}}{\partial \zeta} = \frac{\partial}{\partial \zeta} \left(\sum_{i=1}^4 \mathbf{y}_i N_i(\eta, \zeta) \right) = -\mathbf{y}_1(1 - \eta) + \mathbf{y}_2(1 - \eta) + \mathbf{y}_3\eta - \mathbf{y}_4\eta \\ &= \begin{bmatrix} y_2 - y_1 \\ z_2 - z_1 \end{bmatrix} (1 - \eta) + \begin{bmatrix} y_3 - y_4 \\ z_3 - z_4 \end{bmatrix} \eta \quad (4.4.155) \end{aligned}$$

In an analogous way, it is valid for the annular element:

$$\begin{bmatrix} \frac{\partial y}{\partial \eta} \\ \frac{\partial r}{\partial \eta} \end{bmatrix} = \frac{\partial \mathbf{y}}{\partial \eta} = \begin{bmatrix} y_4 - y_1 \\ r_4 - r_1 \end{bmatrix} (1 - \zeta) + \begin{bmatrix} y_3 - y_2 \\ r_3 - r_2 \end{bmatrix} \zeta \quad (4.4.156)$$

$$\begin{bmatrix} \frac{\partial y}{\partial \zeta} \\ \frac{\partial r}{\partial \zeta} \end{bmatrix} = \frac{\partial \mathbf{y}}{\partial \zeta} = \begin{bmatrix} y_2 - y_1 \\ r_2 - r_1 \end{bmatrix} (1 - \eta) + \begin{bmatrix} y_3 - y_4 \\ r_3 - r_4 \end{bmatrix} \eta \quad (4.4.157)$$

For the distribution of the displacements of the area, the same shape functions $N_i(\eta, \zeta)$ are used. Thereby, the element based on this approach is an isoparametric element. Furthermore, the same

shape functions are used for the displacements in all three coordinate directions. For the prismatic element, the following formulation is obtained:

$$\mathbf{w}_K(\eta, \zeta) = \sum_{i=1}^4 \underbrace{\begin{bmatrix} U_{i,K} \\ V_{i,K} \\ W_{i,K} \end{bmatrix}}_{\mathbf{w}_{i,K}^e} N_i(\eta, \zeta) = \sum_{i=1}^4 \underbrace{\mathbf{I} N_i(\eta, \zeta)}_{\hat{\mathbf{N}}_i(\eta, \zeta)} \mathbf{w}_{i,K}^e \quad (4.4.158)$$

In an analogous way, the following formulation is used for the annular element:

$$\mathbf{u}_K(\eta, \zeta) = \sum_{i=1}^4 \underbrace{\begin{bmatrix} T_{i,K} \\ V_{i,K} \\ R_{i,K} \end{bmatrix}}_{\mathbf{u}_{i,K}^e} N_i(\eta, \zeta) = \sum_{i=1}^4 \underbrace{\mathbf{I} N_i(\eta, \zeta)}_{\hat{\mathbf{N}}_i(\eta, \zeta)} \mathbf{u}_{i,K}^e \quad (4.4.159)$$

In the sections 4.2 and 4.3, the strain matrices $\hat{\mathbf{B}}_K$ have been formulated in the following way according to (4.2.57) and (4.3.118):

$$\hat{\mathbf{B}}_K(y, z) = \mathbf{T}_x \hat{\mathbf{N}}(y, z) iK \frac{2\pi}{\ell} + \mathbf{T}_y \frac{\partial}{\partial y} \hat{\mathbf{N}}(y, z) + \mathbf{T}_z \frac{\partial}{\partial z} \hat{\mathbf{N}}(y, z) \quad (4.4.160)$$

$$\hat{\mathbf{B}}_K(r, y) = \frac{1}{r} [\mathbf{T}_0 + \mathbf{T}_\phi iK] \hat{\mathbf{N}}(r, y) + \mathbf{T}_r \frac{\partial}{\partial r} \hat{\mathbf{N}}(r, y) + \mathbf{T}_y \frac{\partial}{\partial y} \hat{\mathbf{N}}(r, y) \quad (4.4.161)$$

It can be seen that for the strain matrices the derivatives of the shape functions $\hat{\mathbf{N}}$ with respect to y and to z or r are required. According to (4.4.145), the shape functions N_i are formulated for the local coordinates η and ζ . Based on the chain rule it is valid:

$$\frac{\partial N_i}{\partial \eta} = \frac{\partial N_i}{\partial y} \frac{\partial y}{\partial \eta} + \frac{\partial N_i}{\partial z} \frac{\partial z}{\partial \eta} \quad (4.4.162)$$

$$\frac{\partial N_i}{\partial \zeta} = \frac{\partial N_i}{\partial y} \frac{\partial y}{\partial \zeta} + \frac{\partial N_i}{\partial z} \frac{\partial z}{\partial \zeta} \quad (4.4.163)$$

Resolving these equations for the wanted derivatives $\frac{\partial N_i}{\partial y}$ and $\frac{\partial N_i}{\partial z}$ gives:

$$\begin{aligned} \frac{\partial N_i}{\partial \eta} \frac{\partial z}{\partial \zeta} - \frac{\partial N_i}{\partial \zeta} \frac{\partial z}{\partial \eta} &= \left[\frac{\partial N_i}{\partial y} \frac{\partial y}{\partial \eta} + \frac{\partial N_i}{\partial z} \frac{\partial z}{\partial \eta} \right] \frac{\partial z}{\partial \zeta} - \left[\frac{\partial N_i}{\partial y} \frac{\partial y}{\partial \zeta} + \frac{\partial N_i}{\partial z} \frac{\partial z}{\partial \zeta} \right] \frac{\partial z}{\partial \eta} = \frac{\partial N_i}{\partial y} \underbrace{\left[\frac{\partial y}{\partial \eta} \frac{\partial z}{\partial \zeta} - \frac{\partial y}{\partial \zeta} \frac{\partial z}{\partial \eta} \right]}_J \\ \Rightarrow \frac{\partial N_i}{\partial y} &= \frac{1}{J} \left[\frac{\partial N_i}{\partial \eta} \frac{\partial z}{\partial \zeta} - \frac{\partial N_i}{\partial \zeta} \frac{\partial z}{\partial \eta} \right] \end{aligned} \quad (4.4.164)$$

$$\begin{aligned} -\frac{\partial N_i}{\partial \eta} \frac{\partial y}{\partial \zeta} + \frac{\partial N_i}{\partial \zeta} \frac{\partial y}{\partial \eta} &= -\left[\frac{\partial N_i}{\partial y} \frac{\partial y}{\partial \eta} + \frac{\partial N_i}{\partial z} \frac{\partial z}{\partial \eta} \right] \frac{\partial y}{\partial \zeta} + \left[\frac{\partial N_i}{\partial y} \frac{\partial y}{\partial \zeta} + \frac{\partial N_i}{\partial z} \frac{\partial z}{\partial \zeta} \right] \frac{\partial y}{\partial \eta} = \frac{\partial N_i}{\partial z} \underbrace{\left[\frac{\partial z}{\partial \zeta} \frac{\partial y}{\partial \eta} - \frac{\partial z}{\partial \eta} \frac{\partial y}{\partial \zeta} \right]}_J \\ \Rightarrow \frac{\partial N_i}{\partial z} &= \frac{1}{J} \left[-\frac{\partial N_i}{\partial \eta} \frac{\partial y}{\partial \zeta} + \frac{\partial N_i}{\partial \zeta} \frac{\partial y}{\partial \eta} \right] \end{aligned} \quad (4.4.165)$$

According to (4.4.154) and (4.4.155), it is valid:

$$\begin{aligned} \begin{bmatrix} \frac{\partial y}{\partial \eta} \\ \frac{\partial z}{\partial \eta} \end{bmatrix} &= \begin{bmatrix} y_4 - y_1 \\ z_4 - z_1 \end{bmatrix} (1 - \zeta) + \begin{bmatrix} y_3 - y_2 \\ z_3 - z_2 \end{bmatrix} \zeta, \quad \begin{bmatrix} \frac{\partial y}{\partial \zeta} \\ \frac{\partial z}{\partial \zeta} \end{bmatrix} = \begin{bmatrix} y_2 - y_1 \\ z_2 - z_1 \end{bmatrix} (1 - \eta) + \begin{bmatrix} y_3 - y_4 \\ z_3 - z_4 \end{bmatrix} \eta \\ \det \mathbf{J} &= \frac{\partial y}{\partial \eta} \frac{\partial z}{\partial \zeta} - \frac{\partial y}{\partial \zeta} \frac{\partial z}{\partial \eta} \end{aligned} \quad (4.4.166)$$

Thereby, the right-hand sides of (4.4.164) and (4.4.165) contain only functions depending on the local coordinates η and ζ so that the derivatives $\frac{\partial N_i}{\partial y}$ and $\frac{\partial N_i}{\partial z}$ of the shape functions can now be determined for any given values of the coordinates η and ζ .

4.5 Formulation of the semi-analytic elements

By combining the fundamentals for the prismatic structure developed in section 4.2 and for the axisymmetric structure developed in section 4.3 with the bilinear interpolation developed in section 4.4 the semi-analytic elements can now be formulated. In the following subsections, the required expressions are developed; afterwards, the evaluation is discussed.

4.5.1 Bilinear prism element

The basic equations for the stiffness matrix and for the mass matrix of a prism element, which have been derived in section 4.2, are given by:

$$\begin{aligned} \delta \mathbf{w}^e \mathbf{T} & \left(\int_{V^e} \mathbf{B}(\mathbf{x})^T \mathbf{D} \mathbf{B}(\mathbf{x}) dV \mathbf{w}^e + \int_{V^e} \mathbf{N}(\mathbf{x})^T \rho \mathbf{N}(\mathbf{x}) dV \ddot{\mathbf{w}}^e \right) \\ & = \sum_K \delta \mathbf{w}_{-K}^e \mathbf{T} [\mathbf{K}_K^e \ell \mathbf{w}_K^e + \mathbf{M}^e \ell \ddot{\mathbf{w}}_K^e] \\ & = \sum_{i=1}^{n_N} \sum_{k=1}^{n_N} \delta \mathbf{w}_{i,K}^e \mathbf{T} [\mathbf{K}_{i|k,K}^e \mathbf{w}_{k,K}^e + \mathbf{M}_{i|k}^e \ddot{\mathbf{w}}_{k,K}^e] \end{aligned} \quad (4.5.167)$$

As derived in section 4.4, the reference position of a point in the cross-sectional area A_C , which is indicated by \mathbf{y} , and the distribution of the displacements \mathbf{w} over the cross-sectional area A_C are formulated for the local coordinates η and ζ in the following way:

$$\mathbf{y}(\eta, \zeta) = \sum_{i=1}^4 \underbrace{\begin{bmatrix} y_i \\ z_i \end{bmatrix}}_{\mathbf{y}_i} N_i(\eta, \zeta), \quad \mathbf{w}_K(\eta, \zeta) = \sum_{i=1}^4 \underbrace{\begin{bmatrix} U_{i,K} \\ V_{i,K} \\ W_{i,K} \end{bmatrix}}_{\mathbf{w}_{i,K}^e} N_i(\eta, \zeta) = \sum_{i=1}^4 \underbrace{\mathbf{I} N_i(\eta, \zeta)}_{\hat{\mathbf{N}}_i(\eta, \zeta)} \mathbf{w}_{i,K}^e \quad (4.5.168)$$

$$N_1(\eta, \zeta) = (1 - \eta)(1 - \zeta), \quad N_2(\eta, \zeta) = (1 - \eta)\zeta, \quad N_3(\eta, \zeta) = \eta\zeta, \quad N_4(\eta, \zeta) = \eta(1 - \zeta) \quad (4.5.169)$$

Since for the displacement in each direction the same shape function is used, it is advantageous to use the submatrix formulation. As derived in section 4.2, the submatrices $\mathbf{M}_{i|k}^e$ and $\mathbf{K}_{i|k,K}^e$ are determined in the following way:

$$\mathbf{M}_{i|k}^e = \int_{A_C} \hat{\mathbf{N}}_i(y, z)^T \rho \hat{\mathbf{N}}_k(y, z) dy dz \quad (4.5.170)$$

$$\begin{aligned} \mathbf{K}_{i|k,K}^e & = K^2 \left(\frac{2\pi}{\ell} \right)^2 \int_{A_C} \hat{\mathbf{N}}_i^T \mathbf{T}_x^T \mathbf{D} \mathbf{T}_x \hat{\mathbf{N}}_k dy dz - iK \frac{2\pi}{\ell} \int_{A_C} \hat{\mathbf{N}}_i^T \mathbf{T}_x^T \mathbf{D} \left(\mathbf{T}_y \frac{\partial \hat{\mathbf{N}}_k}{\partial y} + \mathbf{T}_z \frac{\partial \hat{\mathbf{N}}_k}{\partial z} \right) dy dz \\ & + iK \frac{2\pi}{\ell} \int_{A_C} \left(\frac{\partial \hat{\mathbf{N}}_i}{\partial y} \mathbf{T}_y^T + \frac{\partial \hat{\mathbf{N}}_i}{\partial z} \mathbf{T}_z^T \right) \mathbf{D} \mathbf{T}_x \hat{\mathbf{N}}_k dy dz \\ & + \int_{A_C} \left(\frac{\partial \hat{\mathbf{N}}_i}{\partial y} \mathbf{T}_y^T + \frac{\partial \hat{\mathbf{N}}_i}{\partial z} \mathbf{T}_z^T \right) \mathbf{D} \left(\mathbf{T}_y \frac{\partial \hat{\mathbf{N}}_k}{\partial y} + \mathbf{T}_z \frac{\partial \hat{\mathbf{N}}_k}{\partial z} \right) dy dz \end{aligned} \quad (4.5.171)$$

Inserting the shape functions $\hat{N}_i = \mathbf{I}N_i$ according to (4.5.168) leads to:

$$\mathbf{M}_{i|k}^e = \rho \mathbf{I} \int_{AC} N_i N_k dy dz \quad (4.5.172)$$

$$\begin{aligned} \mathbf{K}_{i|k,K}^e &= K^2 \left(\frac{2\pi}{\ell} \right)^2 \mathbf{T}_x^T \mathbf{D} \mathbf{T}_x \int_{AC} N_i N_k dy dz \\ &\quad - iK \frac{2\pi}{\ell} \left(\mathbf{T}_x^T \mathbf{D} \mathbf{T}_y \int_{AC} N_i \frac{\partial N_k}{\partial y} dy dz + \mathbf{T}_x^T \mathbf{D} \mathbf{T}_z \int_{AC} N_i \frac{\partial N_k}{\partial z} dy dz \right) \\ &\quad + iK \frac{2\pi}{\ell} \left(\mathbf{T}_y^T \mathbf{D} \mathbf{T}_x \int_{AC} \frac{\partial N_i}{\partial y} N_k dy dz + \mathbf{T}_z^T \mathbf{D} \mathbf{T}_x \int_{AC} \frac{\partial N_i}{\partial z} N_k dy dz \right) \\ &\quad + \mathbf{T}_y^T \mathbf{D} \mathbf{T}_y \int_{AC} \frac{\partial N_i}{\partial y} \frac{\partial N_k}{\partial y} dy dz + \mathbf{T}_y^T \mathbf{D} \mathbf{T}_z \int_{AC} \frac{\partial N_i}{\partial y} \frac{\partial N_k}{\partial z} dy dz \\ &\quad + \mathbf{T}_z^T \mathbf{D} \mathbf{T}_y \int_{AC} \frac{\partial N_i}{\partial z} \frac{\partial N_k}{\partial y} dy dz + \mathbf{T}_z^T \mathbf{D} \mathbf{T}_z \int_{AC} \frac{\partial N_i}{\partial z} \frac{\partial N_k}{\partial z} dy dz \end{aligned} \quad (4.5.173)$$

As already mentioned in section 4.2, there are three types of integrals, namely

1. integrals of the product of two shape functions:

$$\int_{AC} N_i N_k dy dz \quad (4.5.174)$$

2. integrals of the product of a shape function and a derivative:

$$\int_{AC} N_i \frac{\partial N_k}{\partial y} dy dz, \int_{AC} N_i \frac{\partial N_k}{\partial z} dy dz, \int_{AC} \frac{\partial N_i}{\partial y} N_k dy dz, \int_{AC} \frac{\partial N_i}{\partial z} N_k dy dz \quad (4.5.175)$$

3. integrals of the product of two derivatives:

$$\int_{AC} \frac{\partial N_i}{\partial y} \frac{\partial N_k}{\partial y} dy dz, \int_{AC} \frac{\partial N_i}{\partial y} \frac{\partial N_k}{\partial z} dy dz, \int_{AC} \frac{\partial N_i}{\partial z} \frac{\partial N_k}{\partial y} dy dz, \int_{AC} \frac{\partial N_i}{\partial z} \frac{\partial N_k}{\partial z} dy dz \quad (4.5.176)$$

In section 4.4 it has been determined:

$$\frac{\partial N_i}{\partial y} = \frac{1}{\frac{\partial y}{\partial \eta} \frac{\partial z}{\partial \zeta} - \frac{\partial y}{\partial \zeta} \frac{\partial z}{\partial \eta}} \left[\frac{\partial N_i}{\partial \eta} \frac{\partial z}{\partial \zeta} - \frac{\partial N_i}{\partial \zeta} \frac{\partial z}{\partial \eta} \right] = \frac{1}{\det \mathbf{J}} \left[\frac{\partial N_i}{\partial \eta} \frac{\partial z}{\partial \zeta} - \frac{\partial N_i}{\partial \zeta} \frac{\partial z}{\partial \eta} \right] \quad (4.5.177)$$

$$\frac{\partial N_i}{\partial z} = \frac{1}{\frac{\partial z}{\partial \zeta} \frac{\partial y}{\partial \eta} - \frac{\partial z}{\partial \eta} \frac{\partial y}{\partial \zeta}} \left[-\frac{\partial N_i}{\partial \eta} \frac{\partial y}{\partial \zeta} + \frac{\partial N_i}{\partial \zeta} \frac{\partial y}{\partial \eta} \right] = \frac{1}{\det \mathbf{J}} \left[-\frac{\partial N_i}{\partial \eta} \frac{\partial y}{\partial \zeta} + \frac{\partial N_i}{\partial \zeta} \frac{\partial y}{\partial \eta} \right] \quad (4.5.178)$$

Furthermore, it is valid:

$$dy dz = \left(\frac{\partial z}{\partial \zeta} \frac{\partial y}{\partial \eta} - \frac{\partial z}{\partial \eta} \frac{\partial y}{\partial \zeta} \right) d\eta d\zeta = \det \mathbf{J} d\eta d\zeta \quad (4.5.179)$$

From this, it follows:

$$\frac{\partial N_k}{\partial y} dy dz = \frac{1}{\det \mathbf{J}} \left[\frac{\partial N_i}{\partial \eta} \frac{\partial z}{\partial \zeta} - \frac{\partial N_i}{\partial \zeta} \frac{\partial z}{\partial \eta} \right] \det \mathbf{J} d\eta d\zeta = \left[\frac{\partial N_i}{\partial \eta} \frac{\partial z}{\partial \zeta} - \frac{\partial N_i}{\partial \zeta} \frac{\partial z}{\partial \eta} \right] d\eta d\zeta \quad (4.5.180)$$

$$\frac{\partial N_k}{\partial z} dy dz = \frac{1}{\det \mathbf{J}} \left[-\frac{\partial N_k}{\partial \eta} \frac{\partial y}{\partial \zeta} + \frac{\partial N_k}{\partial \zeta} \frac{\partial y}{\partial \eta} \right] \det \mathbf{J} d\eta d\zeta = \left[-\frac{\partial N_k}{\partial \eta} \frac{\partial y}{\partial \zeta} + \frac{\partial N_k}{\partial \zeta} \frac{\partial y}{\partial \eta} \right] d\eta d\zeta \quad (4.5.181)$$

It can be seen that the determinant $\det \mathbf{J}$ of the Jacobian is cancelled from the expressions. Based on this, it can be formulated for the integrals:

$$\int_{A_C} N_i N_k dy dz = \int_0^1 \int_0^1 N_i N_k \det \mathbf{J} d\eta d\zeta \quad (4.5.182)$$

$$\int_{A_C} N_i \frac{\partial N_k}{\partial y} dy dz = \int_0^1 \int_0^1 N_i \left[\frac{\partial N_i}{\partial \eta} \frac{\partial z}{\partial \zeta} - \frac{\partial N_i}{\partial \zeta} \frac{\partial z}{\partial \eta} \right] d\eta d\zeta \quad (4.5.183)$$

$$\int_{A_C} N_i \frac{\partial N_k}{\partial y} dy dz = \int_0^1 \int_0^1 N_i \left[-\frac{\partial N_k}{\partial \eta} \frac{\partial y}{\partial \zeta} + \frac{\partial N_k}{\partial \zeta} \frac{\partial y}{\partial \eta} \right] d\eta d\zeta \quad (4.5.184)$$

$$\int_{A_C} \frac{\partial N_i}{\partial y} \frac{\partial N_k}{\partial y} dy dz = \int_0^1 \int_0^1 \frac{1}{\det \mathbf{J}} \left[\frac{\partial N_i}{\partial \eta} \frac{\partial z}{\partial \zeta} - \frac{\partial N_i}{\partial \zeta} \frac{\partial z}{\partial \eta} \right] \left[\frac{\partial N_k}{\partial \eta} \frac{\partial z}{\partial \zeta} - \frac{\partial N_k}{\partial \zeta} \frac{\partial z}{\partial \eta} \right] d\eta d\zeta \quad (4.5.185)$$

$$\int_{A_C} \frac{\partial N_i}{\partial y} \frac{\partial N_k}{\partial z} dy dz = \int_0^1 \int_0^1 \frac{1}{\det \mathbf{J}} \left[\frac{\partial N_i}{\partial \eta} \frac{\partial z}{\partial \zeta} - \frac{\partial N_i}{\partial \zeta} \frac{\partial z}{\partial \eta} \right] \left[-\frac{\partial N_k}{\partial \eta} \frac{\partial y}{\partial \zeta} + \frac{\partial N_k}{\partial \zeta} \frac{\partial y}{\partial \eta} \right] d\eta d\zeta \quad (4.5.186)$$

$$\int_{A_C} \frac{\partial N_i}{\partial z} \frac{\partial N_k}{\partial z} dy dz = \int_0^1 \int_0^1 \frac{1}{\det \mathbf{J}} \left[-\frac{\partial N_i}{\partial \eta} \frac{\partial y}{\partial \zeta} + \frac{\partial N_i}{\partial \zeta} \frac{\partial y}{\partial \eta} \right] \left[-\frac{\partial N_k}{\partial \eta} \frac{\partial y}{\partial \zeta} + \frac{\partial N_k}{\partial \zeta} \frac{\partial y}{\partial \eta} \right] d\eta d\zeta \quad (4.5.187)$$

4.5.2 Bilinear annular element

In section 4.3, the following basic equations for the stiffness matrix and for the mass matrix of an annular element have been developed:

$$\begin{aligned} \delta \mathbf{u}^e \mathbf{T} & \left(\int_{V^e} \mathbf{B}(\mathbf{x})^T \mathbf{D} \mathbf{B}(\mathbf{x}) dV \mathbf{u}^e + \int_{V^e} \mathbf{N}(\mathbf{x})^T \rho \mathbf{N}(\mathbf{x}) dV \ddot{\mathbf{u}}^e \right) \\ & = \sum_K \delta \mathbf{u}_{-K}^e \mathbf{T} [2\pi \mathbf{K}_K^e \mathbf{u}_K^e + 2\pi \mathbf{M}^e \ddot{\mathbf{u}}_K^e] \\ & = \sum_{i=1}^{n_N} \sum_{k=1}^{n_N} \delta \mathbf{u}_{i,K}^e \mathbf{T} [2\pi \mathbf{K}_{i|k,K}^e \mathbf{u}_{k,K}^e + 2\pi \mathbf{M}_{i|k}^e \ddot{\mathbf{u}}_{k,K}^e] \end{aligned} \quad (4.5.188)$$

The position \mathbf{y} within the cross-sectional area A_C and the distribution of the displacements \mathbf{u} over the cross-sectional area A_C are described by the bilinear approach developed in section 4.4. Using the local coordinates η and ζ , the :

$$\mathbf{y}(\eta, \zeta) = \sum_{i=1}^4 \underbrace{\begin{bmatrix} y_i \\ r_i \end{bmatrix}}_{\mathbf{y}_i} N_i(\eta, \zeta), \quad \mathbf{u}_K(\eta, \zeta) = \sum_{i=1}^4 \underbrace{\begin{bmatrix} T_{i,K} \\ V_{i,K} \\ R_{i,K} \end{bmatrix}}_{\mathbf{u}_{i,K}^e} N_i(\eta, \zeta) = \sum_{i=1}^4 \underbrace{\mathbf{I} N_i(\eta, \zeta)}_{\hat{\mathbf{N}}_i(\eta, \zeta)} \mathbf{u}_{i,K}^e \quad (4.5.189)$$

$$N_1(\eta, \zeta) = (1 - \eta)(1 - \zeta), \quad N_2(\eta, \zeta) = (1 - \eta)\zeta, \quad N_3(\eta, \zeta) = \eta\zeta, \quad N_4(\eta, \zeta) = \eta(1 - \zeta) \quad (4.5.190)$$

Since for the displacement in each direction the same shape function is used, it is advantageous to use the submatrix formulation. As derived in section 4.3, the submatrices $\mathbf{M}_{i|k}^e$ and $\mathbf{K}_{i|k,K}^e$ are

determined in the following way:

$$\mathbf{M}_{i|k}^e = \int_{A_C} \hat{\mathbf{N}}_i(y,r)^T \rho \hat{\mathbf{N}}_k(y,r) r dy dr \quad (4.5.191)$$

$$\begin{aligned} \mathbf{K}_{i|k,K}^e &= \int_{A_C} \hat{\mathbf{B}}_{i,-K}(r,y)^T \mathbf{D} \hat{\mathbf{B}}_{k,K}(r,y) r dr dy \\ &= \int_{A_C} \frac{1}{r} \hat{\mathbf{N}}_i^T [\mathbf{T}_0^T - iK \mathbf{T}_\phi^T] \mathbf{D} [\mathbf{T}_0 + iK \mathbf{T}_\phi] \hat{\mathbf{N}}_k dr dy \\ &\quad + \int_{A_C} \hat{\mathbf{N}}_i^T [\mathbf{T}_0^T - iK \mathbf{T}_\phi^T] \mathbf{D} \left[\mathbf{T}_r \frac{\partial \hat{\mathbf{N}}_k}{\partial r} + \mathbf{T}_y \frac{\partial \hat{\mathbf{N}}_k}{\partial y} \right] dr dy \\ &\quad + \int_{A_C} \left[\frac{\partial \hat{\mathbf{N}}_i}{\partial r}^T \mathbf{T}_r^T + \frac{\partial \hat{\mathbf{N}}_i}{\partial y}^T \mathbf{T}_y^T \right] \mathbf{D} [\mathbf{T}_0 + iK \mathbf{T}_\phi] \hat{\mathbf{N}}_k dr dy \\ &\quad + \int_{A_C} \left[\frac{\partial \hat{\mathbf{N}}_i}{\partial r}^T \mathbf{T}_r^T + \frac{\partial \hat{\mathbf{N}}_i}{\partial y}^T \mathbf{T}_y^T \right] \mathbf{D} \left[\mathbf{T}_r \frac{\partial \hat{\mathbf{N}}_k}{\partial r} + \mathbf{T}_y \frac{\partial \hat{\mathbf{N}}_k}{\partial y} \right] r dr dy \end{aligned} \quad (4.5.192)$$

Inserting the shape functions $\hat{N}_i = \mathbf{I} N_i$ according to (4.5.189) leads to:

$$\mathbf{M}_{i|k}^e = \rho \mathbf{I} \int_{A_C} N_i N_k r dy dr \quad (4.5.193)$$

$$\begin{aligned} \mathbf{K}_{i|k,K}^e &= [\mathbf{T}_0^T - iK \mathbf{T}_\phi^T] \mathbf{D} [\mathbf{T}_0 + iK \mathbf{T}_\phi] \int_{A_C} \frac{1}{r} N_i N_k dy dz \\ &\quad + [\mathbf{T}_0^T - iK \mathbf{T}_\phi^T] \mathbf{D} \mathbf{T}_y \int_{A_C} N_i \frac{\partial N_k}{\partial y} dy dr + [\mathbf{T}_0^T - iK \mathbf{T}_\phi^T] \mathbf{D} \mathbf{T}_r \int_{A_C} N_i \frac{\partial N_k}{\partial r} dy dr \\ &\quad + \mathbf{T}_y^T \mathbf{D} [\mathbf{T}_0 + iK \mathbf{T}_\phi] \int_{A_C} \frac{\partial N_i}{\partial y} N_k dy dr + \mathbf{T}_r^T \mathbf{D} [\mathbf{T}_0 + iK \mathbf{T}_\phi] \int_{A_C} \frac{\partial N_i}{\partial r} N_k dy dr \\ &\quad + \mathbf{T}_y^T \mathbf{D} \mathbf{T}_y \int_{A_C} \frac{\partial N_i}{\partial y} \frac{\partial N_k}{\partial y} r dy dr + \mathbf{T}_y^T \mathbf{D} \mathbf{T}_r \int_{A_C} \frac{\partial N_i}{\partial y} \frac{\partial N_k}{\partial r} r dy dr \\ &\quad + \mathbf{T}_r^T \mathbf{D} \mathbf{T}_y \int_{A_C} \frac{\partial N_i}{\partial r} \frac{\partial N_k}{\partial y} r dy dr + \mathbf{T}_r^T \mathbf{D} \mathbf{T}_r \int_{A_C} \frac{\partial N_i}{\partial r} \frac{\partial N_k}{\partial r} r dy dr \end{aligned} \quad (4.5.194)$$

Here, four different types of integrals have to be distinguished

1. integrals of the product of two shape functions and the radius r :

$$\int_{A_C} N_i N_k r dy dr \quad (4.5.195)$$

2. integrals of the product of two shape functions and the reciprocal value of the radius r :

$$\int_{A_C} \frac{1}{r} N_i N_k dy dr \quad (4.5.196)$$

3. integrals of the product of a shape function and a derivative:

$$\int_{A_C} N_i \frac{\partial N_k}{\partial y} dy dz, \int_{A_C} N_i \frac{\partial N_k}{\partial z} dy dz, \int_{A_C} \frac{\partial N_i}{\partial y} N_k dy dz, \int_{A_C} \frac{\partial N_i}{\partial z} N_k dy dz \quad (4.5.197)$$

4. integrals of the product of two derivatives:

$$\int_{A_C} \frac{\partial N_i}{\partial y} \frac{\partial N_k}{\partial y} r dy dr, \int_{A_C} \frac{\partial N_i}{\partial y} \frac{\partial N_k}{\partial z} r dy dr, \int_{A_C} \frac{\partial N_i}{\partial z} \frac{\partial N_k}{\partial y} r dy dr, \int_{A_C} \frac{\partial N_i}{\partial z} \frac{\partial N_k}{\partial z} r dy dr \quad (4.5.198)$$

The product of a derivative and the infinitesimal area element $dy dr$ can be derived from the results

of (4.5.180) and (4.5.181) by replacing the coordinate z with r . Thereby, it is obtained:

$$\frac{\partial N_k}{\partial y} dy dr = \frac{1}{\det \mathbf{J}} \left[\frac{\partial N_i}{\partial \eta} \frac{\partial r}{\partial \zeta} - \frac{\partial N_i}{\partial \zeta} \frac{\partial r}{\partial \eta} \right] \det \mathbf{J} d\eta d\zeta = \left[\frac{\partial N_i}{\partial \eta} \frac{\partial r}{\partial \zeta} - \frac{\partial N_i}{\partial \zeta} \frac{\partial r}{\partial \eta} \right] d\eta d\zeta \quad (4.5.199)$$

$$\frac{\partial N_k}{\partial r} dy dr = \frac{1}{\det \mathbf{J}} \left[-\frac{\partial N_k}{\partial \eta} \frac{\partial y}{\partial \zeta} + \frac{\partial N_k}{\partial \zeta} \frac{\partial y}{\partial \eta} \right] \det \mathbf{J} d\eta d\zeta = \left[-\frac{\partial N_k}{\partial \eta} \frac{\partial y}{\partial \zeta} + \frac{\partial N_k}{\partial \zeta} \frac{\partial y}{\partial \eta} \right] d\eta d\zeta \quad (4.5.200)$$

It can be seen that the determinant $\det \mathbf{J}$ of the Jacobian is cancelled from the expressions. Based on this, it can be formulated for the integrals:

$$\int_{AC} N_i N_k r dy dr = \int_0^1 \int_0^1 N_i N_k \det \mathbf{J} r d\eta d\zeta \quad (4.5.201)$$

$$\int_{AC} \frac{1}{r} N_i N_k dy dr = \int_0^1 \int_0^1 \frac{1}{r} N_i N_k \det \mathbf{J} d\eta d\zeta \quad (4.5.202)$$

$$\int_{AC} N_i \frac{\partial N_k}{\partial y} dy dr = \int_0^1 \int_0^1 N_i \left[\frac{\partial N_i}{\partial \eta} \frac{\partial r}{\partial \zeta} - \frac{\partial N_i}{\partial \zeta} \frac{\partial r}{\partial \eta} \right] d\eta d\zeta \quad (4.5.203)$$

$$\int_{AC} N_i \frac{\partial N_k}{\partial r} dy dr = \int_0^1 \int_0^1 N_i \left[-\frac{\partial N_k}{\partial \eta} \frac{\partial y}{\partial \zeta} + \frac{\partial N_k}{\partial \zeta} \frac{\partial y}{\partial \eta} \right] d\eta d\zeta \quad (4.5.204)$$

$$\int_{AC} \frac{\partial N_i}{\partial y} \frac{\partial N_k}{\partial r} r dy dr = \int_0^1 \int_0^1 \frac{1}{\det \mathbf{J}} \left[\frac{\partial N_i}{\partial \eta} \frac{\partial r}{\partial \zeta} - \frac{\partial N_i}{\partial \zeta} \frac{\partial r}{\partial \eta} \right] \left[\frac{\partial N_k}{\partial \eta} \frac{\partial r}{\partial \zeta} - \frac{\partial N_k}{\partial \zeta} \frac{\partial r}{\partial \eta} \right] r d\eta d\zeta \quad (4.5.205)$$

$$\int_{AC} \frac{\partial N_i}{\partial y} \frac{\partial N_k}{\partial r} r dy dr = \int_0^1 \int_0^1 \frac{1}{\det \mathbf{J}} \left[\frac{\partial N_i}{\partial \eta} \frac{\partial r}{\partial \zeta} - \frac{\partial N_i}{\partial \zeta} \frac{\partial r}{\partial \eta} \right] \left[-\frac{\partial N_k}{\partial \eta} \frac{\partial y}{\partial \zeta} + \frac{\partial N_k}{\partial \zeta} \frac{\partial y}{\partial \eta} \right] r d\eta d\zeta \quad (4.5.206)$$

$$\int_{AC} \frac{\partial N_i}{\partial r} \frac{\partial N_k}{\partial r} r dy dr = \int_0^1 \int_0^1 \frac{1}{\det \mathbf{J}} \left[-\frac{\partial N_i}{\partial \eta} \frac{\partial y}{\partial \zeta} + \frac{\partial N_i}{\partial \zeta} \frac{\partial y}{\partial \eta} \right] \left[-\frac{\partial N_k}{\partial \eta} \frac{\partial y}{\partial \zeta} + \frac{\partial N_k}{\partial \zeta} \frac{\partial y}{\partial \eta} \right] r d\eta d\zeta \quad (4.5.207)$$

4.5.3 Numerical integration

In the sections 4.5.1 and 4.5.2 the integrals for the mass matrix and for the stiffness matrix have been developed. For some of these integrals, an analytical solution is not possible. This is especially the case for those integrals, which contain reciprocal values of the determinant $\det \mathbf{J}$ of the Jacobian or of the radial coordinate r . Thus, a numerical evaluation is used. A widely used method is the Gauss integration. Here, the integral of a function f over a domain D is approximated by weighted function values at certain points given by ξ_i and η_i :

$$\int_D f(\xi, \eta) d\xi d\eta = \sum_{i=1}^N f(\xi_i, \eta_i) w_i \quad (4.5.208)$$

For the integration over the unit square, Schwarz [67] gives the following coordinates and weights for the integration points:

In Fig.4.5.5 the positions of the integration points within the unit square are displayed.

Using these parameters, the integral of the function f over the unit square is approximated by:

$$\int_0^1 \int_0^1 f(\eta, \zeta) d\eta d\zeta = \sum_{i=1}^4 \sum_{j=1}^4 f(\sigma_i, \sigma_j) \sigma_i \sigma_j \quad (4.5.209)$$

i	σ_i	w_i
1	0.069 431 8442	0.172 927 4226
2	0.330 009 4782	0.326 072 5774
3	0.669 990 5218	0.326 072 5774
4	0.930 568 1558	0.172 927 4226

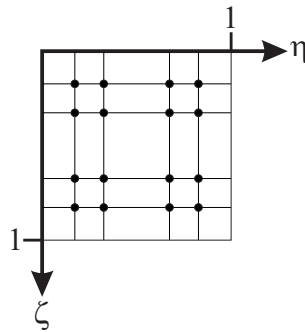


Figure 4.5.5: Position of the integration points for the Gauss integration

Chapter 5

Description of the rotating flexible wheelset

The description of the wheelset is developed by combining the floating frame of reference formulation for a flexible body with the concept of cyclic systems. In section 5.1 the basic kinematics of the wheelset are presented. The consideration of a cyclic structure and the related generalization by an n -tuple of identical particles are developed in section 5.2. In the section 5.3 the formulation for the cyclic structure is modified by using a description in an intermediate frame. Based on this, a transformation between the two formulations is derived; in the section 5.4 this transformation is applied to the equations of motion of a linear cyclic system, which have been developed in the section 3.2. Furthermore, in the section 5.5, the description of the flexible wheelset by a modal synthesis is adapted to the transformation derived in the section 3.2. The shape functions required for the modal synthesis are gained from a finite element model of the wheelset, which is described in the section 5.6. In the section 5.7 the basic principle of the inertia terms for the n -tuple is developed and applied to the formulation using the intermediate frame. In the sections 5.8, some basic characteristics of the inertia terms for the three groups will be discussed. Finally, the description of external forces for the rotating wheelset is discussed in the section 5.9.

5.1 Kinematics of the wheelset

The basis for the kinematics is the floating frame of reference formulation:

$$\mathbf{r}_{OP}^I = \mathbf{r}_{OR}^I + \mathbf{S}^{I\mathcal{R}} \mathbf{r}_{RP}^{\mathcal{R}} \quad (5.1.1)$$

For the description of the wheelset the body-fixed frame \mathcal{B}_W is used as the floating frame of reference \mathcal{R} . The reference point R_W lies on the centre of the axis of the rotational symmetry of the wheelset. Thereby, the position of a particle belonging to the wheelset, which is currently located at the point P is described in the following way:

$$\mathbf{r}_{OP}^I = \mathbf{r}_{OR_W}^I + \mathbf{S}^{I\mathcal{B}_W} \mathbf{r}_{R_W P}^{\mathcal{B}_W} \quad (5.1.2)$$

The point R_W and the frame \mathcal{B}_W define the current spatial position of the wheelset. In the following considerations the kinematics of this motion will be developed. Special characteristics of the kinematics are:

- splitting of the motion into one part given by the motion along the track and another part describing the relative; this is generally used in railway dynamics

- introducing an intermediate frame performing all motions of the wheelset except the large rotation due to overturning and special treatment of the overturning motion
- describing the relative kinematics by cylindrical coordinates to exploit the rotational symmetry

5.1.1 Rigid body motions

As usual in railway dynamics, the kinematics is split into two parts: The first part is given by the trajectory of the track; here, the track point T and the track frame \mathcal{T} are used. The geometry of the trajectory is described by the position vector \mathbf{r}_{OT}^I and the transformation matrix \mathbf{S}^{IT} , which both depend on the arc length s :

$$\mathbf{r}_{OT}^I = \mathbf{r}_{OT}^I(s), \mathbf{S}^{IT} = \mathbf{S}^{IT}(s) \quad (5.1.3)$$

The matrix \mathbf{S}^{IT} describes the orientation of the track. Changes of the orientation are caused by curves, superelevations and gradients of the track. The individual coordinate $s_W = s_W(t)$ indicates the current position of the wheelset on the trajectory, which describes the track. This position is determined by the track point T_W and the rotation matrix \mathbf{S}^{IT_W} of the wheelset. It is valid:

$$s = s_W(t) \Rightarrow \mathbf{r}_{OT_W}^I = \mathbf{r}_{OT}^I(s_W), \mathbf{S}^{IT_W} = \mathbf{S}^{IT}(s_W) \quad (5.1.4)$$

The second part describes the motions of the wheelset relative to the track. As mentioned before, the current position and orientation of the wheelset is described by the reference point R_W and the body-fixed reference frame \mathcal{B}_W of the wheelset. The relative translations are therefore expressed by the vector $\mathbf{r}_{T_W R_W}^{\mathcal{T}}$:

$$\mathbf{r}_{T_W R_W}^{\mathcal{T}} = \begin{bmatrix} 0 \\ y_W(t) \\ z_W(t) \end{bmatrix} \quad (5.1.5)$$

Here, y_W and z_W indicate the lateral and the vertical displacement of the wheelset, respectively. – The rotation of the wheelset relative to the track is described by the matrix $\mathbf{S}^{\mathcal{T}_W \mathcal{B}_W}$ describes the rotation of the entire wheelset with respect to the track. As already mentioned before, the wheelset is considered as a rotational symmetric structure, whereas the 2-axis of the frame \mathcal{B}_W is the axis of symmetry. Furthermore, the wheelset performs a large rotation due to its overturning motion around its 2-axis. Therefore, it is sensible to modify the usual sequence of the Cardan angles 1-2-3 in such a way that the rotation around the 2-axis is the last in the sequence. By using the roll angle ϕ_W , the yaw angle ψ_W and the overturning angle χ_W the matrix can be composed from elementary rotation matrices in the following way:

$$\mathbf{S}^{\mathcal{T}_W \mathcal{B}_W} = \mathbf{S}_3(\psi_W(t)) \mathbf{S}_1(\phi_W(t)) \mathbf{S}_2(\chi_W(t)) \quad (5.1.6)$$

For the sake of brevity and for a better overview, the dependency of the arc length coordinate $s_W(t)$, of the translations $y_W(t)$ and $z_W(t)$ and of the rotation angles $\phi_W(t)$, $\psi_W(t)$, and $\chi_W(t)$ will not be indicated explicitly in the following considerations. – The matrix $\mathbf{S}^{\mathcal{T}_W \mathcal{B}_W}$ can be split into two parts:

$$\begin{aligned} \mathbf{S}^{\mathcal{T}_W \mathcal{B}_W} &= \underbrace{\mathbf{S}_3(\psi_W) \mathbf{S}_1(\phi_W)}_{\mathbf{S}^{\mathcal{T}_W \mathcal{A}_W}} \underbrace{\mathbf{S}_2(\chi_W)}_{\mathbf{S}^{\mathcal{A}_W \mathcal{B}_W}} \\ &= \begin{bmatrix} \cos \psi_W & -\cos \phi_W \sin \psi_W & -\sin \phi_W \sin \psi_W \\ \sin \psi_W & \cos \phi_W \cos \psi_W & \cos \phi_W \sin \psi_W \\ 0 & \sin \phi_W & \cos \phi_W \end{bmatrix} \begin{bmatrix} \cos \chi_W & 0 & \sin \chi_W \\ 0 & 1 & 0 \\ -\sin \chi_W & 0 & \cos \chi_W \end{bmatrix} \end{aligned} \quad (5.1.7)$$

Thereby, an intermediate frame \mathcal{A}_W is defined, which performs all motions of the undeformed wheelset except the overturning motion χ_W . Thus, the frame \mathcal{A}_W will be referenced as the sliding frame. – It should be pointed out that the roll angle ϕ_W and the yaw angle ψ_W are usually quite small and stay in a certain range around zero. In contrast to this, the overturning angle χ_W is a large angle, which grows while the vehicle is running¹.

In total, the rigid body kinematics of the wheelset is formulated in the following way:

$$\mathbf{r}_{OR_W}^I = \mathbf{r}_{OT}^I(s_W) + \mathbf{S}^{IT}(s_W) \mathbf{r}_{TWR_W}^{\mathcal{T}_W}(y_W, z_W) \quad (5.1.8)$$

$$\mathbf{S}^{IB_W} = \mathbf{S}^{IT}(s_W) \mathbf{S}^{\mathcal{T}_W \mathcal{A}_W}(\phi_W, \psi_W) \mathbf{S}^{\mathcal{A}_W \mathcal{B}_W}(\chi_W) \quad (5.1.9)$$

This formulation shows the influence of the degrees of freedom.

The angular velocity of the wheelset can be formulated by superposing the relative angular velocities. It is valid:

$$\tilde{\omega}_{IT_W}^I = \frac{\partial \mathbf{S}^{IT}(s_W)}{\partial s_W} \dot{s}_W \mathbf{S}^{IT}(s_W)^T = \tilde{\omega}_{IT_W}^I(\dot{s}_W, s_W) \Rightarrow \omega_{IT_W}^I = \omega_{IT_W}^I(\dot{s}_W, s_W) \quad (5.1.10)$$

$$\omega_{\mathcal{T}_W \mathcal{A}_W}^{\mathcal{T}_W} = \begin{bmatrix} \dot{\phi}_W \cos \psi_W \\ \dot{\phi}_W \sin \psi_W \\ \dot{\psi}_W \end{bmatrix} = \omega_{\mathcal{T}_W \mathcal{A}_W}^{\mathcal{T}_W}(\dot{\phi}_W, \dot{\psi}_W, \phi_W, \psi_W) \quad (5.1.11)$$

$$\omega_{\mathcal{A}_W \mathcal{B}_W}^{\mathcal{A}_W} = \omega_{\mathcal{A}_W \mathcal{B}_W}^{\mathcal{B}_W} = \begin{bmatrix} 0 \\ \dot{\chi}_W \\ 0 \end{bmatrix} = \dot{\chi}_W \mathbf{e}_2 \quad (5.1.12)$$

The absolute angular velocity $\omega_{IB_W}^I$ can be composed in the following way:

$$\omega_{IB_W}^I = \omega_{IT_W}^I(\dot{s}_W, s_W) + \mathbf{S}^{IT}(s_W) \left[\omega_{\mathcal{T}_W \mathcal{A}_W}^{\mathcal{T}_W}(\dot{\phi}_W, \dot{\psi}_W, \phi_W, \psi_W) + \mathbf{S}^{\mathcal{T}_W \mathcal{A}_W}(\phi_W, \psi_W) \dot{\chi}_W \mathbf{e}_2 \right] \quad (5.1.13)$$

Here, an advantage of the chosen formulation becomes visible: In the description in the inertial frame I the absolute angular velocity $\omega_{IB_W}^I$ of the wheelset contains the angular velocity $\dot{\chi}_W$, but not the angle χ_W and thereby also not the functions $\sin(\chi_W)$ and $\cos(\chi_W)$. This aspect is especially interesting in the context of linearization, as discussed by Vohla [77].

5.1.2 Relative motions

The relative position of a particle with respect to the body reference point R is described in the reference frame \mathcal{R} by:

$$\mathbf{r}_{RP}^{\mathcal{R}} = \mathbf{x}^{\mathcal{R}} + \mathbf{w}^{\mathcal{R}}(\mathbf{x}^{\mathcal{R}}, t) \quad (5.1.14)$$

Here, the vector $\mathbf{x}^{\mathcal{R}}$ describes the position of the particle in the reference state, usually the undeformed state. The vector $\mathbf{w}^{\mathcal{R}}$ describes the deformation field, by which the particle is shifted from its reference position to its current position. In the present case, the body-fixed frame \mathcal{B}_W of the wheelset is chosen as the reference frame. Thereby, the relative kinematics is formulated in the following way:

$$\mathbf{r}_{RP}^{\mathcal{B}_W} = \mathbf{x}^{\mathcal{B}_W} + \mathbf{w}^{\mathcal{B}_W}(\mathbf{x}^{\mathcal{B}_W}, t) \quad (5.1.15)$$

¹In the context of the wheelset the expression “pitch motion” for the rotation around the 2-axis is a bit misleading, since “pitch” suggests a small periodic motion around a reference state, as it is known e.g. for the carbody of a vehicle. Therefore, the wheelset’s rotation around its 2-axis will be referenced as “overturning motion”; this also underlines that it is a large motion, which grows while the vehicle is running.

The wheelset is considered as a rotational symmetric structure, whereas the 2-axis is the axis of symmetry. Therefore, it is obvious to use cylindrical coordinates for the description of the kinematics. In the body-fixed frame \mathcal{B} , the axial coordinate y , the radial coordinate r and the azimuth ϕ are used as cylindrical coordinates. Thereby, the reference position of a particle can be expressed in the following way:

$$\mathbf{x}^{\mathcal{B}_w} = \begin{bmatrix} r \sin \phi \\ y \\ r \cos \phi \end{bmatrix} = \underbrace{\begin{bmatrix} \cos \phi & 0 & \sin \phi \\ 0 & 1 & 0 \\ -\sin \phi & 0 & \cos \phi \end{bmatrix}}_{\mathbf{S}_2(\phi)} \underbrace{\begin{bmatrix} 0 \\ y \\ r \end{bmatrix}}_{\mathbf{c}} = \mathbf{x}^{\mathcal{B}_w}(r, \phi, y) \quad (5.1.16)$$

Since the azimuth ϕ appears as an argument of the trigonometric functions $\sin \phi$ and $\cos \phi$, it is evident that the coordinate triples $\langle r, \phi, y \rangle$ and $\langle r, \phi + 2\pi k, y \rangle$, $k \in \mathbb{Z}$ denote the same reference point. It should be pointed out that the coordinate triple $\langle \mathbf{c}, \phi \rangle$, which is used in the body-fixed frame describes a certain particle; thereby, these coordinates are material coordinates. The radial coordinate r and the axial coordinate y are contained in the vector \mathbf{c} . To keep the expressions short, this vector will be used in the following:

$$\mathbf{x}^{\mathcal{B}_w} = \mathbf{x}^{\mathcal{B}_w}(r, \phi, y) = \mathbf{x}^{\mathcal{B}_w}(\mathbf{c}, \phi) \quad (5.1.17)$$

For the deformation vector $\mathbf{w}^{\mathcal{B}_w}(\mathbf{x}^{\mathcal{B}_w}, t)$, the reference position vector $\mathbf{x}^{\mathcal{B}_w}$ is an argument. Since the reference position vector depends on the cylindrical coordinates $\langle \mathbf{c}, \phi \rangle$, the deformation field can also be formulated using these coordinates:

$$\mathbf{x}^{\mathcal{B}_w} = \mathbf{x}^{\mathcal{B}_w}(\mathbf{c}, \phi) \Rightarrow \mathbf{w}^{\mathcal{B}_w}(\mathbf{x}^{\mathcal{B}_w}, t) = \mathbf{w}^{\mathcal{B}_w}(\mathbf{c}, \phi, t) \quad (5.1.18)$$

The deformation is also described based on cylindrical coordinates. For this sake, the axial deformation V , the radial deformation R and the tangential deformation T are used. Thereby, it is obtained:

$$\mathbf{w}^{\mathcal{B}_w}(\mathbf{c}, \phi, t) = \begin{bmatrix} T(\mathbf{c}, \phi, t) \cos \phi + R(\mathbf{c}, \phi, t) \sin \phi \\ V(\mathbf{c}, \phi, t) \\ R(\mathbf{c}, \phi, t) \cos \phi - T(\mathbf{c}, \phi, t) \sin \phi \end{bmatrix} = \underbrace{\begin{bmatrix} \cos \phi & 0 & \sin \phi \\ 0 & 1 & 0 \\ -\sin \phi & 0 & \cos \phi \end{bmatrix}}_{\mathbf{S}_2(\phi)} \underbrace{\begin{bmatrix} T(\mathbf{c}, \phi, t) \\ V(\mathbf{c}, \phi, t) \\ R(\mathbf{c}, \phi, t) \end{bmatrix}}_{\mathbf{u}(\mathbf{c}, \phi, t)} \quad (5.1.19)$$

In the following considerations, the symbols \mathbf{c} and \mathbf{u} indicate the reference position and the deformation, respectively, using the directions of cylindrical coordinates. For the description in the direction of cartesian coordinates, the symbols \mathbf{x} and \mathbf{w} will be used.

In total, the relative position of the particle with respect to the reference point is expressed by:

$$\begin{aligned} \mathbf{r}_{R_w P}^{\mathcal{B}_w} &= \mathbf{x}^{\mathcal{B}_w} + \mathbf{w}^{\mathcal{B}_w}(\mathbf{x}^{\mathcal{B}_w}, t) \\ &= \mathbf{S}_2(\phi) \mathbf{c} + \mathbf{S}_2(\phi) \mathbf{u}(\mathbf{c}, \phi, t) \\ &= \mathbf{S}_2(\phi) [\mathbf{c} + \mathbf{u}(\mathbf{c}, \phi, t)] \end{aligned} \quad (5.1.20)$$

It should be noted that the rotation matrix $\mathbf{S}_2(\phi)$ is constant. Therefore it is valid:

$$\dot{\mathbf{r}}_{R_w P}^{\mathcal{B}_w} = \mathbf{S}_2(\phi) \dot{\mathbf{u}}(\mathbf{c}, \phi, t), \quad \delta' \mathbf{r}_{R_w P}^{\mathcal{B}_w} = \mathbf{S}_2(\phi) \delta' \mathbf{u}(\mathbf{c}, \phi, t), \quad \ddot{\mathbf{r}}_{R_w P}^{\mathcal{B}_w} = \mathbf{S}_2(\phi) \ddot{\mathbf{u}}(\mathbf{c}, \phi, t), \quad (5.1.21)$$

5.1.3 Summary

By combining the following elements formulated in the previous sections 5.1.1 and 5.1.2

- absolute position of the reference point R_W of the wheelset:

$$\mathbf{r}_{OR_W}^I = \mathbf{r}_{OT_W}^I(s_W) + \mathbf{S}^{IT_W}(s_W) \mathbf{r}_{T_W R_W}^{T_W}(y_W, z_W) \quad (5.1.22)$$

- rotation of the body-fixed frame \mathcal{B}_W of the wheelset, which is used as the floating frame of reference:

$$\mathbf{S}^{IB_W} = \mathbf{S}^{IT_W}(s_W) \mathbf{S}^{T_W \mathcal{A}_W}(\phi_W, \psi_W) \mathbf{S}^{\mathcal{A}_W \mathcal{B}_W}(\chi_W) \quad (5.1.23)$$

- relative position of the point P with respect to the reference point R_W :

$$\mathbf{r}_{R_W P}^{\mathcal{B}_W} = \mathbf{S}_2(\phi) [\mathbf{c} + \mathbf{u}(\mathbf{c}, \phi, t)] \quad (5.1.24)$$

the current position of a particle, which is located at the point P can be described:

$$\begin{aligned} \mathbf{r}_{OP}^I &= \mathbf{r}_{OR_W}^I + \mathbf{S}^{IB_W} \mathbf{r}_{R_W P}^{\mathcal{B}_W} \\ &= \mathbf{r}_{OT_W}^I + \mathbf{S}^{IT_W} \mathbf{r}_{T_W R_W}^{T_W} + \mathbf{S}^{IT_W} \mathbf{S}^{T_W \mathcal{A}_W} \mathbf{S}^{\mathcal{A}_W \mathcal{B}_W} \mathbf{S}_2(\phi) [\mathbf{c} + \mathbf{u}(\mathbf{c}, \phi, t)] \end{aligned} \quad (5.1.25)$$

This formulation is the base for the following considerations. Since these considerations deal only with the wheelset, the index w , which indicates the wheelset, is skipped for the sake of brevity and for a better overview if there is no possibility of an ambiguity.

A general overview on the kinematics, which uses the intermediate sliding frame \mathcal{A} and cylindrical coordinates, is given in Fig.5.1.1.

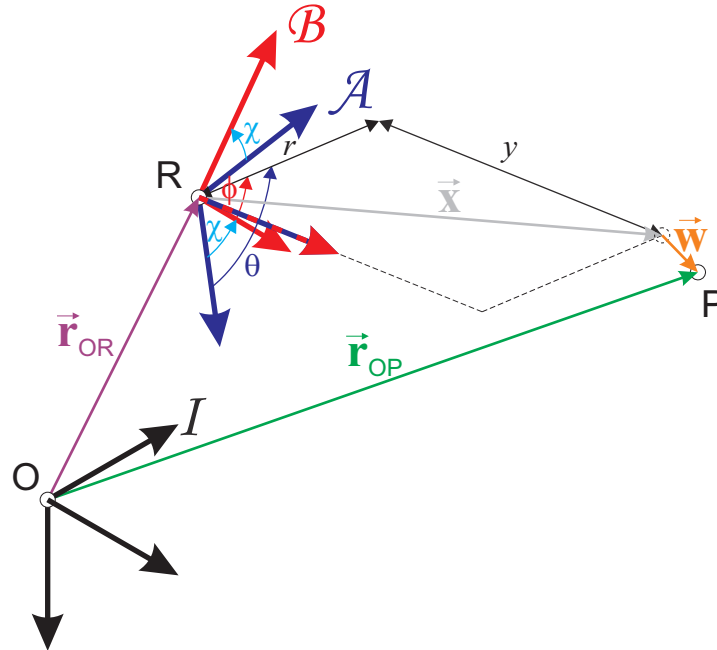


Figure 5.1.1: Kinematics of a particle located at the point P.

It can be seen that the two sequent rotations with the overturning angle χ and the azimuth ϕ are both carried out around the 2-axis. Thereby, the two rotations can be merged into one; here, the

new angle $\theta = \chi + \phi$ is introduced. In total, the kinematics of the point P is formulated in the following way, whereas the index \bar{W} is skipped as mentioned before:

$$\begin{aligned} \mathbf{r}_{OP}^I &= \mathbf{r}_{OR}^I + \mathbf{S}^{IT} \mathbf{S}^{T\mathcal{A}} \mathbf{S}^{\mathcal{A}B} \mathbf{S}_2(\phi) [\mathbf{c} + \mathbf{u}(\mathbf{c}, \phi, t)] \\ &= \mathbf{r}_{OR}^I + \mathbf{S}^{I\mathcal{A}} \underbrace{\mathbf{S}_2(\chi) \mathbf{S}_2(\phi)}_{\mathbf{S}_2(\chi+\phi)} [\mathbf{c} + \mathbf{u}(\mathbf{c}, \phi, t)] = \mathbf{r}_{OR}^I + \mathbf{S}^{I\mathcal{A}} \mathbf{S}_2(\theta) [\mathbf{c} + \mathbf{u}(\mathbf{c}, \phi, t)] \end{aligned} \quad (5.1.26)$$

This description, which uses the sliding frame \mathcal{A} as the reference frame, will be discussed later.

5.2 Generalization of a cyclic structure: The n -tuple of particles

Generally, the equations of motion for a flexible structure are developed by considering a basic element of the structure. In the general case of a flexible body this basic element is an infinitesimal mass particle. This strategy is also applied if the flexible body is considered as a cyclic structure; in this case, however, the basic element can be extended.

As already described, a cyclic system consists of n identical segments, which are arranged in a circular way. Rotors having such a cyclic structure are not rare in technical applications. Examples are bladed discs as used for turbines and turbocompressores, spoked wheels, and disc wheels. For the following consideration the rotational symmetry is exploited. If the zeroth segment contains a particle, then each other segment contains a corresponding particle. These corresponding particles form an n -tuple, which can be seen as a basic unit for the cyclic structure, as shown in Fig.5.2.2

An n -tuple of n identical particles is the most basic generalization of a cyclic structure. The reference position of the j -th particle of the n -tuple is given by:

$$\mathbf{x}^{(j)} = \mathbf{S}_2(\phi_j) \mathbf{c}, \quad \phi_j = \phi_0 + \frac{2\pi}{n} j \quad (5.2.27)$$

The n -tuple is uniquely defined by the vector \mathbf{c} and the initial azimuth ϕ_0 .

A perfectly rotational symmetric structure like a disc wheel can also be described based on this consideration. However, for such a structure the choice of the number of segments n is arbitrary as shown in Fig.5.2.3

An overview of the particles belonging to one n -tuple is given in Figure 5.2.4. In the reference state the particles are located in equidistant way on a circle defined by its radius r and by the distance y between the reference point R and the circle's centre. The azimuth ϕ_0 of the zeroth particle with respect to the 3-axis of the body-fixed frame is given by ϕ_0 . Because of the equidistant distribution of the particles along the circumference the n -tuple is uniquely defined by the coordinates y , r , and ϕ_0 . In the body-fixed frame \mathcal{B} the position of the j -th particle in the reference state is described by the following vector:

$$\mathbf{x}^{\mathcal{B}}(\mathbf{c}, \phi_j) = \mathbf{x}_j^{\mathcal{B}} = \mathbf{S}_2(\phi_j) \mathbf{c}, \quad \phi_j = \phi_0 + \frac{2\pi}{n} j. \quad (5.2.28)$$

The motions are described in the directions of cylindrical coordinates, since these directions have the same orientation for each segment; this is an important aspect regarding the description as a cyclic structure. The displacement of the j -th particle is formulated in the following way:

$$\mathbf{w}^{\mathcal{B}}(\mathbf{c}, \phi_j) = \mathbf{w}_j^{\mathcal{B}} = \mathbf{S}_2(\phi_j) \mathbf{u}(\mathbf{c}, \phi_j) = \mathbf{S}_2(\phi_j) \mathbf{u}^{(j)} \quad (5.2.29)$$

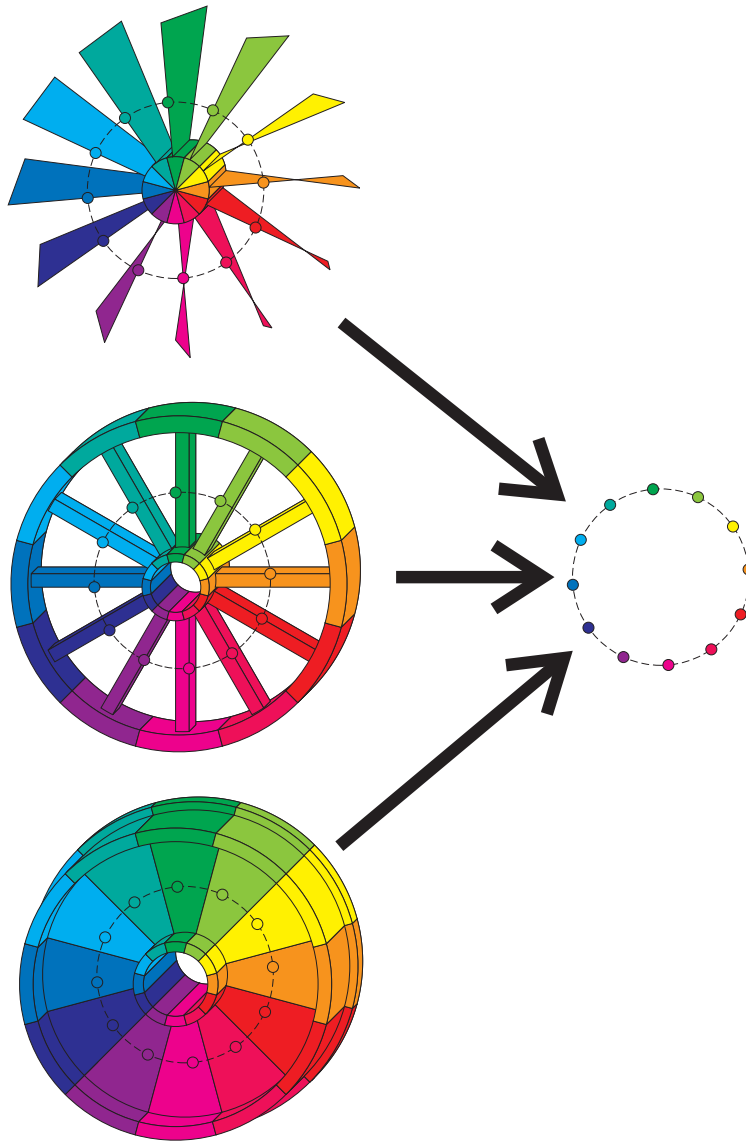


Figure 5.2.2: Examples for cyclic structures and generalization by an n -tuple of corresponding particles; above: bladed disc; middle: spoked wheel; below: disc wheel.

The displacement $\mathbf{u}^{(j)}$ for the j -th particle is introduced for the sake of brevity. If the considered particle is the j -th particle of an n -tuple, which is uniquely defined by ϕ_0 and \mathbf{c} , then the reference coordinates of the particle are given by ϕ_j and \mathbf{c} . Furthermore, if the particles of one arbitrary n -tuple are considered, the dependency on ϕ_0 and \mathbf{c} does not have to be indicated explicitly, since these coordinates define the n -tuple and are therefore valid for all of its particles.

In the following considerations, a formulation using the body-fixed frame \mathcal{B} as the floating frame of reference will be derived to describe the kinematics for the particles of one n -tuple. The current absolute position of the j -th particle is indicated by the point P_j . It can be formulated:

$$\mathbf{r}_{OP_j}^I = \mathbf{r}_{OR}^I + \mathbf{S}^{IB} \left(\mathbf{x}_j^B + \mathbf{w}_j^B \right) = \mathbf{r}_{OR}^I + \mathbf{S}^{IB} \mathbf{S}_2(\phi_j) \left(\mathbf{c} + \mathbf{u}^{(j)} \right) \quad (5.2.30)$$

It should be pointed out that the vectors and matrices, which are used in (5.2.30) for describing the position of the particle, are real; therefore, it is valid:

$$\mathbf{r}_{OR}^I, \mathbf{c}, \mathbf{u}^{(j)} \in \mathbb{R}^3, \mathbf{S}^{IB}, \mathbf{S}_2(\phi_j) \in \mathbb{R}^{3 \times 3} \quad (5.2.31)$$

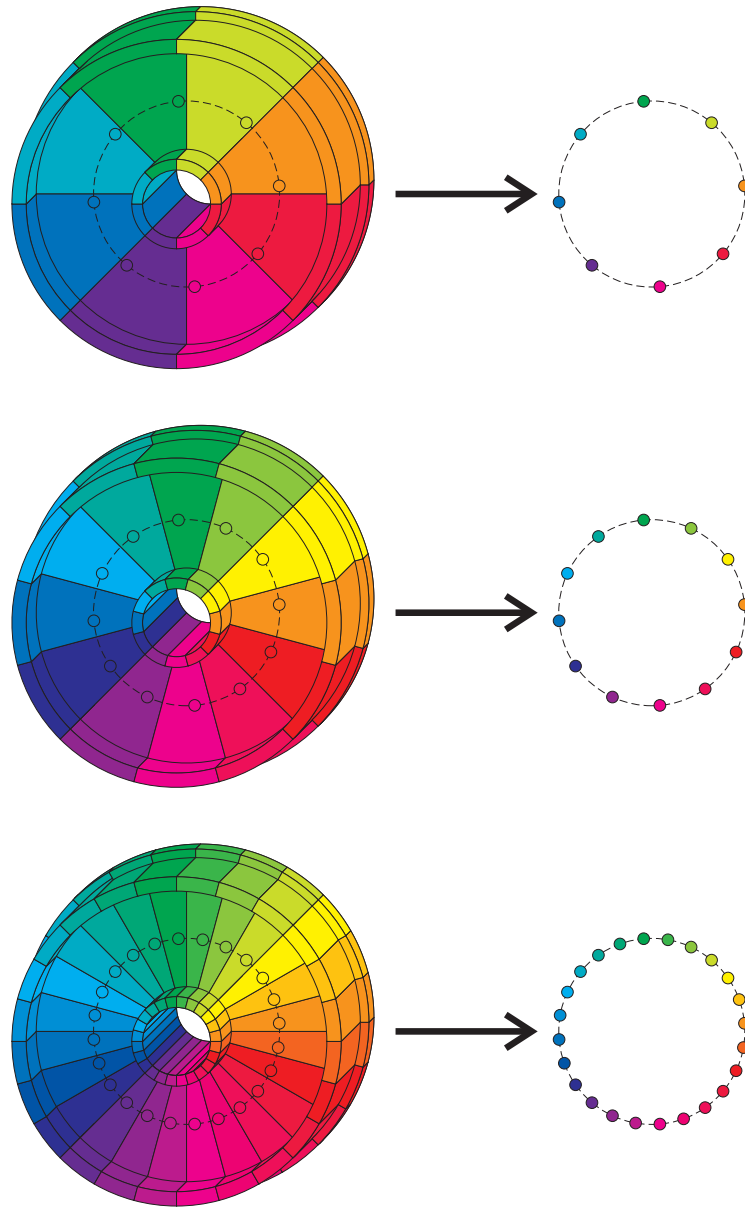


Figure 5.2.3: Arbitrary segmentation for a rotational symmetric structure; above: $n = 8$; middle: $n = 12$; below: $n = 24$.

An overview on the kinematics of the particles belonging to one n -tuple is given in Fig.5.2.5.

According to the concept of cyclic structures discussed in the section 3, the positions of the particles belonging to one n -tuple are described by a discrete Fourier series. For the angle ϕ_j it is valid:

$$\phi_j = \phi_0 + \frac{2\pi}{n}j \Rightarrow \phi_j - \phi_0 = \frac{2\pi}{n}j \Rightarrow e^{ik(\phi_j - \phi_0)} = e^{ik\frac{2\pi}{n}j} = \left(e^{i\frac{2\pi}{n}}\right)^{kj} = \zeta^{kj}, \zeta = e^{i\frac{2\pi}{n}} \quad (5.2.32)$$

Here, $\zeta = e^{i\frac{2\pi}{n}}$ is the root of unity. Based on this, the displacement $\mathbf{u}^{(j)}$ of the j -th particle is expressed in the following way:

$$\mathbf{u}^{(j)} = \sum_{k=k_{\min}}^{k_{\max}} \mathbf{u}_k^{\mathcal{B}} \zeta^{kj} = \sum_{k=k_{\min}}^{k_{\max}} \mathbf{u}_k^{\mathcal{B}} e^{ik(\phi_j - \phi_0)}, k_{\max} - k_{\min} = n - 1 \quad (5.2.33)$$

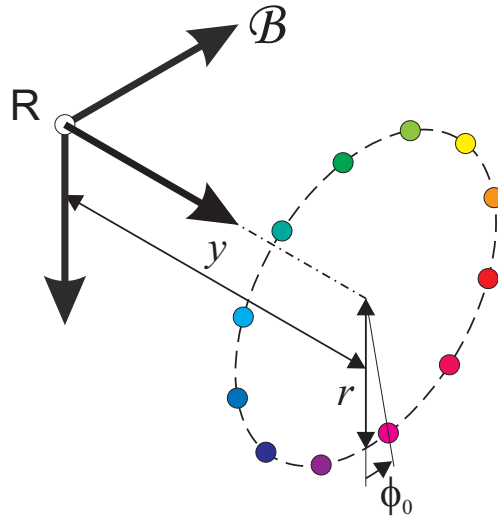


Figure 5.2.4: Corresponding particles forming an n -tuple defined by y , r , and ϕ_0 .

As indicated in (5.2.31), the vectors \mathbf{c} and $\mathbf{u}^{(j)}$ and thereby also the vector $\mathbf{p}^{(j)} = \mathbf{c} + \mathbf{u}^{(j)}$ are real vectors. In the section 3.1.3 the problem of a discrete Fourier series for n values $f_j \in \mathbb{R}$ has been considered; in this context it is reasonable to use certain values for the bounds k_{\min} and k_{\max} . Here, it has to be distinguished whether n is an even or an odd number.

$$\frac{n}{2} \notin \mathbb{N} \wedge n \in \mathbb{N}, \mathbf{u}^{(j)} \in \mathbb{R}^3 : \mathbf{u}^{(j)} = \sum_{k=k_{\min}}^{k_{\max}} \mathbf{u}_k^{\mathcal{B}} \zeta^{kj}, k_{\max} = \frac{n-1}{2}, k_{\min} = -k_{\max} \quad (5.2.34)$$

$$\frac{n}{2} \in \mathbb{N} \wedge n \in \mathbb{N}, \mathbf{u}^{(j)} \in \mathbb{R}^3 : \mathbf{u}^{(j)} = \sum_{k=k_{\min}}^{k_{\max}} \mathbf{u}_k^{\mathcal{B}} \zeta^{kj}, k_{\max} = \frac{n}{2}, k_{\min} = -k_{\max} + 1 \quad (5.2.35)$$

If the bounds k_{\min} and k_{\max} are selected in this way, then it is valid:

$$\mathbf{u}^{(j)} \in \mathbb{R}^3 \Rightarrow \Im \mathbf{u}_0^{\mathcal{B}} = \mathbf{0}, \mathbf{u}_{-k}^{\mathcal{B}} = \overline{\mathbf{u}_k^{\mathcal{B}}}, \Im \mathbf{u}_{\frac{n}{2}}^{\mathcal{B}} = \mathbf{0} \quad (5.2.36)$$

In the body-fixed frame \mathcal{B} the relative position of the j -th particle with respect to the reference point R is given by:

$$\mathbf{r}_{\text{RP}_j}^{\mathcal{B}} = \mathbf{S}_2(\phi_j) (\mathbf{c} + \mathbf{u}^{(j)}) \quad (5.2.37)$$

It will turn out to be useful to formulate the position for the direction of cylindrical coordinates in the following way:

$$\mathbf{c} + \mathbf{u}^{(j)} = \mathbf{c} + \sum_{k=k_{\min}}^{k_{\max}} \mathbf{u}_k^{\mathcal{B}} e^{ik(\phi_j - \phi_0)} = \sum_{k=k_{\min}}^{-1} \underbrace{\mathbf{u}_k^{\mathcal{B}} e^{-ik\phi_0}}_{\mathbf{p}_k^{\mathcal{B}}} e^{ik\phi_j} + \underbrace{\mathbf{c} + \mathbf{u}_0^{\mathcal{B}}}_{\mathbf{p}_0^{\mathcal{B}}} + \sum_{k=1}^{k_{\max}} \underbrace{\mathbf{u}_k^{\mathcal{B}} e^{-ik\phi_0}}_{\mathbf{p}_k^{\mathcal{B}}} e^{ik\phi_j} = \sum_{k=k_{\min}}^{k_{\max}} \mathbf{p}_k^{\mathcal{B}} e^{ik\phi_j} \quad (5.2.38)$$

Thereby, the position $\mathbf{p}^{(j)}$ for the j -th particle is expressed by:

$$\mathbf{p}^{(j)} = \mathbf{c} + \mathbf{u}^{(j)} = \sum_{k=k_{\min}}^{k_{\max}} \mathbf{p}_k^{\mathcal{B}} = e^{ik\phi_j}, \mathbf{p}_k^{\mathcal{B}} = \begin{cases} \mathbf{c} + \mathbf{u}_0^{\mathcal{B}} & \text{for } k = 0 \\ \mathbf{u}_k^{\mathcal{B}} e^{-ik\phi_0} & \text{for } k \neq 0 \end{cases} \quad (5.2.39)$$

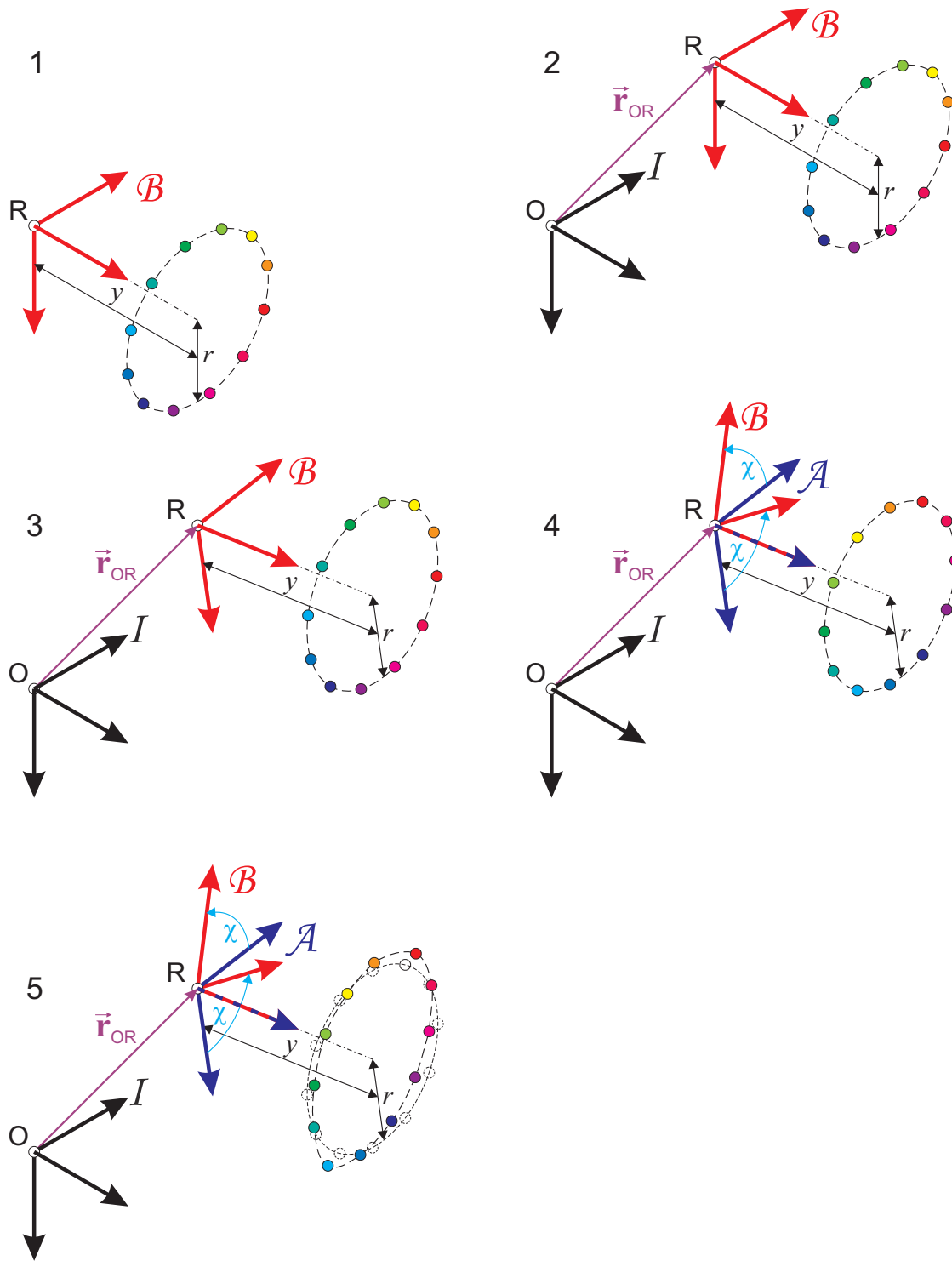


Figure 5.2.5: Kinematics of the particles belonging to one n -tuple; 1: Reference configuration of the n -tuple; 2: Rigid body translation; 3: Rigid body rotation except the overturning motion; 4: Rigid body rotation due to the overturning motion; 5: Relative motions due to deformations.

5.3 Description in the sliding frame

In section 5.1.1 the following matrix describing the rotation of the body-fixed frame \mathcal{B}_W with respect to the inertial frame I has been formulated.

$$\mathbf{S}^{I\mathcal{B}_W} = \mathbf{S}^{I\mathcal{I}_W(s_W)} \mathbf{S}^{\mathcal{I}_W\mathcal{A}_W}(\varphi_W, \psi_W) \mathbf{S}^{\mathcal{A}_W\mathcal{B}_W}(\chi_W) \quad (5.3.40)$$

For the sake of brevity, the index w referring to the wheelset is omitted and the matrices \mathbf{S}^{IT_w} and $\mathbf{S}^{T_w \mathcal{A}_w}$ for the following considerations:

$$\mathbf{S}^{IB} = \mathbf{S}^{IT(s)} \mathbf{S}^{T\mathcal{A}}(\varphi, \psi) \mathbf{S}^{\mathcal{A}B}(\chi) = \mathbf{S}^{I\mathcal{A}}(s, \varphi, \psi) \mathbf{S}^{\mathcal{A}B}(\chi), \quad \mathbf{S}^{\mathcal{A}B} = \mathbf{S}_2(\chi) \quad (5.3.41)$$

Since the rotation from the sliding frame \mathcal{A} to the body-fixed frame \mathcal{B} is the last one in the sequence of rotations, the sliding frame \mathcal{A} performs all motions of the wheelset except the large rotation with the overturning angle χ around the 2-axis.

In section 5.1.3, the following formulation for the absolute position of a particle located at the point P_j has been developed; this formulation is based on the floating frame of reference formulation, which uses the body-fixed frame \mathcal{B} as the reference frame, and the description of the relative position by cylindrical coordinates:

$$\mathbf{r}_{OP_j}^I = \mathbf{r}_{OR}^I + \mathbf{S}^{IB} \mathbf{S}_2(\phi_j) (\mathbf{c} + \mathbf{u}^{(j)}) = \mathbf{r}_{OR}^I + \mathbf{S}^{IB} \mathbf{S}_2(\phi_j) \mathbf{p}^{(j)} \quad (5.3.42)$$

Based on the matrix decomposition according to (5.3.41) the matrix product contained in (5.3.42) can be reformulated in the following way:

$$\mathbf{S}^{IB} \mathbf{S}_2(\phi) = \mathbf{S}^{I\mathcal{A}} \mathbf{S}^{\mathcal{A}B} \mathbf{S}_2(\phi) = \mathbf{S}^{I\mathcal{A}} \mathbf{S}_2(\chi) \mathbf{S}_2(\phi) = \mathbf{S}^{I\mathcal{A}} \mathbf{S}_2(\chi + \phi) = \mathbf{S}^{I\mathcal{A}} \mathbf{S}_2(\theta) \quad (5.3.43)$$

Here, the new azimuth $\theta = \chi + \phi$, which is used in the sliding frame \mathcal{A} , is introduced. By introducing the azimuth θ_j for the j -th particle:

$$\theta = \chi + \phi \Rightarrow \theta_j = \chi + \phi_j \Rightarrow \phi_j = \theta_j - \chi \quad (5.3.44)$$

the description of the position is reformulated in the following way:

$$\mathbf{S}^{IB} \mathbf{S}_2(\phi_j) = \mathbf{S}^{I\mathcal{A}} \mathbf{S}_2(\theta_j) \Rightarrow \mathbf{r}_{OP_j}^I = \mathbf{r}_{OR}^I + \mathbf{S}^{IB} \mathbf{S}_2(\phi_j) \mathbf{p}^{(j)} = \mathbf{r}_{OR}^I + \mathbf{S}^{I\mathcal{A}} \mathbf{S}_2(\theta_j) \mathbf{p}^{(j)} \quad (5.3.45)$$

In the previous section 5.2 the position vector $\mathbf{p}^{(j)}$ has been described by the following expression:

$$\mathbf{p}^{(j)} = \mathbf{c} + \mathbf{u}^{(j)} = \sum_{k=k_{\min}}^{k_{\max}} \mathbf{p}_k^{\mathcal{B}} e^{ik\phi_j} \quad (5.3.46)$$

In order to complete the formulation for the new azimuth θ_j in the sliding frame \mathcal{A} , the azimuth ϕ_j has to be eliminated. By using the relation (5.3.44), the terms $e^{ik\phi_j}$ are reformulated in the following way:

$$e^{ik\phi_j} = e^{ik(\theta_j - \chi)} = e^{ik\theta_j - ik\chi} = e^{-ik\chi} e^{ik\theta_j} \quad (5.3.47)$$

Inserting this into (5.3.46) leads to:

$$\mathbf{p}^{(j)} = \sum_{k=k_{\min}}^{k_{\max}} \mathbf{p}_k^{\mathcal{B}} e^{ik\phi_j} = \sum_{k=k_{\min}}^{k_{\max}} \underbrace{\mathbf{p}_k^{\mathcal{B}} e^{-ik\chi}}_{\mathbf{p}_k^{\mathcal{A}}} e^{ik\theta_j} = \sum_{k=k_{\min}}^{k_{\max}} \mathbf{p}_k^{\mathcal{A}} e^{ik\theta_j} \quad (5.3.48)$$

Thereby the new vectors $\mathbf{p}_k^{\mathcal{A}}$ are introduced. The relation between the vectors $\mathbf{p}_k^{\mathcal{A}}$ and $\mathbf{p}_k^{\mathcal{B}}$, which are used for the formulations using the sliding frame \mathcal{A} and the body-fixed frame \mathcal{B} , respectively, is given by:

$$\mathbf{p}_k^{\mathcal{A}} = \mathbf{p}_k^{\mathcal{B}} e^{-ik\chi} \Leftrightarrow \mathbf{p}_k^{\mathcal{B}} = \mathbf{p}_k^{\mathcal{A}} e^{ik\chi} \quad (5.3.49)$$

By inserting the definition for the vectors $\mathbf{p}_k^{\mathcal{B}}$ according to (5.2.39) it can be formulated:

$$k = 0 : \mathbf{p}_0^{\mathcal{A}} = \mathbf{p}_0^{\mathcal{B}} \underbrace{e^{-i \cdot 0 \cdot \chi}}_1 = \mathbf{c} + \mathbf{u}_0^{\mathcal{B}} = \mathbf{c} + \mathbf{u}_0^{\mathcal{A}} \quad (5.3.50)$$

$$k \neq 0 : \mathbf{p}_k^{\mathcal{A}} = \mathbf{p}_k^{\mathcal{B}} e^{-ik\chi} = \mathbf{u}_k^{\mathcal{B}} e^{-ik\phi_0} e^{-ik\chi} = \underbrace{\mathbf{u}_k^{\mathcal{B}} e^{-ik\chi}}_{\mathbf{u}_k^{\mathcal{A}}} e^{-ik\phi_0} = \mathbf{u}_k^{\mathcal{A}} e^{-ik\phi_0} \quad (5.3.51)$$

From this, the relation between the deformation vectors $\mathbf{u}_k^{\mathcal{A}}$ and $\mathbf{u}_k^{\mathcal{B}}$ is derived:

$$\mathbf{u}_k^{\mathcal{A}} = \mathbf{u}_k^{\mathcal{B}} e^{-ik\chi} \Leftrightarrow \mathbf{u}_k^{\mathcal{B}} = \mathbf{u}_k^{\mathcal{A}} e^{ik\chi} \quad (5.3.52)$$

Because of $e^{i \cdot 0 \cdot \chi} = e^0 = 1$ the generalized relation (5.3.52) also covers the case $\mathbf{u}_0^{\mathcal{A}} = \mathbf{u}_0^{\mathcal{B}}$ applied in (5.3.50). – As introduced in the section 5.2, the displacement $\mathbf{u}^{(j)}$ is a real vector; thereby, it is valid for the vectors $\mathbf{u}_k^{\mathcal{B}}$ of the Fourier series:

$$\overline{\mathbf{u}_k^{\mathcal{B}}} = \mathbf{u}_{-k}^{\mathcal{B}} \quad (5.3.53)$$

From this it follows for the new vectors $\mathbf{u}_k^{\mathcal{A}}$

$$\overline{\mathbf{u}_k^{\mathcal{A}}} = \overline{\mathbf{u}_k^{\mathcal{B}} e^{-ik\chi}} = \overline{\mathbf{u}_k^{\mathcal{B}}} e^{ik\chi} = \mathbf{u}_{-k}^{\mathcal{B}} e^{-i(-k)\chi} = \mathbf{u}_{-k}^{\mathcal{A}} \Rightarrow \overline{\mathbf{u}_k^{\mathcal{A}}} = \mathbf{u}_{-k}^{\mathcal{A}} \quad (5.3.54)$$

For the derivatives it is valid:

$$\mathbf{u}_k^{\mathcal{B}} = \mathbf{u}_k^{\mathcal{A}} e^{ik\chi} \quad (5.3.55)$$

$$\dot{\mathbf{u}}_k^{\mathcal{B}} = \frac{d}{dt} \left(\mathbf{u}_k^{\mathcal{A}} e^{ik\chi} \right) = \left(\dot{\mathbf{u}}_k^{\mathcal{A}} + ik\dot{\chi} \mathbf{u}_k^{\mathcal{A}} \right) e^{ik\chi} = \mathbf{u}_k^{*\mathcal{A}} e^{ik\chi} \quad (5.3.56)$$

$$\ddot{\mathbf{u}}_k^{\mathcal{B}} = \frac{d^2}{dt^2} \left(\mathbf{u}_k^{\mathcal{A}} e^{ik\chi} \right) = \left(\ddot{\mathbf{u}}_k^{\mathcal{A}} + 2ik\dot{\chi} \dot{\mathbf{u}}_k^{\mathcal{A}} + ik\ddot{\chi} \mathbf{u}_k^{\mathcal{A}} - k^2 \dot{\chi}^2 \mathbf{u}_k^{\mathcal{A}} \right) e^{ik\chi} = \mathbf{u}_k^{**\mathcal{A}} e^{ik\chi} \quad (5.3.57)$$

The vectors $\mathbf{u}_k^{*\mathcal{A}}$ and $\mathbf{u}_k^{**\mathcal{A}}$ represent the expressions contained in the brackets. In the following considerations, they will be used repeatedly for the sake of brevity and a better overview.

Regarding the derivatives of the position vector $\mathbf{p}^{(j)}$ it has to be taken into account that the azimuth $\theta = \chi + \phi$ contains the large angle $\chi = \chi(t)$ of the overturning motion. Therefore, it is valid for the derivative of the power $e^{ik\theta_j}$:

$$\frac{d}{dt} e^{ik\theta_j} = \frac{d}{dt} e^{ik(\chi + \phi_j)} = e^{ik(\chi + \phi_j)} ik\dot{\chi} = e^{ik\theta_j} ik\dot{\chi} \quad (5.3.58)$$

From this it follows for the derivatives of the position vector $\mathbf{p}^{(j)}$:

$$\mathbf{p}^{(j)} = \sum_{k=k_{\min}}^{k_{\max}} \mathbf{p}_k^{\mathcal{B}} e^{ik\phi_j} = \sum_{k=k_{\min}}^{k_{\max}} \mathbf{p}_k^{\mathcal{A}} e^{ik\theta_j} \quad (5.3.59)$$

$$\dot{\mathbf{p}}^{(j)} = \sum_{k=k_{\min}}^{k_{\max}} \dot{\mathbf{p}}_k^{\mathcal{B}} e^{ik\phi_j} = \sum_{k=k_{\min}}^{k_{\max}} \left(\dot{\mathbf{p}}_k^{\mathcal{A}} + ik\dot{\chi} \mathbf{p}_k^{\mathcal{A}} \right) e^{ik\theta_j} \quad (5.3.60)$$

$$\ddot{\mathbf{p}}^{(j)} = \sum_{k=k_{\min}}^{k_{\max}} \ddot{\mathbf{p}}_k^{\mathcal{B}} e^{ik\phi_j} = \sum_{k=k_{\min}}^{k_{\max}} \left(\ddot{\mathbf{p}}_k^{\mathcal{A}} + 2ik\dot{\chi} \dot{\mathbf{p}}_k^{\mathcal{A}} + ik\ddot{\chi} \mathbf{p}_k^{\mathcal{A}} - k^2 \dot{\chi}^2 \mathbf{p}_k^{\mathcal{A}} \right) e^{ik\theta_j} \quad (5.3.61)$$

From (5.3.60) the virtual velocity is derived:

$$\delta \dot{\mathbf{p}}^{(j)} = \sum_{k=k_{\min}}^{k_{\max}} \dot{\mathbf{p}}_k^{\mathcal{B}} e^{ik\phi_j} = \sum_{k=k_{\min}}^{k_{\max}} \left(\dot{\mathbf{p}}_k^{\mathcal{A}} + ik\dot{\chi} \mathbf{p}_k^{\mathcal{A}} \right) e^{ik\theta_j} \quad (5.3.62)$$

5.4 Transformation of the linear cyclic system

In the section 3 the description of a linear cyclic system has been discussed. The equation of motion of a linear cyclic system is given by:

$$\mathbf{M}_C \ddot{\mathbf{y}}_C(t) + \mathbf{P}_C \dot{\mathbf{y}}_C(t) + \mathbf{Q}_C \mathbf{y}_C(t) = \mathbf{h}_C(t) \quad (5.4.63)$$

The matrices \mathbf{M}_C , \mathbf{P}_C and \mathbf{Q}_C have the following structure, which is explained for the generalized matrix \mathbf{C}_C :

$$\mathbf{C}_C = \begin{bmatrix} \mathbf{C}^{(0)} & \mathbf{C}^{(1)} & \mathbf{0} & \dots & \mathbf{0} & \mathbf{C}^{(-1)} \\ \mathbf{C}^{(-1)} & \mathbf{C}^{(0)} & \mathbf{C}^{(1)} & \dots & \mathbf{0} & \mathbf{0} \\ \mathbf{0} & \mathbf{C}^{(-1)} & \mathbf{C}^{(0)} & \dots & \mathbf{0} & \mathbf{0} \\ \vdots & \vdots & \vdots & \ddots & \vdots & \vdots \\ \mathbf{0} & \mathbf{0} & \mathbf{0} & \dots & \mathbf{C}^{(0)} & \mathbf{C}^{(1)} \\ \mathbf{C}^{(1)} & \mathbf{0} & \mathbf{0} & \dots & \mathbf{C}^{(-1)} & \mathbf{C}^{(0)} \end{bmatrix} \quad (5.4.64)$$

The matrices \mathbf{M}_C , \mathbf{P}_C and \mathbf{Q}_C are derived from the matrix \mathbf{C}_C by replacing the submatrices $\mathbf{C}^{(l)}$ by the matrices $\mathbf{M}^{(l)}$, $\mathbf{P}^{(l)}$ and $\mathbf{Q}^{(l)}$, respectively. All matrices are assumed to be real matrices, i.e. $\Im \mathbf{M}_C = \mathbf{0}$, $\Im \mathbf{P}_C = \mathbf{0}$, $\Im \mathbf{Q}_C = \mathbf{0}$ and $\Im \mathbf{C}_C = \mathbf{0}$.

The vector $\mathbf{y}_C(t)$ is composed of subvectors; the subvector $\mathbf{y}^{(j)}(t)$ describes the displacement of the j -th segment. The subvectors can be expressed by a discrete Fourier series:

$$\mathbf{y}_C(t) = \begin{bmatrix} \mathbf{y}^{(0)}(t) \\ \vdots \\ \mathbf{y}^{(j)}(t) \\ \vdots \\ \mathbf{y}^{(n-1)}(t) \end{bmatrix}, \quad \mathbf{y}^{(j)}(t) = \sum_{k=k_{\min}}^{k_{\max}} \mathbf{y}_k(t) \zeta^{kj}, \quad \zeta = e^{\frac{2\pi i}{n}}, \quad k_{\max} - k_{\min} = n - 1 \quad (5.4.65)$$

Using this formulation, the equation of motion according to (5.4.63) can be transformed. It is assumed that the vector $\delta' \dot{\mathbf{y}}_C$ is a real vector so that its transpose $\delta' \dot{\mathbf{y}}_C^T$ is equal to its Hermitean transpose $\delta' \dot{\mathbf{y}}_C^H$. The transformation leads to:

$$\begin{aligned} \delta' \dot{\mathbf{y}}_C^T (\mathbf{M}_C \ddot{\mathbf{y}}_C + \mathbf{P}_C \dot{\mathbf{y}}_C + \mathbf{Q}_C \mathbf{y}_C) &= \delta' \dot{\mathbf{y}}_F^H (\mathbf{T}_{CF}^H \mathbf{M}_C \mathbf{T}_{CF} \ddot{\mathbf{y}}_F + \mathbf{T}_{CF}^H \mathbf{P}_C \mathbf{T}_{CF} \dot{\mathbf{y}}_F + \mathbf{T}_{CF}^H \mathbf{Q}_C \mathbf{T}_{CF} \mathbf{y}_F) \\ &= n \sum_{k=k_{\min}}^{k_{\max}} \delta' \dot{\mathbf{y}}_k^H (\mathbf{M}_k \ddot{\mathbf{y}}_k + \mathbf{P}_k \dot{\mathbf{y}}_k + \mathbf{Q}_k \mathbf{y}_k) \end{aligned} \quad (5.4.66)$$

In section 5.3, the following description for the displacement of the j -th particle of an n -tuple by a discrete Fourier series has been developed:

$$\mathbf{u}^{(j)} = \sum_{k=k_{\min}}^{k_{\max}} \mathbf{u}_k^B \zeta^{kj}, \quad k_{\max} - k_{\min} = n - 1, \quad \Im \mathbf{u}^{(j)} = \mathbf{0} \Rightarrow \mathbf{u}_{-k}^B = \overline{\mathbf{u}_k^B}, \quad \Im \mathbf{u}_0^B = \mathbf{0}, \quad \Im \mathbf{u}_{\frac{n}{2}}^B = \mathbf{0} \quad (5.4.67)$$

This description is valid for the body-fixed frame \mathcal{B} . Based on geometrical considerations a formulation for the sliding frame \mathcal{A} has been developed. Here, the relation between the vectors $\mathbf{u}_k^{\mathcal{A}}$ used in the frame \mathcal{A} and the original vectors $\mathbf{u}_k^{\mathcal{B}}$ is given by:

$$\mathbf{u}_k^{\mathcal{B}} e^{-ik\chi} = \mathbf{u}_k^{\mathcal{A}} \Leftrightarrow \mathbf{u}_k^{\mathcal{B}} = \mathbf{u}_k^{\mathcal{A}} e^{ik\chi} \quad (5.4.68)$$

For the derivatives with respect to the time t it is valid:

$$\mathbf{u}_k^{\mathcal{B}} = \mathbf{u}_k^{\mathcal{A}} e^{ik\chi} \quad (5.4.69)$$

$$\dot{\mathbf{u}}_k^{\mathcal{B}} = \left(\dot{\mathbf{u}}_k^{\mathcal{A}} + ik\dot{\chi}\mathbf{u}_k^{\mathcal{A}} \right) e^{ik\chi} \quad (5.4.70)$$

$$\ddot{\mathbf{u}}_k^{\mathcal{B}} = \left(\ddot{\mathbf{u}}_k^{\mathcal{A}} + 2ik\dot{\chi}\dot{\mathbf{u}}_k^{\mathcal{A}} + ik\ddot{\chi}\mathbf{u}_k^{\mathcal{A}} - k^2\dot{\chi}^2\mathbf{u}_k^{\mathcal{A}} \right) e^{ik\chi} \quad (5.4.71)$$

Since the vectors $\mathbf{y}^{(j)}(t)$ describe displacements of particles belonging to the j -th segment, it is obvious to apply the relations (5.4.69), (5.4.69) and (5.4.69), which are valid for single particles, to the vectors \mathbf{y}_k . This leads to:

$$\mathbf{y}_k^{\mathcal{B}} = \mathbf{y}_k^{\mathcal{A}} e^{ik\chi} \quad (5.4.72)$$

$$\dot{\mathbf{y}}_k^{\mathcal{B}} = \left(\dot{\mathbf{y}}_k^{\mathcal{A}} + ik\dot{\chi}\mathbf{y}_k^{\mathcal{A}} \right) e^{ik\chi} \quad (5.4.73)$$

$$\ddot{\mathbf{y}}_k^{\mathcal{B}} = \left(\ddot{\mathbf{y}}_k^{\mathcal{A}} + 2ik\dot{\chi}\dot{\mathbf{y}}_k^{\mathcal{A}} + ik\ddot{\chi}\mathbf{y}_k^{\mathcal{A}} - k^2\dot{\chi}^2\mathbf{y}_k^{\mathcal{A}} \right) e^{ik\chi} \quad (5.4.74)$$

For the vector of the virtual velocity it is derived from (5.4.73):

$$\delta'\dot{\mathbf{y}}_k^{\mathcal{B}} = \left(\delta'\dot{\mathbf{y}}_k^{\mathcal{A}} + ik\delta'\dot{\chi}\mathbf{y}_k^{\mathcal{A}} \right) e^{ik\chi} \quad (5.4.75)$$

The Hermitean transpose is obtained to:

$$\delta'\dot{\mathbf{y}}_k^{\mathcal{B}\text{H}} = \left(\delta'\dot{\mathbf{y}}_k^{\mathcal{A}\text{H}} - ik\delta'\dot{\chi}\mathbf{y}_k^{\mathcal{A}\text{H}} \right) e^{-ik\chi} \quad (5.4.76)$$

Now, the vectors for \mathcal{B} can be replaced. By factoring out the scalar term and collecting the terms separately for the virtual velocities $\delta'\dot{\mathbf{y}}_k^{\mathcal{A}}$ and for the virtual angular velocity $\delta'\dot{\chi}$, the transformation leads to the following result:

$$\begin{aligned} & \delta'\dot{\mathbf{y}}_k^{\mathcal{B}\text{H}} \left(\mathbf{M}_k \ddot{\mathbf{y}}_k^{\mathcal{B}} + \mathbf{P}_k \dot{\mathbf{y}}_k^{\mathcal{B}} + \mathbf{Q}_k \mathbf{y}_k^{\mathcal{B}} \right) \\ &= \left[\delta'\dot{\mathbf{y}}_k^{\mathcal{A}\text{H}} - ik\delta'\dot{\chi}\mathbf{y}_k^{\mathcal{A}\text{H}} \right] e^{-ik\chi} \left(\mathbf{M}_k \left[\ddot{\mathbf{y}}_k^{\mathcal{A}} + 2ik\dot{\chi}\dot{\mathbf{y}}_k^{\mathcal{A}} + ik\ddot{\chi}\mathbf{y}_k^{\mathcal{A}} - k^2\dot{\chi}^2\mathbf{y}_k^{\mathcal{A}} \right] e^{ik\chi} \right. \\ & \quad \left. + \mathbf{P}_k \left[\dot{\mathbf{y}}_k^{\mathcal{A}} + ik\dot{\chi}\mathbf{y}_k^{\mathcal{A}} \right] e^{ik\chi} + \mathbf{Q}_k \mathbf{y}_k^{\mathcal{A}} e^{ik\chi} \right) \\ &= \left[\delta'\dot{\mathbf{y}}_k^{\mathcal{A}\text{H}} - ik\delta'\dot{\chi}\mathbf{y}_k^{\mathcal{A}\text{H}} \right] \left(\mathbf{M}_k \left[\ddot{\mathbf{y}}_k^{\mathcal{A}} + 2ik\dot{\chi}\dot{\mathbf{y}}_k^{\mathcal{A}} + ik\ddot{\chi}\mathbf{y}_k^{\mathcal{A}} - k^2\dot{\chi}^2\mathbf{y}_k^{\mathcal{A}} \right] \right. \\ & \quad \left. + \mathbf{P}_k \left[\dot{\mathbf{y}}_k^{\mathcal{A}} + ik\dot{\chi}\mathbf{y}_k^{\mathcal{A}} \right] + \mathbf{Q}_k \mathbf{y}_k^{\mathcal{A}} \right) \underbrace{e^{ik\chi} e^{-ik\chi}}_1 \\ &= \delta'\dot{\mathbf{y}}_k^{\mathcal{A}\text{H}} \left(\mathbf{M}_k \left[\ddot{\mathbf{y}}_k^{\mathcal{A}} + 2ik\dot{\chi}\dot{\mathbf{y}}_k^{\mathcal{A}} + ik\ddot{\chi}\mathbf{y}_k^{\mathcal{A}} - k^2\dot{\chi}^2\mathbf{y}_k^{\mathcal{A}} \right] + \mathbf{P}_k \left[\dot{\mathbf{y}}_k^{\mathcal{A}} + ik\dot{\chi}\mathbf{y}_k^{\mathcal{A}} \right] + \mathbf{Q}_k \mathbf{y}_k^{\mathcal{A}} \right) \\ & \quad - ik\delta'\dot{\chi}\mathbf{y}_k^{\mathcal{A}\text{H}} \left(\mathbf{M}_k \left[\ddot{\mathbf{y}}_k^{\mathcal{A}} + 2ik\dot{\chi}\dot{\mathbf{y}}_k^{\mathcal{A}} + ik\ddot{\chi}\mathbf{y}_k^{\mathcal{A}} - k^2\dot{\chi}^2\mathbf{y}_k^{\mathcal{A}} \right] + \mathbf{P}_k \left[\dot{\mathbf{y}}_k^{\mathcal{A}} + ik\dot{\chi}\mathbf{y}_k^{\mathcal{A}} \right] + \mathbf{Q}_k \mathbf{y}_k^{\mathcal{A}} \right) \end{aligned} \quad (5.4.77)$$

The final result of (5.4.77) shows that the functions $e^{ik\chi}$ and $e^{-ik\chi}$ are eliminated so that the overturning angle $\chi = \chi(t)$ does not appear as an argument of a nonlinear function. In order to formulate the terms for the complete system, the expression (5.4.77) has to be summed over all periodicities k . Since the virtual velocity $\delta'\dot{\chi}$ does not depend on k , it can be factored out from the

sum. Thereby, it is obtained:

$$\begin{aligned}
& \delta' \dot{\mathbf{y}}_C^T (\mathbf{M}_C \ddot{\mathbf{y}}_C + \mathbf{P}_C \dot{\mathbf{y}}_C + \mathbf{Q}_C \mathbf{y}_C) \\
&= \sum_{k=k_{\min}}^{k_{\max}} \delta' \dot{\mathbf{y}}_k^B H \left(\mathbf{M}_k \ddot{\mathbf{y}}_k^B + \mathbf{P}_k \dot{\mathbf{y}}_k^B + \mathbf{Q}_k \mathbf{y}_k^B \right) \\
&= \sum_{k=k_{\min}}^{k_{\max}} \delta' \dot{\mathbf{y}}_k^A H \left(\mathbf{M}_k \left[\ddot{\mathbf{y}}_k^A + 2ik \dot{\chi} \dot{\mathbf{y}}_k^A + ik \ddot{\chi} \mathbf{y}_k^A - k^2 \dot{\chi}^2 \mathbf{y}_k^A \right] + \mathbf{P}_k \left[\dot{\mathbf{y}}_k^A + ik \dot{\chi} \mathbf{y}_k^A \right] + \mathbf{Q}_k \mathbf{y}_k^A \right) \\
&\quad - \delta' \dot{\chi} \sum_{k=k_{\min}}^{k_{\max}} ik \mathbf{y}_k^A H \left(\mathbf{M}_k \left[\ddot{\mathbf{y}}_k^A + 2ik \dot{\chi} \dot{\mathbf{y}}_k^A + ik \ddot{\chi} \mathbf{y}_k^A - k^2 \dot{\chi}^2 \mathbf{y}_k^A \right] + \mathbf{P}_k \left[\dot{\mathbf{y}}_k^A + ik \dot{\chi} \mathbf{y}_k^A \right] + \mathbf{Q}_k \mathbf{y}_k^A \right)
\end{aligned} \tag{5.4.78}$$

In the case of the flexible wheelset, no circulatoric forces are acting within the structure, i.e. $\mathbf{N}_C = \mathbf{0}$ so that it is valid $\mathbf{Q}_C = \mathbf{K}_C$. Effects, which result from the inertia, are described by the mass matrix \mathbf{M}_C and by the gyroscopic matrix \mathbf{G}_C ; these terms will be considered in a separate section. Beneath the mass matrix and the gyroscopic matrix the stiffness matrix \mathbf{K} is an essential term in the context of a flexible body. Therefore, this term shall be considered more in detail here. For the transformation it is valid:

$$\begin{aligned}
\delta' \dot{\mathbf{y}}_C^T \mathbf{K}_C \mathbf{y}_C &= n \sum_{k=k_{\min}}^{k_{\max}} \delta' \dot{\mathbf{y}}_k^B H \mathbf{K}_k \mathbf{y}_k^B = n \sum_{k=k_{\min}}^{k_{\max}} \left[\delta' \dot{\mathbf{y}}_k^A H - ik \delta' \dot{\chi} \mathbf{y}_k^A H \right] e^{-ik\chi} \mathbf{K}_k \mathbf{y}_k^A e^{ik\chi} \\
&= n \sum_{k=k_{\min}}^{k_{\max}} \left[\delta' \dot{\mathbf{y}}_k^A H \mathbf{K}_k \mathbf{y}_k^A - ik \delta' \dot{\chi} \mathbf{y}_k^A H \mathbf{K}_k \mathbf{y}_k^A \right] \underbrace{e^{-ik\chi} e^{ik\chi}}_1 \\
&= n \sum_{k=k_{\min}}^{k_{\max}} \delta' \dot{\mathbf{y}}_k^A H \mathbf{K}_k \mathbf{y}_k^A - i \delta' \dot{\chi} n \sum_{k=k_{\min}}^{k_{\max}} k \mathbf{y}_k^A H \mathbf{K}_k \mathbf{y}_k^A
\end{aligned} \tag{5.4.79}$$

It can be seen that the terms $\delta' \dot{\mathbf{y}}_k^B H \mathbf{K}_k \mathbf{y}_k^B$ and $\delta' \dot{\mathbf{y}}_k^A H \mathbf{K}_k \mathbf{y}_k^A$, which express the conservative part of the deformation forces for the deformational motions, have an analogous structure. In order to evaluate the second partial sum, the sum is reformulated using the following relation, which is derived in the appendix A.1:

$$\sum_{k=-\hat{k}}^{\hat{k}} X_k = X_0 + \sum_{l=1}^{\hat{k}} (X_l + X_{-l}) \tag{5.4.80}$$

Resolving the Hermitean transposes and applying this transformation leads to:

$$\sum_{k=-\hat{k}}^{\hat{k}} k \mathbf{y}_k^A H \mathbf{K}_k \mathbf{y}_k^A = \sum_{k=-\hat{k}}^{\hat{k}} k \overline{\mathbf{y}}_k^A T \mathbf{K}_k \mathbf{y}_k^A = \underbrace{0 \cdot \overline{\mathbf{y}}_0^A T \mathbf{K}_0 \mathbf{y}_0^A}_0 + \sum_{l=1}^{\hat{k}} \left(l \overline{\mathbf{y}}_l^A T \mathbf{K}_l \mathbf{y}_l^A - l \overline{\mathbf{y}}_{-l}^A T \mathbf{K}_{-l} \mathbf{y}_{-l}^A \right) \tag{5.4.81}$$

The result of the product $\overline{\mathbf{y}}_k^A T \mathbf{K}_k \mathbf{y}_k^A$ is a scalar; therefore, it is not affected by a transposition:

$$\overline{\mathbf{y}}_k^A T \mathbf{K}_k \mathbf{y}_k^A = \left(\overline{\mathbf{y}}_k^A T \mathbf{K}_k \mathbf{y}_k^A \right)^T = \mathbf{y}_k^A T \mathbf{K}_k^T \overline{\mathbf{y}}_k^A \tag{5.4.82}$$

By applying this relation and factoring out the periodicity l it is obtained:

$$\sum_{k=-\hat{k}}^{\hat{k}} k \mathbf{y}_k^A H \mathbf{K}_k \mathbf{y}_k^A = \sum_{l=1}^{\hat{k}} \left(l \overline{\mathbf{y}}_l^A T \mathbf{K}_l \mathbf{y}_l^A - l \overline{\mathbf{y}}_{-l}^A T \mathbf{K}_{-l} \mathbf{y}_{-l}^A \right) = \sum_{l=1}^{\hat{k}} l \left(\overline{\mathbf{y}}_l^A T \mathbf{K}_l \mathbf{y}_l^A - \mathbf{y}_{-l}^A T \mathbf{K}_{-l} \overline{\mathbf{y}}_{-l}^A \right) \tag{5.4.83}$$

With the exception of $k = \frac{n}{2}$ it is valid for the vectors $\mathbf{y}_k^{\mathcal{A}}$:

$$\mathbf{y}_{-k}^{\mathcal{A}} = \overline{\mathbf{y}_k^{\mathcal{A}}} \quad (5.4.84)$$

In the section 3.3.3, the following relation has been determined for the matrices \mathbf{K}_k :

$$\mathbf{K}_k = \mathbf{K}_k^{\text{H}} = \mathbf{K}_{-k}^{\text{T}} \Rightarrow \mathbf{K}_k - \mathbf{K}_{-k}^{\text{T}} = \mathbf{0} \quad (5.4.85)$$

In total it is valid:

$$\begin{aligned} \sum_{k=-\hat{k}}^{\hat{k}} k \mathbf{y}_k^{\mathcal{A}\text{H}} \mathbf{K}_k \mathbf{y}_k^{\mathcal{A}} &= \sum_{l=1}^{\hat{k}} l \left(\overline{\mathbf{y}_l^{\mathcal{A}}}^{\text{T}} \mathbf{K}_l \mathbf{y}_l^{\mathcal{A}} - \mathbf{y}_{-l}^{\mathcal{A}\text{T}} \mathbf{K}_{-l} \mathbf{y}_{-l}^{\mathcal{A}} \right) = \sum_{l=1}^{\hat{k}} l \left(\overline{\mathbf{y}_l^{\mathcal{A}}}^{\text{T}} \mathbf{K}_l \mathbf{y}_l^{\mathcal{A}} - \overline{\mathbf{y}_l^{\mathcal{A}}}^{\text{T}} \mathbf{K}_{-l} \mathbf{y}_l^{\mathcal{A}} \right) \\ &= \sum_{l=1}^{\hat{k}} l \mathbf{y}_l^{\mathcal{A}\text{H}} \underbrace{(\mathbf{K}_l - \mathbf{K}_{-l}^{\text{T}})}_{\mathbf{0}} \mathbf{y}_l^{\mathcal{A}} = 0 \end{aligned} \quad (5.4.86)$$

For the final evaluation, the cases of an odd and an even number n have to be distinguished. For an odd number n , the lower bound k_{\min} and the upper bound k_{\max} only differ by their signs:

$$n \in \mathbb{N} \wedge \frac{n}{2} \notin \mathbb{N} : k_{\max} = \frac{n-1}{2}, k_{\min} = -\frac{n-1}{2} = -k_{\max} \quad (5.4.87)$$

Therefore, the relation (5.4.86) can be applied immediately so that it is obtained:

$$\begin{aligned} \delta' \dot{\mathbf{y}}_{\text{C}}^{\text{T}} \mathbf{K}_{\text{C}} \mathbf{y}_{\text{C}} &= n \sum_{k=k_{\min}}^{k_{\max}} \delta' \dot{\mathbf{y}}_k^{\mathcal{B}\text{H}} \mathbf{K}_k \mathbf{y}_k^{\mathcal{B}} = n \sum_{k=k_{\min}}^{k_{\max}} \delta' \dot{\mathbf{y}}_k^{\mathcal{A}\text{H}} \mathbf{K}_k \mathbf{y}_k^{\mathcal{A}} - i \delta' \dot{\chi} n \sum_{k=k_{\min}}^{k_{\max}} k \mathbf{y}_k^{\mathcal{A}\text{H}} \mathbf{K}_k \mathbf{y}_k^{\mathcal{A}} \\ &= n \sum_{k=k_{\min}}^{k_{\max}} \delta' \dot{\mathbf{y}}_k^{\mathcal{A}\text{H}} \mathbf{K}_k \mathbf{y}_k^{\mathcal{A}} - i \delta' \dot{\chi} n \underbrace{\sum_{k=-k_{\max}}^{k_{\max}} k \mathbf{y}_k^{\mathcal{A}\text{H}} \mathbf{K}_k \mathbf{y}_k^{\mathcal{A}}}_{\mathbf{0}} \end{aligned} \quad (5.4.88)$$

For an even number n the bounds are given by:

$$\frac{n}{2} \in \mathbb{N} : k_{\max} = \frac{n}{2}, k_{\min} = -\frac{n}{2} + 1 \quad (5.4.89)$$

In this case, the sum over k has to be split up before the transformation (5.4.86) can be applied. Thereby, it is obtained:

$$\frac{n}{2} \in \mathbb{N} : \sum_{k=k_{\min}}^{k_{\max}} k \mathbf{y}_k^{\mathcal{A}\text{H}} \mathbf{K}_k \mathbf{y}_k^{\mathcal{A}} = \sum_{k=-\frac{n}{2}+1}^{\frac{n}{2}} k \mathbf{y}_k^{\mathcal{A}\text{H}} \mathbf{K}_k \mathbf{y}_k^{\mathcal{A}} = \underbrace{\sum_{k=-\frac{n}{2}+1}^{\frac{n}{2}-1} k \mathbf{y}_k^{\mathcal{A}\text{H}} \mathbf{K}_k \mathbf{y}_k^{\mathcal{A}}}_{\mathbf{0}} + \mathbf{y}_{\frac{n}{2}}^{\mathcal{A}\text{H}} \mathbf{K}_{\frac{n}{2}} \mathbf{y}_{\frac{n}{2}}^{\mathcal{A}} \quad (5.4.90)$$

5.5 Modal synthesis

The purpose of the modal synthesis is the description of the deformation field. Here, shape functions $\mathbf{W}_I(\mathbf{x}^{\mathcal{B}})$, which depend on the reference location indicated by $\mathbf{x}^{\mathcal{B}}$, are scaled by the modal coordinates $q_I(t)$ and superimposed:

$$\mathbf{w}^{\mathcal{B}}(\mathbf{x}^{\mathcal{B}}, t) = \sum_{I=1}^{N_{\mathcal{B}}} \mathbf{W}_I(\mathbf{x}^{\mathcal{B}}) q_I^{\mathcal{B}}(t) \quad (5.5.91)$$

Generally, the minimum requirement for the shape functions $\mathbf{W}_I(\mathbf{x}^B)$ is that they fulfil the geometric boundary conditions. Usually, selected eigenmodes of the flexible structure are used as shape functions.

Also in the present case, the eigenmodes of the wheelset shall be used; more precisely, it is reasonable to use the eigenmodes of the non-rotating wheelset. Of course, the wheelset performs a large rotation χ , whereby the angular velocity $\dot{\chi}$ can be rather high so that the eigenfrequencies may change due to gyroscopic effects; however, the angular velocity χ depends on the current running speed of the vehicle, which can vary.

In the section 3.3.2 it has been shown that for a cyclic system an eigenvector \mathbf{y}_{CI} has the following structure:

$$\left(\mathbf{M}_C \lambda_I^2 + \mathbf{P}_C \lambda_I + \mathbf{Q}_C \right) \underbrace{\begin{bmatrix} \mathbf{y}_I^{(0)} \\ \mathbf{y}_I^{(1)} \\ \vdots \\ \mathbf{y}_I^{(n-1)} \end{bmatrix}}_{\mathbf{y}_{CI}} = \mathbf{0}, \quad \mathbf{y}_I^{(j)} = \mathbf{Y}_I \zeta^{k_I j} \quad (5.5.92)$$

Each eigenvector \mathbf{y}_{CI} has one and only one periodicity k_I . Furthermore, it has been shown in the section 3.3.3 that for a damped cyclic system double eigenvalues $\lambda_I = \lambda_J$, $I \neq J$, occur for $k \neq 0$; it is valid:

$$\left(\mathbf{M}_C \lambda_I^2 + \mathbf{D}_C \lambda_I + \mathbf{K}_C \right) \mathbf{y}_{CI} = \mathbf{0}, \quad \mathbf{y}_I^{(j)} = \mathbf{Y}_I \zeta^{k_I j} \quad (5.5.93)$$

$$\left(\mathbf{M}_C \lambda_I^2 + \mathbf{D}_C \lambda_I + \mathbf{K}_C \right) \mathbf{y}_{CJ} = \mathbf{0}, \quad \mathbf{y}_J^{(j)} = \mathbf{Y}_J \zeta^{-k_I j} \quad (5.5.94)$$

As described in the section 3.3.3, the double eigenvectors reflect the isotropy of the cyclic structure. Due to this isotropy, the structure has no preferred orientation so that for $k_I \neq 0$ an eigenvibration with the associated eigenfrequency can occur for any spatial orientation. Thereby, two parameters are required in order to determine the actual amplitude and the actual orientation. From the isotropy of the cyclic structure, it also follows that for the modal synthesis where selected eigenmodes are used as shape functions always both eigenmodes associated with a double eigenvalue have to be used; otherwise, an ‘‘artificial anisotropy’’ would be generated.

In the case of the wheelset, the internal damping of the structure is very weak so that it can be neglected and the damping matrix \mathbf{D}_C vanishes. For such an undamped cyclic system, as generally for undamped systems, the eigenvibration is a harmonic motion so that the eigenvalues $\lambda_I = i\omega_I$ are imaginary. In this case, it is valid:

$$\lambda_I = i\omega_I \Rightarrow \left(-\mathbf{M}_C \omega_I^2 + \mathbf{K}_C \right) \mathbf{y}_{CI} = \mathbf{0}, \quad \mathbf{y}_I^{(j)} = \mathbf{Y}_I \zeta^{k_I j} \quad (5.5.95)$$

The matrices \mathbf{M}_C and \mathbf{K}_C and the eigenfrequency $\frac{\omega_I}{2\pi}$ are real; thereby, the conjugation of the eigenvector problem leads to:

$$\mathbf{0} = \overline{\left(-\mathbf{M}_C \omega_I^2 + \mathbf{K}_C \right) \mathbf{y}_{CI}} = \left(-\mathbf{M}_C \omega_I^2 + \mathbf{K}_C \right) \overline{\mathbf{y}_{CI}}, \quad \overline{\mathbf{y}_I^{(j)}} = \overline{\mathbf{Y}_I \zeta^{k_I j}} = \overline{\mathbf{Y}_I} \zeta^{-k_I j} = \mathbf{y}_J^{(j)} \quad (5.5.96)$$

Apparently, for the undamped cyclic system the relation $\mathbf{y}_{CJ} = \overline{\mathbf{y}_{CI}}$ is valid for the two eigenvectors belonging to the double eigenvalue $\lambda_I = \lambda_J = i\omega_I$.

By applying the structure of the cyclic system to the present case, the shape functions \mathbf{U}_I which describe the displacements in the directions of cylindrical coordinates can be formulated in the following way:

$$\mathbf{U}_I(\mathbf{c}, \phi_j) = \mathbf{U}_I(\mathbf{c}, \phi_0) \zeta^{k_I j} = \mathbf{U}_I(\mathbf{c}, \phi_0) e^{ik_I(\phi_j - \phi_0)} \quad (5.5.97)$$

In the section 5.3 a transformation between the descriptions in the body-fixed frame \mathcal{B} and in the sliding frame \mathcal{A} has been developed. For the description in the sliding frame \mathcal{A} the kinematics has to be formulated using the azimuth θ , for which it is valid:

$$\theta = \chi + \phi \Rightarrow \phi_j - \chi \quad (5.5.98)$$

By applying this relation it can be formulated:

$$\begin{aligned} \mathbf{u}(\mathbf{c}, \phi_j, t) &= \sum_{I=1}^{N_B} \mathbf{U}_I(\mathbf{c}, \phi_j) q_I^{\mathcal{B}}(t) = \sum_{I=1}^{N_B} \mathbf{U}_I(\mathbf{c}, \phi_0) e^{ik_I(\phi_j - \phi_0)} q_I^{\mathcal{B}}(t) \\ &= \sum_{I=1}^{N_B} \mathbf{U}_I(\mathbf{c}, \phi_0) e^{ik_I(\theta_j - \chi - \phi_0)} q_I^{\mathcal{B}}(t) = \sum_{I=1}^{N_B} \underbrace{\mathbf{U}_I(\mathbf{c}, \phi_0) e^{ik_I(\theta_j - \phi_0)}}_{\mathbf{U}_I(\mathbf{c}, \theta_j)} \underbrace{e^{-ik_I\chi}}_{q_I^{\mathcal{A}}(t)} q_I^{\mathcal{B}}(t) \end{aligned} \quad (5.5.99)$$

Thereby, the new modal coordinates $q_I^{\mathcal{A}}(t)$ for the formulation in the sliding frame \mathcal{A} are introduced; their relation to the modal coordinates $q_I^{\mathcal{B}}(t)$ used in the body-fixed frame \mathcal{B} is given by:

$$q_I^{\mathcal{A}}(t) = q_I^{\mathcal{B}}(t) e^{-ik_I\chi} \Leftrightarrow q_I^{\mathcal{B}}(t) = q_I^{\mathcal{A}}(t) e^{ik_I\chi} \quad (5.5.100)$$

With respect to the derivatives it has to be taken into account that the azimuth θ_j contains the large rotation angle χ and thereby depends on the time t . Therefore, it is valid:

$$\frac{d}{dt} \mathbf{U}_I(\mathbf{c}, \theta_j) = \frac{d}{d\theta_j} \left(\mathbf{U}_I(\mathbf{c}, \phi_0) e^{ik_I(\theta_j - \phi_0)} \right) \frac{d\theta_j}{dt} = \mathbf{U}_I(\mathbf{c}, \phi_0) e^{ik_I(\theta_j - \phi_0)} ik_I \dot{\chi} = \mathbf{U}_I(\mathbf{c}, \theta_j) ik_I \dot{\chi} \quad (5.5.101)$$

From this, it follows for the deformation velocity $\dot{\mathbf{u}}$ and the deformation acceleration $\ddot{\mathbf{u}}$:

$$\mathbf{u}(\mathbf{c}, \phi_j, t) = \sum_{I=1}^{N_B} \mathbf{U}_I(\mathbf{c}, \phi_j) q_I^{\mathcal{B}} = \sum_{I=1}^{N_B} \mathbf{U}_I(\mathbf{c}, \theta_j) q_I^{\mathcal{A}} \quad (5.5.102)$$

$$\dot{\mathbf{u}}(\mathbf{c}, \phi_j, t) = \sum_{I=1}^{N_B} \mathbf{U}_I(\mathbf{c}, \phi_j) \dot{q}_I^{\mathcal{B}} = \sum_{I=1}^{N_B} \mathbf{U}_I(\mathbf{c}, \theta_j) \left(\dot{q}_I^{\mathcal{A}} + ik_I \dot{\chi} q_I^{\mathcal{A}} \right) \quad (5.5.103)$$

$$\ddot{\mathbf{u}}(\mathbf{c}, \phi_j, t) = \sum_{I=1}^{N_B} \mathbf{U}_I(\mathbf{c}, \phi_j) \ddot{q}_I^{\mathcal{B}} = \sum_{I=1}^{N_B} \mathbf{U}_I(\mathbf{c}, \theta_j) \left(\ddot{q}_I^{\mathcal{A}} + 2ik_I \dot{\chi} \dot{q}_I^{\mathcal{A}} + ik_I \ddot{\chi} q_I^{\mathcal{A}} - k_I^2 \dot{\chi}^2 q_I^{\mathcal{A}} \right) \quad (5.5.104)$$

For the virtual velocity $\delta' \dot{\mathbf{u}}$ it is valid:

$$\delta' \dot{\mathbf{u}}(\mathbf{c}, \phi_j, t) = \sum_{I=1}^{N_B} \mathbf{U}_I(\mathbf{c}, \phi_j) \delta' \dot{q}_I^{\mathcal{B}} = \sum_{I=1}^{N_B} \mathbf{U}_I(\mathbf{c}, \theta_j) \left(\delta' \dot{q}_I^{\mathcal{A}} + ik_I \delta' \dot{\chi} q_I^{\mathcal{A}} \right) \quad (5.5.105)$$

The vector \mathbf{u} describes the deformations in the directions of cylindrical coordinates; therefore, it is equal for both frames \mathcal{B} and \mathcal{A} . The formulation for the directions of cartesian coordinates is obtained to:

$$\mathbf{w}^{\mathcal{B}}(\mathbf{c}, \phi_j, t) = \mathbf{S}_2(\phi_j) \mathbf{u}(\mathbf{c}, \phi_j, t) = \sum_{I=1}^{N_B} \underbrace{\mathbf{S}_2(\phi_j) \mathbf{U}_I(\mathbf{c}, \phi_j)}_{\mathbf{W}_I(\mathbf{c}, \phi_j)} q_I^{\mathcal{B}} = \sum_{I=1}^{N_B} \mathbf{W}_I(\mathbf{c}, \phi_j) q_I^{\mathcal{B}} \quad (5.5.106)$$

Thereby, the shape functions $\mathbf{W}_I(\mathbf{c}, \phi_j) = \mathbf{S}_2(\phi_j) \mathbf{U}_I(\mathbf{c}, \phi_j)$ for cartesian coordinates are defined. The deformation and their derivatives shall now be transformed into the sliding frame \mathcal{A} . Here, the following relation is used:

$$\mathbf{S}^{\mathcal{A}\mathcal{B}} \mathbf{S}_2(\phi_j) = \mathbf{S}_2(\chi) \mathbf{S}_2(\phi_j) = \mathbf{S}_2(\chi + \phi_j) = \mathbf{S}_2(\theta_j) \quad (5.5.107)$$

By applying this relation it is obtained:

$$\mathbf{S}^{\mathcal{A}\mathcal{B}} \mathbf{w}^{\mathcal{B}} = \underbrace{\mathbf{S}^{\mathcal{A}\mathcal{B}} \mathbf{S}_2(\phi_j)}_{\mathbf{S}_2(\theta_j)} \mathbf{u}(\mathbf{c}, \phi_j, t) = \sum_{I=1}^{N_B} \underbrace{\mathbf{S}_2(\theta_j) \mathbf{U}_I(\mathbf{c}, \theta_j)}_{\mathbf{W}_I(\mathbf{c}, \theta_j)} q_I^{\mathcal{A}} \quad (5.5.108)$$

$$\mathbf{S}^{\mathcal{A}\mathcal{B}} \dot{\mathbf{w}}^{\mathcal{B}} = \underbrace{\mathbf{S}^{\mathcal{A}\mathcal{B}} \mathbf{S}_2(\phi_j)}_{\mathbf{S}_2(\theta_j)} \dot{\mathbf{u}}(\mathbf{c}, \phi_j, t) = \sum_{I=1}^{N_B} \underbrace{\mathbf{S}_2(\theta_j) \mathbf{U}_I(\mathbf{c}, \theta_j)}_{\mathbf{W}_I(\mathbf{c}, \theta_j)} \left(\dot{q}_I^{\mathcal{A}} + ik_I \dot{\chi} q_I^{\mathcal{A}} \right) \quad (5.5.109)$$

$$\mathbf{S}^{\mathcal{A}\mathcal{B}} \ddot{\mathbf{w}}^{\mathcal{B}} = \underbrace{\mathbf{S}^{\mathcal{A}\mathcal{B}} \mathbf{S}_2(\phi_j)}_{\mathbf{S}_2(\theta_j)} \ddot{\mathbf{u}}(\mathbf{c}, \phi_j, t) = \sum_{I=1}^{N_B} \underbrace{\mathbf{S}_2(\theta_j) \mathbf{U}_I(\mathbf{c}, \theta_j)}_{\mathbf{W}_I(\mathbf{c}, \theta_j)} \left(\ddot{q}_I^{\mathcal{A}} + 2ik_I \dot{\chi} \dot{q}_I^{\mathcal{A}} + ik_I \ddot{\chi} q_I^{\mathcal{A}} - k_I^2 \dot{\chi}^2 q_I^{\mathcal{A}} \right) \quad (5.5.110)$$

Here, the notations $\mathbf{S}^{\mathcal{A}\mathcal{B}} \dot{\mathbf{w}}^{\mathcal{B}}$ and $\mathbf{S}^{\mathcal{A}\mathcal{B}} \ddot{\mathbf{w}}^{\mathcal{B}}$, which might appear unnecessary complicated, are used in order to point out that these expressions describe the deformation velocity and the deformation acceleration in the sliding frame \mathcal{A} . In contrast to this, the vectors $\dot{\mathbf{w}}^{\mathcal{A}}$ and $\ddot{\mathbf{w}}^{\mathcal{A}}$ contain derivatives of the rotation matrix $\mathbf{S}^{\mathcal{A}\mathcal{B}}$ and thereby also the relative angular velocity $\omega_{\mathcal{A}\mathcal{B}}^{\mathcal{A}}$ between the frames \mathcal{A} and \mathcal{B} .

According to (5.5.97) the shape functions $\mathbf{U}_I(\mathbf{c}, \phi_j)$ have been formulated in the following way:

$$\mathbf{U}_I(\mathbf{c}, \phi_j) = \mathbf{U}_I(\mathbf{c}, \phi_0) \zeta^{k_I j} = \mathbf{U}_I(\mathbf{c}, \phi_0) e^{ik_I(\phi_j - \phi_0)} \quad (5.5.111)$$

Regarding the derivation of the equations, this formulation is very compact. For practical applications, however, a formulation using real vectors is more useful. This formulation shall be derived next. For $k_I \neq 0$ the eigenmodes, which are used as the shape functions, are associated to double eigenvalues $\lambda_I = \lambda_J$, $I \neq J$. Furthermore, it can be derived from the eigenvector problem (5.5.96) for an undamped cyclic system, the second eigenvector $\mathbf{U}_J(\mathbf{c}, \phi_j)$ is obtained as the complex conjugate of the first eigenvector $\mathbf{U}_I(\mathbf{c}, \phi_j)$. For the pair of the two terms, which use the double eigenmodes as the shape functions, it is valid:

$$\begin{aligned} \mathbf{U}_I(\mathbf{c}, \phi_j) q_I^{\mathcal{B}} + \mathbf{U}_J(\mathbf{c}, \phi_j) q_J^{\mathcal{B}} &= \mathbf{U}_I(\mathbf{c}, \phi_j) q_I^{\mathcal{B}} + \overline{\mathbf{U}_I(\mathbf{c}, \phi_j)} q_J^{\mathcal{B}} \\ &= \underbrace{\Re \mathbf{U}_I(\mathbf{c}, \phi_j)}_{\mathbf{U}_{I1}(\mathbf{c}, \phi_j)} \underbrace{\left(q_I^{\mathcal{B}} + q_J^{\mathcal{B}} \right)}_{q_{I1}^{\mathcal{B}}} + \underbrace{\Im \mathbf{U}_I(\mathbf{c}, \phi_j)}_{\mathbf{U}_{I2}(\mathbf{c}, \phi_j)} \underbrace{\left(q_I^{\mathcal{B}} - q_J^{\mathcal{B}} \right)}_{q_{I2}^{\mathcal{B}}} \end{aligned} \quad (5.5.112)$$

Thereby, the real shape functions $\mathbf{U}_{I1}(\mathbf{c}, \phi_j) = \Re \mathbf{U}_I(\mathbf{c}, \phi_j)$ and $\mathbf{U}_{I2}(\mathbf{c}, \phi_j) = \Im \mathbf{U}_I(\mathbf{c}, \phi_j)$ and the real modal coordinates $q_{I1}^{\mathcal{B}} = q_I^{\mathcal{B}} + q_J^{\mathcal{B}}$ and $q_{I2}^{\mathcal{B}} = i(q_I^{\mathcal{B}} - q_J^{\mathcal{B}})$ are introduced. In an analogous way, the real shape functions $\mathbf{U}_{I1}(\mathbf{c}, \theta_j)$ and $\mathbf{U}_{I2}(\mathbf{c}, \theta_j)$ and the real modal coordinates $q_{I1}^{\mathcal{A}}$ and $q_{I2}^{\mathcal{A}}$ used for the description in the sliding frame \mathcal{A} are defined:

$$\mathbf{U}_{I1}(\mathbf{c}, \theta_j) = \Re \mathbf{U}_I(\mathbf{c}, \theta_j), \quad \mathbf{U}_{I2}(\mathbf{c}, \theta_j) = \Im \mathbf{U}_I(\mathbf{c}, \theta_j), \quad q_{I1}^{\mathcal{A}} = q_I^{\mathcal{A}} + q_J^{\mathcal{A}}, \quad q_{I2}^{\mathcal{A}} = i \left(q_I^{\mathcal{A}} - q_J^{\mathcal{A}} \right) \quad (5.5.113)$$

Based on this, the terms according to (5.5.102), (5.5.103) and (5.5.104) using a pair of eigenmodes belonging to a double eigenvalue can be reformulated in the following way:

$$\begin{aligned} \mathbf{U}_I(\mathbf{c}, \phi_j) \dot{q}_I^B + \mathbf{U}_J(\mathbf{c}, \phi_j) \dot{q}_J^B &= \mathbf{U}_I(\mathbf{c}, \theta_j) \dot{q}_I^A + \mathbf{U}_J(\mathbf{c}, \theta_j) \dot{q}_J^A \\ &= \mathbf{U}_{I1}(\mathbf{c}, \theta_j) \dot{q}_{I1}^A + \mathbf{U}_{I2}(\mathbf{c}, \theta_j) \dot{q}_{I2}^A \end{aligned} \quad (5.5.114)$$

$$\begin{aligned} \mathbf{U}_I(\mathbf{c}, \phi_j) \ddot{q}_I^B + \mathbf{U}_J(\mathbf{c}, \phi_j) \ddot{q}_J^B &= \mathbf{U}_I(\mathbf{c}, \theta_j) \left(\ddot{q}_I^A + ik_I \dot{\chi} \dot{q}_I^A \right) + \mathbf{U}_J(\mathbf{c}, \theta_j) \left(\ddot{q}_J^A + ik_J \dot{\chi} \dot{q}_J^A \right) \\ &= \mathbf{U}_{I1}(\mathbf{c}, \theta_j) \left(\ddot{q}_{I1}^A + k_I \dot{\chi} \dot{q}_{I2}^A \right) + \mathbf{U}_{I2}(\mathbf{c}, \theta_j) \left(\ddot{q}_{I2}^A - k_I \dot{\chi} \dot{q}_{I1}^A \right) \end{aligned} \quad (5.5.115)$$

$$\begin{aligned} \mathbf{U}_I(\mathbf{c}, \phi_j) \ddot{q}_I^B + \mathbf{U}_J(\mathbf{c}, \phi_j) \ddot{q}_J^B &= \mathbf{U}_I(\mathbf{c}, \theta_j) \left(\ddot{q}_I^A + 2ik_I \dot{\chi} \dot{q}_I^A + ik_I \ddot{\chi} \dot{q}_I^A - k_I^2 \dot{\chi}^2 \dot{q}_I^A \right) \\ &\quad + \mathbf{U}_J(\mathbf{c}, \theta_j) \left(\ddot{q}_J^A + 2ik_J \dot{\chi} \dot{q}_J^A + ik_J \ddot{\chi} \dot{q}_J^A - k_J^2 \dot{\chi}^2 \dot{q}_J^A \right) \\ &= \mathbf{U}_{I1}(\mathbf{c}, \theta_j) \left(\ddot{q}_{I1}^A + 2k_I \dot{\chi} \dot{q}_{I2}^A + k_I \ddot{\chi} \dot{q}_{I2}^A - k_I^2 \dot{\chi}^2 \dot{q}_{I1}^A \right) \\ &\quad + \mathbf{U}_{I2}(\mathbf{c}, \theta_j) \left(\ddot{q}_{I2}^A - 2k_I \dot{\chi} \dot{q}_{I1}^A + k_I \ddot{\chi} \dot{q}_{I1}^A - k_I^2 \dot{\chi}^2 \dot{q}_{I2}^A \right) \end{aligned} \quad (5.5.116)$$

5.6 Structural dynamics model of the wheelset

To describe the flexible body by a modal synthesis, shape functions are required. For these shape functions, eigenmodes of the body are often used. In this section a structural dynamics model of the wheelset, from which the eigenmodes are obtained, is developed. This model is based on the finite element method. As described in section 2.1.2, the finite element method is a numerical method for boundary value problems. Although the problem of determining eigenmodes of a flexible structure cannot be solved analytically in the present case of the wheelset, it should be noted that numerical methods generally introduce certain errors into the solution; these errors usually grow with the order of the problem to be solved. Therefore, it is desirable to reduce the order of the numerical problem. By exploiting symmetry properties this can be done without loss of accuracy.

In Fig.5.6.6 the wheelset is displayed. This wheelset is a trailing wheelset equipped with two brake discs. It is used by DB (Deutsche Bahn = German Railways) in passenger coaches for long distance traffic; it is suitable for running speeds up to 200 km/h. The axle, the wheels, and the hubs of the brake discs consist of steel, while the brake discs except their hubs consist of cast iron. The original brake discs possess fins for the cooling; in the present model these fins are not modelled explicitly, but their influence is considered by multiplying the density and the shear modulus with reduction factor equal to the filling grade. Furthermore, also the inner rings of the roller bearings, which also consist of steel, are taken into account, since these components cause a strong increase of the bending stiffness of the journals.

From Fig.5.6.6 it can be seen that the wheelset is rotational symmetric with respect to the y-axis. Therefore, a semianalytic solution for rotational symmetric structures will be developed in the following sections. Furthermore the present wheelset is symmetric with respect to the middle cross plain, i.e. the plain spanned by the x- and the z-axis; this symmetry is independent of the rotational symmetry. As it will turn out, both symmetries can be exploited to reduce the order of the finite element model without loss of accuracy.

The basis for the structural dynamics are Navier's equations for a linear elastic material. For the

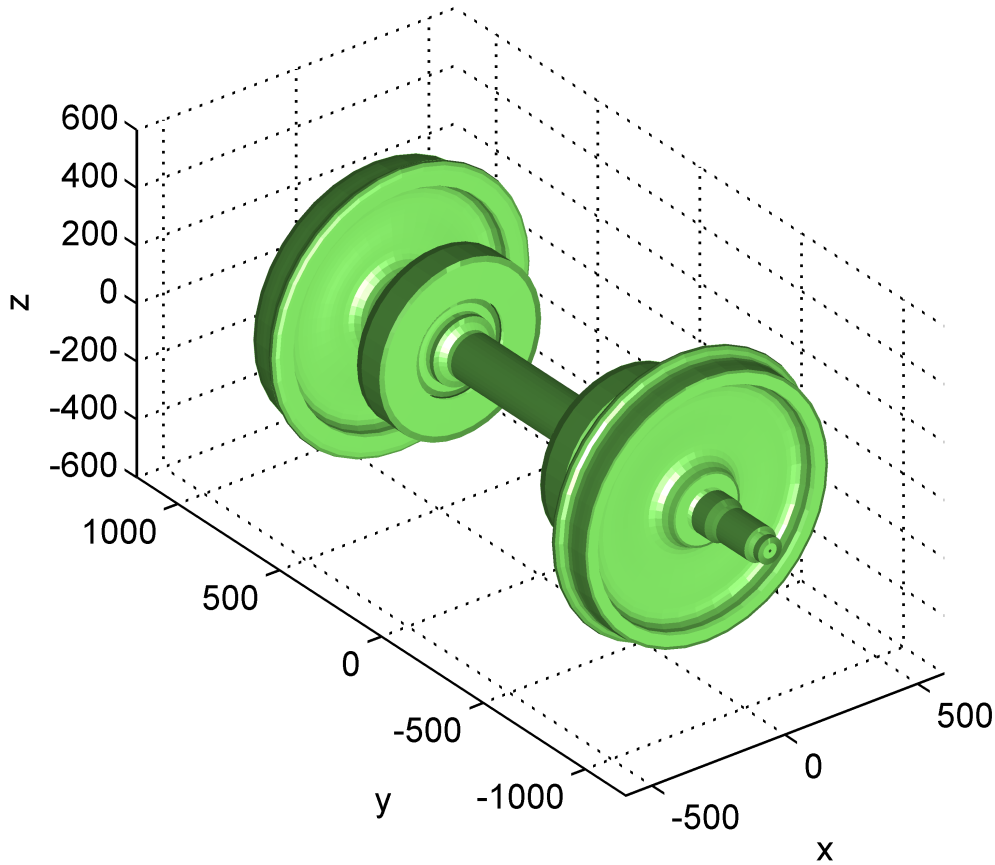


Figure 5.6.6: Geometric shape of the wheelset.

deformations in the directions of Cartesian coordinates, they are given by:

$$\frac{\partial^2 U}{\partial x^2} + \frac{\partial^2 U}{\partial y^2} + \frac{\partial^2 U}{\partial z^2} + \frac{1}{1-2\nu} \frac{\partial}{\partial x} \left(\frac{\partial U}{\partial x} + \frac{\partial V}{\partial y} + \frac{\partial W}{\partial z} \right) - \frac{\rho}{G} \frac{\partial^2 U}{\partial t^2} = 0 \quad (5.6.117)$$

$$\frac{\partial^2 V}{\partial x^2} + \frac{\partial^2 V}{\partial y^2} + \frac{\partial^2 V}{\partial z^2} + \frac{1}{1-2\nu} \frac{\partial}{\partial y} \left(\frac{\partial U}{\partial x} + \frac{\partial V}{\partial y} + \frac{\partial W}{\partial z} \right) - \frac{\rho}{G} \frac{\partial^2 V}{\partial t^2} = 0 \quad (5.6.118)$$

$$\frac{\partial^2 W}{\partial x^2} + \frac{\partial^2 W}{\partial y^2} + \frac{\partial^2 W}{\partial z^2} + \frac{1}{1-2\nu} \frac{\partial}{\partial z} \left(\frac{\partial U}{\partial x} + \frac{\partial V}{\partial y} + \frac{\partial W}{\partial z} \right) - \frac{\rho}{G} \frac{\partial^2 W}{\partial t^2} = 0 \quad (5.6.119)$$

Here, G , ν and ρ denote the shear modulus, Poisson's ratio and the density of the material, respectively. – As described in section 5.1.2 the reference position of a particle of the wheelset described in the body-fixed frame \mathcal{B} is given by:

$$\mathbf{x}^{\mathcal{B}} = \mathbf{S}_2(\phi) \mathbf{c} = \begin{bmatrix} r \sin \phi \\ y \\ r \cos \phi \end{bmatrix} = \begin{bmatrix} x \\ y \\ z \end{bmatrix} \quad (5.6.120)$$

Thereby the relation between the Cartesian coordinates x and z in the transversal directions on the one hand and the polar coordinates r and ϕ on the other hand is given by:

$$x = r \sin \phi, \quad z = r \cos \phi \quad (5.6.121)$$

In the following considerations, the wheelset is regarded as a rotational symmetric structure. Therefore, Navier's equations are expressed in cylindrical coordinates. The derivation of Navier's equation for cylindrical coordinates is quite tedious. Thus, the detailed derivation can be found in the appendix B.4. As a result, the following three scalar equations are obtained:

$$0 = \frac{1}{r^2} \frac{\partial^2 T}{\partial \phi^2} + \frac{2}{r^2} \frac{\partial R}{\partial \phi} - \frac{T}{r^2} + \frac{1}{r} \frac{\partial T}{\partial r} + \frac{\partial^2 T}{\partial r^2} + \frac{\partial^2 T}{\partial y^2} + \frac{1}{1-2\nu} \frac{1}{r} \frac{\partial}{\partial \phi} \left(\frac{1}{r} \frac{\partial T}{\partial \phi} + \frac{R}{r} + \frac{\partial R}{\partial r} + \frac{\partial V}{\partial y} \right) - \frac{\rho}{G} \frac{\partial^2 T}{\partial t^2} \quad (5.6.122)$$

$$0 = \frac{1}{r^2} \frac{\partial^2 V}{\partial \phi^2} + \frac{1}{r} \frac{\partial V}{\partial r} + \frac{\partial^2 V}{\partial r^2} + \frac{\partial^2 V}{\partial y^2} + \frac{1}{1-2\nu} \frac{\partial}{\partial y} \left(\frac{1}{r} \frac{\partial T}{\partial \phi} + \frac{R}{r} + \frac{\partial R}{\partial r} + \frac{\partial V}{\partial y} \right) - \frac{\rho}{G} \frac{\partial^2 V}{\partial t^2} \quad (5.6.123)$$

$$0 = \frac{1}{r^2} \frac{\partial^2 R}{\partial \phi^2} - \frac{2}{r^2} \frac{\partial T}{\partial \phi} - \frac{R}{r^2} + \frac{1}{r} \frac{\partial R}{\partial r} + \frac{\partial^2 R}{\partial r^2} + \frac{\partial^2 R}{\partial y^2} + \frac{1}{1-2\nu} \frac{\partial}{\partial r} \left(\frac{1}{r} \frac{\partial T}{\partial \phi} + \frac{R}{r} + \frac{\partial R}{\partial r} + \frac{\partial V}{\partial y} \right) - \frac{\rho}{G} \frac{\partial^2 R}{\partial t^2} \quad (5.6.124)$$

For a rotational symmetric structure the material parameters G , ν and ρ do not depend on the angle ϕ , but only on the radial coordinate r and the axial coordinate y :

$$G = G(r, y), \quad \nu = \nu(r, y), \quad \rho = \rho(r, y) \quad (5.6.125)$$

As it has been shown in section 4.2, Navier's equations can be reduced by the following semi-analytic solution:

$$\mathbf{u} = \underbrace{\mathbf{u}_k(r, \phi, y)}_{\hat{\mathbf{u}}_k(y, z)} e^{ik\phi} e^{i\omega_k t} = \underbrace{\hat{\mathbf{u}}_k(r, y)}_{\mathbf{u}_k(r, \phi, y)} e^{ik\phi} e^{i\omega_k t}, \quad k \in \mathbb{Z} \quad (5.6.126)$$

As a result, it is obtained:

$$0 = -\frac{k^2+1}{r^2} T_k + \frac{\partial^2 T_k}{\partial y^2} + \frac{\partial^2 T_k}{\partial r^2} - \frac{1}{r} \frac{\partial T_k}{\partial r} + \frac{2ik}{r^2} R_k + \frac{1}{1-2\nu} \frac{ik}{r} \left(\frac{ik}{r} T_k + \frac{R_k}{r} + \frac{\partial R_k}{\partial r} + \frac{\partial V_k}{\partial y} \right) + \omega_k^2 T_k \quad (5.6.127)$$

$$0 = -\frac{k^2}{r^2} V_k + \frac{\partial^2 V_k}{\partial y^2} + \frac{\partial^2 V_k}{\partial r^2} - \frac{1}{r} \frac{\partial V_k}{\partial r} + \frac{1}{1-2\nu} \frac{\partial}{\partial y} \left(\frac{ik}{r} T_k + \frac{R_k}{r} + \frac{\partial R_k}{\partial r} + \frac{\partial V_k}{\partial y} \right) + \omega_k^2 V_k \quad (5.6.128)$$

$$0 = -\frac{k^2+1}{r^2} R_k + \frac{\partial^2 R_k}{\partial y^2} + \frac{\partial^2 R_k}{\partial r^2} - \frac{1}{r} \frac{\partial R_k}{\partial r} - \frac{2ik}{r^2} T_k + \frac{1}{1-2\nu} \frac{\partial}{\partial r} \left(\frac{ik}{r} T_k + \frac{R_k}{r} + \frac{\partial R_k}{\partial r} + \frac{\partial V_k}{\partial y} \right) + \omega_k^2 R_k \quad (5.6.129)$$

In section 4.5.2 an annular finite element with a quadrilateral cross section is developed based on this semi-analytic solution.

In total, exploitation of the rotational symmetry and the plain symmetry enables a drastical reduction of the grid used for the finite element model; this grid is displayed in Fig.5.6.7. The grid is inspired by the model by Heiß presented in [17], but slightly refined. In total the grid possesses 499 nodes and 386 elements. As the grid shows, the half wheelset consists of an axle, one wheel and one brake disc.

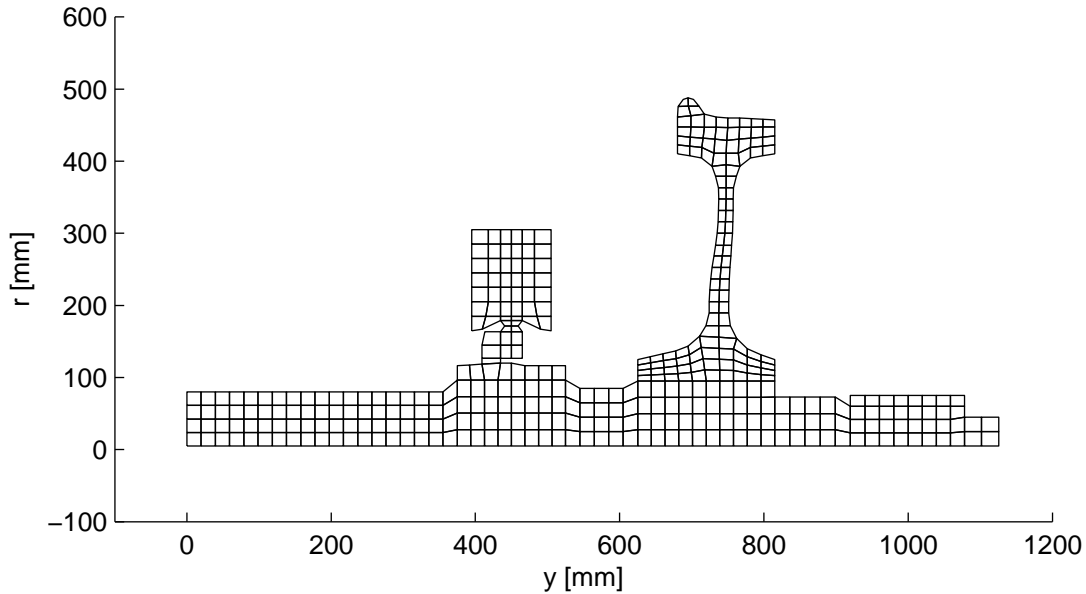


Figure 5.6.7: Finite element grid for the wheelset.

the eigenmodes can be classified by two properties regarding the symmetry, i.e. the periodicity k regarding the rotational symmetry on the one hand and the symmetric or antimetric shape regarding the symmetry with respect to the middle cross plain on the other hand. In this section, some eigenmodes illustrating these properties will be shown. It should be noted that a detailed analysis of the eigenmodes of a wheelset very similar to the one treated here has been given by Heiss in his thesis [17]; the most important results of the work by Heiss are also presented and discussed in the book by Gasch, Knothe, and Liebich [15]. Therefore, the following discussion of the results can be kept comparatively brief.

In Table 5.6.1 some symmetric and antimetric eigenmodes for different periodicities k are displayed. It can be seen that for the periodicities $k \geq 2$ nearly identical eigenfrequencies occur for the symmetric and antimetric eigenmodes. Furthermore, for these eigenmodes the motions are limited to the wheels, while the axle remains nearly unaffected. The explanation can be obtained from the consideration of one n -tuple: The resulting centre of gravity of one n -tuple is only influenced by displacements having the periodicities $k = 0$ or $k = 1$; for $k \geq 2$ the resulting centre of gravity is unaffected by the displacements. In the present case this means that no resulting force is exchanged between the axle and the wheels. As a result, for $k \geq 2$ the wheels vibrate as if they were clamped at their hubs.

In Tab.5.6.2 the eigenmodes associated with the four lowest eigenfrequencies for $k = 1$ are displayed. The eigenmodes associated with the eigenfrequencies of 83.376 Hz and 239.78 Hz are symmetric, while those associated with the eigenfrequencies of 147.20 Hz and 414.65 Hz are antimetric. The images show that these eigenmodes are mainly characterized by bending deformations of the axle and inclinations of the wheels and the brake discs. Furthermore, as discussed in section 3.3.3, double eigenvalues occur; Tab.5.6.2 illustrates the relation between the two eigenmodes associated with a double eigenvalue: For the present case of the periodicity $k = 1$ the two eigenmodes are rotated against each other by an angle of 90° or $\pi/2$.

In Table 5.6.3 some symmetric eigenmodes for different periodicities $k \geq 2$ are displayed. Also here, double eigenmodes occur, which are rotated against each other.

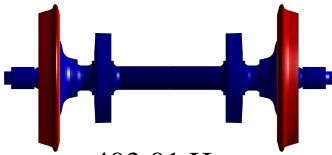
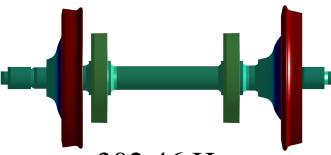
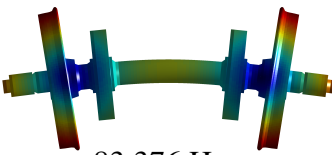





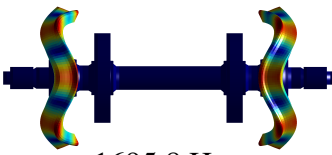
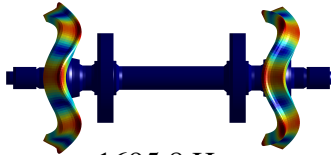
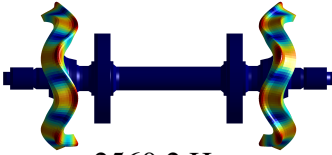
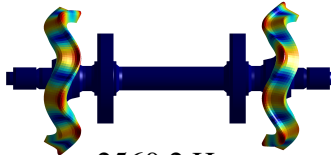
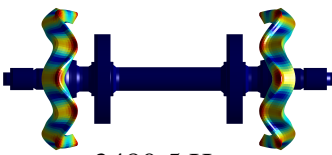
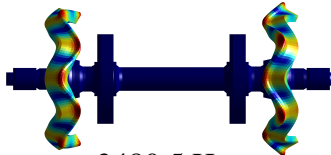
	symmetric	antimetric
$k = 0$	 403.01 Hz	 302.46 Hz
$k = 1$	 83.376 Hz	 147.20 Hz
$k = 2$	 344.63 Hz	 344.63 Hz
$k = 3$	 931.03 Hz	 931.03 Hz
$k = 4$	 1695.8 Hz	 1695.8 Hz
$k = 5$	 2560.2 Hz	 2560.2 Hz
$k = 6$	 3480.5 Hz	 3480.5 Hz

Table 5.6.1: Symmetric and antimetric eigenmodes of the wheelset for different periodicities k

5.7 Inertia terms for a cyclic structure: General principle

For a flexible body described by the floating frame of reference formulation, the inertia terms according to Jourdain's principle are obtained by integrating the scalar product of the absolute

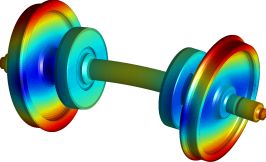
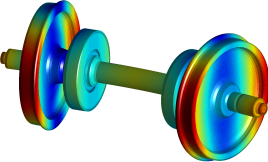
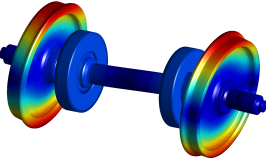
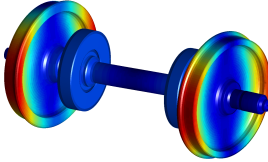
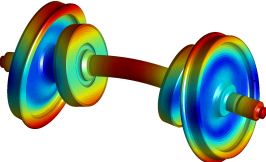
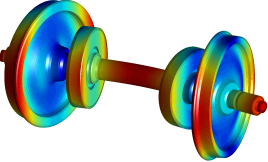
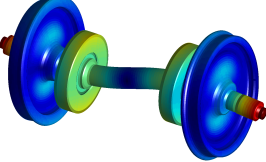
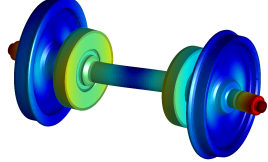
 <p>83.376 Hz</p>	 <p>83.376 Hz</p>
 <p>147.20 Hz</p>	 <p>147.20 Hz</p>
 <p>239.78 Hz</p>	 <p>239.78 Hz</p>
 <p>414.65 Hz</p>	 <p>414.65 Hz</p>

Table 5.6.2: Double bending eigenmodes of the wheelset ($k = 1$)

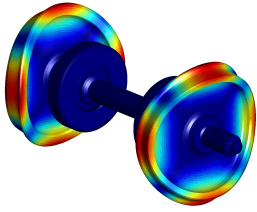
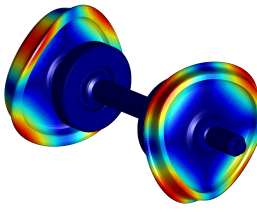
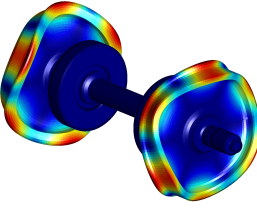
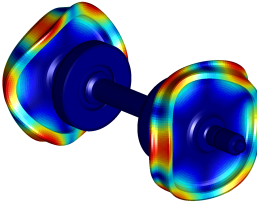
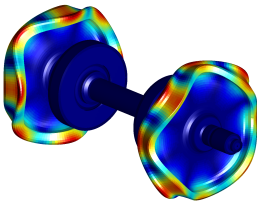
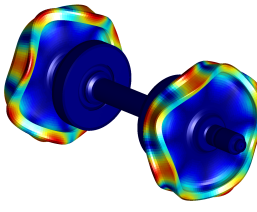
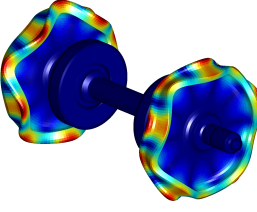
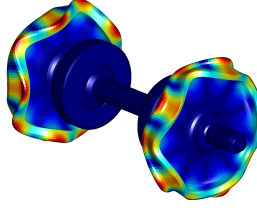
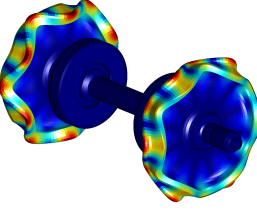
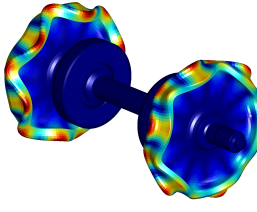
$k = 2$	 <p>344.63 Hz</p>	 <p>344.63 Hz</p>
$k = 3$	 <p>931.03 Hz</p>	 <p>931.03 Hz</p>
$k = 4$	 <p>1695.8 Hz</p>	 <p>1695.8 Hz</p>
$k = 5$	 <p>2560.2 Hz</p>	 <p>2560.2 Hz</p>
$k = 6$	 <p>3480.5 Hz</p>	 <p>3480.5 Hz</p>

Table 5.6.3: Double eigenmodes of the wheelset for periodicities $k \geq 2$

virtual velocity $\delta' \mathbf{v}_{OP}^I$ and the absolute acceleration \mathbf{a}_{OP}^I for all particles of the body B; the particles have the infinitesimal mass dm .

An integral can be considered as a the sum of an infinite number of infinitesimal summands. Therefore, the properties which are valid for the addition can also be applied to the integration. One of these properties is the associative property of the addition, i.e. the sequence of the additions is arbitrary:

$$(x + y) + z = x + (y + z) \Rightarrow (a + b) + (c + d) = (a + c) + (b + d) \quad (5.7.130)$$

Therefore, it is possible to evaluate partial sums, which again are summed up to the entire sum.

If the flexible body is considered as a cyclic structure, then it consists of n identical segments S_j , $0 \leq j \leq n - 1$, which are circularly arranged. Based on the associative property, the integral over the entire body B can be determined by carrying out the integration over each segments and afterwards summing up the integrals obtained for each segment.

$$\int_B \delta' \mathbf{v}_{OP}^I \mathbf{T} \mathbf{a}_{OP}^I dm = \sum_{j=0}^{n-1} \int_{S_j} \delta' \mathbf{v}_{OP_j}^I \mathbf{T} \mathbf{a}_{OP_j}^I dm, P_j \in S_j \quad (5.7.131)$$

Furthermore, since the segments S_j forming the cyclic structure are identical, the particles form n -tuples of corresponding particles. Here, the point P_j belonging to the j -th segment S_j is defined by the triple $\langle r, y, \phi_0 + \frac{2\pi}{n} j \rangle$ of cylindrical coordinates. Also, due to the associative property the sequence of the integration and the summation can be modified without affecting the result. Therefore, instead of integrating the product $\delta' \mathbf{v}_{OP}^I \mathbf{T} \mathbf{a}_{OP}^I$ over each segment S_j and summing up the individual integrals the inertia terms can also be determined by summing up the products for the n -tuple first and subsequently integrating the resulting sum over the zeroth segment S_0 . Since the segment are identical, the domain of r and y is equal for each segment and the domain for the angle ϕ_j is shifted by $\frac{2\pi}{n} j$. Therefore, it is valid:

$$\sum_{j=0}^{n-1} \int_{S_j} \delta' \mathbf{v}_{OP_j}^I \mathbf{T} \mathbf{a}_{OP_j}^I dm = \int_{S_0} \left(\sum_{j=0}^{n-1} \delta' \mathbf{v}_{OP_j}^I \mathbf{T} \mathbf{a}_{OP_j}^I \right) dm \quad (5.7.132)$$

If the resulting sum has a certain characteristic property, which is independent from the chosen n -tuple, then this is also a property of the integral. More concretely, if a certain term is eliminated from the sum $\delta' \mathbf{v}_{OP_j}^I \mathbf{T} \mathbf{a}_{OP_j}^I$ over the n -tuple of corresponding particles, then this term is also not contained in the integral over all mass particles of the body B. Therefore, the evaluation of the sum over the n -tuple of corresponding particles will turn out to be useful in order to determine some characteristics of the inertia terms for a cyclic structure.

According to the floating frame of reference formulation, whereby the body-fixed frame \mathcal{B} is used as the reference frame, the current position of a particle located at the point P is given by:

$$\mathbf{r}_{OP}^I = \mathbf{r}_{OR}^I + \mathbf{S}^{IB} \mathbf{r}_{RP}^I \quad (5.7.133)$$

As described in the appendix C.1, the virtual velocity $\delta' \mathbf{v}_{OP}^I$ and the acceleration \mathbf{a}_{OP}^I for the particle are obtained to:

$$\delta' \mathbf{v}_{OP}^I = \delta' \mathbf{v}_{OR}^I + \delta' \tilde{\omega}_{IB}^I \mathbf{S}^{IB} \mathbf{r}_{RP}^B + \tilde{\omega}_{IB}^I \mathbf{S}^{IB} \delta' \dot{\mathbf{r}}_{RP}^B \quad (5.7.134)$$

$$\mathbf{a}_{OP}^I = \mathbf{a}_{OR}^I + \left(\tilde{\omega}_{IB}^I + \tilde{\omega}_{IB}^I \tilde{\omega}_{IB}^I \right) \mathbf{S}^{IB} \mathbf{r}_{RP}^B + 2 \tilde{\omega}_{IB}^I \mathbf{S}^{IB} \dot{\mathbf{r}}_{RP}^B + \mathbf{S}^{IB} \ddot{\mathbf{r}}_{RP}^B \quad (5.7.135)$$

Due to the overturning motion of the wheelset, the body-fixed frame \mathcal{B} performs a large rotation; thereby, the rotation matrix \mathbf{S}^{IB} contains the trigonometric functions $\sin\chi$ and $\cos\chi$. In contrast to this, the sliding frame \mathcal{A} does not perform the large rotation; therefore, the inertia terms for this formulation shall be considered.

By splitting the rotation matrix \mathbf{S}^{IB} , the current position of a particle located at the point P_j is given by:

$$\mathbf{r}_{OP_j}^I = \mathbf{r}_{OR}^I + \mathbf{S}^{IB} \mathbf{S}_2(\phi_j) \mathbf{p}^{(j)} = \mathbf{r}_{OR}^I + \underbrace{\mathbf{S}^{IA} \mathbf{S}^{AB} \mathbf{S}_2(\phi_j) \mathbf{p}^{(j)}}_{\mathbf{r}_{RP_j}^A} \quad (5.7.136)$$

For the vector $\mathbf{r}_{RP_j}^A$, which describes the relative position of the j -th particle in the sliding frame, it is valid:

$$\mathbf{r}_{RP_j}^A = \mathbf{S}^{AB} \mathbf{S}_2(\phi_j) \mathbf{p}^{(j)} = \mathbf{S}_2(\chi) \mathbf{S}_2(\phi_j) \mathbf{p}^{(j)} = \mathbf{S}_2(\chi + \phi_j) \mathbf{p}^{(j)} = \mathbf{S}_2(\theta_j) \mathbf{p}^{(j)} \quad (5.7.137)$$

In order to describe the kinematics of the particle in the sliding frame \mathcal{A} , the position vector $\mathbf{p}^{(j)}$ has to be formulated using the azimuth θ_j . In the section 5.3, the following expression has been derived:

$$\mathbf{p}^{(j)} = \sum_{k=k_{\min}}^{k_{\max}} \mathbf{p}_k^A e^{ik(\theta_j - \phi_0)} \quad (5.7.138)$$

The relation between the description of position in the directions of cylindrical coordinates and the one in the directions of cartesian coordinates is given by the rotation matrix $\mathbf{S}_2(\theta_j)$. In a rotation matrix, the rotation angle appears as the argument of the sine and the cosine function. Therefore, the rotation matrix $\mathbf{S}_2(\beta)$ can be decomposed in the following way:

$$\mathbf{S}_2(\beta) = \begin{bmatrix} \cos\beta & 0 & \sin\beta \\ 0 & 1 & 0 \\ -\sin\beta & 0 & \cos\beta \end{bmatrix} = \underbrace{\begin{bmatrix} 0 & 0 & 0 \\ 0 & 1 & 0 \\ 0 & 0 & 0 \end{bmatrix}}_{\mathbf{S}_{2,0}} + \cos\beta \underbrace{\begin{bmatrix} 1 & 0 & 0 \\ 0 & 0 & 0 \\ 0 & 0 & 1 \end{bmatrix}}_{\mathbf{S}_{2,C}} + \sin\beta \underbrace{\begin{bmatrix} 0 & 0 & 1 \\ 0 & 0 & 0 \\ -1 & 0 & 0 \end{bmatrix}}_{\mathbf{S}_{2,S}} \quad (5.7.139)$$

By applying the relation between the exponential function $e^{i\phi}$ and the trigonometric functions $\cos\beta$ and $\sin\beta$

$$\cos\beta = \frac{e^{i\beta} + e^{-i\beta}}{2}, \quad \sin\beta = \frac{e^{i\beta} - e^{-i\beta}}{2i} = -i \frac{e^{i\beta} - e^{-i\beta}}{2} \quad (5.7.140)$$

it can be formulated:

$$\begin{aligned} \mathbf{S}_2(\beta) &= \mathbf{S}_{2,0} + \cos\beta \mathbf{S}_{2,C} + \sin\beta \mathbf{S}_{2,S} = \mathbf{S}_{2,0} + \frac{e^{i\beta} + e^{-i\beta}}{2} \mathbf{S}_{2,C} - i \frac{e^{i\beta} - e^{-i\beta}}{2} \mathbf{S}_{2,S} \\ &= \mathbf{S}_{2,0} + \underbrace{\frac{1}{2} (\mathbf{S}_{2,C} - i \mathbf{S}_{2,S})}_{\mathbf{S}_{2,1}} e^{i\beta} + \underbrace{\frac{1}{2} (\mathbf{S}_{2,C} + i \mathbf{S}_{2,S})}_{\mathbf{S}_{2,-1}} e^{-i\beta} = \sum_{c=-1}^c \mathbf{S}_{2,c} e^{ic\beta} \end{aligned} \quad (5.7.141)$$

Thereby, the rotation matrix $\mathbf{S}_2(\beta)$ is formulated as a Fourier series. Based on this, the position vector $\mathbf{r}_{RP_j}^A$, too, can be expressed by a Fourier polynomial obtained from the product of two Fourier series. In the formulation for $\mathbf{p}^{(j)}$ according to (5.7.138) the difference $\theta_j - \phi_0$ is used as the argument. In order to adapt the Fourier series for the rotation matrix $\mathbf{S}_2(\theta_j)$, the rotation around the angle θ_j is split up into two parts $\theta_j - \phi_0$ and θ_0 . Applying the matrix decomposition

according to (5.7.141) to the matrix $\mathbf{S}_2(\theta_j - \phi_0)$ and inserting the Fourier series for $\mathbf{p}^{(j)}$ according to (5.7.138) leads to:

$$\mathbf{r}_{\text{RP}_j}^{\mathcal{A}} = \mathbf{S}_2(\theta_j) \mathbf{p}^{(j)} = \left(\sum_{c=-1}^c \mathbf{S}_{2,c} e^{ic\theta_j} \right) \left(\sum_{k=k_{\min}}^{k_{\max}} \mathbf{p}_k^{\mathcal{A}} e^{ik\theta_j} \right) = \sum_{c=-1}^c \sum_{k=k_{\min}}^{k_{\max}} \mathbf{S}_{2,c} \mathbf{p}_k^{\mathcal{A}} e^{i(k+c)\theta_j} \quad (5.7.142)$$

Based on the index shift, which is derived in the appendix A.1, the inner sum over k is reformulated in the following way.

$$\sum_{k=k_{\min}}^{k_{\max}} X_k = \sum_{K=k_{\min}+c}^{k_{\max}+c} X_{K-c} \Rightarrow \sum_{k=k_{\min}}^{k_{\max}} \mathbf{S}_{2,c} \mathbf{p}_k^{\mathcal{A}} e^{i(k+c)\theta_j} = \sum_{K=k_{\min}+c}^{k_{\max}+c} \mathbf{S}_{2,c} \mathbf{p}_{K-c}^{\mathcal{A}} e^{iK\theta_j} \quad (5.7.143)$$

Resolving the outer sum over c and merging the resulting sums over K leads to:

$$\begin{aligned} \mathbf{r}_{\text{RP}_j}^{\mathcal{A}} &= \sum_{c=-1}^1 \sum_{k=k_{\min}}^{k_{\max}} \mathbf{S}_{2,c} \mathbf{p}_k^{\mathcal{A}} e^{i(k+c)\theta_j} = \sum_{c=-1}^1 \sum_{K=k_{\min}+c}^{k_{\max}+c} \mathbf{S}_{2,c} \mathbf{p}_{K-c}^{\mathcal{A}} e^{iK\theta_j} \\ &= \sum_{K=k_{\min}-1}^{k_{\max}-1} \mathbf{S}_{2,-1} \mathbf{p}_{K+1}^{\mathcal{A}} e^{iK\theta_j} + \sum_{K=k_{\min}}^{k_{\max}} \mathbf{S}_{2,0} \mathbf{p}_K^{\mathcal{A}} e^{iK\theta_j} + \sum_{K=k_{\min}+1}^{k_{\max}+1} \mathbf{S}_{2,1} \mathbf{p}_{K-1}^{\mathcal{A}} e^{iK\theta_j} \\ &= \mathbf{S}_{2,-1} \mathbf{p}_{k_{\min}}^{\mathcal{A}} e^{i(k_{\min}-1)\theta_j} + \left(\mathbf{S}_{2,-1} \mathbf{p}_{k_{\min}+1}^{\mathcal{A}} + \mathbf{S}_{2,0} \mathbf{p}_{k_{\min}}^{\mathcal{A}} \right) e^{ik_{\min}\theta_j} \\ &\quad + \sum_{K=k_{\min}+1}^{k_{\max}-1} \left(\mathbf{S}_{2,-1} \mathbf{p}_{K+1}^{\mathcal{A}} + \mathbf{S}_{2,0} \mathbf{p}_K^{\mathcal{A}} + \mathbf{S}_{2,1} \mathbf{p}_{K-1}^{\mathcal{A}} \right) e^{iK\theta_j} \\ &\quad + \left(\mathbf{S}_{2,0} \mathbf{p}_{k_{\max}}^{\mathcal{A}} + \mathbf{S}_{2,1} \mathbf{p}_{k_{\max}-1}^{\mathcal{A}} \right) e^{ik_{\max}\theta_j} + \mathbf{S}_{2,1} \mathbf{p}_{k_{\max}}^{\mathcal{A}} e^{i(k_{\max}+1)\theta_j} \\ &= \sum_{K=k_{\min}-1}^{k_{\max}+1} \mathbf{r}_{\mathcal{A},K}^{\mathcal{A}} e^{iK\theta_j} \end{aligned} \quad (5.7.144)$$

Here, the new vectors $\mathbf{r}_{\mathcal{A},K}^{\mathcal{A}}$ are defined in the following way:

$$\mathbf{r}_{\mathcal{A},K}^{\mathcal{A}} = \begin{cases} \mathbf{S}_2(\phi_0) \mathbf{S}_{2,-1} \mathbf{p}_{k_{\min}}^{\mathcal{A}} & \text{for } K = k_{\min} - 1 \\ \mathbf{S}_{2,-1} \mathbf{p}_{k_{\min}+1}^{\mathcal{A}} + \mathbf{S}_{2,0} \mathbf{p}_{k_{\min}}^{\mathcal{A}} & \text{for } K = k_{\min} \\ \mathbf{S}_{2,-1} \mathbf{p}_{K+1}^{\mathcal{A}} + \mathbf{S}_{2,0} \mathbf{p}_K^{\mathcal{A}} + \mathbf{S}_{2,1} \mathbf{p}_{K-1}^{\mathcal{A}} & \text{for } k_{\min} + 1 \leq K \leq k_{\max} - 1 \\ \mathbf{S}_{2,0} \mathbf{p}_{k_{\max}}^{\mathcal{A}} + \mathbf{S}_{2,1} \mathbf{p}_{k_{\max}-1}^{\mathcal{A}} & \text{for } K = k_{\max} \\ \mathbf{S}_{2,1} \mathbf{p}_{k_{\max}}^{\mathcal{A}} & \text{for } K = k_{\max} + 1 \end{cases} \quad (5.7.145)$$

By transforming the vector $\mathbf{r}_{\text{RP}_j}^{\mathcal{A}}$ into the inertial frame I it is obtained:

$$\mathbf{r}_{\text{RP}_j}^I = \mathbf{S}^{I\mathcal{A}} \mathbf{r}_{\text{RP}_j}^{\mathcal{A}} = \mathbf{S}^{I\mathcal{A}} \sum_{K=k_{\min}-1}^{k_{\max}+1} \mathbf{r}_{\mathcal{A},K}^{\mathcal{A}} e^{iK(\theta_j - \phi_0)} = \sum_{K=k_{\min}-1}^{k_{\max}+1} \mathbf{S}^{I\mathcal{A}} \mathbf{r}_{\mathcal{A},K}^{\mathcal{A}} e^{iK\theta_j} = \sum_{K=k_{\min}-1}^{k_{\max}+1} \mathbf{r}_{\mathcal{A},K}^I e^{iK\theta_j} \quad (5.7.146)$$

For the new vectors $\mathbf{r}_{\mathcal{A},K}^I$ it is valid:

$$\mathbf{r}_{\mathcal{A},K}^I = \mathbf{S}^{I\mathcal{A}} \mathbf{r}_{\mathcal{A},K}^{\mathcal{A}} \quad (5.7.147)$$

It should be pointed out that in this formulation (5.7.146) the large overturning angle $\chi = \chi(t)$ is implicitly contained in the azimuth θ_j , but not in the vectors $\mathbf{r}_{\mathcal{A},K}^I$. This has to be taken into account for the derivative with respect to the time t . For the derivative of the power $e^{iK(\theta_j - \phi_0)}$ it is valid:

$$\theta_j = \chi(t) + \phi_0 + \frac{2\pi}{n} j \Rightarrow \frac{d}{dt} \left(e^{iK\theta_j} \right) = \frac{d}{d\theta_j} \left(e^{iK\theta_j} \right) \frac{d\theta_j}{dt} = e^{iK\theta_j} iK \dot{\chi}(t) \quad (5.7.148)$$

Based on this, the velocity $\mathbf{v}_{\text{RP}_j}^I$ and the acceleration $\mathbf{a}_{\text{RP}_j}^I$ are obtained to:

$$\mathbf{r}_{\text{RP}_j}^I = \sum_{K=k_{\min}-1}^{k_{\max}+1} \mathbf{r}_{\mathcal{A},K}^I e^{iK\theta_j} \quad (5.7.149)$$

$$\mathbf{v}_{\text{RP}_j}^I = \sum_{K=k_{\min}-1}^{k_{\max}+1} \left(\dot{\mathbf{r}}_{\mathcal{A},K}^I + iK\dot{\chi} \mathbf{r}_{\mathcal{A},K}^I \right) e^{iK\theta_j} = \sum_{K=k_{\min}-1}^{k_{\max}+1} \mathbf{v}_{\mathcal{A},K}^I e^{iK\theta_j} \quad (5.7.150)$$

$$\mathbf{a}_{\text{RP}_j}^I = \sum_{K=k_{\min}-1}^{k_{\max}+1} \left(\ddot{\mathbf{r}}_{\mathcal{A},K}^I + 2iK\dot{\chi} \dot{\mathbf{r}}_{\mathcal{A},K}^I + (iK\ddot{\chi} - K^2\dot{\chi}^2) \mathbf{r}_{\mathcal{A},K}^I \right) e^{iK\theta_j} = \sum_{K=k_{\min}-1}^{k_{\max}+1} \mathbf{a}_{\mathcal{A},K}^I e^{iK\theta_j} \quad (5.7.151)$$

The vector of the virtual velocity $\delta' \mathbf{v}_{\text{RP}_j}^I$ is derived from (5.7.150):

$$\delta' \mathbf{v}_{\text{RP}_j}^I = \sum_{K=k_{\min}-1}^{k_{\max}+1} \delta' \mathbf{v}_{\mathcal{A},K}^I e^{iK(\theta_j - \phi_0)} \quad (5.7.152)$$

Based on this the sum of the product $\delta' \mathbf{v}_{\text{OP}_j}^I \mathbf{a}_{\text{OP}_j}^I$ over the n -tuple of corresponding particles can now be evaluated. It is valid:

$$\begin{aligned} \sum_{j=0}^{n-1} \delta' \mathbf{v}_{\text{OP}_j}^I \mathbf{a}_{\text{OP}_j}^I &= \sum_{j=0}^{n-1} \left(\delta' \mathbf{v}_{\text{OR}}^I + \delta' \mathbf{v}_{\text{RP}_j}^I \right) \mathbf{a}_{\text{OR}}^I + \sum_{j=0}^{n-1} \delta' \mathbf{v}_{\text{RP}_j}^I \mathbf{a}_{\text{RP}_j}^I \\ &= \delta' \mathbf{v}_{\text{OP}_j}^I \mathbf{a}_{\text{OR}}^I \sum_{j=0}^{n-1} 1 + \sum_{j=0}^{n-1} \delta' \mathbf{v}_{\text{RP}_j}^I \mathbf{a}_{\text{RP}_j}^I \end{aligned} \quad (5.7.153)$$

For the powers $e^{iK\theta_j}$ contained in the Fourier polynomials for $\delta' \mathbf{v}_{\text{RP}_j}^I$ and $\mathbf{a}_{\text{RP}_j}^I$ it is valid:

$$\theta_j = \chi + \phi_j = \chi + \phi_0 + \frac{2\pi}{n}j \Rightarrow e^{iK\theta_j} = e^{iK(\chi + \phi_0 + \frac{2\pi}{n}j)} = e^{iK(\chi + \phi_0)} e^{iK\frac{2\pi}{n}j} = e^{iK(\chi + \phi_0)} \zeta^{Kj} \quad (5.7.154)$$

The evaluation is based on the following relation:

$$\sum_{j=0}^{n-1} \zeta^{pj} = \begin{cases} n & \text{for } \frac{p}{n} \in \mathbb{Z} \\ 0 & \text{for } \frac{p}{n} \notin \mathbb{Z} \end{cases} \quad (5.7.155)$$

As derived in section 3.1.3, it is valid for the periodicity:

$$-\frac{n}{2} + \frac{1}{2} \leq k_{\min} \leq k \leq k_{\max} \leq \frac{n}{2} \quad (5.7.156)$$

It is assumed that the cyclic structure consists of $n > 2$ segments; from this, it can be derived:

$$2 < n \Rightarrow \frac{1}{2} > \frac{1}{n} \Rightarrow \frac{1}{4} > \frac{1}{2n} \Rightarrow -\frac{1}{4} < -\frac{1}{2n} \quad (5.7.157)$$

From this, it follows for the bounds of K :

$$k_{\min} \geq -\frac{n}{2} + \frac{1}{2} \Rightarrow k_{\min} - 1 \geq -\frac{n}{2} - \frac{1}{2} \Rightarrow \frac{k_{\min} - 1}{n} \geq -\frac{1}{2} - \frac{1}{2n} > -\frac{3}{4} \quad (5.7.158)$$

$$k_{\max} \leq \frac{n}{2} \Rightarrow k_{\max} + 1 \leq \frac{n}{2} + 1 \Rightarrow \frac{k_{\max} + 1}{n} \leq \frac{1}{2} + \frac{1}{n} < 1 \quad (5.7.159)$$

Thereby, the range of the quotient $\frac{K}{n}$ is obtained to:

$$k_{\min} - 1 \leq K \leq k_{\max} + 1 \Rightarrow -\frac{3}{4} \leq \frac{k_{\min} - 1}{n} \leq \frac{K}{n} \leq \frac{k_{\max} + 1}{n} < 1 \Rightarrow -\frac{3}{4} < \frac{K}{n} < 1 \quad (5.7.160)$$

According to (5.7.155), the sum of the powers ζ^{pj} does not vanish if the quotient $\frac{p}{n}$ is an integer. Applying this to the present case leads to:

$$-\frac{3}{4} < \frac{K}{n} < 1 \wedge \frac{K}{n} \in \mathbb{Z} \Rightarrow K = 0 \Rightarrow \sum_{j=0}^{n-1} \zeta^{Kj} = \begin{cases} n & \text{for } K = 0 \\ 0 & \text{for } K \neq 0 \end{cases} \quad (5.7.161)$$

Based on this, it is obtained for the sum of $\mathbf{a}_{\text{RP}_j}^I$:

$$\begin{aligned} \sum_{j=0}^{n-1} \mathbf{a}_{\text{RP}_j}^I &= \sum_{j=0}^{n-1} \sum_{K=k_{\min}-1}^{k_{\max}+1} \mathbf{a}_{\mathcal{A},K}^I e^{iK\theta_j} = \sum_{K=k_{\min}-1}^{k_{\max}+1} \sum_{j=0}^{n-1} \mathbf{a}_{\mathcal{A},K}^I e^{iK(\chi+\phi_0)} \zeta^{Kj} \\ &= \sum_{K=k_{\min}-1}^{k_{\max}+1} \left(\mathbf{a}_{\mathcal{A},K}^I e^{iK(\chi+\phi_0)} \left(\sum_{j=0}^{n-1} \zeta^{Kj} \right) \right) = n \mathbf{a}_{\mathcal{A},0}^I \underbrace{e^{i \cdot 0 \cdot (\chi+\phi_0)}}_1 = n \mathbf{a}_{\mathcal{A},0}^I \end{aligned} \quad (5.7.162)$$

In an analogous way it is obtained for the sum of $\delta' \mathbf{v}_{\text{RP}_j}^I$:

$$\sum_{j=0}^{n-1} \delta' \mathbf{v}_{\text{RP}_j}^I = \sum_{K=k_{\min}-1}^{k_{\max}+1} \left(\delta' \mathbf{v}_{\mathcal{A},K}^I e^{iK(\chi+\phi_0)} \left(\sum_{j=0}^{n-1} \zeta^{Kj} \right) \right) = n \delta' \mathbf{v}_{\mathcal{A},0}^I \underbrace{e^{i \cdot 0 \cdot (\chi+\phi_0)}}_1 = n \delta' \mathbf{v}_{\mathcal{A},0}^I \quad (5.7.163)$$

Inserting these results into (5.7.153) leads to:

$$\begin{aligned} \sum_{j=0}^{n-1} \delta' \mathbf{v}_{\text{OP}_j}^I \mathbf{a}_{\text{OP}_j}^I &= \delta' \mathbf{v}_{\text{OP}_j}^I \mathbf{T} \left(\mathbf{a}_{\text{OR}}^I \sum_{j=0}^{n-1} 1 + \sum_{j=0}^{n-1} \mathbf{a}_{\text{RP}_j}^I \right) + \left(\sum_{j=0}^{n-1} \delta' \mathbf{v}_{\text{RP}_j}^I \mathbf{T} \right) \mathbf{a}_{\text{OR}}^I + \sum_{j=0}^{n-1} \delta' \mathbf{v}_{\text{RP}_j}^I \mathbf{T} \mathbf{a}_{\text{RP}_j}^I \\ &= \delta' \mathbf{v}_{\text{OP}_j}^I \mathbf{T} \left(n \mathbf{a}_{\text{OR}}^I + n \mathbf{a}_{\mathcal{A},0}^I \right) + n \delta' \mathbf{v}_{\mathcal{A},0}^I \mathbf{T} \mathbf{a}_{\text{OR}}^I + \sum_{j=0}^{n-1} \delta' \mathbf{v}_{\text{RP}_j}^I \mathbf{T} \mathbf{a}_{\text{RP}_j}^I \end{aligned} \quad (5.7.164)$$

The result indicates that the inertia terms for the translational motions and the coupling terms between the translational motions on the one hand and the rotational motions and relative motions on the other hand do not contain the large overturning angle χ .

The evaluation of the remaining sum is more complicated since in this case the product of two Fourier polynomials has to be summed up. The vector $\mathbf{r}_{\text{RP}_j}^I$ which describes the current position of the j -th particle with respect to the reference point R is a geometric vector and thereby a real vector; therefore, also the vectors $\mathbf{v}_{\text{RP}_j}^I$ for the velocity and $\delta' \mathbf{v}_{\text{RP}_j}^I$ for the virtual velocity are real vectors. A real vector is equal to its complex conjugate so that it can be formulated:

$$\Im \mathbf{r}_{\text{RP}_j}^I = \mathbf{0} \Rightarrow \mathbf{r}_{\text{RP}_j}^I = \overline{\mathbf{r}_{\text{RP}_j}^I} \Rightarrow \delta' \mathbf{v}_{\text{RP}_j}^I = \overline{\delta' \mathbf{v}_{\text{RP}_j}^I} \Rightarrow \delta' \mathbf{v}_{\text{RP}_j}^I \mathbf{T} = \overline{\delta' \mathbf{v}_{\text{RP}_j}^I \mathbf{T}} = \delta' \mathbf{v}_{\text{RP}_j}^I \mathbf{H} \quad (5.7.165)$$

For the Hermitean transpose $\delta' \mathbf{v}_{\text{RP}_j}^I \mathbf{H}$ it is valid:

$$\delta' \mathbf{v}_{\text{RP}_j}^I \mathbf{T} = \delta' \mathbf{v}_{\text{RP}_j}^I \mathbf{H} = \sum_{K=k_{\min}-1}^{k_{\max}+1} \delta' \mathbf{v}_{\mathcal{A},K}^I \mathbf{H} e^{iK\theta_j} = \sum_{K=k_{\min}-1}^{k_{\max}+1} \delta' \mathbf{v}_{\mathcal{A},K}^I \mathbf{H} e^{-iK\theta_j} \quad (5.7.166)$$

The periodicities of the two Fourier polynomials which describe the virtual velocity $\delta'v_{RP_j}^I$ and the acceleration $\mathbf{a}_{RP_j}^I$ are independent from each other. Therefore, a separate periodicity L is used for the acceleration, while the bounds remain unchanged. Thereby, the remaining sum over j can be formulated in the following way:

$$\begin{aligned}
\sum_{j=0}^{n-1} \delta'v_{RP_j}^I \mathbf{T} \mathbf{a}_{RP_j}^I &= \sum_{j=0}^{n-1} \left(\sum_{K=k_{\min}-1}^{k_{\max}+1} \delta'v_{\mathcal{A},K}^I \mathbf{H} e^{-iK\theta_j} \right) \left(\sum_{L=k_{\min}-1}^{k_{\max}+1} \mathbf{a}_{\mathcal{A},L}^I e^{iL\theta_j} \right) \\
&= \sum_{j=0}^{n-1} \sum_{K=k_{\min}-1}^{k_{\max}+1} \sum_{L=k_{\min}-1}^{k_{\max}+1} \delta'v_{\mathcal{A},K}^I \mathbf{H} \mathbf{a}_{\mathcal{A},L}^I e^{i(-K+L)\theta_j} \\
&= \sum_{K=k_{\min}-1}^{k_{\max}+1} \sum_{L=k_{\min}-1}^{k_{\max}+1} \left(\delta'v_{\mathcal{A},K}^I \mathbf{H} \mathbf{a}_{\mathcal{A},L}^I \left(\sum_{j=0}^{n-1} e^{i(L-K)\theta_j} \right) \right) \quad (5.7.167)
\end{aligned}$$

For the sum over j it is valid:

$$\begin{aligned}
\theta_j = \chi + \phi_0 + \frac{2\pi}{n}j &\Rightarrow \sum_{j=0}^{n-1} e^{i(L-K)\theta_j} = \sum_{j=0}^{n-1} e^{i(L-K)(\chi + \phi_0 + \frac{2\pi}{n}j)} = \sum_{j=0}^{n-1} e^{i(L-K)(\chi + \phi_0)} e^{i(L-K)\frac{2\pi}{n}j} \\
&= e^{i(L-K)(\chi + \phi_0)} \sum_{j=0}^{n-1} \zeta^{(L-K)j} \quad (5.7.168)
\end{aligned}$$

Also here, the sum over j is evaluated based on (5.7.155); to this end, it has to be determined, for which pairs $\langle K, L \rangle$ the sum of the powers $\zeta^{(L-K)j}$ does not vanish. From (5.7.155) it follows for the present case that for a non-vanishing result the quotient $\frac{L-K}{n}$ is an integer; this is the first condition for the pairs $\langle K, L \rangle$:

$$\frac{L-K}{n} \in \mathbb{Z} \quad (5.7.169)$$

Furthermore, the ranges of the periodicities K and L are limited by the bounds of the sums:

$$\delta'v_{RP_j}^I \mathbf{T} = \sum_{K=k_{\min}-1}^{k_{\max}+1} \delta'v_{\mathcal{A},K}^I \mathbf{H} e^{-iK\theta_j} \Rightarrow k_{\min}-1 \leq K \leq k_{\max}+1 \quad (5.7.170)$$

$$\sum_{L=k_{\min}-1}^{k_{\max}+1} \mathbf{a}_{\mathcal{A},L}^I e^{iL\theta_j} \Rightarrow k_{\min}-1 \leq L \leq k_{\max}+1 \quad (5.7.171)$$

Thereby, two other conditions for the pairs $\langle K, L \rangle$ are given.

In order to determine the wanted pairs $\langle K, L \rangle$, the range of the quotient $\frac{L-K}{n}$ has to be determined. Multiplying the condition for K according to (5.7.171) by -1

$$k_{\min}-1 \leq K \leq k_{\max}+1 \Leftrightarrow -k_{\min}+1 \geq -K \geq -k_{\max}-1 \quad (5.7.172)$$

and combining the result with the condition for L according to (5.7.171) leads to:

$$\begin{aligned}
-k_{\max}-1 \leq -K \leq -k_{\min}+1 \wedge k_{\min}-1 \leq L \leq k_{\max}+1 \\
\Rightarrow -k_{\max}+k_{\min}-2 = -(k_{\max}-k_{\min}+2) \leq L-K \leq k_{\max}-k_{\min}+2 \quad (5.7.173)
\end{aligned}$$

The relation between the bounds k_{\min} and k_{\max} of the original Fourier series is given by:

$$k_{\min}+n = k_{\max}+1 \Rightarrow n-1 = k_{\max}-k_{\min} \Rightarrow n+1 = k_{\max}-k_{\min}+2 \quad (5.7.174)$$

By applying this relation the range of the quotient $\frac{L-K}{n}$ is obtained to:

$$\underbrace{-(k_{\max} - k_{\min} + 2)}_{-n-1} \leq L - K \leq \underbrace{k_{\max} - k_{\min} + 2}_{n+1} \Rightarrow -1 - \frac{1}{n} = -\left(1 + \frac{1}{n}\right) \leq \frac{L-K}{n} \leq 1 + \frac{1}{n} \quad (5.7.175)$$

Since the n -tuple consists of $n > 2$ particles, it is valid:

$$n > 2 \Rightarrow \frac{1}{n} < \frac{1}{2} \Rightarrow 1 + \frac{1}{n} < \frac{3}{2} \Rightarrow -\frac{3}{2} < -\left(1 + \frac{1}{n}\right) \leq \frac{L-K}{n} = M \leq 1 + \frac{1}{n} < \frac{3}{2} \quad (5.7.176)$$

From this it follows:

$$-\frac{3}{2} < \frac{L-K}{n} = M < \frac{3}{2} \wedge M \in \mathbb{Z} \Rightarrow M \in \{-1, 0, 1\} \quad (5.7.177)$$

This result indicates that for the given ranges of K and L the quotient $\frac{L-K}{n}$ can have three different integer values. For a given value M the relation between K and L is obtained to:

$$\frac{L-K}{n} = M \Rightarrow -K + L = Mn \Rightarrow L = K + Mn \quad (5.7.178)$$

By inserting this into the condition (5.7.171) it is obtained:

$$k_{\min} - 1 \leq L = K + Mn \leq k_{\max} + 1 \Rightarrow k_{\min} - 1 - Mn \leq K \leq k_{\max} + 1 - Mn \quad (5.7.179)$$

Thereby, a second condition for K in addition to (5.7.170) is obtained. By using the maximum function $\max(a, b)$ and the minimum function $\min(a, b)$:

$$\max(a, b) = \begin{cases} a & \text{for } a \geq b \\ b & \text{for } a < b \end{cases}, \min(a, b) = \begin{cases} b & \text{for } a \geq b \\ a & \text{for } a < b \end{cases} \quad (5.7.180)$$

it can be formulated:

$$k_{\min} - 1 \leq K \leq k_{\max} + 1 \wedge k_{\min} - 1 - Mn \leq K \leq k_{\max} + 1 - Mn \quad (5.7.181)$$

$$\Rightarrow \max(k_{\min} - 1, k_{\min} - 1 - Mn) \leq K \leq \min(k_{\max} + 1, k_{\max} + 1 - Mn) \quad (5.7.182)$$

As a result, for each value M a range of K is determined for which the values L are obtained from the relation (5.7.178). Thereby, the wanted pairs $\langle K, L \rangle$, for which the sum

$$\sum_{j=0}^{n-1} e^{i(L-K)\theta_j} = e^{i(L-K)(\chi+\phi_0)} \sum_{j=0}^{n-1} \zeta^{(L-K)j} \quad (5.7.183)$$

does not vanish, can now be determined. In order to simplify the results, the relation between the bounds k_{\min} and k_{\max} of the original Fourier series will be applied:

$$k_{\min} + n = k_{\max} + 1 \Leftrightarrow k_{\min} - 1 + n = k_{\max} \Leftrightarrow k_{\min} = k_{\max} + 1 - n \quad (5.7.184)$$

The evaluation of the range of K , the relation between K and L and the function $e^{i(L-K)(\chi+\phi_0)}$ for the three values of M leads to:

	$M = -1$	$M = 0$	$M = 1$
$\max(k_{\min} - 1, k_{\min} - 1 - Mn)$	$k_{\min} - 1 + n = k_{\max}$	$k_{\min} - 1$	$k_{\min} - 1$
$\min(k_{\max} + 1, k_{\max} + 1 - Mn)$	$k_{\max} + 1$	$k_{\max} + 1$	$k_{\max} + 1 - n = k_{\min}$
$L = K + Mn$	$L = K - n$	$L = K$	$L = K + n$
$e^{i(L-K)(\chi+\phi_0)}$	$e^{-in(\chi+\phi_0)}$	$e^{i \cdot 0 \cdot (\chi+\phi_0)} = 1$	$e^{in(\chi+\phi_0)}$

Based on these results the three sets \mathbb{K}_M , which contain the wanted pairs $\langle K, L \rangle$, are determined:

$$M = -1 : \langle K, L \rangle \in \mathbb{K}_{-1} = \{K, L \in \mathbb{Z} | k_{\max} \leq K \leq k_{\max} + 1 \wedge L = K - n\} \quad (5.7.185)$$

$$M = 0 : \langle K, L \rangle \in \mathbb{K}_0 = \{K, L \in \mathbb{Z} | k_{\min} - 1 \leq K \leq k_{\max} + 1 \wedge L = K\} \quad (5.7.186)$$

$$M = 1 : \langle K, L \rangle \in \mathbb{K}_1 = \{K, L \in \mathbb{Z} | k_{\min} - 1 \leq K \leq k_{\min} \wedge L = K + n\} \quad (5.7.187)$$

The sets \mathbb{K}_{-1} and \mathbb{K}_1 contain only two pairs $\langle K, L \rangle$; by applying the relation (5.7.184) it is obtained:

$$\mathbb{K}_{-1} = \{\langle k_{\max}, k_{\max} - n \rangle, \langle k_{\max} + 1, k_{\max} + 1 - n \rangle\} = \{\langle k_{\max}, k_{\min} - 1 \rangle, \langle k_{\max} + 1, k_{\min} \rangle\} \quad (5.7.188)$$

$$\mathbb{K}_1 = \{\langle k_{\min} - 1, k_{\min} - 1 + n \rangle, \langle k_{\min}, k_{\min} + n \rangle\} = \{\langle k_{\min} - 1, k_{\max} \rangle, \langle k_{\min}, k_{\max} + 1 \rangle\} \quad (5.7.189)$$

In total it is obtained for the sum of the product $\delta' \mathbf{v}_{\text{RP}_j}^I \mathbf{a}_{\text{RP}_j}^I$ over the corresponding particles of the n -tuple:

$$\begin{aligned} \sum_{j=0}^{n-1} \delta' \mathbf{v}_{\text{RP}_j}^I \mathbf{a}_{\text{RP}_j}^I &= \sum_{K=k_{\min}-1}^{k_{\max}+1} \sum_{L=k_{\min}-1}^{k_{\max}+1} \left(\delta' \mathbf{v}_{\mathcal{A},K}^I \mathbf{a}_{\mathcal{A},L}^I \left(\sum_{j=0}^{n-1} e^{i(L-K)\theta_j} \right) \right) \\ &= \underbrace{\sum_{K=k_{\min}-1}^{k_{\max}+1} \delta' \mathbf{v}_{\mathcal{A},K}^I \mathbf{a}_{\mathcal{A},K}^I n}_{M=0} + \underbrace{\left(\delta' \mathbf{v}_{\mathcal{A},k_{\min}-1}^I \mathbf{a}_{\mathcal{A},k_{\max}}^I + \delta' \mathbf{v}_{\mathcal{A},k_{\min}}^I \mathbf{a}_{\mathcal{A},k_{\max}+1}^I \right) n e^{in(\chi+\phi_0)}}_{M=1} \\ &\quad + \underbrace{\left(\delta' \mathbf{v}_{\mathcal{A},k_{\max}}^I \mathbf{a}_{\mathcal{A},k_{\min}-1}^I + \delta' \mathbf{v}_{\mathcal{A},k_{\max}+1}^I \mathbf{a}_{\mathcal{A},k_{\min}}^I \right) n e^{-in(\chi+\phi_0)}}_{M=-1} \end{aligned} \quad (5.7.190)$$

By inserting this result into (5.7.164) it is obtained for the complete inertia terms of the n -tuple:

$$\begin{aligned} \sum_{j=0}^{n-1} \delta' \mathbf{v}_{\text{OP}_j}^I \mathbf{a}_{\text{OP}_j}^I &= \delta' \mathbf{v}_{\text{OR}}^I \mathbf{a}_{\text{OR}}^I \left(\sum_{j=0}^{n-1} \mathbf{1} + \sum_{j=0}^{n-1} \mathbf{a}_{\text{RP}_j}^I \right) + \left(\sum_{j=0}^{n-1} \delta' \mathbf{v}_{\text{RP}_j}^I \mathbf{a}_{\text{RP}_j}^I \right) \mathbf{a}_{\text{OR}}^I + \sum_{j=0}^{n-1} \delta' \mathbf{v}_{\text{RP}_j}^I \mathbf{a}_{\text{RP}_j}^I \\ &= n \left(\delta' \mathbf{v}_{\text{OR}}^I \mathbf{a}_{\text{OR}}^I + \mathbf{a}_{\mathcal{A},0}^I \right) + \delta' \mathbf{v}_{\mathcal{A},0}^I \mathbf{a}_{\text{OR}}^I + \sum_{K=k_{\min}-1}^{k_{\max}+1} \delta' \mathbf{v}_{\mathcal{A},K}^I \mathbf{a}_{\mathcal{A},K}^I \\ &\quad + n \left(\delta' \mathbf{v}_{\mathcal{A},k_{\min}-1}^I \mathbf{a}_{\mathcal{A},k_{\max}}^I + \delta' \mathbf{v}_{\mathcal{A},k_{\min}}^I \mathbf{a}_{\mathcal{A},k_{\max}+1}^I \right) e^{in\phi_0} e^{in\chi} \\ &\quad + n \left(\delta' \mathbf{v}_{\mathcal{A},k_{\max}}^I \mathbf{a}_{\mathcal{A},k_{\min}-1}^I + \delta' \mathbf{v}_{\mathcal{A},k_{\max}+1}^I \mathbf{a}_{\mathcal{A},k_{\min}}^I \right) e^{-in\phi_0} e^{-in\chi} \end{aligned} \quad (5.7.191)$$

The result indicates that for the formulation of the inertia terms in the sliding frame \mathcal{A} the large angle χ , which describes the overturning motion of the wheelset, is nearly completely eliminated; only the terms which

5.8 Inertia terms for a cyclic structure: Structure of the terms

In the previous section 5.7 the inertia terms for an n -tuple of corresponding particles have been determined for a formulation which uses the sliding frame \mathcal{A} as the reference frame. It turned out that for this case the large overturning angle χ can be eliminated nearly completely; only very few

terms, which are associated to the highest periodicities k_{\min} and k_{\max} contain the functions $e^{in\chi}$ and $e^{-in\chi}$. However, in the Fourier polynomials, which have been used for this consideration, the rotational motions and the relative motions of the particles were not treated separately. Therefore, in the following sections, the inertia terms for the different types of motions shall be considered separately. The full derivation of the inertia terms is given in the appendix C.

Generally, the motions of a flexible body can be divided into three groups, namely translational motions, rotational motions and relative motions. Here, the translational motions and the rotational motions are motions of the entire body, which are also known as rigid body motions, while relative motions usually describe deformations. For the inertia terms, the product of the virtual velocity $\delta'v_{OP}^B$ and the acceleration \mathbf{a}_{OP}^I have to be integrated over all infinitesimal masses dm of the body. For the floating frame of reference formulation where the body-fixed frame \mathcal{B} is used as the reference frame the virtual velocity $\delta'v_{OP}^B$ is given by:

$$\delta'v_{OP}^I = \delta'v_{OR}^I - \tilde{\mathbf{r}}_{RP}^I \delta'\omega_{IB}^I + \delta'\dot{\mathbf{r}}_{RP}^I \quad (5.8.192)$$

Thereby, the integrand for the inertia terms can be split up in the following way:

$$\delta'v_{OP}^{I\ T} \mathbf{a}_{OP}^I = \delta'v_{OR}^{I\ T} \mathbf{a}_{OP}^I + \delta'\omega_{IB}^{I\ T} \tilde{\mathbf{r}}_{RP}^I \mathbf{a}_{OP}^I + \delta'\dot{\mathbf{r}}_{RP}^{I\ T} \mathbf{a}_{OP}^I \quad (5.8.193)$$

The acceleration is given by:

$$\mathbf{a}_{OP}^I = \mathbf{a}_{OR}^I + \left(\dot{\tilde{\omega}}_{IB}^I + \tilde{\omega}_{IB}^I \tilde{\omega}_{IB}^I \right) \mathbf{S}^{IB} \mathbf{r}_{RP}^B + 2 \tilde{\omega}_{IB}^I \mathbf{S}^{IB} \dot{\mathbf{r}}_{RP}^B + \mathbf{S}^{IB} \ddot{\mathbf{r}}_{RP}^B \quad (5.8.194)$$

By factoring out the vectors and matrices $\delta'v_{OR}^I$, \mathbf{a}_{OR}^I , \mathbf{S}^{IB} , $\tilde{\omega}_{IB}^I$ and $\dot{\tilde{\omega}}_{IB}^I$, which are equal for all particles, the inertia terms for the translational motions can be formulated in the following way:

$$\begin{aligned} \int_B \delta'v_{OR}^{I\ T} \mathbf{a}_{OP}^I dm &= \delta'v_{OR}^{I\ T} \left(m_B \mathbf{a}_{OR}^I + \left(\dot{\tilde{\omega}}_{IB}^I + \tilde{\omega}_{IB}^I \tilde{\omega}_{IB}^I \right) \mathbf{S}^{IB} \int_B \mathbf{r}_{RP}^B dm \right. \\ &\quad \left. + 2 \tilde{\omega}_{IB}^I \mathbf{S}^{IB} \int_B \dot{\mathbf{r}}_{RP}^B dm + \mathbf{S}^{IB} \int_B \ddot{\mathbf{r}}_{RP}^B dm \right) \quad (5.8.195) \end{aligned}$$

For the rotational motions the inertia terms are obtained to:

$$\begin{aligned} \int_B \delta'\omega_{IB}^{I\ T} \tilde{\mathbf{r}}_{RP}^I \mathbf{a}_{OP}^I &= \delta'\omega_{IB}^{I\ T} \left(\mathbf{S}^{IB} \int_B \tilde{\mathbf{r}}_{RP}^B dm \mathbf{S}^{BI} \mathbf{a}_{OR}^I - \mathbf{S}^{IB} \int_B \tilde{\mathbf{r}}_{RP}^B \tilde{\mathbf{r}}_{RP}^B dm \mathbf{S}^{BI} \dot{\omega}_{IB}^I \right. \\ &\quad \left. - \tilde{\omega}_{IB}^I \mathbf{S}^{IB} \int_B \tilde{\mathbf{r}}_{RP}^B \tilde{\mathbf{r}}_{RP}^B dm \mathbf{S}^{BI} \omega_{IB}^I \right. \\ &\quad \left. + 2 \mathbf{S}^{IB} \int_B \tilde{\mathbf{r}}_{RP}^B \dot{\tilde{\mathbf{r}}}_{RP}^B dm \mathbf{S}^{BI} \omega_{IB}^I + \mathbf{S}^{IB} \int_B \tilde{\mathbf{r}}_{RP}^B \ddot{\mathbf{r}}_{RP}^B dm \right) \quad (5.8.196) \end{aligned}$$

For the relative motions it is obtained:

$$\begin{aligned} \int_B \delta'\dot{\mathbf{r}}_{RP}^{I\ T} \mathbf{a}_{OP}^I dm &= \int_B \delta'\dot{\mathbf{r}}_{RP}^{B\ T} dm \mathbf{S}^{BI} \mathbf{a}_{OP}^I - \int_B \delta'\dot{\mathbf{r}}_{RP}^{B\ T} \tilde{\mathbf{r}}_{RP}^B dm \mathbf{S}^{BI} \dot{\omega}_{IB}^I \\ &\quad + \omega_{IB}^{I\ T} \mathbf{S}^{IB} \int_B \delta'\dot{\mathbf{r}}_{RP}^{B\ T} \tilde{\mathbf{r}}_{RP}^B dm \mathbf{S}^{BI} \omega_{IB}^I \\ &\quad - \int_B \delta'\dot{\mathbf{r}}_{RP}^{B\ T} \tilde{\mathbf{r}}_{RP}^B dm \mathbf{S}^{BI} \omega_{IB}^I + \int_B \delta'\dot{\mathbf{r}}_{RP}^{B\ T} \ddot{\mathbf{r}}_{RP}^B dm \quad (5.8.197) \end{aligned}$$

The relative position is described by the sum of the reference position vector \mathbf{x}^B and the deformation field $\mathbf{w}^B(\mathbf{x}^B, t)$:

$$\mathbf{r}_{RP}^B = \mathbf{x}^B + \mathbf{w}^B(\mathbf{x}^B, t) \quad (5.8.198)$$

In the body-fixed frame \mathcal{B} the reference position vector is constant so that its derivative with respect to the time t vanishes; thereby, it is valid for the vectors $\mathbf{r}_{\text{RP}}^{\mathcal{B}}$ and $\dot{\mathbf{r}}_{\text{RP}}^{\mathcal{B}}$

$$\mathbf{r}_{\text{RP}}^{\mathcal{B}} = \mathbf{x}^{\mathcal{B}} + \sum_{I=1}^{N_{\mathcal{B}}} \mathbf{W}_I(\mathbf{x}^{\mathcal{B}}) q_I \Rightarrow \dot{\mathbf{r}}_{\text{RP}}^{\mathcal{B}} = \sum_{I=1}^{N_{\mathcal{B}}} \mathbf{W}_I(\mathbf{x}^{\mathcal{B}}) \dot{q}_I \Rightarrow \ddot{\mathbf{r}}_{\text{RP}}^{\mathcal{B}} = \sum_{I=1}^{N_{\mathcal{B}}} \mathbf{W}_I(\mathbf{x}^{\mathcal{B}}) \ddot{q}_I \quad (5.8.199)$$

From this it follows for the integrals, which are contained in the inertia terms for the translational motions:

$$\int_{\mathcal{B}} \mathbf{r}_{\text{RP}}^{\mathcal{B}} dm = \int_{\mathcal{B}} \mathbf{x}^{\mathcal{B}} dm + \sum_{I=1}^{N_{\mathcal{B}}} \int_{\mathcal{B}} \mathbf{W}_I(\mathbf{x}^{\mathcal{B}}) dm q_I \quad (5.8.200)$$

$$\int_{\mathcal{B}} \dot{\mathbf{r}}_{\text{RP}}^{\mathcal{B}} dm = \sum_{I=1}^{N_{\mathcal{B}}} \int_{\mathcal{B}} \mathbf{W}_I(\mathbf{x}^{\mathcal{B}}) dm \dot{q}_I \quad (5.8.201)$$

$$\int_{\mathcal{B}} \ddot{\mathbf{r}}_{\text{RP}}^{\mathcal{B}} dm = \sum_{I=1}^{N_{\mathcal{B}}} \int_{\mathcal{B}} \mathbf{W}_I(\mathbf{x}^{\mathcal{B}}) dm \ddot{q}_I \quad (5.8.202)$$

The integrals contained in the inertia terms for the rotational motions are reformulated in the following way:

$$\begin{aligned} \int_{\mathcal{B}} \tilde{\mathbf{r}}_{\text{RP}}^{\mathcal{B}} \tilde{\mathbf{r}}_{\text{RP}}^{\mathcal{B}} dm &= \int_{\mathcal{B}} (\tilde{\mathbf{x}}^{\mathcal{B}} + \tilde{\mathbf{w}}^{\mathcal{B}}) (\tilde{\mathbf{x}}^{\mathcal{B}} + \tilde{\mathbf{w}}^{\mathcal{B}}) dm \\ &= \int_{\mathcal{B}} \tilde{\mathbf{x}}^{\mathcal{B}} \tilde{\mathbf{x}}^{\mathcal{B}} dm + \int_{\mathcal{B}} (\tilde{\mathbf{x}}^{\mathcal{B}} \tilde{\mathbf{w}}^{\mathcal{B}} + \tilde{\mathbf{w}}^{\mathcal{B}} \tilde{\mathbf{x}}^{\mathcal{B}}) dm + \int_{\mathcal{B}} \tilde{\mathbf{w}}^{\mathcal{B}} \tilde{\mathbf{w}}^{\mathcal{B}} dm \end{aligned} \quad (5.8.203)$$

$$\int_{\mathcal{B}} \tilde{\mathbf{r}}_{\text{RP}}^{\mathcal{B}} \dot{\tilde{\mathbf{r}}}_{\text{RP}}^{\mathcal{B}} dm = \int_{\mathcal{B}} (\tilde{\mathbf{x}}^{\mathcal{B}} + \tilde{\mathbf{w}}^{\mathcal{B}}) \dot{\tilde{\mathbf{w}}}^{\mathcal{B}} dm = \int_{\mathcal{B}} \tilde{\mathbf{x}}^{\mathcal{B}} \dot{\tilde{\mathbf{w}}}^{\mathcal{B}} dm + \int_{\mathcal{B}} \tilde{\mathbf{w}}^{\mathcal{B}} \dot{\tilde{\mathbf{w}}}^{\mathcal{B}} dm \quad (5.8.204)$$

$$\int_{\mathcal{B}} \tilde{\mathbf{r}}_{\text{RP}}^{\mathcal{B}} \ddot{\tilde{\mathbf{r}}}_{\text{RP}}^{\mathcal{B}} dm = \int_{\mathcal{B}} (\tilde{\mathbf{x}}^{\mathcal{B}} + \tilde{\mathbf{w}}^{\mathcal{B}}) \ddot{\tilde{\mathbf{w}}}^{\mathcal{B}} dm = \int_{\mathcal{B}} \tilde{\mathbf{x}}^{\mathcal{B}} \ddot{\tilde{\mathbf{w}}}^{\mathcal{B}} dm + \int_{\mathcal{B}} \tilde{\mathbf{w}}^{\mathcal{B}} \ddot{\tilde{\mathbf{w}}}^{\mathcal{B}} dm \quad (5.8.205)$$

Applying the modal synthesis leads to:

$$\begin{aligned} \int_{\mathcal{B}} \tilde{\mathbf{r}}_{\text{RP}}^{\mathcal{B}} \tilde{\mathbf{r}}_{\text{RP}}^{\mathcal{B}} dm &= \int_{\mathcal{B}} \tilde{\mathbf{x}}^{\mathcal{B}} \tilde{\mathbf{x}}^{\mathcal{B}} dm + \sum_{I=1}^{N_{\mathcal{B}}} \int_{\mathcal{B}} (\tilde{\mathbf{x}}^{\mathcal{B}} \tilde{\mathbf{W}}_I(\mathbf{x}^{\mathcal{B}}) + \tilde{\mathbf{W}}_I(\mathbf{x}^{\mathcal{B}}) \tilde{\mathbf{x}}^{\mathcal{B}}) dm q_I \\ &\quad + \sum_{v=1}^{N_{\mathcal{B}}} \sum_{I=1}^{N_{\mathcal{B}}} \int_{\mathcal{B}} \tilde{\mathbf{W}}_v(\mathbf{x}^{\mathcal{B}}) \tilde{\mathbf{W}}_I(\mathbf{x}^{\mathcal{B}}) dm q_v q_I \end{aligned} \quad (5.8.206)$$

$$\int_{\mathcal{B}} \tilde{\mathbf{r}}_{\text{RP}}^{\mathcal{B}} \dot{\tilde{\mathbf{r}}}_{\text{RP}}^{\mathcal{B}} dm = \sum_{I=1}^{N_{\mathcal{B}}} \int_{\mathcal{B}} \tilde{\mathbf{x}}^{\mathcal{B}} \tilde{\mathbf{W}}_I(\mathbf{x}^{\mathcal{B}}) dm \dot{q}_I + \sum_{v=1}^{N_{\mathcal{B}}} \sum_{I=1}^{N_{\mathcal{B}}} \int_{\mathcal{B}} \tilde{\mathbf{W}}_v(\mathbf{x}^{\mathcal{B}}) \tilde{\mathbf{W}}_I(\mathbf{x}^{\mathcal{B}}) dm q_v \dot{q}_I \quad (5.8.207)$$

$$\int_{\mathcal{B}} \tilde{\mathbf{r}}_{\text{RP}}^{\mathcal{B}} \ddot{\tilde{\mathbf{r}}}_{\text{RP}}^{\mathcal{B}} dm = \sum_{I=1}^{N_{\mathcal{B}}} \int_{\mathcal{B}} \tilde{\mathbf{x}}^{\mathcal{B}} \mathbf{W}_I(\mathbf{x}^{\mathcal{B}}) dm \ddot{q}_I + \sum_{v=1}^{N_{\mathcal{B}}} \sum_{I=1}^{N_{\mathcal{B}}} \int_{\mathcal{B}} \tilde{\mathbf{W}}_v(\mathbf{x}^{\mathcal{B}}) \mathbf{W}_I(\mathbf{x}^{\mathcal{B}}) dm q_v \ddot{q}_I \quad (5.8.208)$$

For the terms which contain products of deformations, a second independent index v in addition to the index I is introduced. – For the inertia terms for the relative motions it is valid:

$$\int_{\mathcal{B}} \delta' \tilde{\mathbf{r}}_{\text{RP}}^{\mathcal{B}T} \tilde{\mathbf{r}}_{\text{RP}}^{\mathcal{B}} dm = \int_{\mathcal{B}} \delta' \tilde{\mathbf{w}}^{\mathcal{B}T} (\tilde{\mathbf{x}}^{\mathcal{B}} + \tilde{\mathbf{w}}^{\mathcal{B}}) dm = \int_{\mathcal{B}} \delta' \tilde{\mathbf{w}}^{\mathcal{B}T} \tilde{\mathbf{x}}^{\mathcal{B}} dm + \int_{\mathcal{B}} \delta' \tilde{\mathbf{w}}^{\mathcal{B}T} \tilde{\mathbf{w}}^{\mathcal{B}} dm \quad (5.8.209)$$

$$\int_{\mathcal{B}} \delta' \dot{\tilde{\mathbf{r}}}_{\text{RP}}^{\mathcal{B}T} \tilde{\mathbf{r}}_{\text{RP}}^{\mathcal{B}} dm = \int_{\mathcal{B}} \delta' \dot{\tilde{\mathbf{w}}}^{\mathcal{B}T} (\tilde{\mathbf{x}}^{\mathcal{B}} + \tilde{\mathbf{w}}^{\mathcal{B}}) dm = \int_{\mathcal{B}} \delta' \dot{\tilde{\mathbf{w}}}^{\mathcal{B}T} \tilde{\mathbf{x}}^{\mathcal{B}} dm + \int_{\mathcal{B}} \delta' \dot{\tilde{\mathbf{w}}}^{\mathcal{B}T} \tilde{\mathbf{w}}^{\mathcal{B}} dm \quad (5.8.210)$$

$$\int_{\mathcal{B}} \delta' \tilde{\mathbf{r}}_{\text{RP}}^{\mathcal{B}T} \dot{\tilde{\mathbf{r}}}_{\text{RP}}^{\mathcal{B}} dm = \int_{\mathcal{B}} \delta' \tilde{\mathbf{w}}^{\mathcal{B}T} \dot{\tilde{\mathbf{w}}}^{\mathcal{B}} dm \quad (5.8.211)$$

$$\int_{\mathcal{B}} \delta' \ddot{\tilde{\mathbf{r}}}_{\text{RP}}^{\mathcal{B}T} \tilde{\mathbf{r}}_{\text{RP}}^{\mathcal{B}} dm = \int_{\mathcal{B}} \delta' \tilde{\mathbf{w}}^{\mathcal{B}T} \ddot{\tilde{\mathbf{w}}}^{\mathcal{B}} dm \quad (5.8.212)$$

Here, the application of the modal synthesis leads to the following formulation:

$$\int_B \delta' \mathbf{r}_{RP}^{\mathcal{B}T} \tilde{\mathbf{r}}_{RP}^{\mathcal{B}} dm = \sum_{v=1}^{N_B} \left(\int_B \mathbf{W}_v(\mathbf{x}^{\mathcal{B}})^T \tilde{\mathbf{x}}^{\mathcal{B}} dm + \sum_{I=1}^{N_B} \int_B \mathbf{W}_v(\mathbf{x}^{\mathcal{B}})^T \tilde{\mathbf{W}}_I(\mathbf{x}^{\mathcal{B}}) dm q_I \right) \delta' \dot{q}_v \quad (5.8.213)$$

$$\int_B \delta' \tilde{\mathbf{r}}_{RP}^{\mathcal{B}} \tilde{\mathbf{r}}_{RP}^{\mathcal{B}} dm = \sum_{v=1}^{N_B} \left(\int_B \tilde{\mathbf{W}}_v(\mathbf{x}^{\mathcal{B}}) \tilde{\mathbf{x}}^{\mathcal{B}} dm + \sum_{I=1}^{N_B} \int_B \tilde{\mathbf{W}}_v(\mathbf{x}^{\mathcal{B}}) \tilde{\mathbf{W}}_I(\mathbf{x}^{\mathcal{B}}) dm q_I \right) \delta' \dot{q}_v \quad (5.8.214)$$

$$\int_B \delta' \mathbf{r}_{RP}^{\mathcal{B}T} \dot{\tilde{\mathbf{r}}}_{RP}^{\mathcal{B}} dm = \sum_{v=1}^{N_B} \sum_{I=1}^{N_B} \int_B \mathbf{W}_v(\mathbf{x}^{\mathcal{B}})^T \tilde{\mathbf{W}}_I(\mathbf{x}^{\mathcal{B}}) dm \dot{q}_I \delta' \dot{q}_v \quad (5.8.215)$$

$$\int_B \delta' \mathbf{r}_{RP}^{\mathcal{B}T} \ddot{\tilde{\mathbf{r}}}_{RP}^{\mathcal{B}} dm = \sum_{v=1}^{N_B} \sum_{I=1}^{N_B} \int_B \mathbf{W}_v(\mathbf{x}^{\mathcal{B}})^T \mathbf{W}_I(\mathbf{x}^{\mathcal{B}}) dm \ddot{q}_I \delta' \dot{q}_v \quad (5.8.216)$$

5.8.1 Rigid body terms

For the rigid body terms, the integrand contains only the vector $\mathbf{x}^{\mathcal{B}}$. Using cylindrical the coordinates $\mathbf{c} = \mathbf{c}(r, y)$ and ϕ it is valid:

$$\mathbf{x}^{\mathcal{B}} = \mathbf{S}_2(\phi) \mathbf{c} \Rightarrow \tilde{\mathbf{x}}^{\mathcal{B}} = \mathbf{S}_2(\phi) \tilde{\mathbf{c}} \mathbf{S}_2(\phi)^T \Rightarrow \tilde{\mathbf{x}}^{\mathcal{B}} \tilde{\mathbf{x}}^{\mathcal{B}} = \mathbf{S}_2(\phi) \tilde{\mathbf{c}} \underbrace{\mathbf{S}_2(\phi)^T \mathbf{S}_2(\phi)}_{\mathbf{I}} \tilde{\mathbf{c}} \mathbf{S}_2(\phi)^T \quad (5.8.217)$$

Inserting the formulation of the rotation matrix $\mathbf{S}_2(\phi)$ as a Fourier series leads to:

$$\begin{aligned} \tilde{\mathbf{x}}^{\mathcal{B}} \tilde{\mathbf{x}}^{\mathcal{B}} &= \mathbf{S}_2(\phi) \tilde{\mathbf{c}} \tilde{\mathbf{c}} \mathbf{S}_2(\phi)^T = \mathbf{S}_2(\phi) \tilde{\mathbf{c}} \tilde{\mathbf{c}} \mathbf{S}_2(-\phi) \\ &= \left(\sum_{b=-1}^1 \mathbf{S}_{2,b} e^{ib\phi} \right) \tilde{\mathbf{c}} \tilde{\mathbf{c}} \left(\sum_{c=-1}^1 \mathbf{S}_{2,c} e^{-ic\phi} \right) = \sum_{b=-1}^1 \sum_{c=-1}^1 \mathbf{S}_{2,b} \tilde{\mathbf{c}} \tilde{\mathbf{c}} \mathbf{S}_{2,c} e^{i(b-c)\phi} \end{aligned} \quad (5.8.218)$$

From this it follows for the sums over the corresponding particles of the n -tuple:

$$\sum_{j=0}^{n-1} \mathbf{x}_j^{\mathcal{B}} = \sum_{j=0}^{n-1} \left(\sum_{b=-1}^1 \mathbf{S}_{2,b} e^{ib\phi_j} \right) \mathbf{c} = \sum_{j=0}^{n-1} \sum_{b=-1}^1 \mathbf{S}_{2,b} e^{ib\phi_j} \mathbf{c} = \sum_{b=-1}^1 \left(\mathbf{S}_{2,b} \mathbf{c} \left(\sum_{j=0}^{n-1} e^{ib\phi_j} \right) \right) \quad (5.8.219)$$

$$\sum_{j=0}^{n-1} \tilde{\mathbf{x}}_j^{\mathcal{B}} \tilde{\mathbf{x}}_j^{\mathcal{B}} = \sum_{j=0}^{n-1} \sum_{b=-1}^1 \sum_{c=-1}^1 \mathbf{S}_{2,b} \tilde{\mathbf{c}} \tilde{\mathbf{c}} \mathbf{S}_{2,c} e^{i(b-c)\phi_j} = \sum_{b=-1}^1 \sum_{c=-1}^1 \left(\mathbf{S}_{2,b} \tilde{\mathbf{c}} \tilde{\mathbf{c}} \mathbf{S}_{2,c} \left(\sum_{j=0}^{n-1} e^{i(b-c)\phi_j} \right) \right) \quad (5.8.220)$$

The sums over j are evaluated based on the following relation, which contains the evaluation of the geometric series:

$$\sum_{j=0}^{n-1} e^{ip\phi_j} = \sum_{j=0}^{n-1} e^{ip\phi_0} e^{ip(\phi_j - \phi_0)} = e^{ip\phi_0} \left(\sum_{j=0}^{n-1} \zeta^{pj} \right) = \begin{cases} ne^{ip\phi_0} & \text{for } \frac{p}{n} \in \mathbb{Z} \\ 0 & \text{for } \frac{p}{n} \notin \mathbb{Z} \end{cases} \quad (5.8.221)$$

It is assumed that the cyclic structure consists of $n > 2$ segments; therefore, it is valid:

$$n > 2 \Rightarrow \frac{1}{n} < \frac{1}{2} \Rightarrow \frac{2}{n} < 1 \quad (5.8.222)$$

For the range of b it is valid:

$$-1 \leq b \leq 1 \Rightarrow -\frac{1}{2} < -\frac{1}{n} \leq \frac{b}{n} \leq \frac{1}{n} < \frac{1}{2} \Rightarrow -\frac{1}{2} < \frac{b}{n} < \frac{1}{2} \quad (5.8.223)$$

From this it follows:

$$-\frac{1}{2} < \frac{b}{n} < \frac{1}{2} \wedge \frac{b}{n} \in \mathbb{Z} \Rightarrow \frac{b}{n} = 0 \Rightarrow b = 0 \quad (5.8.224)$$

Thereby, the evaluation of the sum of \mathbf{x}_j^B leads to:

$$\sum_{j=0}^{n-1} \mathbf{x}_j^B = \sum_{b=-1}^1 \left(\mathbf{S}_{2,b} \mathbf{c} \left(\sum_{j=0}^{n-1} e^{ib\phi_j} \right) \right) = \mathbf{S}_{2,0} \mathbf{c} n = n \begin{bmatrix} 0 & 0 & 0 \\ 0 & 1 & 0 \\ 0 & 0 & 0 \end{bmatrix} \begin{bmatrix} 0 \\ y \\ r \end{bmatrix} = n \begin{bmatrix} 0 \\ y \\ 0 \end{bmatrix} \quad (5.8.225)$$

The result indicates that the centre of mass of the cyclic structure lies on the 2-axis, which is in this case the axis of the rotational symmetry. Furthermore, the result does not depend on the angle ϕ_0 .

The expression for the inertia tensor contains two sums over the indices b and c . Since the ranges of b and c are equal, it is valid based on (5.8.223):

$$-1 \leq c \leq 1 \Rightarrow -\frac{1}{2} < \frac{c}{n} < \frac{1}{2} \Rightarrow \frac{1}{2} > -\frac{c}{n} > -\frac{1}{2} \quad (5.8.226)$$

From this, it can be derived:

$$-\frac{1}{2} < \frac{b}{n} < \frac{1}{2} \wedge -\frac{1}{2} < -\frac{c}{n} < \frac{1}{2} \Rightarrow 1 < \frac{b-c}{n} < 1 \quad (5.8.227)$$

Based on this, it can be derived:

$$-1 < \frac{b-c}{n} < 1 \wedge \frac{b-c}{n} \in \mathbb{Z} \Rightarrow \frac{b-c}{n} = 0 \Rightarrow b-c = 0 \Rightarrow b = c \quad (5.8.228)$$

From this, it follows:

$$\begin{aligned} \sum_{j=0}^{n-1} \tilde{\mathbf{x}}_j^B \tilde{\mathbf{x}}_j^B &= \sum_{b=-1}^1 \sum_{c=-1}^1 \left(\mathbf{S}_{2,b} \tilde{\mathbf{c}} \tilde{\mathbf{c}} \mathbf{S}_{2,c} \left(\sum_{j=0}^{n-1} e^{i(b-c)\phi_j} \right) \right) = \sum_{b=-1}^1 \mathbf{S}_{2,b} \tilde{\mathbf{c}} \tilde{\mathbf{c}} \mathbf{S}_{2,b} n \\ &= n (\mathbf{S}_{2,-1} \tilde{\mathbf{c}} \tilde{\mathbf{c}} \mathbf{S}_{2,-1} + \mathbf{S}_{2,0} \tilde{\mathbf{c}} \tilde{\mathbf{c}} \mathbf{S}_{2,0} + \mathbf{S}_{2,1} \tilde{\mathbf{c}} \tilde{\mathbf{c}} \mathbf{S}_{2,1}) \end{aligned} \quad (5.8.229)$$

With the following matrices:

$$\mathbf{S}_{2,-1} = \frac{1}{2} \begin{bmatrix} 1 & 0 & -i \\ 0 & 0 & 0 \\ i & 0 & 1 \end{bmatrix}, \mathbf{S}_{2,0} = \begin{bmatrix} 0 & 0 & 0 \\ 0 & 1 & 0 \\ 0 & 0 & 0 \end{bmatrix}, \mathbf{S}_{2,1} = \frac{1}{2} \begin{bmatrix} 1 & 0 & i \\ 0 & 0 & 0 \\ -i & 0 & 1 \end{bmatrix}, \tilde{\mathbf{c}} \tilde{\mathbf{c}} = \begin{bmatrix} -r^2 - y^2 & 0 & 0 \\ 0 & -r^2 & ry \\ 0 & ry & -y^2 \end{bmatrix} \quad (5.8.230)$$

it is obtained:

$$\begin{aligned} \sum_{j=0}^{n-1} \tilde{\mathbf{x}}_j^B \tilde{\mathbf{x}}_j^B &= n (\mathbf{S}_{2,-1} \tilde{\mathbf{c}} \tilde{\mathbf{c}} \mathbf{S}_{2,-1} + \mathbf{S}_{2,0} \tilde{\mathbf{c}} \tilde{\mathbf{c}} \mathbf{S}_{2,0} + \mathbf{S}_{2,1} \tilde{\mathbf{c}} \tilde{\mathbf{c}} \mathbf{S}_{2,1}) \\ &= -\frac{n}{2} \begin{bmatrix} r^2 + 2y^2 & 0 & 0 \\ 0 & 2r^2 & 0 \\ 0 & 0 & r^2 + 2y^2 \end{bmatrix} \end{aligned} \quad (5.8.231)$$

The result is a diagonal matrix, whereby the first and the third diagonal element are equal. Since the 1-axis and the 3-axis are the transverse axes of the cyclic structure, this result indicates that in the undeformed reference state the moment of inertia is equal for each transverse axis.

5.8.2 Terms of first order

In the present case, terms of first order are those terms in which the shape function \mathbf{W}_I appears one time as a factor. These terms are the following integrals, which appear in the inertia terms for the translational and rotational motions:

$$\int_B \mathbf{W}_I(\mathbf{x}^B) dm, \int_B \tilde{\mathbf{x}}^B \mathbf{W}_I(\mathbf{x}^B) dm, \int_B \tilde{\mathbf{x}}^B \tilde{\mathbf{W}}_I(\mathbf{x}^B) dm, \int_B \left(\tilde{\mathbf{x}}^B \tilde{\mathbf{W}}_I(\mathbf{x}^B) + \tilde{\mathbf{W}}_I(\mathbf{x}^B) \tilde{\mathbf{x}}^B \right) dm \quad (5.8.232)$$

From these terms, the following integrals contained in the inertia terms for the relative motions can be derived:

$$\int_B \mathbf{W}_v(\mathbf{x}^B)^T \tilde{\mathbf{x}}^B dm, \int_B \tilde{\mathbf{W}}_v(\mathbf{x}^B) \tilde{\mathbf{x}}^B dm \quad (5.8.233)$$

With the exception of a very small region around the reference point, the absolute value $|\mathbf{x}^B|$ of the reference position vector is far greater than the absolute value $|\mathbf{w}^B|$ of the deformation vector; therefore, the first order terms are the dominant coupling terms between the translational and rotational motions on the one hand and the deformational motions on the other hand.

In the previous section 5.8.1 it has already been derived for the matrix $\tilde{\mathbf{x}}^B$:

$$\mathbf{x}^B = \mathbf{S}_2(\phi) \mathbf{c} \Rightarrow \tilde{\mathbf{x}}^B = \mathbf{S}_2(\phi) \tilde{\mathbf{c}} \mathbf{S}_2(\phi)^T \quad (5.8.234)$$

As derived in the section 5.5 it is valid for the shape functions:

$$\mathbf{W}_I(\mathbf{x}^B) = \mathbf{W}_I(\mathbf{c}, \phi) = \mathbf{S}_2(\phi) \mathbf{U}_I(\mathbf{c}, \phi) \Rightarrow \tilde{\mathbf{W}}_I(\mathbf{x}^B) = \mathbf{S}_2(\phi) \tilde{\mathbf{U}}_I(\mathbf{c}, \phi) \mathbf{S}_2(\phi)^T \quad (5.8.235)$$

By inserting this into the integrands of (5.8.232) and applying the relation:

$$\mathbf{S}_2(\phi)^T \mathbf{S}_2(\phi) = \mathbf{I} \quad (5.8.236)$$

it is obtained:

$$\tilde{\mathbf{x}}^B \mathbf{W}_I(\mathbf{x}^B) = \mathbf{S}_2(\phi) \tilde{\mathbf{c}} \mathbf{S}_2(\phi)^T \mathbf{S}_2(\phi) \mathbf{U}_I(\mathbf{c}, \phi) = \mathbf{S}_2(\phi) \tilde{\mathbf{c}} \mathbf{U}_I(\mathbf{c}, \phi) \quad (5.8.237)$$

$$\tilde{\mathbf{x}}^B \tilde{\mathbf{W}}_I(\mathbf{x}^B) = \mathbf{S}_2(\phi) \tilde{\mathbf{c}} \mathbf{S}_2(\phi)^T \mathbf{S}_2(\phi) \tilde{\mathbf{U}}_I(\mathbf{c}, \phi) \mathbf{S}_2(\phi)^T = \mathbf{S}_2(\phi) \tilde{\mathbf{c}} \tilde{\mathbf{U}}_I(\mathbf{c}, \phi) \mathbf{S}_2(-\phi) \quad (5.8.238)$$

$$\tilde{\mathbf{W}}_I(\mathbf{x}^B) \tilde{\mathbf{x}}^B = \mathbf{S}_2(\phi) \tilde{\mathbf{U}}_I(\mathbf{c}, \phi) \mathbf{S}_2(\phi)^T \mathbf{S}_2(\phi) \tilde{\mathbf{c}} \mathbf{S}_2(\phi)^T = \mathbf{S}_2(\phi) \tilde{\mathbf{U}}_I(\mathbf{c}, \phi) \tilde{\mathbf{c}} \mathbf{S}_2(-\phi) \quad (5.8.239)$$

First, the terms, which contain only one rotation matrix, shall be considered. For the corresponding particles of an n -tuple the eigenmode \mathbf{U}_I is given by:

$$\mathbf{U}_I(\mathbf{c}, \phi_j) = \mathbf{U}_I(\mathbf{c}, \phi_0) \zeta^{k_I j} \quad (5.8.240)$$

The matrix $\mathbf{S}_2(\phi_j)$ is formulated in the following way:

$$\mathbf{S}_2(\phi_j) = \sum_{b=-1}^1 \mathbf{S}_{2,b} e^{ib\phi_j} = \sum_{b=-1}^1 \mathbf{S}_{2,b} e^{ib\phi_0} e^{ib(\phi_j-\phi_0)} = \sum_{b=-1}^1 \mathbf{S}_{2,b} e^{ib\phi_0} \zeta^{bj} \quad (5.8.241)$$

Based on this, it can be formulated:

$$\begin{aligned} \mathbf{W}(\mathbf{x}_j^B) &= \mathbf{S}_2(\phi_j) \mathbf{U}_I(\mathbf{c}, \phi_j) \\ &= \left(\sum_{b=-1}^1 \mathbf{S}_{2,b} e^{ib\phi_0} \zeta^{bj} \right) \mathbf{U}_I(\mathbf{c}, \phi_0) \zeta^{k_I j} = \sum_{b=-1}^1 \mathbf{S}_{2,b} \mathbf{U}_I(\mathbf{c}, \phi_0) e^{ib\phi_0} \zeta^{(k_I+b)j} \end{aligned} \quad (5.8.242)$$

$$\begin{aligned} \tilde{\mathbf{x}}_j^B \tilde{\mathbf{W}}_I(\mathbf{x}_j^B) &= \mathbf{S}_2(\phi_j) \tilde{\mathbf{c}} \mathbf{U}_I(\mathbf{c}, \phi_j) \\ &= \left(\sum_{b=-1}^1 \mathbf{S}_{2,b} e^{ib\phi_0} \zeta^{bj} \right) \tilde{\mathbf{c}} \mathbf{U}_I(\mathbf{c}, \phi_0) \zeta^{k_I j} = \sum_{b=-1}^1 \mathbf{S}_{2,b} \tilde{\mathbf{c}} \mathbf{U}_I(\mathbf{c}, \phi_0) e^{ib\phi_0} \zeta^{(k_I+b)j} \end{aligned} \quad (5.8.243)$$

The summation over the corresponding particles leads to:

$$\sum_{j=1}^{n-1} \mathbf{W}(\mathbf{x}_j^{\mathcal{B}}) = \sum_{b=-1}^1 \left(\mathbf{S}_{2,b} \mathbf{U}_I(\mathbf{c}, \phi_0) e^{ib\phi_0} \left(\sum_{j=0}^{n-1} \zeta^{(k_I+b)j} \right) \right) \quad (5.8.244)$$

$$\sum_{j=1}^{n-1} \tilde{\mathbf{x}}_j^{\mathcal{B}} \tilde{\mathbf{W}}_I(\mathbf{x}_j^{\mathcal{B}}) = \sum_{b=-1}^1 \left(\mathbf{S}_{2,b} \tilde{\mathbf{c}} \mathbf{U}_I(\mathbf{c}, \phi_0) e^{ib\phi_0} \left(\sum_{j=0}^{n-1} \zeta^{(k_I+b)j} \right) \right) \quad (5.8.245)$$

Again, the following rule for the geometric series is applied:

$$\sum_{j=0}^{n-1} \zeta^{pj} = \begin{cases} n & \text{for } \frac{p}{n} \in \mathbb{Z} \\ 0 & \text{for } \frac{p}{n} \notin \mathbb{Z} \end{cases} \quad (5.8.246)$$

As derived in the section 3.1.2 it is valid for the periodicity k_I :

$$-\frac{n}{2} + \frac{1}{2} \leq k_{\min} \leq k_I \leq k_{\max} \leq \frac{n}{2} \Rightarrow -\frac{1}{2} + \frac{1}{2n} \leq \frac{k_I}{n} \leq \frac{1}{2} \quad (5.8.247)$$

This range is now combined with the range of $\frac{b}{n}$ according to (5.8.223). Furthermore, because of $n \in \mathbb{N}$ the number n is positive so that also the fraction $\frac{1}{2n}$ is positive. Thereby, it is obtained:

$$-\frac{1}{2} + \frac{1}{2n} \leq \frac{k_I}{n} \leq \frac{1}{2} \wedge -\frac{1}{2} < \frac{b}{n} < \frac{1}{2} \Rightarrow -1 < -1 + \frac{1}{2n} < \frac{k_I+b}{n} < 1 \quad (5.8.248)$$

The sum over j doesn't vanish if the fraction $\frac{k_I+b}{n}$ is an integer. Therefore, it is valid:

$$-1 < \frac{k_I+b}{n} < 1 \wedge \frac{k_I+b}{n} \in \mathbb{Z} \Rightarrow \frac{k_I+b}{n} = 0 \Rightarrow k_I+b=0 \Rightarrow k_I = -b \quad (5.8.249)$$

Because of $b \in \{-1, 0, 1\}$ it follows that the sums (5.8.244) and (5.8.245) do not vanish for $k_I \in \{-1, 0, 1\}$. Conversely, this means that the following integrals

$$\int_{\mathcal{B}} \mathbf{W}_I(\mathbf{x}^{\mathcal{B}}) dm, \int_{\mathcal{B}} \tilde{\mathbf{x}}^{\mathcal{B}} \tilde{\mathbf{W}}_I(\mathbf{x}^{\mathcal{B}}) dm \quad (5.8.250)$$

always vanish for $k_I \notin \{-1, 0, 1\}$.

For the integrands, which contain two rotation matrices, it is valid:

$$\begin{aligned} \tilde{\mathbf{x}}_j^{\mathcal{B}} \tilde{\mathbf{W}}_I(\mathbf{x}_j^{\mathcal{B}}) &= \mathbf{S}_{2}(\phi_j) \tilde{\mathbf{c}} \tilde{\mathbf{U}}_I(\mathbf{c}, \phi_j) \mathbf{S}_{2}(-\phi_j) \\ &= \left(\sum_{b=-1}^1 \mathbf{S}_{2,b} e^{ib\phi_0} \zeta^{bj} \right) \tilde{\mathbf{c}} \tilde{\mathbf{U}}_I(\mathbf{c}, \phi_0) \zeta^{k_I j} \left(\sum_{c=-1}^1 \mathbf{S}_{2,c} e^{-ic\phi_0} \zeta^{-bj} \right) \\ &= \sum_{b=-1}^1 \sum_{c=-1}^1 \mathbf{S}_{2,b} \tilde{\mathbf{c}} \tilde{\mathbf{U}}_I(\mathbf{c}, \phi_0) \mathbf{S}_{2,c} e^{i(b-c)\phi_0} \zeta^{(k_I+b-c)j} \end{aligned} \quad (5.8.251)$$

$$\tilde{\mathbf{W}}_I(\mathbf{x}_j^{\mathcal{B}}) \tilde{\mathbf{x}}_j^{\mathcal{B}} = \sum_{b=-1}^1 \sum_{c=-1}^1 \mathbf{S}_{2,b} \tilde{\mathbf{U}}_I(\mathbf{c}, \phi_0) \tilde{\mathbf{c}} \mathbf{S}_{2,c} e^{i(b-c)\phi_0} \zeta^{(k_I+b-c)j} \quad (5.8.252)$$

The summation over the corresponding particles leads to:

$$\sum_{j=0}^{n-1} \tilde{\mathbf{x}}_j^{\mathcal{B}} \tilde{\mathbf{W}}_I(\mathbf{x}_j^{\mathcal{B}}) = \sum_{b=-1}^1 \sum_{c=-1}^1 \left(\mathbf{S}_{2,b} \tilde{\mathbf{c}} \tilde{\mathbf{U}}_I(\mathbf{c}, \phi_0) \mathbf{S}_{2,c} e^{i(b-c)\phi_0} \left(\sum_{j=0}^{n-1} \zeta^{(k_I+b-c)j} \right) \right) \quad (5.8.253)$$

$$\sum_{j=0}^{n-1} \tilde{\mathbf{W}}_I(\mathbf{x}_j^{\mathcal{B}}) \tilde{\mathbf{x}}_j^{\mathcal{B}} = \sum_{b=-1}^1 \sum_{c=-1}^1 \left(\mathbf{S}_{2,b} \tilde{\mathbf{U}}_I(\mathbf{c}, \phi_0) \tilde{\mathbf{c}} \mathbf{S}_{2,c} e^{i(b-c)\phi_0} \left(\sum_{j=0}^{n-1} \zeta^{(k_I+b-c)j} \right) \right) \quad (5.8.254)$$

Also here, the rule (5.8.246) is applied for the evaluation. For the range of $\frac{k_I+b-c}{n}$ it is obtained:

$$-\frac{n}{2} + \frac{1}{2} \leq k_I \leq \frac{n}{2} \wedge -1 \leq b \leq 1 \wedge -1 \leq -c \leq 1 \Rightarrow -\frac{1}{2} - \frac{3}{2n} \leq \frac{k_I+b-c}{n} \leq \frac{1}{2} + \frac{2}{n} \quad (5.8.255)$$

Here, the two segment numbers $n = 3$ and $n = 4$ turn out to be special cases, which shall not be discussed here. For $n > 4$ it is valid:

$$n > 4 \Rightarrow \frac{1}{n} < \frac{1}{4} \Rightarrow \frac{2}{n} < \frac{1}{2} \Rightarrow \frac{1}{2} + \frac{2}{n} < 1 \quad (5.8.256)$$

$$n > 4 \Rightarrow \frac{1}{n} < \frac{1}{4} \Rightarrow -\frac{3}{2n} > -\frac{3}{8} \Rightarrow -\frac{1}{2} - \frac{3}{2n} > -\frac{7}{8} > -1 \quad (5.8.257)$$

Based on this, it can be determined for the fraction $\frac{k_I+b-c}{n}$:

$$\begin{aligned} -1 < -\frac{1}{2} - \frac{3}{2n} \leq \frac{k_I+b-c}{n} \leq \frac{1}{2} + \frac{2}{n} < 1 \wedge \frac{k_I+b-c}{n} \in \mathbb{Z} \\ \Rightarrow \frac{k_I+b-c}{n} = 0 \Rightarrow k_I+b-c = 0 \Rightarrow k_I = c-b \end{aligned} \quad (5.8.258)$$

For the difference $c - b$ it is valid:

$$b \in \{-1, 0, 1\} \wedge c \in \{-1, 0, 1\} \Rightarrow c - b \in \{-2, -1, 0, 1, 2\} \quad (5.8.259)$$

From this it follows that for shape functions having the periodicity $k_I \notin \{-2, -1, 0, 1, 2\}$ the following integrals

$$\int_{\mathcal{B}} \widetilde{\mathbf{x}}^{\mathcal{B}} \widetilde{\mathbf{W}}_I(\mathbf{x}^{\mathcal{B}}) dm, \int_{\mathcal{B}} \left(\widetilde{\mathbf{x}}^{\mathcal{B}} \widetilde{\mathbf{W}}_I(\mathbf{x}^{\mathcal{B}}) + \widetilde{\mathbf{W}}_I(\mathbf{x}^{\mathcal{B}}) \widetilde{\mathbf{x}}^{\mathcal{B}} \right) dm \quad (5.8.260)$$

generally vanish.

In total it can be concluded that the first order terms, which are dominant for the coupling between the rigid body motions and the relative motions, can only be different from zero for shape functions having the periodicity $k_I \in \{-2, -1, 0, 1, 2\}$; conversely, this means that for shape functions having the periodicity $|k_I| > 2$ the coupling to the rigid body motions is relatively weak.

5.8.3 Terms of second order

For terms of second order, the integrand contains a product of two shape functions $\mathbf{W}_v(\mathbf{x}^{\mathcal{B}})$ and $\mathbf{W}_I(\mathbf{x}^{\mathcal{B}})$. Due to the greater range of the periodicities k_I the complete evaluation requires a considerable effort. However, regarding the relative motions, some dominant terms shall be considered here. As it can be seen from (5.8.197) several terms contain the angular velocity $\omega_{I\mathcal{B}}^I$, which can be split up into the absolute angular velocity $\omega_{I\mathcal{A}}^I$ of the sliding frame \mathcal{A} and the relative angular velocity $\omega_{\mathcal{A}\mathcal{B}}^{\mathcal{A}}$ between the sliding frame \mathcal{A} and the body-fixed frame \mathcal{B} :

$$\omega_{I\mathcal{B}}^I = \omega_{I\mathcal{A}}^I + \mathbf{S}^{I\mathcal{A}} \omega_{\mathcal{A}\mathcal{B}}^{\mathcal{A}} \Rightarrow \omega_{I\mathcal{B}}^{\mathcal{B}} = \mathbf{S}^{\mathcal{B}I} \omega_{I\mathcal{B}}^I = \mathbf{S}^{\mathcal{B}I} \omega_{\mathcal{A}\mathcal{B}}^{\mathcal{A}} + \omega_{\mathcal{A}\mathcal{B}}^{\mathcal{B}} \quad (5.8.261)$$

Using the unit vector \mathbf{e}_2 , which points in the direction of the 2-axis, the relative angular velocity $\omega_{\mathcal{A}\mathcal{B}}^{\mathcal{B}}$ can be formulated in the following way:

$$\omega_{\mathcal{A}\mathcal{B}}^{\mathcal{B}} = \dot{\chi} \mathbf{e}_2 \quad (5.8.262)$$

Since the vector $\omega_{\mathcal{A}\mathcal{B}}^{\mathcal{B}}$ contains the large angular velocity $\dot{\chi}$ of the overturning motion, its absolute value can be considered to be greater than the one of the angular velocity $\omega_{I\mathcal{A}}^I$ of the sliding frame, i.e. $|\omega_{\mathcal{A}\mathcal{B}}^{\mathcal{B}}| = |\dot{\chi}| \gg |\omega_{I\mathcal{A}}^I|$. Therefore, the terms, which contain the angular velocity $\omega_{\mathcal{A}\mathcal{B}}^{\mathcal{B}}$ shall be considered here. Another important term is the integral containing the acceleration $\ddot{\mathbf{w}}^{\mathcal{B}}$. The integrands of these terms can be reformulated in the following way:

$$\begin{aligned} \omega_{\mathcal{A}\mathcal{B}}^{\mathcal{A}T} \mathbf{S}^{\mathcal{A}\mathcal{B}} \widetilde{\mathbf{W}}_{\mathbf{v}}(\mathbf{x}^{\mathcal{B}}) \widetilde{\mathbf{W}}_I(\mathbf{x}^{\mathcal{B}}) \mathbf{S}^{\mathcal{B}\mathcal{A}} \omega_{\mathcal{A}\mathcal{B}}^{\mathcal{A}} &= \omega_{\mathcal{A}\mathcal{B}}^{\mathcal{B}T} \mathbf{S}_2(\phi) \widetilde{\mathbf{U}}_{\mathbf{v}}(\mathbf{c}, \phi) \mathbf{S}_2(\phi)^T \mathbf{S}_2(\phi) \widetilde{\mathbf{U}}_I(\mathbf{c}, \phi) \mathbf{S}_2(\phi)^T \omega_{\mathcal{A}\mathcal{B}}^{\mathcal{B}} \\ &= \chi^2 \mathbf{e}_2^T \mathbf{S}_2(\phi) \widetilde{\mathbf{U}}_{\mathbf{v}}(\mathbf{c}, \phi) \widetilde{\mathbf{U}}_I(\mathbf{c}, \phi) \mathbf{S}_2(-\phi) \mathbf{e}_2 \end{aligned} \quad (5.8.263)$$

$$\begin{aligned} \mathbf{W}_{\mathbf{v}}(\mathbf{x}^{\mathcal{B}})^T \widetilde{\mathbf{W}}_I(\mathbf{x}^{\mathcal{B}}) \mathbf{S}^{\mathcal{B}\mathcal{A}} \omega_{\mathcal{A}\mathcal{B}}^{\mathcal{A}} &= \mathbf{U}_{\mathbf{v}}(\mathbf{c}, \phi)^T \mathbf{S}_2(\phi)^T \mathbf{S}_2(\phi) \widetilde{\mathbf{U}}_I(\mathbf{c}, \phi) \mathbf{S}_2(\phi)^T \omega_{\mathcal{A}\mathcal{B}}^{\mathcal{B}} \\ &= \mathbf{U}_{\mathbf{v}}(\mathbf{c}, \phi)^T \widetilde{\mathbf{U}}_I(\mathbf{c}, \phi) \mathbf{S}_2(-\phi) \mathbf{e}_2 \dot{\chi} \end{aligned} \quad (5.8.264)$$

$$\mathbf{W}_{\mathbf{v}}(\mathbf{x}^{\mathcal{B}})^T \mathbf{W}_I(\mathbf{x}^{\mathcal{B}}) = \mathbf{U}_{\mathbf{v}}(\mathbf{c}, \phi)^T \mathbf{S}_2(\phi)^T \mathbf{S}_2(\phi) \mathbf{U}_I(\mathbf{c}, \phi) = \mathbf{U}_{\mathbf{v}}(\mathbf{c}, \phi)^T \mathbf{U}_I(\mathbf{c}, \phi) \quad (5.8.265)$$

If the rotation matrix $\mathbf{S}_i(\beta)$ describes a rotation around the i -axis, the unit vector \mathbf{e}_i , which points into the direction of this axis, is not affected by the rotation, i.e. it is valid:

$$\mathbf{S}_i(\beta) \mathbf{e}_i = \mathbf{e}_i \quad (5.8.266)$$

Therefore, it is valid:

$$\begin{aligned} \omega_{\mathcal{A}\mathcal{B}}^{\mathcal{A}T} \mathbf{S}^{\mathcal{A}\mathcal{B}} \widetilde{\mathbf{W}}_{\mathbf{v}}(\mathbf{x}^{\mathcal{B}}) \widetilde{\mathbf{W}}_I(\mathbf{x}^{\mathcal{B}}) \mathbf{S}^{\mathcal{B}\mathcal{A}} \omega_{\mathcal{A}\mathcal{B}}^{\mathcal{A}} &= \chi^2 \mathbf{e}_2^T \mathbf{S}_2(\phi) \widetilde{\mathbf{U}}_{\mathbf{v}}(\mathbf{c}, \phi) \widetilde{\mathbf{U}}_I(\mathbf{c}, \phi) \mathbf{S}_2(-\phi) \mathbf{e}_2 \\ &= \chi^2 \mathbf{e}_2^T \widetilde{\mathbf{U}}_{\mathbf{v}}(\mathbf{c}, \phi) \widetilde{\mathbf{U}}_I(\mathbf{c}, \phi) \mathbf{e}_2 \end{aligned} \quad (5.8.267)$$

$$\begin{aligned} \mathbf{W}_{\mathbf{v}}(\mathbf{x}^{\mathcal{B}})^T \widetilde{\mathbf{W}}_I(\mathbf{x}^{\mathcal{B}}) \mathbf{S}^{\mathcal{B}\mathcal{A}} \omega_{\mathcal{A}\mathcal{B}}^{\mathcal{A}} &= \mathbf{U}_{\mathbf{v}}(\mathbf{c}, \phi)^T \widetilde{\mathbf{U}}_I(\mathbf{c}, \phi) \mathbf{S}_2(-\phi) \mathbf{e}_2 \dot{\chi} \\ &= \mathbf{U}_{\mathbf{v}}(\mathbf{c}, \phi)^T \widetilde{\mathbf{U}}_I(\mathbf{c}, \phi) \mathbf{e}_2 \dot{\chi} \end{aligned} \quad (5.8.268)$$

Thereby, the rotation matrices $\mathbf{S}_2(\phi)$ are eliminated. For the corresponding particles of the n -tuple it is obtained:

$$\begin{aligned} \omega_{\mathcal{A}\mathcal{B}}^{\mathcal{A}T} \mathbf{S}^{\mathcal{A}\mathcal{B}} \widetilde{\mathbf{W}}_{\mathbf{v}}(\mathbf{x}_j^{\mathcal{B}}) \widetilde{\mathbf{W}}_I(\mathbf{x}_j^{\mathcal{B}}) \mathbf{S}^{\mathcal{B}\mathcal{A}} \omega_{\mathcal{A}\mathcal{B}}^{\mathcal{A}} &= \chi^2 \mathbf{e}_2^T \widetilde{\mathbf{U}}_{\mathbf{v}}(\mathbf{c}, \phi_j) \widetilde{\mathbf{U}}_I(\mathbf{c}, \phi_j) \mathbf{e}_2 \\ &= \chi^2 \mathbf{e}_2^T \widetilde{\mathbf{U}}_{\mathbf{v}}(\mathbf{c}, \phi_0) \zeta^{k_{\mathbf{v}}j} \widetilde{\mathbf{U}}_I(\mathbf{c}, \phi_0) \zeta^{k_I j} \mathbf{e}_2 \\ &= \chi^2 \mathbf{e}_2^T \widetilde{\mathbf{U}}_{\mathbf{v}}(\mathbf{c}, \phi_0) \widetilde{\mathbf{U}}_I(\mathbf{c}, \phi_0) \mathbf{e}_2 \zeta^{(k_{\mathbf{v}}+k_I)j} \end{aligned} \quad (5.8.269)$$

$$\begin{aligned} \mathbf{W}_{\mathbf{v}}(\mathbf{x}_j^{\mathcal{B}})^T \widetilde{\mathbf{W}}_I(\mathbf{x}_j^{\mathcal{B}}) \mathbf{S}^{\mathcal{B}\mathcal{A}} \omega_{\mathcal{A}\mathcal{B}}^{\mathcal{A}} &= \mathbf{U}_{\mathbf{v}}(\mathbf{c}, \phi_j)^T \widetilde{\mathbf{U}}_I(\mathbf{c}, \phi_j) \mathbf{e}_2 \dot{\chi} \\ &= \mathbf{U}_{\mathbf{v}}(\mathbf{c}, \phi_0)^T \zeta^{k_{\mathbf{v}}j} \widetilde{\mathbf{U}}_I(\mathbf{c}, \phi) \zeta^{k_{\mathbf{v}}j} \mathbf{e}_2 \dot{\chi} \\ &= \mathbf{U}_{\mathbf{v}}(\mathbf{c}, \phi_0)^T \widetilde{\mathbf{U}}_I(\mathbf{c}, \phi) \mathbf{e}_2 \dot{\chi} \zeta^{(k_{\mathbf{v}}+k_I)j} \end{aligned} \quad (5.8.270)$$

$$\begin{aligned} \mathbf{W}_{\mathbf{v}}(\mathbf{x}_j^{\mathcal{B}})^T \mathbf{W}_I(\mathbf{x}_j^{\mathcal{B}}) &= \mathbf{U}_{\mathbf{v}}(\mathbf{c}, \phi_j)^T \mathbf{U}_I(\mathbf{c}, \phi_j) = \mathbf{U}_{\mathbf{v}}(\mathbf{c}, \phi_0)^T \zeta^{k_{\mathbf{v}}j} \mathbf{U}_I(\mathbf{c}, \phi_0) \zeta^{k_I j} \\ &= \mathbf{U}_{\mathbf{v}}(\mathbf{c}, \phi_0)^T \mathbf{U}_I(\mathbf{c}, \phi_0) \zeta^{(k_{\mathbf{v}}+k_I)j} \end{aligned} \quad (5.8.271)$$

In all three cases, the sum of the powers $\zeta^{(k_{\mathbf{v}}+k_I)j}$ has to be evaluated. For the periodicities $k_{\mathbf{v}}$ and k_I it is valid:

$$-\frac{n}{2} + \frac{1}{2} \leq k_{\mathbf{v}} \leq \frac{n}{2} \wedge -\frac{n}{2} + \frac{1}{2} \leq k_I \leq \frac{n}{2} \Rightarrow -1 + \frac{1}{2n} \leq \frac{k_{\mathbf{v}} + k_I}{n} \leq 1 \quad (5.8.272)$$

By combining this with the condition that the fraction $\frac{k_{\mathbf{v}}+k_I}{n}$ is an integer it is obtained:

$$-1 + \frac{1}{2n} \leq \frac{k_{\mathbf{v}} + k_I}{n} \leq 1 \wedge \frac{k_{\mathbf{v}} + k_I}{n} \in \mathbb{Z} \Rightarrow \frac{k_{\mathbf{v}} + k_I}{n} \in \{0, 1\} \quad (5.8.273)$$

The case $\frac{k_v+k_I}{n} = 1$ only occurs for $k_v = k_I = \frac{n}{2}$. For all other periodicities it is valid:

$$\frac{k_v + k_I}{n} = 0 \Rightarrow k_v + k_I = 0 \Rightarrow k_v = -k_I \quad (5.8.274)$$

This result indicates that the terms (5.8.269), (5.8.270) and (5.8.271) can only be different from zero for $k_v = -k_I$, i.e. if the periodicities k_v and k_I of both shape functions \mathbf{W}_v and \mathbf{W}_I only differ by the sign. This corresponds to the result, which has been derived in the section 3.2. The reason for this decoupling also with respect to the centrifugal terms (5.8.269) and the gyroscopic terms (5.8.270) the angular velocity $\omega_{AB}^B = \chi \mathbf{e}_2$ does not depend on the azimuth ϕ , but is equal for all particles so that the basic property of the cyclic system that all segments are equal is maintained.

5.9 External forces

Generally, the wheelset of a railway vehicle can be subjected to four kinds of external forces:

1. Wheel-rail contact forces: The wheel-rail contact forces act on the running surfaces of the wheels. They are the only forces between the wheelset and the track and thereby also the only ones acting between the vehicle and the track. In regular operation, the wheel-rail forces act permanently; at least, they have to support the vehicle's weight. they vanish only in the case that the solid contact between the wheel and the rail is lost, e.g. due to wheel lift or derailment.
2. Bearing forces: The bearing forces act between the wheelset's journals and the bearing; via the bearing and the primary suspension the wheelset is connected to the rest of the vehicle, i.e. either to a bogie frame or directly to the carbody, if the vehicle has a single-stage suspension. Also in this case, a force acts permanently since the bearings have to transmit the weight of the rest of the vehicle, in particular the carbody.
3. Braking forces: The braking force acts between the wheelset and the braking device, which is either connected to the bogie frame or to the carbody. The location on the wheelset depends on the type of construction of the brake. If the wheelset is equipped with disc brakes, the braking force acts on the intended surface of the discs; if it is equipped with tread brakes, the force acts on the running surfaces of the wheels. Of course, the braking forces act only, when the brake is activated. In the present work, the running with released brakes is investigated so that no braking forces are taken into account. However, the demonstrated methodology can also be applied for these forces.
4. Driving forces: Driving forces only occur if the wheelset is connected to a propulsion system. Also here, the exact location, where the driving force acts, depends on the construction, e.g. a gear wheel or a hollow driving shaft, also known as a quill. In the present case, a non-driven wheelset is considered so no driving forces have to be taken into account.

In the following sections, the terms describing the impact of the wheel-rail contact forces and of the bearing forces on the wheelset will be developed.

5.9.1 Wheel-rail contact forces

Actually, the wheel-rail contact is a small area, in which distributed stresses are acting. However, this area is rather small compared to the main dimensions of the wheelset so that in the present consideration of the wheelset as a body the wheel-rail contact forces are described by a discrete force \mathbf{f}_{WR}^I and a discrete moment \mathbf{m}_{WR}^I , which are acting at the point P_I . For the sake of brevity, only the force will be considered in the following.

Generally, the virtual power $\delta'P_F$ of an external discrete force \mathbf{f}^I acting on a flexible body at the point F is described by the scalar product of the force and the virtual velocity $\delta'\mathbf{v}_{OF}^I$ of the body at this point.

$$\delta'P_I = \mathbf{f}^I \cdot \delta'\mathbf{v}_{OF}^I \quad (5.9.275)$$

If the floating frame of reference formulation (FFRF) is used and the body-fixed frame \mathcal{B} is chosen as the reference frame, then the virtual velocity at the point F is given by:

$$\delta'\mathbf{v}_{OF}^I = \delta'\mathbf{v}_{OR}^I + \delta'\tilde{\omega}_{IB}^I \mathbf{S}^{IB} \left(\mathbf{x}_F^{\mathcal{B}} + \mathbf{w}^{\mathcal{B}}(\mathbf{x}_F^{\mathcal{B}}) \right) + \mathbf{S}^{IB} \delta'\dot{\mathbf{w}}^{\mathcal{B}}(\mathbf{x}_F^{\mathcal{B}}) \quad (5.9.276)$$

Usually, the deformation field $\mathbf{w}^{\mathcal{B}}(\mathbf{x}^{\mathcal{B}})$ is described by a modal synthesis, in which N shape functions $\mathbf{W}_I^{\mathcal{B}}(\mathbf{x}^{\mathcal{B}})$ are scaled by modal coordinates q_I and superposed.

$$\mathbf{w}^{\mathcal{B}}(\mathbf{x}^{\mathcal{B}}) = \sum_{I=1}^{N_B} \mathbf{W}_I^{\mathcal{B}}(\mathbf{x}^{\mathcal{B}}) q_I(t) \Rightarrow \delta'\dot{\mathbf{w}}^{\mathcal{B}}(\mathbf{x}_F^{\mathcal{B}}) = \sum_{I=1}^{N_B} \mathbf{W}_I^{\mathcal{B}}(\mathbf{x}_F^{\mathcal{B}}) \delta'q_I \quad (5.9.277)$$

In order to explore the problem of modelling a rolling wheel as a flexible body, the simplified case of a cylindrical wheel rolling on a plane ground shall be considered. In Figure 5.9.8, this case where the contact force \mathbf{f} acts at the point F is illustrated.

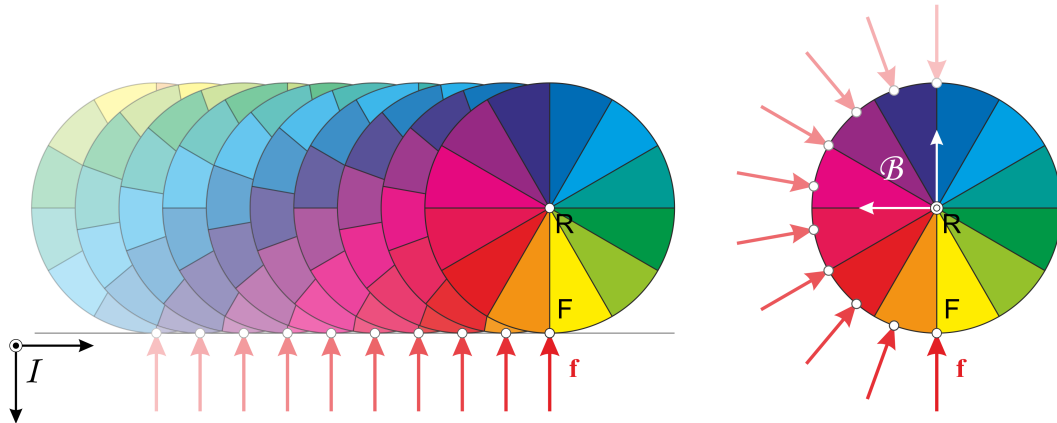


Figure 5.9.8: Rolling wheel and contact force; left: observation in the inertia frame I ; right: observation in the body-fixed frame \mathcal{B} .

It is evident that the contact moves around the wheel's circumference so that the vector $\mathbf{x}_F^{\mathcal{B}}$, which describes the current position of the contact point in the body-fixed frame \mathcal{B} , is not constant, but a function of the circumferential angle ϕ , i.e. $\mathbf{x}_F^{\mathcal{B}} = \mathbf{x}_F^{\mathcal{B}}(\phi)$. Based on this and by using the formulations (5.9.276) and (5.9.277) the required virtual velocity $\delta'\mathbf{v}_{OF}^I$ at the contact point F , which is required for the virtual power of the force \mathbf{f}^I is obtained to:

$$\delta'\mathbf{v}_{OF}^I = \delta'\mathbf{v}_{OR}^I + \delta'\tilde{\omega}_{IB}^I \mathbf{S}^{IB} \left(\mathbf{x}_F^{\mathcal{B}}(\phi) + \sum_{I=1}^{N_B} \mathbf{W}_I^{\mathcal{B}}(\mathbf{x}_F^{\mathcal{B}}(\phi)) q_I \right) + \mathbf{S}^{IB} \sum_{I=1}^{N_B} \mathbf{W}_I^{\mathcal{B}}(\mathbf{x}_F^{\mathcal{B}}(\phi)) \delta'q_I \quad (5.9.278)$$

Here, the main problem of describing a rolling wheel as a flexible body becomes visible. Since the angle ϕ doesn't have a constant value, the shape functions $\mathbf{W}_I^B(\mathbf{x}^B)$ have to be provided as continuous functions of the angle ϕ , i.e. $\mathbf{W}_I^B(\mathbf{x}_F^B(\phi)) = \mathbf{W}_I^B(\phi)$, and not just for one single point. For the sake of clarity, Figure 5.9.8 shows only a rotation of the wheel around 180 degrees; actually, due to the rolling of the wheel the contact moves around the full circumference of the wheel. Since the angles $\phi = \phi_0$ and $\phi = \phi_0 + 2\pi$ denote the same point on the circumference, it is obvious to describe the shape functions \mathbf{W}_I^B as a Fourier series:

$$\mathbf{x}_F^B(\phi) = \mathbf{x}_F^B(\phi + 2\pi) \Rightarrow \mathbf{W}_I^B(\mathbf{x}_F^B(\phi)) = \mathbf{W}_I^B(\phi) = \mathbf{W}_I^B(\phi + 2\pi) = \sum_{K=-\infty}^{\infty} \mathbf{W}_{I,K}^B e^{iK\phi} \quad (5.9.279)$$

It should also be noted that the shape functions for a flexible body are usually calculated by a finite element (FE) model. Due to the discretization used by the FE method, the deformations are calculated for discrete points; between these points local interpolation functions are applied. This method of evaluating the shape functions $\mathbf{W}_i^B(\phi)$ for the current value of ϕ appears rather laborious, since the current interpolation interval has to be determined due to the local interpolation functions. Therefore, a description of the shape functions $\mathbf{W}_i^B(\phi)$ as continuous functions of ϕ seems to be useful. As already mentioned, in an FE model the displacements are known for the nodes, i.e. for discrete points. If the values of the function $f(\phi)$ are given for N equidistant points² indicated by $\phi = \phi_j = \phi_0 + \frac{2\pi}{n}j$, $0 \leq j \leq N-1$, then the values $f(\phi_j)$ can be expressed by the following discrete Fourier series as it has been derived in the section 3.1.2:

$$K_{\min} \leq K \leq K_{\max} = K_{\min} + N - 1, \quad \zeta^{Kj} = e^{i\frac{2\pi}{N}Kj}$$

$$c_K = \frac{1}{N} \left(\sum_{j=0}^{n-1} f(\phi_j) \zeta^{-Kj} \right) \Rightarrow f(\phi_j) = \sum_{K=K_{\min}}^{K_{\max}} c_K \zeta^{Kj} \quad (5.9.280)$$

The formulation for a scalar function $f(\phi)$ can easily be extended to a vector. In the case of the wheel the circle, on which the force moves, is defined by the cylindrical coordinates r and y so that the points for the following vector \mathbf{x}_j^B have to be evaluated:

$$\mathbf{x}_j^B = \underbrace{\begin{bmatrix} \cos \phi_j & 0 & \sin \phi_j \\ 0 & 1 & 0 \\ -\sin \phi_j & 0 & \cos \phi_j \end{bmatrix}}_{\mathbf{S}_2(\phi_j)} \underbrace{\begin{bmatrix} 0 \\ y \\ r \end{bmatrix}}_{\mathbf{c}(r,y)} = \mathbf{x}^B(\mathbf{c}, \phi_j) \quad (5.9.281)$$

Since the vector \mathbf{c} contains the cylindrical coordinates r and y , it will be used as an argument in the following considerations for the sake of brevity instead of indicating the coordinates r and y separately. Based on this, the following vectors $\mathbf{W}_{I,K}^B$ are obtained from the given values for the shape function $\mathbf{W}_I^B(\mathbf{x}_j^B)$:

$$\mathbf{W}_{I,K}^B(\mathbf{c}) e^{iK\phi_0} = \frac{1}{N} \left(\sum_{j=0}^{N-1} \mathbf{W}_I^B(\mathbf{x}_j^B) \zeta^{-Kj} \right) \Leftrightarrow \mathbf{W}_{I,K}^B(r,y) = \frac{e^{-iK\phi_0}}{N} \left(\sum_{j=0}^{N-1} \mathbf{W}_I^B(\mathbf{x}_j^B) \zeta^{-Kj} \right) \quad (5.9.282)$$

²Since here the general case of a discrete Fourier series is considered, the number N is introduced in order to avoid confusion with the number n which in this chapter denotes the number of segments of a cyclic system. For the same reason, the upcase letter K is used for the periodicity here.

The correction factor $e^{-iK\phi_0}$ which takes into account the initial angle ϕ_0 is introduced in order to enable a simpler formulation of the resulting Fourier series. By using the relation between the power ζ^{Kj} and the angle ϕ_j it can be formulated:

$$e^{iK\phi_0} \zeta^{Kj} = e^{iK\phi_0} e^{i\frac{2\pi}{n}Kj} = e^{iK(\phi_0 + \frac{2\pi}{n}j)} = e^{iK\phi_j}$$

$$\Rightarrow \mathbf{W}_I^B(\mathbf{c}, \phi_j) = \mathbf{W}_I^B(\mathbf{x}_j^B) = \sum_{K=K_{\min}}^{K_{\max}} \mathbf{W}_{I,K}^B(\mathbf{c}) e^{iK\phi_0} \zeta^{Kj} = \sum_{K=K_{\min}}^{K_{\max}} \mathbf{W}_{I,K}^B(\mathbf{c}) e^{iK\phi_j} \quad (5.9.283)$$

For the discrete values $\phi_j = \phi_0 + \frac{2\pi}{n}j$ the discrete Fourier series (5.9.283) produces the given values $\mathbf{W}_I^B(r, y, \phi_j)$. By extending the range of ϕ from the n discrete values $\phi = \phi_j$ to the entire set of real numbers, i.e. to $\phi \in \mathbb{R}$, the expression according to (5.9.283) can be used as an interpolation:

$$\mathbf{W}_I^B(\mathbf{c}, \phi) = \sum_{K=K_{\min}}^{K_{\max}} \mathbf{W}_{I,K}^B(\mathbf{c}) e^{iK\phi}, \quad \mathbf{W}_{I,K}^B = \frac{e^{-iK\phi_0}}{N} \left(\sum_{j=0}^{N-1} \mathbf{W}_I^B(\mathbf{c}, \phi_j) \zeta^{-Kj} \right) \quad (5.9.284)$$

Since the Fourier series according to (5.9.284) is an interpolation, it contains only a finite number of terms in contrast to the exact formulation according to (5.9.279).

It can be assumed that in the sliding frame \mathcal{A} the angle θ_F where the force acts is constant. Based on the relation between the azimuths ϕ and θ it is valid:

$$\theta = \chi + \phi \Rightarrow \phi = \theta - \chi \Rightarrow \phi_F(t) = \theta_F - \chi(t) \quad (5.9.285)$$

For the sake of clarity, the dependency on the time t is indicated explicitly here. Based on Thereby, the required displacement vector is obtained to:

$$\mathbf{w}^B(\mathbf{x}_F^B) = \mathbf{w}^B(\mathbf{c}, \phi_F) = \sum_{I=1}^{N_B} \left(\sum_{K=K_{\min}}^{K_{\max}} \mathbf{W}_{I,K}^B(\mathbf{c}) e^{iK\phi_F(t)} \right) q_I(t) = \sum_{I=1}^{N_B} \left(\sum_{K=K_{\min}}^{K_{\max}} \mathbf{W}_{I,K}^B(\mathbf{c}) e^{iK(\theta_F - \chi(t))} \right) q_I(t) \quad (5.9.286)$$

It should be noted out that for the kinematics of the point F the displacement field is evaluated for the current coordinates of F which are indicated by \mathbf{c} and ϕ_F . The point F is not a material point, i.e. due the rotation around the increasing angle χ a different particle is located at the point F at any time. If the current velocity $\dot{\mathbf{w}}^B(\mathbf{x}_F^B)$ at the point F is of interest, then the velocity field has to be determined first and after this the coordinates of F have to be inserted into the velocity field. In other words, the dependency of ϕ_F on the time t which represents the permanent change of particles located at F must not be taken into account for the differentiation. Thereby, it is obtained for the velocity $\dot{\mathbf{w}}^B(\mathbf{x}_F^B)$ and for the virtual velocity $\delta' \dot{\mathbf{w}}^B(\mathbf{x}_F^B)$:

$$\dot{\mathbf{w}}^B(\mathbf{x}_F^B) = \dot{\mathbf{w}}^B(\mathbf{c}, \phi_F) = \sum_{I=1}^{N_B} \left(\sum_{K=K_{\min}}^{K_{\max}} \mathbf{W}_{I,K}^B(\mathbf{c}) e^{iK(\theta_F - \chi(t))} \right) \dot{q}_I(t) \quad (5.9.287)$$

$$\delta' \dot{\mathbf{w}}^B(\mathbf{x}_F^B) = \delta' \dot{\mathbf{w}}^B(\mathbf{c}, \phi_F) = \sum_{I=1}^{N_B} \left(\sum_{K=K_{\min}}^{K_{\max}} \mathbf{W}_{I,K}^B(\mathbf{c}) e^{iK(\theta_F - \chi(t))} \right) \delta' \dot{q}_I \quad (5.9.288)$$

Up to here, the Fourier series has been used for providing a formulation for the moving load based on continuous functions. Based on this, the special case of a cyclic structure shall be considered in the following. In this context it is useful to formulate the shape functions \mathbf{W}_I^B which are valid for cartesian coordinates in an alternative way which uses cylindrical coordinates:

$$\mathbf{W}_I^B(\mathbf{c}, \phi) = \mathbf{S}_2(\phi) \mathbf{U}_I(\mathbf{c}, \phi) \quad (5.9.289)$$

In order to apply the transformation, which has been derived in the section 5.3, the shape function $\mathbf{U}_I(\mathbf{c}, \phi)$ have to fulfill the following condition:

$$\phi_j = \phi_0 + \frac{2\pi}{n}j : \mathbf{U}_I^{\mathcal{B}}(\mathbf{c}, \phi_j) = \mathbf{U}_I^{\mathcal{B}}(\mathbf{c}, \phi_0) e^{ik_I(\phi_j - \phi_0)} = \mathbf{U}_I^{\mathcal{B}}(\mathbf{c}, \phi_0) \zeta^{ik_I j} \quad (5.9.290)$$

As discussed in the section 3.1.2, the evaluation of the function $e^{iK\phi}$ for discrete values ϕ_j can be carried out by using the formulation $K = k + mn$ whereby the basic periodicity $k_{\min} \leq k \leq k_{\max}$ is used:

$$e^{iK\phi_j} = e^{iK(\phi_0 + \frac{2\pi}{n}j)} = e^{iK\phi_0} e^{i(k+mn)\frac{2\pi}{n}j} = e^{iK\phi_0} \underbrace{e^{i\frac{2\pi}{n}kj}}_{\zeta^{kj}} \underbrace{e^{2\pi imj}}_1 \quad (5.9.291)$$

Based on this, the continuous shape function $\mathbf{U}_I^{\mathcal{B}}(r, y, \phi)$ for a cyclic structure can be formulated in the following way:

$$\mathbf{U}_I^{\mathcal{B}}(\mathbf{c}, \phi) = \sum_{m=-\infty}^{\infty} \mathbf{U}_{I,m}(\mathbf{c}) e^{i(k+mn)\phi} \quad (5.9.292)$$

Using the relation (5.9.291) it is obtained for $\mathbf{U}_I^{\mathcal{B}}(\mathbf{c}, \phi_j)$:

$$\mathbf{U}_I^{\mathcal{B}}(\mathbf{c}, \phi_j) = \sum_{m=-\infty}^{\infty} \mathbf{U}_{I,m}(\mathbf{c}) e^{i(k_I+mn)\phi_j} = \sum_{m=-\infty}^{\infty} \mathbf{U}_{I,m}(\mathbf{c}) e^{ik_I\phi_0} \zeta^{k_I j} = \underbrace{\left(\sum_{m=-\infty}^{\infty} \mathbf{U}_{I,m}(\mathbf{c}) e^{ik_I\phi_0} \right)}_{\mathbf{U}_I^{\mathcal{B}}(\mathbf{c}, \phi_0)} \zeta^{k_I j} \quad (5.9.293)$$

Thereby, it is shown that the formulation (5.9.292) fulfils the condition (5.9.290).

By using the shape functions, which fulfill the condition (5.9.290), the displacement $\mathbf{u}(\mathbf{c}, \phi)$ is obtained to:

$$\mathbf{u}(\mathbf{c}, \phi) = \sum_{I=1}^{N_B} \mathbf{U}_I^{\mathcal{B}}(\mathbf{c}, \phi) q_I^{\mathcal{B}} = \sum_{I=1}^{N_B} \left(\sum_{m=-\infty}^{\infty} \mathbf{U}_{I,m}(\mathbf{c}) e^{i(k_I+mn)\phi} \right) q_I^{\mathcal{B}} \quad (5.9.294)$$

The evaluation of the displacement field for the angle ϕ_F leads to:

$$\begin{aligned} \mathbf{u}(\mathbf{c}, \phi_F) &= \sum_{I=1}^{N_B} \left(\sum_{m=-\infty}^{\infty} \mathbf{U}_{I,m}(\mathbf{c}) e^{i(k_I+mn)\phi_F} \right) q_I^{\mathcal{B}} = \sum_{I=1}^{N_B} \left(\sum_{m=-\infty}^{\infty} \mathbf{U}_{I,m}(\mathbf{c}) e^{i(k_I+mn)(\theta_F - \chi)} \right) q_I^{\mathcal{B}} \\ &= \sum_{I=1}^{N_B} \left(\sum_{m=-\infty}^{\infty} \mathbf{U}_{I,m}(\mathbf{c}) e^{i(k_I+mn)(\theta_F - \chi)} \right) q_I^{\mathcal{B}} \\ &= \sum_{I=1}^{N_B} \left(\sum_{m=-\infty}^{\infty} \mathbf{U}_{I,m}(\mathbf{c}) e^{i(k_I+mn)\theta_F} e^{-imn\chi} \right) \underbrace{e^{-ik_I\chi} q_I^{\mathcal{B}}}_{q_I^{\mathcal{A}}} \end{aligned} \quad (5.9.295)$$

Thereby, the displacement is expressed by using the transformed modal coordinates $q_I^{\mathcal{A}}$ which have been introduced in the section 5.3. The only remaining terms, in which the large overturning angle χ is contained, are the functions $e^{-imn\chi}$. For $m = 0$, the term $e^{-imn\chi}$ is equal to 1 and thereby constant. Since the overturning angle of the wheel increases monotonously over time, the terms $e^{-imn\chi}$ oscillate with strongly increasing frequency for growing absolute values of m and with the number of segments n . If n goes tends to infinity, then the cyclic structure becomes an axisymmetric structure; in this case, the shape functions are given by:

$$n \rightarrow \infty : \mathbf{U}_I(\mathbf{c}, \phi) = \mathbf{U}_I(\mathbf{c}) e^{ik_I\phi} \quad (5.9.296)$$

In the case of a wheelset, the wheel rim is a relatively massive axisymmetric part. Therefore, the solution according to (5.9.296) can be considered as a good approximation of its deformations so that the terms for $m \neq 0$ can be neglected. In this case it is valid:

$$\mathbf{u}(\mathbf{c}_{\text{WR}}, \phi_{\text{F}}) \approx \sum_{I=1}^{N_{\text{B}}} \mathbf{U}_{I,0}(\mathbf{c}_{\text{WR}}) e^{ik_I \phi_{\text{F}}} q_I^{\text{B}} = \sum_{I=1}^{N_{\text{B}}} \mathbf{U}_{I,0}(\mathbf{c}_{\text{WR}}) e^{ik_I(\theta_{\text{F}} - \chi)} q_I^{\text{B}} = \sum_{I=1}^{N_{\text{B}}} \underbrace{\mathbf{U}_{I,0}(\mathbf{c}_{\text{WR}}) e^{ik_I \theta_{\text{F}}}}_{\mathbf{U}_I(\mathbf{c}_{\text{WR}}, \theta_{\text{F}})} \underbrace{e^{-ik_I \chi}}_{q_I^{\text{A}}} q_I^{\text{B}} \quad (5.9.297)$$

By using this approximation, the angle χ is eliminated completely. For the formulation in the sliding frame \mathcal{A} it is valid:

$$\begin{aligned} \mathbf{w}^{\mathcal{A}}(\mathbf{c}_{\text{WR}}, \theta_{\text{F}}) &= \mathbf{S}^{\mathcal{A}\text{B}} \mathbf{w}^{\text{B}}(\mathbf{c}_{\text{WR}}, \phi_{\text{F}}) = \underbrace{\mathbf{S}_2(\chi) \mathbf{S}_2(\phi_{\text{F}})}_{\mathbf{S}_2(\chi + \phi_{\text{F}})} \left(\sum_{I=1}^{N_{\text{B}}} \mathbf{U}_I(\mathbf{c}_{\text{WR}}, \theta_{\text{F}}) q_I^{\text{A}} \right) \\ &= \sum_{I=1}^{N_{\text{B}}} \mathbf{S}_2(\theta_{\text{F}}) \mathbf{U}_I(\mathbf{c}_{\text{WR}}, \theta_{\text{F}}) q_I^{\text{A}} = \sum_{I=1}^{N_{\text{B}}} \mathbf{W}_I^{\text{B}}(\mathbf{c}_{\text{WR}}, \theta_{\text{F}}) q_I^{\text{A}} \end{aligned} \quad (5.9.298)$$

5.9.2 Bearing forces

A bearing encloses the shaft, to which it is mounted. Furthermore, the diameter of the bearing is relatively small compared to the entire wheelset. Therefore, it is reasonable to define the virtual velocity for the bearing force by the medium value of the deformations over the circumference:

$$\delta'v_{\text{B}I}^I = \frac{1}{2\pi} \int_0^{2\pi} \delta'v_{\text{OP}_I}^I d\phi = \frac{1}{2\pi} \int_0^{2\pi} (\delta'v_{\text{OR}}^I + \delta'v_{\text{RP}_I}^I) d\phi = \delta'v_{\text{OR}}^I \underbrace{\frac{1}{2\pi} \int_0^{2\pi} d\phi}_1 + \frac{1}{2\pi} \int_0^{2\pi} \delta'v_{\text{RP}_I}^I d\phi \quad (5.9.299)$$

The evaluation of the remaining term can be reduced to the consideration of the n -tuple for the inertia terms. In the section 5.7 it has been determined:

$$\sum_{j=0}^{n-1} \delta'v_{\text{RP}_j}^I = \sum_{K=k_{\text{min}}-1}^{k_{\text{max}}+1} \left(\delta'v_{\mathcal{A},K}^I e^{iK(\chi + \phi_0)} \left(\sum_{j=0}^{n-1} \zeta^{Kj} \right) \right) = n \delta'v_{\mathcal{A},0}^I \underbrace{e^{i \cdot 0 \cdot (\chi + \phi_0)}}_1 = n \delta'v_{\mathcal{A},0}^I \quad (5.9.300)$$

For the vectors $\delta'v_{\mathcal{A},K}^I$ it is valid:

$$\mathbf{r}_{\mathcal{A},K}^I = \mathbf{S}^{I\mathcal{A}} \mathbf{r}_{\mathcal{A},K}^I \Rightarrow \mathbf{v}_{\mathcal{A},K}^I = \tilde{\omega}_{I\mathcal{A}}^I \mathbf{S}^{I\mathcal{A}} \mathbf{r}_{\mathcal{A},K}^{\mathcal{A}} + \mathbf{S}^{I\mathcal{A}} \dot{\mathbf{r}}_{\mathcal{A},K}^{\mathcal{A}} \Rightarrow \delta'v_{\mathcal{A},K}^I = \delta' \tilde{\omega}_{I\mathcal{A}}^I \mathbf{S}^{I\mathcal{A}} \mathbf{r}_{\mathcal{A},K}^{\mathcal{A}} + \mathbf{S}^{I\mathcal{A}} \delta' \dot{\mathbf{r}}_{\mathcal{A},K}^{\mathcal{A}} \quad (5.9.301)$$

For $k_{\text{min}} + 1 \leq K \leq k_{\text{max}} - 1$, which includes the case $K = 0$, the vector $\mathbf{r}_{\mathcal{A},K}^{\mathcal{A}}$ is defined in the following way:

$$\mathbf{r}_{\mathcal{A},K}^{\mathcal{A}} = \mathbf{S}_{2,-1} \mathbf{p}_{K+1}^{\mathcal{A}} + \mathbf{S}_{2,0} \mathbf{p}_K^{\mathcal{A}} + \mathbf{S}_{2,1} \mathbf{p}_{K-1}^{\mathcal{A}} \quad (5.9.302)$$

Setting $K = 0$ and inserting the result into (5.9.301) leads to:

$$\begin{aligned} \delta'v_{\mathcal{A},0}^I &= \delta' \tilde{\omega}_{I\mathcal{A}}^I \mathbf{S}^{I\mathcal{A}} \mathbf{r}_{\mathcal{A},0}^{\mathcal{A}} + \mathbf{S}^{I\mathcal{A}} \delta' \dot{\mathbf{r}}_{\mathcal{A},0}^{\mathcal{A}} \\ &= \delta' \tilde{\omega}_{I\mathcal{A}}^I \mathbf{S}^{I\mathcal{A}} \left(\mathbf{S}_{2,-1} \mathbf{p}_1^{\mathcal{A}} + \mathbf{S}_{2,0} \mathbf{p}_0^{\mathcal{A}} + \mathbf{S}_{2,1} \mathbf{p}_{-1}^{\mathcal{A}} \right) + \mathbf{S}^{I\mathcal{A}} \left(\mathbf{S}_{2,-1} \delta' \dot{\mathbf{p}}_1^{\mathcal{A}} + \mathbf{S}_{2,0} \delta' \dot{\mathbf{p}}_0^{\mathcal{A}} + \mathbf{S}_{2,1} \delta' \dot{\mathbf{p}}_{-1}^{\mathcal{A}} \right) \end{aligned} \quad (5.9.303)$$

From this, it becomes evident that the medium value of the displacement over the circumference can only be different from zero for motions having the periodicities $k = -1$, $k = 0$ or $k = 1$.

Chapter 6

Modelling of the track

The track model, which will be developed in this section, has to fulfill the following requirements:

1. The track model must be suitable for calculating non-periodic solutions.
2. The track model must be able to describe the running of the vehicle at high speed during a longer time interval.
3. The track model must describe the vertical and the lateral dynamics of the track.

In order to fulfill the requirement 1 the track model has to be a time-domain model. From this it follows that the track model also has to be finite, since an infinite track model can only be handled in the frequency domain.

If the track model is finite, then the requirement 2 can only be fulfilled by a moving track model. Once again an example may underline this: If the vehicle is running at a speed of $v_0 = 270$ km/h, which is not uncommon in real operation of high-speed railways, then it covers a distance of 75 m in one second. In order to study phenomena like the hunting motion, a simulation time of several seconds is required to make sure that transient motions have nearly completely died out. For a time interval of 10 s a track length of at least 750 m is required for an inertially fixed track model.

6.1 Structure of the track model

The basis for the track model, which will be presented in this section, is the model developed by Ripke [58]. Regarding the classifications, which have been discussed in section 2.3, this model is a **structural model**, which consists of the components “rails”, “sleepers”, “pads” and “underground” so that it reproduces the actual structure of a real track. Furthermore, the model can be classified as a **two-layer model**, i.e. the motions of the rails and of the sleepers are independent regarding the kinematics; the motions of the ballast and the underground, however, are not described by degrees of freedom.

The modelling of the four components, which have already been mentioned, shall be briefly discussed. The **rail** are modelled as flexible body by using finite elements. For the vertical bending, Ripke uses the Timoshenko beam theory; furthermore, longitudinal vibrations are taken into account by modelling the rail as a rod. With respect to the lateral bending and to the torsion, the cross section of the rail is resolved; here, the head and the foot of the rail are modelled by beams,

which can also perform torsional motions. The web connecting the head and the foot of the rail is modelled as a plate. Thereby, also deformations of the cross section can be described.

The rails are supported by discrete **pads** and **sleepers**. In his work, Ripke models the sleepers as rigid bodies, which can perform three translations and three rotations. The pads, which connect the rails to the sleepers, are modelled by discrete compact force elements, i.e. the fastening between a rail and a sleeper is modelled by a single force element, which describes forces and moments acting between the rail and the sleeper; the moments take clamping effect due to the spatial dimension of the actual pad into account. The force elements representing the pads have linear characteristics for the forces and moments. In a similar way, the **underground** is also modelled by a linear compact force element; each sleeper is connected by such a force element to the rigid ground.

The complete track model is **linear**; therefore, a modal decomposition is possible. Ripke exploits several symmetries of the model to split it up into independent partial models. The model is symmetric with respect to the vertical longitudinal plane; thereby, it can be split into a symmetric and antimetric part. Furthermore, the cant angle of the rail, i.e. its inclination towards the middle of the track, is neglected; as a result, the symmetric model is split into one part describing vertical bending and longitudinal motions and another part describing lateral bending and torsion.

In his model, Ripke uses **equal boundary conditions** at the rails' ends so that the track model forms a ring. Thereby, the behaviour of an infinite track model, which is determined by the radiation of waves and the lack of reflection at the ends, can be approximated by a finite model with a sufficient length. The ring model enables the simulation of the system's behaviour over a longer time interval, e.g. to make sure that transient effects die out. Since the ring model has no ends, where a wave reflection would occur, the results are valid for the complete length. Furthermore, Ripke considers the track as a **cyclic structure**, which consists of n identical segments. Each segment represents one sleeper bay. Thus, the relation between the length ℓ_T of the track model, the number n of the sleeper bays, and the sleeper spacing Δs_S is given by:

$$\ell_T = n \cdot \Delta s_S \Leftrightarrow \Delta s_S = \frac{\ell_T}{n} \quad (6.1.1)$$

Together with the aforementioned exploitation of the symmetries, this provides a drastic reduction of the computational effort.

The track model, which will be developed in the present chapter, is based on the model by Ripke. However, it is enhanced in three aspects:

- The rails are modelled by a semi-analytic finite element model using volume elements. By using an exponential function for the distribution of the deformations along the rail's length, the three dimensional problem is reduced to a two dimensional one, which is solved by discretizing the cross section. In his work, Ripke points out that especially the thickness of the plate representing the rail web has to be chosen very carefully. The rail model, which will be presented here, is a three dimensional volume model, which requires only a very slight simplification of the original geometry of the rail; thereby, the problem of choosing an appropriate simplified geometry is circumvented.
- Each pad, which connects a rail and a sleeper, is modelled by discrete force elements, which are distributed across the rail seat, where the rail is supported by the sleeper. Regarding the consistency of the model, this modelling appears to be more appropriate to the refined finite element model of the rail than a single compact element
- The rail cant is taken into account. As a result, some possibilities to split up the model into decoupled subsystems are lost. However, regarding the available computational power, this

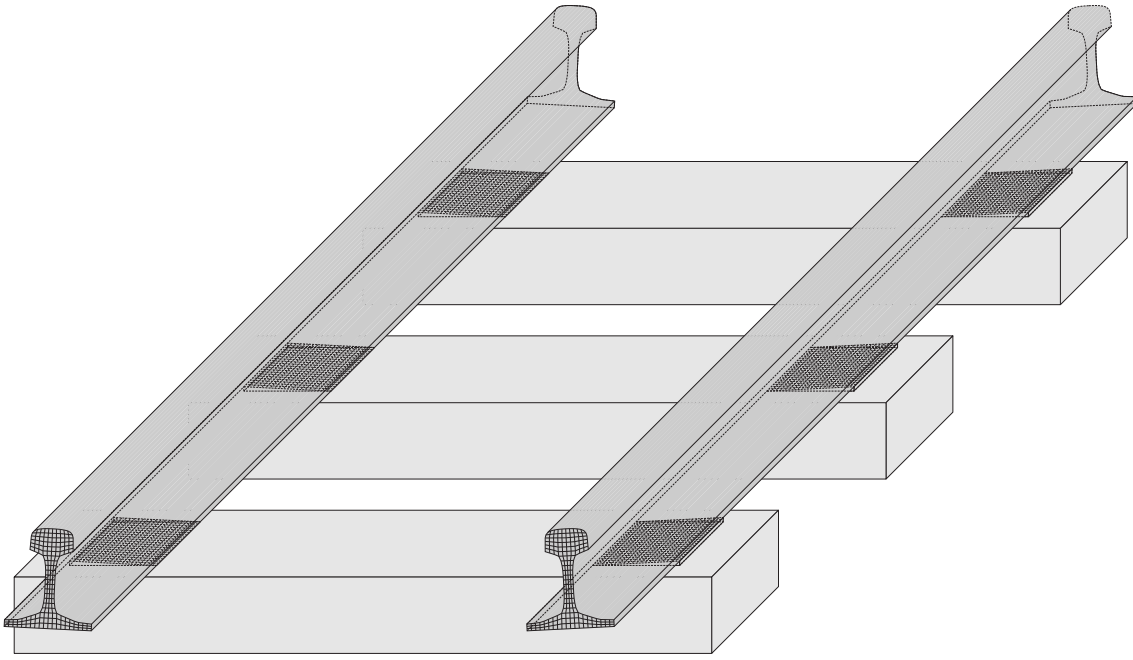


Figure 6.1.1: Overview of the track model

doesn't pose a problem. Ripke mentions that his model focuses on the vertical dynamics. However, in the present work, also the lateral dynamics will be investigated. Thereby, the consideration of the rail cant appears to be appropriate.

In Figure 6.1.1 three segments of the track model are displayed.

6.2 Modelling of the rail

The rail is modelled as a flexible body. Usually, the motions of a flexible body are described using the floating frame of reference formulation. The current position of a particle located at the point P is expressed in the following way:

$$\mathbf{r}_{OP}^I = \mathbf{r}_{OR}^I + \mathbf{S}^{I\mathcal{R}_R} \mathbf{r}_{RP}^{\mathcal{R}_R} = \mathbf{r}_{OR}^I + \mathbf{S}^{I\mathcal{R}_R} \left[\mathbf{x}^{\mathcal{R}_R} + \mathbf{w}^{\mathcal{R}_R}(\mathbf{x}^{\mathcal{R}_R}, t) \right] \quad (6.2.2)$$

Here, the vector $\mathbf{x}^{\mathcal{R}_R}$ indicates the reference position of the considered particle; the displacement is expressed by the deformation field $\mathbf{w}^{\mathcal{R}_R}(\mathbf{x}^{\mathcal{R}_R}, t)$.

In the present case of the track model, all motions are considered to be small. Therefore, deformational motions are in the same order of magnitude as motions of the complete body. The absolute position of the reference point R_R is assumed to be constant. The spatial orientation of the reference frame \mathcal{R}_R is assumed to be constant, too; with respect to the inertia frame I , the frame \mathcal{R}_R is inclined at the cant angle ϕ_R around the 1-axis, which is considered to be the longitudinal axis of the rail. As a result, the motion of a particle of the rail is described in the following way:

$$\mathbf{r}_{OP_R}^I = \mathbf{r}_{OR_R}^I + \mathbf{S}^{I\mathcal{R}_R} \mathbf{r}_{P_R P_R}^{\mathcal{R}_R} = \mathbf{r}_{OR_R}^I + \mathbf{S}_1(\phi_R) [\mathbf{x}_R + \mathbf{w}_R(\mathbf{x}_R, t)] \quad (6.2.3)$$

Since the position vector $\mathbf{r}_{OR_R}^I$ of the reference point, the reference position vector \mathbf{x}_R of the particle and the cant angle ϕ_R are constant, it is valid for the velocity:

$$\frac{d}{dt} \mathbf{r}_{OR_R}^I = \mathbf{0}, \quad \frac{d}{dt} \mathbf{x}_R = \mathbf{0}, \quad \frac{d}{dt} \mathbf{S}_1(\phi_R) = \mathbf{0} \Rightarrow \mathbf{v}_{OP_R}^I = \mathbf{S}_1(\phi_R) \dot{\mathbf{w}}_R(\mathbf{x}_R, t) \quad (6.2.4)$$

The deformation field $\mathbf{w}_R(\mathbf{x}_R, t)$ is described by a modal synthesis; here, shape functions $\mathbf{w}_{RI}(\mathbf{x}_R)$, which depend on the reference position \mathbf{x}_R of the considered particle, are scaled by time-dependent modal coordinates $q_{RI}(t)$ and superposed:

$$\mathbf{w}_R(\mathbf{x}_R, t) = \sum_I \mathbf{w}_{RI}(\mathbf{x}_R) q_{RI}(t) \quad (6.2.5)$$

In order to gain the required shape functions $\mathbf{w}_{RI}(\mathbf{x}_R)$, a structural dynamics model of the rail is needed. Here, a model is used, which is based on a semi-analytic solution of Navier's equation; these equations, which describe the behaviour of a three-dimensional linear elastic continuum, are given by:

$$\frac{\partial^2 U}{\partial x^2} + \frac{\partial^2 U}{\partial y^2} + \frac{\partial^2 U}{\partial z^2} + \frac{1}{1-2\nu} \frac{\partial}{\partial x} \left(\frac{\partial U}{\partial x} + \frac{\partial V}{\partial y} + \frac{\partial W}{\partial z} \right) - \frac{\rho}{G} \frac{\partial^2 U}{\partial t^2} = 0 \quad (6.2.6)$$

$$\frac{\partial^2 V}{\partial x^2} + \frac{\partial^2 V}{\partial y^2} + \frac{\partial^2 V}{\partial z^2} + \frac{1}{1-2\nu} \frac{\partial}{\partial y} \left(\frac{\partial U}{\partial x} + \frac{\partial V}{\partial y} + \frac{\partial W}{\partial z} \right) - \frac{\rho}{G} \frac{\partial^2 V}{\partial t^2} = 0 \quad (6.2.7)$$

$$\frac{\partial^2 W}{\partial x^2} + \frac{\partial^2 W}{\partial y^2} + \frac{\partial^2 W}{\partial z^2} + \frac{1}{1-2\nu} \frac{\partial}{\partial z} \left(\frac{\partial U}{\partial x} + \frac{\partial V}{\partial y} + \frac{\partial W}{\partial z} \right) - \frac{\rho}{G} \frac{\partial^2 W}{\partial t^2} = 0 \quad (6.2.8)$$

Here, G , ν and ρ denote the shear modulus, Poisson's ratio and the density of the material, respectively. By using the following semi-analytic solution:

$$\mathbf{w} = \mathbf{w}_k(x, y, z, t) = \underbrace{\begin{bmatrix} U_k(y, z) \\ V_k(y, z) \\ W_k(y, z) \end{bmatrix}}_{\hat{\mathbf{w}}_k(y, z)} e^{ik\kappa x} e^{i\omega_k t} = \underbrace{\hat{\mathbf{w}}_k(y, z)}_{\mathbf{w}_k(x, y, z)} e^{ik\kappa x} e^{i\omega_k t}, \quad \kappa = \frac{2\pi}{\ell}, \quad k \in \mathbb{Z} \quad (6.2.9)$$

the equations (6.2.6), (6.2.7) and (6.2.8) are reduced to the following expressions:

$$0 = -k^2 \kappa^2 U_k + \frac{\partial^2 U_k}{\partial y^2} + \frac{\partial^2 U_k}{\partial z^2} + \frac{ik\kappa}{1-2\nu} \left(ik\kappa U_k + \frac{\partial V_k}{\partial y} + \frac{\partial W_k}{\partial z} \right) + \frac{\rho}{G} U_k \omega_k^2 \quad (6.2.10)$$

$$0 = -k^2 \kappa^2 V_k + \frac{\partial^2 V_k}{\partial y^2} + \frac{\partial^2 V_k}{\partial z^2} + \frac{1}{1-2\nu} \frac{\partial}{\partial y} \left(ik\kappa U_k + \frac{\partial V_k}{\partial y} + \frac{\partial W_k}{\partial z} \right) + \frac{\rho}{G} V_k \omega_k^2 \quad (6.2.11)$$

$$0 = -k^2 \kappa^2 W_k + \frac{\partial^2 W_k}{\partial y^2} + \frac{\partial^2 W_k}{\partial z^2} + \frac{1}{1-2\nu} \frac{\partial}{\partial z} \left(ik\kappa U_k + \frac{\partial V_k}{\partial y} + \frac{\partial W_k}{\partial z} \right) + \frac{\rho}{G} W_k \omega_k^2 \quad (6.2.12)$$

As it can be seen from (6.2.9), the functions $U_k(y, z)$, $V_k(y, z)$ and $W_k(y, z)$ depend on the cross-sectional coordinates y and z , so that the original three-dimensional field problem has been reduced to a two-dimensional one.

In order to solve the problem, a finite prism element, which is based on the solution (6.2.9), is used. This is a quadrilateral element, which uses a bilinear interpolation. The derivation of the element can be found in chapter 4. In Figure 6.2.2, the discretization of the cross section by quadrilateral finite elements is shown. For each element, the displacement field $\mathbf{w}(x, y, z, t)$ and the strain field $\boldsymbol{\varepsilon}(x, y, z, t)$ are formulated in the following way:

$$\mathbf{w}(x, y, z, t) = \sum_K \hat{\mathbf{N}}(y, z) e^{iK \frac{2\pi}{\ell} x} \mathbf{w}_K^e, \quad \boldsymbol{\varepsilon}(x, y, z, t) = \sum_K \hat{\mathbf{B}}_K(y, z) e^{iK \frac{2\pi}{\ell} x} \mathbf{w}_K^e \quad (6.2.13)$$

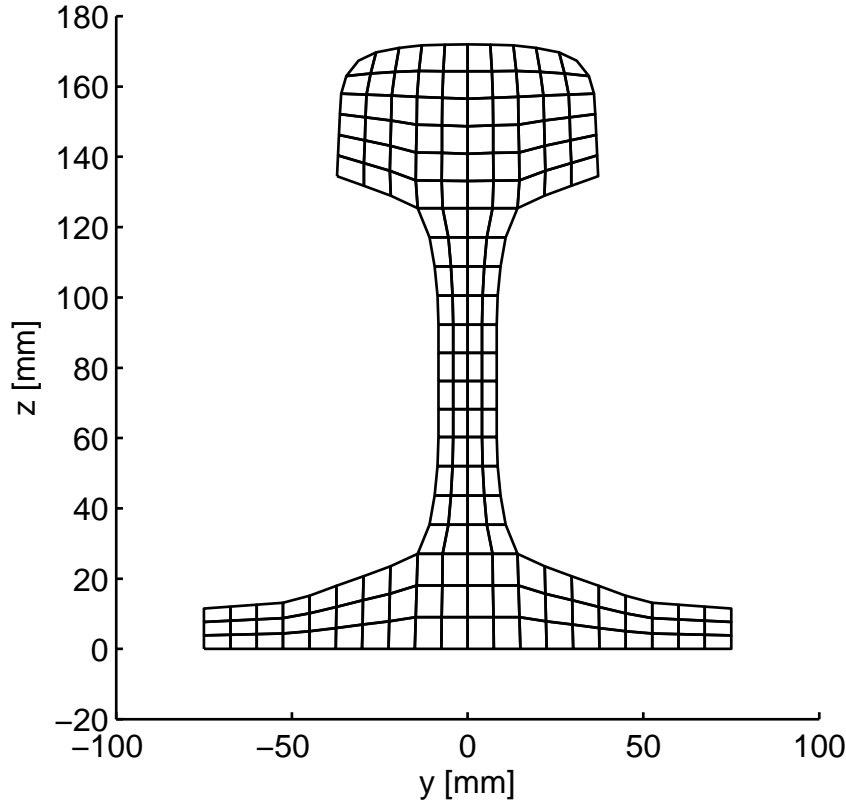


Figure 6.2.2: Discretization of the rail's cross section by quadrilateral finite elements

Here, the vector \mathbf{w}_K^e contains the nodal displacements. Based on this, the following inertia terms and stiffness terms for one prism element are derived:

$$\begin{aligned}
 & \int_{V^e} \left(\delta \tilde{\mathbf{e}}(\mathbf{x})^T \mathbf{D} \tilde{\mathbf{e}}(\mathbf{x}) + \delta \tilde{\mathbf{w}}(\mathbf{x})^T \rho \ddot{\tilde{\mathbf{w}}}(\mathbf{x}) \right) dV \\
 &= \sum_L \delta \mathbf{w}_L^e{}^T \left(\int_{A_C} \hat{\mathbf{B}}_L(y, z)^T \mathbf{D} \hat{\mathbf{B}}_L(y, z) dy dz \ell \mathbf{w}_L^e + \int_{A_C} \hat{\mathbf{N}}(y, z)^T \rho \hat{\mathbf{N}}(y, z) dy dz \ell \ddot{\mathbf{w}}_L^e \right) \\
 &= \sum_K \delta \mathbf{w}_{-K}^e{}^T \left(\int_{A_C} \hat{\mathbf{B}}_{-K}(y, z)^T \mathbf{D} \hat{\mathbf{B}}_{-K}(y, z) dy dz \ell \mathbf{w}_K^e + \int_{A_C} \hat{\mathbf{N}}(y, z)^T \rho \hat{\mathbf{N}}(y, z) dy dz \ell \ddot{\mathbf{w}}_K^e \right) \\
 &= \sum_K \delta \mathbf{w}_{-K}^e{}^T \left(\mathbf{K}_K^e \ell \mathbf{w}_K^e + \mathbf{M}^e \ell \ddot{\mathbf{w}}_K^e \right) \tag{6.2.14}
 \end{aligned}$$

Here, the matrices \mathbf{K}_K^e and \mathbf{M}^e are the element stiffness matrices and the element mass matrices, respectively; since the mass matrix \mathbf{M}^e is independent from the periodicity K , no index K is required. Due to the orthogonality of the functions $e^{iK\frac{2\pi}{\ell}x}$ and $e^{iL\frac{2\pi}{\ell}x}$ for $K \neq L$ the inertia terms and the stiffness terms are decoupled for each periodicity K .

Based on the terms for the prism elements, the inertia and stiffness terms for the rail can be formulated in the following way:

$$\int_{V_R} \left(\delta \tilde{\mathbf{e}}(\mathbf{x})^T \mathbf{D} \tilde{\mathbf{e}}(\mathbf{x}) + \delta \tilde{\mathbf{w}}(\mathbf{x})^T \rho \ddot{\tilde{\mathbf{w}}}(\mathbf{x}) \right) dV = \sum_K \delta \mathbf{w}_{\text{FE}|K}^e{}^T \left(\ell \mathbf{M}_{\text{FE}|K} \ddot{\mathbf{w}}_{\text{FE}|K}(t) + \ell \mathbf{K}_{\text{FE}|K} \mathbf{w}_{\text{FE}|K}(t) \right) \tag{6.2.15}$$

By applying the solution:

$$\mathbf{w}_{\text{FE}|K}(t) = \mathbf{W}_{\text{R}|K,I} e^{i\omega_{K,I}t} \quad (6.2.16)$$

the homogeneous equation of motion can be reduced to the following algebraic eigenvector problem:

$$\ell \left(-\mathbf{M}_{\text{FE}} \omega_{K,I}^2 + \mathbf{K}_{\text{FE}|K} \right) \mathbf{W}_{\text{R}|K,I} = \mathbf{0}, \quad \mathbf{W}_{\text{R}|K,I} \neq \mathbf{0} \quad (6.2.17)$$

As it will be discussed later, the eigenfrequencies $\frac{\omega_{K,I}}{2\pi}$ of the rail have to be calculated for a very high number of periodicities. In order to get an impression, the results for two wavelengths will be discussed. In Figure 6.2.3 the eigenmodes associated with the eight lowest eigenfrequencies for the wavelength $\lambda = 3.6$ m are shown. For a better visibility, the eigenmodes are displayed for a part having the length of 1.8 m, i.e. a half wave is shown. Since the rail profile has a maximum width of 150 mm and a height of 172 mm, the condition for a slender beam is fulfilled, i.e. the length of the beam is at least ten times its maximum dimension of the cross section.

The four lowest eigenfrequencies are associated with the deformations of a one-dimensional continuum, i.e. the lateral bending (64 Hz), the vertical bending (152 Hz), the torsion (232 Hz) and the longitudinal expansion and compression (1442 Hz). The eigenmodes associated with the fifth eigenfrequency (1448 Hz) and the sixth eigenfrequency (4192 Hz) show distinct deformations of the cross section; an inclination of the rail head is clearly visible. For the seventh eigenfrequency (5246 Hz) and the eighth eigenfrequency (5442 Hz) bending motions of the rail foot occur.

In Figure 6.2.4 the eigenmodes associated with the eight lowest eigenfrequencies for the wavelength $\lambda = 1.2$ m are shown. This wavelength is two times the sleeper spacing so that these modes are important for the so-called pinned-pinned mode of the track; for the pinned-pinned mode the wave nodes are located above the sleepers so that vibrations of the rail are relatively weakly damped. Again, the eigenmodes are displayed for a part having the length of 1.8 m so that in this case one and a half full waves are shown.

The two lowest eigenfrequencies are associated with the lateral bending (508 Hz) and the torsion (848 Hz). A closer look to the eigenmode of the lateral bending reveals an inclination of the profile, i.e. the separation of lateral translation for the bending on the one hand and the rotation for the torsion on the other hand is lost. Apparently, the “classical theories” for the one-dimensional continuum reach the limits of their validity, when the wavelength approaches the dimension of the cross section. The third eigenfrequency (1069 Hz) is associated with the vertical bending of the rail. For the fourth eigenfrequency (1911 Hz) a distinct deformation of the cross section occurs. This eigenfrequency is considerably lower than the fifth eigenfrequency (4288 Hz), which is associated with the longitudinal expansion and compression of the rail.

6.3 Modelling of the sleeper

In the present model the sleeper is modelled as a rigid body, which is supported by a visco-elastic layer representing the underground. All motions of the sleeper are considered to be small so that both the kinematics and the equations of motion can be linearized.

The rails are supported by equidistant sleepers, to which they are connected by force elements representing the rail pads. However, since all sleepers are considered to be equal, one single sleeper will be considered; for the sake of brevity, the indices which identify the individual sleepers of the track will be introduced later. In the following sections, the kinematics and the inertia of a single sleeper and the forces of the visco-elastic layer supporting it will be derived.

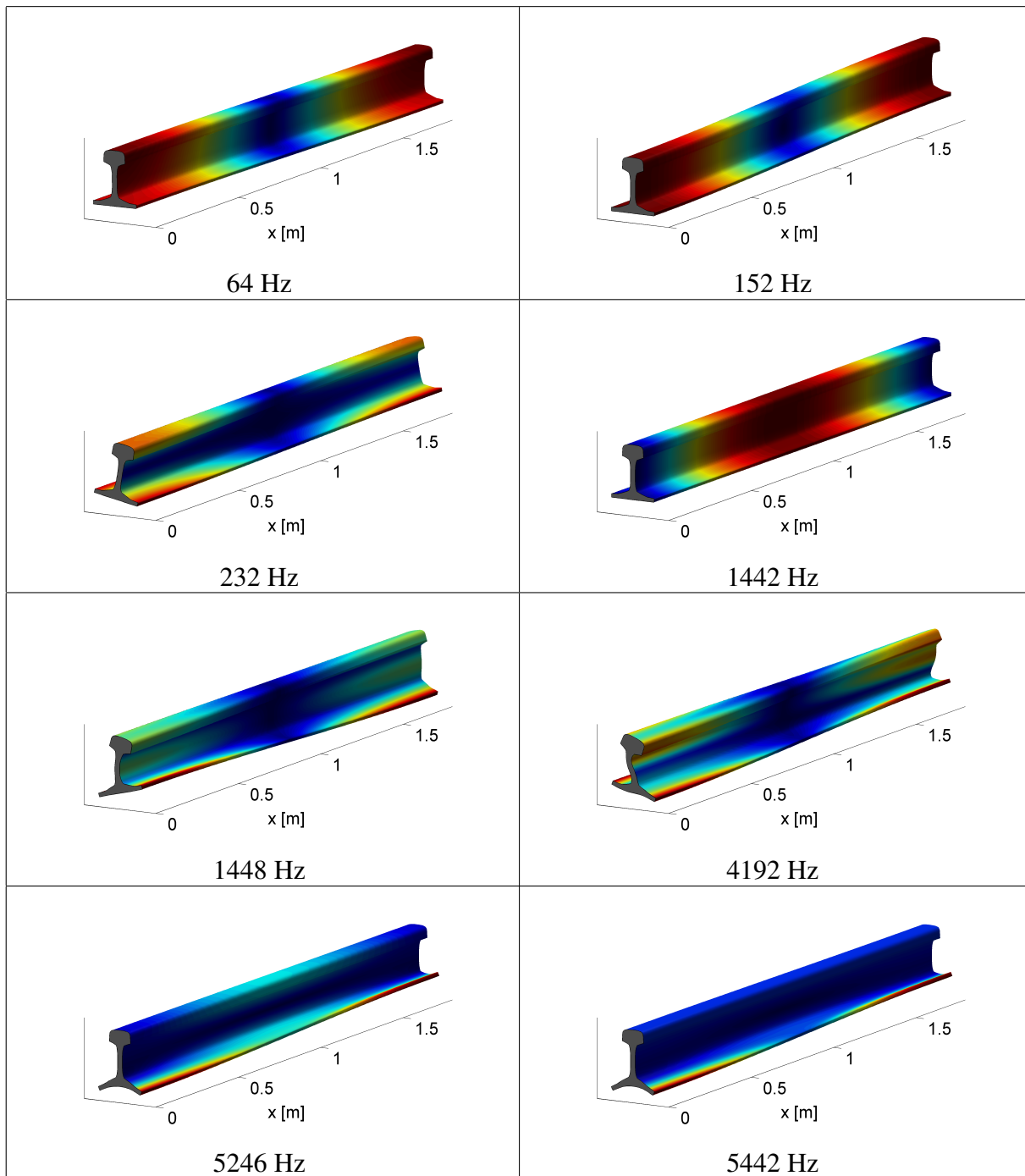


Figure 6.2.3: Rail modes for the wavelength $\lambda = 3.6$ m

6.3.1 Kinematics of the sleeper

The sleeper has the six degrees of freedom of a rigid body. The three translations are the longitudinal displacement $x_S(t)$, the lateral displacement $y_S(t)$ and the vertical displacement $z_S(t)$; these translations describe the displacement of the sleeper's reference point R from its reference position which is defined by the longitudinal distance X_{S0} and the vertical distance Z_{S0} . The three rotations are the roll angle $\varphi_S(t)$, the pitch angle $\vartheta_S(t)$ and the yaw angle $\psi_S(t)$. For the sake of brevity, the dependency of x_S , y_S , z_S , φ_S , ϑ_S and ψ_S on the time t will not always be indicated explicitly. By using the three angles as cardan angles the rotation of the body-fixed frame S of the sleeper, which is used as the reference frame, with respect to the inertial frame I is described. In total, the

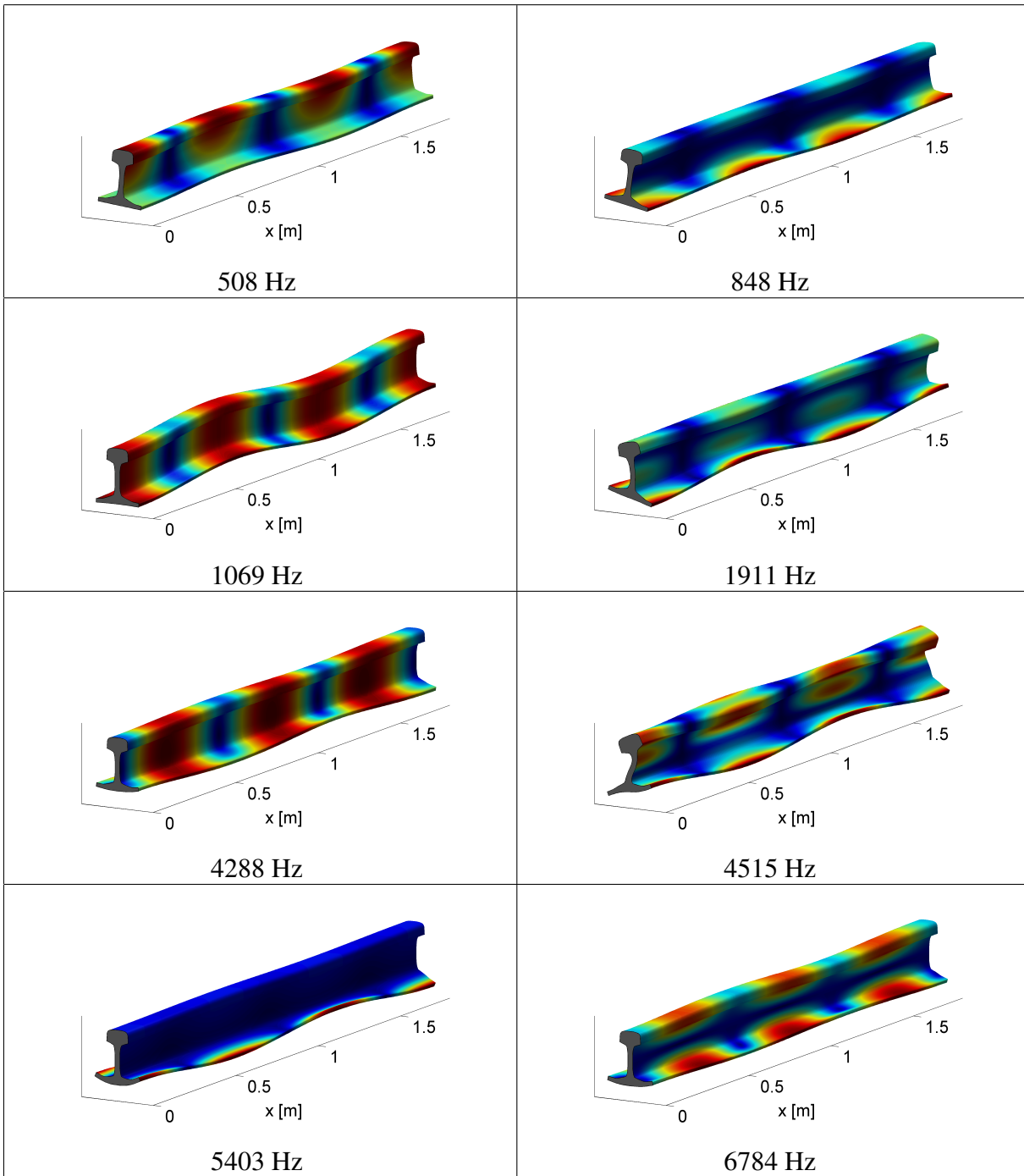


Figure 6.2.4: Rail modes for the wavelength $\lambda = 1.2$ m

current position of a point P, which is indicated by the sleeper's body-fixed coordinates x , y and z , is formulated in the following way:

$$\begin{aligned}
 \mathbf{r}_{OP}^I &= \mathbf{r}_{OR}^I + \mathbf{S}^{IS} \mathbf{x}^S = \begin{bmatrix} X_{S0} + x_S \\ y_S \\ Z_{S0} + z_S \end{bmatrix} + \mathbf{S}_1(\varphi_S) \mathbf{S}_2(\vartheta_S) \mathbf{S}_3(\psi_S) \begin{bmatrix} x \\ y \\ z \end{bmatrix} \\
 &= \begin{bmatrix} X_{S0} + x_S + \cos \vartheta_S (\cos \psi_S x - \sin \psi_S y) + \sin \vartheta_S z \\ y_S + \cos \varphi_S (\sin \psi_S x + \cos \psi_S y) - \sin \varphi_S (-\sin \vartheta_S (\cos \psi_S x - \sin \psi_S y) + \cos \vartheta_S z) \\ Z_{S0} + z_S + \sin \varphi_S (\sin \psi_S x + \cos \psi_S y) + \cos \varphi_S (-\sin \vartheta_S (\cos \psi_S x - \sin \psi_S y) + \cos \vartheta_S z) \end{bmatrix}
 \end{aligned} \tag{6.3.18}$$

As mentioned before, it is assumed that the motions of the sleeper are small; for a small angle ϕ the following approximation can be used:

$$\phi \ll 1 \Rightarrow \sin \phi \approx \phi, \cos \phi \approx 1 \quad (6.3.19)$$

By applying this to the vector \mathbf{r}_{OP}^I according to (6.3.18) it is obtained:

$$\begin{aligned} \mathbf{r}_{OP}^I &\approx \begin{bmatrix} X_{S0} + x_S + x - \psi_S y + \vartheta_S z \\ y_S + \psi_S x + y - \phi_S (-\vartheta_S (x - \psi_S y) + z) \\ Z_{S0} + z_S + \phi_S (\psi_S x + y) - \vartheta_S (x - \psi_S y) + z \end{bmatrix} \\ &\approx \begin{bmatrix} X_{S0} + x_S + x - \psi_S y + \vartheta_S z \\ y_S + (\psi_S + \phi_S \vartheta_S) x + (1 - \phi_S \vartheta_S \psi_S) y - \phi_S z \\ Z_{S0} + z_S + (\phi_S \psi_S - \vartheta_S) x + (\phi_S + \vartheta_S \psi_S) y + z \end{bmatrix} \end{aligned} \quad (6.3.20)$$

Neglecting small terms and regrouping the terms leads to:

$$\mathbf{r}_{OP}^I \approx \underbrace{\begin{bmatrix} X_{S0} + x \\ y \\ Z_{S0} + z \end{bmatrix}}_{\mathbf{r}_{OP_0}^I} + \underbrace{\begin{bmatrix} x_S(t) - \psi_S(t) y + \vartheta_S(t) z \\ y_S(t) + \psi_S(t) x - \phi_S z(t) \\ z_S(t) - \vartheta_S(t) x + \phi_S(t) y \end{bmatrix}}_{\mathbf{w}_P^I} = \mathbf{r}_{OP_0}^I + \underbrace{\begin{bmatrix} 1 & 0 & 0 & 0 & z & -y \\ 0 & 1 & 0 & -z & 0 & x \\ 0 & 0 & 1 & y & -x & 0 \end{bmatrix}}_{\mathbf{C}_S^I(\mathbf{x}^S)} \underbrace{\begin{bmatrix} x_S(t) \\ y_S(t) \\ z_S(t) \\ \phi_S(t) \\ \vartheta_S(t) \\ \psi_S(t) \end{bmatrix}}_{\mathbf{q}_S(t)} \quad (6.3.21)$$

This linearized formulation of the kinematics will be used for the points at which the sleeper is connected to other elements.

6.3.2 Inertia terms for the sleeper

In the appendix C, the following inertia terms for a rigid body B in the formulation for the body-fixed frame \mathcal{B} have been derived:

$$\begin{aligned} \int_B \delta' \mathbf{v}_{OP}^I \mathbf{T} \mathbf{a}_{OP}^I dm &= \delta' \mathbf{v}_{OR}^I \mathbf{T} \left[m_B \mathbf{a}_{OR}^I + \mathbf{S}^{IB} \left(\dot{\tilde{\omega}}_{IB}^B + \tilde{\omega}_{IB}^B \tilde{\omega}_{IB}^B \right) \int_B \mathbf{x}_{RP}^B dm \right] \\ &+ \delta' \omega_{IB}^B \mathbf{T} \left[\int_B \tilde{\mathbf{x}}_{RP}^B dm \mathbf{S}^{BI} \mathbf{a}_{OR}^I + \mathbf{J}_{B,(R)}^B \dot{\omega}_{IB}^B + \tilde{\omega}_{IB}^B \mathbf{J}_{B,(R)}^B \omega_{IB}^B \right] \end{aligned} \quad (6.3.22)$$

Here, m_B is the mass of the body. The matrix $\mathbf{J}_{B,(R)}^B$ denotes the inertia tensor with respect to the reference point R described in the body-fixed frame \mathcal{B} . If the centre of gravity C_B is used as the reference point R, then it is valid:

$$\int_B \mathbf{x}_{C_B P}^B dm = \mathbf{0} \quad (6.3.23)$$

$$\Rightarrow \int_B \delta' \mathbf{v}_{OP}^I \mathbf{T} \mathbf{a}_{OP}^I dm = \delta' \mathbf{v}_{OC_B}^I \mathbf{T} m_B \mathbf{a}_{OC_B}^I + \delta' \omega_{IB}^B \mathbf{T} \left[\mathbf{J}_{B,(C_B)}^B \dot{\omega}_{IB}^B + \tilde{\omega}_{IB}^B \mathbf{J}_{B,(C_B)}^B \omega_{IB}^B \right] \quad (6.3.24)$$

In this case, the coupling terms between the translational and the rotational motions vanish. As a result, the inertia terms can be written as:

$$\int_B \delta' \mathbf{v}_{OP}^I \mathbf{T} \mathbf{a}_{OP}^I dm = \delta' \mathbf{v}_{OC_B}^I \mathbf{T} m_B \mathbf{a}_{OC_B}^I + \delta' \omega_{IB}^B \mathbf{T} \left[\mathbf{J}_{B,(C_B)}^B \dot{\omega}_{IB}^B + \tilde{\omega}_{IB}^B \mathbf{J}_{B,(C_B)}^B \omega_{IB}^B \right] \quad (6.3.25)$$

For the sleeper, the rotation matrix \mathbf{S}^{IS} between the inertial frame I and the body-fixed frame S of the sleeper has been formulated in the previous section 6.3.1:

$$\mathbf{S}^{IS} = \mathbf{S}_1(\varphi_S) \mathbf{S}_2(\vartheta_S) \mathbf{S}_3(\psi_S) \quad (6.3.26)$$

From this, the following angular velocity ω_{IS}^I is obtained:

$$\tilde{\omega}_{IS}^I = \dot{\mathbf{S}}^{IS} \mathbf{S}^{IS\top} \Rightarrow \omega_{IS}^I = \begin{bmatrix} \dot{\varphi}_S + \dot{\psi}_S \sin \vartheta_S \\ \dot{\vartheta}_S \cos \varphi_S - \dot{\psi}_S \cos \vartheta_S \sin \varphi_S \\ \dot{\psi}_S \cos \vartheta_S \cos \varphi_S + \dot{\vartheta}_S \sin \varphi_S \end{bmatrix} \quad (6.3.27)$$

The transformation into the body-fixed frame S leads to:

$$\omega_{IS}^S = \mathbf{S}^{SI} \omega_{IS}^I = \mathbf{S}^{IS\top} \omega_{IS}^I = \begin{bmatrix} \dot{\varphi}_S \cos \vartheta_S \cos \psi_S + \dot{\vartheta}_S \sin \psi_S \\ -\dot{\varphi}_S \cos \vartheta_S \sin \psi_S + \dot{\vartheta}_S \cos \psi_S \\ \dot{\psi}_S + \dot{\varphi}_S \sin \vartheta_S \end{bmatrix} \quad (6.3.28)$$

The angular acceleration $\dot{\omega}_{IS}^S$ is obtained to:

$$\dot{\omega}_{IS}^S = \begin{bmatrix} (\ddot{\varphi}_S \cos \vartheta_S - \dot{\varphi}_S \dot{\vartheta}_S \sin \vartheta_S + \dot{\vartheta}_S \dot{\psi}_S) \cos \psi_S + (\ddot{\vartheta}_S - \dot{\varphi}_S \dot{\psi}_S \cos \vartheta_S) \sin \psi_S \\ -(\ddot{\varphi}_S \cos \vartheta_S - \dot{\varphi}_S \dot{\vartheta}_S \sin \vartheta_S + \dot{\vartheta}_S \dot{\psi}_S) \sin \psi_S + (\ddot{\vartheta}_S - \dot{\varphi}_S \dot{\psi}_S \cos \vartheta_S) \cos \psi_S \\ \ddot{\psi}_S + \dot{\varphi}_S \dot{\vartheta}_S \sin \vartheta_S + \dot{\varphi}_S \dot{\vartheta}_S \cos \vartheta_S \end{bmatrix} \quad (6.3.29)$$

Applying the approximation for small angles

$$\phi \ll 1 \Rightarrow \sin \phi \approx \phi, \cos \phi \approx 1 \quad (6.3.30)$$

and neglecting small terms leads to:

$$\omega_{IS}^S \approx \begin{bmatrix} \dot{\varphi}_S + \dot{\vartheta}_S \psi_S \\ -\dot{\varphi}_S \psi_S + \dot{\vartheta}_S \\ \dot{\psi}_S + \dot{\varphi}_S \vartheta_S \end{bmatrix} \approx \begin{bmatrix} \dot{\varphi}_S \\ \dot{\vartheta}_S \\ \dot{\psi}_S \end{bmatrix} \quad (6.3.31)$$

$$\dot{\omega}_{IS}^S \approx \begin{bmatrix} \ddot{\varphi}_S - \dot{\varphi}_S \dot{\vartheta}_S \vartheta_S + \dot{\vartheta}_S \dot{\psi}_S + (\ddot{\vartheta}_S - \dot{\varphi}_S \dot{\psi}_S) \psi_S \\ -(\ddot{\varphi}_S - \dot{\varphi}_S \dot{\vartheta}_S \vartheta_S + \dot{\vartheta}_S \dot{\psi}_S) \psi_S + \ddot{\vartheta}_S - \dot{\varphi}_S \dot{\psi}_S \\ \ddot{\psi}_S + \dot{\varphi}_S \dot{\vartheta}_S + \dot{\varphi}_S \dot{\vartheta}_S \end{bmatrix} \approx \begin{bmatrix} \ddot{\varphi}_S \\ \ddot{\vartheta}_S \\ \ddot{\psi}_S \end{bmatrix} \quad (6.3.32)$$

These terms are now inserted into the inertia terms according to (6.3.22); by again neglecting small terms, the following linearized inertia terms for the sleeper are obtained:

$$\begin{aligned} \int_S \delta' \mathbf{v}_{OP}^I \top \mathbf{a}_{OP}^I dm &= \delta' \mathbf{v}_{OC_S}^I \top m_S \mathbf{a}_{OC_S}^I + \delta' \omega_{IS}^S \top \left(\mathbf{J}_S^S \dot{\omega}_{IS}^S + \tilde{\omega}_{IS}^S \mathbf{J}_S^{B_S} \omega_{IS}^S \right) \\ &\approx \delta' \mathbf{v}_{OC_S}^I \top m_S \mathbf{a}_{OC_S}^I + \delta' \omega_{IS}^S \top \mathbf{J}_S^S \dot{\omega}_{IS}^S \\ &\approx \begin{bmatrix} \delta' \dot{x}_S \\ \delta' \dot{y}_S \\ \delta' \dot{z}_S \end{bmatrix} \top m_S \begin{bmatrix} \ddot{x}_S \\ \ddot{y}_S \\ \ddot{z}_S \end{bmatrix} + \begin{bmatrix} \delta' \dot{\varphi}_S \\ \delta' \dot{\vartheta}_S \\ \delta' \dot{\psi}_S \end{bmatrix} \top \begin{bmatrix} I_{xx,S} & 0 & 0 \\ 0 & I_{yy,S} & 0 \\ 0 & 0 & I_{zz,S} \end{bmatrix} \begin{bmatrix} \ddot{\varphi}_S \\ \ddot{\vartheta}_S \\ \ddot{\psi}_S \end{bmatrix} \\ &\approx \underbrace{\begin{bmatrix} \delta' \dot{x}_S \\ \delta' \dot{y}_S \\ \delta' \dot{z}_S \\ \delta' \dot{\varphi}_S \\ \delta' \dot{\vartheta}_S \\ \delta' \dot{\psi}_S \end{bmatrix} \top}_{\delta' \dot{\mathbf{q}}_S \top} \underbrace{\begin{bmatrix} m_S & 0 & 0 & 0 & 0 & 0 \\ 0 & m_S & 0 & 0 & 0 & 0 \\ 0 & 0 & m_S & 0 & 0 & 0 \\ 0 & 0 & 0 & I_{xx,S} & 0 & 0 \\ 0 & 0 & 0 & 0 & I_{yy,S} & 0 \\ 0 & 0 & 0 & 0 & 0 & I_{zz,S} \end{bmatrix}}_{\mathbf{M}_S} \underbrace{\begin{bmatrix} \ddot{x}_S \\ \ddot{y}_S \\ \ddot{z}_S \\ \ddot{\varphi}_S \\ \ddot{\vartheta}_S \\ \ddot{\psi}_S \end{bmatrix}}_{\dot{\mathbf{q}}_S} \end{aligned} \quad (6.3.33)$$

6.3.3 Modelling of the underground

The underground is modelled as a viscoelastic layer which is located between the rigid ground and the bottom face A_S of the sleeper. The bottom face A_S is a rectangle having the length L_S in the direction of y and the width W_S in the direction of x ; its vertical distance below the sleeper's reference point is indicated by the constant value z_U . Thereby, the vector \mathbf{x}_U^S describing the bottom face in the body-fixed frame \mathcal{S} is given by:

$$\mathbf{x}_U^S = \begin{bmatrix} x \\ y \\ z_U \end{bmatrix}, \quad -\frac{L_S}{2} \leq y \leq \frac{L_S}{2}, \quad -\frac{W_S}{2} \leq x \leq \frac{W_S}{2} \quad (6.3.34)$$

The local stress of the visco-elastic layer consists of an elastic part and a viscous part. The elastic part is obtained by multiplying the local displacement $\mathbf{w}_S^I(\mathbf{x}_U^S)$ with the stiffness matrix $\bar{\mathbf{K}}_U$. For the viscous part, the local displacement velocity $\dot{\mathbf{w}}_S^I(\mathbf{x}_U^S)$ is multiplied with the damping matrix $\bar{\mathbf{D}}_U$. By multiplying the local stress with an infinitesimal area having the edge lengths dx and dy the following infinitesimal force $d\mathbf{f}$ is obtained:

$$d\mathbf{f}_U^I = \underbrace{\begin{bmatrix} \bar{c}_x & 0 & 0 \\ 0 & \bar{c}_y & 0 \\ 0 & 0 & \bar{c}_z \end{bmatrix}}_{\bar{\mathbf{K}}_U} \mathbf{w}_S^I(\mathbf{x}_U^S) dx dy + \underbrace{\begin{bmatrix} \bar{b}_x & 0 & 0 \\ 0 & \bar{b}_y & 0 \\ 0 & 0 & \bar{b}_z \end{bmatrix}}_{\bar{\mathbf{D}}_U} \dot{\mathbf{w}}_S^I(\mathbf{x}_U^S) dx dy \quad (6.3.35)$$

The layer is assumed to be homogeneous so that the matrices $\bar{\mathbf{K}}_U$ and $\bar{\mathbf{D}}_U$ are constant.

The complete virtual power $\delta'P_U$ for the viscoelastic layer is obtained by integrating the scalar product of the local virtual velocity $\delta'\dot{\mathbf{w}}_S^I(\mathbf{x}_U^S)$ and the infinitesimal force $d\mathbf{f}_U^I$ over the area A_S of the bottom face:

$$\delta'P_U = \int_{A_S} \delta'\dot{\mathbf{w}}_S^I(\mathbf{x}_U^S)^T d\mathbf{f}_U^I \quad (6.3.36)$$

Inserting the relation for the linearized kinematics developed in the section 6.3.1

$$\mathbf{w}_S^I(\mathbf{x}_U^S) = \mathbf{C}_S^I(\mathbf{x}_U^S) \mathbf{q}_S \Rightarrow \dot{\mathbf{w}}_S^I(\mathbf{x}_U^S) = \mathbf{C}_S^I(\mathbf{x}_U^S) \dot{\mathbf{q}}_S \Rightarrow \delta'\dot{\mathbf{w}}_S^I(\mathbf{x}_U^S) = \mathbf{C}_S^I(\mathbf{x}_U^S) \delta'\dot{\mathbf{q}}_S \quad (6.3.37)$$

leads to:

$$\begin{aligned} \delta'P_U &= \int_{A_S} \delta'\dot{\mathbf{q}}_S^T \mathbf{C}_S^I(\mathbf{x}_U^S)^T \left(\bar{\mathbf{K}}_U \mathbf{C}_S^I(\mathbf{x}_U^S) \mathbf{q}_S + \bar{\mathbf{D}}_U \mathbf{C}_S^I(\mathbf{x}_U^S) \dot{\mathbf{q}}_S \right) dx dy \\ &= \delta'\dot{\mathbf{q}}_S^T \underbrace{\int_{A_S} \mathbf{C}_S^I(\mathbf{x}_U^S)^T \bar{\mathbf{K}}_U \mathbf{C}_S^I(\mathbf{x}_U^S) dx dy}_{\mathbf{K}_U} \mathbf{q}_S + \delta'\dot{\mathbf{q}}_S^T \underbrace{\int_{A_S} \mathbf{C}_S^I(\mathbf{x}_U^S)^T \bar{\mathbf{D}}_U \mathbf{C}_S^I(\mathbf{x}_U^S) dx dy}_{\mathbf{D}_U} \dot{\mathbf{q}}_S \end{aligned} \quad (6.3.38)$$

For the matrix $\mathbf{C}_S^I(\mathbf{x}_U^S)$ it is valid:

$$\mathbf{C}_S^I(\mathbf{x}_U^S) = \begin{bmatrix} 1 & 0 & 0 & 0 & z_U & -y \\ 0 & 1 & 0 & -z_U & 0 & x \\ 0 & 0 & 1 & y & -x & 0 \end{bmatrix} \quad (6.3.39)$$

By inserting the matrices $\mathbf{C}_S^I(\mathbf{x}_U^S)$ and $\bar{\mathbf{K}}_U$ and integrating the product over the area A_S according to (6.3.34) it is obtained for the stiffness matrix \mathbf{K}_U :

$$\begin{aligned} \mathbf{K}_U &= \int_{A_S} \mathbf{C}_S^I(\mathbf{x}_U^S)^T \bar{\mathbf{K}}_U \mathbf{C}_S^I(\mathbf{x}_U^S) dx dy \\ &= \int_{-L_S/2}^{L_S/2} \int_{-W_S/2}^{W_S/2} \begin{bmatrix} \bar{c}_x & 0 & 0 & 0 & \bar{c}_x z_U & -\bar{c}_x y \\ 0 & \bar{c}_y & 0 & -\bar{c}_y z_U & 0 & \bar{c}_y x \\ 0 & 0 & \bar{c}_z & \bar{c}_z y & -\bar{c}_z x & 0 \\ 0 & -\bar{c}_y z_U & \bar{c}_z y & \bar{c}_y z_U^2 + \bar{c}_z y^2 & -\bar{c}_z x y & -\bar{c}_y x z_U \\ \bar{c}_x z_U & 0 & -\bar{c}_z x & -\bar{c}_z x y & \bar{c}_x z_U^2 + \bar{c}_z x^2 & -\bar{c}_x y z_U \\ -\bar{c}_x y & \bar{c}_y x & 0 & -\bar{c}_y x z_U & -\bar{c}_x y z_U & \bar{c}_x y^2 + \bar{c}_y x^2 \end{bmatrix} dx dy \\ &= W_S L_S \begin{bmatrix} \bar{c}_x & 0 & 0 & 0 & \bar{c}_x z_U & 0 \\ 0 & \bar{c}_y & 0 & -\bar{c}_y z_U & 0 & 0 \\ 0 & 0 & \bar{c}_z & 0 & 0 & 0 \\ 0 & -\bar{c}_y z_U & 0 & z_U^2 \bar{c}_y + \frac{1}{12} \bar{c}_z L_S^2 & 0 & 0 \\ \bar{c}_x z_U & 0 & 0 & 0 & \bar{c}_x z_U^2 + \frac{1}{12} \bar{c}_z W_S^2 & 0 \\ 0 & 0 & 0 & 0 & 0 & \frac{1}{12} \bar{c}_x L_S^2 + \frac{1}{12} \bar{c}_y W_S^2 \end{bmatrix} \end{aligned} \quad (6.3.40)$$

By defining the following stiffnesses:

$$c_{Ux} = \bar{c}_x W_S L_S, \quad c_{Uy} = \bar{c}_y W_S L_S, \quad c_{Uz} = \bar{c}_z W_S L_S \quad (6.3.41)$$

the resulting stiffness matrix \mathbf{K}_U for the layer representing the underground is formulated in the following way:

$$\mathbf{K}_U = \begin{bmatrix} c_{Ux} & 0 & 0 & 0 & c_{Ux} z_U & 0 \\ 0 & c_{Uy} & 0 & -c_{Uy} z_U & 0 & 0 \\ 0 & 0 & c_{Uz} & 0 & 0 & 0 \\ 0 & -c_{Uy} z_U & 0 & z_U^2 c_{Uy} + \frac{1}{12} c_{Uz} L_S^2 & 0 & 0 \\ c_{Ux} z_U & 0 & 0 & 0 & c_{Ux} z_U^2 + \frac{1}{12} c_{Uz} W_S^2 & 0 \\ 0 & 0 & 0 & 0 & 0 & \frac{1}{12} c_{Ux} L_S^2 + \frac{1}{12} c_{Uy} W_S^2 \end{bmatrix} \quad (6.3.42)$$

From (6.3.38) it can be seen that the structure of the damping matrix \mathbf{D}_U is analogous to the one of the stiffness matrix \mathbf{K}_U so that the matrix \mathbf{D}_U can be derived from the matrix \mathbf{K}_U by simply replacing the matrix $\bar{\mathbf{K}}_U$ with the matrix $\bar{\mathbf{D}}_U$. From the comparison of the matrices $\bar{\mathbf{K}}_U$ and $\bar{\mathbf{D}}_U$ as indicated in (6.3.35) it follows that replacing the matrix $\bar{\mathbf{K}}_U$ with the matrix $\bar{\mathbf{D}}_U$ means to substitute the stiffnesses \bar{c}_x , \bar{c}_y and \bar{c}_z by the damping coefficients \bar{b}_x , \bar{b}_y and \bar{b}_z . By defining the following damping coefficients:

$$b_{Ux} = \bar{b}_x W_S L_S, \quad b_{Uy} = \bar{b}_y W_S L_S, \quad b_{Uz} = \bar{b}_z W_S L_S \quad (6.3.43)$$

the damping matrix \mathbf{D}_U for the visco-elastic layer can be expressed in the following way:

$$\mathbf{D}_U = \begin{bmatrix} b_{Ux} & 0 & 0 & 0 & b_{Ux} z_U & 0 \\ 0 & b_{Uy} & 0 & -b_{Uy} z_U & 0 & 0 \\ 0 & 0 & b_{Uz} & 0 & 0 & 0 \\ 0 & -b_{Uy} z_U & 0 & z_U^2 b_{Uy} + \frac{1}{12} b_{Uz} L_S^2 & 0 & 0 \\ b_{Ux} z_U & 0 & 0 & 0 & b_{Ux} z_U^2 + \frac{1}{12} b_{Uz} W_S^2 & 0 \\ 0 & 0 & 0 & 0 & 0 & \frac{1}{12} b_{Ux} L_S^2 + \frac{1}{12} b_{Uy} W_S^2 \end{bmatrix} \quad (6.3.44)$$

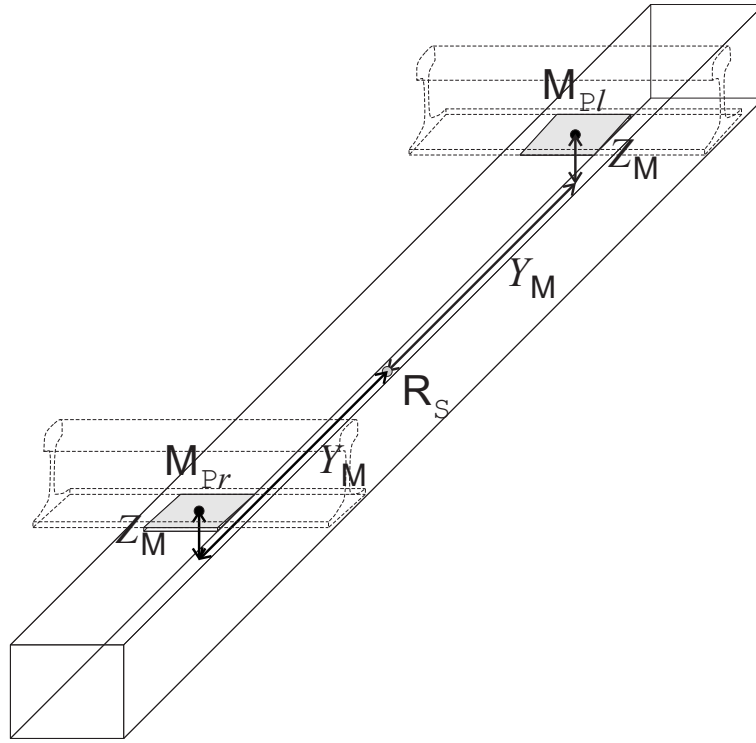


Figure 6.3.5: Position of the rail seats (grey) on the sleeper; M_{Pr} : centre of the right rail seat; M_{Pl} : centre of the left rail seat; R_S : reference point of the sleeper

6.3.4 Rail seat

The rail seat is a plane on the top of the sleeper; here, the sleeper is connected to the rail via the pad. The rail seat is inclined with the rail cant ϕ_R . In Figure 6.3.5, the location of the two rail seats on a sleeper is shown. As displayed in Figure 6.3.6, a point P_I is indicated by the local coordinates x_I and y_I relative to the centre M of the rail seat.

By using the centre M_{Pr} of the right rail seat, the relative position of a point P_{SI} at the rail seat with respect to the reference point R_S is described in the following way:

$$\mathbf{x}_I^S \equiv \mathbf{r}_{R_S P_{SI}}^S = \mathbf{r}_{R_S M_{Pr}}^S + \mathbf{r}_{M_{Pr} P_{SI}}^S = \underbrace{\begin{bmatrix} 0 \\ Y_M \\ Z_M \end{bmatrix}}_{\mathbf{r}_{R_S M_S}^S} + \underbrace{\begin{bmatrix} 1 & 0 & 0 \\ 0 & \cos \phi_R & -\sin \phi_R \\ 0 & \sin \phi_R & \cos \phi_R \end{bmatrix}}_{\mathbf{S}_I(\phi_R)} \underbrace{\begin{bmatrix} x_I \\ y_I \\ 0 \end{bmatrix}}_{\mathbf{r}_{M_S P_{SI}}^S} = \begin{bmatrix} x_I \\ Y_M + y_I \cos \phi_R \\ Z_M + y_I \sin \phi_R \end{bmatrix} \quad (6.3.45)$$

In section 6.3, the following linearized formulation for the displacement \mathbf{w}_P^I of a point P belonging to the sleeper S has been developed:

$$\mathbf{x}^S = \begin{bmatrix} x \\ y \\ z \end{bmatrix} \Rightarrow \mathbf{w}_P^I(\mathbf{x}^S) = \underbrace{\begin{bmatrix} 1 & 0 & 0 & 0 & z & -y \\ 0 & 1 & 0 & -z & 0 & x \\ 0 & 0 & 1 & y & -x & 0 \end{bmatrix}}_{\mathbf{C}_S^I(\mathbf{x}^S)} \underbrace{\begin{bmatrix} x_S(t) \\ y_S(t) \\ z_S(t) \\ \phi_S(t) \\ \vartheta_S(t) \\ \psi_S(t) \end{bmatrix}}_{\mathbf{q}_S(t)} \quad (6.3.46)$$

The expression (6.3.46) describes the displacement in the inertial frame I . In order to determine

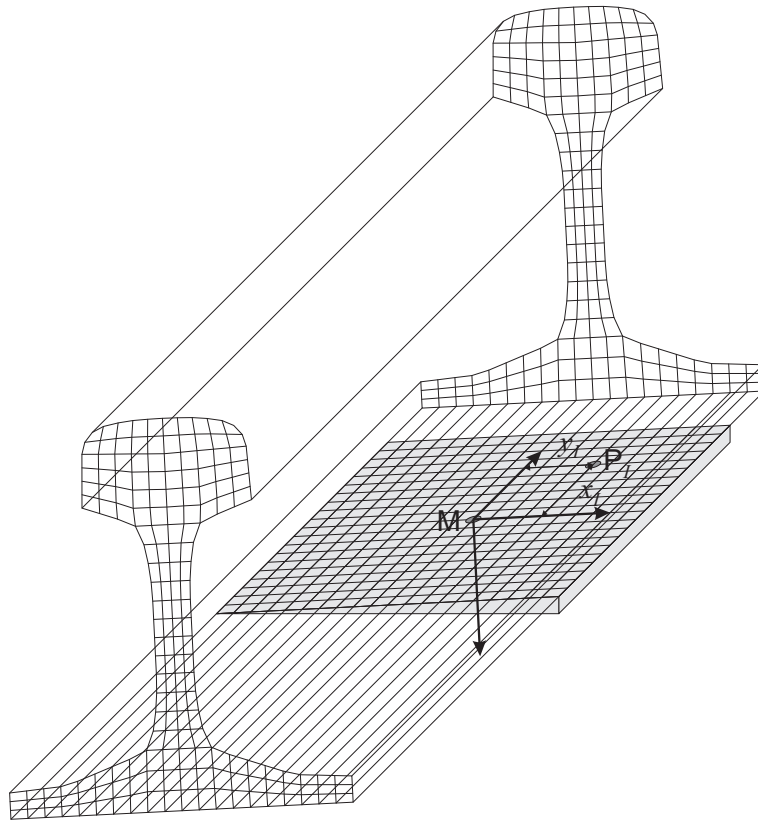


Figure 6.3.6: Overview of the rail seat and the rail foot; M : centre of the rail seat; P_I : considered point defined by local coordinates x_I and y_I

the kinematics of the pad, the displacement has to be transformed into the rail frame \mathcal{R} ; since the rail is inclined by the constant angle ϕ_R around its 1-axis, it is valid:

$$\mathbf{S}^{\mathcal{R}I} = \mathbf{S}^{\mathcal{R}I^{-1}} = \mathbf{S}_1(\phi_R)^{-1} = \mathbf{S}_1(-\phi_R) \quad (6.3.47)$$

Thereby, the displacement \mathbf{w}_{SP_I} of the point P_I , which is required for the kinematics of the pad, is obtained to:

$$\mathbf{w}_{SP_I} \equiv \mathbf{w}_P^{\mathcal{R}}(\mathbf{x}_I^S) = \mathbf{S}^{\mathcal{R}I} \mathbf{w}_P^I(\mathbf{x}_I^S) = \underbrace{\mathbf{S}_1(-\phi_R) \mathbf{C}_S^I(\mathbf{x}_I^S)}_{\mathbf{C}_{SP_I}} \mathbf{q}_S(t) = \mathbf{C}_{SP_I} \mathbf{q}_S(t) \quad (6.3.48)$$

Here, the matrix \mathbf{C}_{SP_I} establishes a relation between the displacement of the sleeper at the rail seat and the generalized motion coordinates of the sleeper. This matrix is given by:

$$\begin{aligned} \mathbf{C}_{SP_I} &= \underbrace{\begin{bmatrix} 1 & 0 & 0 \\ 0 & \cos \phi_R & \sin \phi_R \\ 0 & -\sin \phi_R & \cos \phi_R \end{bmatrix}}_{\mathbf{S}_1(-\phi_R)} \underbrace{\begin{bmatrix} 1 & 0 & 0 & 0 & Z_M + y_I \sin \phi_R & -Y_M - y_I \cos \phi_R \\ 0 & 1 & 0 & -Z_M - y_I \sin \phi_R & 0 & x \\ 0 & 0 & 1 & Y_M + y_I \cos \phi_R & -x & 0 \end{bmatrix}}_{\mathbf{C}_S^I(\mathbf{x}_I^S)} \\ &= \begin{bmatrix} 1 & 0 & 0 & 0 & Z_M + y_I \sin \phi_R & -Y_M - y_I \cos \phi_R \\ 0 & \cos \phi_R & \sin \phi_R & -Z_M \cos \phi_R + Y_M \sin \phi_R & -x_I \sin \phi_R & x_I \cos \phi_R \\ 0 & -\sin \phi_R & \cos \phi_R & Y_M \cos \phi_R + Z_M \sin \phi_R + y_I & -x_I \cos \phi_R & -x_I \sin \phi_R \end{bmatrix} \quad (6.3.49) \end{aligned}$$

The kinematics for the left rail seat is obtained in an analogous way. As it can be seen from Figure 6.3.5, the signs of the lateral distance Y_M and of the rail cant ϕ_R have to be changed.

6.4 The track as a cyclic structure

The track consists of prismatic rails supported by sleepers, which have identical properties and equidistant positions; thereby, the track can be partitioned into equal segments, as shown in Figure 6.4.7. As the figure shows, each segment contains one sleeper, i.e. it is clear, to which segment

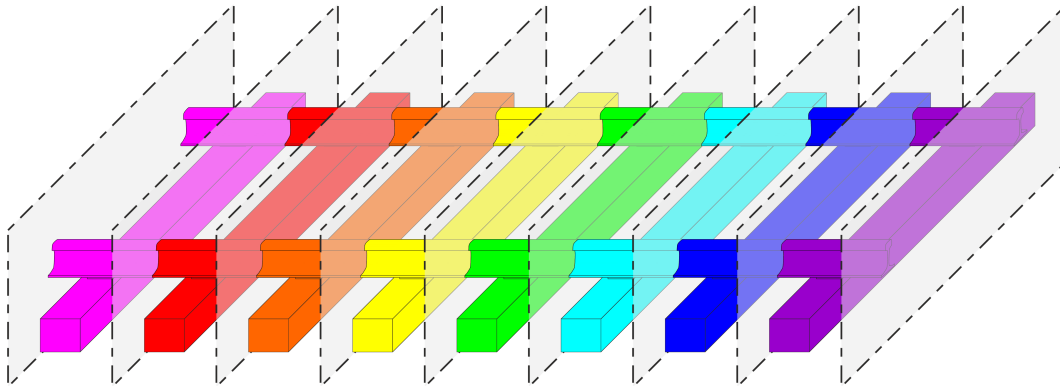


Figure 6.4.7: Cyclic track structure

a certain sleeper belongs. In contrast to this, the rails are continuous elements; therefore, the rails have to be divided into sections so that one section of each rail belongs to a uniquely defined segment.

In the previous sections 6.2 and 6.3 the terms for the individual components have been derived. In this section, these formulations will be adapted to the description of cyclic systems developed in the chapter 3.

6.4.1 Rails

The rail is considered as a prismatic structure; therefore, its displacement field can be formulated as a continuous Fourier series:

$$\mathbf{w}_R^{\mathcal{R}}(x, y, z, t) = \sum_{K=-\infty}^{\infty} \mathbf{w}_{R|K}^{\mathcal{R}}(y, z, t) e^{iK\kappa x}, \quad \kappa = \frac{2\pi}{\ell} \quad (6.4.50)$$

In the section 6.2, it has been shown that each term $\mathbf{w}_{R|K}^{\mathcal{R}}(y, z, t) e^{iK\kappa x}$ is a semi-analytic solution of Navier's equation for a prismatic structure. Furthermore, it can be shown based on the considerations given in the section 3.1.1 that for $K \neq -L$ the functions $e^{iK\kappa x}$ and $e^{i(K+L)\kappa x}$ are orthogonal:

$$\int_0^{\ell} e^{iK\kappa x} e^{iL\kappa x} dx = \int_0^{\ell} e^{i(K+L)\kappa x} dx = \left. \frac{e^{i(K+L)\kappa x}}{i(K+L)\kappa} \right|_0^{\ell} = \frac{e^{i(K+L)\kappa \ell} - e^0}{i(K+L)\kappa} = \frac{\overbrace{e^{2\pi i(K+L)}}^1 - 1}{i(K+L)\kappa} = 0 \quad (6.4.51)$$

By using the prismatic finite element described in the section 4.2, a separate problem is formulated for each periodicity K :

$$\int_R \delta' \mathbf{r}^T \ddot{\mathbf{r}} dm + \int_R \delta' \dot{\boldsymbol{\varepsilon}}^T \boldsymbol{\sigma} dV = \sum_{K=-\infty}^{\infty} \delta' \mathbf{w}_{FE|K}^H (\ell \mathbf{M}_{FE} \ddot{\mathbf{w}}_{FE|K} + \ell \mathbf{K}_{FE|K} \mathbf{w}_{FE|K}), \quad \mathbf{w}_{FE|K} = \begin{bmatrix} \mathbf{w}_{1,K}^e \\ \mathbf{w}_{2,K}^e \\ \vdots \\ \mathbf{w}_{N,K}^e \end{bmatrix} \quad (6.4.52)$$

Here, the vectors $\mathbf{w}_{j,K}^e$ denote the nodal displacements for the j -th node.

It should be pointed out that by applying the semi-analytic solution (6.4.50) the entire cyclic structure is already transformed into a formulation of a cyclic system, which has in this case an infinite number of segments. This solution has to be adapted to the finite number of segments given by the discrete support by the sleepers. As mentioned before, the rail is partitioned into sections whereby each section belongs to a segment. Also here, the consideration using an n -tuple of corresponding particles can be applied. In this case the reference coordinates are given by:

$$\mathbf{x}_j^{\mathcal{R}} = \mathbf{x}^{\mathcal{R}}(x_j, y, z) = \begin{bmatrix} x_0 + j \cdot \Delta s \\ y \\ z \end{bmatrix} \quad (6.4.53)$$

The values for the coordinates y and z are equal for each particle. The displacement of the rail for the j -th corresponding particle is formulated in the following way:

$$\mathbf{w}_R^{(j)} \equiv \mathbf{w}^{\mathcal{R}}(x_j, y, z) = \sum_{K=-\infty}^{\infty} \mathbf{w}_{R|K}^{\mathcal{R}}(y, z) e^{iK\kappa(x_0 + j \cdot \Delta s)} \quad (6.4.54)$$

Practically, this means that the continuous Fourier series has to be evaluated at discrete equidistant points. As described in the section 3.1.2, the periodicity K is expressed as $K = k + mn$, whereby

$k_{\min} \leq k \leq k_{\max}$ is the periodicity for the cyclic system. For the powers it is valid:

$$\kappa = \frac{2\pi}{n \cdot \Delta s} \Rightarrow \kappa \cdot j \cdot \Delta s = \frac{2\pi}{n \cdot \Delta s} j \cdot \Delta s = \frac{2\pi}{n} j \Rightarrow e^{i\kappa \cdot j \cdot \Delta s} = e^{i(k+mn)\frac{2\pi}{n}j} = \underbrace{e^{i\frac{2\pi}{n}kj}}_{\zeta^{kj}} \underbrace{e^{2\pi i m j}}_1 = \zeta^{kj} \quad (6.4.55)$$

Thereby, the displacement for the corresponding points of the rail can be formulated in the following way:

$$\begin{aligned} \mathbf{w}_R^{(j)} &= \sum_{K=-\infty}^{\infty} \mathbf{w}_{R|K}(y, z) e^{iK\kappa(x_0+j\Delta s)} = \sum_{K=-\infty}^{\infty} \mathbf{w}_{R|K}(y, z) e^{iK\kappa x_0} e^{iK\kappa \cdot j \cdot \Delta s} \\ &= \sum_{k=k_{\min}}^{k_{\max}} \underbrace{\left(\sum_{m=-\infty}^{\infty} \mathbf{w}_{R|k+mn}(y, z) e^{i(k+mn)\kappa x_0} \right)}_{\mathbf{w}_{R,k}^{\mathcal{R}}(x_0, y, z)} \zeta^{kj} = \sum_{k=k_{\min}}^{k_{\max}} \mathbf{w}_{R,k}^{\mathcal{R}}(x_0, y, z) \zeta^{kj} \end{aligned} \quad (6.4.56)$$

Here, each vector $\mathbf{w}_{R|k+mn}(y, z) e^{i(k+mn)\kappa x_0}$ is described by a modal synthesis of the following form:

$$\mathbf{w}_{R|k+mn}(y, z) = \sum_{I=1}^{N_R} \mathbf{W}_{R|k+mn, I}(y, z) \mathbf{q}_{R|k+mn, I} \quad (6.4.57)$$

Here, $\mathbf{W}_{R|k+mn, I}(y, z)$ are the eigenmodes of the finite element model of the rail according to (6.2.17).

6.4.2 Sleepers

As described in section the kinematics of the sleeper is described by the vector $\mathbf{q}_S(t)$ which contains the degrees of freedom of the sleeper. By applying the formulation of the kinematics as a discrete Fourier series the vector $\mathbf{q}_S^{(j)}(t)$ which describes the motions of the j -th sleeper is expressed in the following way:

$$\mathbf{q}_S^{(j)}(t) = \sum_{k=k_{\min}}^{k_{\max}} \mathbf{q}_{S|k}(t) \zeta^{kj} \quad (6.4.58)$$

Based on this, the inertia terms for the sleeper and the inertia and damping terms of the underground can be formulated since these terms are governed only by the motions of the sleeper. By inserting the Fourier series for the displacement vector $\mathbf{q}_S^{(j)}$, for the velocity vector $\dot{\mathbf{q}}_S^{(j)}$ and for the acceleration vector $\ddot{\mathbf{q}}_S^{(j)}$ it is obtained:

$$\begin{aligned} &\sum_{j=0}^{n-1} \delta' \dot{\mathbf{q}}_S^{(j)T} \left(\mathbf{M}_S \ddot{\mathbf{q}}_S^{(j)} + \mathbf{D}_U \dot{\mathbf{q}}_S^{(j)} + \mathbf{K}_U \mathbf{q}_S^{(j)} \right) \\ &= \sum_{j=0}^{n-1} \left(\sum_{k=k_{\min}}^{k_{\max}} \delta' \dot{\mathbf{q}}_{S|k}^H \zeta^{-kj} \right) \left(\sum_{l=k_{\min}}^{k_{\max}} (\mathbf{M}_S \ddot{\mathbf{q}}_{S|l} + \mathbf{D}_U \dot{\mathbf{q}}_{S|l} + \mathbf{K}_U \mathbf{q}_{S|l}) \zeta^{lj} \right) \\ &= \sum_{j=0}^{n-1} \sum_{k=k_{\min}}^{k_{\max}} \sum_{l=k_{\min}}^{k_{\max}} \delta' \dot{\mathbf{q}}_{S|k}^H (\mathbf{M}_S \ddot{\mathbf{q}}_{S|l} + \mathbf{D}_U \dot{\mathbf{q}}_{S|l} + \mathbf{K}_U \mathbf{q}_{S|l}) \zeta^{(-k+l)j} \\ &= \sum_{k=k_{\min}}^{k_{\max}} \sum_{l=k_{\min}}^{k_{\max}} \left(\delta' \dot{\mathbf{q}}_{S|k}^H (\mathbf{M}_S \ddot{\mathbf{q}}_{S|l} + \mathbf{D}_U \dot{\mathbf{q}}_{S|l} + \mathbf{K}_U \mathbf{q}_{S|l}) \left(\sum_{j=0}^{n-1} \zeta^{(-k+l)j} \right) \right) \end{aligned} \quad (6.4.59)$$

The expression is evaluated based on the relation (3.1.70), which has been developed in the section 3.1.2:

$$k_{\min} \leq k \leq k_{\max} \wedge k_{\min} \leq l \leq k_{\max} : \sum_{j=0}^{n-1} \zeta_5^{(-k+l)j} = \begin{cases} 0 & \text{for } k \neq l \\ n & \text{for } k = l \end{cases} \quad (6.4.60)$$

Thereby, the following result is obtained:

$$\sum_{j=0}^{n-1} \delta' \dot{\mathbf{q}}_S^{(j)T} \left(\mathbf{M}_S \ddot{\mathbf{q}}_S^{(j)} + \mathbf{D}_U \dot{\mathbf{q}}_S^{(j)} + \mathbf{K}_U \mathbf{q}_S^{(j)} \right) = \sum_{k=k_{\min}}^{k_{\max}} n \delta' \dot{\mathbf{q}}_{S|k}^H \left(\mathbf{M}_S \ddot{\mathbf{q}}_{S|l} + \mathbf{D}_U \dot{\mathbf{q}}_{S|l} + \mathbf{K}_U \mathbf{q}_{S|l} \right) \quad (6.4.61)$$

It can clearly be seen that the terms for different periodicities k are decoupled. In the present case the

6.4.3 Modelling of the pads

In a real track, pads, which consist of a comparatively soft material like polymers, are located in the fastening system between the rail foot and the rail seat of the sleeper; they enable relative motions between the rails and the sleepers to reduce dynamic forces. In the present track model, the a pad is modelled by distributed discrete linear visco-elastic elements. These elements are acting between the rail seat of the sleeper and the bottom surface of the rail. Due to the refined rail model, modeling the pad by distributed elements appear to be more appropriate then modeling it by just one compact force element.

In order to determine the forces acting between the rail and the sleeper the kinematics of the points between the discrete visco-elastic elements representing the pads act. Here, the points P_I at the n pads form an n -tuple of corresponding points. The pad acts at the bottom surface of the rail. This surface is a horizontal plane, which is defined by $z^{\mathcal{R}} = z_{\text{RP}}$. Based on the discrete Fourier series (6.4.56), the displacement of the rail for the j -th pad is given by:

$$\begin{aligned} \mathbf{w}_{\text{RPI}}^{(j)} &\equiv \mathbf{w}^{\mathcal{R}}(j \cdot \Delta s_S + x_I, y_I, z_{\text{RP}}) = \sum_{K=-\infty}^{\infty} \mathbf{w}_{\text{R}|K}(y_I, z_{\text{RP}}) e^{iK\kappa(j \cdot \Delta s_S + x_I)} \\ &= \sum_{k=k_{\min}}^{k_{\max}} \underbrace{\left(\sum_{m=-\infty}^{\infty} \mathbf{w}_{\text{R}|k+mn}(y_I, z_{\text{RP}}) e^{i(k+mn)\kappa x_I} \right)}_{\mathbf{w}_{\text{RPI},k}} \zeta^{kj} = \sum_{k=k_{\min}}^{k_{\max}} \mathbf{w}_{\text{RPI},k} \zeta^{kj} \end{aligned} \quad (6.4.62)$$

In the section 6.3.4 the kinematics of the sleeper at the railseat has been considered. As a result it has been obtained:

$$\mathbf{w}_{\text{SPI}} \equiv \mathbf{w}_{\text{P}}^{\mathcal{R}}(\mathbf{x}_I^S) = \mathbf{S}^{\mathcal{R}I} \mathbf{w}_{\text{P}}^I(\mathbf{x}_I^S) = \underbrace{\mathbf{S}_1(-\phi_{\text{R}})}_{\mathbf{C}_{\text{SPI}}} \mathbf{C}_{\text{S}}^I(\mathbf{x}_I^S) \mathbf{q}_{\text{S}}(t) = \mathbf{C}_{\text{SPI}} \mathbf{q}_{\text{S}}(t) \quad (6.4.63)$$

By inserting the discrete Fourier series according to (6.4.58) the displacement at the j -th pad is formulated in the following way:

$$\mathbf{w}_{\text{SPI}}^{(j)} = \mathbf{C}_{\text{SPI}} \mathbf{q}_{\text{S}}^{(j)}(t) = \sum_{k=k_{\min}}^{k_{\max}} \mathbf{C}_{\text{SPI}} \mathbf{q}_{\text{S}|k}(t) \zeta^{kj} \quad (6.4.64)$$

Based on this, the relative motion between the two points is given by:

$$\mathbf{w}_{PI}^{(j)} = \mathbf{w}_{SPI}^{(j)} - \mathbf{w}_{RPI}^{(j)} = \sum_{k=k_{\min}}^{k_{\max}} (\mathbf{C}_{SPI} \mathbf{q}_{S|k} - \mathbf{w}_{RPI,k}) \zeta^{kj} = \sum_{k=k_{\min}}^{k_{\max}} \mathbf{w}_{PI|k} \zeta^{kj} \quad (6.4.65)$$

As already mentioned, the pads is modelled by distributed linear visco-elastic force elements. The force acting at the I -th point in the j -th pad is given by:

$$\mathbf{f}_{PI}^{(j)} = \mathbf{K}_{PI} \mathbf{w}_{PI}^{(j)} + \mathbf{D}_{PI} \dot{\mathbf{w}}_{PI}^{(j)} \quad (6.4.66)$$

Here, the matrices of the force element are given by:

$$\mathbf{K}_{PI} = \begin{bmatrix} c_{Px} & 0 & 0 \\ 0 & c_{Py} & 0 \\ 0 & 0 & c_{Pz} \end{bmatrix}, \quad \mathbf{D}_{PI} = \begin{bmatrix} b_{Px} & 0 & 0 \\ 0 & b_{Py} & 0 \\ 0 & 0 & b_{Pz} \end{bmatrix} \quad (6.4.67)$$

The virtual power of the force element is determined to:

$$\delta' P_{PI}^{(j)} = \delta' \dot{\mathbf{w}}_{PI}^{(j)T} \mathbf{f}_{PI}^{(j)} = \delta' \dot{\mathbf{w}}_{PI}^{(j)T} \mathbf{K}_{PI} \mathbf{w}_{PI}^{(j)} + \delta' \dot{\mathbf{w}}_{PI}^{(j)T} \mathbf{D}_{PI} \dot{\mathbf{w}}_{PI}^{(j)} \quad (6.4.68)$$

For the n -tuple of the corresponding force elements it is obtained:

$$P_{PI} = \sum_{j=0}^{n-1} \delta' P_{PI}^{(j)} = \sum_{j=0}^{n-1} \left(\delta' \dot{\mathbf{w}}_{PI}^{(j)T} \mathbf{K}_{PI} \mathbf{w}_{PI}^{(j)} + \delta' \dot{\mathbf{w}}_{PI}^{(j)T} \mathbf{D}_{PI} \dot{\mathbf{w}}_{PI}^{(j)} \right) \quad (6.4.69)$$

Also here, it is assumed that the virtual deformation velocity $\delta' \dot{\mathbf{w}}_{PI}^{(j)}$ is a real vector so that the transpose is equal to the Hermitian transpose. By applying the transformation derived in the section 3.2 it is obtained:

$$\delta' P_{PI} = \sum_{j=0}^{n-1} \left(\delta' \dot{\mathbf{w}}_{PI}^{(j)H} \mathbf{K}_{PI} \mathbf{w}_{PI}^{(j)} + \delta' \dot{\mathbf{w}}_{PI}^{(j)H} \mathbf{D}_{PI} \dot{\mathbf{w}}_{PI}^{(j)} \right) = n \sum_{k=k_{\min}}^{k_{\max}} \delta' \dot{\mathbf{w}}_{PI|k}^H (\mathbf{K}_{PI} \mathbf{w}_{PI|k} + \mathbf{D}_{PI} \dot{\mathbf{w}}_{PI|k}) \quad (6.4.70)$$

Since the pad is resolved into distributed visco-elastic elements, the virtual power $\delta' P_{PI}$ has to be summed up over all individual elements.

6.4.4 Equations of motion

Based on the models for the individual components, which have been shown in the previous sections, the homogenous equation of motion for the track model can now be formulated in the following way:

$$\mathbf{0} = n \begin{bmatrix} \mathbf{M}_R & \mathbf{0} & \mathbf{0} \\ \mathbf{0} & \mathbf{M}_R & \mathbf{0} \\ \mathbf{0} & \mathbf{0} & \mathbf{M}_S \end{bmatrix} \begin{bmatrix} \ddot{\mathbf{q}}_{Rr|[k]} \\ \ddot{\mathbf{q}}_{Rl|[k]} \\ \ddot{\mathbf{q}}_{S|k} \end{bmatrix} + n \begin{bmatrix} \mathbf{D}_{P|RR,[k]} & \mathbf{0} & \mathbf{D}_{P|RSr,[k]} \\ \mathbf{0} & \mathbf{D}_{P|RR,[k]} & \mathbf{D}_{P|RSl,[k]} \\ \mathbf{D}_{P|RSr,[k]}^T & \mathbf{D}_{P|RSl,[k]}^T & \mathbf{D}_{P|Sr} + \mathbf{D}_{P|Sl} + \mathbf{D}_U \end{bmatrix} \begin{bmatrix} \dot{\mathbf{q}}_{Rr|[k]} \\ \dot{\mathbf{q}}_{Rl|[k]} \\ \dot{\mathbf{q}}_{S|[k]} \end{bmatrix} \\ + n \begin{bmatrix} \mathbf{K}_{R,[k]} + \mathbf{K}_{P|RR,[k]} & \mathbf{0} & \mathbf{K}_{P|RSr,[k]} \\ \mathbf{0} & \mathbf{K}_{R,[k]} + \mathbf{K}_{P|RR,[k]} & \mathbf{K}_{P|RSl,[k]} \\ \mathbf{K}_{P|RSr,[k]}^T & \mathbf{K}_{P|RSl,[k]}^T & \mathbf{K}_{P|Sr} + \mathbf{K}_{P|Sl} + \mathbf{K}_U \end{bmatrix} \begin{bmatrix} \mathbf{q}_{Rr|[k]} \\ \mathbf{q}_{Rl|[k]} \\ \mathbf{q}_{S|[k]} \end{bmatrix} \quad (6.4.71)$$

Here, the vector $\mathbf{q}_{S|k}$ describes the motion of the sleeper as introduced in (6.4.58). The matrices \mathbf{M}_S , \mathbf{D}_U and \mathbf{K}_U denote the inertia of the sleeper and the damping and the stiffness of the underground; as it can be seen from (6.4.61) the matrices are equal for each periodicity k .

The vectors $\mathbf{q}_{Rr|k}$ and $\mathbf{q}_{Rl|k}$ contain the modal coordinates for the right and for the left rail, respectively. Each vector $\mathbf{q}_{Ri|k}$, $i = r, l$ is composed of subvectors in the following way:

$$\mathbf{q}_{Ri|[k]} = \begin{bmatrix} \vdots \\ \mathbf{q}_{Ri|k-2n} \\ \mathbf{q}_{Ri|k-n} \\ \mathbf{q}_{Ri|k} \\ \mathbf{q}_{Ri|k+n} \\ \mathbf{q}_{Ri|k+2n} \\ \vdots \end{bmatrix} \quad (6.4.72)$$

Each subvector $\mathbf{q}_{Rr|K}$ contains the modal coordinates for the shape functions of the rail having the periodicity $K = k + mn$. The matrices \mathbf{M}_R and $\mathbf{K}_{R|[k]}$ contain the modal masses and the modal stiffnesses of the rail; as it has been derived in the section 4.2, the mass matrix of the prism elements does not depend on the periodicity K so no index is required. As it can be seen from (6.2.17), the equation contains the factor ℓ , whereby it is valid for the track length $\ell = n \cdot \Delta s$; thereby, the number of segments n can be factored out. The matrices $\mathbf{D}_{P\dots}$ and $\mathbf{K}_{P\dots}$ represent the forces of the pads. The displacements at the rail foot, where the pads act, depend on the shape functions and thereby on the periodicity K .

For each basic periodicity k shape functions having the periodicities $K = k + mn$ are used for the rails. Although the shape functions for the rails are decoupled for different periodicities $K \neq L$, an interaction occurs due to the coupling by the discrete support. Thereby, for each eigenvector of the entire track the deformation field \mathbf{w}_T of the rails contains several periodicities:

$$\mathbf{w}_{TI}(x, y, z) = \sum_{m=m_{I,\min}}^{m_{I,\max}} \mathbf{w}_{TI,m}(y, z) e^{i k_I + m n \kappa x} \quad (6.4.73)$$

6.5 Influence of the length of the track model

The length ℓ_T of the track is related to the number of sleepers n_{S1} , whereas one sleeper bay has a length of $\Delta s = 0.6$ m. The track length can be varied in a particularly simple way if powers of 2 are used for the number of sleepers. In the present case the following numbers n are used:

- $n = 16 \Rightarrow \ell_T = n \cdot \Delta s = 9.6$ m
- $n = 32 \Rightarrow \ell_T = n \cdot \Delta s = 19.2$ m
- $n = 64 \Rightarrow \ell_T = n \cdot \Delta s = 38.4$ m
- $n = 128 \Rightarrow \ell_T = n \cdot \Delta s = 76.8$ m

In Fig.6.5.8 und Fig.6.5.9 the frequency response functions for a symmetric excitation by vertical forces above one sleeper and in the middle of a sleeper bay, respectively, are displayed.

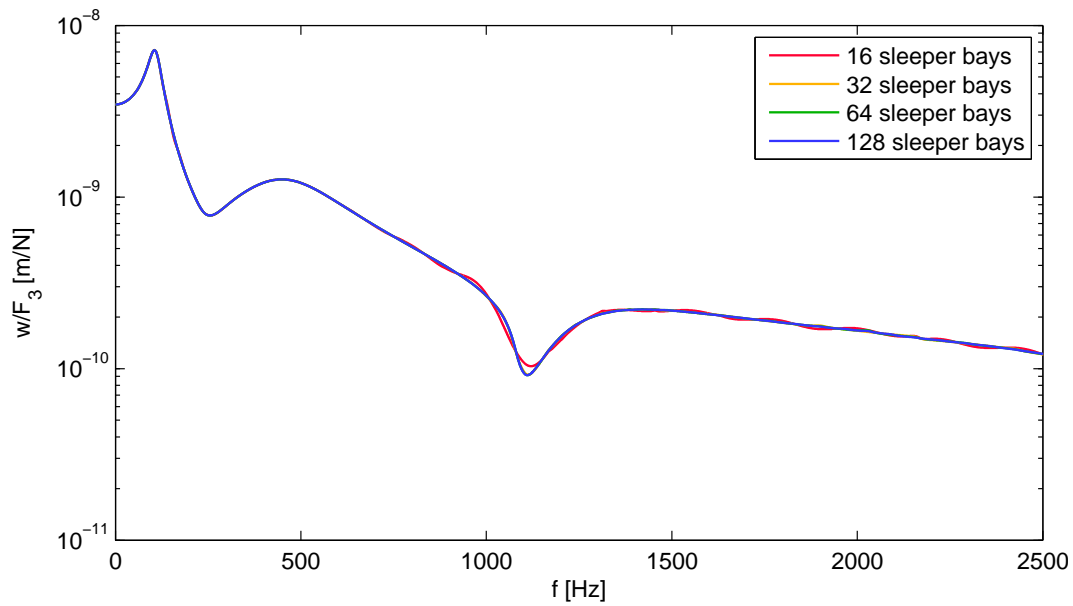


Figure 6.5.8: Frequency response of the track model for a symmetric excitation by vertical forces above one sleeper

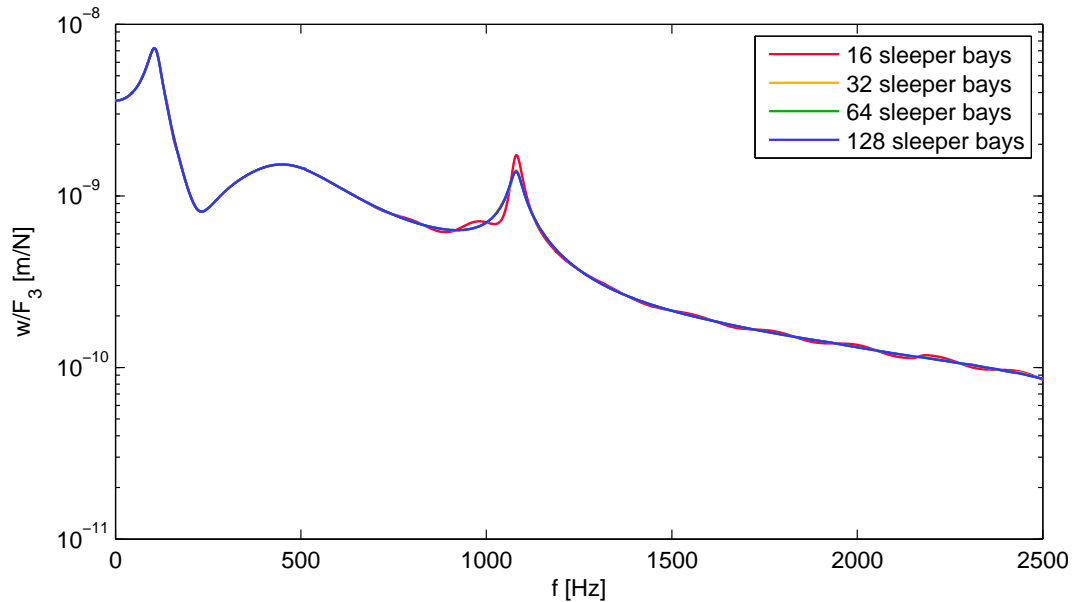


Figure 6.5.9: Frequency response of the track model for a symmetric excitation by vertical forces in the middle of a sleeper bay

The curves for $n = 32$ and $n = 64$ are hardly visible, since both curves are lying under the curve for $n = 128$; in other words, the curves for $n = 32$, $n = 64$, and $n = 128$ are nearly equal. In contrast to this, the curve for $n = 16$ shows distinct deviations from the aforementioned curves. The strongest deviation occurs at the peak at approx. 1100 Hz for the excitation in the middle of the sleeper bay shown in Fig.6.5.9; further deviations can be seen in the frequency range between 700 Hz and 3000 Hz. The yellow and the green curve representing the result for $n = 32$ and $n = 64$ are nearly completely covered by the blue line indicating the result for $n = 128$. This means that doubling the number of sleepers from $n = 32$ to $n = 64$ and again to $n = 128$ hardly causes any change of the curve so that a number of $n = 32$ seems to be sufficient.

For a better overview on the dynamic behaviour the frequency response functions obtained for the two different positions of the excitation forces are compared in Fig.6.5.10; for both calculation the

track model possessing $n = 128$ sleeper bays is used. Below 200 Hz the position of the excitation

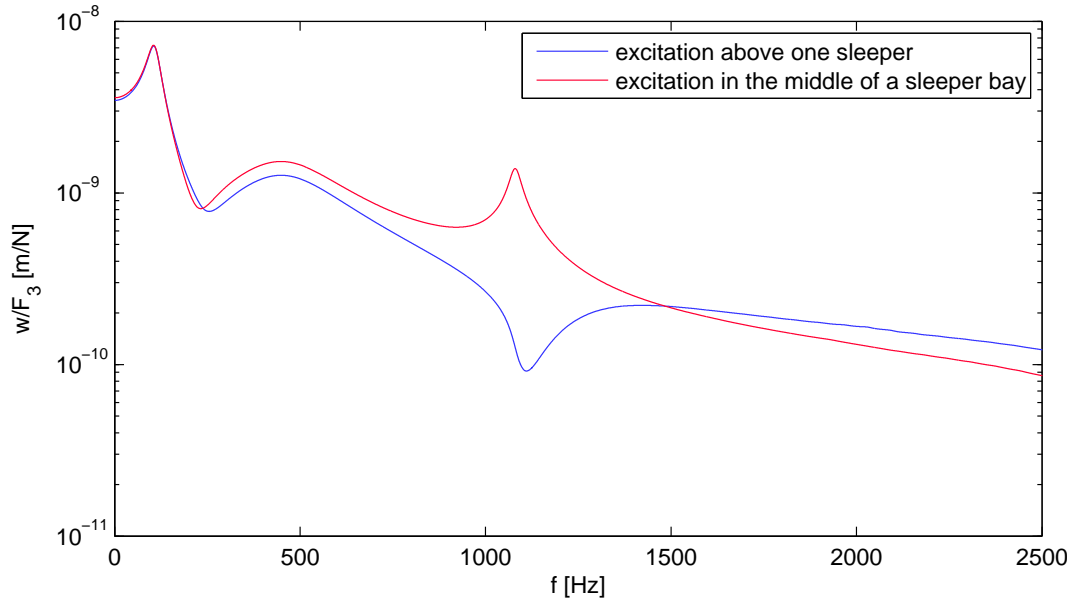


Figure 6.5.10: Frequency response of the track model for a symmetric excitation by vertical forces above one sleeper and in the middle of a sleeper bay; $n = 128$ sleeper bays

forces hardly affects the frequency response. In contrast to this, strong differences can be seen especially in the range around 1100 Hz: For the excitation above the sleeper a minimum occurs, while the excitation in the middle of the sleeper bay leads to a maximum.

The frequency responses for an antimetric excitation by lateral forces are displayed in Fig.6.5.11 and Fig.6.5.12; also here, the two cases of an excitation above one sleeper and in the middle of a sleeper bay are considered.

Below 140 Hz the curves are nearly lying above each other so that the deviations between the curves are very small. However, above this frequency strong differences between the curves occur. In the range between 140 Hz and 1500 Hz the red curve obtained for $n = 16$ shows a series of distinct peaks; these peaks have a nearly equidistant distribution over the frequency. If the number of sleeper bays is doubled to $n = 32$ the peaks become smaller, while new peaks occur in the middle between the peaks for $n = 16$, i.e. at the location of the minima. By further doubling the number of sleeper bays to $n = 64$ and $n = 128$, this effect again occurs so that the curves become smoother with an increasing number of sleeper bays n .

This behaviour can be explained with the finiteness of the structure. For an infinite structure the waves are propagating along the structure without being reflected, since the structure has no boundaries causing a reflection; this effect is also known as “geometric damping.” In contrast to this, for a finite structure standing waves or stationary waves occur; these standing waves cause the maxima. Nevertheless the waves become weaker while propagating through the track because of the damping. In order to approximate the behaviour of an infinite structure by using a finite one, the finite structure has to be long enough so that the waves returning to the point of observation of the finite structure have been weakened enough to neglect their influence.

In Fig.6.5.13 the frequency response functions obtained for $n = 128$ sleeper bays and for the two different positions of the excitation forces are compared in order to investigate the influence of the position. Also in this case, the position of the excitation force has hardly an influence on the frequency response for low frequencies, here below 200 Hz. Moreover, also here a force acting in

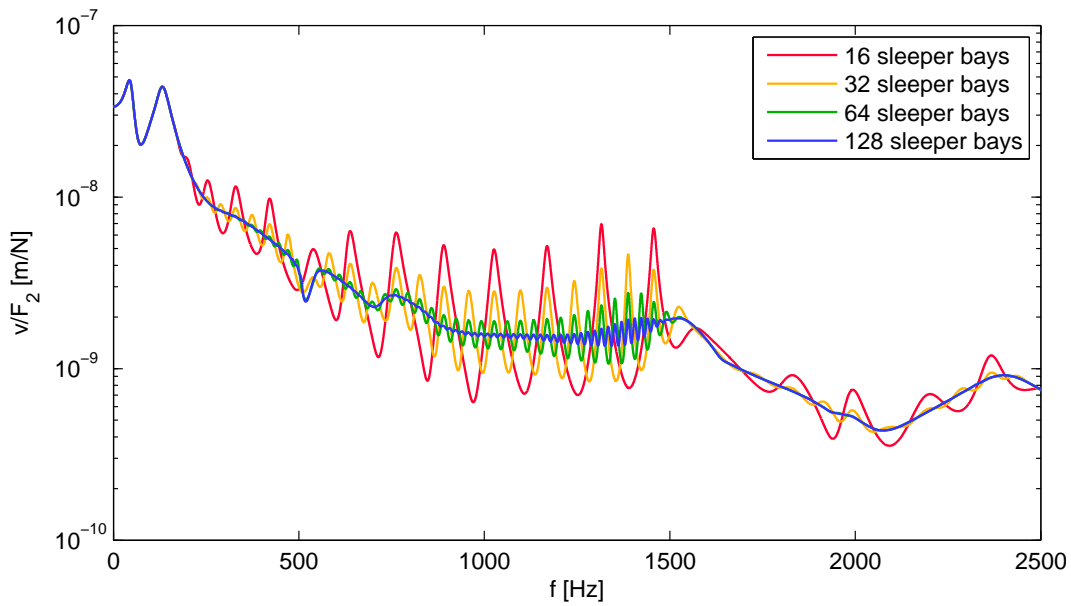


Figure 6.5.11: Frequency response of the track model for an antimetric excitation by lateral forces above one sleeper

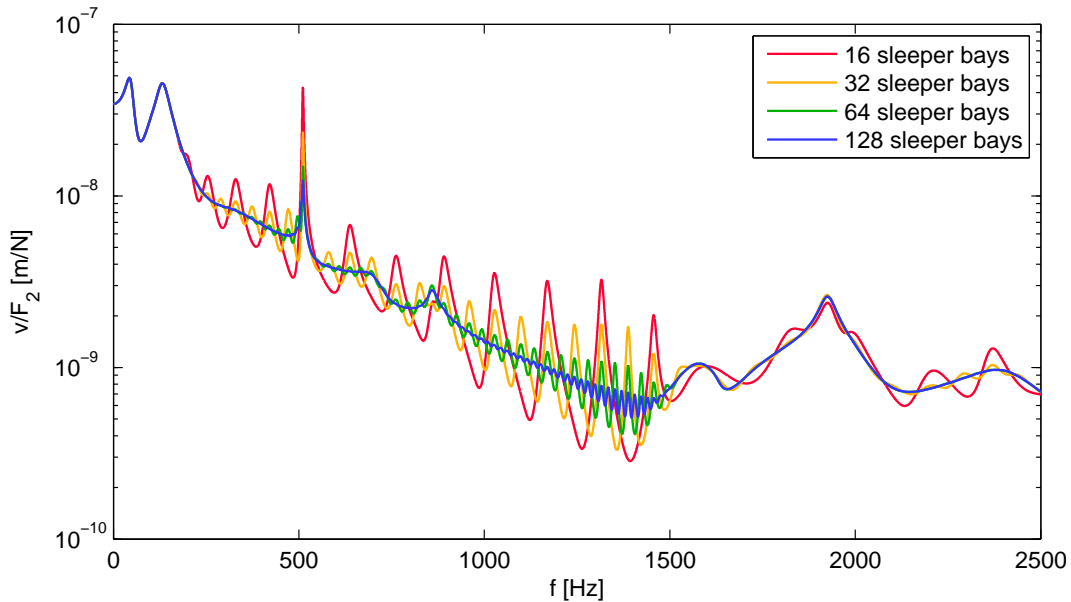


Figure 6.5.12: Frequency response of the track model for a symmetric excitation by lateral forces in the middle of a sleeper bay

the middle of a sleeper bay causes an excitation of a pinned-pinned mode; this leads to the peak at 500 Hz of the curve for the excitation in the middle of the sleeper bay.

By comparing the results obtained for vertical and lateral excitation, it turns out that the frequency response for lateral excitation is more sensitive to the number of sleeper bays than the one for vertical excitation: For the vertical excitation the curve for $n = 16$ sleepers has a slightly wavy shape resulting from the finiteness of the structure; this “waviness” already vanishes nearly completely for $n = 32$ sleeper bays. The curves for $n = 64$, $n = 64$, and $n = 128$ hardly differ from each other. Thus, for this excitation a track model having $n = 32$ can be considered as a quite good approximation for an infinite track model; in other words, in this case the convergence behaviour is good. For a lateral excitation, however, the convergence behaviour is worse. Even for $n = 64$ sleeper bays a wavy shape of the frequency response can be seen above 400 Hz. Only for $n = 128$

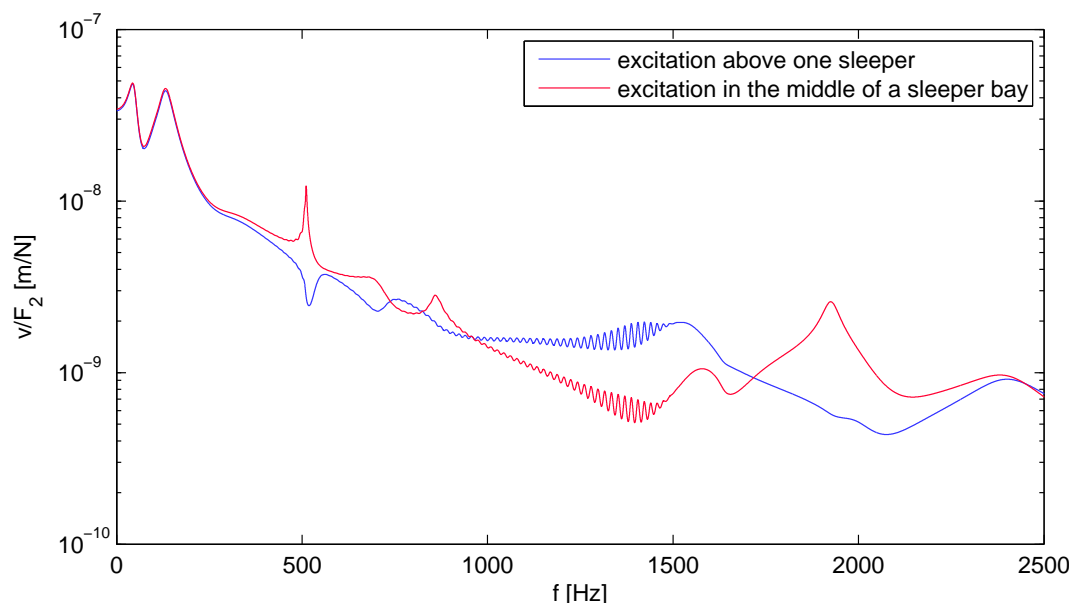


Figure 6.5.13: Frequency response of the track model for an antimetric excitation by lateral forces above one sleeper and in the middle of a sleeper bay; $n = 128$ sleeper bays

a nearly smooth curve is obtained for the frequency response is obtained up to approx. 800 Hz; above this frequency, the curve again becomes wavy and shows peaks resulting from the finiteness of the structure.

Apparently, the lateral motions of the rail head are distinctly less damped than the vertical motions. Regarding vertical motions the cross section of the rail is very stiff so that for vertical motions of the rail head also vertical motions of the rail foot occur. Thereby, the pads and for low frequencies also the underground layer are compressed and stretched; this causes a considerable damping, since the pads and the underground layer are the damping components of the track. For lateral excitations the cross section of the rail can perform a combination of lateral translations and rotations around the rail's longitudinal axis. If the resulting instant centre of rotation is located near the rail foot, the rail pads are only slightly deformed so that only a weak damping occurs. Furthermore, the web of the rail is comparatively thin so that relative rotations between the rail head and the rail foot can be expected. Thereby, the motions of the rail foot are lower so that the damping effect of the pads connected to the rail foot is weaker.

Chapter 7

Modelling of the wheel-rail contact

In reality the wheel-rail contact is a limited area, in which normal and tangential stresses act between the surfaces of the wheel and the rail. The area of the wheel-rail contact is usually a few square centimeters large, i.e. it is quite small compared to the main dimensions of the wheelset and the rail. The wheel-rail contact is moving around the wheel due to the wheel's overturning motion and along the rail due to the running of the vehicle. Furthermore, the wheel-rail contact is moving laterally on the running surfaces of wheel and rail due to the contact geometry.

The stresses acting in the wheel-rail contact are related to the deformations of wheel and rail in the contact zone. It is, however, sensible and advantageous to treat the “local deformations” in the contact zone separately from the “global deformations” of the structural dynamics, because for these two problems different aspects are important. Simply spoken, it could be said that the analysis of the structural flexibility and dynamics considers the entire structure, whereas small changes of the geometry hardly affect the result, e.g. the eigenfrequency of the structure, while the contact mechanics is focused on a small region of the structure, where a highly precise description of the geometry is required.

An example may illustrate the impact of local deviations of the geometry on the results: In the standard EN 13674-1 the rail profiles 60E1 and 60E2 are defined. The only difference between these two profiles is the profile of the rail head. The standard also contains the area A , the mass per length ρA and the moments of inertia I_{xx} and I_{yy} for the cross section. According to the Euler-Bernoulli beam theory, the first bending eigenfrequency for a beam, which is supported at both ends as shown in Fig.7.0.1, is given by:

$$f = \frac{\pi}{2} \sqrt{\frac{EI}{\rho AL^4}} \quad (7.0.1)$$

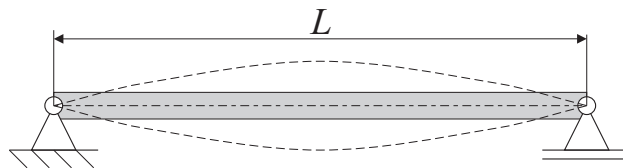


Figure 7.0.1: Supported beam; dashed lines: First bending eigenmode

The Euler-Bernoulli beam theory is valid for slender beams, i.e. the length of the beam is at least ten times the dimension of the cross section. Both profiles have a height of 170 mm and a width of 150 mm. Therefore, the length is set to $L = 2$ m in the following example. For Young's modulus

E of steel the value $E = 210$ MPa is used. In Tab. 7.0.1 the geometries of the two profiles and the bending eigenfrequencies of a rail having one of the two profiles are listed.

Profile	60E1	60E2
Cross sectional area A	76.70 mm ²	76.48 mm ²
Mass per length ρA	60.21 kg/m	60.03 kg/m
Moment of inertia I_{xx}	3038.3 cm ⁴	3021.5 cm ⁴
$f_{xx} = \frac{\pi}{2} \sqrt{\frac{EI_{xx}}{\rho AL^4}}$	127.8352268 Hz	127.6722937 Hz
Moment of inertia I_{yy}	512.3 cm ⁴	510.5 cm ⁴
$f_{yy} = \frac{\pi}{2} \sqrt{\frac{EI_{yy}}{\rho AL^4}}$	52.49251697 Hz	52.47872013 Hz

Table 7.0.1: Comparison of the geometry and the structural dynamics for a rail having the profiles 60E1 or 60E2 according to EN 13674-1; $L = 2$ m; $E = 210$ MPa

Using the mean value as the reference value the relative differences between the corresponding frequencies are $\frac{2|f_{xx,60E1} - f_{xx,60E2}|}{f_{xx,60E1} + f_{xx,60E2}} = 0.001275$ and $\frac{2|f_{yy,60E1} - f_{yy,60E2}|}{f_{yy,60E1} + f_{yy,60E2}} = 0.000263$. Here, it becomes evident that the impact of the difference between the two geometries on the structural dynamics is negligible. It can therefore be expected that, if all other parameters like the mass of the sleepers or the stiffnesses of the pads are unchanged, the dynamical behaviour of a track is nearly the same, if rails of the type 60E1 or of the type 60E2 are used. It can also be expected that the structural eigenfrequencies of a wheelset hardly change if a different profile is applied on the wheels.

The impact on the contact, however, is strong. In Fig.7.0.2 the pressure distribution is shown for the centred position of a wheelset.

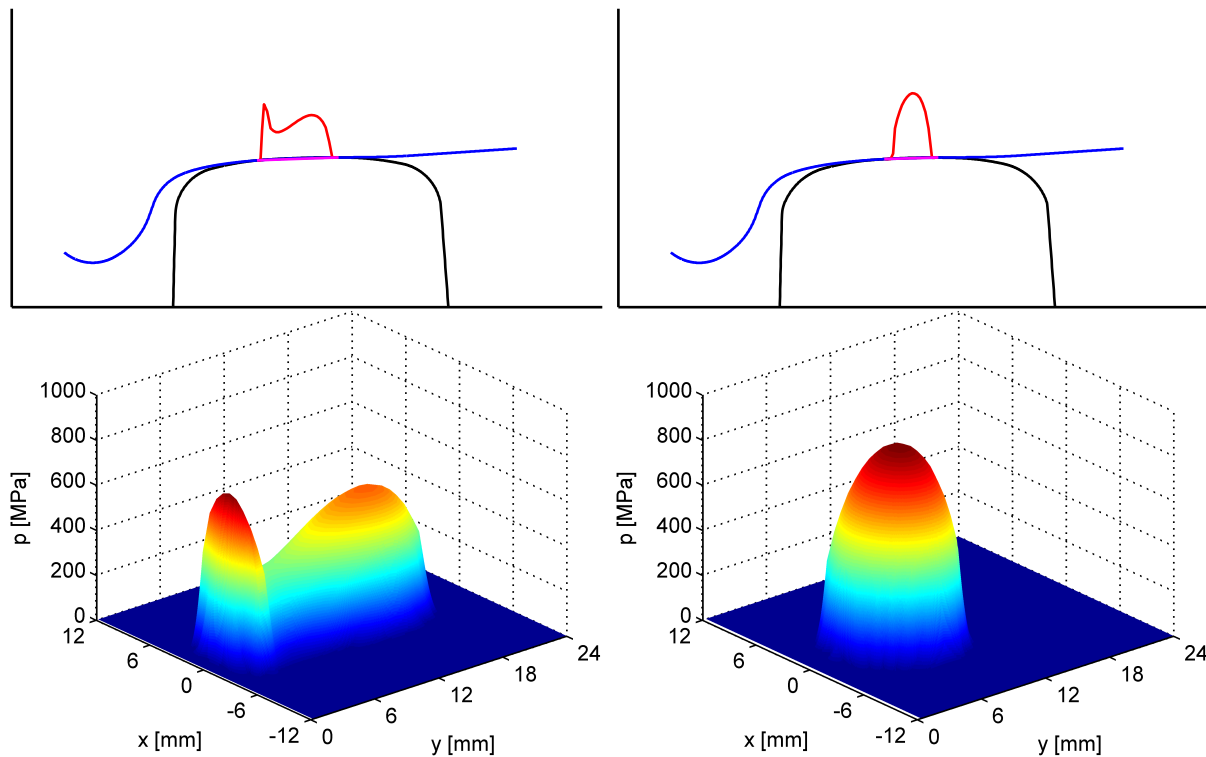


Figure 7.0.2: Pressure distribution in the wheel-rail contact for the centred position of the wheelset; left: rail profile 60E1; right: rail profile 60E2. Wheel profile: S1002; cant 1:40

The different shapes of the profiles cause a different pressure distribution; the results will be discussed in detail in section 8.1. Nevertheless, the comparison of the results for the structural dynamics on the one hand and for the contact mechanics on the other hand shows that a separate treatment of these two problems is sensible.

In this chapter, a wheel-rail contact model will be developed. The analysis of the contact geometry is mainly based on the work by Netter [48]; the basics for the contact mechanics and for the formulation of the contact problem follows the fundamental book by Kalker [26].

7.1 Kinematics

In the reference frame \mathcal{R} , the deformation is expressed by a field $\mathbf{w}^{\mathcal{R}}(\mathbf{x}^{\mathcal{R}}, t)$. If the reference position of the marker is indicated by the vector $\mathbf{x}_M^{\mathcal{R}}$, then the absolute position of the marker is given by

$$\mathbf{r}_{OM}^I = \mathbf{r}_{OR}^I + \mathbf{S}^{I\mathcal{R}} \left(\mathbf{x}_M^{\mathcal{R}} + \mathbf{w}^{\mathcal{R}}(\mathbf{x}_M^{\mathcal{R}}, t) \right) \quad (7.1.2)$$

Therefore, the determination of the kinematics for the translational motion of the marker doesn't pose a problem. For the rotational motions, however, the determination of the kinematics is less evident, in particular for a three-dimensional continuum, while for some other modelling concepts like beams angles describing rotations are used.

One possibility to determine a rotation for a three-dimensional continuum is based on the consideration of the deformation gradient. The following consideration is a very brief comprehension of the formulation given by Schiehlen and Eberhardt. The gradient \mathbf{F} is given by:

$$\mathbf{x}^{\mathcal{R}} = \begin{bmatrix} x \\ y \\ z \end{bmatrix}, \quad \mathbf{w}^{\mathcal{R}} = \begin{bmatrix} u(x, y, z) \\ v(x, y, z) \\ w(x, y, z) \end{bmatrix}, \quad \mathbf{F} = \begin{bmatrix} 1 + \frac{\partial u}{\partial x} & \frac{\partial u}{\partial y} & \frac{\partial u}{\partial z} \\ \frac{\partial v}{\partial x} & 1 + \frac{\partial v}{\partial y} & \frac{\partial v}{\partial z} \\ \frac{\partial w}{\partial x} & \frac{\partial w}{\partial y} & 1 + \frac{\partial w}{\partial z} \end{bmatrix} \quad (7.1.3)$$

The deformation gradient can be expressed as a product of a rotation tensor \mathbf{S} and a stretch tensor. Here, two formulations are possible:

$$\mathbf{F} = \mathbf{S}\mathbf{U} = \mathbf{V}\mathbf{S} \quad (7.1.4)$$

Here, the rotation tensor \mathbf{S} is an orthogonal matrix, i.e. $\mathbf{S}^T = \mathbf{S}^{-1}$, while the stretch tensors \mathbf{U} and \mathbf{V} are symmetric matrices, i.e. $\mathbf{U} = \mathbf{U}^T$ and $\mathbf{V} = \mathbf{V}^T$. For small deformations the rotation tensor \mathbf{S} can be approximated by the sum of the identity matrix \mathbf{I} and the skew-symmetric part of the deformation gradient \mathbf{F} :

$$\mathbf{S} \approx \mathbf{I} + \frac{1}{2}(\mathbf{F} - \mathbf{F}^T) = \begin{bmatrix} 1 & \frac{1}{2}\left(\frac{\partial u}{\partial y} - \frac{\partial v}{\partial x}\right) & \frac{1}{2}\left(\frac{\partial u}{\partial z} - \frac{\partial w}{\partial x}\right) \\ \frac{1}{2}\left(\frac{\partial v}{\partial x} - \frac{\partial u}{\partial y}\right) & 1 & \frac{1}{2}\left(\frac{\partial v}{\partial z} - \frac{\partial w}{\partial y}\right) \\ \frac{1}{2}\left(\frac{\partial w}{\partial x} - \frac{\partial u}{\partial z}\right) & \frac{1}{2}\left(\frac{\partial w}{\partial y} - \frac{\partial v}{\partial z}\right) & 1 \end{bmatrix} = \begin{bmatrix} 1 & -\gamma & \beta \\ \gamma & 1 & -\alpha \\ -\beta & \alpha & 1 \end{bmatrix} \quad (7.1.5)$$

For the tensor of the angular velocity \mathbf{W} it is valid:

$$\mathbf{W} = \dot{\mathbf{S}}\mathbf{S}^T \quad (7.1.6)$$

By using the approximation according to (7.1.5) it is obtained for small deformations:

$$\dot{\mathbf{S}}\mathbf{S}^T \approx \begin{bmatrix} 0 & -\dot{\gamma} & \dot{\beta} \\ \dot{\gamma} & 0 & -\dot{\alpha} \\ -\dot{\beta} & \dot{\alpha} & 0 \end{bmatrix} \begin{bmatrix} 1 & \gamma & -\beta \\ -\gamma & 1 & \alpha \\ \beta & -\alpha & 1 \end{bmatrix} = \begin{bmatrix} 0 & -\dot{\gamma} & \dot{\beta} \\ \dot{\gamma} & 0 & -\dot{\alpha} \\ -\dot{\beta} & \dot{\alpha} & 0 \end{bmatrix} + \begin{bmatrix} \dot{\gamma}\gamma + \dot{\beta}\beta & -\dot{\beta}\alpha & -\dot{\gamma}\alpha \\ -\dot{\alpha}\beta & \dot{\gamma}\gamma + \dot{\alpha}\alpha & -\dot{\gamma}\beta \\ -\dot{\alpha}\gamma & -\dot{\beta}\gamma & \dot{\beta}\beta + \dot{\alpha}\alpha \end{bmatrix} \quad (7.1.7)$$

By assuming that the angles are small, i.e. $\alpha \ll 1$, $\beta \ll 1$ and $\gamma \ll 1$, the coefficients of the second matrix are much less than those of the first one and can therefore be neglected. Thereby, the tensor \mathbf{W} of the angular velocity is approximated in the following way:

$$\mathbf{W} = \dot{\mathbf{S}}\mathbf{S}^T \approx \begin{bmatrix} 0 & -\dot{\gamma} & \dot{\beta} \\ \dot{\gamma} & 0 & -\dot{\alpha} \\ -\dot{\beta} & \dot{\alpha} & 0 \end{bmatrix} \quad (7.1.8)$$

The rotation tensor is described by a skew-symmetric matrix of the order 3×3 . Here, the multiplication of \mathbf{W} with a vector \mathbf{r} can alternatively be formulated as the vector product of a vector $\boldsymbol{\omega}$ and \mathbf{x} .

$$\underbrace{\begin{bmatrix} 0 & -\dot{\gamma} & \dot{\beta} \\ \dot{\gamma} & 0 & -\dot{\alpha} \\ -\dot{\beta} & \dot{\alpha} & 0 \end{bmatrix}}_{\mathbf{W}} \underbrace{\begin{bmatrix} X \\ Y \\ Z \end{bmatrix}}_{\mathbf{r}} = \begin{bmatrix} -\dot{\gamma}Y + \dot{\beta}Z \\ \dot{\gamma}X - \dot{\alpha}Z \\ -\dot{\beta}X + \dot{\alpha}Y \end{bmatrix} = \underbrace{\begin{bmatrix} \dot{\alpha} \\ \dot{\beta} \\ \dot{\gamma} \end{bmatrix}}_{\boldsymbol{\omega}} \times \underbrace{\begin{bmatrix} X \\ Y \\ Z \end{bmatrix}}_{\mathbf{r}} \quad (7.1.9)$$

In the present case of the wheel-rail contact, however, the determination of the rotation angles α , β and γ by according to (7.1.5) can lead to results, which do not adequately describe the kinematics of the flexible structure. In order to illustrate this problem, a rather simple example of a rectangular bar shall be considered; similar to the rail, this bar can be seen as a prismatic shape. In this example, the bar performs a shear deformation in its longitudinal direction; for the sake of simplicity, it is assumed that the distribution of the longitudinal displacement u only depends on the lateral coordinate y . In Figure 7.1.3, the bar is shown in its deformed and its undeformed state; furthermore, the bar's cross section is indicated.

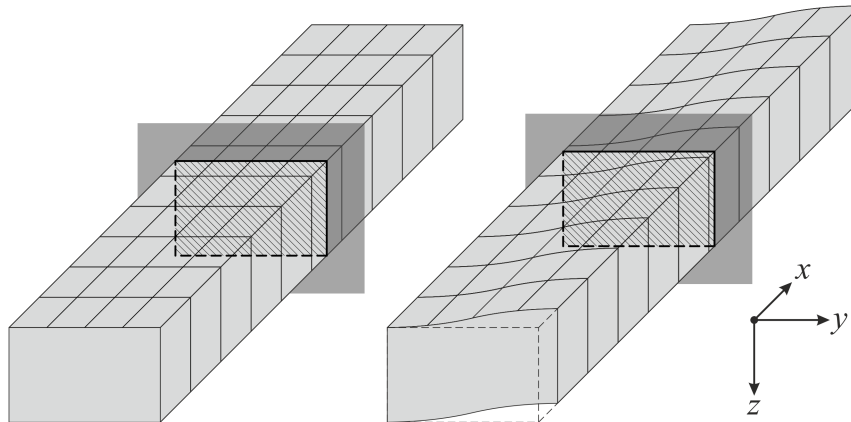


Figure 7.1.3: Rectangular bar; left: undeformed reference state; right: shear deformation; hatched area: cross section of the bar determined as the intersection with the dark grey plain.

Using the body-fixed frame \mathcal{B} of the bar as the reference frame, it is obtained for the reference position $\mathbf{x}^{\mathcal{B}}$ and for the deformation $\mathbf{w}^{\mathcal{B}}$:

$$\mathbf{x}^{\mathcal{B}} = \begin{bmatrix} x \\ y \\ z \end{bmatrix}, \quad \mathbf{w}^{\mathcal{B}} = \begin{bmatrix} u(y) \\ 0 \\ 0 \end{bmatrix} \quad (7.1.10)$$

The displacements v and w in the lateral and the vertical directions and thereby also their derivatives are zero. According to (7.1.5), it is obtained for the rotation angles:

$$\alpha = \frac{1}{2} \left(\frac{\partial w}{\partial y} - \frac{\partial v}{\partial z} \right) = 0, \quad \beta = \frac{1}{2} \left(\frac{\partial u}{\partial z} - \frac{\partial w}{\partial x} \right) = 0, \quad \gamma = \frac{1}{2} \left(\frac{\partial v}{\partial x} - \frac{\partial u}{\partial y} \right) = -\frac{1}{2} \frac{\partial u}{\partial y} = -u_y \quad (7.1.11)$$

Here, the variable u_y denoting the partial derivative of u with respect to y is introduced for the sake of brevity. The result indicates a rotation around the vertical axis occurs. However, as it can be seen from Figure 7.1.3, the shape of the bar's cross section, which is indicated as the intersection with a transversal plain, and thereby the shape of its surface remain unchanged. Therefore, with respect to the analysis of the wheel-rail contact geometry, the determination of the rotation based on the deformation gradient leads to an incorrect input. Therefore, an alternative approach, which produces a more adequate result, will be presented in the following sections.

The angular velocities can be derived directly from the angles according to (7.1.11); thereby, it is obtained for the vector $\boldsymbol{\omega}$:

$$\dot{\alpha} = 0, \dot{\beta} = 0, \dot{\gamma} = -\frac{1}{2} \frac{\partial^2 u}{\partial y \partial t} = -\frac{1}{2} \dot{u}_y \Rightarrow \boldsymbol{\omega} = -\frac{1}{2} \dot{u}_y \begin{bmatrix} 0 \\ 0 \\ 1 \end{bmatrix} \quad (7.1.12)$$

In contrast to the angular displacement, this result is plausible; in the deformed state of the bar displayed in Figure 7.1.3 the shear deformation, which can be interpreted as a superposition of a rotation and the actual deformation, is clearly visible. Apparently, for the wheel-rail contact, which shall be coupled to a flexible body, the kinematics shows some inconsistencies in the sense that the angular velocity is not necessarily the derivative of the angular position. Also this aspect will be taken into account in the following considerations.

7.1.1 Rotation of the surface

Since the wheel-rail contact acts at the surfaces of the wheel and the rail, it is obvious to determine the rotational motions of the markers from the orientation of the surfaces of these two bodies. The main problem to be solved is to determine a rotation matrix $\mathbf{S}^{\mathcal{R}\mathcal{S}}$, which describes the rotation between the reference frame \mathcal{R} and the surface frame \mathcal{S} .

In the reference frame \mathcal{R} the surface of the body is described by the vector $\mathbf{x}_S^{\mathcal{R}}$. Since a surface is a two-dimensional structure, its points can be indicated by two independent parameters ξ and η :

$$\mathbf{x}_S^{\mathcal{R}} = \mathbf{x}_S^{\mathcal{R}}(\xi, \eta) \quad (7.1.13)$$

The deformation is given as a field depending on the reference position, i.e. $\mathbf{w}^{\mathcal{R}}(\mathbf{x}^{\mathcal{R}})$. Therefore, the position of a point S belonging to the surface can be formulated as a function depending on the two parameters ξ and η of the surface:

$$\mathbf{r}_S^{\mathcal{R}} = \mathbf{x}_S^{\mathcal{R}}(\xi, \eta) + \mathbf{w}^{\mathcal{R}}(\mathbf{x}_S^{\mathcal{R}}(\xi, \eta)) = \mathbf{r}_S^{\mathcal{R}}(\xi, \eta) \quad (7.1.14)$$

The orientation of the surface is determined based on the tangential vectors \mathbf{t}_ξ and \mathbf{t}_η , which are obtained as the partial derivatives of the position vector $\mathbf{r}_S^{\mathcal{R}}$ with respect to the two parameters ξ and η :

$$\mathbf{t}_\xi^{\mathcal{R}} = \frac{\partial \mathbf{r}_S^{\mathcal{R}}}{\partial \xi}, \quad \mathbf{t}_\eta^{\mathcal{R}} = \frac{\partial \mathbf{r}_S^{\mathcal{R}}}{\partial \eta} \quad (7.1.15)$$

The tangential vectors $\mathbf{t}_\xi^{\mathcal{R}}$ and $\mathbf{t}_\eta^{\mathcal{R}}$ span a tangential plain to the surface. Therefore, all vectors $\mathbf{y}_T^{\mathcal{R}}$ lying in this plain can be described by a linear combination of the two tangential vectors:

$$\mathbf{y}_T^{\mathcal{R}} = c_\xi \mathbf{t}_\xi^{\mathcal{R}} + c_\eta \mathbf{t}_\eta^{\mathcal{R}}, \quad c_\xi \neq 0 \vee c_\eta \neq 0 \Rightarrow \mathbf{y}_T^{\mathcal{R}} \neq \mathbf{0} \quad (7.1.16)$$

Although it is assumed that the tangential vectors $\mathbf{t}_\xi^{\mathcal{R}}$ and $\mathbf{t}_\eta^{\mathcal{R}}$ are linearly independent, they are not necessarily orthogonal. The scalar factors c_ξ and c_η can be chosen arbitrarily; however, it has to be ensured that the tangential vector $\mathbf{y}_T^{\mathcal{R}}$ is not equal to the zero vector.

For vectors of the three-dimensional space the cross product is a very convenient way to generate orthogonal vectors; it is valid:

$$\mathbf{c} = \mathbf{a} \times \mathbf{b} \Rightarrow \mathbf{a} \cdot \mathbf{c} = 0 \wedge \mathbf{b} \cdot \mathbf{c} = 0 \quad (7.1.17)$$

This characteristic property will be applied several times in the following considerations. Based on this, the normal vector $\mathbf{n}^{\mathcal{R}}$, which is orthogonal to the surface, can be determined by:

$$\mathbf{n}^{\mathcal{R}} = \mathbf{t}_\xi^{\mathcal{R}} \times \mathbf{t}_\eta^{\mathcal{R}} \Rightarrow \mathbf{n}^{\mathcal{R}} \cdot \mathbf{t}_\xi^{\mathcal{R}} = 0 \wedge \mathbf{n}^{\mathcal{R}} \cdot \mathbf{t}_\eta^{\mathcal{R}} = 0 \quad (7.1.18)$$

$$\mathbf{n}^{\mathcal{R}} = \mathbf{t}_\xi^{\mathcal{R}} \times \mathbf{t}_\eta^{\mathcal{R}} \Rightarrow \mathbf{n}^{\mathcal{R}} \cdot \mathbf{t}_\xi^{\mathcal{R}} = 0 \wedge \mathbf{n}^{\mathcal{R}} \cdot \mathbf{t}_\eta^{\mathcal{R}} = 0 \quad (7.1.19)$$

Therefore, the normal vector $\mathbf{n}^{\mathcal{R}}$ is also orthogonal to all linear combinations of the tangential vectors $\mathbf{t}_\xi^{\mathcal{R}}$ and $\mathbf{t}_\eta^{\mathcal{R}}$:

$$\mathbf{n}^{\mathcal{R}} \cdot \mathbf{y}_T^{\mathcal{R}} = \mathbf{n}^{\mathcal{R}} \cdot (c_\xi \mathbf{t}_\xi^{\mathcal{R}} + c_\eta \mathbf{t}_\eta^{\mathcal{R}}) = \mathbf{n}^{\mathcal{R}} \cdot c_\xi \mathbf{t}_\xi^{\mathcal{R}} + \mathbf{n}^{\mathcal{R}} \cdot c_\eta \mathbf{t}_\eta^{\mathcal{R}} = c_\xi \underbrace{\mathbf{n}^{\mathcal{R}} \cdot \mathbf{t}_\xi^{\mathcal{R}}}_0 + c_\eta \underbrace{\mathbf{n}^{\mathcal{R}} \cdot \mathbf{t}_\eta^{\mathcal{R}}}_0 = 0 \quad (7.1.20)$$

The three vectors $\mathbf{t}_\xi^{\mathcal{R}}$, $\mathbf{t}_\eta^{\mathcal{R}}$ and $\mathbf{n}^{\mathcal{R}}$ are obtained from the geometric analysis of the surface in its current state so they are considered to be the given input for the determination of the wanted rotation matrix $\mathbf{S}^{\mathcal{R}\mathcal{S}}$.

Generally, the orientation of a frame in the three-dimensional space can be described by its three basis vectors. In the frame itself, the vectors are the canonical basis vectors. Therefore, it is valid for the surface frame \mathcal{S} :

$$\mathbf{e}_{S1}^{\mathcal{S}} = \begin{bmatrix} 1 \\ 0 \\ 0 \end{bmatrix}, \mathbf{e}_{S2}^{\mathcal{S}} = \begin{bmatrix} 0 \\ 1 \\ 0 \end{bmatrix}, \mathbf{e}_{S3}^{\mathcal{S}} = \begin{bmatrix} 0 \\ 0 \\ 1 \end{bmatrix} \quad (7.1.21)$$

For each vector $\mathbf{e}_{SI}^{\mathcal{S}}$ the I -th coordinate has the value 1, while the two other coordinates are zero; thereby, it is evident that the vectors $\mathbf{e}_{S1}^{\mathcal{S}}$, $\mathbf{e}_{S2}^{\mathcal{S}}$ and $\mathbf{e}_{S3}^{\mathcal{S}}$ are unit vectors. By applying the transformation matrix $\mathbf{S}^{\mathcal{R}\mathcal{S}}$ the vectors are transformed from the surface frame \mathcal{S} into the reference frame \mathcal{R} :

$$\mathbf{e}_{S1}^{\mathcal{R}} = \mathbf{S}^{\mathcal{R}\mathcal{S}} \mathbf{e}_{S1}^{\mathcal{S}} = \begin{bmatrix} s_{11} & s_{12} & s_{13} \\ s_{21} & s_{22} & s_{23} \\ s_{31} & s_{32} & s_{33} \end{bmatrix} \begin{bmatrix} 1 \\ 0 \\ 0 \end{bmatrix} = \begin{bmatrix} s_{11} \\ s_{21} \\ s_{31} \end{bmatrix} \quad (7.1.22)$$

$$\mathbf{e}_{S2}^{\mathcal{R}} = \mathbf{S}^{\mathcal{R}\mathcal{S}} \mathbf{e}_{S2}^{\mathcal{S}} = \begin{bmatrix} s_{11} & s_{12} & s_{13} \\ s_{21} & s_{22} & s_{23} \\ s_{31} & s_{32} & s_{33} \end{bmatrix} \begin{bmatrix} 0 \\ 1 \\ 0 \end{bmatrix} = \begin{bmatrix} s_{12} \\ s_{22} \\ s_{32} \end{bmatrix} \quad (7.1.23)$$

$$\mathbf{e}_{S3}^{\mathcal{R}} = \mathbf{S}^{\mathcal{R}\mathcal{S}} \mathbf{e}_{S3}^{\mathcal{S}} = \begin{bmatrix} s_{11} & s_{12} & s_{13} \\ s_{21} & s_{22} & s_{23} \\ s_{31} & s_{32} & s_{33} \end{bmatrix} \begin{bmatrix} 0 \\ 0 \\ 1 \end{bmatrix} = \begin{bmatrix} s_{13} \\ s_{23} \\ s_{33} \end{bmatrix} \quad (7.1.24)$$

Thereby, the rotation matrix $\mathbf{S}^{\mathcal{RS}}$ can be expressed by arranging the transformed vectors $\mathbf{e}_{S1}^{\mathcal{R}}$, $\mathbf{e}_{S2}^{\mathcal{R}}$ and $\mathbf{e}_{S3}^{\mathcal{R}}$ as the columns of the matrix:

$$\mathbf{S}^{\mathcal{RS}} = \begin{bmatrix} \mathbf{e}_{S1}^{\mathcal{R}} & \mathbf{e}_{S2}^{\mathcal{R}} & \mathbf{e}_{S3}^{\mathcal{R}} \end{bmatrix} \quad (7.1.25)$$

The conditions for the column vectors $\mathbf{e}_{S1}^{\mathcal{R}}$, $\mathbf{e}_{S2}^{\mathcal{R}}$ and $\mathbf{e}_{S3}^{\mathcal{R}}$ follow from the properties of the rotation matrix $\mathbf{S}^{\mathcal{RS}}$. In the appendix D these properties are derived in detail for a rotation matrix \mathbf{R}_N , while here only the essential properties and relations, which are required for developing the wanted rotation matrix $\mathbf{S}^{\mathcal{RS}}$ are presented. The rotation matrix \mathbf{R}_N can be formulated in two ways, namely by its column vectors \mathbf{e}_1 , \mathbf{e}_2 and \mathbf{e}_3 and as a product of N elementary rotation matrices:

$$\mathbf{R}_N = \begin{bmatrix} \mathbf{e}_1 & \mathbf{e}_2 & \mathbf{e}_3 \end{bmatrix} = \prod_{k=1}^N \mathbf{S}_{I_k}(\phi_k), \quad I_k = 1, 2, 3 \quad (7.1.26)$$

In the appendix D, two characteristic properties for the rotation matrix \mathbf{R}_N are shown:

1. The rotation matrix \mathbf{R}_N is an orthogonal matrix, i.e. its transpose is equal to its inverse:

$$\mathbf{R}_N^T = \mathbf{R}_N^{-1} \quad (7.1.27)$$

2. The determinant of the rotation matrix \mathbf{R}_N is equal to 1:

$$\det \mathbf{R}_N = 1 \quad (7.1.28)$$

From this, it can be derived for the column vectors \mathbf{e}_1 , \mathbf{e}_2 and \mathbf{e}_3 of the rotation matrix \mathbf{R}_N :

1. The column vectors \mathbf{e}_1 , \mathbf{e}_2 and \mathbf{e}_3 are orthogonal unit vectors:

$$\mathbf{e}_k^T \mathbf{e}_l = \mathbf{e}_k \cdot \mathbf{e}_l = \begin{cases} 1 & \text{for } k = l \\ 0 & \text{for } k \neq l \end{cases} \Rightarrow |\mathbf{e}_k| = \sqrt{\mathbf{e}_k \cdot \mathbf{e}_k} = 1 \quad (7.1.29)$$

2. The following relations between the column vectors \mathbf{e}_1 , \mathbf{e}_2 and \mathbf{e}_3 are valid:

$$\mathbf{e}_1 = \mathbf{e}_2 \times \mathbf{e}_3, \quad \mathbf{e}_2 = \mathbf{e}_3 \times \mathbf{e}_1, \quad \mathbf{e}_3 = \mathbf{e}_1 \times \mathbf{e}_2 \quad (7.1.30)$$

Alternatively, these relations can be formulated in the following way:

$$\mathbf{e}_j = \mathbf{e}_k \times \mathbf{e}_l, \quad \langle j, k, l \rangle \in \{ \langle 1, 2, 3 \rangle, \langle 2, 3, 1 \rangle, \langle 3, 1, 2 \rangle \} \quad (7.1.31)$$

Based on these conditions, the column vectors $\mathbf{e}_{S1}^{\mathcal{R}}$, $\mathbf{e}_{S2}^{\mathcal{R}}$ and $\mathbf{e}_{S3}^{\mathcal{R}}$ of the wanted rotation matrix $\mathbf{S}^{\mathcal{RS}}$ can be determined based on the tangential vector $\mathbf{y}_T^{\mathcal{R}}$ and the normal vector $\mathbf{n}^{\mathcal{R}}$ according to (7.1.16) and (7.1.19), respectively, which can again be determined from the tangential vectors $\mathbf{t}_\xi^{\mathcal{R}}$ and $\mathbf{t}_\eta^{\mathcal{R}}$.

The column vectors $\mathbf{e}_{S1}^{\mathcal{R}}$, $\mathbf{e}_{S2}^{\mathcal{R}}$ and $\mathbf{e}_{S3}^{\mathcal{R}}$ are unit vectors; from a given vector $\mathbf{y}_i^{\mathcal{R}} \neq \mathbf{0}$ a unit vector $\mathbf{e}_i^{\mathcal{R}}$, which has the same orientation as $\mathbf{y}_i^{\mathcal{R}}$, is obtained by normalizing $\mathbf{y}_i^{\mathcal{R}}$, i.e. multiplying it with the reciprocal value of the norm $|\mathbf{y}_i^{\mathcal{R}}|$:

$$\mathbf{y}_i^{\mathcal{R}} \neq \mathbf{0} \Rightarrow \mathbf{e}_i^{\mathcal{R}} = \frac{1}{|\mathbf{y}_i^{\mathcal{R}}|} \mathbf{y}_i^{\mathcal{R}} = \frac{\mathbf{y}_i^{\mathcal{R}}}{|\mathbf{y}_i^{\mathcal{R}}|} \quad (7.1.32)$$

Based on this, the three column vectors are obtained by the following steps:

1. One vector $\mathbf{e}_{SI}^{\mathcal{R}}$ is obtained by normalizing the normal vector $\mathbf{n}^{\mathcal{R}}$:

$$\mathbf{y}_I^{\mathcal{R}} = c_N \mathbf{n}^{\mathcal{R}} = c_N \mathbf{t}_\xi^{\mathcal{R}} \times \mathbf{t}_\eta^{\mathcal{R}}, \mathbf{e}_{SI}^{\mathcal{R}} = \frac{\mathbf{y}_I^{\mathcal{R}}}{|\mathbf{y}_I^{\mathcal{R}}|} \quad (7.1.33)$$

Since the vector product is not commutative, the chosen sequence $\mathbf{t}_\xi^{\mathcal{R}} \times \mathbf{t}_\eta^{\mathcal{R}}$ has an influence on the orientation of the normal vector $\mathbf{n}^{\mathcal{R}}$. Since in principle this choice is arbitrary, an additional scalar factor c_N is introduced; by choosing $c_N = -1$, the orientation of the vector $\mathbf{y}_I^{\mathcal{R}}$ can be changed into the opposite direction.

2. Another vector $\mathbf{e}_{SJ}^{\mathcal{R}}$ is obtained by normalizing a linear combination $\mathbf{y}_T^{\mathcal{R}}$ of the tangential vectors $\mathbf{t}_\xi^{\mathcal{R}}$ and $\mathbf{t}_\eta^{\mathcal{R}}$; due to (7.1.19) and (7.1.20) it is ensured that the vectors $\mathbf{y}_I^{\mathcal{R}}$ and $\mathbf{y}_J^{\mathcal{R}}$ and thereby also the unit vectors $\mathbf{e}_{SI}^{\mathcal{R}}$ and $\mathbf{e}_{SJ}^{\mathcal{R}}$ are orthogonal.

$$\mathbf{y}_J^{\mathcal{R}} = \mathbf{y}_T^{\mathcal{R}} = c_\xi \mathbf{t}_\xi^{\mathcal{R}} + c_\eta \mathbf{t}_\eta^{\mathcal{R}}, \mathbf{e}_{SJ}^{\mathcal{R}} = \frac{\mathbf{y}_J^{\mathcal{R}}}{|\mathbf{y}_J^{\mathcal{R}}|} \quad (7.1.34)$$

3. The third vector $\mathbf{e}_{SK}^{\mathcal{R}}$ is obtained from the cross product of the vectors $\mathbf{e}_{SI}^{\mathcal{R}}$ and $\mathbf{e}_{SJ}^{\mathcal{R}}$; this ensures that $\mathbf{e}_{SK}^{\mathcal{R}}$ is orthogonal to both $\mathbf{e}_{SI}^{\mathcal{R}}$ and $\mathbf{e}_{SJ}^{\mathcal{R}}$ according to (7.1.17). Depending on how the indices I and J are chosen, the corresponding triple $\langle j, k, l \rangle$ has to be selected from the following ones, as derived in section D.3:

$$\mathbf{e}_{SK}^{\mathcal{R}} = \mathbf{e}_{SI}^{\mathcal{R}} \times \mathbf{e}_{SJ}^{\mathcal{R}}, \langle j, k, l \rangle \in \{ \langle 1, 2, 3 \rangle, \langle 2, 3, 1 \rangle, \langle 3, 1, 2 \rangle \} \quad (7.1.35)$$

It should be noted that the vectors $\mathbf{e}_{Si}^{\mathcal{R}}$, $i = 1, 2, 3$, which form the rotation matrix $\mathbf{S}^{\mathcal{R}\mathcal{S}}$, are not uniquely defined. It is evident that the vectors $\mathbf{y}_I^{\mathcal{R}}$ and $\mathbf{y}_J^{\mathcal{R}}$, to which the normal vector $\mathbf{n}^{\mathcal{R}}$ and $\mathbf{y}_T^{\mathcal{R}}$ are assigned, can in principle be selected arbitrarily. Furthermore, the scalar factors c_ξ and c_η , which determine the orientation of the tangential vector $\mathbf{y}_T^{\mathcal{R}}$ can be chosen arbitrarily as long as the vector $\mathbf{y}_T^{\mathcal{R}}$ is not equal to the zero vector. This second aspect shall be discussed later.

The method derived up to here shall now be applied to a practical example, which is based on the case discussed before in section 7.1. In this case, the top surface of the rectangular bar shall be considered. Here, it is obvious to use the coordinates x and y as parameters of this surface so that the tangential vectors $\mathbf{t}_x^{\mathcal{B}}$ and $\mathbf{t}_y^{\mathcal{B}}$ have to be determined. The geometrical analysis leads to the following result:

$$\mathbf{r}^{\mathcal{B}} = \mathbf{x}^{\mathcal{B}} + \mathbf{w}^{\mathcal{B}} = \begin{bmatrix} x + u(y) \\ y \\ z \end{bmatrix} \Rightarrow \mathbf{t}_x^{\mathcal{B}} = \frac{\partial \mathbf{r}^{\mathcal{B}}}{\partial x} = \begin{bmatrix} 1 \\ 0 \\ 0 \end{bmatrix}, \mathbf{t}_y^{\mathcal{B}} = \frac{\partial \mathbf{r}^{\mathcal{B}}}{\partial y} = \begin{bmatrix} \frac{\partial u}{\partial y} \\ 1 \\ 0 \end{bmatrix} = \begin{bmatrix} u_y \\ 1 \\ 0 \end{bmatrix}, u_y = \frac{\partial u}{\partial y} \quad (7.1.36)$$

Here, the expression u_y denoting the partial derivative of the longitudinal displacement $u(x, y)$ with respect to the lateral coordinate is introduced for the sake of brevity. For the normal vector $\mathbf{n}^{\mathcal{B}}$ it is obtained:

$$\mathbf{n}^{\mathcal{B}} = \mathbf{t}_x^{\mathcal{B}} \times \mathbf{t}_y^{\mathcal{B}} = \begin{bmatrix} 1 \\ 0 \\ 0 \end{bmatrix} \times \begin{bmatrix} u_y \\ 1 \\ 0 \end{bmatrix} = \begin{bmatrix} 0 \\ 0 \\ 1 \end{bmatrix} \quad (7.1.37)$$

Thereby, the “geometric vectors” are known and will be considered to be given for the determination of the matrix \mathbf{S}^{BS} , which describes the rotation between the body-fixed frame \mathcal{B} and the surface frame \mathcal{S} . The expression “geometric vectors”, which is used here and in the following, shall indicate that these vectors are obtained from the geometrical analysis.

Since in the present case the normal vector \mathbf{n}^B is pointing in the direction of the 3-axis of the body-fixed frame \mathcal{B} , it is reasonable to assign it to the vector \mathbf{y}_3^B , i.e. setting the scalar factor used in (7.1.33) to $c_N = 1$; thereby, it is obtained for the vector \mathbf{e}_{S3}^B :

$$\mathbf{y}_3^B = \mathbf{n}^B = \begin{bmatrix} 0 \\ 0 \\ 1 \end{bmatrix} \Rightarrow \mathbf{e}_{S3}^{\mathcal{R}} = \frac{\mathbf{n}^{\mathcal{R}}}{|\mathbf{n}^{\mathcal{R}}|} = \begin{bmatrix} 0 \\ 0 \\ 1 \end{bmatrix} \quad (7.1.38)$$

For the determination of the two other vectors \mathbf{e}_{S1}^B and \mathbf{e}_{S2}^B there are two rather obvious possibilities. One possibility is to assign the tangential vector \mathbf{t}_x^B , i.e. the derivative with respect to the longitudinal coordinate x , to the vector \mathbf{y}_1^B ; regarding (7.1.34) the scalar factors are set to $x_x = 1$ and $c_y = 0$. Since the vector \mathbf{e}_{S2}^B is determined as the cross product of the vectors \mathbf{e}_{S1}^B and \mathbf{e}_{S3}^B , according to (7.1.35) the triple $\langle j, k, l \rangle = \langle 2, 3, 1 \rangle$ has to be used for the product $\mathbf{e}_{Sj}^{\mathcal{R}} = \mathbf{e}_{Sk}^{\mathcal{R}} \times \mathbf{e}_{Sl}^{\mathcal{R}}$. In total, it is obtained:

$$\mathbf{y}_1^B = \mathbf{t}_x^B = \begin{bmatrix} 1 \\ 0 \\ 0 \end{bmatrix} \Rightarrow \mathbf{e}_{S1}^{\mathcal{R}} = \frac{\mathbf{t}_x^B}{|\mathbf{t}_x^B|} = \begin{bmatrix} 1 \\ 0 \\ 0 \end{bmatrix} \Rightarrow \mathbf{e}_{S2}^{\mathcal{R}} = \mathbf{e}_{S3}^{\mathcal{R}} \times \mathbf{e}_{S1}^{\mathcal{R}} = \begin{bmatrix} 0 \\ 0 \\ 1 \end{bmatrix} \times \begin{bmatrix} 1 \\ 0 \\ 0 \end{bmatrix} = \begin{bmatrix} 0 \\ 1 \\ 0 \end{bmatrix} \quad (7.1.39)$$

$$\Rightarrow \mathbf{S}^{BS} = [\mathbf{e}_{S1}^B \quad \mathbf{e}_{S2}^B \quad \mathbf{e}_{S3}^B] = \begin{bmatrix} 1 & 0 & 0 \\ 0 & 1 & 0 \\ 0 & 0 & 1 \end{bmatrix} \quad (7.1.40)$$

A second rather obvious possibility is to assign the tangential vector \mathbf{t}_y^B , i.e. the derivative with respect to the lateral coordinate y , to the vector \mathbf{y}_2^B ; in this case, the scalar factors are set to $x_x = 0$ and $c_y = 1$ for (7.1.34). For the determination of the vector \mathbf{e}_{S1}^B the triple $\langle j, k, l \rangle = \langle 1, 2, 3 \rangle$ has to be chosen. This leads to:

$$\mathbf{y}_2^B = \mathbf{t}_y^B = \begin{bmatrix} u_y \\ 1 \\ 0 \end{bmatrix} \Rightarrow \mathbf{e}_{S2}^{\mathcal{R}} = \frac{\mathbf{t}_y^B}{|\mathbf{t}_y^B|} = \frac{1}{\sqrt{1+u_y^2}} \begin{bmatrix} u_y \\ 1 \\ 0 \end{bmatrix} \quad (7.1.41)$$

$$\Rightarrow \mathbf{e}_{S1}^{\mathcal{R}} = \mathbf{e}_{S2}^{\mathcal{R}} \times \mathbf{e}_{S3}^{\mathcal{R}} = \frac{1}{\sqrt{1+u_y^2}} \begin{bmatrix} u_y \\ 1 \\ 0 \end{bmatrix} \times \begin{bmatrix} 0 \\ 0 \\ 1 \end{bmatrix} = \frac{1}{\sqrt{1+u_y^2}} \begin{bmatrix} 1 \\ -u_y \\ 0 \end{bmatrix} \quad (7.1.42)$$

$$\Rightarrow \mathbf{S}^{BS} = [\mathbf{e}_{S1}^B \quad \mathbf{e}_{S2}^B \quad \mathbf{e}_{S3}^B] = \begin{bmatrix} \frac{1}{\sqrt{1+u_y^2}} & \frac{u_y}{\sqrt{1+u_y^2}} & 0 \\ -\frac{u_y}{\sqrt{1+u_y^2}} & \frac{1}{\sqrt{1+u_y^2}} & 0 \\ 0 & 0 & 1 \end{bmatrix} \quad (7.1.43)$$

By comparing this result with the three elementary rotation matrices for the three-dimensional space, it becomes clear that the matrix \mathbf{S}^{BS} according to (7.1.43) describes a rotation around the 3-axis, i.e. around the vertical axis:

$$\mathbf{S}_3 = \begin{bmatrix} \cos \gamma & -\sin \gamma & 0 \\ \sin \gamma & \cos \gamma & 0 \\ 0 & 0 & 1 \end{bmatrix} \Rightarrow \sin \gamma = \frac{-u_y}{\sqrt{1+u_y^2}}, \quad \cos \gamma = \frac{1}{\sqrt{1+u_y^2}} \quad (7.1.44)$$

It is evident that the resulting matrix \mathbf{S}^{BS} depends on the choice of the vectors. By assigning the tangential vector \mathbf{t}_x^B to the vector \mathbf{y}_1^B the matrix \mathbf{S}^{BS} is equal to the identity matrix, i.e. the matrix \mathbf{S}^{BS} is not influenced by the longitudinal shear deformation of the bar. Apparently, this is the correct description of the scenario shown in Figure 7.1.3, where the bar's cross section in fact remains unchanged. If, however, the tangential vector \mathbf{t}^B is assigned to the vector \mathbf{y}_2^B , then the matrix \mathbf{S}^{BS} describes a rotation around the 3-axis, which is evidently wrong regarding the cross section. The different results for the matrix \mathbf{S}^{BS} are a consequence of the fact that due to the shear deformation of the bar the angle between the two geometric tangential vectors \mathbf{t}_x^B and \mathbf{t}_y^B varies. This becomes evident by comparing the vectors \mathbf{t}_x^B and \mathbf{t}_y^B determined in (7.1.36): While the vector \mathbf{t}_x^B is constant, the vector \mathbf{t}_y^B changes its direction depending on u_y . For the basis vectors of the surface frame, however, it is assumed that they are always orthogonal.

The bar, which is chosen here as an example, and the rail, to which this formulation will finally be applied, can also be interpreted as an extrusion of a cross section along a path curve. Since the path curve can be considered as a description of the local orientation of the structure, it is reasonable to use this direction as a reference and therefore to choose the tangential vector, which has to be selected, in such a way that it points into the direction of the path curve.

7.1.2 Angular velocity of the surface

If the rotation of a frame \mathcal{K} relative to the frame \mathcal{J} is described by the matrix $\mathbf{S}^{J\mathcal{K}}$, then the angular velocity of \mathcal{K} relative to \mathcal{J} is determined by:

$$\tilde{\omega}_{J\mathcal{K}}^J = \dot{\mathbf{S}}^{J\mathcal{K}} \mathbf{S}^{J\mathcal{K}T} \quad (7.1.45)$$

The relation between the vector $\omega_{J\mathcal{K}}^J$ and the tilde matrix $\tilde{\omega}_{J\mathcal{K}}^J$ is given by:

$$\omega_{J\mathcal{K}}^J = \begin{bmatrix} \omega_1 \\ \omega_2 \\ \omega_3 \end{bmatrix} \Leftrightarrow \tilde{\omega}_{J\mathcal{K}}^J = \begin{bmatrix} 0 & -\omega_3 & \omega_2 \\ \omega_3 & 0 & -\omega_1 \\ -\omega_2 & \omega_1 & 0 \end{bmatrix} \quad (7.1.46)$$

In appendix D.4 the rotation matrix $\mathbf{S}^{J\mathcal{K}}$ has been formulated as a rotation matrix \mathbf{R}_N , which is described by its column vectors; for this case, the corresponding angular velocity has been derived. Here, only the result shall be presented. The tilde matrix $\tilde{\omega}_{J\mathcal{K}}^J$ is obtained to:

$$\mathbf{S}^{J\mathcal{K}} = \mathbf{R}_N = [\mathbf{e}_1 \quad \mathbf{e}_2 \quad \mathbf{e}_3] \Rightarrow \tilde{\omega}_{J\mathcal{K}}^J = \dot{\mathbf{R}}_N \mathbf{R}_N^T = \mathbf{R}_N \begin{bmatrix} 0 & -\mathbf{e}_2 \cdot \dot{\mathbf{e}}_1 & \mathbf{e}_1 \cdot \dot{\mathbf{e}}_3 \\ \mathbf{e}_2 \cdot \dot{\mathbf{e}}_1 & 0 & -\mathbf{e}_3 \cdot \dot{\mathbf{e}}_2 \\ -\mathbf{e}_1 \cdot \dot{\mathbf{e}}_3 & \mathbf{e}_3 \cdot \dot{\mathbf{e}}_2 & 0 \end{bmatrix} \mathbf{R}_N^T \quad (7.1.47)$$

From this, the following formulation of the angular velocity as a vector $\omega_{J\mathcal{K}}^J$ can be derived:

$$\omega_{J\mathcal{K}}^J = \mathbf{R}_N \begin{bmatrix} \dot{\mathbf{e}}_2 \cdot \mathbf{e}_3 \\ \dot{\mathbf{e}}_3 \cdot \mathbf{e}_1 \\ \dot{\mathbf{e}}_1 \cdot \mathbf{e}_2 \end{bmatrix} = (\dot{\mathbf{e}}_2 \cdot \mathbf{e}_3) \mathbf{e}_1 + (\dot{\mathbf{e}}_3 \cdot \mathbf{e}_1) \mathbf{e}_2 + (\dot{\mathbf{e}}_1 \cdot \mathbf{e}_2) \mathbf{e}_3 \quad (7.1.48)$$

Applying this to the rotation of the surface frame \mathcal{S} relative to the reference frame \mathcal{R} leads to:

$$\omega_{\mathcal{R}\mathcal{S}}^{\mathcal{R}} = \left(\dot{\mathbf{e}}_{S2}^{\mathcal{R}} \cdot \mathbf{e}_{S3}^{\mathcal{R}} \right) \mathbf{e}_{S1}^{\mathcal{R}} + \left(\dot{\mathbf{e}}_{S3}^{\mathcal{R}} \cdot \mathbf{e}_{S1}^{\mathcal{R}} \right) \mathbf{e}_{S2}^{\mathcal{R}} + \left(\dot{\mathbf{e}}_{S1}^{\mathcal{R}} \cdot \mathbf{e}_{S2}^{\mathcal{R}} \right) \mathbf{e}_{S3}^{\mathcal{R}} \quad (7.1.49)$$

It can be seen that the formulation of the vector $\boldsymbol{\omega}_{\mathcal{R}\mathcal{S}}^{\mathcal{R}}$ contains the vectors $\dot{\mathbf{e}}_{S1}^{\mathcal{R}}$, $\dot{\mathbf{e}}_{S2}^{\mathcal{R}}$ and $\dot{\mathbf{e}}_{S3}^{\mathcal{R}}$, i.e. the derivatives of all three basis vectors. In the methodology developed in section 7.1.1, however, the matrix $\mathbf{S}^{\mathcal{R}\mathcal{S}}$ is determined by normalizing the vectors $c_N \mathbf{n}^{\mathcal{R}}$ and $c_\xi \mathbf{t}_\xi^{\mathcal{R}} + c_\eta \mathbf{t}_\eta^{\mathcal{R}}$ and assigning them to two column vectors $\mathbf{e}_{S1}^{\mathcal{R}}$ and $\mathbf{e}_{S2}^{\mathcal{R}}$, while the third vector $\mathbf{e}_{S3}^{\mathcal{R}}$ is determined by applying the following relation for the correct index triple $\langle j, k, l \rangle$:

$$\mathbf{e}_{Sj}^{\mathcal{R}} = \mathbf{e}_{Sk}^{\mathcal{R}} \times \mathbf{e}_{Sl}^{\mathcal{R}}, \langle j, k, l \rangle \in \{\langle 1, 2, 3 \rangle, \langle 2, 3, 1 \rangle, \langle 3, 1, 2 \rangle\} \quad (7.1.50)$$

Therefore, the goal of the following transformation is to express the angular velocity only by the two chosen vectors; this also shows, how the choice of the two vectors influences the obtained angular velocity. To this end, it is useful to formulate the vector $\boldsymbol{\omega}_{\mathcal{R}\mathcal{S}}^{\mathcal{R}}$ given by (7.1.49) in a generalized way similar to (7.1.50). This generalized formulation is given by:

$$\boldsymbol{\omega}_{\mathcal{R}\mathcal{S}}^{\mathcal{R}} = \left(\dot{\mathbf{e}}_{Sj}^{\mathcal{R}} \cdot \mathbf{e}_{Sk}^{\mathcal{R}} \right) \mathbf{e}_{Sl}^{\mathcal{R}} + \left(\dot{\mathbf{e}}_{Sk}^{\mathcal{R}} \cdot \mathbf{e}_{Sl}^{\mathcal{R}} \right) \mathbf{e}_{Sj}^{\mathcal{R}} + \left(\dot{\mathbf{e}}_{Sl}^{\mathcal{R}} \cdot \mathbf{e}_{Sj}^{\mathcal{R}} \right) \mathbf{e}_{Sk}^{\mathcal{R}}, \langle j, k, l \rangle \in \{\langle 1, 2, 3 \rangle, \langle 2, 3, 1 \rangle, \langle 3, 1, 2 \rangle\} \quad (7.1.51)$$

The evaluation of this formulation leads to:

$$\langle j, k, l \rangle = \langle 1, 2, 3 \rangle : \boldsymbol{\omega}_{\mathcal{R}\mathcal{S}}^{\mathcal{R}} = \left(\dot{\mathbf{e}}_{S1}^{\mathcal{R}} \cdot \mathbf{e}_{S2}^{\mathcal{R}} \right) \mathbf{e}_{S3}^{\mathcal{R}} + \left(\dot{\mathbf{e}}_{S2}^{\mathcal{R}} \cdot \mathbf{e}_{S3}^{\mathcal{R}} \right) \mathbf{e}_{S1}^{\mathcal{R}} + \left(\dot{\mathbf{e}}_{S3}^{\mathcal{R}} \cdot \mathbf{e}_{S1}^{\mathcal{R}} \right) \mathbf{e}_{S2}^{\mathcal{R}} \quad (7.1.52)$$

$$\langle j, k, l \rangle = \langle 2, 3, 1 \rangle : \boldsymbol{\omega}_{\mathcal{R}\mathcal{S}}^{\mathcal{R}} = \left(\dot{\mathbf{e}}_{S2}^{\mathcal{R}} \cdot \mathbf{e}_{S3}^{\mathcal{R}} \right) \mathbf{e}_{S1}^{\mathcal{R}} + \left(\dot{\mathbf{e}}_{S3}^{\mathcal{R}} \cdot \mathbf{e}_{S1}^{\mathcal{R}} \right) \mathbf{e}_{S2}^{\mathcal{R}} + \left(\dot{\mathbf{e}}_{S1}^{\mathcal{R}} \cdot \mathbf{e}_{S2}^{\mathcal{R}} \right) \mathbf{e}_{S3}^{\mathcal{R}} \quad (7.1.53)$$

$$\langle j, k, l \rangle = \langle 3, 1, 2 \rangle : \boldsymbol{\omega}_{\mathcal{R}\mathcal{S}}^{\mathcal{R}} = \left(\dot{\mathbf{e}}_{S3}^{\mathcal{R}} \cdot \mathbf{e}_{S1}^{\mathcal{R}} \right) \mathbf{e}_{S2}^{\mathcal{R}} + \left(\dot{\mathbf{e}}_{S1}^{\mathcal{R}} \cdot \mathbf{e}_{S2}^{\mathcal{R}} \right) \mathbf{e}_{S3}^{\mathcal{R}} + \left(\dot{\mathbf{e}}_{S2}^{\mathcal{R}} \cdot \mathbf{e}_{S3}^{\mathcal{R}} \right) \mathbf{e}_{S1}^{\mathcal{R}} \quad (7.1.54)$$

Since the addition is commutative, it is shown that for all three index triples $\langle j, k, l \rangle$ the generalized formulation according to (7.1.51) leads to the same result, which is equal to (7.1.49).

For the following considerations, a relation between the column vectors and their derivatives is required. According to (7.1.29), the column vectors of a rotation matrix are orthogonal unit vectors; therefore, it is valid for the present case:

$$\mathbf{e}_{Sk}^{\mathcal{R}\text{T}} \mathbf{e}_{Sl}^{\mathcal{R}} = \mathbf{e}_{Sk}^{\mathcal{R}} \cdot \mathbf{e}_{Sl}^{\mathcal{R}} = \begin{cases} 1 & \text{for } k = l \\ 0 & \text{for } k \neq l \end{cases} \Rightarrow \left| \mathbf{e}_{Sk}^{\mathcal{R}} \right| = \sqrt{\mathbf{e}_{Sk}^{\mathcal{R}} \cdot \mathbf{e}_{Sk}^{\mathcal{R}}} = 1 \quad (7.1.55)$$

Differentiating the relation (7.1.55) for $k \neq l$ and subsequently applying the commutativity of the scalar product leads to:

$$0 = \mathbf{e}_{Sk}^{\mathcal{R}} \cdot \mathbf{e}_{Sl}^{\mathcal{R}} \Rightarrow 0 = \frac{d}{dt} \left(\mathbf{e}_{Sk}^{\mathcal{R}} \cdot \mathbf{e}_{Sl}^{\mathcal{R}} \right) = \dot{\mathbf{e}}_{Sk}^{\mathcal{R}} \cdot \mathbf{e}_{Sl}^{\mathcal{R}} + \mathbf{e}_{Sk}^{\mathcal{R}} \cdot \dot{\mathbf{e}}_{Sl}^{\mathcal{R}} \Rightarrow -\dot{\mathbf{e}}_{Sk}^{\mathcal{R}} \cdot \mathbf{e}_{Sl}^{\mathcal{R}} = \mathbf{e}_{Sk}^{\mathcal{R}} \cdot \dot{\mathbf{e}}_{Sl}^{\mathcal{R}} = \dot{\mathbf{e}}_{Sl}^{\mathcal{R}} \cdot \mathbf{e}_{Sk}^{\mathcal{R}} \quad (7.1.56)$$

By adapting this result to $j \neq l$:

$$-\dot{\mathbf{e}}_{Sj}^{\mathcal{R}} \cdot \mathbf{e}_{Sl}^{\mathcal{R}} = \dot{\mathbf{e}}_{Sl}^{\mathcal{R}} \cdot \mathbf{e}_{Sj}^{\mathcal{R}} \quad (7.1.57)$$

and inserting this relation and by applying the vector triple product:

$$\mathbf{a} \times (\mathbf{b} \times \mathbf{c}) = (\mathbf{a} \cdot \mathbf{c}) \mathbf{b} - (\mathbf{a} \cdot \mathbf{b}) \mathbf{c} \quad (7.1.58)$$

the sum of the first and the third term of (7.1.51) can be reformulated in the following way:

$$\left(\dot{\mathbf{e}}_{Sj}^{\mathcal{R}} \cdot \mathbf{e}_{Sk}^{\mathcal{R}} \right) \mathbf{e}_{Sl}^{\mathcal{R}} + \left(\dot{\mathbf{e}}_{Sl}^{\mathcal{R}} \cdot \mathbf{e}_{Sj}^{\mathcal{R}} \right) \mathbf{e}_{Sk}^{\mathcal{R}} = \left(\dot{\mathbf{e}}_{Sj}^{\mathcal{R}} \cdot \mathbf{e}_{Sk}^{\mathcal{R}} \right) \mathbf{e}_{Sl}^{\mathcal{R}} - \left(\dot{\mathbf{e}}_{Sj}^{\mathcal{R}} \cdot \mathbf{e}_{Sl}^{\mathcal{R}} \right) \mathbf{e}_{Sk}^{\mathcal{R}} = \dot{\mathbf{e}}_{Sj}^{\mathcal{R}} \times \left(\mathbf{e}_{Sl}^{\mathcal{R}} \times \mathbf{e}_{Sk}^{\mathcal{R}} \right) \quad (7.1.59)$$

Applying the anticommutativity of the cross product and the relation (7.1.50) leads to:

$$\begin{aligned} \left(\dot{\mathbf{e}}_{Sj}^{\mathcal{R}} \cdot \mathbf{e}_{Sk}^{\mathcal{R}}\right) \mathbf{e}_{Sl}^{\mathcal{R}} + \left(\dot{\mathbf{e}}_{Sl}^{\mathcal{R}} \cdot \mathbf{e}_{Sj}^{\mathcal{R}}\right) \mathbf{e}_{Sk}^{\mathcal{R}} &= \dot{\mathbf{e}}_{Sj}^{\mathcal{R}} \times \left(\mathbf{e}_{Sl}^{\mathcal{R}} \times \mathbf{e}_{Sk}^{\mathcal{R}}\right) = -\left(-\mathbf{e}_{Sk}^{\mathcal{R}} \times \mathbf{e}_{Sl}^{\mathcal{R}}\right) \times \dot{\mathbf{e}}_{Sj}^{\mathcal{R}} \\ &= \underbrace{\left(\mathbf{e}_{Sk}^{\mathcal{R}} \times \mathbf{e}_{Sl}^{\mathcal{R}}\right)}_{\mathbf{e}_{Sj}^{\mathcal{R}}} \times \dot{\mathbf{e}}_{Sj}^{\mathcal{R}} = \mathbf{e}_{Sj}^{\mathcal{R}} \times \dot{\mathbf{e}}_{Sj}^{\mathcal{R}} \end{aligned} \quad (7.1.60)$$

Apparently, the sum of the first and the third term of the angular velocity $\omega_{\mathcal{R}\mathcal{S}}^{\mathcal{R}}$ can be expressed by just one column vector and its derivative. As a result, it is obtained:

$$\omega_{\mathcal{R}\mathcal{S}}^{\mathcal{R}} = \left(\dot{\mathbf{e}}_{Sj}^{\mathcal{R}} \cdot \mathbf{e}_{Sk}^{\mathcal{R}}\right) \mathbf{e}_{Sl}^{\mathcal{R}} + \left(\dot{\mathbf{e}}_{Sk}^{\mathcal{R}} \cdot \mathbf{e}_{Sl}^{\mathcal{R}}\right) \mathbf{e}_{Sj}^{\mathcal{R}} + \left(\dot{\mathbf{e}}_{Sl}^{\mathcal{R}} \cdot \mathbf{e}_{Sj}^{\mathcal{R}}\right) \mathbf{e}_{Sk}^{\mathcal{R}} = \mathbf{e}_{Sj}^{\mathcal{R}} \times \dot{\mathbf{e}}_{Sj}^{\mathcal{R}} + \left(\dot{\mathbf{e}}_{Sk}^{\mathcal{R}} \cdot \mathbf{e}_{Sl}^{\mathcal{R}}\right) \mathbf{e}_{Sj}^{\mathcal{R}} \quad (7.1.61)$$

In order to complete the formulation, either the vector $\dot{\mathbf{e}}_{Sk}^{\mathcal{R}}$ or the vector $\mathbf{e}_{Sl}^{\mathcal{R}}$ has to be eliminated. Here, the consideration of the products $\mathbf{e}_{Sk}^{\mathcal{R}} \times \mathbf{e}_{Sj}^{\mathcal{R}}$ and $\mathbf{e}_{Sl}^{\mathcal{R}} \times \mathbf{e}_{Sj}^{\mathcal{R}}$ is useful; by inserting the relation (7.1.50) between the column vectors, applying the vector triple product and taking advantage of the fact that the column vectors are orthogonal unit vectors it is obtained:

$$\mathbf{e}_{Sk}^{\mathcal{R}} \times \mathbf{e}_{Sj}^{\mathcal{R}} = \mathbf{e}_{Sk}^{\mathcal{R}} \times \left(\mathbf{e}_{Sk}^{\mathcal{R}} \times \mathbf{e}_{Sl}^{\mathcal{R}}\right) = \underbrace{\left(\mathbf{e}_{Sk}^{\mathcal{R}} \cdot \mathbf{e}_{Sl}^{\mathcal{R}}\right)}_0 \mathbf{e}_{Sk}^{\mathcal{R}} - \underbrace{\left(\mathbf{e}_{Sk}^{\mathcal{R}} \cdot \mathbf{e}_{Sk}^{\mathcal{R}}\right)}_1 \mathbf{e}_{Sl}^{\mathcal{R}} = -\mathbf{e}_{Sl}^{\mathcal{R}} \quad (7.1.62)$$

$$\mathbf{e}_{Sl}^{\mathcal{R}} \times \mathbf{e}_{Sj}^{\mathcal{R}} = \mathbf{e}_{Sl}^{\mathcal{R}} \times \left(\mathbf{e}_{Sk}^{\mathcal{R}} \times \mathbf{e}_{Sl}^{\mathcal{R}}\right) = \underbrace{\left(\mathbf{e}_{Sl}^{\mathcal{R}} \cdot \mathbf{e}_{Sl}^{\mathcal{R}}\right)}_1 \mathbf{e}_{Sk}^{\mathcal{R}} - \underbrace{\left(\mathbf{e}_{Sl}^{\mathcal{R}} \cdot \mathbf{e}_{Sk}^{\mathcal{R}}\right)}_0 \mathbf{e}_{Sl}^{\mathcal{R}} = \mathbf{e}_{Sk}^{\mathcal{R}} \quad (7.1.63)$$

Furthermore, the commutativity of the scalar triple product, which is proven in appendix A.5.2, is required:

$$\mathbf{a} \cdot (\mathbf{b} \times \mathbf{c}) = \mathbf{b} \cdot (\mathbf{c} \times \mathbf{a}) = \mathbf{c} \cdot (\mathbf{a} \times \mathbf{b}) \quad (7.1.64)$$

The product $\dot{\mathbf{e}}_{Sk}^{\mathcal{R}} \cdot \mathbf{e}_{Sl}^{\mathcal{R}}$ can now be reformulated by subsequently applying the relation (7.1.62), the anticommutativity of the cross product and the commutativity of the scalar triple product according to (7.1.64). This leads to:

$$\dot{\mathbf{e}}_{Sk}^{\mathcal{R}} \cdot \mathbf{e}_{Sl}^{\mathcal{R}} = \dot{\mathbf{e}}_{Sk}^{\mathcal{R}} \cdot \left(-\mathbf{e}_{Sk}^{\mathcal{R}} \times \mathbf{e}_{Sj}^{\mathcal{R}}\right) = \dot{\mathbf{e}}_{Sk}^{\mathcal{R}} \cdot \left(\mathbf{e}_{Sj}^{\mathcal{R}} \times \mathbf{e}_{Sk}^{\mathcal{R}}\right) = \mathbf{e}_{Sj}^{\mathcal{R}} \cdot \left(\mathbf{e}_{Sk}^{\mathcal{R}} \times \dot{\mathbf{e}}_{Sk}^{\mathcal{R}}\right) \quad (7.1.65)$$

Alternatively, the product can be reformulated by subsequently applying the relation (7.1.56), the relation (7.1.63), the commutativity of the triple scalar product according to (7.1.64) and the anticommutativity of the vector product; this results in:

$$\dot{\mathbf{e}}_{Sk}^{\mathcal{R}} \cdot \mathbf{e}_{Sl}^{\mathcal{R}} = -\dot{\mathbf{e}}_{Sl}^{\mathcal{R}} \cdot \mathbf{e}_{Sk}^{\mathcal{R}} = -\dot{\mathbf{e}}_{Sl}^{\mathcal{R}} \cdot \left(\mathbf{e}_{Sl}^{\mathcal{R}} \times \mathbf{e}_{Sj}^{\mathcal{R}}\right) = \mathbf{e}_{Sj}^{\mathcal{R}} \cdot \left(-\dot{\mathbf{e}}_{Sl}^{\mathcal{R}} \times \mathbf{e}_{Sl}^{\mathcal{R}}\right) = \mathbf{e}_{Sj}^{\mathcal{R}} \cdot \left(\mathbf{e}_{Sl}^{\mathcal{R}} \times \dot{\mathbf{e}}_{Sl}^{\mathcal{R}}\right) \quad (7.1.66)$$

In total, two formulations for the angular velocity are obtained, which use only two of the three column vectors:

$$\omega_{\mathcal{R}\mathcal{S}}^{\mathcal{R}} = \mathbf{e}_{Sj}^{\mathcal{R}} \times \dot{\mathbf{e}}_{Sj}^{\mathcal{R}} + \left(\dot{\mathbf{e}}_{Sk}^{\mathcal{R}} \cdot \mathbf{e}_{Sl}^{\mathcal{R}}\right) \mathbf{e}_{Sj}^{\mathcal{R}} = \mathbf{e}_{Sj}^{\mathcal{R}} \times \dot{\mathbf{e}}_{Sj}^{\mathcal{R}} + \left(\mathbf{e}_{Sj}^{\mathcal{R}} \cdot \left[\mathbf{e}_{Sk}^{\mathcal{R}} \times \dot{\mathbf{e}}_{Sk}^{\mathcal{R}}\right]\right) \mathbf{e}_{Sj}^{\mathcal{R}} \quad (7.1.67)$$

$$= \mathbf{e}_{Sj}^{\mathcal{R}} \times \dot{\mathbf{e}}_{Sj}^{\mathcal{R}} + \left(\mathbf{e}_{Sj}^{\mathcal{R}} \cdot \left[\mathbf{e}_{Sl}^{\mathcal{R}} \times \dot{\mathbf{e}}_{Sl}^{\mathcal{R}}\right]\right) \mathbf{e}_{Sj}^{\mathcal{R}} \quad (7.1.68)$$

It should be pointed out that both formulations (7.1.67) and (7.1.68) are valid for all index triples $\langle j, k, l \rangle$ given by:

$$\langle j, k, l \rangle \in \{\langle 1, 2, 3 \rangle, \langle 2, 3, 1 \rangle, \langle 3, 1, 2 \rangle\} \quad (7.1.69)$$

Therefore, the index j can have the values $j = 1$, $j = 2$ and $j = 3$ so that each of the vectors $\mathbf{e}_{S1}^{\mathcal{R}}$, $\mathbf{e}_{S2}^{\mathcal{R}}$ and $\mathbf{e}_{S3}^{\mathcal{R}}$ can be used as the vector $\mathbf{e}_{Sj}^{\mathcal{R}}$. Furthermore, it can be seen that both formulations (7.1.67) and (7.1.67) have an analogous structure, i.e. the formulation (7.1.67) can be transformed into the formulation (7.1.67) by simply replacing the vector $\mathbf{e}_{Sk}^{\mathcal{R}}$ by the vector $\mathbf{e}_{Sl}^{\mathcal{R}}$. This means that for the second term of the angular velocity any vector $\mathbf{e}_{Sk}^{\mathcal{R}}$ or $\mathbf{e}_{Sl}^{\mathcal{R}}$ except the already chosen vector $\mathbf{e}_{Sj}^{\mathcal{R}}$ can be used. For the present case this means that for the angular velocity the normalized normal vector $c_N \mathbf{n}^{\mathcal{R}}$ can be assigned to the vector $\mathbf{e}_{Sj}^{\mathcal{R}}$ and any normalized tangential vector $c_\xi \mathbf{t}_\xi^{\mathcal{R}} + c_\eta \mathbf{t}_\eta^{\mathcal{R}}$ can be assigned to the vector $\mathbf{e}_{Sk}^{\mathcal{R}}$ or $\mathbf{e}_{Sl}^{\mathcal{R}}$; however, the actual indices of the axes, to which the vectors are assigned, do not matter. By defining the normal unit vector $\mathbf{e}_N^{\mathcal{R}}$ and the tangential unit vector $\mathbf{e}_T^{\mathcal{R}}$

$$\mathbf{y}_N^{\mathcal{R}} = c_N \mathbf{n}^{\mathcal{R}} \Rightarrow \mathbf{e}_N^{\mathcal{R}} = \frac{\mathbf{y}_N^{\mathcal{R}}}{|\mathbf{y}_N^{\mathcal{R}}|}, \quad \mathbf{y}_T^{\mathcal{R}} = c_\xi \mathbf{t}_\xi^{\mathcal{R}} + c_\eta \mathbf{t}_\eta^{\mathcal{R}} \Rightarrow \mathbf{e}_T^{\mathcal{R}} = \frac{\mathbf{y}_T^{\mathcal{R}}}{|\mathbf{y}_T^{\mathcal{R}}|} \quad (7.1.70)$$

the angular velocity at the surface can be formulated in the following way:

$$\omega_{\mathcal{R}S}^{\mathcal{R}} = \mathbf{e}_N^{\mathcal{R}} \times \dot{\mathbf{e}}_N^{\mathcal{R}} + \left(\mathbf{e}_N^{\mathcal{R}} \cdot \left[\mathbf{e}_T^{\mathcal{R}} \times \dot{\mathbf{e}}_T^{\mathcal{R}} \right] \right) \mathbf{e}_N^{\mathcal{R}} \quad (7.1.71)$$

The angular velocity $\omega_{\mathcal{R}S}^{\mathcal{R}}$ contains two products of the structure $\mathbf{e}_I^{\mathcal{R}} \times \dot{\mathbf{e}}_I^{\mathcal{R}}$; therefore, this product will be analyzed in the following considerations. For a unit vector \mathbf{e}_I , which is obtained by normalizing the vector $\mathbf{y}_I \neq \mathbf{0}$, it is valid:

$$|\mathbf{y}_I| = \sqrt{\mathbf{y}_I \cdot \mathbf{y}_I} = (\mathbf{y}_I \cdot \mathbf{y}_I)^{\frac{1}{2}} \Rightarrow \mathbf{e}_I = \frac{1}{|\mathbf{y}_I|} \mathbf{y}_I = \frac{1}{\sqrt{\mathbf{y}_I \cdot \mathbf{y}_I}} \mathbf{y}_I = (\mathbf{y}_I \cdot \mathbf{y}_I)^{-\frac{1}{2}} \mathbf{y}_I \quad (7.1.72)$$

Using this formulation, the derivative $\dot{\mathbf{e}}_I$ of the unit vector \mathbf{e}_I is obtained to:

$$\begin{aligned} \dot{\mathbf{e}}_I &= \frac{d\mathbf{e}_I}{dt} = \frac{d}{dt} \left((\mathbf{y}_I \cdot \mathbf{y}_I)^{-\frac{1}{2}} \mathbf{y}_I \right) = \frac{d}{dt} \left((\mathbf{y}_I \cdot \mathbf{y}_I)^{-\frac{1}{2}} \right) \mathbf{y}_I + (\mathbf{y}_I \cdot \mathbf{y}_I)^{-\frac{1}{2}} \frac{d\mathbf{y}_I}{dt} \\ &= -\frac{1}{2} (\mathbf{y}_I \cdot \mathbf{y}_I)^{-\frac{3}{2}} (\dot{\mathbf{y}}_I \cdot \mathbf{y}_I + \mathbf{y}_I \cdot \dot{\mathbf{y}}_I) \mathbf{y}_I + (\mathbf{y}_I \cdot \mathbf{y}_I)^{-\frac{1}{2}} \dot{\mathbf{y}}_I \end{aligned} \quad (7.1.73)$$

Based on this result, the cross product $\mathbf{e}_I \times \dot{\mathbf{e}}_I$ can be evaluated; in this context it should be noted that the cross product of two equal vectors is the zero vector, i.e. $\mathbf{r} \times \mathbf{r} = \mathbf{0}$.

$$\begin{aligned} \mathbf{e}_I \times \dot{\mathbf{e}}_I &= (\mathbf{y}_I \cdot \mathbf{y}_I)^{-\frac{1}{2}} \mathbf{y}_I \times \left(-\frac{1}{2} (\mathbf{y}_I \cdot \mathbf{y}_I)^{-\frac{3}{2}} (\dot{\mathbf{y}}_I \cdot \mathbf{y}_I + \mathbf{y}_I \cdot \dot{\mathbf{y}}_I) \mathbf{y}_I + (\mathbf{y}_I \cdot \mathbf{y}_I)^{-\frac{1}{2}} \dot{\mathbf{y}}_I \right) \\ &= -\frac{1}{2} (\mathbf{y}_I \cdot \mathbf{y}_I)^{-2} (\dot{\mathbf{y}}_I \cdot \mathbf{y}_I + \mathbf{y}_I \cdot \dot{\mathbf{y}}_I) \underbrace{\mathbf{y}_I \times \mathbf{y}_I}_{\mathbf{0}} + (\mathbf{y}_I \cdot \mathbf{y}_I)^{-1} \mathbf{y}_I \times \dot{\mathbf{y}}_I = \frac{\mathbf{y}_I \times \dot{\mathbf{y}}_I}{\mathbf{y}_I \cdot \mathbf{y}_I} \end{aligned} \quad (7.1.74)$$

Based on this, the first term of (7.1.71) can be evaluated; it is valid:

$$\mathbf{e}_N^{\mathcal{R}} \times \dot{\mathbf{e}}_N^{\mathcal{R}} = \frac{\mathbf{y}_N^{\mathcal{R}} \times \dot{\mathbf{y}}_N^{\mathcal{R}}}{\mathbf{y}_N^{\mathcal{R}} \cdot \mathbf{y}_N^{\mathcal{R}}} = \frac{(c_N \mathbf{n}^{\mathcal{R}}) \times (c_N \dot{\mathbf{n}}^{\mathcal{R}})}{(c_N \mathbf{n}^{\mathcal{R}}) \cdot (c_N \dot{\mathbf{n}}^{\mathcal{R}})} = \frac{c_N^2 \mathbf{n}^{\mathcal{R}} \times \dot{\mathbf{n}}^{\mathcal{R}}}{c_N^2 \mathbf{n}^{\mathcal{R}} \cdot \dot{\mathbf{n}}^{\mathcal{R}}} = \frac{\mathbf{n}^{\mathcal{R}} \times \dot{\mathbf{n}}^{\mathcal{R}}}{\mathbf{n}^{\mathcal{R}} \cdot \dot{\mathbf{n}}^{\mathcal{R}}} \quad (7.1.75)$$

It turns out that the factor c_N , which has been introduced in order to change the orientation of the normal vector $\mathbf{n}^{\mathcal{R}}$ is eliminated so it does not matter whether the normal vector is determined by $\mathbf{n}^{\mathcal{R}} = \mathbf{t}_\xi^{\mathcal{R}} \times \mathbf{t}_\eta^{\mathcal{R}}$ or by $\mathbf{n}^{\mathcal{R}} = \mathbf{t}_\eta^{\mathcal{R}} \times \mathbf{t}_\xi^{\mathcal{R}}$. Thereby, the first term $\mathbf{e}_N^{\mathcal{R}} \times \dot{\mathbf{e}}_N^{\mathcal{R}}$ of the angular velocity $\omega_{\mathcal{R}S}^{\mathcal{R}}$ is uniquely defined.

By applying the relation (7.1.74) and the definition of the unit vector it is obtained for the second term of (7.1.71):

$$\left(\mathbf{e}_N^{\mathcal{R}} \cdot \left[\mathbf{e}_T^{\mathcal{R}} \times \dot{\mathbf{e}}_T^{\mathcal{R}}\right]\right) \mathbf{e}_N^{\mathcal{R}} = \left(\frac{\mathbf{y}_N^{\mathcal{R}}}{\sqrt{\mathbf{y}_N^{\mathcal{R}} \cdot \mathbf{y}_N^{\mathcal{R}}}} \cdot \frac{\mathbf{y}_T^{\mathcal{R}} \times \dot{\mathbf{y}}_T^{\mathcal{R}}}{\mathbf{y}_T^{\mathcal{R}} \cdot \dot{\mathbf{y}}_T^{\mathcal{R}}}\right) \frac{\mathbf{y}_N^{\mathcal{R}}}{\sqrt{\mathbf{y}_N^{\mathcal{R}} \cdot \mathbf{y}_N^{\mathcal{R}}}} = \frac{\mathbf{y}_N^{\mathcal{R}} \cdot \left[\mathbf{y}_T^{\mathcal{R}} \times \dot{\mathbf{y}}_T^{\mathcal{R}}\right]}{\left(\mathbf{y}_N^{\mathcal{R}} \cdot \mathbf{y}_N^{\mathcal{R}}\right) \left(\mathbf{y}_T^{\mathcal{R}} \cdot \dot{\mathbf{y}}_T^{\mathcal{R}}\right)} \mathbf{y}_N^{\mathcal{R}} \quad (7.1.76)$$

Inserting the relation $\mathbf{y}_N^{\mathcal{R}} = c_N \mathbf{n}^{\mathcal{R}}$ according to (7.1.70) leads to:

$$\begin{aligned} \left(\mathbf{e}_N^{\mathcal{R}} \cdot \left[\mathbf{e}_T^{\mathcal{R}} \times \dot{\mathbf{e}}_T^{\mathcal{R}}\right]\right) \mathbf{e}_N^{\mathcal{R}} &= \frac{\mathbf{y}_N^{\mathcal{R}} \cdot \left[\mathbf{y}_T^{\mathcal{R}} \times \dot{\mathbf{y}}_T^{\mathcal{R}}\right]}{\left(\mathbf{y}_N^{\mathcal{R}} \cdot \mathbf{y}_N^{\mathcal{R}}\right) \left(\mathbf{y}_T^{\mathcal{R}} \cdot \dot{\mathbf{y}}_T^{\mathcal{R}}\right)} \mathbf{y}_N^{\mathcal{R}} = \frac{c_N \mathbf{n}^{\mathcal{R}} \cdot \left[\mathbf{y}_T^{\mathcal{R}} \times \dot{\mathbf{y}}_T^{\mathcal{R}}\right]}{\left(c_N \mathbf{n}^{\mathcal{R}} \cdot c_N \mathbf{n}^{\mathcal{R}}\right) \left(\mathbf{y}_T^{\mathcal{R}} \cdot \dot{\mathbf{y}}_T^{\mathcal{R}}\right)} c_N \mathbf{n}^{\mathcal{R}} \\ &= \frac{c_N^2 \mathbf{n}^{\mathcal{R}} \cdot \left(\mathbf{y}_T^{\mathcal{R}} \times \dot{\mathbf{y}}_T^{\mathcal{R}}\right)}{c_N^2 \left(\mathbf{n}^{\mathcal{R}} \cdot \mathbf{n}^{\mathcal{R}}\right) \left(\mathbf{y}_T^{\mathcal{R}} \cdot \dot{\mathbf{y}}_T^{\mathcal{R}}\right)} \mathbf{n}^{\mathcal{R}} = \frac{\mathbf{n}^{\mathcal{R}} \cdot \left(\mathbf{y}_T^{\mathcal{R}} \times \dot{\mathbf{y}}_T^{\mathcal{R}}\right)}{\left(\mathbf{n}^{\mathcal{R}} \cdot \mathbf{n}^{\mathcal{R}}\right) \left(\mathbf{y}_T^{\mathcal{R}} \cdot \dot{\mathbf{y}}_T^{\mathcal{R}}\right)} \mathbf{n}^{\mathcal{R}} \end{aligned} \quad (7.1.77)$$

Also here, the scalar factor c_N for the normal vector is eliminated. In total, it is obtained for the angular velocity at the surface:

$$\omega_{\mathcal{R}\mathcal{S}}^{\mathcal{R}} = \mathbf{e}_N^{\mathcal{R}} \times \dot{\mathbf{e}}_N^{\mathcal{R}} + \left(\mathbf{e}_N^{\mathcal{R}} \cdot \left[\mathbf{e}_T^{\mathcal{R}} \times \dot{\mathbf{e}}_T^{\mathcal{R}}\right]\right) \mathbf{e}_N^{\mathcal{R}} = \frac{\mathbf{n}^{\mathcal{R}} \times \dot{\mathbf{n}}^{\mathcal{R}}}{\mathbf{n}^{\mathcal{R}} \cdot \mathbf{n}^{\mathcal{R}}} + \frac{\mathbf{n}^{\mathcal{R}} \cdot \left(\mathbf{y}_T^{\mathcal{R}} \times \dot{\mathbf{y}}_T^{\mathcal{R}}\right)}{\left(\mathbf{n}^{\mathcal{R}} \cdot \mathbf{n}^{\mathcal{R}}\right) \left(\mathbf{y}_T^{\mathcal{R}} \cdot \dot{\mathbf{y}}_T^{\mathcal{R}}\right)} \mathbf{n}^{\mathcal{R}} \quad (7.1.78)$$

Also for the angular velocity, the case of the rectangular bar shall be considered as a example; again, the body-fixed frame \mathcal{B} is used as the reference frame \mathcal{R} . For the vectors $\mathbf{t}_x^{\mathcal{B}}$, $\mathbf{t}_y^{\mathcal{B}}$, $\mathbf{n}^{\mathcal{B}}$ and their derivatives it is valid:

$$\mathbf{t}_x^{\mathcal{B}} = \begin{bmatrix} 1 \\ 0 \\ 0 \end{bmatrix} \Rightarrow \dot{\mathbf{t}}_x^{\mathcal{B}} = \mathbf{0}, \quad \mathbf{t}_y^{\mathcal{B}} = \begin{bmatrix} u_y \\ 1 \\ 0 \end{bmatrix} \Rightarrow \dot{\mathbf{t}}_y^{\mathcal{B}} = \begin{bmatrix} \dot{u}_y \\ 0 \\ 0 \end{bmatrix}, \quad \mathbf{n}^{\mathcal{B}} = \begin{bmatrix} 0 \\ 0 \\ 1 \end{bmatrix} \Rightarrow \dot{\mathbf{n}}^{\mathcal{B}} = \mathbf{0} \Rightarrow \mathbf{n}^{\mathcal{B}} \times \dot{\mathbf{n}}^{\mathcal{B}} = \mathbf{0} \quad (7.1.79)$$

In the present case, the normal vector $\mathbf{n}^{\mathcal{B}}$ and the tangential vector $\mathbf{t}_x^{\mathcal{B}}$ are constant; thereby, their derivatives $\dot{\mathbf{n}}^{\mathcal{B}}$ and $\dot{\mathbf{t}}_x^{\mathcal{B}}$ are zero vectors. Because of $\dot{\mathbf{n}} = \mathbf{0}$, the first term of the angular velocity according to (7.1.78) vanishes. According to (7.1.70) each linear combination of the “geometric” tangential vectors $\mathbf{t}_\xi^{\mathcal{R}}$ and $\mathbf{t}_\eta^{\mathcal{R}}$ can be used as the tangential vector $\mathbf{y}_T^{\mathcal{R}}$. As done in the previous section 7.1.1 two obvious possibilities shall be considered. One possibility is to use the vector $\mathbf{t}_x^{\mathcal{B}}$ as the tangential vector $\mathbf{y}_T^{\mathcal{B}}$. Since the vector $\mathbf{t}_x^{\mathcal{B}}$ is constant, its derivative $\dot{\mathbf{t}}_x^{\mathcal{B}}$ is equal to the zero vector so that the entire angular velocity is zero:

$$\mathbf{y}_T^{\mathcal{B}} = \mathbf{t}_x^{\mathcal{B}} \Rightarrow \dot{\mathbf{y}}_T^{\mathcal{B}} = \dot{\mathbf{t}}_x^{\mathcal{B}} = \mathbf{0} \Rightarrow \mathbf{y}_T^{\mathcal{B}} \times \dot{\mathbf{y}}_T^{\mathcal{B}} = \mathbf{0} \Rightarrow \omega_{\mathcal{B}\mathcal{S},x}^{\mathcal{B}} = \mathbf{0} \quad (7.1.80)$$

Another obvious possibility is to use the vector $\mathbf{t}_y^{\mathcal{B}}$ as the tangential vector $\mathbf{y}_T^{\mathcal{B}}$. In this case, it is obtained for the numerator of the fraction contained in (7.1.78):

$$\mathbf{y}_T^{\mathcal{B}} = \mathbf{t}_y^{\mathcal{B}} \Rightarrow \mathbf{n}^{\mathcal{B}} \cdot \left(\mathbf{y}_T^{\mathcal{B}} \times \dot{\mathbf{y}}_T^{\mathcal{B}}\right) = \mathbf{n}^{\mathcal{B}} \cdot \left(\mathbf{t}_y^{\mathcal{B}} \times \dot{\mathbf{t}}_y^{\mathcal{B}}\right) = \mathbf{n}^{\mathcal{B}} \cdot \left(\begin{bmatrix} u_y \\ 1 \\ 0 \end{bmatrix} \times \begin{bmatrix} \dot{u}_y \\ 0 \\ 0 \end{bmatrix}\right) = \begin{bmatrix} 0 \\ 0 \\ 1 \end{bmatrix} \cdot \begin{bmatrix} 0 \\ 0 \\ -\dot{u}_y \end{bmatrix} = -\dot{u}_y \quad (7.1.81)$$

Finally, it is obtained for the angular velocity:

$$\mathbf{n}^B \cdot \mathbf{n}^B = 1, \mathbf{t}_y^B \cdot \mathbf{t}_y^B = 1 + u_y^2 \Rightarrow \omega_{BS,y}^B = \frac{\mathbf{n}^B \times \dot{\mathbf{n}}^B}{\underbrace{\mathbf{n}^B \cdot \mathbf{n}^B}_0} + \frac{\mathbf{n}^B \cdot (\mathbf{t}_y^B \times \dot{\mathbf{t}}_y^B)}{(\mathbf{n}^B \cdot \mathbf{n}^B) (\mathbf{t}_y^B \cdot \mathbf{t}_y^B)} \mathbf{n}^B = \frac{-\dot{u}_y}{1 + u_y^2} \begin{bmatrix} 0 \\ 0 \\ 1 \end{bmatrix} \quad (7.1.82)$$

The tangential vector \mathbf{t}_y^B changes its direction due to the deformation of the bar so that a rotation is obtained.

Due to the shear deformation the angle between the tangential vectors \mathbf{t}_x^B and \mathbf{t}_y^B is not constant, or in other words, both tangential vectors are rotating with different angular velocities. For the rotation of a frame consisting of several vectors it is required that the vectors maintain their orientation relative to each other. Therefore, it is reasonable to use the medium value of the two results; in the present case this leads to:

$$\omega_{BS}^B = \frac{1}{2} (\omega_{BS,x}^B + \omega_{BS,y}^B) = \frac{1}{2} \frac{-\dot{u}_y}{1 + u_y^2} \begin{bmatrix} 0 \\ 0 \\ 1 \end{bmatrix} \quad (7.1.83)$$

By using the approximative method based on the deformation gradient, which has been shown in the section 7.1, the following result has been obtained according to (7.1.12):

$$\boldsymbol{\omega} = -\frac{1}{2} \dot{u}_y \begin{bmatrix} 0 \\ 0 \\ 1 \end{bmatrix} \quad (7.1.84)$$

By assuming that the deformations are very small, it is valid $u_y \ll 1$; from this it follows $1 + u_y^2 \approx 1$ so that the two results (7.1.83) and (7.1.84) are nearly equal.

Based on this, it is reasonable to determine the second term of (7.1.78) as a medium value of the terms, which are obtained for setting the tangential vector \mathbf{y}_T^R equal to one of the “geometric” tangential vectors \mathbf{t}_ξ^B and \mathbf{t}_η^B . This leads to:

$$\mathbf{y}_T^R = \mathbf{t}_\xi^R \Rightarrow \omega_{RS}^R = \frac{\mathbf{n}^R \times \dot{\mathbf{n}}^R}{\mathbf{n}^R \cdot \mathbf{n}^R} + \frac{\mathbf{n}^R \cdot (\mathbf{t}_\xi^R \times \dot{\mathbf{t}}_\xi^R)}{(\mathbf{n}^R \cdot \mathbf{n}^R) (\mathbf{t}_\xi^R \cdot \mathbf{t}_\xi^R)} \mathbf{n}^R \quad (7.1.85)$$

$$\mathbf{y}_T^R = \mathbf{t}_\eta^R \Rightarrow \omega_{RS}^R = \frac{\mathbf{n}^R \times \dot{\mathbf{n}}^R}{\mathbf{n}^R \cdot \mathbf{n}^R} + \frac{\mathbf{n}^R \cdot (\mathbf{t}_\eta^R \times \dot{\mathbf{t}}_\eta^R)}{(\mathbf{n}^R \cdot \mathbf{n}^R) (\mathbf{t}_\eta^R \cdot \mathbf{t}_\eta^R)} \mathbf{n}^R \quad (7.1.86)$$

$$\Rightarrow \omega_{RS}^R = \frac{\mathbf{n}^R \times \dot{\mathbf{n}}^R}{\mathbf{n}^R \cdot \mathbf{n}^R} + \frac{1}{2} \left(\frac{\mathbf{n}^R \cdot (\mathbf{t}_\xi^R \times \dot{\mathbf{t}}_\xi^R)}{(\mathbf{t}_\xi^R \cdot \mathbf{t}_\xi^R)} + \frac{\mathbf{n}^R \cdot (\mathbf{t}_\eta^R \times \dot{\mathbf{t}}_\eta^R)}{(\mathbf{t}_\eta^R \cdot \mathbf{t}_\eta^R)} \right) \frac{\mathbf{n}^R}{\mathbf{n}^R \cdot \mathbf{n}^R} \quad (7.1.87)$$

Thereby, a formulation for the angular velocity at the surface on the flexible body is obtained. Once again, it should be pointed out that this formulation is ultimately based on the tangential vectors \mathbf{t}_ξ^R and \mathbf{t}_η^R and their derivatives $\dot{\mathbf{t}}_\xi^R$ and $\dot{\mathbf{t}}_\eta^R$. The normal vector \mathbf{n}^R is determined by the vector product of the tangential vectors, whereby the sequence of the vectors, which affects the sign of the product, is not prescribed, but has to be used consistently. This means that one of the formulations $\mathbf{n}^R = \mathbf{t}_\xi^R \times \mathbf{t}_\eta^R$ or $\mathbf{n}^R = \mathbf{t}_\eta^R \times \mathbf{t}_\xi^R$ has to be selected and the selected formulation has to be used consistently.

7.1.3 Application to the rail

The methods, which have been developed in the previous sections 7.1.1 and 7.1.2, shall now be applied to the flexible bodies representing the rail in order to determine the kinematics of the frame \mathcal{M}_{Ri} . In this context it should be noticed that the frame \mathcal{M}_{Ri} is not necessarily identical to the surface frame \mathcal{S} which has been considered in the previous sections. Therefore, a further rotation matrix $\mathbf{S}^{S\mathcal{M}_{Ri}}$ is introduced so that the rotation between the reference frame \mathcal{R} of the rail and the frame \mathcal{M}_{Ri} is formulated in the following way:

$$\mathbf{S}^{\mathcal{R}\mathcal{M}_{Ri}} = \mathbf{S}^{\mathcal{R}\mathcal{S}} \mathbf{S}^{S\mathcal{M}_{Ri}} \quad (7.1.88)$$

The matrix $\mathbf{S}^{S\mathcal{M}_{Ri}}$ only expresses the different orientations of the surface and the marker so that it is constant. Therefore, it has to be calculated only once and it can be determined by considering the reference state which is usually the undeformed state of the flexible body; the matrices for this state will be denoted by the index 0. In this case, the matrix $\mathbf{S}_0^{\mathcal{R}\mathcal{M}_{Ri}}$ is given; e.g. by the frame in which the profile function is defined. Then, the matrix $\mathbf{S}^{S\mathcal{M}_{Ri}}$ is obtained to:

$$\mathbf{S}_0^{\mathcal{R}\mathcal{M}_{Ri}} = \mathbf{S}_0^{\mathcal{R}\mathcal{S}} \mathbf{S}^{S\mathcal{M}_{Ri}} \Rightarrow \mathbf{S}^{S\mathcal{M}_{Ri}} = \mathbf{S}_0^{\mathcal{R}\mathcal{S}^{-1}} \mathbf{S}_0^{\mathcal{R}\mathcal{M}_{Ri}} = \mathbf{S}_0^{\mathcal{R}\mathcal{S}^T} \mathbf{S}_0^{\mathcal{R}\mathcal{M}_{Ri}} \quad (7.1.89)$$

Since the matrix $\mathbf{S}^{S\mathcal{M}_{Ri}}$ is constant, its derivative vanishes, i.e. $\dot{\mathbf{S}}^{S\mathcal{M}_{Ri}} = \mathbf{0}$, so that it has no influence on the angular velocity of the frame. Therefore, it is valid:

$$\tilde{\omega}_{\mathcal{R}\mathcal{M}_{Ri}}^{\mathcal{R}} = \dot{\mathbf{S}}^{\mathcal{R}\mathcal{M}_{Ri}} \mathbf{S}^{\mathcal{R}\mathcal{M}_{Ri}T} = \dot{\mathbf{S}}^{\mathcal{R}\mathcal{S}} \underbrace{\mathbf{S}^{S\mathcal{M}_{Ri}} \mathbf{S}^{S\mathcal{M}_{Ri}T}}_{\mathbf{I}} \mathbf{S}^{\mathcal{R}\mathcal{S}T} = \dot{\mathbf{S}}^{\mathcal{R}\mathcal{S}} \mathbf{S}^{\mathcal{R}\mathcal{S}T} = \tilde{\omega}_{\mathcal{R}\mathcal{S}}^{\mathcal{R}} \Rightarrow \tilde{\omega}_{\mathcal{R}\mathcal{M}_{Ri}}^{\mathcal{R}} = \tilde{\omega}_{\mathcal{R}\mathcal{S}}^{\mathcal{R}} \quad (7.1.90)$$

Now, the rotation matrix $\mathbf{S}^{\mathcal{R}\mathcal{S}}$ and the angular velocity $\omega_{\mathcal{R}\mathcal{S}}^{\mathcal{R}}$ shall be determined. As described in the previous sections 7.1.1 and 7.1.2, the surface, for which the rotation shall be determined, has to be described by two parameters. In the case of the running surface of the rail, it is obvious to use the longitudinal coordinate x as one parameter; the choice of the second parameter will be discussed later.

The wheel-rail contact moves along the track due to the forward motion of the vehicle; thereby, the coordinate x_{wRi} indicating the current position of the i -th wheel-rail contact grows with the time. Therefore, the displacement \mathbf{w}_{M_R} for the marker M_R , which is located in the running surface at the rail head, has to be provided as a function of x . If the track is modelled as a cyclic structure, the use of a Fourier series is obvious and advantageous. For a straight track, the reference position of the marker is given by the coordinates $\langle x, y_{M_R}, z_{M_R} \rangle$, whereby the y_{M_R} and z_{M_R} are constant. Thereby, the trajectory, on which the marker M_R moves, is given by:

$$\mathbf{r}_{RM_R}^{\mathcal{R}} = \begin{bmatrix} x \\ y_{M_R} \\ z_{M_R} \end{bmatrix} + \mathbf{w}^{\mathcal{R}}(x, y_{M_R}, z_{M_R}, t) = \begin{bmatrix} x \\ y_{M_R} \\ z_{M_R} \end{bmatrix} + \sum_{K=-\infty}^{\infty} \mathbf{w}_K^{\mathcal{R}}(y_{M_R}, z_{M_R}, t) e^{iK\kappa x} \quad (7.1.91)$$

The exponential function, from which the sine and the cosine function are derived, is a smooth function, which can be differentiated without problems; in the present case, this is useful for the determination of the tangential vector $\mathbf{t}_x^{\mathcal{R}}$, which is obtained as the partial derivative of $\mathbf{r}_{RM_R}^{\mathcal{R}}$ with respect to the longitudinal coordinate x .

$$\mathbf{t}_x^{\mathcal{R}}(x) = \frac{\partial}{\partial x} \mathbf{r}_{RM_R}^{\mathcal{R}} = \underbrace{\begin{bmatrix} 1 \\ 0 \\ 0 \end{bmatrix}}_{\mathbf{t}_{0x}^{\mathcal{R}}} + \sum_{K=-\infty}^{\infty} \mathbf{w}_K^{\mathcal{R}}(y_{M_R}, z_{M_R}, t) iK\kappa e^{iK\kappa x} \quad (7.1.92)$$

The tangential vector required for the analysis is obtained by for the current position x_{WRi} of the i -th contact, i.e. $\mathbf{t}_x^{\mathcal{R}} = \mathbf{t}_x^{\mathcal{R}}(x_{WRi})$.

For the determination of the second tangential vector $\mathbf{t}_\eta^{\mathcal{R}}$, the modelling of the rail has to be considered. As described in the section 6.2, the cross section of the rail is discretized using finite elements. In the present case, bilinear elements, which have a shape of a quadrilateral, are used. For the analysis of the structural dynamics, this approximation is adequate and suitable; for the description of the local geometry, which is required here, it can be problematic, because the discretization by the bilinear elements generates vertices or corners, while the surfaces of the wheel and the rail are smooth. Also, the interpolation based on the local shape functions doesn't seem very helpful here, since at the borders between the elements including the nodes discontinuities of the derivatives can occur, in particular for linear elements.

A possibility to approximate the partial derivative in the lateral direction is the use of an interpolation curve. This interpolation curve will be determined by the centred node S_0 , which is identical to the marker M_R , and its two neighbouring nodes S_{-1} and S_1 , which are also lying at the surface of the rail. This is shown in Figure 7.1.4.

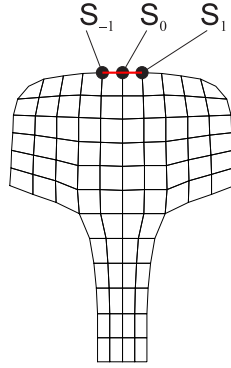


Figure 7.1.4: Interpolation nodes S_{-1} , S_0 and S_1 for the discretized cross section of the rail; red: interpolation curve.

The curve is described by a parameter η so that for the parameter η_i the point K_i is described. If the vector $\mathbf{r}_{RS_i}^{\mathcal{B}}$ describes the position of the i -th surface node, then it is valid:

$$\mathbf{r}(\eta_{-1}) = \mathbf{r}_{RS_{-1}}^{\mathcal{B}}, \quad \mathbf{r}(\eta_0) = \mathbf{r}_{RS_0}^{\mathcal{B}}, \quad \mathbf{r}(\eta_1) = \mathbf{r}_{RS_1}^{\mathcal{B}} \quad (7.1.93)$$

The continuous function $\mathbf{r}(\eta)$ can be formulated using Lagrangian polynomials $\ell_j(\eta)$.

$$\mathbf{r}_{RS}^{\mathcal{R}}(\eta) = \mathbf{r}_{RS_{-1}}^{\mathcal{R}} \ell_{-1}(\eta) + \mathbf{r}_{RS_0}^{\mathcal{R}} \ell_0(\eta) + \mathbf{r}_{RS_1}^{\mathcal{B}} \ell_1(\eta), \quad \ell_i(\eta_k) = \begin{cases} 1 & \text{for } i = k \\ 0 & \text{for } i \neq k \end{cases} \quad (7.1.94)$$

The Lagrangian polynomials are continuous smooth functions; therefore, they can be differentiated, which leads to the following approximation for the tangential vector \mathbf{t}_η :

$$\mathbf{t}_\eta^{\mathcal{R}} = \frac{\partial}{\partial \eta} \mathbf{r}_{RS}^{\mathcal{B}}(\eta) = \mathbf{r}_{RS_{-1}}^{\mathcal{R}} \ell'_{-1}(\eta) + \mathbf{r}_{RS_0}^{\mathcal{R}} \ell'_0(\eta) + \mathbf{r}_{RS_1}^{\mathcal{R}} \ell'_1(\eta), \quad \ell'_i = \frac{d\ell_i(\eta)}{d\eta} \quad (7.1.95)$$

The values η_i for the parameter η at the given points can be chosen nearly arbitrarily as long as the sequence of the values represents the sequence of the points, through which the curve passes. In the present case, it is obvious to set the value η_i equal to its index i , i.e. $\eta_i = i$.

The construction of the Lagrangian polynomials is fully derived in the appendix A.4; here, only the result shall be presented. For the three given arguments $\eta_{-1} = -1$, $\eta_0 = 0$ and $\eta_1 = 1$ the following polynomials $\ell_i(\eta)$ are determined:

$$\ell_{-1}(\eta) = \frac{1}{2}\eta^2 - \frac{1}{2}\eta, \quad \ell_0(\eta) = -\eta^2 + \eta, \quad \ell_1(\eta) = \frac{1}{2}\eta^2 + \frac{1}{2}\eta \quad (7.1.96)$$

The derivatives $\ell'_i(\eta)$ are obtained to:

$$\ell'_{-1}(\eta) = \eta - \frac{1}{2}, \quad \ell'_0(\eta) = -2\eta + 1, \quad \ell'_1(\eta) = \eta + \frac{1}{2} \quad (7.1.97)$$

Based on this, the tangential vector \mathbf{t}_η^B to the curve at the point S_0 is obtained to:

$$\mathbf{t}_\eta^{\mathcal{R}}(\eta = 0) = \mathbf{r}_{\mathcal{R}S_{-1}}^{\mathcal{R}} \ell'_{-1}(\eta = 0) + \mathbf{r}_{\mathcal{R}S_0}^{\mathcal{R}} \ell'_0(\eta = 0) + \mathbf{r}_{\mathcal{R}S_1}^{\mathcal{R}} \ell'_1(\eta = 0) = \frac{1}{2} \left(\mathbf{r}_{\mathcal{R}S_1}^{\mathcal{R}} - \mathbf{r}_{\mathcal{R}S_{-1}}^{\mathcal{R}} \right) \quad (7.1.98)$$

The result indicates that based on this approximation the tangential vector \mathbf{t}^B is half the vector, which describes distance from the point S_{-1} to the point S_1 . Thereby, the tangential vector \mathbf{t}_η^B , which is required for the determination of the rotation of the surface, is determined solely based on the positions of discrete points so this approximation can be applied to the finite element models representing the wheelset and the rail.

The kinematics is treated in the same way as for the marker M_R . Regarding the cross section, the coordinates for the nodes S_I are given by the constant values $\langle y_{S_I}, z_{S_I} \rangle$, $I = 1, -1$; inserting these coordinates into (7.1.91) leads to:

$$\mathbf{r}_{\mathcal{R}S_I}^{\mathcal{R}} = \begin{bmatrix} x \\ y_{S_I} \\ z_{S_I} \end{bmatrix} + \mathbf{w}^{\mathcal{R}}(x, y_{S_I}, z_{S_I}, t) = \begin{bmatrix} x \\ y_{S_I} \\ z_{S_I} \end{bmatrix} + \sum_{K=-\infty}^{\infty} \mathbf{w}_K^{\mathcal{R}}(y_{S_I}, z_{S_I}, t) e^{iK\kappa x} \quad (7.1.99)$$

By inserting this into (7.1.98) the tangential vector $\mathbf{t}_\eta^{\mathcal{R}}(x)$ at the node $S_0 \equiv M_R$ is obtained:

$$\begin{aligned} \mathbf{t}_\eta^{\mathcal{R}}(x) &= \frac{1}{2} \left(\mathbf{r}_{\mathcal{R}S_1}^{\mathcal{R}} - \mathbf{r}_{\mathcal{R}S_{-1}}^{\mathcal{R}} \right) = \frac{1}{2} \left(\begin{bmatrix} x \\ y_{S_1} \\ z_{S_1} \end{bmatrix} + \mathbf{w}^{\mathcal{R}}(x, y_{S_1}, z_{S_1}, t) - \begin{bmatrix} x \\ y_{S_{-1}} \\ z_{S_{-1}} \end{bmatrix} - \mathbf{w}^{\mathcal{R}}(x, y_{S_{-1}}, z_{S_{-1}}, t) \right) \\ &= \frac{1}{2} \underbrace{\begin{bmatrix} 0 \\ y_{S_1} - y_{S_{-1}} \\ z_{S_1} - z_{S_{-1}} \end{bmatrix}}_{\mathbf{t}_{0\eta}^{\mathcal{R}}} + \sum_{K=-\infty}^{\infty} \frac{1}{2} \underbrace{\left(\mathbf{w}_K^{\mathcal{R}}(y_{S_1}, z_{S_1}, t) - \mathbf{w}_K^{\mathcal{R}}(y_{S_{-1}}, z_{S_{-1}}, t) \right)}_{\mathbf{t}_{\eta|K}^{\mathcal{R}}} e^{iK\kappa x} \end{aligned} \quad (7.1.100)$$

Also here, the tangential vector, which is required for the determination of the rotation at the surface, is obtained for the current position x_{wRi} of the i -th wheel-rail contact, i.e. $\mathbf{t}_\eta^{\mathcal{R}} = \mathbf{t}_\eta^{\mathcal{R}}(x_{wRi})$.

The motions of the track model, which includes the rail, are described by a modal synthesis. Here, the deformation field of the rail is described by a superposition of shape functions $\mathbf{w}_{TI}(x, y, z)$, whereby each shape function is formulated as a continuous Fourier series.

$$\mathbf{w}_R^{\mathcal{R}}(x, y, z, t) = \sum_I \mathbf{w}_{TI}^{\mathcal{R}}(x, y, z) q_{TI}(t) = \sum_I \left(\sum_{K=K_{I,\min}}^{K_{I,\max}} \mathbf{w}_{TI,K}^{\mathcal{R}}(y, z) e^{iK\kappa x} \right) q_{TI}(t) \quad (7.1.101)$$

The position of the marker M_{Ri} is defined by the values y_{M_R} and z_{M_R} of the cross-sectional coordinates and the value x_{WRi} indicating the current position of the i -th wheel-rail contact. Using the modal synthesis, this displacement is obtained to:

$$\mathbf{w}_R^{\mathcal{R}}(x_{WRi}, y_{M_R}, z_{M_R}, t) = \sum_I \left(\sum_{K=K_{I,\min}}^{K_{I,\max}} \mathbf{w}_{TI,K}^{\mathcal{R}}(y_{M_R}, z_{M_R}) e^{iK \kappa x_{WRi}} \right) q_{TI}(t) \quad (7.1.102)$$

The tangential vector $\mathbf{t}_{x,i}^{\mathcal{R}}$ with respect to the longitudinal coordinate x is obtained by inserting the modal synthesis (7.1.101) into the formulation (7.1.92) and setting $x = x_{WRi}$; this leads to:

$$\mathbf{t}_{x,i}^{\mathcal{R}} = \begin{bmatrix} 1 \\ 0 \\ 0 \end{bmatrix} + \sum_I \left(\sum_{K=K_{I,\min}}^{K_{I,\max}} \mathbf{w}_{TI,K}^{\mathcal{R}}(y_{M_R}, z_{M_R}) iK \kappa e^{iK \kappa x_{WRi}} \right) q_{TI}(t) \quad (7.1.103)$$

In a similar way, the tangential vector $\mathbf{t}_{\eta}^{\mathcal{R}}$ with respect to the transverse coordinate η is obtained based on the formulation (7.1.100).

$$\mathbf{t}_{\eta,i}^{\mathcal{R}} = \frac{1}{2} \begin{bmatrix} 0 \\ y_{S_1} - y_{S_{-1}} \\ z_{S_1} - z_{S_{-1}} \end{bmatrix} + \sum_I \left(\sum_{K=K_{I,\min}}^{K_{I,\max}} \frac{1}{2} \left(\mathbf{w}_{TI,K}^{\mathcal{R}}(y_{S_1}, z_{S_1}) - \mathbf{w}_{TI,K}^{\mathcal{R}}(y_{S_{-1}}, z_{S_{-1}}) \right) e^{iK \kappa x_{WRi}} \right) q_{TI}(t) \quad (7.1.104)$$

By using the following definitions:

$$\mathbf{w}_{TI,K}^{\mathcal{R}}(y_{M_R}, z_{M_R}) = \mathbf{w}_{M_R|I,K}, \quad \frac{1}{2} \left(\mathbf{w}_{TI,K}^{\mathcal{R}}(y_{S_1}, z_{S_1}) - \mathbf{w}_{TI,K}^{\mathcal{R}}(y_{S_{-1}}, z_{S_{-1}}) \right) = \mathbf{t}_{\eta|I,K} \quad (7.1.105)$$

it can be written:

$$\mathbf{w}_R^{\mathcal{R}}(x_{WRi}, y_{M_R}, z_{M_R}, t) = \sum_I \left(\sum_{K=K_{I,\min}}^{K_{I,\max}} \mathbf{w}_{M_R|I,K} e^{iK \kappa x_{WRi}} \right) q_{TI}(t) \quad (7.1.106)$$

$$\mathbf{t}_{x,i}^{\mathcal{R}} = \mathbf{t}_{0x}^{\mathcal{R}} + \sum_I \left(\sum_{K=K_{I,\min}}^{K_{I,\max}} \mathbf{w}_{M_R|I,K} iK \kappa e^{iK \kappa x_{WRi}} \right) q_{TI}(t), \quad \mathbf{t}_{0x}^{\mathcal{R}} = \begin{bmatrix} 1 \\ 0 \\ 0 \end{bmatrix} \quad (7.1.107)$$

$$\mathbf{t}_{\eta,i}^{\mathcal{R}} = \mathbf{t}_{0\eta}^{\mathcal{R}} + \sum_I \left(\sum_{K=K_{I,\min}}^{K_{I,\max}} \mathbf{t}_{\eta|I,K} e^{iK \kappa x_{WRi}} \right) q_{TI}(t), \quad \mathbf{t}_{0\eta}^{\mathcal{R}} = \frac{1}{2} \begin{bmatrix} 0 \\ y_{S_1} - y_{S_{-1}} \\ z_{S_1} - z_{S_{-1}} \end{bmatrix} \quad (7.1.108)$$

Based on the ‘‘geometrical’’ tangential vectors $\mathbf{t}_{x,i}^{\mathcal{R}}$ and $\mathbf{t}_{\eta,i}^{\mathcal{R}}$ the rotation matrix which describes the angular position of the frame \mathcal{M}_{Ri} can now be determined. First, the vector product of the constant parts $\mathbf{t}_{0x}^{\mathcal{R}}$ and $\mathbf{t}_{0\eta}^{\mathcal{R}}$ of the tangential vectors shall be considered:

$$\mathbf{t}_{0x}^{\mathcal{R}} \times \mathbf{t}_{0\eta}^{\mathcal{R}} = \begin{bmatrix} 1 \\ 0 \\ 0 \end{bmatrix} \times \frac{1}{2} \begin{bmatrix} 0 \\ y_{S_1} - y_{S_{-1}} \\ z_{S_1} - z_{S_{-1}} \end{bmatrix} = \frac{1}{2} \begin{bmatrix} 0 \\ -(z_{S_1} - z_{S_{-1}}) \\ y_{S_1} - y_{S_{-1}} \end{bmatrix} \quad (7.1.109)$$

If the surface points S_{-1} and S_1 are selected in such a way that it is valid $y_{S_1} > y_{S_{-1}} \Leftrightarrow y_{S_1} - y_{S_{-1}} > 0$, then the third coordinate of the product is positive, i.e. a part of the product points in the positive direction of the 3-axis. Therefore, it is reasonable to define the normal vector $\mathbf{n}_i^{\mathcal{R}}$ in the following way:

$$\mathbf{n}_i^{\mathcal{R}} = \mathbf{t}_{x,i}^{\mathcal{R}} \times \mathbf{t}_{\eta,i}^{\mathcal{R}} \quad (7.1.110)$$

Based on the method developed in the section 7.1.1, the rotation matrix $\mathbf{S}^{\mathcal{R}\mathcal{S}}$ between the reference frame \mathcal{R} and the surface frame \mathcal{S} for the marker M_{Ri} is now formulated in the following way using the vectors $\mathbf{t}_{x,i}^{\mathcal{R}}$ and $\mathbf{t}_{\eta,i}^{\mathcal{R}}$ which have been determined according to (7.1.107) and (7.1.108), respectively:

$$\mathbf{y}_3 = \mathbf{n}_i^{\mathcal{R}} = \mathbf{t}_{x,i}^{\mathcal{R}} \times \mathbf{t}_{\eta,i}^{\mathcal{R}} \Rightarrow \mathbf{e}_{S3}^{\mathcal{R}} = \frac{\mathbf{n}_i^{\mathcal{R}}}{|\mathbf{n}_i^{\mathcal{R}}|}, \mathbf{y}_1 = \mathbf{t}_{x,i}^{\mathcal{R}} \Rightarrow \mathbf{e}_{S1}^{\mathcal{R}} = \frac{\mathbf{t}_{x,i}^{\mathcal{R}}}{|\mathbf{t}_{x,i}^{\mathcal{R}}|}, \mathbf{e}_{S2}^{\mathcal{R}} = \mathbf{e}_{S3}^{\mathcal{R}} \times \mathbf{e}_{S1}^{\mathcal{R}} \quad (7.1.111)$$

$$\Rightarrow \mathbf{S}^{\mathcal{R}\mathcal{S}} = \begin{bmatrix} \mathbf{e}_{S1}^{\mathcal{R}} & \mathbf{e}_{S2}^{\mathcal{R}} & \mathbf{e}_{S3}^{\mathcal{R}} \end{bmatrix} \quad (7.1.112)$$

Thereby, the rotation matrix between the body-fixed frame \mathcal{R} of the rail and the surface frame \mathcal{S} is obtained. It should, however, be noticed that the surface frame \mathcal{S} is not necessarily identical to the frame \mathcal{M}_{Ri} of the marker; therefore, a correction by a constant matrix $\mathbf{S}^{\mathcal{S}\mathcal{M}_{Ri}}$ may be necessary. In the case of the rail, the frame \mathcal{M}_{Ri} , in which the profile function is defined, has the same orientation as the body-fixed frame \mathcal{R} for the undeformed state. By using the index 0 for the matrices describing the undeformed state it is valid:

$$\mathbf{I} = \mathbf{S}_0^{\mathcal{R}\mathcal{M}_{Ri}} = \mathbf{S}_0^{\mathcal{R}\mathcal{S}} \mathbf{S}^{\mathcal{S}\mathcal{M}_{Ri}} \Rightarrow \mathbf{S}^{\mathcal{S}\mathcal{M}_{Ri}} = \mathbf{S}_0^{\mathcal{R}\mathcal{S}-1} = \mathbf{S}_0^{\mathcal{R}\mathcal{S}\text{T}} \quad (7.1.113)$$

The matrix $\mathbf{S}_0^{\mathcal{R}\mathcal{S}}$ is determined in an analogous way as the matrix $\mathbf{S}^{\mathcal{R}\mathcal{S}}$; here, however, only the constant parts $\mathbf{t}_{0x}^{\mathcal{R}}$ and $\mathbf{t}_{0\eta}^{\mathcal{R}}$ of the tangential vectors are used:

$$\mathbf{y}_{30} = \mathbf{n}_0^{\mathcal{R}} = \mathbf{t}_{0x}^{\mathcal{R}} \times \mathbf{t}_{0\eta}^{\mathcal{R}} \Rightarrow \mathbf{e}_{S30}^{\mathcal{R}} = \frac{\mathbf{n}_0^{\mathcal{R}}}{|\mathbf{n}_0^{\mathcal{R}}|}, \mathbf{y}_{10} = \mathbf{t}_{0x}^{\mathcal{R}} \Rightarrow \mathbf{e}_{S10}^{\mathcal{R}} = \frac{\mathbf{t}_{0x}^{\mathcal{R}}}{|\mathbf{t}_{0x}^{\mathcal{R}}|}, \mathbf{e}_{S20}^{\mathcal{R}} = \mathbf{e}_{S30}^{\mathcal{R}} \times \mathbf{e}_{S10}^{\mathcal{R}} \quad (7.1.114)$$

$$\Rightarrow \mathbf{S}_0^{\mathcal{R}\mathcal{S}} = \begin{bmatrix} \mathbf{e}_{S10}^{\mathcal{R}} & \mathbf{e}_{S20}^{\mathcal{R}} & \mathbf{e}_{S30}^{\mathcal{R}} \end{bmatrix} \quad (7.1.115)$$

Since the vectors $\mathbf{t}_{0x}^{\mathcal{R}}$ and $\mathbf{t}_{0\eta}^{\mathcal{R}}$ are constant, the matrix $\mathbf{S}_0^{\mathcal{R}\mathcal{S}}$ has to be determined only once. Finally, the rotation matrix $\mathbf{S}^{\mathcal{R}\mathcal{M}_{Ri}}$ is obtained to:

$$\mathbf{S}^{\mathcal{R}\mathcal{M}_{Ri}} = \mathbf{S}^{\mathcal{R}\mathcal{S}} \mathbf{S}^{\mathcal{S}\mathcal{M}_{Ri}} = \mathbf{S}^{\mathcal{R}\mathcal{S}} \mathbf{S}_0^{\mathcal{R}\mathcal{S}\text{T}} \quad (7.1.116)$$

In the section 7.1.2 the following expression for the angular velocity at the surface of a flexible body has been derived:

$$\omega_{\mathcal{R}\mathcal{S}}^{\mathcal{R}} = \frac{\mathbf{n}^{\mathcal{R}} \times \dot{\mathbf{n}}^{\mathcal{R}}}{\mathbf{n}^{\mathcal{R}} \cdot \mathbf{n}^{\mathcal{R}}} + \frac{1}{2} \left(\frac{\mathbf{n}^{\mathcal{R}} \cdot (\mathbf{t}_{\xi}^{\mathcal{R}} \times \dot{\mathbf{t}}_{\xi}^{\mathcal{R}})}{\mathbf{t}_{\xi}^{\mathcal{R}} \cdot \mathbf{t}_{\xi}^{\mathcal{R}}} + \frac{\mathbf{n}^{\mathcal{R}} \cdot (\mathbf{t}_{\eta}^{\mathcal{R}} \times \dot{\mathbf{t}}_{\eta}^{\mathcal{R}})}{\mathbf{t}_{\eta}^{\mathcal{R}} \cdot \mathbf{t}_{\eta}^{\mathcal{R}}} \right) \frac{\mathbf{n}^{\mathcal{R}}}{\mathbf{n}^{\mathcal{R}} \cdot \mathbf{n}^{\mathcal{R}}} \quad (7.1.117)$$

As shown in (7.1.90), the matrix $\mathbf{S}^{\mathcal{R}\mathcal{M}_{Ri}}$ has no influence on the angular velocity $\omega_{\mathcal{R}\mathcal{M}_{Ri}}^{\mathcal{R}}$ because it is constant. By using the tangential vectors with respect to the coordinates x and η , it is valid:

$$\omega_{\mathcal{R}\mathcal{M}_{Ri}}^{\mathcal{R}} = \omega_{\mathcal{R}\mathcal{S}}^{\mathcal{R}} = \frac{\mathbf{n}^{\mathcal{R}} \times \dot{\mathbf{n}}^{\mathcal{R}}}{\mathbf{n}^{\mathcal{R}} \cdot \mathbf{n}^{\mathcal{R}}} + \frac{1}{2} \left(\frac{\mathbf{n}^{\mathcal{R}} \cdot (\mathbf{t}_x^{\mathcal{R}} \times \dot{\mathbf{t}}_x^{\mathcal{R}})}{\mathbf{t}_x^{\mathcal{R}} \cdot \mathbf{t}_x^{\mathcal{R}}} + \frac{\mathbf{n}^{\mathcal{R}} \cdot (\mathbf{t}_{\eta}^{\mathcal{R}} \times \dot{\mathbf{t}}_{\eta}^{\mathcal{R}})}{\mathbf{t}_{\eta}^{\mathcal{R}} \cdot \mathbf{t}_{\eta}^{\mathcal{R}}} \right) \frac{\mathbf{n}^{\mathcal{R}}}{\mathbf{n}^{\mathcal{R}} \cdot \mathbf{n}^{\mathcal{R}}} \quad (7.1.118)$$

The expression is relatively complex. In the present case of the rail the deformations are relatively small so that it can be assumed that the difference between the current tangential vectors $\mathbf{t}_x^{\mathcal{R}}$ and $\mathbf{t}_{\eta}^{\mathcal{R}}$ on the one hand and the tangential vectors $\mathbf{t}_{0x}^{\mathcal{R}}$ and $\mathbf{t}_{0\eta}^{\mathcal{R}}$ on the other hand is very small:

$$\left| \mathbf{t}_x^{\mathcal{R}} - \mathbf{t}_{0x}^{\mathcal{R}} \right| \ll \left| \mathbf{t}_{0x}^{\mathcal{R}} \right| \Rightarrow \mathbf{t}_x^{\mathcal{R}} \approx \mathbf{t}_{0x}^{\mathcal{R}}, \left| \mathbf{t}_{\eta}^{\mathcal{R}} - \mathbf{t}_{0\eta}^{\mathcal{R}} \right| \ll \left| \mathbf{t}_{0\eta}^{\mathcal{R}} \right| \Rightarrow \mathbf{t}_{\eta}^{\mathcal{R}} \approx \mathbf{t}_{0\eta}^{\mathcal{R}} \quad (7.1.119)$$

From this it follows for the normal vector:

$$\mathbf{n}^{\mathcal{R}} = \mathbf{t}_x^{\mathcal{R}} \times \mathbf{t}_\eta^{\mathcal{R}} \approx \mathbf{t}_{0x}^{\mathcal{R}} \times \mathbf{t}_{0\eta}^{\mathcal{R}} = \mathbf{n}_0^{\mathcal{R}} \quad (7.1.120)$$

For the derivative $\dot{\mathbf{n}}^{\mathcal{R}}$ of the normal vector it is valid:

$$\mathbf{n}^{\mathcal{R}} = \mathbf{t}_x^{\mathcal{R}} \times \mathbf{t}_\eta^{\mathcal{R}} \Rightarrow \dot{\mathbf{n}}^{\mathcal{R}} = \dot{\mathbf{t}}_x^{\mathcal{R}} \times \mathbf{t}_\eta^{\mathcal{R}} + \mathbf{t}_x^{\mathcal{R}} \times \dot{\mathbf{t}}_\eta^{\mathcal{R}} \approx \dot{\mathbf{t}}_x^{\mathcal{R}} \times \mathbf{t}_{0\eta}^{\mathcal{R}} + \mathbf{t}_{0x}^{\mathcal{R}} \times \dot{\mathbf{t}}_\eta^{\mathcal{R}} \quad (7.1.121)$$

Thereby, the expression for the angular velocity can be simplified in the following way:

$$\omega_{\mathcal{R}\mathcal{M}_{Ri}}^{\mathcal{R}} \approx \frac{\mathbf{n}_0^{\mathcal{R}} \times (\dot{\mathbf{t}}_x^{\mathcal{R}} \times \mathbf{t}_{0\eta}^{\mathcal{R}} + \mathbf{t}_{0x}^{\mathcal{R}} \times \dot{\mathbf{t}}_\eta^{\mathcal{R}})}{\mathbf{n}_0^{\mathcal{R}} \cdot \mathbf{n}_0^{\mathcal{R}}} + \frac{1}{2} \left(\frac{\mathbf{n}_0^{\mathcal{R}} \cdot (\mathbf{t}_{0x}^{\mathcal{R}} \times \dot{\mathbf{t}}_x^{\mathcal{R}})}{\mathbf{t}_{0x}^{\mathcal{R}} \cdot \mathbf{t}_{0x}^{\mathcal{R}}} + \frac{\mathbf{n}_0^{\mathcal{R}} \cdot (\mathbf{t}_{0\eta}^{\mathcal{R}} \times \dot{\mathbf{t}}_\eta^{\mathcal{R}})}{\mathbf{t}_{0\eta}^{\mathcal{R}} \cdot \mathbf{t}_{0\eta}^{\mathcal{R}}} \right) \frac{\mathbf{n}_0^{\mathcal{R}}}{\mathbf{n}_0^{\mathcal{R}} \cdot \mathbf{n}_0^{\mathcal{R}}} \quad (7.1.122)$$

The vectors $\dot{\mathbf{t}}_x^{\mathcal{R}}$ and $\dot{\mathbf{t}}_\eta^{\mathcal{R}}$ are derived from (7.1.107) and (7.1.108), respectively; it is obtained:

$$\dot{\mathbf{t}}_{x,i}^{\mathcal{R}} = \sum_I \left(\sum_{K=K_{I,\min}}^{K_{I,\max}} \mathbf{w}_{M_{R|I,K}} \mathbf{i}K \kappa e^{iK \kappa x_{WRi}} \right) \dot{q}_{TI}(t) = \sum_I \left(\sum_{K=K_{I,\min}}^{K_{I,\max}} \mathbf{t}_{x|I,K} e^{iK \kappa x_{WRi}} \right) \dot{q}_{TI}(t) \quad (7.1.123)$$

$$\dot{\mathbf{t}}_{\eta,i}^{\mathcal{R}} = \sum_I \left(\sum_{K=K_{I,\min}}^{K_{I,\max}} \mathbf{t}_{\eta|I,K} e^{iK \kappa x_{WRi}} \right) \dot{q}_{TI}(t) \quad (7.1.124)$$

Here, the following abbreviation has been introduced for a better overview:

$$\mathbf{t}_{x|I,K} = \mathbf{w}_{M_{R|I,K}} \mathbf{i}K \kappa \quad (7.1.125)$$

Based on this, the terms for the angular velocity can be formulated by a modal synthesis:

$$\frac{\mathbf{n}_0^{\mathcal{R}} \times (\dot{\mathbf{t}}_x^{\mathcal{R}} \times \mathbf{t}_{0\eta}^{\mathcal{R}} + \mathbf{t}_{0x}^{\mathcal{R}} \times \dot{\mathbf{t}}_\eta^{\mathcal{R}})}{\mathbf{n}_0^{\mathcal{R}} \cdot \mathbf{n}_0^{\mathcal{R}}} = \sum_I \left(\sum_{K=K_{I,\min}}^{K_{I,\max}} \frac{\mathbf{n}_0^{\mathcal{R}} \times (\mathbf{t}_{x|I,K} \times \mathbf{t}_{0\eta}^{\mathcal{R}} + \mathbf{t}_{0x}^{\mathcal{R}} \times \mathbf{t}_{\eta|I,K})}{\mathbf{n}_0^{\mathcal{R}} \cdot \mathbf{n}_0^{\mathcal{R}}} e^{iK \kappa x_{WRi}} \right) \dot{q}_I(t) \quad (7.1.126)$$

$$\frac{\mathbf{n}_0^{\mathcal{R}} \cdot (\mathbf{t}_{0x}^{\mathcal{R}} \times \dot{\mathbf{t}}_x^{\mathcal{R}})}{\mathbf{t}_{0x}^{\mathcal{R}} \cdot \mathbf{t}_{0x}^{\mathcal{R}}} \frac{\mathbf{n}_0^{\mathcal{R}}}{\mathbf{n}_0^{\mathcal{R}} \cdot \mathbf{n}_0^{\mathcal{R}}} = \sum_I \left(\sum_{K=K_{I,\min}}^{K_{I,\max}} \frac{\mathbf{n}_0^{\mathcal{R}} \cdot (\mathbf{t}_{0x}^{\mathcal{R}} \times \mathbf{t}_{x|I,K})}{\mathbf{t}_{0x}^{\mathcal{R}} \cdot \mathbf{t}_{0x}^{\mathcal{R}}} \frac{\mathbf{n}_0^{\mathcal{R}}}{\mathbf{n}_0^{\mathcal{R}} \cdot \mathbf{n}_0^{\mathcal{R}}} e^{iK \kappa x_{WRi}} \right) \dot{q}_I(t) \quad (7.1.127)$$

$$\frac{\mathbf{n}_0^{\mathcal{R}} \cdot (\mathbf{t}_{0\eta}^{\mathcal{R}} \times \dot{\mathbf{t}}_\eta^{\mathcal{R}})}{\mathbf{t}_{0\eta}^{\mathcal{R}} \cdot \mathbf{t}_{0\eta}^{\mathcal{R}}} \frac{\mathbf{n}_0^{\mathcal{R}}}{\mathbf{n}_0^{\mathcal{R}} \cdot \mathbf{n}_0^{\mathcal{R}}} = \sum_I \left(\sum_{K=K_{I,\min}}^{K_{I,\max}} \frac{\mathbf{n}_0^{\mathcal{R}} \cdot (\mathbf{t}_{0\eta}^{\mathcal{R}} \times \mathbf{t}_{\eta|I,K})}{\mathbf{t}_{0\eta}^{\mathcal{R}} \cdot \mathbf{t}_{0\eta}^{\mathcal{R}}} \frac{\mathbf{n}_0^{\mathcal{R}}}{\mathbf{n}_0^{\mathcal{R}} \cdot \mathbf{n}_0^{\mathcal{R}}} e^{iK \kappa x_{WRi}} \right) \dot{q}_I(t) \quad (7.1.128)$$

By defining:

$$\Omega_{I,K} = \frac{\mathbf{n}_0^{\mathcal{R}} \times (\mathbf{t}_{x|I,K} \times \mathbf{t}_{0\eta}^{\mathcal{R}} + \mathbf{t}_{0x}^{\mathcal{R}} \times \mathbf{t}_{\eta|I,K})}{\mathbf{n}_0^{\mathcal{R}} \cdot \mathbf{n}_0^{\mathcal{R}}} + \frac{1}{2} \left(\frac{\mathbf{n}_0^{\mathcal{R}} \cdot (\mathbf{t}_{0x}^{\mathcal{R}} \times \mathbf{t}_{x|I,K})}{\mathbf{t}_{0x}^{\mathcal{R}} \cdot \mathbf{t}_{0x}^{\mathcal{R}}} + \frac{\mathbf{n}_0^{\mathcal{R}} \cdot (\mathbf{t}_{0\eta}^{\mathcal{R}} \times \mathbf{t}_{\eta|I,K})}{\mathbf{t}_{0\eta}^{\mathcal{R}} \cdot \mathbf{t}_{0\eta}^{\mathcal{R}}} \right) \frac{\mathbf{n}_0^{\mathcal{R}}}{\mathbf{n}_0^{\mathcal{R}} \cdot \mathbf{n}_0^{\mathcal{R}}} \quad (7.1.129)$$

it can finally be formulated:

$$\omega_{\mathcal{R}\mathcal{S}}^{\mathcal{R}} \approx \sum_I \left(\sum_{K=K_{I,\min}}^{K_{I,\max}} \Omega_{I,K} e^{iK \kappa x_{WRi}} \right) \dot{q}_I(t) \quad (7.1.130)$$

It should be noted that due to the approximation $\mathbf{t}_x^{\mathcal{R}} \approx \mathbf{t}_{0x}^{\mathcal{R}}$ and $\mathbf{t}_\eta^{\mathcal{R}} \approx \mathbf{t}_{0\eta}^{\mathcal{R}}$ the vectors $\Omega_{I,K}$ are constant so that the expression (7.1.129) has to be evaluated only once at the beginning of the calculation.

7.1.4 Application to the wheel

The rotation of the marker frame \mathcal{M}_{wi} , which is attached to the surface of the wheel, is determined in a similar way as for the frame \mathcal{M}_{Ri} . Also here, the rotation matrix $\mathbf{S}^{\mathcal{B}\mathcal{M}_{wi}}$ is expressed by multiplying the matrix $\mathbf{S}^{\mathcal{B}\mathcal{S}}$, which describes the rotation of the surface frame \mathcal{S} relative to the body-fixed frame \mathcal{B} , and the constant matrix $\mathbf{S}^{\mathcal{S}\mathcal{M}_{wi}}$ expressing the different orientations of the surface and the marker.

$$\mathbf{S}^{\mathcal{B}\mathcal{M}_{wi}} = \mathbf{S}^{\mathcal{B}\mathcal{S}} \mathbf{S}^{\mathcal{S}\mathcal{M}_{wi}} \quad (7.1.131)$$

Also for the wheel, the matrix $\mathbf{S}^{\mathcal{S}\mathcal{M}_{wi}}$ is determined from the given matrix $\mathbf{S}_0^{\mathcal{B}\mathcal{M}_{wi}}$ and the matrix $\mathbf{S}_0^{\mathcal{B}\mathcal{S}}$ which are both valid for the reference state, i.e. the undeformed state:

$$\mathbf{S}_0^{\mathcal{B}\mathcal{M}_{wi}} = \mathbf{S}_0^{\mathcal{B}\mathcal{S}} \mathbf{S}^{\mathcal{S}\mathcal{M}_{wi}} \Rightarrow \mathbf{S}^{\mathcal{S}\mathcal{M}_{wi}} = \mathbf{S}_0^{\mathcal{B}\mathcal{S}^{-1}} \mathbf{S}_0^{\mathcal{B}\mathcal{M}_{wi}} = \mathbf{S}_0^{\mathcal{B}\mathcal{S}^T} \mathbf{S}_0^{\mathcal{B}\mathcal{M}_{wi}} \quad (7.1.132)$$

While kinematics of the rail was described by cartesian coordinates $\langle x, y, z \rangle$, for the wheel the description using cylindrical coordinates $\langle r, y, \phi \rangle$ is more suitable. In the body-fixed frame \mathcal{B} the reference position $\mathbf{x}_{M_{wi}}^{\mathcal{B}}$ of the marker M_{wi} is lying on a circle defined by the constant values $r_{M_{wi}} > 0$ and $y_{M_{wi}}$.

$$\mathbf{x}_{M_{wi}}^{\mathcal{B}} = \begin{bmatrix} x_{M_{wi}} \\ y_{M_{wi}} \\ z_{M_{wi}} \end{bmatrix} = \underbrace{\begin{bmatrix} \cos \phi & 0 & \sin \phi \\ 0 & 1 & 0 \\ -\sin \phi & 0 & \cos \phi \end{bmatrix}}_{\mathbf{S}_2(\phi)} \underbrace{\begin{bmatrix} 0 \\ y_{M_{wi}} \\ r_{M_{wi}} \end{bmatrix}}_{\mathbf{c}_{M_{wi}}} = \begin{bmatrix} r_{M_{wi}} \sin \phi \\ y_{M_{wi}} \\ r_{M_{wi}} \cos \phi \end{bmatrix} = \mathbf{x}^{\mathcal{B}}(\mathbf{c}_{M_{wi}}, \phi) \quad (7.1.133)$$

As introduced in the section 5.1.2, the vector $\mathbf{c}_{M_{wi}}$ is indicated for the sake of brevity instead of indicating the coordinates $r_{M_{wi}}$ and $y_{M_{wi}}$ separately. – The trajectory of the marker M_{wi} is given by:

$$\mathbf{r}_{RM_{wi}}^{\mathcal{B}} = \mathbf{x}^{\mathcal{B}}(\mathbf{c}_{M_{wi}}, \phi) + \mathbf{w}^{\mathcal{B}}(\mathbf{c}_{M_{wi}}, \phi, t) = \begin{bmatrix} r_{M_{wi}} \sin \phi \\ y_{M_{wi}} \\ r_{M_{wi}} \cos \phi \end{bmatrix} + \sum_{K=-\infty}^{\infty} \mathbf{w}_K^{\mathcal{B}}(\mathbf{c}_{M_{wi}}, t) e^{iK\phi} \quad (7.1.134)$$

The tangential vector $\mathbf{t}_{\phi}^{\mathcal{B}}$ with respect to the angle ϕ is obtained to:

$$\mathbf{t}_{\phi}^{\mathcal{B}}(\phi) = \frac{\partial}{\partial \phi} \mathbf{r}_{RM_{wi}}^{\mathcal{B}} = \underbrace{\begin{bmatrix} r_{M_{wi}} \cos \phi \\ 0 \\ -r_{M_{wi}} \sin \phi \end{bmatrix}}_{\mathbf{t}_{0\phi}^{\mathcal{R}}} + \sum_{K=-\infty}^{\infty} \mathbf{w}_K^{\mathcal{B}}(\mathbf{c}_{M_{wi}}, t) iK e^{iK\phi} \quad (7.1.135)$$

The constant part $\mathbf{t}_{0\phi}^{\mathcal{R}}$ can be formulated in the following way:

$$\mathbf{t}_{0\phi}^{\mathcal{R}} = \begin{bmatrix} r_{M_{wi}} \cos \phi \\ 0 \\ -r_{M_{wi}} \sin \phi \end{bmatrix} = r_{M_{wi}} \begin{bmatrix} \cos \phi \\ 0 \\ -\sin \phi \end{bmatrix} = r_{M_{wi}} \underbrace{\begin{bmatrix} \cos \phi & 0 & \sin \phi \\ 0 & 1 & 0 \\ -\sin \phi & 0 & \cos \phi \end{bmatrix}}_{\mathbf{S}_2(\phi)} \underbrace{\begin{bmatrix} 1 \\ 0 \\ 0 \end{bmatrix}}_{\mathbf{e}_1} \quad (7.1.136)$$

Also here, the cross section of the wheel is discretized by finite elements; therefore, the tangential vector with respect to the lateral coordinate is determined in an analogous way as for the rail. Also here, three nodes S_{-1} , S_0 and S_1 which are located at the surface are chosen; in Figure 7.1.5 the position of the nodes is displayed.

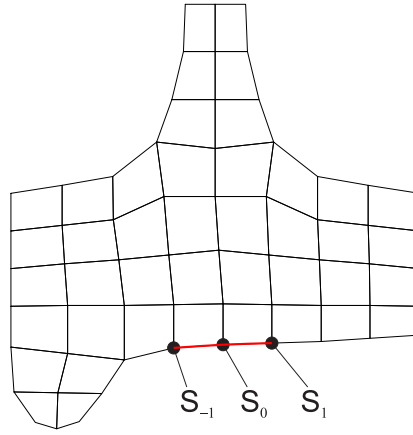


Figure 7.1.5: Interpolation nodes S_{-1} , S_0 and S_1 for the discretized cross section of the wheel; red: interpolation curve.

For the node S_I the current relative position is obtained to:

$$\mathbf{r}_{RS_I}^B = \begin{bmatrix} r_{S_I} \sin \phi \\ y_{S_I} \\ r_{S_I} \cos \phi \end{bmatrix} + \mathbf{w}^B(r_{S_I}, y_{S_I}, \phi, t) = \begin{bmatrix} r_{S_I} \sin \phi \\ y_{S_I} \\ r_{S_I} \cos \phi \end{bmatrix} + \sum_{K=-\infty}^{\infty} \mathbf{w}_K^B(r_{S_I}, y_{S_I}, t) e^{iK\phi} \quad (7.1.137)$$

If the curve connecting the three nodes is described by Lagrangian interpolation polynomials, then the tangential vector to the curve at the central node S_0 is obtained as half the vector describing the distance between the outer nodes S_{-1} and S_1 ; this has been shown in the previous section 7.1.3. In the present case for the wheel it is obtained for the tangential vector \mathbf{t}_{η}^B with respect to the lateral coordinate η :

$$\begin{aligned} \mathbf{t}_{\eta}^B(\phi) &= \frac{1}{2} (\mathbf{r}_{RS_1}^B - \mathbf{r}_{RS_{-1}}^B) \\ &= \frac{1}{2} \left(\begin{bmatrix} r_{S_1} \sin \phi \\ y_{S_1} \\ r_{S_1} \cos \phi \end{bmatrix} + \mathbf{w}^B(y_{S_1}, r_{S_1}, \phi, t) - \begin{bmatrix} r_{S_{-1}} \sin \phi \\ y_{S_{-1}} \\ r_{S_{-1}} \cos \phi \end{bmatrix} - \mathbf{w}^B(y_{S_{-1}}, r_{S_{-1}}, \phi, t) \right) \\ &= \frac{1}{2} \underbrace{\begin{bmatrix} (r_{S_1} - r_{S_{-1}}) \sin \phi \\ y_{S_1} - y_{S_{-1}} \\ (r_{S_1} - r_{S_{-1}}) \cos \phi \end{bmatrix}}_{\mathbf{t}_{0\eta}^B} + \sum_{K=-\infty}^{\infty} \frac{1}{2} \underbrace{(\mathbf{w}_K^B(r_{S_1}, y_{S_1}, t) - \mathbf{w}_K^B(r_{S_{-1}}, y_{S_{-1}}, t))}_{\mathbf{t}_{\eta|K}^B} e^{iK\phi} \quad (7.1.138) \end{aligned}$$

For the sake of brevity the following abbreviations shall be introduced:

$$r_{S_1} - r_{S_{-1}} = \Delta r_S, \quad y_{S_1} - y_{S_{-1}} = \Delta y_S \Rightarrow \mathbf{t}_{0\eta}^B = \frac{1}{2} \begin{bmatrix} (r_{S_1} - r_{S_{-1}}) \sin \phi \\ y_{S_1} - y_{S_{-1}} \\ (r_{S_1} - r_{S_{-1}}) \cos \phi \end{bmatrix} = \frac{1}{2} \begin{bmatrix} \Delta r_S \sin \phi \\ \Delta y_S \\ \Delta r_S \cos \phi \end{bmatrix} \quad (7.1.139)$$

Furthermore, the tangential vector $\mathbf{t}_{0\eta}^B$ can be formulated in the following way:

$$\mathbf{t}_{0\eta}^B = \frac{1}{2} (\mathbf{x}^B(\mathbf{c}_{S_1}, \phi) - \mathbf{x}^B(\mathbf{c}_{S_{-1}}, \phi)) = \frac{1}{2} (\mathbf{S}_2(\phi) \mathbf{c}_{S_1} - \mathbf{S}_2(\phi) \mathbf{c}_{S_{-1}}) = \frac{1}{2} \mathbf{S}_2(\phi) (\mathbf{c}_{S_1} - \mathbf{c}_{S_{-1}}) \quad (7.1.140)$$

The deformation field of the flexible wheelset is described by a modal synthesis. As described in the section 5.9.1, it is reasonable to formulate the distribution of the deformations over the

circumference of a circle defined by $\mathbf{c} = \mathbf{c}(r, y)$ as a continuous Fourier series. Thereby, it is valid:

$$\mathbf{w}^B(\mathbf{c}, \phi, t) = \sum_I \mathbf{W}_I^B(\mathbf{c}, \phi) q_I^B(t) = \sum_I \left(\sum_{K=K_{I,\min}}^{K_{I,\max}} \mathbf{W}_{I,K}^B(\mathbf{c}) e^{iK\phi} \right) q_I^B(t) \quad (7.1.141)$$

Based on this, the tangential vector \mathbf{t}_ϕ^B with respect to the azimuth ϕ is obtained to:

$$\mathbf{t}_\phi^B = \begin{bmatrix} r_{M_{wi}} \cos \phi \\ 0 \\ -r_{M_{wi}} \sin \phi \end{bmatrix} + \sum_I \left(\sum_{K=K_{I,\min}}^{K_{I,\max}} \mathbf{W}_{I,K}^B(\mathbf{c}_{M_{wi}}) iK e^{iK\phi} \right) q_I^B(t) \quad (7.1.142)$$

The tangential vector \mathbf{t}_η^B with respect to the lateral coordinate η is obtained to:

$$\mathbf{t}_\eta^B = \underbrace{\frac{1}{2} \mathbf{S}_2(\phi) (\mathbf{c}_{S_1} - \mathbf{c}_{S_{-1}})}_{\mathbf{t}_{0\eta}^B} + \sum_I \left(\sum_{K=K_{I,\min}}^{K_{I,\max}} \frac{1}{2} \left(\mathbf{W}_{I,K}^B(\mathbf{c}_{S_1}) - \mathbf{W}_{I,K}^B(\mathbf{c}_{S_{-1}}) \right) e^{iK\phi} \right) q_I^B(t) \quad (7.1.143)$$

The normal vector is determined by the cross product of the tangential vectors. In order to find the suitable sequence, the following cross product of the vectors $\mathbf{t}_{0\phi}^B$ and $\mathbf{t}_{0\eta}^B$ is considered:

$$\begin{aligned} \mathbf{t}_{0\phi}^B \times \mathbf{t}_{0\eta}^B &= \begin{bmatrix} r_{M_{wi}} \cos \phi \\ 0 \\ -r_{M_{wi}} \sin \phi \end{bmatrix} \times \frac{1}{2} \begin{bmatrix} \Delta r_S \sin \phi \\ \Delta y_S \\ \Delta r_S \cos \phi \end{bmatrix} = \frac{1}{2} \begin{bmatrix} \Delta y_S r_{M_{wi}} \sin \phi \\ \Delta r_S r_{M_{wi}} (-\sin^2 \phi - \cos^2 \phi) \\ \Delta y_S r_{M_{wi}} \cos \phi \end{bmatrix} \\ &= \frac{1}{2} \begin{bmatrix} \Delta y_S r_{M_{wi}} \sin \phi \\ -\Delta r_S r_{M_{wi}} \\ \Delta y_S r_{M_{wi}} \cos \phi \end{bmatrix} = \underbrace{\begin{bmatrix} \cos \phi & 0 & \sin \phi \\ 0 & 1 & 0 \\ -\sin \phi & 0 & \cos \phi \end{bmatrix}}_{\mathbf{S}_2(\phi)} \underbrace{\begin{bmatrix} 0 \\ -\Delta r_S \\ \Delta y_S \end{bmatrix}}_{\mathbf{c}_{0n}} \end{aligned} \quad (7.1.144)$$

According to (7.1.133) the radius $r_{M_{wi}}$ is positive. If the nodes S_{-1} and S_1 are chosen in such a way that it is valid $y_{S_1} < y_{S_{-1}}$, i.e. the node S_{-1} is lying left of the node S_1 , then the third coordinate of the vector \mathbf{c}_{0n} is positive as it is the case for the vector $\mathbf{c}_{M_{wi}}$ according to (7.1.133), i.e. both vectors $\mathbf{c}_{M_{wi}}$ and \mathbf{c}_{0n} are pointing outwards. Therefore, the chosen sequence in the vector product $\mathbf{t}_{0\phi}^B \times \mathbf{t}_{0\eta}^B$ which describes the normal vector to the undeformed surface is reasonable.

Based on the tangential vectors which are calculated according to (7.1.142) and (7.1.143) the rotation matrix \mathbf{S}^{BS} can now be determined based on the method developed in the section 7.1.1. Here, the trajectory curve, for which the azimuth ϕ is the parameter, is the path curve; therefore, the tangential vector \mathbf{t}_ϕ^B is assigned to the vector \mathbf{y}_1 :

$$\mathbf{y}_3 = \mathbf{n}_i^B = \mathbf{t}_{\phi,i}^B \times \mathbf{t}_{\eta,i}^B \Rightarrow \mathbf{e}_{S3}^B = \frac{\mathbf{n}_i^B}{|\mathbf{n}_i^B|}, \quad \mathbf{y}_1 = \mathbf{t}_{\phi,i}^B \Rightarrow \mathbf{e}_{S1}^B = \frac{\mathbf{t}_{x,i}^B}{|\mathbf{t}_{x,i}^B|}, \quad \mathbf{e}_{S2}^B = \mathbf{e}_{S3}^B \times \mathbf{e}_{S1}^B \quad (7.1.145)$$

$$\Rightarrow \mathbf{S}^{BS} = [\mathbf{e}_{S1}^B \quad \mathbf{e}_{S2}^B \quad \mathbf{e}_{S3}^B] \quad (7.1.146)$$

In an analogous way, the matrix \mathbf{S}_0^{BS} is determined. For the absolute values of the vector $\mathbf{n}_0^B = \mathbf{t}_{0\phi}^B \times \mathbf{t}_{0\eta}^B$ it is valid:

$$\begin{aligned} \mathbf{n}_0^B = \mathbf{t}_{0\phi}^B \times \mathbf{t}_{0\eta}^B &= \frac{r_{M_{wi}}}{2} \mathbf{S}_2(\phi) \mathbf{c}_{0n} \Rightarrow \mathbf{n}_0^{B^T} \mathbf{n}_0^B = \frac{r_{M_{wi}}^2}{4} \mathbf{c}_{0n}^T \underbrace{\mathbf{S}_2(\phi)^T \mathbf{S}_2(\phi)}_{\mathbf{I}} \mathbf{c}_{0n} \\ \Rightarrow |\mathbf{n}_0^B| &= \sqrt{\mathbf{n}_0^{B^T} \mathbf{n}_0^B} = \frac{r_{M_{wi}}}{2} \sqrt{\mathbf{c}_{0n}^T \mathbf{c}_{0n}} = \frac{r_{M_{wi}}}{2} |\mathbf{c}_{0n}| = \frac{r_{M_{wi}}}{2} \sqrt{\Delta y_S^2 + \Delta r_S^2} \end{aligned} \quad (7.1.147)$$

Thereby, it is obtained for the vector \mathbf{e}_{S30}^B :

$$\mathbf{e}_{S30}^B = \frac{\mathbf{n}_0^B}{|\mathbf{n}_0^B|} = \mathbf{S}_2(\phi) \frac{\mathbf{c}_{0n}}{|\mathbf{c}_{0n}|} = \mathbf{S}_2(\phi) \underbrace{\frac{1}{\sqrt{\Delta y_S^2 + \Delta r_S^2}} \begin{bmatrix} 0 \\ -\Delta r_S \\ \Delta y_S \end{bmatrix}}_{\mathbf{e}_{S3}} = \frac{1}{\sqrt{\Delta y_S^2 + \Delta r_S^2}} \begin{bmatrix} \Delta y_S \sin \phi \\ -\Delta r_S \\ \Delta y_S \cos \phi \end{bmatrix} \quad (7.1.148)$$

Since the radius $r_{M_{wi}}$ is positive, i.e. $r_{M_{wi}} > 0$, and since it is valid $\sin^2 \phi + \cos^2 \phi = 1$, the vector \mathbf{e}_{S10}^B is easily obtained from normalizing the vector $\mathbf{t}_{\phi 0}^B$:

$$\mathbf{t}_{\phi 0}^{\mathcal{R}} = r_{M_{wi}} \begin{bmatrix} \cos \phi \\ 0 \\ -\sin \phi \end{bmatrix} = r_{M_{wi}} \mathbf{S}_2(\phi) \underbrace{\begin{bmatrix} 1 \\ 0 \\ 0 \end{bmatrix}}_{\mathbf{e}_1} \Rightarrow \mathbf{e}_{S10}^B = \frac{\mathbf{t}_{\phi 0}^{\mathcal{R}}}{|\mathbf{t}_{\phi 0}^{\mathcal{R}}|} = \begin{bmatrix} \cos \phi \\ 0 \\ -\sin \phi \end{bmatrix} = \mathbf{S}_2(\phi) \mathbf{e}_1 \quad (7.1.149)$$

The third vector \mathbf{e}_{S20}^B is determined in the following way:

$$\begin{aligned} \mathbf{e}_{S20}^B &= \frac{1}{\sqrt{\Delta y_S^2 + \Delta r_S^2}} \begin{bmatrix} \Delta y_S \sin \phi \\ -\Delta r_S \\ \Delta y_S \cos \phi \end{bmatrix} \times \begin{bmatrix} \cos \phi \\ 0 \\ -\sin \phi \end{bmatrix} = \frac{1}{\sqrt{\Delta y_S^2 + \Delta r_S^2}} \begin{bmatrix} \Delta r_S \sin \phi \\ \Delta y_S \sin^2 \phi + \Delta y_S \cos^2 \phi \\ \Delta r_S \cos \phi \end{bmatrix} \\ &= \frac{1}{\sqrt{\Delta y_S^2 + \Delta r_S^2}} \begin{bmatrix} \Delta r_S \sin \phi \\ \Delta y_S \\ \Delta r_S \cos \phi \end{bmatrix} = \underbrace{\begin{bmatrix} \cos \phi & 0 & \sin \phi \\ 0 & 1 & 0 \\ -\sin \phi & 0 & \cos \phi \end{bmatrix}}_{\mathbf{S}_2(\phi)} \underbrace{\frac{1}{\sqrt{\Delta y_S^2 + \Delta r_S^2}} \begin{bmatrix} 0 \\ \Delta y_S \\ \Delta r_S \end{bmatrix}}_{\mathbf{e}_{S2}} \end{aligned} \quad (7.1.150)$$

In total, the matrix \mathbf{S}_0^{BS} is obtained to:

$$\mathbf{S}_0^{BS} = [\mathbf{e}_{S10}^B \quad \mathbf{e}_{S20}^B \quad \mathbf{e}_{S30}^B] = [\mathbf{S}_2(\phi) \mathbf{e}_1 \quad \mathbf{S}_2(\phi) \mathbf{e}_{S2} \quad \mathbf{S}_2(\phi) \mathbf{e}_{S3}] = \mathbf{S}_2(\phi) [\mathbf{e}_1 \quad \mathbf{e}_{S2} \quad \mathbf{e}_{S3}] \quad (7.1.151)$$

If in the reference state the 2-axis of the frame \mathcal{M}_{wi} is parallel to the 2-axis of the wheelset, then it is valid for the matrix $\mathbf{S}_0^{B\mathcal{M}_{wi}}$:

$$\mathbf{S}_0^{B\mathcal{M}_{wi}} = \mathbf{S}_0^{BS} \mathbf{S}^{S\mathcal{M}_{wi}} = \mathbf{S}_2(\phi) \quad (7.1.152)$$

From this it follows for the matrix $\mathbf{S}^{S\mathcal{M}_{wi}}$:

$$\mathbf{S}^{S\mathcal{M}_{wi}} = \mathbf{S}_0^{BS^{-1}} \mathbf{S}_0^{B\mathcal{M}_{wi}} = \mathbf{S}_0^{BS^T} \mathbf{S}_2(\phi) = \begin{bmatrix} \mathbf{e}_1^T \\ \mathbf{e}_{S2}^T \\ \mathbf{e}_{S3}^T \end{bmatrix} \underbrace{\mathbf{S}_2(\phi)^T \mathbf{S}_2(\phi)}_{\mathbf{I}} \Rightarrow \mathbf{S}^{S\mathcal{M}_{wi}} = \begin{bmatrix} \mathbf{e}_1^T \\ \mathbf{e}_{S2}^T \\ \mathbf{e}_{S3}^T \end{bmatrix} \quad (7.1.153)$$

Thereby, the matrix $\mathbf{S}^{S\mathcal{M}_{wi}}$ is known so that the rotation matrix between the body-fixed frame \mathcal{B} and the frame \mathcal{M}_{wi} can be calculated:

$$\mathbf{S}^{B\mathcal{M}_{wi}} = \mathbf{S}^{BS} \mathbf{S}^{S\mathcal{M}_{wi}} \quad (7.1.154)$$

Also here, the angular velocity is determined based on the following expression derived in the section 7.1.2:

$$\boldsymbol{\omega}_{\mathcal{R}S}^{\mathcal{R}} = \frac{\mathbf{n}^{\mathcal{R}} \times \dot{\mathbf{n}}^{\mathcal{R}}}{\mathbf{n}^{\mathcal{R}} \cdot \mathbf{n}^{\mathcal{R}}} + \frac{1}{2} \left(\frac{\mathbf{n}^{\mathcal{R}} \cdot (\mathbf{t}_{\xi}^{\mathcal{R}} \times \dot{\mathbf{t}}_{\xi}^{\mathcal{R}})}{\mathbf{t}_{\xi}^{\mathcal{R}} \cdot \mathbf{t}_{\xi}^{\mathcal{R}}} + \frac{\mathbf{n}^{\mathcal{R}} \cdot (\mathbf{t}_{\eta}^{\mathcal{R}} \times \dot{\mathbf{t}}_{\eta}^{\mathcal{R}})}{\mathbf{t}_{\eta}^{\mathcal{R}} \cdot \mathbf{t}_{\eta}^{\mathcal{R}}} \right) \frac{\mathbf{n}^{\mathcal{R}}}{\mathbf{n}^{\mathcal{R}} \cdot \mathbf{n}^{\mathcal{R}}} \quad (7.1.155)$$

Similar to the case of the rail, the constant matrix $\mathbf{S}^{SM_{wi}}$ has no influence on the angular velocity. Therefore, it is valid for the angular velocity $\omega_{\mathcal{B}M_{wi}}^{\mathcal{B}}$:

$$\omega_{\mathcal{B}M_{wi}}^{\mathcal{B}} = \omega_{\mathcal{B}S}^{\mathcal{B}} = \frac{\mathbf{n}^{\mathcal{B}} \times \dot{\mathbf{n}}^{\mathcal{B}}}{\mathbf{n}^{\mathcal{B}} \cdot \mathbf{n}^{\mathcal{B}}} + \frac{1}{2} \left(\frac{\mathbf{n}^{\mathcal{B}} \cdot (\mathbf{t}_{\phi}^{\mathcal{B}} \times \dot{\mathbf{t}}_{\phi}^{\mathcal{B}})}{\mathbf{t}_{\phi}^{\mathcal{B}} \cdot \mathbf{t}_{\phi}^{\mathcal{B}}} + \frac{\mathbf{n}^{\mathcal{B}} \cdot (\mathbf{t}_{\eta}^{\mathcal{B}} \times \dot{\mathbf{t}}_{\eta}^{\mathcal{B}})}{\mathbf{t}_{\eta}^{\mathcal{B}} \cdot \mathbf{t}_{\eta}^{\mathcal{B}}} \right) \frac{\mathbf{n}^{\mathcal{B}}}{\mathbf{n}^{\mathcal{B}} \cdot \mathbf{n}^{\mathcal{B}}} \quad (7.1.156)$$

Also here, the angular velocity shall be simplified:

$$\omega_{\mathcal{B}M_{wi}}^{\mathcal{B}} \approx \frac{\mathbf{n}_0^{\mathcal{B}} \times \dot{\mathbf{n}}_0^{\mathcal{B}}}{\mathbf{n}_0^{\mathcal{B}} \cdot \mathbf{n}_0^{\mathcal{B}}} + \frac{1}{2} \left(\frac{\mathbf{n}_0^{\mathcal{B}} \cdot (\mathbf{t}_{\phi 0}^{\mathcal{B}} \times \dot{\mathbf{t}}_{\phi 0}^{\mathcal{B}})}{\mathbf{t}_{\phi 0}^{\mathcal{B}} \cdot \mathbf{t}_{\phi 0}^{\mathcal{B}}} + \frac{\mathbf{n}_0^{\mathcal{B}} \cdot (\mathbf{t}_{\eta 0}^{\mathcal{B}} \times \dot{\mathbf{t}}_{\eta 0}^{\mathcal{B}})}{\mathbf{t}_{\eta 0}^{\mathcal{B}} \cdot \mathbf{t}_{\eta 0}^{\mathcal{B}}} \right) \frac{\mathbf{n}_0^{\mathcal{B}}}{\mathbf{n}_0^{\mathcal{B}} \cdot \mathbf{n}_0^{\mathcal{B}}} \quad (7.1.157)$$

Thereby, it is set for the normal vector $\mathbf{n}^{\mathcal{B}}$:

$$\mathbf{n}^{\mathcal{B}} = \mathbf{t}_{\phi}^{\mathcal{B}} \times \mathbf{t}_{\eta}^{\mathcal{R}} \approx \mathbf{t}_{0\phi}^{\mathcal{B}} \times \mathbf{t}_{0\eta}^{\mathcal{B}} = \mathbf{n}_0^{\mathcal{B}} \quad (7.1.158)$$

The derivative $\dot{\mathbf{n}}^{\mathcal{R}}$ of the normal vector is approximated in the following way:

$$\mathbf{n}^{\mathcal{B}} = \mathbf{t}_{\phi}^{\mathcal{B}} \times \mathbf{t}_{\eta}^{\mathcal{B}} \Rightarrow \dot{\mathbf{n}}^{\mathcal{B}} = \dot{\mathbf{t}}_{\phi}^{\mathcal{B}} \times \mathbf{t}_{\eta}^{\mathcal{B}} + \mathbf{t}_{\phi}^{\mathcal{B}} \times \dot{\mathbf{t}}_{\eta}^{\mathcal{B}} \approx \dot{\mathbf{t}}_x^{\mathcal{B}} \times \mathbf{t}_{0\eta}^{\mathcal{B}} + \mathbf{t}_{0\phi}^{\mathcal{R}} \times \dot{\mathbf{t}}_{\eta}^{\mathcal{B}} \quad (7.1.159)$$

The vectors $\dot{\mathbf{t}}_{\phi}^{\mathcal{B}}$ and $\dot{\mathbf{t}}_{\eta}^{\mathcal{B}}$ are derived from (7.1.142) and (7.1.143), respectively; it is obtained:

$$\dot{\mathbf{t}}_{\phi,i}^{\mathcal{R}} = \sum_I \left(\sum_{K=K_{I,\min}}^{K_{I,\max}} \mathbf{w}_{M_{R|I,K}} iK e^{iK \phi_{WRi}} \right) \dot{q}_I^{\mathcal{B}}(t) = \sum_I \left(\sum_{K=K_{I,\min}}^{K_{I,\max}} \mathbf{t}_{\phi|I,K} e^{iK \phi_{WRi}} \right) \dot{q}_I^{\mathcal{B}}(t) \quad (7.1.160)$$

$$\dot{\mathbf{t}}_{\eta,i}^{\mathcal{R}} = \sum_I \left(\sum_{K=K_{I,\min}}^{K_{I,\max}} \mathbf{t}_{\eta|I,K} e^{iK \phi_{WRi}} \right) \dot{q}_I^{\mathcal{B}}(t) \quad (7.1.161)$$

Here, the following abbreviation has been introduced for a better overview:

$$\mathbf{t}_{\phi|I,K} = \mathbf{w}_{M_{R|I,K}} iK \quad (7.1.162)$$

Based on this, the terms for the angular velocity can be formulated by a modal synthesis:

$$\frac{\mathbf{n}_0^{\mathcal{B}} \times (\dot{\mathbf{t}}_{\phi}^{\mathcal{B}} \times \mathbf{t}_{0\eta}^{\mathcal{B}} + \mathbf{t}_{0\phi}^{\mathcal{B}} \times \dot{\mathbf{t}}_{\eta}^{\mathcal{B}})}{\mathbf{n}_0^{\mathcal{B}} \cdot \mathbf{n}_0^{\mathcal{B}}} = \sum_I \left(\sum_{K=K_{I,\min}}^{K_{I,\max}} \frac{\mathbf{n}_0^{\mathcal{B}} \times (\mathbf{t}_{\phi|I,K}^{\mathcal{B}} \times \mathbf{t}_{0\eta}^{\mathcal{B}} + \mathbf{t}_{0\phi}^{\mathcal{B}} \times \mathbf{t}_{\eta|I,K}^{\mathcal{B}})}{\mathbf{n}_0^{\mathcal{B}} \cdot \mathbf{n}_0^{\mathcal{B}}} e^{iK \phi_{WRi}} \right) \dot{q}_I^{\mathcal{B}}(t) \quad (7.1.163)$$

$$\frac{\mathbf{n}_0^{\mathcal{B}} \cdot (\mathbf{t}_{0\phi}^{\mathcal{B}} \times \dot{\mathbf{t}}_{\phi}^{\mathcal{B}})}{\mathbf{t}_{0\phi}^{\mathcal{B}} \cdot \mathbf{t}_{0\phi}^{\mathcal{B}}} \frac{\mathbf{n}_0^{\mathcal{B}}}{\mathbf{n}_0^{\mathcal{B}} \cdot \mathbf{n}_0^{\mathcal{B}}} = \sum_I \left(\sum_{K=K_{I,\min}}^{K_{I,\max}} \frac{\mathbf{n}_0^{\mathcal{B}} \cdot (\mathbf{t}_{0\phi}^{\mathcal{B}} \times \mathbf{t}_{\phi|I,K}^{\mathcal{B}})}{\mathbf{t}_{0\phi}^{\mathcal{B}} \cdot \mathbf{t}_{0\phi}^{\mathcal{B}}} \frac{\mathbf{n}_0^{\mathcal{B}}}{\mathbf{n}_0^{\mathcal{B}} \cdot \mathbf{n}_0^{\mathcal{B}}} e^{iK \phi_{WRi}} \right) \dot{q}_I^{\mathcal{B}}(t) \quad (7.1.164)$$

$$\frac{\mathbf{n}_0^{\mathcal{B}} \cdot (\mathbf{t}_{0\eta}^{\mathcal{B}} \times \dot{\mathbf{t}}_{\eta}^{\mathcal{B}})}{\mathbf{t}_{0\eta}^{\mathcal{B}} \cdot \mathbf{t}_{0\eta}^{\mathcal{B}}} \frac{\mathbf{n}_0^{\mathcal{B}}}{\mathbf{n}_0^{\mathcal{B}} \cdot \mathbf{n}_0^{\mathcal{B}}} = \sum_I \left(\sum_{K=K_{I,\min}}^{K_{I,\max}} \frac{\mathbf{n}_0^{\mathcal{B}} \cdot (\mathbf{t}_{0\eta}^{\mathcal{B}} \times \mathbf{t}_{\eta|I,K}^{\mathcal{B}})}{\mathbf{t}_{0\eta}^{\mathcal{B}} \cdot \mathbf{t}_{0\eta}^{\mathcal{B}}} \frac{\mathbf{n}_0^{\mathcal{B}}}{\mathbf{n}_0^{\mathcal{B}} \cdot \mathbf{n}_0^{\mathcal{B}}} e^{iK \phi_{WRi}} \right) \dot{q}_I^{\mathcal{B}}(t) \quad (7.1.165)$$

Similar to the rail, the following modal coefficients are defined:

$$\Omega_{I,K}^{\mathcal{B}} = \frac{\mathbf{n}_0^{\mathcal{B}} \times (\mathbf{t}_{\phi|I,K}^{\mathcal{B}} \times \mathbf{t}_{0\eta}^{\mathcal{B}} + \mathbf{t}_{0\phi}^{\mathcal{B}} \times \mathbf{t}_{\eta|I,K}^{\mathcal{B}})}{\mathbf{n}_0^{\mathcal{B}} \cdot \mathbf{n}_0^{\mathcal{B}}} + \frac{1}{2} \left(\frac{\mathbf{n}_0^{\mathcal{B}} \cdot (\mathbf{t}_{0\phi}^{\mathcal{B}} \times \mathbf{t}_{\phi|I,K}^{\mathcal{B}})}{\mathbf{t}_{0\phi}^{\mathcal{B}} \cdot \mathbf{t}_{0\phi}^{\mathcal{B}}} + \frac{\mathbf{n}_0^{\mathcal{B}} \cdot (\mathbf{t}_{0\eta}^{\mathcal{B}} \times \mathbf{t}_{\eta|I,K}^{\mathcal{B}})}{\mathbf{t}_{0\eta}^{\mathcal{B}} \cdot \mathbf{t}_{0\eta}^{\mathcal{B}}} \right) \frac{\mathbf{n}_0^{\mathcal{B}}}{\mathbf{n}_0^{\mathcal{B}} \cdot \mathbf{n}_0^{\mathcal{B}}} \quad (7.1.166)$$

Based on this, it can finally be formulated:

$$\omega_{\mathcal{B}M_{wi}}^{\mathcal{B}} \approx \sum_I \left(\sum_{K=K_{I,\min}}^{K_{I,\max}} \Omega_{I,K}^{\mathcal{B}} e^{iK \phi_{WRi}} \right) \dot{q}_I^{\mathcal{B}}(t) \quad (7.1.167)$$

7.2 Geometry and kinematics of the contact

Based on the relative kinematics of the coupling points K_W and K_R the contact zone itself and the kinematics inside this zone are determined. As already mentioned the surfaces of the wheel contact body and of the rail contact body are assumed to be rotational symmetric and prismatic, respectively. The following considerations are based on the work of Netter [48].

The rail surface is assumed to be the lateral surface of a prism. The axis of extrusion is the 1-axis, while the 2- and the 3-axis form the cross section. If the rail profile is defined by the profile function $z_R = z_R(y_R)$ depending on the lateral coordinate y_R , then the rail surface is described by:

$$\mathbf{r}_{K_R P_R}^{\mathcal{R}} \equiv \mathbf{x}_R(\xi, y_R) = \begin{bmatrix} \xi \\ y_R \\ z_R(y_R) \end{bmatrix} \quad (7.2.168)$$

The wheel surface is considered as a rotational symmetric surface. Using the nominal radius r_0 and the profile function $z_W = z_W(y_W)$ the surface can be described by:

$$\mathbf{r}_{M_W P_W}^{\mathcal{W}} = \begin{bmatrix} [r_0 + z_W(y_W)] \sin \theta \\ y_W \\ [r_0 + z_W(y_W)] \cos \theta \end{bmatrix} = \underbrace{\begin{bmatrix} \cos \theta & 0 & \sin \theta \\ 0 & 1 & 0 \\ -\sin \theta & 0 & \cos \theta \end{bmatrix}}_{\mathbf{S}_2(\theta)} \underbrace{\begin{bmatrix} 0 \\ y_W \\ r_W \end{bmatrix}}_{\mathbf{p}_W(y_W)}, \quad r_W = r_0 + z_W(y_W) \quad (7.2.169)$$

Here, the vector $\mathbf{p}_W = \mathbf{p}_W(y_W)$, which contains the profile function for the wheel, is introduced. It is furthermore assumed that the radius r_W is strictly positive, i.e.:

$$r_W = r_0 + z_W(y_W) > 0 \quad (7.2.170)$$

In the following considerations the dependency of the vertical profile coordinates z_W and z_R on the lateral profile coordinates y_W and y_R , respectively, are not mentioned explicitly for a better overview.

The surface of the wheel contact body is described for the centre point M_W of the wheel. For the taper circle, the lateral coordinate is $y_W = 0$ and the radius is equal to the nominal rolling radius. The coupling point K_W is located on the taper circle. Therefore, it is valid:

$$\mathbf{r}_{K_W P_W}^{\mathcal{W}} = \mathbf{r}_{K_W M_W}^{\mathcal{W}} + \mathbf{r}_{M_W P_W}^{\mathcal{W}} = \begin{bmatrix} 0 \\ 0 \\ -r_0 \end{bmatrix} + \mathbf{S}_2(\theta) \mathbf{p}_W(y_W) \quad (7.2.171)$$

Therefore, the resulting vector between the rail coupling point K_R and the centre point of the wheel M_W is expressed in the rail profile frame in the following way:

$$\mathbf{r}_{K_R M_W}^{\mathcal{R}} = \mathbf{r}_{K_R K_W}^{\mathcal{R}} + \mathbf{S}^{\mathcal{R}\mathcal{W}} \mathbf{r}_{K_W M_W}^{\mathcal{W}} = \begin{bmatrix} \Delta X_{RW} \\ \Delta Y_{RW} \\ \Delta Z_{RW} \end{bmatrix} \quad (7.2.172)$$

The relative displacement and the relative rotation are described by the vector $\mathbf{r}_{K_R K_W}^{\mathcal{R}}$ and the matrix $\mathbf{S}^{\mathcal{R}\mathcal{W}}$, respectively, which belong to the kinematical input of the contact model. Since the vector $\mathbf{r}_{K_W M_W}^{\mathcal{W}}$ is constant, the relative displacement $\mathbf{r}_{K_R M_W}^{\mathcal{R}}$ is calculated directly without iteration.

Since the rail surface is considered as a prism with its extrusion oriented in the direction of the 1-axis of the rail frame, it is obvious to project the wheel surface into the 2,3-plane of the rail frame

\mathcal{R} . In a first step, the description of the wheel surface in the frame \mathcal{R} is required. The rotation matrix $\mathbf{S}^{\mathcal{R}\mathcal{W}}$ used for the transformation is composed of three rotations around the 1-, the 2- and the 3-axis. Since the extrusion of the prism is oriented in the direction of the 1-axis of the rail profile frame \mathcal{R} , it is advantageous to choose the rotation around the 1-axis with the angle α as the first rotation in the sequence. The wheel surface is a rotational symmetric surface with the 2-axis as the axis of symmetry. Therefore it is obvious to choose the rotation around the 2-axis with the angle β as the last rotation in the sequence. The remaining rotation around the 3-axis with the angle γ is therefore the second rotation. In total, the rotation matrix $\mathbf{S}^{\mathcal{R}\mathcal{W}}$ is composed in the following way:

$$\begin{aligned}\mathbf{S}^{\mathcal{R}\mathcal{W}} &= \mathbf{S}_1(\alpha)\mathbf{S}_3(\gamma)\mathbf{S}_2(\beta) \\ &= \begin{bmatrix} \cos\gamma\cos\beta & -\sin\gamma & \cos\gamma\sin\beta \\ \cos\alpha\sin\gamma\cos\beta + \sin\alpha\sin\beta & \cos\alpha\cos\gamma & \cos\alpha\sin\gamma\sin\beta - \sin\alpha\cos\beta \\ \sin\alpha\sin\gamma\cos\beta - \cos\alpha\sin\beta & \sin\alpha\cos\gamma & \sin\alpha\sin\gamma\sin\beta + \cos\alpha\cos\beta \end{bmatrix}\end{aligned}\quad (7.2.173)$$

As already mentioned, the matrix $\mathbf{S}^{\mathcal{R}\mathcal{W}}$ is given by the kinematics used as the input. By comparing the given matrix $\mathbf{S}^{\mathcal{R}\mathcal{W}}$

$$\mathbf{S}^{\mathcal{R}\mathcal{W}} = \begin{bmatrix} s_{11}^{\mathcal{R}\mathcal{W}} & s_{12}^{\mathcal{R}\mathcal{W}} & s_{13}^{\mathcal{R}\mathcal{W}} \\ s_{21}^{\mathcal{R}\mathcal{W}} & s_{22}^{\mathcal{R}\mathcal{W}} & s_{23}^{\mathcal{R}\mathcal{W}} \\ s_{31}^{\mathcal{R}\mathcal{W}} & s_{32}^{\mathcal{R}\mathcal{W}} & s_{33}^{\mathcal{R}\mathcal{W}} \end{bmatrix}\quad (7.2.174)$$

to the formulation according to (7.2.173), the trigonometric functions of the angles α , β and γ can be determined in the following way:

$$\begin{aligned}s_{22}^{\mathcal{R}\mathcal{W}} &= \cos\alpha\cos\gamma, \quad s_{32}^{\mathcal{R}\mathcal{W}} = \sin\alpha\cos\gamma \\ \Rightarrow \frac{s_{32}^{\mathcal{R}\mathcal{W}}}{s_{22}^{\mathcal{R}\mathcal{W}}} &= \frac{\sin\alpha\cos\gamma}{\cos\alpha\cos\gamma} = \tan\alpha \Rightarrow \cos\alpha = \frac{1}{\sqrt{1+\tan^2\alpha}}, \quad \sin\alpha = \frac{\sin\alpha}{\sqrt{1+\tan^2\alpha}}\end{aligned}\quad (7.2.175)$$

$$\begin{aligned}s_{11}^{\mathcal{R}\mathcal{W}} &= \cos\gamma\cos\beta, \quad s_{13}^{\mathcal{R}\mathcal{W}} = \cos\gamma\sin\beta \\ \Rightarrow \frac{s_{13}^{\mathcal{R}\mathcal{W}}}{s_{11}^{\mathcal{R}\mathcal{W}}} &= \frac{\cos\gamma\sin\beta}{\cos\gamma\cos\beta} = \tan\beta \Rightarrow \cos\beta = \frac{1}{\sqrt{1+\tan^2\beta}}, \quad \sin\beta = \frac{\sin\beta}{\sqrt{1+\tan^2\beta}}\end{aligned}\quad (7.2.176)$$

$$s_{12}^{\mathcal{R}\mathcal{W}} = -\sin\gamma \Rightarrow \cos\gamma = \sqrt{1-\sin^2\gamma}, \quad \tan\gamma = \frac{\sin\gamma}{\sqrt{1-\sin^2\gamma}}\quad (7.2.177)$$

Thereby, the expressions $\sin\alpha$, $\cos\alpha$, $\sin\beta$, $\cos\beta$, $\sin\gamma$ and $\cos\gamma$, which are required for the following considerations, are known.

Using the relative vector $\mathbf{r}_{\mathcal{K}_R\mathcal{M}_W}^{\mathcal{R}}$ describing the relative translation between the reference point of the rail and the centre of the wheel, the description of the wheel surface in the rail profile frame \mathcal{R} is obtained by:

$$\mathbf{r}_{\mathcal{K}_R\mathcal{P}_W}^{\mathcal{R}} = \mathbf{r}_{\mathcal{K}_R\mathcal{M}_W}^{\mathcal{R}} + \mathbf{S}^{\mathcal{R}\mathcal{W}}\mathbf{r}_{\mathcal{M}_W\mathcal{P}_W}^{\mathcal{W}} = \mathbf{r}_{\mathcal{K}_R\mathcal{M}_W}^{\mathcal{R}} + \mathbf{S}_1(\alpha)\mathbf{S}_3(\gamma)\mathbf{S}_2(\beta)\mathbf{r}_{\mathcal{M}_W\mathcal{P}_W}^{\mathcal{R}}\quad (7.2.178)$$

The evaluation of the product of the matrices $\mathbf{S}_1(\alpha)$ and $\mathbf{S}_3(\gamma)$ gives:

$$\mathbf{S}_1(\alpha)\mathbf{S}_3(\gamma) = \begin{bmatrix} 1 & 0 & 0 \\ 0 & \cos\alpha & -\sin\alpha \\ 0 & \sin\alpha & \cos\alpha \end{bmatrix} \begin{bmatrix} \cos\gamma & -\sin\gamma & 0 \\ \sin\gamma & \cos\gamma & 0 \\ 0 & 0 & 1 \end{bmatrix} = \begin{bmatrix} \cos\gamma & -\sin\gamma & 0 \\ \cos\alpha\sin\gamma & \cos\alpha\cos\gamma & -\sin\alpha \\ \sin\alpha\sin\gamma & \sin\alpha\cos\gamma & \cos\alpha \end{bmatrix}\quad (7.2.179)$$

The transformation of the wheel surface vector into the rail frame \mathcal{R} leads to:

$$\begin{aligned} \mathbf{r}_{M_W P_W}^{\mathcal{R}} &= \mathbf{S}^{\mathcal{R}\mathcal{W}} \mathbf{r}_{M_W P_W}^{\mathcal{W}} = \mathbf{S}_1(\alpha) \mathbf{S}_3(\gamma) \underbrace{\mathbf{S}_2(\beta) \mathbf{S}_2(\theta)}_{\mathbf{S}_2(\beta+\theta)} \mathbf{p}_W(y_W) \\ &= \begin{bmatrix} \cos \gamma & -\sin \gamma & 0 \\ \cos \alpha \sin \gamma & \cos \alpha \cos \gamma & -\sin \alpha \\ \sin \alpha \sin \gamma & \sin \alpha \cos \gamma & \cos \alpha \end{bmatrix} \begin{bmatrix} r_W \sin(\beta + \theta) \\ y_W \\ r_W \cos(\beta + \theta) \end{bmatrix} \end{aligned} \quad (7.2.180)$$

7.2.1 Determination of the wheel envelope

The projection of the wheel surface into the 2,3-plane of the rail frame \mathcal{R} is done by the envelope of the wheel. To determine of the wheel the normal vector of the wheel surface is required. This normal vector calculated by a cross product of the tangential vectors of the surface, which are obtained as the derivatives of the wheel surface vector with respect to the two parameters of the surface. These two parameters are the circumferential angle θ and the lateral coordinate y_W . Thereby, for the tangential vectors it is obtained:

$$\frac{\partial \mathbf{r}_{M_W P_W}^{\mathcal{W}}}{\partial \theta} = \begin{bmatrix} r_W \cos \theta \\ 0 \\ -r_W \sin \theta \end{bmatrix}, \quad \frac{\partial \mathbf{r}_{M_W P_W}^{\mathcal{W}}}{\partial y_W} = \begin{bmatrix} r'_W \sin \theta \\ 1 \\ r'_W \cos \theta \end{bmatrix} = \begin{bmatrix} z'_W \sin \theta \\ 1 \\ z'_W \cos \theta \end{bmatrix} \quad (7.2.181)$$

Here, the following relation is used:

$$r'_W = \frac{dr_W}{dy_W} = \frac{d}{dy_W} [r_0 + z_W(y_W)] = \underbrace{\frac{dr_0}{dy_W}}_0 + \underbrace{\frac{dz_W(y_W)}{dy_W}}_{z'_W} = z'_W \quad (7.2.182)$$

As already mentioned, the normal vector $\mathbf{n}^{\mathcal{R}}$ is obtained from the cross product of the tangential vectors:

$$\begin{aligned} \mathbf{n}_W^{\mathcal{W}} &= \frac{\partial \mathbf{r}_{M_W P_W}^{\mathcal{W}}}{\partial \theta} \times \frac{\partial \mathbf{r}_{M_W P_W}^{\mathcal{W}}}{\partial y_W} = \begin{bmatrix} r_W \cos \theta \\ 0 \\ -r_W \sin \theta \end{bmatrix} \times \begin{bmatrix} z'_W \sin \theta \\ 1 \\ z'_W \cos \theta \end{bmatrix} = \begin{bmatrix} r_W \sin \theta \\ -r_W z'_W \sin^2 \theta - r_W z'_W \cos^2 \theta \\ r_W \cos \theta \end{bmatrix} \\ &= \begin{bmatrix} r_W \sin \theta \\ -r_W z'_W \\ r_W \cos \theta \end{bmatrix} = \mathbf{S}_2(\theta) \begin{bmatrix} 0 \\ -z'_W \\ 1 \end{bmatrix} r_W \end{aligned} \quad (7.2.183)$$

The transformation of the normal vector into the rail profile frame \mathcal{R} gives:

$$\begin{aligned} \mathbf{n}_W^{\mathcal{R}} &= \mathbf{S}^{\mathcal{R}\mathcal{W}} \mathbf{n}_W^{\mathcal{W}} = \mathbf{S}_1(\alpha) \mathbf{S}_3(\gamma) \underbrace{\mathbf{S}_2(\beta) \mathbf{S}_2(\theta)}_{\mathbf{S}_2(\beta+\theta)} \begin{bmatrix} 0 \\ -z'_W \\ 1 \end{bmatrix} r_W \\ &= \begin{bmatrix} \cos \gamma & -\sin \gamma & 0 \\ \cos \alpha \sin \gamma & \cos \alpha \cos \gamma & -\sin \alpha \\ \sin \alpha \sin \gamma & \sin \alpha \cos \gamma & \cos \alpha \end{bmatrix} \begin{bmatrix} \sin(\beta + \theta) \\ -z'_W \\ \cos(\beta + \theta) \end{bmatrix} r_W \end{aligned} \quad (7.2.184)$$

If a point of the wheel surface belongs to the wheel envelope, the normal vector $\mathbf{n}_{W,E}^{\mathcal{R}} = \mathbf{n}_W^{\mathcal{R}}(y_R, \theta_E)$ at this point lies in the 2,3-plane of the rail profile frame \mathcal{R} . Therefore, it must be possible to

express the vector $\mathbf{n}_{W,E}^{\mathcal{R}}$ in the following way:

$$\mathbf{n}_{W,E}^{\mathcal{R}} = \mathbf{S}_1(\Phi_E) \begin{bmatrix} 0 \\ 0 \\ \ell \end{bmatrix} = \begin{bmatrix} 1 & 0 & 0 \\ 0 & \cos \Phi_E & -\sin \Phi_E \\ 0 & \sin \Phi_E & \cos \Phi_E \end{bmatrix} \begin{bmatrix} 0 \\ 0 \\ \ell \end{bmatrix} = \begin{bmatrix} 0 \\ -\ell \sin \Phi_E \\ \ell \cos \Phi_E \end{bmatrix} \quad (7.2.185)$$

For the sake of brevity, the angle ε will be used in the following considerations; this angle is defined in the following way:

$$\varepsilon = \beta + \theta_E \quad (7.2.186)$$

Thereby, the normal vector $\mathbf{n}_{W,E}^{\mathcal{R}}$ can be written as:

$$\mathbf{n}_{W,E}^{\mathcal{R}} = \mathbf{n}_W^{\mathcal{R}}(y_R, \theta_E) = \mathbf{S}_1(\alpha) \mathbf{S}_3(\gamma) \mathbf{S}_2(\beta + \theta_E) \begin{bmatrix} 0 \\ -z'_W \\ 1 \end{bmatrix} r_W = \mathbf{S}_1(\alpha) \mathbf{S}_3(\gamma) \mathbf{S}_2(\varepsilon) \begin{bmatrix} 0 \\ -z'_W \\ 1 \end{bmatrix} r_W \quad (7.2.187)$$

By applying this condition to the normal vector it is obtained:

$$\mathbf{n}_{W,E}^{\mathcal{R}} = \begin{bmatrix} 0 \\ -\ell \sin \Phi_E \\ \ell \cos \Phi_E \end{bmatrix} = \begin{bmatrix} \cos \gamma \sin \varepsilon + \sin \gamma z'_W \\ \cos \alpha \sin \gamma \sin \varepsilon - \cos \alpha \cos \gamma z'_W - \sin \alpha \cos \varepsilon \\ \sin \alpha \sin \gamma \sin \varepsilon - \sin \alpha \cos \gamma z'_W + \cos \alpha \cos \varepsilon \end{bmatrix} r_W \quad (7.2.188)$$

From the comparison of the first components of the vectors, the condition for the angle θ_E can be found. Since the wheel radius r_W is assumed to be strictly positive according to (7.2.170), it is valid:

$$r_W > 0, [\cos \gamma \sin \varepsilon + \sin \gamma z'_W] r_W = 0 \Rightarrow \cos \gamma \sin \varepsilon = -\sin \gamma z'_W \Rightarrow \sin \varepsilon = -\tan \gamma z'_W \quad (7.2.189)$$

Thereby, the envelope can be described in the rail profile frame \mathcal{R} in the following form:

$$\mathbf{r}_{K_R P_{WE}}^{\mathcal{R}} = \mathbf{r}_{K_R M_W}^{\mathcal{R}} + \begin{bmatrix} \cos \gamma & -\sin \gamma & 0 \\ \cos \alpha \sin \gamma & \cos \alpha \cos \gamma & -\sin \alpha \\ \sin \alpha \sin \gamma & \sin \alpha \cos \gamma & \cos \alpha \end{bmatrix} \begin{bmatrix} r_W \sin \varepsilon \\ y_W \\ r_W \cos \varepsilon \end{bmatrix} \quad (7.2.190)$$

$$\sin \varepsilon = -\tan \gamma z'_W, \cos \varepsilon = \sqrt{1 - (\tan \gamma z'_W)^2}$$

Since the terms $\sin \varepsilon$ and $\cos \varepsilon$ depend on $z'_W = z'_W(y_W)$ and thereby on the profile coordinate y_W , the envelope itself depends only on y_W , i.e. on only one parameter. – By comparing the second and the third components for the two descriptions of the normal vector $\mathbf{n}_{W,E}^{\mathcal{R}}$, the inclination angle Φ_E of the wheel envelope can be determined:

$$\begin{aligned} -\ell \sin \Phi_E &= [\cos \alpha \sin \gamma \sin \varepsilon - \cos \alpha \cos \gamma z'_W - \sin \alpha \cos \varepsilon] r_W \\ \ell \cos \Phi_E &= [\sin \alpha \sin \gamma \sin \varepsilon - \sin \alpha \cos \gamma z'_W + \cos \alpha \cos \varepsilon] r_W \\ \Rightarrow \tan \Phi_E &= -\frac{[\cos \alpha \sin \gamma \sin \varepsilon - \cos \alpha \cos \gamma z'_W - \sin \alpha \cos \varepsilon] r_W}{[\sin \alpha \sin \gamma \sin \varepsilon - \sin \alpha \cos \gamma z'_W + \cos \alpha \cos \varepsilon] r_W} \\ &= -\frac{\sin \gamma \sin \varepsilon - \cos \gamma z'_W - \tan \alpha \cos \varepsilon}{\tan \alpha [\sin \gamma \sin \varepsilon - \cos \gamma z'_W] + \cos \varepsilon} \end{aligned} \quad (7.2.191)$$

By using the condition (7.2.189) the following expression can be simplified:

$$\sin \gamma \sin \varepsilon - \cos \gamma z'_W = -\sin \gamma \tan \gamma z'_W - \cos \gamma z'_W = -\left(\frac{\sin^2 \gamma}{\cos \gamma} + \frac{\cos^2 \gamma}{\cos \gamma}\right) z'_W = -\frac{z'_W}{\cos \gamma} \quad (7.2.192)$$

Inserting this relation gives the following expression for the inclination angle of the wheel envelope:

$$\tan \Phi_E = -\frac{\sin \gamma \sin \varepsilon - \cos \gamma z'_W - \tan \alpha \cos \varepsilon}{\tan \alpha [\sin \gamma \sin \varepsilon - \cos \gamma z'_W] + \cos \varepsilon} = -\frac{-\frac{z'_W}{\cos \gamma} - \tan \alpha \cos \varepsilon}{-\tan \alpha \frac{z'_W}{\cos \gamma} + \cos \varepsilon} = \frac{z'_W + \tan \alpha \cos \gamma \cos \varepsilon}{-\tan \alpha z'_W + \cos \gamma \cos \varepsilon} \quad (7.2.193)$$

7.2.2 Determination of the interpenetration

To determine the contact area, the intersection of the undeformed surfaces of wheel and rail is considered. The condition for the intersection can be formulated as:

$$\begin{aligned} \mathbf{r}_{K_R P_R}^{\mathcal{R}} &= \mathbf{r}_{K_R P_W}^{\mathcal{R}} \\ \begin{bmatrix} \xi \\ y_R \\ z_R \end{bmatrix} &= \begin{bmatrix} \Delta X_{RW} \\ \Delta Y_{RW} \\ \Delta Z_{RW} \end{bmatrix} + \begin{bmatrix} \cos \gamma & -\sin \gamma & 0 \\ \cos \alpha \sin \gamma & \cos \alpha \cos \gamma & -\sin \alpha \\ \sin \alpha \sin \gamma & \sin \alpha \cos \gamma & \cos \alpha \end{bmatrix} \begin{bmatrix} r_W \sin(\beta + \theta) \\ y_W \\ r_W \cos(\beta + \theta) \end{bmatrix} \end{aligned} \quad (7.2.194)$$

As already mentioned, the intersection is considered in the 2,3-plane of the rail profile system \mathcal{R} . Here, the envelope of the wheel is used; this curve is obtained for $\theta + \beta = \varepsilon$. The first step is to determine the intersection points P_l and P_r between the wheel envelope and the rail profile. The conditions for the intersection in the 2,3-plane are formulated as:

$$y_R = \Delta Y_{RW} + \cos \alpha \sin \gamma r_W \sin \varepsilon + \cos \alpha \cos \gamma y_W - \sin \alpha r_W \cos \varepsilon \quad (7.2.195)$$

$$z_R = \Delta Z_{RW} + \sin \alpha \sin \gamma r_W \sin \varepsilon + \sin \alpha \cos \gamma y_W + \cos \alpha r_W \cos \varepsilon \quad (7.2.196)$$

Usually, the profiles of wheel and rail are given by the functions $z_W = z_W(y_W)$ and $z_R = z_R(y_R)$, respectively. Based on this formulation, the problem can be solved by defining an error function $f(y_W)$. For a given value y_W this function is calculated in the following steps:

1. Evaluate the wheel profile function: $r_W = r_0 + z_W(y_W)$, $z'_W = z'_W(y_W)$
2. Determine the trigonometric terms depending on the angle ε :
 - (a) $\sin \varepsilon = -\tan \gamma z'_W$
 - (b) $\cos \varepsilon = \sqrt{1 - (\tan \gamma z'_W)^2}$
3. Set $y_R^* = \Delta Y_{RW} + \cos \alpha \sin \gamma r_W \sin \varepsilon + \cos \alpha \cos \gamma y_W - \sin \alpha r_W \cos \varepsilon$
4. Evaluate the rail profile function: $z_R^* = z_R(y_R^*)$
5. Set $f(y_W) = \Delta Z_{RW} + \sin \alpha \sin \gamma r_W \sin \varepsilon + \sin \alpha \cos \gamma y_W + \cos \alpha r_W \cos \varepsilon - z_R^*$

Thereby, the problem can be reduced to the solution of the equation $f(y_W) = 0$, i.e. to the solution of only one non-linear equation depending on one variable y_W . A suitable algorithm is the regula falsi or methods derived from it like the Illinois algorithm. As a result a set of solutions $y_{W,i}$ is obtained:

$$f(y_{W,i}) = 0 \quad (7.2.197)$$

The values y_{Wl} and y_{Wr} for the left and the right point P_l and P_r are obtained as the minimum and the maximum value of the set of solutions, respectively. As a result of the calculation of the error function $f(y_R)$ also the other coordinates at the left and the right intersection points are available.

$$\begin{aligned} y_{Wl} = \min_i(y_{W,i}) \Rightarrow z_{Wl} = z_W(y_{Wl}), z'_{Wl} = z'_W(y_{Wl}), \sin \varepsilon_l = -\tan \gamma z'_{Wl}, \cos \varepsilon_l = \sqrt{1 - (\tan \gamma z'_{Wl})^2} \\ y_{Rl} = \Delta Y_{RW} + \cos \alpha \cos \gamma y_{Wl} + [\cos \alpha \sin \gamma \sin \varepsilon_l - \sin \alpha \cos \varepsilon_l] (r_0 + z_{Wl}), \\ z_{Rl} = z_R(y_{Rl}), \xi_l = \Delta X_{RW} + \cos \gamma \sin \varepsilon_l (r_0 + z_{Wl}) - \sin \gamma y_{Wl} \end{aligned} \quad (7.2.198)$$

$$\begin{aligned} y_{Wr} = \max_i(y_{W,i}) \Rightarrow z_{Wr} = z_W(y_{Wr}), z'_{Wr} = z'_W(y_{Wr}), \sin \varepsilon_r = -\tan \gamma z'_{Wr}, \cos \varepsilon_r = \sqrt{1 - (\tan \gamma z'_{Wr})^2} \\ y_{Rr} = \Delta Y_{RW} + \cos \alpha \cos \gamma y_{Wr} + [\cos \alpha \sin \gamma \sin \varepsilon_r - \sin \alpha \cos \varepsilon_r] (r_0 + z_{Wr}), \\ z_{Rr} = z_R(y_{Rr}), \xi_r = \Delta X_{RW} + \cos \gamma \sin \varepsilon_r (r_0 + z_{Wr}) - \sin \gamma y_{Wr} \end{aligned} \quad (7.2.199)$$

The secant connecting the two intersection points P_l and P_r is used to define the contact frame \mathcal{C} . Here, the secant is used as the 2-axis, while the 1-axis coincides with the 1-axis of the 1-axis of the rail profile frame \mathcal{R} . Thereby, the transformation matrix $\mathbf{S}^{\mathcal{R}\mathcal{C}}$ is given by:

$$\tan \Phi_C = \frac{z_{Rr} - z_{Rl}}{y_{Rr} - y_{Rl}} \Rightarrow \sin \Phi_C = \frac{\tan \Phi_C}{\sqrt{1 + \tan^2 \Phi_C}}, \cos \Phi_C = \frac{1}{\sqrt{1 + \tan^2 \Phi_C}} \quad (7.2.200)$$

$$\Rightarrow \mathbf{S}^{\mathcal{R}\mathcal{C}} = \mathbf{S}_1(\Phi_C) = \begin{bmatrix} 1 & 0 & 0 \\ 0 & \cos \Phi_C & -\sin \Phi_C \\ 0 & \sin \Phi_C & \cos \Phi_C \end{bmatrix} \quad (7.2.201)$$

An overview on the intersection points P_l and P_r , the secant and the contact frame is given in Fig.7.2.6

The interpenetration of the surfaces of wheel and rail are now determined in the contact frame \mathcal{C} . The left intersection point P_l is defined as the reference point. The relative position of the points P_W and P_R lying on the surfaces of the wheel and the rail, respectively, can be described by the following vectors:

$$\mathbf{r}_{P_l P_W}^{\mathcal{C}} = \begin{bmatrix} x \\ y \\ \zeta_W(x, y) \end{bmatrix}, \mathbf{r}_{P_l P_R}^{\mathcal{C}} = \begin{bmatrix} x \\ y \\ \zeta_R(x, y) \end{bmatrix} \quad (7.2.202)$$

The interpenetration field $\delta(x, y)$ is now defined in the following way:

$$\mathbf{r}_{P_R P_W}^{\mathcal{C}} = \mathbf{r}_{P_l P_W}^{\mathcal{C}} - \mathbf{r}_{P_l P_R}^{\mathcal{C}} = [0 \ 0 \ \delta(x, y)]^T = [0 \ 0 \ \zeta_W(x, y) - \zeta_R(x, y)]^T \quad (7.2.203)$$

According to (7.2.168) the rail surface is described by the following vector:

$$\mathbf{r}_{K_R P_R}^{\mathcal{R}} \equiv \mathbf{x}_R(\xi, y_R) = \begin{bmatrix} \xi \\ y_R \\ z_R(y_R) \end{bmatrix} \quad (7.2.204)$$

The transformation of this vector into the contact frame \mathcal{C} gives:

$$\mathbf{r}_{K_R P_R}^{\mathcal{C}} = \mathbf{S}^{\mathcal{C}\mathcal{R}} \mathbf{r}_{K_R P_R}^{\mathcal{R}} = \mathbf{S}_1(-\Phi_C) \mathbf{x}_R(\xi, y_R) \quad (7.2.205)$$

The left intersection point P_l is defined by $\xi = \xi_l$ and $y_R = y_{Rl}$. In the contact frame \mathcal{C} , the distance between the point P_l and a point P_R , which lies on the surface of the rail, is obtained by:

$$\begin{aligned} \mathbf{r}_{P_l P_R}^{\mathcal{C}} &= \mathbf{r}_{K_R P_R}^{\mathcal{C}} - \mathbf{r}_{K_R P_l}^{\mathcal{C}} = \mathbf{S}_1(-\Phi_C) \mathbf{x}_R(\xi, y_R) - \mathbf{S}_1(-\Phi_C) \mathbf{x}_R(\xi_l, y_{Rl}) \\ &= \mathbf{S}_1(-\Phi_C) [\mathbf{x}_R(\xi, y_R) - \mathbf{x}_R(\xi_l, y_{Rl})] = \begin{bmatrix} 1 & 0 & 0 \\ 0 & \cos \Phi_C & \sin \Phi_C \\ 0 & -\sin \Phi_C & \cos \Phi_C \end{bmatrix} \begin{bmatrix} \xi - \xi_l \\ y_R - y_{Rl} \\ z_R - z_{Rl} \end{bmatrix} \end{aligned} \quad (7.2.206)$$

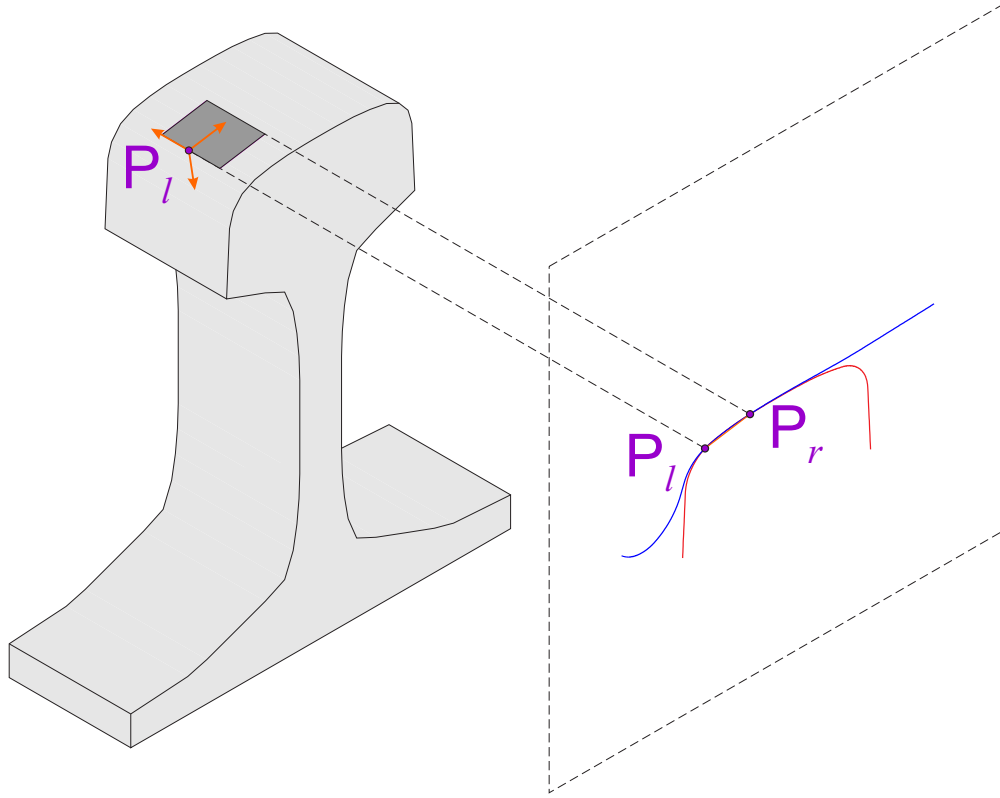


Figure 7.2.6: Left (P_l) and right (P_r) intersection points of the wheel envelope (blue) and the rail profile (red) and the resulting contact frame \mathcal{C} (orange)

For the point P_{Ri} , which is defined by the coordinates $x^C = x_i$ and $y^C = y_i$ it is therefore valid:

$$\mathbf{r}_{P_l P_{Ri}}^C = \begin{bmatrix} x_i \\ y_i \\ \zeta_{Ri} \end{bmatrix} = \begin{bmatrix} 1 & 0 & 0 \\ 0 & \cos \Phi_C & \sin \Phi_C \\ 0 & -\sin \Phi_C & \cos \Phi_C \end{bmatrix} \begin{bmatrix} \xi_i - \xi_l \\ y_{Ri} - y_{Rl} \\ z_R(y_{Ri}) - z_{Rl} \end{bmatrix} \quad (7.2.207)$$

For the given values x_i and y_i the variables ξ_i , y_{Ri} and $z_{Ri} = z_R(y_{Ri})$ have to be determined by solving the following equations, which are obtained from the first and the second coordinate of the vector equation (7.2.207):

$$0 = \xi_i - \xi_l - x_i \quad (7.2.208)$$

$$0 = \cos \Phi_C (y_{Ri} - y_{Rl}) + \sin \Phi_C (z_R(y_{Ri}) - z_{Rl}) - y_i = f_R(y_{Ri}) \quad (7.2.209)$$

While the value ξ_i can be calculated directly, the value y_{Ri} is determined by solving a single non-linear equation, which can be done with the Newton method. Based on the values y_{Ri} and z_{Ri} the vertical distance $\zeta_R(x_i, y_i)$ for the rail surface is obtained:

$$\zeta_R(x_i, y_i) = -\sin \Phi_C (y_{Ri} - y_{Rl}) + \cos \Phi_C (z_R(y_{Ri}) - z_{Rl}) \quad (7.2.210)$$

The position of a point P_W on the wheel surface is given by:

$$\mathbf{r}_{K_R P_W}^{\mathcal{R}} = \mathbf{r}_{K_R M_W}^{\mathcal{R}} + \mathbf{r}_{M_W P_W}^{\mathcal{R}}(\theta, y_W) = \mathbf{r}_{K_R M_W}^{\mathcal{R}} + \mathbf{S}_1(\alpha) \mathbf{S}_3(\gamma) \mathbf{S}_2(\beta + \theta) \mathbf{p}_W(y_W) \quad (7.2.211)$$

The transformation into the contact frame \mathcal{C} gives:

$$\mathbf{r}_{K_R P_W}^C = \mathbf{S}^{C\mathcal{R}} \mathbf{r}_{K_R P_W}^{\mathcal{R}} = \mathbf{S}_1(-\Phi_C) \left[\mathbf{r}_{K_R M_W}^{\mathcal{R}} + \mathbf{r}_{M_W P_W}^{\mathcal{R}}(\theta, y_W) \right] \quad (7.2.212)$$

Using the formulation of the wheel surface, the left intersection point P_l is defined by $\theta_{El} + \beta = \varepsilon_l$ and $y_w = y_{wl}$. Thereby the distance between the points P_w and P_l is given by:

$$\begin{aligned}
\mathbf{r}_{P_l P_w}^C &= \mathbf{r}_{K_R P_w}^C - \mathbf{r}_{K_R P_l}^C \\
&= \mathbf{S}_1(-\Phi_C) \left[\mathbf{r}_{K_R M_w}^R + \mathbf{r}_{M_w P_w}^R(\theta, y_w) \right] - \mathbf{S}_1(-\Phi_C) \left[\mathbf{r}_{K_R M_w}^R + \mathbf{r}_{M_w P_w}^R(\theta_{El}, y_{wl}) \right] \\
&= \mathbf{S}_1(-\Phi_C) \left[\mathbf{r}_{M_w P_w}^R(\theta, y_w) - \mathbf{r}_{M_w P_w}^R(\theta_{El}, y_{wl}) \right] \\
&= \mathbf{S}_1(-\Phi_C) \left[\mathbf{S}_1(\alpha) \mathbf{S}_3(\gamma) \mathbf{S}_2(\beta + \theta) \mathbf{p}_w(y_w) - \mathbf{S}_1(\alpha) \mathbf{S}_3(\gamma) \mathbf{S}_2(\beta + \theta_{El}) \mathbf{p}_w(y_{wl}) \right] \\
&= \underbrace{\mathbf{S}_1(-\Phi_C) \mathbf{S}_1(\alpha)}_{\mathbf{S}_1(\alpha - \Phi_C)} \mathbf{S}_3(\gamma) \left[\mathbf{S}_2(\beta + \theta) \mathbf{p}_w(y_w) - \mathbf{S}_2(\varepsilon_l) \mathbf{p}_w(y_{wl}) \right] \tag{7.2.213}
\end{aligned}$$

From this it follows:

$$\begin{aligned}
\mathbf{r}_{P_l P_w}^C &= \mathbf{r}_{K_R P_w}^C - \mathbf{r}_{K_R P_l}^C = \mathbf{S}_1(\alpha - \Phi_C) \mathbf{S}_3(\gamma) \left[\mathbf{S}_2(\beta + \theta) \mathbf{p}_w(y_w) - \mathbf{S}_2(\varepsilon_l) \mathbf{p}_w(y_{wl}) \right] \\
&= \begin{bmatrix} \cos \gamma & -\sin \gamma & 0 \\ \cos(\alpha - \Phi_C) \sin \gamma & \cos(\alpha - \Phi_C) \cos \gamma & -\sin(\alpha - \Phi_C) \\ \sin(\alpha - \Phi_C) \sin \gamma & \sin(\alpha - \Phi_C) \cos \gamma & \cos(\alpha - \Phi_C) \end{bmatrix} \begin{bmatrix} r_w \sin(\beta + \theta) - r_{wl} \sin \varepsilon_l \\ y_w - y_{wl} \\ r_w \cos(\beta + \theta) - r_{wl} \cos \varepsilon_l \end{bmatrix} \tag{7.2.214}
\end{aligned}$$

For the point P_{wi} it is valid:

$$\mathbf{r}_{P_l P_{wi}}^C = \mathbf{S}_1(\alpha - \Phi_C) \mathbf{S}_3(\gamma) \left[\mathbf{S}_2(\beta + \theta_i) \mathbf{p}_w(y_{wi}) - \mathbf{S}_2(\varepsilon_l) \mathbf{p}_w(y_{wl}) \right] = \begin{bmatrix} x_i \\ y_i \\ \zeta_{wi} \end{bmatrix} \tag{7.2.215}$$

Using the relation (7.2.214), it can be formulated:

$$\begin{bmatrix} x_i \\ y_i \\ \zeta_{wi} \end{bmatrix} = \begin{bmatrix} \cos \gamma & -\sin \gamma & 0 \\ \cos(\alpha - \Phi_C) \sin \gamma & \cos(\alpha - \Phi_C) \cos \gamma & -\sin(\alpha - \Phi_C) \\ \sin(\alpha - \Phi_C) \sin \gamma & \sin(\alpha - \Phi_C) \cos \gamma & \cos(\alpha - \Phi_C) \end{bmatrix} \begin{bmatrix} r_{wi} \sin(\beta + \theta_i) - r_{wl} \sin \varepsilon_l \\ y_{wi} - y_{wl} \\ r_{wi} \cos(\beta + \theta_i) - r_{wl} \cos \varepsilon_l \end{bmatrix} \tag{7.2.216}$$

The first and the second components give the conditions for the coordinates y_{wi} and θ_i of the point. The angle θ_i only appears in the functions $\sin(\beta + \theta_i)$ and $\cos(\beta + \theta_i)$. For the sake of brevity, it is defined:

$$s_i = \sin(\beta + \theta_i) \Rightarrow \cos(\beta + \theta_i) = \sqrt{1 - \sin^2(\beta + \theta_i)} = \sqrt{1 - s_i^2} \tag{7.2.217}$$

The radius r_{wi} is defined by:

$$r_{wi} = r_0 + z_w(y_{wi}) \tag{7.2.218}$$

By using these definitions, the two conditions for the coordinates y_{wi} and θ_i can be formulated in the following way:

$$\begin{aligned}
0 &= \cos \gamma \left[(r_0 + z_w(y_{wi})) s_i - r_{wl} \sin \varepsilon_l \right] - \sin \gamma \left[y_{wi} - y_{wl} \right] - x_i \\
&= f_w(y_{wi}, s_i) \tag{7.2.219}
\end{aligned}$$

$$\begin{aligned}
0 &= \cos(\alpha - \Phi_C) \sin \gamma \left[(r_0 + z_w(y_{wi})) s_i - r_{wl} \sin \varepsilon_l \right] + \cos(\alpha - \Phi_C) \cos \gamma \left[y_{wi} - y_{wl} \right] \\
&\quad - \sin(\alpha - \Phi_C) \left[(r_0 + z_w(y_{wi})) \sqrt{1 - s_i^2} - r_{wl} \cos \varepsilon_l \right] - y_i \\
&= g_w(y_{wi}, s_i) \tag{7.2.220}
\end{aligned}$$

As a result, a system of two nonlinear equations is obtained:

$$\mathbf{f}_w(y_{wi}, s_i) = \begin{bmatrix} f_w(y_{wi}, s_i) \\ g_w(y_{wi}, s_i) \end{bmatrix} = \mathbf{0} \quad (7.2.221)$$

This system can be solved e.g. by Newton's method. Solving these equations gives the values y_{wi} and θ_i . By inserting the solutions y_{wi} and θ_i into the third equation, the required vertical distance ζ_{wi} is determined:

$$\begin{aligned} \zeta_w(x_i, y_i) = & \sin(\alpha - \Phi_C) \sin \gamma [(r_0 + z_w(y_{wi})) s_i - r_{wl} \sin \epsilon_l] + \sin(\alpha - \Phi_C) \cos \gamma [y_{wi} - y_{wl}] \\ & + \cos(\alpha - \Phi_C) \left[(r_0 + z_w(y_{wi})) \sqrt{1 - s_i^2} - r_{wl} \cos \epsilon_l \right] \end{aligned} \quad (7.2.222)$$

Finally, the interpenetration is obtained as the difference of the vertical distances:

$$\delta(x_i, y_i) = \zeta_w(x_i, y_i) - \zeta_r(x_i, y_i) \quad (7.2.223)$$

7.3 Contact mechanics

To analyze the contact problem a relation between the deformations \mathbf{u}_i and the tensions $\boldsymbol{\sigma}_i$ is required. As already mentioned the wheel and the rail are considered as half-spaces consisting of linear elastic material. Under this assumption this relation is given by the equations of Boussinesq and Cerruti, given e.g. in the fundamental book by Kalker [26]. The tensions are the tangential stresses $\tau_1(x, y)$ and $\tau_2(x, y)$ acting in longitudinal and lateral direction, respectively, and the pressure $p(x, y)$ acting in vertical direction. As a result of the stresses, deformations u_1 , u_2 and w in longitudinal, lateral and vertical direction, respectively, occur. The stresses are described by fields, i.e. $\tau_1 = \tau_1(x, y)$, $\tau_2 = \tau_2(x, y)$ and $p = p(x, y)$.

$$\underbrace{\begin{bmatrix} u_1(X, Y) \\ u_2(X, Y) \\ w(X, Y) \end{bmatrix}}_{\mathbf{u}(X, Y)} = \int_A \underbrace{\begin{bmatrix} H_{11}(X-x, Y-y) & H_{12}(X-x, Y-y) & H_{13}(X-x, Y-y) \\ H_{12}(X-x, Y-y) & H_{22}(X-x, Y-y) & H_{23}(X-x, Y-y) \\ H_{13}(X-x, Y-y) & H_{23}(X-x, Y-y) & H_{33}(X-x, Y-y) \end{bmatrix}}_{\mathbf{H}(X-x, Y-y)} \underbrace{\begin{bmatrix} \tau_1(x, y) \\ \tau_2(x, y) \\ p(x, y) \end{bmatrix}}_{\boldsymbol{\sigma}(x, y)} dA \quad (7.3.224)$$

The matrix $\mathbf{H}(X-x, Y-y)$ contains the influence functions $H_{IK}(X-x, Y-y)$, which are given by:

$$H_{11}(X-x, Y-y) = \frac{1}{\pi G} \left[\frac{1-\nu}{[(X-x)^2 + (Y-y)^2]^{1/2}} + \frac{\nu(X-x)^2}{[(X-x)^2 + (Y-y)^2]^{3/2}} \right] \quad (7.3.225)$$

$$H_{12}(X-x, Y-y) = H_{21}(X-x, Y-y) = \frac{\nu}{\pi G} \frac{(X-x)(Y-y)}{[(X-x)^2 + (Y-y)^2]^{3/2}} \quad (7.3.226)$$

$$H_{13}(X-x, Y-y) = -H_{31}(X-x, Y-y) = \frac{K}{\pi G} \frac{(X-x)}{[(X-x)^2 + (Y-y)^2]} \quad (7.3.227)$$

$$H_{22}(X-x, Y-y) = \frac{1}{\pi G} \left[\frac{1-\nu}{[(X-x)^2 + (Y-y)^2]^{1/2}} + \frac{\nu(Y-y)^2}{[(X-x)^2 + (Y-y)^2]^{3/2}} \right] \quad (7.3.228)$$

$$H_{23}(X-x, Y-y) = -H_{32}(X-x, Y-y) = \frac{K}{\pi G} \frac{(Y-y)}{[(X-x)^2 + (Y-y)^2]} \quad (7.3.229)$$

$$H_{33}(X-x, Y-y) = \frac{1}{\pi G} \frac{1-\nu}{[(X-x)^2 + (Y-y)^2]^{1/2}} \quad (7.3.230)$$

Here, the coefficients G , ν and K are the combined material parameters. If G_i and ν_i are the shear modulus and Poisson's ratio for the material of the body i , then the combined material parameters are obtained by:

$$\frac{1}{G} = \frac{1}{2} \left(\frac{1}{G_1} + \frac{1}{G_2} \right), \quad \frac{\nu}{G} = \frac{1}{2} \left(\frac{\nu_1}{G_1} + \frac{\nu_2}{G_2} \right), \quad \frac{K}{G} = \frac{1}{4} \left(\frac{1-2\nu_1}{G_1} - \frac{1-2\nu_2}{G_2} \right) \quad (7.3.231)$$

For the contact model, which is developed here, it is assumed that both the wheel and the rail consist of steel so that the shear modulus G_i and Poisson's ratio ν_i is equal for both bodies. From this it follows:

$$G_1 = G_2, \quad \nu_1 = \nu_2 \Rightarrow \frac{1}{G_1} = \frac{1}{G_2} = \frac{1}{G}, \quad \frac{\nu_1}{G_1} = \frac{\nu_2}{G_2} = \frac{\nu}{G}, \quad \frac{K}{G} = 0 \quad (7.3.232)$$

The difference parameter K vanishes; as a result, the functions $H_{13}(X-x, Y-y)$ and $H_{23}(X-x, Y-y)$ vanish so that the normal contact problem on the one hand and the tangential contact problem on the other hand are decoupled from each other:

$$\begin{bmatrix} u_1(X, Y) \\ u_2(X, Y) \\ w(X, Y) \end{bmatrix} = \int_A \begin{bmatrix} H_{11}(X-x, Y-y) & H_{12}(X-x, Y-y) & 0 \\ H_{12}(X-x, Y-y) & H_{22}(X-x, Y-y) & 0 \\ 0 & 0 & H_{33}(X-x, Y-y) \end{bmatrix} \begin{bmatrix} \tau_1(x, y) \\ \tau_2(x, y) \\ p(x, y) \end{bmatrix} dA \quad (7.3.233)$$

7.4 Discretization of the contact problem

To discretise the problem a grid having the grid constant Δa is defined. Using the offsets x_O and y_O and the integers \bar{x}_i and \bar{y}_i , the i -th gridpoint has the following coordinates in the contact frame \mathcal{C} :

$$\mathbf{r}_{P_0 P_i}^{\mathcal{C}} = \begin{bmatrix} x_i \\ y_i \\ 0 \end{bmatrix} = \begin{bmatrix} x_O + \bar{x}_i \Delta a \\ y_O + \bar{y}_i \Delta a \\ 0 \end{bmatrix}, \quad \bar{x}_i, \bar{y}_i \in \mathbb{Z} \quad (7.4.234)$$

At these gridpoints the deformations and the tensions are considered:

$$\mathbf{u}(x_i, y_i) = \begin{bmatrix} u_1(x_i, y_i) \\ u_2(x_i, y_i) \\ w(x_i, y_i) \end{bmatrix} = \begin{bmatrix} u_{1,i} \\ u_{2,i} \\ w_i \end{bmatrix} = \mathbf{u}_i, \quad \boldsymbol{\sigma}(x_i, y_i) = \begin{bmatrix} \tau_1(x_i, y_i) \\ \tau_2(x_i, y_i) \\ p(x_i, y_i) \end{bmatrix} = \begin{bmatrix} \tau_{1,i} \\ \tau_{2,i} \\ p_i \end{bmatrix} = \boldsymbol{\sigma}_i \quad (7.4.235)$$

Regarding the deformations the values at the gridpoints $\mathbf{u}_i = \mathbf{u}(x_i, y_i)$ are sufficient. However, as it will turn out, for the stresses a field $\boldsymbol{\sigma}(x, y)$ describing the stress distribution on the surface is required. This field can be formulated by superposing local functions $f_k(x, y)$, which are scaled with the tensions $\boldsymbol{\sigma}_k = \boldsymbol{\sigma}(x_k, y_k)$ at the k -th gridpoint:

$$\begin{bmatrix} \tau_1(x, y) \\ \tau_2(x, y) \\ p(x, y) \end{bmatrix} = \boldsymbol{\sigma}(x, y) = \sum_k f_k(x, y) \boldsymbol{\sigma}_k = \sum_k f_k(x, y) \begin{bmatrix} \tau_{1,k} \\ \tau_{2,k} \\ p_k \end{bmatrix} \quad (7.4.236)$$

For this formulation the function f_k must have the value 1 at the k -th gridpoint and it must vanish at all other gridpoints, i.e. for $i \neq k$. Thus it is valid:

$$f_k(x_i, y_i) = \begin{cases} 1 & \text{for } i = k \\ 0 & \text{for } i \neq k \end{cases} \Rightarrow \boldsymbol{\sigma}(x_k, y_k) = \sum_{i, i \neq k} \underbrace{\boldsymbol{\sigma}_i f_i(x_k, y_k)}_0 + \underbrace{\boldsymbol{\sigma}_k f_k(x_k, y_k)}_1 = \boldsymbol{\sigma}_k \quad (7.4.237)$$

In the present case a linear distribution of the tensions between two gridpoints is used. Therefore, a local bilinear function of the following form is used for $f_k(x, y)$:

$$f_k = \begin{cases} \left(1 - \frac{|x-x_k|}{\Delta a}\right) \left(1 - \frac{|y-y_k|}{\Delta a}\right) & \text{for } |x-x_k| \leq \Delta a \wedge |y-y_k| \leq \Delta a \\ 0 & \text{for } |x-x_k| > \Delta a \vee |y-y_k| > \Delta a \end{cases} \quad (7.4.238)$$

Since the grid constant Δa is strictly positive, i.e. $\Delta a > 0$, it is valid:

$$|x-x_k| \leq \Delta a \Rightarrow \frac{|x-x_k|}{\Delta a} \leq 1 \Rightarrow -\frac{|x-x_k|}{\Delta a} \geq -1 \Rightarrow 1 - \frac{|x-x_k|}{\Delta a} \geq 0 \quad (7.4.239)$$

$$|y-y_k| \leq \Delta a \Rightarrow \frac{|y-y_k|}{\Delta a} \leq 1 \Rightarrow -\frac{|y-y_k|}{\Delta a} \geq -1 \Rightarrow 1 - \frac{|y-y_k|}{\Delta a} \geq 0 \quad (7.4.240)$$

$$\Rightarrow f_k(x, y) = \underbrace{\left(1 - \frac{|x-x_k|}{\Delta a}\right)}_{\geq 0} \underbrace{\left(1 - \frac{|y-y_k|}{\Delta a}\right)}_{\geq 0} \geq 0 \text{ for } |x-x_k| \leq \Delta a \wedge |y-y_k| \leq \Delta a \quad (7.4.241)$$

From this it follows that the function $f_k(x, y)$ is non-negative for the following domain D_k :

$$D_k = \{(x, y) \in \mathbb{R}^2 \mid |x-x_k| \leq \Delta a, |y-y_k| \leq \Delta a\} \quad (7.4.242)$$

The conditions for x and y can be reformulated in the following way:

$$\begin{aligned} x-x_k \geq 0 &\Leftrightarrow x \geq x_k : |x-x_k| = x-x_k \leq \Delta a \Rightarrow x_k \leq x \leq x_k + \Delta a \\ x-x_k < 0 &\Leftrightarrow x < x_k : |x-x_k| = -(x-x_k) = -x+x_k \leq \Delta a \Rightarrow x_k - \Delta a \leq x < x_k \\ &\Rightarrow x_k - \Delta a \leq x \leq x_k + \Delta a \end{aligned} \quad (7.4.243)$$

$$\begin{aligned} y-y_k \geq 0 &\Leftrightarrow y \geq y_k : |y-y_k| = y-y_k \leq \Delta a \Rightarrow y_k \leq y \leq y_k + \Delta a \\ y-y_k < 0 &\Leftrightarrow y < y_k : |y-y_k| = -(y-y_k) = -y+y_k \leq \Delta a \Rightarrow y_k - \Delta a \leq y < y_k \\ &\Rightarrow y_k - \Delta a \leq y \leq y_k + \Delta a \end{aligned} \quad (7.4.244)$$

$$\Rightarrow D_k = \{(x, y) \in \mathbb{R}^2 \mid x_k - \Delta a \leq x \leq x_k + \Delta a, y_k - \Delta a \leq y \leq y_k + \Delta a\} \quad (7.4.245)$$

This domain is a square having the edge length $2\Delta a$ and the centre $\langle x_k, y_k \rangle$. In Fig.7.4.7 the function $f_k(x, y)$ is displayed. According to (7.4.238) the chosen function $f_k(x, y)$ vanishes at the borders of

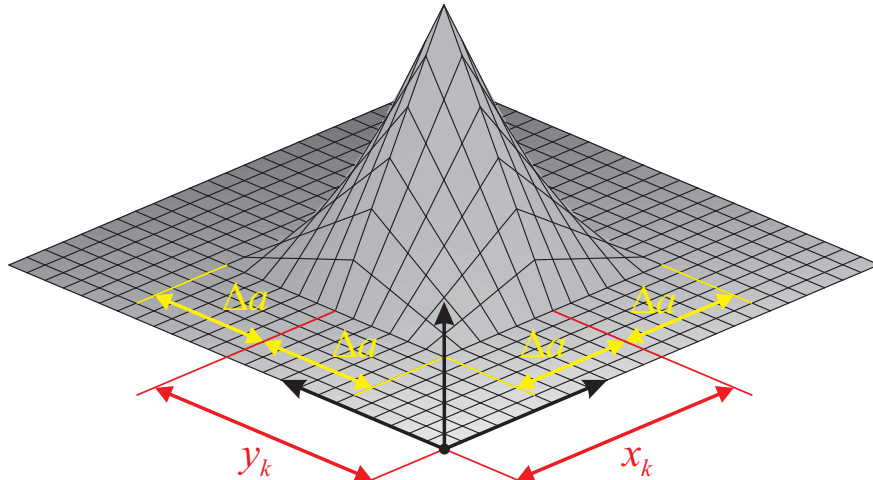


Figure 7.4.7: Local bilinear interpolation function $f_k(x, y)$

the domain D_k :

$$x = x_k - \Delta a \Leftrightarrow x - x_k = -\Delta a \Rightarrow 1 - \frac{|x - x_k|}{\Delta a} = 1 - \frac{|-\Delta a|}{\Delta a} = 0 \Rightarrow f_k(x_k - \Delta a, y) = 0 \quad (7.4.246)$$

$$x = x_k + \Delta a \Leftrightarrow x - x_k = \Delta a \Rightarrow 1 - \frac{|x - x_k|}{\Delta a} = 1 - \frac{|\Delta a|}{\Delta a} = 0 \Rightarrow f_k(x_k + \Delta a, y) = 0 \quad (7.4.247)$$

$$y = y_k - \Delta a \Leftrightarrow y - y_k = -\Delta a \Rightarrow 1 - \frac{|y - y_k|}{\Delta a} = 1 - \frac{|-\Delta a|}{\Delta a} = 0 \Rightarrow f_k(x, y_k - \Delta a) = 0 \quad (7.4.248)$$

$$y = y_k + \Delta a \Leftrightarrow y - y_k = \Delta a \Rightarrow 1 - \frac{|y - y_k|}{\Delta a} = 1 - \frac{|\Delta a|}{\Delta a} = 0 \Rightarrow f_k(x, y_k + \Delta a) = 0 \quad (7.4.249)$$

The gridpoints, which are adjacent to the k -th gridpoint, are lying on these borders; all other gridpoints are located outside the domain D_k , i.e. they are located in the complement $A \setminus D_k$ of the domain D_k in A . For the k -th gridpoint being the centre of the domain D_k it is valid:

$$f_k(x_k, y_k) = \underbrace{\left(1 - \frac{|x_k - x_k|}{\Delta a}\right)}_1 \underbrace{\left(1 - \frac{|y_k - y_k|}{\Delta a}\right)}_1 = 1 \quad (7.4.250)$$

Thereby, the chosen function according to (7.4.238) vanishes for all gridpoints except the k -th one so that it fulfills the aforementioned conditions $f_k(x_i, y_i) = 0$ for $i \neq k$ and $f_k(x_k, y_k) = 1$, which are required by the discretization according to (7.4.237).

In section 7.3 the following relation between the displacement \mathbf{u} and the tension $\boldsymbol{\sigma}$ has been presented:

$$\mathbf{u}(X, Y) = \int_A \mathbf{H}(X - x, Y - y) \boldsymbol{\sigma}(x, y) dA \quad (7.4.251)$$

Here, the matrix $\mathbf{H}(X - x, Y - y)$ contains the influence functions $H_{IK}(X - x, Y - y)$. By inserting the discretized distribution of the tensions according to (7.4.237) into (7.4.251) and factoring out the vectors $\boldsymbol{\sigma}_k$ from the integral the deformation \mathbf{u}_i at the i -th gridpoint is obtained to:

$$\begin{aligned} \mathbf{u}_i = \mathbf{u}(x_i, y_i) &= \int_A \mathbf{H}(x_i - x, y_i - y) \boldsymbol{\sigma}(x, y) dA = \int_A \mathbf{H}(x_i - x, y_i - y) \sum_k f_k(x, y) \boldsymbol{\sigma}_k dA \\ &= \sum_k \underbrace{\int_A \mathbf{H}(x_i - x, y_i - y) f_k(x, y) dA}_{\mathbf{H}_{i|k}} \boldsymbol{\sigma}_k = \sum_k \mathbf{H}_{i|k} \boldsymbol{\sigma}_k \end{aligned} \quad (7.4.252)$$

For the wheel-rail contact it is assumed that the wheel and the rail consist of the same material so that the shear modulus G and Poisson's ratio ν are equal for both bodies. In this case, it is valid:

$$\mathbf{H}(X - x, Y - y) = \begin{bmatrix} H_{11}(X - x, Y - y) & H_{12}(X - x, Y - y) & 0 \\ H_{12}(X - x, Y - y) & H_{22}(X - x, Y - y) & 0 \\ 0 & 0 & H_{33}(X - x, Y - y) \end{bmatrix} \quad (7.4.253)$$

Thus, the normal contact problem on the one hand and the tangential contact problem on the other hand are decoupled from each other. As a result, the complete system of linear equations according to (7.4.252) can be split up into two independent systems. The system of equations,

which describes the normal contact problem, can be written as:

$$\begin{bmatrix} \vdots \\ w_{i-1} \\ w_i \\ w_{i+1} \\ \vdots \end{bmatrix} = \begin{bmatrix} \ddots & \vdots & \vdots & \vdots & \vdots \\ \cdots & H_{i-1|k-1}^{[33]} & H_{i-1|k}^{[33]} & H_{i-1|k+1}^{[33]} & \cdots \\ \cdots & H_{i|k-1}^{[33]} & H_{i|k}^{[33]} & H_{i|k+1}^{[33]} & \cdots \\ \cdots & H_{i+1|k-1}^{[33]} & H_{i+1|k}^{[33]} & H_{i+1|k+1}^{[33]} & \cdots \\ \vdots & \vdots & \vdots & \vdots & \ddots \end{bmatrix} \begin{bmatrix} \vdots \\ p_{k-1} \\ p_k \\ p_{k+1} \\ \vdots \end{bmatrix} \quad (7.4.254)$$

The system of linear equations, which describes the discretized tangential contact problem, can be formulated in the following way:

$$\begin{bmatrix} \vdots \\ u_{1,i-1} \\ u_{2,i-1} \\ u_{1,i} \\ u_{2,i} \\ u_{1,i+1} \\ u_{2,i+1} \\ \vdots \end{bmatrix} = \begin{bmatrix} \ddots & \vdots & \vdots & \vdots & \vdots & \vdots & \vdots \\ \cdots & H_{i-1|k-1}^{[11]} & H_{i-1|k-1}^{[12]} & H_{i-1|k}^{[11]} & H_{i-1|k}^{[12]} & H_{i-1|k+1}^{[11]} & H_{i-1|k+1}^{[12]} & \cdots \\ \cdots & H_{i-1|k-1}^{[12]} & H_{i-1|k-1}^{[22]} & H_{i-1|k}^{[12]} & H_{i-1|k}^{[22]} & H_{i-1|k+1}^{[12]} & H_{i-1|k+1}^{[22]} & \cdots \\ \cdots & H_{i|k-1}^{[11]} & H_{i|k-1}^{[12]} & H_{i|k}^{[11]} & H_{i|k}^{[12]} & H_{i|k+1}^{[11]} & H_{i|k+1}^{[12]} & \cdots \\ \cdots & H_{i|k-1}^{[12]} & H_{i|k-1}^{[22]} & H_{i|k}^{[12]} & H_{i|k}^{[22]} & H_{i|k+1}^{[12]} & H_{i|k+1}^{[22]} & \cdots \\ \cdots & H_{i+1|k-1}^{[11]} & H_{i+1|k-1}^{[12]} & H_{i+1|k}^{[11]} & H_{i+1|k}^{[12]} & H_{i+1|k+1}^{[11]} & H_{i+1|k+1}^{[12]} & \cdots \\ \cdots & H_{i+1|k-1}^{[12]} & H_{i+1|k-1}^{[22]} & H_{i+1|k}^{[12]} & H_{i+1|k}^{[22]} & H_{i+1|k+1}^{[12]} & H_{i+1|k+1}^{[22]} & \cdots \\ \vdots & \vdots & \vdots & \vdots & \vdots & \vdots & \vdots & \ddots \end{bmatrix} \begin{bmatrix} \vdots \\ \tau_{1,k-1} \\ \tau_{2,k-1} \\ \tau_{1,k} \\ \tau_{2,k} \\ \tau_{1,k+1} \\ \tau_{2,k+1} \\ \vdots \end{bmatrix} \quad (7.4.255)$$

In order to formulate the two systems of linear equations, the coefficients $H_{i|k}^{[IK]}$ are required. As discussed before, the function $f_k(x, y)$ generally vanishes outside the domain D_k , i.e. it vanishes in the complement $A \setminus D_k$ of the domain D_k in A . Since the integrand for the coefficients $H_{i|k}^{[IK]}$ contains the function $f_k(x, y)$ as a factor, it vanishes in the complement $A \setminus D_k$, too. Therefore, it is valid:

$$\begin{aligned} H_{i|k}^{[IK]} &= \int_A H_{IK}(x_i - x, y_i - y) f_k(x, y) dA \\ &= \int_{D_k} H_{IK}(x_i - x, y_i - y) f_k(x, y) dA + \underbrace{\int_{A \setminus D_k} H_{IK}(x_i - x, y_i - y) \overbrace{f_k(x, y)}^{=0} dA}_{=0} \end{aligned} \quad (7.4.256)$$

Thus, the integration has to be carried out for the domain D_k only. By inserting the influence functions H_{11} , H_{12} , H_{22} and H_{33} according to (7.3.225), (7.3.226), (7.3.228) and (7.3.230) into the remaining integral of (7.4.256), the integrals, from which the coefficients $H_{i|k}^{[IK]}$ are obtained, are

formulated:

$$H_{i|k}^{[11]} = \int_{D_k} \left[\frac{1-\nu}{\pi G} \frac{1}{[(x_i-x)^2 + (y_i-y)^2]^{1/2}} + \frac{\nu}{\pi G} \frac{(x_i-x)^2}{[(x_i-x)^2 + (y_i-y)^2]^{3/2}} \right] f_k(x,y) dA \quad (7.4.257)$$

$$H_{i|k}^{[12]} = \int_{D_k} \frac{\nu}{\pi G} \frac{(x_i-x)(y_i-y)}{[(x_i-x)^2 + (y_i-y)^2]^{3/2}} f_k(x,y) dA \quad (7.4.258)$$

$$H_{i|k}^{[22]} = \int_{D_k} \left[\frac{1-\nu}{\pi G} \frac{1}{[(x_i-x)^2 + (y_i-y)^2]^{1/2}} + \frac{\nu}{\pi G} \frac{(y_i-y)^2}{[(x_i-x)^2 + (y_i-y)^2]^{3/2}} \right] f_k(x,y) dA \quad (7.4.259)$$

$$H_{i|k}^{[33]} = \int_{D_k} \frac{1-\nu}{\pi G} \frac{1}{[(x_i-x)^2 + (y_i-y)^2]^{1/2}} f_k(x,y) dA \quad (7.4.260)$$

After splitting up the integrals and factoring out the terms containing the constant material parameters G and ν the required compliance coefficients $H_{i|k}^{[11]}$, $H_{i|k}^{[12]}$, $H_{i|k}^{[22]}$ and $H_{i|k}^{[33]}$ can be formulated as linear combinations of four integrals $h_{i|k}^{[11]}$, $h_{i|k}^{[12]}$, $h_{i|k}^{[22]}$ and $h_{i|k}^{[33]}$:

$$h_{i|k}^{[11]} = \int_{D_k} \frac{(x_i-x)^2 f_k(x,y)}{[(x_i-x)^2 + (y_i-y)^2]^{3/2}} dA, \quad h_{i|k}^{[12]} = \int_{D_k} \frac{(x_i-x)(y_i-y) f_k(x,y)}{[(x_i-x)^2 + (y_i-y)^2]^{3/2}} dA, \quad (7.4.261)$$

$$h_{i|k}^{[22]} = \int_{D_k} \frac{(y_i-y)^2 f_k(x,y)}{[(x_i-x)^2 + (y_i-y)^2]^{3/2}} dA, \quad h_{i|k}^{[33]} = \int_{D_k} \frac{f_k(x,y)}{[(x_i-x)^2 + (y_i-y)^2]^{1/2}} dA \quad (7.4.262)$$

$$H_{i|k}^{[11]} = \frac{1-\nu}{\pi G} h_{i|k}^{[33]} + \frac{\nu}{\pi G} h_{i|k}^{[11]}, \quad H_{i|k}^{[12]} = \frac{\nu}{\pi G} h_{i|k}^{[12]} \quad (7.4.263)$$

$$H_{i|k}^{[22]} = \frac{1-\nu}{\pi G} h_{i|k}^{[33]} + \frac{\nu}{\pi G} h_{i|k}^{[22]}, \quad H_{i|k}^{[33]} = \frac{1-\nu}{\pi G} h_{i|k}^{[33]} \quad (7.4.264)$$

It is advantageous to formulate the integrals for local coordinates ξ and η . The origin of the local coordinates is the point P_i , where the deformations $u_{1,i}$, $u_{2,i}$ and w_i have to be determined. Furthermore, the coordinates are normalized by the grid constant Δa :

$$x = x_i + \xi \Delta a, \quad y = y_i + \eta \Delta a \quad (7.4.265)$$

Using the normalized distances $\bar{x}_{i|k}$ and $\bar{y}_{i|k}$ it can be formulated:

$$x - x_k = x_i - x_k + \xi \Delta a = \bar{x}_{i|k} \Delta a + \xi \Delta a = \Delta a (\xi - \bar{x}_{k|i}) \Rightarrow \frac{x - x_k}{\Delta a} = \xi - \bar{x}_{k|i} \quad (7.4.266)$$

$$y - y_k = y_i - y_k + \eta \Delta a = \bar{y}_{i|k} \Delta a + \eta \Delta a = \Delta a (\eta - \bar{y}_{k|i}) \Rightarrow \frac{y - y_k}{\Delta a} = \eta - \bar{y}_{k|i} \quad (7.4.267)$$

Thereby, the shape function f_k can be reformulated to:

$$f_k = \left(1 - \left| \frac{x - x_k}{\Delta a} \right| \right) \left(1 - \left| \frac{y - y_k}{\Delta a} \right| \right) = (1 - |\xi - \bar{x}_{k|i}|) (1 - |\eta - \bar{y}_{k|i}|) = f_{k|i}(\xi, \eta) \quad (7.4.268)$$

The intervals for the domain are adapted in the following way:

$$\begin{aligned} x_k - \Delta a \leq x \leq x_k + \Delta a &\Rightarrow -\Delta a \leq x - x_k \leq \Delta a \\ &\Rightarrow -1 \leq \frac{x - x_k}{\Delta a} = \xi - \bar{x}_{k|i} \leq 1 \Rightarrow \bar{x}_{k|i} - 1 \leq \xi \leq \bar{x}_{k|i} + 1 \end{aligned} \quad (7.4.269)$$

$$\begin{aligned} y_k - \Delta a \leq y \leq y_k + \Delta a &\Rightarrow -\Delta a \leq y - y_k \leq \Delta a \\ &\Rightarrow -1 \leq \frac{y - y_k}{\Delta a} = \eta - \bar{y}_{k|i} \leq 1 \Rightarrow \bar{y}_{k|i} - 1 \leq \eta \leq \bar{y}_{k|i} + 1 \end{aligned} \quad (7.4.270)$$

Thereby, the domain D_k is formulated using the coordinates ξ and η :

$$D_k = \{ (\xi, \eta) \in \mathbb{R}^2 \mid \bar{x}_{k|i} - 1 \leq \xi \leq \bar{x}_{k|i} + 1, \bar{y}_{k|i} - 1 \leq \eta \leq \bar{y}_{k|i} + 1 \} \quad (7.4.271)$$

For the infinitesimal area element dA it is valid:

$$dA = dx dy = \frac{\partial x}{\partial \xi} d\xi \cdot \frac{\partial y}{\partial \eta} d\eta = \Delta a^2 d\xi d\eta \quad (7.4.272)$$

In order to adapt the influence functions to the new coordinates, it is determined:

$$x = x_i + \Delta a \xi \Rightarrow x_i - x = -\Delta a \xi \Rightarrow (x_i - x)^2 = \xi^2 \Delta a^2 \quad (7.4.273)$$

$$y = y_i + \Delta a \eta \Rightarrow y_i - y = -\Delta a \eta \Rightarrow (y_i - y)^2 = \eta^2 \Delta a^2 \quad (7.4.274)$$

$$\Rightarrow [(x_i - x)^2 + (y_i - y)^2]^{1/2} = [\xi^2 \Delta a^2 + \eta^2 \Delta a^2]^{1/2} = [\xi^2 + \eta^2]^{1/2} \Delta a \quad (7.4.275)$$

Thereby, the integrals $h_{i|k}^{[11]}$, $h_{i|k}^{[12]}$, $h_{i|k}^{[22]}$ and $h_{i|k}^{[33]}$ are reformulated in the following way:

$$h_{i|k}^{[11]} = \int_{D_k} \frac{(x_i - x)^2 f_k(x, y)}{[(x_i - x)^2 + (y_i - y)^2]^{3/2}} dA = \int_{\bar{y}_{k|i}-1}^{\bar{y}_{k|i}+1} \int_{\bar{x}_{k|i}-1}^{\bar{x}_{k|i}+1} \frac{\xi^2 f_{k|i}(\xi, \eta)}{[\xi^2 + \eta^2]^{3/2}} \Delta a d\xi d\eta \quad (7.4.276)$$

$$h_{i|k}^{[12]} = \int_{D_k} \frac{(x_i - x)(y_i - y) f_k(x, y)}{[(x_i - x)^2 + (y_i - y)^2]^{3/2}} dA = \int_{\bar{y}_{k|i}-1}^{\bar{y}_{k|i}+1} \int_{\bar{x}_{k|i}-1}^{\bar{x}_{k|i}+1} \frac{\xi \eta f_{k|i}(\xi, \eta)}{[\xi^2 + \eta^2]^{3/2}} \Delta a d\xi d\eta \quad (7.4.277)$$

$$h_{i|k}^{[22]} = \int_{D_k} \frac{(y_i - y)^2 f_k(x, y)}{[(x_i - x)^2 + (y_i - y)^2]^{3/2}} dA = \int_{\bar{y}_{k|i}-1}^{\bar{y}_{k|i}+1} \int_{\bar{x}_{k|i}-1}^{\bar{x}_{k|i}+1} \frac{\eta^2 f_{k|i}(\xi, \eta)}{[\xi^2 + \eta^2]^{3/2}} \Delta a d\xi d\eta \quad (7.4.278)$$

$$h_{i|k}^{[33]} = \int_{D_k} \frac{f_k(x, y)}{[(x_i - x)^2 + (y_i - y)^2]^{1/2}} dA = \int_{\bar{y}_{k|i}-1}^{\bar{y}_{k|i}+1} \int_{\bar{x}_{k|i}-1}^{\bar{x}_{k|i}+1} \frac{f_{k|i}(\xi, \eta)}{[\xi^2 + \eta^2]^{1/2}} \Delta a d\xi d\eta \quad (7.4.279)$$

It will turn out later that the coefficients $H_{i|i}^{[11]}$, $H_{i|i}^{[12]}$, $H_{i|i}^{[22]}$ are of special interest; therefore, they will be considered here. Since the normalized distances $\bar{x}_{i|i} = 0$ and $\bar{y}_{i|i} = 0$ vanish, it is valid for the integrals:

$$f_{i|i}(\xi, \eta) = (1 - |\xi - \bar{x}_{i|i}|) (1 - |\eta - \bar{y}_{i|i}|) = (1 - |\xi|) (1 - |\eta|) \quad (7.4.280)$$

$$h_{i|i}^{[11]} = \int_{\bar{y}_{i|i}-1}^{\bar{y}_{i|i}+1} \int_{\bar{x}_{i|i}-1}^{\bar{x}_{i|i}+1} \frac{\xi^2 f_{i|i}(\xi, \eta)}{[\xi^2 + \eta^2]^{3/2}} \Delta a d\xi d\eta = \int_{-1}^1 \int_{-1}^1 \frac{\xi^2 (1 - |\xi|) (1 - |\eta|)}{[\xi^2 + \eta^2]^{3/2}} \Delta a d\xi d\eta \quad (7.4.281)$$

$$h_{i|i}^{[12]} = \int_{\bar{y}_{i|i}-1}^{\bar{y}_{i|i}+1} \int_{\bar{x}_{i|i}-1}^{\bar{x}_{i|i}+1} \frac{\xi \eta f_{i|i}(\xi, \eta)}{[\xi^2 + \eta^2]^{3/2}} \Delta a d\xi d\eta = \int_{-1}^1 \int_{-1}^1 \frac{\xi \eta (1 - |\xi|) (1 - |\eta|)}{[\xi^2 + \eta^2]^{3/2}} \Delta a d\xi d\eta \quad (7.4.282)$$

$$h_{i|i}^{[22]} = \int_{\bar{y}_{i|i}-1}^{\bar{y}_{i|i}+1} \int_{\bar{x}_{i|i}-1}^{\bar{x}_{i|i}+1} \frac{\eta^2 f_{i|i}(\xi, \eta)}{[\xi^2 + \eta^2]^{3/2}} \Delta a d\xi d\eta = \int_{-1}^1 \int_{-1}^1 \frac{\eta^2 (1 - |\xi|) (1 - |\eta|)}{[\xi^2 + \eta^2]^{3/2}} \Delta a d\xi d\eta \quad (7.4.283)$$

$$h_{i|i}^{[33]} = \int_{\bar{y}_{i|i}-1}^{\bar{y}_{i|i}+1} \int_{\bar{x}_{i|i}-1}^{\bar{x}_{i|i}+1} \frac{f_{i|i}(\xi, \eta)}{[\xi^2 + \eta^2]^{1/2}} \Delta a d\xi d\eta = \int_{-1}^1 \int_{-1}^1 \frac{(1 - |\xi|) (1 - |\eta|)}{[\xi^2 + \eta^2]^{1/2}} \Delta a d\xi d\eta \quad (7.4.284)$$

It can be seen that the integrands of $h_{i|i}^{[11]}$ and $h_{i|i}^{[22]}$ can be converted into each other by interchanging the arguments ξ and η . Furthermore, both integrations over ξ and η have to be carried out over the same interval $[-1, 1]$. Thereby, the two integrals are equal:

$$h_{i|i}^{[11]} = h_{i|i}^{[22]} \quad (7.4.285)$$

From this it follows that the coefficients $H_{i|i}^{[11]}$ and $H_{i|i}^{[22]}$ are equal:

$$H_{i|i}^{[11]} = \frac{1-\nu}{\pi G} h_{i|i}^{[33]} + \frac{\nu}{\pi G} h_{i|i}^{[11]} = \frac{1-\nu}{\pi G} h_{i|i}^{[33]} + \frac{\nu}{\pi G} h_{i|i}^{[22]} = H_{i|i}^{[22]} \quad (7.4.286)$$

The integrand $g_{12}(\xi, \eta)$ of the integral $h_{i|i}^{[12]}$ is an odd function with respect to both variables ξ and η :

$$g_{12}(-\xi, \eta) = \frac{(-\xi)\eta(1-|-\xi|)(1-|\eta|)}{[(-\xi)^2 + \eta^2]^{3/2}} = -\frac{\xi\eta(1-|\xi|)(1-|\eta|)}{[\xi^2 + \eta^2]^{3/2}} = -g_{12}(\xi, \eta) \quad (7.4.287)$$

$$g_{12}(\xi, -\eta) = \frac{\xi(-\eta)(1-|\xi|)(1-|-\eta|)}{[\xi^2 + (-\eta)^2]^{3/2}} = -\frac{\xi\eta(1-|\xi|)(1-|\eta|)}{[\xi^2 + \eta^2]^{3/2}} = -g_{12}(\xi, \eta) \quad (7.4.288)$$

The interval $[-1, 1]$, over which both integrations for ξ and η have to be carried out, is a symmetric interval. The integral of an odd function $f(-x) = -f(x)$ over a symmetric interval $[-b, b]$ always vanishes. Therefore, it is valid:

$$f(-x) = -f(x) \Rightarrow \int_{-b}^b f(x) dx = 0 \Rightarrow h_{i|i}^{[12]} = \int_{-1}^1 \int_{-1}^1 \frac{\xi\eta(1-|\xi|)(1-|\eta|)}{[\xi^2 + \eta^2]^{3/2}} \Delta a d\xi d\eta = 0 \quad (7.4.289)$$

Therefore, the coefficient $H_{i|i}^{[12]} = 0$ vanishes.

The complete evaluation of the integrals is a bit laborious. Therefore, the full evaluation is contained in the Appendix E, while here only the most important steps and the solution are presented. These steps can be described briefly in the following way:

1. The shape function $f_{k|i}(\xi, \eta)$ is reformulated and the domain D_k is split up into four subdomains $D_{k,n}$.
2. The local cartesian coordinates ξ and η are replaced by local normalized polar coordinates.
3. The integration over the subdomains $D_{k,n}$ is carried out by superposing integrals over triangular domains, which can be solved analytically.

The shape function $f_{k|i}(\xi, \eta)$ contains absolute values; therefore, the integrals have to be evaluated piecewise. To this end, the domain D_k is split up into four subdomains $D_{k,1}$, $D_{k,2}$, $D_{k,3}$ and $D_{k,4}$ and the shape function is reformulated in the following way:

$$f_{k|i}(\xi, \eta) = (1 - |\xi - \bar{x}_{k|i}|) (1 - |\eta - \bar{y}_{k|i}|) = (1 - c_\xi [\xi - \bar{x}_{k|i}]) (1 - c_\eta [\eta - \bar{y}_{k|i}]) \quad (7.4.290)$$

The subdomains $D_{k,n}$ are chosen in such a way that the coefficients c_X and c_Y are constant within each subdomain. In total it is valid:

	$\bar{x}_{k i} - 1 \leq \xi \leq \bar{x}_{k i}$	$\bar{x}_{k i} \leq \xi \leq \bar{x}_{k i} + 1$
$\bar{y}_{k i} \leq \eta \leq \bar{y}_{k i} + 1$	Subdomain $D_{k,2}$ $c_\xi = -1, c_\eta = 1$	Subdomain $D_{k,1}$ $c_\xi = 1, c_\eta = 1$
$\bar{y}_{k i} - 1 \leq \eta \leq \bar{y}_{k i}$	Subdomain $D_{k,3}$ $c_\xi = -1, c_\eta = -1$	Subdomain $D_{k,4}$ $c_\xi = 1, c_\eta = -1$

The integrals over the complete domain D_k are obtained by summing up the integrals over the subdomains $D_{k,n}$. Based on this, the integrals $h_{i|k}^{[11]}$, $h_{i|k}^{[12]}$, $h_{i|k}^{[22]}$ and $h_{i|k}^{[33]}$ are obtained in the following way:

$$h_{i|k}^{[11]} = \sum_{n=1}^4 \iint_{D_{k,n}} \frac{\xi^2 f_{k|i}(\xi, \eta)}{[\xi^2 + \eta^2]^{3/2}} \Delta a d\xi d\eta = \sum_{n=1}^4 h_{i|k,n}^{[11]} \quad (7.4.291)$$

$$h_{i|k}^{[12]} = \sum_{n=1}^4 \iint_{D_{k,n}} \frac{\xi \eta f_{k|i}(\xi, \eta)}{[\xi^2 + \eta^2]^{3/2}} \Delta a d\xi d\eta = \sum_{n=1}^4 h_{i|k,n}^{[12]} \quad (7.4.292)$$

$$h_{i|k}^{[22]} = \sum_{n=1}^4 \iint_{D_{k,n}} \frac{\eta^2 f_{k|i}(\xi, \eta)}{[\xi^2 + \eta^2]^{3/2}} \Delta a d\xi d\eta = \sum_{n=1}^4 h_{i|k,n}^{[22]} \quad (7.4.293)$$

$$h_{i|k}^{[33]} = \sum_{n=1}^4 \iint_{D_{k,n}} \frac{f_{k|i}(\xi, \eta)}{[\xi^2 + \eta^2]^{1/2}} \Delta a d\xi d\eta = \sum_{n=1}^4 h_{i|k,n}^{[33]} \quad (7.4.294)$$

For further evaluation, the local cartesian coordinates ξ and η are expressed by the polar coordinates r and ϕ in the following way:

$$\xi = r \cos \phi, \quad \eta = r \sin \phi, \quad r \geq 0 \quad (7.4.295)$$

An overview on the coordinates x and y of the contact frame C , the local cartesian coordinates ξ and η , the local polar coordinates r and ϕ and the subdomains $D_{k,1}$, $D_{k,2}$, $D_{k,3}$ and $D_{k,4}$ is given in Fig.7.4.8. Using the new polar coordinates, the terms contained in the integrands of $h_{i|k,n}^{[K]}$ are reformulated:

$$\xi^2 = r^2 \cos^2 \phi, \quad \eta^2 = r^2 \sin^2 \phi \Rightarrow [\xi^2 + \eta^2]^{1/2} = [r^2 \cos^2 \phi + r^2 \sin^2 \phi]^{1/2} = r \quad (7.4.296)$$

For the infinitesimal area element it is valid:

$$d\xi d\eta = r dr d\phi \quad (7.4.297)$$

The shape function $f_{k|i}$ is expressed in the following way:

$$\begin{aligned} f_{k|i}(\xi, \eta) &= (1 - c_\xi [\xi - \bar{x}_{k|i}]) (1 - c_\eta [\eta - \bar{y}_{k|i}]) \\ &= (1 - c_\xi [r \cos \phi - \bar{x}_{k|i}]) (1 - c_\eta [r \sin \phi - \bar{y}_{k|i}]) \\ &= (1 + c_\xi \bar{x}_{k|i}) (1 + c_\eta \bar{y}_{k|i}) - c_\xi (1 + c_\eta \bar{y}_{k|i}) r \cos \phi \\ &\quad - c_\eta (1 + c_\xi \bar{x}_{k|i}) r \sin \phi + c_\xi c_\eta r^2 \sin \phi \cos \phi \\ &= f_{k|i,0} + f_{k|i,1} r \cos \phi + f_{k|i,2} r \sin \phi + f_{12} r^2 \sin \phi \cos \phi = f_{k|i}(r, \phi) \end{aligned} \quad (7.4.298)$$

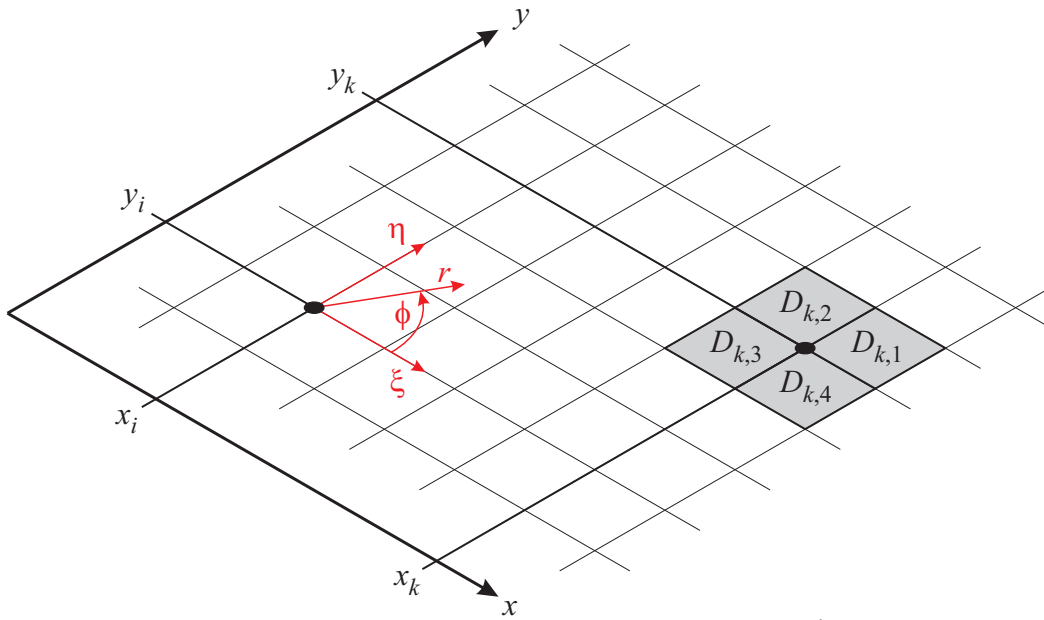


Figure 7.4.8: Global coordinates x and y , local cartesian coordinates ξ and η , local polar coordinates r and ϕ and subdomains $D_{k,1}$, $D_{k,2}$, $D_{k,3}$ and $D_{k,4}$ for the function f_k .

Thereby, the four integrands can be formulated in the following way:

$$\frac{\xi^2 f_{k|i}(\xi, \eta)}{[\xi^2 + \eta^2]^{3/2}} \Delta a d\xi d\eta = \frac{r^2 \cos^2 \phi f_{k|i}(r, \phi)}{r^3} \Delta a r dr d\phi = \Delta a f_{k|i}(r, \phi) \cos^2 \phi dr d\phi \quad (7.4.299)$$

$$\frac{\xi \eta f_{k|i}(\xi, \eta)}{[\xi^2 + \eta^2]^{3/2}} \Delta a d\xi d\eta = \frac{r \cos \phi r \sin \phi f_{k|i}(r, \phi)}{r^3} \Delta a r dr d\phi = \Delta a f_{k|i}(r, \phi) \cos \phi \sin \phi dr d\phi \quad (7.4.300)$$

$$\frac{\eta^2 f_{k|i}(\xi, \eta)}{[\xi^2 + \eta^2]^{3/2}} \Delta a d\xi d\eta = \frac{r^2 \sin^2 \phi f_{k|i}(r, \phi)}{r^3} \Delta a r dr d\phi = \Delta a f_{k|i}(r, \phi) \sin^2 \phi dr d\phi \quad (7.4.301)$$

$$\frac{f_{k|i}(\xi, \eta)}{[\xi^2 + \eta^2]^{1/2}} \Delta a d\xi d\eta = \frac{f_{k|i}(r, \phi)}{r} \Delta a r dr d\phi = \Delta a f_{k|i}(r, \phi) dr d\phi \quad (7.4.302)$$

Here, the big advantage of the polar coordinates becomes visible: The denominator has been eliminated so that for the reformulated integrands no singularities occur. Furthermore, it should be noted that in the reformulated integrands the shape function $f_k(r, \phi)$ is the only term depending on the radial coordinate r . In the following, the following generalized integral will be considered:

$$h_{ik}^{[IK]} = \iint_{D_{k,n}} \Delta a f_k(r, \phi) \sin^M \phi \cos^N \phi dr d\phi, \quad M, N \in \{0, 1, 2\} \quad (7.4.303)$$

If a function $g(r, \phi)$, which is defined for polar coordinates as the arguments, shall be integrated over a two-dimensional domain, the simplest case is the case of a domain D_{AB} , which is limited by two rays defined by the angles ϕ_A and ϕ_B and a curve defined by $R(\phi)$ as displayed in Figure 7.4.9. Then, the integral of the function $g(r, \phi)$ over the domain D_{AB} is determined by the following expression:

$$\iint_{D_{AB}} g(r, \phi) dA = \int_{\phi_A}^{\phi_B} \int_0^{R(\phi)} g(r, \phi) r dr d\phi \quad (7.4.304)$$

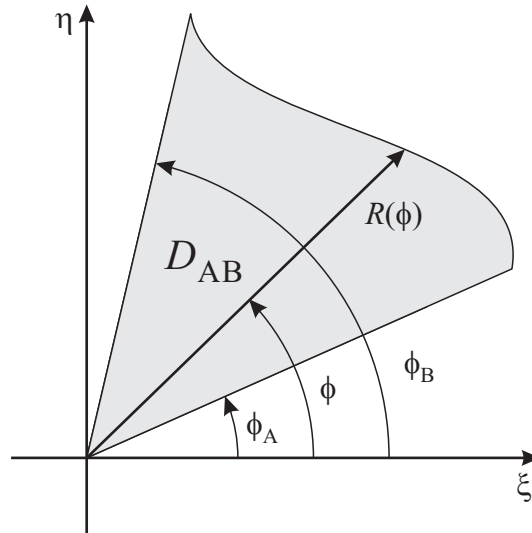


Figure 7.4.9: Domain D_{AB} described in polar coordinates

The limits of the subdomains $D_{k,n}$ given by a constant value either for x or for y ; thereby, each subdomain $D_{k,n}$ is a rectangle, whereas the edges are parallel to the axes of the global coordinates x and y and also the axes of the local cartesian coordinates ξ and η .

Now, a rectangular domain D is considered. Its corners are given by the points P_1 , P_2 , P_3 and P_4 and its edges are parallel to the ξ -axis or the η -axis, as it is the case for the subdomains $D_{k,n}$. The edges $\overline{P_1P_2}$ and $\overline{P_3P_4}$ are the horizontal edges defined by the constant values η_A and η_B , respectively. The edges $\overline{P_2P_3}$ and $\overline{P_4P_1}$ are the vertical edges; they are defined by the constant values ξ_A and ξ_B , respectively. The integral over the rectangular domain D can now be expressed by superposing integrals over triangular domains T_{AB} . Here, the three corners of the triangle T_{AB} are given by the origin of the coordinates and the edge $\overline{P_AP_B}$ of the rectangle. Using a generalized formulation for the integrands (7.4.299), (7.4.300), (7.4.301) and (7.4.302) the integral for the triangular domain T_{AB} is expressed in the following way:

$$\begin{aligned} F_{M,N}(P_A \rightarrow P_B) &= \iint_{T_{AB}} \Delta a f_{i|k}(r, \phi) \sin^M \phi \cos^N \phi dr d\phi \\ &= \int_{\phi_A}^{\phi_B} \int_0^{R_{AB}(\phi)} \Delta a f_{i|k}(r, \phi) \sin^M \phi \cos^N \phi dr d\phi, \quad M, N \in \{0, 1, 2\} \end{aligned} \quad (7.4.305)$$

It is important to note that the integral $F_{M,N}(P_A \rightarrow P_B)$ is counted positively if the end angle ϕ_B is greater than the start angle ϕ_A . In the reverse, i.e. if the end angle ϕ_B is greater than the start angle ϕ_A , the integral $F_{M,N}(P_A \rightarrow P_B)$ is counted negatively. Altogether, the principle to determine the integral over the rectangular domain D by superposing the integrals over the triangular domains T_{12} , T_{23} , T_{34} and T_{41} is illustrated in Figure 7.4.10.

Because of $\phi_3 > \phi_2$ and $\phi_4 > \phi_3$, the integrals $F_{M,N}(P_2 \rightarrow P_3)$ and $F_{M,N}(P_3 \rightarrow P_4)$ over the triangular domains T_{23} and T_{34} , respectively, are counted positively. In contrast to this, the integrals $F_{M,N}(P_1 \rightarrow P_2)$ and $F_{M,N}(P_4 \rightarrow P_1)$ over the triangular domains T_{12} and T_{41} are counted negatively because of $\phi_2 < \phi_1$ and $\phi_4 < \phi_1$. Thereby, the $F_{M,N}(P_1 \rightarrow P_2)$ and $F_{M,N}(P_4 \rightarrow P_1)$ partially cancel the integrals $F_{M,N}(P_2 \rightarrow P_3)$ and $F_{M,N}(P_3 \rightarrow P_4)$ out. As a result, the integral $F_{M,N}(D)$ over the rectangular subdomain D having the corners P_1 , P_2 , P_3 and P_4 is obtained to:

$$F_{M,N}(D) = F_{M,N}(P_1 \rightarrow P_2) + F_{M,N}(P_2 \rightarrow P_3) + F_{M,N}(P_3 \rightarrow P_4) + F_{M,N}(P_4 \rightarrow P_1) \quad (7.4.306)$$

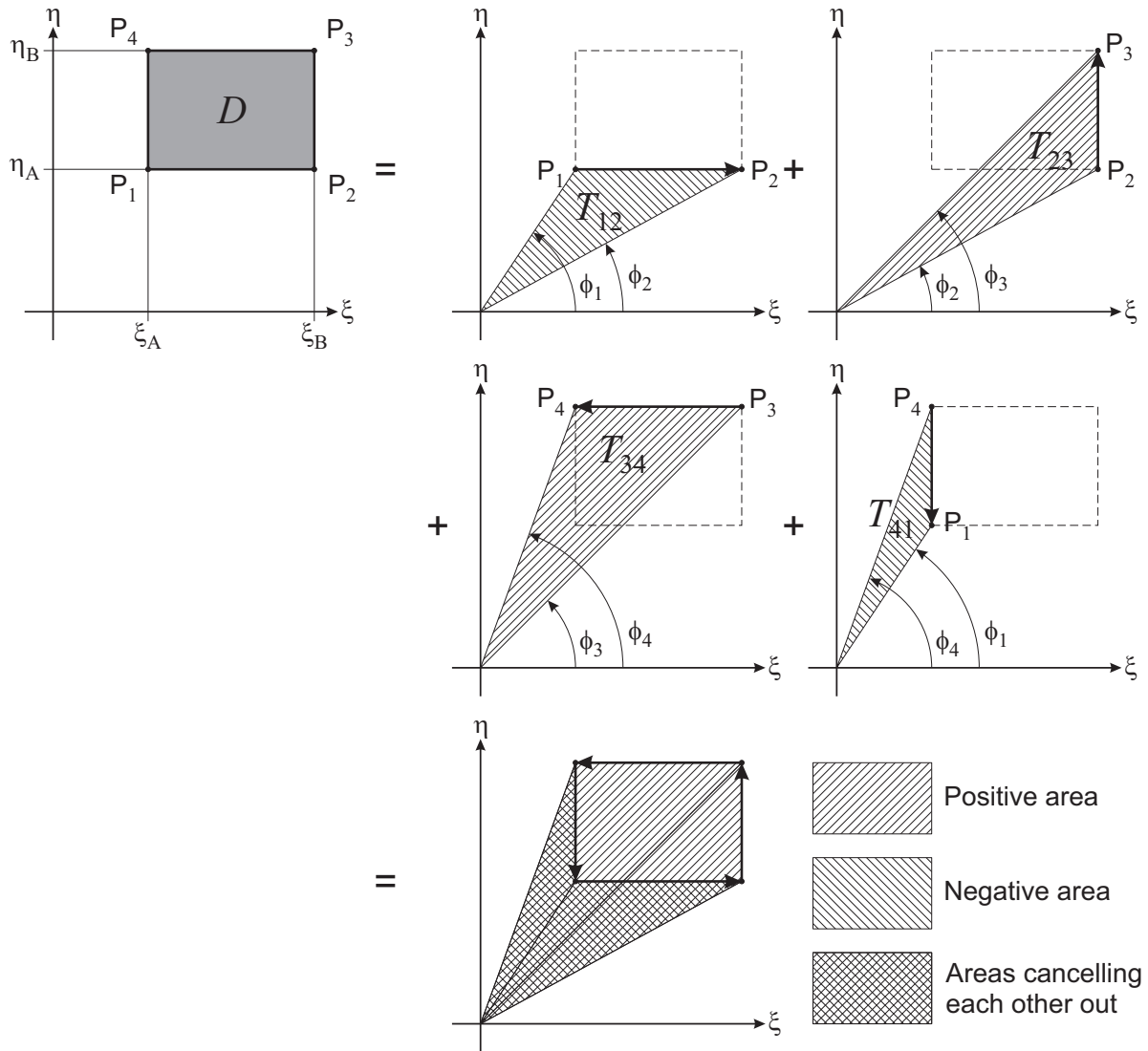


Figure 7.4.10: Description of the rectangular domain D by superposing triangular domains T_{AB} .

Since the edges of the rectangular domain are either horizontal or vertical and therefore defined either by a constant value $\xi_C = \text{const.}$ or a constant value $\eta_C = \text{const.}$, the radius functions $R_{AB}(\phi)$ can be derived directly from the relation between the local cartesian coordinates ξ and η and the polar coordinates r and ϕ :

$$\xi = r \cos \phi, \quad \eta = r \sin \phi \quad (7.4.307)$$

From this it follows for the radius functions:

$$\overline{P_1 P_2} : \eta = \eta_A \Rightarrow R_{12}(\phi) \sin \phi = \eta_A \Rightarrow R_{12}(\phi) = \frac{\eta_A}{\sin \phi} \quad (7.4.308)$$

$$\overline{P_2 P_3} : \xi = \xi_B \Rightarrow R_{23}(\phi) \cos \phi = \xi_B \Rightarrow R_{23}(\phi) = \frac{\xi_B}{\cos \phi} \quad (7.4.309)$$

$$\overline{P_3 P_4} : \eta = \eta_B \Rightarrow R_{34}(\phi) \sin \phi = \eta_B \Rightarrow R_{34}(\phi) = \frac{\eta_B}{\sin \phi} \quad (7.4.310)$$

$$\overline{P_4 P_1} : \xi = \xi_A \Rightarrow R_{41}(\phi) \cos \phi = \xi_A \Rightarrow R_{41}(\phi) = \frac{\xi_A}{\cos \phi} \quad (7.4.311)$$

Using these functions, all integrals required for the compliance coefficients $H_{ik}^{[K]}$ can be expressed

by linear combinations of the following integrals:

$$\begin{aligned} \int_{\phi_I}^{\phi_J} \cos \phi d\phi &= \sin \phi \Big|_{\phi_I}^{\phi_J}, \quad \int_{\phi_I}^{\phi_J} \frac{1}{\cos \phi} d\phi = \ln \left(\frac{1 + \sin \phi}{\cos \phi} \right) \Big|_{\phi_I}^{\phi_J}, \quad \int_{\phi_I}^{\phi_J} \frac{\sin \phi}{\cos^2 \phi} d\phi = \frac{1}{\cos \phi} \Big|_{\phi_I}^{\phi_J} \\ \int_{\phi_I}^{\phi_J} \sin \phi d\phi &= -\cos \phi \Big|_{\phi_I}^{\phi_J}, \quad \int_{\phi_I}^{\phi_J} \frac{1}{\sin \phi} d\phi = \ln \left(\frac{1 - \cos \phi}{\sin \phi} \right) \Big|_{\phi_I}^{\phi_J}, \quad \int_{\phi_I}^{\phi_J} \frac{\cos \phi}{\sin^2 \phi} d\phi = -\frac{1}{\sin \phi} \Big|_{\phi_I}^{\phi_J} \end{aligned} \quad (7.4.312)$$

As already mentioned, a detailed derivation of the expressions, which are necessary to determine the compliance coefficients $H_{i|k}^{[JK]}$, is given in the Appendix E. Here, it shall just be pointed out that for the bilinear shape function $f_k(x, y)$ the compliance coefficients can be determined analytically.

7.5 Normal contact

In section 7.4, a discretized formulation for the contact problem has been developed based on the equations of Boussinesq and Cerruti. For the case that both bodies being in contact have the same material parameters, it has been shown that the normal contact problem and the tangential contact problem are decoupled from each other. Therefore, they can be solved separately, which means an important reduction of the computational effort. The relation between the normal deformations $w_i = w(x_i, y_i)$ and the pressures $p_k = p(x_k, y_k)$ is given by the following system of linear equations:

$$\begin{bmatrix} \vdots \\ w_{i-1} \\ w_i \\ w_{i+1} \\ \vdots \end{bmatrix} = \begin{bmatrix} \ddots & \vdots & \vdots & \vdots & \\ \cdots & H_{i-1|k-1}^{[33]} & H_{i-1|k}^{[33]} & H_{i-1|k+1}^{[33]} & \cdots \\ \cdots & H_{i|k-1}^{[33]} & H_{i|k}^{[33]} & H_{i|k+1}^{[33]} & \cdots \\ \cdots & H_{i+1|k-1}^{[33]} & H_{i+1|k}^{[33]} & H_{i+1|k+1}^{[33]} & \cdots \\ \vdots & \vdots & \vdots & \vdots & \ddots \end{bmatrix} \begin{bmatrix} \vdots \\ p_{k-1} \\ p_k \\ p_{k+1} \\ \vdots \end{bmatrix} \quad (7.5.313)$$

The condition, which has been fulfilled by the solution of the normal contact problem, can be formulated in a very descriptive way. If two bodies are pressed against each other, then their is a geometrical interpenetration δ of their undeformed surfaces. Of course, in reality, the bodies cannot interpenetrate each other, but the geometrical interpenetration δ is compensated by the deformation w of the bodies. The wanted solution of the normal contact problem is a distribution of the pressure p , which causes a deformation w compensating the geometrical interpenetration δ . However, the normal contact can only transmit compression stresses, but no tensile stresses. Furthermore, the pressure p vanishes at those points, where no actual contact occurs, i.e. where the normal deformation w is greater than the interpenetration δ . Based on these considerations, the condition for the normal contact problem can be formulated. Here, C is the domain describing the actual contact area so that the complement $A \setminus C$ describes the region outside the contact area. Then it is valid:

$$(x, y) \in C : \delta(x, y) - w(x, y) = 0 \wedge p(x, y) > 0 \quad (7.5.314)$$

$$(x, y) \in A \setminus C : \delta(x, y) - w(x, y) < 0 \wedge p(x, y) = 0 \quad (7.5.315)$$

For the sake of simplicity, the pressure $p(x, y)$ is defined in such a way that it is non-negative, although compression stresses are usually indicated by a negative sign.

In section 7.4 it has been discussed:

$$p(x, y) = \sum_k p_k f_k(x, y), \quad f_k(x, y) \geq 0, \quad H_{33}(X - x, Y - y) = \frac{1 - \nu}{\pi G} \frac{1}{[(X - x)^2 + (Y - y)^2]^{1/2}} > 0$$

$$\Rightarrow H_{i|k}^{[33]} = \iint_A H_{33}(x_i - x, y_i - y) f_k(x, y) dA > 0 \quad (7.5.316)$$

The interpenetration $\delta_i = \delta(x_i, y_i)$ is determined in the following way:

1. Determine the normal distance ζ_{Ri} for the given values x_i and y_i :

$$\mathbf{r}_{P_{Ri}P_l}^C = \mathbf{S}_1(-\Phi_C) \left[\mathbf{r}_R^{\mathcal{R}}(\xi_i, y_{Ri}) - \mathbf{r}_R^{\mathcal{R}}(\xi_l, y_{Rl}) \right] = [x_i \quad y_i \quad \zeta_{Ri}]^T \quad (7.5.317)$$

2. Determine the normal distance ζ_{Wi} for the given values x_i and y_i :

$$\mathbf{r}_{P_{Wi}P_l}^C = \mathbf{S}_1(\alpha - \Phi_C) \mathbf{S}_3(\gamma) [\mathbf{S}_2(\Theta_i) \mathbf{p}_W(y_{Wi}) - \mathbf{S}_2(\epsilon_l) \mathbf{p}_W(y_{Wl})] = [x_i \quad y_i \quad \zeta_{Wi}]^T \quad (7.5.318)$$

3. Set $\delta_i = \zeta_{Wi} - \zeta_{Ri}$.

7.5.1 Solving algorithm

As derived before, the discretized normal contact problem based on the equations of Boussinesq and Cerrutti is formulated as a system of linear equations; the most generalized formulation of such a system is given by:

$$\mathbf{A} \mathbf{x} = \mathbf{b} \quad (7.5.319)$$

Generally, there are two basic strategies to determine the solution vector \mathbf{x} of a system of linear equations **direct calculation** and **iterative calculation**. These two strategies and their advantages and disadvantages will be considered and briefly discussed in the following.

The basic idea of the **direct calculation** is to transform the system of linear equations in such a way that all but one of the unknown elements of the wanted vector \mathbf{x} are eliminated from the equations. This transformation is done by a finite number of steps depending on the order N of the system. As a result, the exact solution vector \mathbf{x} is obtained. A well-known method is to decompose the matrix \mathbf{A} into a product of a lower left matrix \mathbf{L} and an upper right matrix \mathbf{U} :

$$\mathbf{A} = \mathbf{L} \mathbf{U}, \quad \mathbf{L} = \begin{bmatrix} l_{11} & 0 & 0 & \dots & 0 \\ l_{21} & l_{22} & 0 & \dots & 0 \\ l_{31} & l_{32} & l_{33} & \dots & 0 \\ \vdots & \vdots & \vdots & \ddots & \vdots \\ l_{N1} & l_{N2} & l_{N3} & \dots & l_{NN} \end{bmatrix}, \quad \mathbf{U} = \begin{bmatrix} u_{11} & u_{12} & u_{13} & \dots & u_{1N} \\ 0 & u_{22} & u_{23} & \dots & u_{2N} \\ 0 & 0 & u_{33} & \dots & u_{3N} \\ \vdots & \vdots & \vdots & \ddots & \vdots \\ 0 & 0 & 0 & \dots & u_{NN} \end{bmatrix}. \quad (7.5.320)$$

Because of the structure of the matrices this decomposition is called LU decomposition. There are different possibilities for the decomposition of the matrix \mathbf{A} . If the matrix \mathbf{A} is symmetric and positive definite, the Cholesky decomposition can be used. Here, the upper right matrix \mathbf{U} is set equal to the transposed lower left matrix \mathbf{L} , i.e. $\mathbf{U} = \mathbf{L}^T$, so that the matrix \mathbf{A} is decomposed

in the way $\mathbf{A} = \mathbf{L}\mathbf{L}^T$. If the matrix \mathbf{A} is non-symmetric and not positive definite, a general LU decomposition is used, whereas the diagonal elements l_{ii} are set equal to 1. – Now, an intermediate vector \mathbf{y} is introduced in the following way:

$$\mathbf{U}\mathbf{x} = \mathbf{y} \Rightarrow \mathbf{A}\mathbf{x} = \mathbf{L}\mathbf{U}\mathbf{x} = \mathbf{L}\mathbf{y} = \mathbf{b} \quad (7.5.321)$$

The intermediate vector \mathbf{y} and the solution vector \mathbf{x} are now determined using a recursive calculation scheme:

$$\begin{aligned} \mathbf{L}\mathbf{y} = \mathbf{b} : \quad & l_{11}y_1 = b_1 \Rightarrow y_1 = \frac{b_1}{l_{11}}, \\ & l_{21}y_1 + l_{22}y_2 = b_2 \Rightarrow y_2 = \frac{b_2 - l_{21}y_1}{l_{22}}, \\ & l_{31}y_1 + l_{32}y_2 + l_{33}y_3 = b_3 \Rightarrow y_3 = \frac{b_3 - l_{31}y_1 - l_{32}y_2}{l_{33}}, \dots \end{aligned} \quad (7.5.322)$$

$$\begin{aligned} \mathbf{U}\mathbf{x} = \mathbf{y} : \quad & u_{NN}x_N = y_N \Rightarrow x_N = \frac{y_N}{u_{NN}}, \\ & u_{N-1|N-1}x_{N-1} + u_{N-1|N}x_N = y_{N-1} \Rightarrow x_{N-1} = \frac{y_{N-1} - u_{N-1|N}x_N}{u_{N-1|N-1}}, \\ & u_{N-2|N-2}x_{N-2} + u_{N-2|N-1}x_{N-1} + u_{N-2|N}x_N = y_{N-2} \\ & \Rightarrow x_{N-2} = \frac{y_{N-2} - u_{N-2|N-1}x_{N-1} - u_{N-2|N}x_N}{u_{N-2|N-2}}, \dots \end{aligned} \quad (7.5.323)$$

Regarding the implementation as a computer code, with growing order N the number of the required floating point operations asymptotically approaches $2N^3/3$ for the LU decomposition and $2N^2$ for the recursive determination of the vectors \mathbf{y} and \mathbf{x} , see e.g. [60]. This means that for a sufficiently high order N the main part of the computational effort is required by the LU decomposition.

The advantage of the direct calculation is that it determines the exact solution after a certain number of steps. For an implementation as a computer code a subsequent iterative improvement of the solution is often useful in order to minimize numerical errors; nevertheless, the basic process of the direct calculation doesn't use any iteration. This also means that no initial approximation of the solution is necessary to start the direct calculation. The main disadvantage of the direct calculation is that for any changes of the matrix \mathbf{A} the LU decomposition has to be carried out again.

For the **iterative calculation**, a system of equations given by

$$\mathbf{g}(\mathbf{x}) = \mathbf{0} \quad (7.5.324)$$

is transformed into the following form:

$$\mathbf{x} = \mathbf{f}(\mathbf{x}) \Rightarrow \mathbf{x}^{(n+1)} = \mathbf{f}(\mathbf{x}^{(n)}) \quad (7.5.325)$$

Starting with an initial approximation $\mathbf{x}^{(0)}$, a sequence of the approximations $\mathbf{x}^{(n)}$ converging towards the wanted solution \mathbf{x} is obtained.

A very instructive way to obtain the iteration scheme for a system of linear equations can be derived by resolving the k -th equation of the system to the k -th component x_k of the wanted solution vector \mathbf{x} .

$$\sum_{i=1}^N a_{k|i}x_i = b_k \Rightarrow x_k = \frac{1}{a_{k|k}} \left[b_k - \sum_{i=1}^{k-1} a_{k|i}x_i - \sum_{i=k+1}^N a_{k|i}x_i \right] \quad (7.5.326)$$

Here, a property, which will be important with respect to the solution of the normal contact problem, becomes visible: The coefficients $a_{i|k}$ of the matrix \mathbf{A} remain unchanged; in contrast to the LU decomposition used for the direct calculation no new matrix coefficients are calculated.

The simplest iteration scheme based on the reformulated equation (7.5.326) is the Jacobi iteration. Here, the components $x_k^{(n+1)}$ of the new approximation vector $\mathbf{x}^{(n+1)}$ are obtained from the existing approximation vector $\mathbf{x}^{(n)}$ in the following way:

$$x_k^{(n+1)} = \frac{1}{a_{k|k}} \left[b_k - \sum_{i=1}^{k-1} a_{k|i} x_i^{(n)} - \sum_{i=k+1}^N a_{k|i} x_i^{(n)} \right] \quad (7.5.327)$$

The Jacobi iteration is characterized by the fact that the new approximation $x_k^{(n+1)}$ is calculated from the existing approximation $x_i^{(n)}$ only.

If the new approximations $x_k^{(n+1)}$ are calculated sequentially, i.e. starting with $k = 1$, then the new approximations $x_i^{(n+1)}$, $i < k$ are already available, when the component $x_k^{(n+1)}$ is calculated. Thus the iteration method (7.5.327) can be improved by using the available new approximations $x_i^{(n+1)}$ for the calculation of $x_k^{(n+1)}$. This leads to the following iteration scheme, which is known as the Gauss-Seidel iteration.

$$x_k^{(n+1)} = \frac{1}{a_{k|k}} \left[b_k - \sum_{i=1}^{k-1} a_{k|i} x_i^{(n+1)} - \sum_{i=k+1}^N a_{k|i} x_i^{(n)} \right] \quad (7.5.328)$$

The Gauss-Seidel iteration method shows a better convergence than the Jacobi iteration method.

The convergence of the Gauss-Seidel iteration can be improved by introducing a relaxation. Here, the new approximation $x_k^{(n+1)}$ is obtained by adding a correction $\Delta x_k^{(n+1)}$ to the existing approximation $x_k^{(n)}$:

$$x_k^{(n+1)} = x_k^{(n)} + \Delta x_k^{(n+1)} = \frac{1}{a_{k|k}} \left[b_k - \sum_{i=1}^{k-1} a_{k|i} x_i^{(n+1)} - \sum_{i=k+1}^N a_{k|i} x_i^{(n)} \right] \quad (7.5.329)$$

The correction $\Delta x_k^{(n+1)}$ is obtained by:

$$\begin{aligned} \Delta x_k^{(n+1)} &= \frac{1}{a_{k|k}} \left[b_k - \sum_{i=1}^{k-1} a_{k|i} x_i^{(n+1)} - a_{k|k} x_k^{(n)} - \sum_{i=k+1}^N a_{k|i} x_i^{(n)} \right] \\ &= \frac{1}{a_{k|k}} \left[b_k - \sum_{i=1}^{k-1} a_{k|i} x_i^{(n+1)} - \sum_{i=k}^N a_{k|i} x_i^{(n)} \right] \end{aligned} \quad (7.5.330)$$

Now a relaxation factor ω is introduced so that the new approximation is obtained to:

$$x_k^{(n+1)} = x_k^{(n)} + \omega \Delta x_k^{(n+1)} = x_k^{(n)} + \frac{\omega}{a_{k|k}} \left[b_k - \sum_{i=1}^{k-1} a_{k|i} x_i^{(n+1)} - \sum_{i=k}^N a_{k|i} x_i^{(n)} \right] \quad (7.5.331)$$

The iteration scheme (7.5.331) is known as the successive over-relaxation method or SOR method. The Gauss-Seidel method can be seen as a special case of the SOR method for $\omega = 1$. – The numerical effort required for an iterative method depends on several factors. First, it depends on the

initial approximation $\mathbf{x}^{(0)}$; if $\mathbf{x}^{(0)}$ is closer to the exact solution \mathbf{x} , fewer iteration steps and therefore a lesser numerical effort are required. Second, it depends on the filling of the matrix \mathbf{A} ; as the iterative schemes (7.5.327), (7.5.328), and (7.5.331) show, fewer multiplications $a_{k|i}x_i$ and fewer additions are necessary, if more coefficients $a_{k|i}$ of the matrix vanish so that the multiplications with these coefficients can be skipped. Thereby, iterative methods are especially well suited for sparse matrices.

To compare the applicability of these two basic strategies on the normal contact problem, it should be pointed out what the solution of the problem consists in. The normal contact problem is formulated in the following way:

$$\mathbf{H}_{33}\mathbf{p} = \mathbf{w}, \quad \begin{array}{ll} w_i - \delta_i = 0 \wedge p_i > 0 & \text{inside the contact area} \\ w_i - \delta_i > 0 \wedge p_i = 0 & \text{outside the contact area} \end{array} \quad (7.5.332)$$

The wanted solution of the normal contact problem is the vector \mathbf{p} , more precise: its non-vanishing components $p_i > 0$. At these grid points $\langle x_i, y_i \rangle$ the normal deformation w_i compensates the interpenetration δ_i of the undeformed surfaces; this characterizes the actual contact area. The condition $w_i - \delta_i > 0$ describes a separation of the deformed surfaces; at the gridpoints $\langle x_i, y_i \rangle$, where this condition is fulfilled, the pressure vanishes, i.e. $p_i = 0$. It should be emphasized that for the wanted solution of the contact problem only the condition $w_i - \delta_i > 0 \Leftrightarrow w_i > \delta_i$ is important, but not the exact value of the deformation w_i .

In this context it turns out that the direct calculation method is less suited for the solution of the normal contact problem: The direct calculation method solves a system of *equations* in its literal sense, i.e. to obtain the vector \mathbf{p} the vector \mathbf{w} on the right hand side has to be fully known. This means that for the points $\langle x_i, y_i \rangle$ outside the actual contact area the deformations $w_i > \delta_i$ have to be determined in such a way that the pressure p_i vanishes; this requires additional computational effort. Of course, the system of equations could be reformulated for the potential contact points by skipping the equations for the grid points $\langle x_i, y_i \rangle$, which are currently regarded to be outside the contact area. However, if the system of equations is changed, the LU decomposition has to be carried out again, which requires a considerable computational effort.

Compared to this, an iterative calculation method is far better suited to take the additional conditions into account: To determine the new approximation $p_k^{(n+1)}$ it is assumed that contact occurs. Therefore, the normal deformation w_k is set equal to the interpenetration δ_k . Then the SOR method gives the following expression for the initial value $\tilde{p}_k^{(n+1)}$ of new approximation:

$$\tilde{p}_k^{(n+1)} = p_k^{(n)} + \frac{\omega}{H_{k|k}^{[33]}} \left[\delta_k - \sum_{i=1}^{k-1} H_{k|i}^{[33]} p_i^{(n+1)} - \sum_{i=k}^N H_{k|i}^{[33]} p_i^{(n)} \right] \quad (7.5.333)$$

According to the additional condition given in (7.5.332) the pressure p_k is either positive or zero, but it cannot be negative. If (7.5.333) gives a non-negative initial value $\tilde{p}_k^{(n+1)}$, this value is taken for the new approximation $p_k^{(n+1)}$; otherwise, $p_k^{(n+1)}$ is simply set to zero:

$$p_k^{(n+1)} = \begin{cases} \tilde{p}_k^{(n+1)} & \text{for } \tilde{p}_k^{(n+1)} \geq 0 \\ 0 & \text{for } \tilde{p}_k^{(n+1)} < 0 \end{cases} \quad (7.5.334)$$

The additional computational effort for the check and the correction according to (7.5.334) is very low. Therefore, an iterative calculation method is chosen for the solution of the normal contact problem.

It should however be kept in mind that because of $H_{i|k}^{[33]} > 0$ the matrix \mathbf{H}_{33} is completely filled. This is highly disadvantageous regarding the computational effort for an iterative calculation method. Therefore two additional measures to reduce the solution effort of the normal contact problem will be presented in the following.

Generally, the sequence of the equations forming a system of linear equations has no influence on the solution and can therefore be changed. Regarding this fact it is obvious to change the sequence, in which the equations are treated, in such a way that the equations having a high defect are treated first, while those equations, which are nearly fulfilled, are treated later. This, however, requires that the defect of each equation is known. For the present case the defect is simply the required correction $\Delta p_k^{(n+1)}$. In the iteration scheme (7.5.333) the $k-1$ corrected values $p_i^{(n+1)}$, $i < k-1$ and the $N-k+1$ uncorrected values $p_i^{(n)}$, $i \geq k$ are used. These values form the current vector $\mathbf{p}^{(m)}$:

$$\mathbf{p}^{(m)} = \left[p_1^{(n+1)} \quad \dots \quad p_{k-1}^{(n+1)} \quad p_k^{(n)} \quad \dots \quad p_N^{(n)} \right]^T \quad (7.5.335)$$

For a given distribution $\mathbf{p}^{(m)}$ of the pressure distribution the related normal deformation $\mathbf{w}^{(m)}$ is obtained by:

$$\mathbf{H}_{33} \mathbf{p}^{(m)} = \mathbf{w}^{(m)} \Rightarrow w_k^{(m)} = \sum_{i=1}^N H_{k|i}^{[33]} p_i^{(m)} = \sum_{i=1}^{k-1} H_{k|i}^{[33]} p_i^{(n+1)} + \sum_{i=k}^N H_{k|i}^{[33]} p_i^{(n)} \quad (7.5.336)$$

Here, the vector $\mathbf{w}^{(m)}$ describes the current normal deformation obtained for the current pressure vector $\mathbf{p}^{(m)}$. Using the current deformation $w_k^{(m)}$ at the k -th gridpoint the expression (7.5.333) yielding the initial value $\tilde{p}_k^{(n+1)}$ can be reformulated to:

$$\begin{aligned} \tilde{p}_k^{(m+1)} &= p_k^{(m)} + \frac{\omega}{H_{k|k}^{[33]}} \left[\delta_k - \sum_{i=1}^{k-1} H_{k|i}^{[33]} p_i^{(n+1)} - \sum_{i=k}^N H_{k|i}^{[33]} p_i^{(n)} \right] \\ &= p_k^{(m)} + \frac{\omega}{H_{k|k}^{[33]}} \left[\delta_k - \sum_{i=1}^N H_{k|i}^{[33]} p_i^{(m)} \right] = p_k^{(m)} + \frac{\omega}{H_{k|k}^{[33]}} \left[\delta_k - w_k^{(m)} \right] \end{aligned} \quad (7.5.337)$$

The corrected value for the new approximation is obtained in a way analogous to (7.5.334):

$$\bar{p}_k^{(m+1)} = \begin{cases} \tilde{p}_k^{(m)} & \text{for } \tilde{p}_k^{(m)} \geq 0 \\ 0 & \text{for } \tilde{p}_k^{(m)} < 0 \end{cases} \quad (7.5.338)$$

The defect $\Delta p_k^{(m+1)}$ is now determined as the difference between the current value $p_k^{(m)}$ and the corrected value $\bar{p}_k^{(m+1)}$:

$$\Delta p_k^{(m+1)} = \bar{p}_k^{(m+1)} - p_k^{(m)} \quad (7.5.339)$$

The correction is now performed the K -th gridpoint, at which the largest absolute value of the defect occurs. As a result, the elements of the new current vector $\mathbf{p}^{(m+1)}$ are:

$$p_k^{(m+1)} = \begin{cases} \bar{p}_K^{(m+1)} & \text{for } k = K \\ p_k^{(m)} & \text{for } k \neq K \end{cases} \quad (7.5.340)$$

Using the definition of the defect (7.5.339) the new approximation vector $\mathbf{p}^{(m+1)}$ can also be expressed in the following way:

$$\begin{aligned}\mathbf{p}^{(m+1)} &= \left[\dots p_{K-1}^{(m)} \bar{p}_K^{(m+1)} p_{K-1}^{(m)} \dots \right]^T \\ &= \left[\dots p_{K-1}^{(m)} p_K^{(m)} p_{K-1}^{(m)} \dots \right]^T + \left[\dots 0 \Delta p_K^{(m+1)} 0 \dots \right]^T \\ &= \mathbf{p}^{(m)} + \Delta \mathbf{p}^{(m+1)}\end{aligned}\quad (7.5.341)$$

Based on this description it is obtained for the new current deformation $\mathbf{w}^{(m+1)}$:

$$\mathbf{w}^{(m+1)} = \mathbf{H}_{33} \mathbf{p}^{(m+1)} = \mathbf{H}_{33} \mathbf{p}^{(m)} + \mathbf{H}_{33} \Delta \mathbf{p}^{(m+1)} = \mathbf{w}^{(m)} + \mathbf{H}_{33} \Delta \mathbf{p}^{(m+1)} \quad (7.5.342)$$

The only non-vanishing element of the vector $\Delta \mathbf{p}^{(m+1)}$ is the K -th component $\Delta p_K^{(m+1)}$. Thus, the update of the deformation is easily obtained by:

$$w_i^{(m+1)} = w_i^{(m)} + H_{i|k}^{[33]} \Delta p_K^{(m+1)} \quad (7.5.343)$$

Based on these considerations a modified solving algorithm can be formulated. For an initial guess $\mathbf{p}^{(0)}$ the related normal deformation $\mathbf{w}^{(0)} = \mathbf{H}_{33} \mathbf{p}^{(0)}$ is calculated. A single iteration cycle consists of the following steps:

1. Determine the corrected values $\bar{p}_k^{(m+1)}$ for the pressure distribution:

$$\bar{p}_k^{(m+1)} = p_k^{(m)} + \frac{\omega}{H_{k|k}^{[33]}} \left[\delta_k - w_k^{(m)} \right], \quad \bar{p}_k^{(m+1)} = \begin{cases} \tilde{p}_k^{(m)} & \text{for } \tilde{p}_k^{(m)} \geq 0 \\ 0 & \text{for } \tilde{p}_k^{(m)} < 0 \end{cases} \quad (7.5.344)$$

2. Calculate the defect for each gridpoint and determine the K -th gridpoint, at which the largest absolute defect occurs:

$$\Delta p_k^{(m+1)} = \bar{p}_k^{(m+1)} - p_k^{(m)}, \quad \left| \Delta p_K^{(m+1)} \right| = \max_k \left| \Delta p_k^{(m+1)} \right| \quad (7.5.345)$$

3. Set the new approximation value $p_K^{(m+1)}$ at the K -th gridpoint equal to the corrected value $\bar{p}_K^{(m+1)}$, leave all other values $p_k^{(m)}$, $k \neq K$ unchanged and update the current deformation:

$$p_k^{(m+1)} = \begin{cases} \bar{p}_K^{(m+1)} & \text{for } k = K \\ p_k^{(m)} & \text{for } k \neq K \end{cases}, \quad w_k^{(m+1)} = w_k^{(m)} + H_{k|k}^{[33]} \Delta p_K^{(m+1)} \quad (7.5.346)$$

By performing the actual correction only at the K -th gridpoint, where the highest absolute defect currently occurs, the number of iteration steps and thereby the computational effort are distinctly reduced. The presented algorithm was found in a heuristic way. Therefore, no mathematical proof for the convergence can be given here. However, in all cases, which were treated in the context of this work, the algorithm has never failed.

It is evident that the computational effort depends on the order N of the system of linear equations. Thus a further measure to reduce the computational effort is to reduce the order of the system. In the case of the normal contact problem the order of the complete problem is the number of the gridpoints, where a positive interpenetration $\delta_i > 0$ has been determined. A reduction of the

system's order can be achieved if a subset of potential contact points is chosen so that the iterative solution only has to be carried out for this subset.

According to the formulation of the normal contact problem for points $\langle x_i, y_i \rangle$ located outside the actual contact area two conditions have to be fulfilled: The pressure p_i vanishes and the deformation w_i is greater than the interpenetration δ_i :

$$p_i = 0 \wedge w_i - \delta_i > 0 \quad (7.5.347)$$

By inverting this condition all points $\langle x_j, y_j \rangle$, where the pressure p_j doesn't vanish or the deformation w_j is lesser than or equal to the interpenetration δ_j , are considered as potential contact points:

$$p_j > 0 \vee w_j - \delta_j \leq 0 \quad (7.5.348)$$

The case of $p_j < 0$ cannot occur due to (7.5.334).

During the progress of the iteration described by the steps (7.5.344), (7.5.345), and (7.5.346) numerical errors will accumulate in the deformation vector $\mathbf{w}^{(m)}$. Such errors can be expected due to the decreasing magnitude of the defect $\Delta p_K^{(m)}$ used for the correction. The magnitude of the defects has to decrease; otherwise, the iteration doesn't converge. It is therefore sensible to recalculate the deformation vector \mathbf{w} after a certain number of iteration cycles to eliminate the accumulated numerical errors. After this recalculation the condition (7.5.348) is checked for all gridpoints and the subset is formed from those gridpoints $\langle x_j, y_j \rangle$, where this condition is fulfilled. The following n_{iter} iteration cycles are only carried out for the subset. After the n_{iter} iteration cycles the deformation vector \mathbf{w} is recalculated for the original set including all gridpoints $\langle x_i, y_i \rangle$, at which a positive interpenetration $\delta_i > 0$ occurs. This also ensures that no potential contact points, which may turn out to be actual contact points, are overlooked and left out.

In total the solution algorithm consists of an outer loop for the selection of the potential contact points and an inner loop for the correction of the pressure at the potential contact points. The algorithm starts with the current pressure $\mathbf{p}^{(m)}$ and the related deformation $\mathbf{w}^{(m)} = \mathbf{H}_{33} \mathbf{p}^{(m)}$ for all gridpoints $\langle x_i, y_i \rangle$ with $\delta_i > 0$. Then the following steps are carried out:

1. Select a subset of all potential contact points $\langle x_j, y_j \rangle$ fulfilling the following condition:

$$p_j^{(m)} > 0 \vee w_j^{(m)} - \delta_j \leq 0 \quad (7.5.349)$$

2. Perform n_{iter} cycles of the following iteration steps for the subset of the potential contact points $\langle x_j, y_j \rangle$:

- (a) Determine the corrected values $\bar{p}_j^{(m+1)}$ for the pressure distribution:

$$\bar{p}_j^{(m+1)} = p_j^{(m)} + \frac{\omega}{H_{j|j}^{[33]}} [\delta_j - w_j^{(m)}], \quad \bar{p}_j^{(m+1)} = \begin{cases} \bar{p}_j^{(m)} & \text{for } \bar{p}_j^{(m)} \geq 0 \\ 0 & \text{for } \bar{p}_j^{(m)} < 0 \end{cases} \quad (7.5.350)$$

- (b) Calculate the defect for each gridpoint of the subset and determine the J -th gridpoint, at which the largest absolute defect occurs:

$$\Delta p_j^{(m+1)} = \bar{p}_j^{(m+1)} - p_j^{(m)}, \quad \left| \Delta p_J^{(m+1)} \right| = \max_j \left| \Delta p_j^{(m+1)} \right| \quad (7.5.351)$$

- (c) Set the new approximation value $p_j^{(m+1)}$ at the J -th gridpoint equal to the corrected value $\bar{p}_J^{(m+1)}$, leave all other values $p_j^{(m)}$, $j \neq J$ unchanged and update the current deformation:

$$p_j^{(m+1)} = \begin{cases} \bar{p}_J^{(m+1)} & \text{for } j = J \\ p_j^{(m)} & \text{for } j \neq J \end{cases}, w_j^{(m+1)} = w_j^{(m)} + H_{j|j}^{[33]} \Delta p_J^{(m+1)} \quad (7.5.352)$$

3. Recalculate the deformation $\mathbf{w}^{(m+n_{iter})}$ for all gridpoints $\langle x_i, y_i \rangle$:

$$\mathbf{w}^{(m+n_{iter})} = \mathbf{H}_{33} \mathbf{p}^{(m+n_{iter})} \quad (7.5.353)$$

The additional effort required by the recalculation is lesser than it may seem. The numerical efficiency can be improved if the subset of those gridpoints $\langle x_k, y_k \rangle$, where the pressure doesn't vanish, i.e. $p_k^{(m+n_{iter})} > 0$, is used for the recalculation. The number N_p of these gridpoints is always lower than the total number N of gridpoints in the interpenetration area. Then the recalculation of the deformation $w_i^{(m+n_{iter})}$ at the i -th gridpoint uses the following procedure:

$$w_i^{(m+n_{iter})} = \sum_{K=1}^{N_p} H_{i|K}^{[33]} p_K^{(m+n_{iter})} \quad (7.5.354)$$

Furthermore the reduced numerical effort for the inner loop due to the smaller subset of the potential contact points outweighs the additional effort for the recalculation.

7.6 Tangential contact

For the tangential contact problem, the relative velocities of wheel and rail in the contact area have to be considered. In the following considerations, the indices $I = 1$ and $I = 2$ will be used to denote kinematics and stresses in the direction of the 1-axis and the 2-axis, respectively, of the contact frame C . Since only the contact frame C is considered in the following, the superscript C indicating this frame will be skipped.

The velocity v_{WI} of the wheel in the contact is expressed by superposing the velocity V_{RI} of the rigid body motion and the deformation velocity \dot{u}_{WI} :

$$v_{WI}(x, y) = V_{WI}(x, y) + \dot{u}_{WI}(x, y), \quad I = 1, 2 \quad (7.6.355)$$

In an analogous way, the velocity v_{RI} for the rail in the contact area is described:

$$v_{RI}(x, y) = V_{RI}(x, y) + \dot{u}_{RI}(x, y), \quad I = 1, 2 \quad (7.6.356)$$

The relative velocity between wheel and rail in the contact is obtained to:

$$\begin{aligned} v_I(x, y) &= v_R(x, y) - v_W(x, y) \\ &= [V_{RI}(x, y) + \dot{u}_{RI}(x, y)] - [V_{WI}(x, y) + \dot{u}_{WI}(x, y)] \\ &= [V_{RI}(x, y) - V_{WI}(x, y)] + [\dot{u}_{RI}(x, y) - \dot{u}_{WI}(x, y)] \\ &= V_I(x, y) + \dot{u}_I(x, y), \quad I = 1, 2 \end{aligned} \quad (7.6.357)$$

Thereby, the relative velocity V_I of the rigid body motion and the resulting deformation u_I are defined. The deformation velocity can be approximated based on the deformation

$u_I^*(x, y) = u_I(x, y, t - \Delta t)$ at an earlier time $t - \Delta t$ and the wanted deformation $u_I(x, y) = u_I(x, y, t)$ at the current time t :

$$u_I(x, y) = u_I(x, y, t), u_I^*(x, y) = u_I(x, y, t - \Delta t) \Rightarrow \dot{u}_I = \dot{u}_I(x, y) \approx \frac{u_I(x, y) - u_I^*(x, y)}{\Delta t} \quad (7.6.358)$$

Using this approximation, the current relative velocity $v_I(x, y) = v_I(x, y, t)$ can be formulated in the following way:

$$v_I(x, y) = V_I(x, y) + \dot{u}_I(x, y) = V_I(x, y) + \frac{u_I(x, y) - u_I^*(x, y)}{\Delta t}, \quad I = 1, 2 \quad (7.6.359)$$

For the further considerations, the deformation $u_I^*(x, y)$ at an earlier time will generally considered to be known so that the solution of the tangential contact problem are the current tangential deformations $u_I(x, y) = u_I(x, y, t)$ and the current tangential stresses $\tau_I(x, y) = \tau_I(x, y, t)$. Furthermore, a condition formulated for $u_I(x, y)$, $\dot{u}_I(x, y)$ or $\tau_I(x, y)$ will be considered to be valid for both coordinate directions, i.e. for $I = 1$ and for $I = 2$, if it is not explicitly stated otherwise.

Regarding the tangential contact, there are two possible states for a point denoted by the coordinates x and y ; these two states are adhesion and sliding. In this context, the resulting tangential stress $\tau(x, y)$ transmitted at this point is an important value; this value is defined by:

$$\tau(x, y) = \sqrt{\tau_1(x, y)^2 + \tau_2(x, y)^2} \geq 0 \quad (7.6.360)$$

The absolute value $\tau(x, y)$ cannot exceed the maximum transmittable tangential stress $\tau_{\max}(x, y)$ at the considered point, which is determined by the local normal pressure $p(x, y)$ and the local friction coefficient $\mu(x, y)$:

$$\tau(x, y) \leq \tau_{\max}(x, y) = \mu(x, y) p(x, y) \quad (7.6.361)$$

In the present case, it has been assumed that both bodies, which are in contact, consist of materials having the same material parameters G and ν . In this case, the normal contact problem is decoupled from the tangential contact problem so that the normal contact problem, as shown in section 7.3. Therefore, the normal contact problem is solved first so that the distribution of the normal pressure $p(x, y)$ is known at the beginning of solving the tangential contact problem.

Now, the conditions can be formulated for the two states of adhesion and sliding.

- In the case of adhesion, the relative velocity vanishes, i.e. both components $v_I(x, y)$ vanish. The resulting tangential stress is less or equal to the maximum transmittable stress:

$$v_I(x, y) = V_I(x, y) + \frac{u_I(x, y) - u_I^*(x, y)}{\Delta t} = 0 \quad (7.6.362)$$

$$\tau(x, y) = \sqrt{\tau_1(x, y)^2 + \tau_2(x, y)^2} \leq \tau_{\max}(x, y) \quad (7.6.363)$$

The condition (7.6.362) can be reformulated to:

$$u_I(x, y) = u_I^*(x, y) - V_I(x, y) \Delta t \quad (7.6.364)$$

- In the case of adhesion, there is a relative velocity, i.e. at least one component of the relative velocity $v_I(x, y)$ does not vanish. The transmitted tangential stress acts in the opposite direction to the relative velocity and its absolute value, i.e. the resulting tangential stress, is equal to the maximum transmittable stress.

$$\tau_I(x, y) = -C \cdot v_I(x, y), \quad C > 0 \quad (7.6.365)$$

$$\tau(x, y) = \sqrt{\tau_1(x, y)^2 + \tau_2(x, y)^2} = \tau_{\max}(x, y) \quad (7.6.366)$$

The constant C contained in the condition (7.6.365) is eliminated in the following way:

$$\tau_1(x, y) = -C \cdot v_1(x, y) \Rightarrow \tau_1(x, y) v_2(x, y) = -C \cdot v_1(x, y) v_2(x, y) \quad (7.6.367)$$

$$\tau_2(x, y) = -C \cdot v_2(x, y) \Rightarrow \tau_2(x, y) v_1(x, y) = -C \cdot v_1(x, y) v_2(x, y) \quad (7.6.368)$$

$$\Rightarrow \tau_1(x, y) v_2(x, y) - \tau_2(x, y) v_1(x, y) = 0 \quad (7.6.369)$$

Inserting the expression for the relative velocity according to (7.6.359) leads to:

$$\begin{aligned} 0 &= \tau_1(x, y) \left[V_2(x, y) + \frac{u_2(x, y) - u_2^*(x, y)}{\Delta t} \right] - \tau_2(x, y) \left[V_1(x, y) + \frac{u_1(x, y) - u_1^*(x, y)}{\Delta t} \right] \\ \Rightarrow 0 &= \tau_1(x, y) [V_2(x, y) \Delta t + u_2(x, y) - u_2^*(x, y)] \\ &\quad - \tau_2(x, y) [V_1(x, y) \Delta t + u_1(x, y) - u_1^*(x, y)] \end{aligned} \quad (7.6.370)$$

These conditions are now applied to the discretized tangential contact problem. The deformations and the tangential stresses at the i -th gridpoint, which are considered as the wanted solution for the current state, have already been defined in the context of the discretization shown in section 7.4:

$$u_{1,i} = u_1(x_i, y_i, t), \quad u_{2,i} = u_2(x_i, y_i, t), \quad \tau_{1,i} = \tau_1(x_i, y_i, t), \quad \tau_{2,i} = \tau_2(x_i, y_i, t) \quad (7.6.371)$$

In an analogous way, the previous deformation and the rigid body velocity are defined:

$$u_{1,i}^* = u_1(x_i, y_i, t - \Delta t), \quad u_{2,i}^* = u_2(x_i, y_i, t - \Delta t), \quad V_{1,i} = V_1(x_i, y_i, t), \quad V_{2,i} = V_2(x_i, y_i, t) \quad (7.6.372)$$

For the sake of simplicity it is assumed that the friction coefficient μ is constant for the complete contact and that it is equal for adhesion and sliding. Then it is valid:

$$\tau_{\max,i} = \tau_{\max}(x_i, y_i) = \mu p(x_i, y_i) = \mu p_i \quad (7.6.373)$$

Using these definitions, the conditions for the two states can be formulated:

$$\text{Adhesion:} \quad u_{1,i} = u_{1,i}^* - V_{1,i} \Delta t, \quad u_{2,i} = u_{2,i}^* - V_{2,i} \Delta t, \quad \sqrt{\tau_{1,i}^2 + \tau_{2,i}^2} \leq \tau_{\max,i} \quad (7.6.374)$$

$$\text{Sliding:} \quad 0 = \tau_{1,i} [V_{2,i} \Delta t + u_{2,i} - u_{2,i}^*] - \tau_{2,i} [V_{1,i} \Delta t + u_{1,i} - u_{1,i}^*], \quad \sqrt{\tau_{1,i}^2 + \tau_{2,i}^2} = \tau_{\max,i} \quad (7.6.375)$$

7.6.1 Solving algorithm

Similar to the normal contact problem discussed in section 7.5, the tangential contact problem is formulated as a system of linear equations and nonlinear conditions. In this case, the nonlinear condition is given by the fact that the resulting tangential stress cannot exceed the maximum transmittable stress.

In section 7.5.1, several methods for the solution of a system of linear equations have been considered and discussed. For the solution of a system of linear equations with nonlinear conditions, an iterative calculation is more efficient than a direct calculation, since the nonlinear conditions can be taken into account easier by an iteration. One of the methods presented in section 7.5.1 is the Gauss-Seidel algorithm. This algorithm generates a sequence of approximations $x_k^{(n)}$, which

converges towards the exact solutions x_k . A new approximation $x_k^{(n+1)}$ is obtained in the following way:

$$x_k^{(n+1)} = x_k^{(n)} + \Delta x_k^{(n+1)}, \quad \Delta x_k^{(n+1)} = \frac{1}{a_{k|k}} \left[b_k - \sum_{i=1}^{k-1} a_{k|i} x_i^{(n+1)} - \sum_{i=k}^N a_{k|i} x_i^{(n)} \right] \quad (7.6.376)$$

Here, $\Delta x_k^{(n+1)}$ is a correction. Since the new values $x_k^{(n+1)}$ are generated subsequently starting with $k = 1$, the values $x_i^{(n+1)}$ for $i < k$ are already available at the time, when $\Delta x_k^{(n+1)}$ and $x_k^{(n+1)}$ are determined.

Based on the Gauss-Seidel method, the solving algorithm for the tangential contact problem will be developed. However, some modifications are necessary. At the tangential contact problem, there is a nonlinear condition contains both tangential stresses $\tau_{1,k}$ and $\tau_{2,k}$ at the k -th grid point. Therefore, the two new approximations $\tau_{1,k}^{(n+1)}$ and $\tau_{2,k}^{(n+1)}$ have to be determined simultaneously, since the check of the conditions for the states of adhesion and sliding only makes sense, if it is carried out for new approximations for both stresses.

The relation between the tangential deformations $u_{l,i}$ and the tangential stresses $\tau_{l,i}$, which is based on the contact mechanics, is given by the following system of linear equations, which has been derived in section 7.4:

$$u_{1,i} = \sum_{j=1}^n H_{ij}^{[11]} \tau_{1,j} + \sum_{j=1}^n H_{ij}^{[12]} \tau_{2,j} \quad (7.6.377)$$

$$u_{2,i} = \sum_{j=1}^n H_{ij}^{[12]} \tau_{1,j} + \sum_{j=1}^n H_{ij}^{[22]} \tau_{2,j} \quad (7.6.378)$$

For the determination of the new approximations $\tau_{1,k}^{(n+1)}$ and $\tau_{2,k}^{(n+1)}$ at the k -th gridpoint the new values $\tau_{1,i}^{(n+1)}$ and $\tau_{2,i}^{(n+1)}$ for $i < k$ and the old values $\tau_{1,i}^{(n)}$ and $\tau_{2,i}^{(n)}$ for $i \leq k$ are available. In the first step for the correction the current deformations $u_{1,k}^{(n)}$ and $u_{2,k}^{(n)}$ are determined according to . Furthermore, it has been determined in section 7.4:

$$H_{k|k}^{[11]} = H_{k|k}^{[22]} = H_0, \quad H_{k|k}^{[12]} = 0 \quad (7.6.379)$$

Thereby, the current deformations $u_{1,k}^{(n)}$ and $u_{2,k}^{(n)}$ are obtained to:

$$u_{1,k}^{(n)} = \sum_{i=1}^{k-1} \left(H_{k|i}^{[11]} \tau_{1,i}^{(n+1)} + H_{k|i}^{[12]} \tau_{2,i}^{(n+1)} \right) + H_0 \tau_{1,k}^{(n)} + \sum_{i=k+1}^N \left(H_{k|i}^{[11]} \tau_{1,i}^{(n)} + H_{k|i}^{[12]} \tau_{2,i}^{(n)} \right) \quad (7.6.380)$$

$$u_{2,k}^{(n)} = \sum_{i=1}^{k-1} \left(H_{k|i}^{[12]} \tau_{1,i}^{(n+1)} + H_{k|i}^{[22]} \tau_{2,i}^{(n+1)} \right) + H_0 \tau_{2,k}^{(n)} + \sum_{i=k+1}^N \left(H_{k|i}^{[12]} \tau_{1,i}^{(n)} + H_{k|i}^{[22]} \tau_{2,i}^{(n)} \right) \quad (7.6.381)$$

Because of $H_{k|k}^{[12]} = 0$ the stress $\tau_{1,k}$ has no impact on the deformation $u_{2,k}$, while the deformation $u_{1,k}$ is independent of $\tau_{2,k}$. – After the correction, the new values $\tau_k^{(n+1)}$ and $\tau_k^{(n+1)}$ are available. Thereby, the new deformations $u_{l,k}^{(n+1)}$ are calculated in the following way:

$$u_{1,k}^{(n+1)} = \sum_{i=1}^{k-1} \left(H_{k|i}^{[11]} \tau_{1,i}^{(n+1)} + H_{k|i}^{[12]} \tau_{2,i}^{(n+1)} \right) + H_0 \tau_{1,k}^{(n+1)} + \sum_{i=k+1}^N \left(H_{k|i}^{[11]} \tau_{1,i}^{(n)} + H_{k|i}^{[12]} \tau_{2,i}^{(n)} \right) \quad (7.6.382)$$

$$u_{2,k}^{(n+1)} = \sum_{i=1}^{k-1} \left(H_{k|i}^{[12]} \tau_{1,i}^{(n+1)} + H_{k|i}^{[22]} \tau_{2,i}^{(n+1)} \right) + H_0 \tau_{2,k}^{(n+1)} + \sum_{i=k+1}^N \left(H_{k|i}^{[12]} \tau_{1,i}^{(n)} + H_{k|i}^{[22]} \tau_{2,i}^{(n)} \right) \quad (7.6.383)$$

Thereby, the differences between the new and the old values for the deformations are:

$$u_{1,k}^{(n+1)} - u_{1,k}^{(n)} = H_0 \tau_{1,k}^{(n+1)} - H_0 \tau_{1,k}^{(n)} \Rightarrow u_{1,k}^{(n+1)} = u_{1,k}^{(n)} + H_0 \tau_{1,k}^{(n+1)} - H_0 \tau_{1,k}^{(n)} \quad (7.6.384)$$

$$u_{2,k}^{(n+1)} - u_{2,k}^{(n)} = H_0 \tau_{2,k}^{(n+1)} - H_0 \tau_{2,k}^{(n)} \Rightarrow u_{2,k}^{(n+1)} = u_{2,k}^{(n)} + H_0 \tau_{2,k}^{(n+1)} - H_0 \tau_{2,k}^{(n)} \quad (7.6.385)$$

As mentioned before, there are two possible states for each point at the tangential contact. If the state of adhesion is assumed, then the values for the deformations $u_{1,k}$ and $u_{2,k}$ can be determined by: (7.6.374):

$$u_{1,k}^A = u_{1,k}^* - V_{1,k} \Delta t, \quad u_{2,k}^A = u_{2,k}^* - V_{2,k} \Delta t \quad (7.6.386)$$

The superscript A indicates the state of adhesion. By setting the new deformations $u_{I,k}^{(n+1)}$ equal to the assumed deformations $u_{I,k}^A$, the conditions for the corresponding stresses $\tau_{I,k}^A$ are formulated:

$$u_{1,k}^* - V_{1,k} \Delta t - u_{1,k}^{(n)} = H_0 \tau_{1,k}^A - H_0 \tau_{1,k}^{(n)} \Rightarrow \tau_{1,k}^A = \tau_{1,k}^{(n)} + \frac{u_{1,k}^* - V_{1,k} \Delta t - u_{1,k}^{(n)}}{H_0} \quad (7.6.387)$$

$$u_{2,k}^* - V_{2,k} \Delta t - u_{2,k}^{(n)} = H_0 \tau_{2,k}^A - H_0 \tau_{2,k}^{(n)} \Rightarrow \tau_{2,k}^A = \tau_{2,k}^{(n)} + \frac{u_{2,k}^* - V_{2,k} \Delta t - u_{2,k}^{(n)}}{H_0} \quad (7.6.388)$$

The new values $\tau_{1,k}^A$ and $\tau_{2,k}^A$ have been determined by assuming the state of adhesion. Therefore, it has to be checked whether the new values fulfill the second condition for the state of adhesion according to (7.6.363). If the resulting stress for $\tau_{1,k}^A$ and $\tau_{2,k}^A$ does not exceed the maximum transmittable stress $\tau_{\max,k}$ at the considered point, then the assumption of adhesion was correct and the values $\tau_{1,k}^A$ and $\tau_{2,k}^A$ are the new approximations $\tau_{1,k}^{(n+1)}$ and $\tau_{2,k}^{(n+1)}$.

$$\sqrt{\tau_{1,k}^A{}^2 + \tau_{2,k}^A{}^2} \leq \tau_{\max,k} \Rightarrow \tau_{1,k}^{(n+1)} = \tau_{1,k}^A \wedge \tau_{2,k}^{(n+1)} = \tau_{2,k}^A \quad (7.6.389)$$

If the resulting stress exceeds the maximum transmittable stress, i.e.

$$\sqrt{\tau_{1,k}^A{}^2 + \tau_{2,k}^A{}^2} > \tau_{\max,k} \quad (7.6.390)$$

then the assumption of adhesion was wrong, so that actually sliding occurs. In this case, the new approximations $\tau_{1,k}^{(n+1)}$ and $\tau_{2,k}^{(n+1)}$ for the tangential stresses and the corresponding deformations $u_{1,k}^{(n+1)}$ and $u_{2,k}^{(n+1)}$ have to fulfill the condition according to (7.6.370):

$$0 = \tau_{1,k}^{(n+1)} \left[V_{2,k} \Delta t + u_{2,k}^{(n+1)} - u_{2,k}^* \right] - \tau_{2,k}^{(n+1)} \left[V_{1,k} \Delta t + u_{1,k}^{(n+1)} - u_{1,k}^* \right] \quad (7.6.391)$$

In order to eliminate the deformations $u_{I,k}^{(n+1)}$ the relations (7.6.384) and (7.6.385) are used. As a result it is obtained:

$$\begin{aligned} 0 &= \tau_{1,k}^{(n+1)} \left[V_{2,k} \Delta t + u_{2,k}^{(n)} + H_0 \tau_{2,k}^{(n+1)} - H_0 \tau_{2,k}^{(n)} - u_{2,k}^* \right] \\ &\quad - \tau_{2,k}^{(n+1)} \left[V_{1,k} \Delta t + u_{1,k}^{(n)} + H_0 \tau_{1,k}^{(n+1)} - H_0 \tau_{1,k}^{(n)} - u_{1,k}^* \right] \\ &= \tau_{1,k}^{(n+1)} \left[V_{2,k} \Delta t + u_{2,k}^{(n)} - H_0 \tau_{2,k}^{(n)} - u_{2,k}^* \right] - \tau_{2,k}^{(n+1)} \left[V_{1,k} \Delta t + u_{1,k}^{(n)} - H_0 \tau_{1,k}^{(n)} - u_{1,k}^* \right] \end{aligned} \quad (7.6.392)$$

Dividing the equation by H_0 leads to:

$$0 = \tau_{1,k}^{(n+1)} \left[\frac{V_{2,k} \Delta t + u_{2,k}^{(n)} - u_{2,k}^*}{H_0} - \tau_{2,k}^{(n)} \right] - \tau_{2,k}^{(n+1)} \left[\frac{V_{1,k} \Delta t + u_{1,k}^{(n)} - u_{1,k}^*}{H_0} - \tau_{1,k}^{(n)} \right] \quad (7.6.393)$$

By comparing this to the adhesion stresses according to (7.6.387) and (7.6.388)

$$\tau_{1,k}^A = \tau_{1,k}^{(n)} + \frac{u_{1,k}^* - V_{1,k} \Delta t - u_{1,k}^{(n)}}{H_0}, \quad \tau_{2,k}^A = \tau_{2,k}^{(n)} + \frac{u_{2,k}^* - V_{2,k} \Delta t - u_{2,k}^{(n)}}{H_0} \quad (7.6.394)$$

it is obtained:

$$0 = -\tau_{1,k}^{(n+1)} \tau_{2,k}^A + \tau_{2,k}^{(n+1)} \tau_{1,k}^A \quad (7.6.395)$$

According to (7.6.375), in the case of sliding the resulting stress is equal to the maximum transmittable stress, i.e.:

$$\sqrt{\tau_{1,k}^{(n+1)2} + \tau_{2,k}^{(n+1)2}} = \tau_{\max,k} \quad (7.6.396)$$

The solutions $\tau_{I,k}^{(n+1)}$ can be found by scaling the adhesion stresses in the following way:

$$\tau_{1,k}^{(n+1)} = \frac{\tau_{\max,k}}{\sqrt{\tau_{1,k}^{(n+1)2} + \tau_{2,k}^{(n+1)2}}} \tau_{1,k}^A, \quad \tau_{2,k}^{(n+1)} = \frac{\tau_{\max,k}}{\sqrt{\tau_{1,k}^{(n+1)2} + \tau_{2,k}^{(n+1)2}}} \tau_{2,k}^A \quad (7.6.397)$$

By inserting this into the equation (7.6.395) it is shown that the solutions according to (7.6.397) in fact fulfil the condition:

$$-\tau_{1,k}^{(n+1)} \tau_{2,k}^A + \tau_{2,k}^{(n+1)} \tau_{1,k}^A = -\frac{\tau_{\max,k}}{\sqrt{\tau_{1,k}^{(n+1)2} + \tau_{2,k}^{(n+1)2}}} \tau_{1,k}^A \tau_{2,k}^A + \frac{\tau_{\max,k}}{\sqrt{\tau_{1,k}^{(n+1)2} + \tau_{2,k}^{(n+1)2}}} \tau_{2,k}^A \tau_{1,k}^A = 0 \quad (7.6.398)$$

In the present case stationary rolling is assumed, i.e. the state of the rolling contact hardly changes compared to the time, which is required for a particle to move through the contact area. Mathematically spoken, this means that the given velocities $V_{1,i}$ and $V_{2,i}$ are constant during the determination of the solution. Since the 1-axis of the contact frame C is pointing in the direction of the running of the vehicle, the particles are moving through the contact area in negative direction with the velocity equal to the negative running speed v_0 . If the time interval Δt is chosen in the following way:

$$\Delta t = \frac{\Delta a}{v_0} \quad (7.6.399)$$

then the previous deformations $u_1^*(x,y)$ and $u_2^*(x,y)$ are equal to the current deformations $u_1(x + \Delta a, y)$ and $u_2(x + \Delta a, y)$, since at the earlier time the particle, which is currently located at $\langle x, y \rangle$ had been located at the point $\langle x - v_0(-\Delta t) = x + \Delta a, y \rangle$ at the earlier time. If it is set

$$u_1^*(x, y) = u_1(x + \Delta a, y), \quad u_2^*(x, y) = u_2(x + \Delta a, y) \quad (7.6.400)$$

then the gridpoints have to be numbered in such a way that the following condition is fulfilled:

$$x_i = x_{i-1} - \Delta a \Leftrightarrow x_i + \Delta a = x_{i-1} \quad (7.6.401)$$

Thereby, the motion of the particle through the contact area is “tracked”, while the stresses $\tau_{1,i}$ and $\tau_{2,i}$ are successively determined with rising i . In total, the correction step for the k -th gridpoint can be formulated in the following way:

1. Determine the current deformations $u_{1,k}^{(n)}$ and $u_{2,k}^{(n)}$ by using the available new values $\tau_{I,i}^{(n+1)}$ for $i < k$ and the old values $\tau_{I,i}^{(n)}$ for $i \geq k$.

2. Calculate the stresses $\tau_{I,k}^A$ for the assumed state of adhesion:

$$\tau_{I,k}^A = \tau_{I,k}^{(n)} + \frac{u_{I,k-1}^{(n+1)} - V_{I,k} \Delta t - u_{I,k}^{(n)}}{H_0} \quad (7.6.402)$$

Here, $u_{I,k-1}^{(n+1)}$ is the corrected deformation from the previous gridpoint with $x_{k-1} = x_k + \Delta a$.

3. Compare the resulting stress of $\tau_{1,k}^A$ and $\tau_{2,k}^A$. If the condition $\sqrt{\tau_{1,k}^A{}^2 + \tau_{2,k}^A{}^2} \leq \tau_{\max,k}$ is fulfilled, set $\tau_{I,k}^{(n+1)} = \tau_{I,k}^A$
4. If the condition is not fulfilled, then scale the stresses $\tau_{I,k}^A$ with $\tau_{\max,k}$:

$$\tau_{I,k}^{(n+1)} = \frac{\tau_{\max,k}}{\sqrt{\tau_{1,k}^A{}^2 + \tau_{2,k}^A{}^2}} \tau_{I,k}^A \quad (7.6.403)$$

5. Determine the corrected deformations $u_{I,k}^{(n+1)}$, which are required as the earlier deformations at the next gridpoint $k+1$:

$$u_{I,k}^{(n+1)} = u_{I,k}^{(n)} + H_0 \left(\tau_{I,k}^{(n+1)} - \tau_{I,k}^{(n)} \right) \quad (7.6.404)$$

This iteration over all gridpoints is repeated until the differences $\left| \tau_{I,k}^{(n+1)} - \tau_{I,k}^{(n)} \right|$ are small enough to fulfil the required accuracy of the calculation.

Chapter 8

Simulation results

Based on the models and methods derived and discussed in the previous chapters, a coupled vehicle-track model is developed. This model represents a passenger coach running on a straight track. In the Figure 8.0.1 the bodies of which the model consists are displayed. The data for the

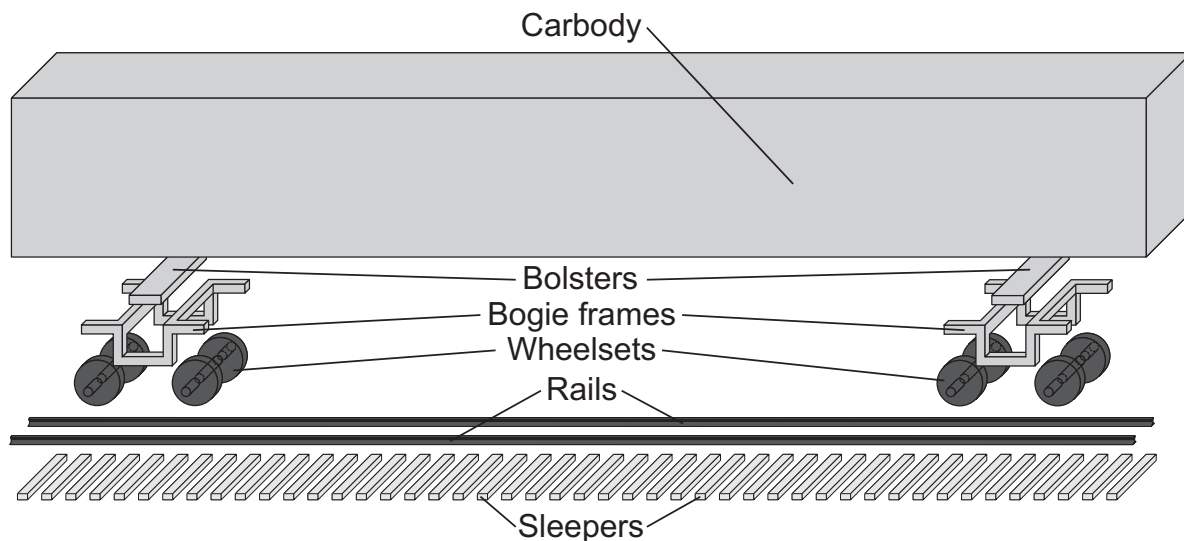


Figure 8.0.1: Bodies of the vehicle-track system. Flexible bodies are displayed in dark colour.

vehicle and for the track are taken from the works by Diepen [11]; and by Ripke [58], respectively. As described in section 2.2.1, the wheelset has two basic attractors: the centred running and the limit cycle hunting. These two scenarios will be investigated in this section. Although the limit cycle hunting is usually avoided in regular operation by a proper mechanical design of the vehicle, this scenario is chosen for two reasons: The nonlinear critical speed $v_{crit,nonlin}$, at which the limit cycle hunting starts, is an important characteristic of the vehicle. Moreover, during hunting the wheel-rail contact covers a wide range of the profiles of wheel and rail. Irregularities of the wheelsets and the rails like track disturbances, worn profiles, or unbalances are generally neglected in these investigations.

A important question in the context of simulating the running behaviour of a railway vehicle is how strong the obtained results are affected by influence factors: On the one hand, such influences can result from the model itself, i.e. the scope of the model (i.e. does the model describe a single running gear, a complete vehicle, or a train consisting of several vehicles interacting with each other?), physical effects, which are taken into account or neglected, the modelling of single

components like the wheel-rail contact or coupling elements like springs and dampers. On the other hand, parameters can have an impact on the results: Some parameters can vary for different regular operation conditions; a typical case is the track geometry covering the track gauge, the rail profiles and the inclination or cant of the rails, which all can affect the conicity and thereby the running behaviour. Other parameters are quite uncertain; a typical example is the friction coefficient in the wheel-rail contact, which depends on environmental conditions like moisture and on the roughness of the running surfaces. The influences of the modelling and of the parameters cannot always be separated from each other: In certain scenarios defined by a set of parameters physical effects or characteristics of the models used for certain components may have an important influence, while these influences are weaker under other conditions.

In the following considerations the influences of three parameters will be investigated and compared:

1. The structural flexibilities of the wheelsets and the rails, since this is an important property of the modelling.
2. The friction coefficient, since this is an uncertain parameter.
3. The conicity, since this can vary for operating the vehicle on different networks.

The consideration of the structural flexibilities is a property of the model. In contrast to this, the friction coefficient and the conicity are parameters. The conicity is a defined parameter, i.e. it depends on the chosen profiles of wheel and rail and on the track geometry. In contrast to this, the friction coefficient is an uncertain parameter.

To investigate the influence of the structural dynamics of the wheelsets and the track, different model configurations are used. The wheelset can be modelled either as a rigid or as a flexible body. For the track, using inertially fixed rails can lead to numerical problems in the solution of the equations of motion. Therefore, a very simple substitution model for the track is used for comparisons. This model will be referred to as “rigid rails” in the following; it is displayed in Figure 8.0.2. The model consists of a rigid body carrying both rail profiles. The rigid body can perform

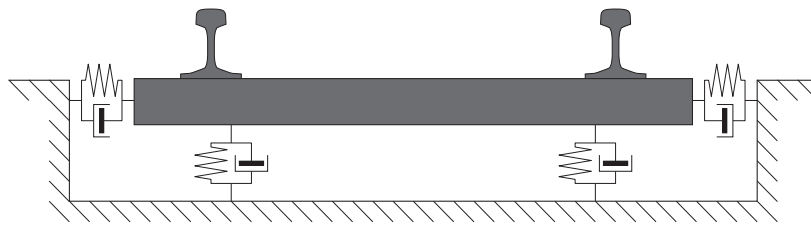


Figure 8.0.2: Simple substitution model for the track (“rigid rails”)

lateral and vertical translations and small roll motions, i.e. rotations around the longitudinal axis of the track. The body is connected to the environment by linear springs and dampers. The values for the parameters are taken from the work by Netter [48]. Each wheelset is supported by such a model, which moves along the trajectory together with the wheelset. Thereby, there are four basic model configurations, which will be considered:

- Rigid wheelsets / rigid rails: *RR*
- Flexible wheelsets / rigid rails: *FR*
- Rigid wheelsets / flexible rails: *RF*

- Flexible wheelsets / flexible rails: *FF*

In order to keep the denotation of the used models short, the configurations will be referenced by the abbreviations given above, which are written in italics. The system behaviour will be investigated for three different wheel-rail geometries:

- wheel profile *S1002*, rail profile *60E1*, rail cant $\tan\Phi_R = 1:40$, track gauge 1435 mm: *S1002 / 60E1 / 1:40*
- wheel profile *S1002*, rail profile *60E1*, rail cant $\tan\Phi_R = 1:20$, track gauge 1435 mm: *S1002 / 60E1 / 1:20*
- wheel profile *S1002*, rail profile *60E2*, rail cant $\tan\Phi_R = 1:40$, track gauge 1435 mm: *S1002 / 60E2 / 1:40*

The mathematical description of the wheel profile *S1002* is taken from the paper by Nefzger [47]. Also here, the used profile geometry will be referenced by the abbreviations written in italics.

8.1 Centred running

The scenario of centred running on a straight track without disturbances can be regarded as the reference state. The distribution of the pressure and the tangential stress were determined for the three contact geometries using the model configurations *RR* and *FF*. The following results for the scenario of centred running were all obtained for constant running speed of $v_0 = 200$ km/ and a friction coefficient of $\mu = 0.4$.

First, the scenario of centred running is investigated for the profile geometry *S1002 / 60E1 / 1:40* is used. In Fig. 8.1.3 the wheel-rail geometry, the pressure distribution and the tangential stress distribution obtained for the models *RR* and *FF* are displayed.

For both model configurations *RR* and *FF* the contact area has a distinctly non-elliptic shape, because it covers the point of $y_R = -10.228$ mm. At this point, the curvature radius of the rail profile *60E1* changes from 80 mm to 300 mm; thereby, the condition of a constant curvature as required for the Hertzian theory, which assumes an elliptical shape of the contact area, is not fulfilled. The vectors describing the tangential stresses form a concentric distribution around the centre of rotation, which is located near the middle of the trailing edge of the contact area. Due to the conical shape of the wheel's tread, the running surface isn't parallel to the vector of the angular velocity, which describes the overturning of the wheelset. As a result, the angular velocity has a component, which is orthogonal to the contact area. This leads to a relative angular velocity between wheel and rail and thereby to a spin creepage. This spin creepage causes the observed circular pattern of the tangential stresses in the contact area.

The comparison of the results shows a considerable influence of the structural flexibilities on the contact area. For the configuration *RR* two distinct pressure maxima occur, the left one showing 792 MPa, the right one showing 619 MPa. For the configuration *FF* the left maximum drastically shrinks to 314 MPa, while the right one increases to 725 MPa. Nevertheless, the contact geometries displayed in Fig. 8.1.3 are nearly identical; a difference is hardly visible. This underlines the sensitivity of the profile combination *S1002 / 60E1 / 1:40* to changes of the relative kinematics.

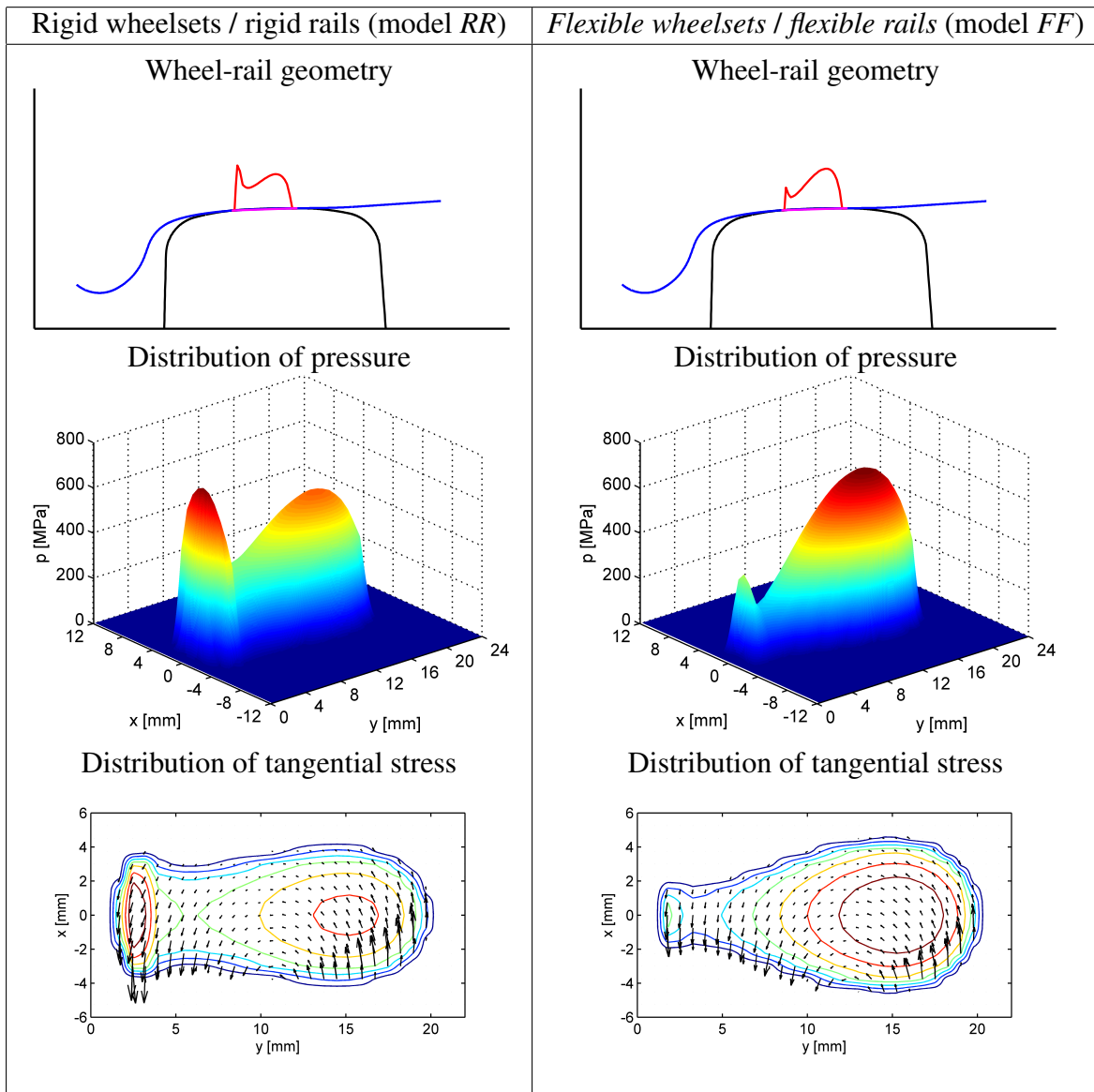


Figure 8.1.3: Influence of the structural flexibilities of wheelsets and rails on the wheel-rail geometry and on the distribution of pressure and tangential stresses for centred running; $v_0 = 200$ km/h; rail profile 60E1; cant 1:40; $\mu = 0.4$.

In the model *FF* the wheelsets and the rails are both modelled as flexible bodies. Thus, the question arises whether the flexibility of the wheelsets or of the rails is mainly responsible for the observed changes of the distributions of the stresses. Therefore, the scenario of centred running was also investigated for the configurations *FR* and *RF*. The wheel-rail geometry and the pressure distribution are displayed in Fig. 8.1.4.

The results obtained for the configurations *RR* and *RF* hardly differ from each other, while also the differences between the results for *FR* and *FF* are very small. This shows that the change of the pressure distribution is mainly caused by the flexibility of the wheelsets. An explanation for this behaviour can be derived from the scheme shown in Fig. 8.1.5.

Due to the vertical forces, which act on the wheelset at the bearings and at the wheel-rail contacts, a bending deformation of the wheelset axle occurs. Thereby, a camber angle of the wheels occurs, which is related to the inclination of the wheel rims.

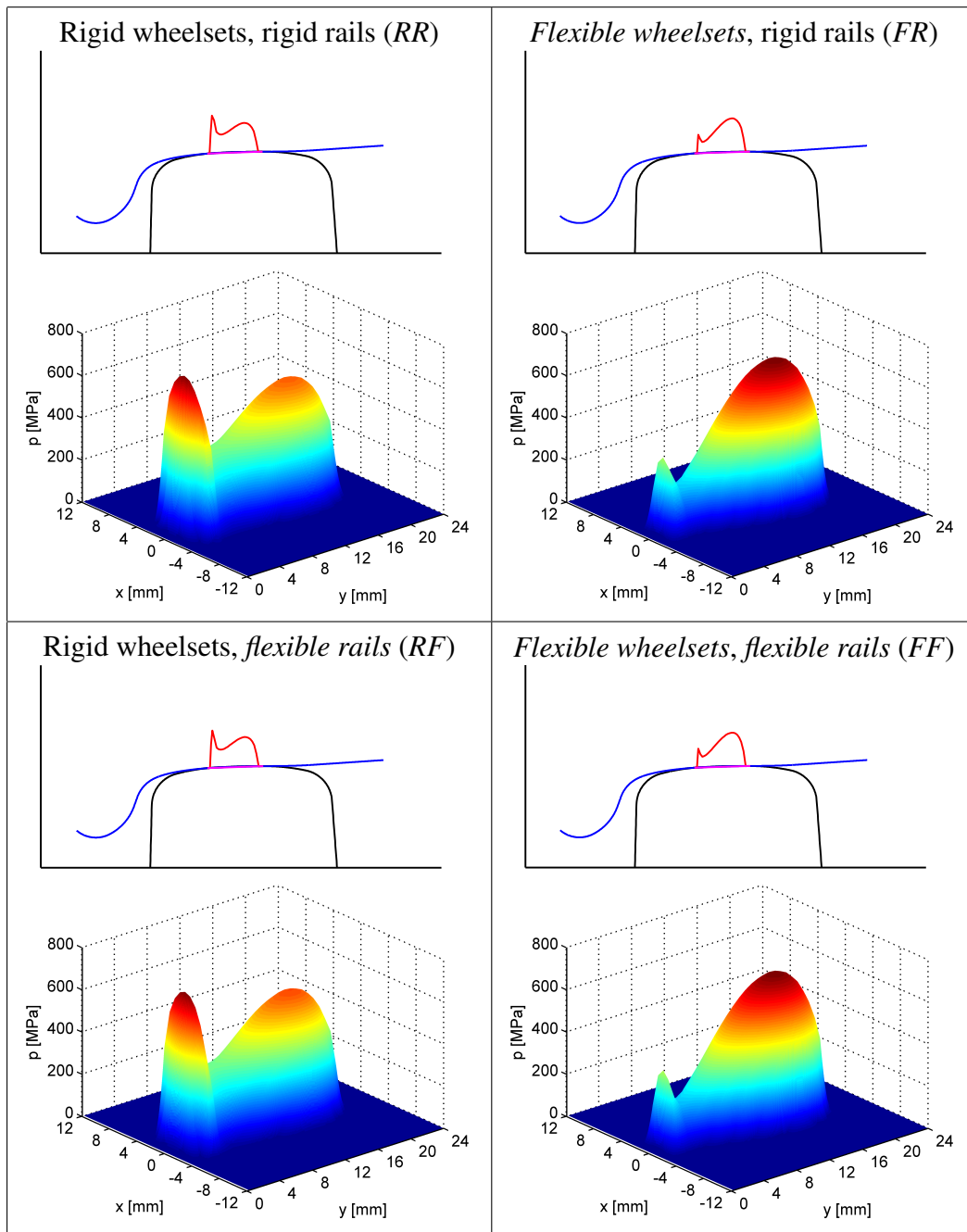


Figure 8.1.4: Influence of the structural flexibilities of wheelsets and rails on the wheel-rail geometry and on the pressure distribution for centred running; $v_0 = 200$ km/h; rail profile 60E1; cant 1:40; $\mu = 0.4$.

Next, the scenario of centred running is investigated for the profile geometry *S1002 / 60E1 / 1:20*. The results obtained for the models *RR* and *FF* are displayed in Fig. 8.1.6.

By comparing these results with those obtained for the profile geometry *S1002 / 60E1 / 1:40* displayed in Fig. 8.1.3, a drastic change of the contact due to the modified cant can be seen. The comparison of the wheel-rail contact geometry shows that the contact zone is shifted outwards. The shape of the contact area also changes strongly: For the profile geometry *S1002 / 60E1 / 1:20* the contact area is about 13 mm long and 6 mm wide; the pressure distribution shows one maximum. In contrast to this, for the profile geometry *S1002 / 60E1 / 1:40* the contact area has a length of 4 mm and a width of 18 mm; two maxima of the pressure distribution occur. Regarding the

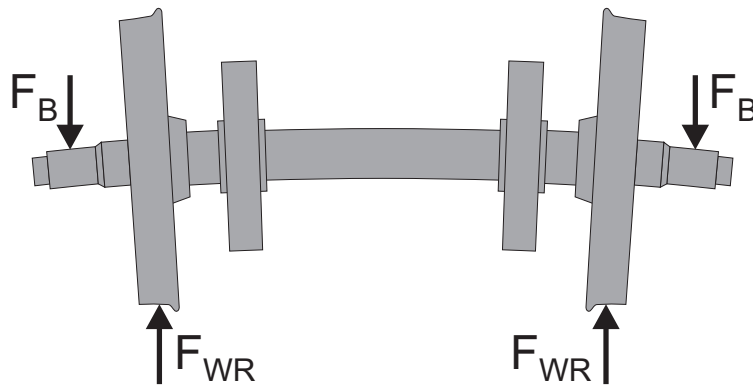


Figure 8.1.5: Bending of the wheelset due to the vertical forces acting at the bearings (F_B) and in the wheel-rail contacts (F_{WR}).

shape of the contact area it can be concluded that for the profile geometry $S1002 / 60E1 / 1:20$ the contact area is longer and narrower while it is shorter and wider for the profile geometry $S1002 / 60E1 / 1:40$.

For the profile geometry $S1002 / 60E1 / 1:20$ the contact zone covers the point of $y_S = 10.228$ mm on the rail head. Here, also an abrupt change of the profile's curvature from a radius of 300 mm to a radius of 80 mm occurs. Because of this discontinuity the contact area is again non-elliptic; this can be seen from the superposition of the distributions of pressure and tangential stresses shown in the lowest diagrams of Fig. 8.1.6.

From Fig. 8.1.6 it can be seen that the difference between the results obtained for the two models RR and FF is quite small; the distributions of the pressure and the tangential stresses are nearly the same. In the scenario of centred running, the distribution of the stresses obtained for the profile geometry $S1002 / 60E1 / 1:20$ is apparently less sensitive to changes of the relative kinematics between the rail head and the wheel rim.

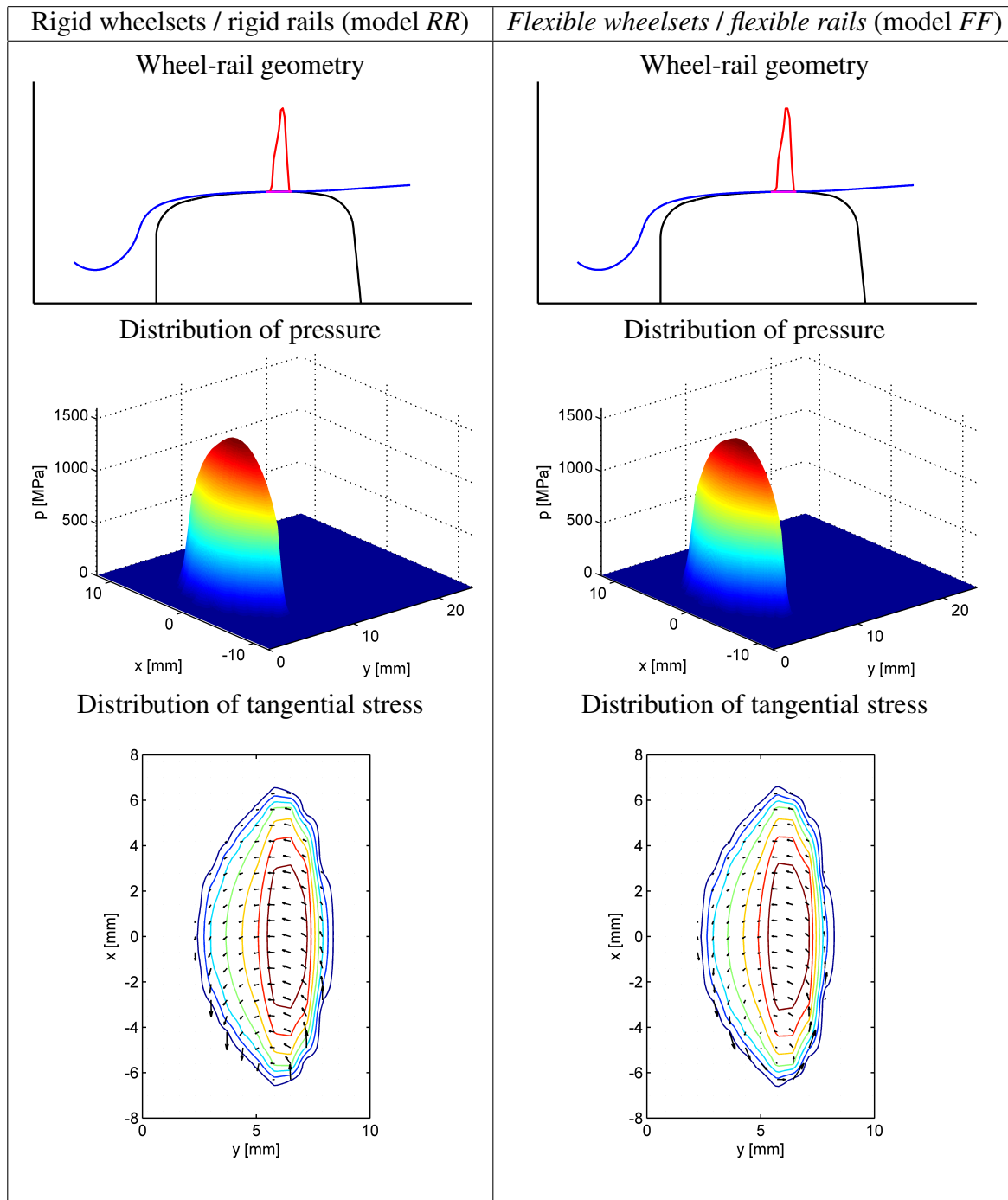


Figure 8.1.6: Influence of the structural flexibilities of wheelsets and rails on the wheel-rail geometry and on the pressure distribution for centred running; $v_0 = 200$ km/h; rail profile 60E1; cant 1:20; $\mu = 0.4$.

In the third case, for which the scenario of centred running is investigated, the profile geometry *S1002 / 60E2 / 1:40* is used. The results are displayed in Fig. 8.1.7.

The results show that for the profile geometry profile geometry *S1002 / 60E2 / 1:40*, a nearly elliptical contact area occurs. This contact area is located between $y_R = -11.889$ mm and $y_R = 11.889$ mm. In this area, the rail profile 60E2 has a constant curvature with the radius 200 mm. Deviations from the perfectly elliptical shape are caused by changes of the curvature of the wheel profile. Here, however, no discontinuities of the curvature occur, as it was the case

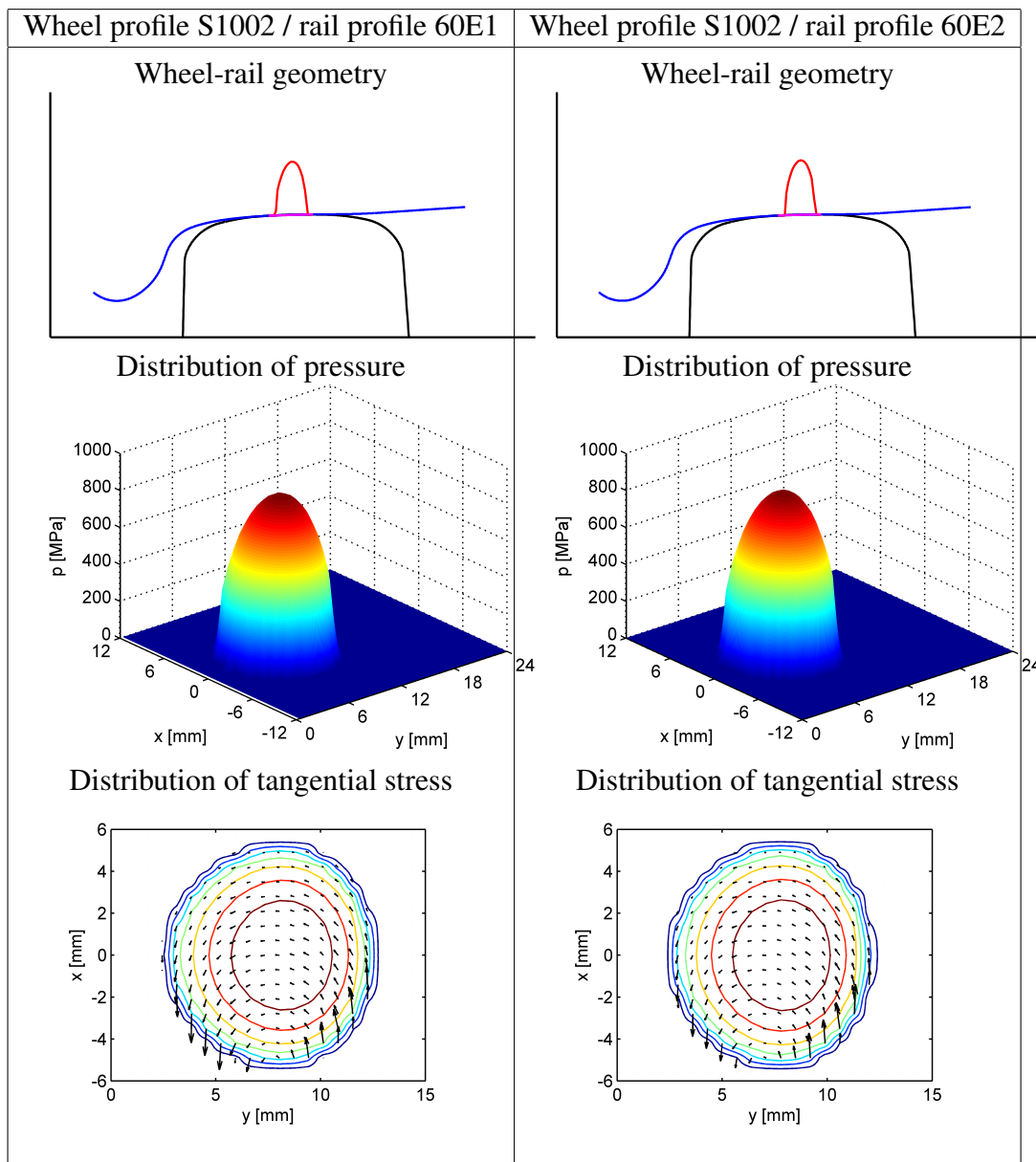


Figure 8.1.7: Influence of the structural flexibilities of wheelsets and rails on the wheel-rail geometry and on the distribution of pressure and tangential stresses for centred running; $v_0 = 200$ km/h; rail profile 60E2; cant 1:40; $\mu = 0.4$.

for the profile geometries $S1002 / 60E1 / 1:40$ and $S1002 / 60E1 / 1:20$. – The results obtained for the two model variants *RR* and *FF* hardly shows any visible differences. This indicates that for the profile geometry $S1002 / 60E2 / 1:40$ the structural flexibilities of wheelsets and rails have a very weak influence on the contact.

For the profile geometry $S1002 / 60E1 / 1:40$ the stress distribution in the contact area for the centred running is quite sensitive to changes of the kinematics caused by the structural deformations; in contrast to this, for the profile geometries $S1002 / 60E1 / 1:20$ and $S1002 / 60E2 / 1:40$ the impact of the structural flexibilities is very weak. Here, the question arises, why this sensitivity not always occurs. In order to answer this question, the results obtained for the three different profile geometries are compared directly In Fig. 8.1.8. Regarding the comparison, it should be noted that for the pressure distribution indicated by the red curve always the same scaling is used.

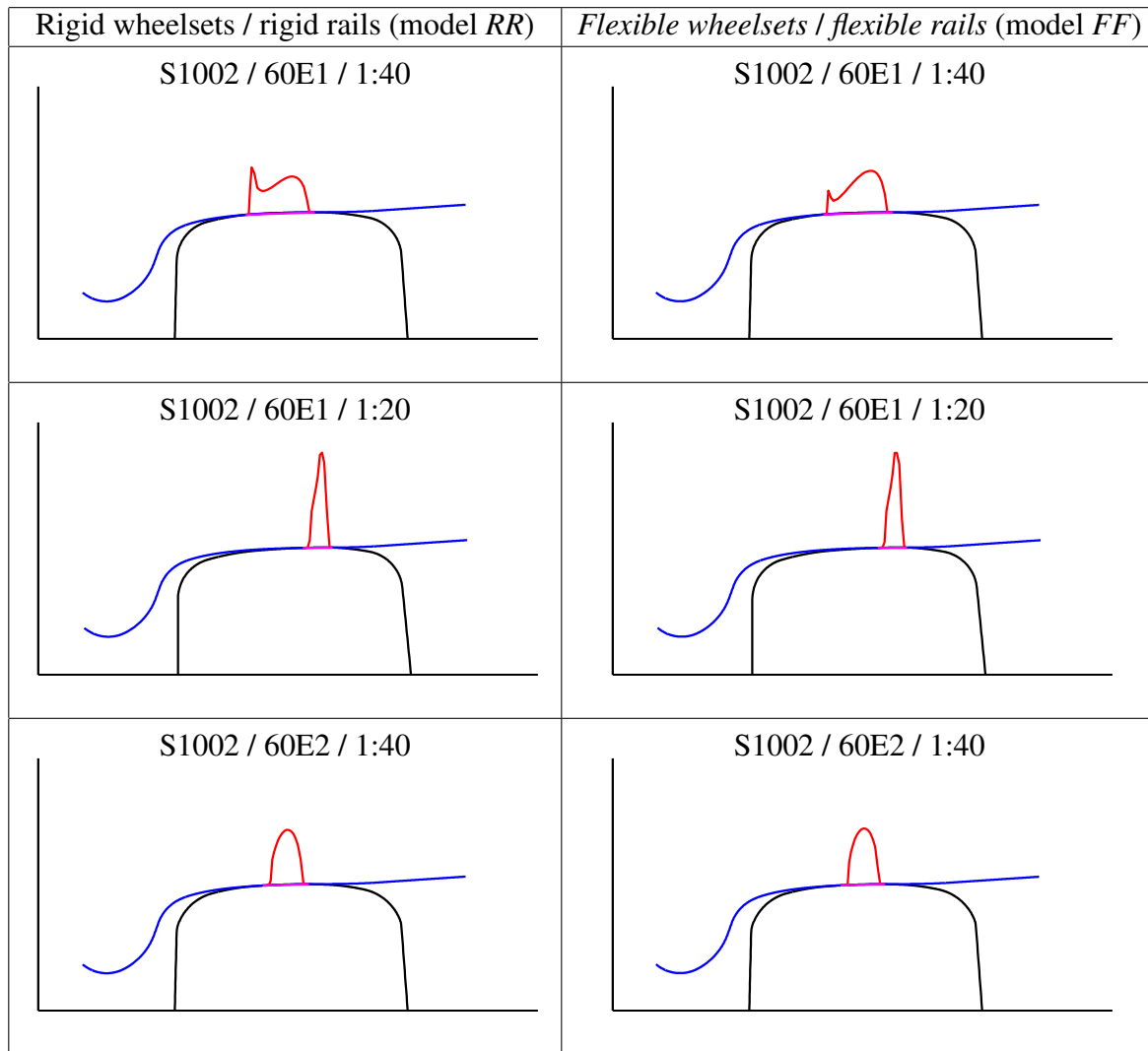


Figure 8.1.8: Influence of the structural flexibilities of wheelsets and rails on the wheel-rail geometry and on the distribution of pressure and tangential stresses for centred running; $v_0 = 200$ km/h; $\mu = 0.4$.

The comparison shows that for the profile geometry *S1002 / 60E1 / 1:40* a relatively wide contact area occurs, while for both profile geometries *S1002 / 60E1 / 1:20* and *S1002 / 60E2 / 1:40* the contact area is distinctly narrower. Apparently, for a wider contact area the pressure distribution is more sensitive to changes of the relative kinematics than for a narrower one.

As a result from the investigation of the centred running it can be concluded:

1. Structural deformations of wheelset and rail can have an impact on the pressure distribution in the contact.
2. The flexibility of the wheelset has a far stronger impact than the one of the rail.
3. If the contact area is wider, which depends on the profile geometry, the impact of the structural flexibilities on the pressure distribution is stronger.

8.2 Hunting behaviour

The hunting is a characteristic motion of a railway vehicle. As discussed in section 2.2.1 the hunting motion is inherent in the traditional guiding mechanism of the railway vehicle, which uses wheelsets. In the section 2.2.1 it has been described that a permanent hunting occurs if the vehicle is running faster than the nonlinear critical speed $v_{\text{crit,nonlin}}$. Usually, this motion should be avoided, since the lateral wheel-rail forces can cause severe damages to the track. In real life, a railway vehicle is excited by irregularities of the track. Therefore, it is difficult to decide, whether vibrations of the vehicle really result from a limit cycle oscillation or whether they are excited by irregularities. Therefore, the running stability is evaluated according to EN 14363. Here, the root mean square (*rms*) value ΣY_{rms} of the guidance forces ΣY of one wheelset is evaluated for a distance of $\Delta s = 100$ m:

$$\Sigma Y_{\text{rms}} = \sqrt{\frac{1}{\Delta s} \int_{s_0}^{s_0+\Delta s} (\Sigma Y)^2 ds} \quad (8.2.1)$$

Since the value ΣY_{rms} is calculated by integrating the square $(\Sigma Y)^2$, it cannot be negative. The standard EN 14363 defines a limit for the lateral forces, which is also known as Prud'homme's limit:

$$\Sigma Y_{\text{max,lim}} = k_1 \left(10 \text{ kN} + \frac{2Q_0}{3} \right) \quad (8.2.2)$$

The factor k_1 is set $k_1 = 1.0$ for locomotives, multiple units, and passenger coaches and $k_1 = 0.85$ for freight cars. Therefore, the value $k_1 = 1.0$ is chosen in the present case. The static wheel load is indicated by Q_0 ; thereby, $2Q_0$ is the static axle load. For vehicles equipped with bogies the criterion for running stability is given by

$$\Sigma Y_{\text{rms,lim}} = \frac{\Sigma Y_{\text{max,lim}}}{2} \quad (8.2.3)$$

In the present case, the static axle load $2Q_0$ is calculated by:

$$2Q_0 = \left[m_{\text{ws}} + 2m_{\text{WB}} + \frac{1}{2}m_{\text{Bf}} + \frac{1}{4}m_{\text{Cb}} \right] g \quad (8.2.4)$$

Here, m_{ws} , m_{WB} , m_{Bf} , and m_{Cb} denote the mass of one wheelset, the mass of one wheelset bearing, the mass of one bogie frame, and the mass of the carbody, respectively. Using the values by Diepen [11] results in a static axle load of $2Q_0 = 100$ kN. Thereby, the limit for the rms value ΣY_{rms} of the lateral forces is:

$$\Sigma Y_{\text{rms,lim}} = \frac{\Sigma Y_{\text{max,lim}}}{2} = \frac{1}{2}k_1 \left(10 \text{ kN} + \frac{2Q_0}{3} \right) = 21.667 \text{ kN} \quad (8.2.5)$$

Furthermore, as already mentioned, it is highly important to avoid damages to the track. Here, the track shift criterion is applied, which is based on a sliding mean value of the guidance forces ΣY over a length of $\Delta s = 2$ m:

$$\Sigma Y_{2\text{m}} = \frac{1}{\Delta s} \int_{s_0}^{s_0+\Delta s} \Sigma Y ds \quad (8.2.6)$$

It should be noted that the resulting force ΣY can change its sign depending on the direction, in which the current lateral wheel-rail forces act. Therefore, in contrast to the root mean square value

ΣY_{rms} the sliding mean value ΣY_{2m} can be negative so that for the evaluation its absolute value will be used. To avoid damage to the track, the absolute value $|\Sigma Y_{2m}|$ must not exceed the limit $\Sigma Y_{\text{max,lim}}$. Using the limit calculated above, the track shift criterion is given in the present case by:

$$|\Sigma Y_{2m}| \leq \Sigma Y_{\text{max,lim}} = k_1 \left(10 \text{ kN} + \frac{2Q_0}{3} \right) = 43.333 \text{ kN} \quad (8.2.7)$$

Since the absolute value $|\Sigma Y_{2m}|$ must not exceed the force limit $\Sigma Y_{\text{max,lim}}$, the maximum values $|\Sigma Y_{2m}|_{\text{max}}$ obtained from the evaluation are the relevant ones.

In the following investigations, three critical running speeds are determined:

- Nonlinear critical speed $v_{\text{crit,nonlin}}$: the lowest running speed, for which a permanent hunting occurs.
- Instability speed $v_{\text{rms,lim}}$: the running speed, at which the limit value $\Sigma Y_{\text{rms,lim}}$ is exceeded by the root mean square value ΣY_{rms} for at least one wheelset.
- Track shift speed $v_{2m,lim}$: the running speed, at which the limit value $\Sigma Y_{\text{max,lim}}$ is exceeded by the maximum absolute value $|\Sigma Y_{2m}|_{\text{max}}$ of the sliding mean value ΣY_{2m} for at least one wheelset.

For the sake of brevity, the expressions “instability speed” and “track shift limit speed” will be used.

8.2.1 Influence of the flexibilities on the hunting

To study the hunting motion, the lateral displacement y_{wsi} of the wheelset’s centre is considered. The phase portrait gives a very good impression of the vibration behaviour: For a monofrequent sinusoidal motion the resulting curve of the phase portrait is an ellipse. Therefore, the more the curve’s shape deviates from an ellipse, the stronger the influence of higher frequent parts is.

The following results were calculated for the profile geometry *S1002 / 60E1 / 1:40*; for this profile geometry, a comparatively high conicity occurs. The friction coefficient was set to $\mu = 0.4$.

In Figure 8.2.9 the phase portraits for the lateral motion y_{ws1} of the front wheelset of the front bogie are displayed for the four model variants *RR*, *FR*, *RF*, and *FF*. The diagrams contain only curves describing a permanent oscillation; if the motion decreases and dies out over time, the resulting curve is not displayed. With growing running speed v_0 the curves become larger; this can be explained qualitatively on the base of Klingel’s equation: In section 2.2.1, it has been shown that the lateral acceleration \ddot{y}_{ws} grows with the square of the running speed v_0^2 .

$$y_{\text{ws}} = \hat{y}_{\text{ws}} \sin \left(\frac{2\pi}{\lambda} x + \beta \right), \quad x = x = v_0 t \Rightarrow \ddot{y}_{\text{ws}} = - \left(\frac{2\pi}{\lambda} v_0 \right)^2 \hat{y}_{\text{ws}} \sin \left(\frac{2\pi}{\lambda} v_0 t + \beta \right) \quad (8.2.8)$$

As a result, also the lateral forces guiding the wheelset increase with growing running speed. Since the magnitude of the curves grows with increasing running speed, colours are only used for the curves obtained for $v_0 = 250$ km/h (blue), $v_0 = 300$ km/h (green), $v_0 = 350$ km/h (yellow), and $v_0 = 400$ km/h (red) for the sake of a better overview.

For the model *RR* the lateral motions are the smallest. The curves show distinct sharp bends or “kinks” at $y_{\text{ws1}} \approx \pm 6.5$ mm. These sharp bends result from the flange contact: When the flange

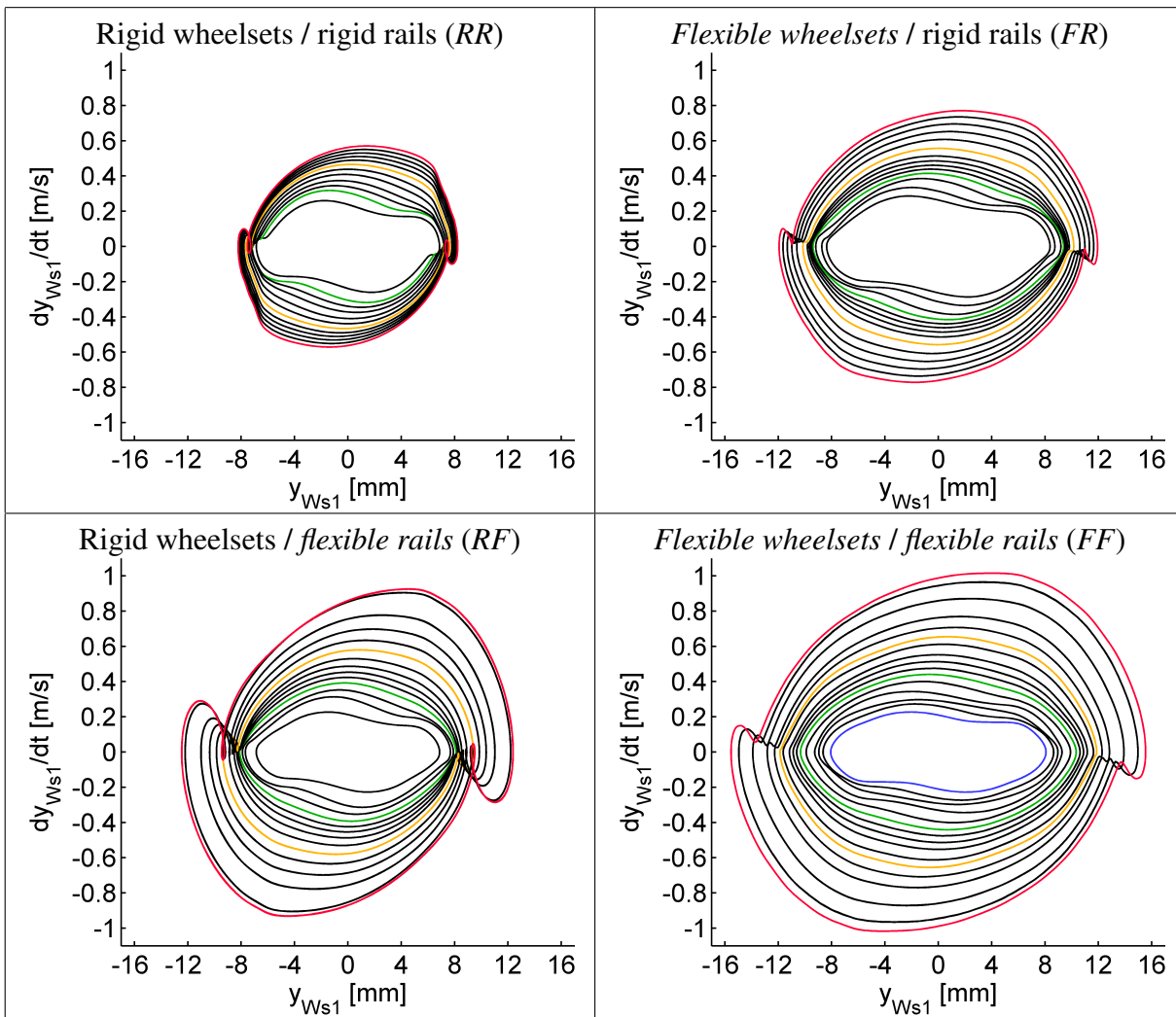


Figure 8.2.9: Lateral motion y_{ws1} for the front wheelset of the front bogie for different model variants. Wheel profile S1002; rail profile 60E1; cant 1:40; $\mu = 0.4$.

touches the rail's corner, a very high lateral force occurs. This force decelerates the wheelset leading to a strong drop of the lateral velocity \dot{y}_{ws1} . The maximum lateral displacement $y_{ws1,max}$ increases only slightly with growing running speed v_0 , since the rigid rails are limiting the lateral displacement relatively strictly, after the lateral clearance between the wheel flange and the railhead has been exhausted. In the track model "rigid rails" the track below each wheelset is modelled by a single rigid track body having a comparatively high inertia; therefore, the track body performs only comparatively small lateral motions. Since for $v_0 < 290$ km/h no permanent hunting motions occur, no curves for this range of the running speed are contained in this diagram.

In the model *FR* the structural flexibility of the wheelsets is taken into account. For this model the curves show larger lateral displacements. Furthermore the curves are smoother: While the "kinks" are still visible for the innermost curve referring to $v_0 = 270$ km/h, they become weaker with increasing running speed and finally vanish nearly completely. This can be explained in the following way: As already mentioned for the model *RR*, large lateral forces occur when the root and the flange of the wheel touch the rail's corner. These forces cause a lateral deformation of the wheelset; thereby, the lateral displacement of the wheelset's centre becomes larger. As it was derived from Klingel's equation in (8.2.8), the wheelset's lateral acceleration \ddot{y}_{ws} grows with increasing running speed v_0 . Thereby, also the lateral forces guiding the wheelset grow with the

running speed. If the lateral forces become larger, also larger deformations of the wheelsets and thereby also a larger lateral displacement of the wheelset's centre can be expected. In fact, the diagram shows that the maximum displacement increases stronger with growing running speed; this will be discussed later. Furthermore, the wheelset is softer than the comparatively stiff wheel-rail contact. Thereby, the impact of the wheel flange hitting the railhead is cushioned by the structural flexibility of the wheelset; as a result, the "kinks" due to the flange contact observed in the diagram for the model *RR* is smoothened. For the model *FR* permanent oscillations occur also at $v_0 = 270$ km/h and $v_0 = 280$ km/h; this indicates that the critical speed $v_{\text{crit,nonlin}}$ is lower when the structural flexibility of the wheelsets is taken into account.

A similar effect can be seen for the model *RF*, which takes the flexibility of the rails into account. Also here, the maximum lateral displacement increases and the "kinks" due to the flange contact vanish. Due to their structural flexibility the rails are also softer than the wheel-rail contact. Furthermore, the rails are connected to the sleepers by the pads and the mass of the rails is lower than the mass of the rigid body used in the "rigid rail" model. Thereby, also lateral deformations caused by the lateral wheel-rail forces occur; furthermore, the impact due to the flange contact is cushioned. Also here, permanent hunting motions occur already at $v_0 = 270$ km/h, i.e. also here the nonlinear critical speed $v_{\text{crit,nonlin}}$ is reduced by the structural flexibilities. However, a comparison of the diagrams for the models *RF* and *FR* shows that the amplitudes obtained for the model *RF* are slightly lower than those obtained for the model *FR*. Apparently, the structural flexibility of the wheelsets has a stronger influence on the running behaviour than the one of the rails. Nevertheless, the influence of the rail's structural flexibility is not negligible.

The results obtained for the model *FF* show the largest lateral motions of the wheelset. Here, the lateral deformations of the wheelsets and the rails are added; this explains the large lateral displacements of the wheelset's centre. A permanent hunting motion occurs already for $v_0 = 250$ km/h; compared to the results obtained with the model *FR* this indicates that taking the flexibility of the rails into account leads to a further reduction of the nonlinear critical speed $v_{\text{crit,nonlin}}$.

The phase portraits for the lateral motion $y_{\text{ws}2}$ of the rear wheelset of the front bogie are displayed in figure 8.2.10. For the rear wheelset the "kink" due to the flange contact is less distinct than for the front wheelset; nevertheless it appears at $y_{\text{ws}2} \approx \pm 6.5$ mm for the model *RR*. The increase of the amplitudes due to the deformations can be observed also here: The smallest amplitudes occur for the model *RR*; the amplitudes obtained for the model *FR* are slightly higher than those obtained for the model *RF*; the largest amplitudes occur for the model *FF*.

The impact of the structural flexibilities on the contact itself is illustrated by Figure 8.2.11. In this figure the pressure distribution on the rail head is displayed for the left contact of wheelset 1; thereby, the "trace" of the wheel-rail contact is visible. The results were calculated for the models *RR* and *FF* using the running speeds $v_0 = 260$ km/h, $v_0 = 300$ km/h, $v_0 = 340$ km/h, and $v_0 = 380$ km/h. As mentioned before, no permanent hunting is obtained for the model variant *RR* at $v_0 = 260$ km/h; thus, the figure for this combination is missing.

It can clearly be seen that for low running speeds the wheel-rail contact moves between the rail head and the rail corner. At $v_0 = 380$ km/h for the model *FF* a flange contact is visible: the contact zone at the rail corner shows a distinct intermission.

A good overview on the system's behaviour is obtained from a bifurcation diagram. In the case investigated here the maximum lateral displacement of the wheelset depending on the running speed is considered. The results, which are presented in the following, are obtained from the calculations using the four aforementioned modelling variants *RR*, *FR*, *RF* and *FF*. A further modelling variant uses the track model including flexible rails, but for the wheelset only eigenmodes for $k = 0$ and

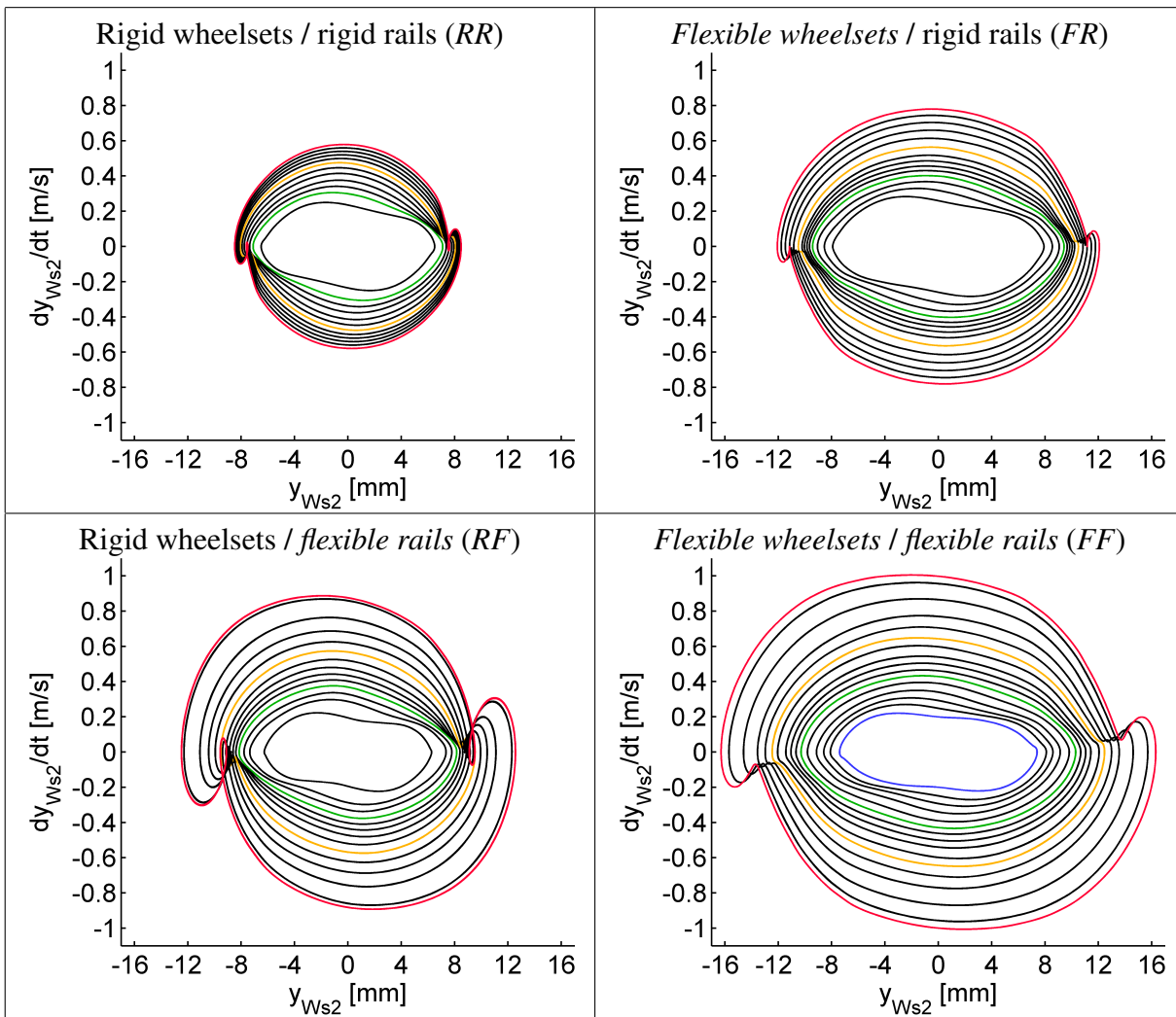


Figure 8.2.10: Lateral motion y_{ws2} for the rear wheelset of the front bogie for different model variants. Wheel profile S1002; rail profile 60E1; cant 1:40; $\mu = 0.4$.

$k = 1$ are taken into account. Eigenmodes for $k = 0$ are rotational symmetric and include torsional and umbrella modes, while eigenmodes for $k = 1$ include bending modes. For $k \geq 2$ the deformations are limited to the wheels; these modes are neglected in this modelling configuration. This variant will be referenced by fF .

In Figure 8.2.12 the maximum lateral displacement of the wheelsets 1 and 2, respectively, versus the running speed is shown for the described different model variants. Figure 8.2.13 displays the hunting frequency for the different model variants. The nonlinear critical speed $v_{crit,nonlin}$, as introduced in section 8.2, for the different model variants are listed in Table 8.2.1.

	$v_{crit,nonlin}$	$\Delta v_{crit,nonlin}$
Rigid wheelsets, rigid rails (<i>RR</i>), reference	289 km/h	
Flexible wheelsets, rigid rails (<i>FR</i>)	264 km/h	25 km/h
Rigid wheelsets, flexible rails (<i>RF</i>)	269 km/h	20 km/h
Flexible wheelsets, flexible rails (<i>FF</i>)	250 km/h	39 km/h

Table 8.2.1: Critical running speeds for different model variants; wheel profile S1002; rail profile 60E1; cant 1:40; $\mu = 0.4$.

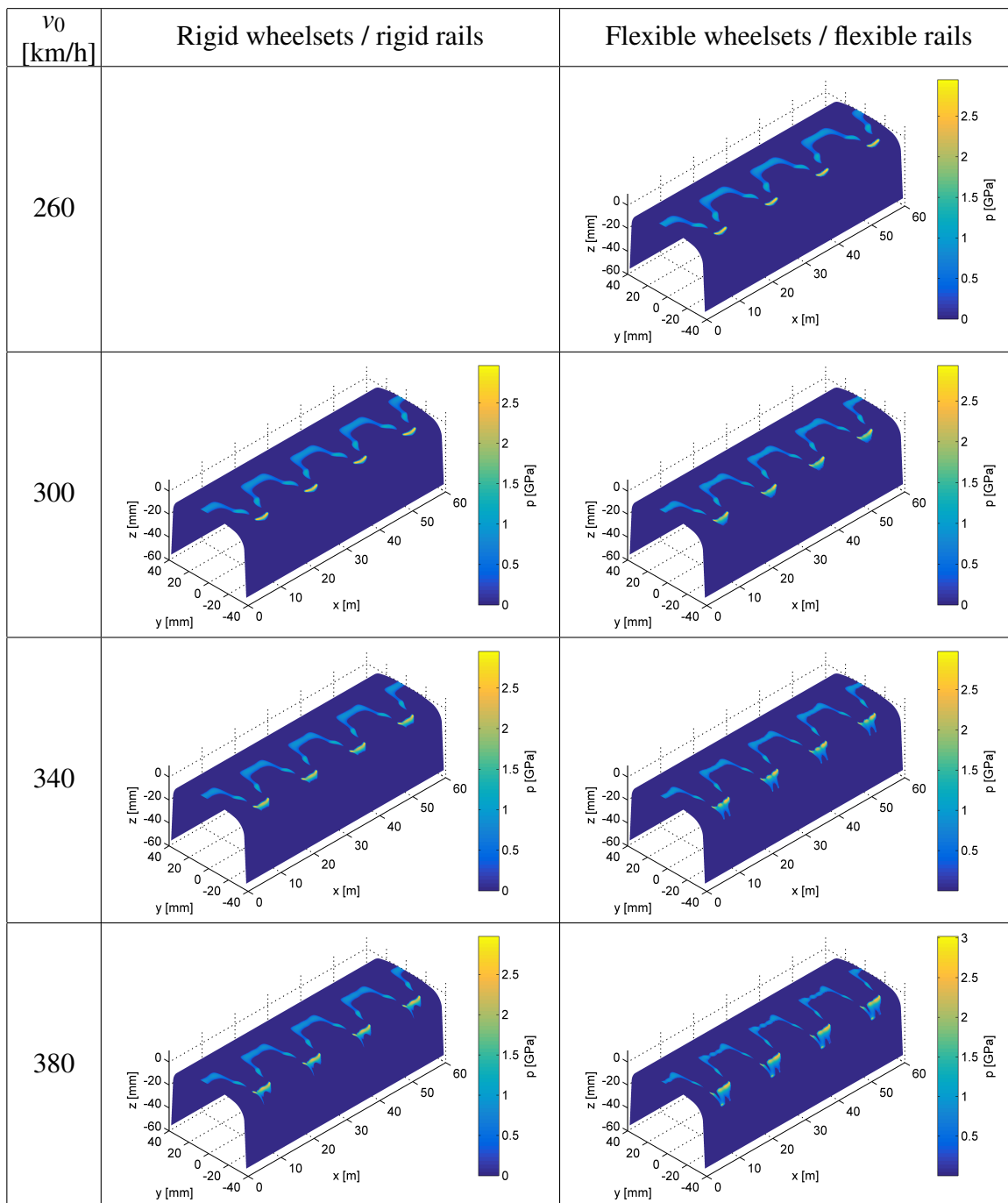


Figure 8.2.11: Pressure distribution on the rail head for the left contact of wheelset 1. Wheel profile S1002; rail profile 60E1; cant 1:40; $\mu = 0.4$.

Generally, the diagrams show that the lateral amplitudes and the frequency increase with the running speed v_0 . The frequency is located in the range between 4.5 Hz and 8 Hz. For the curves it can be concluded:

- Model *RR* (black curves): The permanent hunting starts at $v_0 = 289$ km/h; since this modelling is a widely used standard, the resulting critical speed will be considered as the reference value. The maximum lateral amplitudes of the wheelsets at the beginning of the hunting are $y_{Ws1,max} = 6.9$ mm and $y_{Ws2,max} = 6.9$ mm. The gradient of the curve is comparatively low, i.e. the lateral motions increase only slightly with growing speed.

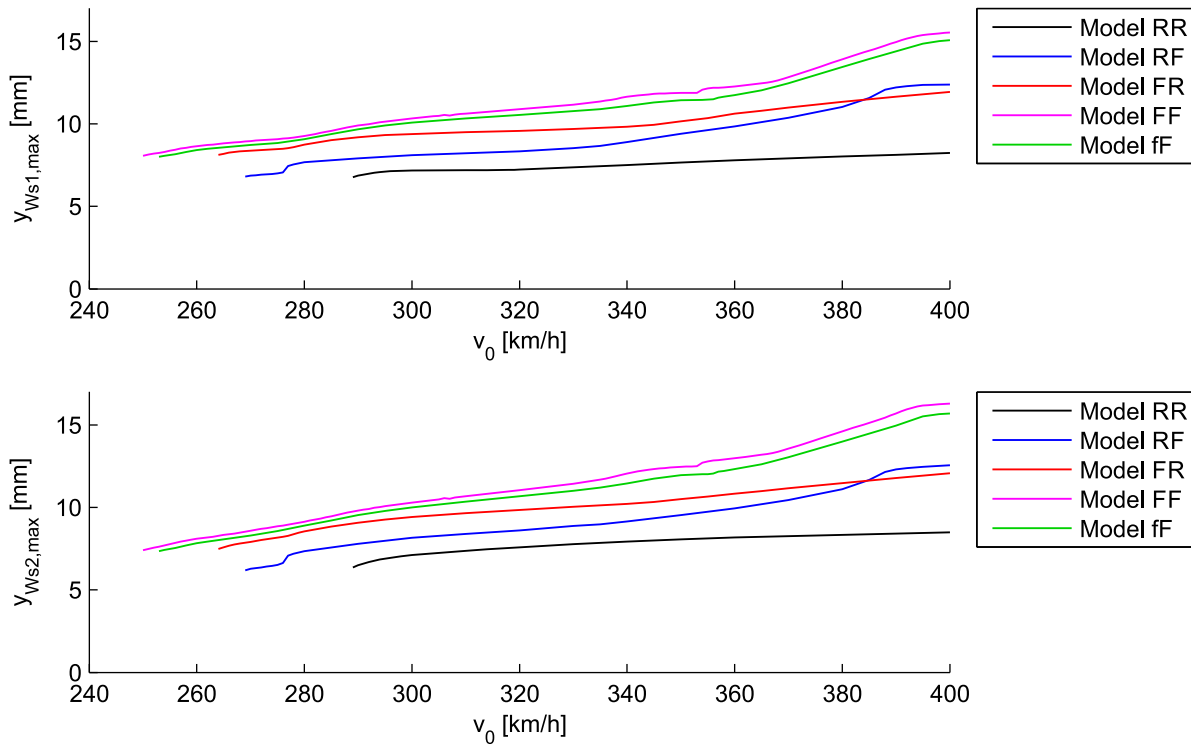


Figure 8.2.12: Maximum lateral displacement for the wheelsets of the front bogie for different model variants; above: front wheelset $y_{ws1,max}$; below: rear wheelset $y_{ws2,max}$; wheel profile S1002; rail profile 60E1; cant 1:40; $\mu = 0.4$.

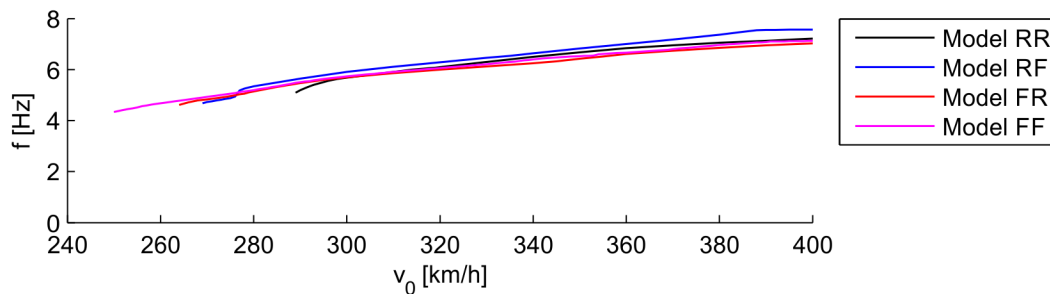


Figure 8.2.13: Hunting frequency for different model variants; wheel profile S1002; rail profile 60E1; cant 1:40; $\mu = 0.4$.

- Model *RF* (blue curves): The permanent hunting starts at $v_0 = 269$ km/h; this indicates that the flexibility of the rails causes a drop of the nonlinear critical speed of 20 km/h. The curves start with an amplitude of $y_{ws1,max} = 6.9$ mm and $y_{ws2,max} = 6.9$ mm, i.e. nearly the same values than for the model *RR*. However, between $v_0 = 276$ km/h and $v_0 = 278$ km/h a sharp increase of the amplitudes occurs. Similar to the curves for the model *FR* also these curves show a larger lateral displacement and a higher gradient than those for the configuration *RR*. This can also be explained by the lateral forces, which increase with the running speed and thereby lead a higher lateral displacement. However, for the configuration *RF* the increase of the amplitudes is lower than for the configuration *FR*: The values for $y_{ws1,max}$ and $y_{ws2,max}$ are only about 1 mm up to 2.5 mm higher than for the standard configuration *RR*. Also the critical speed drops only by 16 km/h down to $v_{crit,nonlin} = 276$ km/h. The hunting frequency increases slightly compared to the standard configuration. In total, the structural flexibility of the rails has a weaker influence than the one of the wheelsets. Nevertheless, the influence

is visible.

- Model *FR* (red curves): For the model *FR*, the curves already start at $v_{\text{crit,nonlin}} = 268$ km/h, which indicates that the structural dynamics of the wheelsets causes a drop of the critical speed $v_{\text{crit,nonlin}}$ of 24 km/h. The amplitudes are about 3 mm up to 4 mm higher than those for the model *RR*; furthermore, the curves show a higher gradient of the amplitude; this can be explained in the following way: With growing running speed the frequency of the hunting increases, as the diagram in Figure 8.2.13 confirms. This also means an increase of the lateral acceleration leading to higher lateral wheel-rail forces. The higher lateral forces cause larger deformations of the flexible wheelset and thereby a larger lateral displacement of the wheelset's centre, where the lateral displacement y_{Ws} is observed.
- Model *FF* (magenta curves): For this model variant the curves show the largest lateral displacements and the highest gradient. Regarding the motion of the wheelset's centre the structural flexibilities of the wheelsets and of the rails can be considered as two springs arranged serially; this means that the deformations of both springs are added and that the resulting stiffness is lower than the one of the softest spring.
- Model *fF* (green curves): The results obtained for this model differ little from those obtained for the model *FF*: The amplitudes for the model *FF* are approximately 0.5 mm higher; the critical speed is 4 km/h lower. This indicates that the bending, umbrella and torsional modes of the wheelset have a dominant influence, while the influence of the modes for $k \geq 2$, which describe deformations of the wheels only, is distinctly weaker.

Furthermore, the resulting lateral forces are evaluated according to the standard EN 14363. In Figure 8.2.14 the root mean square values ΣY_{rms} of the resulting lateral forces, which are calculated according to equation (8.2.1), versus the running speed v_0 are displayed.

For all four model variants, the forces at the wheelsets 1 and 3, which are the leading wheelsets, hardly differ from each other; also for the wheelsets 2 and 4, which are the trailing wheelsets, nearly the same values are obtained. Generally, the forces at the trailing wheelsets 2 and 4 are higher than those at the leading wheelsets 1 and 3.

For the evaluation with respect to the instability criterion, the maximum value $\Sigma Y_{\text{rms,max}}(v_0)$ at the running speed v_0 is relevant. If $\Sigma Y_{\text{rms},i}(v_0)$ is the value at the i -th wheelset, then the value $\Sigma Y_{\text{rms,max}}(v_0)$ is defined by:

$$\Sigma Y_{\text{rms,max}}(v_0) = \max_i (\Sigma Y_{\text{rms},i}(v_0)), \quad i = 1, 2, 3, 4 \quad (8.2.9)$$

In Figure 8.2.15 the maximum values $\Sigma Y_{\text{rms,max}}(v_0)$ versus the running speed v_0 , which are obtained for the four model variants, are shown. The running speeds $v_{\text{lim,rms}}$, at which the limit $\Sigma_{\text{rms,lim}}$ is reached, are listed in Table 8.2.2; furthermore, in this table, the limit speed $v_{\text{lim,rms}}$ is compared to the nonlinear critical speed $v_{\text{crit,nonlin}}$ for each model.

The diagrams shown in Figure 8.2.15 and the values listed in Table 8.2.2 show that for the models *RR*, *FR*, and *RF* the limit value of $\Sigma Y_{\text{rms,lim}} = 25$ kN is exceeded very soon after the permanent hunting has started, i.e. the difference between the critical speed $v_{\text{crit,nonlin}}$ and the limit speed $v_{\text{lim,rms}}$ is comparatively small: 3 km/h for the model *FF* and 4 km/h for the models *RR* and *RF*. Only the model *FF* shows a higher difference of 11 km/h between the nonlinear critical speed and the limit speed according to the instability criterion. It should be pointed out that the difference between the limit speeds $v_{\text{lim,rms}}$ obtained for the two configurations using flexible wheelsets is quite

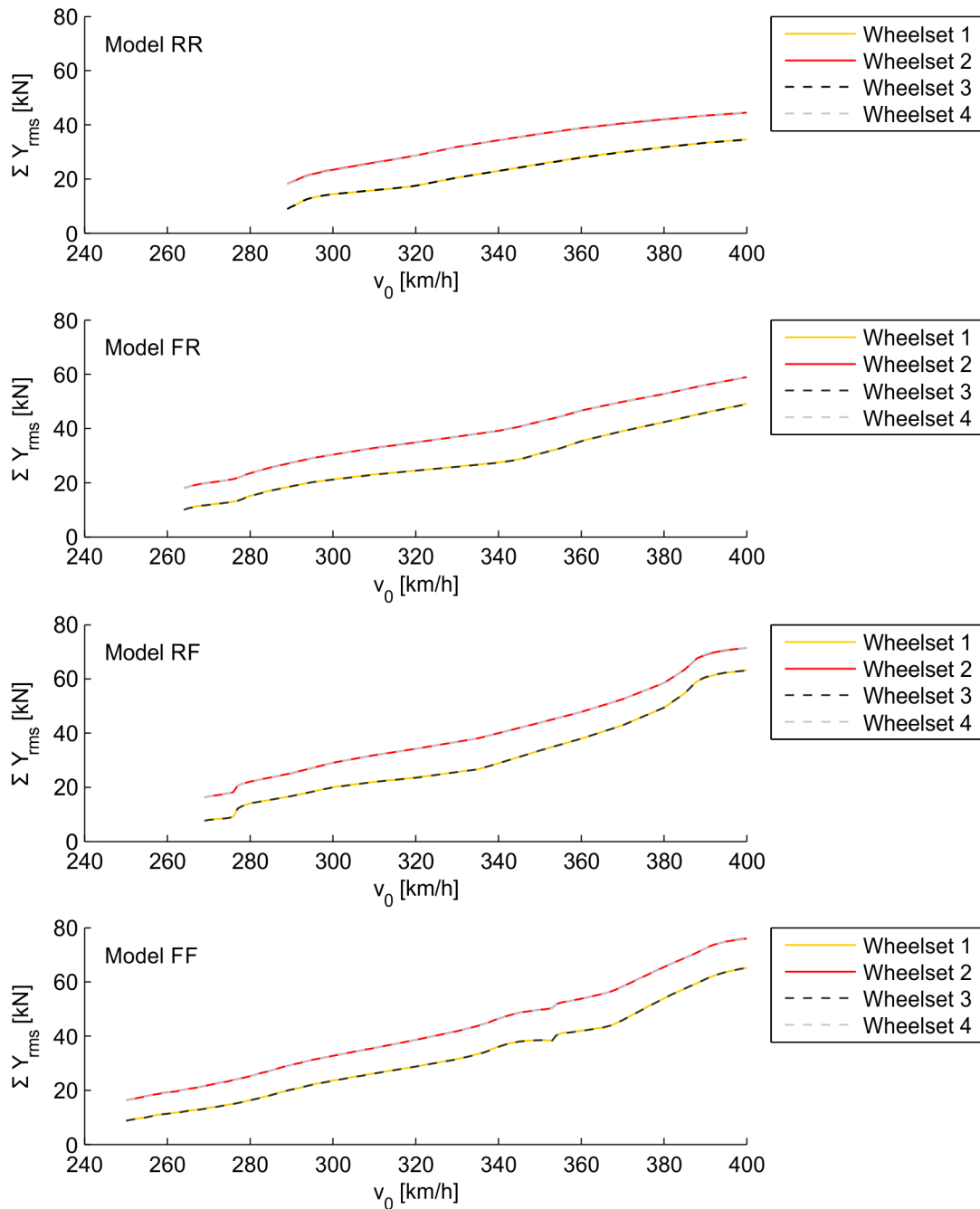


Figure 8.2.14: Root mean square values ΣY_{rms} of the resulting lateral forces for different model variants; wheel profile S1002; rail profile 60E1; cant 1:40; $\mu = 0.4$.

	$v_{lim,rms}$	$\Delta v_{lim,rms}$	$v_{crit,nonlin}$	$v_{lim,rms} - v_{crit,nonlin}$
Model RR, reference	295 km/h		289 km/h	6 km/h
Model FR	275 km/h	20 km/h	264 km/h	9 km/h
Model RF	279 km/h	16 km/h	269 km/h	10 km/h
Model FF	269 km/h	26 km/h	250 km/h	19 km/h

Table 8.2.2: Limit speeds according to the instability criterion (EN 14363) for the different model variants; wheel profile S1002; rail profile 60E1; cant 1:40; $\mu = 0.4$.

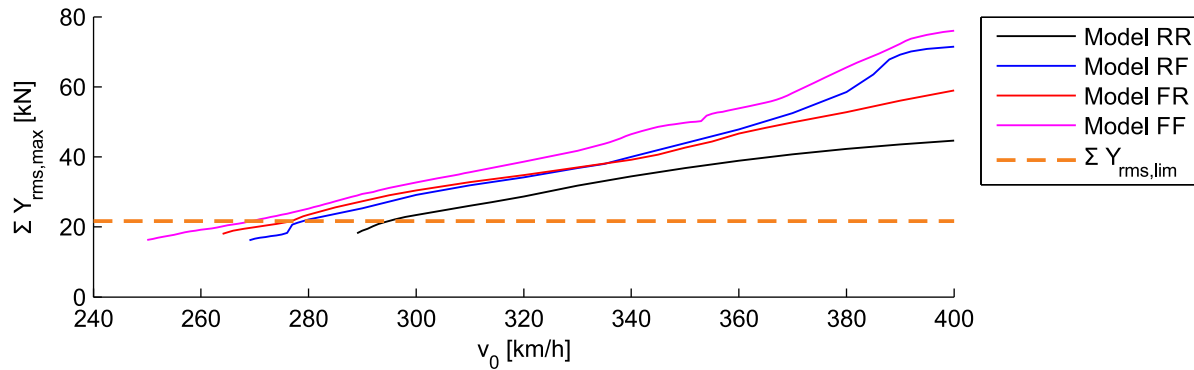


Figure 8.2.15: Maximum root mean square values $\Sigma Y_{\text{rms,max}}$ of the resulting lateral forces ΣY for different model variants; wheel profile S1002; rail profile 60E1; cant 1:40; $\mu = 0.4$.

small: The limit speeds are $v_{\text{lim,rms}} = 266$ km/h for the configuration *FF* and $v_{\text{lim,rms}} = 271$ km/h for the model *FR*. Also this underlines that the structural flexibility of the wheelset has a stronger influence on the running behaviour than the one of the rails.

In an analogous way, the values of the resulting lateral force ΣY are evaluated with respect to the track shift criterion; here, the maximum absolute sliding mean value $|\Sigma Y_{2m}|_{\text{max}}$. In Figure 8.2.16, the maximum absolute sliding mean value $|\Sigma Y_{2m}|_{\text{max}}$ for the four models *RR*, *FR*, *RF* and *FF* are shown as functions of the running speed v_0 and compared to the force limit $\Sigma Y_{\text{max,lim}}$; the values for the speed $v_{\text{lim},2m}$, at which the force limit is exceeded

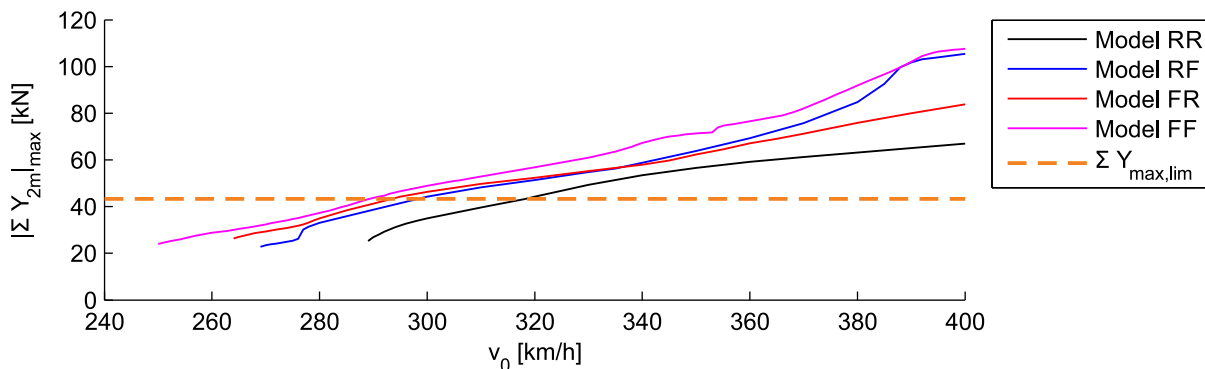


Figure 8.2.16: Maximum absolute sliding mean values $|\Sigma Y_{\text{rms}}|_{\text{max}}$ of the resulting lateral forces ΣY for different model variants; wheel profile S1002; rail profile 60E1; cant 1:40; $\mu = 0.4$.

	$v_{\text{lim},2m}$	$\Delta v_{\text{lim},2m}$	$v_{\text{crit,nonlin}}$	$v_{\text{lim},2m} - v_{\text{crit,nonlin}}$
Model <i>RR</i>, reference	318 km/h		289 km/h	29 km/h
Model <i>FR</i>	293 km/h	25 km/h	264 km/h	19 km/h
Model <i>RF</i>	298 km/h	20 km/h	269 km/h	19 km/h
Model <i>FF</i>	289 km/h	29 km/h	250 km/h	39 km/h

Table 8.2.3: Limit speeds according to the track shift criterion (EN 14363) for the different model variants; wheel profile S1002; rail profile 60E1; cant 1:40; $\mu = 0.4$.

Generally it can be concluded:

- The structural flexibility of the wheelsets has a stronger influence on the running behaviour

than the one of the rails: It causes a larger increase of the lateral amplitudes and a higher drop of the nonlinear critical speed.

- The influence of the structural flexibilities on the hunting frequency is quite weak: The flexibility of the rails causes a slight increase of the frequency, while the flexibility of the wheelset leads to slightly lower frequencies.

8.2.2 Influence of the friction

The friction characteristics occurring in the wheel-rail contact are one of the most uncertain parameters for a railway vehicle. The friction depends e.g. on the roughness of the surfaces as well as on the presence of media like water or dirt. Nevertheless, the characteristics is important for the behaviour of the railway vehicle: The tangential forces, which are responsible for the vehicle's guidance, are transmitted in the wheel-rail contact by friction. As explained in 7, the actual contact area is split into a zone of adhesion and a zone of sliding, if the contact transmits tangential forces, i.e. the limit between sticking and sliding is actually reached locally. Therefore, the influence of the friction is investigated here, also to give an impression, how large the influence of this uncertain parameter is compared to the influence of the structural flexibilities.

For the model versions *RR* and *FF* the calculations were carried out using the following four values of the friction coefficient:

- $\mu = 0.40$
- $\mu = 0.35$
- $\mu = 0.30$
- $\mu = 0.25$

For the calculations the rail profile 60E1 with an inclination of 1:40 was used. In Fig.8.2.17 and Fig.8.2.18 the phase portraits for the lateral motions y_{ws1} and y_{ws2} of the two wheelsets of the front bogie are displayed. As already done in section 8.2.1, colours are only used for the curves obtained for $v_0 = 250$ km/h (blue), $v_0 = 300$ km/h (green), $v_0 = 350$ km/h (yellow), and $v_0 = 400$ km/h (red) for the sake of a better overview.

The comparison of the curves shows that the friction coefficient hardly affects the qualitative shape of the curves. Nevertheless, especially the results obtained for the flexible model *FF* show that a higher friction coefficient leads to larger lateral displacements of the wheelsets.

In Figures 8.2.19 and 8.2.20 the maximum lateral displacements of the wheelsets 1 and 2, respectively, for the different values of the friction coefficients are displayed. It should be pointed out that the limits of the vertical axis have been adapted so that the curves can be distinguished better from each other. The nonlinear critical speed $v_{crit,nonlin}$ obtained for the different model configurations and friction coefficients are listed in Table 8.2.4.

The diagram for the model *RR* shows that with higher friction coefficients the critical speed drops from $v_{crit,nonlin} = 317$ km/h for $\mu = 0.25$ down to $v_{crit,nonlin} = 292$ km/h for $\mu = 0.4$. For the model *FF*, which takes the flexibilities of the wheelsets and the rails into account, also a drop of the critical speed occurs from $v_{crit,nonlin} = 282$ km/h for $\mu = 0.25$ down to $v_{crit,nonlin} = 255$ km/h for $\mu = 0.4$. For the model *RR*, the lateral amplitudes are hardly changed. In contrast to this, the results obtained for the model *FF* show that distinctly larger amplitudes occur if the value of the friction coefficient

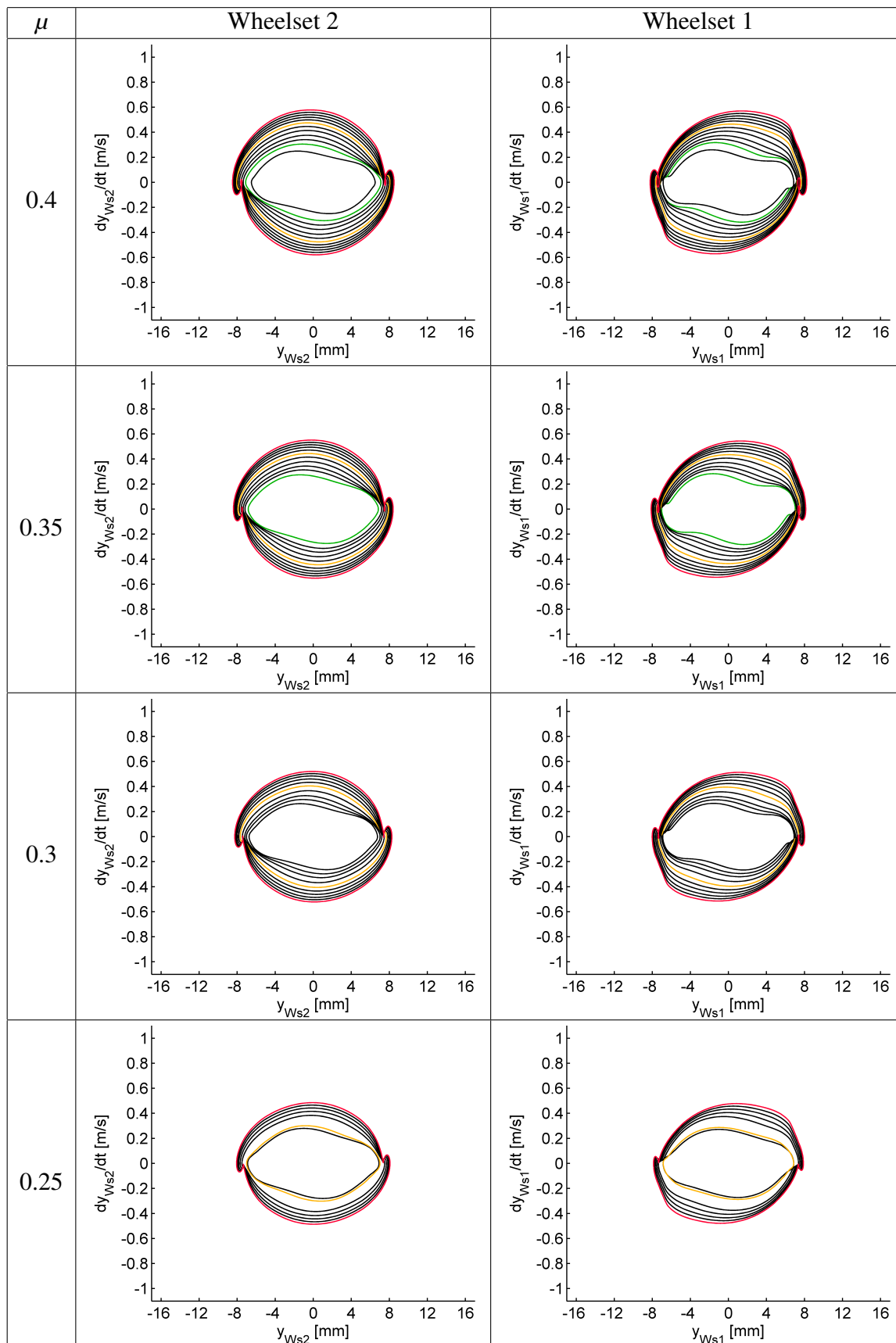


Figure 8.2.17: Phase portraits for the lateral motions of the leading bogie's wheelsets for different friction coefficients μ ; rigid wheelsets / rigid rails; rail profile 60E1; cant 1:40

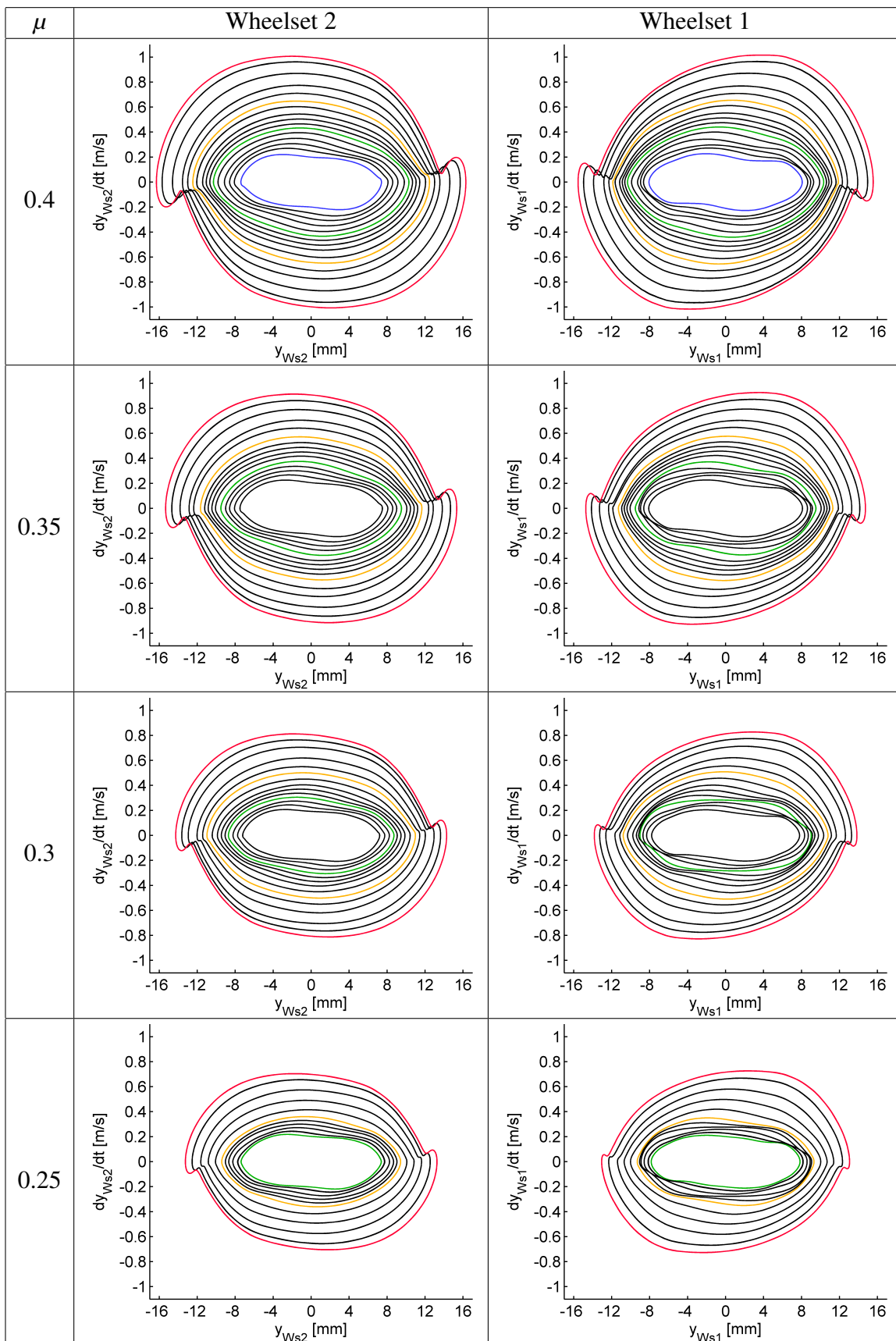


Figure 8.2.18: Phase portraits for the lateral motions of the leading bogie's wheelsets for different friction coefficients μ ; flexible wheelsets / flexible rails; rail profile 60E1; cant 1:40

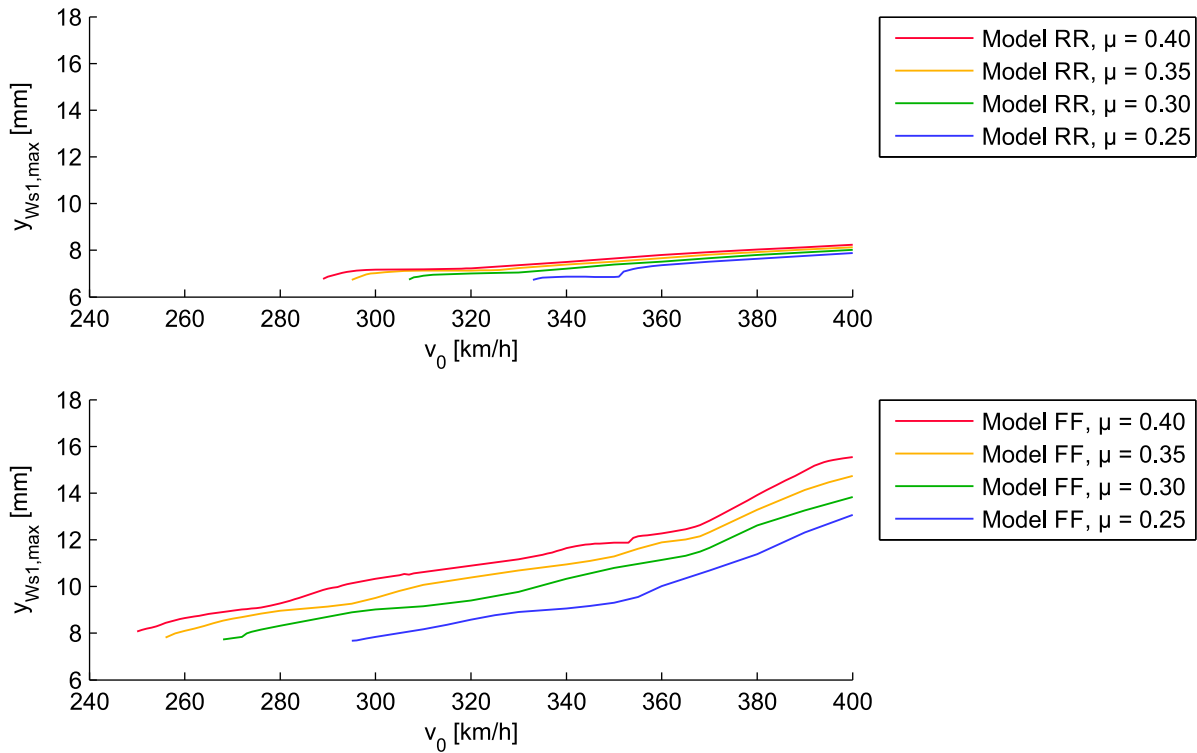


Figure 8.2.19: Maximum lateral displacement $y_{ws1,max}$ for the wheelset 1; above: model *RR*, below: model *FF*; wheel profile S1002; rail profile 60E1; cant 1:40.

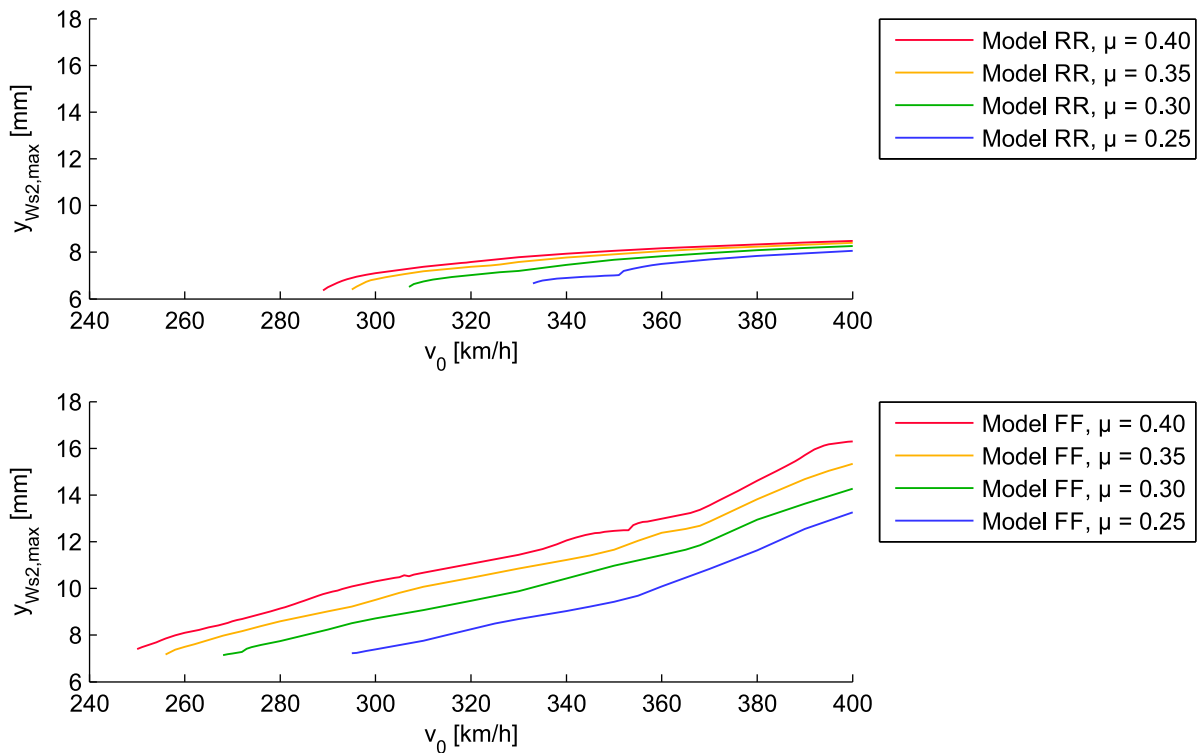


Figure 8.2.20: Maximum lateral displacement $y_{ws2,max}$ for the wheelset 2; above: model *RR*, below: model *FF*; wheel profile S1002; rail profile 60E1; cant 1:40.

is higher. Apparently, for the model taking the structural flexibilities into account the amplitudes are more sensitive to the friction coefficient than for the model using rigid wheelsets and a rigid

	$\mu = 0.25$	$\mu = 0.30$	$\mu = 0.35$	$\mu = 0.40$	$\Delta v_{\text{crit,nonlin}}$
<i>RR</i>	333 km/h	307 km/h	295 km/h	289 km/h	44 km/h
<i>FF</i>	282 km/h	268 km/h	256 km/h	250 km/h	27 km/h
$\Delta v_{\text{crit,nonlin}}$	35 km/h	39 km/h	39 km/h	39 km/h	

Table 8.2.4: Nonlinear critical speeds $v_{\text{crit,nonlin}}$ for different model versions and different values for the friction coefficient μ

track.

Table 8.2.4 shows that the variation of the friction coefficient from $\mu = 0.25$ to $\mu = 0.4$ reduces the nonlinear critical speed $v_{\text{crit,nonlin}}$ by about 25 km/h; the reduction of the critical speed is nearly the same for both model configurations. Taking the structural flexibilities into account leads to a reduction of the nonlinear critical speed $v_{\text{crit,nonlin}}$ by about 35 km/h for all investigated values of the friction coefficient. From this it can be concluded that the impact of the structural flexibilities on the nonlinear critical speed is about 30% higher than the one of varying the friction coefficient; therefore, the influence of the structural flexibilities is not negligible.

Figure 8.2.21 shows the hunting frequency versus the running speed for the two model configurations and for the four values of the friction coefficient. It can be seen that the friction coefficient

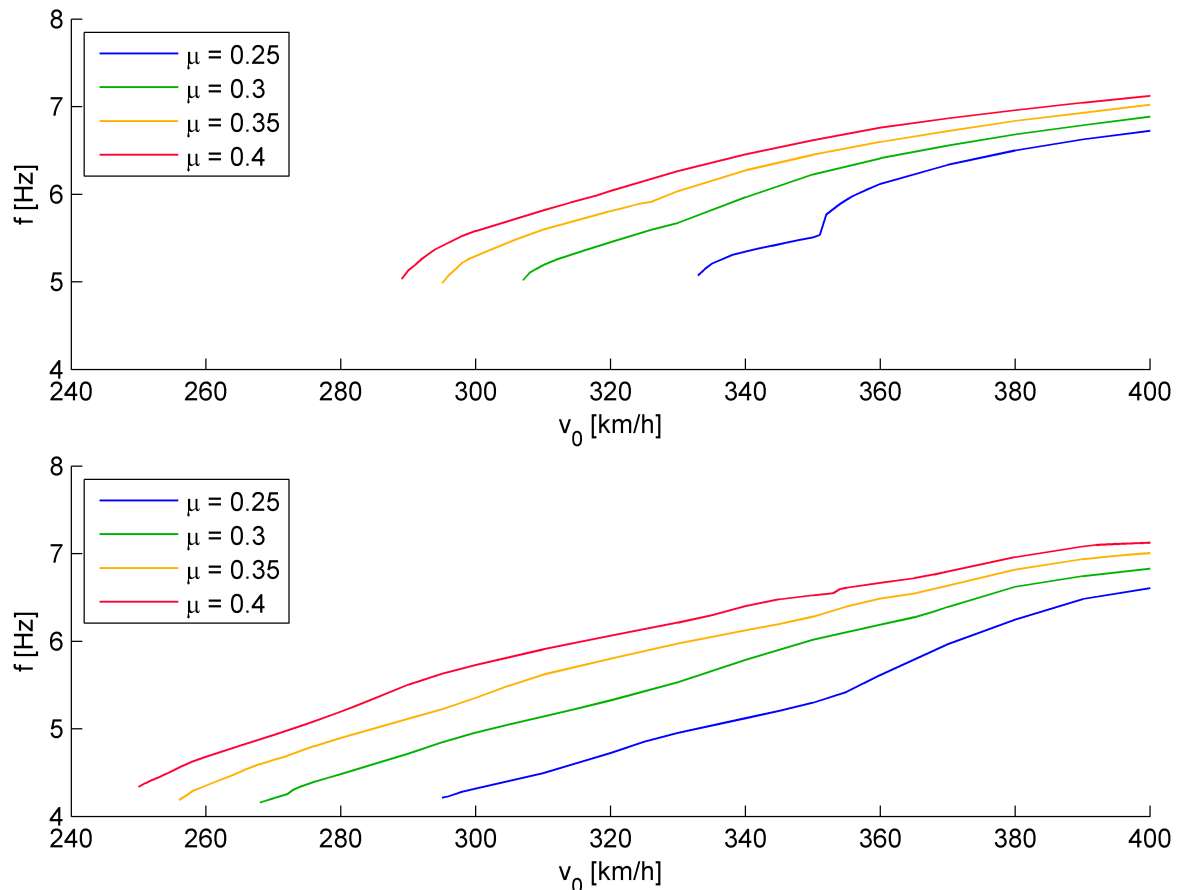


Figure 8.2.21: Hunting frequency; above: model *RR*, below: model *FF*; wheel profile S1002; rail profile 60E1; cant 1:40.

has a distinct impact on the hunting frequency for both configurations: The hunting frequency increases for higher values of the friction coefficient. This effect can be explained by the following consideration: For the hunting motion of the wheelset the tangential forces, which are transmitted

by friction, are essential, since they are guiding the wheelset; this also becomes clear from the linearized equations of motion shown in the section 2.2.1. It is obvious that a higher frequency of the motion means a higher acceleration for the same amplitude. To achieve such a higher acceleration higher forces are required. The friction coefficient μ is limiting the transmittable tangential forces. A lower friction coefficient leads to lower tangential forces and thereby to a lower frequency of the hunting oscillation.

Furthermore, the resulting lateral forces are evaluated according to the standard EN 14363. First, the root mean square value ΣY_{rms} is considered. It turns out that higher values generally occur at the trailing wheelsets, as already seen for the results discussed in section 8.2.1, higher values generally occur at the trailing wheelsets. The maximum values $\Sigma Y_{\text{rms,max}}(v_0)$ versus the running speed v_0 are displayed in Figure 8.2.22. Furthermore, the instability speeds $v_{\text{lim,rms}}$, at which the maximum value $\Sigma Y_{\text{rms,max}}$ reaches the force limit, are listed in Table 8.2.5 for the two model versions and the four values of the friction coefficient.

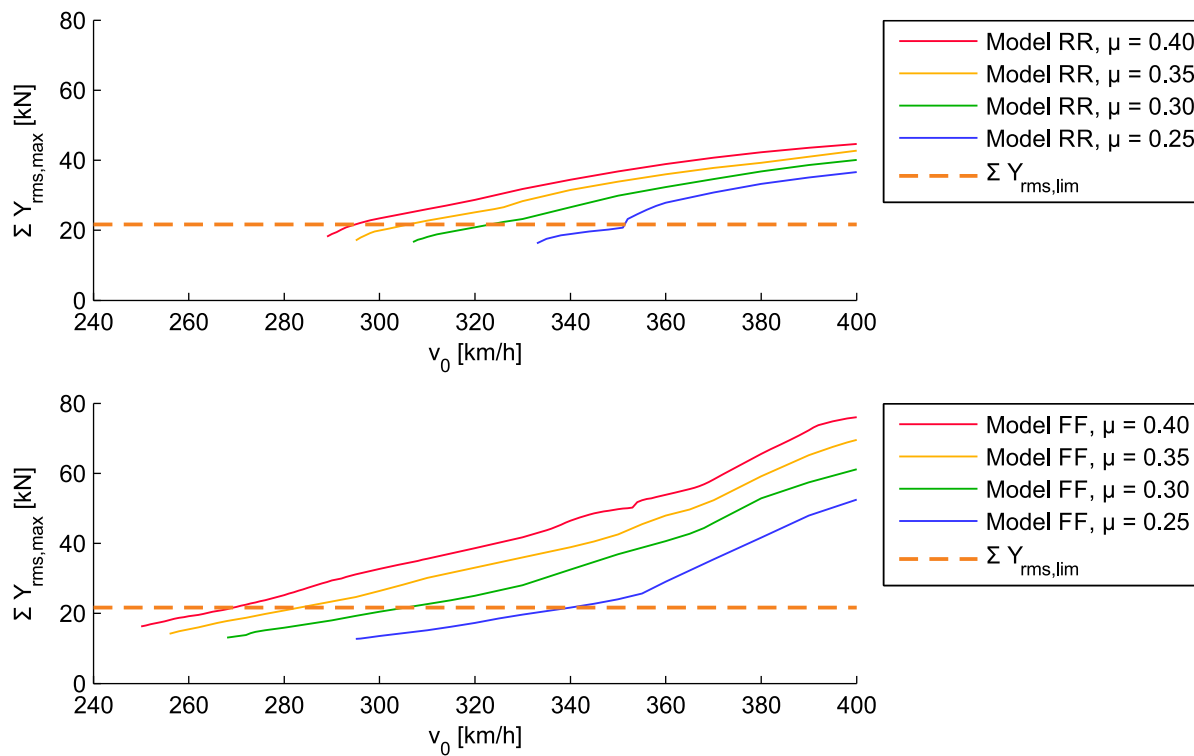


Figure 8.2.22: Maximum root mean square values $\Sigma Y_{\text{rms,max}}$ of the resulting lateral forces ΣY for the model *FF* and different friction coefficients; wheel profile S1002; rail profile 60E1; cant 1:40.

;

	$\mu = 0.25$	$\mu = 0.30$	$\mu = 0.35$	$\mu = 0.40$	$\Delta v_{\text{lim,rms}}$
<i>RR</i>	351 km/h	323 km/h	306 km/h	295 km/h	56 km/h
<i>FF</i>	340 km/h	306 km/h	283 km/h	269 km/h	71 km/h
$\Delta v_{\text{lim,rms}}$	11 km/h	17 km/h	23 km/h	26 km/h	

Table 8.2.5: Instability speeds $v_{\text{lim,rms}}$ for different model versions and different values for the friction coefficient μ

The diagrams contained in the Figures 8.2.22 show that for lower friction coefficients the curves

start at lower values of ΣY_{rms} . Thereby, the difference $\Delta v = v_{\text{lim,rms}} - v_{\text{crit,nonlin}}$ between the non-linear critical speed $v_{\text{crit,nonlin}}$, at which the permanent hunting starts, and the instability speed $v_{\text{lim,rms}}$, at which the force limit is exceeded, is larger for a lower friction coefficient μ : For $\mu = 0.4$ the difference is $\Delta v = 4$ km/h for the model *RR* and $\Delta v = 11$ km/h for the model *FF*. If the friction coefficient is reduced to $\mu = 0.25$, the differences increase to $\Delta v = 25$ km/h for the model *RR* and $\Delta v = 38$ km/h for the model *FF*.

In Figure 8.2.23 the maximum absolute values $|\Sigma Y_{2m}|_{\text{max}}$ versus the running speed v_0 are displayed. The running speeds at which the force limit is exceeded are listed in Table 8.2.6

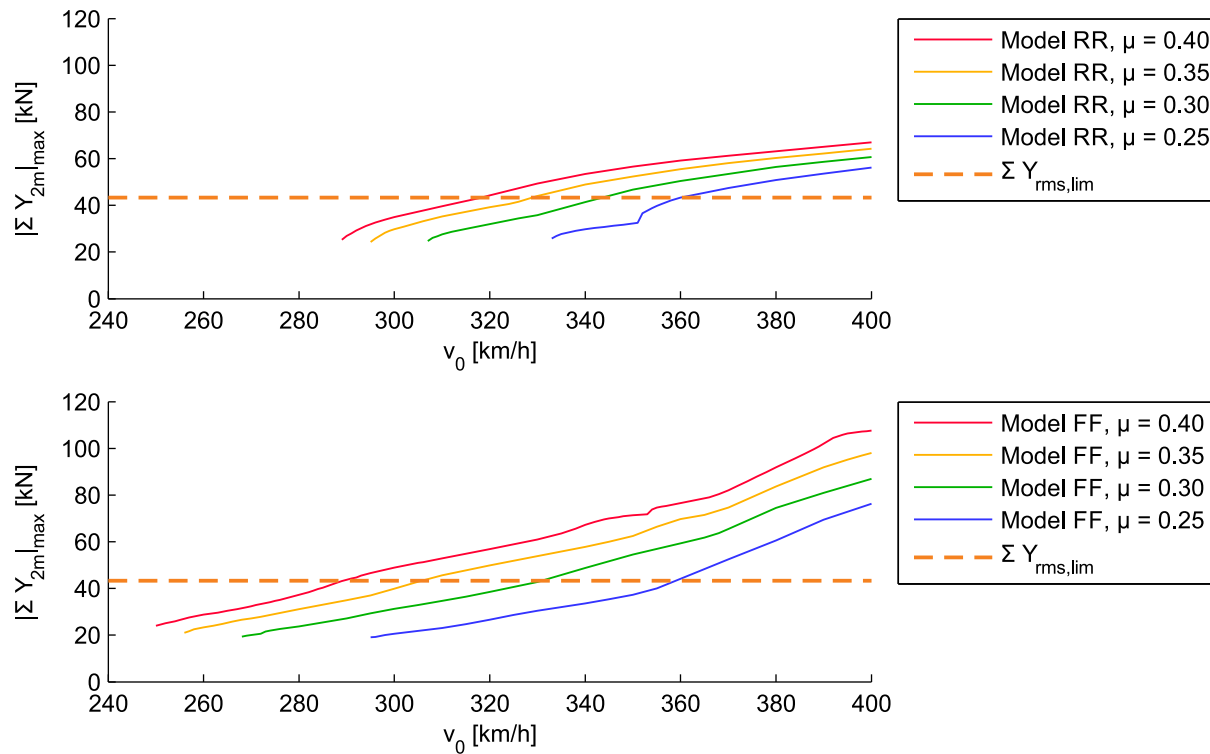


Figure 8.2.23: Maximum track shift forces $|\Sigma Y_{2m}|_{\text{max}}$ of the resulting lateral forces at the wheelset 2; above: model *FF*; below: model *RR*; wheel profile S1002; rail profile 60E1; cant 1:40.

	$\mu = 0.25$	$\mu = 0.30$	$\mu = 0.35$	$\mu = 0.40$	$\Delta v_{2m,lim}$
<i>RR</i>	360 km/h	344 km/h	329 km/h	318 km/h	42 km/h
<i>FF</i>	359 km/h	331 km/h	306 km/h	289 km/h	70 km/h
$\Delta v_{2m,lim}$	1 km/h	13 km/h	23 km/h	31 km/h	

Table 8.2.6: Track shift limit speeds $v_{2m,lim}$ for different model versions and different values for the friction coefficient μ

The results are rather similar to those obtained for ΣY_{rms} . With an increasing value of the friction coefficient μ , the difference between the nonlinear critical speed $v_{\text{crit,nonlin}}$ and the speed $v_{2m,lim}$, at which the force limit is exceeded grows; furthermore, the model *FF* is distinctly more sensitive to changes of μ than the model *RR*.

In total it can be concluded:

- The friction coefficient μ has a distinct impact on the running behaviour: a higher friction

coefficient leads to a lower nonlinear critical speed $v_{\text{crit,nonlin}}$ and to a higher hunting frequency. Since the hunting motion is excited by the tangential forces, which are limited by the friction coefficient, a higher friction coefficient causes a stronger excitation.

- For the model *FF* the lateral amplitudes of the wheelsets are more sensitive to the friction coefficient: For a higher friction coefficient larger amplitudes occur if the structural flexibilities are taken into account, while for the model using rigid wheelsets and rigid rails the amplitudes are hardly affected. If the excitation is stronger and thereby also the frequency is higher, also higher lateral forces occur when the wheel flange hits the rail head; these higher forces cause larger deformations of the wheelsets and the rails.
- For all four values of the friction coefficient μ the nonlinear critical speed $v_{\text{crit,nonlin}}$ is about 35 km/h lower if the structural flexibilities of wheelsets and rails are taken into account. If the friction coefficient is increased from $\mu = 0.25$ to $\mu = 0.4$, the critical speed drops by about 25 km/h for the rigid model as well as for the fully flexible model. Thereby, the reduction of the nonlinear critical speed by taking the structural flexibilities into account is about 30 % higher than the reduction by the increase of the friction coefficient.
- The limit speeds obtained from the instability criterion and from the track shift criterion are strongly affected by the friction coefficient. For the model *RR* the limit speeds obtained for $\mu = 0.25$ and $\mu = 0.4$ differ by about 45 km/h

8.2.3 Influence of the conicity

As discussed in section 2.2.1 the conicity has a strong impact on the running behaviour of the wheelset. The solution of Klingel's equation considered in section 2.2.1

$$y_{\text{ws}}(x) = \hat{y} \cos\left(\frac{2\pi}{\lambda}x + \beta\right), \quad \lambda = 2\pi\sqrt{\frac{a_0 r_0}{\tan \delta_0}} \quad (8.2.10)$$

shows that a higher conicity $\tan \delta_0$ leads to a shorter wavelength λ . By assuming a constant running speed, i.e. $x = v_0 t$, it can be seen that the frequency f of the hunting motion is lower the lower the conicity is:

$$x = v_0 t \Rightarrow \cos\left(\frac{2\pi}{\lambda}x + \beta\right) = \cos\left(\frac{2\pi}{\lambda}v_0 t + \beta\right) = \cos(2\pi f t + \beta) \Rightarrow f = \frac{v_0}{\lambda} = v_0 \sqrt{\frac{\tan \delta_0}{a_0 r_0}} \quad (8.2.11)$$

By setting $x = v_0 t$ the lateral acceleration is obtained to:

$$y_{\text{ws}}(t) = \hat{y} \cos\left(\frac{2\pi}{\lambda}v_0 t + \beta\right) \Rightarrow \ddot{y}_{\text{ws}}(t) = - \underbrace{\left(\frac{2\pi}{\lambda}v_0\right)^2}_{\hat{y}_{\text{ws}}} \hat{y} \cos\left(\frac{2\pi}{\lambda}v_0 t + \beta\right) \quad (8.2.12)$$

By inserting the expression for the wavelength λ , the amplitude of the lateral acceleration \hat{y}_{ws} can be formulated in the following way:

$$\hat{y}_{\text{ws}} = \frac{\tan \delta_0}{a_0 r_0} v_0^2 \hat{y} \quad (8.2.13)$$

Although Klingel's equation is a comparatively rough approximation, it nevertheless shows that for a lower conicity a lower hunting frequency and a lower lateral acceleration of the wheelset can

be expected. This basic consideration will be used for the interpretation of the results presented in this section.

The conicity is determined by the geometry of the profiles of wheel and rail, i.e. the shape of the profiles, but also their relative position. Usually, the rails are not installed vertically on the sleepers, but are slightly inclined towards the middle of the track. On different railway networks different cants are used: An inclination of $1 : 40 \hat{=} 1.432$ deg is used in Germany, Austria and Switzerland, while an inclination of $1 : 20 \hat{=} 2.862$ deg is used in the UK, France, Italy and Norway. Generally, a higher inclination angle leads to a lower conicity.

In this section, results from calculations using the profile geometry *S1002 / 60E1 / 1:20* are presented. In order to investigate the influence of the conicity on the running behaviour, these results are compared with those obtained for the profile geometry *S1002 / 60E1 / 1:40*, which have been discussed in the previous sections. The results presented and discussed in the following considerations are all obtained for a friction coefficient of $\mu = 0.4$.

First, the general impact of the profile geometry on the system behaviour is investigated. Here, the model *FF* is used. For a direct comparison, a running speed of $v_0 = 255$ km/h was chosen, since for this speed periodic motions were obtained for both profile geometries. In Fig.8.2.24 the phase portraits for the lateral motions y_{Wsi} of all four wheelsets are displayed.

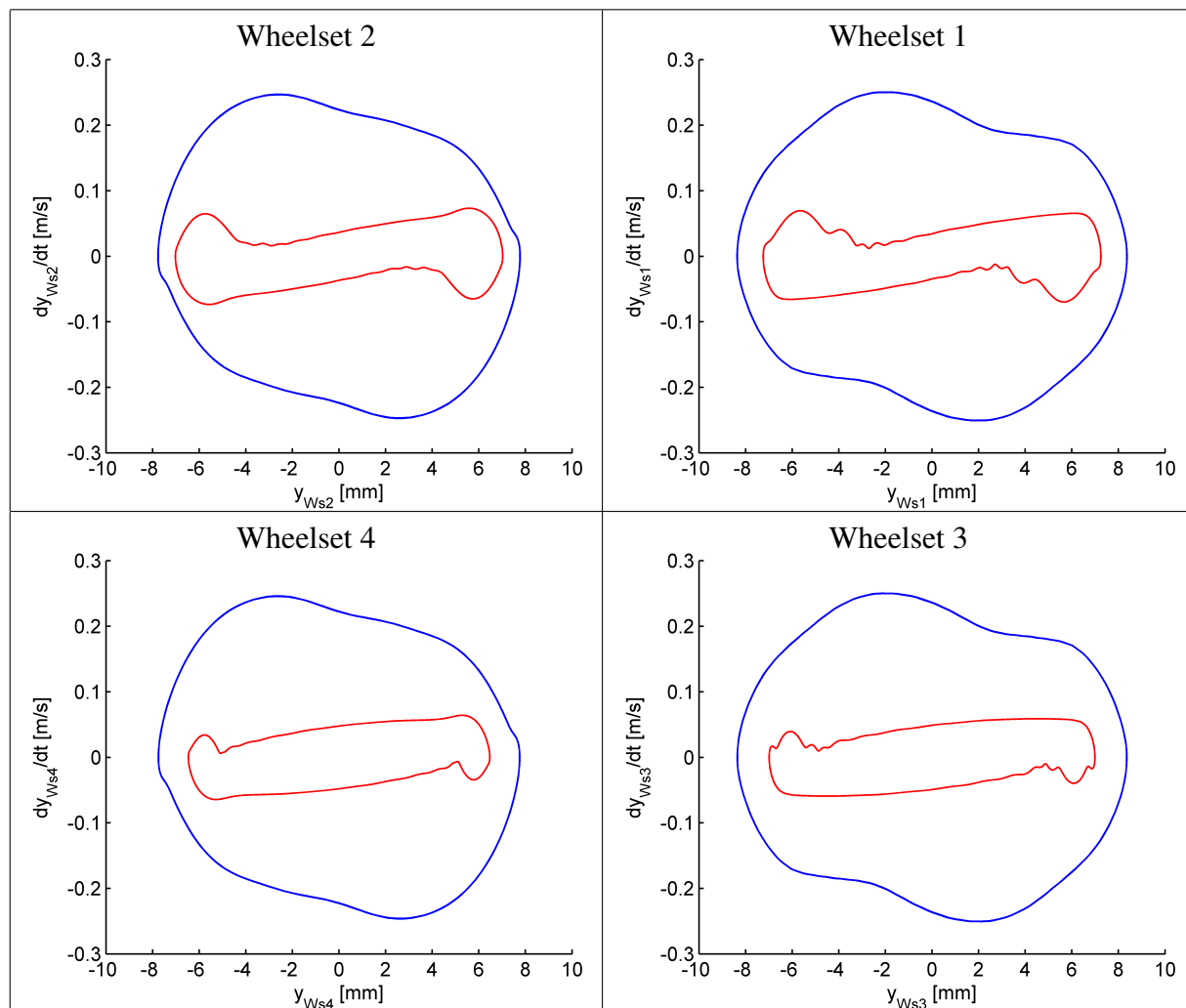


Figure 8.2.24: Lateral motion y_{Wsi} of the wheelsets for different cants. Red: cant 1:20; blue: cant 1:40. $v_0 = 255$ km/h; model *FF*; wheel profile S1002; rail profile 60E1; $\mu = 0.4$.

Generally, for both profile geometries, the maximum lateral displacements of the wheelset are in the same range of magnitude; for the profile geometry $S1002 / 60E1 / 1:40$ slightly higher displacements occur than for $S1002 / 60E1 / 1:20$. However, the lateral velocity of the wheelsets is generally distinctly higher for the profile geometry $S1002 / 60E1 / 1:40$ than for $S1002 / 60E1 / 1:20$. This indicates that for the profile geometry $S1002 / 60E1 / 1:40$ the frequency of the motion is higher. Moreover, it can be seen that for the profile geometry $S1002 / 60E1 / 1:40$ the curves describing the motions of the wheelsets 1 and 3 hardly differ from each other. The same applies to the curves for the wheelsets 2 and 4; also here, for the blue curves obtained for $S1002 / 60E1 / 1:40$ a difference is hardly visible. In contrast to this, the curves for all four wheelsets obtained for the profile geometry $S1002 / 60E1 / 1:20$ differ from each other; although these differences are not tremendous, they are nevertheless clearly visible. The wheelsets 1 and 3 are the front wheelsets of the two bogies, while the wheelsets 2 and 4 are the rear wheelsets of each bogie; for the vehicle, on which the present model is based, both bogies are identical. The fact that for the wheelsets 1 and 3 and for the wheelsets 2 and 4, respectively, nearly the same curves are obtained, if the profile geometry $S1002 / 60E1 / 1:40$ is used, suggests that the bogies hardly interact with each other; the coupling by the carbody is apparently very weak. In contrast to this, the differences, which are observed for the curves for all four wheelsets in the case of the profile geometry $S1002 / 60E1 / 1:20$, indicate an interaction between the two bogies. For a more detailed investigation, the phase portraits of the lateral motion y_{Cb} and the yaw motion ψ_{Cb} are displayed in Fig. 8.2.25.

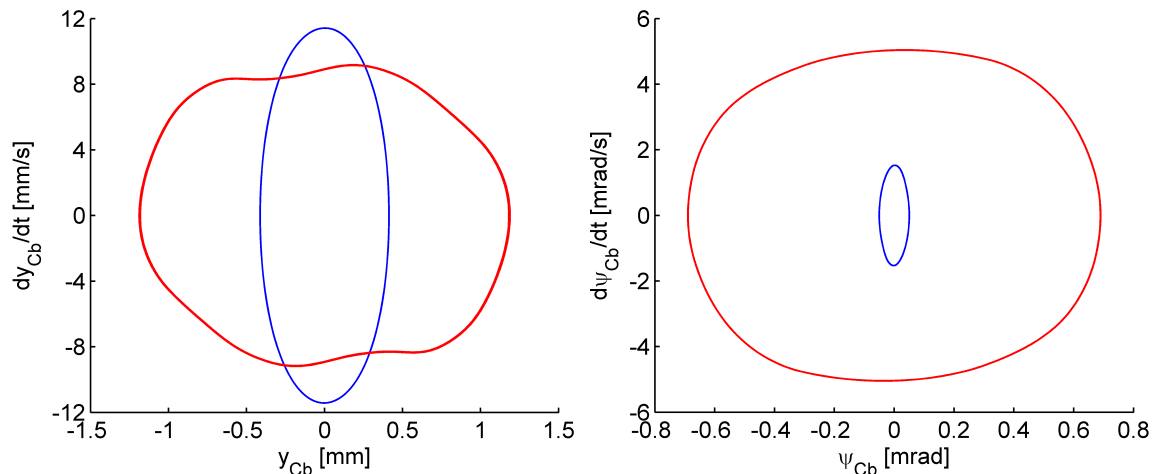


Figure 8.2.25: Lateral motion y_{Cb} (left) and yaw motion ψ_{Cb} of the carbody for different cants. Red: cant 1:20; blue: cant 1:40. $v_0 = 255$ km/h; model FF ; wheel profile $S1002$; rail profile $60E1$; $\mu = 0.4$.

It can clearly be seen that for the profile geometry $S1002 / 60E1 / 1:20$ the carbody performs larger motions than for $S1002 / 60E1 / 1:40$; for the yaw motion the difference of the magnitude is particularly great. This indicates that for the profile geometry $S1002 / 60E1 / 1:20$ there is in fact a coupling of the two bogies by the carbody, while for $S1002 / 60E1 / 1:40$ the interaction of the bogies via the carbody is comparatively weak. The results suggest that for the profile geometry $S1002 / 60E1 / 1:20$ a carbody instability occurs, while for the profile geometry $S1002 / 60E1 / 1:40$ a bogie instability is observed.

In Fig. 8.2.26 the distribution of the pressure on the railhead for the left contact of wheelset 1 is displayed. The change of the contact geometry due to the changed rail cant is clearly visible. For the profile geometry $S1002 / 60E1 / 1:20$ the contact zone hardly changes its lateral position on the rail head. If the wheelset is close to its maximum lateral displacement, a second isolated

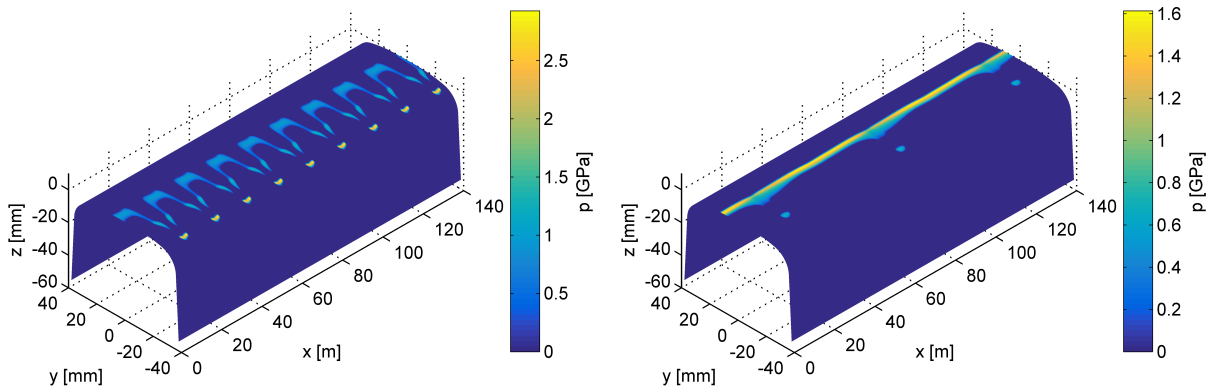


Figure 8.2.26: Distribution of the pressure on the rail head for wheelset 1; left: cant 1:40; right: cant 1:20

contact area appears. In contrast to this, for the profile geometry $S1002 / 60E1 / 1:40$ the contact area moves across the profile between the middle of the tread and the rail corner. Furthermore, it can be seen that for the profile geometry $S1002 / 60E1 / 1:40$ a shorter wavelength occurs than for $S1002 / 60E1 / 1:20$. A shorter wavelength indicates a higher conicity and leads to a higher hunting frequency at the same speed. The higher frequency, which occurs for the profile geometry $S1002 / 60E1 / 1:40$, explains, why the diagrams contained in Fig. 8.2.24 show a higher lateral velocity \dot{y}_{wsi} of the wheelset's centre for $S1002 / 60E1 / 1:40$ than for $S1002 / 60E1 / 1:20$.

Figure 8.2.27 shows the frequency f of the hunting motion versus the running speed v_0 . The dia-

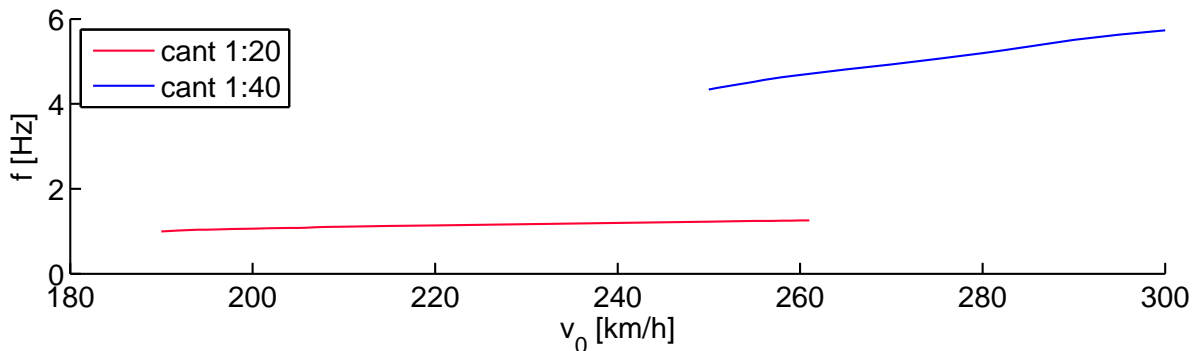


Figure 8.2.27: Hunting frequency. Model FF , rail profile 60E1, $\mu = 0.4$.

gram clearly shows that for the profile geometry $S1002 / 60E1 / 1:40$ the frequency of the hunting motion and the slope indicating the increase of the frequency f with growing running speed v_0 are both distinctly higher than for the profile geometry $S1002 / 60E1 / 1:20$. For the profile geometry $S1002 / 60E1 / 1:20$ permanent hunting occurs in the range of the running speed between $v_0 = 190$ km/h and $v_0 = 261$ km/h; outside this speed interval no permanent hunting motions are observed. In this speed interval the hunting frequency grows from $f = 0.997$ Hz at $v_0 = 190$ km/h up to $f = 1.257$ Hz at $v_0 = 261$ km/h. As discussed in section 8.2.1, for the profile geometry $S1002 / 60E1 / 1:20$ the permanent hunting starts at $v_0 = 250$ km/h. The frequency increases from $f = 4.338$ Hz at $v_0 = 250$ km/h up to $f = 5.730$ Hz at $v_0 = 300$ km/h.

In Figure 8.2.28 and Figure 8.2.29 the maximum lateral displacement $y_{Cb,max}$ and the maximum yaw angle $\psi_{Cb,max}$ of the carbody versus the running speed v_0 are displayed. The curves obtained for the profile geometry $S1002 / 60E1 / 1:20$ show a distinct peak at $v_0 = 205$ km/h for the lateral and the yaw motion and a further one at $v_0 = 195$ km/h for the yaw motion; these peaks indicate resonances of the carbody.

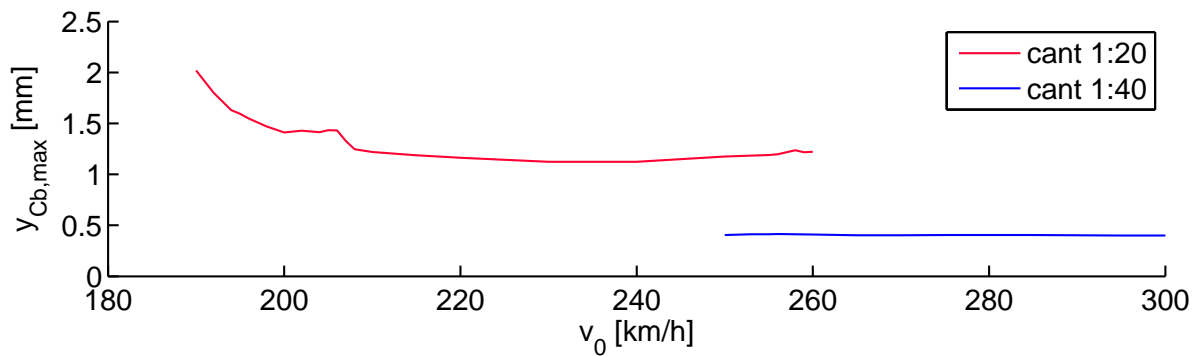


Figure 8.2.28: Maximum lateral displacement of the carbody. Model *FF*, rail profile 60E1, $\mu = 0.4$.

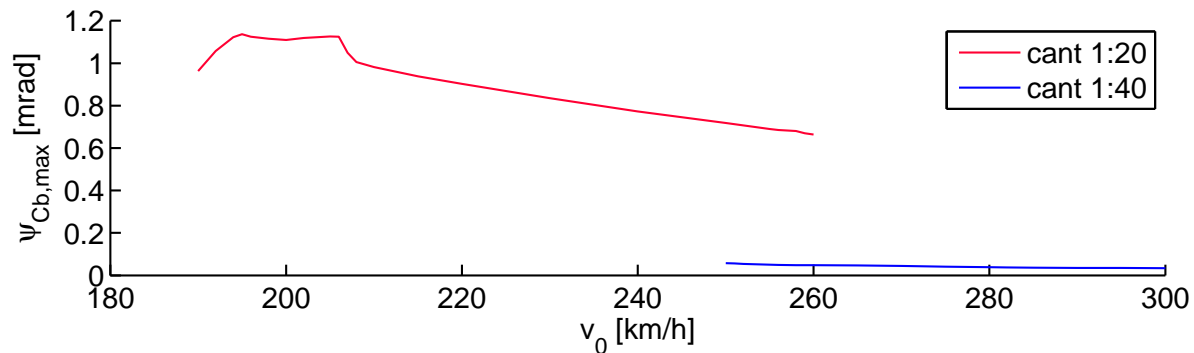


Figure 8.2.29: Maximum yaw angle of the carbody. Model *FF*, rail profile 60E1, $\mu = 0.4$.

In Fig. 8.2.30 the maximum lateral displacement of the wheelsets 1 and 2 versus the running speed v_0 for the two profile geometries *S1002 / 60E1 / 1:20* and *S1002 / 60E1 / 1:40* are displayed. It

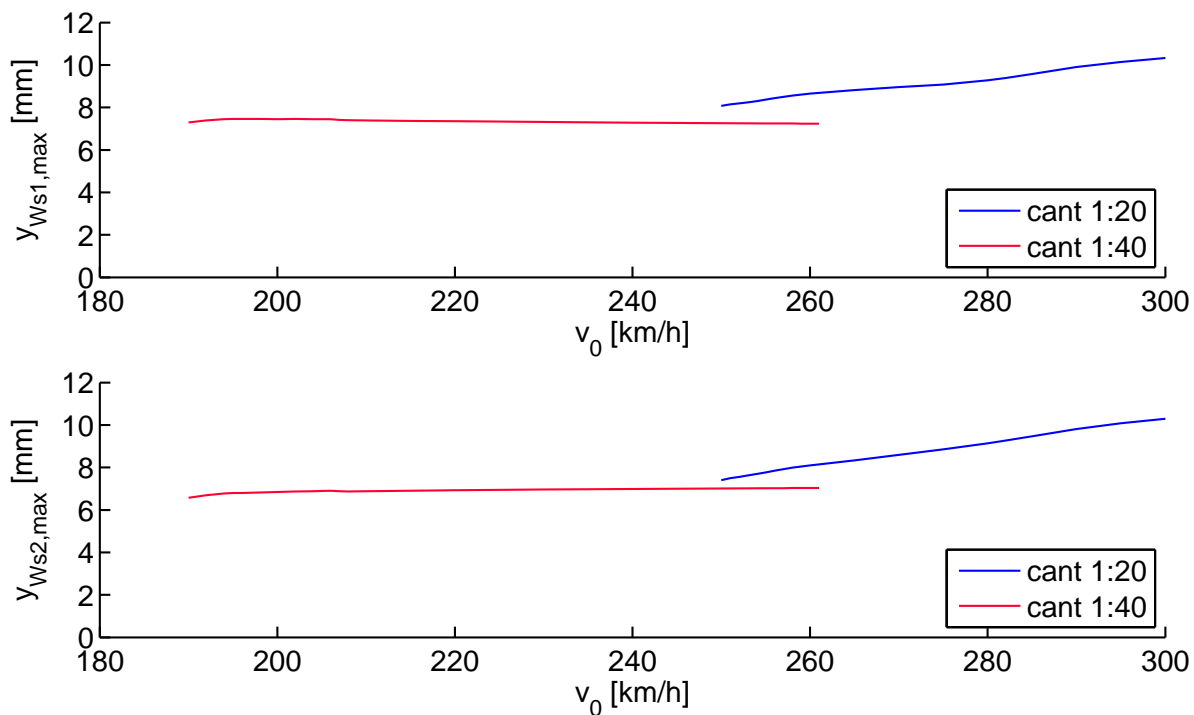


Figure 8.2.30: Maximum lateral displacement of the wheelsets 1 and 2. Model *FF*, rail profile 60E1, $\mu = 0.4$.

can clearly be seen that for the profile geometry *S1002 / 60E1 / 1:20* the maximum lateral dis-

placements $y_{W_s, \max}$ hardly change with varying running speed; the curves are nearly horizontal. In contrast to this the maximum lateral displacements $y_{W_s, \max}$ distinctly grow with the running speed for the profile geometry *S1002 / 60E1 / 1:20*.

Next, the influence of the structural flexibilities is investigated for the lower conicity. Calculations were carried out for the models *RR* and *FF* using a rail cant of 1:20. The phase portraits of the lateral motions of the wheelsets 1 and 2 are shown in Fig.8.2.31 and Fig.8.2.32.

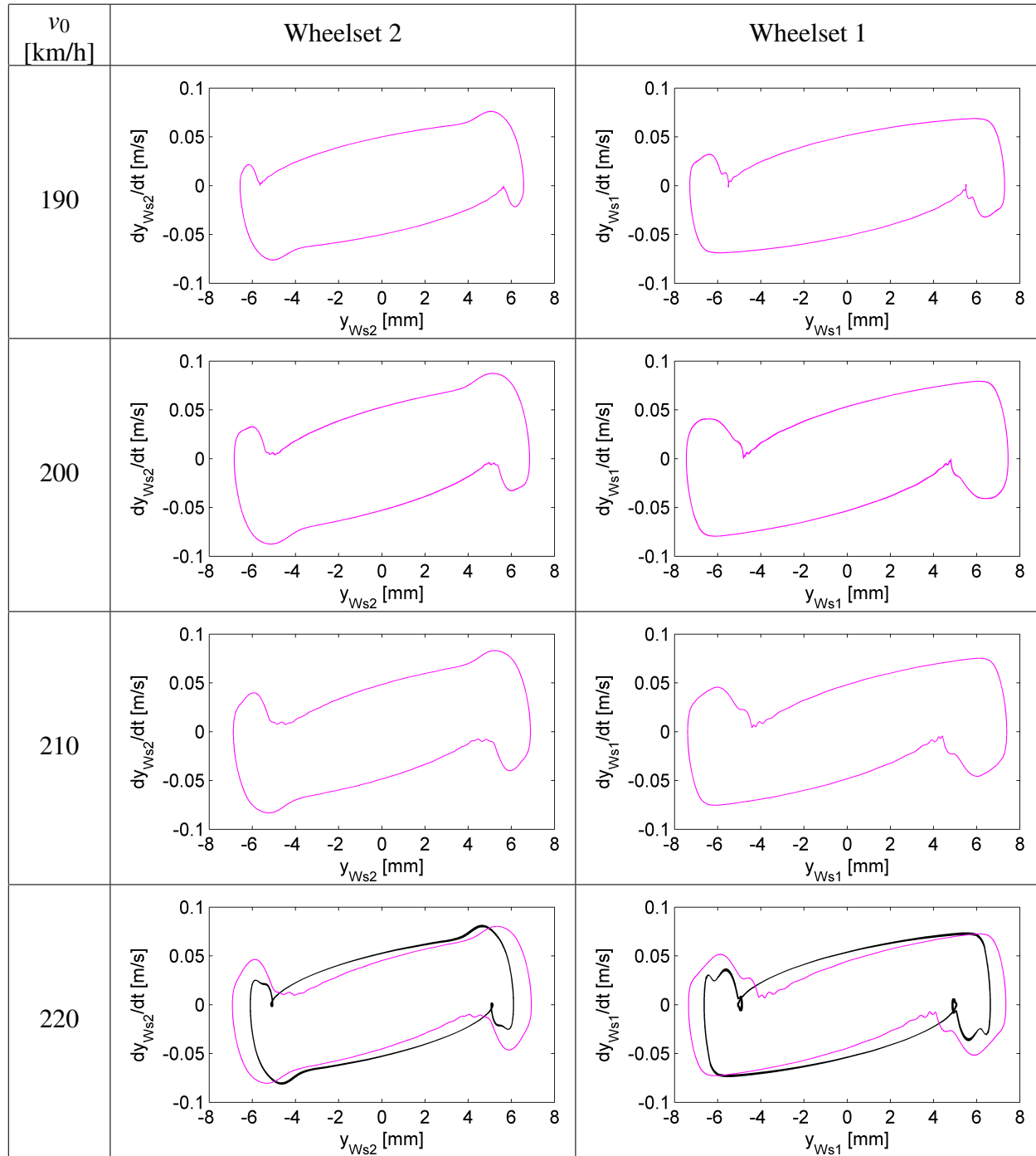


Figure 8.2.31: Phase portraits for the lateral motions y_{W_s1} for the front wheelset and y_{W_s2} for the rear wheelset of the front bogie for different model variants. Black curve: model *RR*, magenta curve: model *FF*; wheel profile *S1002*; rail profile *60E1*; cant 1:20; $\mu = 0.4$.

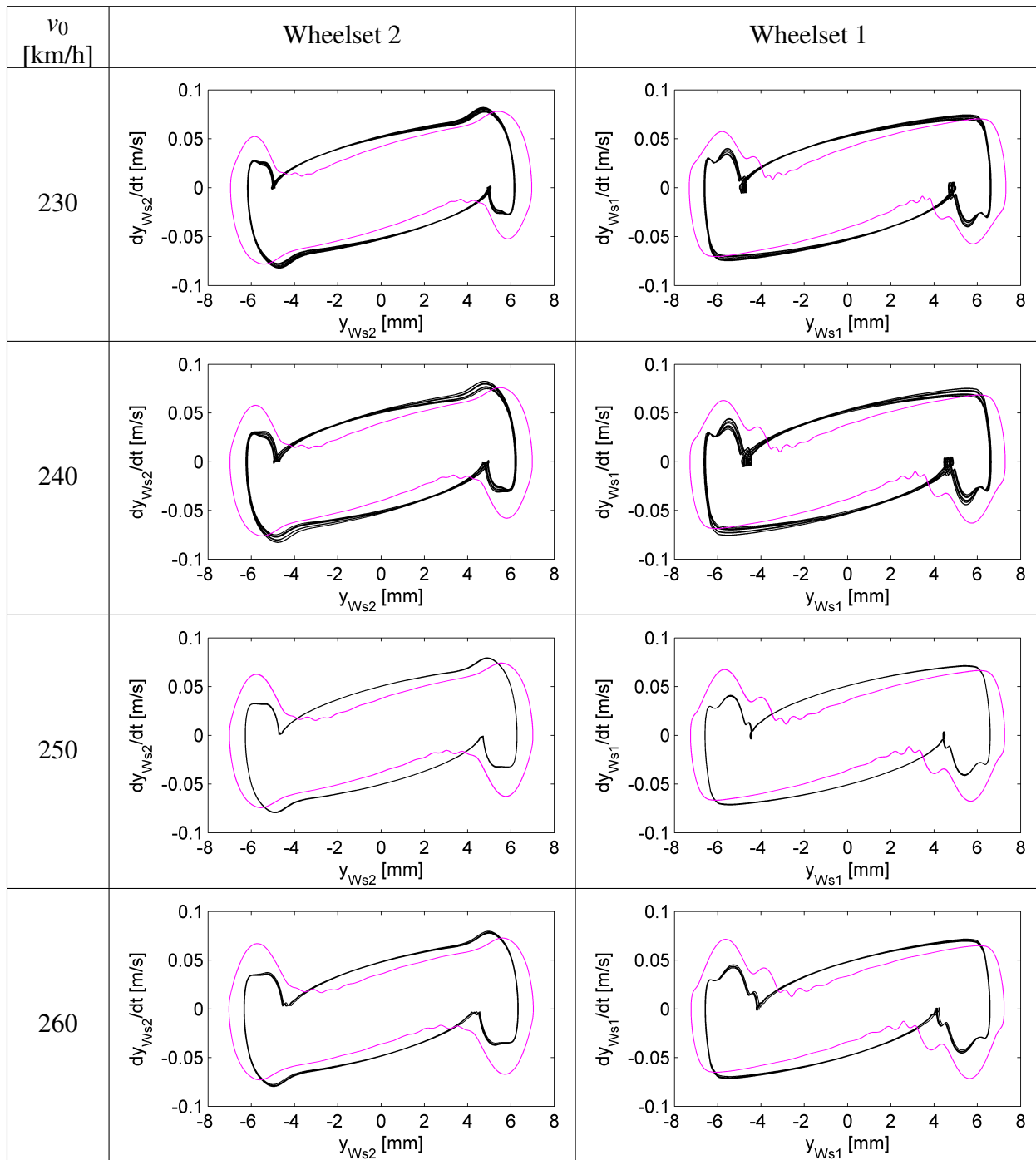


Figure 8.2.32: Phase portraits for the lateral motions y_{ws1} for the front wheelset and y_{ws2} for the rear wheelset of the front bogie for different model variants. Black curve: model *RR*, magenta curve: model *FF*; wheel profile S1002; rail profile 60E1; cant 1:20; $\mu = 0.4$.

The diagrams show that the differences between the results obtained for the models *RR* and *FF* are comparatively small. For the model *FF* the maximum lateral displacement is approximately 0.7 mm higher than for the model *RR*. Furthermore, the “kinks” resulting from the flange contact do not only appear for the model *RR*, but also for the model *FF*. In the region before reaching the maximum displacement the inclination of the curves for the model *FF* with respect to the vertical axis is slightly higher than for the model *RR*. As already discussed, the lateral acceleration and

therefore also the lateral forces are lower for a lower conicity. Since the lateral forces are lower, also the structural deformations caused by these forces are smaller. Therefore, the influence of the structural flexibilities is smaller in the case of a low conicity than for a high conicity as obtained for a rail cant of 1:40.

In Figure 8.2.33 the maximum lateral displacements $y_{ws1,max}$ and $y_{ws2,max}$ of the wheelsets of the front bogie versus the running speed v_0 are displayed. Here, it can clearly be seen that the curves

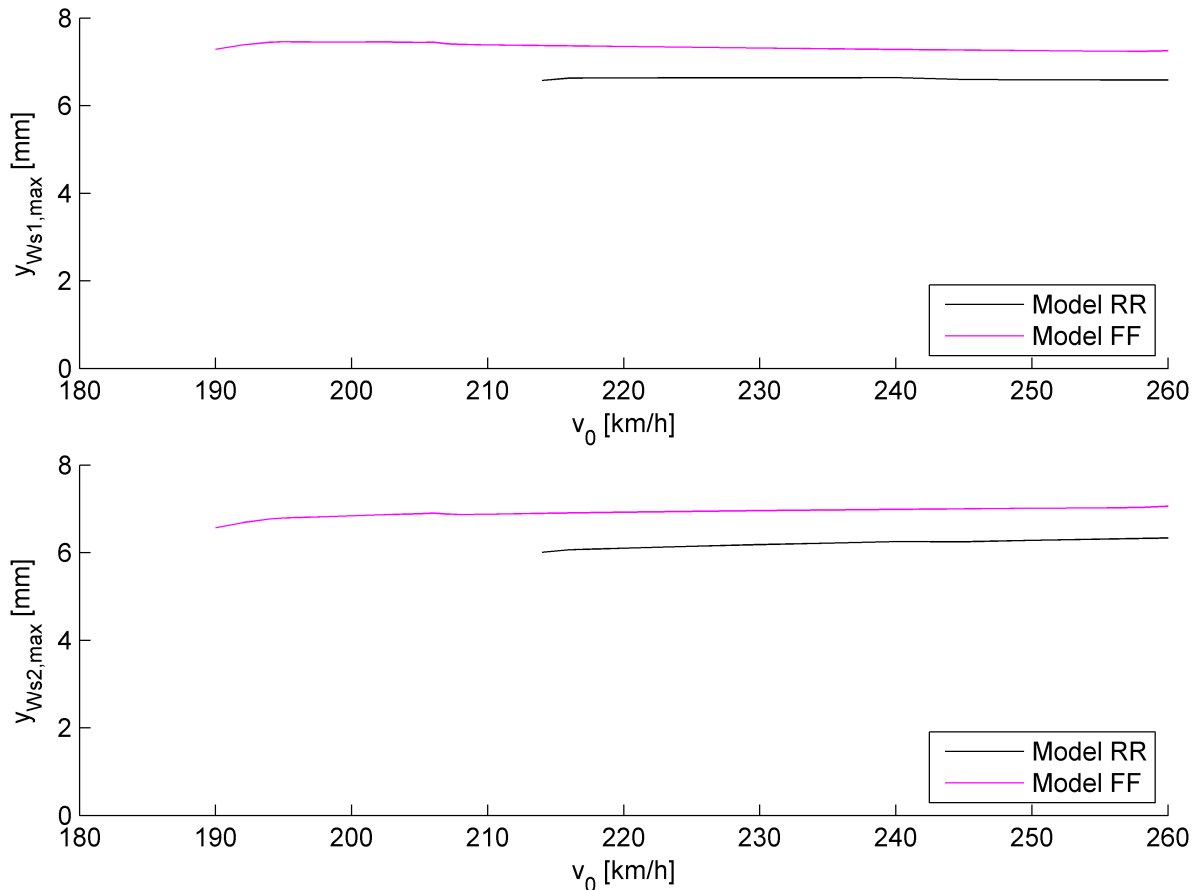


Figure 8.2.33: Maximum lateral displacement for the wheelsets of the front bogie for different model variants; above: front wheelset $y_{ws1,max}$; below: rear wheelset $y_{ws2,max}$; wheel profile S1002; rail profile 60E1; cant 1/40; $\mu = 0.4$.

are nearly horizontal; this indicates that the influence of the running speed v_0 on the maximum lateral displacement is comparatively weak. Also, the diagrams show that maximum lateral displacement of the wheelsets is approx. 0.7 mm higher if the structural flexibilities of the wheelsets and the rails are taken into account; as mentioned before, the influence of the structural flexibilities is quite weak in this case. However, the diagrams show that the nonlinear critical speed $v_{crit,nonlin}$ drops from $v_{crit,nonlin} = 214$ km/h down to $v_{crit,nonlin} = 190$ km/h, if the structural flexibilities are taken into account.

In Fig.8.2.34 the pressure distributions at the left contact of the wheelset 1 are compared for the rigid model *RR* and for the flexible model *FF*. The differences between the two distributions are very small; this too indicates that in this case the impact of the structural deformations on the contact is very weak.

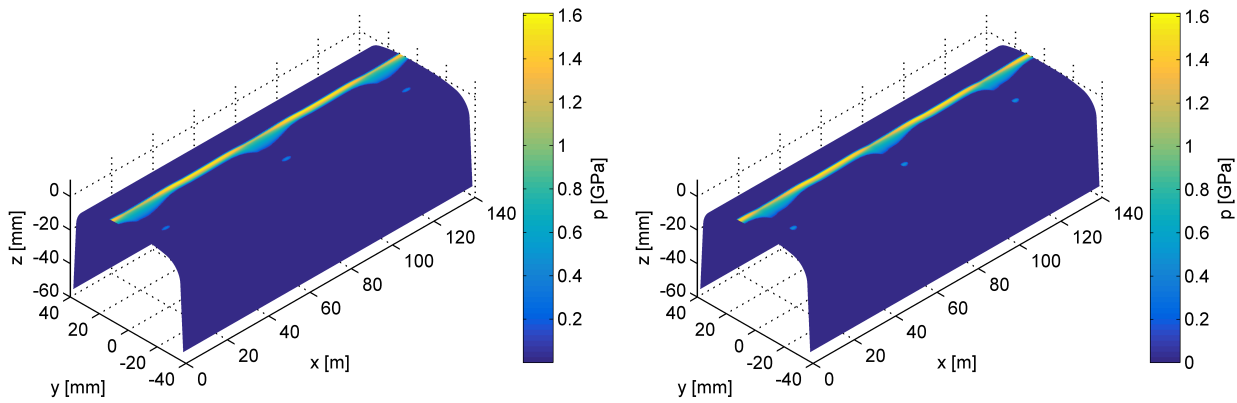


Figure 8.2.34: Distribution of the pressure on the rail head for wheelset 1; left: model *RR*; right: model *FF*; $v_0 = 220$ km/h; cant 1:20; $\mu = 0.4$

8.3 Conclusion

In this chapter, the impact of the structural flexibilities of the wheelsets and the rails on the running behaviour has been investigated. Furthermore, this impact has been compared to the ones of a varying friction coefficient and of different profile geometries.

Regarding the centred running on an undisturbed tangent track, the results show that the structural flexibilities can have a considerable impact on the wheel-rail contact. This impact is particularly strong for a wide contact area, as it is obtained for the profile geometry *S1002 / 60E1 / 1:40*: the shape of the contact area and the stress distribution in the contact are distinctly changed if the structural flexibilities are taken into account. For the profile geometries *S1002 / 60E1 / 1:20* and *S1002 / 60E2 / 1:40*, the contact area is narrower; in this case, the influence of the structural flexibilities is weak. A further investigation for the profile geometry *S1002 / 60E1 / 1:40* shows that the changes are mainly caused by the flexibility of the wheelset. The way, how the contact area's shape and the stress distribution are changed, suggest that these changes are caused by an inclination of the wheel rim due to the bending of the wheelset's axle. This bending is caused by the vertical forces acting at the wheel-rail contacts and at the journals due to the weight of the carbody and the bogie frame. As a result, a kind of camber angle of the wheel occurs.

The structural flexibilities of the wheelsets and the rails also have an impact on the hunting motion. Generally, the flexibilities lead to larger lateral motions of the wheelsets and to a lower nonlinear critical speed, i.e. the permanent hunting already starts at a lower running speed if the structural flexibilities are taken into account. However, the strength of the impact depends on other factors like the profile geometry and the friction coefficient in the wheel-rail contact. Generally, the impact of the structural flexibilities is the stronger for a higher conicity and for a higher friction coefficient. This shall be shortly discussed:

- From Klingel's equation it is known that a higher conicity leads to a shorter wavelength and thereby to a higher hunting frequency at the same running speed. From this, it follows that for a higher conicity also the lateral acceleration of the wheelset is higher. A higher lateral acceleration suggests that also the lateral wheel-rail forces, which guide the wheelset, are higher.
- Regarding the friction coefficient, it is evident that for a higher friction coefficient higher tangential forces can be transmitted in the wheel-rail contact. Furthermore, the self-excitation of the wheelset above the critical speed results from the characteristics of the tangential forces

acting in the wheel-rail contact. From this, it can be deduced that a higher friction coefficient causes a stronger self-excitation of the wheelset and thereby also higher lateral forces.

It can be concluded that a higher conicity and a higher friction both cause higher lateral forces. It is evident that higher forces acting on a flexible structure usually larger deformations. This finally explains why the structural flexibilities have a stronger impact, if the conicity and the friction coefficient are higher.

For the combination of the wheel profile S1002 and the rail profile 60E1 with a cant of 1:40, which has a comparatively high conicity, and for a friction coefficient of $\mu = 0.4$, the structural flexibilities cause an increase of the wheelset's maximum lateral displacement from $y_{WS,max} \approx 7$ mm up to $y_{WS,max} \approx 10$ mm...11 mm and a reduction of the nonlinear critical speed from $v_{crit,nonlin} = 289$ km/h down to $v_{crit,nonlin} = 250$ km/h. These changes are in an order of magnitude that cannot be neglected. Further investigations, in which the flexibilities of the wheelsets and of the rails are taken into account separately, show that the flexibility of the wheelsets has a stronger impact; nevertheless, the impact of the flexibility of the rails is not negligible.

Chapter 9

Conclusion and outlook

In the present work, a refined and enhanced vehicle-track model has been developed. Compared to the “conventional modelling”, which can be done by many commercially available simulation programs, the presented model has mainly three extensions.

The first extension is the modelling of the wheelsets as flexible bodies. A special characteristics of the wheelsets from the mechanical point of view is that they are performing large rotations. At higher speeds the angular velocity generates gyroscopic effects so that this motion cannot be neglected. However, from the mathematical point of view, this large rotation is described by trigonometric functions, so that there are strong nonlinearities. In the present work a formulation is developed which takes advantage from the rotational symmetry of the wheelset. In this formulation, the wheelset is described in a sliding frame, which performs all motions except the large overturning motion. The rotational symmetric body is considered as a cyclic structure, which consists of n circularly arranged identical segments. The generalization of the cyclic structure is an n -tuple of identical particles, which has also been used to determine the characteristic properties of the equations of motion of a cyclic structure. The application of this description is not restricted to wheelsets, but also suitable for other rotating components.

The second extension is the modelling of the track as a flexible structure. This provides a more realistic modelling than the widely used substitution models used in multibody simulation programs. The rails are modelled by a semi-analytical finite element model which takes advantage from the prismatic shape of the rails. The rails are supported by discrete sleepers via pads which are modelled by distributed visco-elastic elements. Also, the rail cant is taken into account. Together with the refined structural model of the rail this provides a high accuracy of the modelling. Although the valid frequency range of the track model is not exploited in this work, the refined modelling nevertheless provides a precise description of the motions of the rail head. This is especially important regarding the lateral dynamics, where the contact geometry can be very sensitive with respect to the relative kinematics between the rail head and the wheel rim.

The third extension is an extended model for the wheel-rail contact. This model is based on the consideration of the wheel and the rail as halfspaces. The discretized contact problem is solved iteratively, i.e. the model contains an actual solution of the equations describing the contact mechanics, not just an estimation of the contact area or the stress distribution. The integration of such a model into a multibody simulation requires a fast solving algorithm; this algorithm is based on the Gauss-Seidel method, but uses several modifications in order to accelerate the solution.

With this enhanced and refined vehicle-track model, two scenarios are investigated. Here, the new model is compared to the “conventional modelling”, where the wheelsets are considered as rigid

bodies and a simple substitution model consisting of masses, springs and dampers is used for the track. For the centred running on an undisturbed track it turns out that for some profile geometries the structural deformations have a considerable impact on the stress distribution in the contact. This impact is especially strong when the contact area is quite wide. Comparisons with different model configurations show that the bending of the wheelset has a strong impact on the contact. The second scenario is the permanent hunting of the vehicle. The results show that the structural flexibilities of the wheelsets and the track can have a strong impact on the running behaviour. If the flexibilities are taken into account, then the lateral displacement of the wheelset grows and the critical speed, i.e. the lowest running speed, at which the permanent hunting starts, is reduced. The influence of the structural flexibilities of the wheelsets and the track on the running behaviour is stronger if the lateral forces are higher. Such high lateral forces occur especially for a high conicity, which leads to a high hunting frequency and thereby high lateral accelerations, and for a high friction coefficient in the wheel rail contact. With lower friction coefficients and lower conicity the impact of the structural flexibilities decreases.

Although it has not been investigated in this work, the model also provides a simultaneous calculation of the wear occurring in the contact due to the refined modelling of the key components of vehicle-track interaction. Usually, the wear is determined in a post-processing of a multibody simulation. Here, models with different detailing and accuracy are used, which can cause problems regarding the adaptation. In the new model, the contact problem is numerically solved during the simulation providing a quite precise determination of the stress distribution in the contact, which is required for the determination of wear. The investigation of wear is an important topic, since this is relevant for the economics of the entire system “railway” consisting of the rolling stock and the infrastructure. Therefore, the new model may lay a new base and new possibilities for the investigation and optimization of the entire system “railway”

Bibliography

- [1] E. Anderson, Z. Bai, C. Bischof, S. Blackford, J. Demmel, J. Dongarra, J. Du Croz, A. Greenbaum, S. Hammarling, A. McKenney, and D. Sorensen. *LAPACK Users' Guide*. Society for Industrial and Applied Mathematics, Philadelphia, PA, third edition, 1999.
- [2] J.B. Ayasse and H. Chollet. Determination of the wheel rail contact patch in semi-hertzian conditions. *Vehicle System Dynamics*, 43:161–172, 2005.
- [3] J.B. Ayasse and H. Chollet. Wheel-rail contact. In S. Iwnicki, editor, *Handbook of railway vehicle dynamics*. CRC Taylor & Francis, 2006.
- [4] L. Baeza and H. Ouyang. A railway track dynamics model based on modal substructuring and a cyclic boundary condition. *Journal of Sound and Vibration*, 330:75–86, 2011.
- [5] K. G. Baur. *Drehgestelle – Bogies*. EK-Verlag, Freiburg, 2006.
- [6] Y. Ben-Othman. *Kurvenquietschen: Untersuchung des Quietschvorgangs und Wege der Minderung*. PhD thesis, Technische Universität Berlin, 2008.
- [7] Y. Bezin, S.D. Iwnicki, and M. Cavalletti. The effect of dynamic rail roll on the wheel-rail contact conditions. *Vehicle System Dynamics Supplement*, 46, 2008.
- [8] S. Bruni, J. Vinolas, M. Berg, O. Polach, and S. Stichel. Modelling of suspension components in a rail vehicle dynamics context. *Vehicle System Dynamics*, 49(7):1021–1072, 2011.
- [9] N. Char and M. Berg. Simulation of vehicle-track interaction with flexible wheelsets, moving track models and field tests. *Vehicle System Dynamics*, 44:sup1:921–931, 2006.
- [10] P. Delfosse. Very-high-speed tests on the french railway track. *Vehicle System Dynamics*, 20:3-4:185–206, 1991.
- [11] P. Diepen. *Horizontaldynamik von Drehgestellfahrzeugen - Berechnung und Optimierung des Laufverhaltens von schnellfahrenden Reisezugwagen mit konventionellen Laufwerken*. PhD thesis, Technische Universität Braunschweig, 1991.
- [12] U. Fingberg. *Ein Modell für das Kurvenquietschen von Schienenfahrzeugen*. Number 140 in VDI-Fortschrittsberichte Reihe 11. VDI-Verlag, Düsseldorf, 1990.
- [13] M. Flach. *Rechnerische Lebensdauerabschätzung für stochastische Lasten im Schienenfahrzeugbau*. Number T 14 in TIM-Forschungsberichte. Forschungszentrum für Multidisziplinäre Analysen und Angewandte Strukturoptimierung der Universität Siegen, Siegen, 1999.
- [14] V.J. Garg and R.V. Dukkipati. *Dynamics of Railway Vehicle Systems*. Academic Press, Toronto, 1984.

- [15] R. Gasch, K. Knothe, and R. Liebich. *Strukturdynamik*. Springer-Verlag Berlin Heidelberg, 2nd edition, 2012.
- [16] W. Hanneforth and W. Fischer. *Laufwerke*. transpress VEB Verlag für Verkehrswesen, Berlin, 1st edition, 1986.
- [17] P. Heiß. *Untersuchungen über das Körperschall- und Abstrahlverhalten eines Reisezugwagenrades*. PhD thesis, Technische Universität Berlin, 1986.
- [18] Studie über ein Schnellverkehrssystem – Systemanalyse und Ergebnisse. Hochleistungs-Schnellbahn Studiengesellschaft mbH (HSB), 1971.
- [19] M. Hughes. *Die Hochgeschwindigkeitsstory*. Alba-Verlag, Düsseldorf, 1994.
- [20] J. Ihme. *Beitrag zur Querdynamik zweiachsiger Schienenfahrzeuge im geraden Gleis*. PhD thesis, Technische Universität Braunschweig, 1983.
- [21] S.D. Iwnicki. Manchester benchmark for rail vehicle simulation. *Vehicle System Dynamics*, 30:295–313, 1998.
- [22] C. Kaas-Petersen. Chaos in a railway bogie. *Acta Mechanica*, 61:89–107, 1986.
- [23] I. Kaiser and K. Popp. Modeling and simulation of the mid-frequency behaviour of an elastic bogie. In K. Popp and W. Schiehlen, editors, *System Dynamics and Long-Term Behaviour of Railway Vehicles, Track and Subgrade*. Springer-Verlag, 2002.
- [24] I. Kaiser and K. Popp. Interaction of elastic wheelsets and elastic rails: modelling and simulation. *Vehicle System Dynamics*, 44:sup1:932–939, 2006.
- [25] J.J. Kalker. A fast algorithm for the simplified theory of rolling contact. *Vehicle System Dynamics*, 11:1–13, 1982.
- [26] J.J. Kalker. *Three-dimensional elastic bodies in rolling contact*. Kluwer Academic Publishers, Dordrecht, 1990.
- [27] J.J. Kalker. Wheel-rail rolling contact theory. *Wear*, 144:243–261, 1991.
- [28] H. Kaps. *S-Transformation zur indirekten Rauheitsmessung bei Schienenfahrzeugen*. Shaker-Verlag, Aachen, 2014.
- [29] W. Kik and J. Piotrowski. A fast, approximate method to calculate normal load at contact between wheel and rail and creep forces during rolling. In *2nd Mini-Conference on Contact Mechanics and Wear of Rail/Wheel Systems, July 29-31, 1996, Budapest, Hungary*, 1996.
- [30] K.-H. Kim. *Verschleißgesetz des Rad-Schiene-Systems*. PhD thesis, Rheinisch-Westfälische Technische Hochschule Aachen, 1996.
- [31] O. Kleiner. *Numerische und experimentelle Untersuchung der Rad-Schiene-Interaktion unter Berücksichtigung mechanischer und thermomechanischer Effekte*. PhD thesis, Technische Universität Kaiserslautern, 2011.
- [32] Klingel. Ueber den Lauf der Eisenbahnwagen auf gerader Bahn. *Organ für die Fortschritte des Eisenbahnwesens*, XX[=20](4):113–123, 1883.

- [33] K. Knothe. *Gleisdynamik*. Ernst & Sohn, Verlag für Architektur und technische Wissenschaften, Berlin, 2001.
- [34] K. Knothe and S.L. Grassie. Modelling of railway track and vehicle/track interaction at high frequencies. *Vehicle System Dynamics*, 22:209–262, 1993.
- [35] K. Knothe and S. Stichel. *Schienenfahrzeugdynamik*. Springer-Verlag, Berlin, 2003.
- [36] R. Kratochwille. *Zum Nutzen schaltbarer Schlingerdämpfer bei Trassierungselementen mit veränderlicher Gleiskrümmung*. PhD thesis, Universität Hannover, 2004.
- [37] B. Kurzeck. *Methoden zur Minderung mittelfrequenter Schwingungen bei Bogenfahrt im Schienennahverkehr*. Shaker-Verlag, Aachen, 2008.
- [38] M. Küsel. *Wellige Verschleißmuster auf Laufflächen von Eisenbahnradern*. Number 47 in Braunschweiger Schriften zur Mechanik. Mechanik-Zentrum der Technischen Universität Braunschweig, Braunschweig, 2002.
- [39] L.D. Landau and E.M. Lifshitz. *Theory of Elasticity*, volume 7 of *Courses of Theoretical Physics*. Pergamon Press, Oxford, 2nd edition, 1970.
- [40] C. Linder. *Verschleiß von Eisenbahnradern mit Unrundheiten*. PhD thesis, ETH Zürich, 1997.
- [41] K. Magnus, K. Popp, and W. Sextro. *Schwingungen*. Springer Vieweg, Wiesbaden, 9th edition, 2013.
- [42] A. Mahr. *Abstimmung der Rad-Schiene-Geometrie mit dem lateralen Fahrzeugverhalten - Methoden und Empfehlungen*. Shaker-Verlag, Aachen, 2002.
- [43] L. Mazzola, S. Bruni, J. Martínez-Casas, and L. Baeza. Numerical estimation of stresses in railway axles using flexible wheelset-track models. In *Proceedings of the 22nd IAVSD Symposium, held at Manchester Metropolitan University, August 14-19, 2011*, 2011.
- [44] M. Mertens. *Trans Europ Express*. Alba-Publikation, Düsseldorf, 1987.
- [45] D. Moelle. *Digitale Grenzykelrechnung zur Untersuchung der Stabilität von Eisenbahndrehgestellen unter dem Einfluß von Nichtlinearitäten*. PhD thesis, Technische Universität Berlin, 1990.
- [46] G.B. Morys. *Zur Entstehung und Verstärkung von Unrundheiten an Eisenbahnradern bei hohen Geschwindigkeiten*. PhD thesis, Technische Universität Karlsruhe, 1998.
- [47] A. Nefzger. Geometrie der Berührung zwischen Radsatz und Gleis. *ETR – Eisenbahntechnische Rundschau*, pages 113–122, März/march 1974.
- [48] H. Netter. *Rad-Schiene-Systeme in differential-algebraischer Darstellung*. Number 352 in VDI-Fortschrittsberichte Reihe 12. VDI-Verlag, Düsseldorf, 1998.
- [49] L. Panning. *Auslegung von Reibelementen zur Schwingungsdämpfung von Turbinenschaufeln*. Number 328 in VDI-Fortschrittsberichte Reihe 11. VDI-Verlag, Düsseldorf, 2005.
- [50] F. Périard. *Wheel-Rail Noise Generation: Curve Squealing by Trams*. PhD thesis, Technische Universiteit Delft, 1998.

- [51] J. Piotrowski and H. Chollet. Wheel-rail contact models for vehicle system dynamics including multi-point contact. *Vehicle System Dynamics*, 43:455–483, 2005.
- [52] M. Pletz, W. Daves, and H. Ossberger. A wheel passing a crossing nose: Dynamic analysis under high axle loads using finite element modelling. *Proceedings of the Institution of Mechanical Engineers, Part F: Journal of Rail and Rapid Transit*, 226(6):603–611, 2012.
- [53] O. Polach and I. Kaiser. Comparison of methods analyzing bifurcation and hunting of complex rail vehicle models. *Journal of Computational and Nonlinear Dynamics*, 7, October 2012.
- [54] K. Popp, K. Knothe, and C. Pöpper. System dynamics and long-term behaviour of railway vehicles, track and subgrade: report on the dfg priority programme in germany and subsequent research. *Vehicle System Dynamics*, 43:485–538, 2005.
- [55] K. Popp and W. Schiehlen. *Fahrzeugdynamik*. Teubner Verlag, Stuttgart, 1993. Revised English edition: K. Popp and W. Schiehlen: *Ground Vehicle Dynamics*, Springer-Verlag Berlin Heidelberg, 2010.
- [56] K. Popp and W. Schiehlen. *Ground Vehicle Dynamics*. Springer-Verlag, Berlin/Heidelberg, 2010.
- [57] X. Quost, M. Sebes, A. Eddhahak, J.B. Ayasse, H. Chollet, P.E. Gautier, and F. Thouverez. Assessment of a semi-hertzian method for determination of wheel-rail contact patch. *Vehicle System Dynamics*, 44:789–814, 2006.
- [58] B. Ripke. *Hochfrequente Gleismodellierung und Simulation der Fahrzeug-Gleis-Dynamik unter Verwendung einer nichtlinearen Kontaktmechanik*. Number 249 in VDI-Fortschrittsberichte Reihe 12. VDI-Verlag, Düsseldorf, 1995.
- [59] R. Roberson and R. Schwertassek. *Dynamics of Multibody Systems*. Springer Verlag, Berlin Heidelberg, 1988.
- [60] H.-G. Roos and H. Schwetlick. *Numerische Mathematik*. Teubner Verlag, Stuttgart, 1999.
- [61] G. Sauvage. Running quality at high speeds. *Vehicle System Dynamics*, 15:sup1:496–508, 1986.
- [62] H. Schelle. *Radverschleißreduzierung für eine Güterzuglokomotive durch optimierte Spurführung*. PhD thesis, Technische Universität Berlin, 2014.
- [63] W. Schiehlen and P. Eberhard. *Applied Dynamics*. Springer, Cham, Heidelberg, New York, Dordrecht, London, 1st edition, 2014.
- [64] W. Schiehlen and P. Eberhard. *Technische Dynamik*. Springer Vieweg, Wiesbaden, 4th edition, 2014.
- [65] E. Schneider. *Schwingungsverhalten und Schallabstrahlung von Schienenrädern*. Number 74 in VDI-Fortschrittsberichte Reihe 11. VDI-Verlag, Düsseldorf, 1985.
- [66] G. Schupp. *Numerische Verzweigungsanalyse mit Anwendungen auf Rad-Schiene-Systeme*. Shaker-Verlag, Aachen, 2004.

- [67] H.R. Schwarz. *Methode der finiten Elemente – eine Einführung unter besonderer Berücksichtigung der Rechenpraxis*. Teubner-Verlag, Stuttgart, 1980.
- [68] A.A. Shabana. *Dynamics of Multibody Systems*. Cambridge University Press, Cambridge, 3rd edition, 2005.
- [69] Z.Y. Shen, J.K. Hedrick, and J.A. Elkins. A comparison of alternative creep force models for rail vehicle dynamic analysis. In J.K. Hedrick, editor, *The Dynamics of Vehicles on Roads and Railway Tracks: Proceedings of the 8th IAVSD Symposium, held at Massachusetts Institute of Technology, Cambridge, MA, August 15-19, 1983*, pages 591–605. Swets Zeitlinger, 1984.
- [70] S. Stichel. *Betriebsfestigkeitsberechnung bei Schienenfahrzeugen anhand von Simulationssrechnungen*. Number 288 in VDI-Fortschrittsberichte Reihe 12. VDI-Verlag, Düsseldorf, 1996.
- [71] G. Strang. *Lineare Algebra*. Springer-Verlag Berlin Heidelberg, 2003. German translation of: G. Strang, *Introduction to Linear Algebra*, Wellesley-Cambridge Press, 1998.
- [72] T. Szolc. Medium frequency dynamic investigation of the railway wheelset-track system using a discrete-continuous model. *Archive of Applied Mechanics*, 68:30–45, 1998.
- [73] T. Szolc. Simulation of dynamic interaction between the railway bogie and the track in the medium frequency range. *Multibody System Dynamics*, 6:99–122, 2001.
- [74] T. Triantafyllidis and B. Prange. Mitgeführte Biegelinie beim Hochgeschwindigkeitszug „ICE“ – Teil I: Theoretische Grundlagen. *Archive of Applied Mechanics*, 64:154–168, 1994.
- [75] T. Triantafyllidis and B. Prange. Mitgeführte Biegelinie beim Hochgeschwindigkeitszug „ICE“ – Teil II: Vergleich zwischen theoretischen und experimentellen Ergebnissen. *Archive of Applied Mechanics*, 64:169–179, 1994.
- [76] P. van Bommel. *Application de la theorie des vibrations non-lineaires sur le probleme du mouvement de lacet d'un vehicule de chemin de fer*. PhD thesis, Technical University Delft, 1964.
- [77] G.K.W. Vohla. *Werkzeuge zur realitätsnahen Simulation der Laufdynamik von Schienenfahrzeugen*. Number 270 in VDI-Fortschrittsberichte Reihe 12. VDI-Verlag, Düsseldorf, 1996.
- [78] E.A.H. Vollebregt, C. Weidemann, and A. Kienberger. Use of “CONTACT” in multi-body vehicle dynamics and profile wear simulation: Initial results. In *Proceedings of the 22nd IAVSD Symposium, held at Manchester Metropolitan University, August 14-19, 2011*, 2011.
- [79] C. Weidemann. *Fahrdynamik und Verschleiß starrer und gummigefederter Eisenbahnräder*. Shaker-Verlag, Aachen, 2001.
- [80] A.H. Wickens. *Fundamentals of Rail Vehicle Dynamics – Guidance and Stability*. Swets & Zeitlinger Publishers, Lisse, 2003.
- [81] Y. Wu. *Semianalytische Gleismodelle zur Simulation der mittel- und hochfrequenten Fahrzeug/Fahrweg-Dynamik*. Number 325 in VDI-Fortschrittsberichte Reihe 12. VDI-Verlag, Düsseldorf, 1997.

-
- [82] X. Xiao, X. Jin, Z. Wen, M. Zhu, and W. Zhang. Effect of tangent track buckle on vehicle derailment. *Multibody System Dynamics*, 25:1–41, 2011.
- [83] W. Zhai, K. Wang, and C. Cai. Fundamentals of vehicle-track coupled dynamics. *Vehicle System Dynamics*, 47:1349–1376, 2009.
- [84] O.C. Zienkiewicz and R.L. Taylor. *The Finite Element Method*, volume 1. Butterworth Heinemann, Oxford, 5th edition, 2000.

Appendix A

Mathematical basics

A.1 Summation

A sum of elements X_k is given by:

$$\sum_{k=k_{\min}}^{k_{\max}} X_k = X_{k_{\min}} + X_{k_{\min}+1} + \dots + X_{k_{\max}-1} + X_{k_{\max}}, \quad k, k_{\min}, k_{\max} \in \mathbb{Z}, \quad k_{\min} \leq k \leq k_{\max} \quad (\text{A.1.1})$$

Here, k is the summation index; its range is limited by the lower bound k_{\min} and the upper bound k_{\max} . In some cases it is useful to adapt the summation index. A frequently used adaptation is the shifting of the summation index; Here, a new summation index l is introduced, for which it is valid:

$$l = k + c \Leftrightarrow k = l - c, \quad c, l \in \mathbb{Z} \quad (\text{A.1.2})$$

The range of the new summation index l is determined in the following way:

$$k_{\min} \leq k = l - c \leq k_{\max} \Rightarrow k_{\min} + c \leq l \leq k_{\max} + c \quad (\text{A.1.3})$$

Based on (A.1.2) and (A.1.3)

$$\sum_{k=k_{\min}}^{k_{\max}} X_k = \sum_{l=k_{\min}+c}^{k_{\max}+c} X_{l-c} \quad (\text{A.1.4})$$

Another possible adaptation is to change the sign of the summation index; here, the following substitution is used:

$$l = -k, \quad k_{\min} \leq k \leq k_{\max} \Rightarrow -k_{\min} \geq -k = l \geq -k_{\max} \Rightarrow -k_{\max} \leq l \leq -k_{\min} \quad (\text{A.1.5})$$

Generally, the upper bound has to be greater or equal the lower bound. Since the addition is a commutative operation, the sequence of the summands does not affect the result. Thereby, it can be formulated:

$$\sum_{k=k_{\min}}^{k_{\max}} X_k = \sum_{l=-k_{\max}}^{-k_{\min}} X_{-l} \quad (\text{A.1.6})$$

Furthermore, a sum can be split up in the following way:

$$k_{\min} \leq k_0 \leq k_{\max} - 1 \Rightarrow \sum_{k=k_{\min}}^{k_{\max}} X_k = \sum_{k=k_{\min}}^{k_0} X_k + \sum_{k=k_0+1}^{k_{\max}} X_k \quad (\text{A.1.7})$$

If the lower bound k_{\min} and the upper bound k_{\max} only differ by the sign, i.e.:

$$k_{\max} = -k_{\min} = \hat{k} > 0 \quad (\text{A.1.8})$$

then the sum can be reformulated by splitting it up into two partial sums and a single summand, applying the substitutions $l = -k$ and $l = k$ to the first and the second partial sum and merging the two partial sums. Thereby, it is obtained:

$$\sum_{k=-\hat{k}}^{\hat{k}} X_k = \sum_{k=-\hat{k}}^{-1} X_k + X_0 + \sum_{k=1}^{\hat{k}} X_k = \sum_{l=1}^{\hat{k}} X_{-l} + X_0 + \sum_{l=1}^{\hat{k}} X_{-l} = X_0 + \sum_{l=1}^{\hat{k}} (X_l + X_{-l}) \quad (\text{A.1.9})$$

This transformation of the sum is particularly useful if there is a special relation between the summands X_l and X_{-l} , e.g. $X_l = X_{-l}$ or $X_l = -X_{-l}$.

A.2 Complex numbers

A complex number $z \in \mathbb{C}$ can be expressed in the following way:

$$z = a + ib = \Re z + i\Im z, \quad a, b \in \mathbb{R}, \quad a = \Re z, \quad b = \Im z, \quad i^2 = -1 \quad (\text{A.2.10})$$

Here, a is the real part of z , b is the imaginary part of z , and i is the imaginary unit. For each complex number z , the geometric sum of the real part and the imaginary part is defined as its absolute value $|z|$:

$$|z| = \sqrt{\Re z^2 + \Im z^2}, \quad |z| \in \mathbb{R} \quad (\text{A.2.11})$$

The addition and the subtraction of two complex numbers z_1 and z_2 are given by:

$$z_1 + z_2 = \underbrace{\Re z_1 + i\Im z_1}_{z_1} + \underbrace{\Re z_2 + i\Im z_2}_{z_2} = \underbrace{\Re z_1 + \Re z_2}_{\Re(z_1+z_2)} + i \underbrace{(\Im z_1 + \Im z_2)}_{\Im(z_1+z_2)} \quad (\text{A.2.12})$$

$$z_1 - z_2 = \underbrace{\Re z_1 + i\Im z_1}_{z_1} - \underbrace{(\Re z_2 + i\Im z_2)}_{z_2} = \underbrace{\Re z_1 - \Re z_2}_{\Re(z_1-z_2)} + i \underbrace{(\Im z_1 - \Im z_2)}_{\Im(z_1-z_2)} \quad (\text{A.2.13})$$

It can be seen that the real parts and the imaginary parts can be added and subtracted separately.

$$\Re(z_1 + z_2) = \Re z_1 + \Re z_2, \quad \Im(z_1 + z_2) = \Im z_1 + \Im z_2 \quad (\text{A.2.14})$$

$$\Re(z_1 - z_2) = \Re z_1 - \Re z_2, \quad \Im(z_1 - z_2) = \Im z_1 - \Im z_2 \quad (\text{A.2.15})$$

By applying the relation $i^2 = -1$ the product of two complex numbers z_1 and z_2 is obtained to:

$$\begin{aligned} z_1 z_2 &= \underbrace{(\Re z_1 + i\Im z_1)}_{z_1} \underbrace{(\Re z_2 + i\Im z_2)}_{z_2} = \Re z_1 \Re z_2 + i\Re z_1 \Im z_2 + i\Im z_1 \Re z_2 + i^2 \Im z_1 \Im z_2 \\ &= \underbrace{\Re z_1 \Re z_2 - \Im z_1 \Im z_2}_{\Re(z_1 z_2)} + i \underbrace{(\Re z_1 \Im z_2 + \Im z_1 \Re z_2)}_{\Im(z_1 z_2)} \end{aligned} \quad (\text{A.2.16})$$

The complex conjugate \bar{z} of a complex number z is obtained by changing the sign of the imaginary part:

$$z = \Re z + i\Im z \Rightarrow \bar{z} = \Re z - i\Im z \quad (\text{A.2.17})$$

From this it follows for the sum and the difference and the product of a complex number z and its conjugate complex \bar{z} :

$$z + \bar{z} = \underbrace{\Re z + i\Im z}_z + \underbrace{\Re z - i\Im z}_{\bar{z}} = 2\Re z \quad (\text{A.2.18})$$

$$z - \bar{z} = \underbrace{\Re z + i\Im z}_z - \underbrace{(\Re z - i\Im z)}_{\bar{z}} = 2i\Im z \quad (\text{A.2.19})$$

The product of z and \bar{z} is obtained to:

$$z\bar{z} = \underbrace{(\Re z + i\Im z)}_z \underbrace{(\Re z - i\Im z)}_{\bar{z}} = \Re z^2 - i^2\Im z^2 = \Re z^2 + \Im z^2 \Rightarrow \sqrt{z\bar{z}} = |z| \quad (\text{A.2.20})$$

For the sum and the difference of two complex conjugates \bar{z}_1 and \bar{z}_2 it is valid:

$$\bar{z}_1 + \bar{z}_2 = \underbrace{\Re z_1 - i\Im z_1}_{\bar{z}_1} + \underbrace{\Re z_2 - i\Im z_2}_{\bar{z}_2} = \underbrace{\Re z_1 + \Re z_2}_{\Re(z_1+z_2)} - i \underbrace{(\Im z_1 + \Im z_2)}_{\Im(z_1+z_2)} = \overline{z_1 + z_2} \quad (\text{A.2.21})$$

$$\bar{z}_1 - \bar{z}_2 = \underbrace{\Re z_1 - i\Im z_1}_{\bar{z}_1} - \underbrace{(\Re z_2 - i\Im z_2)}_{\bar{z}_2} = \underbrace{\Re z_1 - \Re z_2}_{\Re(z_1-z_2)} - i \underbrace{(\Im z_1 - \Im z_2)}_{\Im(z_1-z_2)} = \overline{z_1 - z_2} \quad (\text{A.2.22})$$

The evaluation of the product leads to:

$$\begin{aligned} \bar{z}_1 \bar{z}_2 &= \underbrace{(\Re z_1 - i\Im z_1)}_{\bar{z}_1} \underbrace{(\Re z_2 - i\Im z_2)}_{\bar{z}_2} = \Re z_1 \Re z_2 - i\Re z_1 \Im z_2 - i\Im z_1 \Re z_2 + i^2 \Im z_1 \Im z_2 \\ &= \underbrace{\Re z_1 \Re z_2 - \Im z_1 \Im z_2}_{\Re(z_1 z_2)} - i \underbrace{(\Re z_1 \Im z_2 + \Im z_1 \Re z_2)}_{\Im(z_1 z_2)} = \overline{z_1 z_2} \end{aligned} \quad (\text{A.2.23})$$

It turns out the addition, the subtraction and the multiplication on the one hand and the conjugation on the other hand can be carried out independently, i.e. the sum, the difference and the product of two complex conjugates are equal to the complex conjugates of the sum, the difference and the product, respectively. By combining the relations it is obtained:

$$\overline{z_1 z_2 + z_3 z_4} = \overline{z_1 z_2} + \overline{z_3 z_4} = \bar{z}_1 \bar{z}_2 + \bar{z}_3 \bar{z}_4 \quad (\text{A.2.24})$$

$$\overline{z_1 z_2 - z_3 z_4} = \overline{z_1 z_2} - \overline{z_3 z_4} = \bar{z}_1 \bar{z}_2 - \bar{z}_3 \bar{z}_4 \quad (\text{A.2.25})$$

A.3 Exponential function for complex exponents

For the exponential function it is valid:

$$z \in \mathbb{C} : e^z = e^{\Re z + i\Im z} = e^{\Re z} e^{i\Im z} \quad (\text{A.3.26})$$

The function $e^{i\Im z}$, which has an imaginary exponent, is evaluated by applying Euler's relation:

$$\phi \in \mathbb{R} : e^{i\phi} = \cos \phi + i \sin \phi \Rightarrow \Re e^{i\phi} = \cos \phi, \Im e^{i\phi} = \sin \phi \quad (\text{A.3.27})$$

By applying the symmetry properties of the sine function and of the cosine function it is obtained:

$$e^{-i\phi} = \cos(-\phi) + i \sin(-\phi) = \cos \phi - i \sin \phi = \Re e^{i\phi} - i \Im e^{i\phi} = \overline{e^{i\phi}} \Rightarrow e^{-i\phi} = \overline{e^{i\phi}} \quad (\text{A.3.28})$$

Based on this, the functions $\cos \phi$ and $\sin \phi$ can be expressed in the following way:

$$e^{i\phi} + e^{-i\phi} = \cos \phi + i \sin \phi + \cos \phi - i \sin \phi = 2 \cos \phi \Rightarrow \cos \phi = \frac{e^{i\phi} + e^{-i\phi}}{2} \quad (\text{A.3.29})$$

$$e^{i\phi} - e^{-i\phi} = \cos \phi + i \sin \phi - (\cos \phi - i \sin \phi) = 2i \sin \phi \Rightarrow \sin \phi = \frac{e^{i\phi} - e^{-i\phi}}{2i} \quad (\text{A.3.30})$$

By applying the relation:

$$i^2 = -1 \Rightarrow 1 = -i^2 \Rightarrow i^{-1} = -i^2 \cdot i^{-1} = -i \quad (\text{A.3.31})$$

the expression (A.3.30) can be reformulated in the following way:

$$\sin \phi = \frac{e^{i\phi} - e^{-i\phi}}{2i} = i \frac{e^{-i\phi} - e^{i\phi}}{2} \quad (\text{A.3.32})$$

For the sine function and for the cosine function it is valid:

$$m \in \mathbb{Z} : \sin(2\pi m) = 0, \cos(2\pi m) = 1 \quad (\text{A.3.33})$$

The cosine function $\cos \phi$ assumes the value 1 if and only if ϕ is an integer multiple of 2π . From this, it follows:

$$m \in \mathbb{Z} \Leftrightarrow e^{2\pi m i} = \underbrace{\cos(2\pi m)}_1 + i \underbrace{\sin(2\pi m)}_0 = 1 \quad (\text{A.3.34})$$

It should be pointed out that the deduction can be made in both directions: If m is an integer, then the expression $e^{2\pi m i}$ is equal to 1. Conversely, it can be deduced from $e^{2\pi m i} = 1$ that m is an integer.

A.4 Polynomial interpolation

If a function $f(\xi)$ is given for discrete arguments ξ_i , an interpolation is used to determine the functions for other arguments $\xi \neq \xi_i$ than the given ones. One method for this purpose is the interpolation using Lagrangian polynomials $\ell_k(\xi)$. Here, the function $f(\xi)$ is described in the following way:

$$f(\xi) = \sum_{i=1}^N f(\xi_i) \ell_i(\xi) \quad (\text{A.4.35})$$

It should be noted that the indexing is arbitrary, i.e. the range of i does not necessarily have to start at $i = 1$. The interpolation polynomials are chosen in such a way that it is valid:

$$\ell_i(\xi_k) = \begin{cases} 1 & \text{for } i = k \\ 0 & \text{for } i \neq k \end{cases} \quad (\text{A.4.36})$$

If the arguments $\xi_1, \xi_2, \dots, \xi_{i-1}, \xi_i, \xi_{i+1}, \dots, \xi_{n-1}, \xi_n$ are given, then the polynomial $\ell_i(x)$, which fulfills the criterion (A.4.36) is constructed in the following way:

$$\ell_i(x) = \frac{\xi - \xi_1}{\xi_i - \xi_1} \cdot \frac{\xi - \xi_2}{\xi_i - \xi_2} \cdot \dots \cdot \frac{\xi - \xi_{i-1}}{\xi_i - \xi_{i-1}} \cdot \frac{\xi - \xi_{i+1}}{\xi_i - \xi_{i+1}} \cdot \dots \cdot \frac{\xi - \xi_{n-1}}{\xi_i - \xi_{n-1}} \cdot \frac{\xi - \xi_n}{\xi_i - \xi_n} \quad (\text{A.4.37})$$

For $\xi = \xi_k$, $k \neq i$, the linear factor $\xi - \xi_k$ vanishes, so that the fraction $\frac{\xi - \xi_k}{\xi_i - \xi_k}$ and thereby the complete product are zero. For $\xi = \xi_i$ the numerator and the denominator for each fraction are equal, so that each fraction and thereby the complete product is equal to 1.

The interpolation is also helpful for the approximation of the derivative $f'(\xi)$, since the polynomials $\ell_i(\xi)$ are continuous functions and can therefore be differentiated. Based on (A.4), the derivative $f'(\xi)$ is obtained to:

$$f'(\xi) = \frac{df(\xi)}{d\xi} = \sum_{i=1}^N f(\xi_i) \ell'_i(\xi) \quad (\text{A.4.38})$$

The interpolation can also be applied to vectors in order to describe an interpolation curve between discrete points within space. Here, the variable ξ is used as a curve parameter and the scalar values $f(\xi_i)$ are replaced by the vectors \mathbf{r}_i , which indicate the position of the i -th point within space. Thereby, the curve is described by:

$$\mathbf{r}(\xi) = \sum_{i=1}^N \mathbf{r}_i \ell_i(\xi) \quad (\text{A.4.39})$$

In this case, it is reasonable to use “simple” values for the parameter ξ like e.g. $\xi = i$; in this case, however, the sequence of the given points is important. For instance, a spatial curve shall be described, which successively passes through three points P_{-1} , P_0 and P_1 described by the three vectors \mathbf{r}_{-1} , \mathbf{r}_0 and \mathbf{r}_1 . By using the arguments $\xi_i = i$ the polynomials $\ell_i(\xi)$ are obtained to:

$$\ell_{-1}(\xi) = \frac{\xi - \xi_0}{\xi_{-1} - \xi_0} \frac{\xi - \xi_1}{\xi_{-1} - \xi_1} = \frac{\xi - 0}{-1 - 0} \frac{\xi - 1}{-1 - 1} = \frac{1}{2}\xi(\xi - 1) = \frac{1}{2}\xi^2 - \frac{1}{2}\xi \quad (\text{A.4.40})$$

$$\ell_0(\xi) = \frac{\xi - \xi_{-1}}{\xi_0 - \xi_{-1}} \frac{\xi - \xi_1}{\xi_0 - \xi_1} = \frac{\xi - (-1)}{0 - (-1)} \frac{\xi - 1}{0 - 1} = -(\xi + 1)(\xi - 1) = -\xi^2 + 1 \quad (\text{A.4.41})$$

$$\ell_1(\xi) = \frac{\xi - \xi_{-1}}{\xi_1 - \xi_{-1}} \frac{\xi - \xi_0}{\xi_1 - \xi_0} = \frac{\xi - (-1)}{1 - (-1)} \frac{\xi - 0}{1 - 0} = \frac{1}{2}(\xi + 1)\xi = \frac{1}{2}\xi^2 + \frac{1}{2}\xi \quad (\text{A.4.42})$$

The tangential vector \mathbf{t} is determined by deriving the vector function $\mathbf{r}(\xi)$, which describes the curve, with respect to the curve parameter ξ . For the derivatives $\ell'_i(\xi)$ of the polynomials it is obtained:

$$\ell_{-1}(\xi) = \frac{1}{2}\xi^2 - \frac{1}{2}\xi \Rightarrow \ell'_{-1}(\xi) = \xi - \frac{1}{2} \quad (\text{A.4.43})$$

$$\ell_0(\xi) = -\xi^2 + 1 \Rightarrow \ell'_0(\xi) = -2\xi \quad (\text{A.4.44})$$

$$\ell_1(\xi) = \frac{1}{2}\xi^2 + \frac{1}{2}\xi \Rightarrow \ell'_1(\xi) = \xi + \frac{1}{2} \quad (\text{A.4.45})$$

In total, the curve and the tangential vector are described by the following formulations:

$$\mathbf{r}(\xi) = \frac{1}{2}(\xi^2 - \xi)\mathbf{r}_{-1} + (-\xi^2 + 1)\mathbf{r}_0 + \frac{1}{2}(\xi^2 + \xi)\mathbf{r}_1 \quad (\text{A.4.46})$$

$$\mathbf{t}(\xi) = \mathbf{r}'(\xi) = \left(\xi - \frac{1}{2}\right)\mathbf{r}_{-1} - 2\xi\mathbf{r}_0 + \left(\xi + \frac{1}{2}\right)\mathbf{r}_1 \quad (\text{A.4.47})$$

For the tangential vector at the point P_0 it is obtained:

$$\mathbf{t}(\xi = 0) = -\frac{1}{2}\mathbf{r}_{-1} + \frac{1}{2}\mathbf{r}_1 = \frac{1}{2}(\mathbf{r}_1 - \mathbf{r}_{-1}) \quad (\text{A.4.48})$$

A.5 Matrices and vectors

Matrices and vectors are a very useful notation for many mathematical problems.

In the following sections, some important relations, which are used in this work, shall be developed and considered.

A.5.1 Vector product

The vector product or cross product is defined only for vectors of the three dimensional space. The vector product of the two vectors $\mathbf{a} \in \mathbb{R}^3$ and $\mathbf{b} \in \mathbb{R}^3$ is given by:

$$\mathbf{a} \times \mathbf{b} = \begin{bmatrix} a_1 \\ a_2 \\ a_3 \end{bmatrix} \times \begin{bmatrix} b_1 \\ b_2 \\ b_3 \end{bmatrix} = \begin{bmatrix} a_2b_3 - a_3b_2 \\ a_3b_1 - a_1b_3 \\ a_1b_2 - a_2b_1 \end{bmatrix} \quad (\text{A.5.49})$$

By changing the sequence of the vectors it is obtained:

$$\mathbf{b} \times \mathbf{a} = \begin{bmatrix} b_1 \\ b_2 \\ b_3 \end{bmatrix} \times \begin{bmatrix} a_1 \\ a_2 \\ a_3 \end{bmatrix} = \begin{bmatrix} b_2a_3 - b_3a_2 \\ b_3a_1 - b_1a_3 \\ b_1a_2 - b_2a_1 \end{bmatrix} = - \begin{bmatrix} a_2b_3 - a_3b_2 \\ a_3b_1 - a_1b_3 \\ a_1b_2 - a_2b_1 \end{bmatrix} = -\mathbf{a} \times \mathbf{b} \quad (\text{A.5.50})$$

From this, it follows:

$$\mathbf{b} \times \mathbf{a} = -\mathbf{a} \times \mathbf{b} \Rightarrow \mathbf{a} \times \mathbf{a} = -\mathbf{a} \times \mathbf{a} \Rightarrow 2\mathbf{a} \times \mathbf{a} = \mathbf{0} \Rightarrow \mathbf{a} \times \mathbf{a} = \mathbf{0} \quad (\text{A.5.51})$$

The norm of the vector product is obtained to:

$$(\mathbf{a} \times \mathbf{b}) \cdot (\mathbf{a} \times \mathbf{b}) = (a_2b_3 - a_3b_2)^2 + (a_3b_1 - a_1b_3)^2 + (a_1b_2 - a_2b_1)^2 \quad (\text{A.5.52})$$

$$|\mathbf{a} \times \mathbf{b}| = \sqrt{(\mathbf{a} \times \mathbf{b}) \cdot (\mathbf{a} \times \mathbf{b})} = \sqrt{(a_2b_3 - a_3b_2)^2 + (a_3b_1 - a_1b_3)^2 + (a_1b_2 - a_2b_1)^2} \quad (\text{A.5.53})$$

The three summands can be evaluated according to the following scheme

$$(a_ib_k - a_kb_i)^2 = a_i^2b_k^2 - 2a_ib_ka_kb_i + a_k^2b_i^2 = a_i^2b_k^2 + a_k^2b_i^2 - a_ib_ka_kb_i - a_kb_ka_ib_i \quad (\text{A.5.54})$$

Based on this scheme it is obtained:

$$\begin{aligned} (\mathbf{a} \times \mathbf{b}) \cdot (\mathbf{a} \times \mathbf{b}) &= (a_2b_3 - a_3b_2)^2 + (a_3b_1 - a_1b_3)^2 + (a_1b_2 - a_2b_1)^2 \\ &= a_2^2b_3^2 + a_3^2b_2^2 - a_2b_2a_3b_3 - a_3b_3a_2b_2 \\ &\quad + a_3^2b_1^2 + a_1^2b_3^2 - a_3b_3a_1b_1 - a_1b_1a_3b_3 \\ &\quad + a_1^2b_2^2 + a_2^2b_1^2 - a_1b_1a_2b_2 - a_2b_2a_1b_1 \\ &= a_1^2(b_2^2 + b_3^2) - a_1b_1(a_2b_2 + a_3b_3) \\ &\quad + a_2^2(b_1^2 + b_3^2) - a_2b_2(a_1b_1 + a_3b_3) \\ &\quad + a_3^2(b_1^2 + b_2^2) - a_3b_3(a_1b_1 + a_2b_2) \end{aligned} \quad (\text{A.5.55})$$

For further evaluation terms of the following structure are added:

$$0 = (a_ib_i)^2 - (a_ib_i)^2 = a_i^2b_i^2 - (a_ib_i)^2 \quad (\text{A.5.56})$$

Using this leads to:

$$\begin{aligned}
(\mathbf{a} \times \mathbf{b}) \cdot (\mathbf{a} \times \mathbf{b}) &= a_1^2 (b_2^2 + b_3^2) + a_1^2 b_1^2 - (a_1 b_1)^2 - a_1 b_1 (a_2 b_2 + a_3 b_3) \\
&\quad + a_2^2 (b_1^2 + b_3^2) + a_2^2 b_2^2 - (a_2 b_2)^2 - a_2 b_2 (a_1 b_1 + a_3 b_3) \\
&\quad + a_3^2 (b_1^2 + b_2^2) + a_3^2 b_3^2 - (a_3 b_3)^2 - a_3 b_3 (a_1 b_1 + a_2 b_2) \\
&= a_1^2 (b_1^2 + b_2^2 + b_3^2) - a_1 b_1 (a_1 b_1 + a_2 b_2 + a_3 b_3) \\
&\quad + a_2^2 (b_1^2 + b_2^2 + b_3^2) - a_2 b_2 (a_1 b_1 + a_2 b_2 + a_3 b_3) \\
&\quad + a_3^2 (b_1^2 + b_2^2 + b_3^2) - a_3 b_3 (a_1 b_1 + a_2 b_2 + a_3 b_3) \\
&= (a_1^2 + a_2^2 + a_3^2) (b_1^2 + b_2^2 + b_3^2) \\
&\quad - (a_1 b_1 + a_2 b_2 + a_3 b_3) (a_1 b_1 + a_2 b_2 + a_3 b_3) \\
&= |\mathbf{a}|^2 |\mathbf{b}|^2 - (\mathbf{a} \cdot \mathbf{b})^2
\end{aligned} \tag{A.5.57}$$

In total, it is valid for the norm:

$$|\mathbf{a} \times \mathbf{b}| = \sqrt{(\mathbf{a} \times \mathbf{b}) \cdot (\mathbf{a} \times \mathbf{b})} = \sqrt{|\mathbf{a}|^2 |\mathbf{b}|^2 - (\mathbf{a} \cdot \mathbf{b})^2} \tag{A.5.58}$$

A.5.2 Scalar triple product

The scalar triple product is defined for vectors of the three-dimensional space. For the three vectors $\mathbf{a} \in \mathbb{R}^3$, $\mathbf{b} \in \mathbb{R}^3$ and $\mathbf{c} \in \mathbb{R}^3$ the scalar triple product can be formulated in the following way:

$$\begin{aligned}
\mathbf{a} \cdot (\mathbf{b} \times \mathbf{c}) &= \begin{bmatrix} a_1 \\ a_2 \\ a_3 \end{bmatrix} \cdot \left(\begin{bmatrix} b_1 \\ b_2 \\ b_3 \end{bmatrix} \times \begin{bmatrix} c_1 \\ c_2 \\ c_3 \end{bmatrix} \right) = \begin{bmatrix} a_1 \\ a_2 \\ a_3 \end{bmatrix} \cdot \begin{bmatrix} b_2 c_3 - b_3 c_2 \\ b_3 c_1 - b_1 c_3 \\ b_1 c_2 - b_2 c_1 \end{bmatrix} \\
&= a_1 (b_2 c_3 - b_3 c_2) + a_2 (b_3 c_1 - b_1 c_3) + a_3 (b_1 c_2 - b_2 c_1) \\
&= a_1 b_2 c_3 + a_2 b_3 c_1 + a_3 b_1 c_2 - a_3 b_2 c_1 - a_2 b_1 c_3 - a_1 b_3 c_2
\end{aligned} \tag{A.5.59}$$

An alternative method to evaluate the scalar triple product is to compute the determinant of the matrix composed of the three column vectors \mathbf{a} , \mathbf{b} and \mathbf{c} by using the rule of Sarrus:

$$\begin{aligned}
\det [\mathbf{a} \ \mathbf{b} \ \mathbf{c}] &= \det \begin{bmatrix} a_1 & b_1 & c_1 \\ a_2 & b_2 & c_2 \\ a_3 & b_3 & c_3 \end{bmatrix} \\
&= a_1 b_2 c_3 + b_1 a_2 c_3 + c_1 a_2 b_3 - a_3 b_2 c_1 - b_3 c_2 a_1 - c_3 a_2 b_1 \\
&= a_1 b_2 c_3 + a_2 b_1 c_3 + a_2 b_3 c_1 - a_3 b_2 c_1 - a_2 b_1 c_3 - a_1 b_3 c_2
\end{aligned} \tag{A.5.60}$$

A cyclic permutation of the vectors leads to the following result:

$$\begin{aligned}
\mathbf{b} \cdot (\mathbf{c} \times \mathbf{a}) &= \begin{bmatrix} b_1 \\ b_2 \\ b_3 \end{bmatrix} \cdot \left(\begin{bmatrix} c_1 \\ c_2 \\ c_3 \end{bmatrix} \times \begin{bmatrix} a_1 \\ a_2 \\ a_3 \end{bmatrix} \right) = \begin{bmatrix} b_1 \\ b_2 \\ b_3 \end{bmatrix} \cdot \begin{bmatrix} c_2 a_3 - c_3 a_2 \\ c_3 a_1 - c_1 a_3 \\ c_1 a_2 - c_2 a_1 \end{bmatrix} \\
&= (c_2 a_3 - c_3 a_2) b_1 + (c_3 a_1 - c_1 a_3) b_2 + (c_1 a_2 - c_2 a_1) b_3 \\
&= a_1 b_2 c_3 + a_2 b_3 c_1 + a_3 b_1 c_2 - a_3 b_2 c_1 - a_2 b_1 c_3 - a_1 b_3 c_2
\end{aligned} \tag{A.5.61}$$

$$\begin{aligned}
\mathbf{c} \cdot (\mathbf{a} \times \mathbf{b}) &= \begin{bmatrix} c_1 \\ c_2 \\ c_3 \end{bmatrix} \cdot \left(\begin{bmatrix} a_1 \\ a_2 \\ a_3 \end{bmatrix} \times \begin{bmatrix} b_1 \\ b_2 \\ b_3 \end{bmatrix} \right) = \begin{bmatrix} c_1 \\ c_2 \\ c_3 \end{bmatrix} \cdot \begin{bmatrix} a_2 b_3 - a_3 b_2 \\ a_3 b_1 - a_1 b_3 \\ a_1 b_2 - a_2 b_1 \end{bmatrix} \\
&= c_1 (a_2 b_3 - a_3 b_2) + c_2 (a_3 b_1 - a_1 b_3) + c_3 (a_1 b_2 - a_2 b_1) \\
&= a_1 b_2 c_3 + a_2 b_3 c_1 + a_3 b_1 c_2 - a_3 b_2 c_1 - a_2 b_1 c_3 - a_1 b_3 c_2
\end{aligned} \tag{A.5.62}$$

Therefore, it is valid:

$$\mathbf{a} \cdot (\mathbf{b} \times \mathbf{c}) = \mathbf{b} \cdot (\mathbf{c} \times \mathbf{a}) = \mathbf{c} \cdot (\mathbf{a} \times \mathbf{b}) \quad (\text{A.5.63})$$

If two vectors of the scalar triple product are equal, then the product vanishes:

$$(\mathbf{a} \times \mathbf{b}) \cdot \mathbf{a} = \underbrace{(\mathbf{a} \times \mathbf{a})}_{\mathbf{0}} \cdot \mathbf{b} = 0 \quad (\text{A.5.64})$$

A.5.3 Vector triple product

The vector triple product is based on the vector product so that it can only be applied to three-dimensional vectors. The vector triple product \mathbf{x} of the vectors $\mathbf{a} \in \mathbb{R}^3$, $\mathbf{b} \in \mathbb{R}^3$ and $\mathbf{c} \in \mathbb{R}^3$ is given by:

$$\mathbf{x} = \mathbf{a} \times (\mathbf{b} \times \mathbf{c}) \quad (\text{A.5.65})$$

The evaluation of the product leads to:

$$\begin{aligned} \mathbf{x} &= \begin{bmatrix} a_1 \\ a_2 \\ a_3 \end{bmatrix} \times \left(\begin{bmatrix} b_1 \\ b_2 \\ b_3 \end{bmatrix} \times \begin{bmatrix} c_1 \\ c_2 \\ c_3 \end{bmatrix} \right) = \begin{bmatrix} a_1 \\ a_2 \\ a_3 \end{bmatrix} \times \begin{bmatrix} b_2 c_3 - b_3 c_2 \\ b_3 c_1 - b_1 c_3 \\ b_1 c_2 - b_2 c_1 \end{bmatrix} \\ &= \begin{bmatrix} a_2 (b_1 c_2 - b_2 c_1) - a_3 (b_3 c_1 - b_1 c_3) \\ a_3 (b_2 c_3 - b_3 c_2) - a_1 (b_1 c_2 - b_2 c_1) \\ a_1 (b_3 c_1 - b_1 c_3) - a_2 (b_2 c_3 - b_3 c_2) \end{bmatrix} \end{aligned} \quad (\text{A.5.66})$$

By factoring out b_i and c_i in the i -th component it is obtained:

$$\begin{aligned} \mathbf{x} &= \begin{bmatrix} a_2 (b_1 c_2 - b_2 c_1) - a_3 (b_3 c_1 - b_1 c_3) \\ a_3 (b_2 c_3 - b_3 c_2) - a_1 (b_1 c_2 - b_2 c_1) \\ a_1 (b_3 c_1 - b_1 c_3) - a_2 (b_2 c_3 - b_3 c_2) \end{bmatrix} = \begin{bmatrix} a_2 b_1 c_2 - a_2 b_2 c_1 - a_3 b_3 c_1 + a_3 b_1 c_3 \\ a_3 b_2 c_3 - a_3 b_3 c_2 - a_1 b_1 c_2 + a_1 b_2 c_1 \\ a_1 b_3 c_1 - a_1 b_1 c_3 - a_2 b_2 c_3 + a_2 b_3 c_2 \end{bmatrix} \\ &= \begin{bmatrix} b_1 (a_2 c_2 + a_3 c_3) - c_1 (a_2 b_2 + a_3 b_3) \\ b_2 (a_1 c_1 + a_3 c_3) - c_2 (a_1 b_1 + a_3 b_3) \\ b_3 (a_1 c_1 + a_2 c_2) - c_3 (a_1 b_1 + a_2 b_2) \end{bmatrix} \end{aligned} \quad (\text{A.5.67})$$

Adding $a_i b_i c_i - a_i b_i c_i = 0$ to the i -th component of the vector and again factoring out b_i and c_i leads to:

$$\begin{aligned} \mathbf{x} &= \begin{bmatrix} b_1 (a_2 c_2 + a_3 c_3) + a_1 b_1 c_1 - a_1 b_1 c_1 - c_1 (a_2 b_2 + a_3 b_3) \\ b_2 (a_1 c_1 + a_3 c_3) + a_2 b_2 c_2 - a_2 b_2 c_2 - c_2 (a_1 b_1 + a_3 b_3) \\ b_3 (a_1 c_1 + a_2 c_2) + a_3 b_3 c_3 - a_3 b_3 c_3 - c_3 (a_1 b_1 + a_2 b_2) \end{bmatrix} \\ &= \begin{bmatrix} b_1 (a_1 c_1 + a_2 c_2 + a_3 c_3) - c_1 (a_1 b_1 + a_2 b_2 + a_3 b_3) \\ b_2 (a_1 c_1 + a_2 c_2 + a_3 c_3) - c_2 (a_1 b_1 + a_2 b_2 + a_3 b_3) \\ b_3 (a_1 c_1 + a_2 c_2 + a_3 c_3) - c_3 (a_1 b_1 + a_2 b_2 + a_3 b_3) \end{bmatrix} \end{aligned} \quad (\text{A.5.68})$$

The terms contained in the brackets can be interpreted as the scalar products $\mathbf{a} \cdot \mathbf{c}$ and $\mathbf{a} \cdot \mathbf{b}$. By splitting the vector into two separate vectors and factoring out these terms, it is obtained:

$$\begin{aligned} \mathbf{x} &= \begin{bmatrix} b_1 (a_1 c_1 + a_2 c_2 + a_3 c_3) - c_1 (a_1 b_1 + a_2 b_2 + a_3 b_3) \\ b_2 (a_1 c_1 + a_2 c_2 + a_3 c_3) - c_2 (a_1 b_1 + a_2 b_2 + a_3 b_3) \\ b_3 (a_1 c_1 + a_2 c_2 + a_3 c_3) - c_3 (a_1 b_1 + a_2 b_2 + a_3 b_3) \end{bmatrix} \\ &= \begin{bmatrix} b_1 \\ b_2 \\ b_3 \end{bmatrix} (a_1 c_1 + a_2 c_2 + a_3 c_3) - \begin{bmatrix} c_1 \\ c_2 \\ c_3 \end{bmatrix} (a_1 b_1 + a_2 b_2 + a_3 b_3) \\ &= \mathbf{b} (\mathbf{a} \cdot \mathbf{c}) - \mathbf{c} (\mathbf{a} \cdot \mathbf{b}) \end{aligned} \quad (\text{A.5.69})$$

In total, the vector triple product can be expressed in the following way:

$$\mathbf{a} \times (\mathbf{b} \times \mathbf{c}) = \mathbf{b}(\mathbf{a} \cdot \mathbf{c}) - \mathbf{c}(\mathbf{a} \cdot \mathbf{b}) \quad (\text{A.5.70})$$

A.6 Evaluation of geometric series

A geometric series s_n is given in the following way:

$$s_n = \sum_{j=0}^{n-1} q^j, \quad j \in \mathbb{N}_0, \quad n \in \mathbb{N}, \quad q \in \mathbb{C}, \quad q \neq 0 \quad (\text{A.6.71})$$

The case $q = 0$ is excluded because the expression 0^0 is not defined. The case $q = 1$ can be evaluated immediately; since the sum consists of n summands, it is valid:

$$j \in \mathbb{N}_0 : q = 1 \Rightarrow q^j = 1^j = 1 \Rightarrow s_n = \sum_{j=0}^{n-1} q^j = \sum_{j=0}^{n-1} 1 = n \quad (\text{A.6.72})$$

For the case $q \neq 0 \wedge q \neq 1$ the expression s_{n+1} has to be considered. This expression can be formulated in the following way:

$$s_{n+1} = \sum_{j=0}^n q^j = \sum_{j=0}^{n-1} q^j + q^n = s_n + q^n \quad (\text{A.6.73})$$

Alternatively, the sum s_n can be split up in a different way; after this, the shift $J = j - 1$ is applied for the summation index. This leads to:

$$s_{n+1} = \sum_{j=0}^n q^j = q^0 + \sum_{j=1}^n q^j = q^0 + q \sum_{j=1}^n q^{j-1} = 1 + q \sum_{J=0}^{n-1} q^J = 1 + q s_n \quad (\text{A.6.74})$$

By setting the two expressions for s_{n+1} equal it is obtained for s_n :

$$s_{n+1} = 1 + q s_n = s_n + q^n \Rightarrow 1 - q^n = s_n - q s_n = s_n(1 - q) \Rightarrow s_n = \frac{1 - q^n}{1 - q} \quad (\text{A.6.75})$$

In total it is valid:

$$\sum_{j=0}^{n-1} q^j = \begin{cases} n & \text{for } q = 1 \\ \frac{1 - q^n}{1 - q} & \text{for } q \neq 1 \wedge q \neq 0 \end{cases} \quad (\text{A.6.76})$$

Based on this, the sum of the powers ζ^{pj} , $p \in \mathbb{Z}$, of a root of unity can be evaluated. It is valid:

$$\sum_{j=0}^{n-1} \zeta^{pj} = \sum_{j=0}^{n-1} (\zeta^p)^j \Rightarrow q = \zeta^p = \left(e^{\frac{2\pi i}{n}} \right)^p = e^{2\pi \frac{p}{n} i} = \cos\left(2\pi \frac{p}{n}\right) + i \sin\left(2\pi \frac{p}{n}\right) \quad (\text{A.6.77})$$

For an exponential function e^z having a complex argument $z \in \mathbb{C}$ it is valid:

$$z \in \mathbb{C} : e^z = e^{\Re z + i \Im z} = e^{\Re z} e^{i \Im z} = e^{\Re z} (\cos(\Im z) + i \sin(\Im z)) \quad (\text{A.6.78})$$

First, the case $q = \zeta^p = 1$ shall be considered. For the sine function and for the cosine function it is valid:

$$m \in \mathbb{Z} : \cos(2\pi m) = 1, \quad \sin(2\pi m) = 0 \quad (\text{A.6.79})$$

From this, it follows:

$$\frac{p}{n} \in \mathbb{Z} \Rightarrow q = \zeta^p = \cos\left(2\pi\frac{p}{n}\right) + i \sin\left(2\pi\frac{p}{n}\right) = 1 \quad (\text{A.6.80})$$

Since p is an integer, the power ζ^{pn} can be evaluated based on (A.6.79); this leads to:

$$p \in \mathbb{Z} : \zeta^{pn} = \left(e^{\frac{2\pi i}{n}}\right)^{pn} = e^{2\pi pi} = \cos(2\pi p) + i \sin(2\pi p) = 1 \quad (\text{A.6.81})$$

Using this relation, it is obtained for $q = \zeta^p \neq 1$:

$$q = \zeta^p \neq 1 : \frac{1 - (\zeta^p)^n}{1 - \zeta^p} = \frac{1 - \zeta^{pn}}{1 - \zeta^p} = \frac{1 - 1}{1 - \zeta^p} = 0 \quad (\text{A.6.82})$$

In total, the evaluation of the sum of ζ^{pj} over $0 \leq j \leq n-1$ can be formulated in the following way:

$$\sum_{j=0}^{n-1} \zeta^{pj} = \sum_{j=0}^{n-1} e^{2\pi \frac{p}{n} i j} = \begin{cases} n & \text{for } \frac{p}{n} \in \mathbb{Z} \\ 0 & \text{for } \frac{p}{n} \notin \mathbb{Z} \end{cases} \quad (\text{A.6.83})$$

Appendix B

Description of a continuum in cylindrical coordinates

In order to describe the structural deformations of an axisymmetric structure, it is obvious to use cylindrical coordinates. In the present case, the z -axis of the structure is chosen as the axis of symmetry. Thereby, the coordinate y is used as the axial coordinate and thereby remains unchanged, while the cartesian coordinates y and z are replaced by the polar coordinates r and ϕ in the following way:

$$x = r \sin \phi, \quad z = r \cos \phi \quad (\text{B.0.1})$$

Furthermore, also the description of the displacement is adapted to the cylindrical coordinates so that the displacement is expressed by the radial displacement R in the direction of r , the tangential displacement T in the circumferential direction described by ϕ and the axial displacement V in the direction of y . For the relation between the displacements U , V and W in the direction of cartesian coordinates on the one hand and the displacements R , T and V in the direction of the cylindrical coordinates on the other hand it is valid:

$$U = T \cos \phi + R \sin \phi, \quad W = R \cos \phi - T \sin \phi \Rightarrow \underbrace{\begin{bmatrix} U \\ V \\ W \end{bmatrix}}_{\mathbf{w}} = \underbrace{\begin{bmatrix} \cos \phi & 0 & \sin \phi \\ 0 & 1 & 0 \\ -\sin \phi & 0 & \cos \phi \end{bmatrix}}_{\mathbf{S}_2(\phi)} \underbrace{\begin{bmatrix} T \\ V \\ R \end{bmatrix}}_{\mathbf{u}} \quad (\text{B.0.2})$$

In the following sections, the description of an axisymmetric flexible structure using cylindrical coordinates will be developed.

B.1 Derivatives

Let f be a function depending on n variables y_i . Furthermore, the variables y_i are considered as functions of the n variables x_j .

$$f = f(y_1, \dots, y_n), \quad y_i = y_i(x_1, \dots, x_n) \quad (\text{B.1.3})$$

Then, the derivative for the function f with respect to x_j is obtained by applying the chain rule:

$$\frac{\partial f}{\partial x_j} = \sum_{i=1}^n \frac{\partial f}{\partial y_i} \frac{\partial y_i}{\partial x_j} = \frac{\partial f}{\partial y_1} \frac{\partial y_1}{\partial x_j} + \dots + \frac{\partial f}{\partial y_n} \frac{\partial y_n}{\partial x_j} = \underbrace{\begin{bmatrix} \frac{\partial y_1}{\partial x_j} & \dots & \frac{\partial y_n}{\partial x_j} \end{bmatrix}}_{\mathbf{J}} \begin{bmatrix} \frac{\partial f}{\partial y_1} \\ \vdots \\ \frac{\partial f}{\partial y_n} \end{bmatrix} \quad (\text{B.1.4})$$

By arranging the derivatives $\frac{\partial f}{\partial x_j}$ in a vector and the row vectors containing the derivatives $\frac{\partial y_i}{\partial x_j}$ in a matrix, it is obtained:

$$\begin{bmatrix} \frac{\partial f}{\partial x_1} \\ \vdots \\ \frac{\partial f}{\partial x_n} \end{bmatrix} = \begin{bmatrix} \frac{\partial y_1}{\partial x_1} & \cdots & \frac{\partial y_n}{\partial x_1} \\ \vdots & & \vdots \\ \frac{\partial y_1}{\partial x_n} & \cdots & \frac{\partial y_n}{\partial x_n} \end{bmatrix} \begin{bmatrix} \frac{\partial f}{\partial y_1} \\ \vdots \\ \frac{\partial f}{\partial y_n} \end{bmatrix} \quad (\text{B.1.5})$$

Here, the matrix \mathbf{J} is the Jacobian containing the derivatives $\frac{\partial y_i}{\partial x_j}$.

In the present case, the relation between the cartesian coordinates x and z on the one hand and the polar coordinates r and ϕ on the other hand is given by:

$$x = r \sin \phi, \quad z = r \cos \phi \quad (\text{B.1.6})$$

The coordinate y remains unchanged. Based on (B.1.5), the relation between the derivatives is formulated in the following way:

$$\begin{bmatrix} \frac{\partial f}{\partial \phi} \\ \frac{\partial f}{\partial y} \\ \frac{\partial f}{\partial r} \end{bmatrix} = \underbrace{\begin{bmatrix} \frac{\partial x}{\partial \phi} & \frac{\partial y}{\partial \phi} & \frac{\partial z}{\partial \phi} \\ \frac{\partial x}{\partial y} & \frac{\partial y}{\partial y} & \frac{\partial z}{\partial y} \\ \frac{\partial x}{\partial r} & \frac{\partial y}{\partial r} & \frac{\partial z}{\partial r} \end{bmatrix}}_{\mathbf{J}} \begin{bmatrix} \frac{\partial f}{\partial x} \\ \frac{\partial f}{\partial y} \\ \frac{\partial f}{\partial z} \end{bmatrix} = \begin{bmatrix} r \cos \phi & 0 & -r \sin \phi \\ 0 & 1 & 0 \\ \sin \phi & 0 & \cos \phi \end{bmatrix} \begin{bmatrix} \frac{\partial f}{\partial x} \\ \frac{\partial f}{\partial y} \\ \frac{\partial f}{\partial z} \end{bmatrix} \quad (\text{B.1.7})$$

In this case, the Jacobian \mathbf{J} can be formulated as a product of a diagonal matrix and an elementary rotation matrix:

$$\mathbf{J} = \begin{bmatrix} r \cos \phi & 0 & -r \sin \phi \\ 0 & 1 & 0 \\ \sin \phi & 0 & \cos \phi \end{bmatrix} = \underbrace{\begin{bmatrix} r & 0 & 0 \\ 0 & 1 & 0 \\ 0 & 0 & 1 \end{bmatrix}}_{\text{diag}(r,1,1)} \underbrace{\begin{bmatrix} \cos \phi & 0 & -\sin \phi \\ 0 & 1 & 0 \\ \sin \phi & 0 & \cos \phi \end{bmatrix}}_{\mathbf{S}_2(-\phi)} \quad (\text{B.1.8})$$

Generally, the inverse of a diagonal matrix is a diagonal matrix, where the diagonal elements have the reciprocal values of the elements of the original matrix:

$$\text{diag}(d_1, d_2, \dots, d_{n-1}, d_n)^{-1} = \text{diag}\left(\frac{1}{d_1}, \frac{1}{d_2}, \dots, \frac{1}{d_{n-1}}, \frac{1}{d_n}\right) \quad (\text{B.1.9})$$

The inverse of an elementary rotation matrix can be obtained by changing the sign of the rotation angle:

$$\mathbf{S}_I(\varphi)^{-1} = \mathbf{S}_I(-\varphi) \quad (\text{B.1.10})$$

Generally, it is valid for the inverse of a matrix product:

$$\begin{aligned} \mathbf{A} = \mathbf{B}\mathbf{C} &\Rightarrow \mathbf{A}^{-1} = \mathbf{C}^{-1} \mathbf{B}^{-1} \\ \mathbf{A} \mathbf{A}^{-1} &= \mathbf{B} \underbrace{\mathbf{C} \mathbf{C}^{-1}}_{\mathbf{I}} \mathbf{B}^{-1} = \mathbf{B} \mathbf{B}^{-1} = \mathbf{I} \end{aligned} \quad (\text{B.1.11})$$

Thereby, the inverse \mathbf{J}^{-1} of the Jacobian \mathbf{J} is obtained to:

$$\begin{aligned} \mathbf{J}^{-1} &= [\text{diag}(r, 1, 1) \mathbf{S}_2(-\phi)]^{-1} = \mathbf{S}_2(-\phi)^{-1} \text{diag}(r, 1, 1)^{-1} \\ &= \mathbf{S}_2(\phi) \text{diag}\left(\frac{1}{r}, 1, 1\right) = \begin{bmatrix} \cos \phi & 0 & \sin \phi \\ 0 & 1 & 0 \\ -\sin \phi & 0 & \cos \phi \end{bmatrix} \begin{bmatrix} \frac{1}{r} & 0 & 0 \\ 0 & 1 & 0 \\ 0 & 0 & 1 \end{bmatrix} \end{aligned} \quad (\text{B.1.12})$$

Inserting this leads to:

$$\begin{aligned} \begin{bmatrix} \frac{\partial f}{\partial \phi} \\ \frac{\partial f}{\partial x} \\ \frac{\partial f}{\partial y} \\ \frac{\partial f}{\partial z} \end{bmatrix} &= \mathbf{J} \begin{bmatrix} \frac{\partial f}{\partial x} \\ \frac{\partial f}{\partial y} \\ \frac{\partial f}{\partial z} \end{bmatrix} \Rightarrow \begin{bmatrix} \frac{\partial f}{\partial x} \\ \frac{\partial f}{\partial y} \\ \frac{\partial f}{\partial z} \end{bmatrix} = \mathbf{J}^{-1} \begin{bmatrix} \frac{\partial f}{\partial \phi} \\ \frac{\partial f}{\partial x} \\ \frac{\partial f}{\partial y} \\ \frac{\partial f}{\partial z} \end{bmatrix} = \begin{bmatrix} \cos \phi & 0 & \sin \phi \\ 0 & 1 & 0 \\ -\sin \phi & 0 & \cos \phi \end{bmatrix} \begin{bmatrix} \frac{1}{r} & 0 & 0 \\ 0 & 1 & 0 \\ 0 & 0 & 1 \end{bmatrix} \begin{bmatrix} \frac{\partial f}{\partial \phi} \\ \frac{\partial f}{\partial x} \\ \frac{\partial f}{\partial y} \\ \frac{\partial f}{\partial z} \end{bmatrix} \\ &= \underbrace{\begin{bmatrix} \cos \phi & 0 & \sin \phi \\ 0 & 1 & 0 \\ -\sin \phi & 0 & \cos \phi \end{bmatrix}}_{\mathbf{S}_2(\phi)} \begin{bmatrix} \frac{1}{r} \frac{\partial f}{\partial \phi} \\ \frac{\partial f}{\partial x} \\ \frac{\partial f}{\partial y} \\ \frac{\partial f}{\partial z} \end{bmatrix} \end{aligned} \quad (\text{B.1.13})$$

From this, the following relations between the derivatives with respect to the cartesian coordinates x and z on the one hand and those with respect to the polar coordinates r and ϕ on the other hand are obtained:

$$\frac{\partial f}{\partial x} = \frac{1}{r} \frac{\partial f}{\partial \phi} \cos \phi + \frac{\partial f}{\partial r} \sin \phi, \quad \frac{\partial f}{\partial z} = -\frac{1}{r} \frac{\partial f}{\partial \phi} \sin \phi + \frac{\partial f}{\partial r} \cos \phi \quad (\text{B.1.14})$$

Based on these relations, the second partial derivatives with respect to x and z can be determined by recursion. This leads to:

$$\begin{aligned} \frac{\partial^2 f}{\partial x^2} &= \frac{\partial}{\partial x} \left(\frac{\partial f}{\partial x} \right) = \frac{1}{r} \frac{\partial}{\partial \phi} \left(\frac{1}{r} \frac{\partial f}{\partial \phi} \cos \phi - \frac{\partial f}{\partial r} \sin \phi \right) \cos \phi - \frac{\partial}{\partial r} \left(\frac{1}{r} \frac{\partial f}{\partial \phi} \cos \phi - \frac{\partial f}{\partial r} \sin \phi \right) \sin \phi \\ &= \frac{1}{r} \left(\frac{1}{r} \frac{\partial^2 f}{\partial \phi^2} \cos \phi - \frac{1}{r} \frac{\partial f}{\partial \phi} \sin \phi - \frac{\partial^2 f}{\partial r \partial \phi} \sin \phi - \frac{\partial f}{\partial r} \cos \phi \right) \cos \phi \\ &\quad - \left(-\frac{1}{r^2} \frac{\partial f}{\partial \phi} \cos \phi + \frac{1}{r} \frac{\partial^2 f}{\partial \phi \partial r} \cos \phi - \frac{\partial^2 f}{\partial r^2} \sin \phi \right) \sin \phi \\ &= \frac{1}{r^2} \frac{\partial^2 f}{\partial \phi^2} \cos^2 \phi - \frac{2}{r} \frac{\partial^2 f}{\partial \phi \partial r} \sin \phi \cos \phi - \frac{1}{r} \frac{\partial f}{\partial r} \cos^2 \phi + \frac{\partial^2 f}{\partial r^2} \sin^2 \phi \end{aligned} \quad (\text{B.1.15})$$

$$\begin{aligned} \frac{\partial^2 f}{\partial z^2} &= \frac{\partial}{\partial z} \left(\frac{\partial f}{\partial z} \right) = \frac{1}{r} \frac{\partial}{\partial \phi} \left(\frac{1}{r} \frac{\partial f}{\partial \phi} \sin \phi + \frac{\partial f}{\partial r} \cos \phi \right) \sin \phi + \frac{\partial}{\partial r} \left(\frac{1}{r} \frac{\partial f}{\partial \phi} \sin \phi + \frac{\partial f}{\partial r} \cos \phi \right) \cos \phi \\ &= \frac{1}{r} \left(\frac{1}{r} \frac{\partial^2 f}{\partial \phi^2} \sin \phi + \frac{1}{r} \frac{\partial f}{\partial \phi} \cos \phi + \frac{\partial^2 f}{\partial r \partial \phi} \cos \phi - \frac{\partial f}{\partial r} \sin \phi \right) \sin \phi \\ &\quad + \left(-\frac{1}{r^2} \frac{\partial f}{\partial \phi} \sin \phi + \frac{1}{r} \frac{\partial^2 f}{\partial \phi \partial r} \sin \phi + \frac{\partial^2 f}{\partial r^2} \cos \phi \right) \cos \phi \\ &= \frac{1}{r^2} \frac{\partial^2 f}{\partial \phi^2} \sin^2 \phi + \frac{2}{r} \frac{\partial^2 f}{\partial r \partial \phi} \sin \phi \cos \phi - \frac{1}{r} \frac{\partial f}{\partial r} \sin^2 \phi + \frac{\partial^2 f}{\partial r^2} \cos^2 \phi \end{aligned} \quad (\text{B.1.16})$$

From this, it follows:

$$\begin{aligned} \frac{\partial^2 f}{\partial x^2} + \frac{\partial^2 f}{\partial z^2} &= \frac{1}{r^2} \frac{\partial^2 f}{\partial \phi^2} \cos^2 \phi - \frac{2}{r} \frac{\partial^2 f}{\partial \phi \partial r} \sin \phi \cos \phi - \frac{1}{r} \frac{\partial f}{\partial r} \cos^2 \phi + \frac{\partial^2 f}{\partial r^2} \sin^2 \phi \\ &\quad + \frac{1}{r^2} \frac{\partial^2 f}{\partial \phi^2} \sin^2 \phi + \frac{2}{r} \frac{\partial^2 f}{\partial r \partial \phi} \sin \phi \cos \phi - \frac{1}{r} \frac{\partial f}{\partial r} \sin^2 \phi + \frac{\partial^2 f}{\partial r^2} \cos^2 \phi \\ &= \frac{1}{r^2} \frac{\partial^2 f}{\partial \phi^2} (\cos^2 \phi + \sin^2 \phi) - \frac{1}{r} \frac{\partial f}{\partial r} (\cos^2 \phi + \sin^2 \phi) + \frac{\partial^2 f}{\partial r^2} (\sin^2 \phi + \cos^2 \phi) \\ &= \frac{1}{r^2} \frac{\partial^2 f}{\partial \phi^2} - \frac{1}{r} \frac{\partial f}{\partial r} + \frac{\partial^2 f}{\partial r^2} \end{aligned} \quad (\text{B.1.17})$$

Thereby, the Laplace operator for the cylindrical coordinates is obtained to:

$$\Delta f = \frac{\partial^2 f}{\partial x^2} + \frac{\partial^2 f}{\partial y^2} + \frac{\partial^2 f}{\partial z^2} = \frac{1}{r^2} \frac{\partial^2 f}{\partial \phi^2} + \frac{\partial^2 f}{\partial y^2} + \frac{\partial^2 f}{\partial r^2} - \frac{1}{r} \frac{\partial f}{\partial r} \quad (\text{B.1.18})$$

B.2 Strains

In section B.1 the following relation between the derivatives of a function f with respect to cylindrical coordinates on the one hand and those with respect to cartesian coordinates on the other hand has been derived:

$$\begin{bmatrix} \frac{\partial f}{\partial \phi} \\ \frac{\partial f}{\partial y} \\ \frac{\partial f}{\partial r} \end{bmatrix} = \begin{bmatrix} r \cos \phi & 0 & -r \sin \phi \\ 0 & 1 & 0 \\ \sin \phi & 0 & \cos \phi \end{bmatrix} \begin{bmatrix} \frac{\partial f}{\partial x} \\ \frac{\partial f}{\partial y} \\ \frac{\partial f}{\partial z} \end{bmatrix} = \underbrace{\begin{bmatrix} r & 0 & 0 \\ 0 & 1 & 0 \\ 0 & 0 & 1 \end{bmatrix}}_{\text{diag}(r,1,1)} \underbrace{\begin{bmatrix} \cos \phi & 0 & -\sin \phi \\ 0 & 1 & 0 \\ \sin \phi & 0 & \cos \phi \end{bmatrix}}_{\mathbf{S}_2(-\phi)} \begin{bmatrix} \frac{\partial f}{\partial x} \\ \frac{\partial f}{\partial y} \\ \frac{\partial f}{\partial z} \end{bmatrix} \quad (\text{B.2.19})$$

The transposition of this relation leads to:

$$\begin{bmatrix} \frac{\partial f}{\partial \phi} & \frac{\partial f}{\partial y} & \frac{\partial f}{\partial r} \end{bmatrix} = \begin{bmatrix} \frac{\partial f}{\partial x} & \frac{\partial f}{\partial y} & \frac{\partial f}{\partial z} \end{bmatrix} \underbrace{\begin{bmatrix} \cos \phi & 0 & \sin \phi \\ 0 & 1 & 0 \\ -\sin \phi & 0 & \cos \phi \end{bmatrix}}_{\mathbf{S}_2(-\phi)^T = \mathbf{S}_2(\phi)} \begin{bmatrix} r & 0 & 0 \\ 0 & 1 & 0 \\ 0 & 0 & 1 \end{bmatrix} \quad (\text{B.2.20})$$

Inserting the displacements U , V and W in the directions of cartesian coordinates into the transposed relation and arranging the row vectors to a matrix gives the following result:

$$\begin{bmatrix} \frac{\partial U}{\partial \phi} & \frac{\partial U}{\partial y} & \frac{\partial U}{\partial r} \\ \frac{\partial V}{\partial \phi} & \frac{\partial V}{\partial y} & \frac{\partial V}{\partial r} \\ \frac{\partial W}{\partial \phi} & \frac{\partial W}{\partial y} & \frac{\partial W}{\partial r} \end{bmatrix} = \underbrace{\begin{bmatrix} \frac{\partial U}{\partial x} & \frac{\partial U}{\partial y} & \frac{\partial U}{\partial z} \\ \frac{\partial V}{\partial x} & \frac{\partial V}{\partial y} & \frac{\partial V}{\partial z} \\ \frac{\partial W}{\partial x} & \frac{\partial W}{\partial y} & \frac{\partial W}{\partial z} \end{bmatrix}}_{\mathbf{F}_w} \underbrace{\begin{bmatrix} \cos \phi & 0 & \sin \phi \\ 0 & 1 & 0 \\ -\sin \phi & 0 & \cos \phi \end{bmatrix}}_{\mathbf{S}_2(\phi)} \begin{bmatrix} r & 0 & 0 \\ 0 & 1 & 0 \\ 0 & 0 & 1 \end{bmatrix} = \mathbf{F}_w \mathbf{S}_2(\phi) \begin{bmatrix} r & 0 & 0 \\ 0 & 1 & 0 \\ 0 & 0 & 1 \end{bmatrix} \quad (\text{B.2.21})$$

Here, the matrix \mathbf{F}_w denotes the displacement gradient for the description using cartesian coordinates, as given e.g. by Schiehlen and Eberhard [64], [63]. The index w corresponds to the vector \mathbf{w} , which describes the displacements in the directions of cartesian coordinates.

The left-hand side of (B.2.21) can also be formulated in an alternative way. Here, the relation between the vectors \mathbf{w} and \mathbf{u} describing the displacements in cartesian and cylindrical coordinates, respectively, is used:

$$\underbrace{\begin{bmatrix} U \\ V \\ W \end{bmatrix}}_{\mathbf{w}} = \underbrace{\begin{bmatrix} \cos \phi & 0 & \sin \phi \\ 0 & 1 & 0 \\ -\sin \phi & 0 & \cos \phi \end{bmatrix}}_{\mathbf{S}_2(\phi)} \underbrace{\begin{bmatrix} T \\ V \\ R \end{bmatrix}}_{\mathbf{u}} \quad (\text{B.2.22})$$

The derivatives of the displacement vector \mathbf{w} with respect to the cylindrical coordinates ϕ , y and r

are obtained to:

$$\begin{aligned}\frac{\partial \mathbf{w}}{\partial \phi} &= \frac{\partial}{\partial \phi} (\mathbf{S}_2(\phi) \mathbf{u}) = \frac{\partial \mathbf{S}_2(\phi)}{\partial \phi} \mathbf{u} + \mathbf{S}_2(\phi) \frac{\partial \mathbf{u}}{\partial \phi} = \underbrace{\mathbf{S}_2(\phi) \mathbf{S}_2(-\phi)}_{\mathbf{I}} \frac{\partial \mathbf{S}_2(\phi)}{\partial \phi} \mathbf{u} + \mathbf{S}_2(\phi) \frac{\partial \mathbf{u}}{\partial \phi} \\ &= \mathbf{S}_2(\phi) \left[\mathbf{S}_2(-\phi) \frac{\partial \mathbf{S}_2(\phi)}{\partial \phi} \mathbf{u} + \frac{\partial \mathbf{u}}{\partial \phi} \right]\end{aligned}\quad (\text{B.2.23})$$

$$\frac{\partial \mathbf{w}}{\partial y} = \frac{\partial}{\partial y} (\mathbf{S}_2(\phi) \mathbf{u}) = \mathbf{S}_2(\phi) \frac{\partial \mathbf{u}}{\partial y} \quad (\text{B.2.24})$$

$$\frac{\partial \mathbf{w}}{\partial r} = \frac{\partial}{\partial r} (\mathbf{S}_2(\phi) \mathbf{u}) = \mathbf{S}_2(\phi) \frac{\partial \mathbf{u}}{\partial r} \quad (\text{B.2.25})$$

Here, the result of the derivative (B.2.23) is modified in order to factor the matrix $\mathbf{S}_2(\phi)$ out. The evaluation of the matrix product contained in (B.2.23) gives:

$$\begin{aligned}\mathbf{S}_2(\phi) &= \begin{bmatrix} \cos \phi & 0 & \sin \phi \\ 0 & 1 & 0 \\ -\sin \phi & 0 & \cos \phi \end{bmatrix}, \quad \frac{\partial \mathbf{S}_2(\phi)}{\partial \phi} = \begin{bmatrix} -\sin \phi & 0 & \cos \phi \\ 0 & 0 & 0 \\ -\cos \phi & 0 & -\sin \phi \end{bmatrix} \\ \mathbf{S}_2(-\phi) \frac{\partial \mathbf{S}_2(\phi)}{\partial \phi} &= \begin{bmatrix} \cos \phi & 0 & -\sin \phi \\ 0 & 1 & 0 \\ \sin \phi & 0 & \cos \phi \end{bmatrix} \begin{bmatrix} -\sin \phi & 0 & \cos \phi \\ 0 & 0 & 0 \\ -\cos \phi & 0 & -\sin \phi \end{bmatrix} \\ &= \begin{bmatrix} -\cos \phi \sin \phi + \sin \phi \cos \phi & 0 & \cos^2 \phi + \sin^2 \phi \\ 0 & 0 & 0 \\ -\sin^2 \phi - \cos^2 \phi & 0 & \sin \phi \cos \phi - \cos \phi \sin \phi \end{bmatrix} = \begin{bmatrix} 0 & 0 & 1 \\ 0 & 0 & 0 \\ -1 & 0 & 0 \end{bmatrix}\end{aligned}\quad (\text{B.2.26})$$

The evaluation of the derivatives of the vector \mathbf{w} with respect to the cylindrical coordinates leads to the following expressions:

$$\frac{\partial \mathbf{w}}{\partial \phi} = \begin{bmatrix} \frac{\partial U}{\partial \phi} \\ \frac{\partial V}{\partial \phi} \\ \frac{\partial W}{\partial \phi} \end{bmatrix} = \mathbf{S}_2(\phi) \left(\begin{bmatrix} 0 & 0 & 1 \\ 0 & 0 & 0 \\ -1 & 0 & 0 \end{bmatrix} \begin{bmatrix} T \\ V \\ R \end{bmatrix} + \begin{bmatrix} \frac{\partial T}{\partial \phi} \\ \frac{\partial V}{\partial \phi} \\ \frac{\partial R}{\partial \phi} \end{bmatrix} \right) = \mathbf{S}_2(\phi) \begin{bmatrix} \frac{\partial T}{\partial \phi} + R \\ \frac{\partial V}{\partial \phi} \\ \frac{\partial R}{\partial \phi} - T \end{bmatrix} \quad (\text{B.2.27})$$

$$\frac{\partial \mathbf{w}}{\partial y} = \begin{bmatrix} \frac{\partial U}{\partial y} \\ \frac{\partial V}{\partial y} \\ \frac{\partial W}{\partial y} \end{bmatrix} = \mathbf{S}_2(\phi) \begin{bmatrix} \frac{\partial T}{\partial y} \\ \frac{\partial V}{\partial y} \\ \frac{\partial R}{\partial y} \end{bmatrix} \quad (\text{B.2.28})$$

$$\frac{\partial \mathbf{w}}{\partial r} = \begin{bmatrix} \frac{\partial U}{\partial r} \\ \frac{\partial V}{\partial r} \\ \frac{\partial W}{\partial r} \end{bmatrix} = \mathbf{S}_2(\phi) \begin{bmatrix} \frac{\partial T}{\partial r} \\ \frac{\partial V}{\partial r} \\ \frac{\partial R}{\partial r} \end{bmatrix} \quad (\text{B.2.29})$$

By arranging the three column vectors in a matrix it is obtained:

$$\begin{bmatrix} \frac{\partial U}{\partial \phi} & \frac{\partial U}{\partial y} & \frac{\partial U}{\partial r} \\ \frac{\partial V}{\partial \phi} & \frac{\partial V}{\partial y} & \frac{\partial V}{\partial r} \\ \frac{\partial W}{\partial \phi} & \frac{\partial W}{\partial y} & \frac{\partial W}{\partial r} \end{bmatrix} = \underbrace{\begin{bmatrix} \cos \phi & 0 & \sin \phi \\ 0 & 1 & 0 \\ -\sin \phi & 0 & \cos \phi \end{bmatrix}}_{\mathbf{S}_2(\phi)} \begin{bmatrix} \frac{\partial T}{\partial \phi} + R & \frac{\partial T}{\partial y} & \frac{\partial T}{\partial r} \\ \frac{\partial V}{\partial \phi} & \frac{\partial V}{\partial y} & \frac{\partial V}{\partial r} \\ \frac{\partial R}{\partial \phi} - T & \frac{\partial R}{\partial y} & \frac{\partial R}{\partial r} \end{bmatrix} = \mathbf{S}_2(\phi) \begin{bmatrix} \frac{\partial T}{\partial \phi} + R & \frac{\partial T}{\partial y} & \frac{\partial T}{\partial r} \\ \frac{\partial V}{\partial \phi} & \frac{\partial V}{\partial y} & \frac{\partial V}{\partial r} \\ \frac{\partial R}{\partial \phi} - T & \frac{\partial R}{\partial y} & \frac{\partial R}{\partial r} \end{bmatrix} \quad (\text{B.2.30})$$

The equations (B.2.21) and (B.2.30) have the same left-hand sides so that their right-hand sides can be set equal. This leads to:

$$\underbrace{\begin{bmatrix} \cos\phi & 0 & \sin\phi \\ 0 & 1 & 0 \\ -\sin\phi & 0 & \cos\phi \end{bmatrix}}_{\mathbf{S}_2(\phi)} \begin{bmatrix} \frac{\partial T}{\partial\phi} + R & \frac{\partial T}{\partial y} & \frac{\partial T}{\partial r} \\ \frac{\partial V}{\partial\phi} & \frac{\partial V}{\partial y} & \frac{\partial V}{\partial r} \\ \frac{\partial R}{\partial\phi} - T & \frac{\partial R}{\partial y} & \frac{\partial R}{\partial r} \end{bmatrix} = \begin{bmatrix} \frac{\partial U}{\partial x} & \frac{\partial U}{\partial y} & \frac{\partial U}{\partial z} \\ \frac{\partial V}{\partial x} & \frac{\partial V}{\partial y} & \frac{\partial V}{\partial z} \\ \frac{\partial W}{\partial x} & \frac{\partial W}{\partial y} & \frac{\partial W}{\partial z} \end{bmatrix} \underbrace{\begin{bmatrix} \cos\phi & 0 & \sin\phi \\ 0 & 1 & 0 \\ -\sin\phi & 0 & \cos\phi \end{bmatrix}}_{\mathbf{S}_2(\phi)} \begin{bmatrix} r & 0 & 0 \\ 0 & 1 & 0 \\ 0 & 0 & 1 \end{bmatrix} \quad (\text{B.2.31})$$

By using a left multiplication of the relation (B.2.31) with $\mathbf{S}_2(-\phi)$ the rotation matrix $\mathbf{S}_2(\phi)$ is eliminated on the left-hand side:

$$\begin{aligned} \mathbf{S}_2(\phi) \begin{bmatrix} \frac{\partial T}{\partial\phi} + R & \frac{\partial T}{\partial y} & \frac{\partial T}{\partial r} \\ \frac{\partial V}{\partial\phi} & \frac{\partial V}{\partial y} & \frac{\partial V}{\partial r} \\ \frac{\partial R}{\partial\phi} - T & \frac{\partial R}{\partial y} & \frac{\partial R}{\partial r} \end{bmatrix} &= \begin{bmatrix} \frac{\partial U}{\partial x} & \frac{\partial U}{\partial y} & \frac{\partial U}{\partial z} \\ \frac{\partial V}{\partial x} & \frac{\partial V}{\partial y} & \frac{\partial V}{\partial z} \\ \frac{\partial W}{\partial x} & \frac{\partial W}{\partial y} & \frac{\partial W}{\partial z} \end{bmatrix} \mathbf{S}_2(\phi) \begin{bmatrix} r & 0 & 0 \\ 0 & 1 & 0 \\ 0 & 0 & 1 \end{bmatrix} \\ \Rightarrow \underbrace{\mathbf{S}_2(-\phi)\mathbf{S}_2(\phi)}_{\mathbf{I}} \begin{bmatrix} \frac{\partial T}{\partial\phi} + R & \frac{\partial T}{\partial y} & \frac{\partial T}{\partial r} \\ \frac{\partial V}{\partial\phi} & \frac{\partial V}{\partial y} & \frac{\partial V}{\partial r} \\ \frac{\partial R}{\partial\phi} - T & \frac{\partial R}{\partial y} & \frac{\partial R}{\partial r} \end{bmatrix} &= \mathbf{S}_2(-\phi) \begin{bmatrix} \frac{\partial U}{\partial x} & \frac{\partial U}{\partial y} & \frac{\partial U}{\partial z} \\ \frac{\partial V}{\partial x} & \frac{\partial V}{\partial y} & \frac{\partial V}{\partial z} \\ \frac{\partial W}{\partial x} & \frac{\partial W}{\partial y} & \frac{\partial W}{\partial z} \end{bmatrix} \mathbf{S}_2(\phi) \begin{bmatrix} r & 0 & 0 \\ 0 & 1 & 0 \\ 0 & 0 & 1 \end{bmatrix} \quad (\text{B.2.32}) \end{aligned}$$

Next, the relation (B.2.32) is transformed by a right multiplication with the inverse diagonal matrix. Thereby, the coordinate r is eliminated on the right-hand side of the relation:

$$\begin{aligned} \begin{bmatrix} \frac{\partial T}{\partial\phi} + R & \frac{\partial T}{\partial y} & \frac{\partial T}{\partial r} \\ \frac{\partial V}{\partial\phi} & \frac{\partial V}{\partial y} & \frac{\partial V}{\partial r} \\ \frac{\partial R}{\partial\phi} - T & \frac{\partial R}{\partial y} & \frac{\partial R}{\partial r} \end{bmatrix} &= \mathbf{S}_2(-\phi) \begin{bmatrix} \frac{\partial U}{\partial x} & \frac{\partial U}{\partial y} & \frac{\partial U}{\partial z} \\ \frac{\partial V}{\partial x} & \frac{\partial V}{\partial y} & \frac{\partial V}{\partial z} \\ \frac{\partial W}{\partial x} & \frac{\partial W}{\partial y} & \frac{\partial W}{\partial z} \end{bmatrix} \mathbf{S}_2(\phi) \begin{bmatrix} r & 0 & 0 \\ 0 & 1 & 0 \\ 0 & 0 & 1 \end{bmatrix} \\ \Rightarrow \begin{bmatrix} \frac{\partial T}{\partial\phi} + R & \frac{\partial T}{\partial y} & \frac{\partial T}{\partial r} \\ \frac{\partial V}{\partial\phi} & \frac{\partial V}{\partial y} & \frac{\partial V}{\partial r} \\ \frac{\partial R}{\partial\phi} - T & \frac{\partial R}{\partial y} & \frac{\partial R}{\partial r} \end{bmatrix} \begin{bmatrix} \frac{1}{r} & 0 & 0 \\ 0 & 1 & 0 \\ 0 & 0 & 1 \end{bmatrix} &= \mathbf{S}_2(-\phi) \begin{bmatrix} \frac{\partial U}{\partial x} & \frac{\partial U}{\partial y} & \frac{\partial U}{\partial z} \\ \frac{\partial V}{\partial x} & \frac{\partial V}{\partial y} & \frac{\partial V}{\partial z} \\ \frac{\partial W}{\partial x} & \frac{\partial W}{\partial y} & \frac{\partial W}{\partial z} \end{bmatrix} \mathbf{S}_2(\phi) \underbrace{\begin{bmatrix} r & 0 & 0 \\ 0 & 1 & 0 \\ 0 & 0 & 1 \end{bmatrix} \begin{bmatrix} \frac{1}{r} & 0 & 0 \\ 0 & 1 & 0 \\ 0 & 0 & 1 \end{bmatrix}}_{\mathbf{I}} \quad (\text{B.2.33}) \end{aligned}$$

Finally, the following relation between the derivatives for cylindrical coordinates on the one hand and for cartesian coordinates on the other hand can be formulated:

$$\begin{bmatrix} \frac{\partial T}{\partial\phi} + R & \frac{\partial T}{\partial y} & \frac{\partial T}{\partial r} \\ \frac{\partial V}{\partial\phi} & \frac{\partial V}{\partial y} & \frac{\partial V}{\partial r} \\ \frac{\partial R}{\partial\phi} - T & \frac{\partial R}{\partial y} & \frac{\partial R}{\partial r} \end{bmatrix} \begin{bmatrix} \frac{1}{r} & 0 & 0 \\ 0 & 1 & 0 \\ 0 & 0 & 1 \end{bmatrix} = \underbrace{\begin{bmatrix} \frac{1}{r} \frac{\partial T}{\partial\phi} + \frac{R}{r} & \frac{\partial T}{\partial y} & \frac{\partial T}{\partial r} \\ \frac{1}{r} \frac{\partial V}{\partial\phi} & \frac{\partial V}{\partial y} & \frac{\partial V}{\partial r} \\ \frac{1}{r} \frac{\partial R}{\partial\phi} - \frac{T}{r} & \frac{\partial R}{\partial y} & \frac{\partial R}{\partial r} \end{bmatrix}}_{\mathbf{F}_u} = \mathbf{S}_2(-\phi) \underbrace{\begin{bmatrix} \frac{\partial U}{\partial x} & \frac{\partial U}{\partial y} & \frac{\partial U}{\partial z} \\ \frac{\partial V}{\partial x} & \frac{\partial V}{\partial y} & \frac{\partial V}{\partial z} \\ \frac{\partial W}{\partial x} & \frac{\partial W}{\partial y} & \frac{\partial W}{\partial z} \end{bmatrix}}_{\mathbf{F}_w} \mathbf{S}_2(\phi) \quad (\text{B.2.34})$$

Here, \mathbf{F}_u is the displacement gradient for cylindrical coordinates; its index \mathbf{u} corresponds to the vector \mathbf{u} describing the displacements in the direction of cylindrical coordinates. The relation can be easily resolved for the gradient \mathbf{F}_w by a left multiplication with $\mathbf{S}_2(\phi)$ and a right multiplication with $\mathbf{S}_2(-\phi)$. As a result, it is obtained:

$$\mathbf{F}_u = \mathbf{S}_2(-\phi) \mathbf{F}_w \mathbf{S}_2(\phi) \Rightarrow \mathbf{S}_2(\phi) \mathbf{F}_u \mathbf{S}_2(-\phi) = \underbrace{\mathbf{S}_2(\phi) \mathbf{S}_2(-\phi)}_{\mathbf{I}} \mathbf{F}_w \underbrace{\mathbf{S}_2(\phi) \mathbf{S}_2(-\phi)}_{\mathbf{I}} = \mathbf{F}_w \quad (\text{B.2.35})$$

The transposition of the expressions (B.2.35) and (B.2.34) gives:

$$\mathbf{F}_w = \mathbf{S}_2(\phi) \mathbf{F}_u \mathbf{S}_2(-\phi) \Rightarrow \mathbf{F}_w^T = \mathbf{S}_2(-\phi)^T \mathbf{F}_u^T \mathbf{S}_2(\phi)^T = \mathbf{S}_2(\phi) \mathbf{F}_u^T \mathbf{S}_2(-\phi) \quad (\text{B.2.36})$$

$$\mathbf{F}_u = \mathbf{S}_2(-\phi) \mathbf{F}_w \mathbf{S}_2(\phi) \Rightarrow \mathbf{F}_u^T = \mathbf{S}_2(\phi)^T \mathbf{F}_w^T \mathbf{S}_2(-\phi)^T = \mathbf{S}_2(-\phi) \mathbf{F}_w^T \mathbf{S}_2(\phi) \quad (\text{B.2.37})$$

By adding the deformation tensor and the transposed deformation tensor, the symmetric strain tensor \mathbf{G} is obtained. Based on the relations (B.2.36) and (B.2.37) it is valid:

$$\begin{aligned} \mathbf{G}_w &= \mathbf{F}_w + \mathbf{F}_w^T = \mathbf{S}_2(\phi) \mathbf{F}_u \mathbf{S}_2(-\phi) + \mathbf{S}_2(\phi) \mathbf{F}_u^T \mathbf{S}_2(-\phi) \\ &= \mathbf{S}_2(\phi) \underbrace{(\mathbf{F}_u + \mathbf{F}_u^T)}_{\mathbf{G}_u} \mathbf{S}_2(-\phi) = \mathbf{S}_2(\phi) \mathbf{G}_u \mathbf{S}_2(-\phi) \end{aligned} \quad (\text{B.2.38})$$

$$\begin{aligned} \mathbf{G}_u &= \mathbf{F}_u + \mathbf{F}_u^T = \mathbf{S}_2(-\phi) \mathbf{F}_w \mathbf{S}_2(\phi) + \mathbf{S}_2(-\phi) \mathbf{F}_w^T \mathbf{S}_2(\phi) \\ &= \mathbf{S}_2(-\phi) \underbrace{(\mathbf{F}_w + \mathbf{F}_w^T)}_{\mathbf{G}_w} \mathbf{S}_2(\phi) = \mathbf{S}_2(-\phi) \mathbf{G}_w \mathbf{S}_2(\phi) \end{aligned} \quad (\text{B.2.39})$$

From the deformation tensors \mathbf{F}_w and \mathbf{F}_u , the elements of the strain tensors \mathbf{G}_w and \mathbf{G}_u are determined. It is valid:

$$\mathbf{F}_w = \begin{bmatrix} \frac{\partial U}{\partial x} & \frac{\partial U}{\partial y} & \frac{\partial U}{\partial z} \\ \frac{\partial V}{\partial x} & \frac{\partial V}{\partial y} & \frac{\partial V}{\partial z} \\ \frac{\partial W}{\partial x} & \frac{\partial W}{\partial y} & \frac{\partial W}{\partial z} \end{bmatrix} \Rightarrow \mathbf{G}_w = \begin{bmatrix} 2\frac{\partial U}{\partial x} & \frac{\partial U}{\partial y} + \frac{\partial V}{\partial x} & \frac{\partial U}{\partial z} + \frac{\partial W}{\partial x} \\ \frac{\partial U}{\partial y} + \frac{\partial V}{\partial x} & 2\frac{\partial V}{\partial y} & \frac{\partial V}{\partial z} + \frac{\partial W}{\partial y} \\ \frac{\partial U}{\partial z} + \frac{\partial W}{\partial x} & \frac{\partial V}{\partial z} + \frac{\partial W}{\partial y} & 2\frac{\partial W}{\partial z} \end{bmatrix} \quad (\text{B.2.40})$$

$$\mathbf{F}_u = \begin{bmatrix} \frac{1}{r} \frac{\partial T}{\partial \phi} + \frac{R}{r} & \frac{\partial T}{\partial y} & \frac{\partial T}{\partial r} \\ \frac{1}{r} \frac{\partial V}{\partial \phi} & \frac{\partial V}{\partial y} & \frac{\partial V}{\partial r} \\ \frac{1}{r} \frac{\partial R}{\partial \phi} - \frac{T}{r} & \frac{\partial R}{\partial y} & \frac{\partial R}{\partial r} \end{bmatrix} \Rightarrow \mathbf{G}_u = \begin{bmatrix} \frac{2}{r} \frac{\partial T}{\partial \phi} + \frac{2R}{r} & \frac{1}{r} \frac{\partial V}{\partial \phi} + \frac{\partial T}{\partial y} & \frac{1}{r} \frac{\partial R}{\partial \phi} - \frac{T}{r} + \frac{\partial T}{\partial r} \\ \frac{1}{r} \frac{\partial V}{\partial \phi} + \frac{\partial T}{\partial y} & 2\frac{\partial V}{\partial y} & \frac{\partial V}{\partial r} + \frac{\partial R}{\partial y} \\ \frac{1}{r} \frac{\partial R}{\partial \phi} - \frac{T}{r} + \frac{\partial T}{\partial r} & \frac{\partial V}{\partial r} + \frac{\partial R}{\partial y} & 2\frac{\partial R}{\partial r} \end{bmatrix} \quad (\text{B.2.41})$$

In order to determine the relations between the strains for the formulation in the cartesian coordinates on the one hand and in cylindrical coordinates on the other hand, the relations (B.2.38) and (B.2.39) are used. It is valid:

$$\mathbf{G}_w = \mathbf{S}_2(\phi) \mathbf{G}_u \mathbf{S}_2(-\phi) \quad (\text{B.2.42})$$

$$\mathbf{G}_u = \mathbf{S}_2(-\phi) \mathbf{G}_w \mathbf{S}_2(\phi) \quad (\text{B.2.43})$$

The evaluation is carried out using the following generalized scheme. For the product $\mathbf{S}_2(\phi) \mathbf{A} \mathbf{S}_2(-\phi)$ of the rotation matrix $\mathbf{S}_2(\phi)$, a symmetric matrix $\mathbf{A} = \mathbf{A}^T$ and the inverse rotation matrix $\mathbf{S}_2(-\phi)$ it is valid:

$$\begin{aligned}
\mathbf{S}_2(\phi) \mathbf{A} \mathbf{S}_2(-\phi) &= \begin{bmatrix} \cos \phi & 0 & \sin \phi \\ 0 & 1 & 0 \\ -\sin \phi & 0 & \cos \phi \end{bmatrix} \begin{bmatrix} a_{11} & a_{12} & a_{13} \\ a_{12} & a_{22} & a_{23} \\ a_{13} & a_{23} & a_{33} \end{bmatrix} \begin{bmatrix} \cos \phi & 0 & -\sin \phi \\ 0 & 1 & 0 \\ \sin \phi & 0 & \cos \phi \end{bmatrix} \\
&= \begin{bmatrix} 0 & 0 & 0 \\ 0 & a_{22} & 0 \\ 0 & 0 & 0 \end{bmatrix} + \begin{bmatrix} 0 & a_{12} & 0 \\ a_{12} & 0 & a_{23} \\ 0 & a_{23} & 0 \end{bmatrix} \cos \phi + \begin{bmatrix} 0 & a_{23} & 0 \\ a_{23} & 0 & -a_{12} \\ 0 & -a_{12} & 0 \end{bmatrix} \sin \phi \\
&\quad + \begin{bmatrix} a_{11} & 0 & a_{13} \\ 0 & 0 & 0 \\ a_{13} & 0 & a_{33} \end{bmatrix} \cos^2 \phi + \begin{bmatrix} a_{33} & 0 & -a_{13} \\ 0 & 0 & 0 \\ -a_{13} & 0 & a_{11} \end{bmatrix} \sin^2 \phi \\
&\quad + \begin{bmatrix} 2a_{13} & 0 & a_{33} - a_{11} \\ 0 & 0 & 0 \\ a_{33} - a_{11} & 0 & -2a_{13} \end{bmatrix} \sin \phi \cos \phi \tag{B.2.44}
\end{aligned}$$

Using this scheme, the relations between the strains for cartesian coordinates and those for cylindrical coordinates can be now be determined. From the comparison of the elements of the matrices it is obtained:

$$\begin{aligned}
&\begin{bmatrix} 2\frac{\partial U}{\partial x} & \frac{\partial U}{\partial y} + \frac{\partial V}{\partial x} & \frac{\partial U}{\partial z} + \frac{\partial W}{\partial x} \\ \frac{\partial U}{\partial y} + \frac{\partial V}{\partial x} & 2\frac{\partial V}{\partial y} & \frac{\partial V}{\partial z} + \frac{\partial W}{\partial y} \\ \frac{\partial U}{\partial z} + \frac{\partial W}{\partial x} & \frac{\partial V}{\partial z} + \frac{\partial W}{\partial y} & 2\frac{\partial W}{\partial z} \end{bmatrix} \\
&= \mathbf{S}_2(\phi) \begin{bmatrix} \frac{2}{r} \frac{\partial T}{\partial \phi} + \frac{2R}{r} & \frac{1}{r} \frac{\partial V}{\partial \phi} + \frac{\partial T}{\partial y} & \frac{1}{r} \frac{\partial R}{\partial \phi} - \frac{T}{r} + \frac{\partial T}{\partial r} \\ \frac{1}{r} \frac{\partial V}{\partial \phi} + \frac{\partial T}{\partial y} & 2\frac{\partial V}{\partial y} & \frac{\partial V}{\partial r} + \frac{\partial R}{\partial y} \\ \frac{1}{r} \frac{\partial R}{\partial \phi} - \frac{T}{r} + \frac{\partial T}{\partial r} & \frac{\partial V}{\partial r} + \frac{\partial R}{\partial y} & 2\frac{\partial R}{\partial r} \end{bmatrix} \mathbf{S}_2(-\phi) \\
2\frac{\partial U}{\partial x} &= \frac{2}{r} \left[\frac{\partial T}{\partial \phi} + R \right] \cos^2 \phi + 2\frac{\partial R}{\partial r} \sin^2 \phi + 2 \left(\frac{1}{r} \frac{\partial R}{\partial \phi} - \frac{T}{r} + \frac{\partial T}{\partial r} \right) \sin \phi \cos \phi \\
\Rightarrow \frac{\partial U}{\partial x} &= \frac{1}{r} \left[\frac{\partial T}{\partial \phi} + R \right] \cos^2 \phi + \frac{\partial R}{\partial r} \sin^2 \phi + \left(\frac{1}{r} \frac{\partial R}{\partial \phi} - \frac{T}{r} + \frac{\partial T}{\partial r} \right) \sin \phi \cos \phi \tag{B.2.45}
\end{aligned}$$

$$\begin{aligned}
2\frac{\partial W}{\partial z} &= \frac{2}{r} \left[\frac{\partial T}{\partial \phi} + R \right] \sin^2 \phi + 2\frac{\partial R}{\partial r} \cos^2 \phi - 2 \left(\frac{1}{r} \frac{\partial R}{\partial \phi} - \frac{T}{r} + \frac{\partial T}{\partial r} \right) \sin \phi \cos \phi \\
\Rightarrow \frac{\partial W}{\partial z} &= \frac{1}{r} \left[\frac{\partial T}{\partial \phi} + R \right] \sin^2 \phi + \frac{\partial R}{\partial r} \cos^2 \phi - \left(\frac{1}{r} \frac{\partial R}{\partial \phi} - \frac{T}{r} + \frac{\partial T}{\partial r} \right) \sin \phi \cos \phi \tag{B.2.46}
\end{aligned}$$

$$\frac{\partial U}{\partial y} + \frac{\partial V}{\partial x} = \left(\frac{1}{r} \frac{\partial V}{\partial \phi} + \frac{\partial T}{\partial y} \right) \cos \phi + \left(\frac{\partial V}{\partial r} + \frac{\partial R}{\partial y} \right) \sin \phi \tag{B.2.47}$$

$$\frac{\partial V}{\partial z} + \frac{\partial W}{\partial y} = \left(\frac{\partial V}{\partial r} + \frac{\partial R}{\partial y} \right) \cos \phi - \left(\frac{1}{r} \frac{\partial V}{\partial \phi} + \frac{\partial T}{\partial y} \right) \sin \phi \tag{B.2.48}$$

$$\frac{\partial U}{\partial z} + \frac{\partial W}{\partial x} = \left(\frac{1}{r} \frac{\partial R}{\partial \phi} - \frac{T}{r} + \frac{\partial T}{\partial r} \right) (\cos^2 \phi - \sin^2 \phi) + 2 \left(\frac{\partial R}{\partial r} - \frac{1}{r} \frac{\partial T}{\partial \phi} - \frac{R}{r} \right) \sin \phi \cos \phi \tag{B.2.49}$$

The product $\mathbf{S}_2(-\phi)\mathbf{A}\mathbf{S}_2(\phi)$ can be derived from (B.2.44) by changing the sign of the angle ϕ . This leads to:

$$\begin{aligned}
\mathbf{S}_2(-\phi)\mathbf{A}\mathbf{S}_2(\phi) &= \begin{bmatrix} 0 & 0 & 0 \\ 0 & a_{22} & 0 \\ 0 & 0 & 0 \end{bmatrix} + \begin{bmatrix} 0 & a_{12} & 0 \\ a_{12} & 0 & a_{23} \\ 0 & a_{23} & 0 \end{bmatrix} \cos(-\phi) + \begin{bmatrix} 0 & a_{23} & 0 \\ a_{23} & 0 & -a_{12} \\ 0 & -a_{12} & 0 \end{bmatrix} \sin(-\phi) \\
&+ \begin{bmatrix} a_{11} & 0 & a_{13} \\ 0 & 0 & 0 \\ a_{13} & 0 & a_{33} \end{bmatrix} \cos^2(-\phi) + \begin{bmatrix} a_{33} & 0 & -a_{13} \\ 0 & 0 & 0 \\ -a_{13} & 0 & a_{11} \end{bmatrix} \sin^2(-\phi) \\
&+ \begin{bmatrix} 2a_{13} & 0 & a_{33} - a_{11} \\ 0 & 0 & 0 \\ a_{33} - a_{11} & 0 & -2a_{13} \end{bmatrix} \sin(-\phi) \cos(-\phi) \\
&= \begin{bmatrix} 0 & 0 & 0 \\ 0 & a_{22} & 0 \\ 0 & 0 & 0 \end{bmatrix} + \begin{bmatrix} 0 & a_{12} & 0 \\ a_{12} & 0 & a_{23} \\ 0 & a_{23} & 0 \end{bmatrix} \cos\phi + \begin{bmatrix} 0 & -a_{23} & 0 \\ -a_{23} & 0 & a_{12} \\ 0 & a_{12} & 0 \end{bmatrix} \sin\phi \\
&+ \begin{bmatrix} a_{11} & 0 & a_{13} \\ 0 & 0 & 0 \\ a_{13} & 0 & a_{33} \end{bmatrix} \cos^2\phi + \begin{bmatrix} a_{33} & 0 & -a_{13} \\ 0 & 0 & 0 \\ -a_{13} & 0 & a_{11} \end{bmatrix} \sin^2\phi \\
&+ \begin{bmatrix} -2a_{13} & 0 & a_{11} - a_{33} \\ 0 & 0 & 0 \\ a_{11} - a_{33} & 0 & 2a_{13} \end{bmatrix} \sin\phi \cos\phi \tag{B.2.50}
\end{aligned}$$

Also here, the relation between the strains for cylindrical coordinates and those for cartesian coordinates are determined by using the scheme and comparing the single elements of the matrices.

$$\begin{aligned}
&\begin{bmatrix} \frac{2}{r} \frac{\partial T}{\partial \phi} + \frac{2R}{r} & \frac{1}{r} \frac{\partial V}{\partial \phi} + \frac{\partial T}{\partial y} & \frac{1}{r} \frac{\partial R}{\partial \phi} - \frac{T}{r} + \frac{\partial T}{\partial r} \\ \frac{1}{r} \frac{\partial V}{\partial \phi} + \frac{\partial T}{\partial y} & 2 \frac{\partial V}{\partial y} & \frac{\partial V}{\partial r} + \frac{\partial R}{\partial y} \\ \frac{1}{r} \frac{\partial R}{\partial \phi} - \frac{T}{r} + \frac{\partial T}{\partial r} & \frac{\partial V}{\partial r} + \frac{\partial R}{\partial y} & 2 \frac{\partial R}{\partial r} \end{bmatrix} \\
&= \mathbf{S}_2(-\phi) \begin{bmatrix} 2 \frac{\partial U}{\partial x} & \frac{\partial U}{\partial y} + \frac{\partial V}{\partial x} & \frac{\partial U}{\partial z} + \frac{\partial W}{\partial x} \\ \frac{\partial U}{\partial y} + \frac{\partial V}{\partial x} & 2 \frac{\partial V}{\partial y} & \frac{\partial V}{\partial z} + \frac{\partial W}{\partial y} \\ \frac{\partial U}{\partial z} + \frac{\partial W}{\partial x} & \frac{\partial V}{\partial z} + \frac{\partial W}{\partial y} & 2 \frac{\partial W}{\partial z} \end{bmatrix} \mathbf{S}_2(\phi) \tag{B.2.51}
\end{aligned}$$

$$\begin{aligned}
\frac{2}{r} \left(\frac{\partial T}{\partial \phi} + R \right) &= 2 \frac{\partial U}{\partial x} \cos^2\phi + 2 \frac{\partial W}{\partial z} \sin^2\phi - 2 \left(\frac{\partial U}{\partial z} + \frac{\partial W}{\partial x} \right) \sin\phi \cos\phi \\
\Rightarrow \frac{1}{r} \left(\frac{\partial T}{\partial \phi} + R \right) &= \frac{\partial U}{\partial x} \cos^2\phi + \frac{\partial W}{\partial z} \sin^2\phi - \left(\frac{\partial U}{\partial z} + \frac{\partial W}{\partial x} \right) \sin\phi \cos\phi \tag{B.2.52}
\end{aligned}$$

$$\begin{aligned}
2 \frac{\partial R}{\partial r} &= 2 \frac{\partial U}{\partial x} \sin^2\phi + 2 \frac{\partial W}{\partial z} \cos^2\phi + 2 \left(\frac{\partial U}{\partial z} + \frac{\partial W}{\partial x} \right) \sin\phi \cos\phi \\
\Rightarrow \frac{\partial R}{\partial r} &= \frac{\partial U}{\partial x} \sin^2\phi + \frac{\partial W}{\partial z} \cos^2\phi + \left(\frac{\partial U}{\partial z} + \frac{\partial W}{\partial x} \right) \sin\phi \cos\phi \tag{B.2.53}
\end{aligned}$$

$$\frac{1}{r} \frac{\partial V}{\partial \phi} + \frac{\partial T}{\partial y} = \left(\frac{\partial U}{\partial y} + \frac{\partial V}{\partial x} \right) \cos\phi - \left(\frac{\partial V}{\partial z} + \frac{\partial W}{\partial y} \right) \sin\phi \tag{B.2.54}$$

$$\frac{\partial V}{\partial r} + \frac{\partial R}{\partial y} = \left(\frac{\partial V}{\partial z} + \frac{\partial W}{\partial y} \right) \cos\phi + \left(\frac{\partial U}{\partial y} + \frac{\partial V}{\partial x} \right) \sin\phi \tag{B.2.55}$$

$$\frac{1}{r} \frac{\partial R}{\partial \phi} - \frac{T}{r} + \frac{\partial T}{\partial r} = \left(\frac{\partial U}{\partial z} + \frac{\partial W}{\partial x} \right) (\cos^2\phi - \sin^2\phi) + 2 \left(\frac{\partial U}{\partial x} - \frac{\partial W}{\partial z} \right) \sin\phi \cos\phi \tag{B.2.56}$$

Thereby, the relations between the strains for the formulations using cartesian coordinates on the one hand and using cylindrical coordinates on the other hand are known.

B.3 Virtual work

For a three-dimensional linear elastic material the relations between the stresses and the strains can be expressed by the following relation, which is based¹ on the equations given e.g. by Zienkiewicz and Taylor [84] or by Schiehlen and Eberhard [64], [63].

$$\underbrace{\begin{bmatrix} \sigma_x \\ \sigma_y \\ \sigma_z \\ \tau_{xy} \\ \tau_{yz} \\ \tau_{zx} \end{bmatrix}}_{\boldsymbol{\sigma}} = \frac{G}{1-2\nu} \underbrace{\begin{bmatrix} 2(1-\nu) & 2\nu & 2\nu & 0 & 0 & 0 \\ 2\nu & 2(1-\nu) & 2\nu & 0 & 0 & 0 \\ 2\nu & 2\nu & 2(1-\nu) & 0 & 0 & 0 \\ 0 & 0 & 0 & 1-2\nu & 0 & 0 \\ 0 & 0 & 0 & 0 & 1-2\nu & 0 \\ 0 & 0 & 0 & 0 & 0 & 1-2\nu \end{bmatrix}}_{\mathbf{D}} \underbrace{\begin{bmatrix} \frac{\partial U}{\partial x} \\ \frac{\partial V}{\partial y} \\ \frac{\partial W}{\partial z} \\ \frac{\partial U}{\partial y} + \frac{\partial V}{\partial x} \\ \frac{\partial V}{\partial z} + \frac{\partial W}{\partial y} \\ \frac{\partial W}{\partial x} + \frac{\partial U}{\partial z} \end{bmatrix}}_{\boldsymbol{\varepsilon}} \quad (\text{B.3.57})$$

In detail, the stresses can be formulated in the following way; here, the expressions for the stresses σ_x , σ_y and σ_z are reformulated.

$$\begin{aligned} \sigma_x &= \frac{G}{1-2\nu} \left[2(1-\nu) \frac{\partial U}{\partial x} + 2\nu \frac{\partial V}{\partial y} + 2\nu \frac{\partial W}{\partial z} \right] = \frac{2G}{1-2\nu} \left[(1-2\nu) \frac{\partial U}{\partial x} + \nu \frac{\partial U}{\partial x} + \nu \frac{\partial V}{\partial y} + \nu \frac{\partial W}{\partial z} \right] \\ &= 2G \left[\frac{\partial U}{\partial x} + \frac{\nu}{1-2\nu} \left(\frac{\partial U}{\partial x} + \frac{\partial V}{\partial y} + \frac{\partial W}{\partial z} \right) \right] \end{aligned} \quad (\text{B.3.58})$$

$$\begin{aligned} \sigma_y &= \frac{G}{1-2\nu} \left[2\nu \frac{\partial U}{\partial x} + 2(1-\nu) \frac{\partial V}{\partial y} + 2\nu \frac{\partial W}{\partial z} \right] = \frac{2G}{1-2\nu} \left[\nu \frac{\partial U}{\partial x} + (1-2\nu) \frac{\partial V}{\partial y} + \nu \frac{\partial V}{\partial y} + \nu \frac{\partial W}{\partial z} \right] \\ &= 2G \left[\frac{\partial V}{\partial y} + \frac{\nu}{1-2\nu} \left(\frac{\partial U}{\partial x} + \frac{\partial V}{\partial y} + \frac{\partial W}{\partial z} \right) \right] \end{aligned} \quad (\text{B.3.59})$$

$$\begin{aligned} \sigma_z &= \frac{G}{1-2\nu} \left[2\nu \frac{\partial U}{\partial x} + 2\nu \frac{\partial V}{\partial y} + 2(1-\nu) \frac{\partial W}{\partial z} \right] = \frac{2G}{1-2\nu} \left[\nu \frac{\partial U}{\partial x} + \nu \frac{\partial V}{\partial y} + (1-2\nu) \frac{\partial W}{\partial z} + \nu \frac{\partial W}{\partial z} \right] \\ &= 2G \left[\frac{\partial W}{\partial z} + \frac{\nu}{1-2\nu} \left(\frac{\partial U}{\partial x} + \frac{\partial V}{\partial y} + \frac{\partial W}{\partial z} \right) \right] \end{aligned} \quad (\text{B.3.60})$$

$$\tau_{xy} = G \left[\frac{\partial U}{\partial y} + \frac{\partial V}{\partial x} \right] \quad (\text{B.3.61})$$

$$\tau_{yz} = G \left[\frac{\partial V}{\partial z} + \frac{\partial W}{\partial y} \right] \quad (\text{B.3.62})$$

$$\tau_{zx} = G \left[\frac{\partial W}{\partial x} + \frac{\partial U}{\partial z} \right] \quad (\text{B.3.63})$$

¹In many books like [84], [64] or [63], the relation between the stresses and the strains is formulated using Young's modulus E . In the present work, the shear modulus G is used for the sake of a more compact formulation. The relation between E and G is given by $E = 2G(1+\nu)$.

The integrand for the virtual work of the stresses is given by:

$$\begin{aligned} \delta \boldsymbol{\varepsilon}^T \boldsymbol{\sigma} &= \left[\frac{\partial \delta U}{\partial x} \quad \frac{\partial \delta V}{\partial y} \quad \frac{\partial \delta W}{\partial z} \quad \frac{\partial \delta U}{\partial y} + \frac{\partial \delta V}{\partial x} \quad \frac{\partial \delta V}{\partial z} + \frac{\partial \delta W}{\partial y} \quad \frac{\partial \delta W}{\partial x} + \frac{\partial \delta U}{\partial z} \right] \begin{bmatrix} \sigma_x \\ \sigma_y \\ \sigma_z \\ \tau_{xy} \\ \tau_{yz} \\ \tau_{zx} \end{bmatrix} \\ &= \frac{\partial \delta U}{\partial x} \sigma_x + \frac{\partial \delta V}{\partial y} \sigma_y + \frac{\partial \delta W}{\partial z} \sigma_z \\ &\quad + \left[\frac{\partial \delta U}{\partial y} + \frac{\partial \delta V}{\partial x} \right] \tau_{xy} + \left[\frac{\partial \delta V}{\partial z} + \frac{\partial \delta W}{\partial y} \right] \tau_{yz} + \left[\frac{\partial \delta W}{\partial x} + \frac{\partial \delta U}{\partial z} \right] \tau_{zx} \end{aligned} \quad (\text{B.3.64})$$

The formulas (B.3.57), (B.3.58), (B.3.59), (B.3.60), (B.3.61), (B.3.62), (B.3.63) and (B.3.64) use the cartesian coordinates x , y and z and the displacements U , V and W in the directions of the cartesian coordinates. In the following considerations, the corresponding expressions for cylindrical coordinates will be derived.

In the first step, the virtual strains, i.e. the derivatives of the virtual displacements δU , δV and δW with respect to x , y and z , will be replaced. The basis are the following relations between the formulations for the strains using cartesian coordinates on the one hand and cylindrical coordinates on the other hand have been derived, which have been derived in section B.2:

$$\frac{\partial U}{\partial x} = \left[\frac{1}{r} \frac{\partial T}{\partial \phi} + \frac{R}{r} \right] \cos^2 \phi + \frac{\partial R}{\partial r} \sin^2 \phi + \left[\frac{1}{r} \frac{\partial R}{\partial \phi} - \frac{T}{r} + \frac{\partial T}{\partial r} \right] \sin \phi \cos \phi \quad (\text{B.3.65})$$

$$\frac{\partial W}{\partial z} = \left[\frac{1}{r} \frac{\partial T}{\partial \phi} + \frac{R}{r} \right] \sin^2 \phi + \frac{\partial R}{\partial r} \cos^2 \phi - \left[\frac{1}{r} \frac{\partial R}{\partial \phi} - \frac{T}{r} + \frac{\partial T}{\partial r} \right] \sin \phi \cos \phi \quad (\text{B.3.66})$$

$$\frac{\partial U}{\partial y} + \frac{\partial V}{\partial x} = \left[\frac{1}{r} \frac{\partial V}{\partial \phi} + \frac{\partial T}{\partial y} \right] \cos \phi + \left[\frac{\partial V}{\partial r} + \frac{\partial R}{\partial y} \right] \sin \phi \quad (\text{B.3.67})$$

$$\frac{\partial V}{\partial z} + \frac{\partial W}{\partial y} = \left[\frac{\partial V}{\partial r} + \frac{\partial R}{\partial y} \right] \cos \phi - \left[\frac{1}{r} \frac{\partial V}{\partial \phi} + \frac{\partial T}{\partial y} \right] \sin \phi \quad (\text{B.3.68})$$

$$\frac{\partial U}{\partial z} + \frac{\partial W}{\partial x} = \left[\frac{1}{r} \frac{\partial R}{\partial \phi} - \frac{T}{r} + \frac{\partial T}{\partial r} \right] [\cos^2 \phi - \sin^2 \phi] + 2 \left[\frac{\partial R}{\partial r} - \frac{1}{r} \frac{\partial T}{\partial \phi} - \frac{R}{r} \right] \sin \phi \cos \phi \quad (\text{B.3.69})$$

For a better overview, it is advantageous to treat the terms in certain groups. The first group contains derivatives of the displacement V with respect to x and z and derivatives of the displacements U and W with respect to y . Here, the relations (B.3.67) and (B.3.68) are used. By collecting the terms with respect to the derivatives of δT , δV and δR , it is obtained:

$$\begin{aligned} &\left[\frac{\partial \delta U}{\partial y} + \frac{\partial \delta V}{\partial x} \right] \tau_{xy} + \left[\frac{\partial \delta V}{\partial z} + \frac{\partial \delta W}{\partial y} \right] \tau_{yz} \\ &= \left(\left[\frac{1}{r} \frac{\partial \delta V}{\partial \phi} + \frac{\partial \delta T}{\partial y} \right] \cos \phi + \left[\frac{\partial \delta V}{\partial r} + \frac{\partial \delta R}{\partial y} \right] \sin \phi \right) \tau_{xy} \\ &\quad + \left(\left[\frac{\partial \delta V}{\partial r} + \frac{\partial \delta R}{\partial y} \right] \cos \phi - \left[\frac{1}{r} \frac{\partial \delta V}{\partial \phi} + \frac{\partial \delta T}{\partial y} \right] \sin \phi \right) \tau_{yz} \\ &= \left[\frac{1}{r} \frac{\partial \delta V}{\partial \phi} + \frac{\partial \delta T}{\partial y} \right] [\tau_{xy} \cos \phi - \tau_{yz} \sin \phi] + \left[\frac{\partial \delta V}{\partial r} + \frac{\partial \delta R}{\partial y} \right] [\tau_{xy} \sin \phi + \tau_{yz} \cos \phi] \end{aligned} \quad (\text{B.3.70})$$

In the second group, derivatives of the displacements U and W with respect to x and z are contained. Applying the relations (B.3.65), (B.3.66) and (B.3.69) leads to:

$$\begin{aligned}
& \frac{\partial \delta U}{\partial x} \sigma_x + \frac{\partial \delta W}{\partial z} \sigma_z + \left[\frac{\partial \delta W}{\partial x} + \frac{\partial \delta U}{\partial z} \right] \tau_{zx} \\
&= \left(\left[\frac{1}{r} \frac{\partial \delta T}{\partial \phi} + \frac{\delta R}{r} \right] \cos^2 \phi + \frac{\partial \delta R}{\partial r} \sin^2 \phi + \left[\frac{1}{r} \frac{\partial \delta R}{\partial \phi} - \frac{\delta T}{r} + \frac{\partial \delta T}{\partial r} \right] \sin \phi \cos \phi \right) \sigma_x \\
&+ \left(\left[\frac{1}{r} \frac{\partial \delta T}{\partial \phi} + \frac{\delta R}{r} \right] \sin^2 \phi + \frac{\partial \delta R}{\partial r} \cos^2 \phi - \left[\frac{1}{r} \frac{\partial \delta R}{\partial \phi} - \frac{\delta T}{r} + \frac{\partial \delta T}{\partial r} \right] \sin \phi \cos \phi \right) \sigma_z \\
&+ \left(\left[\frac{1}{r} \frac{\partial \delta R}{\partial \phi} - \frac{\delta T}{r} + \frac{\partial \delta T}{\partial r} \right] [\cos^2 \phi - \sin^2 \phi] + 2 \left[\frac{\partial \delta R}{\partial r} - \frac{1}{r} \frac{\partial \delta T}{\partial \phi} - \frac{\delta R}{r} \right] \sin \phi \cos \phi \right) \tau_{zx} \\
&= \left[\frac{1}{r} \frac{\partial \delta T}{\partial \phi} + \frac{\delta R}{r} \right] [\sigma_x \cos^2 \phi + \sigma_z \sin^2 \phi - 2 \tau_{zx} \sin \phi \cos \phi] \\
&+ \frac{\partial \delta R}{\partial r} [\sigma_x \sin^2 \phi + \sigma_z \cos^2 \phi + 2 \tau_{zx} \sin \phi \cos \phi] \\
&+ \left[\frac{1}{r} \frac{\partial \delta R}{\partial \phi} - \frac{\delta T}{r} + \frac{\partial \delta T}{\partial r} \right] [(\sigma_x - \sigma_z) \sin \phi \cos \phi + \tau_{zx} (\cos^2 \phi - \sin^2 \phi)] \tag{B.3.71}
\end{aligned}$$

The third group contains only the derivative of δV with respect to y . In the first step, this group remains unchanged.

In the second step, the terms containing the stresses will be evaluated using the following relations, which have been derived in section B.2:

$$\frac{1}{r} \frac{\partial T}{\partial \phi} + \frac{R}{r} = \frac{\partial U}{\partial x} \cos^2 \phi + \frac{\partial W}{\partial z} \sin^2 \phi - \left(\frac{\partial U}{\partial z} + \frac{\partial W}{\partial x} \right) \sin \phi \cos \phi \tag{B.3.72}$$

$$\frac{\partial R}{\partial r} = \frac{\partial U}{\partial x} \sin^2 \phi + \frac{\partial W}{\partial z} \cos^2 \phi + \left(\frac{\partial U}{\partial z} + \frac{\partial W}{\partial x} \right) \sin \phi \cos \phi \tag{B.3.73}$$

$$\frac{1}{r} \frac{\partial V}{\partial \phi} + \frac{\partial T}{\partial y} = \left(\frac{\partial U}{\partial y} + \frac{\partial V}{\partial x} \right) \cos \phi - \left(\frac{\partial V}{\partial z} + \frac{\partial W}{\partial y} \right) \sin \phi \tag{B.3.74}$$

$$\frac{\partial V}{\partial r} + \frac{\partial R}{\partial y} = \left(\frac{\partial V}{\partial z} + \frac{\partial W}{\partial y} \right) \cos \phi + \left(\frac{\partial U}{\partial y} + \frac{\partial V}{\partial x} \right) \sin \phi \tag{B.3.75}$$

$$\frac{1}{r} \frac{\partial R}{\partial \phi} - \frac{T}{r} + \frac{\partial T}{\partial r} = \left(\frac{\partial U}{\partial z} + \frac{\partial W}{\partial x} \right) (\cos^2 \phi - \sin^2 \phi) + 2 \left(\frac{\partial U}{\partial x} - \frac{\partial W}{\partial z} \right) \sin \phi \cos \phi \tag{B.3.76}$$

From (B.3.72) and (B.3.73) it follows:

$$\begin{aligned}
\frac{1}{r} \frac{\partial T}{\partial \phi} + \frac{R}{r} + \frac{\partial R}{\partial r} &= \frac{\partial U}{\partial x} \cos^2 \phi + \frac{\partial W}{\partial z} \sin^2 \phi - \left(\frac{\partial U}{\partial z} + \frac{\partial W}{\partial x} \right) \sin \phi \cos \phi \\
&+ \frac{\partial U}{\partial x} \sin^2 \phi + \frac{\partial W}{\partial z} \cos^2 \phi + \left(\frac{\partial U}{\partial z} + \frac{\partial W}{\partial x} \right) \sin \phi \cos \phi \\
&= \frac{\partial U}{\partial x} (\cos^2 \phi + \sin^2 \phi) + \frac{\partial W}{\partial z} (\sin^2 \phi + \cos^2 \phi) = \frac{\partial U}{\partial x} + \frac{\partial W}{\partial z} \tag{B.3.77}
\end{aligned}$$

In order to evaluate the aforementioned third group of terms, the expression (B.3.59) for σ_y is used. Applying the relation (B.3.77) leads to:

$$\begin{aligned}
\frac{\partial \delta V}{\partial y} \sigma_y &= \frac{\partial \delta V}{\partial y} 2G \left[\frac{\partial V}{\partial y} + \frac{\nu}{1-2\nu} \left(\frac{\partial U}{\partial x} + \frac{\partial V}{\partial y} + \frac{\partial W}{\partial z} \right) \right] \\
&= \frac{\partial \delta V}{\partial y} 2G \left[\frac{\partial V}{\partial y} + \frac{\nu}{1-2\nu} \left(\frac{1}{r} \frac{\partial T}{\partial \phi} + \frac{R}{r} + \frac{\partial R}{\partial r} + \frac{\partial V}{\partial y} \right) \right] \tag{B.3.78}
\end{aligned}$$

Next, the first group of terms is considered. Here, the expressions (B.3.61) and (B.3.62) are inserted into the terms contained in (B.3.70) and the relations (B.3.74) and (B.3.75) are applied. This gives the following results:

$$\begin{aligned}\tau_{xy} \cos \phi - \tau_{yz} \sin \phi &= G \left(\frac{\partial U}{\partial y} + \frac{\partial V}{\partial x} \right) \cos \phi - G \left(\frac{\partial V}{\partial z} + \frac{\partial W}{\partial y} \right) \sin \phi \\ &= G \left[\left(\frac{\partial U}{\partial y} + \frac{\partial V}{\partial x} \right) \cos \phi - \left(\frac{\partial V}{\partial z} + \frac{\partial W}{\partial y} \right) \sin \phi \right] = G \left[\frac{1}{r} \frac{\partial V}{\partial \phi} + \frac{\partial T}{\partial y} \right] \quad (\text{B.3.79})\end{aligned}$$

$$\begin{aligned}\tau_{xy} \sin \phi + \tau_{yz} \cos \phi &= G \left(\frac{\partial U}{\partial y} + \frac{\partial V}{\partial x} \right) \sin \phi + G \left(\frac{\partial V}{\partial z} + \frac{\partial W}{\partial y} \right) \cos \phi \\ &= G \left[\left(\frac{\partial U}{\partial y} + \frac{\partial V}{\partial x} \right) \sin \phi + \left(\frac{\partial V}{\partial z} + \frac{\partial W}{\partial y} \right) \cos \phi \right] = G \left[\frac{\partial V}{\partial r} + \frac{\partial R}{\partial y} \right] \quad (\text{B.3.80})\end{aligned}$$

Inserting these expressions into the integrand of the virtual work leads to:

$$\begin{aligned}&\left[\frac{\partial \delta U}{\partial y} + \frac{\partial \delta V}{\partial x} \right] \tau_{xy} + \left[\frac{\partial \delta V}{\partial z} + \frac{\partial \delta W}{\partial y} \right] \tau_{yz} \\ &= \left[\frac{1}{r} \frac{\partial \delta V}{\partial \phi} + \frac{\partial \delta T}{\partial y} \right] [\tau_{xy} \cos \phi - \tau_{yz} \sin \phi] + \left[\frac{\partial \delta V}{\partial r} + \frac{\partial \delta R}{\partial y} \right] [\tau_{xy} \sin \phi + \tau_{yz} \cos \phi] \\ &= \left[\frac{1}{r} \frac{\partial \delta V}{\partial \phi} + \frac{\partial \delta T}{\partial y} \right] G \left[\frac{1}{r} \frac{\partial V}{\partial \phi} + \frac{\partial T}{\partial y} \right] + \left[\frac{\partial \delta V}{\partial r} + \frac{\partial \delta R}{\partial y} \right] G \left[\frac{\partial V}{\partial r} + \frac{\partial R}{\partial y} \right] \quad (\text{B.3.81})\end{aligned}$$

The terms of (B.3.71) contain the stresses σ_x , σ_z and τ_{zx} . By inserting the expressions (B.3.58), (B.3.60) and (B.3.63) and applying the relations (B.3.72), (B.3.73) and (B.3.76), it is obtained:

$$\begin{aligned}&\sigma_x \cos^2 \phi + \sigma_z \sin^2 \phi - 2\tau_{zx} \sin \phi \cos \phi \\ &= 2G \left[\frac{\partial U}{\partial x} + \frac{\nu}{1-2\nu} \left(\frac{\partial U}{\partial x} + \frac{\partial V}{\partial y} + \frac{\partial W}{\partial z} \right) \right] \cos^2 \phi \\ &\quad + 2G \left[\frac{\partial W}{\partial z} + \frac{\nu}{1-2\nu} \left(\frac{\partial U}{\partial x} + \frac{\partial V}{\partial y} + \frac{\partial W}{\partial z} \right) \right] \sin^2 \phi - 2G \left[\frac{\partial W}{\partial x} + \frac{\partial U}{\partial z} \right] \sin \phi \cos \phi \\ &= 2G \left[\frac{\partial U}{\partial x} \cos^2 \phi + \frac{\partial W}{\partial z} \sin^2 \phi - \left(\frac{\partial W}{\partial x} + \frac{\partial U}{\partial z} \right) \sin \phi \cos \phi \right] \\ &\quad + 2G \frac{\nu}{1-2\nu} \left(\frac{\partial U}{\partial x} + \frac{\partial V}{\partial y} + \frac{\partial W}{\partial z} \right) (\cos^2 \phi + \sin^2 \phi) \\ &= 2G \left[\frac{1}{r} \frac{\partial T}{\partial \phi} + \frac{R}{r} + \frac{\nu}{1-2\nu} \left(\frac{1}{r} \frac{\partial T}{\partial \phi} + \frac{R}{r} + \frac{\partial V}{\partial y} + \frac{\partial R}{\partial r} \right) \right] \quad (\text{B.3.82})\end{aligned}$$

$$\begin{aligned}&\sigma_x \sin^2 \phi + \sigma_z \cos^2 \phi + 2\tau_{zx} \sin \phi \cos \phi \\ &= 2G \left[\frac{\partial U}{\partial x} + \frac{\nu}{1-2\nu} \left(\frac{\partial U}{\partial x} + \frac{\partial V}{\partial y} + \frac{\partial W}{\partial z} \right) \right] \sin^2 \phi \\ &\quad + 2G \left[\frac{\partial W}{\partial z} + \frac{\nu}{1-2\nu} \left(\frac{\partial U}{\partial x} + \frac{\partial V}{\partial y} + \frac{\partial W}{\partial z} \right) \right] \cos^2 \phi + 2G \left[\frac{\partial W}{\partial x} + \frac{\partial U}{\partial z} \right] \sin \phi \cos \phi \\ &= 2G \left[\frac{\partial U}{\partial x} \sin^2 \phi + \frac{\partial W}{\partial z} \cos^2 \phi + \left(\frac{\partial W}{\partial x} + \frac{\partial U}{\partial z} \right) \sin \phi \cos \phi \right] \\ &\quad + 2G \frac{\nu}{1-2\nu} \left(\frac{\partial U}{\partial x} + \frac{\partial V}{\partial y} + \frac{\partial W}{\partial z} \right) (\sin^2 \phi + \cos^2 \phi) \\ &= 2G \left[\frac{\partial R}{\partial r} + \frac{\nu}{1-2\nu} \left(\frac{1}{r} \frac{\partial T}{\partial \phi} + \frac{R}{r} + \frac{\partial R}{\partial r} + \frac{\partial V}{\partial y} \right) \right] \quad (\text{B.3.83})\end{aligned}$$

$$\begin{aligned}
& (\sigma_x - \sigma_z) \sin \phi \cos \phi + \tau_{zx} (\cos^2 \phi - \sin^2 \phi) \\
&= 2G \left[\frac{\partial U}{\partial x} + \frac{\nu}{1-2\nu} \left(\frac{\partial U}{\partial x} + \frac{\partial V}{\partial y} + \frac{\partial W}{\partial z} \right) \right] \sin \phi \cos \phi \\
&\quad - 2G \left[\frac{\partial W}{\partial z} + \frac{\nu}{1-2\nu} \left(\frac{\partial U}{\partial x} + \frac{\partial V}{\partial y} + \frac{\partial W}{\partial z} \right) \right] \sin \phi \cos \phi + G \left[\frac{\partial W}{\partial x} + \frac{\partial U}{\partial z} \right] (\cos^2 \phi - \sin^2 \phi) \\
&= G \left[2 \left(\frac{\partial U}{\partial x} - \frac{\partial W}{\partial z} \right) \sin \phi \cos \phi + \left(\frac{\partial W}{\partial x} + \frac{\partial U}{\partial z} \right) (\cos^2 \phi - \sin^2 \phi) \right] \\
&\quad + 2G \frac{\nu}{1-2\nu} \left(\frac{\partial U}{\partial x} + \frac{\partial V}{\partial y} + \frac{\partial W}{\partial z} \right) (\sin^2 \phi + \cos^2 \phi) \\
&= G \left[\frac{1}{r} \frac{\partial R}{\partial \phi} - \frac{T}{r} + \frac{\partial T}{\partial r} \right]
\end{aligned} \tag{B.3.84}$$

Inserting these relations into the second group (B.3.71) gives:

$$\begin{aligned}
& \frac{\partial \delta U}{\partial x} \sigma_x + \frac{\partial \delta W}{\partial z} \sigma_z + \left[\frac{\partial \delta W}{\partial x} + \frac{\partial \delta U}{\partial z} \right] \tau_{zx} \\
&= \left[\frac{1}{r} \frac{\partial \delta T}{\partial \phi} + \frac{\delta R}{r} \right] [\sigma_x \cos^2 \phi + \sigma_z \sin^2 \phi - 2 \tau_{zx} \sin \phi \cos \phi] \\
&\quad + \frac{\partial \delta R}{\partial r} [\sigma_x \sin^2 \phi + \sigma_z \cos^2 \phi + 2 \tau_{zx} \sin \phi \cos \phi] \\
&\quad + \left[\frac{1}{r} \frac{\partial \delta R}{\partial \phi} - \frac{\delta T}{r} + \frac{\partial \delta T}{\partial r} \right] [(\sigma_x - \sigma_z) \sin \phi \cos \phi + \tau_{zx} (\cos^2 \phi - \sin^2 \phi)] \\
&= \left[\frac{1}{r} \frac{\partial \delta T}{\partial \phi} + \frac{\delta R}{r} \right] 2G \left[\frac{1}{r} \frac{\partial T}{\partial \phi} + \frac{R}{r} + \frac{\nu}{1-2\nu} \left(\frac{1}{r} \frac{\partial T}{\partial \phi} + \frac{R}{r} + \frac{\partial V}{\partial y} + \frac{\partial R}{\partial r} \right) \right] \\
&\quad + \frac{\partial \delta R}{\partial r} 2G \left[\frac{\partial R}{\partial r} + \frac{\nu}{1-2\nu} \left(\frac{1}{r} \frac{\partial T}{\partial \phi} + \frac{R}{r} + \frac{\partial V}{\partial y} + \frac{\partial R}{\partial r} \right) \right] \\
&\quad + \left[\frac{1}{r} \frac{\partial \delta R}{\partial \phi} - \frac{\delta T}{r} + \frac{\partial \delta T}{\partial r} \right] G \left[\frac{1}{r} \frac{\partial R}{\partial \phi} - \frac{T}{r} + \frac{\partial T}{\partial r} \right]
\end{aligned} \tag{B.3.85}$$

Now, the complete integrand for the virtual work of the stresses can be formulated for cylindrical coordinates. It is obtained:

$$\begin{aligned}
\delta \varepsilon^T \sigma &= \frac{\partial \delta U}{\partial x} \sigma_x + \frac{\partial \delta V}{\partial y} \sigma_y + \frac{\partial \delta W}{\partial z} \sigma_z \\
&\quad + \left[\frac{\partial \delta U}{\partial y} + \frac{\partial \delta V}{\partial x} \right] \tau_{xy} + \left[\frac{\partial \delta V}{\partial z} + \frac{\partial \delta W}{\partial y} \right] \tau_{yz} + \left[\frac{\partial \delta W}{\partial x} + \frac{\partial \delta U}{\partial z} \right] \tau_{zx} \\
&= \left[\frac{1}{r} \frac{\partial \delta T}{\partial \phi} + \frac{\delta R}{r} \right] 2G \left[\frac{1}{r} \frac{\partial T}{\partial \phi} + \frac{R}{r} + \frac{\nu}{1-2\nu} \left(\frac{1}{r} \frac{\partial T}{\partial \phi} + \frac{R}{r} + \frac{\partial V}{\partial y} + \frac{\partial R}{\partial r} \right) \right] \\
&\quad + \frac{\partial \delta V}{\partial y} 2G \left[\frac{\partial V}{\partial y} + \frac{\nu}{1-2\nu} \left(\frac{1}{r} \frac{\partial T}{\partial \phi} + \frac{R}{r} + \frac{\partial R}{\partial r} + \frac{\partial V}{\partial y} \right) \right] \\
&\quad + \frac{\partial \delta R}{\partial r} 2G \left[\frac{\partial R}{\partial r} + \frac{\nu}{1-2\nu} \left(\frac{1}{r} \frac{\partial T}{\partial \phi} + \frac{R}{r} + \frac{\partial V}{\partial y} + \frac{\partial R}{\partial r} \right) \right] \\
&\quad + \left[\frac{1}{r} \frac{\partial \delta V}{\partial \phi} + \frac{\partial \delta T}{\partial y} \right] G \left[\frac{1}{r} \frac{\partial V}{\partial \phi} + \frac{\partial T}{\partial y} \right] + \left[\frac{\partial \delta V}{\partial r} + \frac{\partial \delta R}{\partial y} \right] G \left[\frac{\partial V}{\partial r} + \frac{\partial R}{\partial y} \right] \\
&\quad + \left[\frac{1}{r} \frac{\partial \delta R}{\partial \phi} - \frac{\delta T}{r} + \frac{\partial \delta T}{\partial r} \right] G \left[\frac{1}{r} \frac{\partial R}{\partial \phi} - \frac{T}{r} + \frac{\partial T}{\partial r} \right]
\end{aligned} \tag{B.3.86}$$

Using vectors, the result can be formulated in the following way:

$$\delta \boldsymbol{\varepsilon}^T \boldsymbol{\sigma} = \underbrace{\begin{bmatrix} \frac{1}{r} \frac{\partial \delta T}{\partial \phi} + \frac{\delta R}{r} \\ \frac{\partial \delta V}{\partial y} \\ \frac{\partial \delta R}{\partial r} \\ \frac{1}{r} \frac{\partial \delta V}{\partial \phi} + \frac{\partial \delta T}{\partial y} \\ \frac{\partial \delta V}{\partial r} + \frac{\partial \delta R}{\partial y} \\ \frac{1}{r} \frac{\partial \delta R}{\partial \phi} - \frac{\delta T}{r} + \frac{\partial \delta T}{\partial r} \end{bmatrix}^T}_{\boldsymbol{\varepsilon}_{cyl}^T} \underbrace{\begin{bmatrix} 2G \left[\frac{1}{r} \frac{\partial T}{\partial \phi} + \frac{R}{r} + \frac{\nu}{1-2\nu} \left(\frac{1}{r} \frac{\partial T}{\partial \phi} + \frac{R}{r} + \frac{\partial V}{\partial y} + \frac{\partial R}{\partial r} \right) \right] \\ 2G \left[\frac{\partial V}{\partial y} + \frac{\nu}{1-2\nu} \left(\frac{1}{r} \frac{\partial T}{\partial \phi} + \frac{R}{r} + \frac{\partial V}{\partial y} + \frac{\partial R}{\partial r} \right) \right] \\ 2G \left[\frac{\partial R}{\partial r} + \frac{\nu}{1-2\nu} \left(\frac{1}{r} \frac{\partial T}{\partial \phi} + \frac{R}{r} + \frac{\partial V}{\partial y} + \frac{\partial R}{\partial r} \right) \right] \\ G \left[\frac{1}{r} \frac{\partial V}{\partial \phi} + \frac{\partial T}{\partial y} \right] \\ G \left[\frac{\partial V}{\partial r} + \frac{\partial R}{\partial y} \right] \\ G \left[\frac{1}{r} \frac{\partial R}{\partial \phi} - \frac{T}{r} + \frac{\partial T}{\partial r} \right] \end{bmatrix}}_{\boldsymbol{\sigma}_{cyl}} = \delta \boldsymbol{\varepsilon}_{cyl}^T \boldsymbol{\sigma}_{cyl} \quad (\text{B.3.87})$$

The relation between the stress vector $\boldsymbol{\sigma}_{cyl}$ for cylindrical coordinates and the strain vector $\boldsymbol{\varepsilon}_{cyl}$ is given by the following equation:

$$\underbrace{\begin{bmatrix} \boldsymbol{\sigma}_t \\ \boldsymbol{\sigma}_y \\ \boldsymbol{\sigma}_r \\ \boldsymbol{\tau}_{ty} \\ \boldsymbol{\tau}_{yr} \\ \boldsymbol{\tau}_{rt} \end{bmatrix}}_{\boldsymbol{\sigma}_{cyl}} = \frac{G}{1-2\nu} \underbrace{\begin{bmatrix} 2(1-\nu) & 2\nu & 2\nu & 0 & 0 & 0 \\ 2\nu & 2(1-\nu) & 2\nu & 0 & 0 & 0 \\ 2\nu & 2\nu & 2(1-\nu) & 0 & 0 & 0 \\ 0 & 0 & 0 & 1-2\nu & 0 & 0 \\ 0 & 0 & 0 & 0 & 1-2\nu & 0 \\ 0 & 0 & 0 & 0 & 0 & 1-2\nu \end{bmatrix}}_{\mathbf{D}} \underbrace{\begin{bmatrix} \frac{1}{r} \frac{\partial T}{\partial \phi} + \frac{R}{r} \\ \frac{\partial V}{\partial y} \\ \frac{\partial R}{\partial r} \\ \frac{1}{r} \frac{\partial V}{\partial \phi} + \frac{\partial T}{\partial y} \\ \frac{\partial V}{\partial r} + \frac{\partial R}{\partial y} \\ \frac{1}{r} \frac{\partial R}{\partial \phi} - \frac{T}{r} + \frac{\partial T}{\partial r} \end{bmatrix}}_{\boldsymbol{\varepsilon}_{cyl}} \quad (\text{B.3.88})$$

In this formulation, the elasticity matrix \mathbf{D} is the same as for cartesian coordinates; this reflects the isotropy of the material, i.e. the material properties are the same for all orientations of coordinates.

B.4 Navier's equation

An isotropic linear elastic three-dimensional continuum is described by the following equation, which is e.g. given by Lifshitz and Landau [39]:

$$\rho \ddot{\mathbf{w}} = \frac{E}{2(1+\nu)} \Delta \mathbf{w} + \frac{E}{2(1+\nu)(1-2\nu)} \mathbf{grad} \operatorname{div} \mathbf{w} \Rightarrow \Delta \mathbf{w} + \frac{1}{1-2\nu} \mathbf{grad} \operatorname{div} \mathbf{w} - \frac{\rho}{G} \ddot{\mathbf{w}} = \mathbf{0} \quad (\text{B.4.89})$$

Here, the displacement \mathbf{w} is formulated for the directions of the cartesian coordinates x, y, z :

$$\mathbf{w} = \begin{bmatrix} U(x, y, z, t) \\ V(x, y, z, t) \\ W(x, y, z, t) \end{bmatrix} \quad (\text{B.4.90})$$

In this section, the equation will be formulated for cylindrical coordinates and for displacements in the direction of cylindrical coordinates. As already shown in section B.2, the relation between the displacements for the two different orientations is given by:

$$\underbrace{\begin{bmatrix} U \\ V \\ W \end{bmatrix}}_{\mathbf{w}} = \underbrace{\begin{bmatrix} \cos \phi & 0 & \sin \phi \\ 0 & 1 & 0 \\ -\sin \phi & 0 & \cos \phi \end{bmatrix}}_{\mathbf{S}_2(\phi)} \underbrace{\begin{bmatrix} T \\ V \\ R \end{bmatrix}}_{\mathbf{u}} \quad (\text{B.4.91})$$

From this relation, it can be derived immediately:

$$\mathbf{w} = \mathbf{S}_2(\phi) \mathbf{u} \Rightarrow \ddot{\mathbf{w}} = \mathbf{S}_2(\phi) \ddot{\mathbf{u}} \quad (\text{B.4.92})$$

In section B.1, the Laplace operator Δ has been derived for cylindrical coordinates r , ϕ , and y , which have the following relation to the cartesian coordinates:

$$x = r \sin \phi, \quad z = r \cos \phi \quad (\text{B.4.93})$$

For this relation, the Laplace operator for a function f is given by:

$$\Delta f = \frac{\partial^2 f}{\partial x^2} + \frac{\partial^2 f}{\partial y^2} + \frac{\partial^2 f}{\partial z^2} = \frac{1}{r^2} \frac{\partial^2 f}{\partial \phi^2} + \frac{\partial^2 f}{\partial y^2} + \frac{\partial^2 f}{\partial r^2} - \frac{1}{r} \frac{\partial f}{\partial r} \quad (\text{B.4.94})$$

Applying the Laplace operator to the displacement vector \mathbf{w} and applying the relation between the displacements \mathbf{w} and \mathbf{u} according to (B.4.91) gives the following result:

$$\begin{aligned} \Delta \mathbf{w} &= \frac{1}{r^2} \frac{\partial^2 \mathbf{w}}{\partial \phi^2} + \frac{\partial^2 \mathbf{w}}{\partial y^2} + \frac{\partial^2 \mathbf{w}}{\partial r^2} - \frac{1}{r} \frac{\partial \mathbf{w}}{\partial r} \\ &= \frac{1}{r^2} \frac{\partial^2}{\partial \phi^2} (\mathbf{S}_2(\phi) \mathbf{u}) + \frac{\partial^2}{\partial y^2} (\mathbf{S}_2(\phi) \mathbf{u}) + \frac{\partial^2}{\partial r^2} (\mathbf{S}_2(\phi) \mathbf{u}) - \frac{1}{r} \frac{\partial}{\partial r} (\mathbf{S}_2(\phi) \mathbf{u}) \\ &= \frac{1}{r^2} \frac{\partial^2}{\partial \phi^2} (\mathbf{S}_2(\phi) \mathbf{u}) + \mathbf{S}_2(\phi) \frac{\partial^2 \mathbf{u}}{\partial y^2} + \mathbf{S}_2(\phi) \frac{\partial^2 \mathbf{u}}{\partial r^2} - \mathbf{S}_2(\phi) \frac{1}{r} \frac{\partial \mathbf{u}}{\partial r} \end{aligned} \quad (\text{B.4.95})$$

For the second partial derivative with respect to the azimuth ϕ it is valid:

$$\begin{aligned} \frac{\partial^2}{\partial \phi^2} (\mathbf{S}_2(\phi) \mathbf{u}) &= \frac{\partial}{\partial \phi} \left(\frac{\partial}{\partial \phi} (\mathbf{S}_2(\phi) \mathbf{u}) \right) = \frac{\partial}{\partial \phi} \left(\frac{\partial \mathbf{S}_2(\phi)}{\partial \phi} \mathbf{u} + \mathbf{S}_2(\phi) \frac{\partial \mathbf{u}}{\partial \phi} \right) \\ &= \frac{\partial^2 \mathbf{S}_2(\phi)}{\partial \phi^2} \mathbf{u} + \frac{\mathbf{S}_2(\phi)}{\partial \phi} \frac{\partial \mathbf{u}}{\partial \phi} + \frac{\mathbf{S}_2(\phi)}{\partial \phi} \frac{\partial \mathbf{u}}{\partial \phi} + \mathbf{S}_2(\phi) \frac{\partial^2 \mathbf{u}}{\partial \phi^2} \\ &= \frac{\partial^2 \mathbf{S}_2(\phi)}{\partial \phi^2} \mathbf{u} + 2 \frac{\mathbf{S}_2(\phi)}{\partial \phi} \frac{\partial \mathbf{u}}{\partial \phi} + \mathbf{S}_2(\phi) \frac{\partial^2 \mathbf{u}}{\partial \phi^2} \end{aligned} \quad (\text{B.4.96})$$

The expression for $\Delta \mathbf{w}$ according to (B.4.95) shows, that all terms except the second partial derivative with respect to ϕ contain the rotation matrix $\mathbf{S}_2(\phi)$ as the first factor. The acceleration $\ddot{\mathbf{w}}$ contains the matrix $\mathbf{S}_2(\phi)$ as the first factor, too, as it can be seen from (B.4.92). Therefore, the expression (B.4.96) is reformulated using the relation:

$$\mathbf{S}_2(\phi) \mathbf{S}_2(-\phi) = \mathbf{I} \quad (\text{B.4.97})$$

By changing the sign of the rotation angle, the inverse of the rotation matrix is obtained. Based on this, it can be formulated:

$$\begin{aligned} \frac{\partial^2}{\partial \phi^2} (\mathbf{S}_2(\phi) \mathbf{u}) &= \frac{\partial^2 \mathbf{S}_2(\phi)}{\partial \phi^2} \mathbf{u} + 2 \frac{\mathbf{S}_2(\phi)}{\partial \phi} \frac{\partial \mathbf{u}}{\partial \phi} + \mathbf{S}_2(\phi) \frac{\partial^2 \mathbf{u}}{\partial \phi^2} \\ &= \underbrace{\mathbf{S}_2(\phi) \mathbf{S}_2(-\phi)}_{\mathbf{I}} \frac{\partial^2 \mathbf{S}_2(\phi)}{\partial \phi^2} \mathbf{u} + 2 \underbrace{\mathbf{S}_2(\phi) \mathbf{S}_2(-\phi)}_{\mathbf{I}} \frac{\mathbf{S}_2(\phi)}{\partial \phi} \frac{\partial \mathbf{u}}{\partial \phi} + \mathbf{S}_2(\phi) \frac{\partial^2 \mathbf{u}}{\partial \phi^2} \\ &= \mathbf{S}_2(\phi) \left(\mathbf{S}_2(-\phi) \frac{\partial^2 \mathbf{S}_2(\phi)}{\partial \phi^2} \mathbf{u} + 2 \mathbf{S}_2(-\phi) \frac{\mathbf{S}_2(\phi)}{\partial \phi} \frac{\partial \mathbf{u}}{\partial \phi} + \frac{\partial^2 \mathbf{u}}{\partial \phi^2} \right) \end{aligned} \quad (\text{B.4.98})$$

As a result, the rotation matrix $\mathbf{S}_2(\phi)$ can now be factored out. Inserting this into (B.4.95) leads to:

$$\begin{aligned}
\Delta \mathbf{w} &= \frac{1}{r^2} \frac{\partial^2}{\partial \phi^2} (\mathbf{S}_2(\phi) \mathbf{u}) + \mathbf{S}_2(\phi) \frac{\partial^2 \mathbf{u}}{\partial y^2} + \mathbf{S}_2(\phi) \frac{\partial^2 \mathbf{u}}{\partial r^2} - \mathbf{S}_2(\phi) \frac{1}{r} \frac{\partial \mathbf{u}}{\partial r} \\
&= \frac{1}{r^2} \mathbf{S}_2(\phi) \left(\mathbf{S}_2(-\phi) \frac{\partial^2 \mathbf{S}_2(\phi)}{\partial \phi^2} \mathbf{u} + 2 \mathbf{S}_2(-\phi) \frac{\mathbf{S}_2(\phi)}{\partial \phi} \frac{\partial \mathbf{u}}{\partial \phi} + \frac{\partial^2 \mathbf{u}}{\partial \phi^2} \right) \\
&\quad + \mathbf{S}_2(\phi) \frac{\partial^2 \mathbf{u}}{\partial y^2} + \mathbf{S}_2(\phi) \frac{\partial^2 \mathbf{u}}{\partial r^2} - \mathbf{S}_2(\phi) \frac{1}{r} \frac{\partial \mathbf{u}}{\partial r} \\
&= \mathbf{S}_2(\phi) \left(\frac{1}{r^2} \mathbf{S}_2(-\phi) \frac{\partial^2 \mathbf{S}_2(\phi)}{\partial \phi^2} \mathbf{u} + \frac{2}{r^2} \mathbf{S}_2(-\phi) \frac{\mathbf{S}_2(\phi)}{\partial \phi} \frac{\partial \mathbf{u}}{\partial \phi} + \frac{1}{r^2} \frac{\partial^2 \mathbf{u}}{\partial \phi^2} + \frac{\partial^2 \mathbf{u}}{\partial y^2} + \frac{\partial^2 \mathbf{u}}{\partial r^2} - \frac{1}{r} \frac{\partial \mathbf{u}}{\partial r} \right)
\end{aligned} \tag{B.4.99}$$

For the rotation matrix $\mathbf{S}_2(\phi)$ and its derivatives it is valid:

$$\mathbf{S}_2(\phi) = \begin{bmatrix} \cos \phi & 0 & -\sin \phi \\ 0 & 1 & 0 \\ \sin \phi & 0 & \cos \phi \end{bmatrix} \tag{B.4.100}$$

$$\frac{\mathbf{S}_2(\phi)}{\partial \phi} = \begin{bmatrix} -\sin \phi & 0 & \cos \phi \\ 0 & 1 & 0 \\ -\cos \phi & 0 & -\sin \phi \end{bmatrix} \tag{B.4.101}$$

$$\frac{\partial^2 \mathbf{S}_2(\phi)}{\partial \phi^2} = \begin{bmatrix} -\cos \phi & 0 & \sin \phi \\ 0 & 0 & 0 \\ -\sin \phi & 0 & -\cos \phi \end{bmatrix} \tag{B.4.102}$$

From this, it follows for the product of the inverse $\mathbf{S}_2(-\phi)$ and the derivatives:

$$\begin{aligned}
\mathbf{S}_2(-\phi) \frac{\partial \mathbf{S}_2(\phi)}{\partial \phi} &= \begin{bmatrix} \cos \phi & 0 & -\sin \phi \\ 0 & 1 & 0 \\ \sin \phi & 0 & \cos \phi \end{bmatrix} \begin{bmatrix} -\sin \phi & 0 & \cos \phi \\ 0 & 1 & 0 \\ -\cos \phi & 0 & -\sin \phi \end{bmatrix} \\
&= \begin{bmatrix} -\cos \phi \sin \phi + \sin \phi \cos \phi & 0 & \cos^2 \phi + \sin^2 \phi \\ 0 & 1 & 0 \\ -\sin^2 \phi - \cos^2 \phi & 0 & \cos \phi \sin \phi - \sin \phi \cos \phi \end{bmatrix} = \begin{bmatrix} 0 & 0 & 1 \\ 0 & 1 & 0 \\ -1 & 0 & 0 \end{bmatrix}
\end{aligned} \tag{B.4.103}$$

$$\begin{aligned}
\mathbf{S}_2(-\phi) \frac{\partial^2 \mathbf{S}_2(\phi)}{\partial \phi^2} &= \begin{bmatrix} \cos \phi & 0 & -\sin \phi \\ 0 & 1 & 0 \\ \sin \phi & 0 & \cos \phi \end{bmatrix} \begin{bmatrix} -\cos \phi & 0 & \sin \phi \\ 0 & 0 & 0 \\ \sin \phi & 0 & -\cos \phi \end{bmatrix} \\
&= \begin{bmatrix} -\cos^2 \phi - \sin^2 \phi & 0 & -\cos \phi \sin \phi + \sin \phi \cos \phi \\ 0 & 1 & 0 \\ -\sin \phi \cos \phi + \cos \phi \sin \phi & 0 & -\sin^2 \phi - \cos^2 \phi \end{bmatrix} = \begin{bmatrix} -1 & 0 & 0 \\ 0 & 1 & 0 \\ 0 & 0 & -1 \end{bmatrix}
\end{aligned} \tag{B.4.104}$$

Thereby, the expression $\Delta \mathbf{w}$ can be formulated in the following way:

$$\begin{aligned}
\Delta \mathbf{w} &= \mathbf{S}_2(\phi) \left(\frac{1}{r^2} \mathbf{S}_2(-\phi) \frac{\partial^2 \mathbf{S}_2(\phi)}{\partial \phi^2} \mathbf{u} + \frac{2}{r^2} \mathbf{S}_2(-\phi) \frac{\mathbf{S}_2(\phi)}{\partial \phi} \frac{\partial \mathbf{u}}{\partial \phi} + \frac{1}{r^2} \frac{\partial^2 \mathbf{u}}{\partial \phi^2} + \frac{\partial^2 \mathbf{u}}{\partial y^2} + \frac{\partial^2 \mathbf{u}}{\partial r^2} - \frac{1}{r} \frac{\partial \mathbf{u}}{\partial r} \right) \\
&= \mathbf{S}_2(\phi) \left(\frac{1}{r^2} \begin{bmatrix} -1 & 0 & 0 \\ 0 & 1 & 0 \\ 0 & 0 & -1 \end{bmatrix} \mathbf{u} + \frac{2}{r^2} \begin{bmatrix} 0 & 0 & 1 \\ 0 & 1 & 0 \\ -1 & 0 & 0 \end{bmatrix} \frac{\partial \mathbf{u}}{\partial \phi} + \frac{1}{r^2} \frac{\partial^2 \mathbf{u}}{\partial \phi^2} + \frac{\partial^2 \mathbf{u}}{\partial y^2} + \frac{\partial^2 \mathbf{u}}{\partial r^2} - \frac{1}{r} \frac{\partial \mathbf{u}}{\partial r} \right)
\end{aligned} \tag{B.4.105}$$

The gradient is directly obtained from the following relation between the derivatives with respect to the cartesian coordinates x , y and z on the one hand and those with respect to the cylindrical coordinates r , ϕ and y on the other hand, which has been derived in section B.1 :

$$\mathbf{grad} f = \begin{bmatrix} \frac{\partial f}{\partial x} \\ \frac{\partial f}{\partial y} \\ \frac{\partial f}{\partial z} \end{bmatrix} = \begin{bmatrix} \cos \phi & 0 & \sin \phi \\ 0 & 1 & 0 \\ -\sin \phi & 0 & \cos \phi \end{bmatrix} \begin{bmatrix} \frac{1}{r} \frac{\partial f}{\partial \phi} \\ \frac{\partial f}{\partial y} \\ \frac{\partial f}{\partial r} \end{bmatrix} = \mathbf{S}_2(\phi) \begin{bmatrix} \frac{1}{r} \frac{\partial f}{\partial \phi} \\ \frac{\partial f}{\partial y} \\ \frac{\partial f}{\partial r} \end{bmatrix} \quad (\text{B.4.106})$$

From this, it follows for the derivatives with respect to x and z :

$$\frac{\partial f}{\partial x} = \frac{1}{r} \frac{\partial f}{\partial \phi} \cos \phi + \frac{\partial f}{\partial r} \sin \phi, \quad \frac{\partial f}{\partial z} = -\frac{1}{r} \frac{\partial f}{\partial \phi} \sin \phi + \frac{\partial f}{\partial r} \cos \phi \quad (\text{B.4.107})$$

Based on this relation and on the following relations according to (B.4.91)

$$U = T \cos \phi + R \sin \phi, \quad W = R \cos \phi - T \sin \phi \quad (\text{B.4.108})$$

it is obtained for the derivatives $\frac{\partial U}{\partial x}$ and $\frac{\partial W}{\partial z}$:

$$\begin{aligned} \frac{\partial U}{\partial x} &= \frac{1}{r} \frac{\partial}{\partial \phi} (T \cos \phi + R \sin \phi) \cos \phi + \frac{\partial}{\partial r} (T \cos \phi + R \sin \phi) \sin \phi \\ &= \frac{1}{r} \left(\frac{\partial T}{\partial \phi} \cos \phi - T \sin \phi + \frac{\partial R}{\partial \phi} \sin \phi + R \cos \phi \right) \cos \phi + \left(\frac{\partial T}{\partial r} \cos \phi + \frac{\partial R}{\partial r} \sin \phi \right) \sin \phi \\ &= \frac{1}{r} \left(\frac{\partial T}{\partial \phi} + R \right) \cos^2 \phi + \left(-\frac{1}{r} T + \frac{1}{r} \frac{\partial R}{\partial \phi} + \frac{\partial T}{\partial r} \right) \sin \phi \cos \phi + \frac{\partial R}{\partial r} \sin^2 \phi \quad (\text{B.4.109}) \end{aligned}$$

$$\begin{aligned} \frac{\partial W}{\partial z} &= -\frac{1}{r} \frac{\partial}{\partial \phi} (R \cos \phi - T \sin \phi) \sin \phi + \frac{\partial}{\partial r} (R \cos \phi - T \sin \phi) \cos \phi \\ &= -\frac{1}{r} \left(\frac{\partial R}{\partial \phi} \cos \phi - R \sin \phi - \frac{\partial T}{\partial \phi} \sin \phi - T \cos \phi \right) \sin \phi + \left(\frac{\partial R}{\partial r} \cos \phi - \frac{\partial T}{\partial r} \sin \phi \right) \cos \phi \\ &= \frac{1}{r} \left(R + \frac{\partial T}{\partial \phi} \right) \sin^2 \phi + \left(-\frac{1}{r} \frac{\partial R}{\partial \phi} + \frac{1}{r} T - \frac{\partial T}{\partial r} \right) \sin \phi \cos \phi + \frac{\partial R}{\partial r} \cos^2 \phi \quad (\text{B.4.110}) \end{aligned}$$

This leads to the following expression for the divergence $\text{div} \mathbf{w}$ of the displacement:

$$\begin{aligned} \text{div} \mathbf{w} &= \frac{\partial U}{\partial x} + \frac{\partial V}{\partial y} + \frac{\partial W}{\partial z} \\ &= \frac{1}{r} \left(\frac{\partial T}{\partial \phi} + R \right) \cos^2 \phi + \left(-\frac{1}{r} T + \frac{1}{r} \frac{\partial R}{\partial \phi} + \frac{\partial T}{\partial r} \right) \sin \phi \cos \phi + \frac{\partial R}{\partial r} \sin^2 \phi + \frac{\partial V}{\partial y} \\ &\quad + \frac{1}{r} \left(R + \frac{\partial T}{\partial \phi} \right) \sin^2 \phi + \left(-\frac{1}{r} \frac{\partial R}{\partial \phi} + \frac{1}{r} T - \frac{\partial T}{\partial r} \right) \sin \phi \cos \phi + \frac{\partial R}{\partial r} \cos^2 \phi \\ &= \frac{1}{r} \left(\frac{\partial T}{\partial \phi} + R \right) (\cos^2 \phi + \sin^2 \phi) + \frac{\partial R}{\partial r} (\sin^2 \phi + \cos^2 \phi) + \frac{\partial V}{\partial y} \\ &= \frac{1}{r} \left(\frac{\partial T}{\partial \phi} + R \right) + \frac{\partial R}{\partial r} + \frac{\partial V}{\partial y} = \frac{1}{r} \frac{\partial T}{\partial \phi} + \frac{R}{r} + \frac{\partial R}{\partial r} + \frac{\partial V}{\partial y} \quad (\text{B.4.111}) \end{aligned}$$

Now, the terms can be inserted into Navier's equation, as given in (B.4.89). This leads to:

$$\begin{aligned}
\mathbf{0} &= \Delta \mathbf{w} + \frac{1}{1-2\nu} \mathbf{grad} \operatorname{div} \mathbf{w} - \frac{\rho}{G} \ddot{\mathbf{w}} \\
&= \mathbf{S}_2(\phi) \left(\frac{1}{r^2} \begin{bmatrix} -1 & 0 & 0 \\ 0 & 0 & 0 \\ 0 & 0 & -1 \end{bmatrix} \mathbf{u} + \frac{2}{r^2} \begin{bmatrix} 0 & 0 & 1 \\ 0 & 0 & 0 \\ -1 & 0 & 0 \end{bmatrix} \frac{\partial \mathbf{u}}{\partial \phi} + \frac{1}{r^2} \frac{\partial^2 \mathbf{u}}{\partial \phi^2} + \frac{\partial^2 \mathbf{u}}{\partial y^2} + \frac{\partial^2 \mathbf{u}}{\partial r^2} - \frac{1}{r} \frac{\partial \mathbf{u}}{\partial r} \right) \\
&\quad + \frac{1}{1-2\nu} \mathbf{S}_2(\phi) \begin{bmatrix} \frac{1}{r} \frac{\partial}{\partial \phi} \\ \frac{\partial}{\partial y} \\ \frac{\partial}{\partial r} \end{bmatrix} \left(\frac{1}{r} \frac{\partial T}{\partial \phi} + \frac{R}{r} + \frac{\partial R}{\partial r} + \frac{\partial V}{\partial y} \right) - \frac{\rho}{G} \mathbf{S}_2(\phi) \ddot{\mathbf{u}} \quad (\text{B.4.112})
\end{aligned}$$

It can be seen that the rotation matrix $\mathbf{S}_2(\phi)$ is the first non-scalar factor in all terms. By multiplying the equation with the inverse $\mathbf{S}_2(\phi)^{-1} = \mathbf{S}_2(-\phi)$ it is obtained:

$$\begin{aligned}
\mathbf{0} &= \frac{1}{r^2} \frac{\partial^2 \mathbf{u}}{\partial \phi^2} + \frac{\partial^2 \mathbf{u}}{\partial y^2} + \frac{\partial^2 \mathbf{u}}{\partial r^2} - \frac{1}{r} \frac{\partial \mathbf{u}}{\partial r} + \frac{1}{r^2} \begin{bmatrix} -1 & 0 & 0 \\ 0 & 0 & 0 \\ 0 & 0 & -1 \end{bmatrix} \mathbf{u} + \frac{2}{r^2} \begin{bmatrix} 0 & 0 & 1 \\ 0 & 0 & 0 \\ -1 & 0 & 0 \end{bmatrix} \frac{\partial \mathbf{u}}{\partial \phi} \\
&\quad + \frac{1}{1-2\nu} \begin{bmatrix} \frac{1}{r} \frac{\partial}{\partial \phi} \\ \frac{\partial}{\partial y} \\ \frac{\partial}{\partial r} \end{bmatrix} \left(\frac{1}{r} \frac{\partial T}{\partial \phi} + \frac{R}{r} + \frac{\partial R}{\partial r} + \frac{\partial V}{\partial y} \right) - \frac{\rho}{G} \ddot{\mathbf{u}} \quad (\text{B.4.113})
\end{aligned}$$

Based on this, the equations for the three components can be formulated. It is obtained:

$$\begin{aligned}
0 &= \frac{1}{r^2} \frac{\partial^2 T}{\partial \phi^2} + \frac{\partial^2 T}{\partial y^2} + \frac{\partial^2 T}{\partial r^2} - \frac{1}{r} \frac{\partial T}{\partial r} - \frac{1}{r^2} T + \frac{2}{r^2} \frac{\partial R}{\partial \phi} \\
&\quad + \frac{1}{1-2\nu} \frac{1}{r} \frac{\partial}{\partial \phi} \left(\frac{1}{r} \frac{\partial T}{\partial \phi} + \frac{R}{r} + \frac{\partial R}{\partial r} + \frac{\partial V}{\partial y} \right) - \frac{\rho}{G} \ddot{T} \quad (\text{B.4.114})
\end{aligned}$$

$$0 = \frac{1}{r^2} \frac{\partial^2 V}{\partial \phi^2} + \frac{\partial^2 V}{\partial y^2} + \frac{\partial^2 V}{\partial r^2} - \frac{1}{r} \frac{\partial V}{\partial r} + \frac{1}{1-2\nu} \frac{\partial}{\partial y} \left(\frac{1}{r} \frac{\partial T}{\partial \phi} + \frac{R}{r} + \frac{\partial R}{\partial r} + \frac{\partial V}{\partial y} \right) - \frac{\rho}{G} \ddot{V} \quad (\text{B.4.115})$$

$$\begin{aligned}
0 &= \frac{1}{r^2} \frac{\partial^2 R}{\partial \phi^2} + \frac{\partial^2 R}{\partial y^2} + \frac{\partial^2 R}{\partial r^2} - \frac{1}{r} \frac{\partial R}{\partial r} - \frac{1}{r^2} R - \frac{2}{r^2} \frac{\partial T}{\partial \phi} \\
&\quad + \frac{1}{1-2\nu} \frac{\partial}{\partial r} \left(\frac{1}{r} \frac{\partial T}{\partial \phi} + \frac{R}{r} + \frac{\partial R}{\partial r} + \frac{\partial V}{\partial y} \right) - \frac{\rho}{G} \ddot{R} \quad (\text{B.4.116})
\end{aligned}$$

Appendix C

Derivation of the kinematics and the inertial terms for a flexible body

C.1 Kinematics: Floating frame of reference formulation

The motion of a point P relative to the origin O of the inertial frame I is considered. The frame \mathcal{P} representing the orientation of the particle is attached to the point P. By using a floating frame of reference \mathcal{R} , which has the origin R, the absolute position of the point P can be described in the following way:

$$\mathbf{r}_{OP}^I = \mathbf{r}_{OR}^I + \mathbf{S}^{I\mathcal{R}} \mathbf{r}_{RP}^{\mathcal{R}} \quad (\text{C.1.1})$$

Here, the vector \mathbf{r}_{OR}^I describes the position of the floating frame's origin R relative to the inertial frame's origin O; this vector is expressed in the coordinates of the inertial frame I . The vector $\mathbf{r}_{RP}^{\mathcal{R}}$ describes the position of the point P relative to the point R, formulated in the coordinates of the floating frame \mathcal{R} . The matrix $\mathbf{S}^{I\mathcal{R}}$ is the rotation matrix, which transforms the floating frame \mathcal{R} into the inertial frame I . The rotation matrix $\mathbf{S}^{I\mathcal{P}}$ between the inertial frame I and the frame \mathcal{P} is obtained by:

$$\mathbf{S}^{I\mathcal{P}} = \mathbf{S}^{I\mathcal{R}} \mathbf{S}^{\mathcal{R}\mathcal{P}} \quad (\text{C.1.2})$$

The velocity and the acceleration are obtained from the first and the second derivative of the position vector with respect to the time t :

$$\mathbf{v}_{OP}^I = \frac{d\mathbf{r}_{OP}^I}{dt} = \mathbf{v}_{OR}^I + \dot{\mathbf{S}}^{I\mathcal{R}} \mathbf{r}_{RP}^{\mathcal{R}} + \mathbf{S}^{I\mathcal{R}} \dot{\mathbf{r}}_{RP}^{\mathcal{R}} \quad (\text{C.1.3})$$

$$\mathbf{a}_{OP}^I = \frac{d^2\mathbf{r}_{OP}^I}{dt^2} = \mathbf{a}_{OR}^I + \ddot{\mathbf{S}}^{I\mathcal{R}} \mathbf{r}_{RP}^{\mathcal{R}} + 2\dot{\mathbf{S}}^{I\mathcal{R}} \dot{\mathbf{r}}_{RP}^{\mathcal{R}} + \mathbf{S}^{I\mathcal{R}} \ddot{\mathbf{r}}_{RP}^{\mathcal{R}} \quad (\text{C.1.4})$$

Here, \mathbf{v}_{OR}^I and \mathbf{a}_{OR}^I denote the absolute velocity and the absolute acceleration, respectively, of the point R with respect to the origin O; also these vectors are expressed in the inertial frame I . The derivative $\dot{\mathbf{S}}^{I\mathcal{R}}$ of the rotation matrix can be replaced in the following way:

$$\dot{\mathbf{S}}^{I\mathcal{R}} = \tilde{\boldsymbol{\omega}}_{I\mathcal{R}}^I \mathbf{S}^{I\mathcal{R}} \quad (\text{C.1.5})$$

The vector $\boldsymbol{\omega}_{I\mathcal{R}}^I$ denotes the angular velocity of the frame \mathcal{R} relative to I expressed in the inertial frame I . By using the tilde operator the cross product or vector product can be expressed by the

multiplication of a matrix and a vector. Thereby, the relation between $\omega_{I\mathcal{R}}^I$ and $\tilde{\omega}_{I\mathcal{R}}^I$ is given by:

$$\tilde{\omega}_{I\mathcal{R}}^I \mathbf{S}^{I\mathcal{R}} \mathbf{r}_{\text{RP}}^{\mathcal{R}} = \omega_{I\mathcal{R}}^I \times \left(\mathbf{S}^{I\mathcal{R}} \mathbf{r}_{\text{RP}}^{\mathcal{R}} \right), \quad \omega_{I\mathcal{R}}^I = \begin{bmatrix} \omega_1 \\ \omega_2 \\ \omega_3 \end{bmatrix} \Rightarrow \tilde{\omega}_{I\mathcal{R}}^I = \begin{bmatrix} 0 & -\omega_3 & \omega_2 \\ \omega_3 & 0 & -\omega_1 \\ -\omega_2 & \omega_1 & 0 \end{bmatrix} \quad (\text{C.1.6})$$

By using a recursion, the second derivative of the rotation matrix can be formulated as:

$$\ddot{\mathbf{S}}^{I\mathcal{R}} = \frac{d}{dt}(\tilde{\omega}_{I\mathcal{R}}^I \mathbf{S}^{I\mathcal{R}}) = \dot{\tilde{\omega}}_{I\mathcal{R}}^I \mathbf{S}^{I\mathcal{R}} + \tilde{\omega}_{I\mathcal{R}}^I \dot{\mathbf{S}}^{I\mathcal{R}} = \dot{\tilde{\omega}}_{I\mathcal{R}}^I \mathbf{S}^{I\mathcal{R}} + \tilde{\omega}_{I\mathcal{R}}^I \tilde{\omega}_{I\mathcal{R}}^I \mathbf{S}^{I\mathcal{R}} \quad (\text{C.1.7})$$

Thereby, the absolute velocity and the absolute acceleration of the point P can be written in the following way:

$$\begin{aligned} \mathbf{v}_{\text{OP}}^I &= \mathbf{v}_{\text{OR}}^I + \dot{\mathbf{S}}^{I\mathcal{R}} \mathbf{r}_{\text{RP}}^{\mathcal{R}} + \mathbf{S}^{I\mathcal{R}} \dot{\mathbf{r}}_{\text{RP}}^{\mathcal{R}} \\ &= \mathbf{v}_{\text{OR}}^I + \tilde{\omega}_{I\mathcal{R}}^I \mathbf{S}^{I\mathcal{R}} \mathbf{r}_{\text{RP}}^{\mathcal{R}} + \mathbf{S}^{I\mathcal{R}} \dot{\mathbf{r}}_{\text{RP}}^{\mathcal{R}} \end{aligned} \quad (\text{C.1.8})$$

$$\begin{aligned} \mathbf{a}_{\text{OP}}^I &= \mathbf{a}_{\text{OR}}^I + \ddot{\mathbf{S}}^{I\mathcal{R}} \mathbf{r}_{\text{RP}}^{\mathcal{R}} + 2\dot{\mathbf{S}}^{I\mathcal{R}} \dot{\mathbf{r}}_{\text{RP}}^{\mathcal{R}} + \mathbf{S}^{I\mathcal{R}} \ddot{\mathbf{r}}_{\text{RP}}^{\mathcal{R}} \\ &= \mathbf{a}_{\text{OR}}^I + \dot{\tilde{\omega}}_{I\mathcal{R}}^I \mathbf{S}^{I\mathcal{R}} \mathbf{r}_{\text{RP}}^{\mathcal{R}} + \tilde{\omega}_{I\mathcal{R}}^I \tilde{\omega}_{I\mathcal{R}}^I \mathbf{S}^{I\mathcal{R}} \mathbf{r}_{\text{RP}}^{\mathcal{R}} + 2\tilde{\omega}_{I\mathcal{R}}^I \mathbf{S}^{I\mathcal{R}} \dot{\mathbf{r}}_{\text{RP}}^{\mathcal{R}} + \mathbf{S}^{I\mathcal{R}} \ddot{\mathbf{r}}_{\text{RP}}^{\mathcal{R}} \end{aligned} \quad (\text{C.1.9})$$

For some considerations it is advantageous to describe the angular velocity in the reference frame \mathcal{R} . It is valid:

$$\omega_{I\mathcal{R}}^{\mathcal{R}} = \mathbf{S}^{\mathcal{R}I} \omega_{I\mathcal{R}}^I \Leftrightarrow \omega_{I\mathcal{R}}^I = \mathbf{S}^{I\mathcal{R}} \omega_{I\mathcal{R}}^{\mathcal{R}} \quad (\text{C.1.10})$$

The tilde matrix is transformed in the following way:

$$\tilde{\omega}_{I\mathcal{R}}^{\mathcal{R}} = \mathbf{S}^{\mathcal{R}I} \tilde{\omega}_{I\mathcal{R}}^I \mathbf{S}^{I\mathcal{R}} \Rightarrow \mathbf{S}^{I\mathcal{R}} \tilde{\omega}_{I\mathcal{R}}^{\mathcal{R}} = \tilde{\omega}_{I\mathcal{R}}^I \mathbf{S}^{I\mathcal{R}} \quad (\text{C.1.11})$$

The angular acceleration $\dot{\omega}_{I\mathcal{R}}^I$ is the derivative of the angular velocity $\tilde{\omega}_{I\mathcal{R}}^I$ with respect to the time t . This leads to:

$$\begin{aligned} \dot{\omega}_{I\mathcal{R}}^I &= \mathbf{S}^{I\mathcal{R}} \dot{\omega}_{I\mathcal{R}}^{\mathcal{R}} \\ \Rightarrow \dot{\omega}_{I\mathcal{R}}^I &= \dot{\mathbf{S}}^{I\mathcal{R}} \omega_{I\mathcal{R}}^{\mathcal{R}} + \mathbf{S}^{I\mathcal{R}} \dot{\omega}_{I\mathcal{R}}^{\mathcal{R}} = \tilde{\omega}_{I\mathcal{R}}^I \mathbf{S}^{I\mathcal{R}} \omega_{I\mathcal{R}}^{\mathcal{R}} + \mathbf{S}^{I\mathcal{R}} \dot{\omega}_{I\mathcal{R}}^{\mathcal{R}} = \tilde{\omega}_{I\mathcal{R}}^I \omega_{I\mathcal{R}}^I + \mathbf{S}^{I\mathcal{R}} \dot{\omega}_{I\mathcal{R}}^{\mathcal{R}} \\ &= \underbrace{\omega_{I\mathcal{R}}^I \times \omega_{I\mathcal{R}}^I}_{\equiv \mathbf{0}} + \mathbf{S}^{I\mathcal{R}} \dot{\omega}_{I\mathcal{R}}^{\mathcal{R}} = \mathbf{S}^{I\mathcal{R}} \dot{\omega}_{I\mathcal{R}}^{\mathcal{R}} \end{aligned} \quad (\text{C.1.12})$$

The transformation of the tilde matrix of the angular acceleration is done in an analogous way to (C.1.11). Thereby it is valid for the angular acceleration:

$$\dot{\tilde{\omega}}_{I\mathcal{R}}^{\mathcal{R}} = \mathbf{S}^{\mathcal{R}I} \dot{\tilde{\omega}}_{I\mathcal{R}}^I \mathbf{S}^{I\mathcal{R}} \Rightarrow \mathbf{S}^{I\mathcal{R}} \dot{\tilde{\omega}}_{I\mathcal{R}}^{\mathcal{R}} = \dot{\tilde{\omega}}_{I\mathcal{R}}^I \mathbf{S}^{I\mathcal{R}} \quad (\text{C.1.13})$$

If the angular velocity and the angular acceleration are described in the reference frame \mathcal{R} , the rotation matrix $\mathbf{S}^{I\mathcal{R}}$ can be factored out, which provides a very compact formulation:

$$\begin{aligned} \mathbf{v}_{\text{OP}}^I &= \mathbf{v}_{\text{OR}}^I + \tilde{\omega}_{I\mathcal{R}}^I \mathbf{S}^{I\mathcal{R}} \mathbf{r}_{\text{RP}}^{\mathcal{R}} + \mathbf{S}^{I\mathcal{R}} \dot{\mathbf{r}}_{\text{RP}}^{\mathcal{R}} \\ &= \mathbf{v}_{\text{OR}}^I + \mathbf{S}^{I\mathcal{R}} \tilde{\omega}_{I\mathcal{R}}^{\mathcal{R}} \mathbf{r}_{\text{RP}}^{\mathcal{R}} + \mathbf{S}^{I\mathcal{R}} \dot{\mathbf{r}}_{\text{RP}}^{\mathcal{R}} \\ &= \mathbf{v}_{\text{OR}}^I + \mathbf{S}^{I\mathcal{R}} \left[\tilde{\omega}_{I\mathcal{R}}^{\mathcal{R}} \mathbf{r}_{\text{RP}}^{\mathcal{R}} + \dot{\mathbf{r}}_{\text{RP}}^{\mathcal{R}} \right] \end{aligned} \quad (\text{C.1.14})$$

$$\begin{aligned} \mathbf{a}_{\text{OP}}^I &= \mathbf{a}_{\text{OR}}^I + \dot{\tilde{\omega}}_{I\mathcal{R}}^I \mathbf{S}^{I\mathcal{R}} \mathbf{r}_{\text{RP}}^{\mathcal{R}} + \tilde{\omega}_{I\mathcal{R}}^I \tilde{\omega}_{I\mathcal{R}}^I \mathbf{S}^{I\mathcal{R}} \mathbf{r}_{\text{RP}}^{\mathcal{R}} + 2\tilde{\omega}_{I\mathcal{R}}^I \mathbf{S}^{I\mathcal{R}} \dot{\mathbf{r}}_{\text{RP}}^{\mathcal{R}} + \mathbf{S}^{I\mathcal{R}} \ddot{\mathbf{r}}_{\text{RP}}^{\mathcal{R}} \\ &= \mathbf{a}_{\text{OR}}^I + \mathbf{S}^{I\mathcal{R}} \dot{\tilde{\omega}}_{I\mathcal{R}}^{\mathcal{R}} \mathbf{r}_{\text{RP}}^{\mathcal{R}} + \mathbf{S}^{I\mathcal{R}} \tilde{\omega}_{I\mathcal{R}}^{\mathcal{R}} \tilde{\omega}_{I\mathcal{R}}^{\mathcal{R}} \mathbf{r}_{\text{RP}}^{\mathcal{R}} + 2\mathbf{S}^{I\mathcal{R}} \tilde{\omega}_{I\mathcal{R}}^{\mathcal{R}} \dot{\mathbf{r}}_{\text{RP}}^{\mathcal{R}} + \mathbf{S}^{I\mathcal{R}} \ddot{\mathbf{r}}_{\text{RP}}^{\mathcal{R}} \\ &= \mathbf{a}_{\text{OR}}^I + \mathbf{S}^{I\mathcal{R}} \left[\dot{\tilde{\omega}}_{I\mathcal{R}}^{\mathcal{R}} \mathbf{r}_{\text{RP}}^{\mathcal{R}} + \tilde{\omega}_{I\mathcal{R}}^{\mathcal{R}} \tilde{\omega}_{I\mathcal{R}}^{\mathcal{R}} \mathbf{r}_{\text{RP}}^{\mathcal{R}} + 2\tilde{\omega}_{I\mathcal{R}}^{\mathcal{R}} \dot{\mathbf{r}}_{\text{RP}}^{\mathcal{R}} + \ddot{\mathbf{r}}_{\text{RP}}^{\mathcal{R}} \right] \end{aligned} \quad (\text{C.1.15})$$

For the principle of virtual power, the virtual velocity $\delta' \mathbf{v}_{OP}^I$ is required. Here, the following rearrangement of the velocity using the commutative rule of the vector product is advantageous:

$$\begin{aligned} \tilde{\mathbf{u}} \mathbf{v} &= \mathbf{u} \times \mathbf{v} = -\mathbf{v} \times \mathbf{u} = -\tilde{\mathbf{v}} \mathbf{u} \\ \Rightarrow \mathbf{v}_{OP}^I &= \mathbf{v}_{OR}^I + \mathbf{S}^{I\mathcal{R}} \left[\tilde{\omega}_{I\mathcal{R}}^{\mathcal{R}} \mathbf{r}_{RP}^{\mathcal{R}} + \dot{\mathbf{r}}_{RP}^{\mathcal{R}} \right] = \mathbf{v}_{OR}^I + \mathbf{S}^{I\mathcal{R}} \left[-\tilde{\mathbf{r}}_{RP}^{\mathcal{R}} \omega_{I\mathcal{R}}^{\mathcal{R}} + \dot{\mathbf{r}}_{RP}^{\mathcal{R}} \right] \end{aligned} \quad (\text{C.1.16})$$

The virtual velocity is now obtained by:

$$\delta' \mathbf{v}_{OP}^I = \delta' \mathbf{v}_{OR}^I + \mathbf{S}^{I\mathcal{R}} \left[-\tilde{\mathbf{r}}_{RP}^{\mathcal{R}} \delta' \omega_{I\mathcal{R}}^{\mathcal{R}} + \delta' \dot{\mathbf{r}}_{RP}^{\mathcal{R}} \right] \quad (\text{C.1.17})$$

The transposition of the vector of the virtual velocity leads to:

$$\begin{aligned} \delta' \mathbf{v}_{OP}^I{}^T &= \delta' \mathbf{v}_{OR}^I{}^T + \left[-\tilde{\mathbf{r}}_{RP}^{\mathcal{R}} \delta' \omega_{I\mathcal{R}}^{\mathcal{R}} + \delta' \dot{\mathbf{r}}_{RP}^{\mathcal{R}} \right]^T \mathbf{S}^{I\mathcal{R}}{}^T \\ &= \delta' \mathbf{v}_{OR}^I{}^T + \left[-\delta' \omega_{I\mathcal{R}}^{\mathcal{R}}{}^T \tilde{\mathbf{r}}_{RP}^{\mathcal{R}}{}^T + \delta' \dot{\mathbf{r}}_{RP}^{\mathcal{R}}{}^T \right] \mathbf{S}^{\mathcal{R}I} \\ &= \delta' \mathbf{v}_{OR}^I{}^T + \left[\delta' \omega_{I\mathcal{R}}^{\mathcal{R}}{}^T \tilde{\mathbf{r}}_{RP}^{\mathcal{R}} + \delta' \dot{\mathbf{r}}_{RP}^{\mathcal{R}}{}^T \right] \mathbf{S}^{\mathcal{R}I} \end{aligned} \quad (\text{C.1.18})$$

This expression for the virtual velocity can be split up: The vectors $\delta' \mathbf{v}_{OR}^I{}^T$ and $\delta' \omega_{I\mathcal{R}}^{\mathcal{R}}{}^T$ denote translational and rotational motions, respectively. Relative motions including deformations contain the vector $\delta' \dot{\mathbf{r}}_{RP}^{\mathcal{R}}{}^T$.

The angular velocity of the frame \mathcal{P} relative to the inertial frame I is obtained by:

$$\begin{aligned} \tilde{\omega}_{IP}^I &= \dot{\mathbf{S}}^{IP} \mathbf{S}^{PI} = \left(\dot{\mathbf{S}}^{I\mathcal{R}} \mathbf{S}^{\mathcal{R}\mathcal{P}} + \mathbf{S}^{I\mathcal{R}} \dot{\mathbf{S}}^{\mathcal{R}\mathcal{P}} \right) \mathbf{S}^{\mathcal{P}\mathcal{R}} \mathbf{S}^{\mathcal{R}I} \\ &= \dot{\mathbf{S}}^{I\mathcal{R}} \underbrace{\mathbf{S}^{\mathcal{R}\mathcal{P}} \mathbf{S}^{\mathcal{P}\mathcal{R}}}_{\mathbf{I}} \mathbf{S}^{\mathcal{R}I} + \mathbf{S}^{I\mathcal{R}} \dot{\mathbf{S}}^{\mathcal{R}\mathcal{P}} \mathbf{S}^{\mathcal{P}\mathcal{R}} \mathbf{S}^{\mathcal{R}I} = \dot{\mathbf{S}}^{I\mathcal{R}} \mathbf{S}^{\mathcal{R}I} + \mathbf{S}^{I\mathcal{R}} \dot{\mathbf{S}}^{\mathcal{R}\mathcal{P}} \mathbf{S}^{\mathcal{P}\mathcal{R}} \mathbf{S}^{\mathcal{R}I} \\ &= \tilde{\omega}_{I\mathcal{R}}^I + \mathbf{S}^{I\mathcal{R}} \tilde{\omega}_{\mathcal{R}\mathcal{P}}^{\mathcal{R}} \mathbf{S}^{\mathcal{R}I} \\ \Rightarrow \omega_{IP}^I &= \omega_{I\mathcal{R}}^I + \mathbf{S}^{I\mathcal{R}} \omega_{\mathcal{R}\mathcal{P}}^{\mathcal{R}} \end{aligned} \quad (\text{C.1.19})$$

Thereby, the virtual angular velocity can be formulated as:

$$\delta' \omega_{IP}^I = \delta' \omega_{I\mathcal{R}}^I + \mathbf{S}^{I\mathcal{R}} \delta' \omega_{\mathcal{R}\mathcal{P}}^{\mathcal{R}} \quad (\text{C.1.20})$$

C.2 Description of the relative kinematics

In section C.1 the kinematics for a particle located at the point P has been developed based on the floating frame of reference formulation. In this formulation, the vector $\mathbf{r}_{RP}^{\mathcal{R}}$ describes the relative position of the point P with respect to the reference point R in the reference frame \mathcal{R} . For a flexible body, this position vector consists of two parts, the reference position $\mathbf{x}^{\mathcal{R}}$ and the displacement $\mathbf{w}^{\mathcal{R}}$. In total it is valid:

$$\mathbf{r}_{RP}^{\mathcal{R}} = \mathbf{x}^{\mathcal{R}} + \mathbf{w}^{\mathcal{R}}(\mathbf{x}^{\mathcal{R}}, t) \quad (\text{C.2.21})$$

The vector $\mathbf{w}^{\mathcal{R}}$ describes a time-dependent displacement field. The vector $\mathbf{x}^{\mathcal{R}}$ describes the reference position of the particle in the reference frame \mathcal{R} ; usually, it describes a constant position.

However, this doesn't necessary mean that the vector is constant with respect to the motion of the particle. If the body-fixed frame \mathcal{B} is chosen as the reference frame, then the vector $\mathbf{x}^{\mathcal{B}}$ can be considered as the material coordinates of a particle. In this case, the vector $\mathbf{x}^{\mathcal{B}}$ is constant so that its derivative with respect to time vanishes. Thereby, it is valid:

$$\mathbf{r}_{\text{RP}}^{\mathcal{B}} = \mathbf{x}^{\mathcal{B}} + \mathbf{w}^{\mathcal{B}}(\mathbf{x}^{\mathcal{B}}, t) \Rightarrow \dot{\mathbf{r}}_{\text{RP}}^{\mathcal{B}} = \dot{\mathbf{w}}^{\mathcal{B}}(\mathbf{x}^{\mathcal{B}}, t) \Rightarrow \ddot{\mathbf{r}}_{\text{RP}}^{\mathcal{B}} = \ddot{\mathbf{w}}^{\mathcal{B}}(\mathbf{x}^{\mathcal{B}}, t) \quad (\text{C.2.22})$$

This formulation is the base for the Lagrangian approach; in this formulation, the motion of a certain particle through the space is observed, i.e. all the time the same particle indicated by $\mathbf{x}^{\mathcal{B}}$ is considered. However, if another frame then the body-fixed frame \mathcal{B} is chosen as the reference frame \mathcal{R} , then the vector $\mathbf{x}^{\mathcal{R}}$ describes a certain position within space, at which a particle is currently located. Since in this approach a particle is observed, which is currently moving through the point P indicated by the reference position $\mathbf{x}^{\mathcal{R}}$, the observed particle is permanently changing, i.e. for each time t another particle is observed. In this case, the coordinates given by the vector $\mathbf{x}^{\mathcal{R}}$ are local coordinates. This is the basic principle for the Eulerian approach and for the Arbitrary Lagrangian-Eulerian approach or ALE approach. In this case it is valid for the derivatives:

$$\mathbf{r}_{\text{RP}}^{\mathcal{R}} = \mathbf{x}^{\mathcal{R}} + \mathbf{w}^{\mathcal{R}}(\mathbf{x}^{\mathcal{R}}, t) \Rightarrow \dot{\mathbf{r}}_{\text{RP}}^{\mathcal{R}} = \frac{\partial \mathbf{w}^{\mathcal{R}}(\mathbf{x}^{\mathcal{R}}, t)}{\partial t} + \frac{\partial \mathbf{w}^{\mathcal{R}}(\mathbf{x}^{\mathcal{R}}, t)}{\partial \mathbf{x}^{\mathcal{R}}} \frac{\partial \mathbf{x}^{\mathcal{R}}}{\partial t} \quad (\text{C.2.23})$$

The following considerations will be focused on the formulation in the body-fixed frame \mathcal{B} , i.e. on the Lagrangian approach.

Generally, a flexible body consists of an infinite number of infinitesimal mass particles; it is a continuum. Such a continuum possesses an infinite number of degrees of freedom (DoF). For practical applications, a discretization is required in order to describe the deformation field $\mathbf{w}^{\mathcal{B}}(\mathbf{x}^{\mathcal{B}}, t)$ at least in an approximative way. For this purpose, a modal synthesis is used very often. In this approach, the displacement $\mathbf{w}^{\mathcal{B}}(\mathbf{x}^{\mathcal{B}}, t)$ of a particle is described by a superposition of shape functions $\mathbf{w}_i^{\mathcal{B}}(\mathbf{x})$, which are scaled by the time-dependent modal coordinates $q_i(t)$. Thereby it is valid:

$$\mathbf{r}_{\text{RP}}^{\mathcal{B}} = \mathbf{x}^{\mathcal{B}} + \mathbf{w}^{\mathcal{B}}(\mathbf{x}^{\mathcal{B}}, t) = \mathbf{x}^{\mathcal{B}} + \sum_{i=1}^N \mathbf{w}_i^{\mathcal{B}}(\mathbf{x}^{\mathcal{B}}) q_i(t) \quad (\text{C.2.24})$$

In this description, the modal coordinates $q_i(t)$ are the degrees of freedom. Of course, the number N of the associated shape functions and modal coordinates is finite. The choice of the shape functions and the number N depend on the type of the structure, on the loads acting on it and on the frequency range, which is of interest. By choosing suitable shape functions and a sufficient number N , a very accurate description of the deformation of the flexible body can be obtained.

From (C.2.24) the expressions for the relative velocity, the virtual relative velocity and the relative acceleration can be derived:

$$\dot{\mathbf{r}}_{\text{RP}}^{\mathcal{B}} = \sum_{i=1}^N \mathbf{w}_i^{\mathcal{B}}(\mathbf{x}^{\mathcal{B}}) \dot{q}_i(t), \quad \delta' \dot{\mathbf{r}}_{\text{RP}}^{\mathcal{B}} = \sum_{i=1}^N \mathbf{w}_i^{\mathcal{B}}(\mathbf{x}^{\mathcal{B}}) \delta' \dot{q}_i, \quad \ddot{\mathbf{r}}_{\text{RP}}^{\mathcal{B}} = \sum_{i=1}^N \mathbf{w}_i^{\mathcal{B}}(\mathbf{x}^{\mathcal{B}}) \ddot{q}_i(t) \quad (\text{C.2.25})$$

For the sake of brevity and for a better overview the arguments $\mathbf{x}^{\mathcal{B}}$ for the shape functions $\mathbf{w}_i^{\mathcal{B}} = \mathbf{w}_i^{\mathcal{B}}(\mathbf{x}^{\mathcal{B}})$ and t for the modal coordinates $q_i = q_i(t)$ and their derivatives will usually not be indicated explicitly in the following considerations.

C.3 Inertia terms

The integrand for the inertia terms is the scalar product of the absolute virtual velocity and the absolute acceleration of one particle. In section C.1 the following expressions for the virtual velocity

and for the acceleration have been derived:

$$\delta' \mathbf{v}_{OP}^I{}^T = \delta' \mathbf{v}_{OR}^I{}^T + \underbrace{\left[\delta' \tilde{\omega}_{I\mathcal{R}}^{\mathcal{R}T} \tilde{\mathbf{r}}_{RP}^{\mathcal{R}} + \delta' \dot{\mathbf{r}}_{RP}^{\mathcal{R}T} \right]}_{\delta' \mathbf{v}_{RP}^I{}^T} \mathbf{S}^{\mathcal{R}I} \quad (\text{C.3.26})$$

$$\mathbf{a}_{OP}^I = \mathbf{a}_{OR}^I + \underbrace{\mathbf{S}^{I\mathcal{R}} \left[\dot{\tilde{\omega}}_{I\mathcal{R}}^{\mathcal{R}} \mathbf{r}_{RP}^{\mathcal{R}} + \tilde{\omega}_{I\mathcal{R}}^{\mathcal{R}} \tilde{\omega}_{I\mathcal{R}}^{\mathcal{R}} \mathbf{r}_{RP}^{\mathcal{R}} + 2 \tilde{\omega}_{I\mathcal{R}}^{\mathcal{R}} \dot{\mathbf{r}}_{RP}^{\mathcal{R}} + \ddot{\mathbf{r}}_{RP}^{\mathcal{R}} \right]}_{\mathbf{a}_{RP}^I} \quad (\text{C.3.27})$$

The evaluation of the scalar product gives:

$$\begin{aligned} \delta' \mathbf{v}_{OP}^I{}^T \mathbf{a}_{OP}^I &= \left(\delta' \mathbf{v}_{OR}^I{}^T + \delta' \mathbf{v}_{RP}^I{}^T \right) \left(\mathbf{a}_{OR}^I + \mathbf{a}_{RP}^I \right) \\ &= \delta' \mathbf{v}_{OR}^I{}^T \left(\mathbf{a}_{OR}^I + \mathbf{a}_{RP}^I \right) + \delta' \mathbf{v}_{RP}^I{}^T \mathbf{a}_{OR}^I + \delta' \mathbf{v}_{RP}^I{}^T \mathbf{a}_{RP}^I \\ &= \delta' \mathbf{v}_{OR}^I{}^T \left(\mathbf{a}_{OR}^I + \mathbf{S}^{I\mathcal{R}} \left[\dot{\tilde{\omega}}_{I\mathcal{R}}^{\mathcal{R}} \mathbf{r}_{RP}^{\mathcal{R}} + \tilde{\omega}_{I\mathcal{R}}^{\mathcal{R}} \tilde{\omega}_{I\mathcal{R}}^{\mathcal{R}} \mathbf{r}_{RP}^{\mathcal{R}} + 2 \tilde{\omega}_{I\mathcal{R}}^{\mathcal{R}} \dot{\mathbf{r}}_{RP}^{\mathcal{R}} + \ddot{\mathbf{r}}_{RP}^{\mathcal{R}} \right] \right) \\ &\quad + \left[\delta' \tilde{\omega}_{I\mathcal{R}}^{\mathcal{R}T} \tilde{\mathbf{r}}_{RP}^{\mathcal{R}} + \delta' \dot{\mathbf{r}}_{RP}^{\mathcal{R}T} \right] \mathbf{S}^{\mathcal{R}I} \mathbf{a}_{OR}^I \\ &\quad + \left[\delta' \tilde{\omega}_{I\mathcal{R}}^{\mathcal{R}T} \tilde{\mathbf{r}}_{RP}^{\mathcal{R}} + \delta' \dot{\mathbf{r}}_{RP}^{\mathcal{R}T} \right] \underbrace{\mathbf{S}^{\mathcal{R}I} \mathbf{S}^{I\mathcal{R}}}_{\mathbf{I}} \left[\dot{\tilde{\omega}}_{I\mathcal{R}}^{\mathcal{R}} \mathbf{r}_{RP}^{\mathcal{R}} + \tilde{\omega}_{I\mathcal{R}}^{\mathcal{R}} \tilde{\omega}_{I\mathcal{R}}^{\mathcal{R}} \mathbf{r}_{RP}^{\mathcal{R}} + 2 \tilde{\omega}_{I\mathcal{R}}^{\mathcal{R}} \dot{\mathbf{r}}_{RP}^{\mathcal{R}} + \ddot{\mathbf{r}}_{RP}^{\mathcal{R}} \right] \end{aligned} \quad (\text{C.3.28})$$

By sorting the terms with respect to the virtual velocities the integrands for the terms belonging to the different kinds of motions are obtained:

$$\begin{aligned} \delta' \mathbf{v}_{OP}^I{}^T \mathbf{a}_{OP}^I &= \delta' \mathbf{v}_{OR}^I{}^T \left(\mathbf{a}_{OR}^I + \mathbf{S}^{I\mathcal{R}} \left[\dot{\tilde{\omega}}_{I\mathcal{R}}^{\mathcal{R}} \mathbf{r}_{RP}^{\mathcal{R}} + \tilde{\omega}_{I\mathcal{R}}^{\mathcal{R}} \tilde{\omega}_{I\mathcal{R}}^{\mathcal{R}} \mathbf{r}_{RP}^{\mathcal{R}} + 2 \tilde{\omega}_{I\mathcal{R}}^{\mathcal{R}} \dot{\mathbf{r}}_{RP}^{\mathcal{R}} + \ddot{\mathbf{r}}_{RP}^{\mathcal{R}} \right] \right) \\ &\quad + \left[\delta' \tilde{\omega}_{I\mathcal{R}}^{\mathcal{R}T} \tilde{\mathbf{r}}_{RP}^{\mathcal{R}} + \delta' \dot{\mathbf{r}}_{RP}^{\mathcal{R}T} \right] \mathbf{S}^{\mathcal{R}I} \mathbf{a}_{OR}^I \\ &\quad + \left[\delta' \tilde{\omega}_{I\mathcal{R}}^{\mathcal{R}T} \tilde{\mathbf{r}}_{RP}^{\mathcal{R}} + \delta' \dot{\mathbf{r}}_{RP}^{\mathcal{R}T} \right] \left[\dot{\tilde{\omega}}_{I\mathcal{R}}^{\mathcal{R}} \mathbf{r}_{RP}^{\mathcal{R}} + \tilde{\omega}_{I\mathcal{R}}^{\mathcal{R}} \tilde{\omega}_{I\mathcal{R}}^{\mathcal{R}} \mathbf{r}_{RP}^{\mathcal{R}} + 2 \tilde{\omega}_{I\mathcal{R}}^{\mathcal{R}} \dot{\mathbf{r}}_{RP}^{\mathcal{R}} + \ddot{\mathbf{r}}_{RP}^{\mathcal{R}} \right] \\ &= \underbrace{\delta' \mathbf{v}_{OR}^I{}^T \left(\mathbf{a}_{OR}^I + \mathbf{S}^{I\mathcal{R}} \left[\dot{\tilde{\omega}}_{I\mathcal{R}}^{\mathcal{R}} \mathbf{r}_{RP}^{\mathcal{R}} + \tilde{\omega}_{I\mathcal{R}}^{\mathcal{R}} \tilde{\omega}_{I\mathcal{R}}^{\mathcal{R}} \mathbf{r}_{RP}^{\mathcal{R}} + 2 \tilde{\omega}_{I\mathcal{R}}^{\mathcal{R}} \dot{\mathbf{r}}_{RP}^{\mathcal{R}} + \ddot{\mathbf{r}}_{RP}^{\mathcal{R}} \right] \right)}_{\text{Translational motions}} \\ &\quad + \underbrace{\delta' \tilde{\omega}_{I\mathcal{R}}^{\mathcal{R}T} \tilde{\mathbf{r}}_{RP}^{\mathcal{R}} \left(\mathbf{S}^{I\mathcal{R}} \mathbf{a}_{OR}^I + \left[\dot{\tilde{\omega}}_{I\mathcal{R}}^{\mathcal{R}} \mathbf{r}_{RP}^{\mathcal{R}} + \tilde{\omega}_{I\mathcal{R}}^{\mathcal{R}} \tilde{\omega}_{I\mathcal{R}}^{\mathcal{R}} \mathbf{r}_{RP}^{\mathcal{R}} + 2 \tilde{\omega}_{I\mathcal{R}}^{\mathcal{R}} \dot{\mathbf{r}}_{RP}^{\mathcal{R}} + \ddot{\mathbf{r}}_{RP}^{\mathcal{R}} \right] \right)}_{\text{Rotational motions}} \\ &\quad + \underbrace{\delta' \dot{\mathbf{r}}_{RP}^{\mathcal{R}T} \left(\mathbf{S}^{I\mathcal{R}} \mathbf{a}_{OR}^I + \left[\dot{\tilde{\omega}}_{I\mathcal{R}}^{\mathcal{R}} \mathbf{r}_{RP}^{\mathcal{R}} + \tilde{\omega}_{I\mathcal{R}}^{\mathcal{R}} \tilde{\omega}_{I\mathcal{R}}^{\mathcal{R}} \mathbf{r}_{RP}^{\mathcal{R}} + 2 \tilde{\omega}_{I\mathcal{R}}^{\mathcal{R}} \dot{\mathbf{r}}_{RP}^{\mathcal{R}} + \ddot{\mathbf{r}}_{RP}^{\mathcal{R}} \right] \right)}_{\text{Relative motions}} \end{aligned} \quad (\text{C.3.29})$$

The terms belonging to the different kinds of motions will be considered separately in the following sections. For all three kinds, the terms will first be developed for an arbitrary reference frame \mathcal{R} . Based on the result, the formulation, which uses the body-fixed frame \mathcal{B} as the reference frame, will be derived. Here, the position vector $\mathbf{r}_{RP}^{\mathcal{B}}$ is split into the constant reference position vector $\mathbf{x}^{\mathcal{B}}$ and the displacement vector $\mathbf{w}^{\mathcal{B}} = \mathbf{w}^{\mathcal{B}}(\mathbf{x}^{\mathcal{B}}, t)$:

$$\mathbf{r}_{RP}^{\mathcal{B}} = \mathbf{x}^{\mathcal{B}} + \mathbf{w}^{\mathcal{B}}(\mathbf{x}^{\mathcal{B}}, t), \quad \frac{d\mathbf{x}^{\mathcal{B}}}{dt} = \mathbf{0} \Rightarrow \dot{\mathbf{r}}_{RP}^{\mathcal{B}} = \dot{\mathbf{w}}^{\mathcal{B}}(\mathbf{x}^{\mathcal{B}}, t) \Rightarrow \ddot{\mathbf{r}}_{RP}^{\mathcal{B}} = \ddot{\mathbf{w}}^{\mathcal{B}}(\mathbf{x}^{\mathcal{B}}, t) \quad (\text{C.3.30})$$

C.3.1 Translational motions

The scalar product of the virtual velocity $\delta' \mathbf{v}_{OR}^I$ of the reference point R and the acceleration \mathbf{a}_{OP}^I can be written as:

$$\begin{aligned} \delta' \mathbf{v}_{OR}^I \mathbf{a}_{OP}^I &= \delta' \mathbf{v}_{OR}^I \mathbf{T} \left(\mathbf{a}_{OR}^I + \mathbf{S}^{I\mathcal{R}} \left[\tilde{\omega}_{I\mathcal{R}}^{\mathcal{R}} \mathbf{r}_{RP}^{\mathcal{R}} + \tilde{\omega}_{I\mathcal{R}}^{\mathcal{R}} \tilde{\omega}_{I\mathcal{R}}^{\mathcal{R}} \mathbf{r}_{RP}^{\mathcal{R}} + 2 \tilde{\omega}_{I\mathcal{R}}^{\mathcal{R}} \dot{\mathbf{r}}_{RP}^{\mathcal{R}} + \ddot{\mathbf{r}}_{RP}^{\mathcal{R}} \right] \right) \\ &= \delta' \mathbf{v}_{OR}^I \mathbf{T} \left(\mathbf{a}_{OR}^I + \mathbf{S}^{I\mathcal{R}} \left[\left(\dot{\tilde{\omega}}_{I\mathcal{R}}^{\mathcal{R}} + \tilde{\omega}_{I\mathcal{R}}^{\mathcal{R}} \tilde{\omega}_{I\mathcal{R}}^{\mathcal{R}} \right) \mathbf{r}_{RP}^{\mathcal{R}} + 2 \tilde{\omega}_{I\mathcal{R}}^{\mathcal{R}} \dot{\mathbf{r}}_{RP}^{\mathcal{R}} + \ddot{\mathbf{r}}_{RP}^{\mathcal{R}} \right] \right) \end{aligned} \quad (\text{C.3.31})$$

By splitting the integrand into summands and factoring out the constant vectors $\delta' \mathbf{v}_{OR}^I$, \mathbf{a}_{OR}^I , $\tilde{\omega}_{I\mathcal{R}}^{\mathcal{R}}$ and $\dot{\tilde{\omega}}_{I\mathcal{R}}^{\mathcal{R}}$ and the matrix $\mathbf{S}^{I\mathcal{R}}$ from the integrals the inertial terms for translational motions can be written as:

$$\begin{aligned} &\int_B \delta' \mathbf{v}_{OR}^I \mathbf{T} \mathbf{a}_{OP}^I dm \\ &= \int_B \delta' \mathbf{v}_{OR}^I \mathbf{T} \left(\mathbf{a}_{OR}^I + \mathbf{S}^{I\mathcal{R}} \left[\left(\dot{\tilde{\omega}}_{I\mathcal{R}}^{\mathcal{R}} + \tilde{\omega}_{I\mathcal{R}}^{\mathcal{R}} \tilde{\omega}_{I\mathcal{R}}^{\mathcal{R}} \right) \mathbf{r}_{RP}^{\mathcal{R}} + 2 \tilde{\omega}_{I\mathcal{R}}^{\mathcal{R}} \dot{\mathbf{r}}_{RP}^{\mathcal{R}} + \ddot{\mathbf{r}}_{RP}^{\mathcal{R}} \right] \right) dm \\ &= \delta' \mathbf{v}_{OR}^I \mathbf{T} \left[\int_B dm \mathbf{a}_{OR}^I + \mathbf{S}^{I\mathcal{R}} \left(\dot{\tilde{\omega}}_{I\mathcal{R}}^{\mathcal{R}} + \tilde{\omega}_{I\mathcal{R}}^{\mathcal{R}} \tilde{\omega}_{I\mathcal{R}}^{\mathcal{R}} \right) \int_B \mathbf{r}_{RP}^{\mathcal{R}} dm + 2 \mathbf{S}^{I\mathcal{R}} \tilde{\omega}_{I\mathcal{R}}^{\mathcal{R}} \int_B \dot{\mathbf{r}}_{RP}^{\mathcal{R}} dm + \mathbf{S}^{I\mathcal{R}} \int_B \ddot{\mathbf{r}}_{RP}^{\mathcal{R}} dm \right] \end{aligned} \quad (\text{C.3.32})$$

The integral over all infinitesimal masses of the body B is the total mass m_B of the body:

$$\int_B dm = m_B \quad (\text{C.3.33})$$

Thereby the inertia terms for the translational motions are formulated in the following way:

$$\begin{aligned} &\int_B \delta' \mathbf{v}_{OR}^I \mathbf{T} \mathbf{a}_{OP}^I dm \\ &= \delta' \mathbf{v}_{OR}^I \mathbf{T} \left[m_B \mathbf{a}_{OR}^I + \mathbf{S}^{I\mathcal{R}} \left(\dot{\tilde{\omega}}_{I\mathcal{R}}^{\mathcal{R}} + \tilde{\omega}_{I\mathcal{R}}^{\mathcal{R}} \tilde{\omega}_{I\mathcal{R}}^{\mathcal{R}} \right) \int_B \mathbf{r}_{RP}^{\mathcal{R}} dm + 2 \mathbf{S}^{I\mathcal{R}} \tilde{\omega}_{I\mathcal{R}}^{\mathcal{R}} \int_B \dot{\mathbf{r}}_{RP}^{\mathcal{R}} dm + \mathbf{S}^{I\mathcal{R}} \int_B \ddot{\mathbf{r}}_{RP}^{\mathcal{R}} dm \right] \end{aligned} \quad (\text{C.3.34})$$

Using the body-fixed frame \mathcal{B} and formulating the relative kinematics according to (C.3.30) leads to:

$$\begin{aligned} &\int_B \delta' \mathbf{v}_{OR}^I \mathbf{T} \mathbf{a}_{OP}^I dm \\ &= \delta' \mathbf{v}_{OR}^I \mathbf{T} \left[m_B \mathbf{a}_{OR}^I + \mathbf{S}^{I\mathcal{B}} \left(\dot{\tilde{\omega}}_{I\mathcal{B}}^{\mathcal{B}} + \tilde{\omega}_{I\mathcal{B}}^{\mathcal{B}} \tilde{\omega}_{I\mathcal{B}}^{\mathcal{B}} \right) \int_B \mathbf{r}_{RP}^{\mathcal{B}} dm + 2 \mathbf{S}^{I\mathcal{B}} \tilde{\omega}_{I\mathcal{B}}^{\mathcal{B}} \int_B \dot{\mathbf{r}}_{RP}^{\mathcal{B}} dm + \mathbf{S}^{I\mathcal{B}} \int_B \ddot{\mathbf{r}}_{RP}^{\mathcal{B}} dm \right] \\ &= \delta' \mathbf{v}_{OR}^I \mathbf{T} \left[m_B \mathbf{a}_{OR}^I + \mathbf{S}^{I\mathcal{B}} \left(\dot{\tilde{\omega}}_{I\mathcal{B}}^{\mathcal{B}} + \tilde{\omega}_{I\mathcal{B}}^{\mathcal{B}} \tilde{\omega}_{I\mathcal{B}}^{\mathcal{B}} \right) \left(\int_B \mathbf{x}^{\mathcal{B}} dm + \int_B \mathbf{w}^{\mathcal{B}} dm \right) \right. \\ &\quad \left. + 2 \mathbf{S}^{I\mathcal{B}} \tilde{\omega}_{I\mathcal{B}}^{\mathcal{B}} \int_B \dot{\mathbf{w}}^{\mathcal{B}} dm + \mathbf{S}^{I\mathcal{B}} \int_B \ddot{\mathbf{w}}^{\mathcal{B}} dm \right] \end{aligned} \quad (\text{C.3.35})$$

For the special case of a rigid body, the displacement vector $\mathbf{w}^{\mathcal{B}}$ and its derivatives $\dot{\mathbf{w}}^{\mathcal{B}}$ and $\ddot{\mathbf{w}}^{\mathcal{B}}$ vanish:

$$\mathbf{r}_{RP}^{\mathcal{B}} = \mathbf{x}^{\mathcal{B}}, \mathbf{w}^{\mathcal{B}} = \mathbf{0} \Rightarrow \dot{\mathbf{r}}_{RP}^{\mathcal{B}} = \dot{\mathbf{w}}^{\mathcal{B}} = \mathbf{0} \Rightarrow \ddot{\mathbf{r}}_{RP}^{\mathcal{B}} = \ddot{\mathbf{w}}^{\mathcal{B}} = \mathbf{0} \quad (\text{C.3.36})$$

Using the body-fixed frame \mathcal{B} as the reference frame the inertial terms for the translational motions according to (C.3.35) can be simplified to:

$$\int_B \delta' \mathbf{v}_{OR}^I \mathbf{T} \mathbf{a}_{OP}^I dm = \delta' \mathbf{v}_{OR}^I \mathbf{T} \left[m_B \mathbf{a}_{OR}^I + \mathbf{S}^{I\mathcal{B}} \left(\dot{\tilde{\omega}}_{I\mathcal{B}}^{\mathcal{B}} + \tilde{\omega}_{I\mathcal{B}}^{\mathcal{B}} \tilde{\omega}_{I\mathcal{B}}^{\mathcal{B}} \right) \int_B \mathbf{x}^{\mathcal{B}} dm \right] \quad (\text{C.3.37})$$

C.3.2 Rotational motions

To formulate the inertial terms for the rotational motions and for the other motions, a reformulation of the acceleration is advantageous so that the constant vectors $\omega_{I\mathcal{R}}^{\mathcal{R}}$ and $\dot{\omega}_{I\mathcal{R}}^{\mathcal{R}}$ can be factored out from the integrals. Here, the commutation rule for the vector product

$$\tilde{\mathbf{u}}\mathbf{v} = \mathbf{u} \times \mathbf{v} = -\mathbf{v} \times \mathbf{u} = -\tilde{\mathbf{v}}\mathbf{u} \quad (\text{C.3.38})$$

is applied on the second and the fourth summand of the acceleration:

$$\begin{aligned} & \delta' \omega_{I\mathcal{R}}^{\mathcal{R}T} \tilde{\mathbf{r}}_{\text{RP}}^{\mathcal{R}} \mathbf{S}^{\mathcal{R}I} \mathbf{a}_{\text{OP}}^I \\ &= \delta' \omega_{I\mathcal{R}}^{\mathcal{R}T} \tilde{\mathbf{r}}_{\text{RP}}^{\mathcal{R}} \left(\mathbf{S}^{\mathcal{R}I} \mathbf{a}_{\text{OR}}^I + \left[\dot{\tilde{\omega}}_{I\mathcal{R}}^{\mathcal{R}} \mathbf{r}_{\text{RP}}^{\mathcal{R}} + \tilde{\omega}_{I\mathcal{R}}^{\mathcal{R}} \tilde{\omega}_{I\mathcal{R}}^{\mathcal{R}} \mathbf{r}_{\text{RP}}^{\mathcal{R}} + 2 \tilde{\omega}_{I\mathcal{R}}^{\mathcal{R}} \dot{\mathbf{r}}_{\text{RP}}^{\mathcal{R}} + \ddot{\mathbf{r}}_{\text{RP}}^{\mathcal{R}} \right] \right) \\ &= \delta' \omega_{I\mathcal{R}}^{\mathcal{R}T} \tilde{\mathbf{r}}_{\text{RP}}^{\mathcal{R}} \left(\mathbf{S}^{\mathcal{R}I} \mathbf{a}_{\text{OR}}^I + \left[-\tilde{\mathbf{r}}_{\text{RP}}^{\mathcal{R}} \dot{\omega}_{I\mathcal{R}}^{\mathcal{R}} + \tilde{\omega}_{I\mathcal{R}}^{\mathcal{R}} \tilde{\omega}_{I\mathcal{R}}^{\mathcal{R}} \mathbf{r}_{\text{RP}}^{\mathcal{R}} - 2 \dot{\tilde{\mathbf{r}}}_{\text{RP}}^{\mathcal{R}} \omega_{I\mathcal{R}}^{\mathcal{R}} + \ddot{\mathbf{r}}_{\text{RP}}^{\mathcal{R}} \right] \right) \\ &= \delta' \omega_{I\mathcal{R}}^{\mathcal{R}T} \left(\tilde{\mathbf{r}}_{\text{RP}}^{\mathcal{R}} \mathbf{S}^{\mathcal{R}I} \mathbf{a}_{\text{OR}}^I - \tilde{\mathbf{r}}_{\text{RP}}^{\mathcal{R}} \tilde{\mathbf{r}}_{\text{RP}}^{\mathcal{R}} \dot{\omega}_{I\mathcal{R}}^{\mathcal{R}} + \tilde{\mathbf{r}}_{\text{RP}}^{\mathcal{R}} \tilde{\omega}_{I\mathcal{R}}^{\mathcal{R}} \tilde{\omega}_{I\mathcal{R}}^{\mathcal{R}} \mathbf{r}_{\text{RP}}^{\mathcal{R}} - 2 \tilde{\mathbf{r}}_{\text{RP}}^{\mathcal{R}} \dot{\tilde{\mathbf{r}}}_{\text{RP}}^{\mathcal{R}} \omega_{I\mathcal{R}}^{\mathcal{R}} + \tilde{\mathbf{r}}_{\text{RP}}^{\mathcal{R}} \ddot{\mathbf{r}}_{\text{RP}}^{\mathcal{R}} \right) \end{aligned} \quad (\text{C.3.39})$$

The third summand contained in the bracket has the structure $\tilde{\mathbf{u}}\tilde{\mathbf{v}}\mathbf{u}$. Using the cross product this expression can be written as:

$$\tilde{\mathbf{u}}\tilde{\mathbf{v}}\mathbf{u} = \mathbf{u} \times (\mathbf{v} \times (\mathbf{v} \times \mathbf{u})) \quad (\text{C.3.40})$$

By using the vector triple product:

$$\vec{a} \times (\vec{b} \times \vec{c}) = (\vec{a} \cdot \vec{c}) \vec{b} - (\vec{a} \cdot \vec{b}) \vec{c} \quad (\text{C.3.41})$$

which is derived in appendix A.5.3, it is obtained for (C.3.40):

$$\vec{u} \times [\vec{v} \times (\vec{v} \times \vec{u})] = \vec{u} \times [(\vec{v} \cdot \vec{u}) \vec{v} - (\vec{v} \cdot \vec{v}) \vec{u}] = (\vec{v} \cdot \vec{u}) \vec{u} \times \vec{v} - (\vec{v} \cdot \vec{v}) \underbrace{\vec{u} \times \vec{u}}_{\vec{0}} = (\vec{v} \cdot \vec{u}) \vec{u} \times \vec{v} \quad (\text{C.3.42})$$

Now, \vec{u} and \vec{v} are commuted. While the scalar product is commutative, the vector product changes the sign, if the factors are commuted. Thereby, it is obtained:

$$\vec{v} \times [\vec{u} \times (\vec{u} \times \vec{v})] = (\vec{u} \cdot \vec{v}) \vec{v} \times \vec{u} = -(\vec{v} \cdot \vec{u}) \vec{u} \times \vec{v} = -\vec{u} \times [\vec{v} \times (\vec{v} \times \vec{u})] \quad (\text{C.3.43})$$

Therefore, it is valid:

$$\tilde{\mathbf{u}}\tilde{\mathbf{v}}\mathbf{u} = -\tilde{\mathbf{v}}\mathbf{u}\vec{u} \quad (\text{C.3.44})$$

The integrand can now be rewritten to:

$$\begin{aligned} & \delta' \omega_{I\mathcal{R}}^{\mathcal{R}T} \tilde{\mathbf{r}}_{\text{RP}}^{\mathcal{R}} \mathbf{S}^{\mathcal{R}I} \mathbf{a}_{\text{OP}}^I \\ &= \delta' \omega_{I\mathcal{R}}^{\mathcal{R}T} \left(\tilde{\mathbf{r}}_{\text{RP}}^{\mathcal{R}} \mathbf{S}^{\mathcal{R}I} \mathbf{a}_{\text{OR}}^I - \tilde{\mathbf{r}}_{\text{RP}}^{\mathcal{R}} \tilde{\mathbf{r}}_{\text{RP}}^{\mathcal{R}} \dot{\omega}_{I\mathcal{R}}^{\mathcal{R}} + \tilde{\mathbf{r}}_{\text{RP}}^{\mathcal{R}} \tilde{\omega}_{I\mathcal{R}}^{\mathcal{R}} \tilde{\omega}_{I\mathcal{R}}^{\mathcal{R}} \mathbf{r}_{\text{RP}}^{\mathcal{R}} - 2 \tilde{\mathbf{r}}_{\text{RP}}^{\mathcal{R}} \dot{\tilde{\mathbf{r}}}_{\text{RP}}^{\mathcal{R}} \omega_{I\mathcal{R}}^{\mathcal{R}} + \tilde{\mathbf{r}}_{\text{RP}}^{\mathcal{R}} \ddot{\mathbf{r}}_{\text{RP}}^{\mathcal{R}} \right) \\ &= \delta' \omega_{I\mathcal{R}}^{\mathcal{R}T} \left(\tilde{\mathbf{r}}_{\text{RP}}^{\mathcal{R}} \mathbf{S}^{\mathcal{R}I} \mathbf{a}_{\text{OR}}^I - \tilde{\mathbf{r}}_{\text{RP}}^{\mathcal{R}} \tilde{\mathbf{r}}_{\text{RP}}^{\mathcal{R}} \dot{\omega}_{I\mathcal{R}}^{\mathcal{R}} - \tilde{\omega}_{I\mathcal{R}}^{\mathcal{R}} \tilde{\mathbf{r}}_{\text{RP}}^{\mathcal{R}} \tilde{\mathbf{r}}_{\text{RP}}^{\mathcal{R}} \omega_{I\mathcal{R}}^{\mathcal{R}} - 2 \tilde{\mathbf{r}}_{\text{RP}}^{\mathcal{R}} \dot{\tilde{\mathbf{r}}}_{\text{RP}}^{\mathcal{R}} \omega_{I\mathcal{R}}^{\mathcal{R}} + \tilde{\mathbf{r}}_{\text{RP}}^{\mathcal{R}} \ddot{\mathbf{r}}_{\text{RP}}^{\mathcal{R}} \right) \end{aligned} \quad (\text{C.3.45})$$

By splitting the integral into several summands and factoring out the vectors \mathbf{a}_{OR}^I , $\delta' \omega_{I\mathcal{R}}^{\mathcal{R}T}$, $\omega_{I\mathcal{R}}^{\mathcal{R}}$ and $\dot{\omega}_{I\mathcal{R}}^{\mathcal{R}}$ the following expression is obtained for the inertial terms for the rotational motions:

$$\begin{aligned}
& \int_B \delta' \omega_{I\mathcal{R}}^{\mathcal{R}T} \tilde{\mathbf{r}}_{RP}^{\mathcal{R}} \mathbf{S}^{\mathcal{R}I} \mathbf{a}_{OP}^I dm \\
&= \int_B \delta' \omega_{I\mathcal{R}}^{\mathcal{R}T} \left(\tilde{\mathbf{r}}_{RP}^{\mathcal{R}} \mathbf{S}^{\mathcal{R}I} \mathbf{a}_{OR}^I - \tilde{\mathbf{r}}_{RP}^{\mathcal{R}} \tilde{\mathbf{r}}_{RP}^{\mathcal{R}} \dot{\omega}_{I\mathcal{R}}^{\mathcal{R}} + \tilde{\mathbf{r}}_{RP}^{\mathcal{R}} \tilde{\omega}_{I\mathcal{R}}^{\mathcal{R}} \tilde{\omega}_{I\mathcal{R}}^{\mathcal{R}} \tilde{\mathbf{r}}_{RP}^{\mathcal{R}} - 2 \tilde{\mathbf{r}}_{RP}^{\mathcal{R}} \dot{\tilde{\mathbf{r}}}_{RP}^{\mathcal{R}} \omega_{I\mathcal{R}}^{\mathcal{R}} + \tilde{\mathbf{r}}_{RP}^{\mathcal{R}} \ddot{\tilde{\mathbf{r}}}_{RP}^{\mathcal{R}} \right) dm \\
&= \delta' \omega_{I\mathcal{R}}^{\mathcal{R}T} \left(\int_B \tilde{\mathbf{r}}_{RP}^{\mathcal{R}} dm \mathbf{S}^{\mathcal{R}I} \mathbf{a}_{OR}^I - \int_B \tilde{\mathbf{r}}_{RP}^{\mathcal{R}} \tilde{\mathbf{r}}_{RP}^{\mathcal{R}} dm \dot{\omega}_{I\mathcal{R}}^{\mathcal{R}} - \tilde{\omega}_{I\mathcal{R}}^{\mathcal{R}} \int_B \tilde{\mathbf{r}}_{RP}^{\mathcal{R}} \tilde{\mathbf{r}}_{RP}^{\mathcal{R}} dm \omega_{I\mathcal{R}}^{\mathcal{R}} \right. \\
&\quad \left. - 2 \int_B \tilde{\mathbf{r}}_{RP}^{\mathcal{R}} \dot{\tilde{\mathbf{r}}}_{RP}^{\mathcal{R}} dm \omega_{I\mathcal{R}}^{\mathcal{R}} + \int_B \tilde{\mathbf{r}}_{RP}^{\mathcal{R}} \ddot{\tilde{\mathbf{r}}}_{RP}^{\mathcal{R}} dm \right) \tag{C.3.46}
\end{aligned}$$

The inertial tensor of the body with respect to the point R expressed in the frame \mathcal{R} is defined by:

$$\mathbf{J}_{B,(R)}^{\mathcal{R}} = - \int_B \tilde{\mathbf{r}}_{RP}^{\mathcal{R}} \tilde{\mathbf{r}}_{RP}^{\mathcal{R}} dm \tag{C.3.47}$$

Using this definition, the inertial terms for the rotational motions can be written as:

$$\begin{aligned}
\int_B \delta' \omega_{I\mathcal{R}}^{\mathcal{R}T} \tilde{\mathbf{r}}_{RP}^{\mathcal{R}} \mathbf{S}^{\mathcal{R}I} \mathbf{a}_{OP}^I dm &= \delta' \omega_{I\mathcal{R}}^{\mathcal{R}T} \left[\int_B \tilde{\mathbf{r}}_{RP}^{\mathcal{R}} dm \mathbf{S}^{\mathcal{R}I} \mathbf{a}_{OR}^I + \mathbf{J}_{B,(R)}^{\mathcal{R}} \dot{\omega}_{I\mathcal{R}}^{\mathcal{R}} + \tilde{\omega}_{I\mathcal{R}}^{\mathcal{R}} \mathbf{J}_{B,(R)}^{\mathcal{R}} \omega_{I\mathcal{R}}^{\mathcal{R}} \right. \\
&\quad \left. - 2 \int_B \tilde{\mathbf{r}}_{RP}^{\mathcal{R}} \dot{\tilde{\mathbf{r}}}_{RP}^{\mathcal{R}} dm \omega_{I\mathcal{R}}^{\mathcal{R}} + \int_B \tilde{\mathbf{r}}_{RP}^{\mathcal{R}} \ddot{\tilde{\mathbf{r}}}_{RP}^{\mathcal{R}} dm \right] \tag{C.3.48}
\end{aligned}$$

If the body-fixed frame \mathcal{B} is used as the reference frame, the inertia terms for the rotational motions are given by:

$$\begin{aligned}
& \int_B \delta' \omega_{I\mathcal{B}}^{\mathcal{B}T} \tilde{\mathbf{r}}_{RP}^{\mathcal{B}} \mathbf{S}^{\mathcal{B}I} \mathbf{a}_{OP}^I dm \\
&= \delta' \omega_{I\mathcal{B}}^{\mathcal{B}T} \left(\int_B \tilde{\mathbf{r}}_{RP}^{\mathcal{B}} dm \mathbf{S}^{\mathcal{B}I} \mathbf{a}_{OR}^I - \int_B \tilde{\mathbf{r}}_{RP}^{\mathcal{B}} \tilde{\mathbf{r}}_{RP}^{\mathcal{B}} dm \dot{\omega}_{I\mathcal{B}}^{\mathcal{B}} - \tilde{\omega}_{I\mathcal{B}}^{\mathcal{B}} \int_B \tilde{\mathbf{r}}_{RP}^{\mathcal{B}} \tilde{\mathbf{r}}_{RP}^{\mathcal{B}} dm \omega_{I\mathcal{B}}^{\mathcal{B}} \right. \\
&\quad \left. - 2 \int_B \tilde{\mathbf{r}}_{RP}^{\mathcal{B}} \dot{\tilde{\mathbf{r}}}_{RP}^{\mathcal{B}} dm \omega_{I\mathcal{B}}^{\mathcal{B}} + \int_B \tilde{\mathbf{r}}_{RP}^{\mathcal{B}} \ddot{\tilde{\mathbf{r}}}_{RP}^{\mathcal{B}} dm \right) \tag{C.3.49}
\end{aligned}$$

Splitting the position vector into the reference position $\mathbf{x}^{\mathcal{B}}$ and the displacement $\mathbf{w}^{\mathcal{B}}$ and sorting the resulting terms depending on how many times the displacement vector $\mathbf{w}^{\mathcal{B}}$ or its derivatives is

contained as a factor leads to:

$$\begin{aligned}
& \int_{\mathbf{B}} \delta' \omega_{IB}^{\mathbf{B} \text{ T}} \tilde{\mathbf{r}}_{\text{RP}}^{\mathbf{B}} \mathbf{S}^{\text{BI}} \mathbf{a}_{\text{OP}}^{\text{I}} dm \\
&= \delta' \omega_{IB}^{\mathbf{B} \text{ T}} \left(\int_{\mathbf{B}} [\tilde{\mathbf{x}}^{\mathbf{B}} + \tilde{\mathbf{w}}^{\mathbf{B}}] dm \mathbf{S}^{\text{BI}} \mathbf{a}_{\text{OR}}^{\text{I}} - \int_{\mathbf{B}} [\tilde{\mathbf{x}}^{\mathbf{B}} + \tilde{\mathbf{w}}^{\mathbf{B}}] [\tilde{\mathbf{x}}^{\mathbf{B}} + \tilde{\mathbf{w}}^{\mathbf{B}}] dm \dot{\omega}_{IB}^{\mathbf{B}} \right. \\
&\quad - \tilde{\omega}_{IB}^{\mathbf{B}} \int_{\mathbf{B}} [\tilde{\mathbf{x}}^{\mathbf{B}} + \tilde{\mathbf{w}}^{\mathbf{B}}] [\tilde{\mathbf{x}}^{\mathbf{B}} + \tilde{\mathbf{w}}^{\mathbf{B}}] dm \omega_{IB}^{\mathbf{B}} \\
&\quad \left. - 2 \int_{\mathbf{B}} [\tilde{\mathbf{x}}^{\mathbf{B}} + \tilde{\mathbf{w}}^{\mathbf{B}}] \dot{\tilde{\mathbf{w}}}^{\mathbf{B}} dm \omega_{IB}^{\mathbf{B}} + \int_{\mathbf{B}} [\tilde{\mathbf{x}}^{\mathbf{B}} + \tilde{\mathbf{w}}^{\mathbf{B}}] \ddot{\mathbf{w}}^{\mathbf{B}} dm \right) \\
&= \delta' \omega_{IB}^{\mathbf{B} \text{ T}} \left(\int_{\mathbf{B}} \tilde{\mathbf{x}}^{\mathbf{B}} dm \mathbf{S}^{\text{BI}} \mathbf{a}_{\text{OR}}^{\text{I}} - \int_{\mathbf{B}} \tilde{\mathbf{x}}^{\mathbf{B}} \tilde{\mathbf{x}}^{\mathbf{B}} dm \dot{\omega}_{IB}^{\mathbf{B}} - \tilde{\omega}_{IB}^{\mathbf{B}} \int_{\mathbf{B}} \tilde{\mathbf{x}}^{\mathbf{B}} \tilde{\mathbf{x}}^{\mathbf{B}} dm \omega_{IB}^{\mathbf{B}} \right) \\
&\quad + \delta' \omega_{IB}^{\mathbf{B} \text{ T}} \left(\int_{\mathbf{B}} \tilde{\mathbf{w}}^{\mathbf{B}} dm \mathbf{S}^{\text{BI}} \mathbf{a}_{\text{OR}}^{\text{I}} - \int_{\mathbf{B}} (\tilde{\mathbf{x}}^{\mathbf{B}} \tilde{\mathbf{w}}^{\mathbf{B}} + \tilde{\mathbf{w}}^{\mathbf{B}} \tilde{\mathbf{x}}^{\mathbf{B}}) dm \dot{\omega}_{IB}^{\mathbf{B}} \right. \\
&\quad \left. - \tilde{\omega}_{IB}^{\mathbf{B}} \int_{\mathbf{B}} (\tilde{\mathbf{x}}^{\mathbf{B}} \tilde{\mathbf{w}}^{\mathbf{B}} + \tilde{\mathbf{w}}^{\mathbf{B}} \tilde{\mathbf{x}}^{\mathbf{B}}) dm \omega_{IB}^{\mathbf{B}} - 2 \int_{\mathbf{B}} \tilde{\mathbf{x}}^{\mathbf{B}} \dot{\tilde{\mathbf{w}}}^{\mathbf{B}} dm \omega_{IB}^{\mathbf{B}} + \int_{\mathbf{B}} \tilde{\mathbf{x}}^{\mathbf{B}} \ddot{\mathbf{w}}^{\mathbf{B}} dm \right) \\
&\quad + \delta' \omega_{IB}^{\mathbf{B} \text{ T}} \left(- \int_{\mathbf{B}} \tilde{\mathbf{w}}^{\mathbf{B}} \tilde{\mathbf{w}}^{\mathbf{B}} dm \dot{\omega}_{IB}^{\mathbf{B}} - \tilde{\omega}_{IB}^{\mathbf{B}} \int_{\mathbf{B}} \tilde{\mathbf{w}}^{\mathbf{B}} \tilde{\mathbf{w}}^{\mathbf{B}} dm \omega_{IB}^{\mathbf{B}} \right. \\
&\quad \left. - 2 \int_{\mathbf{B}} \tilde{\mathbf{w}}^{\mathbf{B}} \dot{\tilde{\mathbf{w}}}^{\mathbf{B}} dm \omega_{IB}^{\mathbf{B}} + \int_{\mathbf{B}} \tilde{\mathbf{w}}^{\mathbf{B}} \ddot{\mathbf{w}}^{\mathbf{B}} dm \right) \tag{C.3.50}
\end{aligned}$$

The terms in the first bracket contain only the reference position vector $\mathbf{x}^{\mathbf{B}}$. These terms describe the characteristics of the undeformed body, i.e. the position of its centre of gravity and its inertia tensor; since these terms don't contain the displacement vector $\mathbf{w}^{\mathbf{B}}$, they will be referenced as zeroth order terms. The second and the third bracket contain the first and the second order terms, respectively. The first order terms are products, in which the vector $\mathbf{w}^{\mathbf{B}}$ or one of its derivatives are contained one time. In the second order terms, the $\mathbf{w}^{\mathbf{B}}$ or one of its derivatives are contained two times, while the reference position vector does not appear at all in these terms.

Also here, the inertia terms for a rigid body are obtained by setting the displacement vector $\mathbf{w}^{\mathbf{B}}$ and its derivatives equal to zero according to (C.3.36). Thereby the inertial terms for the rotational motions of a rigid body can be written as:

$$\begin{aligned}
& \int_{\mathbf{B}} \delta' \omega_{IB}^{\mathbf{B} \text{ T}} \tilde{\mathbf{r}}_{\text{RP}}^{\mathbf{B}} \mathbf{S}^{\text{BI}} \mathbf{a}_{\text{OP}}^{\text{I}} dm \\
&= \delta' \omega_{IB}^{\mathbf{B} \text{ T}} \left(\int_{\mathbf{B}} \tilde{\mathbf{x}}^{\mathbf{B}} dm \mathbf{S}^{\text{BI}} \mathbf{a}_{\text{OR}}^{\text{I}} - \int_{\mathbf{B}} \tilde{\mathbf{x}}^{\mathbf{B}} \tilde{\mathbf{x}}^{\mathbf{B}} dm \dot{\omega}_{IB}^{\mathbf{B}} - \tilde{\omega}_{IB}^{\mathbf{B}} \int_{\mathbf{B}} \tilde{\mathbf{x}}^{\mathbf{B}} \tilde{\mathbf{x}}^{\mathbf{B}} dm \omega_{IB}^{\mathbf{B}} \right) \\
&= \delta' \omega_{IB}^{\mathbf{B} \text{ T}} \left(\int_{\mathbf{B}} \tilde{\mathbf{x}}^{\mathbf{B}} dm \mathbf{S}^{\text{BI}} \mathbf{a}_{\text{OR}}^{\text{I}} - \mathbf{J}_{\mathbf{B},(\text{R})}^{\mathbf{B}} \dot{\omega}_{IB}^{\mathbf{B}} - \tilde{\omega}_{IB}^{\mathbf{B}} \mathbf{J}_{\mathbf{B},(\text{R})}^{\mathbf{B}} \omega_{IB}^{\mathbf{B}} \right) \tag{C.3.51}
\end{aligned}$$

Combining this result with (C.3.37) leads to the complete inertia terms for a rigid body, which are given by:

$$\begin{aligned}
\int_{\mathbf{B}} \delta' \mathbf{v}_{\text{OP}}^{\text{I} \text{ T}} \mathbf{a}_{\text{OP}}^{\text{I}} dm &= \int_{\mathbf{B}} \delta' \mathbf{v}_{\text{OR}}^{\text{I} \text{ T}} \mathbf{a}_{\text{OP}}^{\text{I}} dm + \int_{\mathbf{B}} \delta' \omega_{IB}^{\mathbf{B} \text{ T}} \tilde{\mathbf{r}}_{\text{RP}}^{\mathbf{B}} \mathbf{S}^{\text{BI}} \mathbf{a}_{\text{OP}}^{\text{I}} dm \\
&= \delta' \mathbf{v}_{\text{OR}}^{\text{I} \text{ T}} \left(m_{\mathbf{B}} \mathbf{a}_{\text{OR}}^{\text{I}} + \mathbf{S}^{\text{IB}} \left(\dot{\tilde{\omega}}_{IB}^{\mathbf{B}} + \tilde{\omega}_{IB}^{\mathbf{B}} \tilde{\omega}_{IB}^{\mathbf{B}} \right) \int_{\mathbf{B}} \tilde{\mathbf{x}}^{\mathbf{B}} dm \right) \\
&\quad + \delta' \omega_{IB}^{\mathbf{B} \text{ T}} \left(\int_{\mathbf{B}} \tilde{\mathbf{x}}^{\mathbf{B}} dm \mathbf{S}^{\text{BI}} \mathbf{a}_{\text{OR}}^{\text{I}} - \mathbf{J}_{\mathbf{B},(\text{R})}^{\mathbf{B}} \dot{\omega}_{IB}^{\mathbf{B}} - \tilde{\omega}_{IB}^{\mathbf{B}} \mathbf{J}_{\mathbf{B},(\text{R})}^{\mathbf{B}} \omega_{IB}^{\mathbf{B}} \right) \tag{C.3.52}
\end{aligned}$$

C.3.3 Relative motions

In order to evaluate the inertia terms for the relative motions, the integrand is again reformulated by using the commutativity of the cross product and resolving the bracket:

$$\begin{aligned}
\delta \dot{\mathbf{r}}_{\text{RP}}^{\mathcal{R}T} \mathbf{S}^{\mathcal{R}I} \mathbf{a}_{\text{OP}}^I &= \delta \dot{\mathbf{r}}_{\text{RP}}^{\mathcal{R}T} \left(\mathbf{S}^{\mathcal{R}I} \mathbf{a}_{\text{OR}}^I + \dot{\tilde{\omega}}_{I\mathcal{R}}^{\mathcal{R}} \mathbf{r}_{\text{RP}}^{\mathcal{R}} + \tilde{\omega}_{I\mathcal{R}}^{\mathcal{R}} \tilde{\omega}_{I\mathcal{R}}^{\mathcal{R}} \mathbf{r}_{\text{RP}}^{\mathcal{R}} + 2 \tilde{\omega}_{I\mathcal{R}}^{\mathcal{R}} \dot{\mathbf{r}}_{\text{RP}}^{\mathcal{R}} + \ddot{\mathbf{r}}_{\text{RP}}^{\mathcal{R}} \right) \\
&= \delta \dot{\mathbf{r}}_{\text{RP}}^{\mathcal{R}T} \left(\mathbf{S}^{\mathcal{R}I} \mathbf{a}_{\text{OR}}^I - \dot{\mathbf{r}}_{\text{RP}}^{\mathcal{R}} \dot{\omega}_{I\mathcal{R}}^{\mathcal{R}} - \tilde{\omega}_{I\mathcal{R}}^{\mathcal{R}} \tilde{\mathbf{r}}_{\text{RP}}^{\mathcal{R}} \omega_{I\mathcal{R}}^{\mathcal{R}} - 2 \dot{\mathbf{r}}_{\text{RP}}^{\mathcal{R}} \omega_{I\mathcal{R}}^{\mathcal{R}} + \ddot{\mathbf{r}}_{\text{RP}}^{\mathcal{R}} \right) \\
&= \delta \dot{\mathbf{r}}_{\text{RP}}^{\mathcal{R}T} \mathbf{S}^{\mathcal{R}I} \mathbf{a}_{\text{OR}}^I - \delta \dot{\mathbf{r}}_{\text{RP}}^{\mathcal{R}T} \tilde{\mathbf{r}}_{\text{RP}}^{\mathcal{R}} \dot{\omega}_{I\mathcal{R}}^{\mathcal{R}} - \delta \dot{\mathbf{r}}_{\text{RP}}^{\mathcal{R}T} \tilde{\omega}_{I\mathcal{R}}^{\mathcal{R}} \tilde{\mathbf{r}}_{\text{RP}}^{\mathcal{R}} \omega_{I\mathcal{R}}^{\mathcal{R}} \\
&\quad - 2 \delta \dot{\mathbf{r}}_{\text{RP}}^{\mathcal{R}T} \dot{\tilde{\mathbf{r}}}_{\text{RP}}^{\mathcal{R}} \omega_{I\mathcal{R}}^{\mathcal{R}} + \delta \dot{\mathbf{r}}_{\text{RP}}^{\mathcal{R}T} \ddot{\mathbf{r}}_{\text{RP}}^{\mathcal{R}} \tag{C.3.53}
\end{aligned}$$

From the commutative rule of the cross product it can be deduced:

$$\tilde{\mathbf{u}}\mathbf{v} = -\tilde{\mathbf{v}}\mathbf{u} \Rightarrow (\tilde{\mathbf{u}}\mathbf{v})^T = (-\tilde{\mathbf{v}}\mathbf{u})^T \Rightarrow \mathbf{v}^T \tilde{\mathbf{u}}^T = -\mathbf{u}^T \tilde{\mathbf{v}}^T \Rightarrow \mathbf{v}^T (-\tilde{\mathbf{u}}) = -\mathbf{u}^T (-\tilde{\mathbf{v}}) \Rightarrow \mathbf{v}^T \tilde{\mathbf{u}} = -\mathbf{u}^T \tilde{\mathbf{v}} \tag{C.3.54}$$

Applying this relation to the third term of the integrand leads to:

$$\begin{aligned}
\delta \dot{\mathbf{r}}_{\text{RP}}^{\mathcal{R}T} \mathbf{S}^{\mathcal{R}I} \mathbf{a}_{\text{OP}}^I &= \delta \dot{\mathbf{r}}_{\text{RP}}^{\mathcal{R}T} \mathbf{S}^{\mathcal{R}I} \mathbf{a}_{\text{OR}}^I - \delta \dot{\mathbf{r}}_{\text{RP}}^{\mathcal{R}T} \tilde{\mathbf{r}}_{\text{RP}}^{\mathcal{R}} \dot{\omega}_{I\mathcal{R}}^{\mathcal{R}} - \delta \dot{\mathbf{r}}_{\text{RP}}^{\mathcal{R}T} \tilde{\omega}_{I\mathcal{R}}^{\mathcal{R}} \tilde{\mathbf{r}}_{\text{RP}}^{\mathcal{R}} \omega_{I\mathcal{R}}^{\mathcal{R}} \\
&\quad - 2 \delta \dot{\mathbf{r}}_{\text{RP}}^{\mathcal{R}T} \dot{\tilde{\mathbf{r}}}_{\text{RP}}^{\mathcal{R}} \omega_{I\mathcal{R}}^{\mathcal{R}} + \delta \dot{\mathbf{r}}_{\text{RP}}^{\mathcal{R}T} \ddot{\mathbf{r}}_{\text{RP}}^{\mathcal{R}} \\
&= \delta \dot{\mathbf{r}}_{\text{RP}}^{\mathcal{R}T} \mathbf{S}^{\mathcal{R}I} \mathbf{a}_{\text{OR}}^I - \delta \dot{\mathbf{r}}_{\text{RP}}^{\mathcal{R}T} \tilde{\mathbf{r}}_{\text{RP}}^{\mathcal{R}} \dot{\omega}_{I\mathcal{R}}^{\mathcal{R}} + \omega_{I\mathcal{R}}^{\mathcal{R}T} \delta \dot{\mathbf{r}}_{\text{RP}}^{\mathcal{R}T} \tilde{\mathbf{r}}_{\text{RP}}^{\mathcal{R}} \omega_{I\mathcal{R}}^{\mathcal{R}} \\
&\quad - 2 \delta \dot{\mathbf{r}}_{\text{RP}}^{\mathcal{R}T} \dot{\tilde{\mathbf{r}}}_{\text{RP}}^{\mathcal{R}} \omega_{I\mathcal{R}}^{\mathcal{R}} + \delta \dot{\mathbf{r}}_{\text{RP}}^{\mathcal{R}T} \ddot{\mathbf{r}}_{\text{RP}}^{\mathcal{R}} \tag{C.3.55}
\end{aligned}$$

By splitting the integrand and factoring out the vectors and matrices, which describe the kinematics of the reference point R, from the integrals it is obtained for the inertia terms for the relative motions:

$$\begin{aligned}
\int_{\text{B}} \delta \dot{\mathbf{r}}_{\text{RP}}^{\mathcal{R}T} \mathbf{S}^{\mathcal{R}I} \mathbf{a}_{\text{OP}}^I dm &= \int_{\text{B}} \left[\delta \dot{\mathbf{r}}_{\text{RP}}^{\mathcal{R}T} \mathbf{S}^{\mathcal{R}I} \mathbf{a}_{\text{OR}}^I - \delta \dot{\mathbf{r}}_{\text{RP}}^{\mathcal{R}T} \tilde{\mathbf{r}}_{\text{RP}}^{\mathcal{R}} \dot{\omega}_{I\mathcal{R}}^{\mathcal{R}} + \omega_{I\mathcal{R}}^{\mathcal{R}T} \delta \dot{\mathbf{r}}_{\text{RP}}^{\mathcal{R}T} \tilde{\mathbf{r}}_{\text{RP}}^{\mathcal{R}} \omega_{I\mathcal{R}}^{\mathcal{R}} \right. \\
&\quad \left. - 2 \delta \dot{\mathbf{r}}_{\text{RP}}^{\mathcal{R}T} \dot{\tilde{\mathbf{r}}}_{\text{RP}}^{\mathcal{R}} \omega_{I\mathcal{R}}^{\mathcal{R}} + \delta \dot{\mathbf{r}}_{\text{RP}}^{\mathcal{R}T} \ddot{\mathbf{r}}_{\text{RP}}^{\mathcal{R}} \right] \\
&= \int_{\text{B}} \delta \dot{\mathbf{r}}_{\text{RP}}^{\mathcal{R}T} dm \mathbf{S}^{\mathcal{R}I} \mathbf{a}_{\text{OR}}^I - \int_{\text{B}} \delta \dot{\mathbf{r}}_{\text{RP}}^{\mathcal{R}T} \tilde{\mathbf{r}}_{\text{RP}}^{\mathcal{R}} dm \dot{\omega}_{I\mathcal{R}}^{\mathcal{R}} \\
&\quad + \omega_{I\mathcal{R}}^{\mathcal{R}T} \int_{\text{B}} \delta \dot{\mathbf{r}}_{\text{RP}}^{\mathcal{R}T} \tilde{\mathbf{r}}_{\text{RP}}^{\mathcal{R}} dm \omega_{I\mathcal{R}}^{\mathcal{R}} \\
&\quad - 2 \int_{\text{B}} \delta \dot{\mathbf{r}}_{\text{RP}}^{\mathcal{R}T} \dot{\tilde{\mathbf{r}}}_{\text{RP}}^{\mathcal{R}} dm \omega_{I\mathcal{R}}^{\mathcal{R}} + \int_{\text{B}} \delta \dot{\mathbf{r}}_{\text{RP}}^{\mathcal{R}T} \ddot{\mathbf{r}}_{\text{RP}}^{\mathcal{R}} dm \tag{C.3.56}
\end{aligned}$$

If the body-fixed frame \mathcal{B} is used as the reference frame, the inertia terms for the relative motions are written as:

$$\begin{aligned}
\int_{\text{B}} \delta \dot{\mathbf{r}}_{\text{RP}}^{\mathcal{B}T} \mathbf{S}^{\mathcal{B}I} \mathbf{a}_{\text{OP}}^I dm &= \int_{\text{B}} \delta \dot{\mathbf{r}}_{\text{RP}}^{\mathcal{B}T} dm \mathbf{S}^{\mathcal{B}I} \mathbf{a}_{\text{OR}}^I - \int_{\text{B}} \delta \dot{\mathbf{r}}_{\text{RP}}^{\mathcal{B}T} \tilde{\mathbf{r}}_{\text{RP}}^{\mathcal{B}} dm \dot{\omega}_{I\mathcal{B}}^{\mathcal{B}} \\
&\quad + \omega_{I\mathcal{B}}^{\mathcal{B}T} \int_{\text{B}} \delta \dot{\mathbf{r}}_{\text{RP}}^{\mathcal{B}T} \tilde{\mathbf{r}}_{\text{RP}}^{\mathcal{B}} dm \omega_{I\mathcal{B}}^{\mathcal{B}} \\
&\quad - 2 \int_{\text{B}} \delta \dot{\mathbf{r}}_{\text{RP}}^{\mathcal{B}T} \dot{\tilde{\mathbf{r}}}_{\text{RP}}^{\mathcal{B}} dm \omega_{I\mathcal{B}}^{\mathcal{B}} + \int_{\text{B}} \delta \dot{\mathbf{r}}_{\text{RP}}^{\mathcal{B}T} \ddot{\mathbf{r}}_{\text{RP}}^{\mathcal{B}} dm \tag{C.3.57}
\end{aligned}$$

Splitting the vector $\mathbf{r}_{\text{RP}}^{\text{B}}$ into the reference position \mathbf{x}^{B} and the deformation \mathbf{w}^{B} leads to:

$$\begin{aligned}
& \int_{\text{B}} \delta' \dot{\mathbf{r}}_{\text{RP}}^{\text{B} \text{ T}} \mathbf{S}^{\text{BI}} \mathbf{a}_{\text{OP}}^{\text{I}} dm \\
&= \int_{\text{B}} \delta' \dot{\mathbf{w}}^{\text{B} \text{ T}} \mathbf{S}^{\text{BI}} \mathbf{a}_{\text{OP}}^{\text{I}} dm \\
&= \int_{\text{B}} \delta' \dot{\mathbf{w}}^{\text{B} \text{ T}} dm \mathbf{S}^{\text{BI}} \mathbf{a}_{\text{OR}}^{\text{I}} - \int_{\text{B}} \delta' \dot{\mathbf{w}}^{\text{B} \text{ T}} [\tilde{\mathbf{x}}^{\text{B}} + \tilde{\mathbf{w}}^{\text{B}}] dm \dot{\omega}_{\text{IB}}^{\text{B}} \\
&\quad + \omega_{\text{IB}}^{\text{B} \text{ T}} \int_{\text{B}} \delta' \tilde{\dot{\mathbf{w}}}^{\text{B}} [\tilde{\mathbf{x}}^{\text{B}} + \tilde{\mathbf{w}}^{\text{B}}] dm \omega_{\text{IB}}^{\text{B}} \\
&\quad - 2 \int_{\text{B}} \delta' \dot{\mathbf{w}}^{\text{B} \text{ T}} \tilde{\dot{\mathbf{w}}}_{\text{RP}}^{\text{B}} dm \omega_{\text{IB}}^{\text{B}} + \int_{\text{B}} \delta' \dot{\mathbf{w}}^{\text{B} \text{ T}} \ddot{\mathbf{w}}_{\text{RP}}^{\text{B}} dm \\
&= \int_{\text{B}} \delta' \dot{\mathbf{w}}^{\text{B} \text{ T}} dm \mathbf{S}^{\text{BI}} \mathbf{a}_{\text{OR}}^{\text{I}} - \int_{\text{B}} \delta' \dot{\mathbf{w}}^{\text{B} \text{ T}} \tilde{\mathbf{x}}^{\text{B}} dm \dot{\omega}_{\text{IB}}^{\text{B}} + \omega_{\text{IB}}^{\text{B} \text{ T}} \int_{\text{B}} \delta' \tilde{\dot{\mathbf{w}}}^{\text{B}} \tilde{\mathbf{x}}^{\text{B}} dm \omega_{\text{IB}}^{\text{B}} \\
&\quad - \int_{\text{B}} \delta' \dot{\mathbf{w}}^{\text{B} \text{ T}} \tilde{\mathbf{w}}^{\text{B}} dm \dot{\omega}_{\text{IB}}^{\text{B}} + \omega_{\text{IB}}^{\text{B} \text{ T}} \int_{\text{B}} \delta' \tilde{\dot{\mathbf{w}}}^{\text{B}} \tilde{\mathbf{w}}^{\text{B}} dm \omega_{\text{IB}}^{\text{B}} \\
&\quad - 2 \int_{\text{B}} \delta' \dot{\mathbf{w}}^{\text{B} \text{ T}} \tilde{\dot{\mathbf{w}}}^{\text{B}} dm \omega_{\text{IB}}^{\text{B}} + \int_{\text{B}} \delta' \dot{\mathbf{w}}^{\text{B} \text{ T}} \ddot{\mathbf{w}}^{\text{B}} dm
\end{aligned} \tag{C.3.58}$$

Appendix D

Rotation matrices

Rotation matrices play an important role in the formulation of kinematics. The rotation matrix $\mathbf{S}^{J\mathcal{K}}$ describes the transformation from the frame \mathcal{K} into the frame J . Thereby, the relation between the description \mathbf{r}^J of a vector in the frame J and its description $\mathbf{r}^{\mathcal{K}}$ in the frame \mathcal{K} is given by:

$$\mathbf{r}^J = \mathbf{S}^{J\mathcal{K}} \mathbf{r}^{\mathcal{K}} \quad (\text{D.0.1})$$

The differentiation of this relation with respect to the time t leads to:

$$\dot{\mathbf{r}}^J = \dot{\mathbf{S}}^{J\mathcal{K}} \mathbf{r}^{\mathcal{K}} + \mathbf{S}^{J\mathcal{K}} \dot{\mathbf{r}}^{\mathcal{K}} \quad (\text{D.0.2})$$

As it will be shown in this appendix, the angular velocity of the frame \mathcal{K} relative to the frame J can be determined based on the derivative $\dot{\mathbf{S}}^{J\mathcal{K}}$.

Also, in this work the relations (D.0.1) and (D.0.2) are used very often; in this context, several properties of rotation matrices are frequently exploited. Therefore, these properties shall be considered in this appendix. Since in the present work spatial kinematics is considered, the following considerations will focus on the three-dimensional space.

A general rotation matrix like the aforementioned matrix $\mathbf{S}^{J\mathcal{K}}$ can be expressed as a product of elementary rotation matrices. An elementary rotation matrix $\mathbf{S}_I(\phi)$ describes a single rotation with the angle ϕ around one of the axes of the cartesian coordinates denoted by I .

D.1 Elementary rotation matrices

For the three-dimensional space there are three elementary rotation matrices:

$$\mathbf{S}_1(\alpha) = \begin{bmatrix} 1 & 0 & 0 \\ 0 & \cos \alpha & -\sin \alpha \\ 0 & \sin \alpha & \cos \alpha \end{bmatrix}, \mathbf{S}_2(\beta) = \begin{bmatrix} \cos \beta & 0 & \sin \beta \\ 0 & 1 & 0 \\ -\sin \beta & 0 & \cos \beta \end{bmatrix}, \mathbf{S}_3(\gamma) = \begin{bmatrix} \cos \gamma & -\sin \gamma & 0 \\ \sin \gamma & \cos \gamma & 0 \\ 0 & 0 & 1 \end{bmatrix} \quad (\text{D.1.3})$$

The diagonal elements of each rotation matrix are either 1 or equal to the cosine function of the rotation angle, while all non-diagonal elements are either 0 or equal to the sine function of the rotation angle. Therefore, it is valid:

$$\sin(\phi = 0) = 0, \cos(\phi = 0) = 1 \Rightarrow \mathbf{S}_I(\phi = 0) = \begin{bmatrix} 1 & 0 & 0 \\ 0 & 1 & 0 \\ 0 & 0 & 1 \end{bmatrix} = \mathbf{I}, I = 1, 2, 3 \quad (\text{D.1.4})$$

By applying the symmetry properties of the trigonometric functions:

$$\sin(-\phi) = -\sin \phi, \quad \cos(-\phi) = \cos \phi \quad (\text{D.1.5})$$

it can be derived:

$$\mathbf{S}_1(-\alpha) = \begin{bmatrix} 1 & 0 & 0 \\ 0 & \cos(-\alpha) & -\sin(-\alpha) \\ 0 & \sin(-\alpha) & \cos(-\alpha) \end{bmatrix} = \begin{bmatrix} 1 & 0 & 0 \\ 0 & \cos \alpha & \sin \alpha \\ 0 & -\sin \alpha & \cos \alpha \end{bmatrix} = \mathbf{S}_1(\alpha)^T \quad (\text{D.1.6})$$

$$\mathbf{S}_2(-\beta) = \begin{bmatrix} \cos(-\beta) & 0 & \sin(-\beta) \\ 0 & 1 & 0 \\ -\sin(-\beta) & 0 & \cos(-\beta) \end{bmatrix} = \begin{bmatrix} \cos \beta & 0 & -\sin \beta \\ 0 & 1 & 0 \\ \sin \beta & 0 & \cos \beta \end{bmatrix} = \mathbf{S}_2(\beta)^T \quad (\text{D.1.7})$$

$$\mathbf{S}_3(-\gamma) = \begin{bmatrix} \cos(-\gamma) & -\sin(-\gamma) & 0 \\ \sin(-\gamma) & \cos(-\gamma) & 0 \\ 0 & 0 & 1 \end{bmatrix} = \begin{bmatrix} \cos \gamma & \sin \gamma & 0 \\ -\sin \gamma & \cos \gamma & 0 \\ 0 & 0 & 1 \end{bmatrix} = \mathbf{S}_3(\gamma)^T \quad (\text{D.1.8})$$

In total it is valid for a rotation matrix describing a rotation around the axis I with the angle ϕ :

$$\mathbf{S}_I(-\phi) = \mathbf{S}_I(\phi)^T, \quad I = 1, 2, 3 \quad (\text{D.1.9})$$

Using the theorems for the trigonometric functions:

$$\sin(\phi_i + \phi_k) = \sin \phi_i \cos \phi_k + \cos \phi_i \sin \phi_k, \quad \cos(\phi_i + \phi_k) = \cos \phi_i \cos \phi_k - \sin \phi_i \sin \phi_k \quad (\text{D.1.10})$$

it can be shown for the products of two elementary rotation matrices for the same axis:

$$\begin{aligned} \mathbf{S}_1(\alpha_i) \mathbf{S}_1(\alpha_k) &= \begin{bmatrix} 1 & 0 & 0 \\ 0 & \cos \alpha_i & -\sin \alpha_i \\ 0 & \sin \alpha_i & \cos \alpha_i \end{bmatrix} \begin{bmatrix} 1 & 0 & 0 \\ 0 & \cos \alpha_k & -\sin \alpha_k \\ 0 & \sin \alpha_k & \cos \alpha_k \end{bmatrix} \\ &= \begin{bmatrix} 1 & 0 & 0 \\ 0 & \cos \alpha_i \cos \alpha_k - \sin \alpha_i \sin \alpha_k & -\cos \alpha_i \sin \alpha_k - \sin \alpha_i \cos \alpha_k \\ 0 & \sin \alpha_i \cos \alpha_k + \cos \alpha_i \sin \alpha_k & -\sin \alpha_i \sin \alpha_k + \cos \alpha_i \cos \alpha_k \end{bmatrix} \\ &= \begin{bmatrix} 1 & 0 & 0 \\ 0 & \cos(\alpha_i + \alpha_k) & -\sin(\alpha_i + \alpha_k) \\ 0 & \sin(\alpha_i + \alpha_k) & \cos(\alpha_i + \alpha_k) \end{bmatrix} = \mathbf{S}_1(\alpha_i + \alpha_k) \end{aligned} \quad (\text{D.1.11})$$

$$\begin{aligned} \mathbf{S}_2(\beta_i) \mathbf{S}_2(\beta_k) &= \begin{bmatrix} \cos \beta_i & 0 & \sin \beta_i \\ 0 & 1 & 0 \\ -\sin \beta_i & 0 & \cos \beta_i \end{bmatrix} \begin{bmatrix} \cos \beta_k & 0 & \sin \beta_k \\ 0 & 1 & 0 \\ -\sin \beta_k & 0 & \cos \beta_k \end{bmatrix} \\ &= \begin{bmatrix} \cos \beta_i \cos \beta_k - \sin \beta_i \sin \beta_k & 0 & -\cos \beta_i \sin \beta_k - \sin \beta_i \cos \beta_k \\ 0 & 1 & 0 \\ \sin \beta_i \cos \beta_k + \cos \beta_i \sin \beta_k & 0 & -\sin \beta_i \sin \beta_k + \cos \beta_i \cos \beta_k \end{bmatrix} \\ &= \begin{bmatrix} \cos(\beta_i + \beta_k) & 0 & \sin(\beta_i + \beta_k) \\ 0 & 1 & 0 \\ -\sin(\beta_i + \beta_k) & 0 & \cos(\beta_i + \beta_k) \end{bmatrix} = \mathbf{S}_2(\beta_i + \beta_k) \end{aligned} \quad (\text{D.1.12})$$

$$\begin{aligned}
\mathbf{S}_3(\gamma_i)\mathbf{S}_3(\gamma_k) &= \begin{bmatrix} \cos \gamma_i & -\sin \gamma_i & 0 \\ \sin \gamma_i & \cos \gamma_i & 0 \\ 0 & 0 & 1 \end{bmatrix} \begin{bmatrix} \cos \gamma_k & -\sin \gamma_k & 0 \\ \sin \gamma_k & \cos \gamma_k & 0 \\ 0 & 0 & 1 \end{bmatrix} \\
&= \begin{bmatrix} \cos \gamma_i \cos \gamma_k - \sin \gamma_i \sin \gamma_k & -\cos \gamma_i \sin \gamma_k - \sin \gamma_i \cos \gamma_k & 0 \\ \sin \gamma_i \cos \gamma_k + \cos \gamma_i \sin \gamma_k & -\sin \gamma_i \sin \gamma_k + \cos \gamma_i \cos \gamma_k & 0 \\ 0 & 0 & 1 \end{bmatrix} \\
&= \begin{bmatrix} \cos(\gamma_i + \gamma_k) & -\sin(\gamma_i + \gamma_k) & 0 \\ \sin(\gamma_i + \gamma_k) & \cos(\gamma_i + \gamma_k) & 0 \\ 0 & 0 & 1 \end{bmatrix} = \mathbf{S}_3(\gamma_i + \gamma_k) \quad (\text{D.1.13})
\end{aligned}$$

In total it is valid for two subsequent rotations around the same axis indicated by I with the angles ϕ_i and ϕ_k :

$$\mathbf{S}_I(\phi_i)\mathbf{S}_I(\phi_k) = \mathbf{S}_I(\phi_i + \phi_k), \quad I = 1, 2, 3 \quad (\text{D.1.14})$$

Based on the relations (D.1.4), (D.1.9) and (D.1.14) it can be derived:

$$\mathbf{S}_I(\phi)\mathbf{S}_I(\phi)^\text{T} = \mathbf{S}_I(\phi)\mathbf{S}_I(-\phi) = \mathbf{S}_I(\phi - \phi) = \mathbf{S}_I(0) = \mathbf{I} \quad (\text{D.1.15})$$

From this it follows:

$$\mathbf{S}_I(\phi)\mathbf{S}_I(\phi)^\text{T} = \mathbf{I} = \mathbf{S}_I(\phi)\mathbf{S}_I(\phi)^{-1} \Rightarrow \mathbf{S}_I(\phi)^\text{T} = \mathbf{S}_I(\phi)^{-1} \quad (\text{D.1.16})$$

The result shows that the transpose $\mathbf{S}_I(\phi)^\text{T}$ of an elementary rotation matrix $\mathbf{S}_I(\phi)$ is equal to its inverse $\mathbf{S}_I(\phi)^{-1}$; thereby, an elementary rotation matrix $\mathbf{S}_I(\phi)$ is an orthogonal matrix.

The determinant of an elementary rotation matrix for the three-dimensional space can be determined based on the rule by Sarrus:

$$\det \begin{bmatrix} a_{11} & a_{12} & a_{13} \\ a_{21} & a_{22} & a_{23} \\ a_{31} & a_{32} & a_{33} \end{bmatrix} = a_{11}a_{22}a_{33} + a_{12}a_{23}a_{31} + a_{13}a_{21}a_{32} - a_{31}a_{22}a_{13} - a_{32}a_{23}a_{11} - a_{33}a_{21}a_{12} \quad (\text{D.1.17})$$

Based on this it is obtained:

$$\det \mathbf{S}_1(\alpha) = \det \begin{bmatrix} 1 & 0 & 0 \\ 0 & \cos \alpha & -\sin \alpha \\ 0 & \sin \alpha & \cos \alpha \end{bmatrix} = \cos^2 \alpha - (-\sin^2 \alpha) = \cos^2 \alpha + \sin^2 \alpha = 1 \quad (\text{D.1.18})$$

$$\det \mathbf{S}_2(\beta) = \det \begin{bmatrix} \cos \beta & 0 & \sin \beta \\ 0 & 1 & 0 \\ -\sin \beta & 0 & \cos \beta \end{bmatrix} = \cos^2 \beta - (-\sin^2 \beta) = \cos^2 \beta + \sin^2 \beta = 1 \quad (\text{D.1.19})$$

$$\det \mathbf{S}_3(\gamma) = \det \begin{bmatrix} \cos \gamma & -\sin \gamma & 0 \\ \sin \gamma & \cos \gamma & 0 \\ 0 & 0 & 1 \end{bmatrix} = \cos^2 \gamma - (-\sin^2 \gamma) = \cos^2 \gamma + \sin^2 \gamma = 1 \quad (\text{D.1.20})$$

For further considerations, the following properties of an elementary rotation matrix can be concluded:

- An elementary rotation matrix $\mathbf{S}_I(\phi)$ is an orthogonal matrix, i.e. its transpose is equal to its inverse.

$$\mathbf{S}_I(\phi)^\text{T} = \mathbf{S}_I(\phi)^{-1} \Rightarrow \mathbf{S}_I(\phi)\mathbf{S}_I(\phi)^\text{T} = \mathbf{S}_I(\phi)\mathbf{S}_I(\phi)^{-1} = \mathbf{I} \quad (\text{D.1.21})$$

- The determinant of an elementary rotation matrix $\mathbf{S}_I(\phi)$ is equal to 1.

$$\det \mathbf{S}_I(\phi) = 1 \quad (\text{D.1.22})$$

- Two elementary rotation matrices, which describe two subsequent rotations with the angles ϕ_i and ϕ_k around the same axis I , can be merged into one elementary rotation matrix:

$$\mathbf{S}_I(\phi_i) \mathbf{S}_I(\phi_k) = \mathbf{S}_I(\phi_i + \phi_k) \quad (\text{D.1.23})$$

D.2 Composed rotation matrices

A general rotation matrix \mathbf{R}_N can be formulated as the product of N elementary rotation matrices:

$$\mathbf{R}_N = \prod_{k=1}^N \mathbf{S}_{I_k}(\phi_k), \quad I_k = 1, 2, 3 \quad (\text{D.2.24})$$

For the following considerations, the following recursive formulation of \mathbf{R}_N is used:

$$\mathbf{R}_0 = \mathbf{I}, \quad \mathbf{R}_k = \mathbf{R}_{k-1} \mathbf{S}_{I_k}(\phi_k) \quad (\text{D.2.25})$$

According to Strang [71], the determinant of a product of two matrices is equal to the product of the determinants for each single matrix:

$$\det(\mathbf{A}\mathbf{B}) = \det \mathbf{A} \det \mathbf{B} \quad (\text{D.2.26})$$

In the section D.1 it has been shown that for each elementary rotation matrix the determinant is equal to 1. Therefore, it is valid:

$$\det \mathbf{R}_k = \det(\mathbf{R}_{k-1} \mathbf{S}_{I_k}(\phi_k)) = \det \mathbf{R}_{k-1} \underbrace{\det \mathbf{S}_{I_k}(\phi_k)}_1 \Rightarrow \det \mathbf{R}_k = \det \mathbf{R}_{k-1} \quad (\text{D.2.27})$$

As discussed in the section D.1, the identity matrix \mathbf{I} can be considered as a special case of an elementary rotation matrix $\mathbf{S}_I(\phi)$ for $\phi = 0$. Thereby, also the determinant $\det \mathbf{R}_0$ of the initial matrix \mathbf{R}_0 is equal to 1 so that it is valid:

$$1 = \det \mathbf{R}_0 = \det \mathbf{R}_1 = \dots = \det \mathbf{R}_{N-1} = \det \mathbf{R}_N \quad (\text{D.2.28})$$

Thereby, it is shown that for the product \mathbf{R}_N of elementary rotation matrices the determinant is equal to 1.

For an orthogonal matrix \mathbf{Q} , the transposed \mathbf{Q}^T is equal to the inverse \mathbf{Q}^{-1} ; thereby, it is valid:

$$\mathbf{Q}^T = \mathbf{Q}^{-1} \Rightarrow \mathbf{Q}\mathbf{Q}^T = \mathbf{Q}\mathbf{Q}^{-1} = \mathbf{I} \quad (\text{D.2.29})$$

In the section D.1 it has been shown that an elementary rotation matrix $\mathbf{S}_I(\phi)$ is always an orthogonal matrix. By applying this to the recursive formulation (D.2.25) it is obtained:

$$\mathbf{R}_k \mathbf{R}_k^T = \mathbf{R}_{k-1} \mathbf{S}_{I_k}(\phi_k) (\mathbf{R}_{k-1} \mathbf{S}_{I_k}(\phi_k))^T = \mathbf{R}_{k-1} \underbrace{\mathbf{S}_{I_k}(\phi_k) \mathbf{S}_{I_k}(\phi_k)^T}_{\mathbf{I}} \mathbf{R}_{k-1}^T \Rightarrow \mathbf{R}_k \mathbf{R}_k^T = \mathbf{R}_{k-1} \mathbf{R}_{k-1}^T \quad (\text{D.2.30})$$

Therefore, it is valid for the matrix \mathbf{R}_N :

$$\mathbf{R}_N \mathbf{R}_N^T = \mathbf{R}_{N-1} \mathbf{R}_{N-1}^T = \dots = \mathbf{R}_1 \mathbf{R}_1^T = \mathbf{R}_0 \mathbf{R}_0^T = \mathbf{I} \mathbf{I}^T = \mathbf{I} \quad (\text{D.2.31})$$

From this, it follows:

$$\mathbf{R}_N \mathbf{R}_N^T = \mathbf{I} = \mathbf{R}_N \mathbf{R}_N^{-1} \Rightarrow \mathbf{R}_N^T = \mathbf{R}_N^{-1} \quad (\text{D.2.32})$$

Thereby, it has been shown that the matrix \mathbf{R}_N , which is a product of N elementary rotation matrices, is an orthogonal matrix, too.

D.3 Formulation by column vectors

In the previous section D.2 the properties of a rotation matrix \mathbf{R}_N , which is described as a product of N elementary rotation matrices $\mathbf{S}_i(\phi_i)$, have been discussed. Based on the facts that each elementary rotation matrix $\mathbf{S}_i(\phi_i)$ is an orthogonal matrix and that its determinant is equal two one it has been derived that also the product \mathbf{R}_N is an orthogonal matrix and its determinant $\det \mathbf{R}_N$ is equal to 1.

The formulation of a rotation matrix \mathbf{R}_N as a product of elementary rotation matrices is particularly useful if the individual elementary rotations are given by their rotation axis and their rotation angle. Alternatively, the matrix \mathbf{R}_N can be formulated by its column vectors. Since \mathbf{R}_N is a rotation matrix for the three-dimensional space, its order is 3×3 so that the formulation by column vectors \mathbf{e}_k is given by:

$$\mathbf{R}_N = [\mathbf{e}_1 \quad \mathbf{e}_2 \quad \mathbf{e}_3] \quad (\text{D.3.33})$$

The formulation using the column vectors \mathbf{e}_1 , \mathbf{e}_2 and \mathbf{e}_3 can be useful if a rotation matrix shall be determined for given vectors. In the following considerations, the conditions for the column vectors shall be derived and discussed.

If \mathbf{R}_N is an orthogonal matrix, then its transpose \mathbf{R}_N^T is equal to its inverse \mathbf{R}_N^{-1} . Thereby, it is valid:

$$\mathbf{R}_N^T = \mathbf{R}_N^{-1} \Rightarrow \mathbf{R}_N^T \mathbf{R}_N = \mathbf{R}_N^{-1} \mathbf{R}_N = \mathbf{I} \quad (\text{D.3.34})$$

By using the formulation according to (D.3.33) is it obtained:

$$\mathbf{R}_N^T \mathbf{R}_N = \begin{bmatrix} \mathbf{e}_1^T \\ \mathbf{e}_2^T \\ \mathbf{e}_3^T \end{bmatrix} [\mathbf{e}_1 \quad \mathbf{e}_2 \quad \mathbf{e}_3] = \begin{bmatrix} \mathbf{e}_1^T \mathbf{e}_1 & \mathbf{e}_1^T \mathbf{e}_2 & \mathbf{e}_1^T \mathbf{e}_3 \\ \mathbf{e}_2^T \mathbf{e}_1 & \mathbf{e}_2^T \mathbf{e}_2 & \mathbf{e}_2^T \mathbf{e}_3 \\ \mathbf{e}_3^T \mathbf{e}_1 & \mathbf{e}_3^T \mathbf{e}_2 & \mathbf{e}_3^T \mathbf{e}_3 \end{bmatrix} = \underbrace{\begin{bmatrix} 1 & 0 & 0 \\ 0 & 1 & 0 \\ 0 & 0 & 1 \end{bmatrix}}_{\mathbf{I}} \quad (\text{D.3.35})$$

By comparing the elements of the product $\mathbf{R}_N^T \mathbf{R}_N$ and of the identity matrix \mathbf{I} the following relation can be formulated:

$$\mathbf{S}^T \mathbf{S} = \mathbf{I} \Rightarrow \mathbf{e}_k^T \mathbf{e}_l = \mathbf{e}_k \cdot \mathbf{e}_l = \begin{cases} 1 & \text{for } k = l \\ 0 & \text{for } k \neq l \end{cases} \Rightarrow |\mathbf{e}_k| = \sqrt{\mathbf{e}_k \cdot \mathbf{e}_k} = 1 \quad (\text{D.3.36})$$

The relation (D.3.36) indicates that the column vectors \mathbf{e}_1 , \mathbf{e}_2 and \mathbf{e}_3 of the rotation matrix \mathbf{S} are orthogonal unit vectors. – It should be noted that here and in the further considerations the following two notations of the scalar product are used synonymously:

$$\mathbf{a}^T \mathbf{b} = \mathbf{a} \cdot \mathbf{b} \quad (\text{D.3.37})$$

The second property of the rotation matrix \mathbf{R}_N which has been derived in section D.3 is that the determinant $\det \mathbf{R}_N$ is equal to 1. In order to evaluate this property with respect to the column vectors \mathbf{e}_k , the determinant of a generalized 3×3 -matrix \mathbf{X} , which is composed of the three column vectors \mathbf{a} , \mathbf{b} and \mathbf{c} , shall be considered first:

$$\mathbf{a} = \begin{bmatrix} a_1 \\ a_2 \\ a_3 \end{bmatrix}, \quad \mathbf{b} = \begin{bmatrix} b_1 \\ b_2 \\ b_3 \end{bmatrix}, \quad \mathbf{c} = \begin{bmatrix} c_1 \\ c_2 \\ c_3 \end{bmatrix}, \quad \mathbf{X} = [\mathbf{a} \quad \mathbf{b} \quad \mathbf{c}] = \begin{bmatrix} a_1 & b_1 & c_1 \\ a_2 & b_2 & c_2 \\ a_3 & b_3 & c_3 \end{bmatrix} \quad (\text{D.3.38})$$

By applying the rule of Sarrus the determinant of the matrix \mathbf{X} is obtained to:

$$\det \mathbf{X} = \det \begin{bmatrix} a_1 & b_1 & c_1 \\ a_2 & b_2 & c_2 \\ a_3 & b_3 & c_3 \end{bmatrix} = a_1 b_2 c_3 + b_1 c_2 a_3 + c_1 a_2 b_3 - a_3 b_2 c_1 - b_3 c_2 a_1 - c_3 a_2 b_1 \quad (\text{D.3.39})$$

For a 3×3 -matrix the determinant can also be obtained from the triple scalar product of the column vectors:

$$\begin{aligned} \det \mathbf{X} &= \det [\mathbf{a} \ \mathbf{b} \ \mathbf{c}] = \mathbf{a} \cdot (\mathbf{b} \times \mathbf{c}) = \begin{bmatrix} a_1 \\ a_2 \\ a_3 \end{bmatrix} \cdot \left(\begin{bmatrix} b_1 \\ b_2 \\ b_3 \end{bmatrix} \times \begin{bmatrix} c_1 \\ c_2 \\ c_3 \end{bmatrix} \right) = \begin{bmatrix} a_1 \\ a_2 \\ a_3 \end{bmatrix} \cdot \begin{bmatrix} b_2 c_3 - b_3 c_2 \\ b_3 c_1 - b_1 c_3 \\ b_1 c_2 - b_2 c_1 \end{bmatrix} \\ &= a_1 (b_2 c_3 - b_3 c_2) + a_2 (b_3 c_1 - b_1 c_3) + a_3 (b_1 c_2 - b_2 c_1) \\ &= a_1 b_2 c_3 - b_3 c_2 a_1 + c_1 a_2 b_3 - c_3 a_2 b_1 + b_1 c_2 a_3 - a_3 b_2 c_1 \end{aligned} \quad (\text{D.3.40})$$

The triple scalar product remains unaffected if the vectors \mathbf{a} , \mathbf{b} and \mathbf{c} are cyclically permuted:

$$\mathbf{a} \cdot (\mathbf{b} \times \mathbf{c}) = \mathbf{b} \cdot (\mathbf{c} \times \mathbf{a}) = \mathbf{c} \cdot (\mathbf{a} \times \mathbf{b}) \quad (\text{D.3.41})$$

Based on the relations (D.3.40) and (D.3.41) a second relation between the column vectors \mathbf{e}_k can be formulated:

$$1 = \det \mathbf{R}_N = \det [\mathbf{e}_1 \ \mathbf{e}_2 \ \mathbf{e}_3] = \mathbf{e}_1 \cdot (\mathbf{e}_2 \times \mathbf{e}_3) = \mathbf{e}_2 \cdot (\mathbf{e}_3 \times \mathbf{e}_1) = \mathbf{e}_3 \cdot (\mathbf{e}_1 \times \mathbf{e}_2) \quad (\text{D.3.42})$$

For the following considerations it is advantageous to use a more generalized formulation of the condition (D.3.42); here, the triple $\langle j, k, l \rangle$ of the indices is chosen in such a way that one of the three scalar triple products given in (D.3.41) is obtained:

$$1 = \mathbf{e}_j \cdot (\mathbf{e}_k \times \mathbf{e}_l), \quad \langle j, k, l \rangle \in \{\langle 1, 2, 3 \rangle, \langle 2, 3, 1 \rangle, \langle 3, 1, 2 \rangle\} \quad (\text{D.3.43})$$

The two conditions (D.3.36) and (D.3.43) can be combined by considering the norms of the vectors in the context of the scalar product and of the vector product. As derived in the section A.5.1 the norm $|\mathbf{a} \times \mathbf{b}|$ of the vector product can be formulated in the following way:

$$|\mathbf{a} \times \mathbf{b}| = \sqrt{(\mathbf{a} \times \mathbf{b}) \cdot (\mathbf{a} \times \mathbf{b})} = \sqrt{|\mathbf{a}|^2 |\mathbf{b}|^2 - (\mathbf{a} \cdot \mathbf{b})^2} \quad (\text{D.3.44})$$

According to (D.3.36), the vectors \mathbf{e}_1 , \mathbf{e}_2 and \mathbf{e}_3 are orthogonal unit vectors. Therefore, it is valid for $k \neq l$:

$$\underbrace{|\mathbf{e}_k|^2}_1 \underbrace{|\mathbf{e}_l|^2}_1 - \underbrace{(\mathbf{e}_k \cdot \mathbf{e}_l)^2}_0 = 1 \Rightarrow |\mathbf{e}_k \times \mathbf{e}_l| = \sqrt{|\mathbf{e}_k|^2 |\mathbf{e}_l|^2 - (\mathbf{e}_k \cdot \mathbf{e}_l)^2} = 1 \quad (\text{D.3.45})$$

The result of (D.3.45) shows that the cross product of two orthogonal unit vectors is a unit vector, too. The scalar product of two vectors \mathbf{a} and \mathbf{b} of the three-dimensional, which include the angle ϕ , can be interpreted in the following way:

$$\mathbf{a} \cdot \mathbf{b} = |\mathbf{a}| |\mathbf{b}| \cos \phi \quad (\text{D.3.46})$$

By applying the relation (D.3.46) to the triple scalar product (D.3.43) and evaluating the norms based on (D.3.36) and (D.3.45), it is obtained:

$$1 = \mathbf{e}_j \cdot (\mathbf{e}_k \times \mathbf{e}_l) = \underbrace{|\mathbf{e}_j|}_1 \underbrace{|\mathbf{e}_k \times \mathbf{e}_l|}_1 \cos \phi \Rightarrow \cos \phi = 1 \Rightarrow \phi = 0 \quad (\text{D.3.47})$$

The result indicates that the angle ϕ included between the vector \mathbf{e}_j and the cross product $\mathbf{e}_k \times \mathbf{e}_l$ is zero so that the vectors \mathbf{e}_j and $\mathbf{e}_k \times \mathbf{e}_l$ have the same direction. Furthermore, the norm of both

vectors \mathbf{e}_j and $\mathbf{e}_k \times \mathbf{e}_l$ is equal to 1. If two vectors have the same direction and the same norm, they are equal so that it is valid:

$$\mathbf{e}_j = \mathbf{e}_k \times \mathbf{e}_l \quad (\text{D.3.48})$$

By applying this relation to the three triples $\langle j, k, l \rangle$ indicated in (D.3.43), it is obtained:

$$\mathbf{e}_1 = \mathbf{e}_2 \times \mathbf{e}_3 \quad (\text{D.3.49})$$

$$\mathbf{e}_2 = \mathbf{e}_3 \times \mathbf{e}_1 \quad (\text{D.3.50})$$

$$\mathbf{e}_3 = \mathbf{e}_1 \times \mathbf{e}_2 \quad (\text{D.3.51})$$

D.4 Angular velocity

As indicated in (D.0.1), the relation between the two descriptions \mathbf{r}^J and $\mathbf{r}^{\mathcal{K}}$ of the same vector in the frames J and \mathcal{K} is expressed by the rotation matrix $\mathbf{S}^{J\mathcal{K}}$:

$$\mathbf{r}^J = \mathbf{S}^{J\mathcal{K}} \mathbf{r}^{\mathcal{K}} \quad (\text{D.4.52})$$

Differentiating the equation with respect to the time leads to:

$$\dot{\mathbf{r}}^J = \dot{\mathbf{S}}^{J\mathcal{K}} \mathbf{r}^{\mathcal{K}} + \mathbf{S}^{J\mathcal{K}} \dot{\mathbf{r}}^{\mathcal{K}} \quad (\text{D.4.53})$$

As derived in the previous section D.2 a rotation matrix is an orthogonal matrix so that it is valid:

$$\mathbf{S}^{J\mathcal{K}\text{T}} = \mathbf{S}^{J\mathcal{K}-1} \Rightarrow \mathbf{S}^{J\mathcal{K}\text{T}} \mathbf{S}^{J\mathcal{K}} = \mathbf{S}^{J\mathcal{K}-1} \mathbf{S}^{J\mathcal{K}} = \mathbf{I} \quad (\text{D.4.54})$$

Based on this property, the first term on the right hand side of (D.4.53) can be reformulated in the following way:

$$\dot{\mathbf{S}}^{J\mathcal{K}} \mathbf{r}^{\mathcal{K}} = \dot{\mathbf{S}}^{J\mathcal{K}} \underbrace{\mathbf{S}^{J\mathcal{K}\text{T}} \mathbf{S}^{J\mathcal{K}}}_{\mathbf{I}} \mathbf{r}^{\mathcal{K}} = \underbrace{\dot{\mathbf{S}}^{J\mathcal{K}} \mathbf{S}^{J\mathcal{K}\text{T}}}_{\tilde{\boldsymbol{\omega}}_{J\mathcal{K}}^J} \underbrace{\mathbf{S}^{J\mathcal{K}} \mathbf{r}^{\mathcal{K}}}_{\mathbf{r}^J} = \tilde{\boldsymbol{\omega}}_{J\mathcal{K}}^J \mathbf{r}^J \quad (\text{D.4.55})$$

The product $\dot{\mathbf{S}}^{J\mathcal{K}} \mathbf{S}^{J\mathcal{K}\text{T}}$ can be interpreted as the angular velocity $\tilde{\boldsymbol{\omega}}_{J\mathcal{K}}^J$, which describes the rotation of the frame \mathcal{K} relative to the frame J ; therefore, this product shall be evaluated in the following. It will turn out that in this context the formulation using column vectors is rather useful. Therefore and for the sake of brevity and of a better overview, the matrix $\mathbf{S}^{J\mathcal{K}}$ will be expressed as a composed rotation matrix \mathbf{R}_N , which is described by its column vectors \mathbf{e}_k :

$$\mathbf{S}^{J\mathcal{K}} = \mathbf{R}_N = [\mathbf{e}_1 \quad \mathbf{e}_2 \quad \mathbf{e}_3] \quad (\text{D.4.56})$$

In order to evaluate the angular velocity $\tilde{\boldsymbol{\omega}}_{J\mathcal{K}}^J$, the product $\dot{\mathbf{R}}_N \mathbf{R}_N^{\text{T}}$ is considered. It is valid:

$$\tilde{\boldsymbol{\omega}}_{J\mathcal{K}}^J = \dot{\mathbf{R}}_N \mathbf{R}_N^{\text{T}} = [\dot{\mathbf{e}}_1 \quad \dot{\mathbf{e}}_2 \quad \dot{\mathbf{e}}_3] \begin{bmatrix} \mathbf{e}_1^{\text{T}} \\ \mathbf{e}_2^{\text{T}} \\ \mathbf{e}_3^{\text{T}} \end{bmatrix} \quad (\text{D.4.57})$$

The formulation according to (D.4.57) requires the evaluation of dyadic products $\dot{\mathbf{e}}_k \mathbf{e}_l^{\text{T}}$, which is rather inconvenient. From the orthogonality of the rotation matrix \mathbf{R}_N it can be derived:

$$\mathbf{R}_N^{\text{T}} = \mathbf{R}_N^{-1} \Rightarrow \mathbf{R}_N \mathbf{R}_N^{\text{T}} = \mathbf{R}_N \mathbf{R}_N^{-1} = \mathbf{I} \quad (\text{D.4.58})$$

Using this relation the product $\dot{\mathbf{R}}_N \mathbf{R}_N^T$ is reformulated in the following way:

$$\dot{\mathbf{R}}_N \mathbf{R}_N^T = \underbrace{\mathbf{R}_N \mathbf{R}_N^T}_{\mathbf{I}} \dot{\mathbf{R}}_N \mathbf{R}_N^T = \mathbf{R}_N \begin{bmatrix} \mathbf{e}_1^T \\ \mathbf{e}_2^T \\ \mathbf{e}_3^T \end{bmatrix} [\dot{\mathbf{e}}_1 \quad \dot{\mathbf{e}}_2 \quad \dot{\mathbf{e}}_3] \mathbf{R}_N^T = \mathbf{R}_N \underbrace{\begin{bmatrix} \mathbf{e}_1^T \dot{\mathbf{e}}_1 & \mathbf{e}_1^T \dot{\mathbf{e}}_2 & \mathbf{e}_1^T \dot{\mathbf{e}}_3 \\ \mathbf{e}_2^T \dot{\mathbf{e}}_1 & \mathbf{e}_2^T \dot{\mathbf{e}}_2 & \mathbf{e}_2^T \dot{\mathbf{e}}_3 \\ \mathbf{e}_3^T \dot{\mathbf{e}}_1 & \mathbf{e}_3^T \dot{\mathbf{e}}_2 & \mathbf{e}_3^T \dot{\mathbf{e}}_3 \end{bmatrix}}_{\mathbf{R}_N^T \dot{\mathbf{R}}_N} \mathbf{R}_N^T \quad (\text{D.4.59})$$

As derived in section (D.3) it is valid for the column vectors \mathbf{e}_1 , \mathbf{e}_2 and \mathbf{e}_3 :

$$\mathbf{e}_k^T \mathbf{e}_l = \mathbf{e}_k \cdot \mathbf{e}_l = \begin{cases} 1 & \text{for } k = l \\ 0 & \text{for } k \neq l \end{cases} \quad (\text{D.4.60})$$

For $k \neq l$ the differentiation of the scalar product $\mathbf{e}_k \cdot \mathbf{e}_l$ and the application of the commutativity of the scalar product leads to:

$$\mathbf{e}_k \cdot \mathbf{e}_l = 0 \Rightarrow 0 = \frac{d}{dt} (\mathbf{e}_k \cdot \mathbf{e}_l) = \dot{\mathbf{e}}_k \cdot \mathbf{e}_l + \mathbf{e}_k \cdot \dot{\mathbf{e}}_l \Rightarrow \mathbf{e}_k \cdot \dot{\mathbf{e}}_l = -\dot{\mathbf{e}}_k \cdot \mathbf{e}_l = -\mathbf{e}_l \cdot \dot{\mathbf{e}}_k \quad (\text{D.4.61})$$

For $k = l$ it is obtained:

$$\mathbf{e}_k \cdot \mathbf{e}_k = 1 \Rightarrow 0 = \frac{d}{dt} (\mathbf{e}_k \cdot \mathbf{e}_k) = \dot{\mathbf{e}}_k \cdot \mathbf{e}_k + \mathbf{e}_k \cdot \dot{\mathbf{e}}_k = 2 \mathbf{e}_k \cdot \dot{\mathbf{e}}_k \Rightarrow \mathbf{e}_k \cdot \dot{\mathbf{e}}_k = 0 \quad (\text{D.4.62})$$

Thereby, it is valid for the product $\dot{\mathbf{R}}_N \mathbf{R}_N^T$:

$$\dot{\mathbf{R}}_N \mathbf{R}_N^T = \mathbf{R}_N \underbrace{\begin{bmatrix} \mathbf{e}_1 \cdot \dot{\mathbf{e}}_1 & \mathbf{e}_1 \cdot \dot{\mathbf{e}}_2 & \mathbf{e}_1 \cdot \dot{\mathbf{e}}_3 \\ \mathbf{e}_2 \cdot \dot{\mathbf{e}}_1 & \mathbf{e}_2 \cdot \dot{\mathbf{e}}_2 & \mathbf{e}_2 \cdot \dot{\mathbf{e}}_3 \\ \mathbf{e}_3 \cdot \dot{\mathbf{e}}_1 & \mathbf{e}_3 \cdot \dot{\mathbf{e}}_2 & \mathbf{e}_3 \cdot \dot{\mathbf{e}}_3 \end{bmatrix}}_{\mathbf{R}_N^T \dot{\mathbf{R}}_N} \mathbf{R}_N^T = \mathbf{R}_N \underbrace{\begin{bmatrix} 0 & -\mathbf{e}_2 \cdot \dot{\mathbf{e}}_1 & \mathbf{e}_1 \cdot \dot{\mathbf{e}}_3 \\ \mathbf{e}_2 \cdot \dot{\mathbf{e}}_1 & 0 & -\mathbf{e}_3 \cdot \dot{\mathbf{e}}_2 \\ -\mathbf{e}_1 \cdot \dot{\mathbf{e}}_3 & \mathbf{e}_3 \cdot \dot{\mathbf{e}}_2 & 0 \end{bmatrix}}_{\mathbf{R}_N^T \dot{\mathbf{R}}_N} \mathbf{R}_N^T \quad (\text{D.4.63})$$

It is evident that the product $\mathbf{R}_N^T \dot{\mathbf{R}}_N$ is a skew-symmetric matrix:

$$\mathbf{R}_N^T \dot{\mathbf{R}}_N = -(\mathbf{R}_N^T \dot{\mathbf{R}}_N)^T \quad (\text{D.4.64})$$

From this it follows that also the product $\dot{\mathbf{R}}_N \mathbf{R}_N^T$ is skew-symmetric:

$$(\dot{\mathbf{R}}_N \mathbf{R}_N^T)^T = (\mathbf{R}_N (\mathbf{R}_N^T \dot{\mathbf{R}}_N) \mathbf{R}_N^T)^T = \mathbf{R}_N^T{}^T (\mathbf{R}_N^T \dot{\mathbf{R}}_N)^T \mathbf{R}_N^T = -\mathbf{R}_N (\mathbf{R}_N^T \dot{\mathbf{R}}_N) \mathbf{R}_N^T \quad (\text{D.4.65})$$

The skew-symmetric matrix $\mathbf{R}_N^T \dot{\mathbf{R}}_N$ can be interpreted as a tilde matrix. The tilde matrix $\tilde{\mathbf{x}}$ is derived from the vector \mathbf{y} in the following way, which provides a formulation of the cross product using a matrix multiplication:

$$\mathbf{x} \times \mathbf{y} = \underbrace{\begin{bmatrix} x_1 \\ x_2 \\ x_3 \end{bmatrix}}_{\mathbf{a}} \times \underbrace{\begin{bmatrix} y_1 \\ y_2 \\ y_3 \end{bmatrix}}_{\mathbf{b}} = \begin{bmatrix} x_2 y_3 - x_3 y_2 \\ x_3 y_1 - x_1 y_3 \\ x_1 y_2 - x_2 y_1 \end{bmatrix} = \underbrace{\begin{bmatrix} 0 & -x_3 & x_2 \\ x_3 & 0 & -x_1 \\ -x_2 & x_1 & 0 \end{bmatrix}}_{\tilde{\mathbf{x}}} \underbrace{\begin{bmatrix} y_1 \\ y_2 \\ y_3 \end{bmatrix}}_{\mathbf{y}} = \tilde{\mathbf{x}} \mathbf{y} \quad (\text{D.4.66})$$

In order to interpret the result (D.4.59), the expression $\mathbf{R}_N \tilde{\mathbf{w}} \mathbf{R}_N^T \mathbf{v}$ shall be considered; here, the skew-symmetric product $\mathbf{R}_N^T \dot{\mathbf{R}}_N$ is replaced by the generalized tilde matrix $\tilde{\mathbf{w}}$. It is obtained:

$$\begin{aligned}
\mathbf{R}_N \tilde{\mathbf{w}} \mathbf{R}_N^T \mathbf{v} &= [\mathbf{e}_1 \ \mathbf{e}_2 \ \mathbf{e}_3] \begin{bmatrix} 0 & -w_3 & w_2 \\ w_3 & 0 & -w_1 \\ -w_2 & w_3 & 0 \end{bmatrix} \begin{bmatrix} \mathbf{e}_1^T \\ \mathbf{e}_2^T \\ \mathbf{e}_3^T \end{bmatrix} \mathbf{v} \\
&= [\mathbf{e}_1 \ \mathbf{e}_2 \ \mathbf{e}_3] \begin{bmatrix} 0 & -w_3 & w_2 \\ w_3 & 0 & -w_1 \\ -w_2 & w_1 & 0 \end{bmatrix} \begin{bmatrix} \mathbf{e}_1^T \mathbf{v} \\ \mathbf{e}_2^T \mathbf{v} \\ \mathbf{e}_3^T \mathbf{v} \end{bmatrix} = [\mathbf{e}_1 \ \mathbf{e}_2 \ \mathbf{e}_3] \begin{bmatrix} -w_3 \mathbf{e}_2^T \mathbf{v} + w_2 \mathbf{e}_3^T \mathbf{v} \\ w_3 \mathbf{e}_1^T \mathbf{v} - w_1 \mathbf{e}_3^T \mathbf{v} \\ -w_2 \mathbf{e}_1^T \mathbf{v} + w_1 \mathbf{e}_2^T \mathbf{v} \end{bmatrix} \\
&= (w_2 \mathbf{e}_3 \cdot \mathbf{v} - w_3 \mathbf{e}_2 \cdot \mathbf{v}) \mathbf{e}_1 + (w_3 \mathbf{e}_1 \cdot \mathbf{v} - w_1 \mathbf{e}_3 \cdot \mathbf{v}) \mathbf{e}_2 + (w_1 \mathbf{e}_2 \cdot \mathbf{v} - w_2 \mathbf{e}_1 \cdot \mathbf{v}) \mathbf{e}_3 \\
&= w_1 [(\mathbf{v} \cdot \mathbf{e}_2) \mathbf{e}_3 - (\mathbf{v} \cdot \mathbf{e}_3) \mathbf{e}_2] + w_2 [(\mathbf{v} \cdot \mathbf{e}_3) \mathbf{e}_1 - (\mathbf{v} \cdot \mathbf{e}_1) \mathbf{e}_3] + w_3 [(\mathbf{v} \cdot \mathbf{e}_1) \mathbf{e}_2 - (\mathbf{v} \cdot \mathbf{e}_2) \mathbf{e}_1]
\end{aligned} \tag{D.4.67}$$

The content of the brackets can be reformulated by using the triple vector product:

$$\mathbf{a} \times (\mathbf{b} \times \mathbf{c}) = (\mathbf{a} \cdot \mathbf{c}) \mathbf{b} - (\mathbf{a} \cdot \mathbf{b}) \mathbf{c} \tag{D.4.68}$$

Applying this relation and the anticommutativity of the cross product

$$\mathbf{a} \times \mathbf{b} = -\mathbf{b} \times \mathbf{a} \tag{D.4.69}$$

leads to:

$$\begin{aligned}
\mathbf{R}_N \tilde{\mathbf{w}} \mathbf{R}_N^T \mathbf{v} &= w_1 [(\mathbf{v} \cdot \mathbf{e}_2) \mathbf{e}_3 - (\mathbf{v} \cdot \mathbf{e}_3) \mathbf{e}_2] + w_2 [(\mathbf{v} \cdot \mathbf{e}_3) \mathbf{e}_1 - (\mathbf{v} \cdot \mathbf{e}_1) \mathbf{e}_3] + w_3 [(\mathbf{v} \cdot \mathbf{e}_1) \mathbf{e}_2 - (\mathbf{v} \cdot \mathbf{e}_2) \mathbf{e}_1] \\
&= w_1 \mathbf{v} \times (\mathbf{e}_3 \times \mathbf{e}_2) + w_2 \mathbf{v} \times (\mathbf{e}_1 \times \mathbf{e}_3) + w_3 \mathbf{v} \times (\mathbf{e}_2 \times \mathbf{e}_1) \\
&= -w_1 (\mathbf{e}_3 \times \mathbf{e}_2) \times \mathbf{v} - w_2 (\mathbf{e}_1 \times \mathbf{e}_3) \times \mathbf{v} - w_3 (\mathbf{e}_2 \times \mathbf{e}_1) \times \mathbf{v} \\
&= w_1 (\mathbf{e}_2 \times \mathbf{e}_3) \times \mathbf{v} + w_2 (\mathbf{e}_3 \times \mathbf{e}_1) \times \mathbf{v} + w_3 (\mathbf{e}_1 \times \mathbf{e}_2) \times \mathbf{v}
\end{aligned} \tag{D.4.70}$$

In section D.3 the following relations between the column vectors \mathbf{e}_1 , \mathbf{e}_2 and \mathbf{e}_3 has been derived:

$$\mathbf{e}_1 = \mathbf{e}_2 \times \mathbf{e}_3, \ \mathbf{e}_2 = \mathbf{e}_3 \times \mathbf{e}_1, \ \mathbf{e}_3 = \mathbf{e}_1 \times \mathbf{e}_2 \tag{D.4.71}$$

Based on this, it is finally obtained:

$$\begin{aligned}
\mathbf{R}_N \tilde{\mathbf{w}} \mathbf{R}_N^T \mathbf{v} &= w_1 (\mathbf{e}_2 \times \mathbf{e}_3) \times \mathbf{v} + w_2 (\mathbf{e}_3 \times \mathbf{e}_1) \times \mathbf{v} + w_3 (\mathbf{e}_1 \times \mathbf{e}_2) \times \mathbf{v} \\
&= w_1 \mathbf{e}_1 \times \mathbf{v} + w_2 \mathbf{e}_2 \times \mathbf{v} + w_3 \mathbf{e}_3 \times \mathbf{v}
\end{aligned} \tag{D.4.72}$$

The evaluation of cross product of the product $\mathbf{R}_N \mathbf{w}$ and the vector \mathbf{v} leads to:

$$\begin{aligned}
(\mathbf{R}_N \mathbf{w}) \times \mathbf{v} &= \left([\mathbf{e}_1 \ \mathbf{e}_2 \ \mathbf{e}_3] \begin{bmatrix} w_1 \\ w_2 \\ w_3 \end{bmatrix} \right) \times \mathbf{v} = (w_1 \mathbf{e}_1 + w_2 \mathbf{e}_2 + w_3 \mathbf{e}_3) \times \mathbf{v} \\
&= w_1 \mathbf{e}_1 \times \mathbf{v} + w_2 \mathbf{e}_2 \times \mathbf{v} + w_3 \mathbf{e}_3 \times \mathbf{v} = \mathbf{R}_N \tilde{\mathbf{w}} \mathbf{R}_N^T \mathbf{v}
\end{aligned} \tag{D.4.73}$$

From this it follows that the matrix $\mathbf{R}_N \tilde{\mathbf{w}} \mathbf{R}_N^T$ is the tilde matrix of the vector $\mathbf{R}_N \mathbf{w}$. By setting $\tilde{\mathbf{w}} = \mathbf{R}_N^T \dot{\mathbf{R}}_N$ the corresponding vector \mathbf{w} is determined:

$$\tilde{\mathbf{w}} = \mathbf{R}_N^T \dot{\mathbf{R}}_N = \begin{bmatrix} 0 & -\mathbf{e}_2 \cdot \dot{\mathbf{e}}_1 & \mathbf{e}_1 \cdot \dot{\mathbf{e}}_3 \\ \mathbf{e}_2 \cdot \dot{\mathbf{e}}_1 & 0 & -\mathbf{e}_3 \cdot \dot{\mathbf{e}}_2 \\ -\mathbf{e}_1 \cdot \dot{\mathbf{e}}_3 & \mathbf{e}_3 \cdot \dot{\mathbf{e}}_2 & 0 \end{bmatrix} \Rightarrow \mathbf{w} = \begin{bmatrix} \mathbf{e}_3 \cdot \dot{\mathbf{e}}_2 \\ \mathbf{e}_1 \cdot \dot{\mathbf{e}}_3 \\ \mathbf{e}_2 \cdot \dot{\mathbf{e}}_1 \end{bmatrix} \tag{D.4.74}$$

Thereby, the tilde matrix $\tilde{\omega}_{j\mathcal{K}}^j$ of the angular velocity of the frame \mathcal{K} relative to the frame j can be formulated using the column vectors of the rotation matrix $\mathbf{S}^{\mathcal{R}\mathcal{S}} = \mathbf{R}_N$:

$$\tilde{\omega}_{j\mathcal{K}}^j = \dot{\mathbf{R}}_N \mathbf{R}_N^T = \mathbf{R}_N \underbrace{\begin{bmatrix} 0 & -\mathbf{e}_2 \cdot \dot{\mathbf{e}}_1 & \mathbf{e}_1 \cdot \dot{\mathbf{e}}_3 \\ \mathbf{e}_2 \cdot \dot{\mathbf{e}}_1 & 0 & -\mathbf{e}_3 \cdot \dot{\mathbf{e}}_2 \\ -\mathbf{e}_1 \cdot \dot{\mathbf{e}}_3 & \mathbf{e}_3 \cdot \dot{\mathbf{e}}_2 & 0 \end{bmatrix}}_{\tilde{\mathbf{w}}} \mathbf{R}_N^T \quad (\text{D.4.75})$$

Based on the relation (D.4.73) the vector of the angular velocity $\omega_{j\mathcal{K}}^j$ is finally obtained:

$$\omega_{j\mathcal{K}}^j = \mathbf{R}_N \underbrace{\begin{bmatrix} \mathbf{e}_3 \cdot \dot{\mathbf{e}}_2 \\ \mathbf{e}_1 \cdot \dot{\mathbf{e}}_3 \\ \mathbf{e}_2 \cdot \dot{\mathbf{e}}_1 \end{bmatrix}}_{\mathbf{w}} = (\mathbf{e}_3 \cdot \dot{\mathbf{e}}_2) \mathbf{e}_1 + (\mathbf{e}_1 \cdot \dot{\mathbf{e}}_3) \mathbf{e}_2 + (\mathbf{e}_2 \cdot \dot{\mathbf{e}}_1) \mathbf{e}_3 \quad (\text{D.4.76})$$

Appendix E

Compliance coefficients

In section 7.4, the following expressions were determined for the compliance coefficients:

$$H_{ik}^{[IK]} = \int_A H_{IK}(x_i - x, y_i - y) f_k(x, y) dA \quad (\text{E.0.1})$$

In this chapter, the integral will be evaluated.

The local shape function $f_k(x, y)$ is given by:

$$f_k = \begin{cases} \left(1 - \frac{|x-x_k|}{\Delta a}\right) \left(1 - \frac{|y-y_k|}{\Delta a}\right) & \text{for } |x-x_k| \leq \Delta a \wedge |y-y_k| \leq \Delta a \\ 0 & \text{for } |x-x_k| > \Delta a \vee |y-y_k| > \Delta a \end{cases} \quad (\text{E.0.2})$$

Here, $\Delta a > 0$ is the grid constant; it is a strictly positive number. From the definition of the function $f_k(x, y)$ according to (E.0.2) it is derived:

$$|x-x_k| \leq \Delta a \Rightarrow \frac{|x-x_k|}{\Delta a} \leq 1 \Rightarrow -\frac{|x-x_k|}{\Delta a} \geq -1 \Rightarrow 1 - \frac{|x-x_k|}{\Delta a} \geq 0 \quad (\text{E.0.3})$$

$$|y-y_k| \leq \Delta a \Rightarrow \frac{|y-y_k|}{\Delta a} \leq 1 \Rightarrow -\frac{|y-y_k|}{\Delta a} \geq -1 \Rightarrow 1 - \frac{|y-y_k|}{\Delta a} \geq 0 \quad (\text{E.0.4})$$

$$\Rightarrow f_k(x, y) = \underbrace{\left(1 - \frac{|x-x_k|}{\Delta a}\right)}_{\geq 0} \underbrace{\left(1 - \frac{|y-y_k|}{\Delta a}\right)}_{\geq 0} \geq 0 \text{ for } |x-x_k| \leq \Delta a \wedge |y-y_k| \leq \Delta a \quad (\text{E.0.5})$$

From this it follows that the function $f_k(x, y)$ is non-negative for the following domain D_k :

$$D_k = \{(x, y) \in \mathbb{R}^2 \mid |x-x_k| \leq \Delta a, |y-y_k| \leq \Delta a\} \quad (\text{E.0.6})$$

By reformulating the conditions for x and y it is obtained:

$$\begin{aligned} x-x_k \geq 0 &\Leftrightarrow x \geq x_k : |x-x_k| = x-x_k \leq \Delta a \Rightarrow x_k \leq x \leq x_k + \Delta a \\ x-x_k < 0 &\Leftrightarrow x < x_k : |x-x_k| = -(x-x_k) = -x+x_k \leq \Delta a \Rightarrow x_k - \Delta a \leq x < x_k \\ &\Rightarrow x_k - \Delta a \leq x \leq x_k + \Delta a \end{aligned} \quad (\text{E.0.7})$$

$$\begin{aligned} y-y_k \geq 0 &\Leftrightarrow y \geq y_k : |y-y_k| = y-y_k \leq \Delta a \Rightarrow y_k \leq y \leq y_k + \Delta a \\ y-y_k < 0 &\Leftrightarrow y < y_k : |y-y_k| = -(y-y_k) = -y+y_k \leq \Delta a \Rightarrow y_k - \Delta a \leq y < y_k \\ &\Rightarrow y_k - \Delta a \leq y \leq y_k + \Delta a \end{aligned} \quad (\text{E.0.8})$$

$$\Rightarrow D_k = \{(x, y) \in \mathbb{R}^2 \mid x_k - \Delta a \leq x \leq x_k + \Delta a, y_k - \Delta a \leq y \leq y_k + \Delta a\} \quad (\text{E.0.9})$$

Outside the domain D_k , i.e. in the complement $A \setminus D_k$ of the domain D_k in A , the function $f_k(x, y)$ vanishes. Therefore, it is valid:

$$\begin{aligned} H_{i|k}^{[IK]} &= \int_A H_{IK}(x_i - x, y_i - y) f_k(x, y) dA \\ &= \int_{D_k} H_{IK}(x_i - x, y_i - y) f_k(x, y) dA + \underbrace{\int_{A \setminus D_k} H_{IK}(x_i - x, y_i - y) \overbrace{f_k(x, y)}^{=0} dA}_{=0} \end{aligned} \quad (\text{E.0.10})$$

In order to obtain the integral over the complete surface A , it is sufficient to carry out the integration just for the domain D_k .

Since the function $f_k(x, y)$ contains the absolute values $|x - x_k|$ and $|y - y_k|$, the integrals have to be evaluated piecewise. To this end, the coefficients c_x and c_y , which are piecewise constant, are introduced. Using these coefficients, the absolute values are reformulated in the following way:

$$|x - x_k| = c_x (x - x_k) \quad (\text{E.0.11})$$

$$x - x_k \geq 0 \Leftrightarrow x \geq x_k : |x - x_k| = x - x_k \Rightarrow c_x = 1 \quad (\text{E.0.12})$$

$$x - x_k < 0 \Leftrightarrow x < x_k : |x - x_k| = -(x - x_k) \Rightarrow c_x = -1 \quad (\text{E.0.13})$$

$$|y - y_k| = c_y (y - y_k) \quad (\text{E.0.14})$$

$$y - y_k \geq 0 \Leftrightarrow y \geq y_k : |y - y_k| = y - y_k \Rightarrow c_y = 1 \quad (\text{E.0.15})$$

$$y - y_k < 0 \Leftrightarrow y < y_k : |y - y_k| = -(y - y_k) \Rightarrow c_y = -1 \quad (\text{E.0.16})$$

The domain D_k according to (E.0.7), in which the function f_k doesn't vanish, is divided into four subdomains $D_{k,1}$, $D_{k,2}$, $D_{k,3}$ and $D_{k,4}$. Within each subdomain, the coefficients c_x and c_y are constant. It should be noted that for $x = x_k \Leftrightarrow x - x_k = 0$ the value c_x can be chosen arbitrarily; in an analogous way, an arbitrary value for c_y can be used for $y = y_k \Leftrightarrow y - y_k = 0$. Thus, the subdomains can be defined in such a way that the limits $x = x_k$ and $y = y_k$ belong to both adjacent subdomains. Thereby, c_x and c_y are not functions of x and y in the strict sense. However, this definition spares the discussion using limits of the functions. In total, it is valid:

	$x_k - \Delta a \leq x \leq x_k$	$x_k \leq x \leq x_k + \Delta a$
$y_k \leq y \leq y_k + \Delta a$	Subdomain $D_{k,2}$ $c_x = -1, c_y = 1$	Subdomain $D_{k,1}$ $c_x = 1, c_y = 1$
$y_k - \Delta a \leq y \leq y_k$	Subdomain $D_{k,3}$ $c_x = -1, c_y = -1$	Subdomain $D_{k,4}$ $c_x = 1, c_y = -1$

Based on this consideration, the function f_k is reformulated in the following way:

$$\begin{aligned} &x_k - \Delta a \leq x \leq x_k + \Delta a \wedge y_k - \Delta a \leq y \leq y_k + \Delta a : \\ &f_k = \left(1 - \frac{|x - x_k|}{\Delta a}\right) \left(1 - \frac{|y - y_k|}{\Delta a}\right) = \left(1 - \frac{c_x (x - x_k)}{\Delta a}\right) \left(1 - \frac{c_y (y - y_k)}{\Delta a}\right) \end{aligned} \quad (\text{E.0.17})$$

Since the function $f_k(x, y)$ vanishes outside the four subdomains $D_{k,1}$, $D_{k,2}$, $D_{k,3}$ and $D_{k,4}$, the

integrals over the surface A can be expressed in the following way:

$$\begin{aligned}
 H_{ik}^{[IK]} &= \int_A H_{IK}(x_i - x, y_i - y) f_k(x, y) dA \\
 &= \int_{D_k} H_{IK}(x_i - x, y_i - y) f_k(x, y) dA \\
 &= \sum_{n=1}^4 \int_{D_{k,n}} H_{IK}(x_i - x, y_i - y) f_k(x, y) dA
 \end{aligned} \tag{E.0.18}$$

The influence functions $H_{IK}(x_i - x, y_i - y)$ are given by:

$$H_{11}(x_i - x, y_i - y) = \frac{1}{\pi G} \left[\frac{1 - \nu}{[(x_i - x)^2 + (y_i - y)^2]^{1/2}} + \frac{\nu (x_i - x)^2}{[(x_i - x)^2 + (y_i - y)^2]^{3/2}} \right] \tag{E.0.19}$$

$$H_{22}(x_i - x, y_i - y) = \frac{1}{\pi G} \left[\frac{1 - \nu}{[(x_i - x)^2 + (y_i - y)^2]^{1/2}} + \frac{\nu (y_i - y)^2}{[(x_i - x)^2 + (y_i - y)^2]^{3/2}} \right] \tag{E.0.20}$$

$$H_{33}(x_i - x, y_i - y) = \frac{1}{\pi G} \frac{1 - \nu}{[(x_i - x)^2 + (y_i - y)^2]^{1/2}} \tag{E.0.21}$$

$$H_{12}(x_i - x, y_i - y) = \frac{\nu}{\pi G} \frac{(x_i - x)(y_i - y)}{[(x_i - x)^2 + (y_i - y)^2]^{3/2}} \tag{E.0.22}$$

Inserting the influence functions into the integrals and splitting the integrals leads to:

$$\begin{aligned}
 H_{ik}^{[33]} &= \int_A H_{33}(x_i - x, y_i - y) f_k(x, y) dA = \int_A \frac{1}{\pi G} \frac{1 - \nu}{[(x_i - x)^2 + (y_i - y)^2]^{1/2}} f_k(x, y) dA \\
 &= \sum_{n=1}^4 \frac{1 - \nu}{\pi G} \int_{D_{k,n}} \frac{f_k(x, y)}{[(x_i - x)^2 + (y_i - y)^2]^{1/2}} dA = \sum_{n=1}^4 \frac{1 - \nu}{\pi G} h_{ik,n}^{[33]}
 \end{aligned} \tag{E.0.23}$$

$$\begin{aligned}
 H_{ik}^{[11]} &= \int_A H_{11}(x_i - x, y_i - y) f_k(x, y) dA \\
 &= \int_A \frac{1}{\pi G} \left[\frac{1 - \nu}{[(x_i - x)^2 + (y_i - y)^2]^{1/2}} + \frac{\nu (x_i - x)^2}{[(x_i - x)^2 + (y_i - y)^2]^{3/2}} \right] f_k(x, y) dA \\
 &= \sum_{n=1}^4 \left[\frac{1 - \nu}{\pi G} \int_{D_{k,n}} \frac{f_k(x, y)}{[(x_i - x)^2 + (y_i - y)^2]^{1/2}} dA + \frac{\nu}{\pi G} \int_{D_{k,n}} \frac{(x_i - x)^2 f_k(x, y)}{[(x_i - x)^2 + (y_i - y)^2]^{3/2}} dA \right] \\
 &= \sum_{n=1}^4 \left[\frac{1 - \nu}{\pi G} h_{ik,n}^{[33]} + \frac{\nu}{\pi G} h_{ik,n}^{[11]} \right]
 \end{aligned} \tag{E.0.24}$$

$$\begin{aligned}
 H_{ik}^{[22]} &= \int_A H_{22}(x_i - x, y_i - y) f_k(x, y) dA \\
 &= \int_A \frac{1}{\pi G} \left[\frac{1 - \nu}{[(x_i - x)^2 + (y_i - y)^2]^{1/2}} + \frac{\nu (y_i - y)^2}{[(x_i - x)^2 + (y_i - y)^2]^{3/2}} \right] f_k(x, y) dA \\
 &= \sum_{n=1}^4 \left[\frac{1 - \nu}{\pi G} \int_{D_{k,n}} \frac{f_k(x, y)}{[(x_i - x)^2 + (y_i - y)^2]^{1/2}} dA + \frac{\nu}{\pi G} \int_{D_{k,n}} \frac{(y_i - y)^2 f_k(x, y)}{[(x_i - x)^2 + (y_i - y)^2]^{3/2}} dA \right] \\
 &= \sum_{n=1}^4 \left[\frac{1 - \nu}{\pi G} h_{ik,n}^{[33]} + \frac{\nu}{\pi G} h_{ik,n}^{[22]} \right]
 \end{aligned} \tag{E.0.25}$$

$$\begin{aligned}
H_{ik}^{[12]} &= \int_A H_{12}(x_i - x, y_i - y) f_k(x, y) dA = \int_A \frac{\nu}{\pi G} \frac{(x_i - x)(y_i - y)}{[(x_i - x)^2 + (y_i - y)^2]^{3/2}} f_k(x, y) dA \\
&= \sum_{n=1}^4 \frac{\nu}{\pi G} \int_{D_{k,n}} \frac{(x_i - x)(y_i - y) f_k(x, y)}{[(x_i - x)^2 + (y_i - y)^2]^{3/2}} dA = \sum_{n=1}^4 \frac{\nu}{\pi G} h_{ik,n}^{[12]}
\end{aligned} \tag{E.0.26}$$

In total the coefficients $H_{ik}^{[K]}$ contain the following four basic integrals:

$$h_{ik,n}^{[33]} = \int_{D_{k,n}} \frac{f_k(x, y)}{[(x_i - x)^2 + (y_i - y)^2]^{1/2}} dA \tag{E.0.27}$$

$$h_{ik,n}^{[11]} = \int_{D_{k,n}} \frac{(x_i - x)^2 f_k(x, y)}{[(x_i - x)^2 + (y_i - y)^2]^{3/2}} dA \tag{E.0.28}$$

$$h_{ik,n}^{[22]} = \int_{D_{k,n}} \frac{(y_i - y)^2 f_k(x, y)}{[(x_i - x)^2 + (y_i - y)^2]^{3/2}} dA \tag{E.0.29}$$

$$h_{ik,n}^{[12]} = \int_{D_{k,n}} \frac{(x_i - x)(y_i - y) f_k(x, y)}{[(x_i - x)^2 + (y_i - y)^2]^{3/2}} dA \tag{E.0.30}$$

It can be seen that for $x = x_i \wedge y = y_i$ a singularity occurs; this requires a special treatment of the integrals. – For the integrals $h_{ik,n}^{[11]}$ and $h_{ik,n}^{[22]}$ it is valid:

$$\begin{aligned}
h_{ik,n}^{[11]} + h_{ik,n}^{[22]} &= \int_{D_{k,n}} \frac{(x_i - x)^2 f_k(x, y)}{[(x_i - x)^2 + (y_i - y)^2]^{3/2}} dA + \int_{D_{k,n}} \frac{(y_i - y)^2 f_k(x, y)}{[(x_i - x)^2 + (y_i - y)^2]^{3/2}} dA \\
&= \int_{D_{k,n}} \left[\frac{(x_i - x)^2 f_k(x, y)}{[(x_i - x)^2 + (y_i - y)^2]^{3/2}} + \frac{(y_i - y)^2 f_k(x, y)}{[(x_i - x)^2 + (y_i - y)^2]^{3/2}} \right] dA \\
&= \int_{D_{k,n}} \frac{(x_i - x)^2 f_k(x, y) + (y_i - y)^2 f_k(x, y)}{[(x_i - x)^2 + (y_i - y)^2]^{3/2}} dA \\
&= \int_{D_{k,n}} \frac{[(x_i - x)^2 + (y_i - y)^2] f_k(x, y)}{[(x_i - x)^2 + (y_i - y)^2]^{3/2}} dA \\
&= \int_{D_{k,n}} \frac{f_k(x, y)}{[(x_i - x)^2 + (y_i - y)^2]^{1/2}} dA = h_{ik,n}^{[33]}
\end{aligned} \tag{E.0.31}$$

It will turn out that in some cases the evaluation of the integral $h_{ik,n}^{[11]}$ is simpler, while in other cases the evaluation of the integral $h_{ik,n}^{[22]}$ requires less effort. Therefore, the integral, for which the evaluation is simpler, is determined and the other integral is obtained by using the relation between $h_{ik,n}^{[11]}$ and $h_{ik,n}^{[22]}$

In the following sections the coefficients will be determined.

E.1 Local coordinates

In the first step the global cartesian coordinates x and y are expressed by the normalized local cartesian coordinates ξ and η . The origin of the local coordinates is the point $\langle x_i, y_i \rangle$, for which the

deformation $\mathbf{u}_i = \mathbf{u}(x_i, y_i)$ is determined. Furthermore the coordinates are normalized with the grid constant $\Delta a > 0$. Thereby, the original coordinates x and y are formulated in the following way:

$$x = x_i + \xi \Delta a \Rightarrow x - x_i = \xi \Delta a \quad (\text{E.1.32})$$

$$y = y_i + \eta \Delta a \Rightarrow y - y_i = \eta \Delta a \quad (\text{E.1.33})$$

In the second step, the local cartesian coordinates ξ and η are expressed by the polar coordinates r and ϕ in the following way:

$$\xi = r \cos \phi, \quad \eta = r \sin \phi, \quad r \geq 0 \quad (\text{E.1.34})$$

In total it is valid:

$$x = x_i + \xi \Delta a = x_i + \Delta a r \cos \phi \Rightarrow x - x_i = \Delta a r \cos \phi \quad (\text{E.1.35})$$

$$y = y_i + \eta \Delta a = y_i + \Delta a r \sin \phi \Rightarrow y - y_i = \Delta a r \sin \phi \quad (\text{E.1.36})$$

From the relation between the local cartesian coordinates ξ and η on the one hand and the polar coordinates r and ϕ on the other hand it can be derived:

$$\begin{aligned} \xi &= r \cos \phi, \quad \eta = r \sin \phi \\ \Rightarrow \xi^2 + \eta^2 &= r^2 \cos^2 \phi + r^2 \sin^2 \phi = r^2 \underbrace{(\cos^2 \phi + \sin^2 \phi)}_1 = r^2 \Rightarrow r = \sqrt{\xi^2 + \eta^2} \end{aligned} \quad (\text{E.1.37})$$

$$\Rightarrow \cos \phi = \frac{\xi}{r} = \frac{\xi}{\sqrt{\xi^2 + \eta^2}}, \quad \sin \phi = \frac{\eta}{r} = \frac{\eta}{\sqrt{\xi^2 + \eta^2}} \quad (\text{E.1.38})$$

Based on this, the following term contained in the influence functions is reformulated in the following way:

$$\left([x_i - x]^2 + [y_i - y]^2 \right)^{1/2} = \sqrt{[-\xi \Delta a]^2 + [-\eta \Delta a]^2} = \sqrt{\xi^2 \Delta a^2 + \eta^2 \Delta a^2} = \Delta a \sqrt{\xi^2 + \eta^2} = \Delta a r \quad (\text{E.1.39})$$

The terms $x - x_k$ and $y - y_k$, which are contained in the shape function f_k , expressed in the following way:

$$\begin{aligned} x_i &= x_O + \bar{x}_i \Delta a, \quad x_k = x_O + \bar{x}_k \Delta a, \quad \bar{x}_i, \bar{x}_k \in \mathbb{Z} \\ \Rightarrow x_i - x_k &= x_O + \bar{x}_i \Delta a - x_O - \bar{x}_k \Delta a = (\bar{x}_i - \bar{x}_k) \Delta a = \bar{x}_{ik} \Delta a, \quad \bar{x}_{ik} = \bar{x}_i - \bar{x}_k \in \mathbb{Z} \\ x - x_k &= x - x_i + x_i - x_k = \Delta a r \cos \phi + \Delta a \frac{x_i - x_k}{\Delta a} = \Delta a (r \cos \phi + \bar{x}_{ik}) \end{aligned} \quad (\text{E.1.40})$$

$$\begin{aligned} y_i &= y_O + \bar{y}_i \Delta a, \quad y_k = y_O + \bar{y}_k \Delta a, \quad \bar{y}_i, \bar{y}_k \in \mathbb{Z} \\ \Rightarrow y_i - y_k &= y_O + \bar{y}_i \Delta a - y_O - \bar{y}_k \Delta a = (\bar{y}_i - \bar{y}_k) \Delta a = \bar{y}_{ik} \Delta a, \quad \bar{y}_{ik} = \bar{y}_i - \bar{y}_k \in \mathbb{Z} \\ y - y_k &= y - y_i + y_i - y_k = \Delta a r \sin \phi + \Delta a \frac{y_i - y_k}{\Delta a} = \Delta a (r \sin \phi + \bar{y}_{ik}) \end{aligned} \quad (\text{E.1.41})$$

Using these relations, the shape function f_k is formulated in the following way:

$$\begin{aligned} f_k(x, y) &= \left(1 - c_X \frac{x - x_k}{\Delta a} \right) \left(1 - c_Y \frac{y - y_k}{\Delta a} \right) = (1 - c_X [r \cos \phi + \bar{x}_{ik}]) (1 - c_Y [r \sin \phi + \bar{y}_{ik}]) \\ &= (1 - c_X r \cos \phi - c_X \bar{x}_{ik}) (1 - c_Y r \sin \phi - c_Y \bar{y}_{ik}) \\ &= \underbrace{(1 - c_X \bar{x}_{ik})}_{f_{k,0}} \underbrace{(1 - c_Y \bar{y}_{ik})}_{f_{k,1}} + \underbrace{c_X (c_Y \bar{y}_{ik} - 1)}_{f_{k,1}} r \cos \phi \\ &\quad + \underbrace{(c_X \bar{x}_{ik} - 1)}_{f_{k,2}} c_Y r \sin \phi + \underbrace{c_X c_Y}_{f_{k,12}} r^2 \cos \phi \sin \phi \\ &= f_{k,0} + f_{k,1} r \cos \phi + f_{k,2} r \sin \phi + f_{k,12} r^2 \cos \phi \sin \phi \end{aligned} \quad (\text{E.1.42})$$

From this it follows:

$$\frac{dx}{d\xi} = \Delta a \Rightarrow dx = d\xi \Delta a, \quad \frac{dy}{d\eta} = \Delta a \Rightarrow dy = d\eta \Delta a \Rightarrow dA = dx dy = \Delta a^2 d\xi d\eta \quad (\text{E.1.43})$$

The influence functions H_{11} , H_{22} , H_{12} , and H_{33} contain differences $x_i - x$ and $y_i - y$ and squares of these differences. It is valid

$$x - x_i = \xi \Delta a \Leftrightarrow x_i - x = -\xi \Delta a \quad (\text{E.1.44})$$

$$y - y_i = \eta \Delta a \Leftrightarrow y_i - y = -\eta \Delta a \quad (\text{E.1.45})$$

As derived in the previous section, the local bilinear function f_k , which is used for the description of the discretized stress field, is formulated in the following way:

$$x_k - \Delta a \leq x \leq x_k + \Delta a \wedge y_k - \Delta a \leq y \leq y_k + \Delta a : \\ f_k = \left(1 - \frac{c_x (x - x_k)}{\Delta a}\right) \left(1 - \frac{c_y (y - y_k)}{\Delta a}\right) \quad (\text{E.1.46})$$

Using the local coordinates it is valid:

$$\frac{x - x_k}{\Delta a} = \frac{x_i + \xi \Delta a - x_k}{\Delta a} = \xi - \frac{x_k - x_i}{\Delta a} = \xi - \frac{\bar{x}_k \Delta a - \bar{x}_i \Delta a}{\Delta a} = \xi - (\bar{x}_k - \bar{x}_i) = \xi - \bar{x}_{ki} \quad (\text{E.1.47})$$

$$\frac{y - y_k}{\Delta a} = \frac{y_i + \eta \Delta a - y_k}{\Delta a} = \eta - \frac{y_k - y_i}{\Delta a} = \eta - \frac{\bar{y}_k \Delta a - \bar{y}_i \Delta a}{\Delta a} = \eta - (\bar{y}_k - \bar{y}_i) = \eta - \bar{y}_{ki} \quad (\text{E.1.48})$$

Here the normalized distances $\bar{x}_{ki} = \bar{x}_k - \bar{x}_i$, $\bar{x}_{ki} \in \mathbb{Z}$ and $\bar{y}_{ki} = \bar{y}_k - \bar{y}_i$, $\bar{y}_{ki} \in \mathbb{Z}$ are used. For the further considerations the function is reformulated in the following way:

$$f_k = \left(1 - \frac{c_x (x - x_k)}{\Delta a}\right) \left(1 - \frac{c_y (y - y_k)}{\Delta a}\right) = [1 - c_x (\xi - \bar{x}_{ki})] [1 - c_y (\eta - \bar{y}_{ki})] \\ = [1 + c_x \bar{x}_{ki} - c_x \xi] [1 + c_y \bar{y}_{ki} - c_y \eta] \\ = \underbrace{(1 + c_x \bar{x}_{ki})}_{f_{k,0}} \underbrace{(1 + c_y \bar{y}_{ki})}_{-f_{k,1}} \underbrace{\xi}_{-f_{k,2}} - \underbrace{(1 + c_x \bar{x}_{ki}) c_y}_{-f_{k,2}} \eta + \underbrace{c_x c_y}_{f_{k,12}} \xi \eta \\ = f_{k,0} + f_{k,1} \xi + f_{k,2} \eta + f_{k,12} \xi \eta \quad (\text{E.1.49})$$

In the second step the local cartesian coordinates ξ and η are replaced by polar coordinates in the following way:

$$\xi = r \cos \phi, \quad \eta = r \sin \phi, \quad r \geq 0 \quad (\text{E.1.50})$$

Thereby, the distances $x_i - x$ and $y_i - y$ are expressed in the following way:

$$x_i - x = -\xi \Delta a = -\Delta a r \cos \phi \quad (\text{E.1.51})$$

$$y_i - y = -\eta \Delta a = -\Delta a r \sin \phi \quad (\text{E.1.52})$$

Since the grid constant $\Delta a > 0$ is strictly positive and the radius $r \geq 0$ is non-negative, it is valid:

$$\begin{aligned} \left([x_i - x]^2 + [y_i - y]^2\right)^{1/2} &= \left((-\Delta a r \cos \phi)^2 + (-\Delta a r \sin \phi)^2\right)^{1/2} \\ &= \left(\Delta a^2 r^2 \cos^2 \phi + \Delta a^2 r^2 \sin^2 \phi\right)^{1/2} \\ &= \left(\cos^2 \phi + \sin^2 \phi\right)^{1/2} \Delta a r = \Delta a r \end{aligned} \quad (\text{E.1.53})$$

By inserting the polar coordinates into the terms contained in the influence functions it is obtained:

$$\frac{1}{[(x_i - x)^2 + (y_i - y)^2]^{1/2}} = \frac{1}{\Delta a r} \quad (\text{E.1.54})$$

$$\frac{(x_i - x)^2}{[(x_i - x)^2 + (y_i - y)^2]^{3/2}} = \frac{(-\Delta a r \cos \phi)^2}{(\Delta a r)^3} = \frac{\Delta a^2 r^2 \cos^2 \phi}{\Delta a^3 r^3} = \frac{\cos^2 \phi}{r \Delta a} \quad (\text{E.1.55})$$

$$\frac{(y_i - y)^2}{[(x_i - x)^2 + (y_i - y)^2]^{3/2}} = \frac{(-\Delta a r \sin \phi)^2}{(\Delta a r)^3} = \frac{\Delta a^2 r^2 \sin^2 \phi}{\Delta a^3 r^3} = \frac{\sin^2 \phi}{r \Delta a} \quad (\text{E.1.56})$$

$$\frac{(x_i - x)(y_i - y)}{[(x_i - x)^2 + (y_i - y)^2]^{3/2}} = \frac{(-\Delta a r \cos \phi)(-\Delta a r \sin \phi)}{(\Delta a r)^3} = \frac{\Delta a^2 r^2 \cos \phi \sin \phi}{\Delta a^3 r^3} = \frac{\cos \phi \sin \phi}{r \Delta a} \quad (\text{E.1.57})$$

For the infinitesimal area element it is valid:

$$dA = dx dy = \Delta a^2 d\xi d\eta = \Delta a^2 r dr d\phi \quad (\text{E.1.58})$$

The function f_k is expressed in the following way:

$$\begin{aligned} f_k(x, y) &= \left(1 - \frac{c_x (x - x_k)}{\Delta a}\right) \left(1 - \frac{c_y (y - y_k)}{\Delta a}\right) \\ &= \underbrace{(1 + c_x \bar{x}_{ki}) (1 + c_y \bar{y}_{ki})}_{f_{k,0}} - \underbrace{c_x (1 + c_y \bar{y}_{ki})}_{-f_{k,1}} \xi - \underbrace{(1 + c_x \bar{x}_{ki}) c_y}_{-f_{k,2}} \eta + \underbrace{c_x c_y}_{f_{k,12}} \xi \eta \\ &= f_{k,0} + f_{k,1} \xi + f_{k,2} \eta + f_{k,12} \xi \eta \\ &= f_{k,0} + f_{k,1} r \cos \phi + f_{k,2} r \sin \phi + f_{k,12} r^2 \sin \phi \cos \phi \\ &= f_k(r, \phi) \end{aligned} \quad (\text{E.1.59})$$

Altogether it is valid for the integrands of the compliance coefficients:

$$\frac{f_k(x, y)}{[(x_i - x)^2 + (y_i - y)^2]^{1/2}} dA = \frac{1}{r \Delta a} f_k(r, \phi) \Delta a^2 r dr d\phi = f_k(r, \phi) \Delta a dr d\phi \quad (\text{E.1.60})$$

$$\frac{(x_i - x)^2 f_k(x, y)}{[(x_i - x)^2 + (y_i - y)^2]^{3/2}} dA = \frac{\cos^2 \phi}{r \Delta a} f_k(r, \phi) \Delta a^2 r dr d\phi = \cos^2 \phi f_k(r, \phi) \Delta a dr d\phi \quad (\text{E.1.61})$$

$$\frac{(y_i - y)^2 f_k(x, y)}{[(x_i - x)^2 + (y_i - y)^2]^{3/2}} dA = \frac{\sin^2 \phi}{r \Delta a} f_k(r, \phi) \Delta a^2 r dr d\phi = \sin^2 \phi f_k(r, \phi) \Delta a dr d\phi \quad (\text{E.1.62})$$

$$\frac{(x_i - x)(y_i - y) f_k(x, y)}{[(x_i - x)^2 + (y_i - y)^2]^{3/2}} dA = \frac{\cos \phi \sin \phi}{r \Delta a} f_k(r, \phi) \Delta a^2 r dr d\phi = \cos \phi \sin \phi f_k(r, \phi) \Delta a dr d\phi \quad (\text{E.1.63})$$

Thereby, the denominator is eliminated so that no singularities occur; this is the main advantage of the formulation using polar coordinates. The resulting integrands can be expressed by the following generalized formulation:

$$h_{ik,n}^{[IK]} = \int_{D_{k,n}} \cos^M \phi \sin^N \phi f_k(r, \phi) \Delta a dr d\phi \quad (\text{E.1.64})$$

E.2 Integration over the polar coordinates

As derived in the equations (E.0.23), (E.0.24), (E.0.25) and (E.0.26) the compliance coefficients can be formulated in the following way:

$$H_{ik}^{[11]} = \int_A H_{11}(x_i - x, y_i - y) f_k(x, y) dA = \sum_{n=1}^4 \left[\frac{1-\nu}{\pi G} h_{ik,n}^{[33]} + \frac{\nu}{\pi G} h_{ik,n}^{[11]} \right] \quad (\text{E.2.65})$$

$$H_{ik}^{[22]} = \int_A H_{22}(x_i - x, y_i - y) f_k(x, y) dA = \sum_{n=1}^4 \left[\frac{1-\nu}{\pi G} h_{ik,n}^{[33]} + \frac{\nu}{\pi G} h_{ik,n}^{[22]} \right] \quad (\text{E.2.66})$$

$$H_{33,ik} = \int_A H_{33}(x_i - x, y_i - y) f_k(x, y) dA = \sum_{n=1}^4 \frac{1-\nu}{\pi G} h_{ik,n}^{[33]} \quad (\text{E.2.67})$$

$$H_{12,ik} = \int_A H_{12}(x_i - x, y_i - y) f_k(x, y) dA = \sum_{n=1}^4 \frac{\nu}{\pi G} h_{ik,n}^{[12]} \quad (\text{E.2.68})$$

The four integrals $h_{ik,n}^{[IK]}$ are defined by:

$$h_{ik,n}^{[33]} = \int_{D_{k,n}} \frac{f_k(x, y)}{[(x_i - x)^2 + (y_i - y)^2]^{1/2}} dA \quad (\text{E.2.69})$$

$$h_{ik,n}^{[11]} = \int_{D_{k,n}} \frac{(x_i - x)^2 f_k(x, y)}{[(x_i - x)^2 + (y_i - y)^2]^{3/2}} dA \quad (\text{E.2.70})$$

$$h_{ik,n}^{[22]} = \int_{D_{k,n}} \frac{(y_i - y)^2 f_k(x, y)}{[(x_i - x)^2 + (y_i - y)^2]^{3/2}} dA \quad (\text{E.2.71})$$

$$h_{ik,n}^{[12]} = \int_{D_{k,n}} \frac{(x_i - x)(y_i - y) f_k(x, y)}{[(x_i - x)^2 + (y_i - y)^2]^{3/2}} dA \quad (\text{E.2.72})$$

In section refAppendixCompliance:LocalCoordinates, the integrands of the integrals $h_{ik,n}^{[IK]}$ have been formulated for polar coordinates. The advantage is that for the formulation using polar coordinates the integrands have no singularities. However, the subdomains $D_{k,n}$, over which the integration has to be carried out, have a rectangular shape, whereas the edges of the rectangle are parallel to the x -axis or to the y -axis. With respect to polar coordinates, the integration over a domain having such a shape is, however, more difficult. For the following considerations it is assumed that the four corners of the rectangle are given by the four points $P_1 = \langle \xi_a, \eta_a \rangle$, $P_2 = \langle \xi_b, \eta_a \rangle$, $P_3 = \langle \xi_b, \eta_b \rangle$, $P_4 = \langle \xi_a, \eta_b \rangle$.

If a function $g(r, \phi)$ has to be integrated over an area, the integration is most simple for an area A_{BC} , which is limited by two rays defined by the angles ϕ_B and ϕ_C and a curve defined by $R(\phi)$. It is valid:

$$\int_{A_{BC}} g(r, \phi) dA = \int_{\phi_B}^{\phi_C} \int_0^{R_{BC}(\phi)} g(r, \phi) r dr d\phi \quad (\text{E.2.73})$$

The integral of the function $g(r, \phi)$ over the rectangular area D can now be obtained by summing up the integrals of the function $g(r, \phi)$ over the triangular areas T_{BC} ; in this case, the triangular area T_{BC} is limited by the rays defined by ϕ_B and ϕ_C and the edge of the rectangle connecting the corners P_B and P_C . Thereby, the three corners of the triangle T_{BC} are given by the two points P_B and P_C

and the origin of the coordinates. Then, the integral over a triangular domain T_{BC} is formulated in the following way:

$$G(P_B \rightarrow P_C) = \int_{T_{BC}} g(r \cos \phi, r \sin \phi) r dr d\phi = \int_{\phi_B}^{\phi_C} \int_0^{R_{BC}(\phi)} g(r \cos \phi, r \sin \phi) r dr d\phi \quad (\text{E.2.74})$$

Here, ϕ_B and ϕ_C indicate the start angle and the end angle, respectively. The coordinates ξ_{BC} and η_{BC} of a point P , which is located on the line connecting the points P_B and P_C , are expressed by:

$$\xi_{BC} = R_{BC}(\phi) \cos \phi, \quad \eta_{BC} = R_{BC}(\phi) \sin \phi \quad (\text{E.2.75})$$

Thereby, the radius function $R_{BC}(\phi)$ is defined. The sign of the integral depends on the relation between the angles ϕ_B and ϕ_C : If the end angle is greater than the start angle, i.e. $\phi_C > \phi_B$, then the integral is counted positively; if the end angle is less than the start angle, i.e. $\phi_C < \phi_B$, then it is counted negatively. Since the rectangular domain D has four edges, the integral over the domain D is expressed by the four integrals over the triangular domains T_{12} , T_{23} , T_{34} , T_{41} .

$$\begin{aligned} \int_D g(\xi, \eta) d\xi d\eta &= \int_{T_{12}} g(r \cos \phi, r \sin \phi) r dr d\phi + \int_{T_{23}} g(r \cos \phi, r \sin \phi) r dr d\phi \\ &+ \int_{T_{34}} g(r \cos \phi, r \sin \phi) r dr d\phi + \int_{T_{41}} g(r \cos \phi, r \sin \phi) r dr d\phi \quad (\text{E.2.76}) \end{aligned}$$

An overview is given in Figure E.2.1. Here, the four edges of the rectangle and the radius functions $R_{BC}(\phi)$ are described in the following way:

$$\text{Lower edge : } P_1 = \langle \xi_A, \eta_A \rangle \rightarrow P_2 = \langle \xi_B, \eta_A \rangle, \quad R_{12}(\phi) = \frac{\eta_A}{\sin \phi} \quad (\text{E.2.77})$$

$$\text{Right edge : } P_2 = \langle \xi_B, \eta_A \rangle \rightarrow P_3 = \langle \xi_B, \eta_B \rangle, \quad R_{23}(\phi) = \frac{\xi_B}{\cos \phi} \quad (\text{E.2.78})$$

$$\text{Upper edge : } P_3 = \langle \xi_B, \eta_B \rangle \rightarrow P_4 = \langle \xi_A, \eta_B \rangle, \quad R_{34}(\phi) = \frac{\eta_B}{\sin \phi} \quad (\text{E.2.79})$$

$$\text{Left edge : } P_4 = \langle \xi_A, \eta_B \rangle \rightarrow P_1 = \langle \xi_A, \eta_A \rangle, \quad R_{41}(\phi) = \frac{\xi_B}{\cos \phi} \quad (\text{E.2.80})$$

By applying this integration on the integral $h_{ik,n}^{[IK]}$ defined in (E.1.64) it is obtained:

$$\begin{aligned} h_{ik,n}^{[IK]} &= \int_{D_{k,n}} \cos^M \phi \sin^N \phi f_k(r, \phi) \Delta a dr d\phi \\ &= \underbrace{\int_{T_{12}} \cos^M \phi \sin^N \phi f_k(r, \phi) \Delta a dr d\phi}_{h_{ik,n}^{[IK]}(P_1 \rightarrow P_2)} + \underbrace{\int_{T_{23}} \cos^M \phi \sin^N \phi f_k(r, \phi) \Delta a dr d\phi}_{h_{ik,n}^{[IK]}(P_2 \rightarrow P_3)} \\ &+ \underbrace{\int_{T_{34}} \cos^M \phi \sin^N \phi f_k(r, \phi) \Delta a dr d\phi}_{h_{ik,n}^{[IK]}(P_3 \rightarrow P_4)} + \underbrace{\int_{T_{41}} \cos^M \phi \sin^N \phi f_k(r, \phi) \Delta a dr d\phi}_{h_{ik,n}^{[IK]}(P_4 \rightarrow P_1)} \quad (\text{E.2.81}) \end{aligned}$$

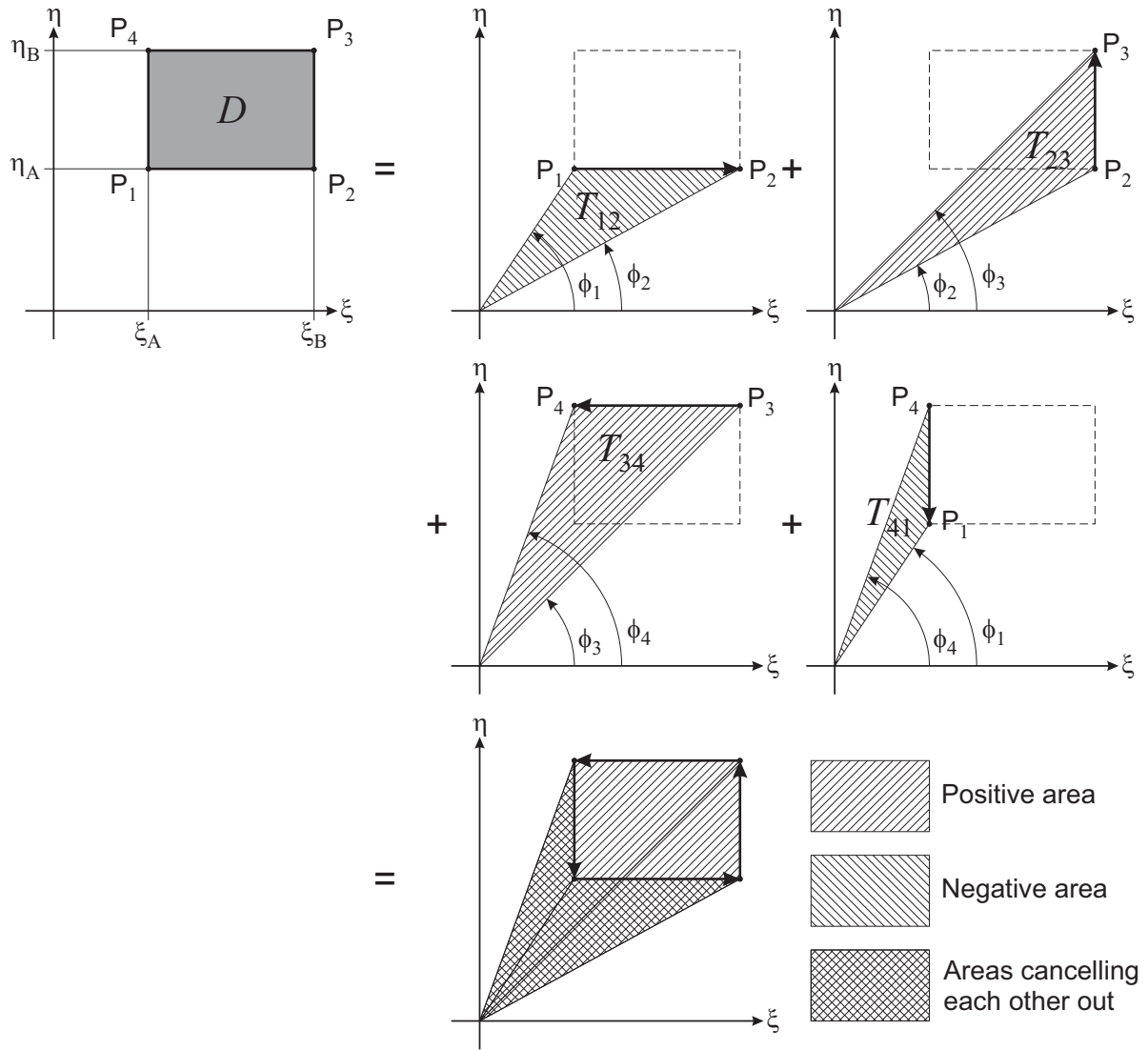


Figure E.2.1: Description of the rectangular domain D by superposing triangular domains T_{AB} .

For the integral over the triangular domain T_{BC} it is valid:

$$\begin{aligned}
 h_{ik,n}^{[IK]}(P_B \rightarrow P_C) &= \int_{T_{BC}} \cos^M \phi \sin^N \phi f_k(r, \phi) \Delta a \, dr \, d\phi \\
 &= \int_{\phi_B}^{\phi_C} \int_0^{R_{BC}(\phi)} \cos^M \phi \sin^N \phi f_k(r, \phi) \Delta a \, dr \, d\phi \\
 &= \Delta a \int_{\phi_B}^{\phi_C} \left[\int_0^{R_{BC}(\phi)} f_k(r, \phi) \, dr \right] \cos^M \phi \sin^N \phi \, d\phi \quad (\text{E.2.82})
 \end{aligned}$$

Since the trigonometric functions $\cos^M \phi$ and $\sin^N \phi$ do not depend on the radial coordinate r , they are factored out from the inner integral over r . The only term of the integrand, which depends on r , is the shape function $f_k(r, \phi)$. Using the formulation for $f_k(r, \phi)$ according to (E.1.59), it is

obtained for the inner integral:

$$\begin{aligned}
\int_0^{R(\phi)} f_k(r, \phi) dr &= \int_0^{R(\phi)} [f_{k,0} + f_{k,1} r \cos \phi + f_{k,2} r \sin \phi + f_{k,12} r^2 \sin \phi \cos \phi] dr \\
&= f_{k,0} \int_0^{R(\phi)} dr + f_{k,1} \cos \phi \int_0^{R(\phi)} r dr + f_{k,2} \sin \phi \int_0^{R(\phi)} r dr + f_{k,12} \cos \phi \sin \phi \int_0^{R(\phi)} r^2 dr \\
&= f_{k,0} r \Big|_0^{R(\phi)} + f_{k,1} \cos \phi \frac{r^2}{2} \Big|_0^{R(\phi)} + f_{k,2} \sin \phi \frac{r^2}{2} \Big|_0^{R(\phi)} + f_{k,12} \cos \phi \sin \phi \frac{r^3}{3} \Big|_0^{R(\phi)} \\
&= f_{k,0} R(\phi) + \frac{1}{2} f_{k,1} \cos \phi R(\phi)^2 + \frac{1}{2} f_{k,2} \sin \phi R(\phi)^2 + \frac{1}{3} f_{k,12} \cos \phi \sin \phi R(\phi)^3
\end{aligned} \tag{E.2.83}$$

E.2.1 Integration for constant ξ

For the integration along $\xi = \text{const.}$ it is valid for the radius $R(\phi)$:

$$\xi = R(\phi) \cos \phi \Rightarrow R(\phi) = \frac{\xi}{\cos \phi} \tag{E.2.84}$$

Inserting this into the result of the inner integral leads to:

$$\begin{aligned}
\int_0^{R(\phi)} f_k(r, \phi) dr &= f_{k,0} R(\phi) + \frac{1}{2} f_{k,1} \cos \phi R(\phi)^2 + \frac{1}{2} f_{k,2} \sin \phi R(\phi)^2 + \frac{1}{3} f_{k,12} \cos \phi \sin \phi R(\phi)^3 \\
&= f_{k,0} \frac{\xi}{\cos \phi} + \frac{1}{2} f_{k,1} \cos \phi \frac{\xi^2}{\cos^2 \phi} + \frac{1}{2} f_{k,2} \sin \phi \frac{\xi^2}{\cos^2 \phi} + \frac{1}{3} f_{k,12} \cos \phi \sin \phi \frac{\xi^3}{\cos^3 \phi} \\
&= f_{k,0} \frac{\xi}{\cos \phi} + \frac{1}{2} f_{k,1} \frac{\xi^2}{\cos \phi} + \frac{1}{2} f_{k,2} \sin \phi \frac{\xi^2}{\cos^2 \phi} + \frac{1}{3} f_{k,12} \sin \phi \frac{\xi^3}{\cos^2 \phi} \\
&= \left(f_{k,0} + \frac{1}{2} f_{k,1} \xi \right) \xi \frac{1}{\cos \phi} + \left(\frac{1}{2} f_{k,2} + \frac{1}{3} f_{k,12} \xi \right) \xi^2 \frac{\sin \phi}{\cos^2 \phi} \\
&= F_{k,\xi,1} \xi \frac{1}{\cos \phi} + F_{k,\xi,2} \xi^2 \frac{\sin \phi}{\cos^2 \phi}
\end{aligned} \tag{E.2.85}$$

For the coefficients $F_{k,\xi,1}$ and $F_{k,\xi,2}$ it is valid:

$$\begin{aligned}
F_{k,\xi,1} &= f_{k,0} + \frac{1}{2} f_{k,1} \xi = \frac{1}{2} [2 f_{k,0} + f_{k,1} \xi] = \frac{1}{2} [2 (1 + c_x \bar{x}_{ki}) (1 + c_y \bar{y}_{ki}) - c_x (1 + c_y \bar{y}_{ki}) \xi] \\
&= \frac{1}{2} [2 (1 + c_x \bar{x}_{ki}) - c_x \xi] (1 + c_y \bar{y}_{ki})
\end{aligned} \tag{E.2.86}$$

$$\begin{aligned}
F_{k,\xi,2} &= \frac{1}{2} f_{k,2} + \frac{1}{3} f_{k,12} \xi = \frac{1}{6} [3 f_{k,2} + 2 f_{k,12} \xi] = \frac{1}{6} [-3 (1 + c_x \bar{x}_{ki}) c_y + 2 c_x c_y \xi] \\
&= \frac{1}{6} [-3 (1 + c_x \bar{x}_{ki}) + 2 c_x \xi] c_y
\end{aligned} \tag{E.2.87}$$

Based on this the integrals over the azimuth ϕ are formulated. Since the factors $F_{k,\xi,1}$ and $F_{k,\xi,2}$ and the coordinate ξ are constant, they are factored out from the integrals. For the integrals $h_{ik,n}^{[33]}$,

$h_{ik,n}^{[11]}$ and $h_{ik,n}^{[22]}$ along a vertical edge indicated by ξ it is obtained:

$$\begin{aligned} h_{ik,n}^{[33]}(\xi, \eta_I \rightarrow \eta_J) &= \Delta a \int_{\phi_I}^{\phi_J} \int_0^{R(\phi)} f_k dr d\phi = \Delta a \int_{\phi_I}^{\phi_J} \left[F_{k,\xi,1} \xi \frac{1}{\cos \phi} + F_{k,\xi,2} \xi^2 \frac{\sin \phi}{\cos^2 \phi} \right] d\phi \\ &= \Delta a \left[F_{k,\xi,1} \int_{\phi_I}^{\phi_J} \frac{1}{\cos \phi} d\phi + F_{k,\xi,2} \xi \int_{\phi_I}^{\phi_J} \frac{\sin \phi}{\cos^2 \phi} d\phi \right] \xi \end{aligned} \quad (\text{E.2.88})$$

$$\begin{aligned} h_{ik,n}^{[11]}(\xi, \eta_I \rightarrow \eta_J) &= \Delta a \int_{\phi_I}^{\phi_J} \int_0^{R(\phi)} f_k dr \cos^2 \phi d\phi = \Delta a \int_{\phi_I}^{\phi_J} \left[F_{k,\xi,1} \xi \frac{1}{\cos \phi} + F_{k,\xi,2} \xi^2 \frac{\sin \phi}{\cos^2 \phi} \right] \cos^2 \phi d\phi \\ &= \Delta a \left[F_{k,\xi,1} \int_{\phi_I}^{\phi_J} \cos \phi d\phi + F_{k,\xi,2} \xi \int_{\phi_I}^{\phi_J} \sin \phi d\phi \right] \xi \end{aligned} \quad (\text{E.2.89})$$

$$\begin{aligned} h_{ik,n}^{[22]}(\xi, \eta_I \rightarrow \eta_J) &= \Delta a \int_{\phi_I}^{\phi_J} \int_0^{R(\phi)} f_k dr \sin^2 \phi d\phi = \Delta a \int_{\phi_I}^{\phi_J} \left[F_{k,\xi,1} \xi \frac{1}{\cos \phi} + F_{k,\xi,2} \xi^2 \frac{\sin \phi}{\cos^2 \phi} \right] \sin^2 \phi d\phi \\ &= \Delta a \left[F_{k,\xi,1} \int_{\phi_I}^{\phi_J} \frac{\sin^2 \phi}{\cos \phi} d\phi + F_{k,\xi,2} \xi \int_{\phi_I}^{\phi_J} \frac{\sin^3 \phi}{\cos^2 \phi} d\phi \right] \xi \end{aligned} \quad (\text{E.2.90})$$

It is evident that the evaluation of the integral $h_{ik,n}^{[22]}(\xi, \eta_I \rightarrow \eta_J)$ requires a higher effort than the evaluation of the integrals $h_{ik,n}^{[11]}(\xi, \eta_I \rightarrow \eta_J)$ and $h_{ik,n}^{[33]}(\xi, \eta_I \rightarrow \eta_J)$. Therefore, this integral is determined by:

$$h_{ik,n}^{[22]}(\xi, \eta_I \rightarrow \eta_J) = h_{ik,n}^{[33]}(\xi, \eta_I \rightarrow \eta_J) - h_{ik,n}^{[11]}(\xi, \eta_I \rightarrow \eta_J) \quad (\text{E.2.91})$$

By using the relation:

$$\int_{\phi_I}^{\phi_J} \frac{\sin^2 \phi}{\cos \phi} d\phi = \int_{\phi_I}^{\phi_J} \frac{1 - \cos^2 \phi}{\cos \phi} d\phi = \int_{\phi_I}^{\phi_J} \frac{1}{\cos \phi} d\phi - \int_{\phi_I}^{\phi_J} \cos \phi d\phi \quad (\text{E.2.92})$$

it is obtained for the integral $h_{ik,n}^{[12]}$:

$$\begin{aligned} h_{ik,n}^{[12]}(\xi, \eta_I \rightarrow \eta_J) &= \Delta a \int_{\phi_I}^{\phi_J} \int_0^{R(\phi)} f_k dr \cos \phi \sin \phi d\phi \\ &= \Delta a \int_{\phi_I}^{\phi_J} \left[F_{k,\xi,1} \xi \frac{1}{\cos \phi} + F_{k,\xi,2} \xi^2 \frac{\sin \phi}{\cos^2 \phi} \right] \cos \phi \sin \phi d\phi \\ &= \Delta a \left[F_{k,\xi,1} \int_{\phi_I}^{\phi_J} \sin \phi d\phi + F_{k,\xi,2} \xi \int_{\phi_I}^{\phi_J} \frac{\sin^2 \phi}{\cos \phi} d\phi \right] \xi \\ &= \Delta a \left[F_{k,\xi,1} \int_{\phi_I}^{\phi_J} \sin \phi d\phi + F_{k,\xi,2} \xi \left(\int_{\phi_I}^{\phi_J} \frac{1}{\cos \phi} d\phi - \int_{\phi_I}^{\phi_J} \cos \phi d\phi \right) \right] \xi \end{aligned} \quad (\text{E.2.93})$$

E.2.2 Integration for constant η

For the integration along $\eta = \text{const.}$ it is valid for the radius $R(\phi)$:

$$\eta = R(\phi) \sin \phi \Rightarrow R(\phi) = \frac{\eta}{\sin \phi} \quad (\text{E.2.94})$$

Inserting this into the result of the inner integral over the radius r leads to:

$$\begin{aligned} \int_0^{R(\phi)} f_k(r, \phi) dr &= f_{k,0} R(\phi) + \frac{1}{2} f_{k,1} \cos \phi R(\phi)^2 + \frac{1}{2} f_{k,2} \sin \phi R(\phi)^2 + \frac{1}{3} f_{k,12} \cos \phi \sin \phi R(\phi)^3 \\ &= f_{k,0} \frac{\eta}{\sin \phi} + \frac{1}{2} f_{k,1} \cos \phi \frac{\eta^2}{\sin^2 \phi} + \frac{1}{2} f_{k,2} \sin \phi \frac{\eta^2}{\sin^2 \phi} + \frac{1}{3} f_{k,12} \cos \phi \sin \phi \frac{\eta^3}{\sin^3 \phi} \\ &= f_{k,0} \frac{\eta}{\sin \phi} + \frac{1}{2} f_{k,1} \cos \phi \frac{\eta^2}{\sin^2 \phi} + \frac{1}{2} f_{k,2} \frac{\eta^2}{\sin \phi} + \frac{1}{3} f_{k,12} \cos \phi \frac{\eta^3}{\sin^2 \phi} \\ &= \left(f_{k,0} + \frac{1}{2} f_{k,2} \eta \right) \eta \frac{1}{\sin \phi} + \left(\frac{1}{2} f_{k,1} + \frac{1}{3} f_{k,12} \eta \right) \eta^2 \frac{\cos \phi}{\sin^2 \phi} \\ &= F_{k,\eta,1} \eta \frac{1}{\sin \phi} + F_{k,\eta,2} \eta^2 \frac{\cos \phi}{\sin^2 \phi} \end{aligned} \quad (\text{E.2.95})$$

The constant coefficients $F_{k,\eta,1}$ and $F_{k,\eta,2}$ are obtained to:

$$\begin{aligned} F_{k,\eta,1} &= f_{k,0} + \frac{1}{2} f_{k,2} \eta = \frac{1}{2} [2 f_{k,0} + f_{k,2} \eta] = \frac{1}{2} [2 (1 + c_x \bar{x}_{ki}) (1 + c_y \bar{y}_{ki}) - (1 + c_x \bar{x}_{ki}) c_y \eta] \\ &= \frac{1}{2} (1 + c_x \bar{x}_{ki}) [2 (1 + c_y \bar{y}_{ki}) - c_y \eta] \end{aligned} \quad (\text{E.2.96})$$

$$\begin{aligned} F_{k,\eta,2} &= \frac{1}{2} f_{k,1} + \frac{1}{3} f_{k,12} \eta = \frac{1}{6} [3 f_{k,1} + 2 f_{k,12} \eta] = \frac{1}{6} [-3 c_x (1 + c_y \bar{y}_{ki}) + 2 c_x c_y \eta] \\ &= \frac{1}{6} c_x [-3 (1 + c_y \bar{y}_{ki}) + 2 c_y \eta] \end{aligned} \quad (\text{E.2.97})$$

Based on this the integrals $h_{ik,n}^{[33]}$, $h_{ik,n}^{[11]}$, $h_{ik,n}^{[22]}$ and $h_{ik,n}^{[12]}$ are formulated:

$$\begin{aligned} h_{ik,n}^{[33]}(\xi_I \rightarrow \xi_J, \eta) &= \Delta a \int_{\phi_I}^{\phi_J} \int_0^{R(\phi)} f_k dr d\phi = \Delta a \int_{\phi_I}^{\phi_J} \left[F_{k,\eta,1} \eta \frac{1}{\sin \phi} + F_{k,\eta,2} \eta^2 \frac{\cos \phi}{\sin^2 \phi} \right] d\phi \\ &= \Delta a \left[F_{k,\eta,1} \int_{\phi_I}^{\phi_J} \frac{1}{\sin \phi} d\phi + F_{k,\eta,2} \eta \int_{\phi_I}^{\phi_J} \frac{\cos \phi}{\sin^2 \phi} d\phi \right] \eta \end{aligned} \quad (\text{E.2.98})$$

$$\begin{aligned} h_{ik,n}^{[11]}(\xi_I \rightarrow \xi_J, \eta) &= \int_{\phi_I}^{\phi_J} \int_0^{R(\phi)} f_k dr \cos^2 \phi d\phi = \Delta a \int_{\phi_I}^{\phi_J} \left[F_{k,\eta,1} \eta \frac{1}{\sin \phi} + F_{k,\eta,2} \eta^2 \frac{\cos \phi}{\sin^2 \phi} \right] \cos^2 \phi d\phi \\ &= \Delta a \left[F_{k,\eta,1} \eta \int_{\phi_I}^{\phi_J} \frac{\cos^2 \phi}{\sin \phi} d\phi + F_{k,\eta,2} \eta^2 \int_{\phi_I}^{\phi_J} \frac{\cos^3 \phi}{\sin^2 \phi} d\phi \right] \end{aligned} \quad (\text{E.2.99})$$

$$\begin{aligned} h_{ik,n}^{[22]}(\xi_I \rightarrow \xi_J, \eta) &= \int_{\phi_I}^{\phi_J} \int_0^{R(\phi)} f_k dr \sin^2 \phi d\phi = \Delta a \int_{\phi_I}^{\phi_J} \left[F_{k,\eta,1} \eta \frac{1}{\sin \phi} + F_{k,\eta,2} \eta^2 \frac{\cos \phi}{\sin^2 \phi} \right] \sin^2 \phi d\phi \\ &= \Delta a \left[F_{k,\eta,1} \int_{\phi_I}^{\phi_J} \sin \phi d\phi + F_{k,\eta,2} \eta \int_{\phi_I}^{\phi_J} \cos \phi d\phi \right] \eta \end{aligned} \quad (\text{E.2.100})$$

In this case the evaluation of the integral $h_{ik,n}^{[11]}(\xi_I \rightarrow \xi_J, \eta)$ is more complicated than those of the integrals $h_{ik,n}^{[33]}(\xi_I \rightarrow \xi_J, \eta)$ and $h_{ik,n}^{[22]}(\xi_I \rightarrow \xi_J, \eta)$ so that the integral $h_{ik,n}^{[11]}(\xi_I \rightarrow \xi_J, \eta)$ is determined by:

$$h_{ik,n}^{[11]}(\xi, \eta_I \rightarrow \eta_J) = h_{ik,n}^{[33]}(\xi, \eta_I \rightarrow \eta_J) - h_{ik,n}^{[22]}(\xi, \eta_I \rightarrow \eta_J) \quad (\text{E.2.101})$$

For the determination of the integral $h_{ik,n}^{[12]}(\xi_I \rightarrow \xi_J, \eta)$ the following relation is used:

$$\int_{\phi_I}^{\phi_J} \frac{\cos^2 \phi}{\sin \phi} d\phi = \int_{\phi_I}^{\phi_J} \frac{1 - \sin^2 \phi}{\sin \phi} d\phi = \int_{\phi_I}^{\phi_J} \frac{1}{\sin \phi} d\phi - \int_{\phi_I}^{\phi_J} \sin \phi d\phi$$

Thereby, it is obtained

$$\begin{aligned} h_{ik,n}^{[12]}(\xi_I \rightarrow \xi_J, \eta) &= \Delta a \int_{\phi_I}^{\phi_J} \int_0^{R(\phi)} f_k dr \cos \phi \sin \phi d\phi \\ &= \Delta a \int_{\phi_I}^{\phi_J} \left[F_{k,\eta,1} \eta \frac{1}{\sin \phi} + F_{k,\eta,2} \eta^2 \frac{\cos \phi}{\sin^2 \phi} \right] \cos \phi \sin \phi d\phi \\ &= \Delta a \left[F_{k,\eta,1} \int_{\phi_I}^{\phi_J} \cos \phi d\phi + F_{k,\eta,2} \eta \int_{\phi_I}^{\phi_J} \frac{\cos^2 \phi}{\sin \phi} d\phi \right] \eta \\ &= \Delta a \left[F_{k,\eta,1} \int_{\phi_I}^{\phi_J} \cos \phi d\phi + F_{k,\eta,2} \eta \left(\int_{\phi_I}^{\phi_J} \frac{1}{\sin \phi} d\phi - \int_{\phi_I}^{\phi_J} \sin \phi d\phi \right) \right] \eta \end{aligned} \quad (\text{E.2.102})$$

E.2.3 Evaluation of the integrals

In sections E.2.1 and E.2.2, it has been shown that the integrals can be formulated as linear combinations of the following integrals:

$$\int_{\phi_I}^{\phi_J} \sin \phi \, d\phi, \int_{\phi_I}^{\phi_J} \cos \phi \, d\phi, \int_{\phi_I}^{\phi_J} \frac{1}{\sin \phi} \, d\phi, \int_{\phi_I}^{\phi_J} \frac{1}{\cos \phi} \, d\phi, \int_{\phi_I}^{\phi_J} \frac{\sin \phi}{\cos^2 \phi} \, d\phi, \int_{\phi_I}^{\phi_J} \frac{\cos \phi}{\sin^2 \phi} \, d\phi \quad (\text{E.2.103})$$

The solution of these integrals is given by:

$$\int \sin(\alpha x) \, dx = -\frac{1}{\alpha} \cos(\alpha x) \quad (\text{E.2.104})$$

$$\int \cos(\alpha x) \, dx = \frac{1}{\alpha} \sin(\alpha x) \quad (\text{E.2.105})$$

$$\begin{aligned} \int \frac{1}{\sin(\alpha x)} \, dx &= \int \csc(\alpha x) \, dx = \frac{1}{\alpha} \ln(\csc(\alpha x) - \cot(\alpha x)) \\ &= \frac{1}{\alpha} \ln\left(\frac{1}{\sin(\alpha x)} - \frac{\cos(\alpha x)}{\sin(\alpha x)}\right) = \frac{1}{\alpha} \ln\left(\frac{1 - \cos(\alpha x)}{\sin(\alpha x)}\right) \end{aligned} \quad (\text{E.2.106})$$

$$\begin{aligned} \int \frac{1}{\cos(\alpha x)} \, dx &= \int \sec(\alpha x) \, dx = \frac{1}{\alpha} \ln(\sec(\alpha x) + \tan(\alpha x)) \\ &= \frac{1}{\alpha} \ln\left(\frac{1}{\cos(\alpha x)} + \frac{\sin(\alpha x)}{\cos(\alpha x)}\right) = \frac{1}{\alpha} \ln\left(\frac{1 + \sin(\alpha x)}{\cos(\alpha x)}\right) \end{aligned} \quad (\text{E.2.107})$$

$$\int \frac{\sin(\alpha x)}{\cos^2(\alpha x)} \, dx = \frac{1}{\alpha \cos(\alpha x)} \quad (\text{E.2.108})$$

$$\int \frac{\cos(\alpha x)}{\sin^2(\alpha x)} \, dx = -\frac{1}{\alpha \sin(\alpha x)} \quad (\text{E.2.109})$$

It can be seen that the solutions of the integrals can be formulated in such a way that the variable x , for which the integration is carried out, only appears as the argument of the functions $\sin(\alpha x)$ and $\cos(\alpha x)$.

In the present case, the parameter α is set to $\alpha = 1$ and the integration variable x is replaced by the angle ϕ . From the relation between the local cartesian coordinates ξ and η on the one hand and the local polar coordinates r and ϕ on the other hand, as it has been introduced in (E.1.34), it can be derived:

$$\begin{aligned} \xi &= r \cos \phi, \quad \eta = r \sin \phi \Rightarrow \xi^2 + \eta^2 = r^2 \cos^2 \phi + r^2 \sin^2 \phi = r^2 (\cos^2 \phi + \sin^2 \phi) = r^2 \\ \Rightarrow \xi &= r \cos \phi \Rightarrow \cos \phi = \frac{\xi}{r} = \frac{\xi}{\sqrt{\xi^2 + \eta^2}}, \quad \eta = r \sin \phi \Rightarrow \sin \phi = \frac{\eta}{r} = \frac{\eta}{\sqrt{\xi^2 + \eta^2}} \end{aligned} \quad (\text{E.2.110})$$

From this it follows:

$$\frac{1 - \cos \phi}{\sin \phi} = \frac{1 - \frac{\xi}{r}}{\frac{\eta}{r}} = \frac{r - \xi}{\eta}, \quad \frac{1 + \sin \phi}{\cos \phi} = \frac{1 + \frac{\eta}{r}}{\frac{\xi}{r}} = \frac{r + \eta}{\xi} \quad (\text{E.2.111})$$

It can be seen that the angles ϕ_I and ϕ_J don't have to be determined at all. Instead of this, the terms containing the trigonometric functions can be expressed in a comparatively simple way using the values ξ_I, η_I, ξ_J and η_J of the cartesian coordinates and the radii $r_I = \sqrt{\xi_I^2 + \eta_I^2}$ and

$r_J = \sqrt{\xi_J^2 + \eta_J^2}$. In total, the solutions for the six basic integrals can be formulated in the following way:

$$\int_{\phi_I}^{\phi_J} \sin \phi \, d\phi = -\cos \phi \Big|_{\phi_I}^{\phi_J} = -(\cos \phi_J - \cos \phi_I) = -\left(\frac{\xi_J}{r_J} - \frac{\xi_I}{r_I}\right) \quad (\text{E.2.112})$$

$$\int_{\phi_I}^{\phi_J} \cos \phi \, d\phi = \sin \phi \Big|_{\phi_I}^{\phi_J} = \sin \phi_J - \sin \phi_I = \frac{\eta_J}{r_J} - \frac{\eta_I}{r_I} \quad (\text{E.2.113})$$

$$\begin{aligned} \int_{\phi_I}^{\phi_J} \frac{1}{\sin \phi} d\phi &= \ln \left(\frac{1 - \cos \phi}{\sin \phi} \right) \Big|_{\phi_I}^{\phi_J} = \ln \left(\frac{1 - \cos \phi_J}{\sin \phi_J} \right) - \ln \left(\frac{1 - \cos \phi_I}{\sin \phi_I} \right) \\ &= \ln \left(\frac{r_J - \xi_J}{\eta_J} \right) - \ln \left(\frac{r_I - \xi_I}{\eta_I} \right) = \ln \left(\frac{r_J - \xi_J}{\eta_J} \frac{\eta_I}{r_I - \xi_I} \right) = \ln \left(\frac{r_J - \xi_J}{r_I - \xi_I} \frac{\eta_I}{\eta_J} \right) \end{aligned} \quad (\text{E.2.114})$$

$$\begin{aligned} \int_{\phi_I}^{\phi_J} \frac{1}{\cos \phi} d\phi &= \ln \left(\frac{1 + \sin \phi}{\cos \phi} \right) \Big|_{\phi_I}^{\phi_J} = \ln \left(\frac{1 + \sin \phi_J}{\cos \phi_J} \right) - \ln \left(\frac{1 + \sin \phi_I}{\cos \phi_I} \right) \\ &= \ln \left(\frac{r_J + \eta_J}{\xi_J} \right) - \ln \left(\frac{r_I + \eta_I}{\xi_I} \right) = \ln \left(\frac{r_J + \eta_J}{\xi_J} \frac{\xi_I}{r_I + \eta_I} \right) = \ln \left(\frac{r_J + \eta_J}{r_I + \eta_I} \frac{\xi_I}{\xi_J} \right) \end{aligned} \quad (\text{E.2.115})$$

$$\int_{\phi_I}^{\phi_J} \frac{\sin \phi}{\cos^2 \phi} d\phi = \frac{1}{\cos \phi} \Big|_{\phi_I}^{\phi_J} = \frac{1}{\cos \phi_J} - \frac{1}{\cos \phi_I} = \frac{r_J}{\xi_J} - \frac{r_I}{\xi_I} \quad (\text{E.2.116})$$

$$\int_{\phi_I}^{\phi_J} \frac{\cos \phi}{\sin^2 \phi} d\phi = -\frac{1}{\sin \phi} \Big|_{\phi_I}^{\phi_J} = -\left(\frac{1}{\sin \phi_J} - \frac{1}{\sin \phi_I} \right) = -\left(\frac{r_J}{\eta_J} - \frac{r_I}{\eta_I} \right) \quad (\text{E.2.117})$$

For $\xi = \text{const.}$ it is valid:

$$\xi_I = \xi_J = \xi$$

$$\int_{\phi_I}^{\phi_J} \sin \phi \, d\phi = - \left(\frac{\xi_J}{r_J} - \frac{\xi_I}{r_I} \right) = - \left(\frac{\xi}{r_J} - \frac{\xi}{r_I} \right) = -\xi \left(\frac{1}{r_J} - \frac{1}{r_I} \right) \quad (\text{E.2.118})$$

$$\int_{\phi_I}^{\phi_J} \frac{1}{\cos \phi} \, d\phi = \ln \left(\frac{r_J + \eta_J \xi_I}{r_I + \eta_I \xi_J} \right) = \ln \left(\frac{r_J + \eta_J \xi}{r_I + \eta_I \xi} \right) = \ln \left(\frac{r_J + \eta_J}{r_I + \eta_I} \right) \quad (\text{E.2.119})$$

$$\int_{\phi_I}^{\phi_J} \frac{\sin \phi}{\cos^2 \phi} \, d\phi = \frac{r_J}{\xi_J} - \frac{r_I}{\xi_I} = \frac{r_J}{\xi} - \frac{r_I}{\xi} = \frac{r_J - r_I}{\xi} \quad (\text{E.2.120})$$

Based on this, the integrals are obtained to:

$$h_{ik,n}^{[33]}(\xi, \eta_I \rightarrow \eta_J) = \Delta a \int_{\phi_I}^{\phi_J} \int_0^{R(\phi)} f_k \, dr \, d\phi = \Delta a \left[F_{k,\xi,1} \int_{\phi_I}^{\phi_J} \frac{1}{\cos \phi} \, d\phi + F_{k,\xi,2} \xi \int_{\phi_I}^{\phi_J} \frac{\sin \phi}{\cos^2 \phi} \, d\phi \right] \xi$$

$$= \Delta a \left[F_{\xi,1} \ln \left(\frac{r_J + \eta_J}{r_I + \eta_I} \right) + F_{k,\xi,2} \xi \frac{r_J - r_I}{\xi} \right] \xi$$

$$= \Delta a \left[F_{\xi,1} \ln \left(\frac{r_J + \eta_J}{r_I + \eta_I} \right) + F_{\xi,2} (r_J - r_I) \right] \xi \quad (\text{E.2.121})$$

$$h_{ik,n}^{[11]}(\xi, \eta_I \rightarrow \eta_J) = \Delta a \int_{\phi_I}^{\phi_J} \int_0^{R(\phi)} f_k \, dr \, \cos^2 \phi \, d\phi = \Delta a \left[F_{\xi,1} \int_{\phi_I}^{\phi_J} \cos \phi \, d\phi + F_{\xi,2} \xi \int_{\phi_I}^{\phi_J} \sin \phi \, d\phi \right] \xi$$

$$= \Delta a \left[F_{\xi,1} \left(\frac{\eta_J}{r_J} - \frac{\eta_I}{r_I} \right) - F_{\xi,2} \xi^2 \left(\frac{1}{r_J} - \frac{1}{r_I} \right) \right] \xi \quad (\text{E.2.122})$$

$$h_{ik,n}^{[12]}(\xi, \eta_I \rightarrow \eta_J) = \Delta a \int_{\phi_I}^{\phi_J} \int_0^{R(\phi)} f_k \, dr \, \cos \phi \, \sin \phi \, d\phi$$

$$= \Delta a \left[F_{k,\xi,1} \int_{\phi_I}^{\phi_J} \sin \phi \, d\phi + F_{k,\xi,2} \xi \left(\int_{\phi_I}^{\phi_J} \frac{1}{\cos \phi} \, d\phi - \int_{\phi_I}^{\phi_J} \cos \phi \, d\phi \right) \right] \xi$$

$$= \Delta a \left[-F_{k,\xi,1} \xi \left(\frac{1}{r_J} - \frac{1}{r_I} \right) + F_{k,\xi,2} \xi \left(\ln \left(\frac{r_J + \eta_J}{r_I + \eta_I} \right) - \left(\frac{\eta_J}{r_J} - \frac{\eta_I}{r_I} \right) \right) \right] \xi$$

$$= \Delta a \left[-F_{k,\xi,1} \left(\frac{1}{r_J} - \frac{1}{r_I} \right) + F_{k,\xi,2} \left(\ln \left(\frac{r_J + \eta_J}{r_I + \eta_I} \right) - \left(\frac{\eta_J}{r_J} - \frac{\eta_I}{r_I} \right) \right) \right] \xi^2 \quad (\text{E.2.123})$$

For $\eta = \text{const.}$ it is valid:

$$\eta_I = \eta_J = \eta$$

$$\int_{\phi_I}^{\phi_J} \cos \phi \, d\phi = \frac{\eta_J}{r_J} - \frac{\eta_I}{r_I} = \frac{\eta}{r_J} - \frac{\eta}{r_I} = \eta \left(\frac{1}{r_J} - \frac{1}{r_I} \right) \quad (\text{E.2.124})$$

$$\int_{\phi_I}^{\phi_J} \frac{1}{\sin \phi} \, d\phi = \ln \left(\frac{r_J - \xi_J \eta_I}{r_I - \xi_I \eta_J} \right) = \ln \left(\frac{r_J - \xi_J \eta}{r_I - \xi_I \eta} \right) = \ln \left(\frac{r_J - \xi_J}{r_I - \xi_I} \right) \quad (\text{E.2.125})$$

$$\int_{\phi_I}^{\phi_J} \frac{\cos \phi}{\sin^2 \phi} \, d\phi = - \left(\frac{r_J}{\eta_J} - \frac{r_I}{\eta_I} \right) = - \left(\frac{r_J}{\eta} - \frac{r_I}{\eta} \right) = - \frac{r_J - r_I}{\eta} \quad (\text{E.2.126})$$

Inserting this into the integrals, which have been determined in section E.2.2, gives the following results:

$$h_{ik,n}^{[33]}(\xi_I \rightarrow \xi_J, \eta) = \Delta a \int_{\phi_I}^{\phi_J} \int_0^{R(\phi)} f_k \, dr \, d\phi = \Delta a \left[F_{k,\eta,1} \int_{\phi_I}^{\phi_J} \frac{1}{\sin \phi} \, d\phi + F_{k,\eta,2} \eta \int_{\phi_I}^{\phi_J} \frac{\cos \phi}{\sin^2 \phi} \, d\phi \right] \eta$$

$$= \Delta a \left[F_{k,\eta,1} \ln \left(\frac{r_J - \xi_J}{r_I - \xi_I} \right) - F_{k,\eta,2} \eta \frac{r_J - r_I}{\eta} \right] \eta$$

$$= \Delta a \left[F_{k,\eta,1} \ln \left(\frac{r_J - \xi_J}{r_I - \xi_I} \right) - F_{k,\eta,2} (r_J - r_I) \right] \eta \quad (\text{E.2.127})$$

$$h_{ik,n}^{[22]}(\xi_I \rightarrow \xi_J, \eta) = \int_{\phi_I}^{\phi_J} \int_0^{R(\phi)} f_k \, dr \, \sin^2 \phi \, d\phi = \Delta a \left[F_{k,\eta,1} \int_{\phi_I}^{\phi_J} \sin \phi \, d\phi + F_{k,\eta,2} \eta \int_{\phi_I}^{\phi_J} \cos \phi \, d\phi \right] \eta$$

$$= \Delta a \left[-F_{k,\eta,1} \left(\frac{\xi_J}{r_J} - \frac{\xi_I}{r_I} \right) + F_{k,\eta,2} \eta^2 \left(\frac{1}{r_J} - \frac{1}{r_I} \right) \right] \eta \quad (\text{E.2.128})$$

$$h_{ik,n}^{[12]}(\xi_I \rightarrow \xi_J, \eta) = \Delta a \int_{\phi_I}^{\phi_J} \int_0^{R(\phi)} f_k \, dr \, \cos \phi \, \sin \phi \, d\phi$$

$$= \Delta a \left[F_{k,\eta,1} \int_{\phi_I}^{\phi_J} \cos \phi \, d\phi + F_{k,\eta,2} \eta \left(\int_{\phi_I}^{\phi_J} \frac{1}{\sin \phi} \, d\phi - \int_{\phi_I}^{\phi_J} \sin \phi \, d\phi \right) \right] \eta$$

$$= \Delta a \left[F_{k,\eta,1} \eta \left(\frac{1}{r_J} - \frac{1}{r_I} \right) + F_{k,\eta,2} \eta \left(\ln \left(\frac{r_J - \xi_J}{r_I - \xi_I} \right) + \left(\frac{\xi_J}{r_J} - \frac{\xi_I}{r_I} \right) \right) \right] \eta$$

$$= \Delta a \left[F_{k,\eta,1} \left(\frac{1}{r_J} - \frac{1}{r_I} \right) + F_{k,\eta,2} \left(\ln \left(\frac{r_J - \xi_J}{r_I - \xi_I} \right) + \left(\frac{\xi_J}{r_J} - \frac{\xi_I}{r_I} \right) \right) \right] \eta^2 \quad (\text{E.2.129})$$

Lebenslauf

Name: Ingo Kaiser

Geburtsdatum: 14. August 1972

Geburtsort: Hannover, Bundesrepublik Deutschland

Staatsangehörigkeit: deutsch

Status: ledig, keine Kinder

Ausbildung

- 1978 – 1982: Grundschule Mengendamm, Hannover
- 1982 – 1984: Orientierungsstufe Birkenstraße, Hannover
- 1984 – 1991: Ratsgymnasium Hannover, Hannover
- 1991: Abitur
- 1991 – 1996: Studium des Maschinenbaus an der Universität Hannover
- 1996: Abschluss des Studiums, Verleihung des Grades „Diplom-Ingenieur“

Berufliche Tätigkeit

- 1996 – 2002: Wissenschaftlicher Mitarbeiter am Institut für Mechanik der Universität Hannover
- 2002 – 2014: Wissenschaftlicher Mitarbeiter am Deutschen Zentrum für Luft- und Raumfahrt (DLR) Oberpfaffenhofen
- 2015 – 2016: Wissenschaftlicher Mitarbeiter an der Escuela Politécnica Superior y Escuela de Arquitectura der Universidad Antonio de Nebrija, Madrid
- Seit 2017: Professor an der Escuela Politécnica Superior y Escuela de Arquitectura der Universidad Antonio de Nebrija, Madrid